Dendron-Mediated Self-Assembly, Disassembly, and Self-Organization of Complex Systems

Brad M. Rosen, Christopher J. Wilson, Daniela A. Wilson, Mihai Peterca, Mohammad R. Imam, and Virgil Percec*

Roy & Diana Vagelos Laboratories, Department of Chemistry, University of Pennsylvania, Philadelphia, Pennsylvania 19104-6323

Received April 19, 2009

Contents

* Corresponding author. E-mail: percec@sas.upenn.edu.

10.1021/cr900157q CCC: $71.50
Published on Web 10/30/2009

1. Introduction

1.1. Background

Dendrimers and dendrons are architectural motifs synthesized by either *divergent* or *convergent* iterative methods, and therefore, they provide monodisperse nonbiological macromolecules with a primary structure of the same level of precision as biological molecules and macromolecules.

Currently dendrimers and dendrons are explored at the interface between chemistry, biology, physics, medicine, complex soft-condensed matter, and nanoscience. While most dendrimers and dendrons are liquids or amorphous solids, they are nevertheless of great interest for many technological applications that are not part of this review. However, by analogy with biological macromolecules, specific primary structures generate programmed dendrons that self-assemble[1−5] into functional supramolecular structures that self-organize into periodic or quasiperiodic arrays. Therefore, through their molecular diversity, self-assembling dendrons and dendrimers provide access to the elucidation of the mechanism of hierarchical transfer of structural information from primary structure to higher structural levels. Ultimately they will answer fundamental questions related to the structural origin of order[6−9] and functions and provide access to the emergence of complex functional systems.[2,5−12] Self-assembling dendrons also mediate the self-assembly and self-organization of diverse polymeric, oligomeric, and monomeric structures with various topologies.

Self-assembly of molecular or macromolecular structures via self-assembling dendrons is preceded by dendron-mediated disassembly from their original three-dimensional arrangement. For example, a linear polymer functionalized with self-assembling dendrons as side groups, commonly named “dendronized polymer”, will disassemble the polymer from its crystal lattice or amorphous aggregate by isolating it in a dendritic coat. The disassembled structure exhibits different functions from those of the assembled structure. This disassembly process may be mediated not only by self-assembling dendrons but also by dendrons that do not self-assemble. In addition, there are situations in which a dendronized structure generated with dendrons that do not self-assemble will mediate the self-assembly of the newly resulting structure. Self-assembly, disassembly, and self-organization directed by dendrons and dendrimers occur either in

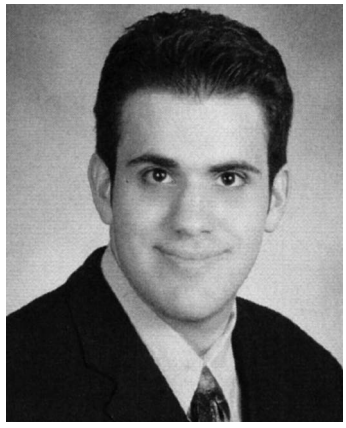

Brad M. Rosen was born in Philadelphia, Pennsylvania. He received his A.B. and A.M. in Chemistry from Harvard University in 2005, where he worked on the synthesis of cyclic enediyne antibiotics under the direction of Professor Andrew G. Myers. He will receive his Ph.D. in 2009 from the University of Pennsylvania. Under the direction of Professor Virgil Percec, his doctoral studies focused on the development of Ni-catalyzed cross-coupling and borylation, synthesis and retrostructural analysis of self-assembling dendrons, and the elaboration of Single-Electron Transfer Living Radical Polymerization. He is the recipient of a Rohm and Haas Graduate Research Fellowship, an NSF Graduate Research Fellowship (2005−2008), an ACS Division of Organic Chemistry Graduate Fellowship (2008−2009, Sponsored by Roche, Inc.), and a University of Pennsylvania Dissertation Fellowship (2009). In 2009, he joined DuPont Central Research and Development in Wilmington, Delaware.

Christopher J. Wilson was born in Wolverhampton in the United Kingdom. He received a M.Chem. (Hons) from the University of Hull in 2004. In 2002 he was awarded a Wellcome Trust grant for undergraduate researchers under the supervision of Dr. Ross Boyle. During his master's year, he worked under the supervision of Professor John Goodby and Dr. Isabel Saez. He completed his Ph.D. under the joint supervision of Dr. Georg H. Mehl and Dr. Ross Boyle, graduating in 2007. Since then he has been a postdoctoral researcher in the group of Professor Virgil Percec at the University of Pennsylvania. His research interests include synthetic organic chemistry, self-assembly of shape-amphiphiles, and soft self-assembly of complex systems.

Daniela A. Wilson (neé Apreutesei) was born in Comanesti, county of Bacau, Romania. She received her B.S. degree (Hon) in chemistry from "A. I. Cuza" University of Iasi, Romania, in 2001 and an M.S. degree (Hon) in environmental chemistry from the same university in 2003. In 2001 she started the Ph.D. program in parallel at "Gh. Asachi" Technical University of Iasi, Department of Organic Chemistry, Romania, under the supervision of Professor Dan Scutaru. During that time she joined in 2003 the group of Professor Shin'ichi Nakatsuji, University of Hyogo, Himeji, Japan, as an exchange Ph.D. student and the group of Dr. Georg Mehl, University of Hull, Hull, U.K., as a Marie Curie Fellow in 2004−2005. In 2006 she defended her Ph.D. thesis with *summa cum laudae* distinction. Since 2007, she was appointed as a postdoctoral researcher in the group of Professor Virgil Percec at the University of Pennsylvania. Her research interests include synthetic organic chemistry, organometallic chemistry, and supramolecular chemistry.

Mihai Peterca received his B.S. in Physics from A. I. Cuza University, Iasi, Romania, in 1997, a M.S. in Physics from University of Miami, Florida, in 2003, and a Ph.D. in Physics at the University of Pennsylvania in 2006 under the direction of Professor Paul A. Heiney. His research interests include self-assembly and self-organization, helicity and chirality, packing in 3 dimensions, and phase transitions. Currently, he is a postdoctoral fellow in Professor Virgil Percec's group working on the development of experimental methods and simulation techniques for the structural analysis of complex soft matter by X-ray diffraction.

solution, in bulk, or both, when the same self-assembled structure is persistent in both solution and bulk.

1.2. Scope of the Review

This review unifies all concepts of dendron-mediated self-assembly and self-organization. The field of dendrimers and dendrons was extensively reviewed in books,[13−16] book series,[17−21] and review series,[22−27] as well as specialized reviews, minireviews, critical reviews, microreviews, topical reviews, perspectives, feature articles, highlights, and accounts. We will discuss briefly those publications that are complementary to the present review as well as those that belong to topics that will not be covered here.

A series of fundamental reviews and highlights discuss synthetic aspects of dendrons and dendrimers,[28−48] and provide an excellent introduction to the field. Two reviews[49,50] and a series of minireviews[51−56] discuss selected topics related to supramolecular dendrimers. In addition, two reviews[57,58] and a large group of minireviews[59−69] on liquid crystal (LC) dendrimers cover complementary work to this review. All publications on LC dendrimers also describe the design of dendritic LCs by the periphery functionalization of conventional dendrimers with mesogenic groups. This class of dendrimers will not be discussed in the current

Mohammad R. Imam was born in Dhaka, Bangladesh. He received his B.Sc. and M.Sc degrees in Chemistry from Dhaka University and obtained his Ph.D. in Organic Chemistry from the University of Pennsylvania in 2008. His Ph.D. thesis work under the supervision of Professor Virgil Percec dealt with dendritic structures self-assembling into helical pyramidal columns and chiral spheres. In 2009 he was a postdoctoral fellow in the group of Professor Virgil Percec and pursued research in molecular recognition, self-assembly, and supramolecular chemistry. He is presently an Assistant Professor of chemistry at the King Fahd University of Petroleum and Minerals (KFUPM) in Dhahran, Saudi Arabia.

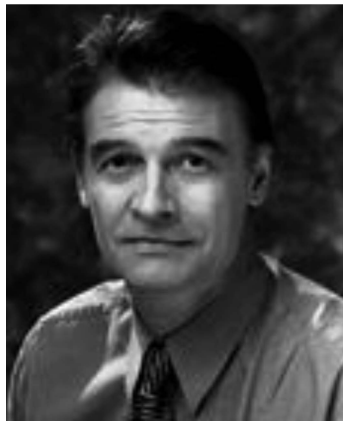

Virgil Percec was born and educated in Romania (Ph.D. 1976). He defected from his native country in 1981 and after short postdoctoral appointments at the University of Freiberg, Germany, and the University of Akron, U.S.A., he joined the Department of Macromolecular Science at Case Western Reserve University in Cleveland (1982) as an Assistant Professor. He was promoted to Associate Professor in 1984, to Professor in 1986, and to Leonard Case Jr. Chair in 1993. In 1999 he moved to the University of Pennsylvania as P. Roy Vagelos Professor of Chemistry. Percec's research interests lie at the interface between organic, bioorganic, supramolecular, and polymer chemistry and liquid crystals, where he contributed over 620 refereed publications, 50 patents, and over 1000 endowed and invited lectures. His list of awards includes Honorary Foreign Member to the Romanian Academy (1993), Humboldt Award (1997), NSF Research Award for Creativity in Research (1990, 1995, 2000), PTN Polymer Award from The Netherlands (2002), the ACS Award in Polymer Chemistry (2004), the Staudinger-Durrer Medal from ETH (2005), the International Award of the Society of Polymer Science from Japan (2007), and the H. F. Mark Medal from the Austrian Research Institute for Chemistry and Technology (2008). He is a Fellow of IUPAC (2001), PMSE Division of ACS (2003), AAAS (2004), and RSC (2008). He is the editor of the *Journal of Polymer Science, Part A: Polymer Chemistry* (since 1996) and of the book series *Liquid Crystals* and serves on the Editorial Boards of 20 international journals.

review. There are numerous reviews[70−78] on dendronized polymers. All examples presented in these reviews refer to dendron-jacketed polymers with limited discussion on self-organizable dendronized polymers. Other dendronized polymer topologies are not mentioned. Several accounts discuss helical chirality mostly on self-organizable dendronized poly(arylacetylenes).[79−81] Polymers dendronized at their chain ends are described only in several brief highlights.[82−85] Recent work on dendronized fullerenes was extensively discussed but only in brief accounts.[86−93] Older contributions on chiral dendrimers and dendrons were reviewed.[94−96] However most of them did not discuss self-assembling dendrons and supramolecular dendrimers. Therefore, they are important mostly from a historical perspective. Nevertheless, the readers are advised to consult recent reviews on the amplification of chirality in supramolecular systems.[97−100] There are a large number of reviews and brief reviews on supramolecular LCs,[101−104] discotic LCs,[105−108] discotic porphyrins, and phthalocyanines.[109,110] Most of these reviews on LCs are very specialized and are concerned with mesophases of interest to the LC community, though some contain sporadic examples of molecules functionalized with what are now termed first-generation Percec-type dendrons. These reviews are recommended for a general introduction to supramolecular LCs. Also as an introduction, we recommend two general reviews on rotaxanes[111,112] and a book on catenanes, rotaxanes, and knots,[113] although they do not discuss dendronized catenanes, rotaxanes, and knots. The reader is also sent to complementary reviews on glycodendrimers,[114−120] peptide dendrimers,[121−123] DNA dendrimers, and dendrimer conjugates.[124,125] Extensive reviews on applications of dendronized materials ranging from light-emitting diodes (LEDs)[126−128] and other electronic materials,[129−131] medicine,[132−141] and catalysis are available.[41,43,130,132,142−146] Topics related to self-assembly of dendritic molecules via transition metal complexes and the application of dendrimers in catalysis are not emphasized in this review.[142,143,147−149]

Historical events that have influenced the evolution of this field will also be discussed. In order to save space within the entire manuscript, we refer to dendrons, dendrimers, and references by mentioning only the corresponding author from that particular laboratory. Reference to dendronized polymers, oligomers, and monomers generated from dendrons that do not self-assemble will be made only when the resulting dendronized structure self-assembles or self-organizes. This review will cover reports in the literature published before April 2009.

The review follows the pattern of the organization in conventional functional polymers, i.e., topology followed by the place where the functional group is incorporated, with the functional group in this publication being replaced with a dendron.[150−155] Figure 1 describes the organization of the linear, cyclic, and star macromolecular topologies and their dendronized architectures, which will be discussed in this review. The first group involves linear polymers and block-copolymers jacketed with dendrons attached to the backbone either directly or via a spacer, or through a covalent or noncovalent bond connected from the dendron apex. The second group contains linear polymers jacketed with dendrons, twin dendrons, and Janus dendrimers attached via their periphery. The third group involves various linear polymers, oligomers, and block-copolymers dendronized at one or both of their chain ends. Cyclic oligomers dendronized with one or multiple dendrons represent the fourth group, while dendronized stars represent the last class. Thus far, examples of the last three topological classes have been limited to dendronization from the apex of the dendron.

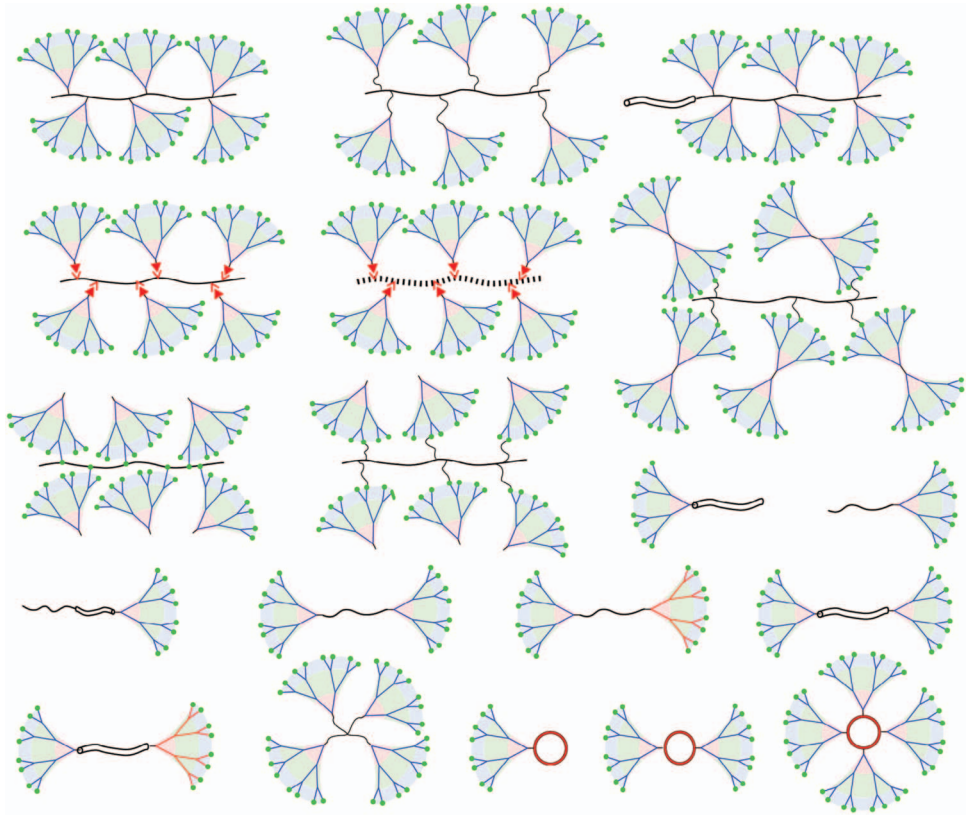

Figure 1. Topologies generated by dendronized linear, star, and macrocyclic polymers. From top left to bottom right: dendron-jacketed polymers with the dendron directly attached to the backbone via the dendron apex, dendron jacketed polymers connected by a flexible spacer, dendron-jacketed block-copolymers, noncovalently dendron-jacketed polymers, dendronized supramolecular polymers, polymers jacketed with dendrimers connected via dendron periphery, polymers jacketed with dendrons connected via dendron periphery, polymers jacketed with dendrons via dendron periphery through a flexible spacer, rigid polymers fuctionalized at one chain end with a dendron, flexible polymers functionalized at one chain end with a dendron, block-copolymers composed of rigid and flexible segments dendronized at one chain end, flexible polymers symmetrically functionalized with dendrons at both chain ends, flexible polymers asymmetrically functionalized with dendrons at both chain ends, rigid polymers symmetrically functionalized with dendrons at both chain ends, rigid polymers asymmetrically functionalized with dendrons at both chain ends, dendronized stars, and dendronized macrocycles. Dendrons (wedges), covalent polymers (long wavy lines), supramolecular polymers (dashed lines), rigid rods segments (wavy tubes), macrocycles (red rings), noncovalent interaction (red triangle and chevron), and their connectivities are pictured.

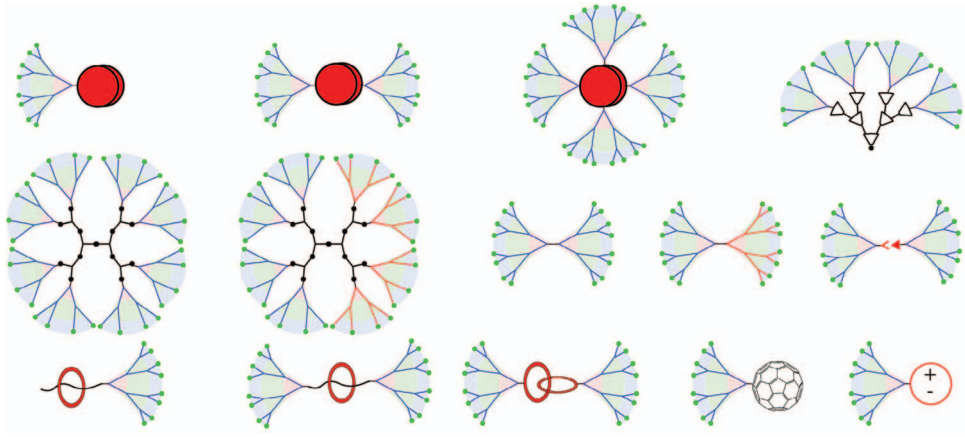

Figure 2. Topologies generated by dendronized polycycles (red discs), dendronized dendrimers (multicolored dendrons connected to black dendrimer framework) and dendrons (multicolored dendrons connected to black wedgelike dendron framework), dendrons dendronized at the apex with identical (twins) or different (Janus) dendrons, pseudorotaxanes, rotaxanes, catenanes, fullerenes, and ionic liquids (red circle with ± inside). Noncovalent interactions are depicted as red triangles next to a red chevron.

Figure 2 classifies the second large group of topologies. They involve dendronized polycycles, dendronized dendrimers, dendrons dendronized with identical (twin-dendrons) or with different (Janus dendrimers) dendrons at the periphery or at the apex, dendronized rotaxanes and catenanes, dendronized fullerenes, and dendronized ionic liquids. Applications derived from all the mentioned classes also will be discussed.

1.3. Definitions and Nomenclature

There are a variety of concepts, that we define below, which are necessary for the discussion of the material enclosed in this review. **Self-Assembly** is the process by which dendrons or dendronized molecules aggregate to form supramolecular objects, i.e., **intermolecular self-assembly**,

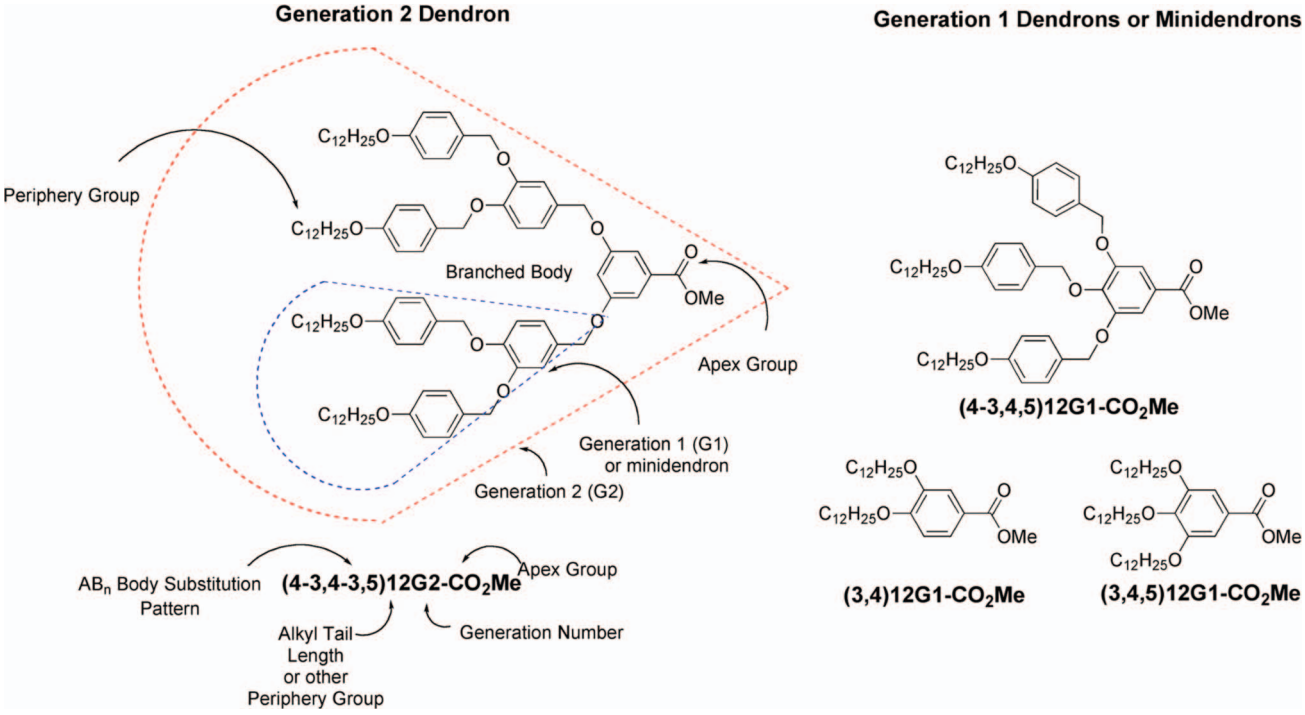

Figure 3. Nomenclature for Percec-type dendrons (left) and generation 1 (G1) dendrons/minidendrons (right).

Table 1. Strengths of Intermolecular Forces; Adapted and Expanded from Ref 162

interaction	strength
ion−ion[163]	100−350 kJ mol^{-1}
ion−dipole	50−200 kJ mol^{-1}
dipole−dipole	5−50 kJ mol^{-1}
hydrogen bonding[164]	4−120 kJ mol^{-1}
cation−π	5−80 kJ mol^{-1}
$\pi-\pi$[166,167]	0−50 kJ mol^{-1}
van der Waals forces	<5 kJ mol^{-1}
(CH_2-CH_2)[168]	(7 kJ/mol per CH_2)

or the process by which dendronized polymers achieve a well-defined 3-D structure, i.e., **intramolecular self-assembly**. **Coassembly** is the assembly of more than one distinct entity into a supramolecular object. **Disassembly**, in the context of this review, has two meanings. The first refers to the reverse of self-assembly, analogous to the reversible formation and denaturating of capsid proteins around the RNA core of the Tobacco Mosaic Virus (TMV).[156] The second meaning of disassembly is the dismantling of the original crystalline, liquid crystalline, or amorphous state of the material prior to self-assembly. Covalent disassembly such as in self-immolative dendrons or equilibration in dynamic combinatorial chemistry represents a different process. **Self-Organization** is the process by which supramolecular or macromolecular objects arrange themselves into periodic lattices or quasiperiodic arrays in solid state or solution. A **quasiperiodic** ordered array exhibits rotational symmetry other than the crystallographically allowed 2, 3, 4, or 6-fold symmetry. **Self-Control**[157,158] is the ability of a molecule to change its shape in response to its environment from a noninteracting (unsociable) to interacting (sociable) conformation. In some circumstances, self-control is equivalent to adaptability. **Quasi-equivalent**[157,158] building blocks are chemically identical subunits that self-control their shape during self-assembly. **Allosteric Regulation** is the influence and ultimate control of a conformation or structure via covalent or noncovalent modification of a chemical subunit.[159−161] **Complex Systems**[11,12] are defined by Ottino:[11]

"A complex system, is a system with a large number of elements, building blocks, or agents, capable of exchanging stimuli with one another and with their environment. The interaction between elements may occur only with immediate neighbors or with distant ones; the agents can be all identical or different; they may move in space or occupy fixed positions, and can be in one state or multiple states. The common characteristic of all complex systems is that they display organization without any external organizing principle being applied. In the most elaborate examples, the agents can learn from past history and modify their states accordingly. Adaptability and robustness are often the byproduct. Part of the system may be altered, and the system may still be able to function.... Complex systems cannot be understood by studying parts in isolation. The very essence of the system lies in the interaction between parts and the overall behavior that emerges from the interactions. The system must be analyzed as a whole."

Examples of complex systems include highways, the Internet, power grids, metabolic pathways, social and political organizations, financial systems, and many physical, biological, and chemical systems. In the relatively trivial example of a highway system, the components can be designed and engineered. However, even in this case, the system is constantly evolving and its emergence is determined by adaptation. Ottino[12] also stresses "that 'complex' is different from 'complicated'. The most elaborate mechanical watches are appropriately called 'très compliqué.' For example, the Star Caliber Patek Phillipe has over 1,000 parts. The pieces in complicated systems can be well understood in isolation, and the whole can be reassembled from its parts." This review pertains to the emergence of complex systems from dendritic buildings blocks. As quoted above, "[the dendritic building blocks] may move in space or occupy fixed positions, and can be in one state or multiple states," i.e., they are quasi-equivalent and exhibit self-control.

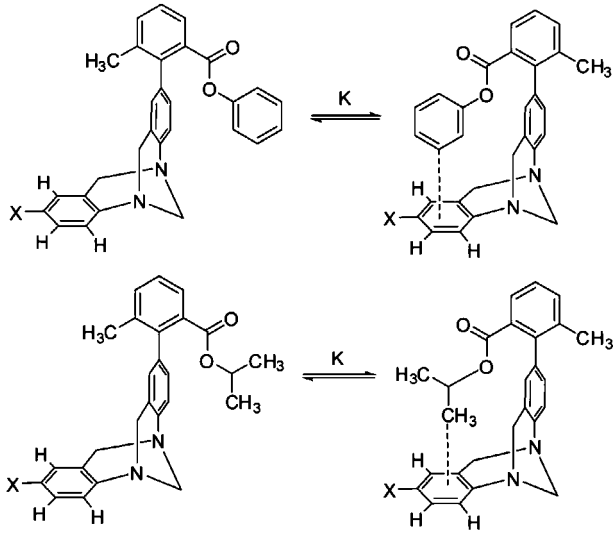

Figure 4. Molecular torsion balance.[167]

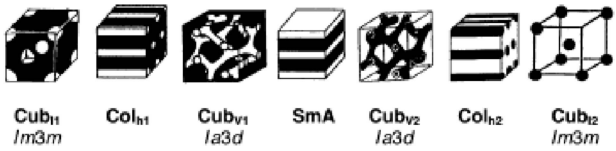

Figure 5. Phase diagram of AB diblock-copolymers.[169]

1.3.1. Nomenclature of Percec-type Dendrons

Self-assembling Percec-type dendrons mediate the self-organization of a variety of dendronized topologies and are, thus, frequently mentioned in this review. Unlike other dendron classes, Percec-type dendrons are prepared with a programmed branching sequence, like the primary structure of a protein, that dictates their self-assembly mechanism. The presence of a branching sequence means that generation number is not the sole determinant of molecular structure. A specific nomenclature has been developed to describe these molecules. For example, examine (4-3,4-3,5)12G2-CO_2Me (Figure 3). The numbers inside the parentheses denote the sequence of AB_n branched building blocks from the periphery to the apex. The number indicates from which position of the phenyl unit the B branches emanate. A descriptor such as Bp or Pr indicates a nonbenzyl branching unit such as biphenyl methyl or phenylpropyl, respectively. The number or descriptor following the parentheses indicates the number of carbons in the aliphatic tail, or alternative periphery unit. Following the periphery descriptor is the generation number. In this case, as there is an AB spacer unit followed by two AB_2 branching units, this molecule is a G2 dendron. The final descriptor is the apex functionality, which in this case is a methyl ester. In earlier reports, (3,4,5)*n*G1, (3,4)*n*G1, and even (4-3,4,5)12G1-CO_2Me were not referred to as dendrons. Later, after higher generations of dendrons and dendrimers generated from these builing blocks were reported by Percec's laboratory, these "minidendrons" were simply referred to as G1 dendrons.

For concision, many acronyms or symbols are used throughout this review to refer to specific polymers, phases, synthetic or analytic techniques, etc. The most frequently used acronyms have been presented in a Glossary at the end of this review. In some places where compounds are numbered within figures or schemes, they will be numbered **X.Y** or *X.Y*, where X is the figure or scheme number, respectively, and Y is the number of the compound within that figure or scheme.

2. Self-Assembling Dendrons as Models for the Design of Self-Organizable Dendronized Polymers

Understanding the self-organization of dendronized polymers is complicated by the broad array of topological classifications and the synergy of dendritic, polymeric, and small-molecule components. Self-assembling dendrons provide a simplified model for the design of self-organizable dendronized polymers. The intermolecular self-assembly of dendrons into supramolecular polymers is similar to the intramolecular self-assembly of linear polymers jacketed with self-assembling and nonself-assembling dendrons. Other topologies, such as linear polymers dendronized at their chain ends, dendronized star polymers, dendronized dendrons and dendronized dendrimers, or dendronized macrocycles, are either structurally similar to self-assembling dendrons or rely on their attachment to mediate self-assembly and self-organization.

Only by understanding the forces[162] (Table 1) responsible for the self-assembly of dendrons and by mastering their design principles can we truly address the self-assembly and self-organization of dendronized polymers.

The forces that govern self-assembly can be divided between directed and nondirected interactions. Directed

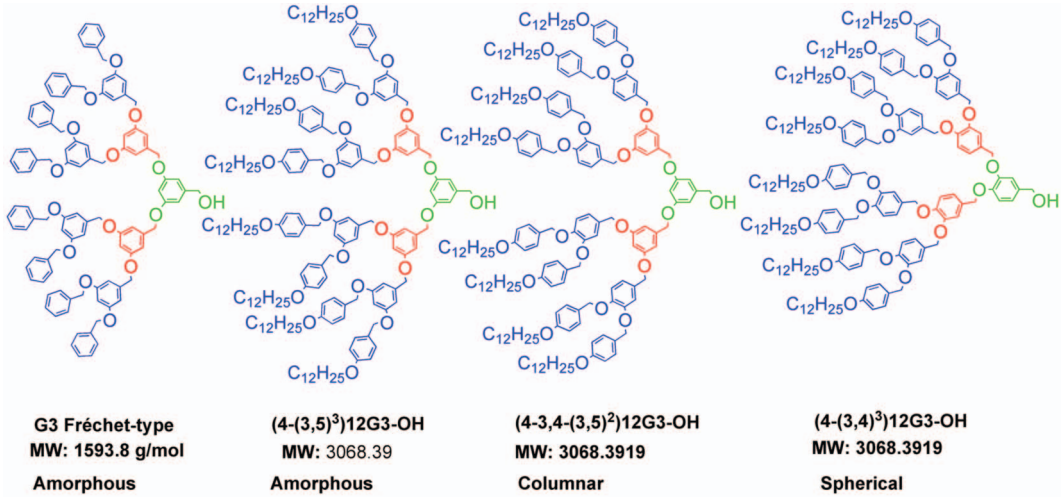

Figure 6. From amorphous benzyl ether dendrons to self-assembling benzyl ether dendrons.

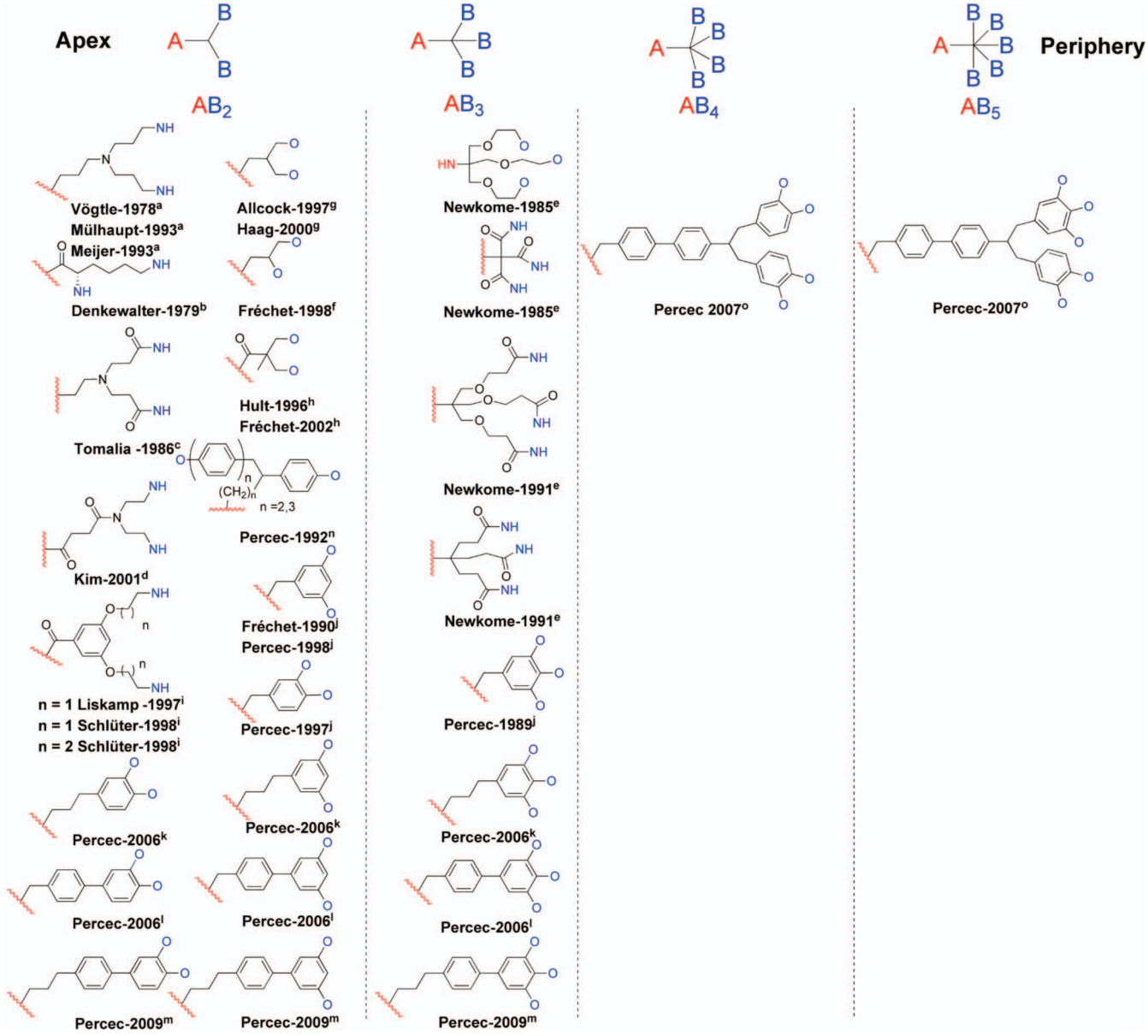

Figure 7. Selected examples of AB_2, AB_3, AB_4, and AB_5 building blocks used in the design of self-assembling dendrons and self-organizable dendronized polymers. [a]Refs 244− 246. [b]Refs 183, 247− 249. [c]Refs 184 and 186. [d]Refs 256 and 257. [e]Refs190, 260, and 261. [f]Refs 264. [g]Refs 262 and 263. [h]Refs 258 and 259. [i]Refs 268, 269, and 270. [j]Refs 192, 195, 265− 267. [k]Refs 273. [l]Refs 274. [m]Ref 181. [n]Refs 215−220 and 221. [o]Refs 275.

Scheme 1. Synthesis of PPI Dendrimers

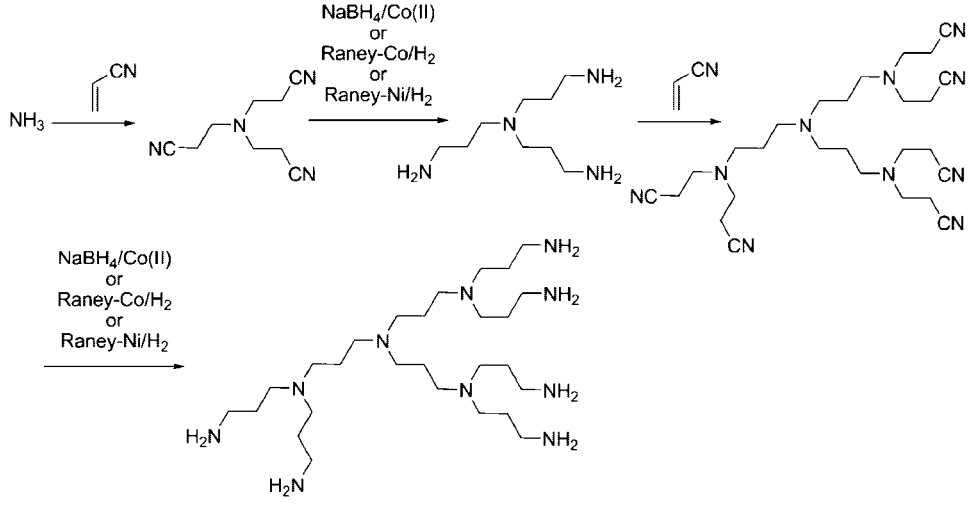

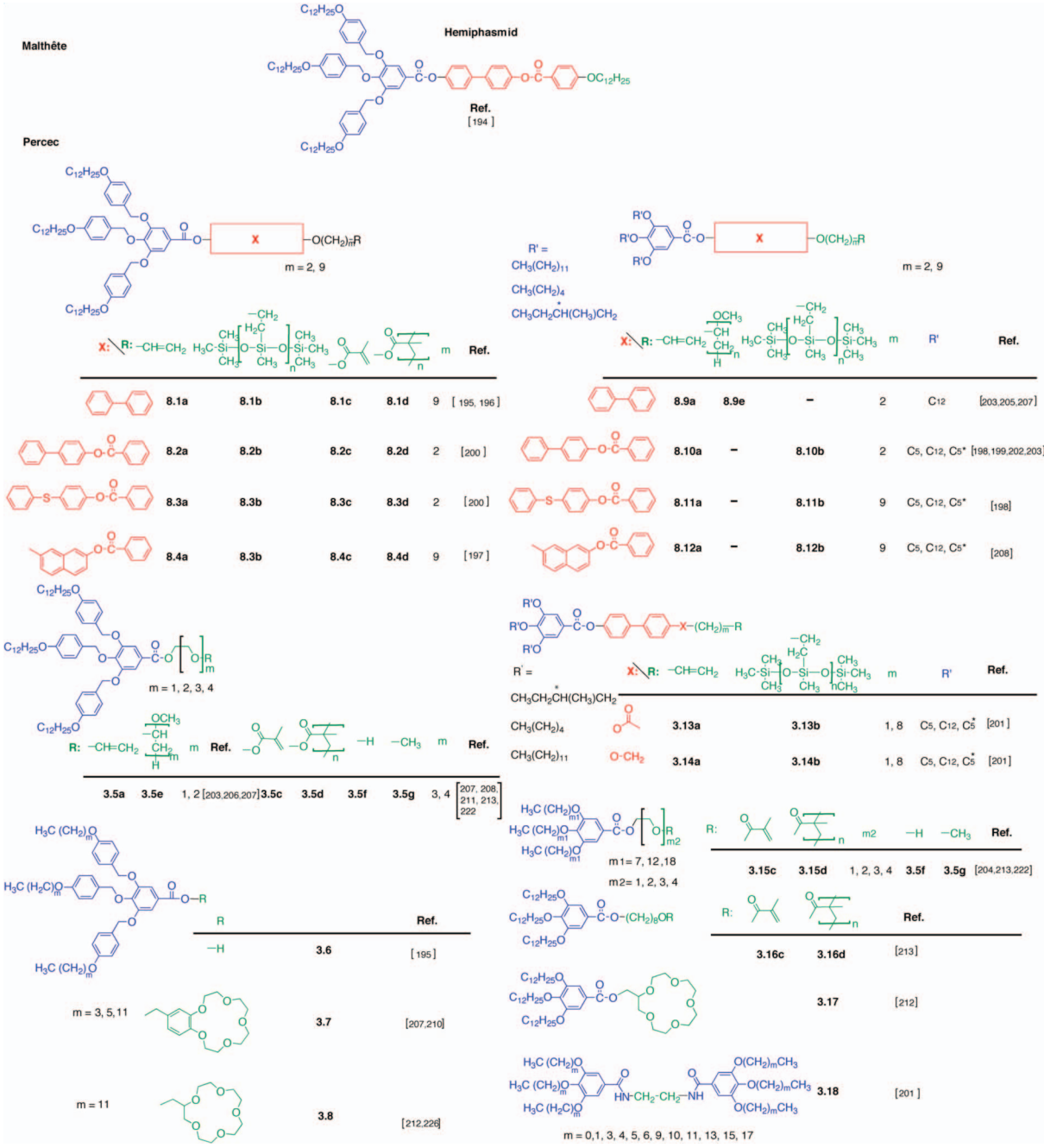

Figure 8. Hemiphasmid reported by Malthête[194] (top) and a selected group of similar first-generation monomers and their polymers reported by Percec.

interactions largely relate to ion−ion,[163] donor−acceptor interactions, H-bonding, and ion−dipole interactions. Ion−ion interactions are of similar magnitude to covalent bonds and, while not traditionally associated with soft condensed matter, are of importance in the formation of ionic liquids, which will be discussed later. H-bonding interactions can be carefully designed through receptor sites, and though their energy is highly variable, they typically contribute between 5 and 30 kJ/mol of stabilization per H-bond pair.[164] Ion−dipole interactions are classic examples of molecular recognition pioneered by Lehn and are intermediate in strength between H-bonds and ion−ion electrostatic interactions.[165] In many cases, directed interactions can be used to manipulate structures or enhance stability. However, there are numerous examples, from our laboratory and others, where modification of chemical structure to reduce or eliminate directed interactions results in retention of self-assembled structure. As such, nondirected interactions between neighboring molecules must contribute significantly to stabilization of self-assembled structures. The relative contributions of each nondirected interaction to self-assembly is still a matter of fundamental research and debate. Sanders and Hunter developed a model that characterized the nature of $\pi-\pi$ interactions via a simplified model of the aromatic system as "positively charged σ-framework between two negatively charged π-electron clouds."[166] This model suggests that the greatest contribution to the $\pi-\pi$ interaction arises from the $\pi-\sigma$ attraction of individual atoms rather than whole molecular π system. Wilcox forwarded an alternative model, drawing support from a "molecular torsion balance" (Figure 4) wherein the folding energies of phenyl esters and isopropyl esters could be quantified.[167] Wilcox concluded that London dispersion forces rather than electrostatic interactions play the most significant role in CH$-\pi$ interactions.

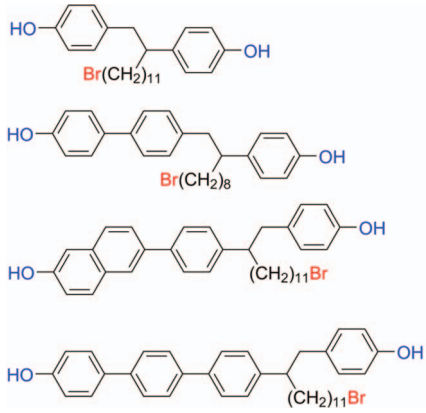

Figure 9. AB_2 building blocks used for the synthesis of hyperbranched polymers and willowlike dendrons and dendrimers.[216−222]

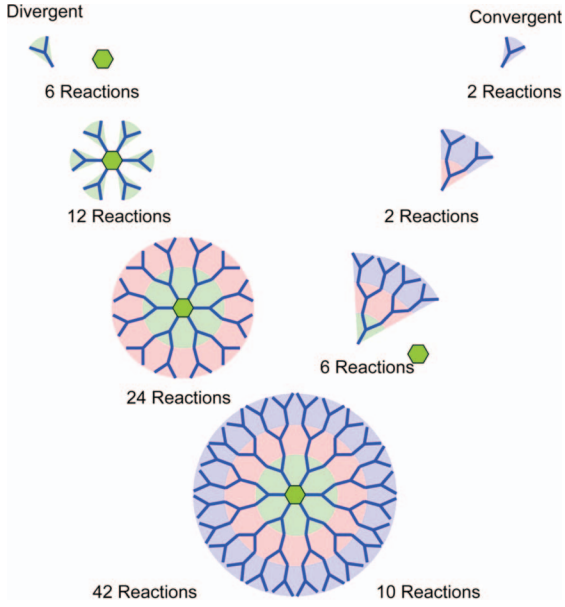

Figure 10. Convergent and divergent synthesis of dendrimers and dendrons.

More significant is the difference between the magnitude of these forces in chemically similar and dissimilar species. Dipole−dipole forces between two hydrophilic domains are stronger than the corresponding interactions between hydrophilic and hydrophobic domains (dipole−induced dipole). Thus, self-assembly can be mediated by the design of molecules composed of multiple domains of different chemical composition, e.g., hydrophilic, aliphatic, and aromatic. In solution, molecules will arrange themselves so as to bury solvophobic portions of the molecule, while in bulk, molecules will orient themselves to maximize the close contact of chemically similar domains. To achieve a specific self-assembled structure, the precursor molecules should be designed to allow optimum close-packing of chemically similar groups. For instance, even in simple examples of alkanethiols on Au surfaces, the close packing of the aliphatic chains allows for 7 kJ/mol of stabilization energy per methylenic group.[168] While the nature of the forces acting upon the self-assembly process are understood, the relative contributions of each force to that process still require significant investigation.

In AB block-copolymers, self-organization occurs when the A and B blocks are immiscible. The type of structure formed is dictated by the weight or volume fraction of the two blocks

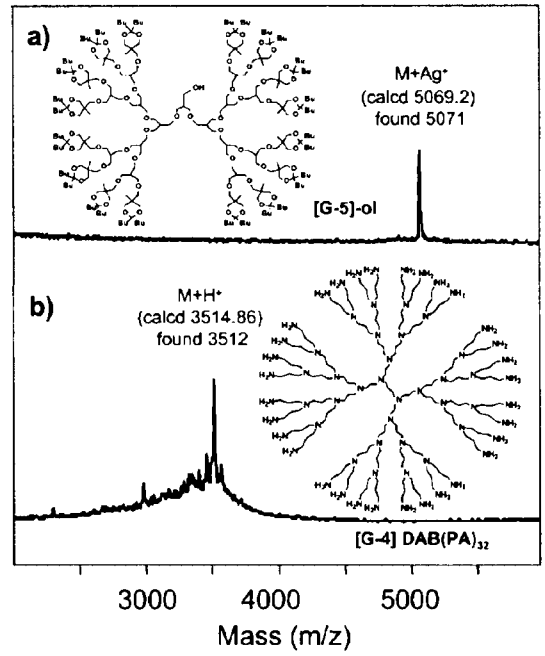

Figure 11. MALDI-TOF spectrum of convergently prepared dendron (a) and divergently prepared dendrimer (b). Reprinted with permission from ref 40. Copyright 2001 American Chemical Society.

(Figure 5).[169] Increasing the weight ratio of the minority block results in a transition from a BCC lattice, to hexagonal perforated lamellar lattice to a cubic gyroid phase, to an S phase. Above 50% weight fraction, the reverse order of phases is observed wherein the blocks are interchanged.

While the self-assembly and self-organization of dendrons often result in microphase-segregated structures, the presence of two immiscible domains is not a strict requirement, and certainly the weight fraction of the immiscible domains is not the primary determinant of structure (Figure 6). G3 Fréchet dendrons do not self-organize and are amorphous liquids. Introduction of a chemically dissimilar aliphatic tail, such as in (4-$(3,5)^3$)12G3−OH, does not mediate self-organization despite ∼50% mass fraction of the tails.[170] However, if the benzyl branching sequence is altered at the periphery while maintaining the ∼50% mass fraction of the aliphatic tails, such as in (4-3,4-$(3,5)^2$)12G3−OH, self-assembly into supramolecular columns followed by self-organization into a Φ_h lattice is observed. Further alteration of the benzyl branching sequence at the apex while maintaining the mass fraction of the aliphatic and aromatic domains, such as in the constitutional isomer (4-$(3,4)^3$)12G3−OH, results in a change in the mechanism of self-assembly so as to form supramolecular spheres that self-organize into a *Cub* lattice. Additionally, it has been shown that the dendronized dipeptide (4-3,4-3,5)*n*G1-CH_2O-Boc-L-Tyr-L-Ala-OMe self-assembles into helical columns that self-organize into a Φ_h lattice, regardless of the length of the aliphatic tail, be it one methylenic unit (∼5% mass fraction) where analogous AB diblock-copolymers would form a spherical structure or 16 methylenic units (∼45% mass fraction) where analogous AB diblock-copolymers would form lamellar structures.[171]

Self-assembly of dendrons is a form of supramolecular polymerization.[172] Unlike H-bonded or coordination polymers, which often follow a multichain open association model of growth dominated by directed interactions, the

Scheme 2. Synthesis of Poly(L-lysine) (PLL) Dendrons[183]

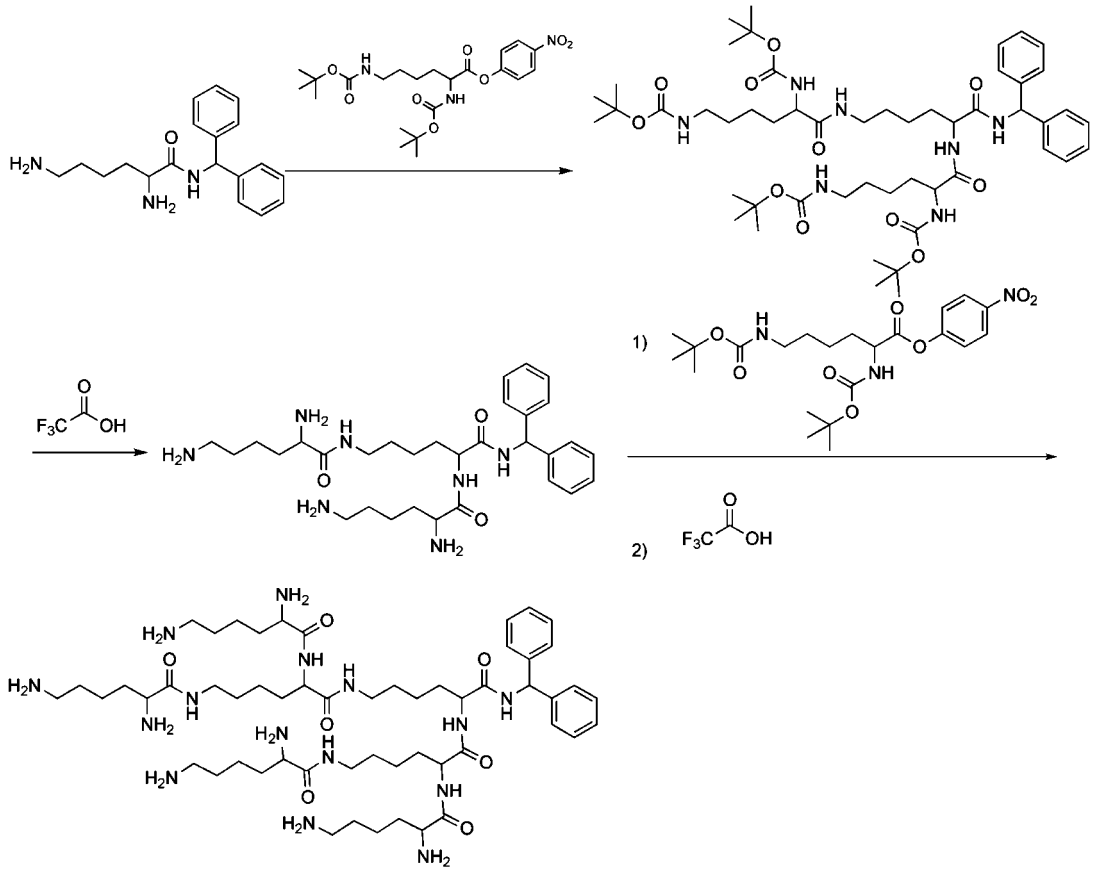

enthalpy term of dendritic self-assembly is strongly influenced by shape interactions and recognition.[101−104,173−175] The growth of the supramolecular assembly is also coupled with and accelerated by the emergence of LC ordering. A universally consistent model for the self-assembly of dendrons and ab initio prediction of structure is not presently available, though work progresses toward the elucidation of such "nanoperiodic" properties.[176] While the presence of directed interactions or immiscible surface and body domains help drive self-assembly and self-organization, molecular shape may be the most critical factor in the formation of 2D and 3D structures.

2.1. Dendrons and Dendrimers

2.1.1. Overview and Historical Background

Structurally, dendrimers consist of a branched core onto which are attached branched arms. The branched arms of dendrimers, which contain nonbranched focal functionality, are named dendrons. Dendrimers and dendrons can be viewed as ideal branched polymers, wherein each monomer repeat unit (mru) introduces a new AB_n bifunctional moiety, where n is the number of branches introduced with each monomer (Figure 7).[177−180] The A domain is connected in the *endo*-direction toward the apex, while the B domain projects outward in the *exo*-direction toward the periphery. For most dendronized topologies encountered, $n = 2$, 3, 4, or 5.

The first low molecular weight dendritic molecules, branched G2-G3 poly(propylene imine) (PPI) dendrimers, were reported by Vögtle[182] in 1978 (see section 2.2 and Scheme 1). In 1979, Denkewalter[183] reported the synthesis of branched L-lysine dendrimers, and in 1984, Tomalia reported in a series of papers and patents the highly influential *divergent* synthesis of higher generation poly(amidoamine) (PAMAM) dendrimers that became a landmark in the field.[184−189] It was Newkome who first reported in 1985 the *grafting* of preformed G1 dendrons onto a branched core to form a G2 dendrimer.[190] In 1990, Fréchet described the first truly *convergent* synthesis of dendrons based on 3,5-dihydroxybenzyl alcohol.[40,191,192] In the same year, Neenan reported the *convergent* synthesis of dendrimers based on 1,3,5-trisubstituted benzenes.[193] Inspired by the hemiphasmid molecule (Figure 8, top left) reported by Malthête in 1986,[194] in 1989 Percec's laboratory reported the synthesis and elaborated the structures of the first libraries of dendritic macromonomers based on (4-3,4,5)12G1, their polymers that represented the first examples of self-organizable dendronized polymers, and the first self-assembling dendrons (Figure 8).[195−213] The rationale of Malthête's and Percec's experiments was briefly discussed in an account[214] and will be detailed in a different subsection.

The self-assembly of these dendrons and dendronized polymers into supramolecular columns was demonstrated in 1989 by differential scanning calorimetry (DSC) and TOPM[195] and in 1991 by X-ray diffraction (XRD) analysis.[199] In 1994, XRD analysis of fibers produced from both macromolecular and supramolecular columns indicated their self-assembly into helical structures, therefore implying that they are chiral.[211] A second class of self-assembling dendrons was designed in Percec's laboratory from conformationally flexible rodlike AB_2 mesogens.[215] One of the two preferred conformations of thse AB_2 repeat units was expected and later demonstrated to self-organize in N and S phases. Libraries of linear and hyperbranched polymers were investigated to select and design in an accelerated fashion the most suitable AB_2 building blocks (Figure 9) that provided

Scheme 3. Synthesis of Tomalia-type PEI Dendrimers[250,35]

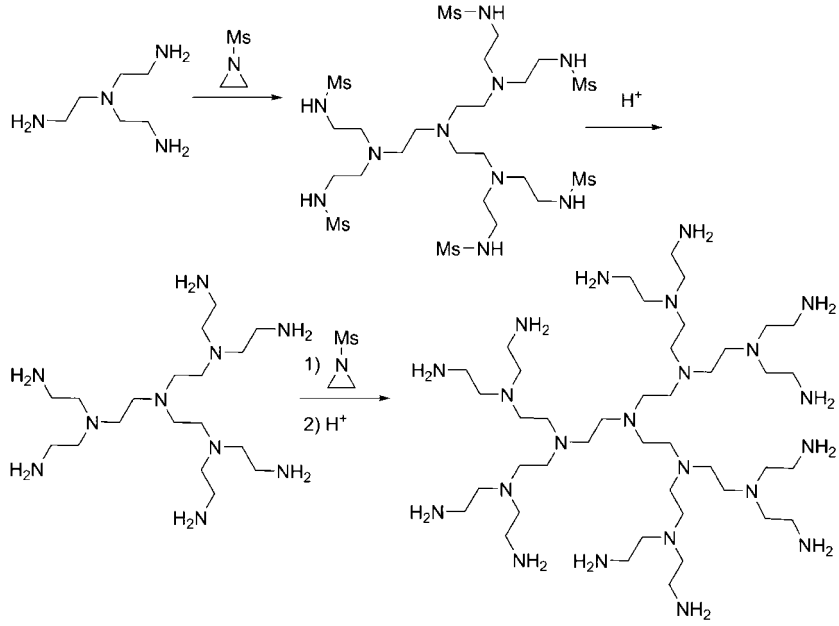

Scheme 4. Synthesis of Tomalia-type PAMAM Dendrimers[186]

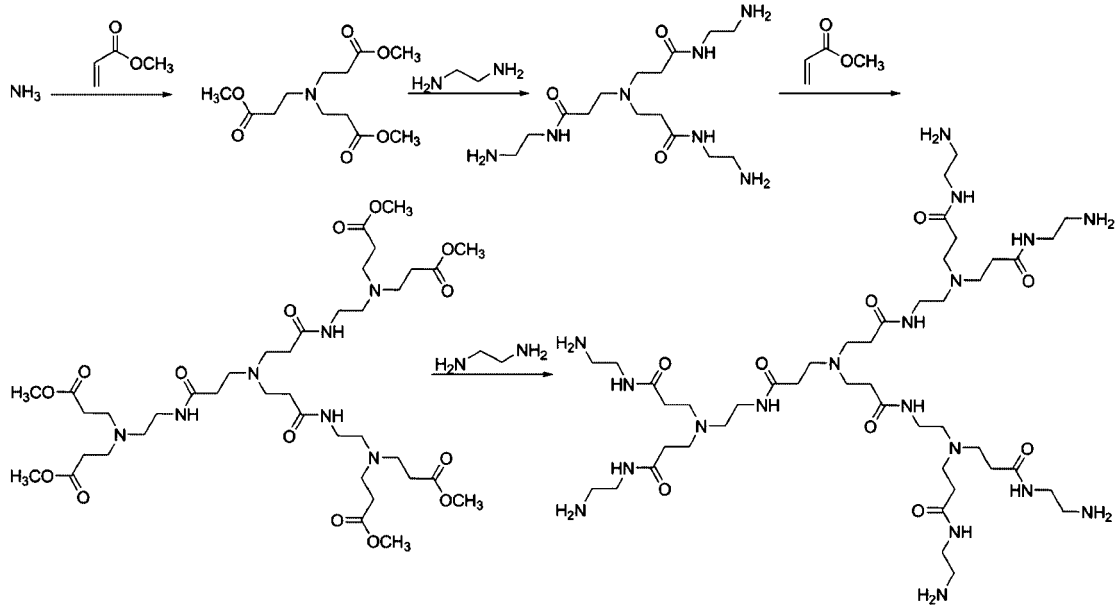

dendrons and dendrimers that were self-organizable in N and S phases.[216−223] As early as 1992, the work from Percec's laboratory was extensively reviewed in conference proceedings and in book chapters.[224−239] While other classes of dendrons and dendrimers do not exhibit the same propensity for self-assembly as Percec-type dendrons, they did in fact provide insight into the role of molecular symmetry.[240] PAMAM dendrimers composed of symmetrical branching units exhibit periodic variation in density with generation number, achieving minimum density at G4.[241] Thus, PAMAM dendrimers of sufficient generation number exhibit solvent-filled intramolecular free volume that can be exploited for encapsulation and delivery of small molecules.[242] Denkewalter's poly(L-lysine) (PLL) dendrons, which are constructed from an asymmetrical branching unit, pack effectively, resulting in less internal solvent-filled void space, and do not vary significantly in density with generation number.[183] Internal solvent-filled void-space in solution may indicate inefficient packing in bulk, providing a partial explanation for why Fréchet dendrons and Percec-type $(3,5)^n12Gn$ dendrons composed of symmetric AB_2 branching units do not self-assemble or self-organize. However, Percec-type dendrons composed of at least one (3,4) AB_2 or (3,4,5) AB_3 asymmetric branching unit self-assemble into supramolecular dendrimers that self-organize into periodic lattices and quasiperiodic arrays.

2.1.2. Synthesis of Dendrons

Dendrons can be prepared through iterative *convergent*[40,191,192] and *divergent*[182,184−190] growth pathways (Figure 10). In the convergent growth strategy, periphery units are sequentially attached to AB_n branching units. With each iteration, the number of total branches is increased by a factor of *n*, where *n* is the number of branches introduced in each branching unit. As *n* is typically between 2 and 4, the total number of attachments per iteration is small and the resulting dendron can typically be prepared as a monodisperse species with

Scheme 5. Convergent Synthesis of PAMAM-like Dendrons; PyBOP = (Benzotriazole-1-yl-oxy-trispyrolidinophosphinium Hexafluorophosphate)[253]

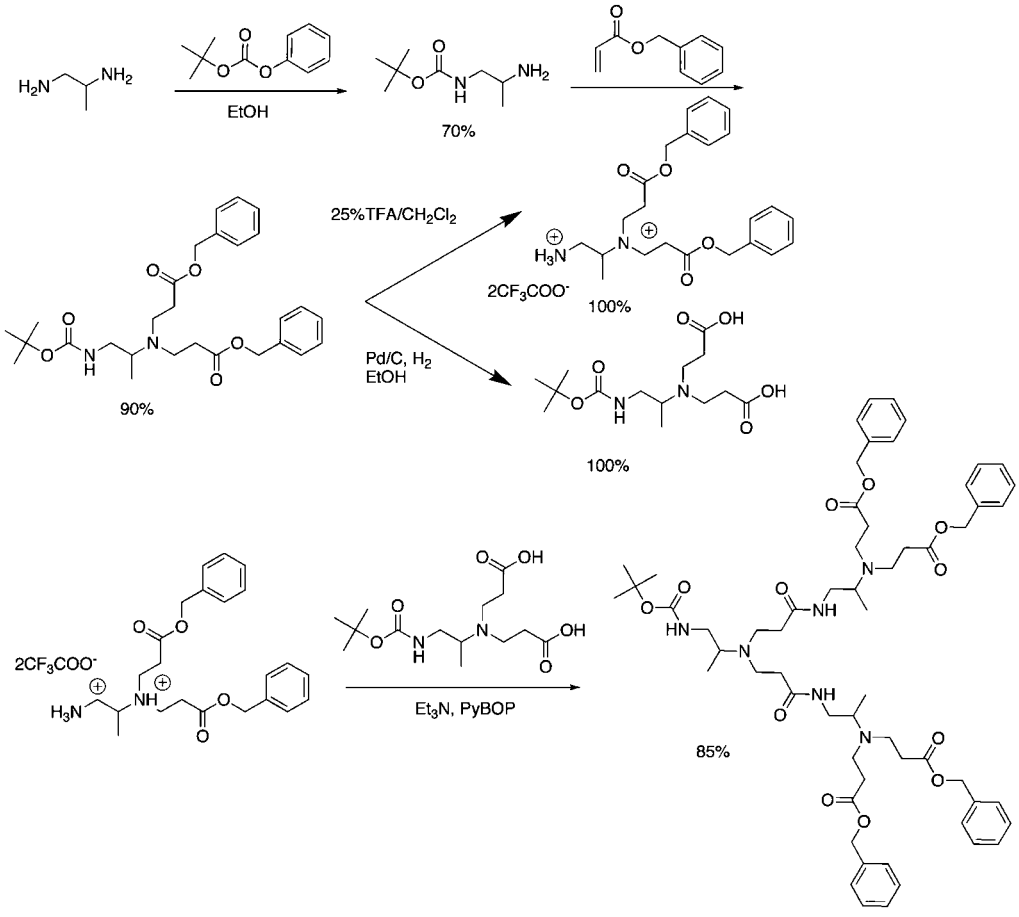

Scheme 6. Synthesis of Kim Amphiphilic Amide Dendrons[256]

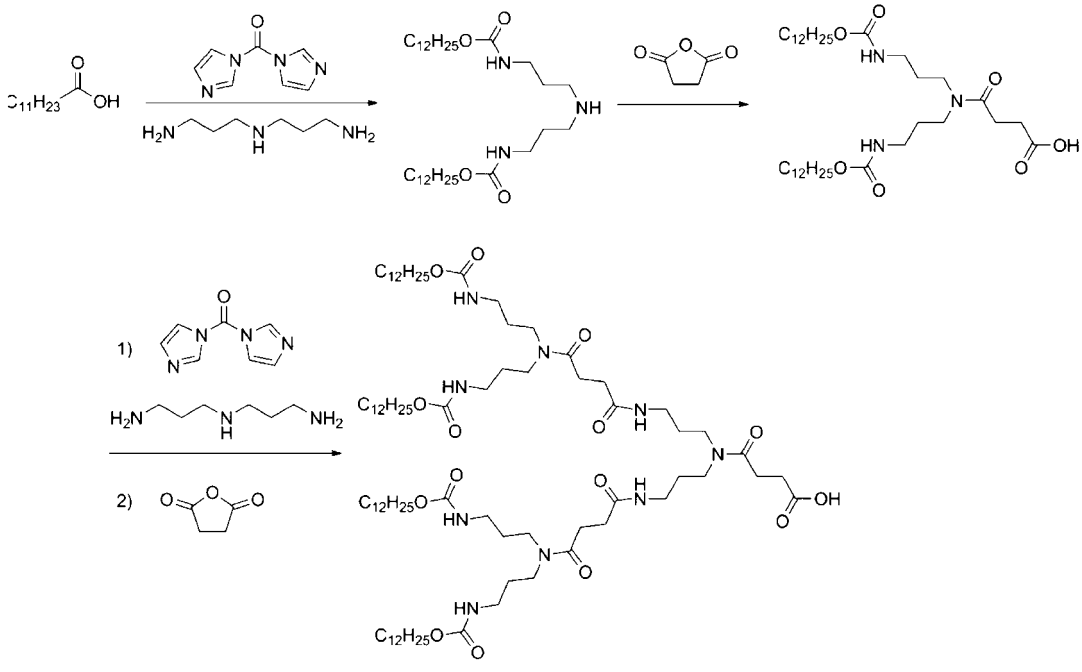

perfect branching that can be confirmed by a combination of analytical techniques including a single peak in MALDI-TOF (Figure 11a).[40] The total number of branches in a dendron produced via a convergent strategy is equal to n^g, where g is the generation number. In the divergent growth strategy, an m-branched core is iteratively decorated with AB_n branching units. The total number of attachments needed for a generation g dendron is equal to $m \times (n^{g-1})$. At low generations, dendrons produced via divergent strategies may be isolable as a monodisperse species, but at higher genera-

Scheme 7. Hult Convergent (Top)[258] and Fréchet Divergent (Bottom)[259] Synthesis of bis(MPA) Dendrons

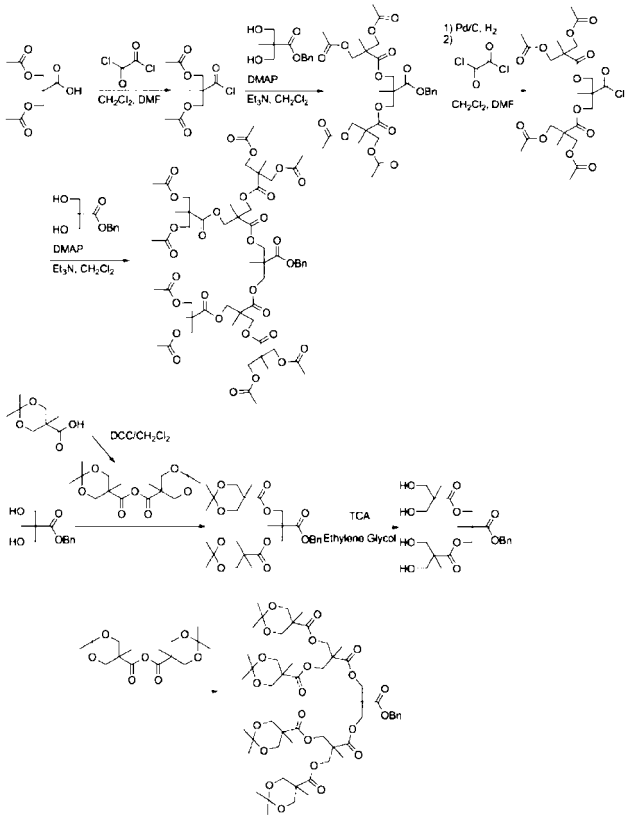

tion, imperfect branching and some polydispersity may be unavoidable, resulting in multiple matrix-assisted laser desorption ionization time-of-flight (MALDI-TOF) peaks (Figure 11b).[40] de Gennes "dense-packing" theory imposes a physical limit on the perfection of divergent growth due to steric crowding at highly functionalized peripheries.[243] Accordingly, steric crowding and the high number of simultaneous periphery functionalizations needed at high generation number limit perfect growth in the divergent approach. Further, the number of reactive surface groups tends to increase the number of deleterious side-reactions. The generation at which a monodisperse structure is no longer attainable is dictated by the efficiency of the attachment chemistry and the length and flexibility of linkages between branching points. The divergent growth strategy results in dendrons with total branching proportional to $m \times (n^g)$. Like supramolecular dendritic polymers, self-organization in dendron-jacketed polymers is partially mediated by *exo*-recognition of the dendrons. Structural imperfections tend to diminish this recognition, and therefore, a high degree of structural uniformity is needed to mediate self-organization. Therefore, the convergent growth strategy is the most frequently employed approach for the synthesis of self-organizing dendrons, dendronized polymers, and other dendronized topologies.

An exhaustive discussion of dendron synthesis is beyond the scope of this review and is available in many other reviews and monographs (see section 1.2). However, a brief but updated instructive overview of the synthesis of the most significant classes of dendrons discussed herein will help readers to follow this review. As will be demonstrated in this chapter, Percec-dendrons more so than any other class have been shown to exhibit rich self-assembly and self-organization behavior in the absence of a polymeric backbone or other intervening core groups. The other classes of dendrons are more notable for their role in self-organization of dendronized polymers and related topologies.

The first reported dendrons were prepared in a divergent manner using AB_2 building blocks. PPI dendrimers, pioneered by Vögtle[182] are prepared through iterative Michael addition of primary amines to acrylonitrile and subsequent nitrile reduction with $NaBH_4$/Co(II) (Scheme 1). The original procedure was improved through the use of Raney-Nickel/H_2 for the reduction step and procedural improvements to

Scheme 8. Synthesis of Newkome-type "Arborols" Dendrimers[190]

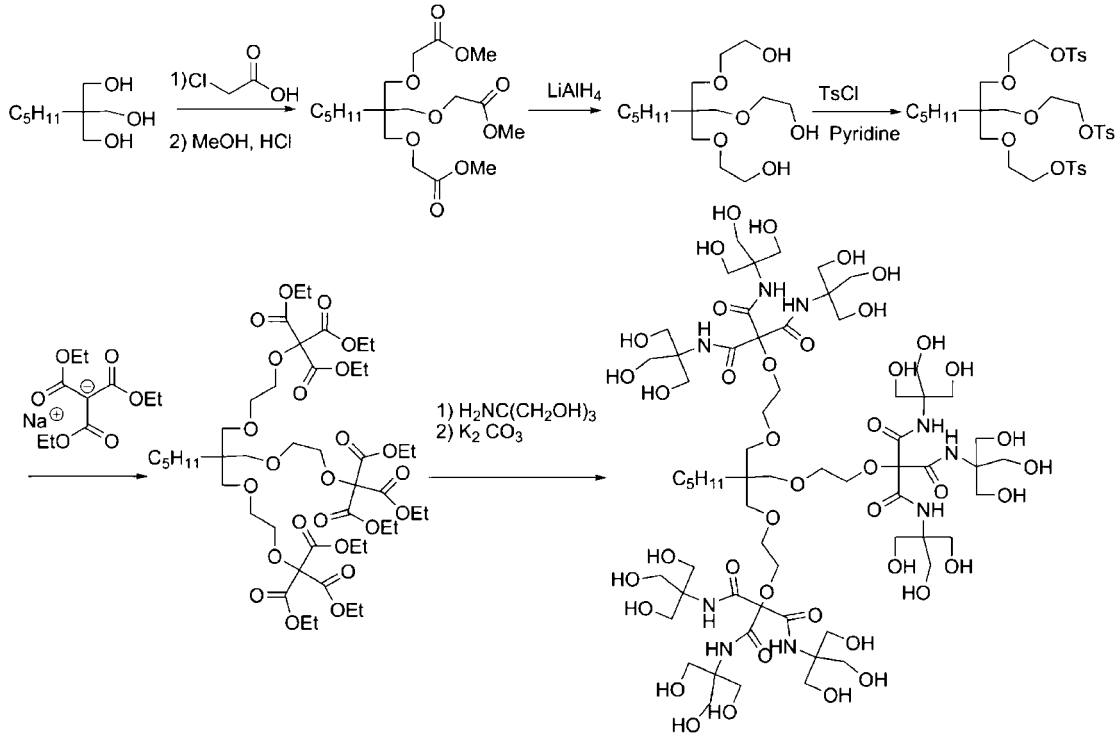

Scheme 9. Newkome Dendrimers Prepared Using Lin's Amine[260]

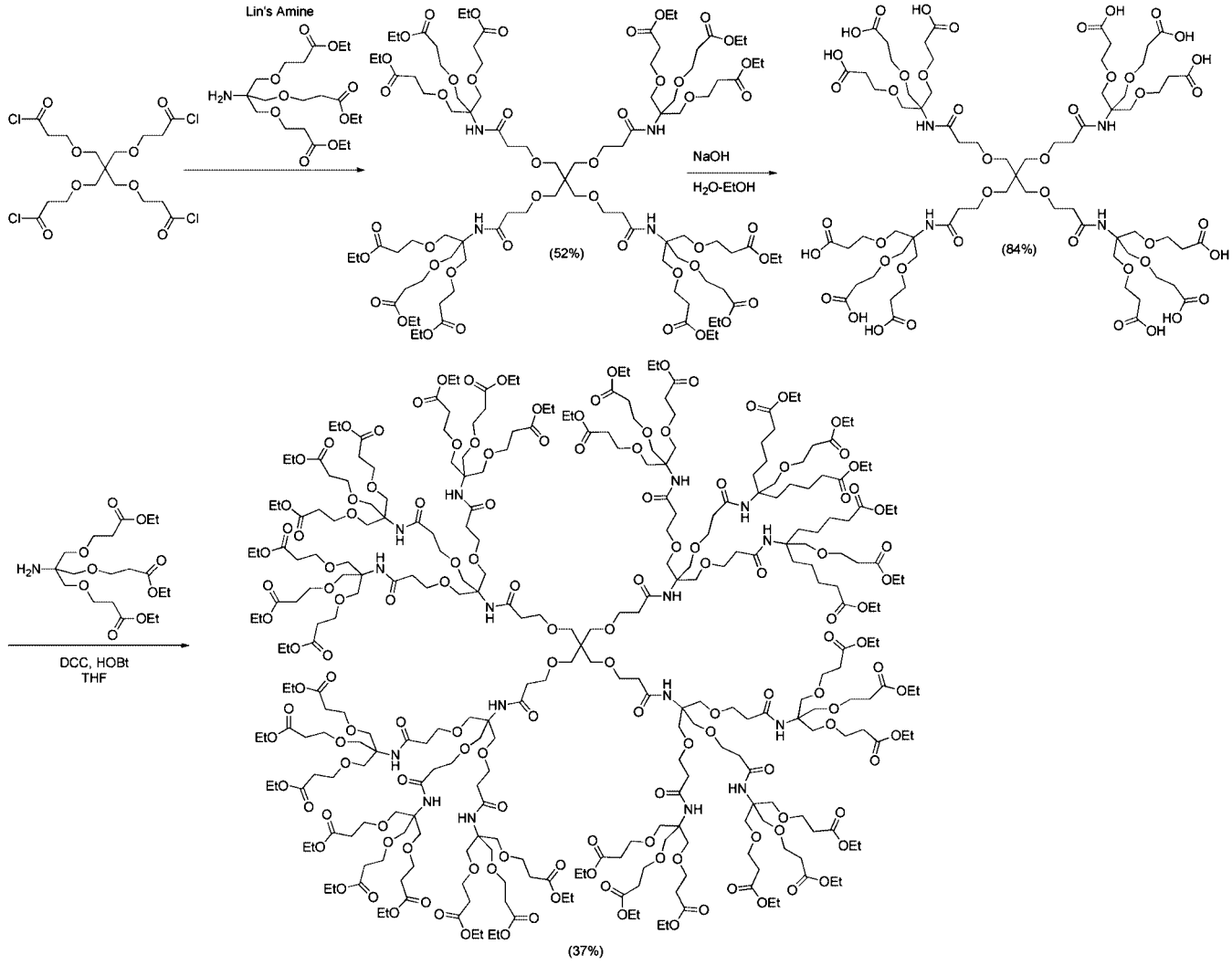

the acrylonitrile addition step, allowing for access to G5 PPI dendrimers with greater structural fidelity.[244] While at DSM, Meijer reported the use of Raney-Co/H_2 for hydrogenation in large-scale PPI dendrimer synthesis. This latter method is by far the most effective approach and was subsequently adopted by DSM for the commercialization of Astromol PPI-type dendrimers.[245] Despite the advantages of the DSM methods, this divergent approach does not result in a single pure molecule due to incomplete branching reactions and competive side-reactions such as retro-Michael addition. While, polydispersity of the G5 PPI dendron is as low as 1.002, ESI-MS studies have shown less than 23% error free dendrons (dendritic purity) of PPI.[246]

In three patents, the first issued in 1979, Denkewalter reported the synthesis of chiral poly(L-lysine) (PLL) dendrons via a divergent methodology (Scheme 2).[183,247−249] Condensation of the primary amine groups of benzhydrylamine protected L-lysine with *p*-nitrophenol activated ester of Boc-protected L-lysine, followed by deprotection of the Boc-groups with trifluoroacetic acid, provides a G2 dendron with four periphery primary amines. The primary amines can serve as grafting sites for iterative synthesis of higher-generation dendrons. Denkewalter's dendrimers have been shown to behave as ideal nondraining and exhibit double molecular weight with each generation, making them suitable markers for size-exclusion chromatography.[247]

Tomalia reported the synthesis of poly(ethylene imine) (PEI) dendrimers via iterative nucleophilic ring-opening of excess *N*-mesylaziridine or *N*-tosyl aziridine with primary amines followed by acidic hydrolysis of the *N*-mesylate (Scheme 3).[35,250] Because of the shorter linkage between branches in PEI dendrimers versus PPI dendrimers, the de Gennes dense-packing limit occurs at G4. As a result, PEI dendrimers have not been as widely used as other classes of dendrimers, though it was shown that treatment of G3 PEI dendrimers with 12 equiv of octanoic acid resulted in the formation of a lamellar lyotropic LC phase.[251]

Tomalia reported the synthesis of poly(amidoamine) (PAMAM) dendrons (Scheme 4).[184−189] Primary amines were treated with methyl acrylate and underwent Michael addition. The resulting ester was amidated with often more than 100-fold molar excess of ethylenediamine, resulting in a new branched primary amine. While up to G9 PAMAM dendrimers prepared by this method are available commercially, electrospray ionization mass spectrometry (ESI-MS)[132] and MALDI-TOF[252] studies have shown that, due to unavoidable *retro*-Michael additions and intramolecular cyclization reactions that also plague the synthesis of PPI dendrimers, dendritic purity at the G4 dendrimer can be lower than 10%. More recently, Christensen developed a convergent approach to PAMAM-like dendrons (Scheme 5).[253] 1,2-Propanediamine is selectively boc-protected at the amino attached to

Scheme 10. Allcock[262] (Top) and Fréchet[264] (Bottom) Synthesis of Dendritic Poly(ethylene oxide)

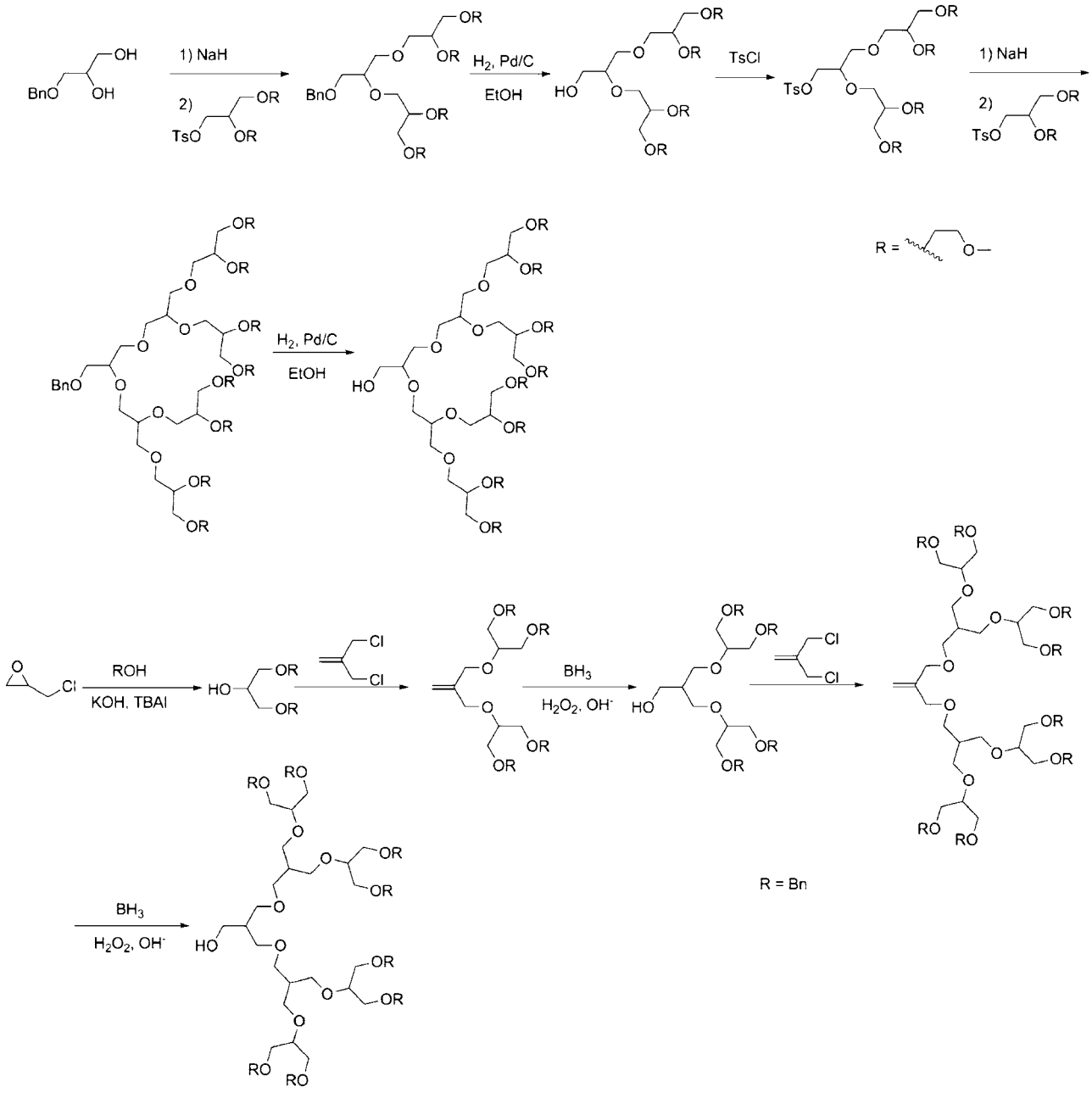

the primary carbon using *tert*-butyl phenyl carbonate.[254,255] The Boc-protected diamine is treated with neat benzyl acrylate to provide the double Michael addition product in very good yield. Treament with 25% TFA in CH_2Cl_2 cleaves the Boc group to provide a free amine and protonates all nitrogens to form a ditrifluoroacetate salt. Alternatively, hydrogenation over Pd/C cleaves the benzyl ester to provide the diacid. Condensation of the diacid with 2 equiv of the free amine in the presence of Et_3N and benzotriazole-1-yl-oxy-trispyrolidinophosphinium hexafluorophosphate (PyBOP) provides the G2 dendron in very good yield. The G2 dendron can be deprotected to the free amine and subjected to a second condensation with G1 diacid to form the G3 dendron in excellent yield. Condensation of the G1, G2, or G3 free amines with tetracarboxylate cores also allowed convergent access to G2, G3, and G4 dendrimers, respectively.

The PAMAM dendrimers of Tomalia were redesigned by Kim to allow access to amphiphilic amide dendrons (Scheme 6).[256] G1 dendrons were prepared through 1,1′-carbonyldiimidazole (CDI)-mediated amidation of lauric acid with *N*-(3-aminopropyl)-1,3-propanediamine followed by treatment with succinic anhydride. G2 dendrons were prepared via iteration of the same technique. G1 dendrons were shown to self-assemble into lamellar structures, while G2 dendrons exhibited Φ_h self-organization. Modification of the periphery alkyl tails to contain diacetylene moieties allowed for stabilization of these structures via photopolymerization.[257]

The first synthesis of 2,2-bis(hydroxymethyl)propionic acid bis(MPA) dendrons followed a *convergent* approach.[258] However, the most efficient variant utilizes a divergent methodology.[259] Hult described the convergent synthesis of dendrons based on monomers derived from bis(MPA) dendrons (Scheme 7, top).[258] Treatment of 2,2-bis(acetoxymethyl)methylpropionic acid with oxalyl chloride produces the corresponding acid chloride. Esterification of the acid chloride with benzyl 2,2-bis(hydroxymethyl)propionoate results in a G2 dendron. Hydrogenative cleavage of the benzyl group with H_2 over Pd/C followed by repetition of

Scheme 11. Haag's Divergent Synthesis of Poly(ethylene glycol) (PEG) Dendrimers

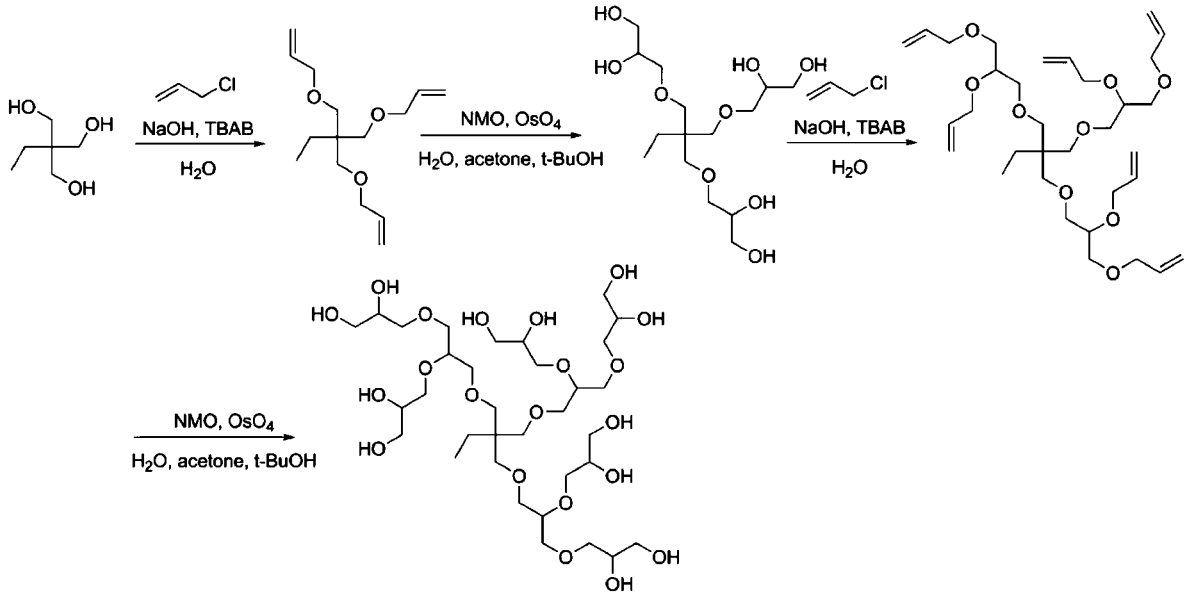

Scheme 12. Synthesis of Fréchet-type Dendrimers and Dendrons[40]

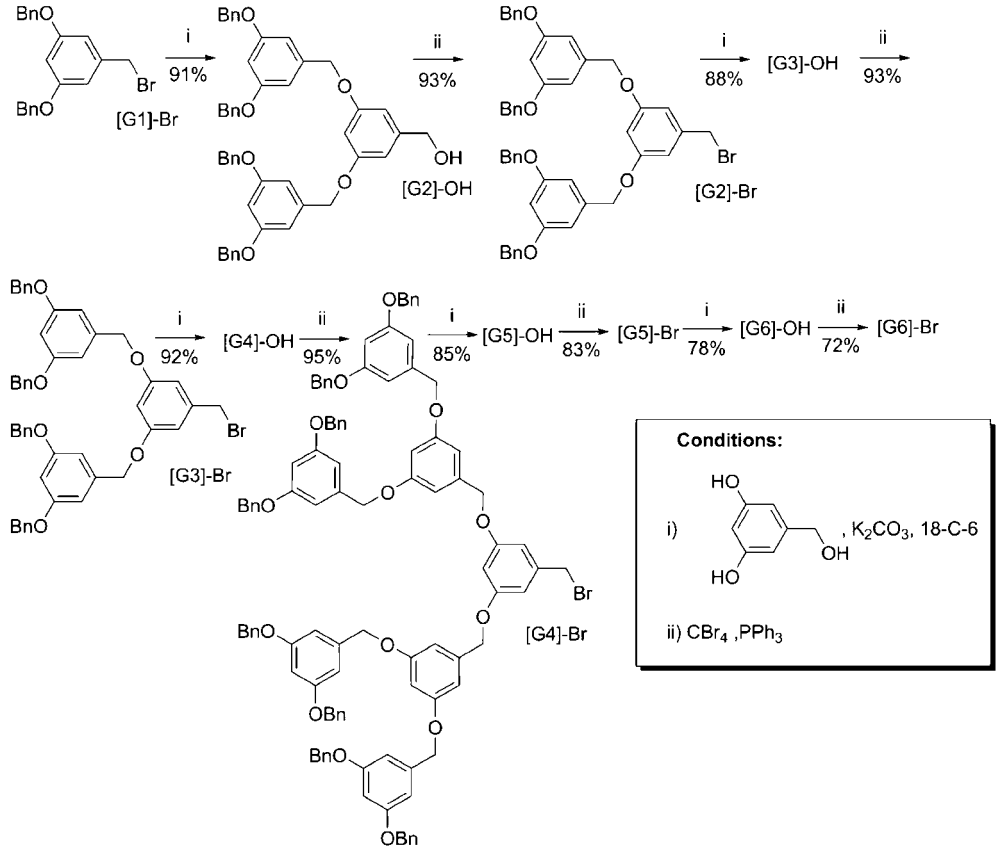

the chlorination and alkylation steps allows access to higher-generation dendrons. G1−G5 bis(MPA) dendrons are commercially available from the Polymer Factory.

In a spectacularly simple experiment, Fréchet described the most efficient divergent route to bis(MPA) dendrons (Scheme 7, bottom).[259] Treatment of benzyl 2,2-bis(hydroxymethyl)propionate with 2,2,5-trimethyl-1,3-dioxane-5-carboxylic anhydride followed by deprotection of the acetonide masked diols with trichloroacetic acid produced a G2 dendron with four hydroxy groups that are available for further grafting.

Divergent synthesis was also used to prepare dendrons constructed from AB_3 building blocks. In 1985, Newkome reported the synthesis of *arborols* (Newkome dendrons) containing repetitive AB_3 branching units based on triethyl methanetricarboxylates and tris(hydroxymethyl)aminomethane (Scheme 8).[190] Triols were *O*-alkylated with chloroacetic acid, esterified to the methyl ester in acidic methanol, and reduced to the corresponding tris(alcohol). The tris(alcohol) was converted to the corresponding tris(tosylate) and alkylated with sodium triethyl methanetricarboxylates. Amidation with tris(hydroxymethyl)aminoethane yielded the G3 den-

Scheme 13. Synthesis of Liskamp Benzamide Dendrimers and Dendrons; BOP = Benzotriazol-1-yloxy-tris(dimethylamino)phosphonium Hexafluorophosphate[268]

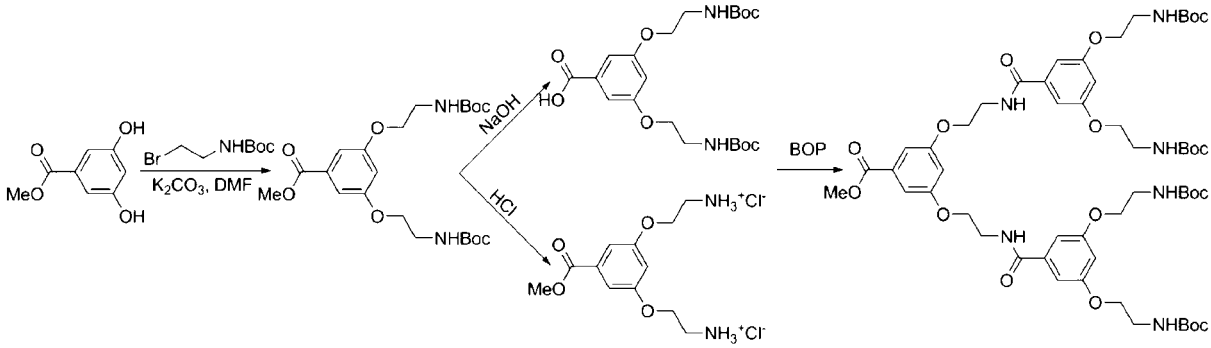

Scheme 14. Synthesis of Liskamp-Modified Benzamide Dendrons Reported by Schlüter; Reagents and Conditions: (a) (1) K_2CO_3, $COCl_2$, Toluene, 0 °C, 30 min; (2) 3-Chloropropylamine Hydrochloride, KOH, Tetrahydrofuran (THF)/Water, 20 °C, 20 H, (65%); (b) K_2CO_3, 18-C-6, Tetrabutyl Ammonium Iodide, Diethyl Ketone, Reflux, 20 h (85%); (c) KOH, Methanol/Water, Reflux, 5 h (95%); (d) (1) 6c, CDI, THF, 40 °C, 24 h; (2) 6d, DBU, CH_2Cl_2, 0 °C, 24 h, (65%); (e) KOH, Methanol/Water, reflux, 8 h, (80%).[270]

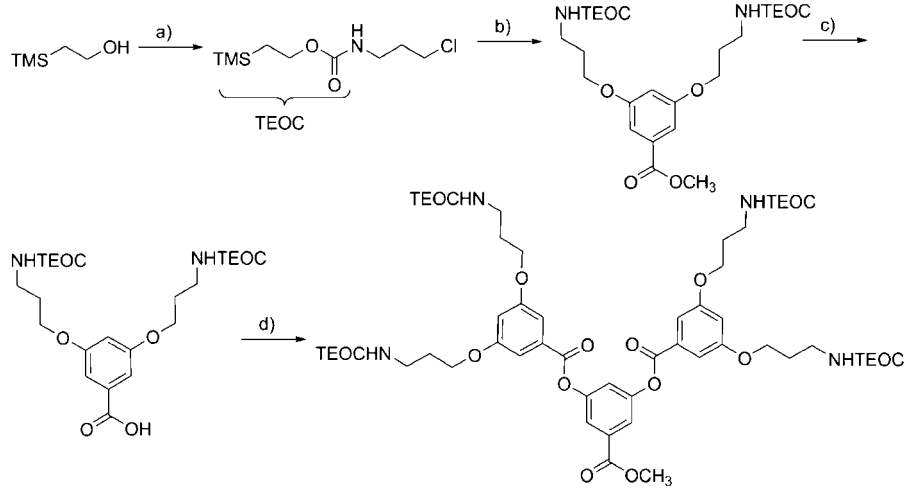

drimer. Newkome has improved this methodology through the use of Lin's amine, $H_2N(CH_2OCH_2CH_2CO_2Et)_3$, as the only branching unit (Scheme 9).[260] Treatment of a tetra-branched acyl chloride core with Lin's amine resulted in the G2 dendrimer in 52% yield, followed by saponification of the 12 surface esters with NaOH in an alcohol−water mixture. Higher-generation dendrimers were prepared through DCC/1-hydroxybenzotriazole (HOBt) peptide coupling of the dendritic acids with Bahera's amine. Up to G6 Newkome dendrimers have been prepared in this fashion. Behera's amine, $H_2NC(CH_2CH_2CO_2CMe)_3$, was employed as an alternative building block for the divergent synthesis of Newkome-type dendrons.[261] G1−G4 dendrons of this type are available from Frontier Scientific under the trade name nTrēons.

For precision dendron synthesis yielding monodisperse building blocks for self-assembly and self-organization, the convergent approach is most suitable. Poly(ethylene oxide) (PEO) dendrons belong to two general classes. The first class, the dendritic PEO linked via branching at 1,2-positions of propane-1,2,3-triols, reported by Allcock, is prepared through alkylation of (benzyloxy)propane-1,2-diol with 2,3-alkoxypropyl tosylate (Scheme 10, top).[262] Hydrogenation over Pd/C provided the dendritic alcohol. Conversion of the dendritic alcohol to the dendritic tosylate allows for iteration of this procedure to make higher-generation dendrons. The same "glycerol" type dendrimers up to at least G4 can be prepared via a divergent route reported by Haag (Scheme 11).[263] 2-Ethyl-2-(hydroxymethyl)propane-1,3-diol was tris-allylated under basic conditions. Exhaustive dihydoxylation with OsO_4 and *N*-methylmorpholine-*N*-oxide provide G2 dendrimer. Repeated allylation and dihydroxylation provide access to higher-generation dendrimers.

Fréchet reported the synthesis of a second class of dendritic PEO using tris(hydroxymethyl)methane.[264] In this approach, epichlorohydrin was bisalkylated via in situ prepared potassium benzoxide. Iterative alkylation onto methallyl dichloride followed by hydroboration provides higher-generation amphiphilic dendrons (Scheme 10, bottom).

Fréchet reported AB_2 branched aryl ether dendrons via a convergent route that became the most important for the scope of this review.[192] Benzyl or substituted benzyl bromides are *O*-alkylated onto 3,5-dihydroxybenzyl alcohol, a rather costly commercial starting material, under phase transfer catalyzed conditions. The benzyl alcohol was transformed to the benzyl bromide via CBr_4/PPh_3. This two-step process can be repeated to achieve higher-generation dendrons. (Scheme 12). At each step, the benzyl bromide or benzyl alcohol oils were purified chromatographically. Very good yields (90+%) were achieved for G1−4 dendrons; however, diminishing yields are achieved for G5 and G6. On the basis of the convergent synthesis of Percec-type dendrons,[265,266] Ueda developed a more facile route to Fréchet-type dendrons.[267] Dendritic benzyl alcohols are activated to the benzyl

Scheme 15. Synthesis of Percec-type Self-Assembling Dendrons

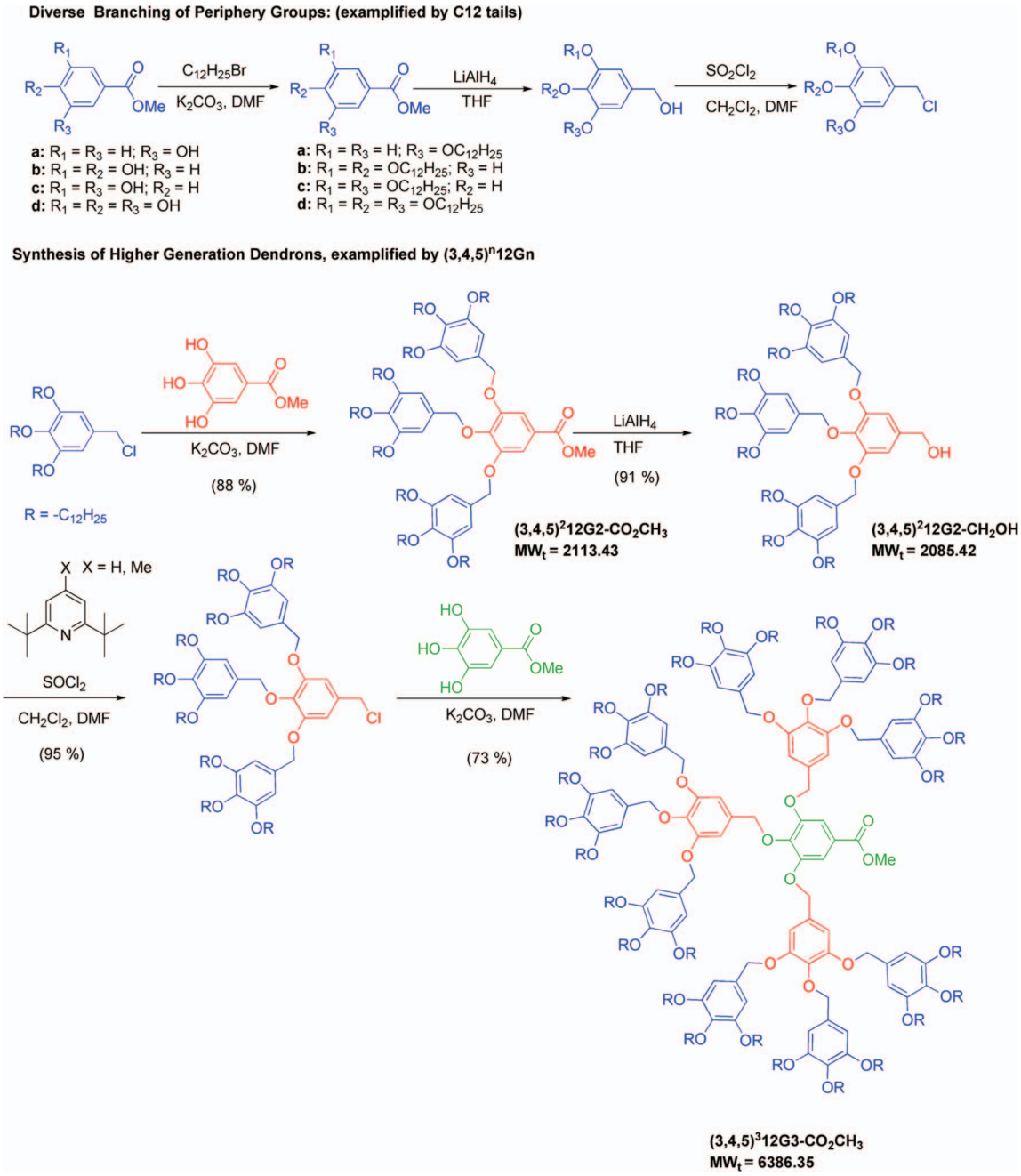

chlorides with thionyl chloride and directly alkylated without purification onto 3,5-dihydroxybenzyl alcohol via Williamson etherification with K_2CO_3 in NMP.

Liskamp reported the synthesis of benzamide dendrons similar in branching architecture to those of Fréchet benzyl ether dendrons (Scheme 13).[268] Methyl 3,5-dihydroxybenzoate was bis(alkylated) with *tert*-butyl 2-bromoethylcarbamate. A portion of the methyl 3,5-bis(2-*tert*-butyloxycarbonylaminoethoxy)benzoate was saponified to the acid, while another portion was acidified to the primary ammonium chloride salt. Condensation of the acid and ammonium chloride with benzotriazol-1-yloxy-tris(dimethylamino)phosphonium hexafluorophosphate (BOP) produced a G2 dendron. Saponification and condensation with primary ammonium salts was used to achieve higher-generation dendrons. BOP coupling was quantitative for the production of G2 Liskamp benzamide dendrons but diminished to 60% for the G5 dendron. Schlüter reported alternatives to the synthesis of Liskamp benzamides, wherein 3,5-dihydroxybenzoic acid was alkylated via Michael addition with acrylonitrile[269] hydrogenated to the free amine and peptide coupling was mediated with carbonyl diimidazole (CDI). Later, Schlüter reported variants of Liskamp dendrons and their corresponding macromonomers and dendronized polymers, containing an extra methylenic group in the linker.[270] These dendrons were prepared via alkylation of 3,5-dihydroxy benzoic acid with *N*-(3-chloropropyl)-3-(trimethylsilyl)propanamide, followed by CDI coupling to form higher-generation dendrons (Scheme 14).

Percec reported the synthesis of self-assembling dendron built from 4-hydroxy-, 3,4-dihydroxy-, 3,5-dihydroxy-, and 3,4,5-trihydroxybenzoates (Scheme 15).[265,266] A diversity of

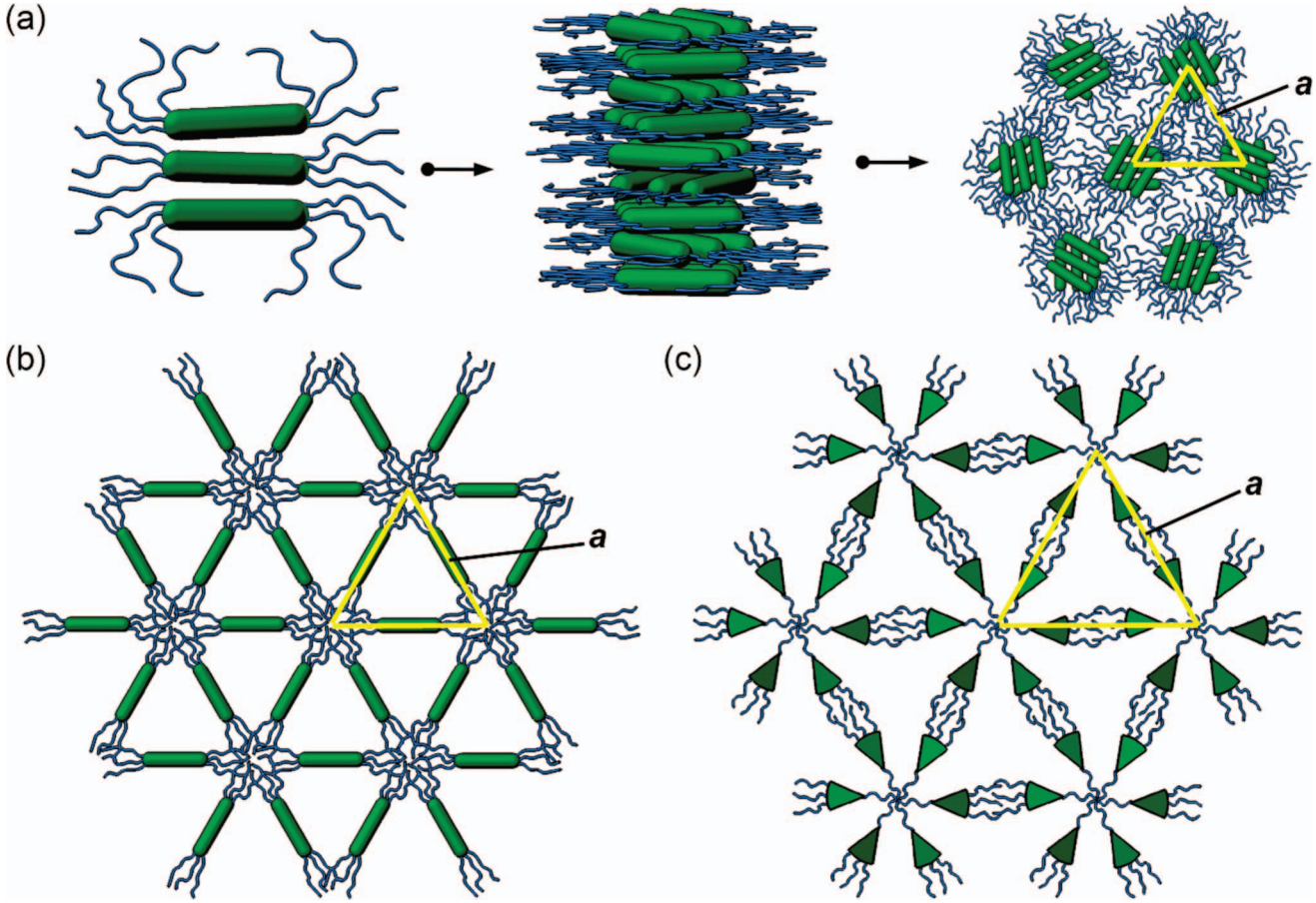

Figure 12. Models for the self-assembly of phasmidic molecules by Malthête[280] (a, b) and Percec (c).

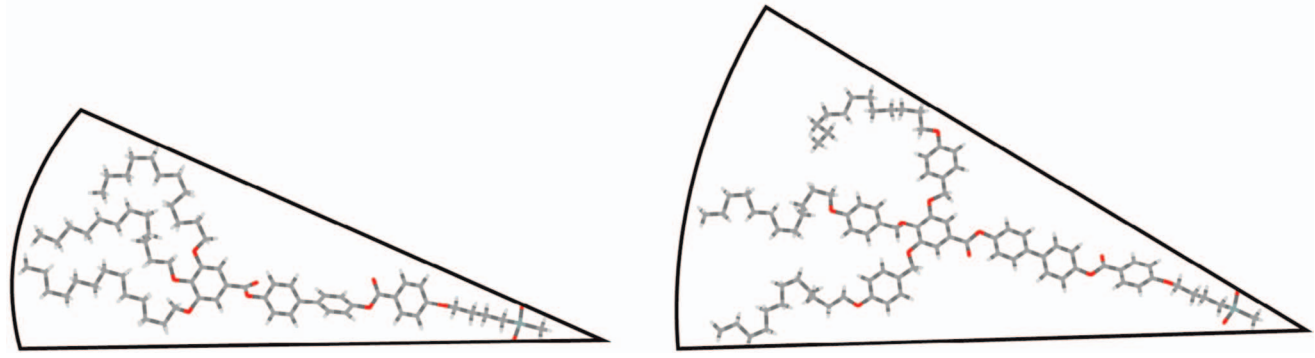

Figure 13. Model of Percec's analogues of Malthête's hemiphasmid.

periphery alkyl groups can be etherified onto inexpensive commercially available methyl 4-hydroxybenzoate, methyl 3,4-dihydroxybenzoate, methyl 3,5-dihydroxybenzoate, and methyl 3,4,5-trihydroxybenzoate. Typically, the hydroxy benzoate, for example, methyl, ethyl, or propyl 3,4,5-trimethoxybenzoate, was alkylated with $C_{12}H_{25}Br$. The resulting dendritic ester, (3,4,5)12G1-CO_2Me, was reduced to the alcohol with $LiAlH_4$ and converted to the benzyl chloride with thionyl chloride. Higher generation Percec-type dendrons can be prepared by alkylation of benzyl chloride dendron (3,4,5)12G1-CH_2Cl onto another hydroxy-branched benzoate, for example, methyl 3,4,5-trihydroxy-benzoate, to form $(3,4,5)^2$12G2-CO_2Me, which can be reduced under similar conditions to $(3,4,5)^2$12G2-CH_2OH. Chlorination with $SOCl_2$ must be performed in the presence of the proton-trap 2,6-di-*tert*-butylpyridine or 2,6-di-*tert*-butyl-4-methylpyridine, to prevent acidic decomposition of the dendron. Further alkylation onto methyl 3,4,5-trihydroxy-benzoate results in G3 dendron $(3,4,5)^3$12G3-CO_2Me. Benzyl chlorides prepared in the synthesis of Percec-type dendrons can be used directly in the subsequent alkylation without further purification. This process can be repeated until the dendrons self-assemble into single dendron spheres, thereby achieving site isolation of the apex functional group.[271] This can occur as early as G5. Additionally, the synthesis of low-generation Percec-type dendrons was optimized for the kilogram scale.[272]

Percec also reported analogous syntheses of phenylpropyl ether,[273] biphenyl methyl ether,[274] as well as AB_4, and AB_5 branched[275] dendrons. These will be discussed later in section 2.2.42.2.4.

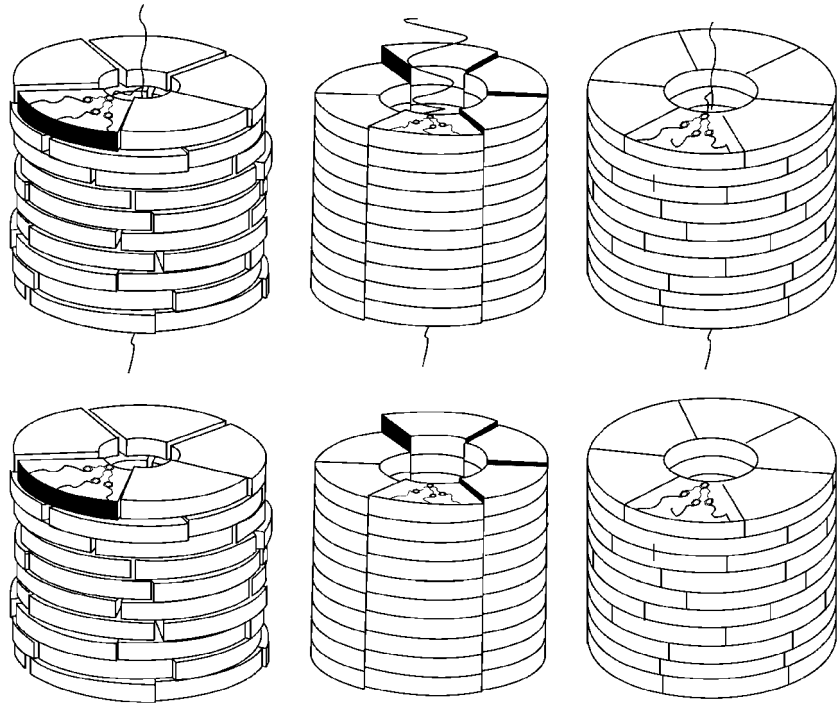

Figure 14. Macromolecular (top) and supramolecular (bottom) columns proposed for model (c) from Figure 12.

2.2. Self-Assembly of Dendrons and Dendrimers

2.2.1. From Malthête Hemiphasmids to Self-Assembling Percec-type Dendrons

In 1985, Chandrasekhar suggested that a molecule consisting of a rod joined to a half-disk might provide access to a biaxial N thermotropic LC phase.[276] During the late 1980s, Saupe came to Percec's office with two publications in hand. Saupe mentioned that Ringdsdorf advised him to discuss these papers with him. The first publication was Saupe's[277] and reported the first lyotropic biaxial N LC, while the second publication was by Malthête[194] and reported what was thought, at that time, to be the first thermotropic biaxial N LC. This molecule was inspired from Chandrasekhar's[276] concept and was named hemiphasmid by Malthête (Figure 8). This molecule was reported to exhibit a very narrow metastable monotropic biaxial N phase.[194] Saupe sought synthetic help to transform the monotropic phase into an enantiotropic one in order to facilitate physical measurements. Ringsdorf convinced him that Percec would be able and willing to provide that help. Jim Heck, a junior graduate student in Percec's laboratory, was assigned to this project, which was expected to be a short endeavor that would involve the synthesis of a monomer as close as possible to Malthête's hemiphasmid. Its polymerization was expected to transform the monotropic biaxial N-phase into an enantiotropic one by the so-called "polymer effect."[278] This project was a complete failure but serendipitously contributed to the development of the field of self-assembling dendrons and self-organizable dendronized polymers and through them to the design of complex functional systems from nonbiological building blocks.

Jim Heck's experiments started with the duplication of the synthesis of Malthête's hemiphasmid followed by its structural analysis and its LC phase behavior performed both in Percec's laboratory at that time at Case Western Reserve University and at the Liquid Crystal Institute of Kent State University. The hemiphasmid reported by Malthête synthesized in Percec's laboratory did not exhibit the monotropic biaxial N phase but rather an S_c phase. This resulted in a later publication that Percec did not want to coauthor.[279] Interestingly, the corresponding polymer displayed an intramolecular self-assembly process to generate a cylindrical macromolecule that self-organized in a Φ_h LC phase.[195] Libraries of monomers and polymers inspired by the work of Malthête on hemiphasmids, phasmids, and other polycatenar mesogens[280−283] were elaborated in an attempt to generate the molecules exhibiting the biaxial LC phase promised to Saupe (Figure 8).

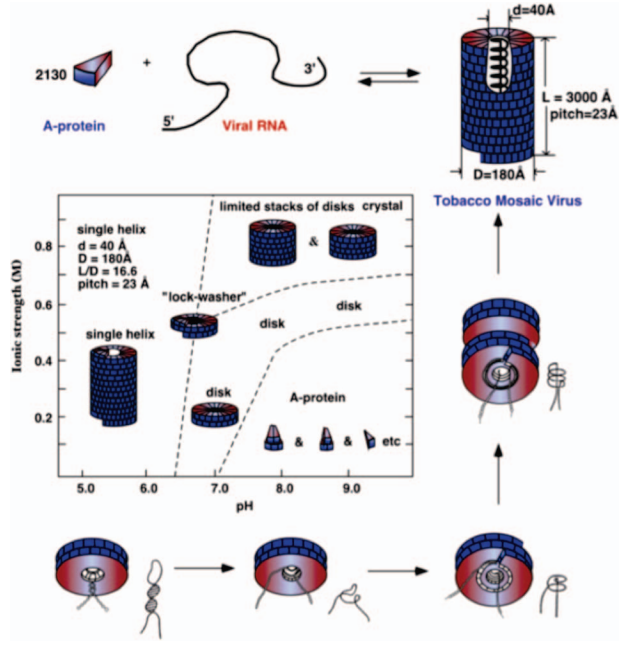

Figure 15. Self-assembly mechanism of TMV. Adapted with permission from refs 156, 304, and 305. Copyright 1983 Wiley-VCH Verlag GmbH & Co. KGaA, 1991 Elsevier, and 1971 Macmillan Publishers Ltd. (Nature New Biology), respectively.

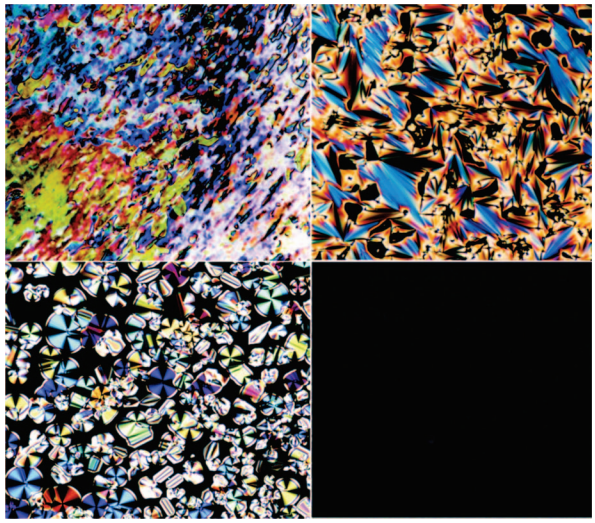

Figure 16. Some characteristic textures of N (top left), S (top right), Φ_h (bottom left), and *Cub* (bottom right) phases.

Simultaneous with the synthesis of hemisphasmids, Malthête elaborated the synthesis and self-assembly of phasmids and other polycatenar molecules in supramolecular columns that self-organize into Φ_h LC phases. Two models were advanced by Malthête for the self-assembly of phasmids into supramolecular columns (Figure 12).[280,282,283] The model from Figure 12a in which the columns are assembled from disklike clusters of rodlike molecules was supported by subsequent work involving XRD experiments combined with experimental densities.[283−286] The model from Figure 12b was considered unacceptable since it created a combination of an unrealistically high density ($\rho > 4.0$) for the aliphatic regions and also empty space in the Φ_h lattice, and subsequently was rejected.[283−286] Percec's laboratory suggested a modification of the model from Figure 12b for the self-organization of supramolecular columns in the Φ_h lattice generated from dendronized polymers and/or from self-assembling dendrons (Figure 12c).[198] This model replaces the intolerably overcrowded high-density paraffinic regions with an acceptable value created by a polymer backbone surrounded by a lower number of alkyl groups. As originally drawn (Figure 12c), the molecule would not allow for the complete filling of the lattice space. However, simulation of the actual 3D structure of the self-assembling hemiphasmidic unit demonstrated a tapered shape that in fact does not generate empty space during self-assembly (Figure 13). Figure 14 illustrates the self-assembly process originally drawn by Jim Heck. The backbone of the dendronized polymer is surrounded by tapered dendrons or hemiphasmids and exhibits a nonhelical or helical supramolecular assembly. A single backbone penetrating through the center of the supramolecular columns is not able to provide the number of tapered side groups forming the cross section of the column unless it adopts a helical conformation. Alternatively, if a very large tapered dendron is used, the conformation of the polymer backbone must extend and, therefore, create a rigid structure. When the self-assembly takes place in the absence of a polymer backbone, helical columns must be obtained wherein the empty space normally occupied by the backbone forms a channel or is filled by a molecular receptor.

Subsequent developments on phasmidic molecules,[282] which have been reviewed,[287−289] established that phasmids and hemiphasmids must contain at least five *p*-linked aromatic rings in the rodlike part of the molecule in order to self-organize into a Φ_h phase.[282] Therefore, the first attempts made to eliminate the self-assembly into supramolecular columns were via the incorporation of nonlinear repeat units in the rigid part of the molecule (Figure 8, **3.3a**,**b**,**c**,**d**, **3.4a**,**b**,**c**,**d**, **3.11a**,**b**, **3.12a**,**b**), by the reduction of the length of the rigid rod (Figure 8, **3.1a**,**b**,**c**,**d**, **3.9a**,**e**, **3.13a**,**b**, **3.14a**,**b**), or by the complete elimination of the rigid aromatic part (Figure 8, **3.5a**,**c**,**d**,**e**,**f**,**g**, **3.6**, **3.15c**,**d**,**f**,**g**, **3.16c**,**d**). Surprisingly, none of the structural variations prevented the self-assembly of the monomer or of the polymer into a supramolecular or macromolecular column. Malthête's hemiphasmid[194] and Percec's molecules from Figure 8 represent the first examples of self-assembling and self-organizable dendronized rod−coils, dendronized rods, dendronized coils, dendrons, and dendronized polymers.

In 1989, it already had been discovered that the first-generation dendron (4-3,4,5)12G1-COOH (Figure 8, **3.6**) self-assembles into supramolecular columns and also mediates the self-assembly of molecular receptors such as oligooxyethylene (Figure 8, **3.5a**,**c**,**d**,**e**,**f**,**g**, **3.15c**,**d**,**f**,**g**) or crown-ethers (Figure 8, **3.7**, **3.8**, **3.17**) into the center of supramolecular columns. In retrospective, these molecules represent the first examples of self-assembling dendronized coils and dendronized macrocycles. When the supramolecular columns do not form a Φ_h LC phase, they exhibt only a Φ_h crystal phase. However, the LC phase could be induced via H-bonding, via ionic interactions, or through exchange of the alkyl groups from the periphery with semifluorinated analogues via the fluorous phase[290−292] or the fluorophobic effect.[293−296] It was not a surprise that the simplest homologue of (4-3,4,5)12G1-X (Figure 8, **3.1**−**3.8**), i.e., (3,4,5)12G1-X (Figure 8, **3.9**−**3.18**) mediated the same self-assembly process except for lower thermal stability of the supramolecular column in its Φ_h LC

Table 2. Expected Reflections for S, Φ_h, $\Phi_{r\text{-}s}$, $\Phi_{r\text{-}c}$, and the Explicit Ratios Between Reciprocal *d*-Spacings for S and Φ_h Relative to the (100) Reflection

(*h*, *k*, *l*)	S[b]	$q_{hkl}{}^a/q_0$ Φ_h	$\Phi_{r\text{-}s}$	$\Phi_{r\text{-}c}$
(1, 0, 0)	1	1	X[c]	
(0, 1, 0)			X	
(1, 1, 0)		$\sqrt{3}$	X	X
(2, 0, 0)	2	2	X	X
(0, 2, 0)			X	X
(1, 2, 0)			X	
(2, 1, 0)		$\sqrt{7}$	X	
(2, 2, 0)		$2\sqrt{2}$	X	X
(0, 3, 0)			X	
(3, 0, 0)	3	3	X	
(1, 3, 0)			X	X
(3, 1, 0)		$\sqrt{13}$	X	X
(2, 3, 0)			X	
(3, 2, 0)		$\sqrt{19}$	X	
(3, 3, 0)		$2\sqrt{2}$	X	X
(0, 4, 0)			X	X
(4, 0, 0)	4	4	X	X
(1, 4, 0)			X	
(4, 1, 0)		$\sqrt{21}$	X	
(0, 5, 0)			X	
(5, 0, 0)	5	5	X	
(2, 4, 0)			X	X
(4, 2, 0)		$2\sqrt{7}$	X	X
(3, 4, 0)			X	
(4, 3, 0)		$\sqrt{37}$	X	
(4, 4, 0)		$4\sqrt{3}$	X	X

[a] q_0 = scattering position of the first nonzero diffraction peak. [b] For S phases, the index is (0, 0, *l*), but for simplicity it is listed as (*h*, 0, 0) [c] X = reflection is observed.

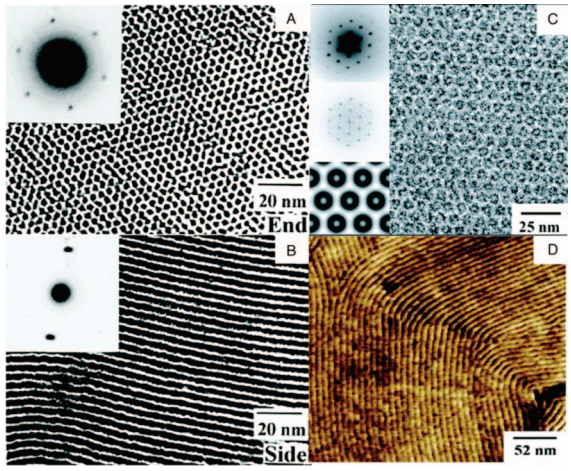

Figure 17. TEM and negative images of homeotropically (a) and parallel (b) aligned (3,4,5)12F8G1−B[15]C5 in the Φ_h. TEM and negative images of hometropically (c) and scanning force microscopy (SFM) image of parallel (d) aligned (4-3,4-3,5)12G1−CH_2−(Boc-L-Tyr-L-Ala-OMe). Reprinted with permission from ref 306. Copyright 1997 American Association for the Advancement of Science and Macmillan Publishers Ltd. (Nature).

phase. The unexpected assembly capability of (3,4,5)12G1-X and later of (3,4)12G1-X made Percec's laboratory decide to name them minidendrons[297,298] since they can be used as models or maquettes for the elaboration of novel architectural motifs from larger generations of dendritic building blocks. The role of these minidendrons was indeed analogous to that of simple peptides used in the understanding of the molecular engineering involved in the assembly of more complex proteins or of maquettes used by sculptors or architects to appreciate various aspects of full-size objects.[299] All these experiments demonstrated the self-assembly of supramolecular polymer backbones via H-bonding, dipole−dipole, and ionic interactions. In 1991, higher generations of $(3,4,5)^n12G_n$−X dendrons were synthesized.[300,301] However, they self-assembled in an unprecedented cubic lattice that took 6 years to solve, and therefore, it was published only in 1997.[265] In 1994, fiber XRD experiments performed on polymer **3.5d** (Figure 8) and its precursor alcohol were shown to self-assemble into helical columns and, therefore, demonstrated that supramolecular columns self-assembled from achiral dendrons and dendronized polymers produce chiral assemblies that are racemic.[211]

The enantiotropic biaxial N phase was never accomplished by this series of experiments. However, the schematic of self-assembly from Figure 14 gave Percec's laboratory the molecular inspiration that his group was looking for since 1982,[214] i.e., to mimic the self-assembly of the Tobacco Mosaic Virus (TMV), which at the time was one of the best understood complex biological systems.[302] In work that became part of his Nobel lecture, Klug demonstrated that TMV exhibits a complex self-nucleating self-assembly mechanism (Figure 15) and self-organizes into a lyotropic Φ_h phase.[156,303−305]

2.2.2. Structural and Retrostructual Analysis of Supramolecular Dendrimers: From 2-D to 3-D Lattices

In the previous subsection, it was noted that the structure of (4-3,4,5)12G1 and (3,4,5)12G1 dendritic acids and metal carboxylates, dendronized crown-ethers, and dendronized oligoethylene oxides self-assemble into supramolecular columns that self-organize into Φ_h lattices. As will be discussed in this subsection and many subsequent sections, the assignment of the lattice and determination of its constituent supramolecular objects is the starting point for the elucidation of the molecular-level structure and self-assembly mechanism. Many techniques will provide information into lattice symmetry and supramolecular shape. Alone, each of these techniques is insufficient and, without other supporting evidence, can be misleading. The determination of the structure is in fact a very complex process that demands attention. The Percec laboratory has developed a rigorous approach to structural and retrostructural analysis encompassing a number of steps including (a) purity determination; (b) thermal analysis by DSC and preliminary phase characterization via thermal optical polarized microscopy (TOPM); (c) small- and wide-angle XRD and electron diffraction (ED) analyses in powder, single domain (single crystal), and fiber that includes electron density maps and histograms, development of a preliminary packing model, and simulation of diffraction to confirm the validity of the model; (d) AFM/TEM/scanning tunneling microscopy (STM)[306] for direct visualization[307] and isomorphous replacement[367] to complement the XRD and ED analysis; and (e) experimental density determination, which is required to complete the structural and retrostructural analysis.

Structural determination cannot proceed until the purity of the dendron is confirmed. Because small molecules have been shown to serve as guests in supramolecular self-assembly, thereby perturbing their structure, the purity demands are high. First, 99.9+% purity must be confirmed

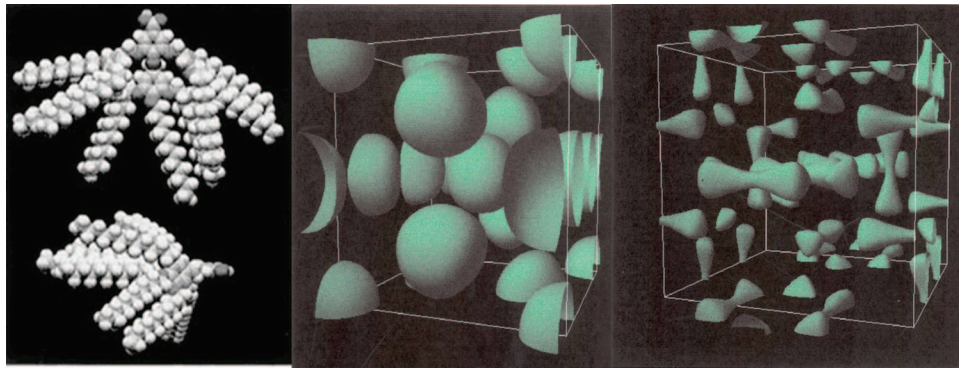

Figure 18. Preferred conical conformation of $(3,4,5)^2$12G2−COOH (left) and micellar supramolecular spheres assembled into a cubic lattice with $Pm\bar{3}n$ symmetry (middle). The regimes of highest electron density (middle) can be compared with the regimes of low electron density (right). Reprinted with permission from ref 314. Copyright 1997 American Chemical Society.

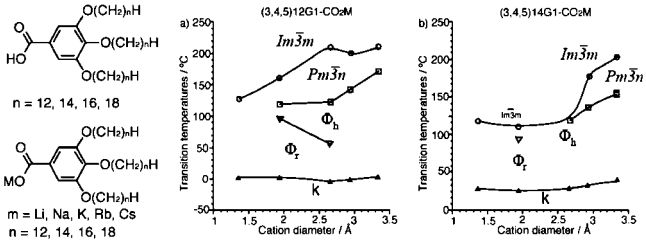

Figure 19. Structure of (3,4,5)*n*G1−COOH and (3,4,5)*n*G1−COOM (left), and phase diagram for varying cation size for (3,4,5)12G1−COOM (a) and (3,4,5)14G1−COOM (b). Reprinted with permission from ref 317. Copyright 2002 Wiley-VCH Verlag GmbH & Co. KGaA.

through a combination of ^{1}H NMR, ^{13}C NMR, size-exclusion chromatography (SEC), and mass spectroscopy (MALDI-TOF).

Following purity assessment, differential scanning calorimetry (DSC) is used to identify ordered phases and determine phase-transition temperatures and their associated enthalpies. Thermal optical polarized microscopy (TOPM) allows for discrimination between 1D, 2D, and 3D ordered phases. While not unambiguous in many cases, TOPM can distinguish between optically isotropic phases (*Cub*, *Tet*, BCC, QLC*)* that exhibit no LC texture (Figure 16, bottom right) and optically anisotropic phases (N, S, Φ_h, $\Phi_{r\text{-}c}$, $\Phi_{r\text{-}s}$) that exhibit a variety of characteristic birefringent textures (Figure 16).

Phases exhibiting optical anisotropy through birefringent TOPM textures are often N, S, or columnar. Texture alone cannot definitively identify the phase. XRD, electron-density histograms, electron-density map reconstruction, and molecular modeling are critical to structural and retrostructural analysis. Powder XRD patterns provide an indication of the lattice symmetry and dimensions. Powder XRD can be viewed as the self-organized structural determination equivalent of NMR molecular structural analysis. In ^{1}H NMR,

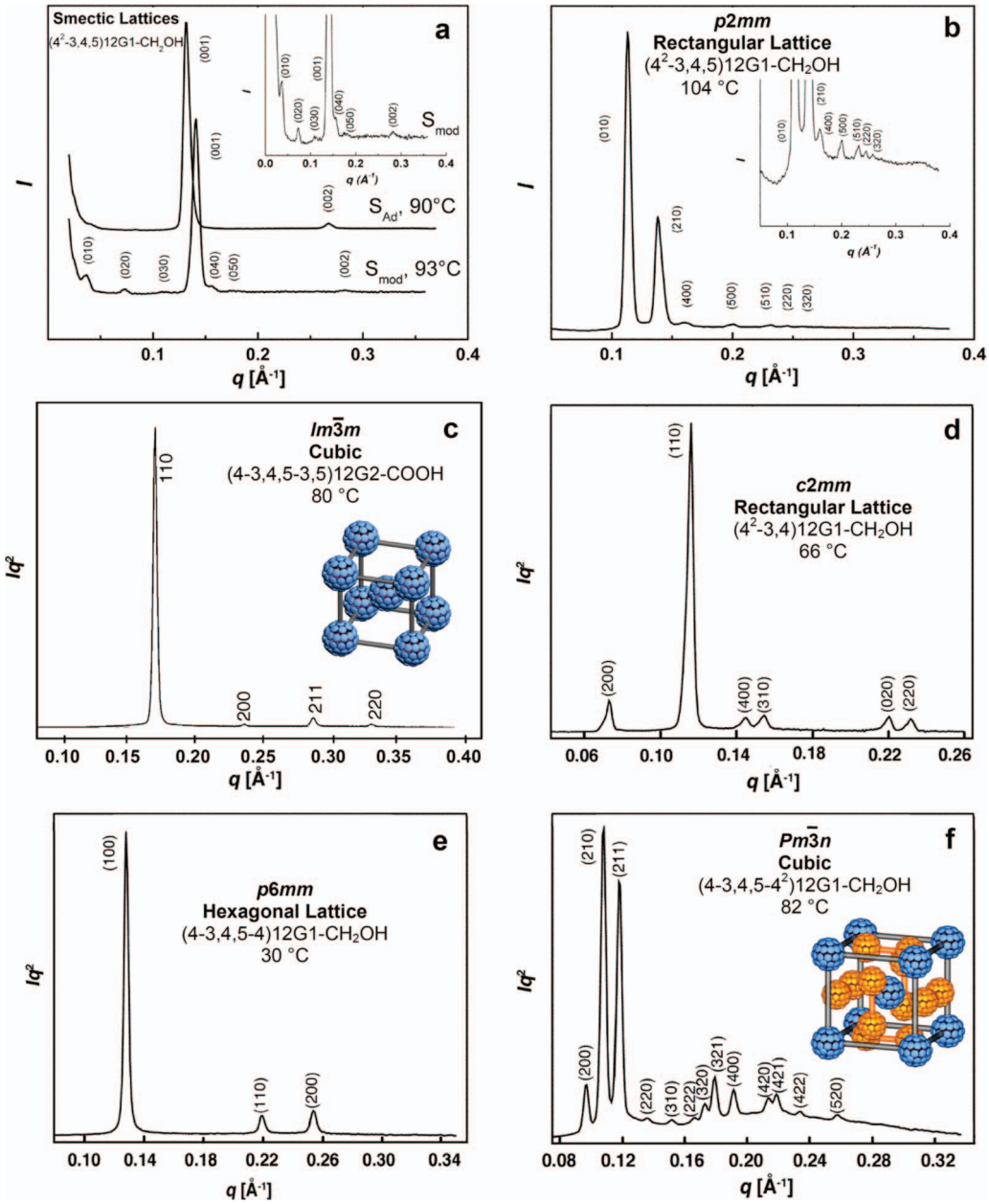

Figure 20. Typical indexed experimental X-ray diffractograms of S_{AD} and S_{mod} phases (a), $\Phi_{r\text{-}s}$ lattice with *p*2*mm* symmetry (b), the BCC lattice with *Im*3̄*m* symmetry (c), the $\Phi_{r\text{-}c}$ lattice with *c*2*mm* symmetry (d), the Φ_h lattice with *p*6*mm* symmetry (e), and the *Cub* lattice with *Pm*3̄*n* symmetry (f). Reprinted with permission from refs 266 and 338. Copyright 2001 and 2004 American Chemical Society.

Table 3. Expected Reflections for Cubic Lattices with *Pm*$\bar{3}$*n*, *Im*$\bar{3}$*m*, and *Ia*$\bar{3}$*d* Symmetry; Ratio of Reciprocal *d*-Spacings for *Pm*$\bar{3}$*n* and *Im*$\bar{3}$*m* Relative to the (110) Reflection and for *Pm*$\bar{3}$*n* Relative to the (211) Reflection

(*h*, *k*, *l*)	q_{hkl}/q_0[a]		
	Pm$\bar{3}$*n* (*Cub*)	*Im*$\bar{3}$*m* (BCC)	*Ia*$\bar{3}$*d* (*Cub*$_{bi}$)
(1, 1, 0)	1	1	
(2, 0, 0)	$\sqrt{2}$	$\sqrt{2}$	
(2, 1, 0)	$\sqrt{(5/2)}$		
(2, 1, 1)	$\sqrt{3}$	$\sqrt{3}$	1
(2, 2, 0)	2	2	$\sqrt{(4/3)}$
(3, 1, 0)	$\sqrt{5}$	$\sqrt{5}$	
(2, 2, 2)	$\sqrt{6}$	$\sqrt{6}$	
(3, 2, 0)	$\sqrt{(13/2)}$		
(3, 2, 1)	$\sqrt{7}$	$\sqrt{7}$	$\sqrt{(7/3)}$
(4, 0, 0)	$2\sqrt{2}$	$2\sqrt{2}$	$\sqrt{(8/3)}$
(4, 1, 0)	$\sqrt{(17/2)}$		
(4, 1, 1)	3	3	
(3, 3, 0)	3	3	
(4, 2, 0)	$\sqrt{10}$	$\sqrt{10}$	$\sqrt{(10/3)}$
(4, 2, 1)	$\sqrt{(21/2)}$		
(3, 3, 2)	$\sqrt{11}$	$\sqrt{11}$	$\sqrt{(11/3)}$
(4, 2, 2)	$2\sqrt{3}$	$2\sqrt{3}$	2
(5, 1, 0)	$\sqrt{13}$	$\sqrt{13}$	
(4, 3, 1)	$\sqrt{13}$	$\sqrt{13}$	$\sqrt{(13/3)}$
(5, 2, 0)	$\sqrt{(29/2)}$		
(4, 3, 2)	$\sqrt{(29/2)}$		
(5, 2, 1)	$\sqrt{15}$	$\sqrt{15}$	$\sqrt{5}$
(4, 4, 0)	4	4	$\sqrt{(16/3)}$

[a] q_0 = scattering position of the first nonzero diffraction peak.

chemical shifts, peak multiplicity, and peak intensities can be used to infer the chemical environment, connectivity, and relative abundance of specific protons. In the context of supporting data, including ^{13}C NMR, Fourier transform infrared (FT-IR) spectroscopy, mass spectrometry, a known reactant structure, and the accessible reaction pathways, the molecular structure of the product can usually be precisely determined. In powder XRD, the scattering intensity I can be plotted versus the reciprocal lattice dimension q. Reciprocal lattice dimensions and actual d-spacings are related: $q = 2\pi/d$. From the peaks present and their relative q values, a lattice type can be assigned, i.e., cubic, tetragonal, orthorhombic, tetragonal, monoclinic, or triclinic. Ideally, using a high-intensity X-ray source such as a synchrotron, the systemic absence of certain reflections will indicate the lattice symmetry and the scattering intensities of the remaining peaks can be used to ascertain the electron-density distribution in the structure. Unfortunately, synchrotron radiation is not always practical for routine analysis, and even so, critical reflections to symmetry determination or even lattice identification may be too low in intensity to detect. Thus, in all cases, like with NMR for small-molecule structure determination, context and supporting data is needed to confidently assign a lattice and begin the process of retrostructural analysis.

N and S phases typically exhibit the simplest diffraction patterns. N phases, which are characterized by 1-D directional alignment but no defined layer spacing, do not exhibit sharp reflections. The most basic S phases show only (00l) diffraction peaks with reciprocal spacings in a ratio of 1:2:3:...:n (Table 2). The layer spacing in S phases is simply equal to d_{001}. For most self-assembling dendrons that self-organize into S phases, only the (001) and the (002)

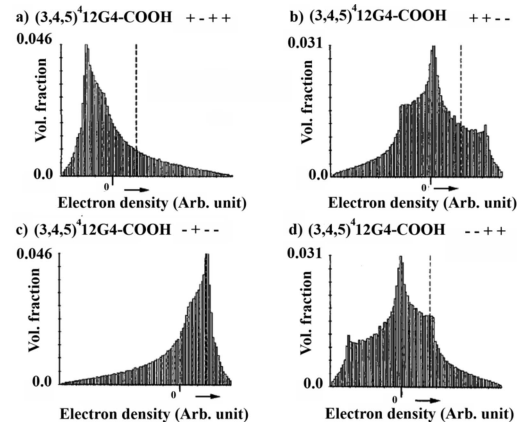

Figure 21. Electron-density histograms for (3,4,5)^{4}12G4−COOH corresponding to the (a) + − + +, (b) + + − −, (c) − + − −, and (d) − − + + phase combinations for the (200), (210), (120), and (211) peaks, respectively. Reprinted with permission from ref 314. Copyright 1997 American Chemical Society.

diffractions are observable via conventional X-ray sources. Notable exceptions[308] exist where higher-order reflections are observed, allowing for greater detail in structure determination.

Among the 2-D arrangements, the hexagonal columnar, Φ_h, lattice with *p*6*mm* symmetry is the simplest, as the lattice parameters a and b are equal. While all h,k values are allowed, the Φ_h lattice typically exhibits a strong (100) diffraction peak and smaller higher-order (110), (200), and (210) diffraction peaks, with reciprocal d-spacings in a ratio of 1:$\sqrt{3}$:2:$\sqrt{7}$ (Table 2). The columnar diameter, D, of the Φ_h lattice can be calculated via $D = 2\langle d_{100}\rangle/\sqrt{3}$. The number of dendrons per column stratum, μ, can be calculated according to $\mu = (\sqrt{3}N_A D^2 t\rho)/2M$, where N_A is Avogadro's number 6.022 × 10^{23} g/mol; t = 4.7 Å, the stacking distance;[309] ρ is the experimental density, and M is the molecular weight of the dendron. As will be discussed later, a low electron density at the column center provides amplification of the higher-order diffraction peaks in Φ_h lattices. In the absence of a low electron-density center, only the (100), (110), and (200) peaks are observed. In certain structures, the (110) diffraction peak can be vanishingly small, thereby giving the impression of S phase with only (100) and (200) reflections. Higher-intensity X-ray sources can reveal these low-intensity reflections. In addition, TEM/STM/AFM is a powerful method to confirm the lattice and the molecular model used to fill it via direct visualization of the supramolecular objects.[306,310] (3,4,5)12F8G1−B[15]C5 and (4-3,4,5)12F8−B[15]C5 were shown by XRD to self-assemble into Φ_h lattices. TEM confirmed this organization in homeotropically and parallel-aligned samples (Figure 17a,b).[311] Dark spots in the center of columns were correlated with the higher electron density of the aromatic and crown-ether phase segments of the dendrons. Later, Percec reported the self-assembly of dendronized dipeptides into helical columns self-organized into a Φ_h lattice.[312] In the case of these hollow columns, a low electron density region is observed at the center of the columns via TEM (Figure 17c). Visualization of parallel-aligned Φ_h assemblies allowed for the determination of the degree of column tilting proximal to a disclination. The permeation length of (4-3,4,5)12F8−B[15]C5 corroborates a model of a column with a rigid aromatic core surrounded by a deformable aliphatic sheath. It must be stressed that, while the standard model for the self-assembly of dendrons, dendron-jacketed poly-

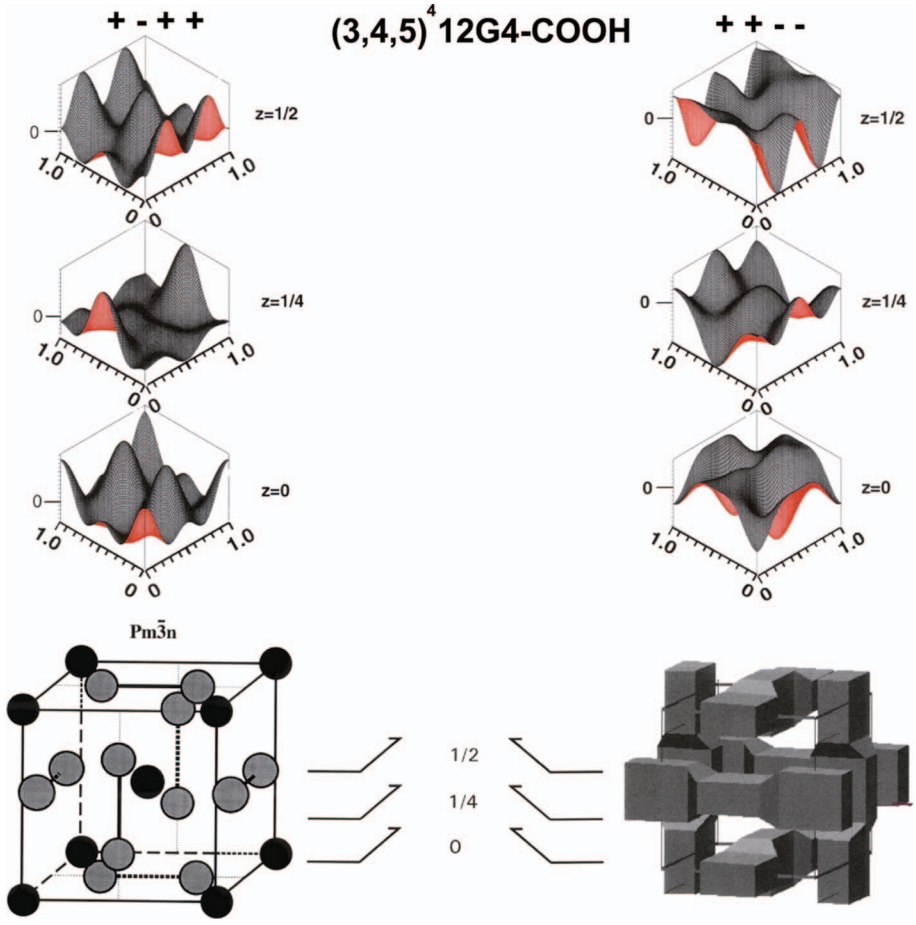

Figure 22. Spherical/micellar model for the + − + + phase assignment (left) and the columnar model for the + + − − phase assignment (right). The corresponding electron-density maps for the $z = 0$, $z = 1/4$, and $z = 1/2$ planes that were used to elaborate the two models are shown above. Discrimination between these two models was accomplished by TEM and isomorphous replacement. Adapted with permission from ref 314. Copyright 1997 American Chemical Society.

mers, and related topologies into columnar assemblies involves the segregation of branched aryl domains in the center of the column and the aliphatic tails on the exterior, this must be rigorously confirmed. Mezzenga recently reported benzamide dendrons and dendrimers noncovalently modified with alkyl sulfonate periphery groups (for related dendronized polymers, see section 3.2.2).[313] Remarkably, it was observed that the surfactant-like alkyl sulfonate groups occupy the interior rather than exterior of the columns. While similar behavior has not been observed for covalently attached alkyl peripheries, it is clear that assuming traditional models of microphase segregation like in block-copolymers is inappropriate.

In addition to Φ_h 2-D lattices, simple rectangular columnar, $\Phi_{r\text{-}s}$, lattices with *p*2*mm* symmetry and centered rectangular columnar, $\Phi_{r\text{-}c}$, phases with *c*2*mm* symmetry can result from the self-organization of dendrons self-assembled in supramolecular columns. For the $\Phi_{r\text{-}s}$ lattice, all *h*, *k* values are allowed, while $\Phi_{r\text{-}c}$ only exhibits diffraction peaks when $h + k =$ even number (Table 2). In both cases, a single numerical ratio for the expected lattice spacings does not exist. Rather, the position of lattice spacing varies according to the ratio of lattice parameters *a* and *b*, according to $q = \sqrt{h^2\times(2\pi/a)^2+k^2\times(2\pi/b)^2}$, where $a = h\langle d_{h00}\rangle$ and $b = k\langle d_{0k0}\rangle$. The $\Phi_{r\text{-}c}$ can usually be distinguished by the lack of (100) and (010) peaks. For the $\Phi_{r\text{-}s}$ lattice, the elliptical column diameters are $D_a = a$ and $D_b = b$, and the number of dendrons per column stratum, μ, can be calculated according to $\mu = (N_A abt\rho)/M$. For the $\Phi_{r\text{-}c}$ lattice, the elliptical column diameters are $D_a \approx a/\sqrt{3}$ and $D_b = b$, and the number of dendrons per column stratum, μ, can be calculated according to $\mu = (N_A abt\rho)/2M$.

The first dendrons reported by Percec self-assemble into supramolecular columns that self-organize into Φ_h lattices. Later, a library of dendrons, (3,4,5)^{n}12Gn−COOH, was designed so that the formation of a taper conformation was sterically restricted.[314] These dendrons preferentially adopt a conical geometry (Figure 18, left). TOPM of the ordered phases of these compounds revealed no birefringence, indicating an optically isotropic lattice. XRD suggested that these dendrons self-organized into a *Cub* lattice with *Pm*$\bar{3}$*n* symmetry. While the shape of the supramolecular objects could not be definitively determined by XRD, this *Cub* lattice was thought to be built of micellar supramolecular spheres (Figure 18, middle).[315,316]

While (3,4,5)^{m}12Gm−COOH dendrons, where $m = 2+$, self-organize into *Cub* lattice, (3,4,5)*m*G1−COOH/CO_2Me/CH_2OH, does not self-assemble or self-organize. However, the corresponding metal carboxylates (3,4,5)*n*G1−COOM, where M = Li, Na, K, Rb, or Cs and $n = 12$, 14, 16, or 18, self-assemble into supramolecular spheres that self-organize into *Cub* phases and a body-centered cubic phase with *Im*$\bar{3}$*m* symmetry (BCC) (Figure 19, left).[317] This lattice had been previously identified in the self-organization of poly(oxazo-

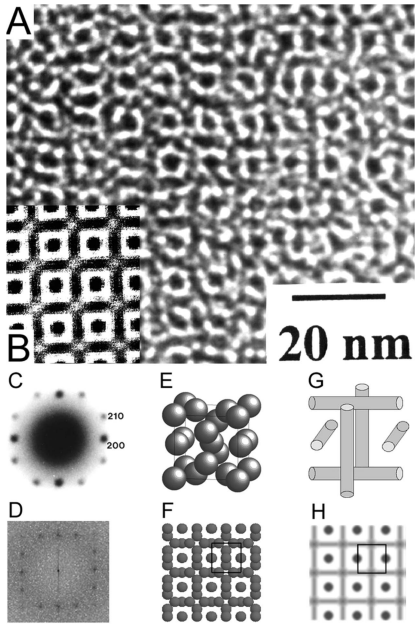

Figure 23. Raw (a) and reconstructed (b) TEM images and (c) ED pattern and (d) Fourier reconstructed power spectrum of (3,4,5-(3,4)^2)12G3−COOH. Also shown is the spherical model (e) for the *Pm*$\bar{3}$*n* phase and its [001] projection (f) and the competiting columnar model (g) and corresponding projection (h). Adapted with permission from ref 306. Copyright 1997 American Association for the Advancement of Science.

line)s jacketed with Percec-type dendrons.[318,319] For $n = 12$, a phase order of $k \rightarrow \Phi_h \rightarrow$ *Cub*$\rightarrow$ BCC is observed for M = K, Rb, and Cs carboxylates. For M = Na, a Φ_r phase is observed before the Φ_h phase, and for M = Li, no *Cub* phase was observed. Increasing the tail length resulted in a steady increase in the dimensions of the self-assembled columns or spheres but also destabilized the Φ_r and *Cub* phases (Figure 19a,b). By $n = 16$, no Φ_r was observed for M = Na, and by $n = 18$, no *Cub* phase was observed for any carboxylate. In the columnar phase, a network of ion−dipole interactions between alkali and carboxylates is believed to constitute the supramolecular backbone.

Powder XRD of the 3-D cubic lattice with *Pm*$\bar{3}$*n* symmetry is described by strong (200), (210), (211), (321), and (400) diffraction peaks and smaller (110), (220), (310), (222), (320), (420), and (421) higher-order diffraction peaks (Figure 20a,f).[265] As will be discussed later, a hollow center to the sphere will typically result in amplification of certain higher-order diffraction peaks. Without a high-intensity X-ray source, the first (110) reflection is usually absent. Reciprocal *d*-spacings follow 1:$\sqrt{2}$:$\sqrt{5}$/2:$\sqrt{3}$:2:$\sqrt{5}$:$\sqrt{6}$:... (Table 3). In addition to the *Cub* lattice, self-assembling dendrons have also been observed to self-organize into a cubic lattice with *Im*$\bar{3}$*m* symmetry, BCC. The BCC lattice has more systematic extinctions than the *Cub* lattice as $h + k + l$ must be even. The BCC lattice typically exhibits a strong (110) reflection and smaller (200), (211), and (220) higher-order reflection with reciprocal *d*-spacings following the ratios of 1:$\sqrt{2}$:$\sqrt{3}$:$\sqrt{4}$...$\sqrt{n}$ (Figure 20c; Table 3).[317] The diameters for the *Cub* and BCC lattices can be calculated from the spherical lattice parameter, $a = (\sqrt{2}d_{100} + \sqrt{4}d_{200} + \sqrt{5}d_{210} + \sqrt{6}d_{211} + \sqrt{8}d_{220} + \sqrt{10}d_{310} + \sqrt{12}d_{222} + \sqrt{13}d_{322} + \sqrt{14}d_{321} + \sqrt{16}d_{400} + \sqrt{20}d_{420})/X$; where X is the number of those reflections observed for either the Cub or BCC lattice. For the Cub lattice, the experimental spherical diameter, D, is calculated according $D = 2\sqrt[3]{3a^3/32\pi}$ and the number of dendrons per spherical dendrimer, μ, can be found according to $\mu = (a^3 N_A \rho)/8M$. For the BCC lattice, $D = 2\sqrt[3]{3a^3/8\pi}$ and the number of dendrons per spherical dendrimer is $\mu = (a^3 N_A \rho)/2M$. In addition to cubic lattices derived from self-assembled spheres, a bicontinuous gyroid phase with *Ia*$\bar{3}$*d* symmetry was observed. This phase can likewise be identified by characteristic reflections with an explicit ratio between reciprocal *d*-spacings (Table 3).

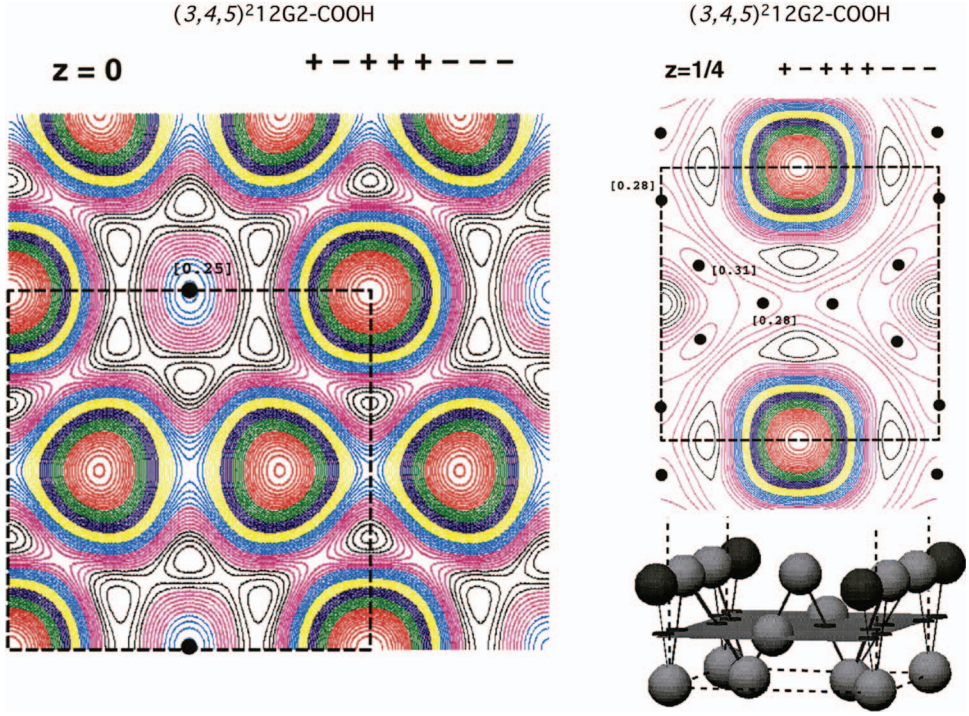

Figure 24. Reconstructed electron-density cross section of the $z = 0$ (left) and $z = 1/4$ planes using the $+ - + +$ phase combination (micellar model) exhibiting quasi-equivalent self-assembly. Reprinted with permission from ref 314. Copyright 1997 American Chemical Society.

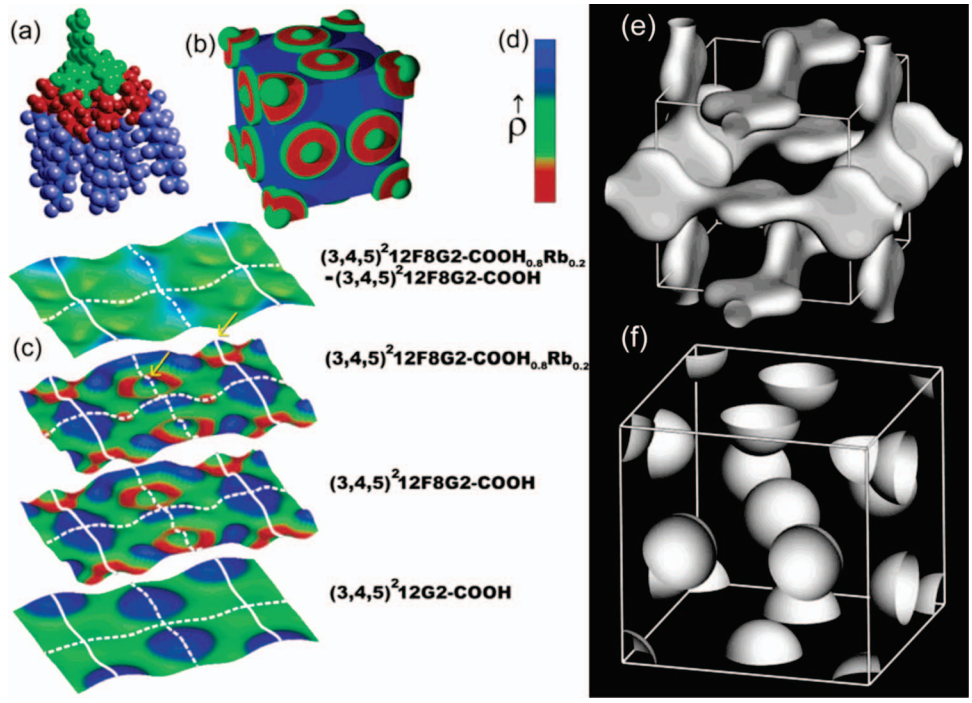

Figure 25. Electron density (ρ) distributions for $(3,4,5)^2$12F8G2−COOH (a) with the lowest ρ aliphatic portions in red, the medium ρ, predominantly aromatic core in green, and the highest ρ fluorinated portions in blue. (b) Expected $\rho(x,y,z)$ distribution in a $Pm\bar{3}n$ unit cell of $(3,4,5)^2$12F8G2−CO_2H according to the spherical model. (c) 2-Dimensional $\rho(x,y)$ maps of the $z = 0$ level for $(3,4,5)^2$12G2−COOH (c, bottom), $(3,4,5)^2$12F8G2−COOH (c, second from bottom), and (3,4,5)212F8G2−$CO_2H_{0.8}Rb_{0.2}$ (c, second from top), and a difference map of $(3,4,5)^2$12F8G2−$COOH_{0.8}Rb_{0.2}$−$(3,4,5)^2$12F8G2−COOH (c, top). Also depicted are the alternative model for the $Pm\bar{3}n$ lattice (e) and the confirmed globular model (f). Reprinted with permission from ref 367. Copyright 2002 American Chemical Society.

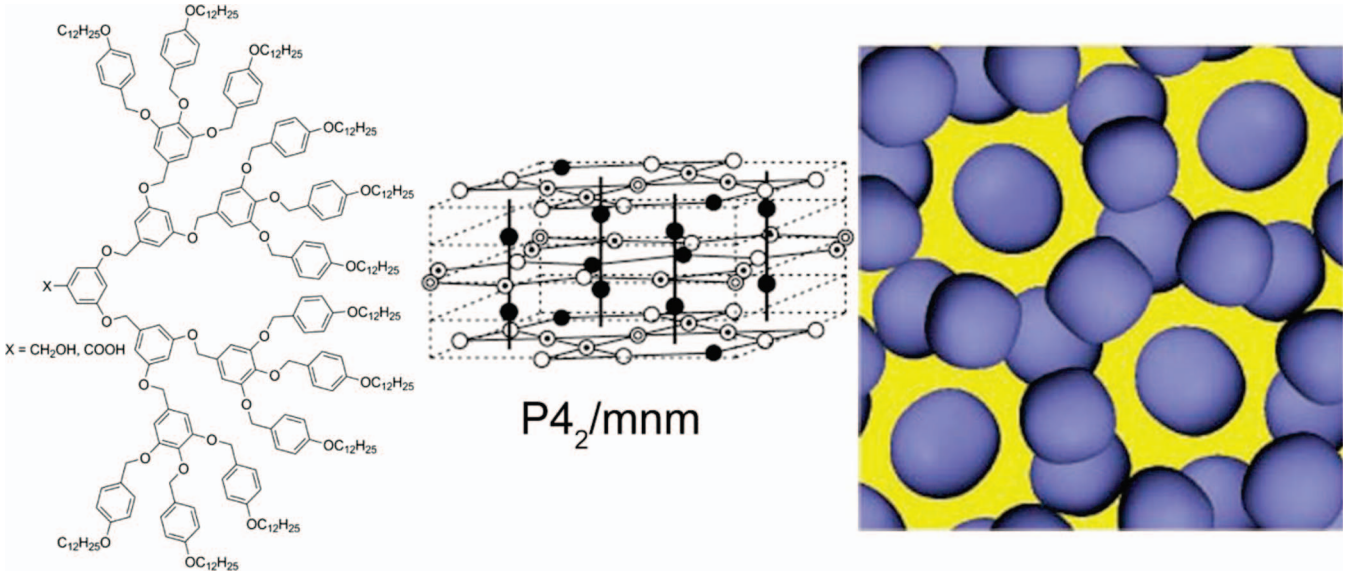

Figure 26. Structures of (4-3,4,5-$(3,5)^2$)12G3−COOH and (4-3,4,5-$(3,5)^2$)12G3−CH_2OH (left), lattice space group diagram (middle), and isoelectron surface exhibiting spherical organization (right). Reprinted with permission from ref 323. Copyright 2003 American Association for the Advancement of Science.

While the self-assembly of Percec-type dendrons in supramolecular spheres and their self-organization into *Cub* lattices was discovered in 1991, it was not until 1997 that these results were published. Largely, this delay was due to ambiguities in the self-assembly mechanism and the true shape of the supramolecular objects that populated the lattice. XRD measurements do not reveal the phase of each reflection. However, in order to generate an electron-density histogram or map from the diffraction data, phase information must be incorporated into the Fourier transform. For small numbers of reflections, a brute force approach can be applied to generate the electron-density histograms for each phase. It is an assumption in the self-assembly of dendrons that the aromatic and aliphatic segments most probably will not mix, and thus, a gradient in electron density should be observed in the electron-density histograms corresponding to these domains. Unfortunately, for the *Cub* lattice

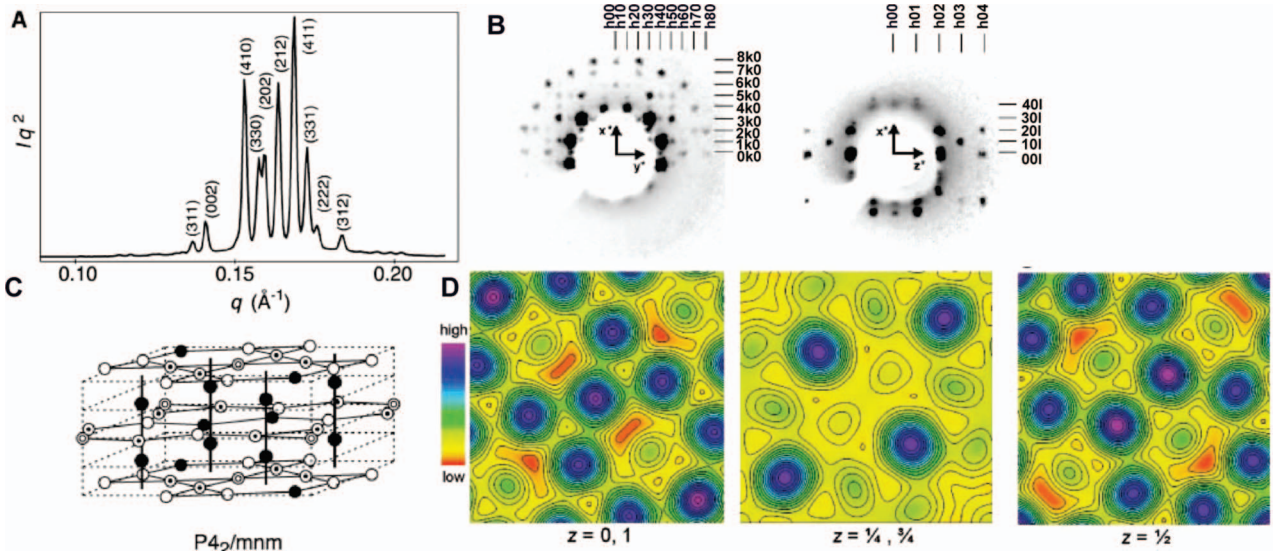

Figure 27. First amphiphilic dendron, (4-3,4,5-(3,5)^2)12G3−CH_2OH, identified to self-organize into the $P4_2/mnm$ tetragonal phase. Small-angle experimental X-ray diffraction powder plot with peak indexing (a); monodomain small-angle experimental X-ray diffraction patterns with indexing (b); schematic of the $P4_2/mnm$ tetragonal unit cell with the 5 different types of spherical clusters (c); and reconstructed electron-density maps at the indicated *z*-axis positions (d). Reprinted with permission from ref 323. Copyright 2003 American Association for the Advancement of Science.

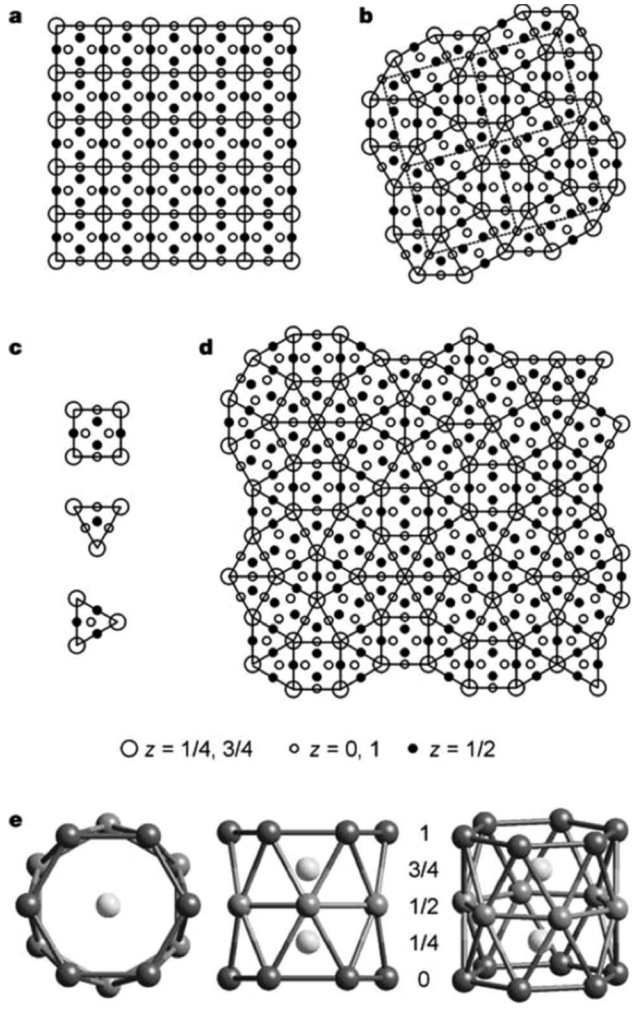

Figure 28. 2D tilings representing tetrahedrally close packed (t.c.p.) lattices such as $Pm\bar{3}n$ (a) and $P4_2/mnm$ (b) using three basic decorated tiles (c). Quasiperiodic arrangement of these tiles (d) results in the proposed model (e) of 12-fold symmetry for the QLC structure of (3,4,5-(3,5)^2)12G3−CH_2OH. Reprinted with permission from ref 325. Copyright 2004 Macmillan Publishers Ltd. (Nature).

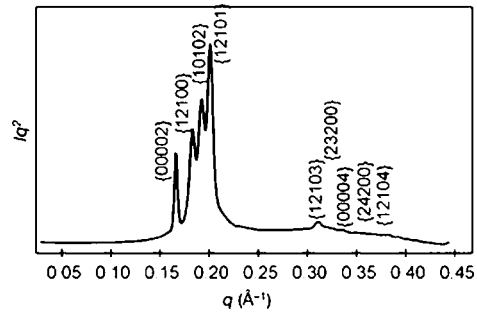

Figure 29. Example of an experimental diffractogram of a QLC lattice. Reprinted with permission from ref 325. Copyright 2004 Macmillan Publishers Ltd. (Nature).

derived from Percec-type self-assembling dendrons, more than one of the phase combinations were consistent with this assumption. The + − + + (and its inverse − + − −) and the + + − − (and its inverse − − + +) phase combinations provided two competing models for self-assembly (Figure 21).[314] For the + + − − phase assignment, an interlocked columnar model was proposed (Figure 22, left), and for the + − + + phase assignment, a spherical micellar-like model was proposed (Figure 22 right). Direct visualization of the *Cub* lattice generated by (3,4,5)^{3}12G3−COOH and (3,4,5-(3,4)^2)12G3−COOH was achieved through TEM and supporting electron diffraction (ED) (Figure 23a).[306,320] Through the use of Fourier filtering of the TEM image (Figure 23b), a spherical model (Figure 23e,f) was found to be more consistent with the image than the rival interlocked columnar model (Figure 23g,h). Quasi-equivalent self-assembly is demonstrated by the tetragonal distortion of the supramolecular spheres shown in the plane $z = 0.25$ (Figure 24).

Despite powder XRD and TEM/ED results, the interlocked columnar model could not be completely discounted in favor of the preferred spherical model. The spherical model was eventually confirmed via the use of isomorphous replacement (Figure 25).[367] (3,4,5)^{2}12G1−COOH was previously determined to self-organize into a *Cub* lattice. By applying the

Table 4. Expected Reflections for the 12-Fold QLC and Ratio of Reciprocal *d*-Spacings Relative to the (00002) Peak

(h_1, h_2, h_3, h_4, h_5)	q/q_0[a] QLC-12-fold
(0, 0, 0, 0, 2)	1.00
(1, 2, 1, 0, 0)	1.08
(1, 0, 1, 0, 2)	1.12
(1, 2, 1, 0, 1)	1.19
(1, 2, 2, 1, 0)	1.52
(1, 2, 1, 0, 3)	1.85
(2, 2, 2, 0, 2)	1.87
(2, 3, 2, 0, 0)	1.87
(2, 3, 2, 0, 1)	1.93
(0, 0, 0, 0, 4)	2.00
(1, 3, 3, 1, 0)	2.08
(2, 4, 2, 0, 0)	2.15
(1, 2, 1, 0, 4)	2.27

[a] q_0 = scattering position of the first nonzero diffraction peak.

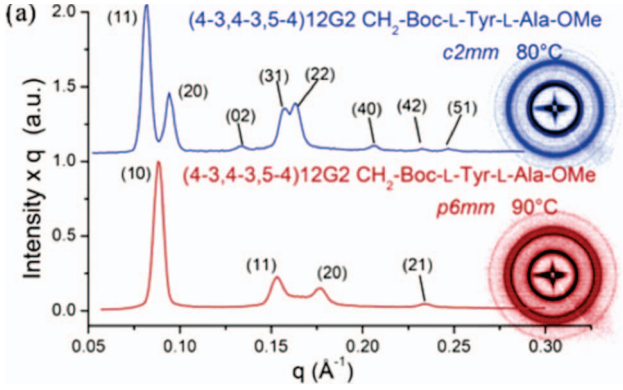

Figure 30. Representative amplification of higher-order diffraction peaks for $\Phi_{r\text{-}c}$ (top) and Φ_h (bottom) lattices. Reprinted with permission from ref 355. Copyright 2006 American Chemical Society.

crystallographic method of isomorphous replacement pioneered by Perutz[321] for globular proteins, where a strongly scattering heavy metal is placed at a known position without perturbation to the 3D structure, more precise determination of the self-assembly mechanism was made possible. Introduction of strong scattering heavy elements was achieved in two ways: (a) partial doping of the carboxylic with Rb by

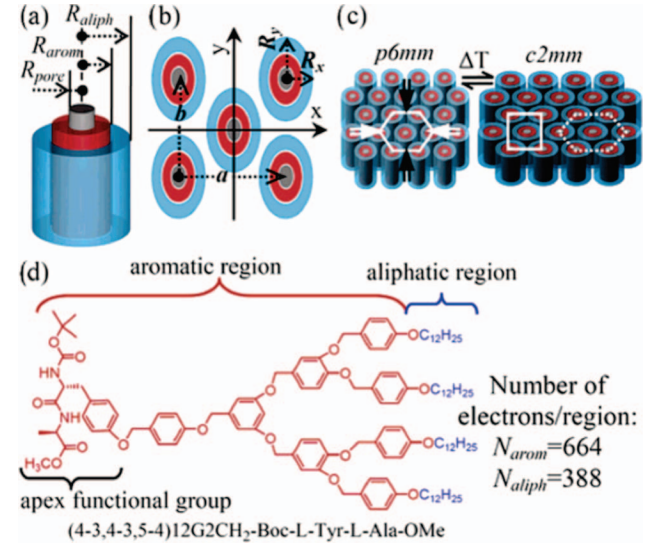

Figure 32. Modeling of the self-assembly of dendrons into hollow columnar structures. (a) Side-on columnar view depicting three concentric shells of differing electron density. (b) Top-down view depicting the hollow, aromatic, and aliphatic shells. (c) Thermoreversible conversion between Φ_h and $\Phi_{r\text{-}c}$ hollow lattices. (d) Electron density-domains of Percec-type dendrons. Color code: hollow core (gray), aromatic (red), aliphatic (blue). Reprinted with permission from ref 355. Copyright 2006 American Chemical Society.

forming the Rb carboxylate and (b) semifluorination of the alkyl tails. The perhydrogenated $(3,4,5)^2$12G1−COOH is only expected to exhibit a bimodal electron-density distribution corresponding to aliphatic and aromatic domains, while the semifluorinated $(3,4,5)^2$12F8−COOH is expected to exhibit a trimodal distribution corresponding to perfluorinated, aliphatic, and aromatic domains. The increased number of features required in the electron-density distribution makes the validation of the chosen phase assignment possible. Once the appropriate phase combination was chosen for a micellar model of XRD of $(3,4,5)^2$12F8−COOH, the system was doped with 20% Rb, $(3,4,5)^2$12F8$COOH_{0.8}Rb_{0.2}$. Electron-density map reconstruction of the resulting XRD demonstrated increased electron density at the center of the micelles where the

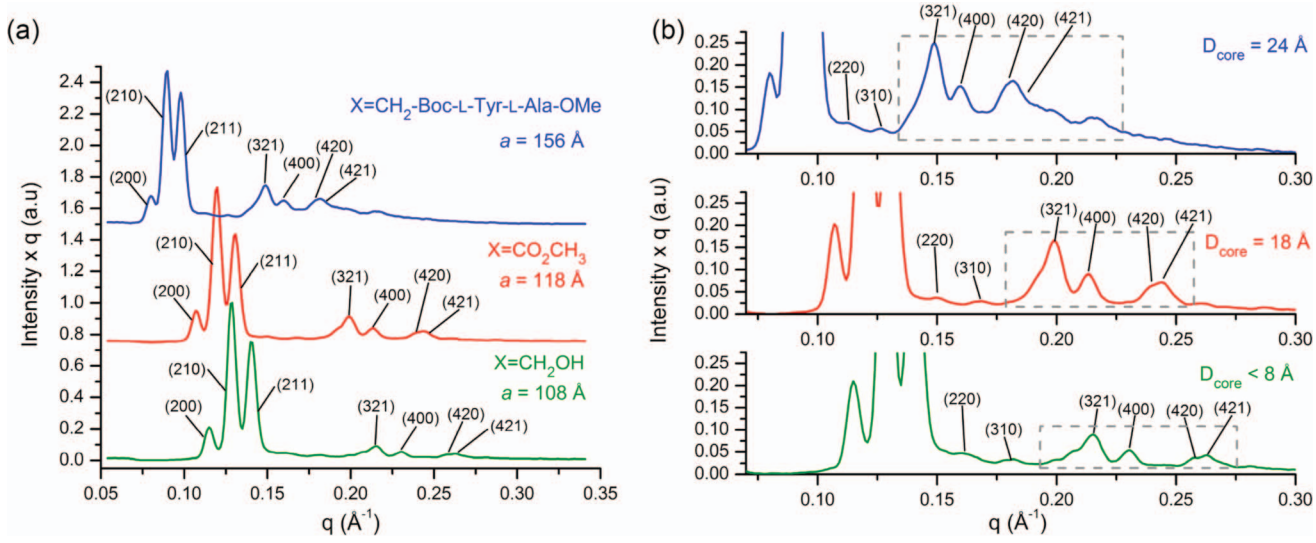

Figure 31. Amplification of higher-order diffraction peaks in the *Cub* phase. (a) Full diffractogram and (b) enlargement of the (321), (400), (420), and (421) reflections. Reprinted with permission from ref 353. Copyright 2006 American Chemical Society.

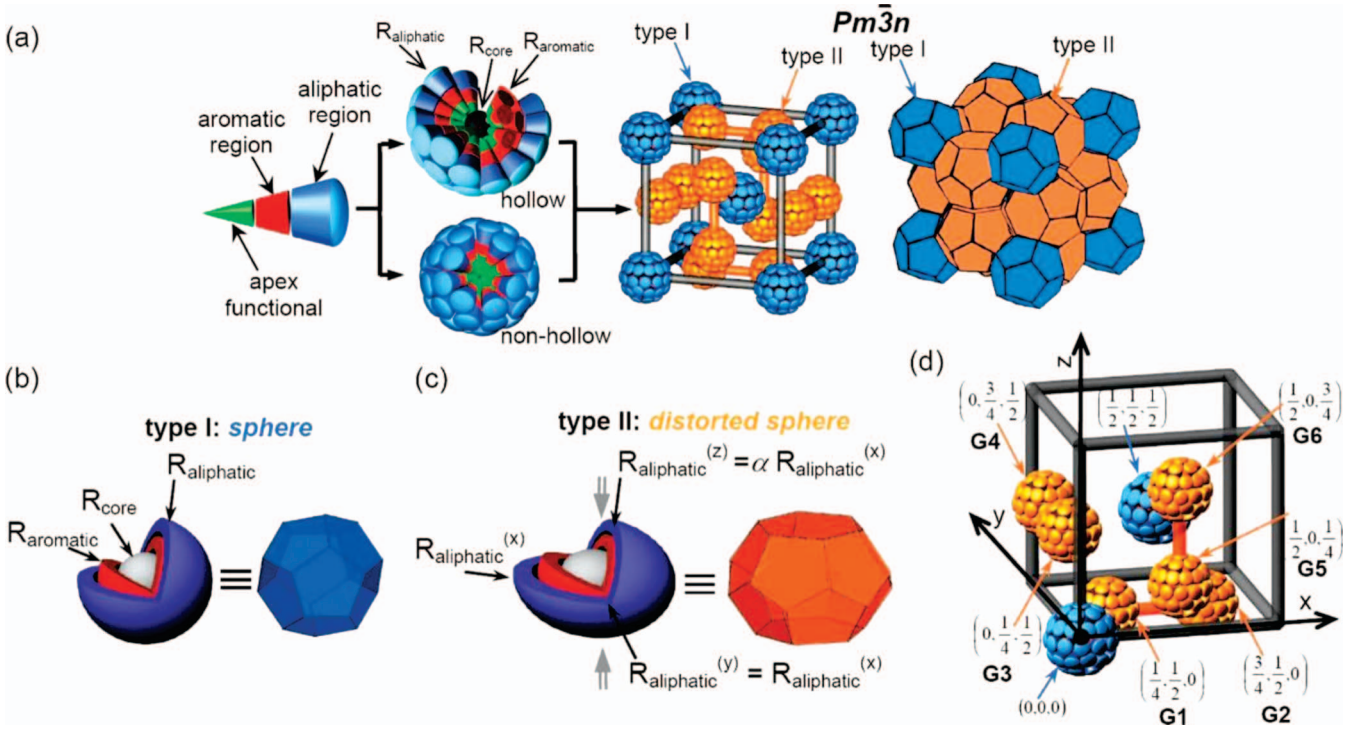

Figure 33. Three shells of constant electron density used to model filled and hollow spherical supramolecular assemblies. (a) Schematic of *Pm*3̄*n* cubic assembly and polyhedron space-filling view of the unit cell. (b, c) Simplified models of (b) spherical and (c) distorted spherical assemblies. (d) Normalized positions of the eight spherical objects that form the *Pm*3̄*n* unit cell. Color code: core region, gray; aromatic region, red; aliphatic region, blue. Reprinted with permission from ref 357. Copyright 2008 American Chemical Society.

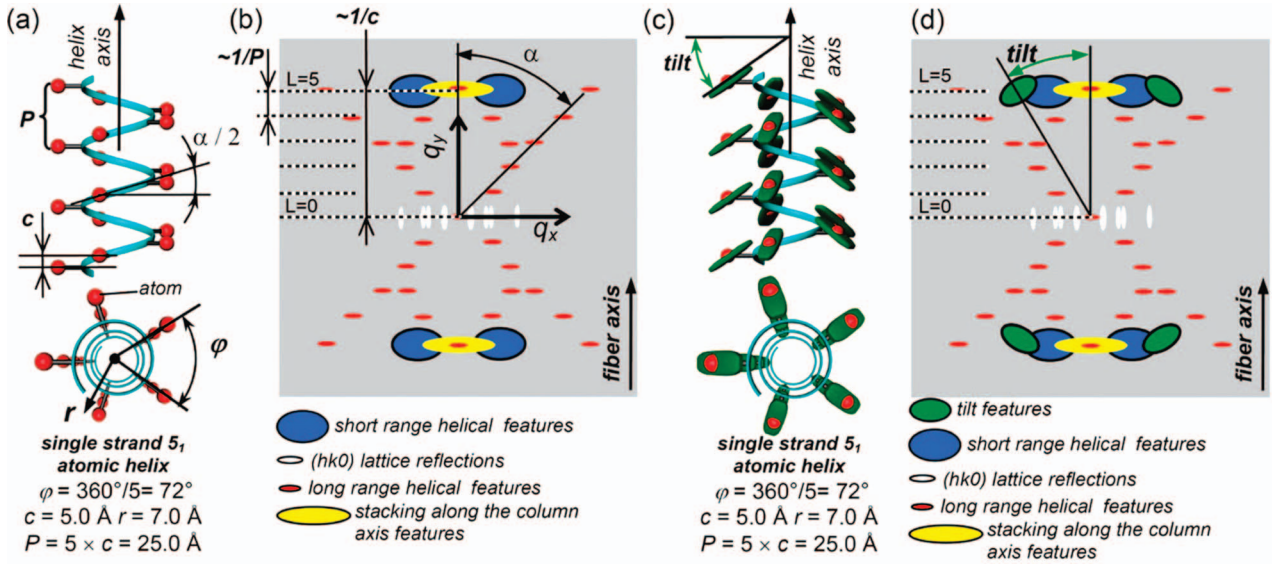

Figure 34. Diffraction by a helical fiber: (a) a 5_1 single-strand atomic helix and its structural parameters; (b) the simplified representation of the fiber diffraction generated for the structure from (a) by using the helical diffraction theory; (c) a 5_1 single-strand atomic helix model generated from tilted groups of atoms and its structural parameters; (d) the simplified representation of the fiber diffraction generated for the structure from (b) by using the helical diffraction theory. Reprinted with permission from ref 330. Copyright 2008 American Chemical Society.

Rb is expected to reside. In addition to proving the spherical model for dendrons self-organized into the *Cub* phase, isomorphous replacement has also been used to confirm the triple-network BCC structure of dendron-rod structures.[322]

Dendrons that self-assemble into spheres were first shown to self-organize into *Cub* lattices, and this lattice has been shown to be the most ubiquitous for Percec-type dendrons. However, other packing arrangements for self-assembled spherical dendrimers have been observed. As mentioned previously for dendritic metal carboxylates, a BCC as well as *Cub* lattices were noted. Noncubic 3-D organization was observed in (4-3,4,5-(3,4)^2)12G3−CO_2CH_3, (4-(3,4,5)^2)12G2−COOH, (3,4-3,4,5)12G2−CH_2OH, (3,4-(3,5)^2)12G3−CH_2OH, (4-3,4,5-3,5)12G2−CH_2OH, (4-3,4,5-(3,5)^2)12G3−COOH, and (4-

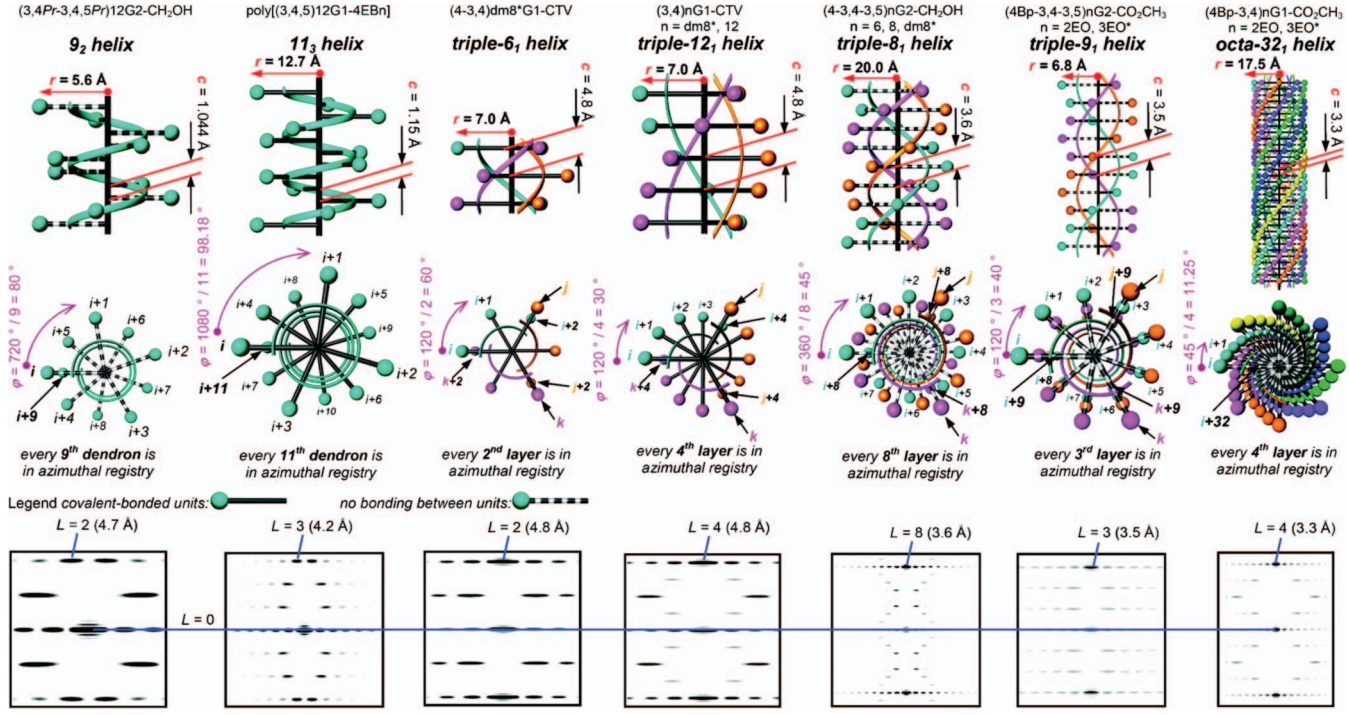

Figure 35. Simulated atomic helices identified for the dendrons self-assembled into helical columnar supramolecular structures. Reprinted with permission from ref 330. Copyright 2008 American Chemical Society.

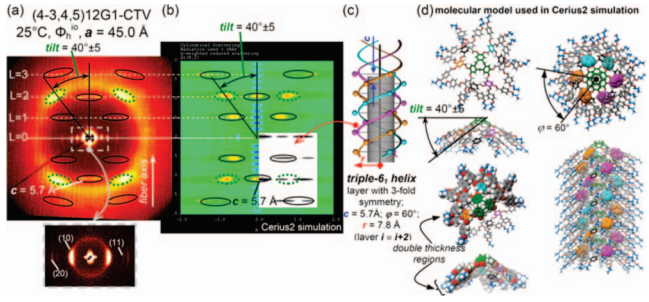

Figure 36. (a) Experimental fiber XRD for (4-3,4,5)12G1−CTV (b) Cerius 2 simulation of the diffractogram generated from a (c) triple-6_1 atomic helix and (d) the corresponding molecular model of self-assembly. Reprinted with permission from ref 330. Copyright 2008 American Chemical Society.

3,4,5-$(3,5)^2$)12G3−C_2HOH. Ungar has performed detailed XRD analysis on the latter two compounds (4-3,4,5-$(3,5)^2$)12G3−COOH and (4-3,4,5-$(3,5)^2$)12G3−CH_2OH, elaborating a giant supramolecular LC lattice with tetragonal $P4_2/mnm$ symmetry (*Tet*) (Figures 26 and 27).[323] The lattice dimensions for the tetragonal unit cell were roughly $a = 17$ nm and $c = 9$ nm. The dendritic acid exhibits this phase exclusively until T_{Iso}, whereas the dendritic alcohol exhibits a series of thermoreversible phases $\Phi_h \rightarrow$ *Cub* $\rightarrow$ *Tet* $\rightarrow$ *I*. The existence of the *Tet* phase was consistent with a similar molecular envelope or distribution of volume with radius d*V*/d*r* with the *Cub* as well as with the taper geometry of highly branched benzyl ether dendron. Close contact of spherical assemblies in the *Tet* is intermediate between that of *Cub* and a BCC lattice. With increasing temperature, close contact between neighboring micelles becomes disfavored, thereby explaining the observed phase order. However, the *Tet* phase can swap places in the thermodynamic phase diagram with *Cub*, depending on the primary structure of the dendritic unit.[324]

The *Tet* lattice with $P4_2/mnm$ symmetry also exhibits a complex diffraction pattern consisting of strong (410), (330), (202), (212), (411), and (331) reflections and weaker (311), (002), (222), and (312) reflections.[323] While not typically observed for self-assembling dendrons self-organized into the *Tet* lattice, other reflections are allowed (consult the International Tables of Crystallography, Space group 36). As with the $\Phi_{r\text{-}s}$ and $\Phi_{r\text{-}c}$ lattices, a simple numerical relationship between the reciprocal lattice reflections is not possible. Rather, the theoretical *d*-spacings must be calculated using the known $a = b$ and c lattice parameters according to $d_{hkl} = \sqrt{(h^2+k^2)/a^2+l^2/c^2}$. The diameter of self-assembled spheres self-organized into $P4_2/mnm$ tetragonal lattice can be calculated from the lattice parameters $a = b$ and c according to, $D = 2\sqrt[3]{(abc/40\pi)}$. The number of dendrons forming a spherical object can be calculated according to $\mu = (abcN_A\rho)/30M$.

An even more complex self-organization of spherical supramolecular dendrimers was observed for (3,4,5-$(3,5)^2$)12G3−CH_2OH.[325−328] On heating (3,4,5-$(3,5)^2$)12G3−CH_2OH exhibits a phase order of X$\rightarrow P4_2/mnm \rightarrow I$. XRD demonstrated 12-fold symmetry, forbidden to classical crystals, in the X phase. Powder XRD analysis utilizing 5 instead of the typical 3 basis vectors confirmed that the X phase is in fact an unprecedented liquid quasicrystal (QLC) (Figure 28). The 12-fold QLC observed for (3,4,5-$(3,5)^2$)12G3−CH_2OH is characterized by strong {00002}, {12100}, {10102}, and {12101} diffraction peaks, as well as smaller {12103}, {23200}, {00004}, {24200}, and {12104} diffraction peaks (Figure 29). The theoretical ratios of the reciprocal *d*-spacings are consistent for 12-fold QLC lattices (Table 4). The experimental diameter of spherical dendrimers in the QLC lattice with 12-fold sym-

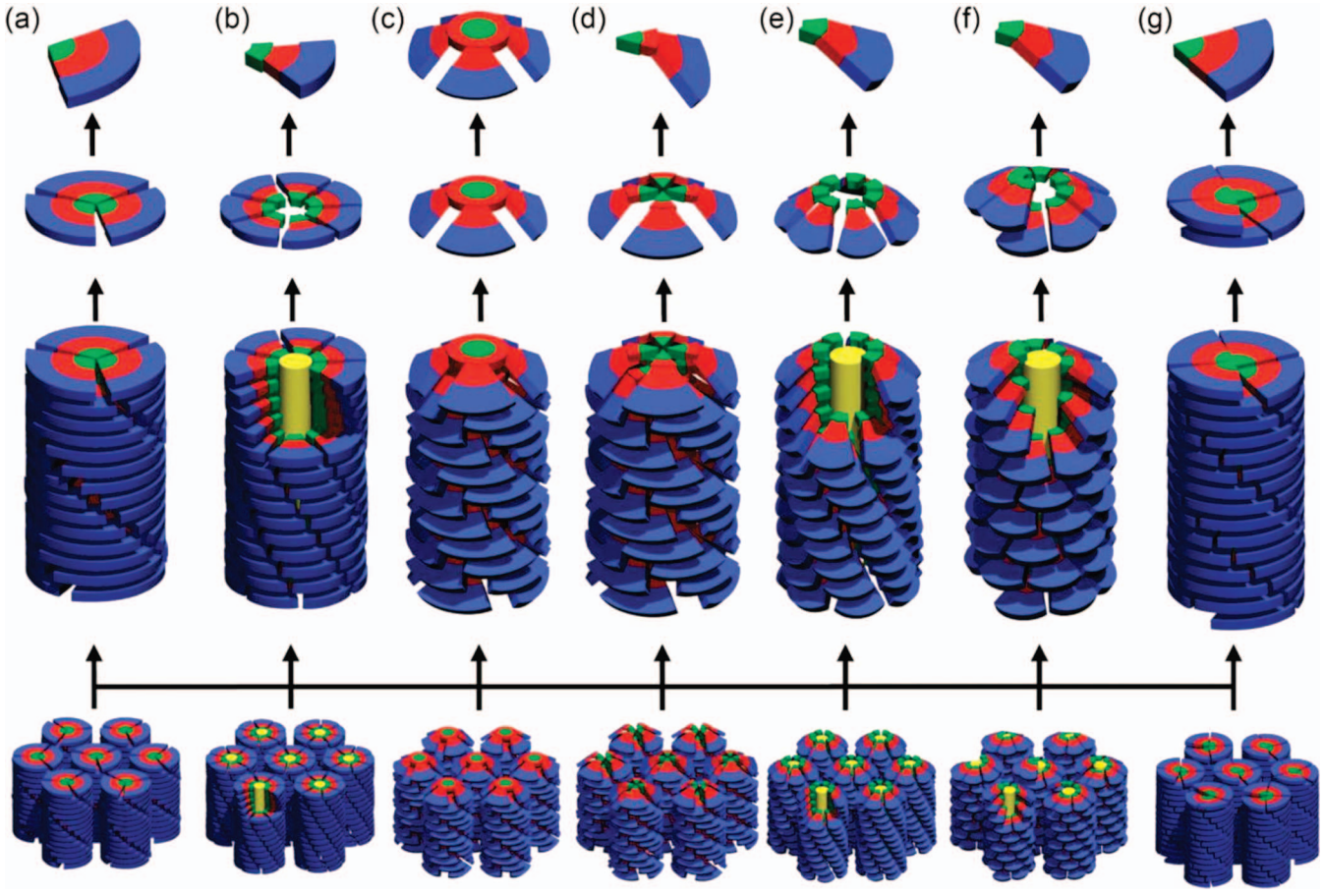

Figure 37. Flat (a,b), pyramidal (c,d,e), and helicene-like (f, g) models of helical self-assembly. Reprinted with permission from ref 330. Copyright 2008 American Chemical Society.

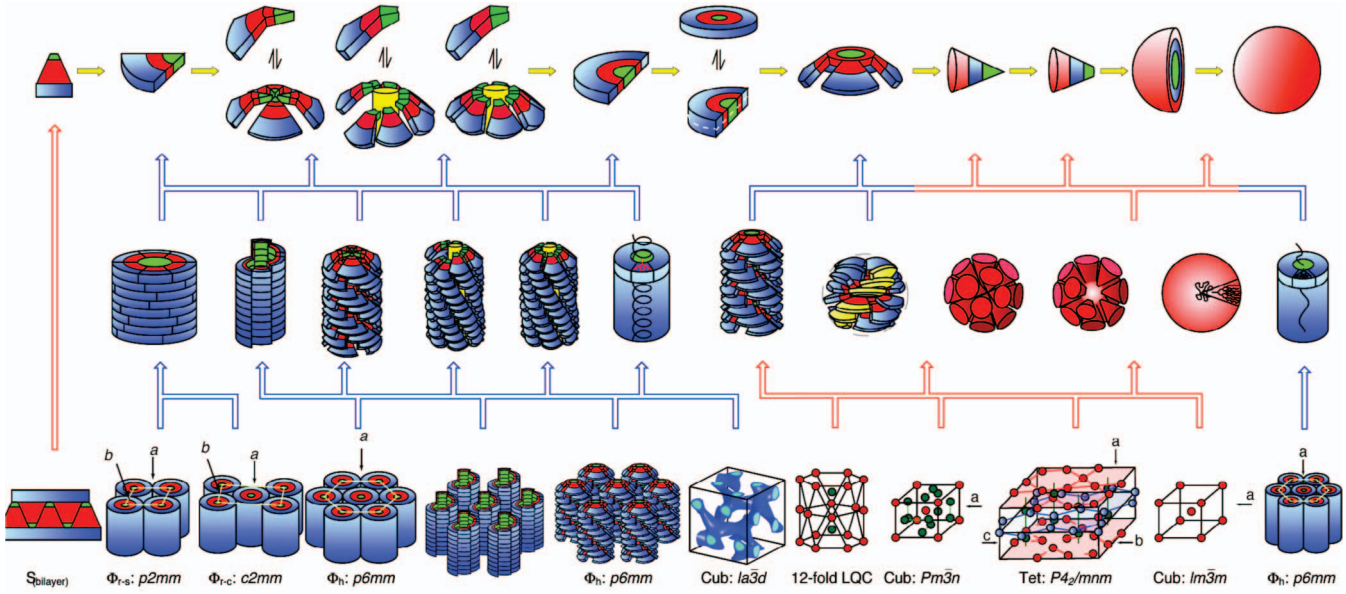

Figure 38. Periodic and quasiperiodic arrays formed via the self-assembly and self-organization of Percec-type dendrons.

metry is $D = 2a/\sqrt[3]{8\pi}$. The total number of dendrons forming a spherical dendrimer is $\mu = (a^3 N_A \rho)/6M$.

Once a periodic or quasi-periodic array is determined, a preliminary molecular model for self-assembly can be produced. As mentioned above, the dimensions of the spherical and columnar objects in each lattice can be obtained as well as the number of dendrons forming a supramolecular sphere or column stratum. A computer model of the self-assembled structures can then be built to match the dimensions derived experimentally. Once a model is constructed, simulation of the powder XRD diffraction pattern allows for comparison of the molecular model with experimental

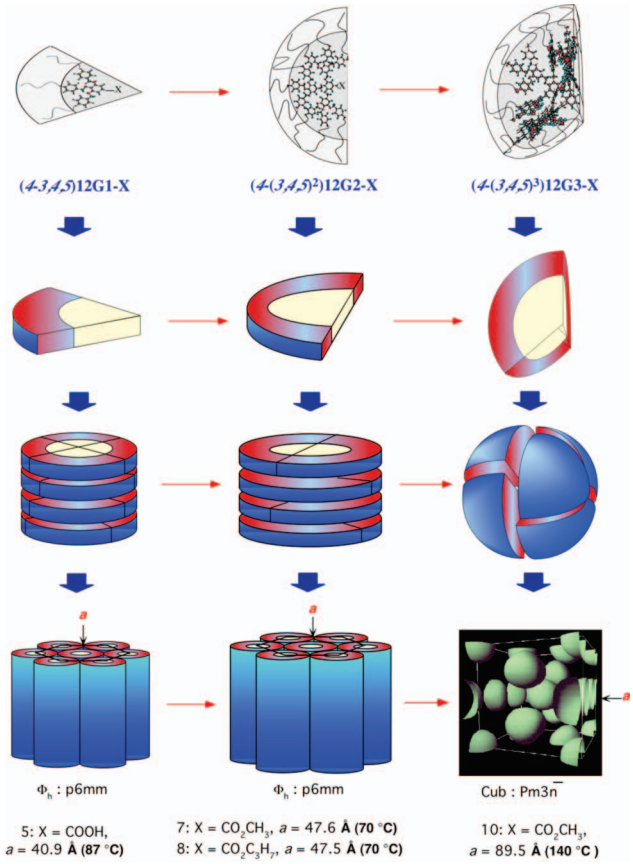

Figure 39. Library of (4-(3,4,5)^n)12Gn−X and their generation-dependent self-assembly into columnar and spherical objects. Reprinted with permission from ref 331. Copyright 1998 American Chemical Society.

diffraction data. The molecular model is then refined until the best possible match between theoretical and experimental diffractograms is reached.

In the particular case of hollow columnar[355] and hollow spherical[357] structures, higher-order diffraction peaks have been observed with greater intensity than in the filled structures. For the $\Phi_{r\text{-}c}$ lattices with a hollow center, an amplification (enhanced intensity) of the (310) and (220) reflections is observed (Figure 30, top) relative to the filled structure. In the *Cub* lattice, a hollow center results in relatively more intense (321), (400), (420), and (421) reflections (Figure 31), relative to the filled spherical model. Increases in the relative size of the pore results in an increase in the amplification of the higher-order reflection peaks. Methods have been developed to accurately predict the diffraction patterns of hollow columnar[355] and hollow spherical structures,[357] allowing for verification of the model. These methods involve the simplification of supramolecular objects into columns (Figure 32) or spheres (Figure 33) built from three concentric shells of varying electron density and simulating their diffraction pattern when self-organized into a given lattice symmetry.

In the case of helical or helical pyramidal columns, details of the internal structure of the column can be ascertained via aligned fiber XRD analysis. Through the application of Cochran, Crick, and Vand helical diffraction theory[329] expanded to tilted self-assembling dendrons,[330] fiber experiments provide information on the helical pitch, helical radius, and tilt of the high electron density aromatic groups, as well as short-range and long-range helical features (Figure 34). Application of this theory allows for the determination of the specific atomic helix formed from the high electron density domains of the self-assembled dendrons (Figure 35). Cerius2 simulation of the aligned-fiber helical diffractogram and comparison with experimental data (Figure 36) provides discrimination between flat, pyramidal, and helicene type self-assembled helical columns (Figure 37), and comparison with experimental fiber-diffractogram allows for the determination of the molecular model of self-assembly.

2.2.3. Molecular Shape Control Through Dendron Branching Structure

As discussed in the previous subsection, a number of self-organized phases can be accessed via the self-assembly of dendrons in columnar or spherical objects (Figure 38). Early on, it was recognized that the primary structure of the dendron dictated whether the self-assembly mechanism would be columnar or spherical. Later, studies were aimed at systematically elaborating which factors are most significant in influencing supramolecular self-assembly.

Molecular shape control through generation can be used to manipulate the mechanism of self-assembly. A library of (4-(3,4,5)^n)12Gn−X dendrons was prepared (Figure 39).[331] (4-3,4,5)12G1−COOH has tapered shape that occupies a quarter-disk as it self-organizes into a Φ_h lattice. (4-(3,4,5)^2)12G2−COOH/CO_2CH_3 also has a tapered shape that occupies a half-disk as it self-assembles into supramolecular columns that self-organize into a Φ_h lattice. However, (4-(3,4,5)^3)12G3−CO_2CH_3 cannot assume a taperlike conformation and, thus, distorts into a conical conformation. The conical segments occupy one-sixth of a sphere and self-organize into *Cub* lattice. Site isolation of the apex X-group was seen at G4.

The phenomenon of increasing molecular taper angle with generation and subsequent transition of columnar to spherical self-assembly was experimentally demonstrated through a library of (3,4-(3,5)$^{n-1}$)12Gn−X dendrons (Figure 40).[332] These experiments supported a previously theoretically predicted concept of molecular shape control via generation number.[35,333] Here the transition to a conical conformation and spherical self-assembly occurs at G5, at which point the apex group achieves site isolation.

The effect of dendron structure on self-assembly was more precisely described via the modulation of its solid angle (Figure 41).[334,335] Here, α' is defined as the projection of the solid angle of the dendron onto a plane and can be determined in all cases according to $\alpha' = 360/\mu$, where μ is the number of dendrons in a column stratum or supramolecular sphere. Increasing the branching via a change in primary structure or increase in generation number of taperlike dendrons increases the α' and the fraction of the disk occupied in columnar self-assembly. At a certain threshold, only unimolecular disks are formed. Above this threshold, further branching results in deformation of the disk into a conical segment with diminished α'. Beyond this point, increased branching increases α' and the fraction of a sphere formed. Ultimately a unimolecular sphere should form. It was recently demonstrated by fiber XRD experiments that many disklike dendrons adopt a crown conformation.[275,330]

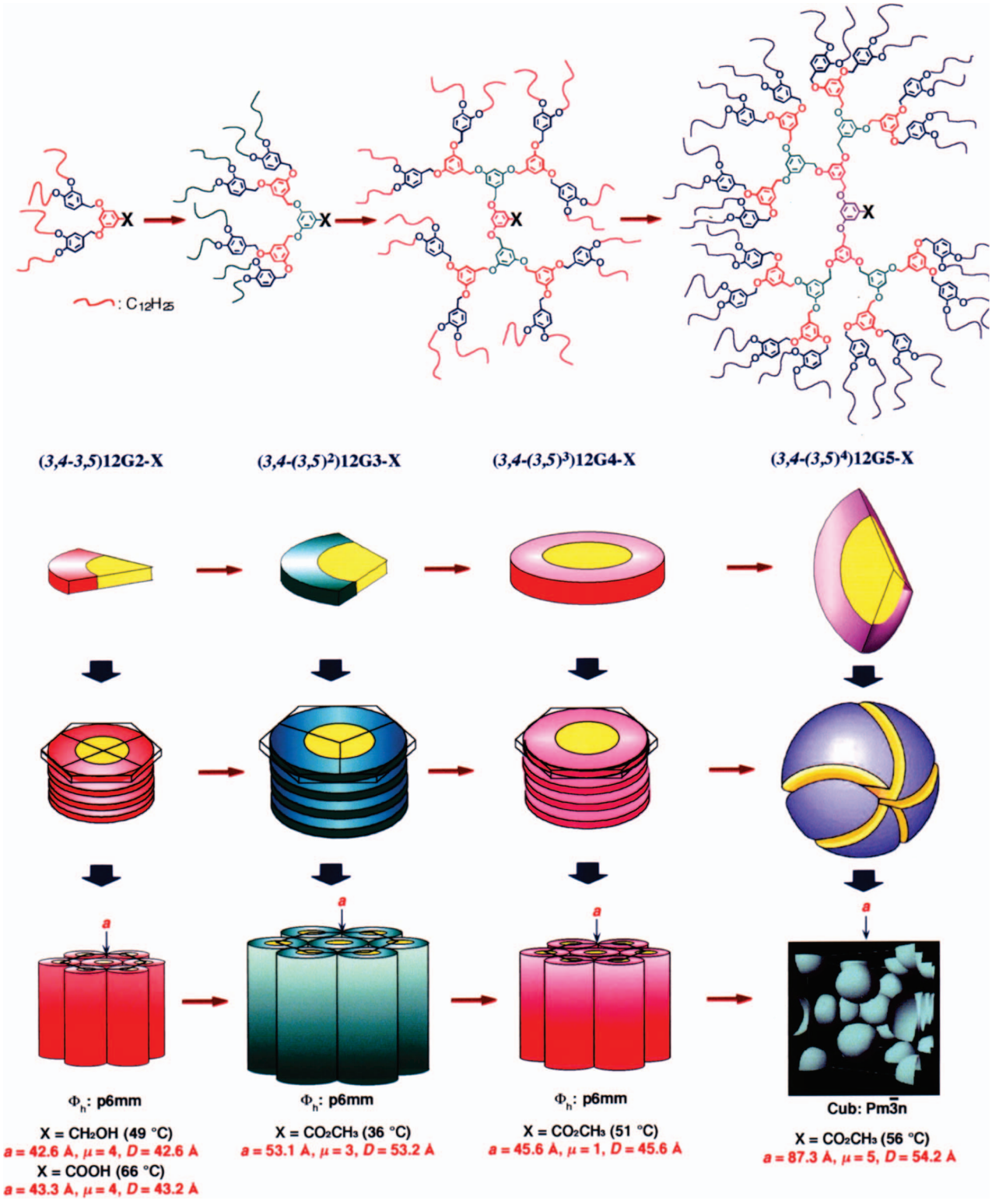

Figure 40. Increasing molecular taper angle with increasing generation number for a library of (3,4-(3,5)$^{n-1}$)12Gn−X. Reprinted with permission from ref 332. Copyright 2000 Wiley-VCH Verlag GmbH & Co. KGaA.

A library of (3,4-(3,4,5)$^{n-1}$)12Gn−X dendrons, where $n = 1-4$, was prepared.[271] In all cases, spherical self-assembly followed by self-organization into a *Cub* lattice was observed (Scheme 16). Increasing generation number, *n*, does not significantly affect the spherical diameter in the *Cub* lattice (Scheme 16 and Figure 42). Rather, increasing generation number decreases the number of dendrons per sphere, μ. At $n = 5$, there is only one dendron per sphere demonstrating the first spherical dendron to self-assemble into a *Cub* lattice. Single dendrons forming a sphere were confirmed via direct visualization using scanning force microscopy (SFM) and XRD experiments (Scheme 16).[271]

Molecular taper angle α, and the projection of the solid angle α', is the primary determinant of the mechanism of self-assembly and related structural parameters. The molecular taper angle can be modulated by changes in structure such as increased branching or increasing the apex volume

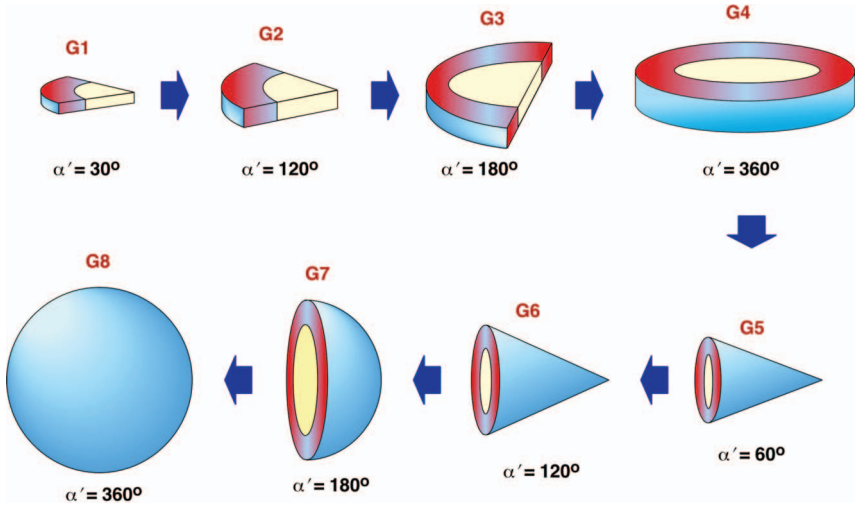

Figure 41. Hierarchical control of self-assembly via molecular solid angle. Reprinted with permission from ref 334. Copyright 2000 American Chemical Society.

Scheme 16. Library of (3,4-(3,4,5)$^{n-1}$)12Gn−X Dendrons and Their Self-Assembly into Supramolecular Spheres and Visualization of Monodendritic Spheres by STM (a, b) (Adapted with Permission from Ref 271; Copyright 2000 American Chemical Society)

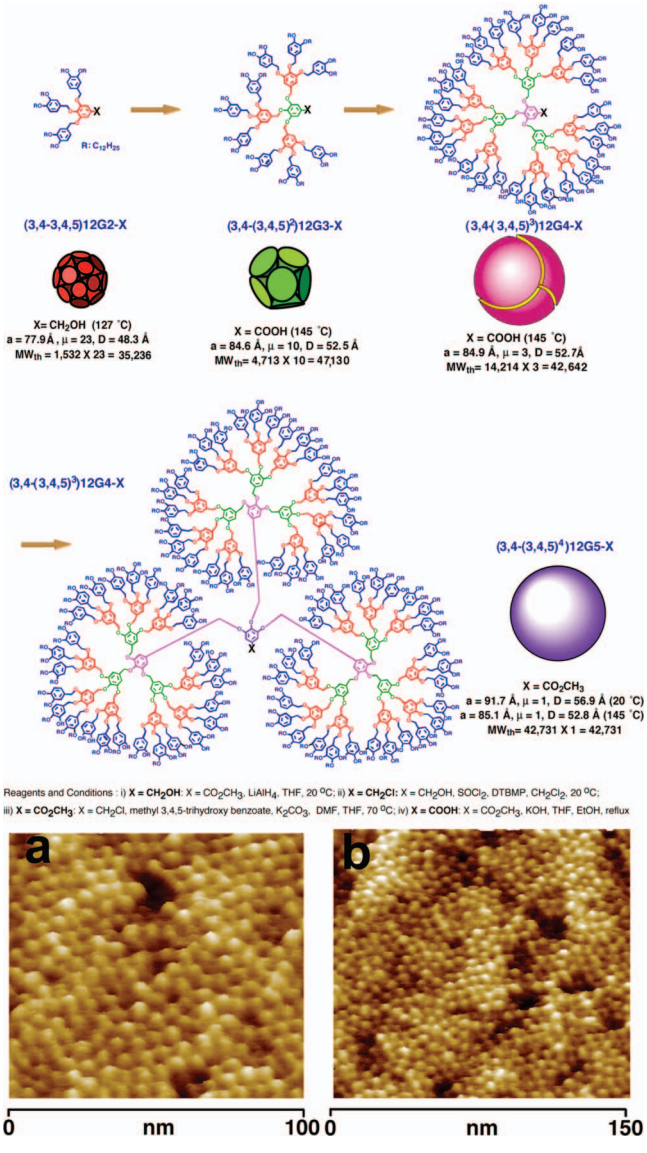

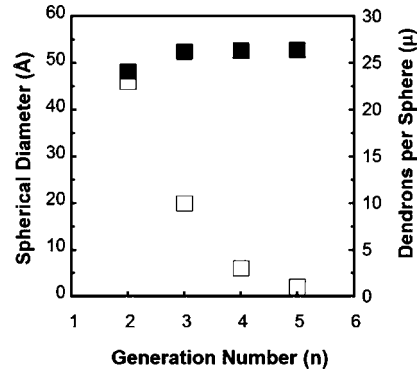

Figure 42. Effect of generation number on spherical diameter (filled squares) and number of Percec-type dendrons per sphere (open squares).[271]

through the use of different metal salts. In addition to structural factors, temperature can also modulate taper angle.[335] Increasing the temperature induces expansion of the molecular taper angle. Rather than increase the size of the self-assembled objects, excess dendrons are most likely excluded from their parent structures and form new ones, assuming that the density is independent of temperature. This process represents a primitive self-replication process and results in diminished object size with increasing temperature or with thermotropic conversion from columns to spheres with increasing temperature.[335]

2.2.4. Generational Library Approach to Discovery

The branching structure and generation number were shown to provide hierarchical control of the self-assembly through manipulation of molecular taper angle. To further elucidate the relationship between molecular and self-assembled structure, libraries of self-assembling Percec-type benzyl ether dendrons were prepared with different branching patterns, generation numbers, and apex functional groups.[266] Typically, libraries are prepared, following a generational approach, wherein a specific G1 periphery dendron (3,4)G1, (3,4,5)12G1, (4-3,4,5)12G1, or (4-3,4)12G1 is iteratively attached to a repeated AB_2 or AB_3 branching unit. What is perhaps most striking about the generational libraries is that, despite the high diversity of connective sequences, a relatively small number of supramolecular structures are

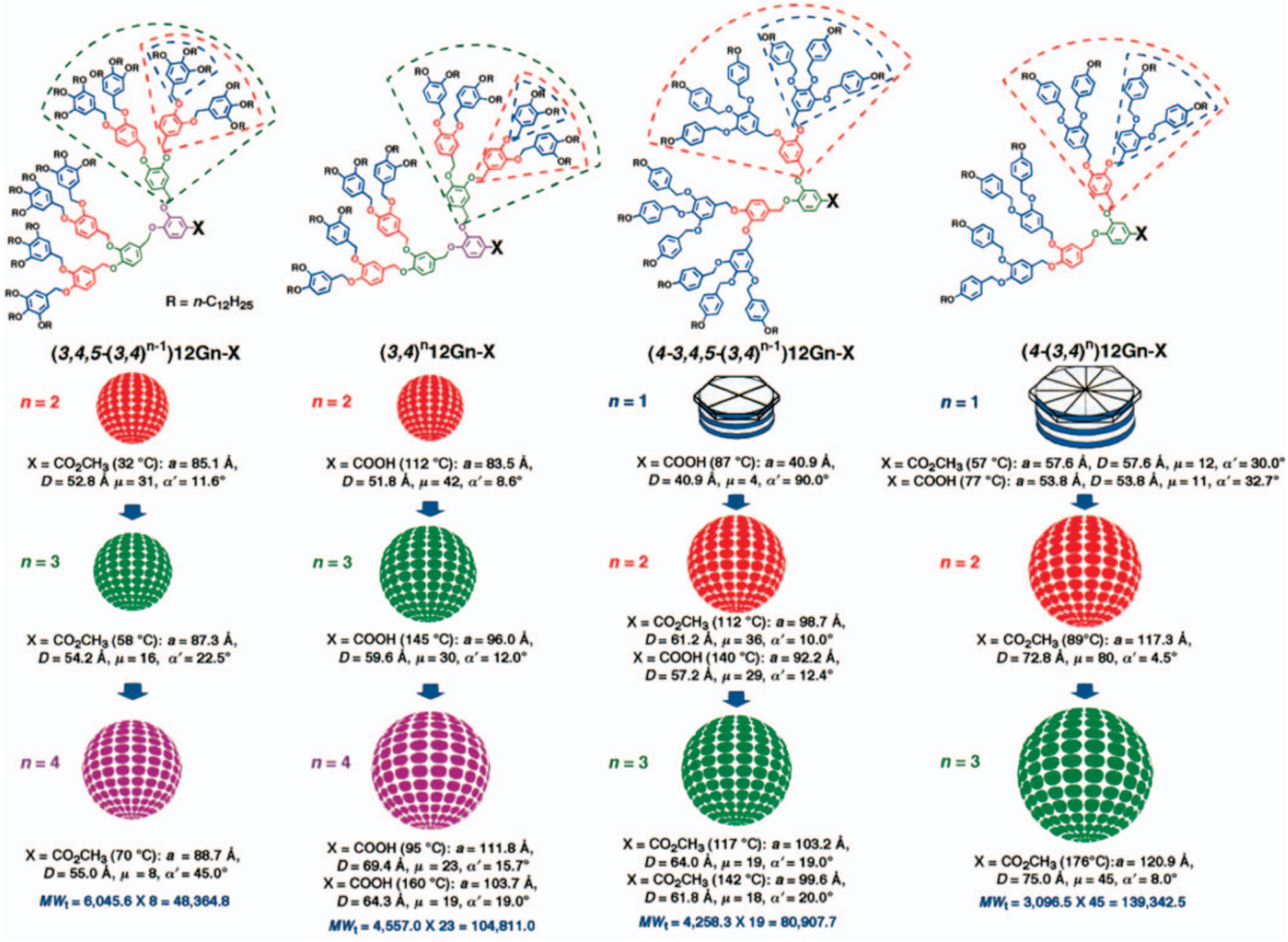

Figure 43. Generational library of dendrons with (3,4) repeating interior branching unit. Self-assembly demonstraties the effect of increased branching and generation number on molecular taper angle. Reprinted with permission from ref 266. Copyright 2001 American Chemical Society.

observed, i.e., columns and spheres. The large difference between the number of available connective sequences (primary structure) and observed 3D structures is in accord with the relationship between the sequence space of proteins and their tertiary structures. Largely, proteins will self-assemble into elongated or globular structures composed of a limited number of secondary structure elements such as α-helices, *β*-sheets, and random coils.[336,337]

It is reiterated in the case of the generational libraries containing a (3,4) interior branching unit that increasing generation number results in an enhanced molecular taper angle, decreasing the number of dendrons in a column stratum or sphere or mediating the transition from columnar to spherical assemblies (Figure 43). With the generational libraries containing a (3,4,5) interior branching unit, it can be seen also that the structure of the periphery branching unit can alter the mechanism of self-assembly (Figure 44). Increased periphery branching favors spherical self-assembly. The use of interior (3,5) branching units strongly predisposes the dendrons to columnar self-assembly and self-organization into Φ_h lattices (Figure 45). Further, it was demonstrated in a large number of examples[181,266,273,274] that self-assembly could be switched between columnar and spherical or globular modes via chemical modification of apex functionality (Figure 46) or temperature variation (Figure 47).

Increasing the generation number of benzyl ether dendrons does not substantially increase the size of the self-assembled object but rather simply reduces the number of dendrons in the column stratum or sphere. Thus, achieving self-assembled dendrimers of larger size requires a different form of molecular design. Hybrid dendrons of the $(AB)_y-AB_n$ were prepared (Figure 48).[338] While in most cases self-assembly of the hybrid dendrons followed similar patterns as traditional Percec-type benzyl ether-dendrons, introduction of AB spacers provided dendrons with larger head-to-tail lengths without increasing α′. This approach provided access to larger self-assembled structures. Further, some small α′ dendrons revealed a new modular smectic phase with additional lateral periodicity, S_{mod} (Figure 49). The self-assembly of some $(AB)_y-AB_n$ into rectangular and oblique lattices in LB films was studied by grazing incidence X-ray diffraction.[339]

In addition to libraries of hybrid $(AB)_y-AB_n$ dendrons, the generality of the self-assembly process of Percec-type dendrons was explored through synthesis of libraries of dendrons constructed from building blocks other than benzyl ethers. A series of libraries of phenylpropyl-type dendrons were prepared, wherein the linker between aromatic branches was extended by two carbon units.[273] Unlike the standard benzyl-ether Percec-type dendrons, phenylpropyl building blocks (Scheme 17, **5** or **12a**,**b**,**c**) are not commercially available. The AB building block was prepared via Knoevenagel addition of malonic acid to 4-hydroxybenzaldehyde followed by hydrogenation over Pd/C and methyl esterifi-

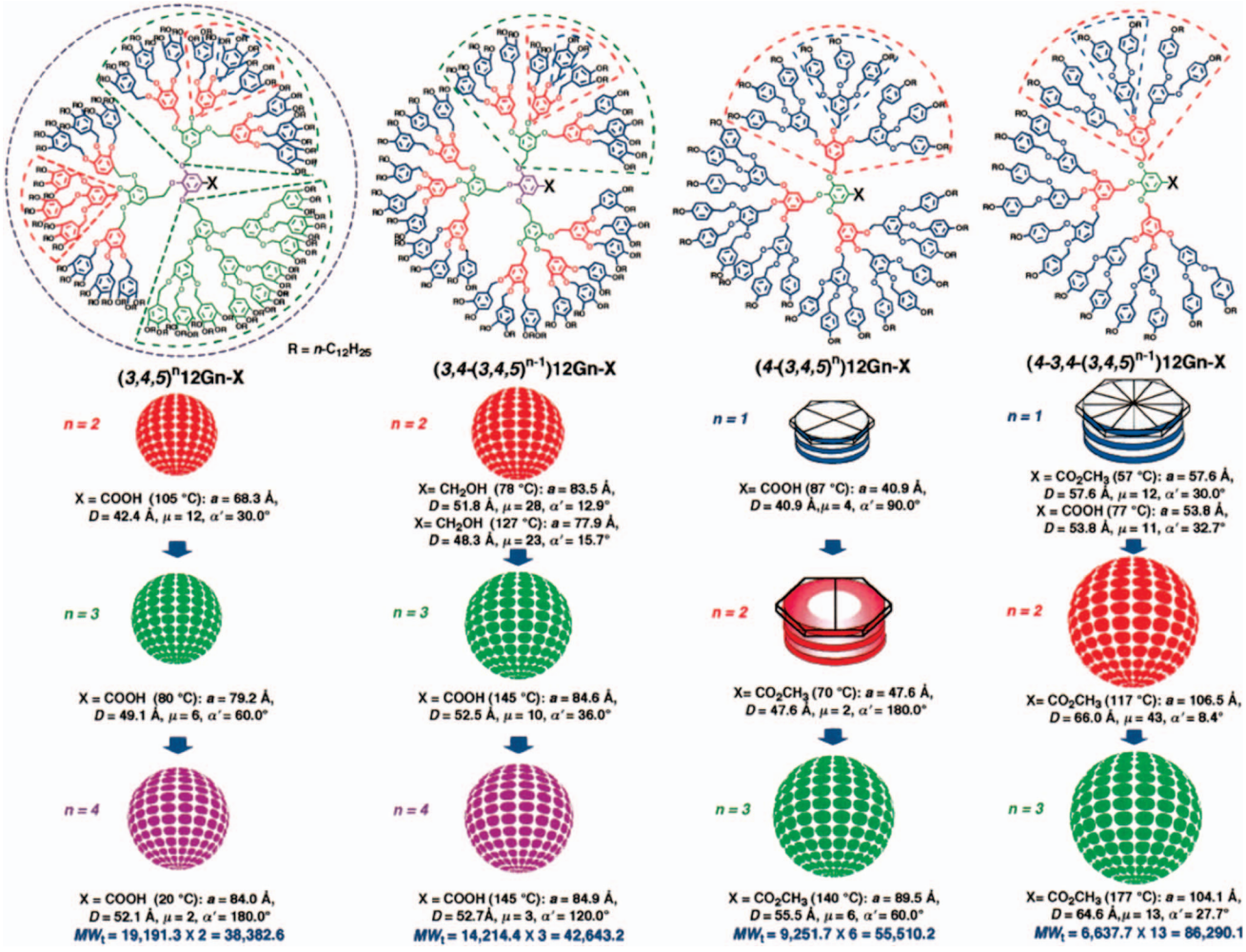

Figure 44. Generational library of dendrons with (3,4,5) repeating interior branching unit, which demonstrates the effect of periphery branching on molecular taper angle and the mechanism of self-assembly. Reprinted with permission from ref 266. Copyright 2001 American Chemical Society.

cation (Scheme 17). AB_n building blocks were prepared through a similar process. 3,4-Dihydroxy-, 3,5-dihydroxy, and 3,4,5-trihydroxybenzoic methyl ester, protected with a benzyl ether, were sequentially reduced to the alcohol and oxidized to the aldehyde, subjected to Knoevenagel expansion with malonic acid, hydrogenated over Pd/C, and etherified (Scheme 17). Phenyl propyl dendron synthesis also requires slight modification from the benzyl ether series (Scheme 18). Tail alkylation and reduction steps were identical to the benzyl ether series. However, in the benzyl ether series, the benzyl alcohol was converted to a benzyl chloride for subsequent alkylation, but aliphatic chlorides are not sufficiently reactive. Therefore, the branched phenylpropanol was converted to the corresponding bromide with CBr_4/PPh_3.

With Percec-type benzyl ether dendrons, it was thought that trans/gauche conformational restriction were required for self-assembly. Retrostructural analysis of the phenylpropyl ether demonstrates that, even with the added flexibility of the propyl linker, self-assembly into all of the previously encountered lattices was observed, including the *Tet*, 12-fold QLC lattice, and hollow-columnar lattices (Figures 50−52). It is important to note that the all-*trans* propyl ether can adopt the same extended conformation as the *trans*-benzyl ether. The effect of odd vs even or longer alkyl linkers on self-assembly will be a topic of future investigation. Further, the phenylpropyl dendrons are more stable under acidic and basic conditions than benzyl ether dendrons and exhibit faster dynamic self-assembly into larger lattices with higher degree of order, but lower T_{iso}. Because of the expansion of the building block, phenylpropyl ether dendrons have a smaller projection of solid angle α' and self-assemble into larger structures than the corresponding benzyl ether dendrons of similar generation number and branching structure.

Other efforts have been made to probe the effect of larger aromatic domains in self-assembly. In 1995 Percec demonstrated the self-assembly of the first nonspherical dendrons and dendrimers into S and N phases.[221,222] These willow-like dendrons and dendrimers were designed according to principles developed from the corresponding hyperbranched polymers[215,217,218] and subsequently prepared through a convergent approach (Schemes 19 and 20). A branched terphenyl was bisalkylated with 1-bromo-10-undecane in *ortho*-dichlorobenzene (*o*-DCB) under phase transfer conditions. The aliphatic alcohol apex group was brominated with CBr_4/PPh_3. This dendritic bromide could then be bisalkylated onto another branched terphenyl and the process could be iterated (Scheme 19). Alkylation onto a trifunctional core provided access to analogous dendrimers (Scheme 20). Self-assembly into S and N phases was mediated by dynamic conformational equilibrium of gauche-dendrons into antidendrons

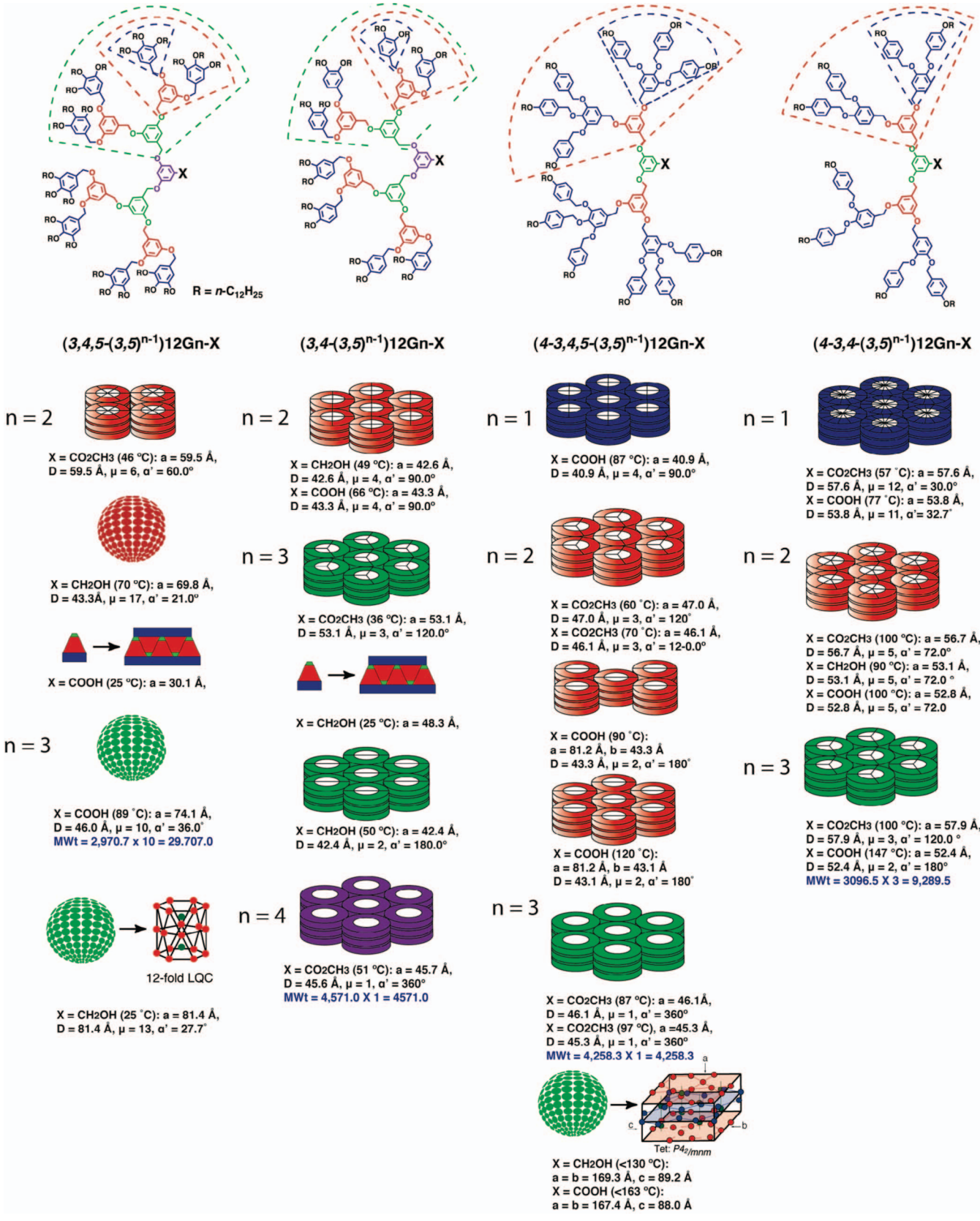

Figure 45. Generational library of dendrons with (3,5) repeating interior unit, which favors columnar self-assembly. Unless otherwise shown, all spherical supramolecular dendrimers self-organinze in a *Cub* lattice. Adapted with permission from ref 266. Copyright 2001 American Chemical Society.

(Figure 53). "Willowlike" dendrons as well as dendrimers self-assemble into the same structures, regardless of their generation number. Flexibility of the dendrons to adopt the anti-conformation allows for interdigitation of the alkyl chains and the formation of elongated structures. In G1−G4 willowlike dendrimers, it was shown that the N−I transition

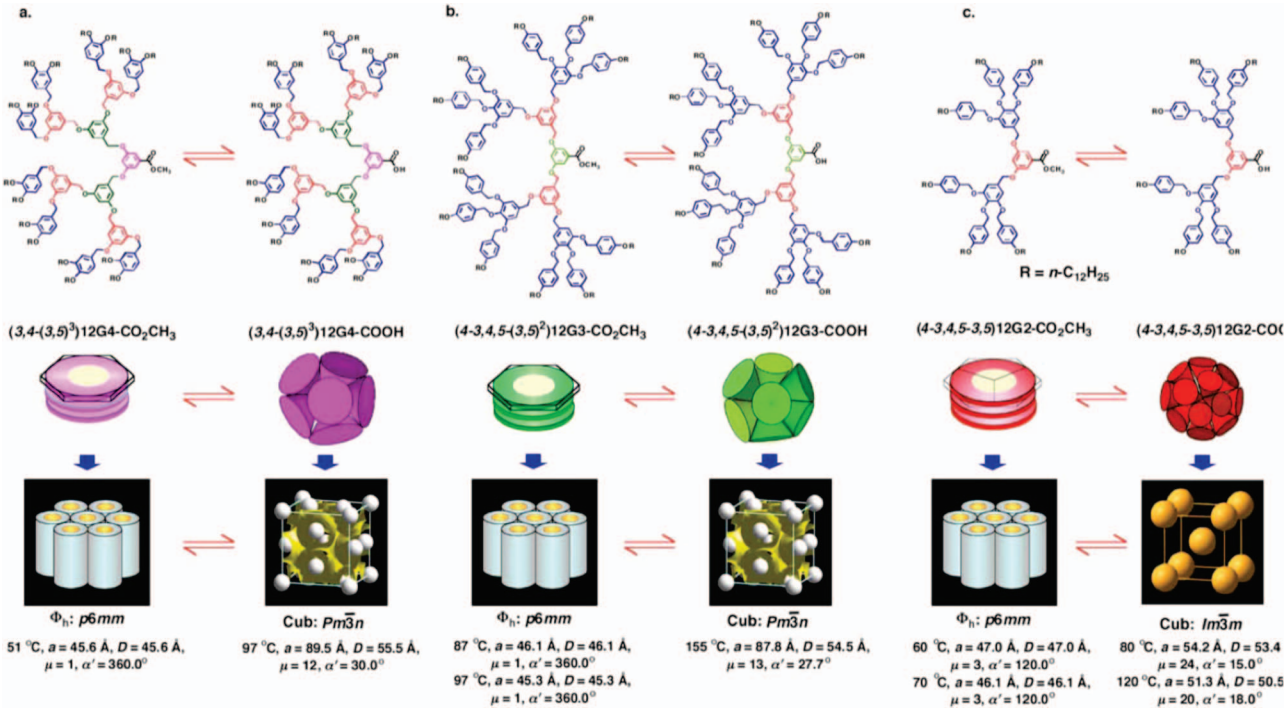

Figure 46. Switching of columnar and spherical self-assembly via chemical modification of apex functionality. Reprinted with permission from ref 266. Copyright 2001 American Chemical Society.

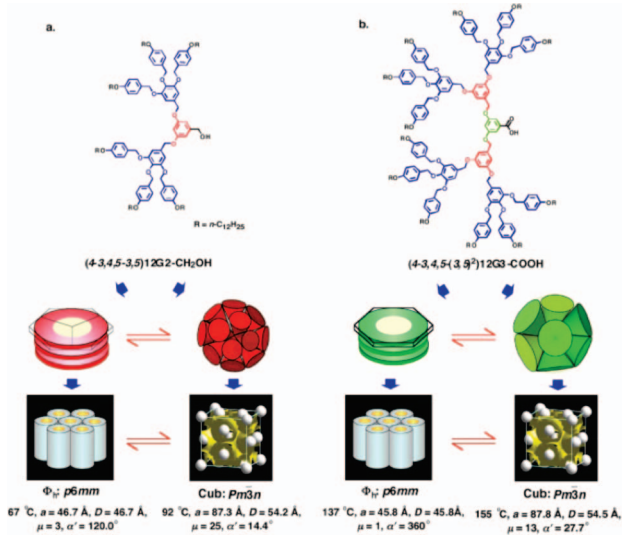

Figure 47. Switching of columnar and spherical self-assembly via chemical and temperature change. Reprinted with permission from ref 266. Copyright 2001 American Chemical Society.

was qualitatively similar to that of low molecular weight liquid crystals.[340] The similarities between low molecular weight LCs and dendrons extend into the self-organized phase.

The bisdendronized monomeric precursor to poly(norbornene)s described in section 3.2.4 also exhibits interesting self-assembly behavior (Figure 54).[341] N phases as described for the willowlike monomers were observed at higher temperatures. However, at low temperature, a hexatic B phase was formed (S_h^B). Ring-opening metathesis polymerization (ROMP) of the bisdendronized norbornene or analogous 7-oxanorbornene provided polymers with DP = 5−10 that self-organize into an unconventional S_C phase (Figure 55).[342] It is important to note that, in this case, self-organizaton results in a structure where the aromatic and aliphatic portions are not segregated, and thus it is concluded that microphase segregation is not guaranteed in dendron-jacketed polymers.

In 1998, it was demonstrated that dendritic acids with polyaromatic groups at the periphery, namely, (4Nf-3,4,5)*n*G1−COOH and (4Bp-3,4,5)12G1−COOH, self-assemble into columns that self-organize into Φ_h lattices (Figure 56).[343]

On the basis of earlier results with terphenyl, naphthyl, and biphenyl-based dendrons, libraries of Percec-type dendrons built from biphenyl-4-methyl ether building blocks were synthesized (Figures 57 and 58).[274] AB_n building blocks were prepared through two Suzuki coupling approaches (Scheme 21). 3,4-Methoxyphenyl-1-boronic acid was cross-coupled with methyl/ethyl 4-bromobenzoate using $Pd(PPh_3)_4$ as catalyst. Selective deprotection of the methyl ethers was achieved with BBr_3. 3,5-Dimethoxy-1-chlorobenzene and 3,4,5-trimethoxy-1-bromobenzene were cross-coupled with toluene boronic acid using $NiCl_2$(dppe)/PPh_3 as catalyst.[344] Benzylic oxidation with $KMnO_4$, followed by methyl esterification and selective deprotection of the methyl ethers with BBr_3, yielded the corresponding AB_2 and AB_3 building blocks.

Similar to phenylpropyl dendrons, the expansion of the aromatic portion of the building block resulted in dendrons with smaller projections of solid angle α′, resulting in larger self-assembled structures than the corresponding benzyl ether dendrons of similar structure and generation number. As with the phenylpropyl ether series, the biphenyl-4 methyl ether dendrons provided evidence of hollow helical columnar architectures without the use of a dipeptide apex group (section 2.2.5). Specifically, (4Bp-3,4Bp-3,5Bp)12G2−CO_2CH_3/CH_2OH, the biphenyl analogue of prototypical dendron used for dendritic dipeptide porous columns, exhibits the large pore, 12−13 Å. Unfortunately, the limited solubility and

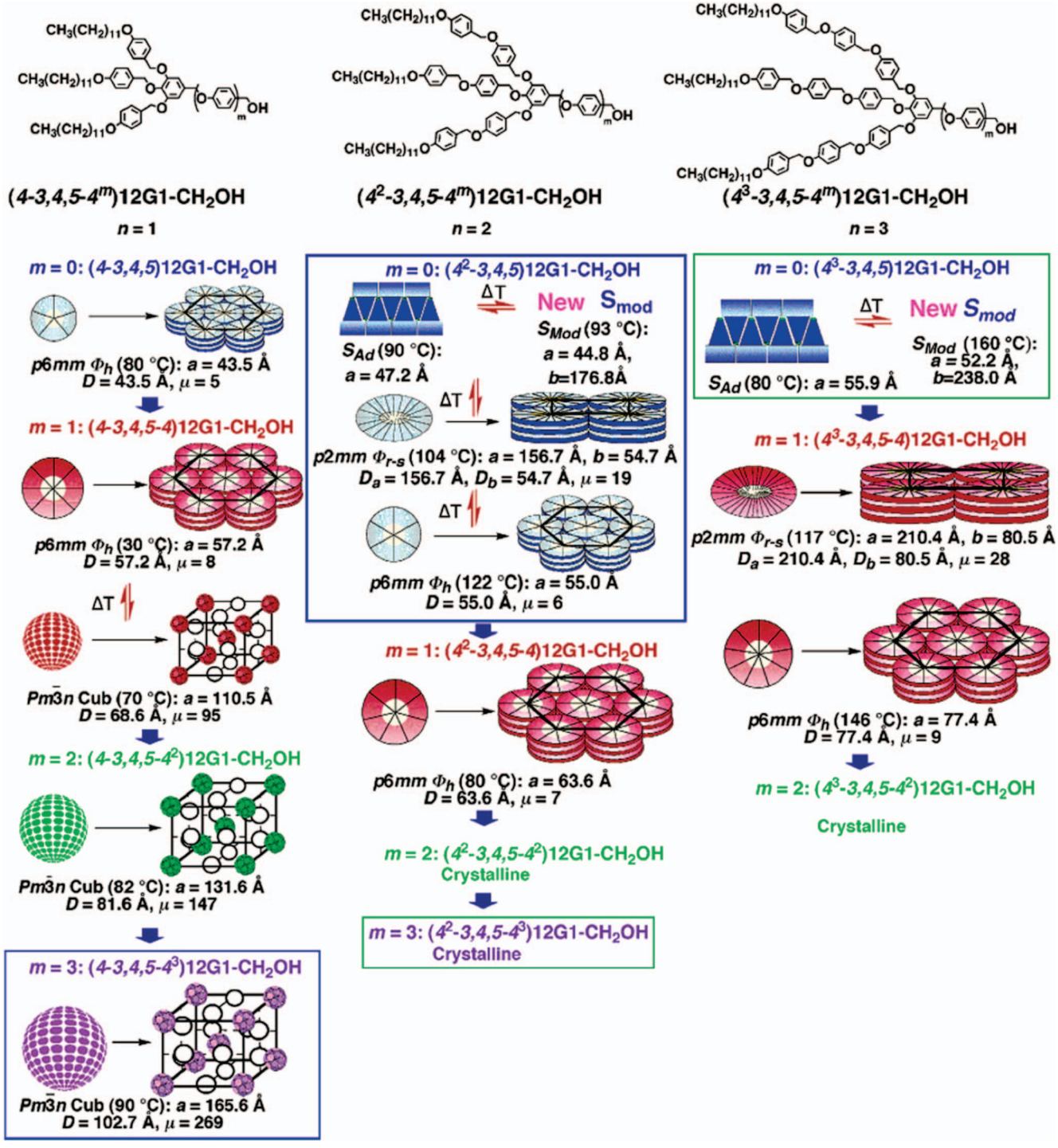

Figure 48. Examples of $(AB)_y-AB_n$ hybrid dendrons exhibiting new S_{mod} phase. Reprinted with permission from ref 338. Copyright 2004 American Chemical Society.

extremely high T_{iso} of biphenyl-4 methyl ether dendrons limited the synthesis of high-generation libraries.

While the biphenyl-based dendrons were limited due to poor solubility, their structural benefits could be harnessed by producing constitutional hybrid dendrons. A library of (4-3,4-3,5)12G2CO_2CH_3 were prepared wherein the benzyl ethers were systematically replaced with biphenyl-4 methyl units and/or additional AB benzyl spacers were introduced.[345] In all cases, a Φ_h, porous Φ_h, or Φ_r lattice was observed via XRD (Figure 59). In particular (4-3,4-4-3,5Bp)12G1−X was shown to be a versatile structure for porous Φ_h self-organization. Regardless of the apex group [X = CO_2Me, CH_2OH, COOK, COOH, $CO_2CH_2CH_2OCH_3$, $CONH_2$, $CONHCH_3$, (*R*)-$CONHCH(CH_3)C_2H_5$, (*S*)-$CONHCH(CH_3)C_2H_5$, or a blend of all apex groups], porous Φ_h was observed and demonstrated that D_{pore} could be tuned by both dendron structure and apex group (Figure 60, left). Further, the introduction of a chiral amide apex-group selected the sense of the helical column and allowed for fiber XRD analysis of the helical porous columns (Figure 60, right). Solution self-assembly of (*R*)-(4-3,4-4-3,5Bp)12G2−$CO_2NHCH(CH_3)C_2H_5$ into helical columns was confirmed by CD/UV−vis in cyclohexanes. Because of the resemblance of cyclohexanes to the interior of lipid bilayers, (4-3,4-4-3,5)12G2−CO_2CH_3 was expected to form cylindrical pores via coassembly with

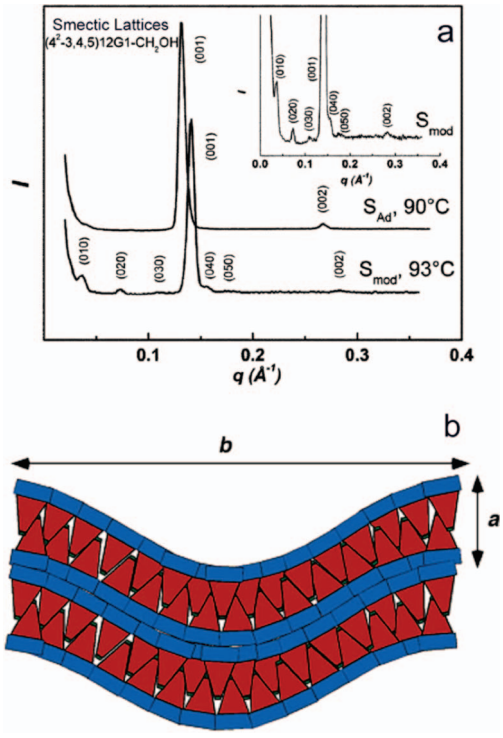

Figure 49. XRD diffractograms comparing typical S with S_{mod} (a) phases and a model of the S_{mod} phase (b). Reprinted with permission from ref 338. Copyright 2004 American Chemical Society.

phospholipids. Preliminary results demonstrated the 1:7 coassembly with L-phophatidylcholine to form porous membranes.

In all previous investigations, self-assembling dendrons were constructed from a combination of AB, AB_2, and AB_3 building blocks. More highly branched dendrons based on AB_4 and AB_5 building blocks have been prepared, demonstrating the robustness of the self-assembly process for Percec-type dendrons.[275] AB_4 and AB_5 building blocks were prepared in a similar fashion by expanding on a previously elaborated synthetic strategy (Scheme 22).[215,217,218] 2-(4-Chlorophenyl)-1-(3,4-dimethoxyphenyl)ethanone was alkylated with 3,4-dimethoxybenzyl bromide or 3,4,5-trimethoxybenzyl chloride using NaOH as a base in TBAH/toluene phase-transfer catalyzed conditions. Reduction of the ketone to methylenic carbon was accomplished via $LiAlH_4/AlCl_3$. The resulting branched aryl chlorides were enlarged via Suzuki coupling 4-methoxycarbonylphenyl-1-boronic acid. For the AB_4 building block, catalysis with $NiCl_2$(dppe)/PPh_3[344] was sufficient; however, for the AB_5 building block, Pd/cyclohexyl JohnPhos (2-(dicyclohexylphosphino)biphenyl)[346] conditions were necessary. Subsequent deprotection with BBr_3 and re-esterification yielded the AB_4 and AB_5 building blocks. Dendron synthesis was performed in a similar fashion to standard benzyl ether Percec-type dendrons. Libraries of dendrons with AB_4 (Figure 61) and AB_5 (Figure 62) apical branching units were prepared. An array of previously encountered flat columnar, pine-tree columnar, pyramidal columnar, and spherical objects were formed that packed into Φ_h, $\Phi_{r\text{-}c}$, $\Phi_{r\text{-}s}$, and *Cub* lattices. The AB_4 and AB_5 building blocks provided access to intriguing new conformations and supramolecular structures. (4-3,4,5-AB_4)12G3$-CO_2CH_3$ was shown to self-assemble via an unprecedented back-folded taper-dendron mechanism into a 7_2 helical column (Figure 63). Here, one (4-3,4,5) branch tucks underneath the other (4-3,4,5) branch. These dendritic sandwiches stack side-by-side to form stratum of twice the thickness of a typical columnar layer. (4-3,4-AB_5)12G3$-CO_2CH_3$ and (4-3,4,5-AB5)12G_3-CO_2Me exhibit crown-conformations that self-assemble into helical pyramidal columns (Figure 62). (4-3,4,5-AB_5)12G3−X (X = CH_2OH, CH_2OAc) was also shown to self-assemble into a 5_1 helical column. In the previous section, it was demonstrated that increasing the generation number mediates a transition from columnar to spherical self-assembly due to steric-restrictions on the taper shape. Never did increasing the generation number mediate a transition from spherical to columnar self-assembly. For the first time, with certain examples of AB_4 and AB_5 dendrons, this reverse order of self-assembly was observed, with spherical structures at lower generation and columnar self-assembly at higher generation, an event that marked the elucidation of a new mechanism of self-assembly. Figures 61−63, show the

Scheme 17. Synthesis of Phenyl Propyl Building Blocks (Reprinted with Permission from Ref 273; Copyright 2006 American Chemical Society)

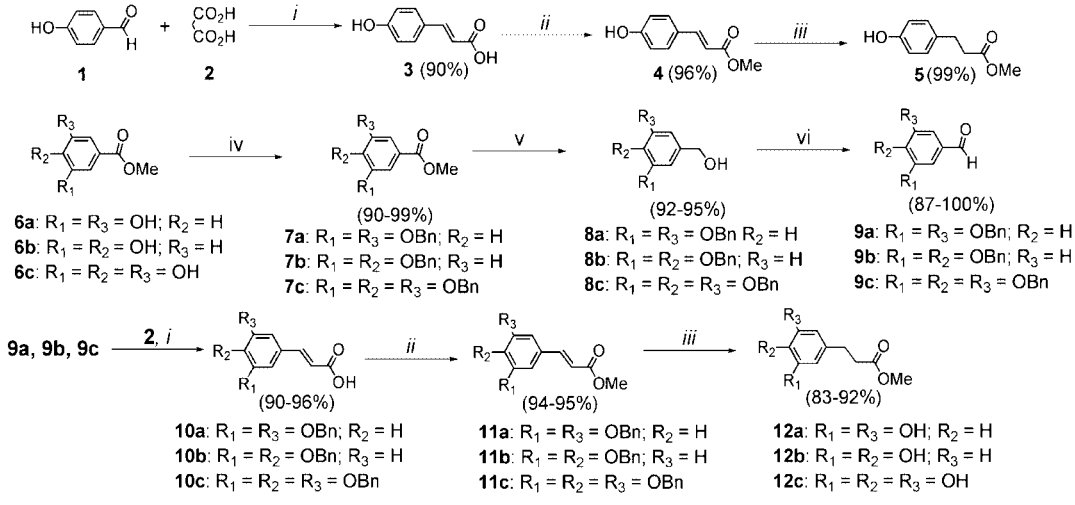

Reagents and conditions: (*i*) morpholine, AcOH, reflux; (*ii*) H_2SO_4 cat./MeOH, reflux; (*iii*) H_2, Pd/C, EtOH; (*iv*) BnCl, DMF, 80 °C; (*v*) $LiAlH_4$, THF; (*vi*) PCC, CH_2Cl_2, 1h.

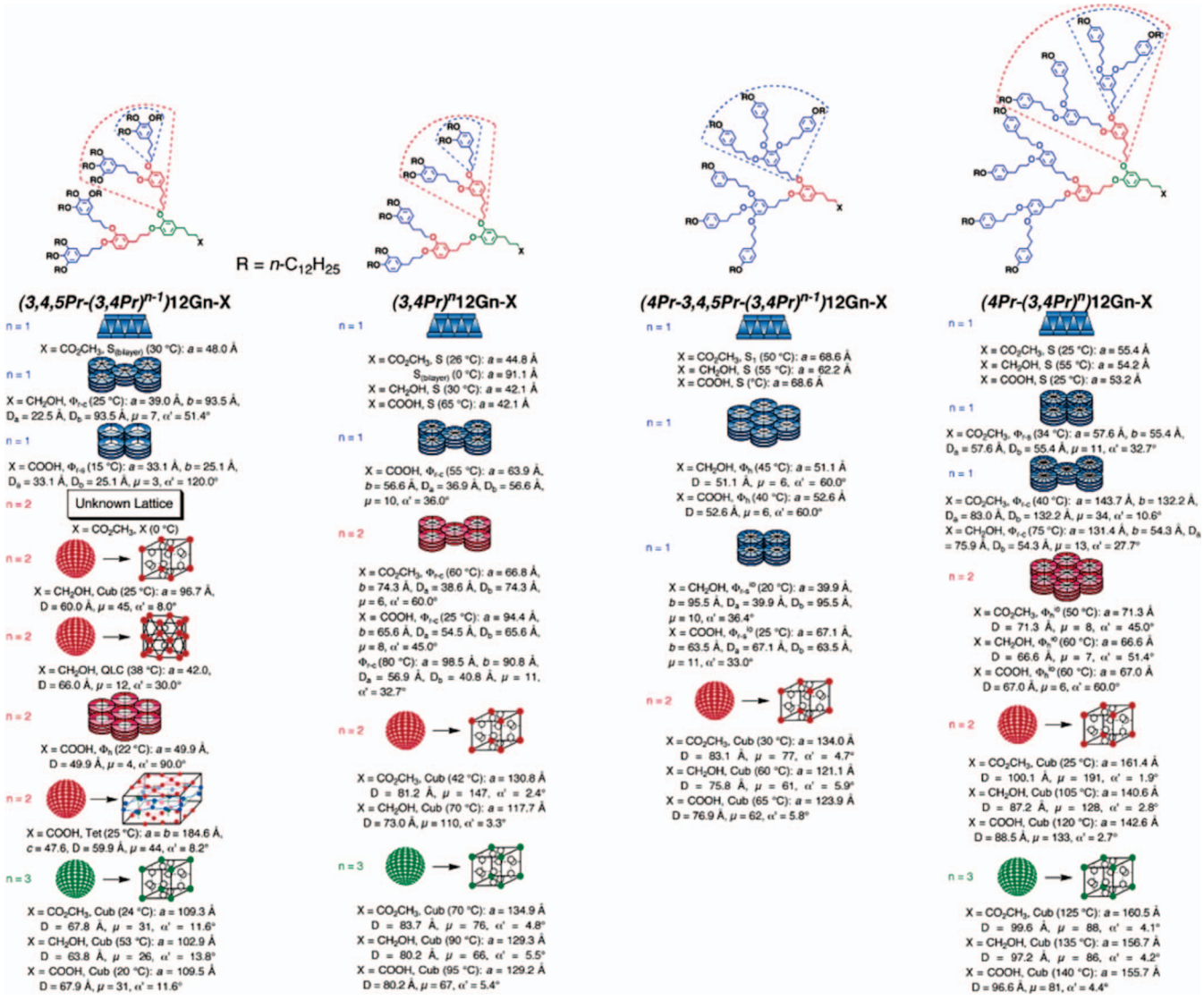

Figure 50. 3,4-Branching library of phenylpropyl ether dendrons exhibiting the full range of self-organized structures including *Cub*, *Tet*, QLC, S, Φ_h, $\Phi_{r\text{-}c}$, and $\Phi_{r\text{-}s}$. Reprinted with permission from ref 273. Copyright 2006 American Chemical Society.

Scheme 18. Phenylpropyl Dendron Synthesis (Reprinted with Permission from Ref 273; Copyright 2006 American Chemical Society)

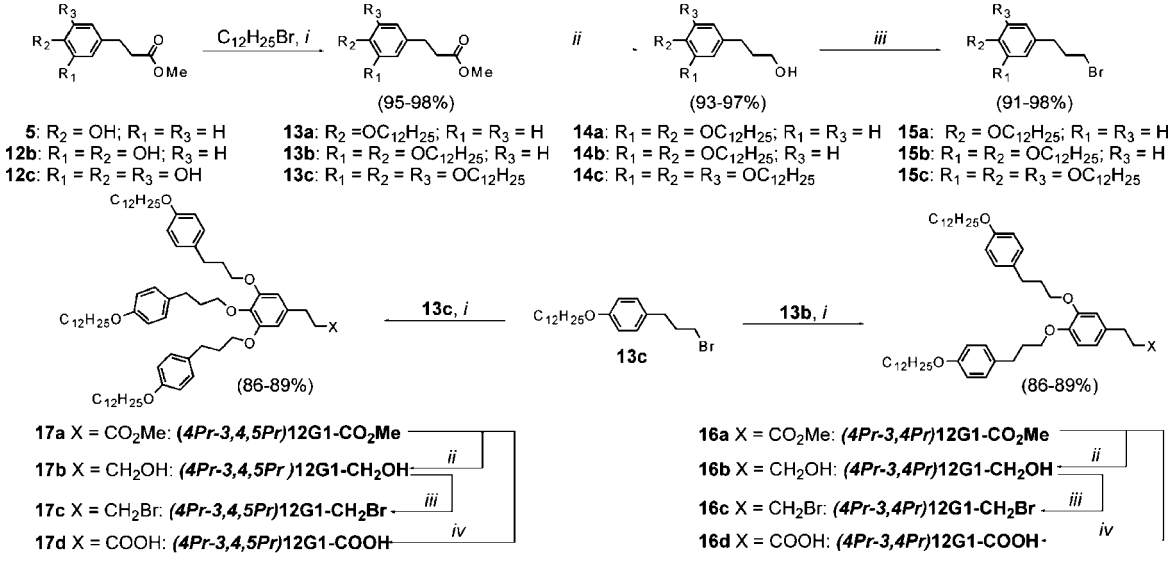

Reagents and conditions: (*i*) K_2CO_3, DMF, 80°C (85-93%); (*ii*) $LiAlH_4$, THF (92-96%); (*iii*) CBr_4, PPh_3, CH_2Cl_2 (90-95%); (*iv*) 1. KOH, THF/EtOH; 2. H_2SO_4 1M (90-95%).

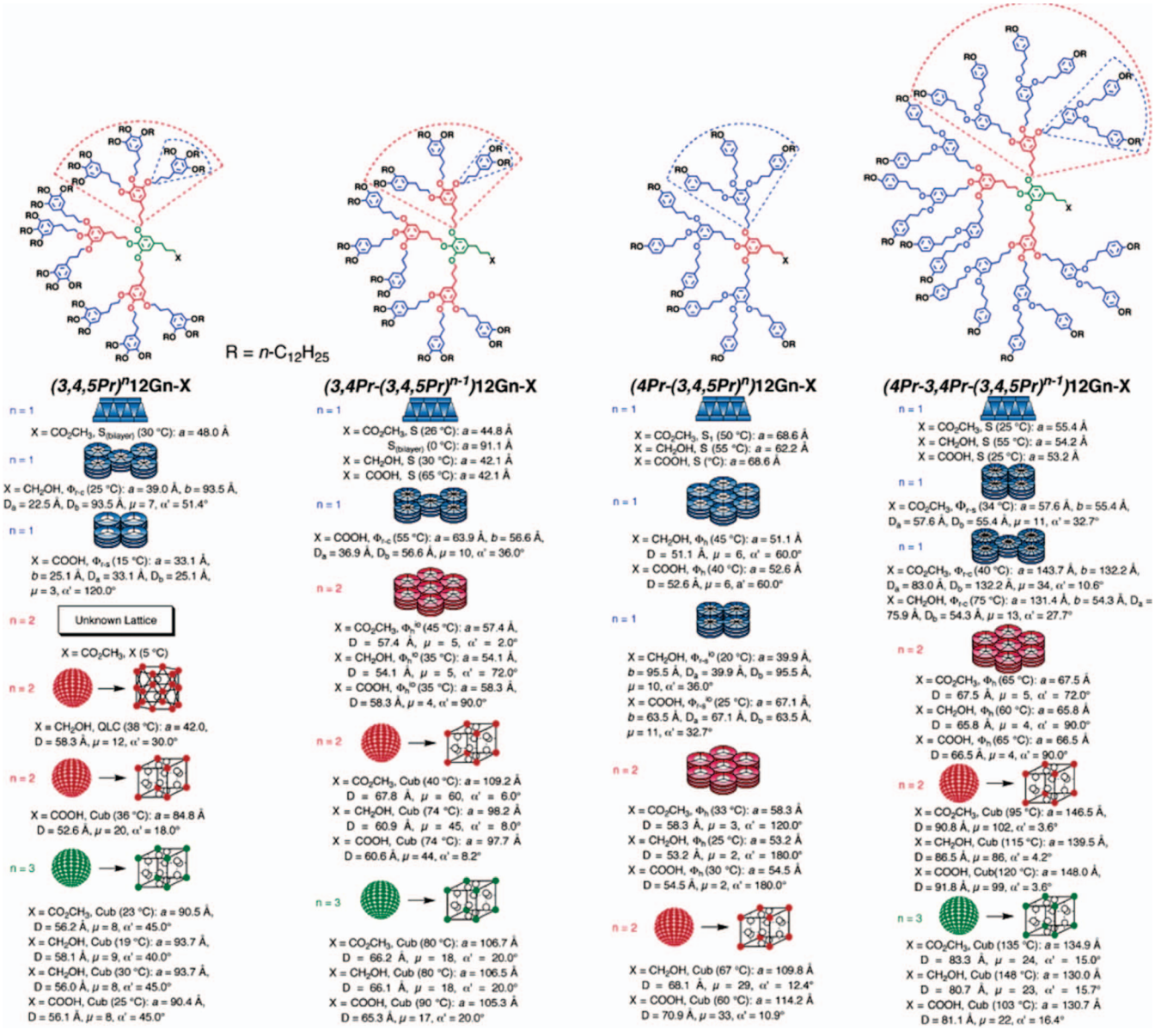

Figure 51. 3,4,5-Branching library phenylpropyl ether dendrons. Reprinted with permission from ref 273. Copyright 2006 American Chemical Society.

discovery of self-assembly of dendritic crowns and of back-folded dendrons into helical pyramidal columns. In addition, (4-AB_4)12G_2−CH_2OH and (4-3,4-AB_4)12G3−X (X = CH_2OH, CO_2Me) self-assembled into hollow spheres that self-organize into a *Cub* lattice (Figure 64), which has been demonstrated to encapsulate small guest molecules such as LiOTf. Previously, encapsulation by spherical self-assembling Percec-type dendrons had only been demonstrated via host−guest interactions with a U-shaped "molecular clip" receptor group at the apex of $(3,4,5)^2$12G2.[347]

2.2.5. Helical Porous Columnar and Spherical Self-Assembly via the Dipeptides from the Apex of Dendritic Dipeptides

(4-3,4-3,5)12G2 was previously shown to be predisposed to columnar self-assembly (Figure 45).[266] In order to test the effect of chirality transfer (allosteric regulation) from the apex to the dendron, Boc-L-Tyr-L-Ala-OMe and Boc-D-Tyr-D-Ala-OMe were attached to (4-3,4-3,5)12G1−CH_2OH via Mitsunobu coupling (Scheme 23).[171,312] NMR and circular dichroism (CD)/UV−vis experiments confirmed self-assembly into helical columnar architectures (Figure 65) in solvophobic solvents that preferentially solvate the aliphatic tails (d_6-cyclohexane and cyclohexane, respectively). Remarkably, XRD in combination with TEM and STM indicated the formation of hollow helical columnar architectures (Figures 17c,d, 66, and 68). Helical porous self-assembly into columns that self-organize into a Φ_h is proposed to be stabilized by a H-bonding network and helical involving the parallel alignment of the dipeptides with the columnar axis (Figure 66). This model is similar to a β-barrel. These structures functioned as aquaporin mimic, mediating water transport via a Grotthuss-type mechanism[348,349] without eliminating H^+ transport across artificial cell membranes such as liposomes[350] or polymersomes[351] (Figure 67). However, these columns do not

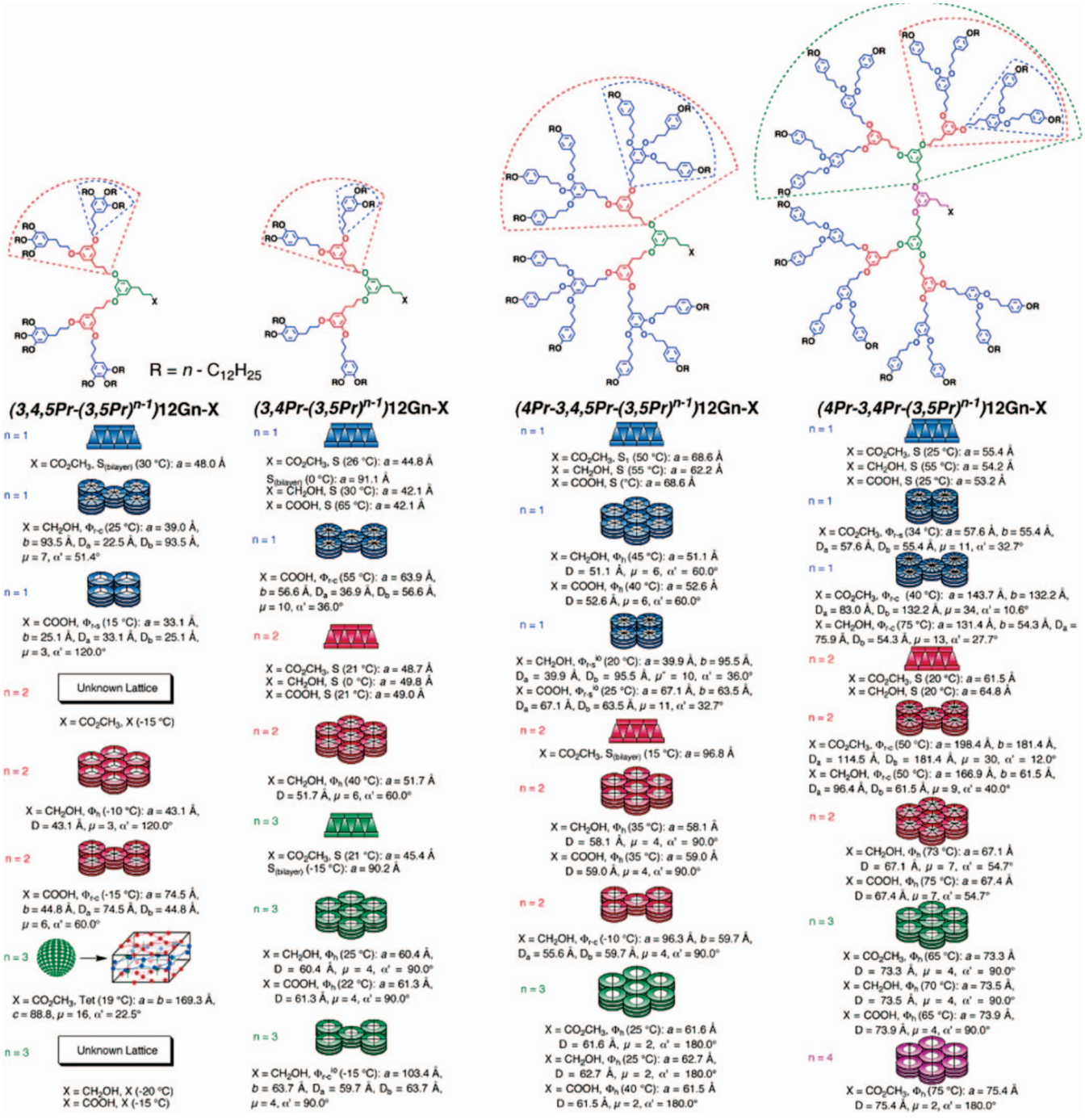

Figure 52. 3,5-Constitutional isomeric branching library of phenylpropyl ether dendrons. Reprinted with permission from ref 273. Copyright 2006 American Chemical Society.

allow transport of Na^+, Li^+, and Cl^- ions. The transport of water across giant vesicular membranes containing dendritic-dipeptide channels was demonstrated through microscopy experiments in hypertonic and hypotonic solutions (Figure 69). Vesicles containing dendritic dipeptides exhibited expansion of the vesicle in hypertonic solution and contraction in hypertonic solution, relative to the vesicles containing no channel, indicating that water is able to permeate the membrane only in the presence of the dendritic dipeptides, allowing for pressure regulation.[350]

It is useful to compare the self-assembly of the parent (4-3,4-3,5)12G1−OH with the corresponding dendritic dipeptide (4-3,4-3,5)12G2−CH_2−Boc-L-Tyr-L-Ala-OMe (Table 5).[171] The parent dendron self-assembles into a supramolecular column with a columnar diameter of 52.6 Å and a negligible pore of <3 Å. Each stratum is composed of six dendrons with a projection of solid angle $\alpha' = 60°$. The supramolecular columns self-organize in a Φ_h lattice. The dendritic dipeptide self-assembles into porous helical supramolecular columns with diameters of 77.1 Å and pore diameters of 13.3 Å. Each column stratum is composed of approximately 11.6 dendrons with a projection of solid angle $\alpha' = 31.0°$. The dendritic dipeptide enhances the overall column diameter thus supporting the stabilization of the pore

Scheme 19. Synthesis of Willowlike Dendrons[221]

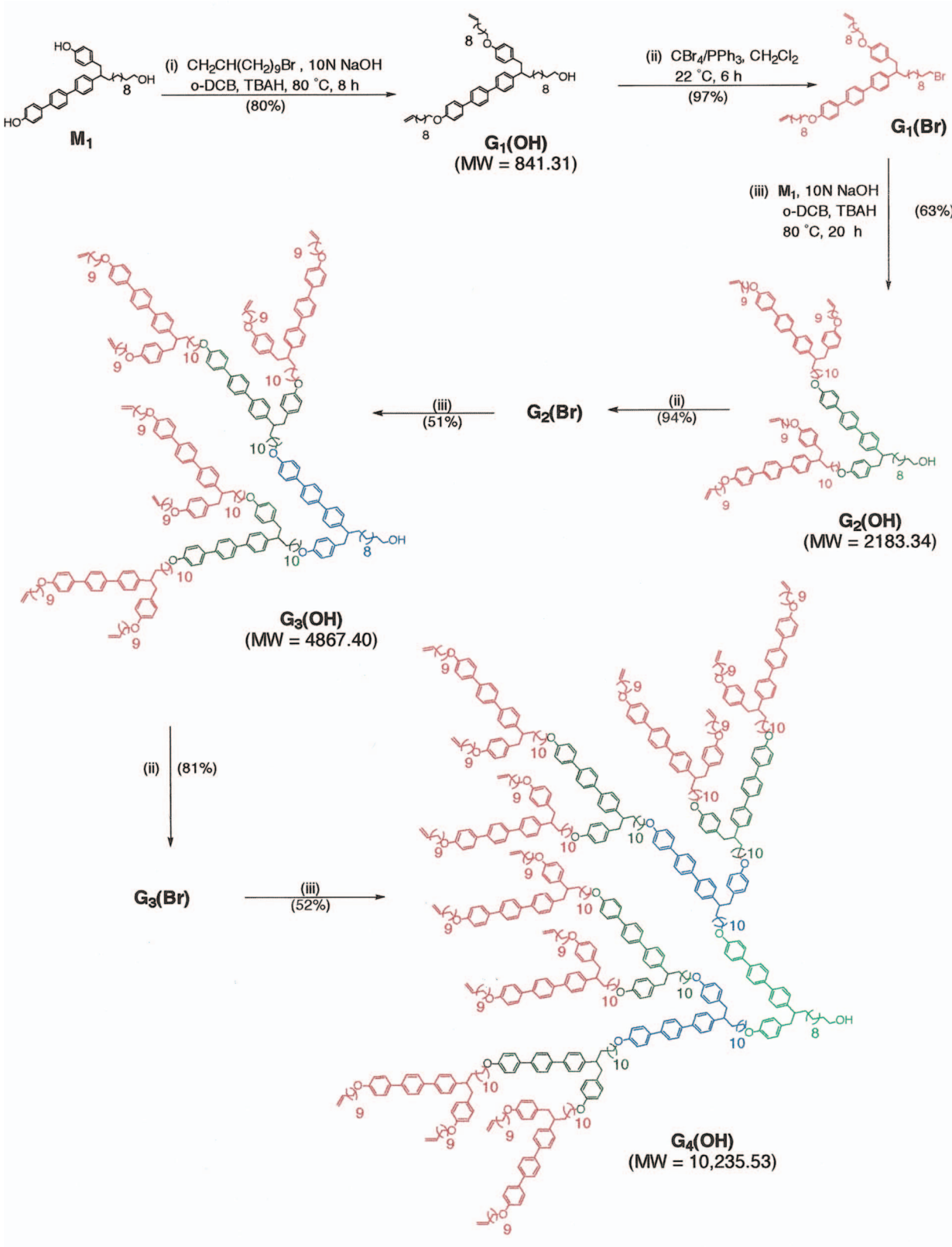

via H-bonding but also by decreasing the molecular taper angle of the dendron, resulting in a lower projection of solid angle and more dendrons per stratum. Like the parent dendritic alcohol, the dendritic dipeptide self-organizes into a Φ_h lattice. For the dendritic dipeptide, it was observed that periphery aliphatic tail length increases the diameter of the column, while it decreases the size of the pore from 15.8 Å at $n = 6-11.7$ Å at $n = 16$. Interestingly, by decreasing the tail length in the parent dendritic alcohol from $n = 16$ to $n = 1$, the pore-size increases from <3 to 6.8 Å. Thus, while the dipeptide does seem to support and enhance pore formation through, it is not a necessary condition.

Scheme 20. Synthesis of Willowlike Dendrimers

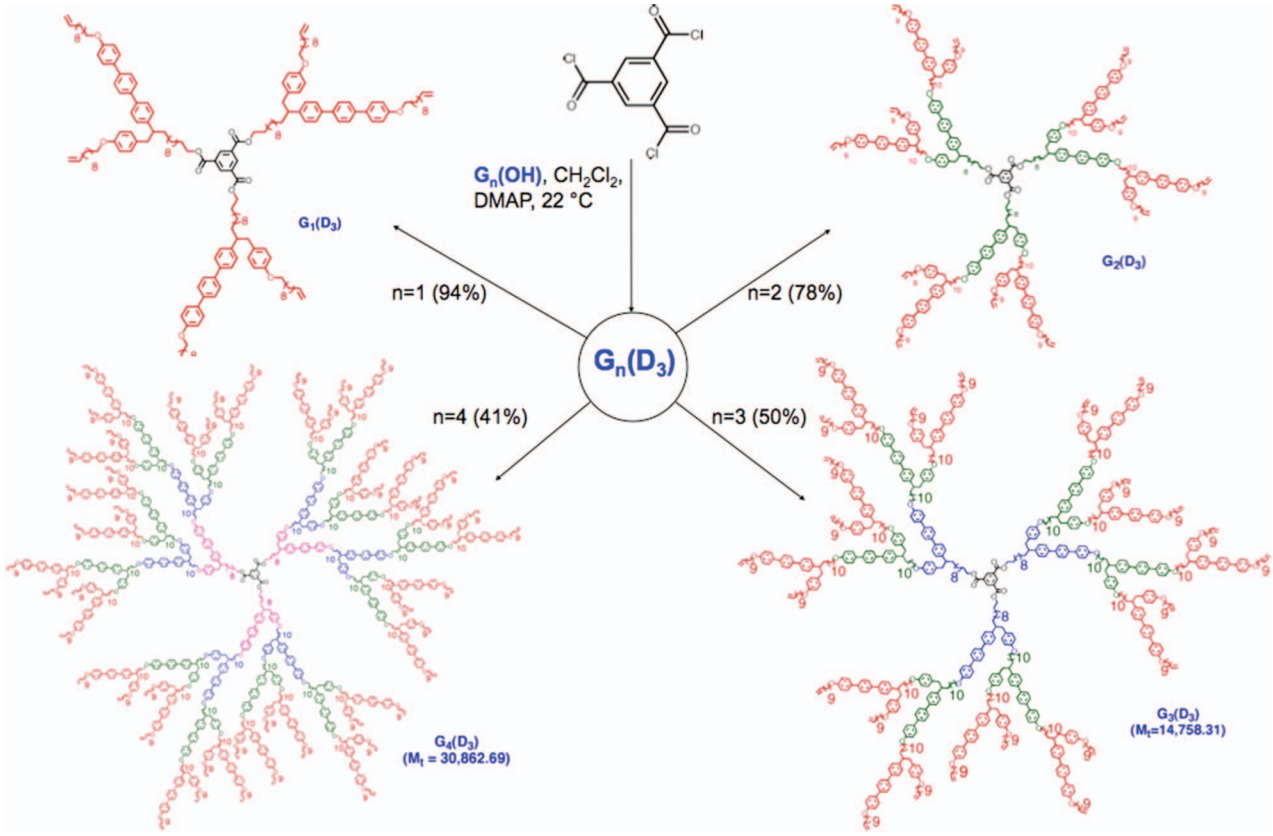

The self-assembly of dendronized dipeptides into helical porous columns can be allosterically programmed by the protecting group on the dipeptide N-terminus (Figure 70).[352] Decreasing the size of the protecting group from X = Boc to X = Moc to X = Ac results in a continual decrease in the H-bond length of the interior network, resulting in enhanced thermal stability of the columnar phase. However, with the decrease in the size of group from the apex comes an increase in the molecular taper angle and a decrease in column size, number of dendrons per stratum, μ, and D_{pore}. Further, in the case of X = Moc, Ac, helical internal order is observed via XRD.

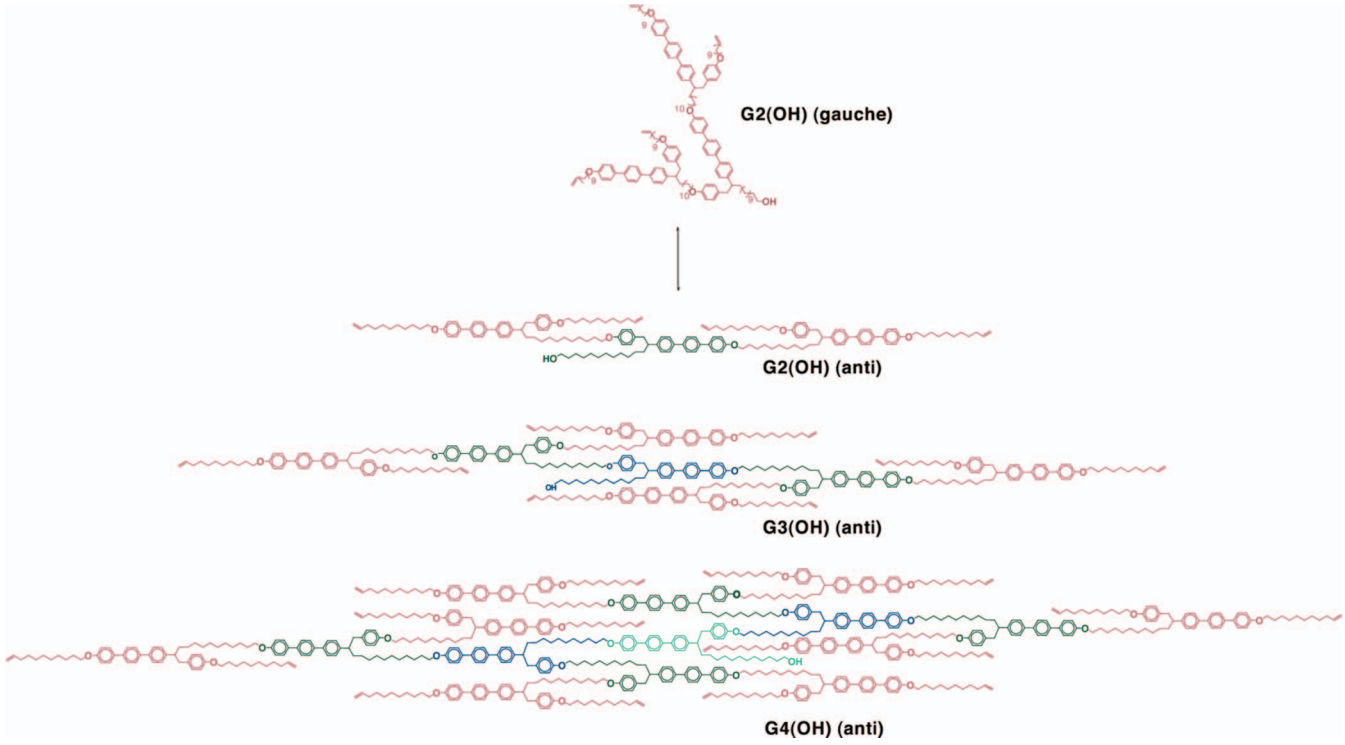

Figure 53. Self-assembly of willowlike dendrons into S and N phases via conformational isomerization. Adapted with permission from ref 221. Copyright 1995 American Chemical Society.

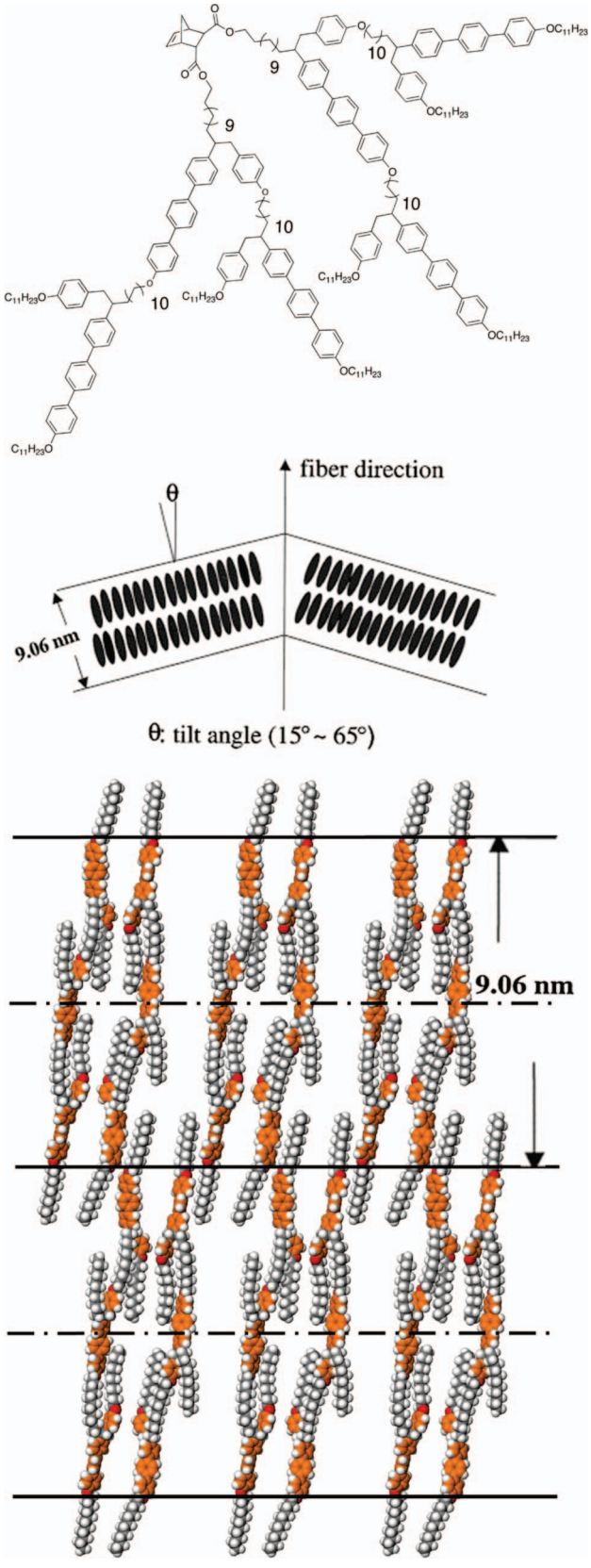

Figure 54. Bisdendronized norbornene monomer (left), schematic of S_h^B self-assembly (middle), and molecular model of layer formation (right). Reprinted with permission from ref 341. Copyright 2002 American Chemical Society.

All four diastereomers of Boc-D/L-Tyr-D/L-Ala-OMe were prepared.[353] It was demonstrated that the helical sense of the self-assembled dendritic dipeptides is determined by the chirality of the Tyr residue that is directly attached to the

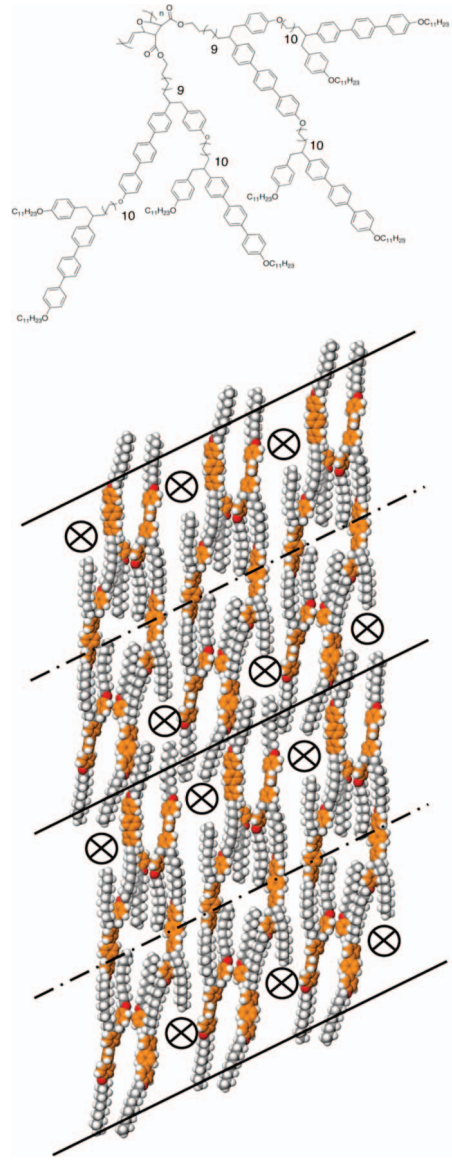

Figure 55. Structure (top) and schematic depicting the nonconventional S phase formed from poly(7-oxanorbornene) bisfunctionalized with willowlike dendrons. X's indicate the polymer backbone running perpendicular to the plane of the page.

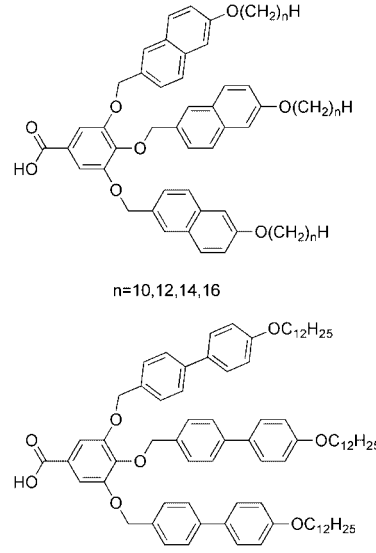

Figure 56. Structures of (4Nf-3,4,5)*n*G1−COOH and (4Bp-3,4,5)12G1−COOH.[343]

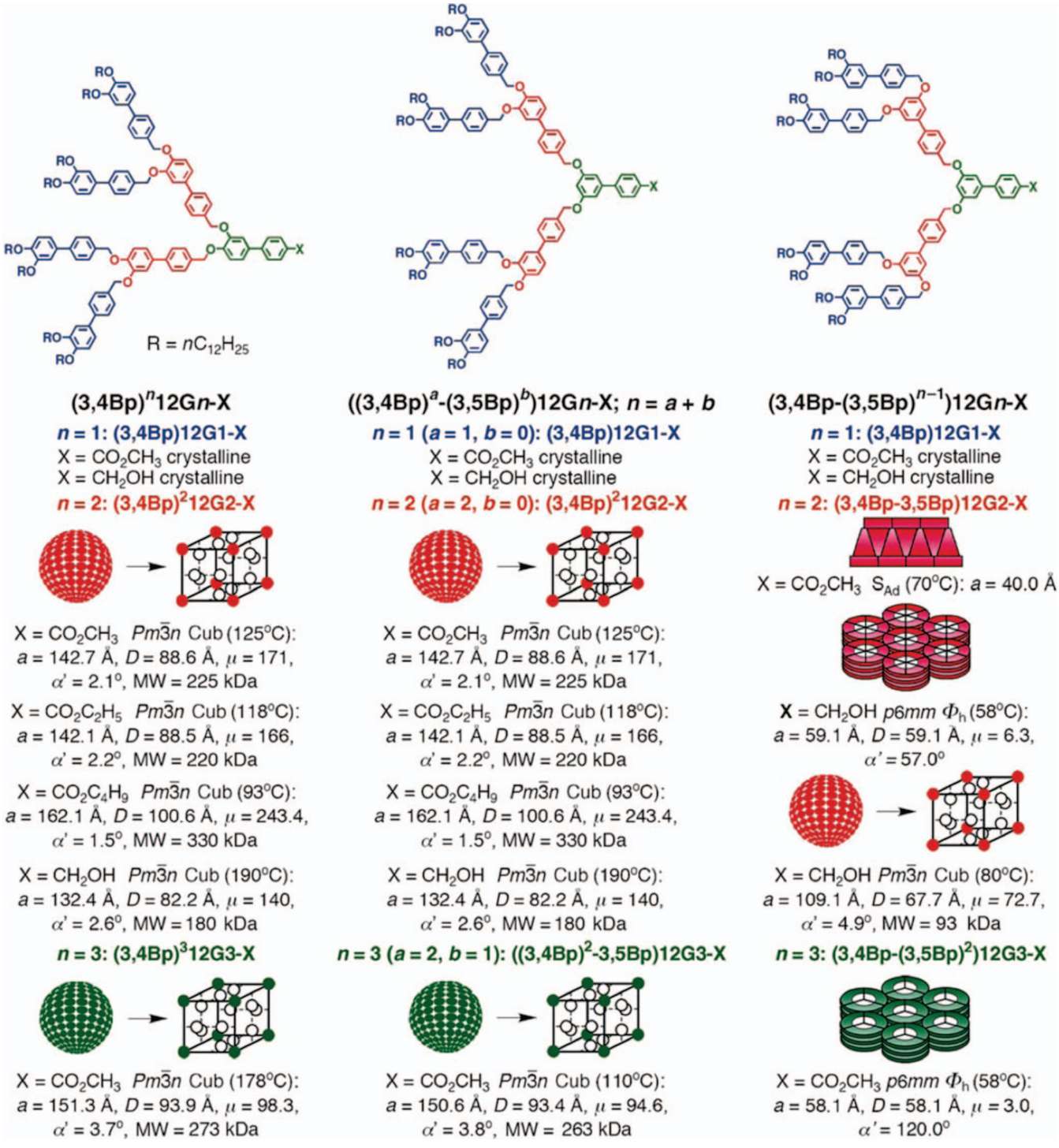

Figure 57. Examples of 3,4-, 3,5-, and 3,4,5-biphenyl-4 methyl ether-based dendrons and their self-assembly. Reprinted with permission from ref 274. Copyright 2006 Wiley-VCH Verlag GmbH & Co. KGaA.

dendron (Figure 71). Crude allosteric regulation[159−161] is operating, wherein modulation of the chirality of the more distant Ala residue also affects the finer features of self-assembly via subtle modulation of the hydrogen-bonding network and pore diameter. Specifically, homochiral dendronized dipeptides L−L/D−D exhibit different self-organized structures than heterochiral dendronized dipeptides L−D and D−L.

The structure and dimensions of the internal pore is also allosterically regulated by substitution of the L-Ala residue with Gly, L-Val, L-Leu, L-Ile, L-Phe, or L-Pro (Figure 72).[354] The helical pore could be tailored from 9 to 15 Å. The largest structural distortion was observed in the case of L-Val at low temperature in which self-organization into $\Phi_{r\text{-}c}$ rather than Φ_h lattice is observed. At elevated temperature, the Φ_h phase emerges. This thermoreversible shape change between ellipsoidal and circular columns was also observed for hybrid dendronized dipeptide (*S*)-(4-3,4-3,5-4)12G2−CH_2−(Boc-L-Tyr-L-Ala-OMe) (Figure 73).[355]

It was shown that attachment of a dipeptide to the apex of a dendron predisposed to columnar self-assembly, (4-3,4-3,5)12G1−CH_2OH, mediated the formation of helical porous

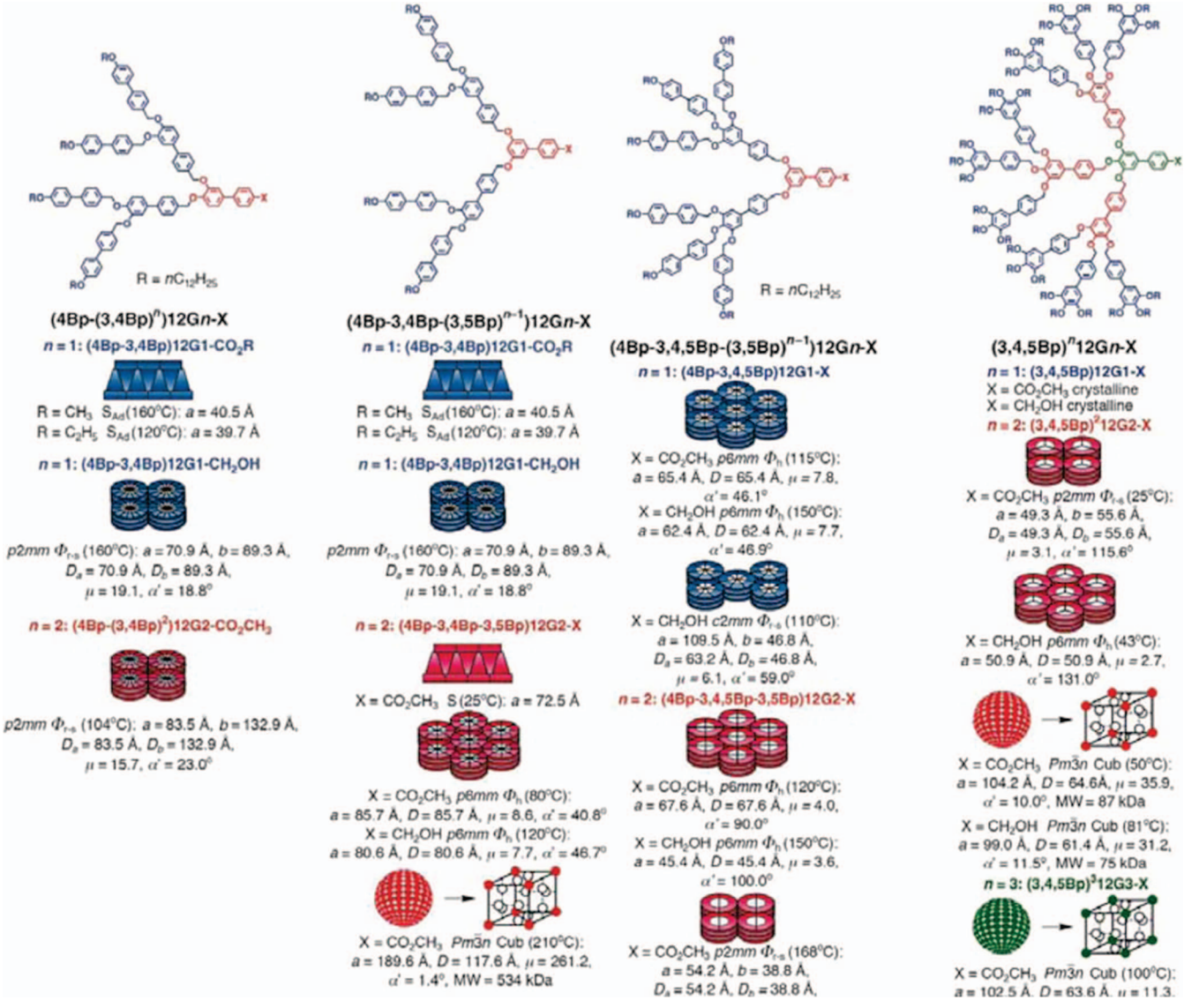

Figure 58. Examples of 3,4-, 3,5-, and 3,4,5-biphenyl-4 methyl ether dendrons and their self-assembly. Reprinted with permission from ref 274. Copyright 2006 Wiley-VCH Verlag GmbH & Co. KGaA.

Scheme 21. Synthesis of 3,4-, 3,5-, and 3,4,5-Biphenyl-4 Methyl Ether Dendritic Building Blocks; Reagents and Conditions: (a) [Pd (PPh$_3$)$_4$], Na$_2$CO$_3$, H$_2$O, Toluene, EtOH, Reflux; (b) BBr$_3$, CH$_2$Cl$_2$, 0−20 °C; (c) [NiCl2 (dppe)]/PPh$_3$, K$_3$PO$_4$, Toluene, 80 °C; (d) KMnO$_4$, Pyridine/H$_2$O (1:1); (e) MeOH, H$_2$SO$_4$ (cat.), Reflux; (f) (i) PyHCl, 190 °C; (ii) EtOH, HCl; (g) (i) NBS, NaH, CHCl$_3$; (ii) Me$_2$SO$_4$, K$_2$CO$_3$ (Reprinted with Permission from Ref 274; Copyright 2006 Wiley-VCH Verlag GmbH & Co. KGaA)

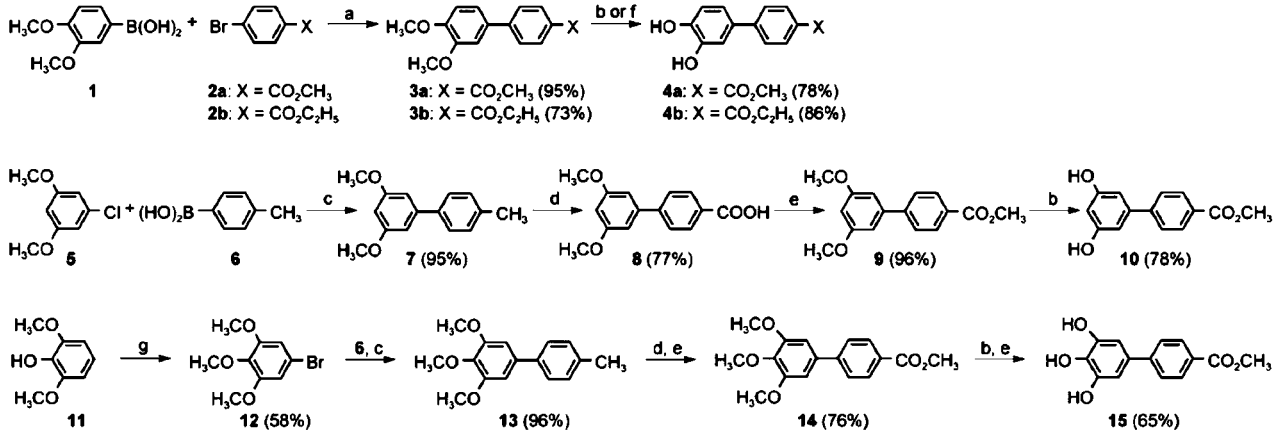

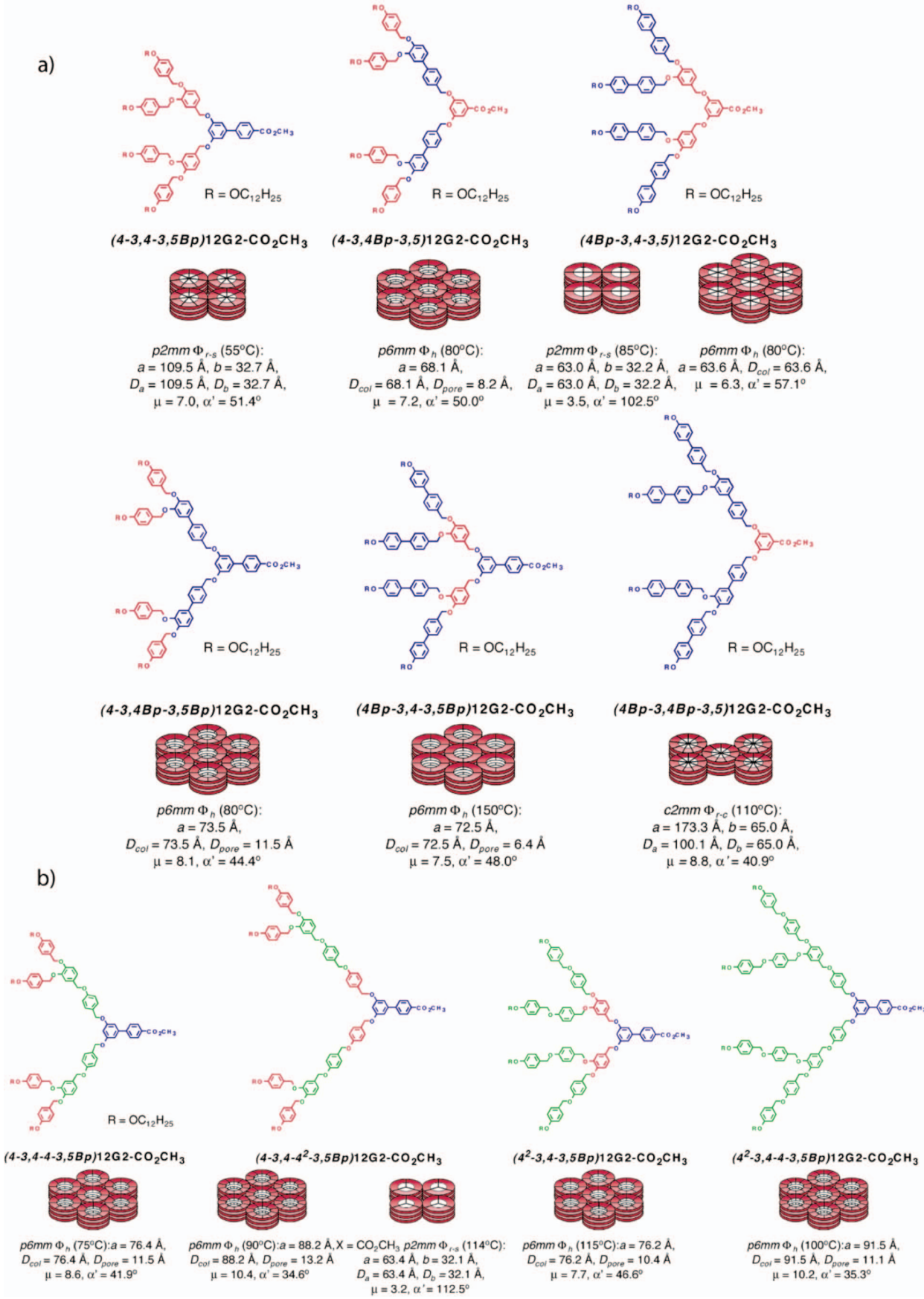

Figure 59. Hybrid 3,4- and 3,5-biphenyl-4 methyl ether dendrons. Reprinted with permission from ref 345. Copyright 2007 Wiley-VCH Verlag GmbH & Co. KGaA.

columns. It was later demonstrated that attachment to other column-forming dendrons such as (4-3,4,5-3,5)12G1−CH_2OH likewise resulted in porous helical columnar structures.[356] Attachment of a dipeptide to the apex

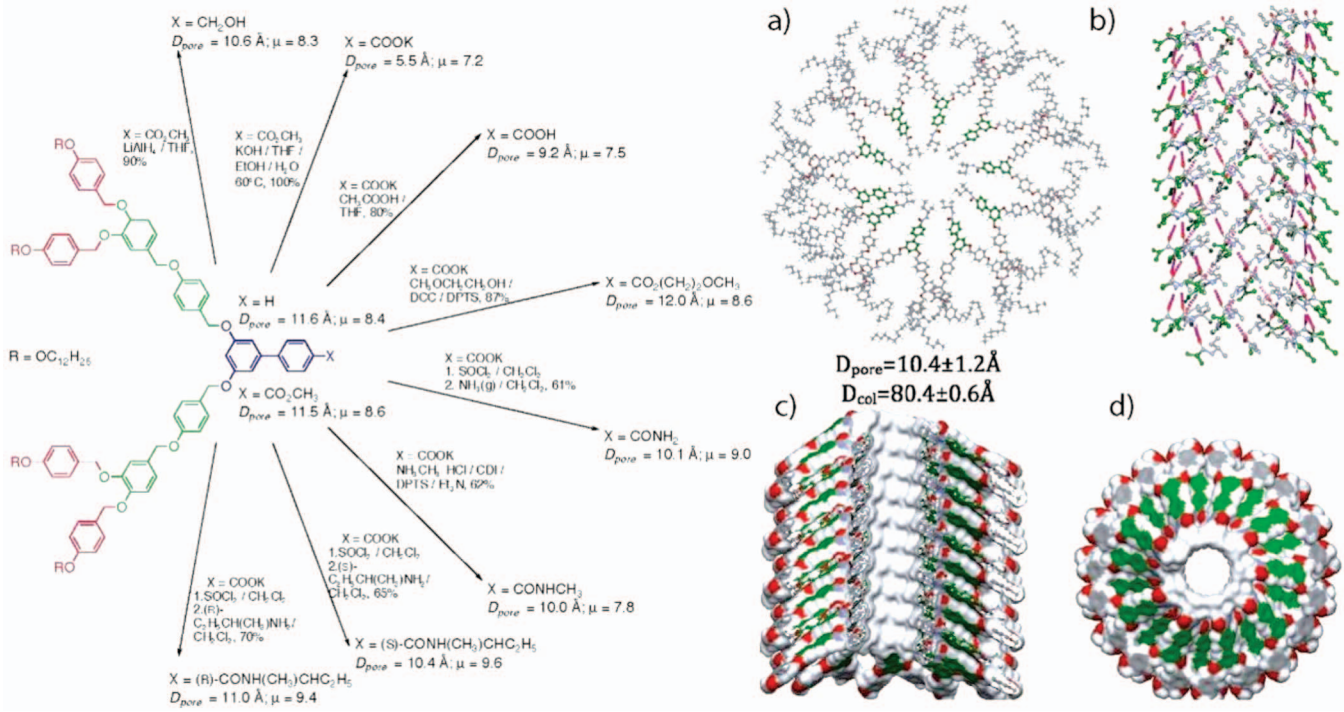

Figure 60. Self-assembly of (4-3,4-4-3,4Bp)12G2−X dendrons into porous columns and the molecular model derived from fiber XRD of (*S*)-(4-3,4-4-3,4Bp)12G2−$CO_2NH_2CH(CH_3)C_2H_5$. Reprinted with permission from ref 345. Copyright 2007 Wiley-VCH Verlag GmbH & Co. KGaA.

Scheme 22. Synthesis of AB_4 and AB_5 Type Dendritic Building Blocks (Reprinted with Permission from Ref 275; Copyright 2007 American Chemical Society)

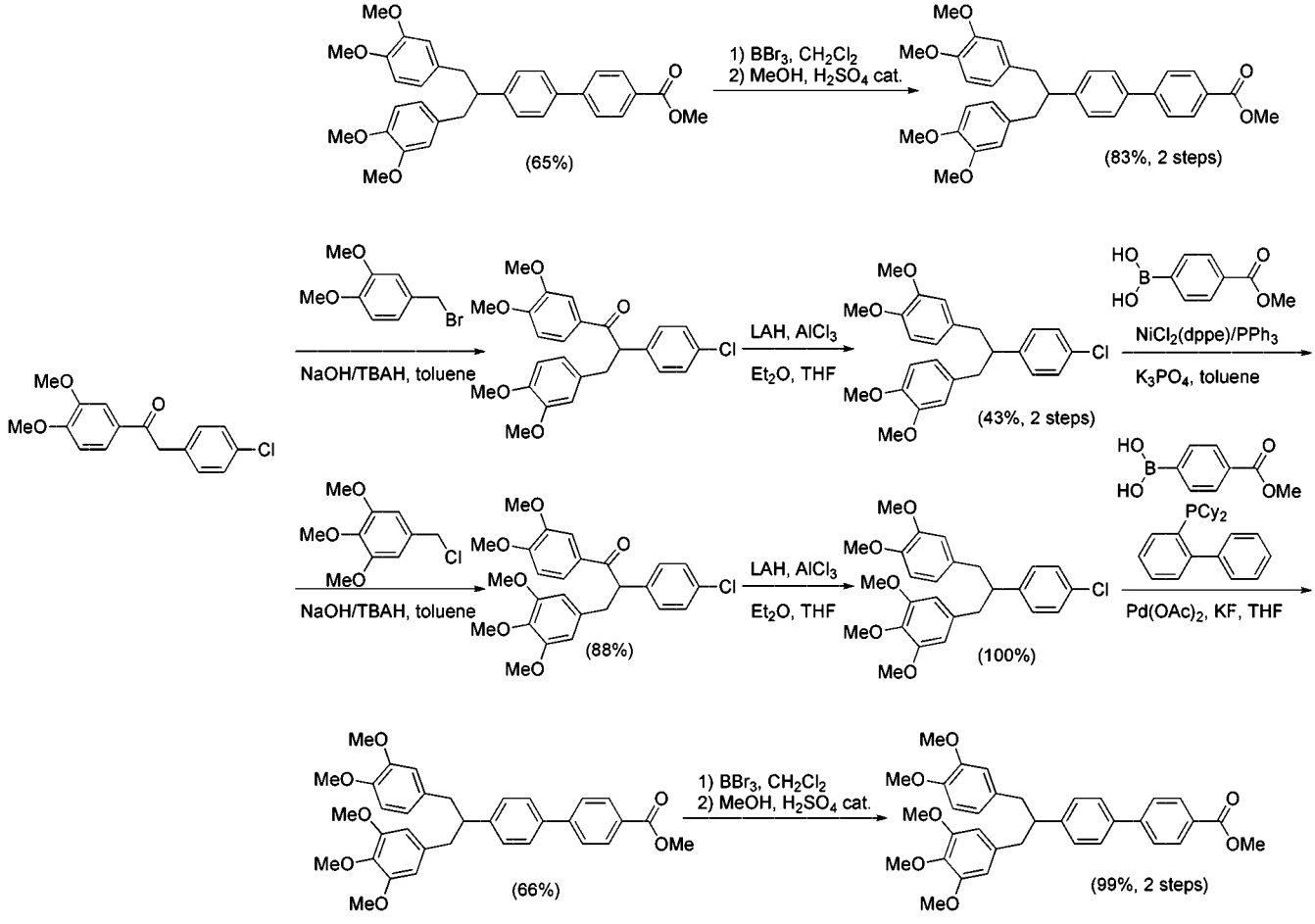

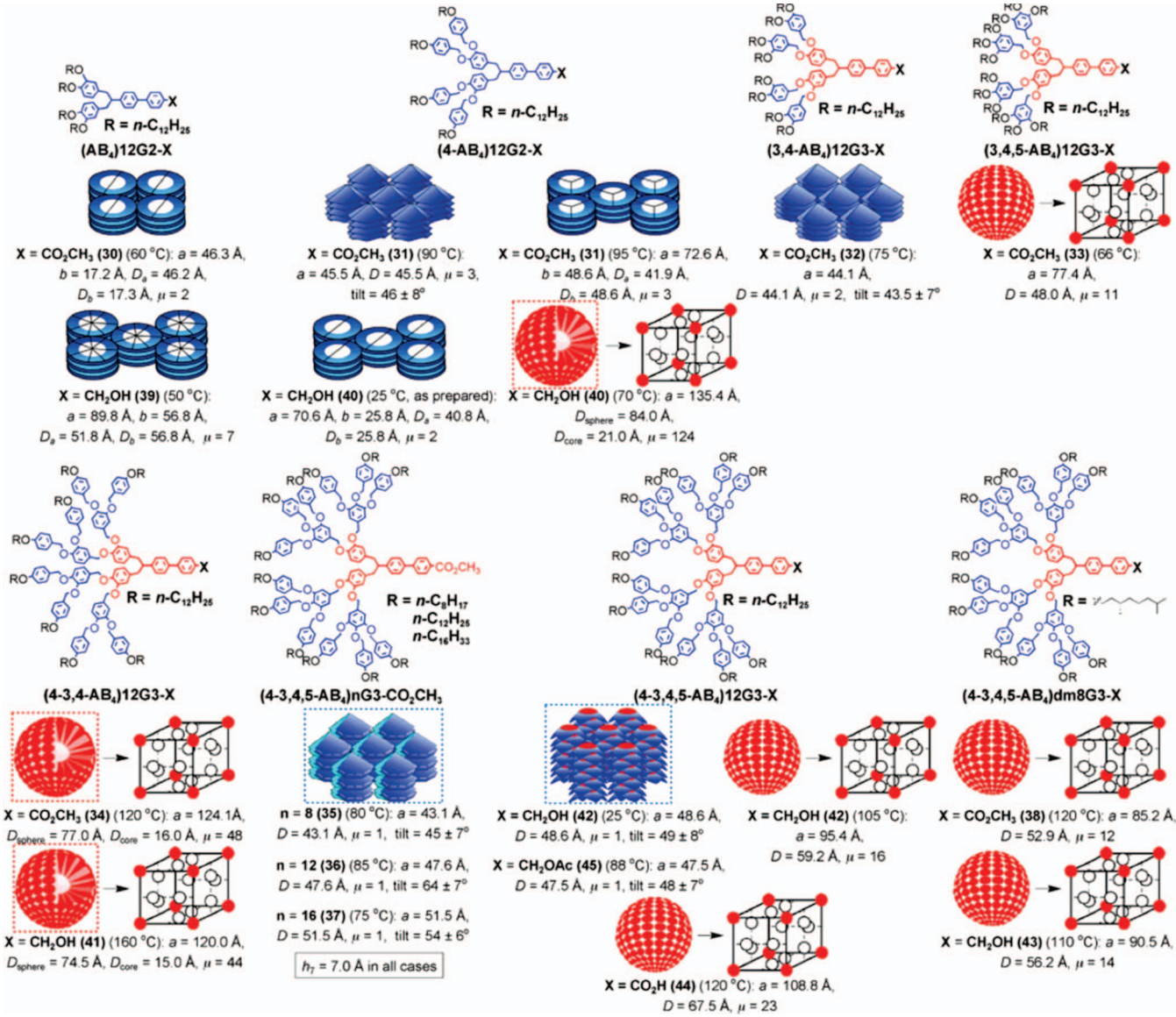

Figure 61. Library of AB_4 based dendrons. Reprinted with permission from ref 275. Copyright 2007 American Chemical Society.

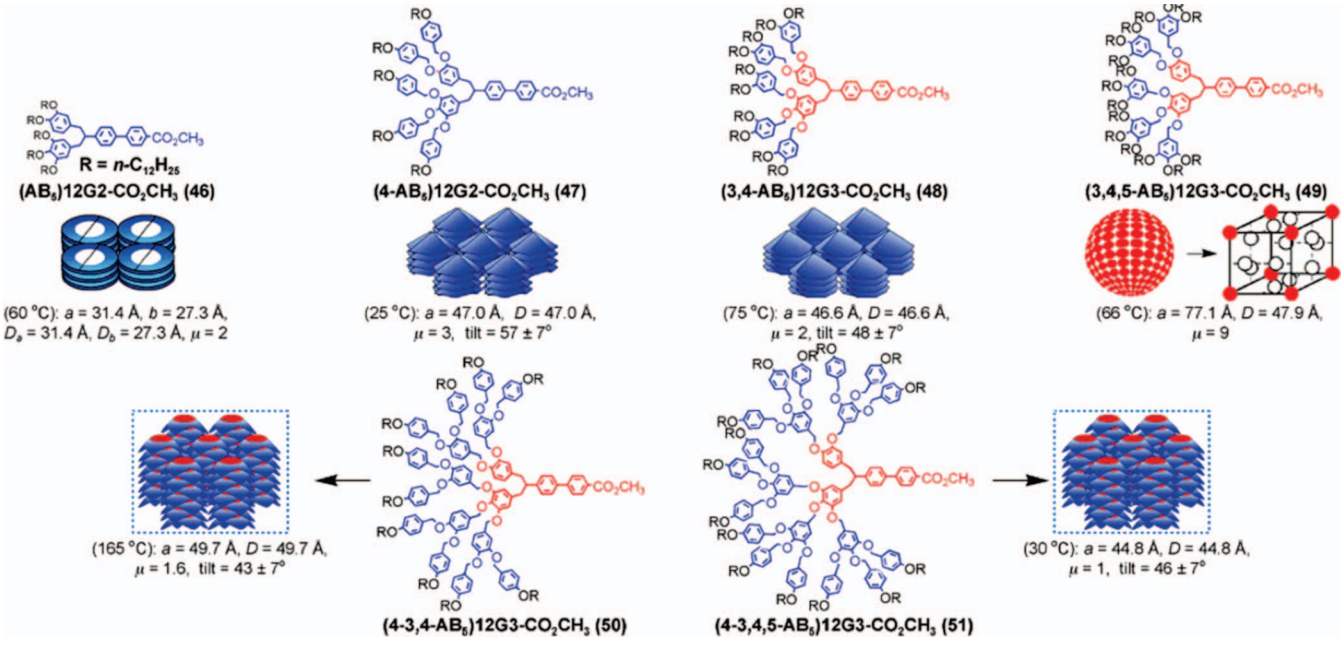

Figure 62. Library of AB_5-based dendrons. Reprinted with permission from ref 275. Copyright 2007 American Chemical Society.

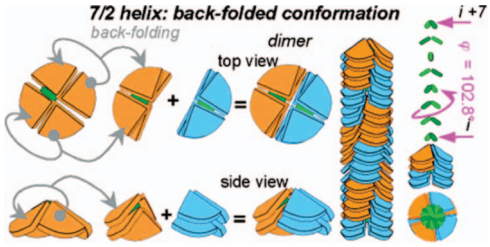

Figure 63. Self-assembly of (4-3,4,5-AB_4)12G3−CO_2CH_3 into a backfolded 7/2-helical column. Reprinted with permission from ref 275. Copyright 2007 American Chemical Society.

of a dendron predisposed to spherical self-assembly, (4-$(3,4)^2$)12G2−CH_2OH, which is the constitutional isomer of (4-3,4-3,5)12G2−CH_2OH, was shown to mediate self-assembly into a chiral hollow sphere (Figure 74).[357] In addition (4-$(3,4)^2$)d*m*8*G2-CO_2Me/CH_2OH and (4-3,4-3,5-4)d*m*8*G2−CO_2Me/CH_2OH were shown to self-assemble in chiral hollow spheres, while (4-$(3,4)^2$)12G_2−CO_2Me/CH_2OH, (4-3,4-3,5-4)*n*G2−CH_2OH (*n* = 4, 6, 12), and (4-3,4-3,5-4^2)*n*G2−CH_2OH (*n* = 4, 6, 8, 10, 12) were shown to self-assemble in nonchiral hollow spheres. Increasing the alkyl tail lengths was shown to diminish the diameter of the hollow core.

2.2.6. Fluorous Phase or Fluorophobic Effect in Self-Assembly

As will be discussed in section 3.2.2, semifluorination of the dendritic periphery enhances the stability of columnar self-organization of dendron-jacketed polymers.[47,293,358] This same phenomenon was observed in the self-assembly of dendrons into supramolecular dendrimers. It was also shown that the fluorophobic effect[290] enhanced the self-organization of (3,4,5)12F*m*G1 dendronized benzo-crown-ethers and crown-ethers into homeotropically aligned Φ_h phases (section 6.1) (Figure 75).[359] Perhydrogenated dendronized crown-ethers only self-organize into Φ_h phases in the presence of alkali salts, thereby forming a virtual polymeric backbone.

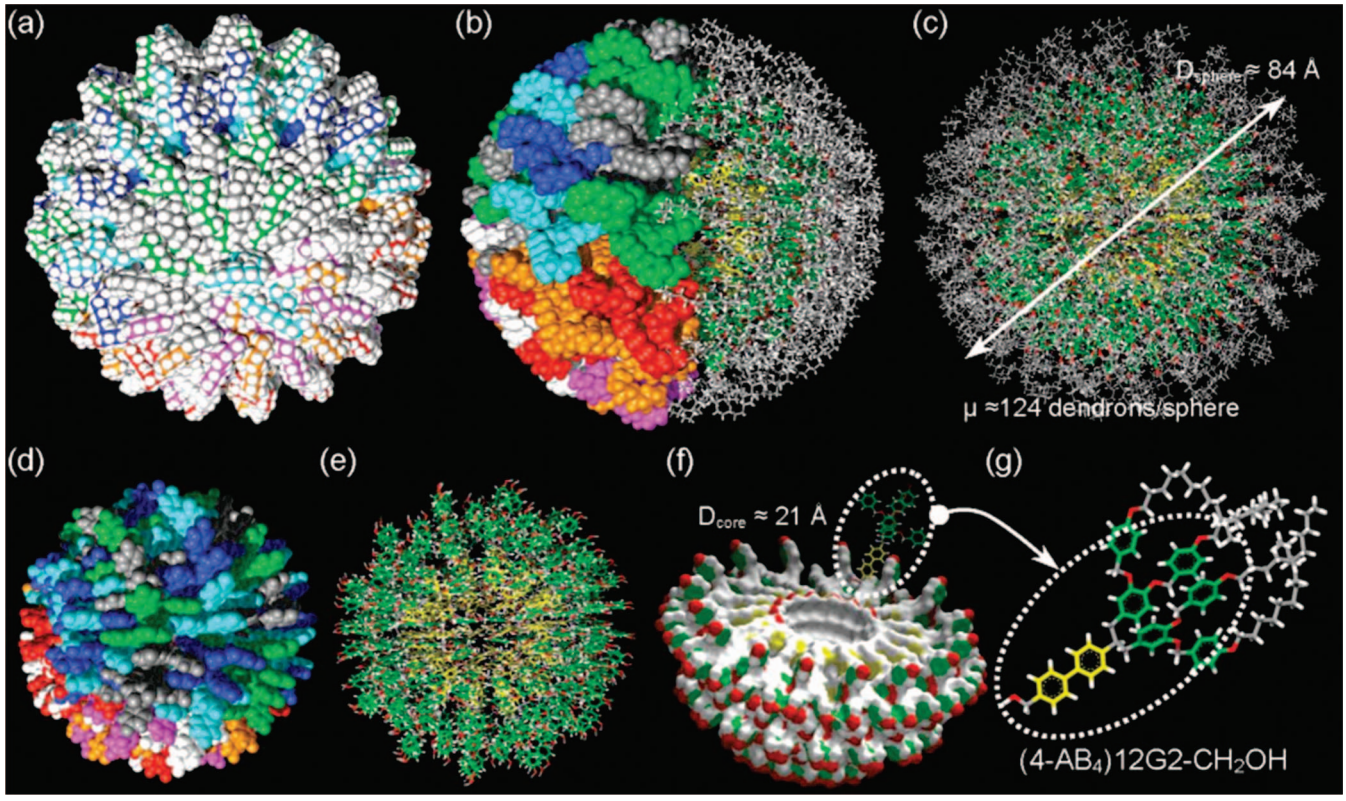

Figure 64. Self-Assembly of (4-AB_4)12G2−CH_2OH into hollow spheres. Reprinted with permission from ref 275. Copyright 2007 American Chemical Society.

Scheme 23. Synthesis of (4-3,4-3,5)12G2−CH_2−(Boc-L-Tyr-L-Ala-OMe)[312]

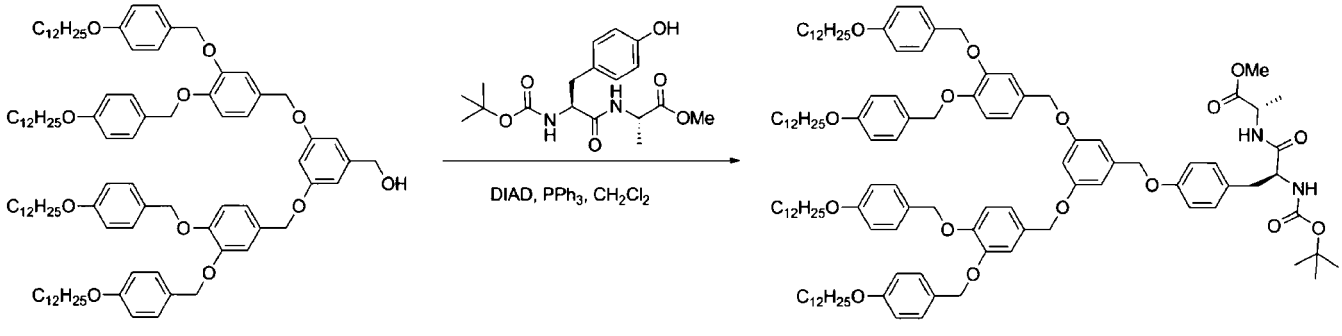

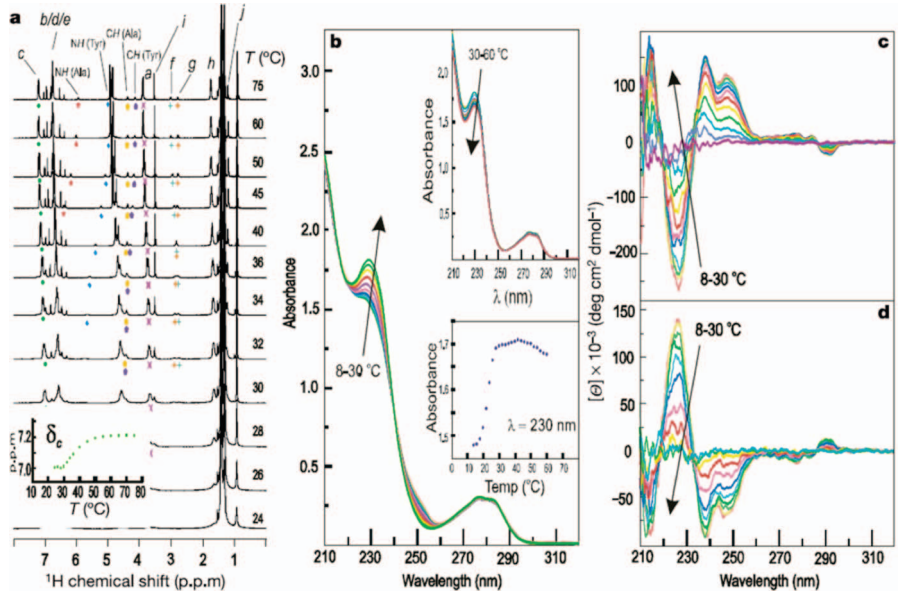

Figure 65. NMR (a) and CD/UV−vis (b, c, d) experiments confirming helical columnar self-assembly of dendronized dipeptides. Reprinted with permission from ref 312. Copyright 2004 Macmillan Publishers Ltd. (Nature).

Semifluorinated dendronized crown-ethers form Φ_h phases even in the absence of salt.

(4-3,4,5)12G1 with oligo-ethylene oxide apex functionality only self-assembles into columnar structures in the presence of alkali salts. Semifluorination of the periphery results in the stabilization of the Φ_h phase, allowing for columnar self-assembly of dendritic acids or dendrons with oligo-oxyethylene apex-functionality (Figure 76).[293] It was later demonstrated that semifluorination of (3,4,5)12G1 dendrons also stabilized the formation of the Φ_h phase in the absence of alkali salts (Figure 77).[360] The stabilization of the Φ_h phase is due to the fluorophobic effect, wherein the immiscibility of the melted perfluorinated and perhydrogenated segments results in greater phase stability. Further, the greater rigidity and cross-sectional area of the perfluorinated segments result in larger column diameters.[360]

The fluorophobic effect not only stabilizes the formation of columns but also can discriminate between spherical and columnar self-assembly (Figure 78).[361,362] Perhydrogenated $(3,4,5)^2$12G2−CO_2Me self-organizes into a *Cub* lattice due to its high degree of branching, which promotes collapse of the high taper angle wedge shape into a lower taper angle conical shape wherein all benzyl units adopt a *trans*-conformation. Semifluorinated $(3,4,5)^2$12F8G2−CO_2Me, on the other hand, forms pyramidal columns that self-organize into a Φ_h lattice. Here, the benzyl groups either adopt an all-*gauche* crown conformation stacking in a unimolecular stratum, or the benzyl groups adopt an all-*trans* conformation self-assembling into pine-tree pyramidal columns (Figures 78 and 79).[361]

As described in section 3.2.3, semifluorinated dendrons attached to electron-donor or -acceptor groups were used to form coassembled pairs of dendronized donors and dendronized acceptors, dendronized donors with acceptor polymers, or dendronized acceptors with donor polymers.[358] All systems self-organized into Φ_h via intercalation of donor arenes and acceptor arenes provided access to complex electronic materials with high electron and hole mobilities. Later, a more detailed XRD analysis of the self-assembly of *n*-type acceptors decorated with semifluorinated dendrons was performed (Figure 80, left).[363] In most cases, self-assembly into pyramidal columns (Figure 37e) was observed, wherein the central column consists of a flat π-stack of the donor, while the pendent dendron is attached to the column with a noticeable tilt angle (Figure 80, right). Self-organization of these pyramidal columns proceeded into Φ_h, $\Phi_{r\text{-}c}$, and $\Phi_{r\text{-}s}$ lattices exhibiting LC phases, Φ_h phases with internal order (Φ_h^{io}), or crystalline phase (Φ_h^{k}).[363] A notable exception was found with the dendronized perylene bisimide. Here, an unprecedented pyramidal architecture was observed, where the perylene units stacked parallel to the columnar axis (Figure 81).

Percec also reported an expanded set of aromatic electron-donors dendronized with either (3,4,5)12F8G1 or (3,4,5)16F8G1 (Figure 82).[364] Donor groups included 3,5-dimethoxybenzene, 3,5-di(pyrrolidine-1-yl)phenol, 2-napthalene, phenothiazine, pyrene, and carbazole (Figure 83). All dendronized donor molecules self-assemble into helical pyramidal columns that self-organize into $\Phi_{r\text{-}s}$, $\Phi_{r\text{-}c}$, or Φ_h lattices. In addition, all molecules exhibit a lower temperature columnar phase that exhibits higher degrees of intracolumnar order. Time-of-flight charge carrier mobility was determined to be $1-3.5 \times 10^{-3}$ cm^2/Vs for the dendronized pyrene and anthracene, and results indicated a polaronic transport mechanism.[365]

In a limited number of examples, fluorophobically driven self-assembly results in noncolumnar structures. (4-3,4,5)12F8−4EO has been shown to self-assemble into an "interlocked" gyroid phase with $Ia\bar{3}d$ symmetry (Figure 84).[366] $(3,4,5)^2$12F8G2−COOH self-assembles into spheres that self-organize in a *Cub* phase .[367] Here the stronger H-bonding is believed to mediate a more compact spherical structure.

In addition to aliphatic tailed biphenyl-methyl ether dendrons reported by Percec, a semifluorinated analogue, (4Bp-3,4,5)12F8G1−CO_2Me, has been prepared by another group.[368] Supramolecular columns of semifluorinated dendrons adopting Φ_h organization could be aligned perpendicular to a magnetic field (Figure 85).

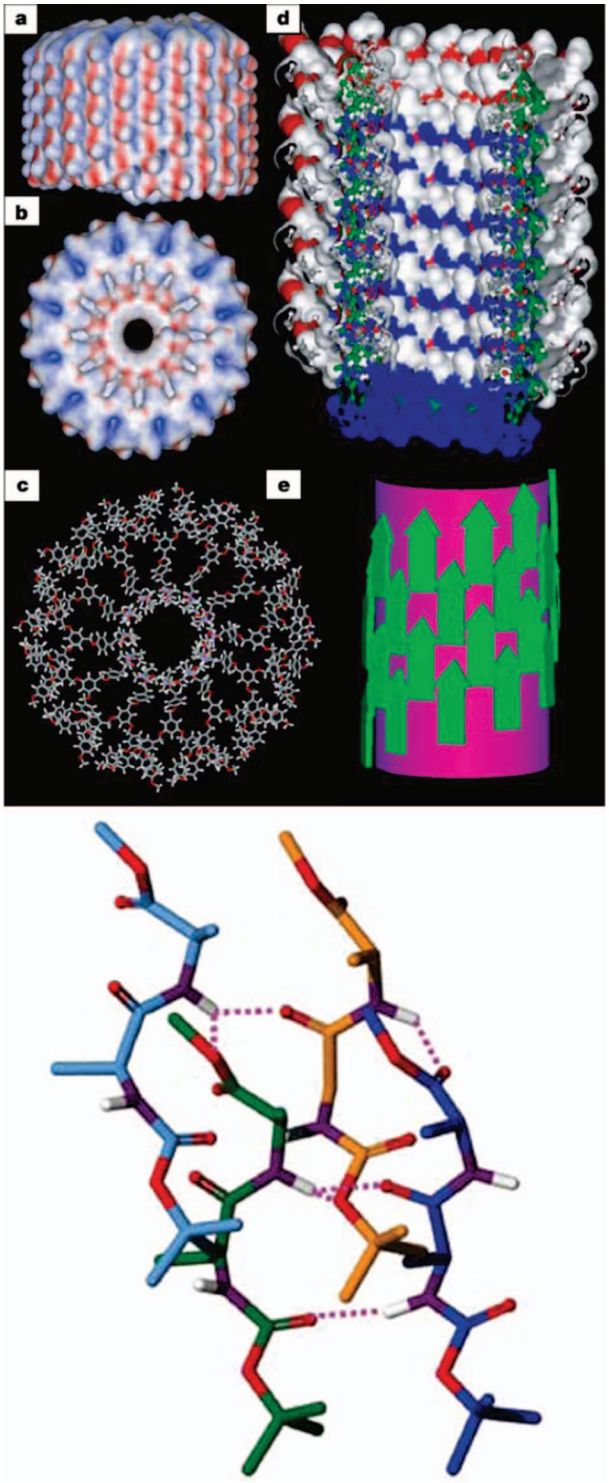

Figure 66. Models of self-assembled helical porous columns from dendritic dipeptides (top, a−d), orientation of dipeptide groups in the column (e), and hydrogen bonding network (bottom). Reprinted with permission from ref 312. Copyright 2004 Macmillan Publishers Ltd. (Nature).

3. Dendron-Jacketed Polymers

3.1. Synthesis of Dendronized Polymers

3.1.1. General Strategies for the Merging of Dendritic and Polymeric Topologies

This review covers a broad array of dendronized polymers and related topologies; the most ubiquitous of them, yet topologically the simplest, is the dendron-jacketed linear polymer (Figure 1, rows 1 and 2 and left half of row 3). Self-assembling dendrons, described in the preceding chapter, serve as supramolecular models of covalently linked dendron-jacketed polymers. Dendron-jacketed polymers were first reported by Tomalia in a seminal patent[369] in 1987 and made available in open literature in 1998.[370] Independent of this work, Percec reported in 1989 examples of self-organizble dendronized polymers prepared via *grafting-onto* and *macromonomer* approaches (vida infra).[195] In 1992, Fréchet and Hawker were able to demonstrate the copolymerization of dendritic *macromonomers* with nondendronized comonomers.[371] Later, Ritter reported the AIBN-mediated homopolymerization of highly functionalized dendritic macromonomers.[372,373] Schlüter expanded the versatility of the *macromonomer* approach toward higher-generation polymerizable dendrons.[374,375] Ritter and Schüter's dendronized polymers do not self-organize. The simplest dendron-jacketed polymers are homopolymers wherein at least one dendritic side group is attached to each

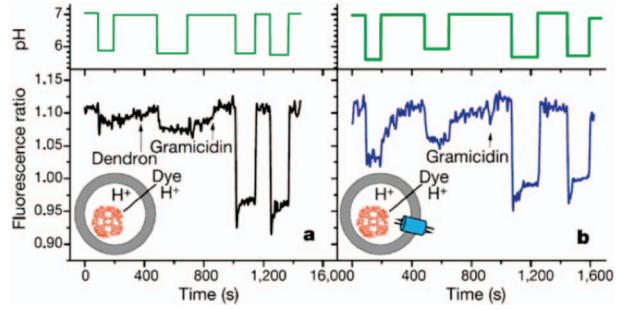

Figure 67. Proton transport experiment comparing a liposome containing an impermeable pH-sensitive fluorescent indicator (left) and a liposome containing a self-assembled dendritic channel (right). Reprinted with permission from ref 312. Copyright 2004 Macmillan Publishers Ltd. (Nature).

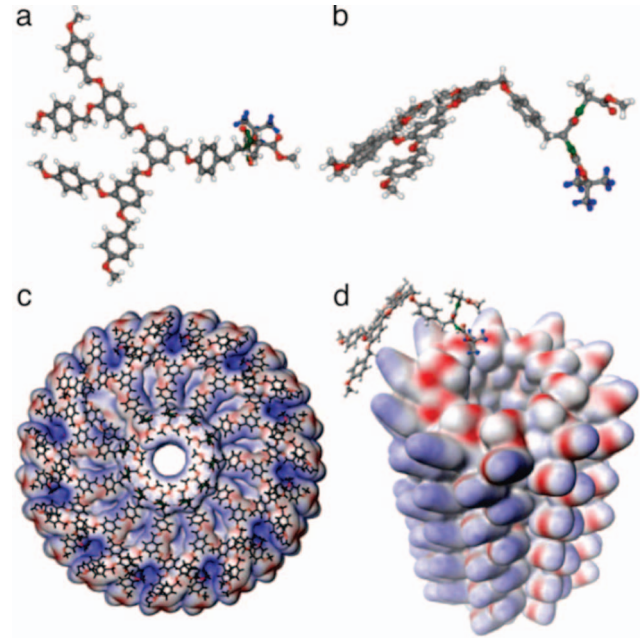

Figure 68. Self-assembly of (4-3,4-3,5)1G2−CH2−Boc-L-Tyr-L-Ala-OMe into helical porous columns. Top (a) and side (b) views of the dendritic dipeptide; (c) top view of the porous column; and (d) view of the pore without dendron. All structures are shown with $-CH_3$ as alkyl groups. Reprinted with permission from ref 171. Copyright 2006 PNAS.

Table 5. Effect of *n* on the Self-Assembly of (4-3,4-3,5)*n*G2−X (Adapted with Permission from Ref 171; Copyright 2006 the PNAS)

n	*T* (°C)	$a = D_{col}$ (Å)	D_{pore} (Å)	ρ_{20} (g/cm^3)	μ^c	α'^d
1[a]	20	36.0	6.8	1.23	5.7	63.2
2[a]	30	38.4	6.8	1.12	5.8	62.1
4[a]	90	42.1	6.7	1.12	5.8	62.1
6[a]	90	44.4	6.6	1.12	5.9	61.0
8[a]	60	46.5	5.1	1.10	6.0	60.0
10[a]	26	49.9	<3	1.05	5.9	61.0
12[a]	26	52.6	<3	1.03	6.0	60.0
14[a]	50	56.7	<3	1.03	5.9	61.0
16[a]	65	60.3	<3	1.06	6.5	55.4
6[b]	30	67.1	15.8	1.12	10.0	36.0
8[b]	30	71.1	15.3	1.10	1.3	35.0
10[b]	30	75.1	14.7	1.07	11.2	32.1
12[b]	25	77.1	13.3	1.02	11.6	31.0
14[b]	30	81.0	12.7	1.07	11.9	30.3
16[b]	30	84.4	11.7	1.07	12.8	28.1

[a] X = OH. [b] X = Boc-L-Tyr-L-Ala-OMe. [c] μ = dendrons per stratum (see section 2.2.2). [d] Projection of the solid angle for tapered monodendrons, $\alpha' = 360/\mu$.

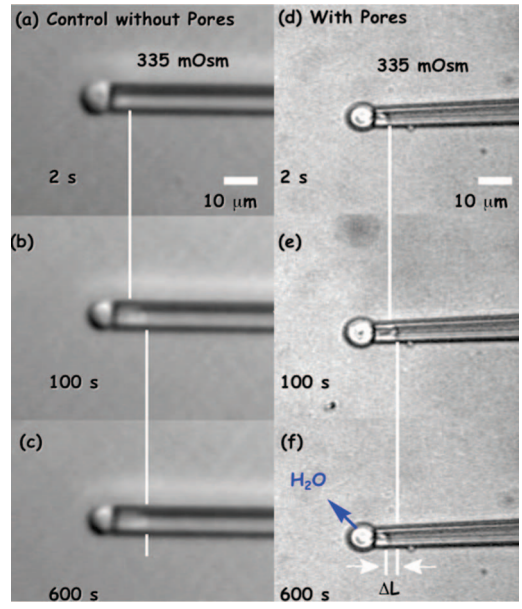

Figure 69. Demonstration of water transport in phospholipid vesicles containing dendritic channels. Giant unilamellar vesicles (GUVs) without dendritic dipeptide (a−c) and vesicles with dendritic dipeptide (d−f) were prepared in 285 mOsm phosphate buffer solution. The vesicles were captured with a micropipet, and their response to hypertonic solution was monitored through optical microscopy. GUVs without dendritic dipeptide expand into the pipet in the presence of 335 mOsm hypertonic solution of phosphate buffer solution (a−c). The GUVs with dendritic dipeptides do not extend nearly as far into the micropipet, indicating water is able to flow through the membrane and equilibrate their pressure. Reprinted with permission from ref 350. Copyright 2007 American Chemical Society.

monomer repeat unit. Alternatively, they can be copolymers built from monomers with and without dendritic side groups. As a form of graft copolymer, the most primitive application of the dendritic jacket is disassembly of the native polymer backbone state, allowing for the suppression of chain−chain interactions including entanglements and chain−chain electronic coupling via steric shielding. This effect can be accompanied, depending on the structure of the dendron and of its repeat unit, by an induced backbone rigidity or helicity. Through the merging of distinct topologies, dendronization of linear polymers can also be a powerful tool to manipulate self-organization. Self-organization of dendron-jacketed polymers is a synergy of the intrinsic main-chain conformation and the spatial requirements and specific interactions of the dendritic side chain. Some dendron architectures have a propensity to self-assemble. These self-assembling dendrons can be used to program structural changes in the random-coil conformation of the polymer backbone enforcing extended-chain or helical conformations,[376] among others. Intramolecular self-assembly of the dendronized polymers into uniform structures can also allow for their self-organization into various lattices. Some polymers have constrained backbones or isotactic backbones that can result in dynamic yet preferred conformations. Polymers possessing higher levels of dynamic order can induce organization in a pendant dendron-jacket, even if that dendron does not exhibit intrinsic self-assembly and self-organization behavior. Random-coil polymers, when jacketed with a dendron that does not exhibit intrinsic self-assembly or self-organization, can result in a dendronized polymer that does in fact self-organize. Molecular dynamics simulations have suggested that, even in linear achiral dendronized polymers, helical conformations[377] and superstructures[378] can arise through the attachment of high-generation dendrons via crowding effects.[379] In all cases, the presence of a dendritic side chain perturbs the polymer organization and vice versa.

The effect of dendron structure on the self-organization of the dendronized polymer as well as the conformation of the main chain will be considered. The strength of the interactions that leads to self-assembly and self-organization in the precursor dendron as well as the mass ratio of dendron side group to the main chain in the monomer repeat unit (mru) largely determines the ability of the dendron to influence the main-chain conformation and stiffness.

Comparing Fréchet-benzyl ether,[40,191,192] Tomalia-PAMAM,[369,370] Liskamp[268]/Liskamp-Schlüter,[270] Percec-type 1 [(3,4,5)^{n}12G$_n$], and Percec-type 2{[4-(3,4,5)^n]12G$_n$}, Newkome-Trēons,[261] Kim-amphiphilic,[256,380] and Fréchet PEG[264] dendrons (Figures 86 and 87),[265,266] it is evident that AB_2 Fréchet, Tomalia-PAMAM, Liskamp, Kim-amphiphilic, and Fréchet PEG dendrons exhibit similar molar masses at a given generation (G). However, because of the combination of increased periphery chain weight as well as an AB_3 branching architecture, Percec-type 2 dendrons have a molar mass at G1 that is about equal to the molar mass of Fréchet and Tomalia-PAMAM dendrons at G2. With increasing generation, this difference increases. By G3, Percec dendrons are of roughly equivalent molar mass to G5 Fréchet and Tomalia-PAMAM dendrons. Percec-type 1 dendrons that contain AB_2 branching subunits have lower molar mass at each generation, and variants of Fréchet and Tomalia-PAMAM dendrons with heavier periphery groups have increased molar mass at each generation than their corresponding archetypes, respectively. Newkome dendrons, which have an AB_3 branching architecture but relatively low periphery mass, have somewhat lower molecular weights than Percec-type 2 dendrons. Attachment of higher molecular tails to Newkome dendrons can reverse this order. Percec dendrons with AB_4 or AB_5 branching architectures will have a higher molar mass at a given generation than Percec-type 1 and Percec-type 2 dendrons.[275] Thus, for a given generation number, Percec-type dendrons will have a more substantial mass effect on the

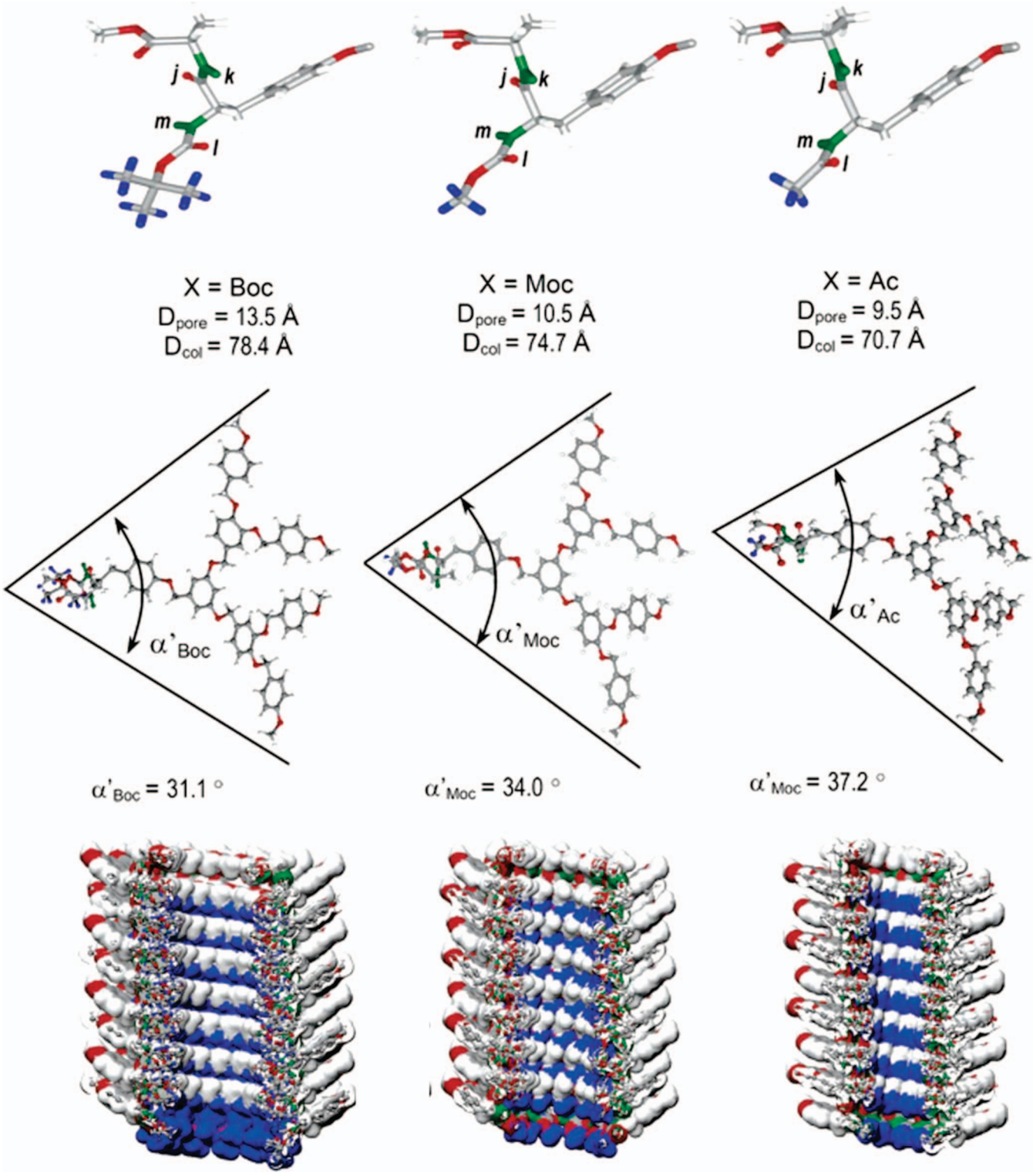

Figure 70. Effect of protecting group on the conformation of the dipeptide segment, molecular taper angle, and self-assembly into helical porous columns. Reprinted with permission from ref 352. Copyright 2005 American Chemical Society.

polymer chain. A larger mass effect accelerates the disassembly process at lower generations and induces self-assembly. However, it is the self-assembly of dendrons that mediates the self-organization of dendronized polymers. Fréchet and Tomalia-PAMAM dendrons of all generations do not self-assemble or self-organize, while Percec-type dendrons self-assemble into a rich array of lamellar, columnar, and spherical structures that self-organize in periodic and quasi-periodic 2-D and 3-D arrays even at G1. The enhanced intrinsic self-assembly and self-organization potential of Percec-type dendrons is a result of *exo*-recognition, self-control and quasi-equivalence,[381] and preferential self-interaction of aliphatic domains through dispersion interaction and aromatic domains via $\pi-\pi$ interaction and, in some cases, via directed interactions at the apex.[382]

More comprehensive reviews of the methods employed in the synthesis of dendronized polymers are available (see section 1.2). However, many structures, their self-

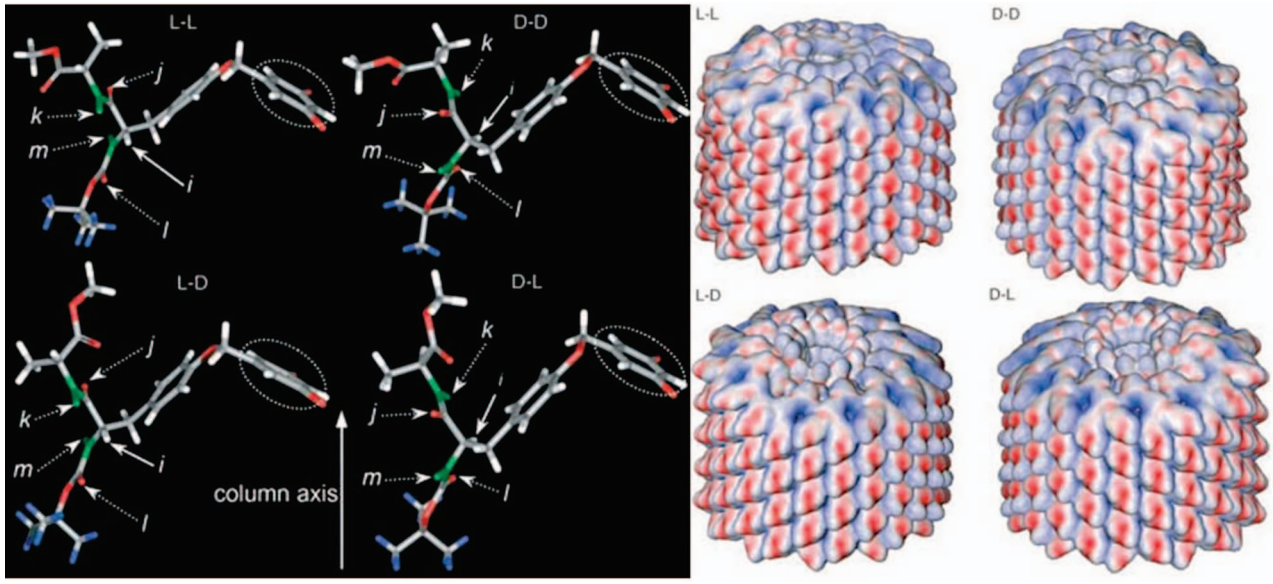

Figure 71. Self-assembly of homochiral and heterochiral dendritic dipeptides is stereochemically controlled and allosterically regulated by the stereochemistry of the dipeptide. Reprinted with permission from ref 353. Copyright 2005 Wiley-VCH Verlag GmbH & Co. KGaA.

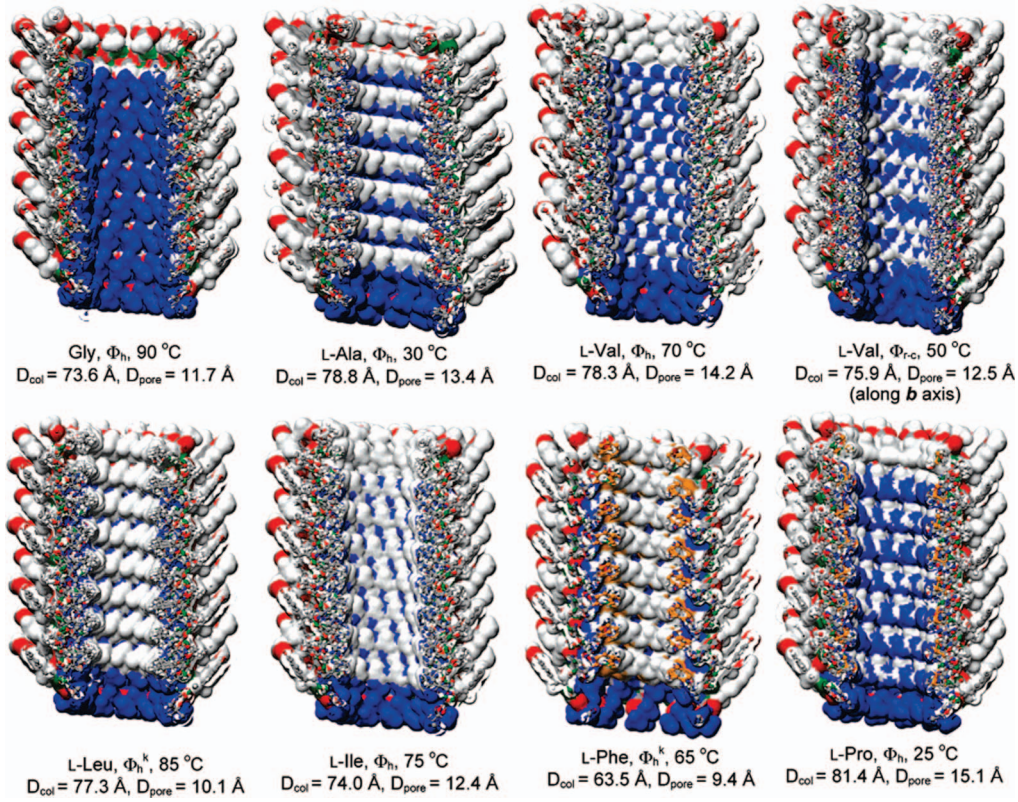

Figure 72. Effect of second dipeptide α-amino acid on helical porous self-assembly. Reprinted with permission from ref 354. Copyright 2007 American Chemical Society.

organization, and resulting functions[29] will be presented in this review. Examination of these examples may inspire the creation of analogous structures. Therefore, it is important to be aware of the strategies employed in dendronized polymer synthesis.

The dendritic and linear polymeric portions are synthesized in separate stages through distinct methods. The dendritic segment is prepared through iterative *convergent*[40,191,192] and *divergent*[182,190,369,370] growth pathways as described in section 2.1.2. By analogy with the synthesis of graft-copolymers,[383−385] the dendritic and polymeric seg-

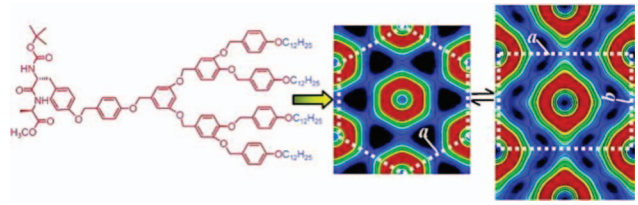

Figure 73. Thermoreversible shape change of circular to ellipsoidal columns as evidenced by cross sections of the reconstructed electron density maps. Reprinted with permission from ref 355. Copyright 2006 American Chemical Society.

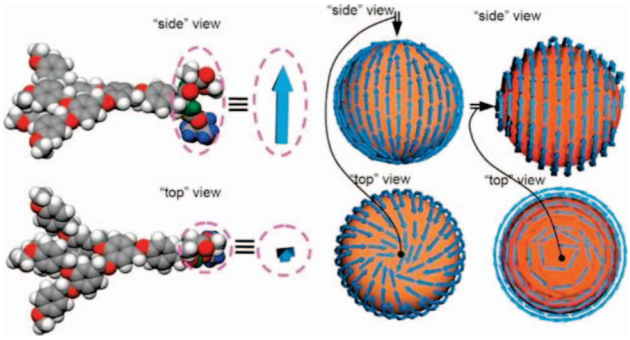

Figure 74. Self-assembly of (4-(3,4)^2)12G2−CH_2−Boc-L-Tyr-L-Ala-OMe in an apple peel, spherical helix, or loxodrome around a hollow core. Reprinted with permission from ref 357. Copyright 2008 American Chemical Society.

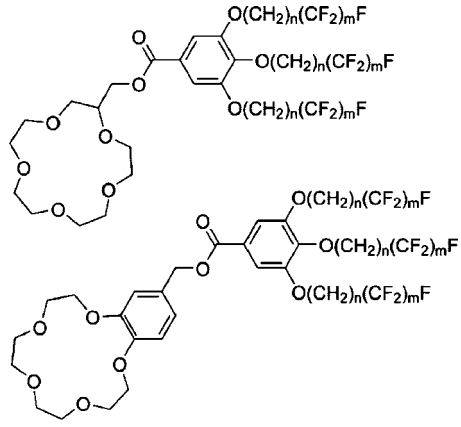

Figure 75. Structures of (3,4,5)12F*m*G1 dendronized benzo-crown and crown-ethers.[359]

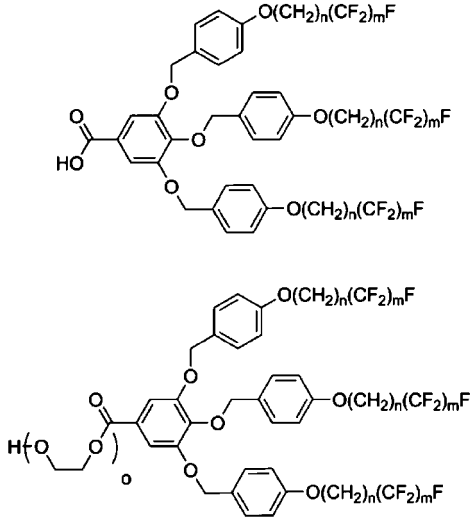

Figure 76. Structures of (4-3,4,5)*n*F*m*G1−COOH and (4-3,4,5)*n*F*m*G1−*o*EO, where *o* is the number of EO repeat units.[293]

ments can be merged via *grafting-onto*, *grafting-from*, or *dendritic macromonomer* strategies (Figure 88). In the grafting-onto strategy, complete dendrons produced via a convergent route are attached to an existing polymer via a variety of ligation approaches. This strategy offers easy adaptation of established convergent strategies, typically through a simple apex functionalization step, and can be useful when the dendritic side groups are incompatible with polymerization conditions.[386] However, the grafting-

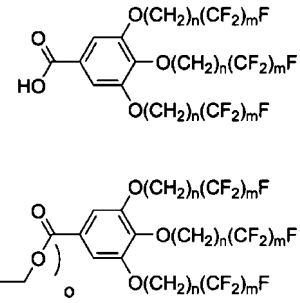

Figure 77. Structures of (3,4,5)12F*m*G1−COOH and (3,4,5)12F*m*G1−*o*EO, where *o* in this case is the number of EO repeat units.[360]

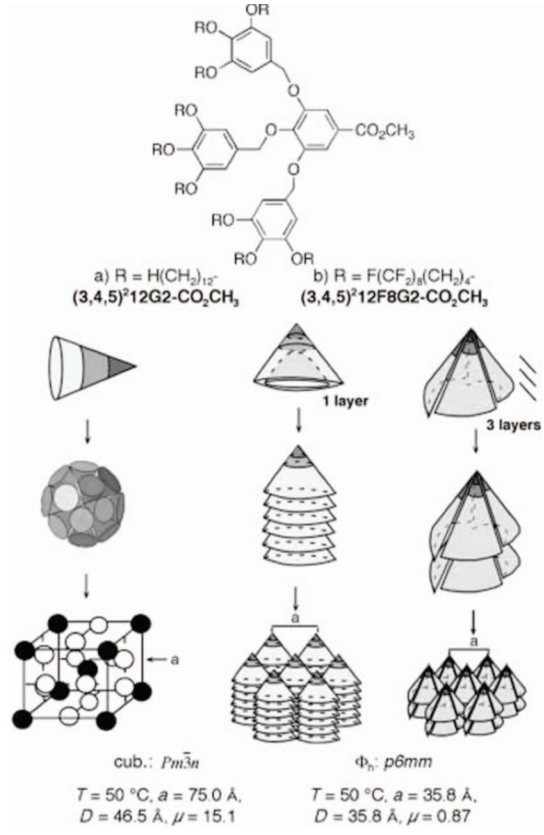

Figure 78. Fluorophobic effect changes the mechanism of self-assembly of G2 benzyl-ether dendrons from spherical to pyramidal columnar. Reprinted with permission from ref 361. Copyright 2003 Wiley-VCH Verlag GmbH & Co. KGaA.

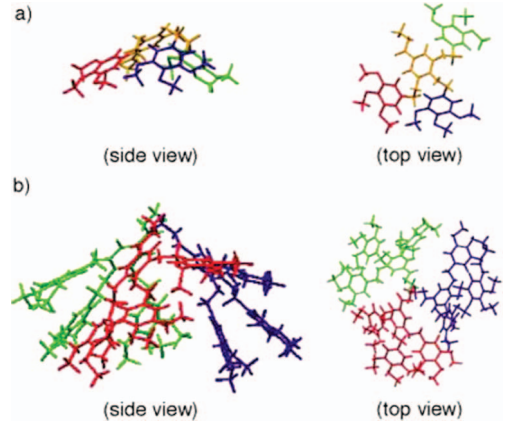

Figure 79. Guache-crown conformation forming pyramidal columns (a) and *trans*-taper conformation forming pine-tree columns (b). Reprinted with permission from ref 361. Copyright 2003 Wiley-VCH Verlag GmbH & Co. KGaA.

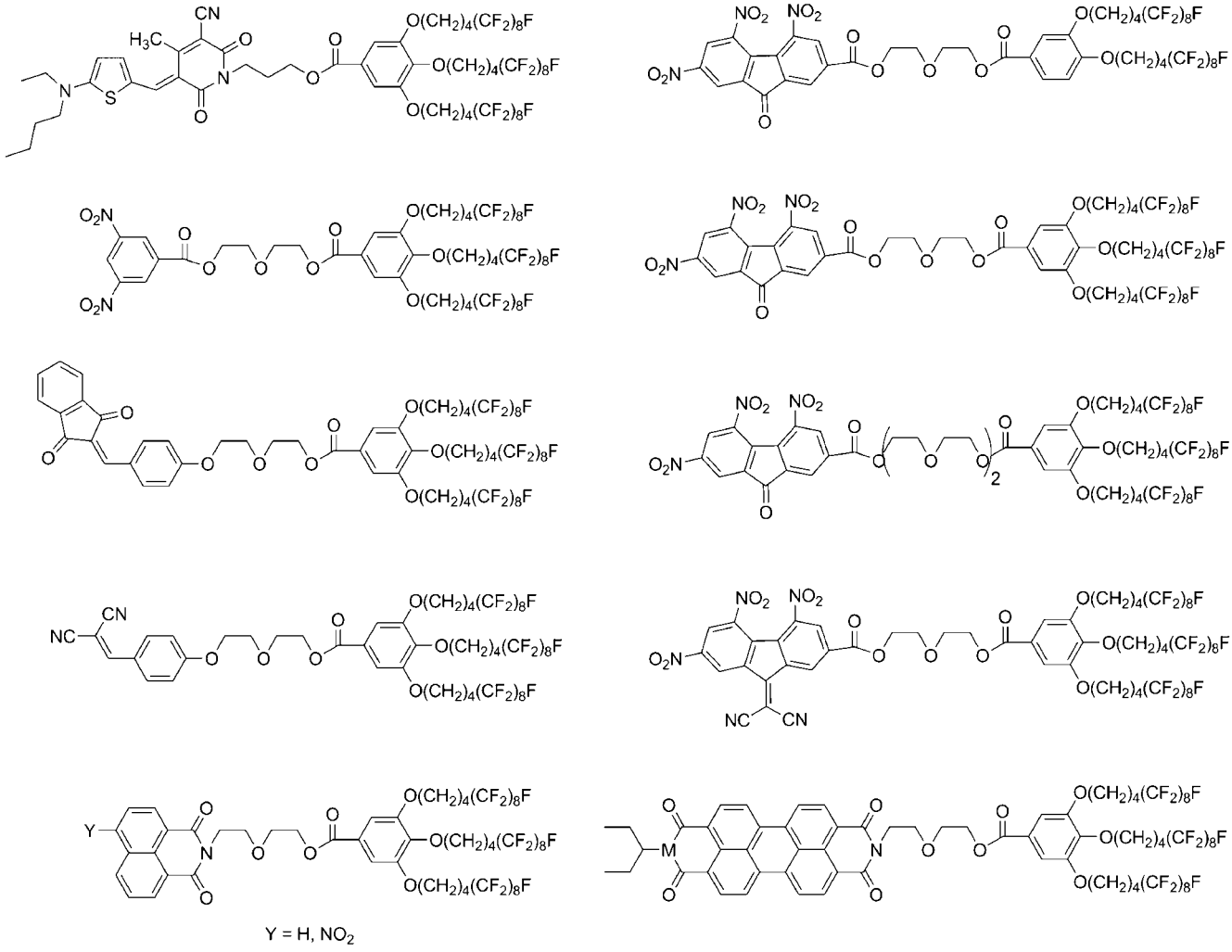

Figure 80. Structures of dendronized *n*-type acceptors.[363]

onto strategy often suffers from incomplete attachment, especially with high-generation dendrons resulting in lower surface coverage. In the grafting-from strategy, pioneered by Tomalia,[369,370] a dendronized polymer with generation one dendritic side chain is first prepared through a formal grafting-onto or macromonomer strategy. The G1 side chain is elaborated to higher-generation dendrons via a divergent growth strategy, and thus, this method suffers from dendritic side-chain polydispersity. As self-organizing dendronized polymers typically require a high degree of dendron structural perfection, i.e., a convergent approach to dendron synthesis, the grafting-from strategy is not typically employed. The macromonomer approach utilizes a dendron, typically constructed via the convergent strategy, which has been functionalized with a polymerizable group at the apex. This dendritic macromonomer is then polymerized or copolymerized to form a dendron-jacketed polymer. A prime advantage of the macromonomer approach is that modification of polymeric materials is not required and perfect dendron surface coverage can be achieved. It must be noted that the use of dendritic macromonomers that do not self-assemble can result in a decrease in the rate of polymerization due to a molecular weight dependent decrease in concentration as well as steric hindrance of the polymerizable group.[372,387,388] Formerly, it was claimed that high-generation nonself-assembling Fréchet-type dendrons do not homopolymerize but copolymerize with nondendritic monomers to some extent.[371,389] However, dendritic macromonomers that do self-assemble in bulk or solution can greatly accelerate the polymerization via an increase in the effective monomer concentration in the self-assembled state.[390]

3.1.2. Polymerization Methods and Implications for Use with Dendritic Macromonomers

The structure of the desired polymeric backbone dictates the method of polymerization to be employed. In the *dendritic macromonomer* approach, the sensitivity of the dendritic side chain to reaction conditions as well as the solubility of the dendritic macromonomer and dendron-jacketed polymer in the polymerization solvent can determine which specific technique is most appropriate. Polymethacrylates, polyacrylates, polystyrenes, and poly(vinyl ether)s are typically prepared through free-radical, anionic, or cationic polymerization or ring-opening metathesis polymerization (ROMP). Greater control can be achieved through a living polymerization[391] such as living anionic polymerization,[392,393] living cationic[394] and living cationic ring-opening polymerization,[395] living ROMP,[396] group-transfer polymerization[397−399] and living radical polymerization. Living radical polymeri-

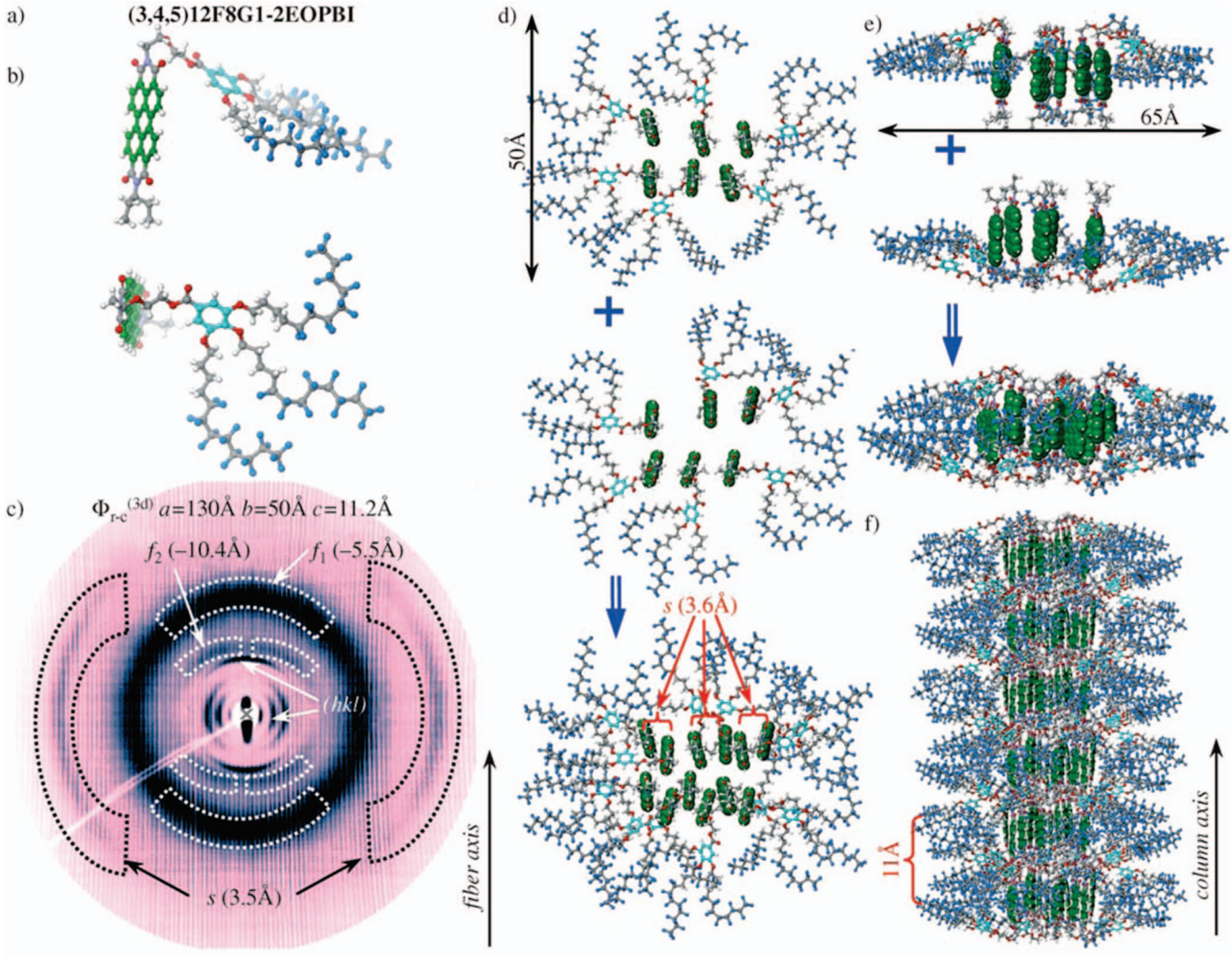

Figure 81. Self-assembly mechanism of (3,4,5)12F8G1−2EOPBI: side-view of dendron (a); top-view of dendron (b); XRD pattern of aligned sample (c); top view schematic of the layers coupling (d); side view of the layers coupling (e); side view of the supramolecular column (f). $s = 3.5$ Å stacking of the PBI core parallel to the column axis; $f_1 = 5.4$ Å average layer thickness correlation features; $f_2 = 10.4$ Å feature corresponding to every $i + 2$ layer registry; (hkl) = reflections of the $\Phi_{r\text{-}c}$ $c2mm$ lattice. Color code: PBI core, green; F, blue; O, red; C, gray; H, white; C of the phenyl ring, light. Reprinted with permission from ref 363. Copyright 2007 Wiley-VCH Verlag GmbH & Co. KGaA.

zation includes a diversity of techniques such as nitroxide mediated polymerization (NMP),[400,401] reversible addition/fragmentation transfer polymerization (RAFT),[402−404] macromolecular design via the interchange of xanthates (MADIX),[405,406] cobalt-mediated living radical polymerization,[407,408] atom-transfer radical polymerization (ATRP),[409] single-electron transfer living radical polymerization (SET-LRP)[410,411] or single-electron transfer degenerative chain transfer living radical polymerization (SET-DTLRP),[412,413] organotelluride mediated LRP (TERP), organostibine mediate LRP (SBRP),[414] or the Iniferter method.[415] Main chain polyethers are often prepared through phase-transfer catalyzed polyetherification.[416]

Conjugated polymers are often prepared via step-growth techniques such as the Suzuki,[417] Sonogashira,[418] and other polycondensation strategies. Under certain conditions, step-growth Suzuki polycondensation can be converted to a living chain-growth mechanism.[419] Poly(arylacetylene)s are prepared via alkyne metathesis polymerization[420] or living insertion polymerization using Noyori's catalyst.[421] Mixed saturated/unsaturated polymers are often prepared via ROMP.

3.2. Linear Polymers Jacketed with Dendrons Attached via their Apex

Dendron-jacketed linear polymers can be divided into three topological categories: (i) linear polymers jacketed with dendrons attached via their apex (Figure 1, first row left and middle and second row left); (ii) linear polymers jacketed with dendrons and dendrimers attached via their periphery (Figure 1, second row right and third row left and middle); (iii) linear-block copolymers jacketed with dendrons (Figure 1, first row right). Linear polymers jacketed with dendrons attached via their apex constitute the majority of systems described. This class of dendronized polymer will be examined first and subdivided according to backbone structure.

3.2.1. Poly(siloxane)s

In 1989 Ringsdorf[422] and Percec[195] described the first liquid crystalline (LC) polymers containing hemiphasmidic side chains, consisting of a half-disk first-generation dendron attached to a rigid-rodlike moiety. In Ringsdorf's polymer,

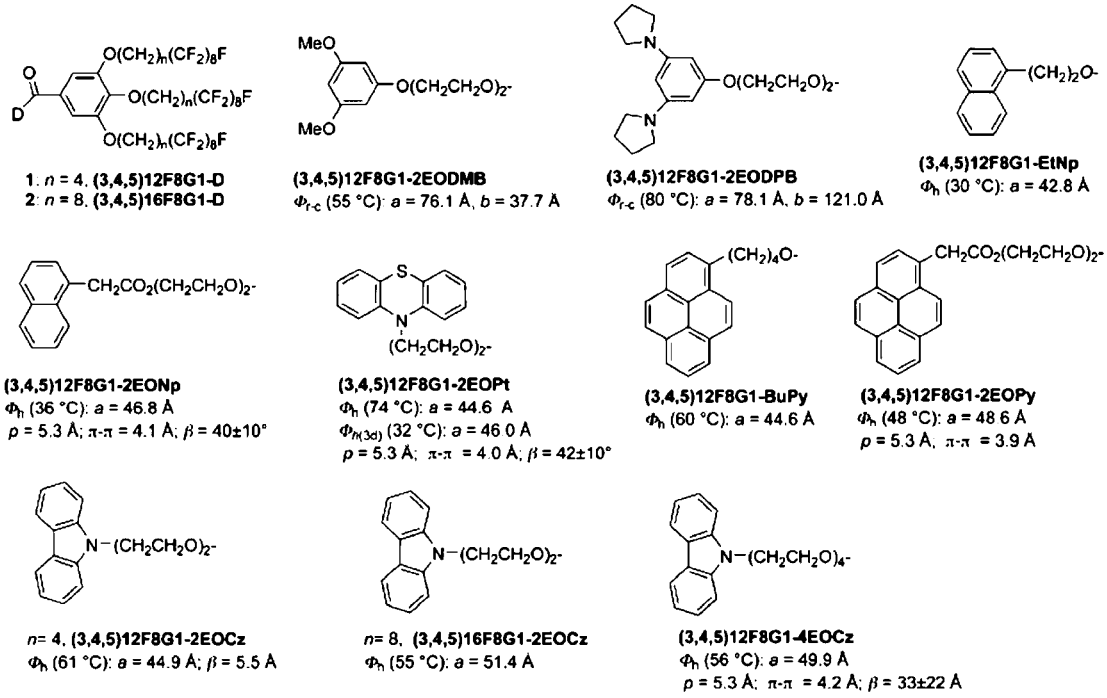

Figure 82. Semifluorinated Percec-type dendrons (top left) and donor apex groups. Reprinted with permission from ref 364. Copyright 2008 Wiley-VCH Verlag GmbH & Co. KGaA.

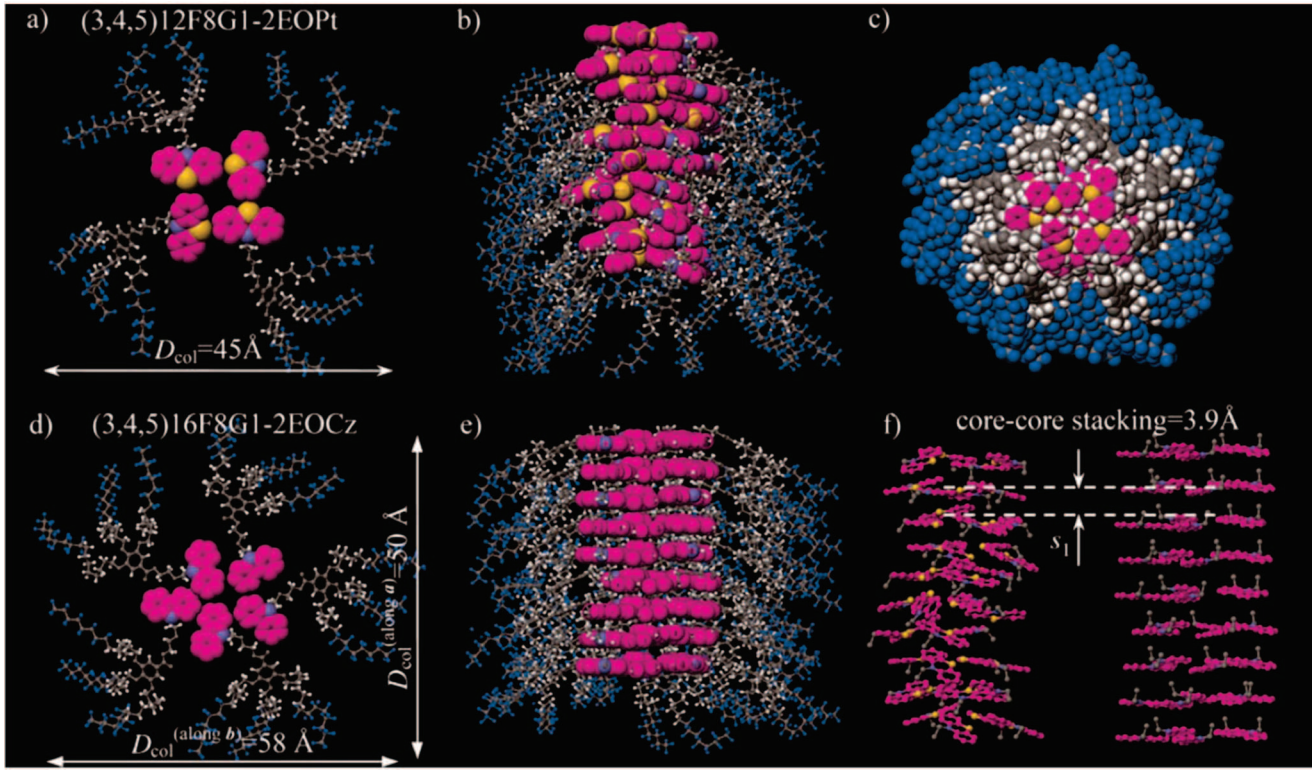

Figure 83. Self-assembly of dendronized phenothiazine and carbazole. Top views of a single stratum (a, d) and side views of the column (b, e). Space-filling top view of the column of dendronized phenothiazine (c). Comparison between columns with (right) and without (left) intracolumnar order (f). Reprinted with permission from ref 364. Copyright 2006 Wiley-VCH Verlag GmbH & Co. KGaA.

which will be referred to as a Class I poly(siloxane) LC polymer, half-phasmidic groups were connected to a flexible poly(methyl siloxane) main chain via a spacer using a grafting-onto approach involving hydrosilylation with a platinum divinyltetramethyldisiloxane complex catalyst (Figure 89, Scheme 24). The resulting polymer exhibited a S phase as determined by TOPM and XRD studies.

Inspired by the paraffin-coated half-phasmidic molecules of Malthête,[423] Percec's laboratory reported two other classes of liquid crystalline polymers containing half-phasmidic sides groups (section 2.2.1 and Figure 8). They were reported in a series of publications from 1989 to 1991 (Figure 89). Using similar grafting-onto chemistry as Ringsdorf, Class II LC polymers[195,197,424] were constructed via attachment of 3,4,5-

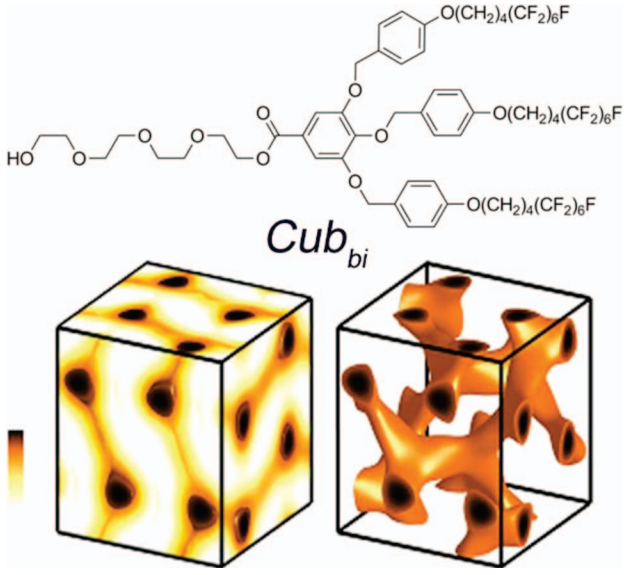

Figure 84. Amphiphilic dendron with semifluorinated periphery that self-organizes into the bicontinuous cubic phase (Cub_{bi}) with $Ia\bar{3}d$ symmetry (a) and corresponding relative electron density volumetric distribution that schematically illustrates the interlocked network of the bicontinuous phases (b).[366]

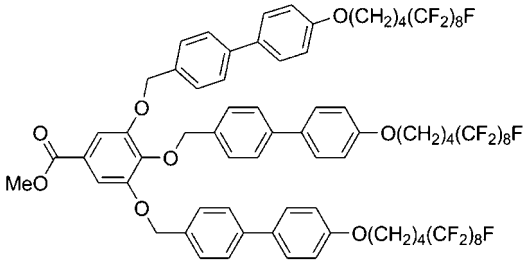

Figure 85. Structure of (4Bp-3,4,5)12F8G1−CO_2Me.[368]

tri[*p*-(*n*-dodecan-1-yl-oxy)benzyloxy]benzoic acid (4-3,4,5)12G1−COOH (formerly referred to as DOBOB) to a vinyl terminated linker. The vinyl periphery was grafted-onto poly(methylsiloxane) via hydrosilylation through platinum divinyltetramethyldisiloxane complex as catalyst. Class III LC polymers[198,199,201−203] were similar to Class I LC polymers described by Ringsdorf, differing only in the nature of the aliphatic periphery and linker groups. Despite some structural similarities between the Class I LC polymers described by Ringsdorf, their self-organization is notably different. Class II LC polymers and copolymers self-organize into a Φ_h phase as evidenced by their focal conic LC texture, while Class I LC polymers were suggested to exhibit a S mesophase. Class III LC polymers self-organize into Φ_h phases but also provided the first examples of LC polymers with thermoreversible Φ_h−S transitions.[201]

Méry prepared poly(methylsiloxane) jacketed with AB_3 carbosilane dendrimers via a grafting-from approach (Figure 89, Scheme 25).[425] Allyltrichlorosilane was grafted-onto poly(methylsiloxane) using platinum divinyltetramethyldisiloxane as catalyst. AB_3 branching was achieved via treatment with allyl magnesium bromide. Higher-generation dendrons could be prepared through Pt-catalyzed hydrosilylation of the terminal alkenes with $HSiCl_3$ and subsequent treatment with allyl magnesium bromide. While wormlike structures were observed, no self-organization was reported. Kim also developed an approach to poly(methylsiloxane) jacketed with a variety of G1 AB_2 carbosilane dendrons,[426] and later, higher-generation AB_3 and hybrid AB_3−AB_2 carbosilane dendrons.[427]

3.2.2. Polymethacrylates, Polyacrylates, Polystyrenes, Poly(vinyl ether)s, Poly(maleimide)s, and Poly(epichlorohydrin)s

In the initial report of Percec-type dendrons grafted-onto poly(siloxane)s, the preparation of poly{[4-(11-methacryoyloxy)undecyloxybenzoyloxy]-4′-[3,4,5-tris(4-(dodecyl-1-oxy)-benzyloxy)benzoate]bipheny} poly[(4-3,4,5)12G1−BpB−C11−MA] via a dendritic macromonomer approach was also disclosed.[195] Poly[(4-3,4,5)12G1−BpB−C11−MA] was shown to self-organize into a Φ_h phase (Figure 90).

Later, a series of poly{4-[(3,4,5)12G1−COO]-4′-[(2-vinyloxy)ethoxy]biphenyl} (poly[(3,4,5)12G1−BP−EO−EVE]) with DP varying from 2.7−8.0 were prepared via living cationic polymerization of the corresponding dendritic vinyl ether macromonomer (Figure 92).[203,205] The polymers with DP ≤ 5 self-assemble via *exo*-recognition of the tapered dendritic side chains into discrete discotic blocks that stack to form columns which self-organize into a Φ_h lattice. For one particular case with DP = 4.4, a re-entrant isotropic (I_{re}) phase was observed when cooling the Φ_h phase (Figure 91).

Similarly, a series of poly[(2-ethoxyvinyl)-OOC-(4-3,4,5)12G1] (poly[(4-3,4,5)12G1−EO−EVE]), with DP varying from 3.7−16, was prepared through living cationic polymerization of the corresponding dendritic macromonomer (Figure 92).[203] At DP ≤ 4, these polymers self-organize into discs that stack to form a Φ_h phase. At DP > 4, these polymers self-assemble directly into columnar architectures that self-organize into a Φ_h lattice. Regardless of the DP, the polymers exhibit an enantiotropic Φ_h phase on heating followed by an N phase. On cooling only an enantiotropic N phase was observed. The temperature of the Φ_h−N transition was largely independent of DP. This process is mimetic of self-assembly process of viral capsid proteins of the tobacco mosaic virus (TMV):[156,428,429] (a) self-organized discs of tapered capsid protein form helical "lock-washers" and (b) RNA threading through the lock-washer is followed by the stack of additional lock-washer supramolecules until the entire RNA length is encapsulated (Figure 15).[224,232]

It was expected that the length and nature of the linkage between the dendritic side chain and the main chain would influence the architecture and self-organization properties of the dendronized polymer. A similar series of poly[(4-3,4,5)12G1COO−*n*EO−MA], where $n = 1-4$ is the length of the oligo(ethylene oxide) (EO) linker, was prepared via free-radical polymerization initiated with AIBN of the corresponding dendritic methacrylate (Figure 93).[208,204] The structures of poly[(4-3,4,5)12G1COO−*n*EO−MA] were compared with those of their monodendritic analogues (4-3,4,5)12G1COO−*n*EO].[227,228,230,234,235,430] Both the dendron-jacketed polymers and the corresponding dendrons self-organized into Φ_h lattices with similar column diameters and numbers of dendrons per column stratum, μ. In all cases, the steric demands of the PMA backbone result in slightly larger column diameters than the corresponding dendron. Increasing the length of the EO spacer increases the diameter of the column and decreases the Φ_h−I transition temperature ($T_{\Phi h\text{-}i}$). Conversely, complete removal of the EO spacer decreases the column diameter and increases the temperature of the Φ_h−I transition.[431] The effect of LiOTf and NaOTf

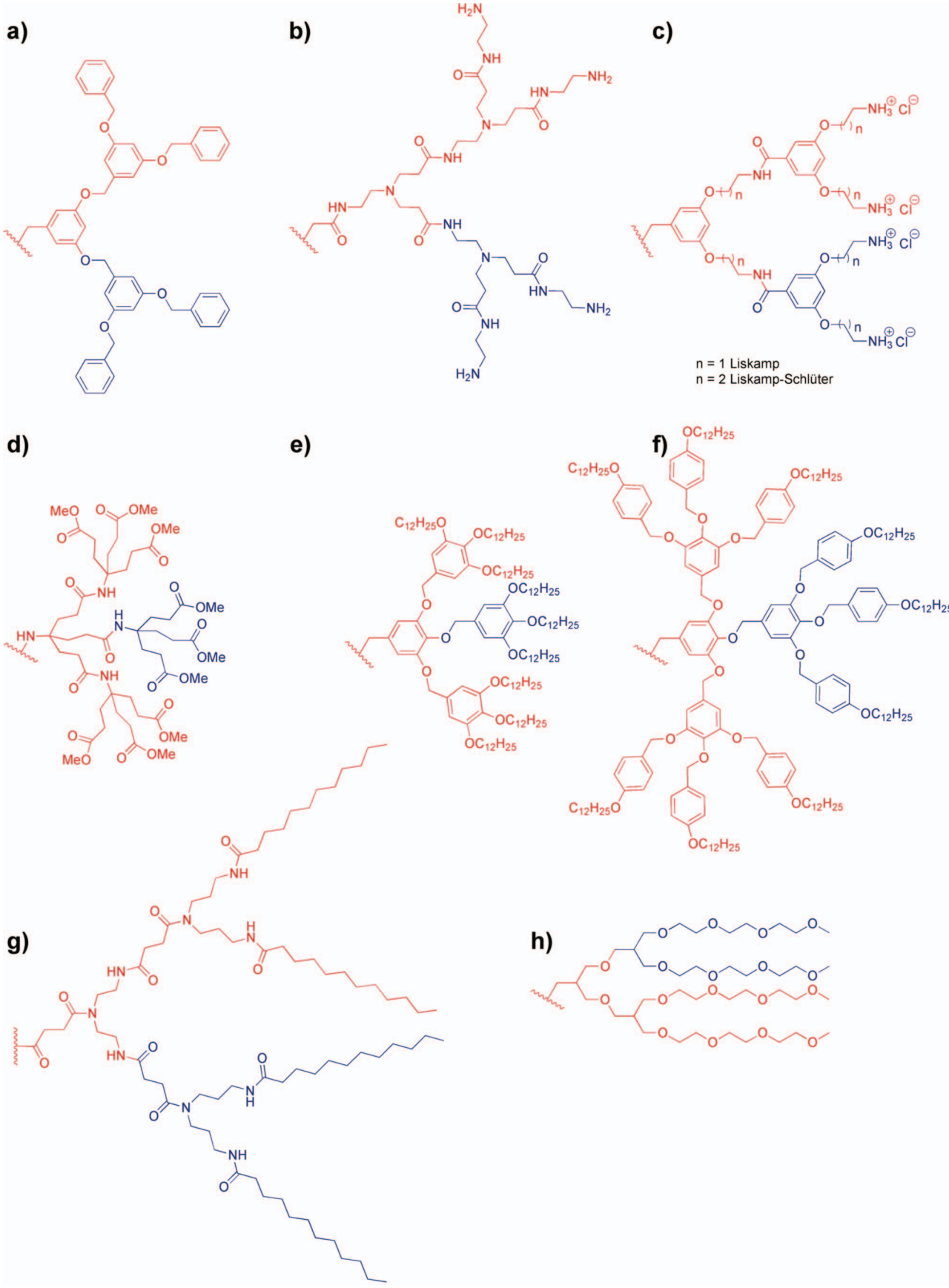

Figure 86. Structure of generation 1 (blue) and generation 2 (red) of Fréchet (a), Tomalia-PAMAM (b), $n = 1$ Liskamp and $n = 2$ Liskamp-Schlüter (c), Newkome dendrons (d), Percec-type 1 dendrons (e), and Percec-type 2 (f) dendrons, Kim amphiphilic dendrons (g), and Fréchet PEO dendrons (h).

salts was also studied.[209] The complexation of the EO spacers with the triflate salts stabilizes the columnar architecture via a network of ion−dipole interactions, thereby increasing the $T_{\Phi h\text{-}i}$. The dendritic analogues were able to accommodate

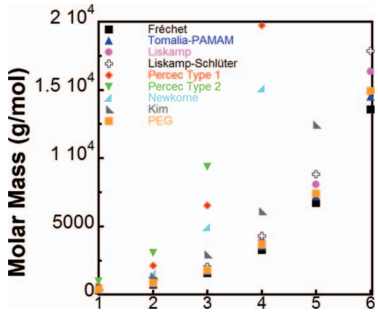

Figure 87. Molecular weight vs generation number for the most frequently employed classes of dendrons (structures shown in Figure 86).

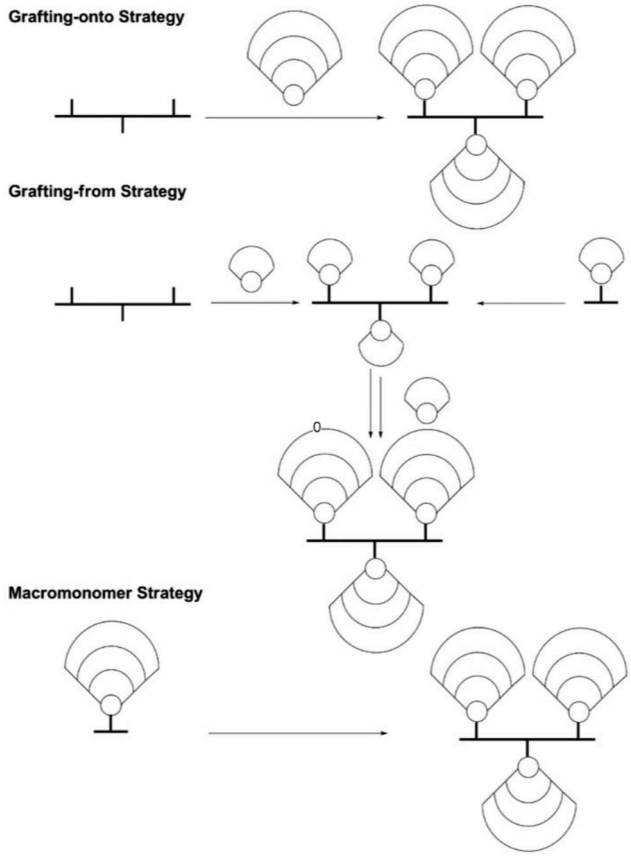

Figure 88. Synthetic strategies for dendronized polymers. Adapted with permission from ref 71. Copyright 1998 Springer Science.

more salt into their column backbone, providing greater increases to $T_{\Phi h\text{-}i}$ per equivalent of salt added. Increasing the length of the EO segment increases the amount of salt uptake possible. No significant difference was observed in the efficacy of Li vs Na. Poly[(3,4,5)*m*G1COO−*n*EO−MA] where $m = 7$, 12, and 18 and $n = 1$, 2, 3, and 4 were studied, yielding similar results.[213] Dendron analogues (3,4,5)*m*G1COO−*n*EO did not self-assemble into Φ_h lattices because of their small taper angle. Complexes of poly[(3,4,5)*m*G1COO−*n*EO−MA] mixed with 2% LiOTf demonstrated relatively high ion conductivity.[442] Interestingly, while there was an increase in conductivity between the crystalline (*k*) and Φ_h phase, continuing to the isotropic phase (I) did not substantially alter the conductivity. Systematic studies on the birefringence and turbidity of (3,4,5)12G1COO−4EO and poly[(3,4,5)12G1COO−4EO−MA] have also been conducted.[432]

Binary mixtures of **P1** poly[(4-3,4,5)12G1COO−*n*EO−MA] and **P2** poly[(4-3,4,5)12G1COO−*m*EO−MA] where $m \neq n$ were also prepared.[433] At low mol % of **P2**, the polymers are miscible and result in a binary composition with a single Φ_h−I transition. Above 40 mol % **P2**, the polymers are largely immiscible, resulting in two distinct Φ_h−I transitions that closely match those of the respective homopolymers. In the same study, binary mixtures of poly[(4-3,4,5)12G1COO−*n*EO−MA] with the dendritic equivalent (4-3,4,5)12G1COO−*n*EO were also prepared. Up until about 40 mol % dendron, the dendron was found to intercalate with the dendronized polymer as indicated by a single Φ_h−I transition at a relatively fixed temperature (Figure 94). Above 40 mol % dendron, a smaller secondary Φ_h−I transition emerged corresponding to dendron that cannot be accommodated inside the saturated dendronized polymer.

Additionally, deuterium-modified poly[(4-3,4,5)12G1COO−4EO−MA] has been prepared wherein the inner phenyl ring has been deuterated and a methoxy branch *ortho* to the dodecyloxy periphery was introduced (Figure 95).[434] Similar Φ_h self-organization was suggested, and these molecules were predicted to exhibit cooperative rotation on account of the methoxy branch, making these dendronized polymers candidates for molecular rotors.

More detailed XRD analysis of the Φ_h formed from poly[(4-3,4,5)12G1COO−4EO−MA] provided greater structural insight.[208] Oriented fibers prepared at 60 °C and cooled to room temperature (RT) exhibited eight equatorial reflections in small-angle X-ray scattering (SAXS) and two additional layer lines in wide-angle X-ray scattering (WAXS), providing for the first time information about the "crystal" structure within the "noncrystallizable" columns. Strong off-meridional maxima suggested that the dendrons were tilted as opposed to perpendicular to the columnar axis, and "pine-tree" models of self-organization with 8_0, 8_1, 8_4 symmetry were proposed (Figure 96).[435,436] 8_0 and 8_4 pine-tree structures are nonhelical, in that each stratum forms a closed disk, while the 8_1 structure is a continuous helical architecture. However, at the time, it was not possible to distinguish between helical and nonhelical columnar assemblies. The structures with helical internal order without long-range column−column correlation are similar to that observed for the TMV (Figure 15).[156] Results to be published soon will demonstrate the helical model to be the correct one.

Increasing the temperature of the oriented fiber from room temperature to the crystalline hexagonal columnar phase ($\Phi_{h,k}$)−Φ_h transition (~40 °C) results in a loss of intracolumnar order.[437,438] Further, the structure decreases in diameter from 60.4 Å at 40 °C to 54 Å at 95 °C,indicating a continual change in the columnar architecture. Compared to the dendron (4-3,4,5)12G1−4EO, the introduction of a covalent PMA backbone does not significantly affect the self-organization, but rather it simply increases the columnar diameter in accordance with the steric demands of the polymeric backbone.[439] On the other hand, transition from a supramolecular to a macromolecular structure results in a significant increase in the Φ_h thermal stability (>40 °C). Because of the more complex kinetics of self-organization of the polymerized macromolecule versus the dendron (4-3,4,5)12G1−4EO precursor, recooling of the fiber from Φ_h to $\Phi_{h,k}$ does not reveal the same structure but rather one with 10% larger column diameter.[440] As-drawn fibers of poly[(4-

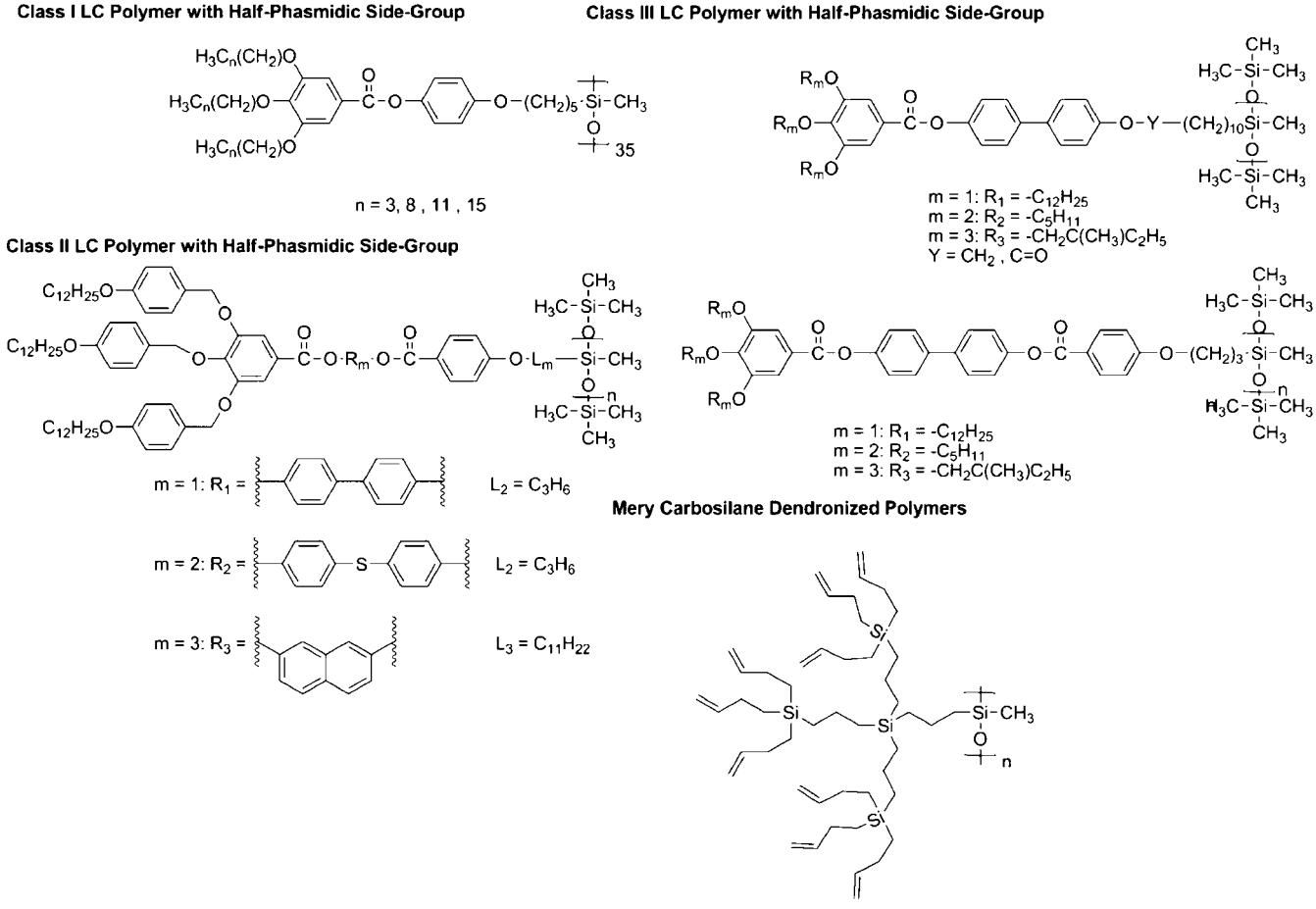

Figure 89. Dendronized poly(siloxane)s.

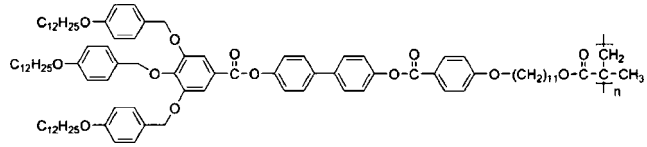

Figure 90. Poly{[4-(11-methacryoyloxy)undecyloxybenzoyloxy]-4′-[3,4,5-tris(4-(dodecyl-1-oxy)benzyloxy)benzoate]biphenyl}.[195]

Scheme 24. Representative Synthesis of Poly(Siloxane)s Jacketed with Percec-type Dendrons[201]

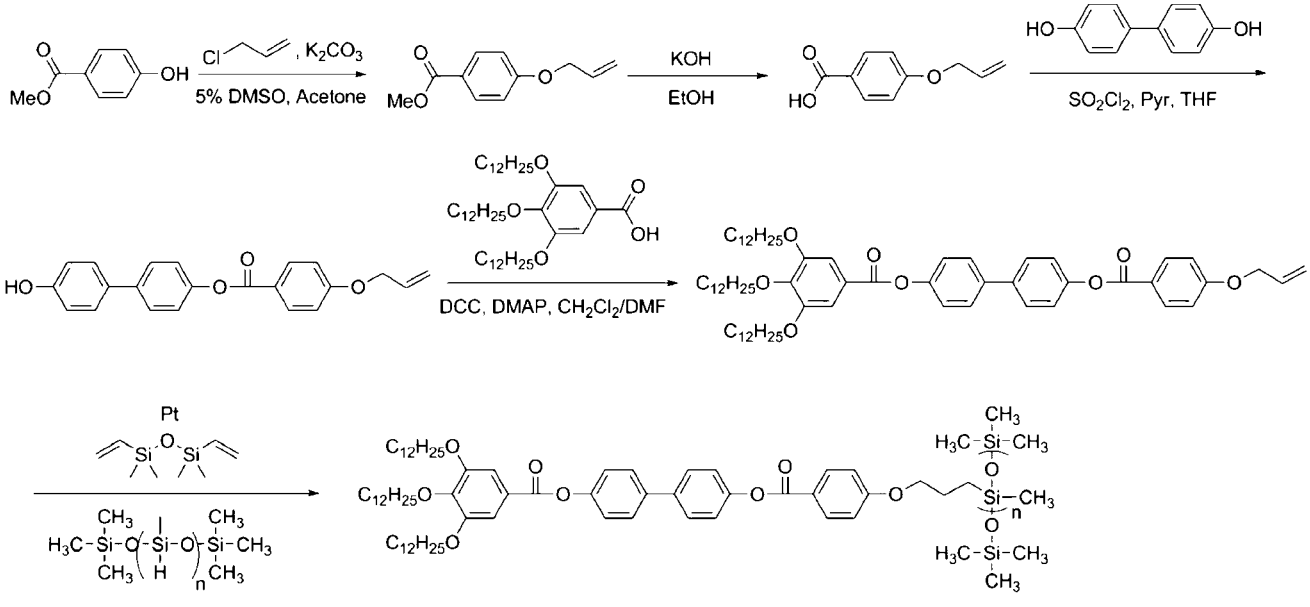

Scheme 25. Synthesis of Poly(siloxane)s Jacketed with Carbosilane Dendrimers[425]

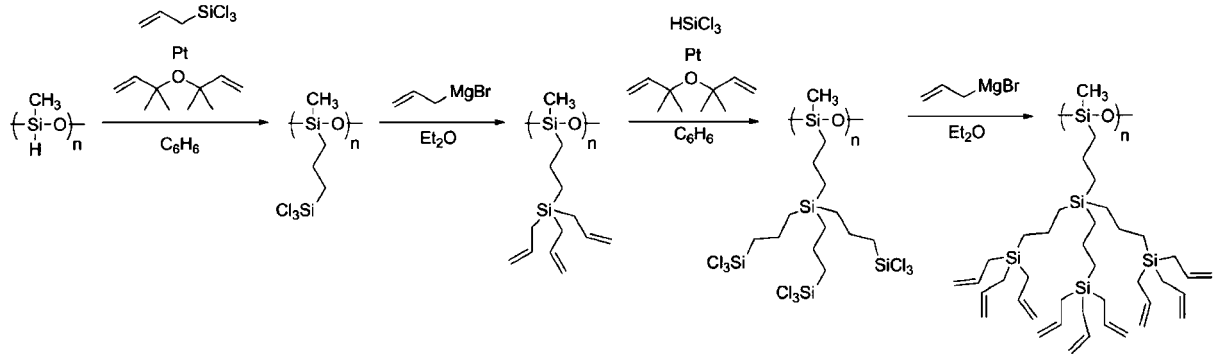

3,4,5)12G1−4EO−MA] revealed extra Bragg reflections that correlated to the coexistence of monoclinic oblique, rather than Φ_h array (Figure 97).[441] This secondary phase is eliminated in successive heating and cooling cycles.

As mentioned in section 2.2.1, Percec demonstrated that self-assembly of (4-3,4,5)12G1 does not require the presence of a covalent polymer backbone. In the presence of Na, K, or Li triflates, (4-3,4,5)12G1 functionalized at the apex with benzo-15-crown-5[210,212,442,443] (section 6.1) or methoxy-terminated oligo(ethylene oxide)[208,209,442,444] (section 4.1.1)

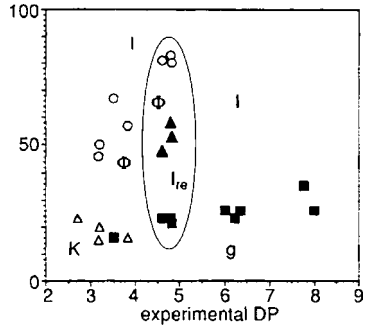

Figure 91. Phase diagram indicating I_{re} when DP = 4.4. Reprinted with permission from ref 205. Copyright 1992 Royal Society of Chemistry.

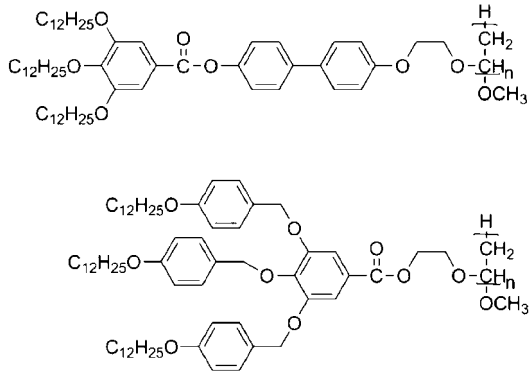

Figure 92. Poly(vinyl ether)s bearing Percec-type dendron side chains.[203]

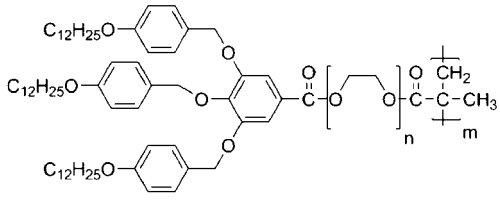

Figure 93. Structure of poly[(4-3,4,5)12G1−*n*EO−MA].[208]

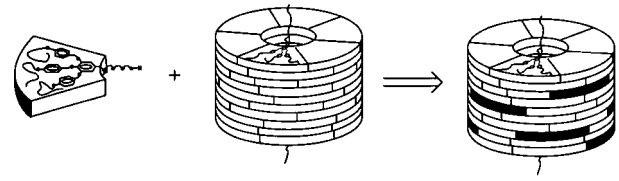

Figure 94. Intercalation of (4-3,4,5)12G1−3EO into poly[(4-3,4,5)12G1−3EO−MA]. Reprinted with permission from ref 433. Copyright 1994 Taylor and Francis.

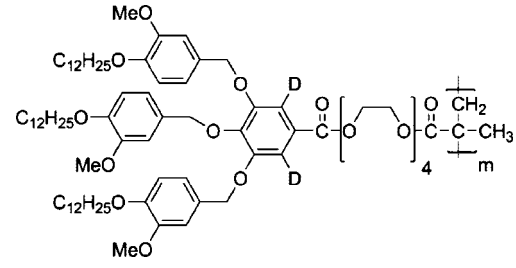

Figure 95. Structure of deuterated and periphery modified poly[(4-3,4,5)12G1−4EO−MA].[434]

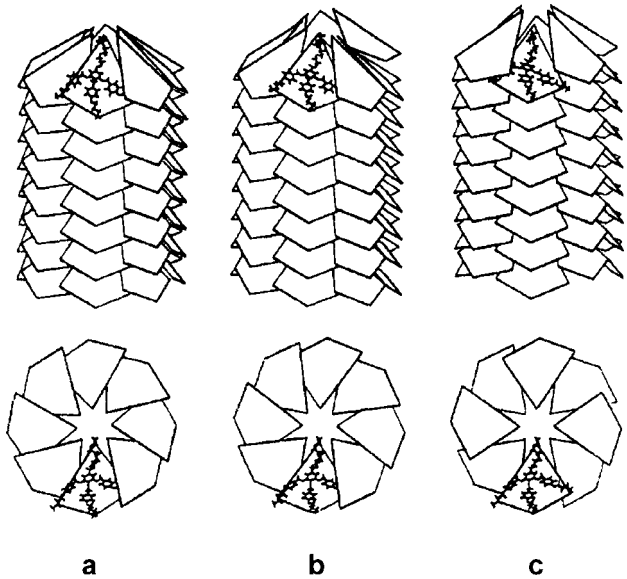

Figure 96. Pine-tree models of poly[(4-3,4,5)12G1−4EO−MA] self-assembly with (a) nonhelical 8_0, (b) helical 8_1, and (c) nonhelical 8_4 symmetry. Reprinted with permission from ref 437. Copyright 1995 American Chemical Society.

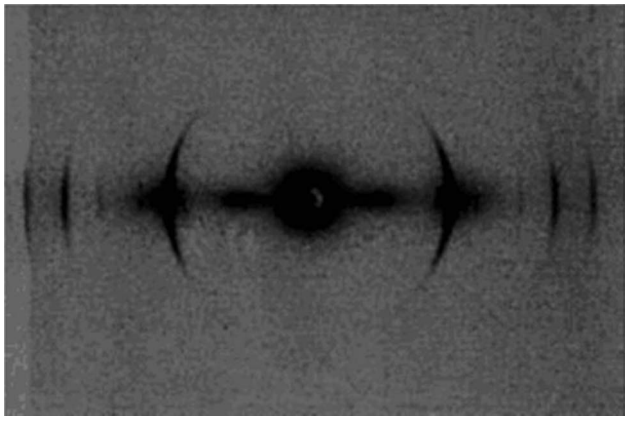

Figure 97. Small-angle X-ray pattern for an as-drawn oriented fiber of poly[(4-3,4,5)12G1−4EO−MA] exhibiting primary and secondary diffractions. Reprinted with permission from ref 441. Copyright 1999 Wiley-VCH Verlag GmbH & Co. KGaA.

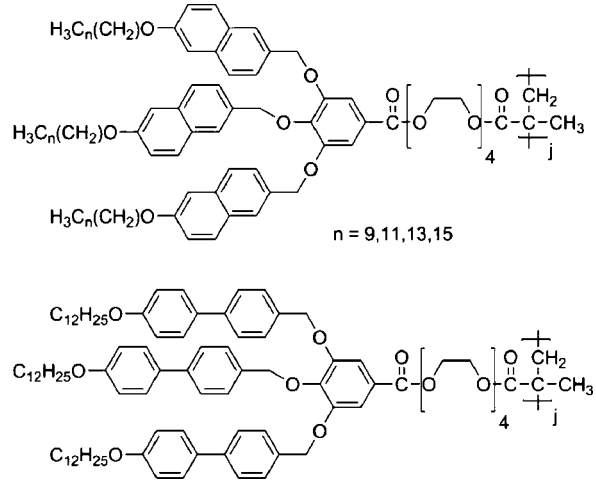

Figure 98. Periphery and aromatic parts modified poly[(4-3,4,5)*n*G1−4EO−MA].[343]

self-assemble into supramolecular helical columns that self-organize into a Φ_h^{io} lattice with internal helical order at low temperature and Φ_h LC phase at elevated temperature. Without alkali salt, only Φ_h^{io} phases are observed. The alkali salt destabilizes the crystalline phase, allowing for LC behavior. The crown-ethers (section 6.1) or *n*EO (section 4.1.1) structures occupy the center of column. Chain-like ion−dipole interactions between the crown-ethers and the alkali salts constitute a virtual supramolecular backbone (Figure 1, second row middle).

The columnar self-assembly of (4-3,4,5)*n*G1 jacketed PMA is robust and tolerates chain-length modification and changes to the molecular framework (Figure 98).[343] Changing the architecture of the dendron to incorporate a larger periphery aryl unit such as naphthalene poly[(4Nf-3,4,5)*m*G1−*n*EO−MA] results in a similar Φ_h architecture with a slightly increased columnar diameter. These studies provided proof of intracolumnar microphase segregation during the self-assembly and self-organization of polymers jacketed with Percec-type dendrons. Figure 99 demonstrates the variation of the dimensions of the overall columnar architecture and the size of each segregated domain in accord with structural modification of alkyl tail, periphery aromatic group, and EO linkage. Increasing the alkyl tail length provides a small linear increase in the overall dimensions of the aliphatic periphery. Increasing the size of the periphery aromatic unit enhances the size of the overall columnar architecture and of the aromatic domain in proportion to the size of the aromatic unit. Elongating the EO spacer increases the size of all domains; however, this increase is not linear, indicating some compaction of longer-chain ethylene oxide spacers. The thermal stabilities of the Φ_h phase also increased with the larger aromatic periphery units and increasing aliphatic tail length.

The effect of branching architecture on the self-organization of dendron-jacketed polymethacrylate and polystyrene was studied through the attachment of a diverse array of Percec-type dendrons (Figure 101).[445] An earlier study,[390,446,447] replicated in this more diverse library, demonstrated that self-assembling dendritic monomers generate a self-encapsulated reactor. Conventional radical polymerization of these dendronized macronomoners provided low molecular weight (MW) polymers with narrow polydispersity (as low as $M_w/M_n \approx 1.05$) at low concentration and very high molecular weight polymers with broader polydispersity at higher concentration. Extremely high MW polymers can be prepared in less than 5 min, though with somewhat broader M_w/M_n. Evidence for a self-encapsulated reactor was provided by the dependence of the rate of polymerization R_p on the dendritic macromonomer concentration. Above a critical concentration of 0.20 mol/L, the R_p rose sharply by 2−3 orders of magnitude (Figure 100). The nonlinear growth of ln R_p versus ln $[M_o]$ indicated an increase in effective monomer concentration by self-encapsulation above the critical monomer concentration.

The polymerization kinetics of self-assembling dendritic macromonomers starkly contrasts earlier studies of nonself-assembling dendritic macromonomers. Homopolymerization of G4 Fréchet dendrons did not proceed.[371,389] However, its copolymerization with a low molar mass comonomer could be accomplished.[371,389] Other nonself-assembling dendritic macromonomers could not be homopolymerized without a long flexible spacer in the macromonomer (Figure 1, first row middle) or extremely long reaction times.[372,387,388,533] Characterization of PMA and PS jacketed with Percec-type dendrons was conducted by size-exclusion chromatography (SEC) with both concentration and multiangle light-scattering detectors (SEC-MALLS) using established methods.[448] First, it was found that the relationship between elution volume V_e or R_g and DP was not linear and high molecular polymers were eluting at multiple volumes including those with low DP fractions. Thus, very high molecular weight dendronized polymers may appear to have artificially low DP. Care must be exercised in ensuring the proper determination of MW in these high molecular weight regions. Further, the radius of gyration R_g and the hydrodynamic radius R_h for PMA and PS jacketed with certain Percec-type dendrons is significantly larger than expected for linear poly(methyl methacrylate) (PMMA) and PS. The enhanced R_g and R_h is due to the formation of rigid-rod structures that are elongated in comparison to the random-coil conformation of the nondendronized polymers.

In all cases except $(3,5)^2$12G2 jacketed PS, Φ_h organization was observed by XRD. Through modification of the primary structure of the dendron, the columnar dimension could be varied from 41 to 50 Å and the number of dendrons forming a stratum could be varied from 1.9 to 7. Structural differences between dendronized PMA and PS were not significant. Direct visualization of these highly "photogenic"[449] molecules

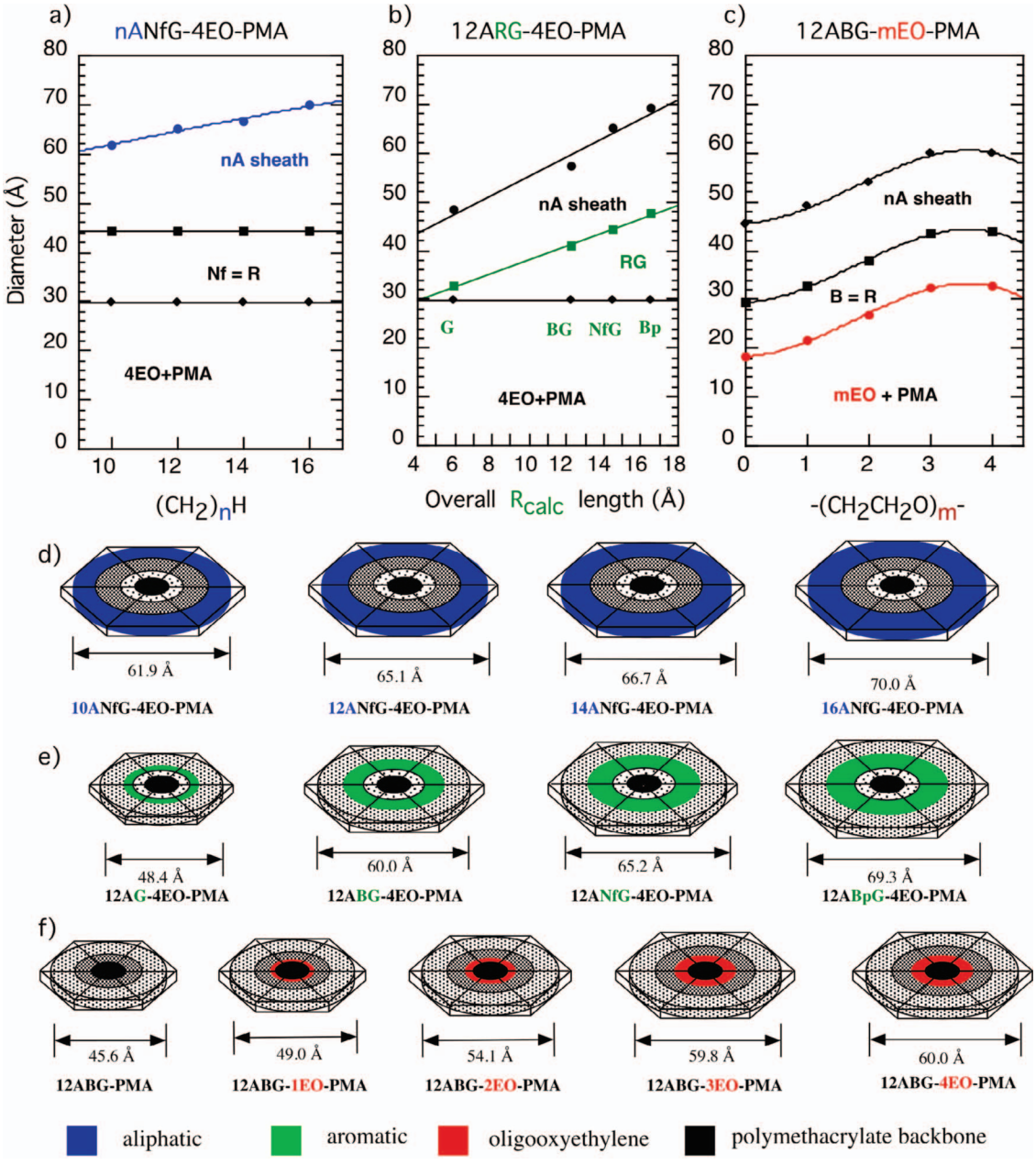

Figure 99. Dependence of the macromolecular column (*a*, Å) diameter and the diameter of its constituent microphase segregated components on (a) alkoxy chain length in the poly[(4NF-3,4,5)12G1−*n*EO−MA] series, (b) overall aromatic group length, which includes the interior and periphery aromatic groups, and (c) oligooxyethylene segment length for the poly[(4-3,4,5)12G1−*m*EO−MA] series (d−f). Schematic representation of a column cross section of polymethacrylates in the Φ_h LC phase. Reprinted with permission from ref 343. Copyright 1998 American Chemical Society.

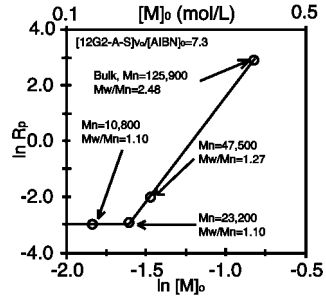

Figure 100. ln R_p vs ln [M_o]. Reprinted with permission from ref 390. Copyright 1997 American Chemical Society.

on surfaces was also performed, confirming cylindrical organization without interpenetration of the side groups (Figure 103).[450,451] Calculation of the persistence length *a′* and Kuhn length l_k indicates extremely stiff polymers with values intermediate between PMA-*g*-PS obtained via PS macromonomers with MW =1740 and 2740, respectively,[452] and far greater than those obtained for PMA jacketed with Fréchet-type dendrons.[374] Furthermore, the visualization of individual polymer chains allowed for the first time direct determination of chain length and diameter. These dimensions were in agreement with those determined by XRD and light-scattering. Direct visualization has since been developed into a powerful tool for the determination of molecular weight distribution and polymer dimensions. Length polydispersity can be calculated (Figure 102b) directly from the histogram of SFM observed contour lengths (Figure 102a).[450]

SFM spin-coated films of (4-3,4,5)14G1- and $(3,4,5)^2$12G2-jacketed polystyrene revealed well-ordered 2-D architectures.[453] Densely branched $(3,4,5)^2$12G2-jacketed PS was not

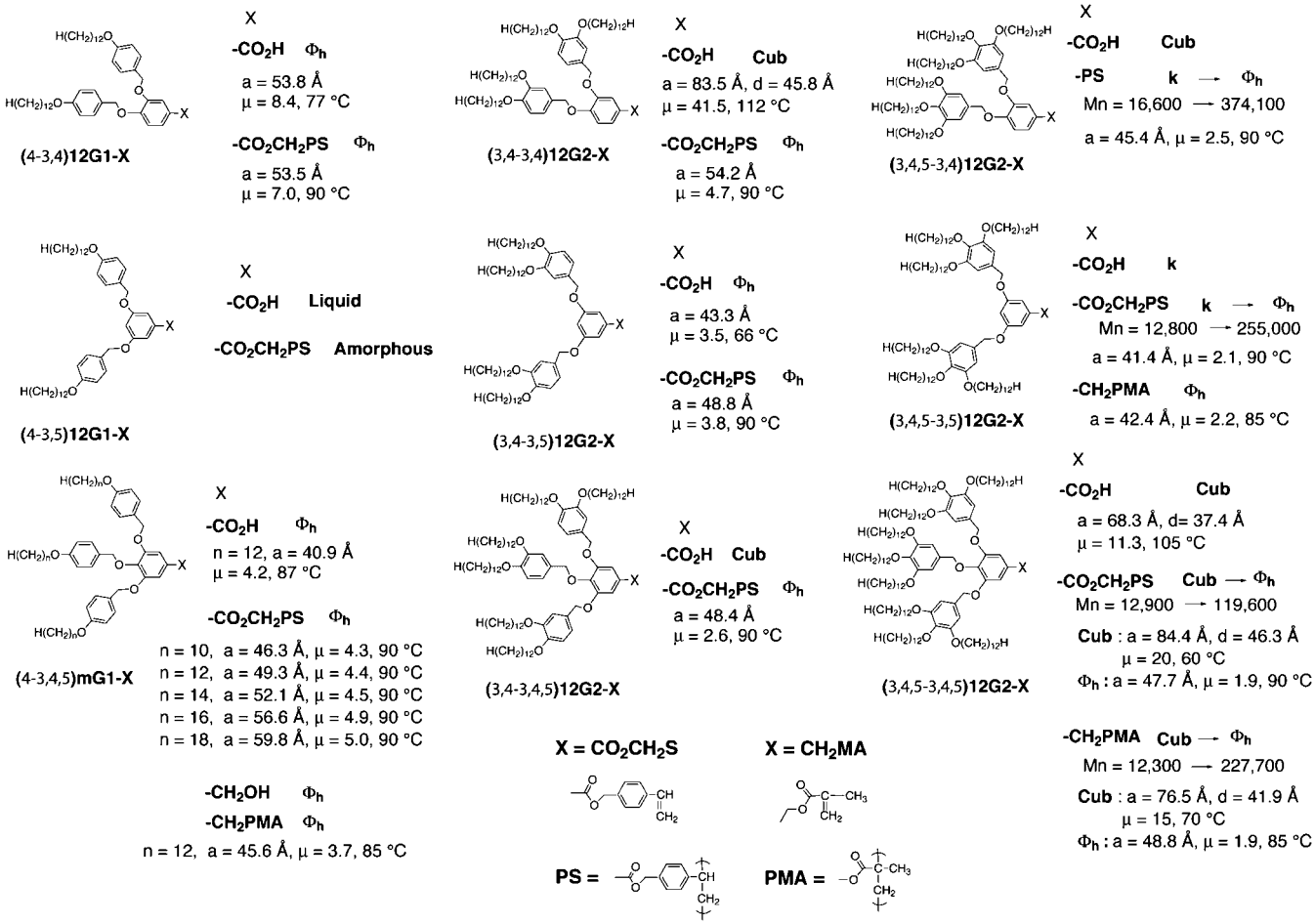

Figure 101. Structures and self-assembly features of a library of dendronized PMA and PS. Reprinted with permission from ref 445. Copyright 1998 American Chemical Society.

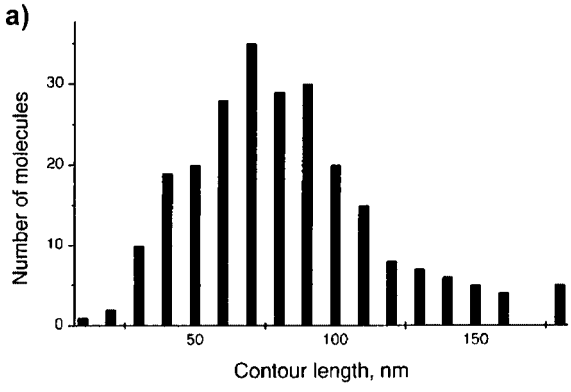

b)

$$L_w = \frac{\sum_i N_i \cdot L_i^2}{\sum_i N_i \cdot L_i}. \quad L_n = \frac{\sum_i N_i \cdot L_i}{\sum_i N_i}. \quad \mathrm{PD} = \frac{L_w}{L_n}$$

Figure 102. Histogram of lengths nonfractionated poly[(4-3,4,5)12G1−S] (a), and the equations for determining the weight-average length, L_w, the number-average length, L_n, and the length polydispersity. N_i are the number of chains with a specific contour length L_i. Reprinted with permission from ref 450. Copyright 1998 Wiley-VCH Verlag GmbH & Co. KGaA.

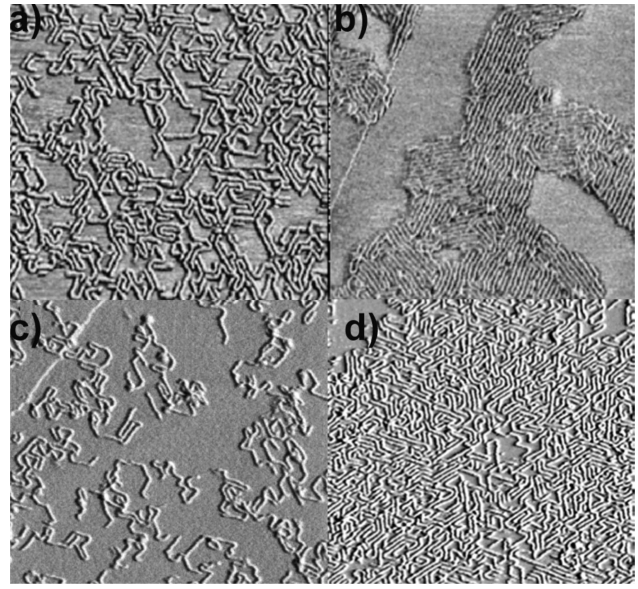

Figure 103. SFM showing individual chains of poly[(4-3,4,5)12G1−S] after spin-casting (a), after annealing at 70 °C for 20 h (b), after semipreparative SEC (c), and at higher concentration (d). Reprinted with permission from refs 445 and 450. Copyright 1998 American Chemical Society and Wiley-VCH Verlag GmbH & Co. KGaA.

affected by surface-type forming wormlike architectures with only short-range orientational order. Less branched (4-3,4,5)12G1-jacketed PS was more dependent on surface type. On mica, (4-3,4,5)12G1-jacketed PS formed plectoneme supercoils. On highly ordered pyrolytic graphite (HOPG), the orientation of the (4-3,4,5)12G1-jacketed PS exhibited

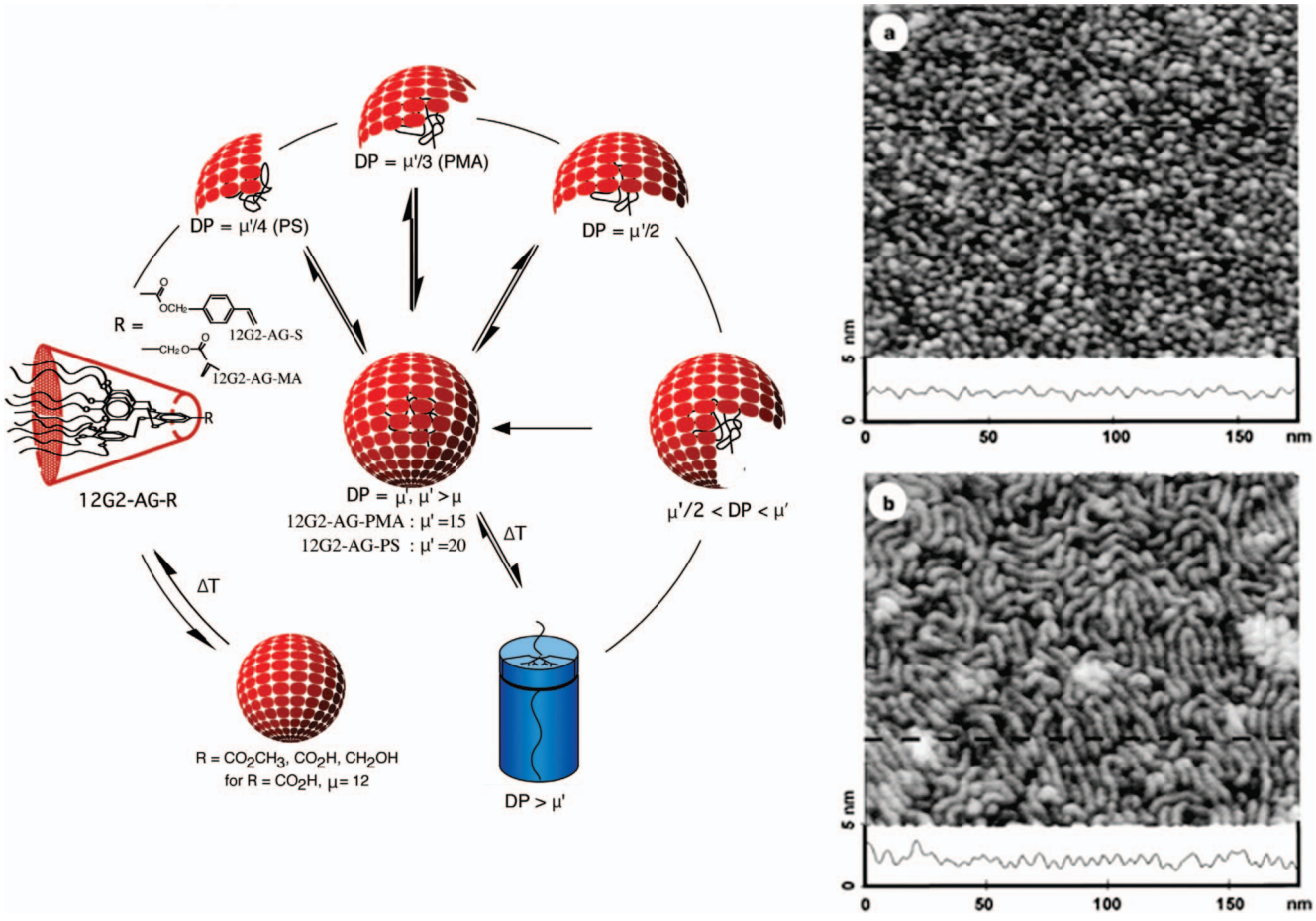

Figure 104. DP-dependent change of dendronized PS from (a) spherical to (b) columnar shapes. Reprinted with permission from ref 446. Copyright 1998 Macmillan Publishers Ltd. (Nature).

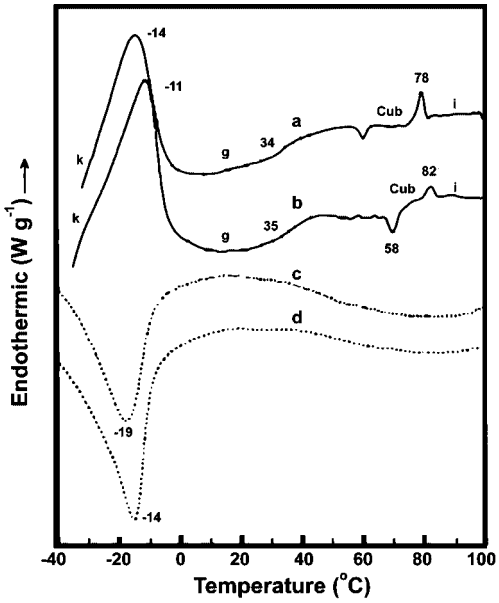

Figure 105. DSC of poly[(3,4,5)^{2}12G2−S] (first heating (a), first cooling (c)) and poly[(3,4,5)^{2}12G2−MA] (first heating (b), first cooling (d)) exhibiting melting and crystallization below a glass transition. Reprinted with permission from ref 446. Copyright 1998 Macmillan Publishers Ltd. (Nature).

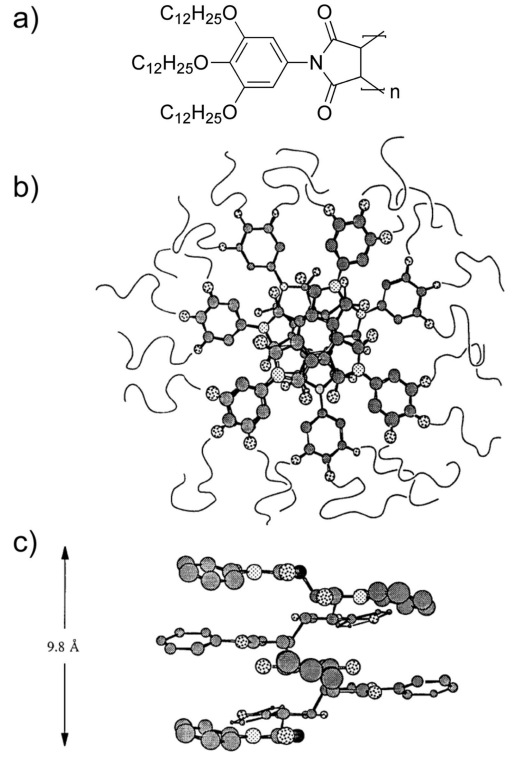

Figure 106. Structure of poly(maleimide) jacketed with a Percec-type dendron (a) and its self-assembly into a 7/2 helical chain conformation as depicted from the top (b) and side (c). Reprinted with permission from ref 456. Copyright 1996 American Chemical Society.

longer-range orientational correlation and followed the surface order.

The self-organization of polymers jacketed with Percec-type dendrons was further elucidated through ^{1}H and ^{13}C

Scheme 26. Poly(pyrrolidinopyridine) Jacketed with bis(MPA)-Dendrons Forming a Rodlike Catalyst (Reprinted with Permission from Ref 457; Copyright 2003 Royal Society of Chemistry)

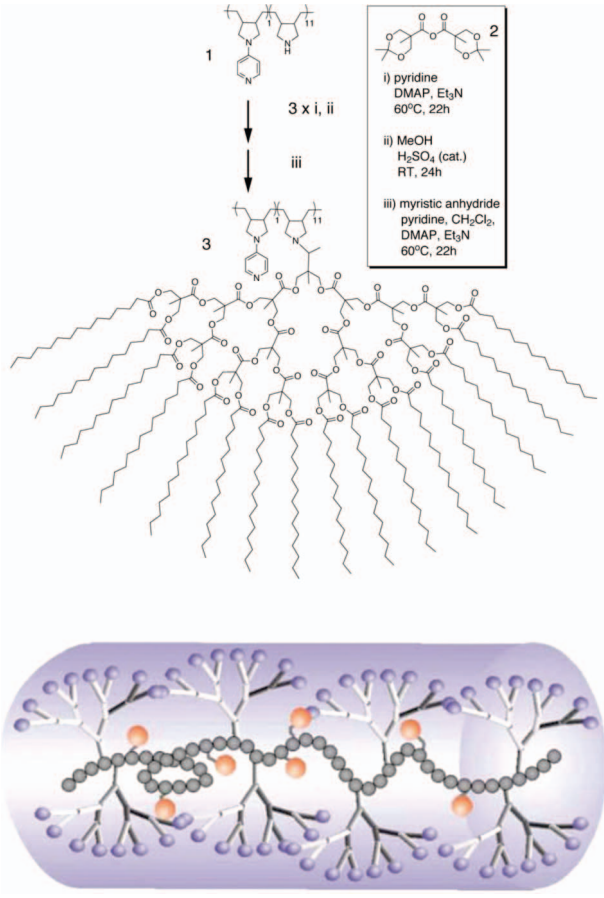

solid-state Magic Angle Spinning (MAS) NMR.[454,455] Four polymers were examined: (a) poly[(4-3,4,5)12G1−MA], (b) poly[(4-3,4,5)12G1−S], (c) poly[$(3,4,5)^2$12G2−MA], and (d) poly[(4-3,4,5)12G1−4EO-MA]. Switching from a PMA backbone in (a) to a PS backbone in (b) had little effect on the T_g values, melting temperatures, or the internal arrangement of aromatic groups as evidenced by equivalent π-shifts for the OCH_2Ph protons. Thus, for PMA- and PS-jacketed with Percec-type dendrons, the backbone appears to have little influence on self-organization. G2 dendrons (c) exhibit less motion than G1 dendrons (a), which is attributed to steric effects from the paraffinic tails. Interestingly the most significant differences are found when an EO spacer was introduced (d). Here, the spacer mechanically decouples the PMA, allowing for access to a favorable orientation of the dendritic side group. Different ring current effects are found

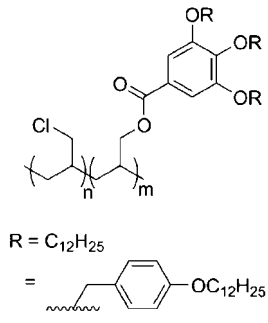

Figure 107. Percec-type dendron jacketed PECH.[460]

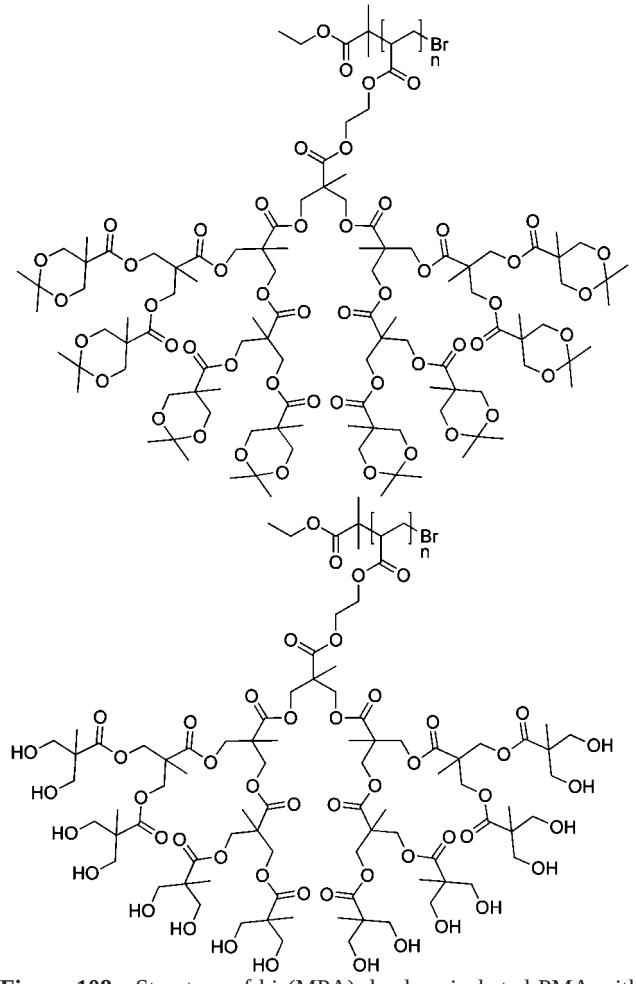

Figure 108. Structure of bis(MPA) dendron jacketed PMA with (top) and without (bottom) hydroxy surface groups.[466,470,471]

for the studied chemical shifts, indicating a different internal structure of the column.

DP-dependent shape change was observed for the first time for PS and PMA jacketed with $(3,4,5)^2$12G1.[446] $(3,4,5)^2$12G1−COOH self-assembles into spheres constructed of 12 quasi-equivalent dendritic subunits. Polymerization of the corresponding styrenic or acrylic dendritic macromonomer results in spherical organization until a critical chain length required to fill the sphere (Figure 104) is reached. At this critical domain, Φ_h and *Cub* exist as neighboring thermoreversible phases. Above the critical DP, only Φ_h is stable. The distinct spherical and columnar architecture can be directly visualized by SFM (Figure 104) and by XRD experiments. DSC revealed a second T_g above the melting/

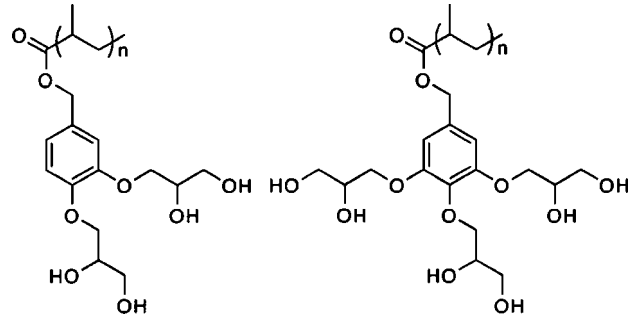

Figure 109. Poly(hydroxylated) dendronized PMA reported by Valiyaveettil.[470−472]

Scheme 27. Synthesis of Aspartic Acid (top) and Biuret Dendronized Polyacrylamide and Polymethacrylate[462−465]

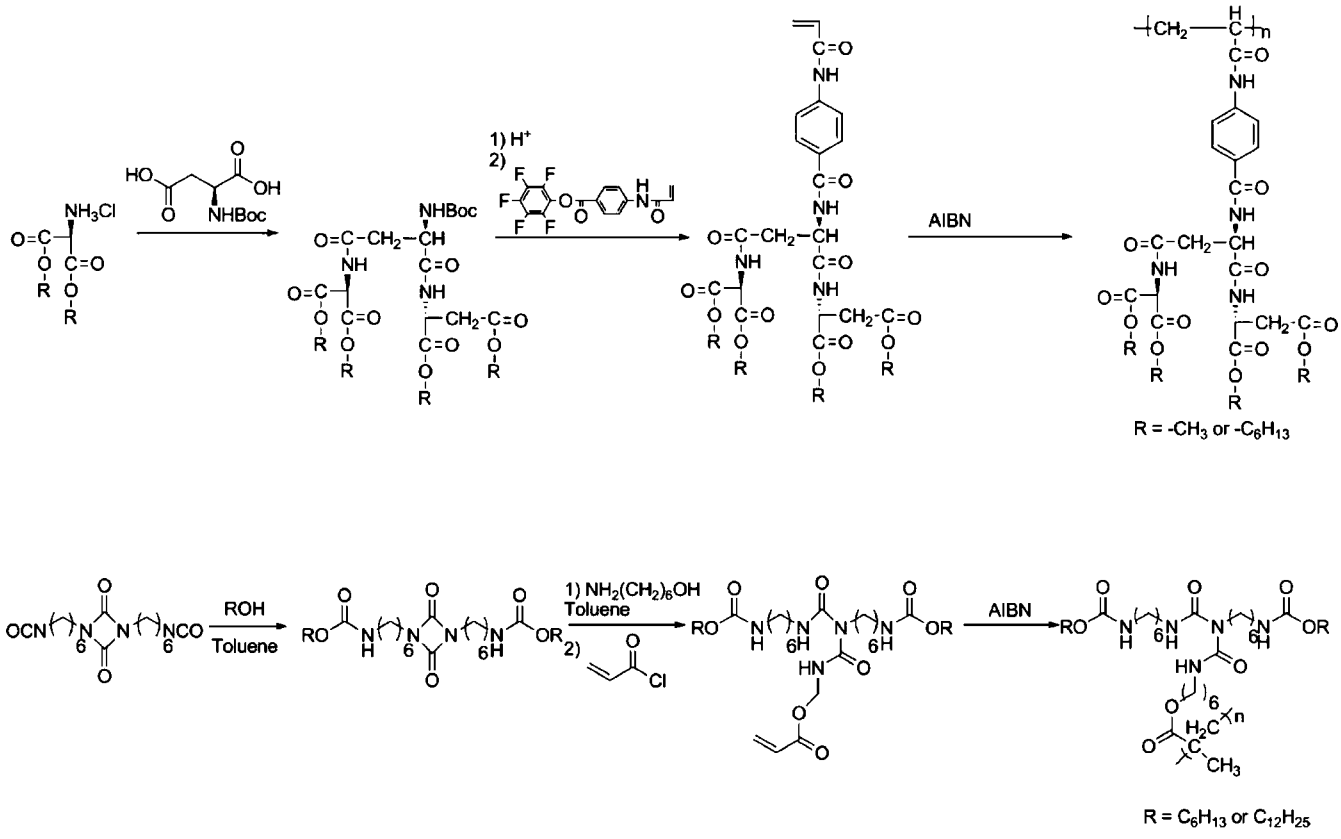

crystallization temperature supporting a microphase-segregated model. In a single-phase system, glass transitions must occur below the melting/crystallization temperature. However, in a microphase-segregated system, the transitions can be reversed since the molecular motion is independent in each phase. In poly[(3,4,5)^{2}12G2−S/MA], melting/crystallization is the transition between crystalline and liquid order in the aliphatic tails, while the glass transition corresponds

Scheme 28. Synthesis of 3EO Linked Aryl Ether Dendronized Polymer; Reagents and Conditions: (a) Me-TEG-Ts, K_2CO_3, KI, DMF, 80 °C (94%); (b) LAH, THF, −5 to 25 °C, (93%); (c) Methacrolyl Chloride, TEA, DMAP, DCM, 0−25 °C, (90%); (d) KI, 15-crown-5, NaH, THF, RT, (44%); (e) (i) *N*-Methylmorpholine, ethyl chloroformate, THF, −15 °C; (ii) $NaBH_4$, −5 °C, (82%); (f) Methacrolyl Chloride, TEA, DMAP, DCM, 0−25 °C (88%) (Adapted with Permission from Ref 474; Copyright 2008 American Chemical Society)

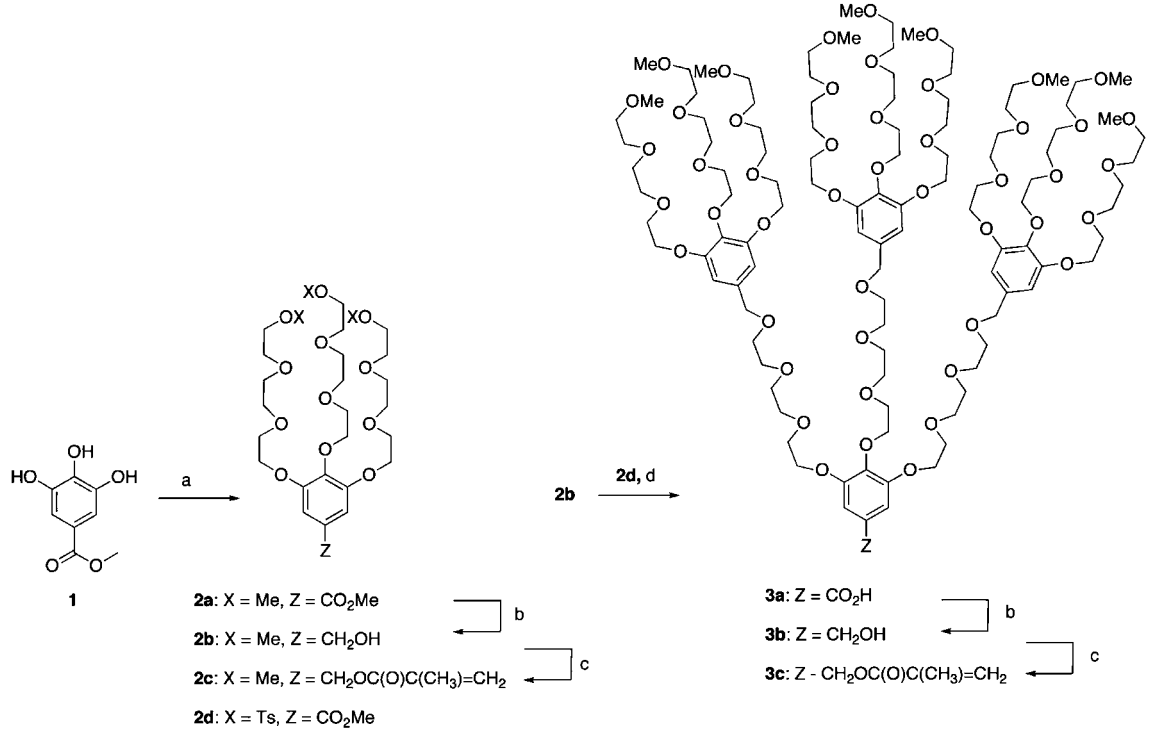

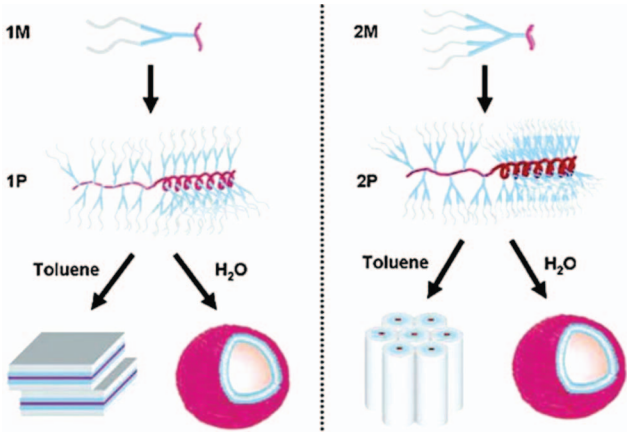

Figure 110. Self-organization of amide dendrons with aliphatic peripheries. Reprinted with permission from ref 380. Copyright 2006 American Chemical Society.

to cooperative motion of the dendritic aromatic units and the polymer backbone.

Poly(maleimide)s jacketed with (3,4,5)12G1 were prepared via free radical polymerization initiated with AIBN and by living anionic polymerization initiated with *t*-BuOK (Figure 106a).[456] Regardless of the polymerization technique employed, the dendronized polymers self-organize into a Φ_h lattice. The Φ_h phase of the dendronized poly(maleimide) is characterized by a 7/2 helical columnar structure formed by optimum packing of the dendritic side groups around a rigid-helical backbone (Figure 106b,c). Alternating copolymers of pyrrolidine jacketed with paraffin capped bis(MPA)-dendrons and pyrrolidinopyridine have been prepared via a grafting-from strategy (Scheme 26).[457] This rodlike dendronized polymer is capable of catalyzing the esterification of tertiary alcohols with pivalic anhydride.

Ronda reported the grafting-onto attachment of Percec-type dendron (3,4,5)12G1 onto poly(epichlorohydrin) (PECH) (Figure 107).[458] Dendronized PECH (DPECH) with a (3,4,5)12G1 dendritic coat exhibited a N phase where the dendron was tilted relative to the columnar axis. Solid-state NMR studies on the conformational dynamics of DPECH suggested that, in the LC state, mobility was isolated to the interior carbons of the aliphatic side chains.[459] A second series of DPECH was prepared via attachment of (4-3,4,5)12G1 to PECH.[460] Attachment efficiency ranged between 39% and 58%. At low attachment efficiency of (4-3,4,5)12G1, DPECH exhibited a nematic-columnar, N_c, mesophase, while at higher attachment efficiency, a Φ_h phase was typically observed, in line with similarly dendronized PS and PMA. In the columnar assembly, the dendrons were found to be tilted between 23 and 45° from the central axis. Ronda also prepared PECH

Scheme 29. Synthesis of Amide Dendrons with Aliphatic Peripheries; CDI = 1,1′-Carbonyl Diimidazole; APPDA = *N*-(3-Aminopropyl)propandiamine; HEMA = 2-Hydroxyethyl Methacrylate (Adapted with Permission from Ref 380; Copyright 2006 American Chemical Society)

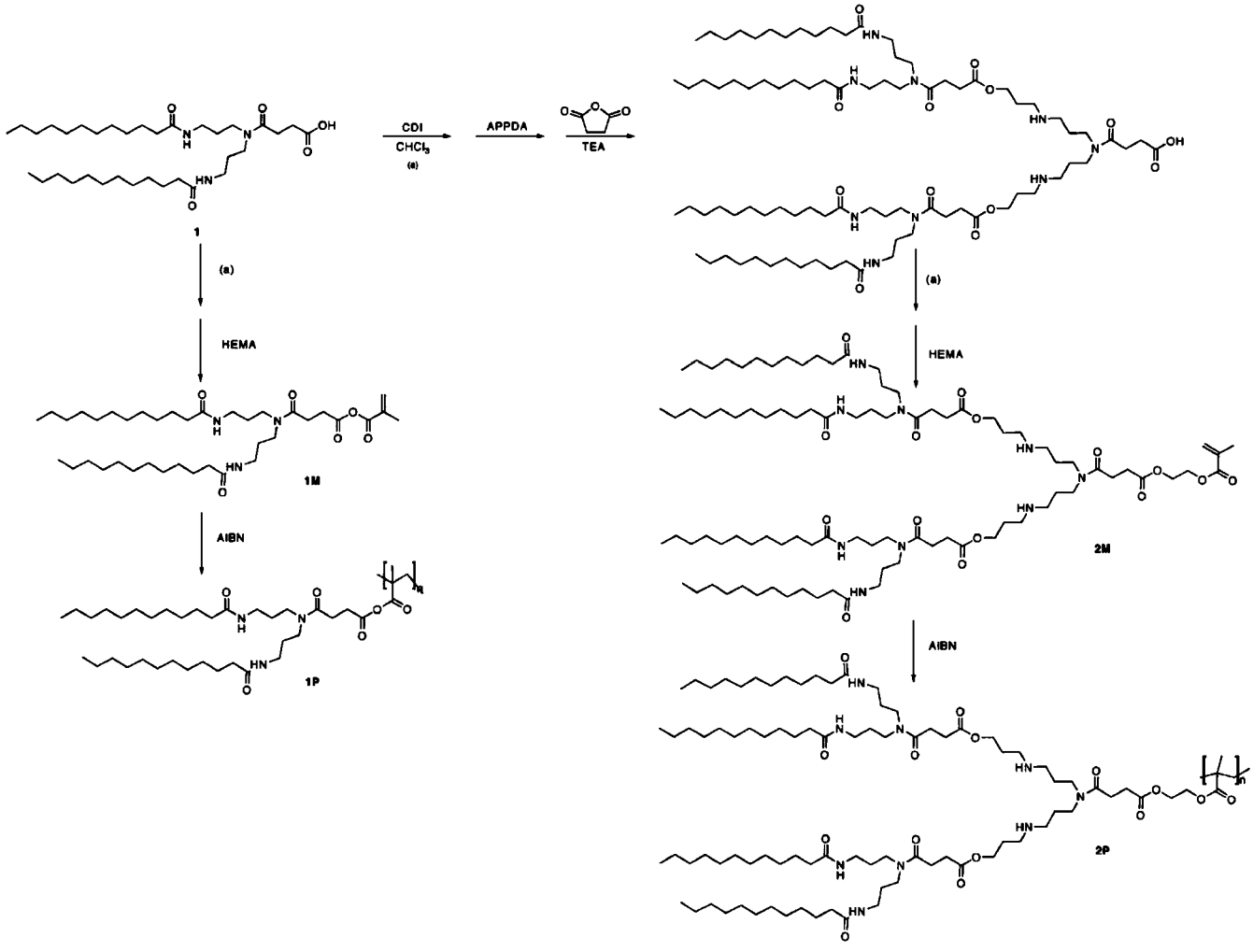

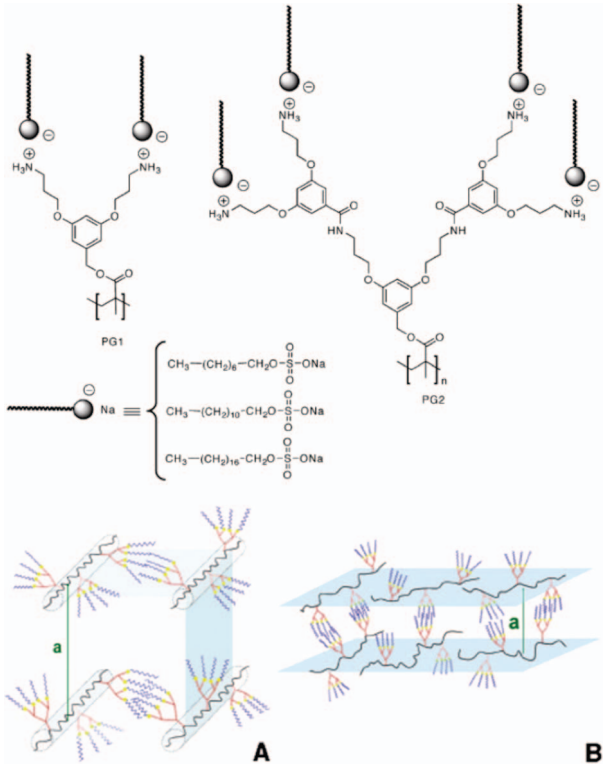

Figure 111. Anionic lipid/dendron complexes and their self-organization. Reprinted with permission from ref 478. Copyright 2007 American Chemical Society.

via a dendritic macromonomer approach using $[(CH_3)_2CHO]_2Al-O-Zn-O-Al[OCH(CH_3)_2]_2$ (Teyssié's Catalyst) or less efficiently with *t*-BuOK as an anionic initiator.[461] PEH jacketed with (4-3,4,5)12G1 and (4-3,5)12G1 exhibited Φ_h organization, while a similar polymer bearing a calamitic side group exhibited a S mesophase.

Self-assembly and self-organizaton of poly(acrylate)s, poly(methacrylate)s, and poly(styrene)s can be mediated through functionalization with other types of dendrons. Polyacrylamide bearing G1 and G2 aspartic acid dendrons[373] with and without paraffinic tails have been shown to adopt a semiflexible rodlike conformation in aqueous media (Scheme 27, top).[462−464] These aspartic acid-based dendrons were prepared via a convergent approach using *N*-Boc-L-aspartic acid and aspartic acid dihexyl ester. Synthesis of the macromonomer was achieved via deprotection of the Boc group and amidation with the active pentafluorophenyl ether of *N*-acrylyl-4-aminobenzoic acid. Radical polymerization was initiated by AIBN. PMA jacketed with diurethane-containing dendrons (biuret) has been prepared and visualized by AFM (Scheme 27, bottom).[465] Dendritic biuret macromonomers were prepared by esterification of hexamethylenediisocyanate (HDI) dimer, HDI−uredione, with hexan-1-ol or dodecan-1-ol, followed by ring-opening with an amino alcohol and treatment with methacrylol chloride. Radical polymerization was initiated by AIBN.

PMA jacketed with aliphatic polyester bis(MPA) dendrons has been prepared through a divergent grafting-from approach (Figure 108).[466] Their rodlike organization has been observed in solution. Aliphatic[467,468] or carborane[469] spacers have also been placed in between the bis(MPA)-dendron and the methacrylate chain. PMA dendronized with G1−G4 polyhydroxylated aryl ether dendrons were prepared but displayed no self-organization,[470,471] though their use in the synthesis of polymer ferrite nanocomposites has been demonstrated (Figure 109).[472] Aliphatic tails have also been affixed to the periphery of bis(MPA) dendrons, though no study of self-organization was reported.[473]

Poly and oligo(ethylene oxide) exhibit the unusual property wherein solubility decreases above a lower critical solution temperature (LCST). Schlüter exploited this phenomenon by preparing PMA jacketed with tri(ethylene glycol) linked aryl ether dendrons (Scheme 28). These dendronized polymers exhibit thermoresponsive behavior where turbidity increases above their LCST.[474] Above this LCST, interesting aggregate morphologies are noted.

Polymerization of aliphatic tailed amide dendrons resulted in dendron-jacketed polymers that form gels in toluene and aqueous conditions (Scheme 29 and Figure 110).[380] The G1 dendron exhibits lamellar architectures via gel formation in toluene, while the G2 dendron generated Φ_h assemblies. In water, both G1 and G2 dendrons form spherical architectures.

Ritter synthesized optically active PA and PMA jacketed with benzamide dendrons with chiral ester functionalized peripheries.[372] Schlüter also reported PMA jacketed with benzamide dendrons.[475] XRD suggested some degree of organization of these semiflexible rodlike molecules, though the exact packing was not determined. Complexation of the surface amine functionality with anionic sulfonate alkyl groups mediates the formation of tetragonal columnar, rectangular columnar, hexagonal columnar, and lamellar architectures (Figure 111).[476,477] This complexation causes the dendron to resemble a $(3,5Pr)^2G2$ Percec-type dendron. Increasing generation number induces lamellar and columnar architectures with larger dimensions, while increasing the length of the anionic lipid tends to favor lamellar architectures.[478] Similar PMA jacketed with G2 and G3 benzamide dendron with tertiary butyl ester and potassium carboxylate periphery groups was prepared.[479] The dendronized polymers with carboxylate surface group formed aggregated structure of roughly half the length of the ester counterpart, indicating self-folding of the chain on itself to form a closed loop. This back-folding is likely due to the favorable interactions of the charged periphery with the polar solvent, leading to solvophobic collapse of the main chain.

Schlüter also reported the polymerization of branched thiophene macromonomers (Scheme 30),[480] which were prepared through a combination of Stille and Kumada cross-couplings of bromo- and tributylstannylthiophenes.[481] Interestingly, the emission properties of the dendron do not shift significantly when going from monomer to polymer, suggesting that conjugated dendrons can be confined into linear architectures without severely perturbing their electronics.

PMA jacketed with dendronized perylene bisimides was prepared by Würthner (Figure 112).[482] Dendronized PBI macromonomers were prepared via one-pot coupling of perylene-3,4,9,10-tetracarboxylic acid bisanhydride with 3,4,5-tris{3-[2-(2-[ethyoxy]ethoxy)ethoxy]-1-propynyl}aniline and 6-aminohexanol in the presence of $Zn(OAc)_2$ followed by treatment with methacroylyl chloride (Scheme 31). Because of the various potential products of the one-pot reaction, the overall yield was low (<5%). Würthner showed that dumbbell shaped dendronized PBIs self-assemble into rodlike structures, whereas wedge-shaped dendronized PBIs form micellar structures (Figure 112). Self-assembly of the dendritic macromonomer provided micelles with 4−6 nm diameter. 8:1 coassembly of the dendritic macromonomer with a dumbbell shaped amphiphilic perylene

Scheme 30. Synthesis of Thiophene-Dendron Jacketed Polymethacrylate[480,481]

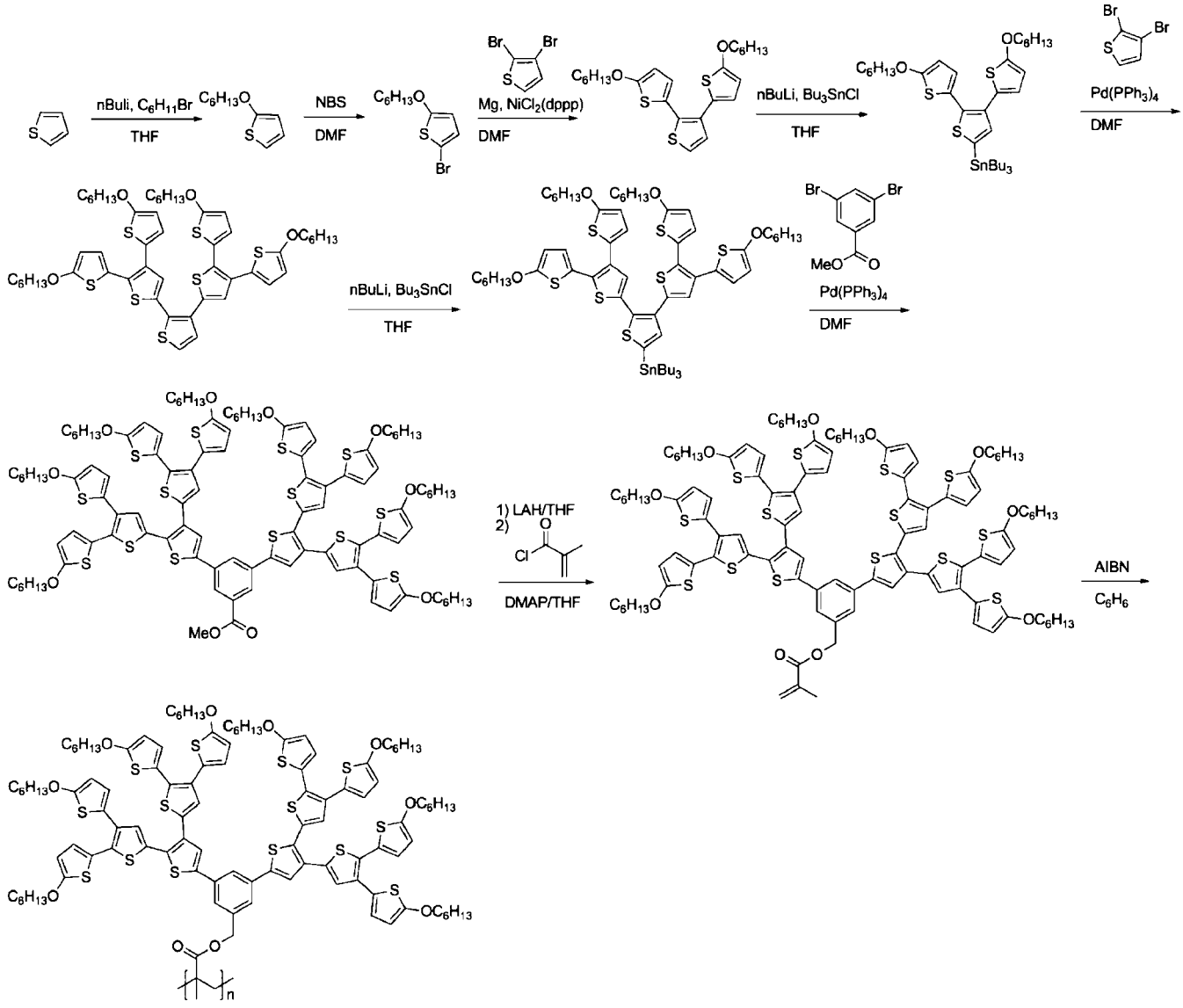

bisimide additive decreased the curvature of the self-assembled architecture, resulting in vesicular structures of approximately 93 nm diameter. Photopolymerization of the vesicular aggregate in the presence of 2,2-dimethoxy-2-phenylacetophenone photoinitiator stabilized the structure without perturbing its size or shape.

Schlüter also reported a 4-aminoproline-based macromonomer that is densely packed with 5-stereocenters (Figure 113).[483] Radical polymerization provided a high molecular weight polymer with T_g > dec (200 °C). CD/UV−vis and molecular modeling assigned a right-hand helical confirmation that persists until decomposition. Molecular modeling suggests that the helical model is compatible with both isotactic and heterotactic sequences in the methacrylate backbone and that chiral amplification is mediated solely by the chiral dendritic side chain and is completely decoupled from the main-chain chirality.

Hawker reported a novel method for the three-dimensional data storage via dendronized polyacrylates (Figure 114).[484] Here, periphery-brominated G1−G3 Fréchet-type dendrons (Figure 115) with a focal acrylate group were photopolymerized in a 1,6-hexamethylenediisocyanate/polypropylene triol (HMDI/PPT) matrix. Diffusion and free-radical polymerization resulted in image generation through the formation of a gradient-refractive index (GRIN) film.

Poly(*p*-hydroxystyrene)s decorated with G1−G5 aliphatic polyester dendrons were prepared.[485,486] Modeling the thermodynamic and dynamic properties of these dendritic polymers has suggested resemblance to a single-chain glassy state,[487] which is in line with the two T_g's observed in poly[(3,4,5)^{2}12G1−MA/S].[446] Alkylation of the hydroxyl periphery with aliphatic tails resulted in increased polymer gelation and allowed for direct visualization of the polymer chains via SFM. Poly(vinylacetylene) has been decorated with G1 Fréchet-type dendrons bearing a focal azide group via Huisgen-cyclization (aka Sharpless "click chemistry").[488] This technique was adapted for the preparation of PMA jacketed with higher-generation dendrons. DCC coupling of the surface hydroxyl groups of a poly(*p*-hydroxystyrene) decorated with a G3 aliphatic polyester dendron with 4-pentynoic acid furnished a polymer jacketed with a terminal alkyne-bearing dendron. Huisgen-cyclization with

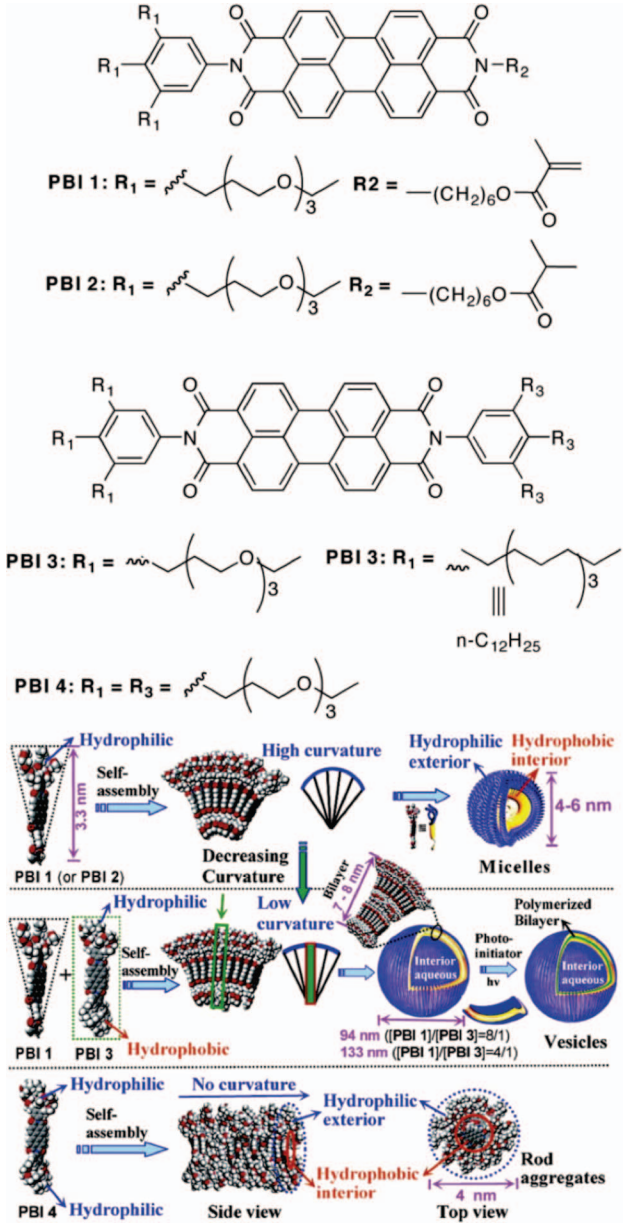

Figure 112. Structures of PBIs 1−4 (top) and schematic of the effect of curvature on the supramolecular structure of self-assembled dendronized PBI reported by Würthner. Reprinted with permission from ref 482. Copyright 2007 American Chemical Society.

a G3 Fréchet dendron bearing an azide apex produced a pseudo-G6 hybrid dendron-jacketed poly(*p*-hydroxystyrene) (Scheme 32).[489] Additionally, Schlüter reported alternating copolymers of methyl acrylate or methyl methacrylate and silylmethylether-substituted [1.1.1]propellane jacketed with G1−G2 Fréchet dendrons.[490] Like random copolymers of PS and PS-jacketed with Fréchet dendrons,[371,491] no self-assembly or self-organization was reported in these cases. Polystyrene functionalized with polypyridine analogues of Fréchet dendrons has also been prepared.[492]

Polystyrene decorated with G1−G5 benzamide dendrons (Figure 116) has been prepared, and direct visualization suggested a nanorod topology.[493] The molecular conformation and stiffness of polystyrene jacketed with benzamide dendrons can be monitored via dielectric spectroscopy in dilute solution.[494]

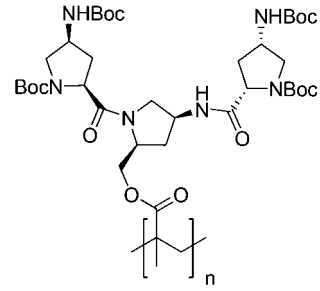

Figure 113. Structure of 4-aminoproline dendron-jacketed polymethacrylate.[483]

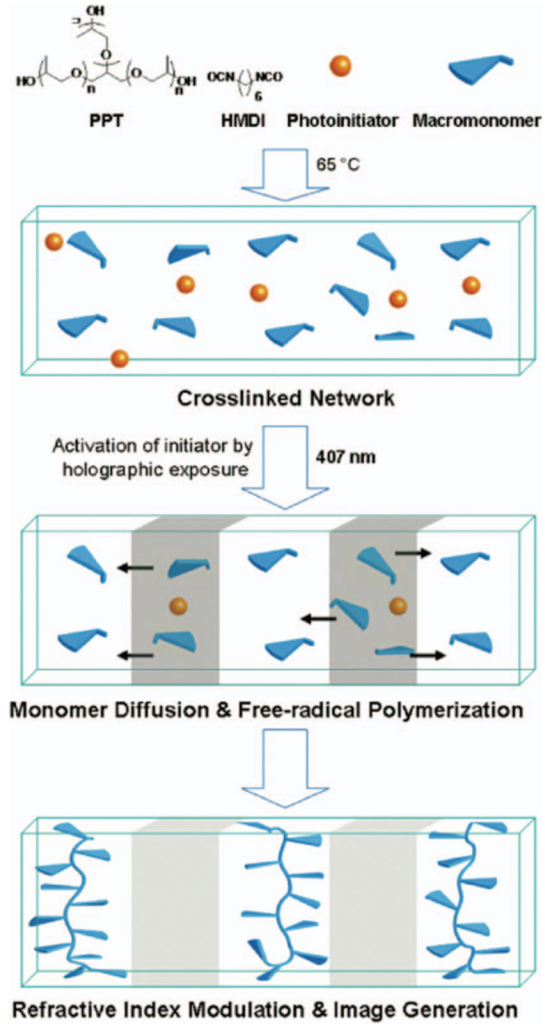

Figure 114. Photocross-linking of brominated Fréchet dendrons. Reprinted with permission from ref 484. Copyright 2009 Royal Society of Chemistry.

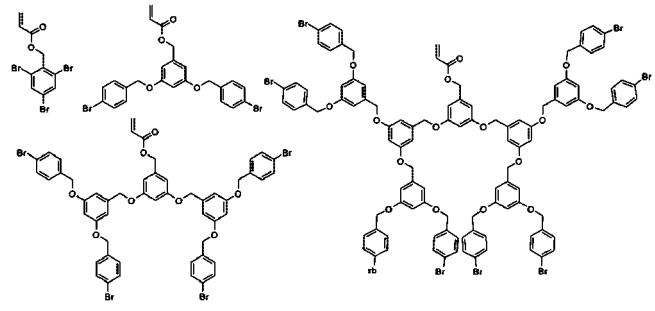

Figure 115. Fréchet dendron utilized in photocross-linking.[484]

Scheme 31. Synthesis of Dendronized PBI-Containing Monomers[482]

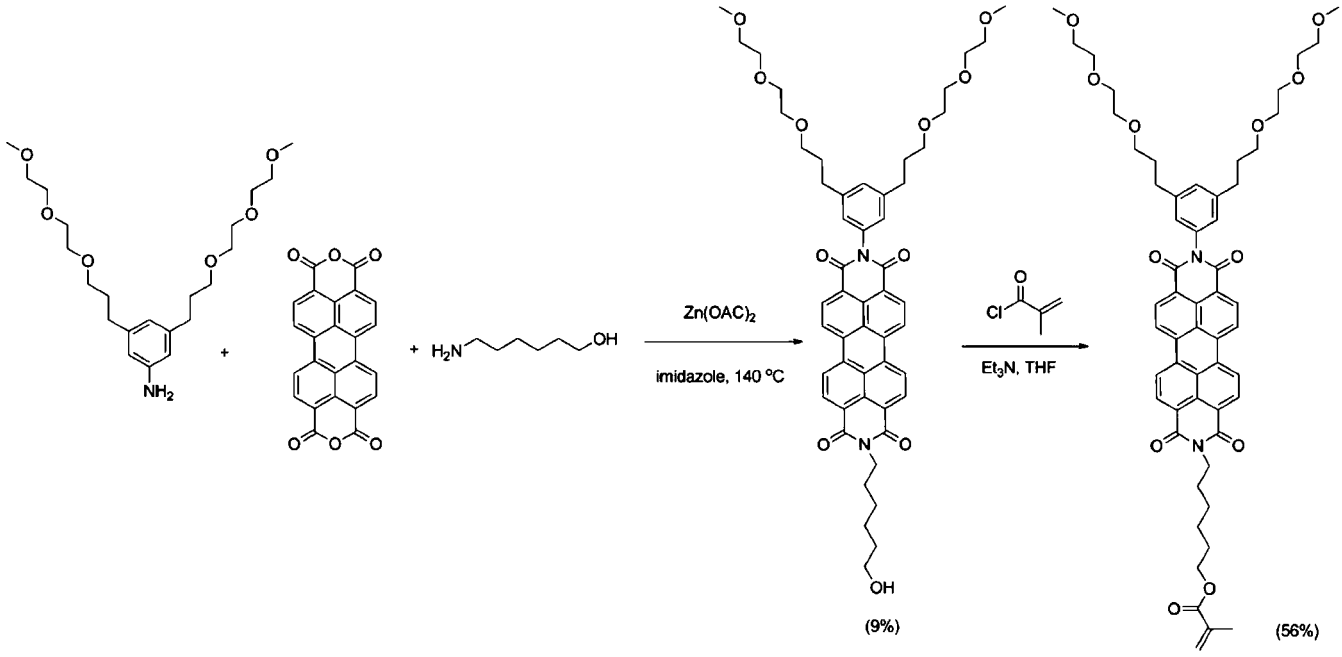

Cryo-TEM of polystyrene jacketed with G3 or G4 benzamide dendrons with surface ammonium groups has suggested the formation of double helical ultrastructures composed of two entwined dendronized polymers (Figure 117).[495] Additionally, replacement of the surface amine groups to Pd/Pt metallopincers allowed for single-site catalysis of Aldol condensation on a dendronized polymer support (Scheme 33).[496] Many examples of PMA/PMMA[497−501] and PS[502−505] jacketed with benzamide dendrons have been reported by Schlüter, and their properties (e.g., stiffness) have been characterized extensively via visualization, though no self-assembly or self-organization was reported.

AFM was used to template the homeotropic arrangement of dendronized polystyrene.[506] AFM was first used to ionically cleave surface α,α-dimethyl-3,5-dimethoxybenzyloxycarbonyl groups, leaving behind free amine sites with a specified pattern. PS jacketed with benzamide dendrons capped with a tetradentate carboxylic acid terminus is noncovalently anchored to the free amines on the surface. Aromatic *ortho*-diyne units at the periphery of the dendrons are irreversibly cross-linked at 140 °C to provide a stable material that can be visualized via AFM to reveal dendronized polymers organized according to the initial patterning (Figure 118).

Méry prepared PS jacketed with multiallylic carbosilane dendrimer side chains via anionic polymerization of dendritic macromonomers.[507] Postpolymerization functionalization of the allylic peripheries can provide a diversity of surface structures (Figure 119).[508] In the case of siloxane or semifluorinated peripheries, the formation of LC mesophase has been noted. An alternative approach to diversely functionalized dendritic polymers utilizes the free radical copolymerization of Fréchet dendritic macromonomers with maleic anhydride.[509] The maleic anhydride is incorporated into the backbone and can be functionalized postpolymerization via hydrolysis to the diacid or by reacting with primary amines or amine-functionalized dendrons. Similarly $(3,4,5)^2$12G2 Percec-type styrenic macromonomers were copolymerized with maleic anhydride (Figure 120).[510] The maleic anhydride groups were subsequently functionalized with bis(MPA)-dendrons. These polymers were found to form single-cylinder structures that could be fashioned into fibers. A hierarchical model for fiber formation was proposed to proceed via single 7 nm cylinder packing into 20 nm hexagonal arrays, which assemble into 200 nm fibrils that aggregate into 100 μm fibers (Figure 120). Additionally, Astruc has reported PS jacketed with G1 carbosilane dendrimers containing ferrocenyl periphery groups (Figure 121)[511] as well as carbosilane dendrimers with triazole-linked ferrocenyl periphery groups.[512] AFM studies of the dendron-jacketed polymer revealed globular structures. Apparently, the dendron was not sufficiently large to induce rigid rodlike structures and disassembly of the amorphous polymer state.

Other exotic dendronized polymers were synthesized for specific applications such as nonlinear optics (NLO).[131,513−517] The dendronized polymers often contain highly conjugated dendritic side chains (Figure 122). Similar polymers have also been prepared using Diels−Alder "click" chemistry[518] employing anthracene and reactive maleimide as a dienophile.[519]

3.2.3. Semifluorinated Dendronized Polymers

Before examining other polymer classes, it is worth noting the effect of semifluorination on the self-organization of dendronized polymers. A similar discussion of the effect of semifluorination in self-assembling dendrons is found in the preceding chapter. Semifluorination of (4-3,4,5)*n*G1 and (3,4,5)*n*G1 dendrons with $-(CH_2)_m(CF_2)_nF$ tails results in stabilization of Φ_h phase of dendrons and dendronized polymethacrylate analogues (Figure 123).[360,520] In addition, it has been shown that dendrons with $m = 4$ and $n = 6$ give rise to gyroid bicontinuous structures.[366] Without the addition of salt, nonpolymerized perhydrogenated (4-3,4,5)*n*G1−4EO and (3,4,5)*n*G1−4EO dendrons organize only into S or *k* phases, while the semifluorinated analogues uniformly self-organize into Φ_h lattices in the absence of salt. Further, the (4-3,4,5)10F6G1−4-EO−MA dendritic macromonomer undergoes thermoreversible transition to a Cub_{bi} lattice at elevated temperature, but polymerization eliminates this

Scheme 32. Hybrid-Dendronized Polymers Prepared via "Click Chemistry" (Reprinted with Permission from Ref 489; Copyright 2005 Royal Society of Chemistry)

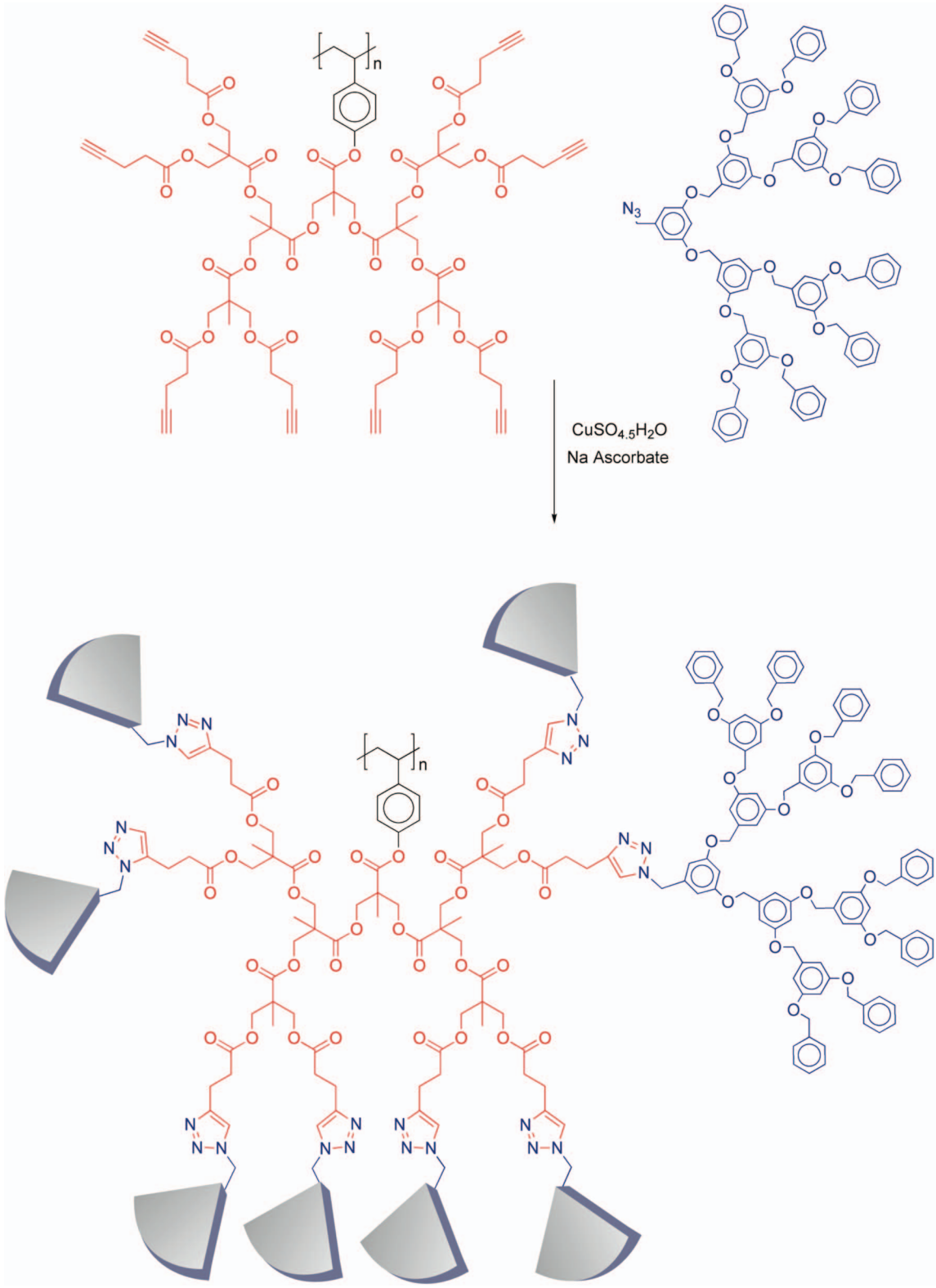

transition.[521] In the dendronized polymers, semifluorination increases the temperature stability of the Φ_h phase by as much as 130 °C through simultaneous increase in isotropization temperature (Figure 124, left) and decrease in crystalline melting temperature (Figure 124, right). Increasing the number of perfluorinated carbons in the dendritic acid (3,4,5)12FnG1−COOH, the dendron with oligoethyleneoxide apex functionality (3,4,5)12F*n*G1−4EO, and the dendronized polymer poly[(3,4,5)12F*n*G1−4EO−MA] results in a monotonic increase in the $T_{\Phi h\text{-}I}$ (Figure 124, left). $T_{\Phi h\text{-}I}$ increased 18, 17, and 10 °C per fluorinated carbon for the dendritic acid, tetraethylene glycol, and dendronized polymer, respectively. Semifluorination results in an increase in isotropization enthalpy. Increasing the number of perfluorinated carbons results in a large decrease in the crystalline melting temperature from $n = 0$ to $n = 4$, and a gradual increase from $n =$

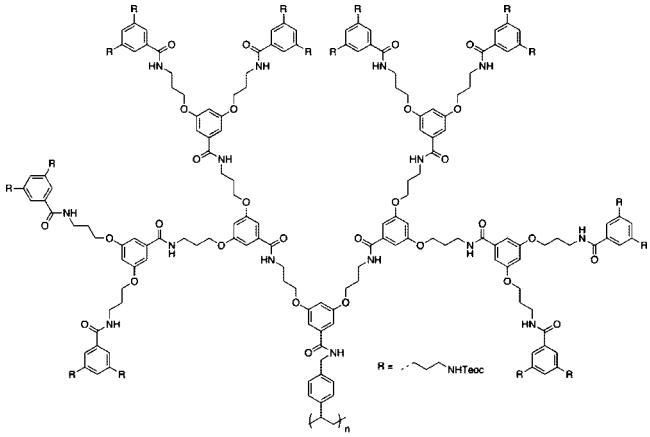

Figure 116. Structure of G4 benzamide dendron explored via direct visualization by SFM.[493]

4 to $n = 8$. The enhancement of Φ_h via semifluorination is thought to be the result of microsegregation of the perfluorinated and perhydrogenated parts of the dendron via the fluorophobic effect as well as the enhanced stiffness of perfluorinated segment resulting in the decrease of liquidlike disorder in the periphery.[360]

Semifluorinated (4-3,4,5)12F8G8G1 dendrons with pendant acceptor groups (4,5,7-trinitrofluorenone-2-carboxylic acid) or donor groups (carbazole, naphthalene, or pyrene) were mixed in 1:1 donor/acceptor ratio with polymers containing donor or acceptor side groups.[358,522] Later, other electron-acceptor groups[363] (aminothienyldioxocyanopyridine, 3,5-dinitrobenzene, naphthalimide, 4-nitro naphthalimide, 1,3-indanedione, malononitrile, and perylenebisimides) and other electron-donor groups[364] (3,5-dimethoxyphenol, 3,5-(dipyrrolidin-1-yl)phenol, and 2-(phenothiazin-10-yl-ethoxy)ethanol) attached to semifluorinated dendrons were

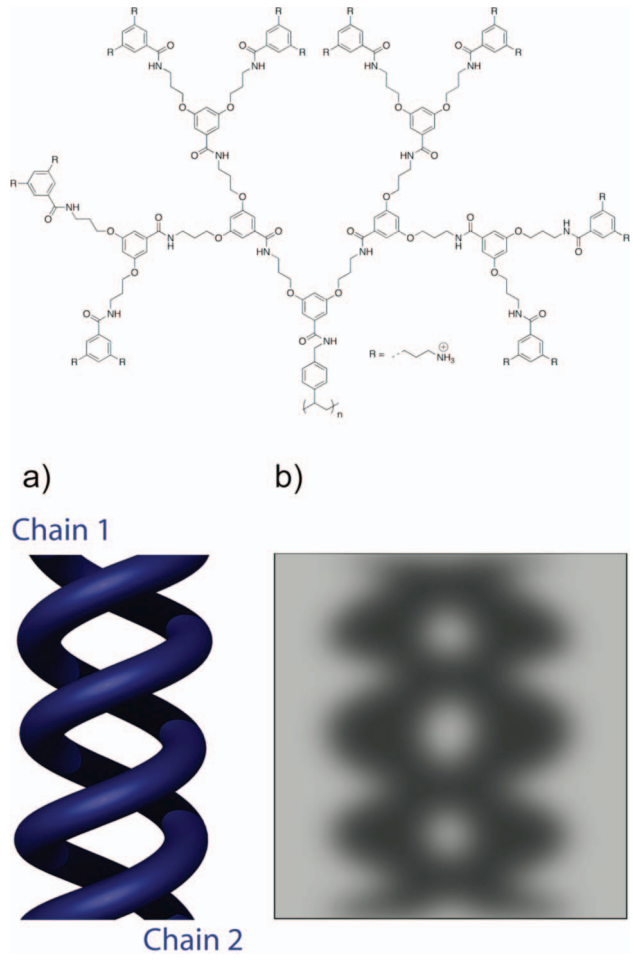

Figure 117. G4 benzamide dendron with ammonium surface and double helical superstructures (a) as suggested by Cryo-TEM depicted in schematic form (b).[495]

Scheme 33. Synthesis of Dendronized Polymers Decorated at the Periphery with Catalytic Metallopincers (Reprinted with Permission from Ref 496; Copyright 2003 American Chemical Society)

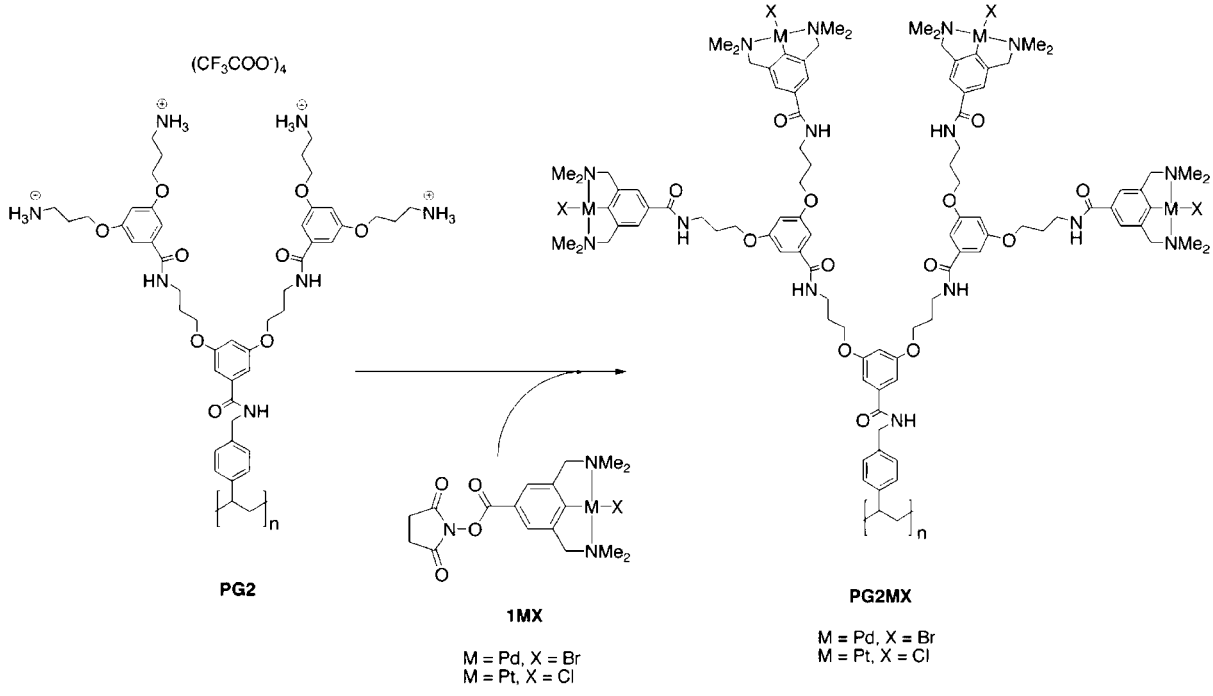

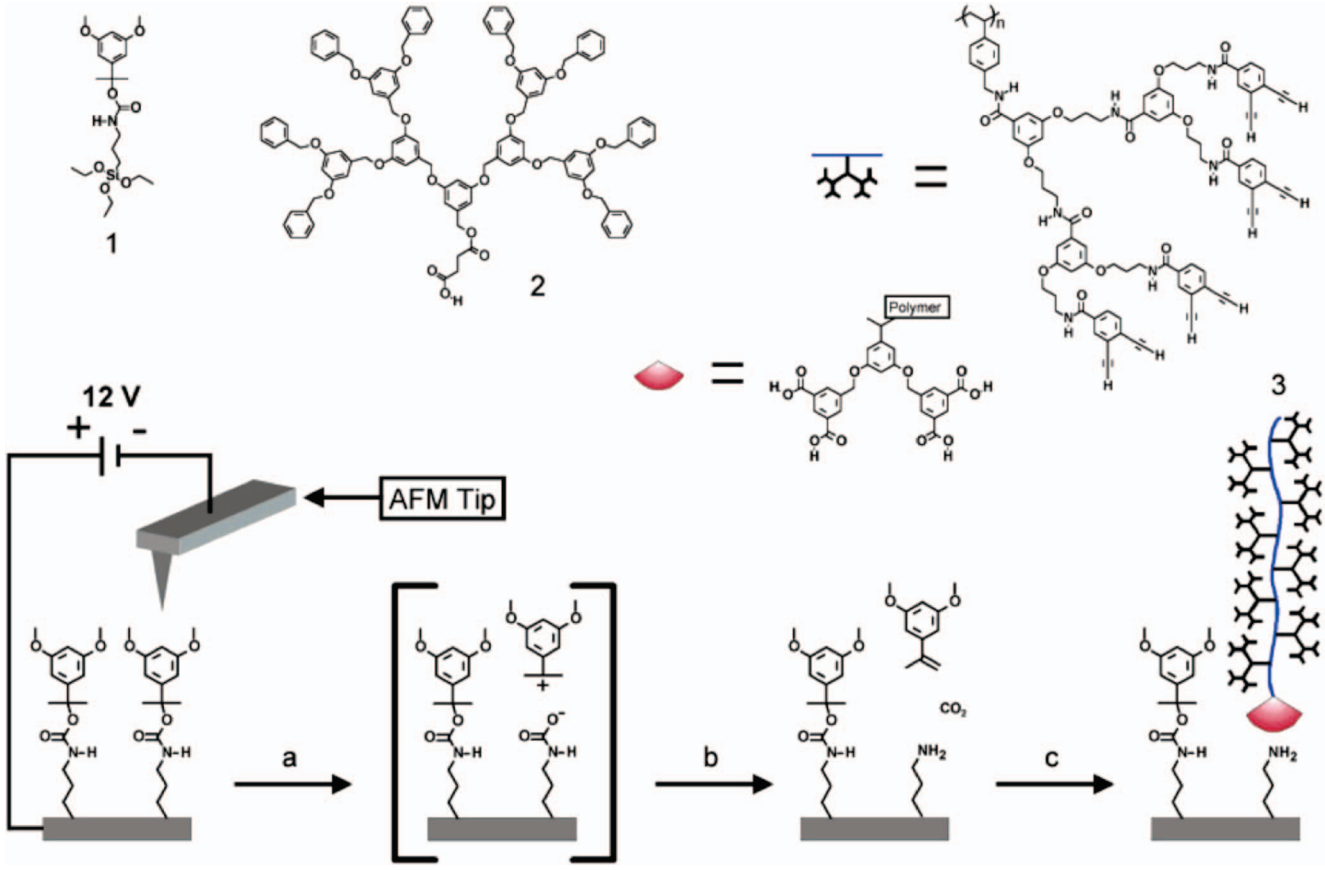

Figure 118. AFM-induced patterning of dendron-jacketed polymers. Reprinted with permission from ref 506. Copyright 2004 American Chemical Society.

shown to self-assemble into helical pyramidal columns. These noncovalent complexes of donor−acceptor dendron with acceptor−donor polymer self-assemble into Φ_h and $\Phi_{r\text{-}c}$ phases via alternating stacking of donor and acceptor moieties (Figure 125). Donor−acceptor complexes formed from 50:50 donor−acceptor mixtures of (4-3,4,5)12F8G1 bearing a carbazole donor group and polymethacrylate bearing trinitrofluorenone-2-carboxylic acid acceptor group provided high and well-balanced hole and electron mobilities ($\mu_{hole} = 2.3 \times 10^{-3}$ cm^2 V^{-1} s^{-1} and $\mu_{electron} = 7.5 \times 10^{-4}$ cm^2 V^{-1} s^{-1}). These electron mobilities represent a 3−5 order of magnitude enhancement over the parent polymer. The inverse complex between (4−3,4,5)12F8G1 bearing a trinitrofluorenone-2-carboxylic acid acceptor group and PMA bearing a carbazole-donor group produced similar results. The alternative organization of donor and acceptor in highly ordered columns mediated by fluorophobically driven self-assembly results in complex supramolecular electronic materials with high charge carrier mobility. Any defects caused by backfolding of the apex functionalized dendrons can be eliminated by a "self-repair" process involving slow cooling from the melt phase (Figure 126).

Ober has investigated block-copolymers wherein one block contains a semifluorinated side chain.[523] Increasing CF_2 number on the semifluorinated chain allows for the organization of the block copolymer into a S_B structure.[524] Similar polymers were prepared wherein two arms and three arms of nonaromatic semifluorinated dendrons were grafted-onto the isoprene block of poly(styrene-*b*-1,2/3,4-isoprene).[525,526] While complete attachment was not achieved (Scheme 34), the dendronized semifluorinated block-copolymers also self-organize into LC mesophases with organization on multiple length scales.[527−529] In one example with 66.3% attachment of 2-armed dendron, large-scale columnar organization (263 Å column diameter) was observed. The columns are composed of the PS block (blue) while the dendritic semifluorinated block is organized into a S_B phase in the intervening space (green) (Figure 127).

Recently, Malmström has reported the modification of cellulose Bio-Fiber with fluorinated dendrons (Scheme 35).[530] Cellulose filter paper was modified with 2-bromoisobutyryl bromide initiator. Surface-initiated ATRP of glycidol methacrylate achieved, followed by acid-catalyzed epoxide hydrolysis and acylations with perhydrogenated and perfluorinated acyl chlorides, provided a cellulose surface coated with perhydrogenated or perfluorinated dendronized PMA. G2 dendronized polymers were prepared through divergent growth of ring-opened epoxide prior to periphery functionalization. Superhydrophobic biofibers were achieved in all cases. The surfaces functionalized with perfluorinated dendronized polymers were also shown to be oleophobic. These modified Bio-Fiber's show promise as self-cleaning textiles.

3.2.4. Poly(norbornene)s, Poly(oxanorbornene)s, and Related Polymers

In 1996, the Percec laboratory reported the dendritic macromonomer approach to the preparation of twin-dendritic bis-(3,4,5)12G1-dendronized poly(7-oxanorbornene) via ROMP (Scheme 36, top).[456,531] Poly(7-oxanorbornene) bis-

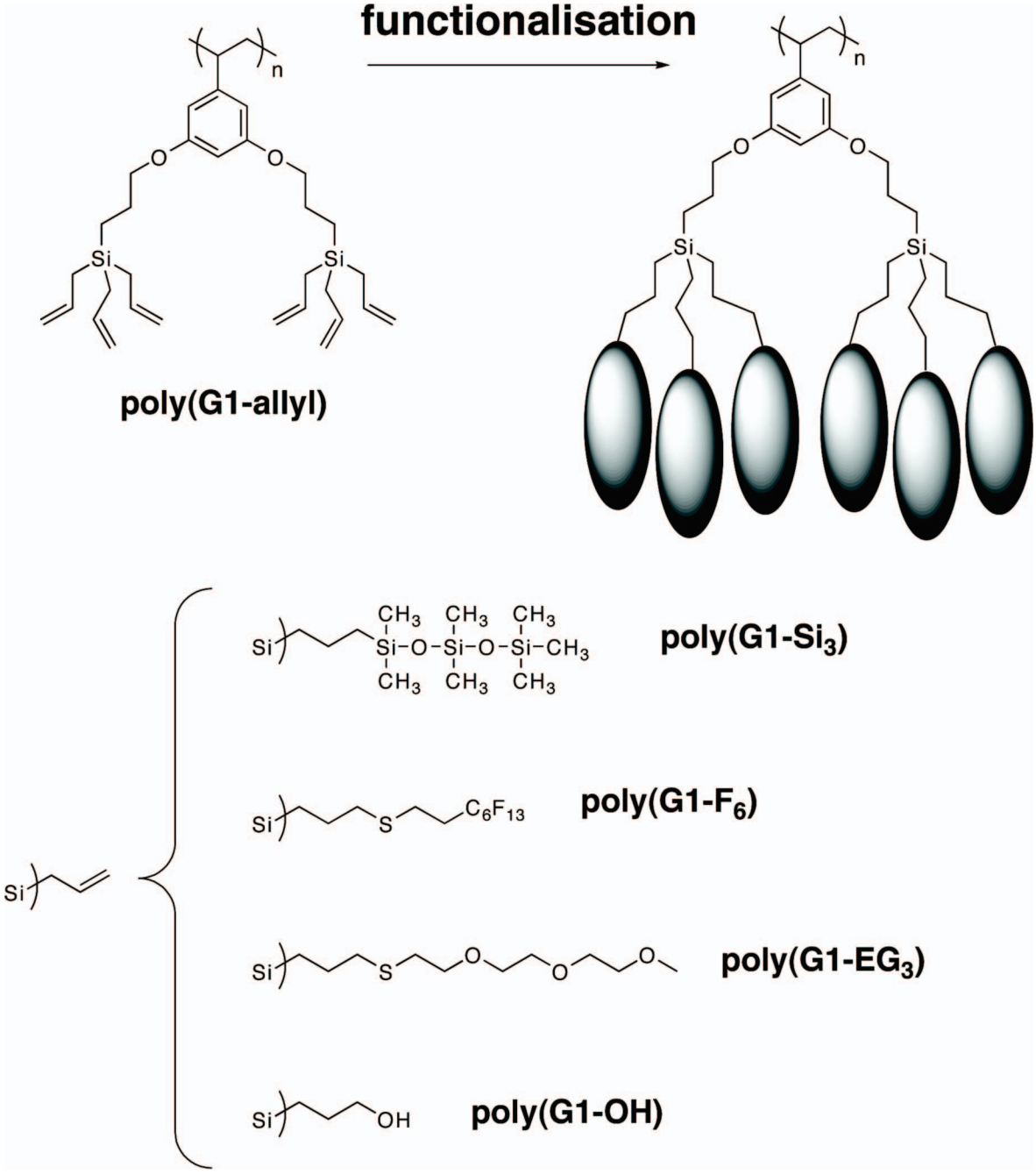

Figure 119. Surface functionalization of polystyrene jacketed with multiallylic carbosilane dendrons. Adapted with permission from ref 508. Copyright 2008 Royal Society of Chemistry.

dendronized with (3,4,5)12G1 (Scheme 36, top) exhibits a Φ_h phase with 3/1 helical columnar structure formed by induction of a helical-chain conformation via the dendritic side group (Figure 128). Shortly, thereafter Fox reported the synthesis of poly(norbornene) jacketed with a single naphthalene-capped dendron via ROMP using Mo(=CH−*t*-Bu)(=*N*-2,6-*i*-$Pr_2C_6H_3$)(*O*-*t*-Bu)$_2$ as catalyst (Scheme 36, bottom).[532] However, this dendron was not rigid enough to prevent excimer formation.

Poly(7-oxanorbornene) bisdendronized with (4-3,4,5)12G1 was also prepared via a dendritic macromonomer approach using $RuCl_2$(=CHPh)$(PCy_3)_2$ as catalyst (Scheme 37).[533] Twin-dendritic polymers with DP ranging from 6−120 were prepared. All exhibit a Φ_h LC phase with a thermal stability that increases with DP until a plateau is reached at DP = 64. Four domains of the ΔH of the Φ_h−I transition can be observed and provide insight into the mechanism of self-assembly. From the monomer to DP = 6, there is a sharp decrease in ΔH of the Φ_h−I transition corresponding to the difference between noncovalent self-assembly into stackable discs and covalent attachment to form similar stackable discs. From DP = 6 to 24, the ΔH of the Φ_h−I transition decreases with a noted odd/even effect and corresponds to a domain of disk stacking. From DP = 24 to 60, ΔH of the Φ_h−I decreases continuously. Above DP = 64, the ΔH of the Φ_h−I plateaus and thus DP = 64 may correspond to an effective persistence length of the polymer.

From a mechanistic standpoint, it is important to note that dendronization of 7-oxanorbornene actually improves the control of ROMP. ROMP of *exo*,*exo*-7-oxabicyclo[2.2.1]hept-

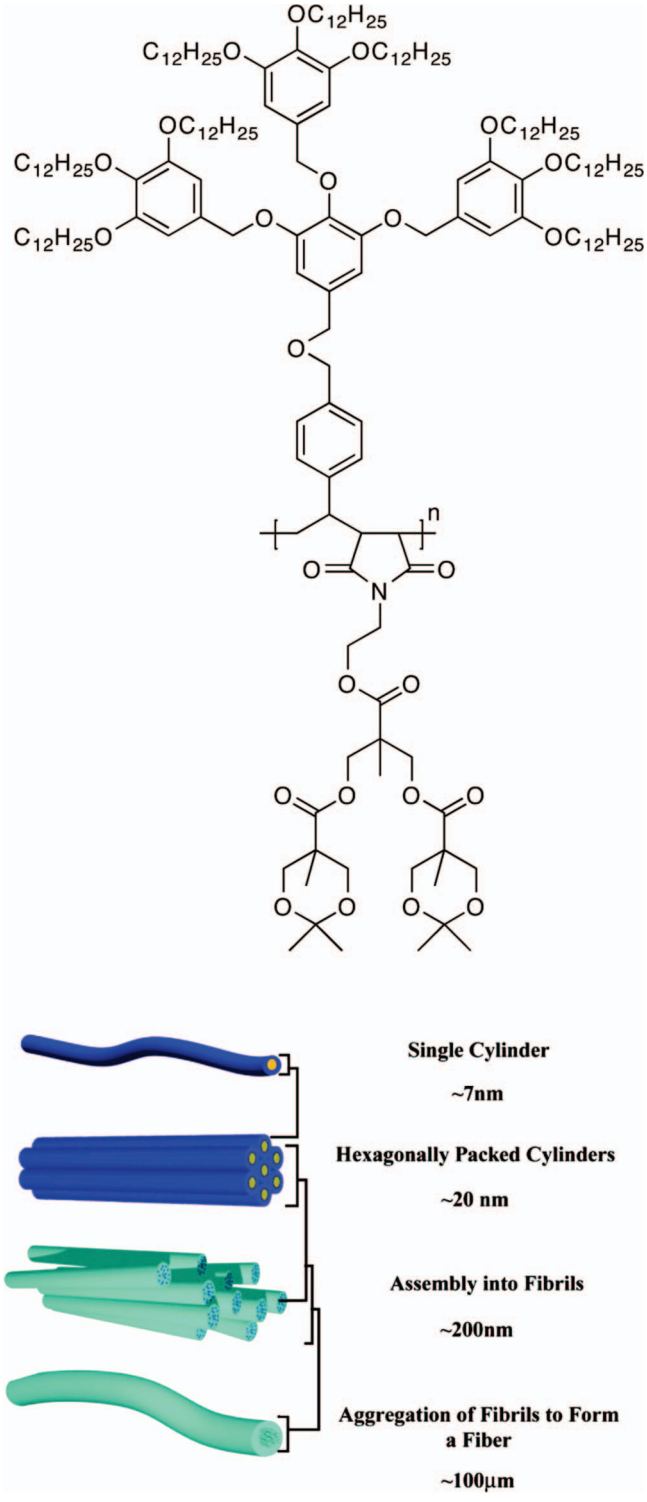

Figure 120. Alternating (3,4,5)12G2, bis-MPA dendronized poly(styrene-co-maleic anhydride). Reprinted with permission from ref 510. Copyright 2009 American Chemical Society.

2-ene-5,6-dicarboxylic acid diethyl ester with Ru(=CHPh)Cl_2(PCy_3)L (L = 1,3-dimesityl-4,5-dihydroimidazol-2-ylidene) resulted in broad molecular weight distribution ($M_w/M_n \approx 2$) due in large part to competition of ROMP with RCM to form cyclic oligomers and polymers. Dendronization significantly decreases the polydispersity. Increasing the steric bulk of the dendritic side chain from (3,4-3,5)12G2 to (3,4,5-3,4)12G2 to $(3,4,5)^2$12G2 results in continual improvement in the control of molecular weight

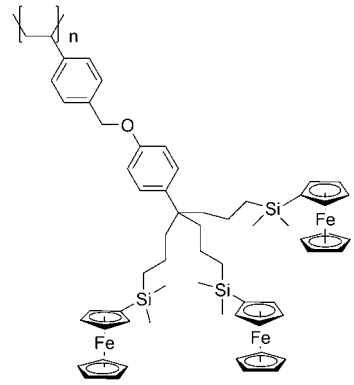

Figure 121. Example ferrocenyl dendronized polymers reported by Astruc.[511]

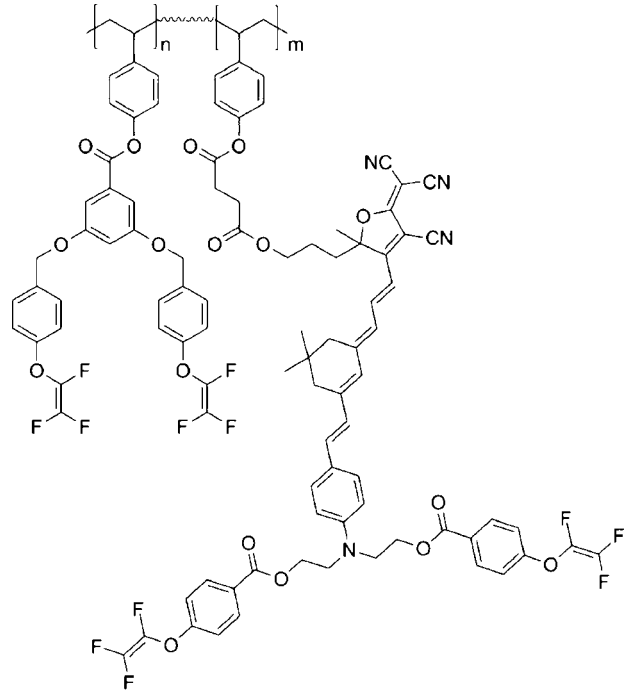

Figure 122. Example of an exotic dendronized polymer for optoelectronics.[514]

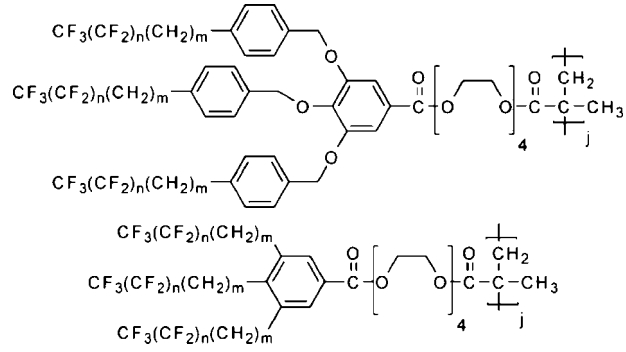

Figure 123. Poly[(4-3,4,5)*m*F*n*G1−4EO−MA] and poly[(3,4,5)*m*F*n*G1−4EO−MA].[360]

evolution, with M_w/M_n as low as 1.03.[534] Further studies demonstrated that shape change from spherical to columnar architectures can be detected during polymerizations via kinetics.[535] Fragments of spheres are more sterically hindered than fragments of columns. As a dendronized polymer with

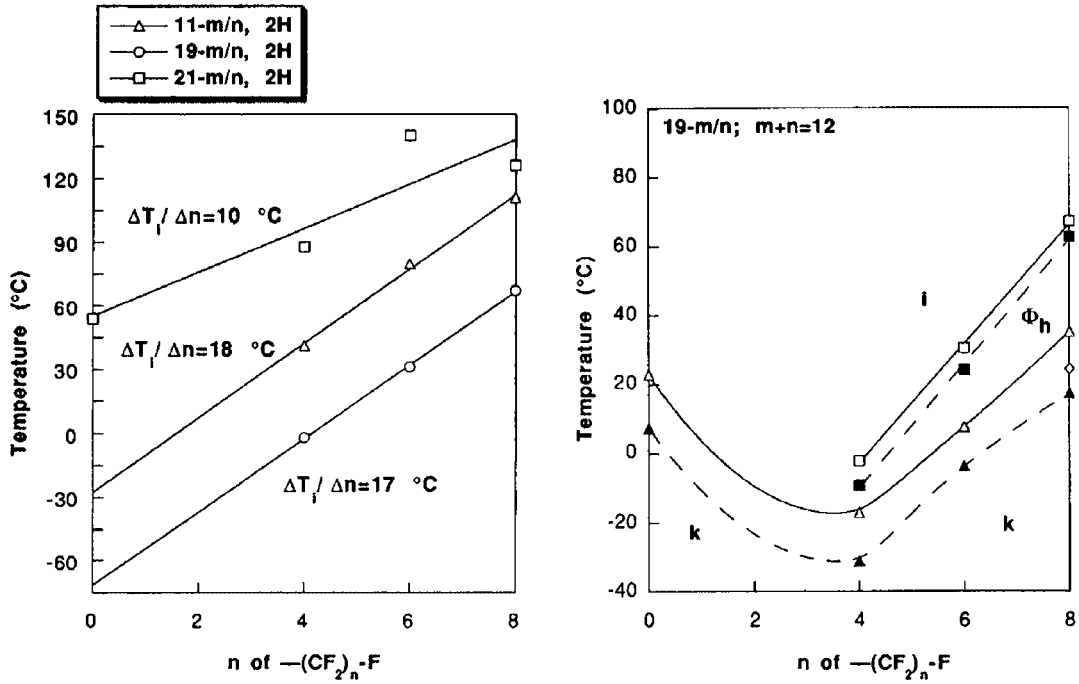

Figure 124. Effect of increasing semifluorination number, *n* (see Figure 123), on the $T_{\Phi h\text{-}I}$ of (3,4,5)12F*n*G1−COOH (11 = *m*/*n*), (3,4,5)12F*n*G1−4EO (19 = *m*/*n*), and poly[(3,4,5)12F*n*G1−4EO−MA] (21 = *m*/*n*) (left). Effect of increasing semifluorination, *n* (see Figure 123), on the phase stabilities of (3,4,5)12F*n*G1−4EO (19 = *m*/*n*). Reprinted with permission from ref 360. Copyright 1996 American Chemical Society.

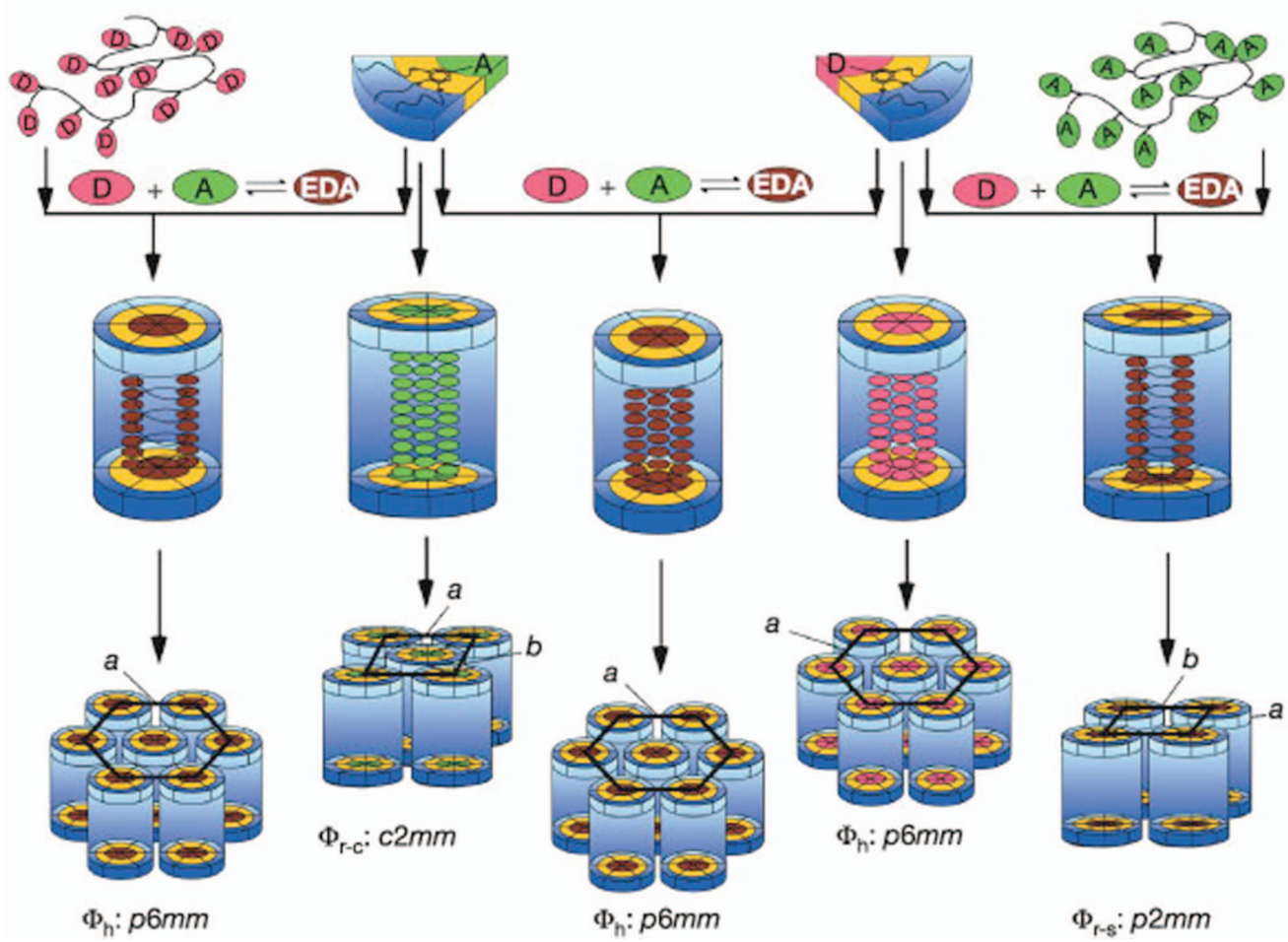

Figure 125. Formation of complex electronic materials via the coassembly of donor/acceptor dendrons and polymers. Reprinted with permission from ref 358. Copyright 2002 Macmillan Publishers Ltd. (Nature).

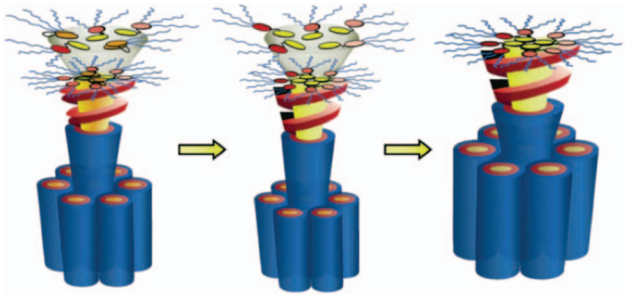

Figure 126. Self-repair mechanism showing the transition from back-folded structural defects (brown discs) to nonfolded aggregates of acceptors, donors, or donor−acceptor complexes in self-assembled electronic materials. Reprinted with permission from ref 363. Copyright 2007 Wiley-VCH Verlag GmbH & Co. KGaA.

a propensity for spherical self-assembly increases in chain length above the critical threshold that can be encapsulated in a sphere, quasi-equivalent motion of the dendron can allow for shape change to a columnar architecture providing rate acceleration of the polymerization. This is exemplified via the ROMP of poly(7-oxanorbornene) dendronized with $(3,4)^2$12G2 (Figure 129). Above DP = 25, the architecture changes from spherical to columnar, resulting in rate acceleration. If, however, the dendronized polymer was less flexible and shape change was not possible, self-interruption of the polymerization at the spherical limit would occur, resulting in perfectly monodisperse polymers.

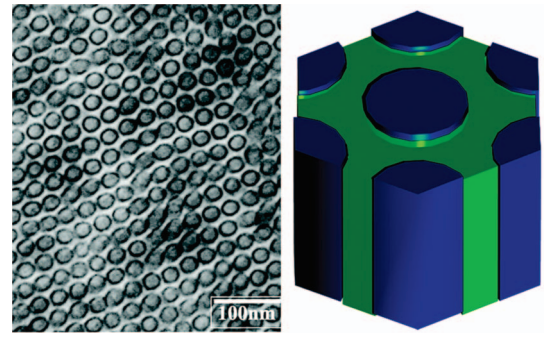

Figure 127. Multiscale organization of dendronized poly(styrene-*b*-isoprene). Reprinted with permission from ref 527. Copyright 2000 American Chemical Society.

Norbornene bisdendronized with willowlike[215,217,218,536] aryl ether dendrons was prepared via ROMP (Scheme 38).[537] TOPM and XRD indicated a progression of LC mesophases on heating from $S_B{}^h \rightarrow S_A \rightarrow N$.

Poly(norbornene)s jacketed with bis(MPA) dendrons were also prepared (Scheme 39).[538] Though they did not exhibit a mesophase, XRD of oriented birefringent fibers did reveal some ordering. Recently, Fréchet and Grubbs reported the ring-expansion metathesis polymerization (REMP) of norbornene analogues functionalized with G2 bis-MPA dendrons to form cyclic polymers (Scheme 40), whose donut topology was observed via AFM.[539]

Scheme 34. General Synthesis and Example Structure of Poly(styrene-*b*-isoprene) with Perfluorinated Dendritic Side Groups[523−526]

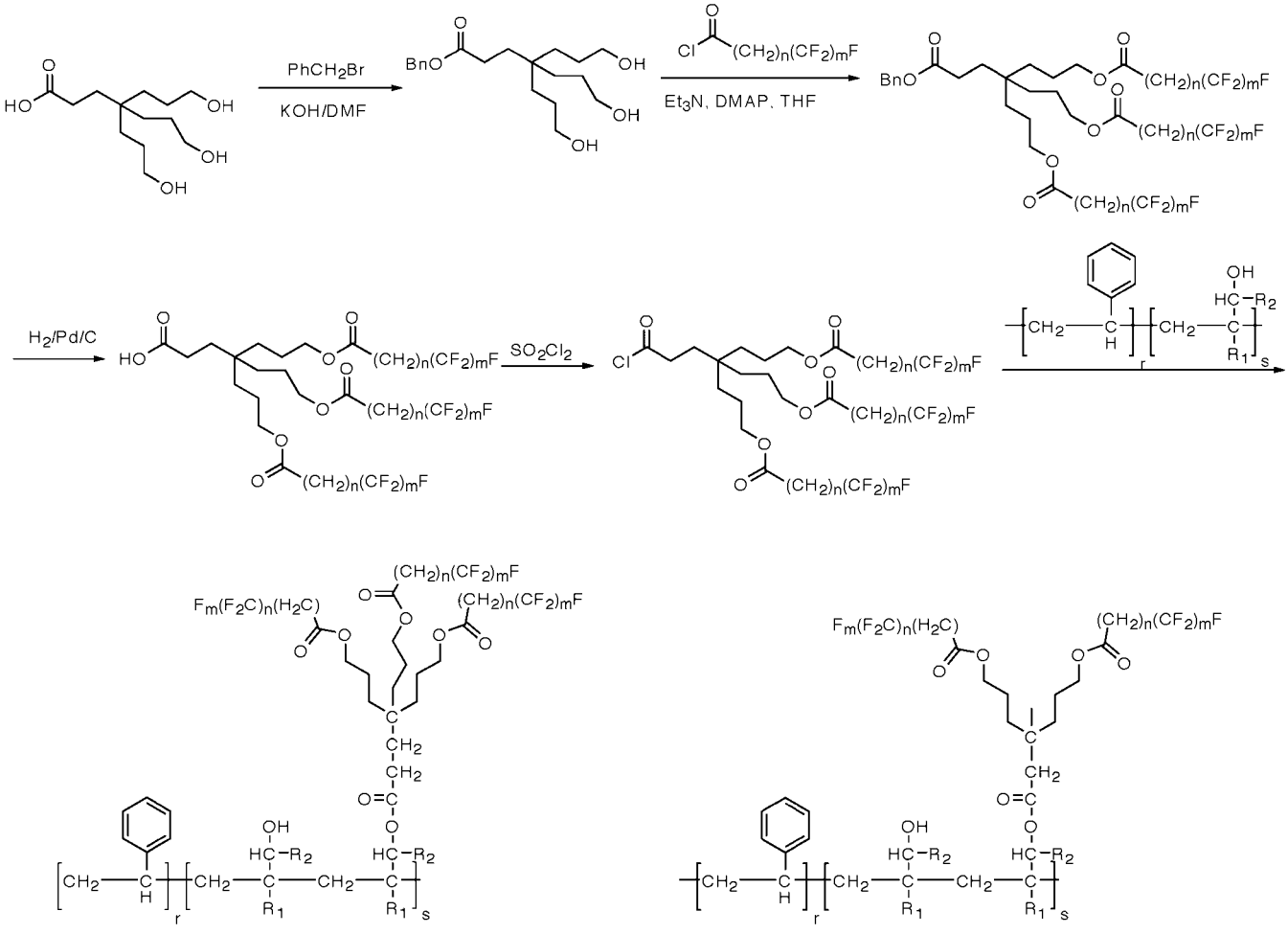

Scheme 35. Synthtesis of Bio-Fiber's Modified with Dendronized Polymers; Reagents and Conditions: (i) GMA, CuCl, $CuBr_2$, PMDETA, Toluene, 30 °C; (ii) Toluene, bis(3-Aminopropyl)-Terminated PDMS, 100 °C; (iii) HCl(aq), THF, RT; (iv) Acid Chloride (R1−R3), TEA, DMAP, DCM, RT (Reprinted with Permission from Ref 530; Copyright 2009 American Chemical Society)

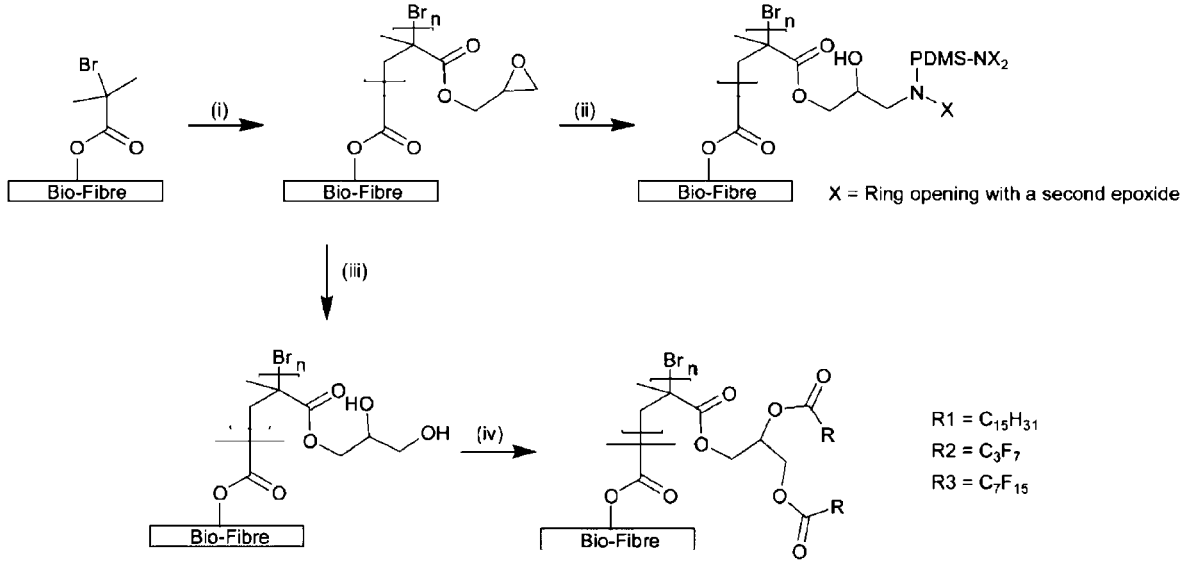

Scheme 36. (3,4,5)12G1-Dendronized Poly(oxanorbornene) and Bisdendronized Poly(7-oxanorbornene) (Top)[456] and Poly(Norbornene) Jacketed with Naphthalene-Capped Dendrons[532]

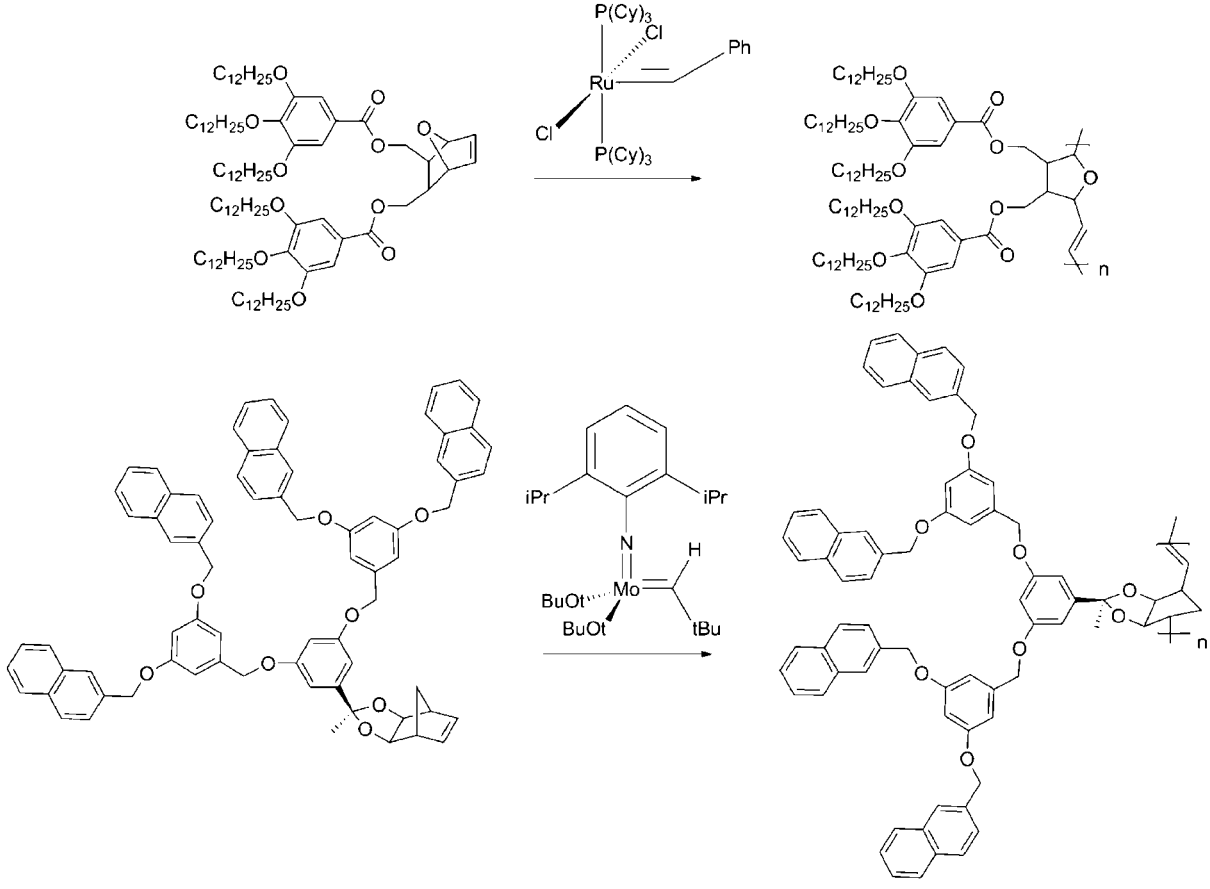

3.2.5. Poly(oxazoline)s

Tomalia reported synthesis of PAMAM jacketed poly(ethylene imine) (produced via hydrolysis of polyoxazoline) via a grafting-from strategy.[369,370] TEM has demonstrated self-organization of rodlike structures into parallel arrays as well as spheroidal architectures. Latterman has reported the synthesis of poly[(*N*-3,4-bis(decyloxy)benzoyl)ethylene imine] which exhibited spherulitic LC texture (Figure 130).[540] Short chain oligomers had been shown to exhibit lamellar and columnar architectures with dendrons bearing shorter-

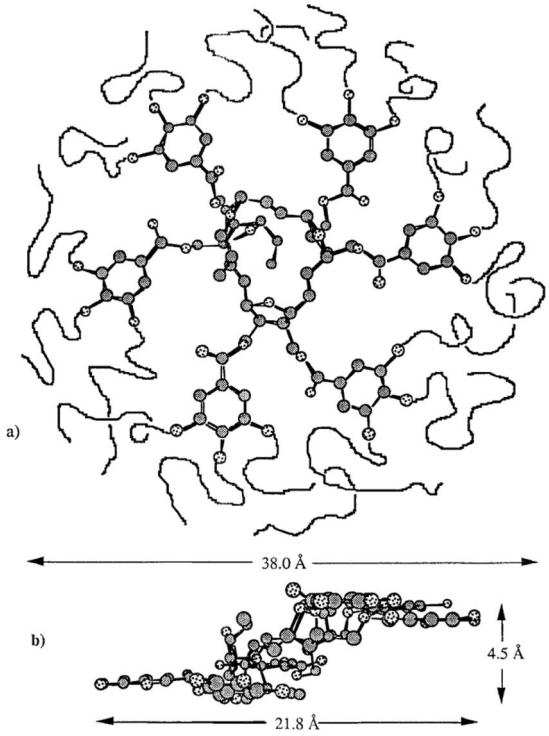

Figure 128. Top (a) and side (b) view of the 3/1 helical model proposed for poly(7-oxanorbornene) bisdendronized with (3,4,5)12G1. Reprinted with permission from ref 456. Copright 1996 American Chemical Society.

chain aliphatic branches.[541] A cubic mesophase was identified via TOPM when the side chains contained 15 or more carbons. XRD was consistent with a BCC lattice, though an insufficient number of reflections were observed to make a definitive assignment. Ringsdorf also examined poly[(*N*-3,4-bis(decyloxy)benzoyl)ethylene imine] and observed a Φ_h structure by XRD.[542,543] LC phases were also observed when poly[(*N*-3,4-bis(decyloxy)benzoyl)ethylene imine] was treated with metal cations.[544] The Percec laboratory also examined poly[(*N*-3,4-bis(decyloxy)benzoyl)ethylene imine] prepared through living cationic ring-opening polymerization (ROP) of the dendronized oxazoline macromonomer.[545] The Φ_h phase was confirmed in samples of DP = 100−500 via XRD and TOPM and direct visualization via TEM and AFM.

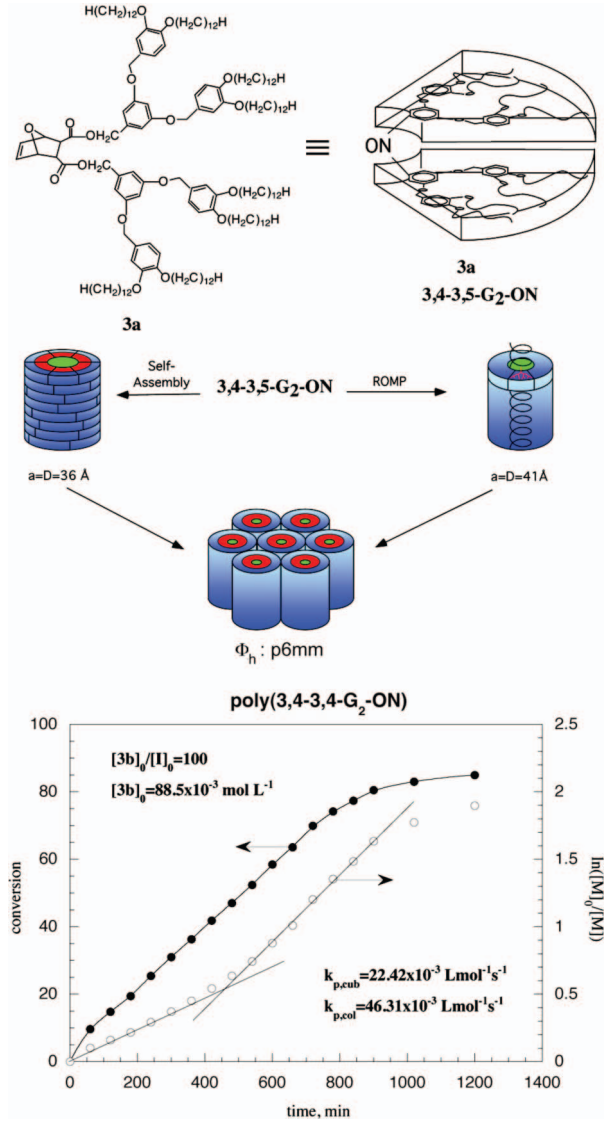

Figure 129. Rate acceleration by shape change from spheres to columns during polymerization. Adapted with permission from ref 535. Copyright 2000 American Chemical Society.

Absent from earlier reports from other groups, it was found that poly(oxazoline) dendronized with (3,4)12G1

Scheme 37. Poly(7-oxanorbornene) Jacketed with (4-3,4,5)12G1[533]

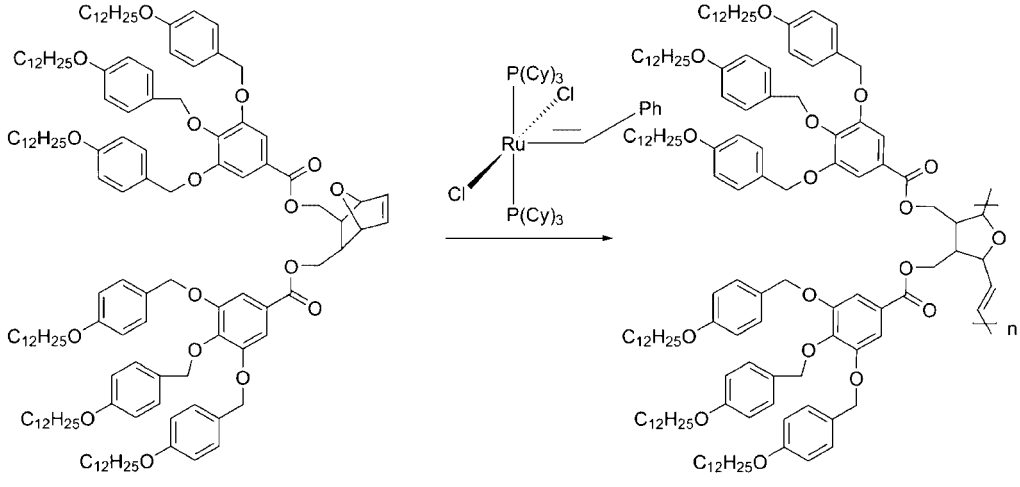

Scheme 38. Willow Dendron Jacket Poly(norbornene) Drawn in Gauche Conformation of the Repeat Unit; In the Self-Organized State, It Is the Anti-Conformer of the Repeat Unit That Dominates[537]

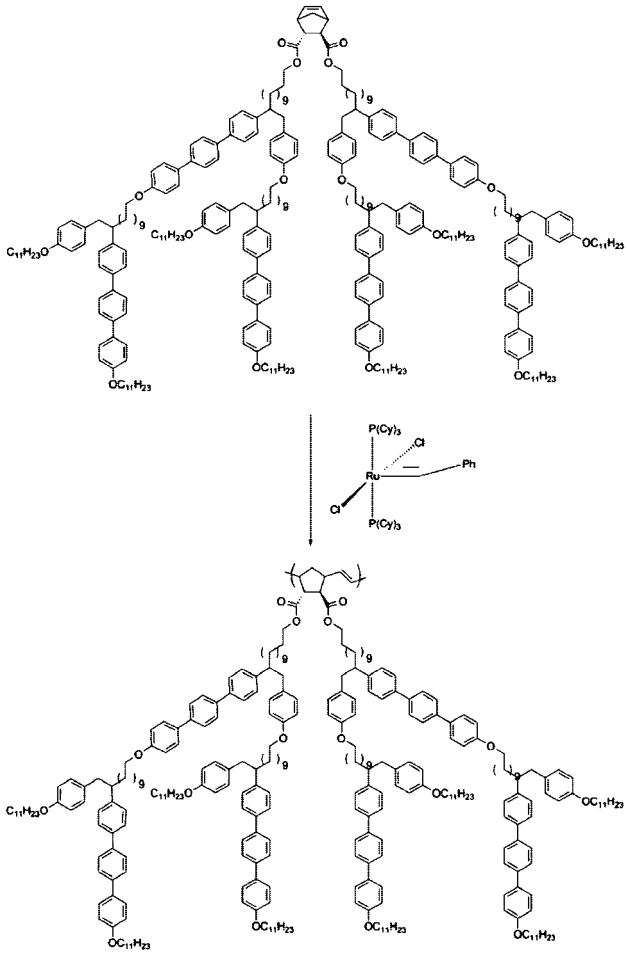

at DP < 70 self-assembles into a spherical architecture that self-organizes into a *Cub* lattice (Figure 131a).[546] At higher DP, a Φ_h architecture emerges, providing the second example of shape change in dendronized polymer mediated by DP. Further it was found that, at low DP, the polymer undergoes thermoreversible shape change from columnar organization at low temperature to spherical organization at temperature just prior to isotropization. XRD analysis indicated that, from DP = 30 to 75, *Cub* lattices coexist with Φ_h lattices. If the polymers were in fact monodisperse, $M_w/M_n = 1.00$, this would not be possible. However, despite the use of living ROP to produce the dendronized poly(oxazolines), they have a measurable polydispersity of $M_w/M_n = 1.09-1.21$. Gel permeation chromatography (GPC) traces (Figure 131b,c) revealed that, due to the low but definitive polydispersity of the polymers produced, at average DP = 30 the polymer mixture begins to contain a small fraction of chains larger than the threshold to be enclosed within a single sphere and, therefore, columnar self-assembly begins to coexist with spherical self-assembly. From average DP = 5−30, the polydispersity of the polymer mixture provides objects with various fractions of a sphere that, due to their quasi-equivalence, self-assemble into spherical objects that are able to self-organize into a *Cub* lattice.

Scheme 40. Cyclic Dendronized Poly(norbornene)s Prepared via REMP

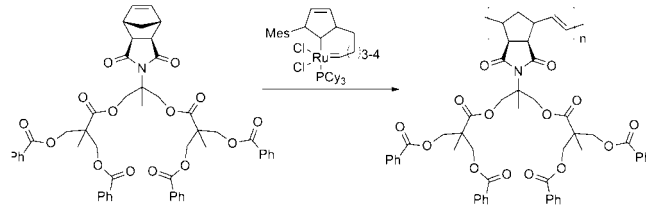

Additionally, the Percec laboratory prepared dendronized PEI through the MeOTf living cationic ROP of dendritic oxazoline macromonomers (Scheme 41). (3,4,5)12G1 dendronized PEI with DP = 20 self-assembled into spheres that self-organized into a BCC "inverse micellar" lattice (Figure 132).[318] A combination of TEM and XRD with electron density map reconstruction definitively assigned the BCC

Scheme 39. Bis(MPA)-Dendronized Poly(norbornene)

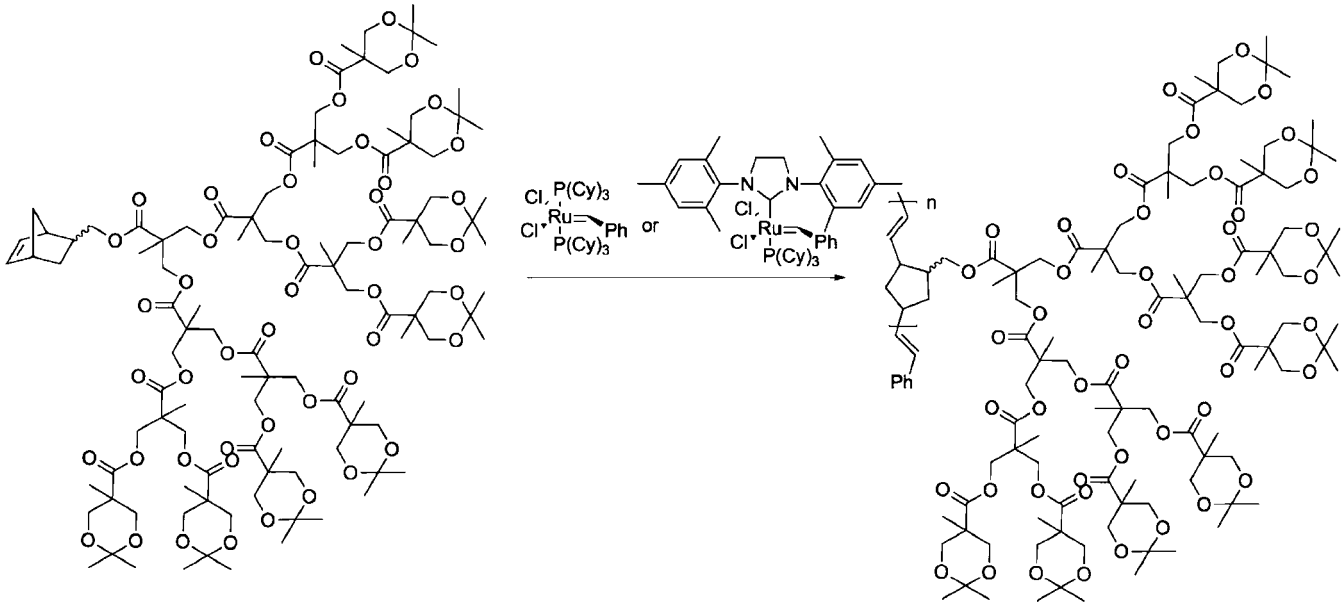

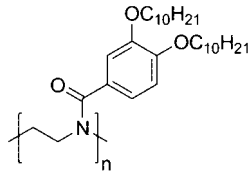

Figure 130. Structure of poly[(*N*-3,4-bis(decyloxy)benzoyl)ethylene imine].[540]

inverse micellar lattice with a phase solution of + + + + (Figure 133).[319]

Scheme 41. Mechanism of Living Cationic ROP of Dendronized Oxazolines[317]

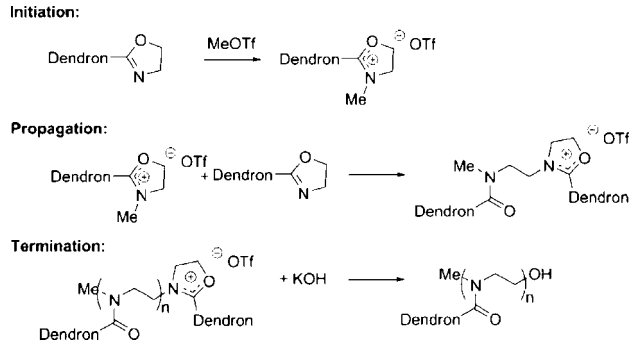

3.2.6. Poly(arylacetylene)s

The backbone of *cis*-transoidal and *cis*-cisoidal poly(phenylacetylene)s (*cis*-PPA)s exhibit multiple conformations, some of them facilitating helical organization and intramolecular electrocyclization.[547−555] While the helical organization of *cis*-PPA is dynamic,[556] chiral side groups can cause the rotation barrier and select the helical sense, and therefore, CD and UV/vis spectroscopy are effective tools for assessing *cis*-PPA backbone conformations.[79,557] As the conformation of *cis*-PPA exhibits dynamic helical order even without dendritic or chiral side groups, it provides an interesting case in which self-organization of analogous dendronized *cis*-PPA is truly a synergy of the intrinsic structure of the polymer

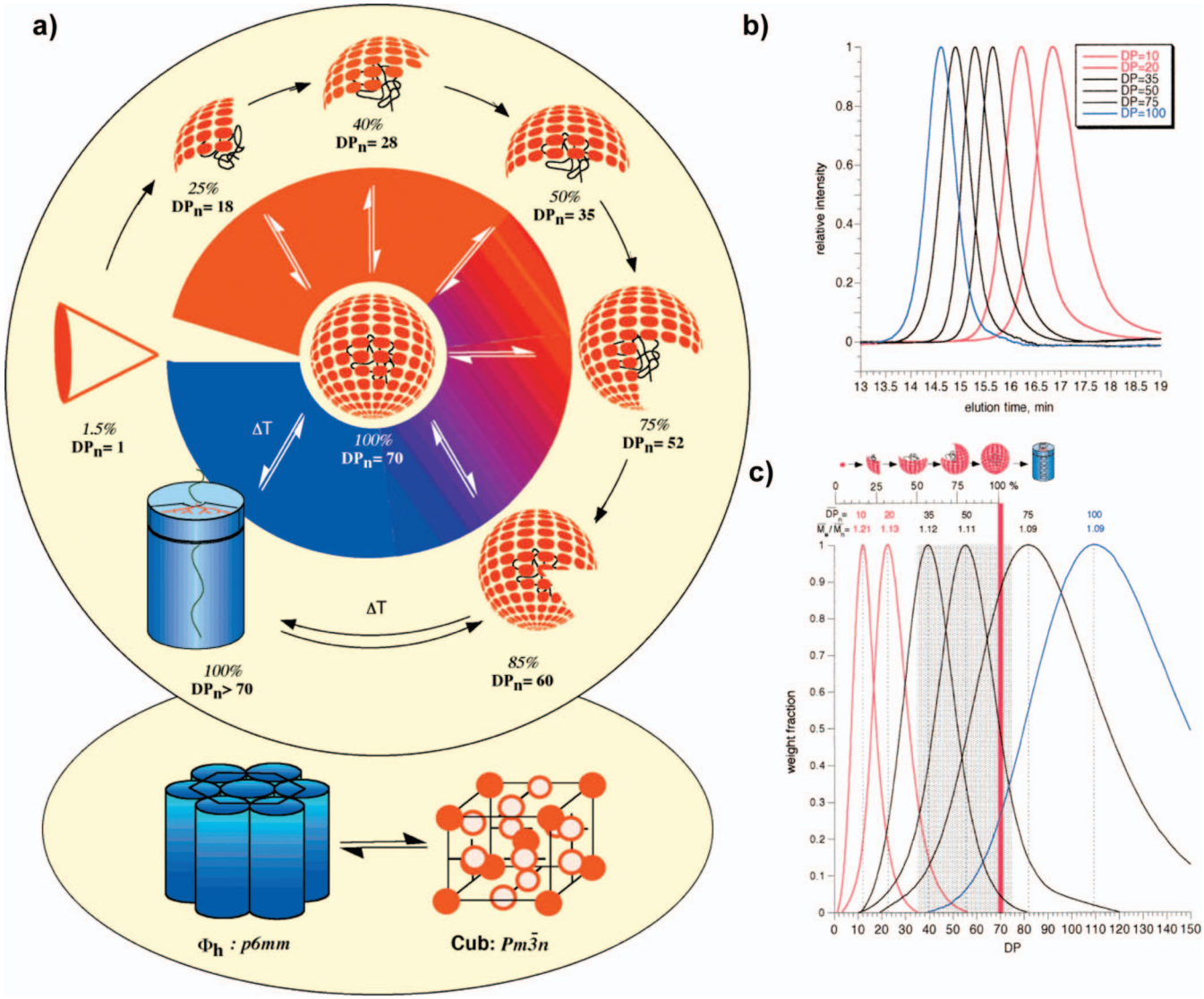

Figure 131. Formation of supramolecular dendrimers via self-assembly and coassembly of macromolecules of different molecular weights (a). Selected GPC traces for poly(oxazoline)s dendronized with (3,4)14G1 (b) and weight fraction as a function of the theoretical DP. The red line represents the threshold for spherical supramolecules, and the shaded area represents the range of DPs for which a biphase was observed by XRD. Reprinted with permission from ref 546. Copyright 2001 American Chemical Society.

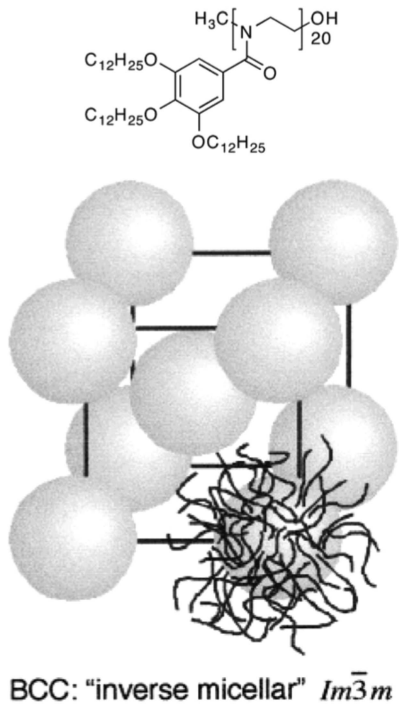

Figure 132. (3,4,5)12G1 dendronized PEI and self-organized BCC lattice. Reprinted with permission from ref 318. Copyright 2000 American Chemical Society.

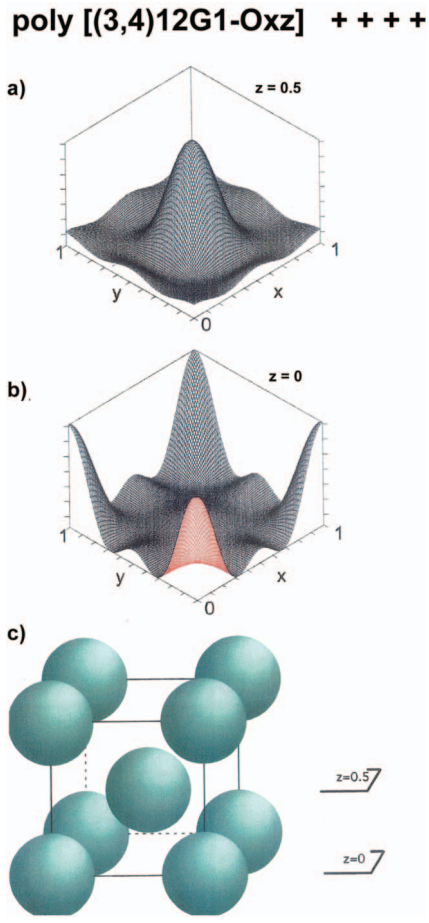

Figure 133. Electron-density maps of the $z = 0.5$ (a) and $z = 0$ (b) planes and a schematic of the BCC unit cell. Reprinted with permission from ref 319. Copyright 2001 Wiley-VCH Verlag GmbH & Co. KGaA.

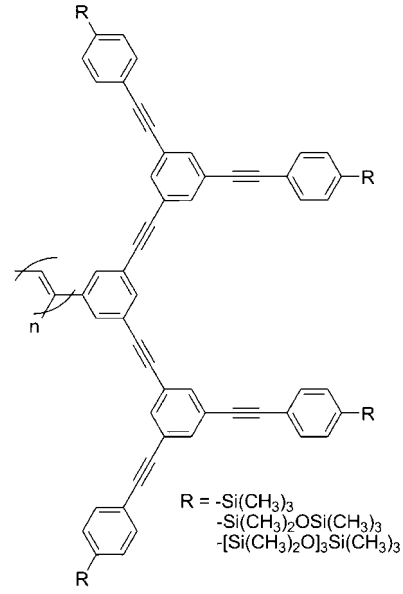

Figure 134. Example of a second-generation phenylacetylene-based dendron.[558,559]

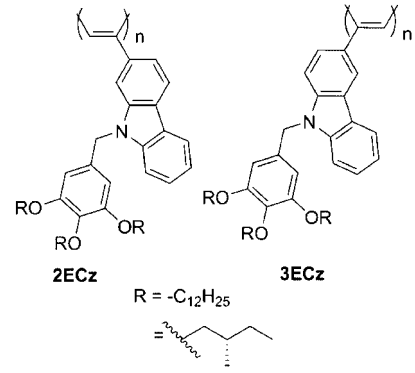

Figure 135. Dendronized poly(ethynyl-carbazole)s.[562]

and structural allosteric regulation via the dendritic side groups. Kaneko was the first to report the synthesis of phenylacetylene-based dendrons (Figure 134).[558,559] The acetylene unit at the apex group of these dendrons was stereoselectively polymerized via $[Rh(C_7H_8)Cl_2]$ to form bisdendronized *cis*-PPA. These bisdendronized *cis*-PPAs self-assemble into Φ_h lattices with columnar diameters ranging from 20.1 to 39.1 Å, corresponding to the first-generation and second-generation macromonomers, respectively. These structures were supported by XRD and AFM studies. Variants of these structures were used as permselective membranes.[560] Ab initio studies of exciton scattering in aryl acetylene dendritic architectures provided a model for the prediction of their electronic transitions.[561]

Percec first reported the synthesis of poly(2-ethynyl-9-substituted carbazole)s (2ECz) and poly(3-ethynyl-9-substituted carbazole)s (3ECz) containing chiral and achiral dendritic substituents (Figure 135).[562] Polymers were prepared from the corresponding acetylenic macromonomer via a living polymerization using $Rh(C{\equiv}CPh)(nbd)(PPh_3)_2$ as catalyst. Poly(*N*-ethynylcarbazole) are also known to a adopt a helical conformation.[563] These *cis*-PPA analogues self-organize into chiral and achiral nematic mesophases, respectively. Neither 2ECz* nor 3ECz* monomers exhibit a CD signature on their own. However, the solution CD studies of the chiral polymers, poly(2ECz*) and poly (3ECz*), demonstrated helical organization, and thus, the achiral

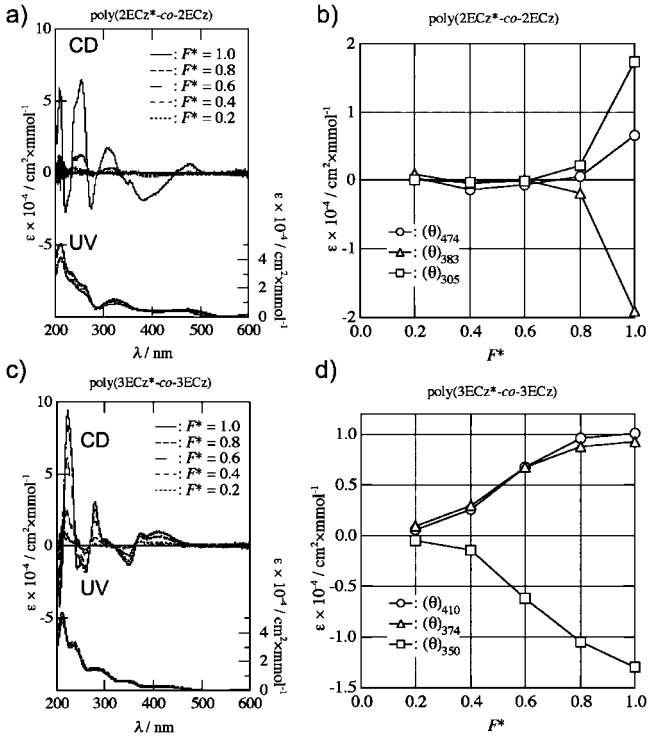

Figure 136. (a) CD (top) and UV (bottom) spectra of 2ECz* and poly(2ECz*-*co*-2ECz) with varying mole fraction of chiral monomer, (b) the θ (ellipticity) dependence on F^* for poly(2ECz*-*co*-2ECz) in THF, (c) CD (top) and UV (bottom) spectra of 3ECz* and poly(3ECz*-*co*-3ECz) with varying mole fraction of chiral monomer, and (d) the θ dependence on F^* for poly(3ECz*-*co*-3ECz) in THF. Reprinted with permission from ref 562. Copyright 2002 John Wiley & Sons, Inc.

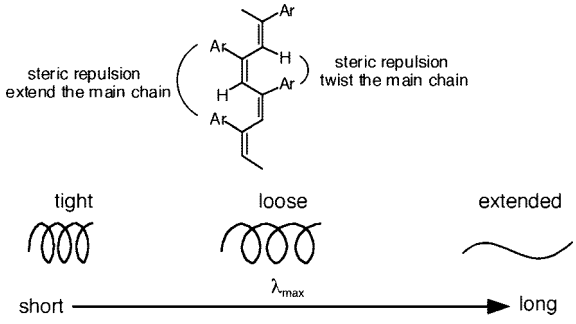

Figure 137. Model explaining the effect of steric repulsion on the helical compression of the main chain. Reprinted with permission from ref 562. Copyright 2002 John Wiley & Sons, Inc.

polymers are presumed to adopt a racemic mixture of helical organization. Random copolymers of 2ECz and 2ECz* as well as 3ECz and 3ECz* were also prepared and studied by CD/UV−vis spectroscopy.(Figure 136). Increasing the mole fraction, F^*, of the chiral monomer in the reactant feed stock prior to polymerization resulted in decreased λ_{max} and increased molar ellipticity. For poly(2ECz*-*co*-2ECz), the ellipticity increases sharply from around $F^* \approx 0.8$ to 1.0. However, for poly(3ECz*-*co*-3ECz), the ellipticity increases gradually from very low F^* and plateaus at ~0.8. It can be concluded, therefore, that the persistence length of the helical conformation is significantly shorter in the case of poly(2ECz) than in that of poly(3ECz). Thus, λ_{max} decreased with increasing F^*. The presence of the chiral side chains compresses the helical backbone. This is reasonable, as the chiral monomer has sterically less demanding alkyl side

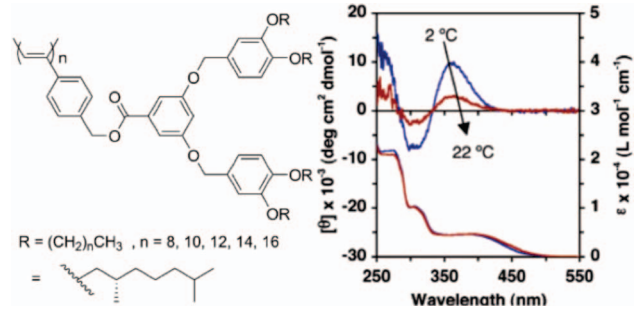

Figure 138. Structure of (3,4-3,5)G2 dendronized cis-PPA (left) and CD (top)/UV−vis (bottom) spectra of *cis*-PPA jacketed with (3,4-3,5)d*m*8G2 in methylcyclohexane. Reprinted with permission from ref 564. Copyright 2005 American Chemical Society.

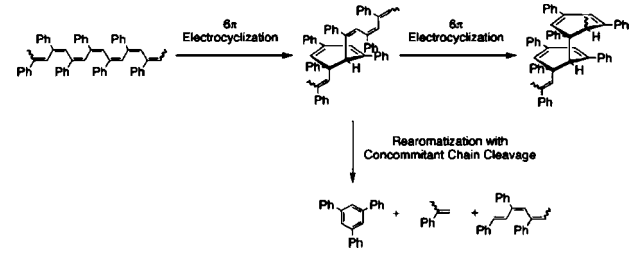

Figure 139. 6π electrocyclization of 1,3-*cis*,5-hexatriene sequences in *cis*-PPA. Reproduced with permission from ref 564. Copyright 2005 American Chemical Society.

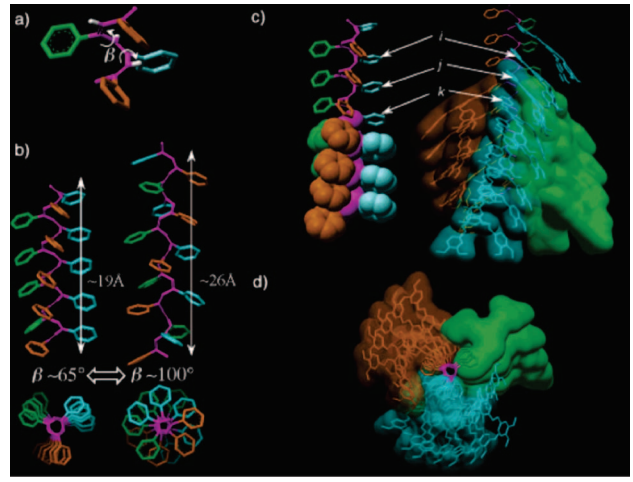

Figure 140. Model of (a) *cis*-PPA dihedral angle, (b) backbone views of *cis*-cioidal (left) and *cis*-transoidal (right) PPA, (c) side view of *cis*-cisoidal PPA indicating helical order, and (d) top view of *cis*-cisoidal PPA showing hollow center. Reproduced with permission from ref 564. Copyright 2005 American Chemical Society.

chains than the achiral monomers, limiting the congestion between neighboring dendron side chains (Figure 137). The compression effect is more pronounced in 2ECz as compared to 3ECz, suggesting that the organization is sensitive to connective geometry. This is in contrast to what is observed for poly[(3,4,5)d*m*8G1−A], where the chiral periphery induced helical expansion rather than contraction. In the latter case, the chiral unit is significantly closer to the helical backbone and is a part of a larger branched aliphatic chain.

Percec prepared a library of (3,4-3,5)*n*G2 self-assembling dendrons with a diversity of achiral and chiral aliphatic tails. These dendron acids were attached to 4-ethynyl benzyl alcohol to form a dendritic macromonomer.[564] Stereoselective living polymerization using Noyori's

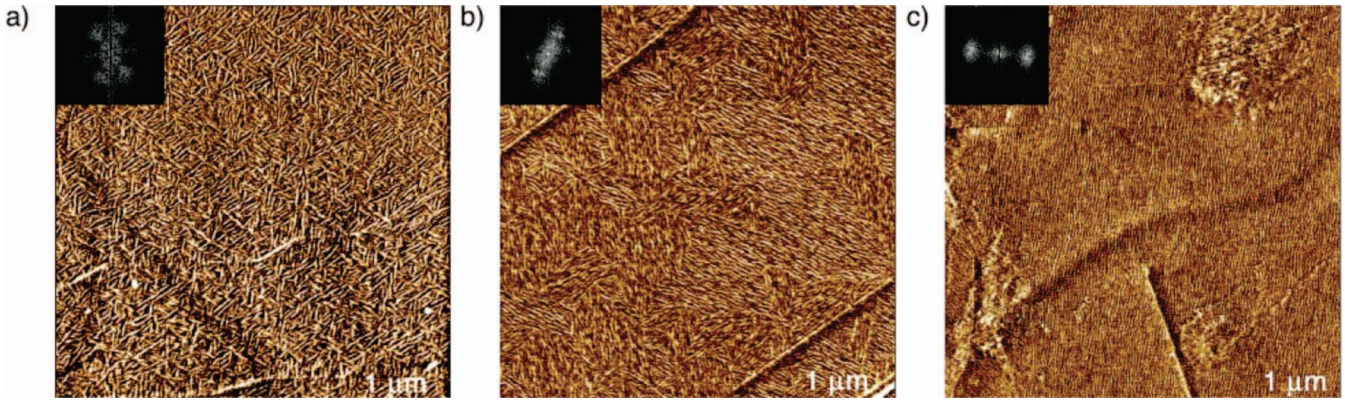

Figure 141. AFM phase image of a single layer of poly[(3,4-3,5)12G2−4EBn] (a) spin-cast on HOPG and after annealing for 1 h at (b) 50 °C and (c) 100 °C. Reprinted with permission from ref 570. Copyright 2006 American Chemical Society.

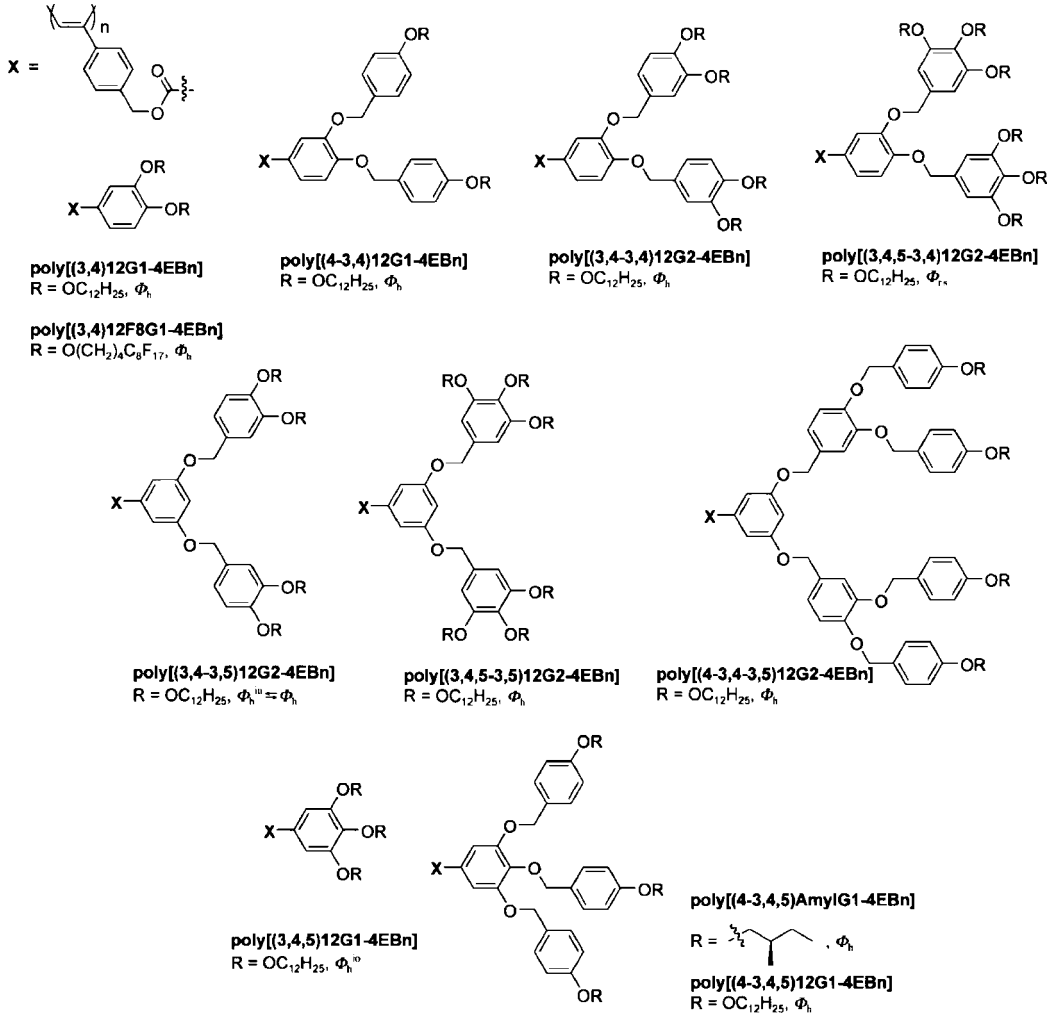

Figure 142. Library of dendronized *cis*-PPA. Reprinted with permission from ref 571. Copyright 2006 Wiley-VCH Verlag GmbH & Co. KGaA.

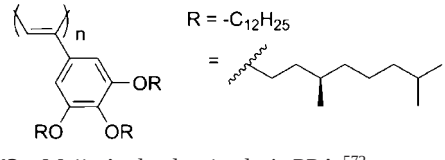

Figure 143. Meijer's dendronized *cis*-PPA.[572]

$Rh(C{\equiv}CPh)(nbd)(PPh_3)_2$ catalyst[421] produced dendronized *cis*-PPA (poly[(3,4-3,5)*n*G2−4EBn]) with DP of 48−52 (Figure 138). Dendronization suppressed 6π electrocyclization, a process recently shown to be accelerated by Lewis acids, and therefore perhaps by the polymerization catalysts as well,[565] of 1,3-*cis*,5-hexatriene sequences in *cis*-PPA (Figure 139) by providing a steric barrier.[566]

CD/UV−vis spectroscopy of the dendronized *cis*-PPA with a chiral tail demonstrates a decrease in chirality with increasing temperature, which is in agreement with the dynamic helical behavior of *cis*-transoidal PPAs (Figure 138).[567−569] All achiral dendronized *cis*-PPA exhibit multiple mesophases with Φ_h organization. In all cases, a thermoreversible transition between hexagonal columnar organization

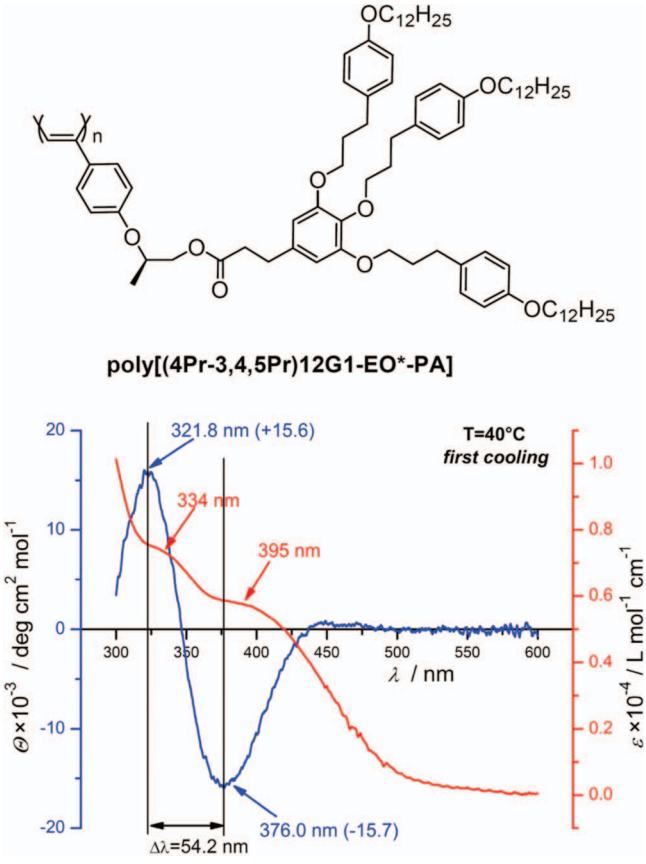

Figure 144. Structure of *cis*-PPA jacketed with phenylpropyl ether dendrons (left) and CD/UV−vis spectra of the helical polymer in methylcyclohexane demonstrating negative exciton coupling. Reprinted with permission from ref 575. Copyright 2007 Wiley-VCH Verlag GmbH & Co. KGaA.

with helical internal order (Φ_h^{io}) at lower temperature and hexagonal columnar organization without internal order (Φ_h) at higher temperatures was observed. In the Φ_h, the aromatic portions of the dendritic side chain exhibit liquidlike disorder. However, in the Φ_h^{io} state, well-defined helicity and dendron tilt features can be observed by XRD, but the internal order and the helical features do not correlate between columns. This phenomenon was explained by an unprecedented thermoreversible conversion of *cis*-cisoidal PPA to *cis*-transoidal PPA. This transition can be viewed as an expansion of dihedral angle, β, of *cis*-PPA from ~65° in *cis*-cisoidal-PPA to ~100° in *cis*-transoidal PPA (Figure 140a). This expansion of the dihedral angle results in overall stretching of the columnar architecture, resulting in a decrease in columnar dimensions in the $\Phi_h^{io} \rightarrow \Phi_h$ transition (Figure 140b). In the Φ_h^{io} organization, the tighter helicity results in a hollow center along the helical axis that becomes filled in the Φ_h phase.

Direct visualization of poly[(3,4-3,5)12G2−4EBn] via AFM was performed on HOPG surfaces.[570] AFM of directly cast films demonstrates alignment with HOPG lattice symmetry via epitaxial adsorption of the peripheral alkyl tails. However, annealing of the sample for 1 h at 50 or 100 °C resulted in the formation of organized domains with 2-D N structure (Figure 141). Results indicate that, on HOPG, *cis*-PPA adopts a conformation that is extended relative to *cis*-cisoidal conformation.

A larger library of dendronized *cis*-PPAs with achiral and chiral aliphatic tails in the self-assembling dendrons was prepared (Figure 142).[571] The corresponding dendrons self-assemble into a diverse array of columnar, spherical, and lamellar architectures. However, when this diverse array of dendritic branching structures are used as side groups in *cis*-PPA, only Φ_h and Φ_h^{io} architectures are observed.

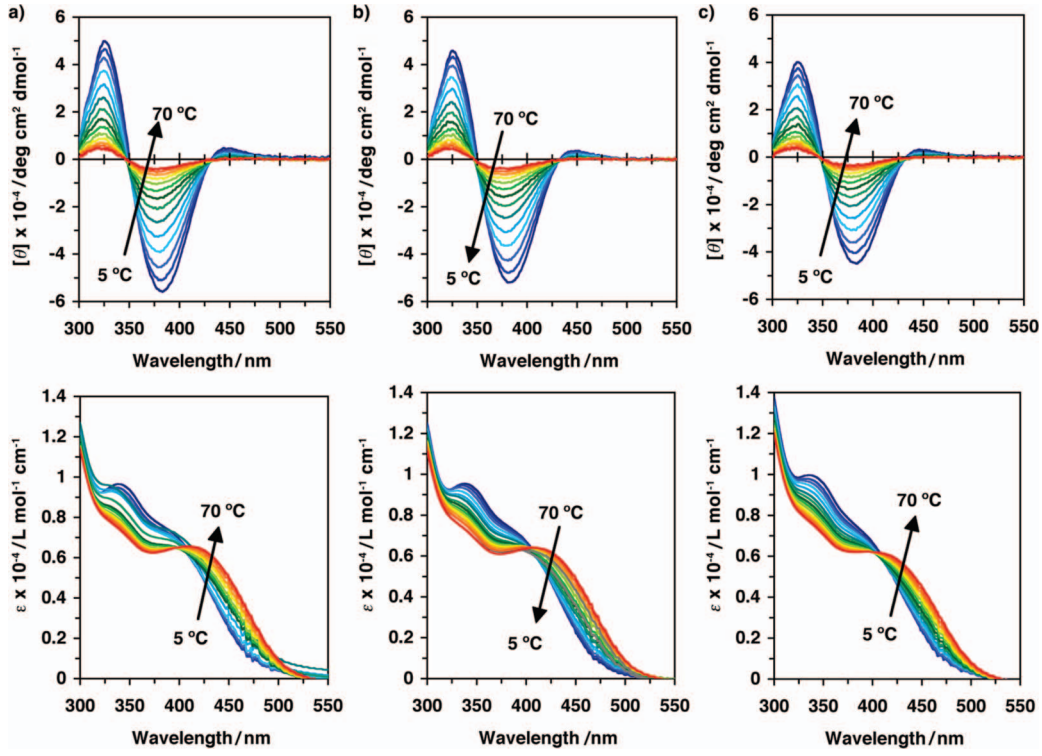

Figure 145. Temperature-dependent CD (top) and UV−vis (bottom) spectra of the helical polymer in methylcyclohexane: (a) first heating, (b) first cooling, and (c) second heating. Reprinted with permission from ref 575. Copyright 2007 Wiley-VCH Verlag GmbH & Co. KGaA.

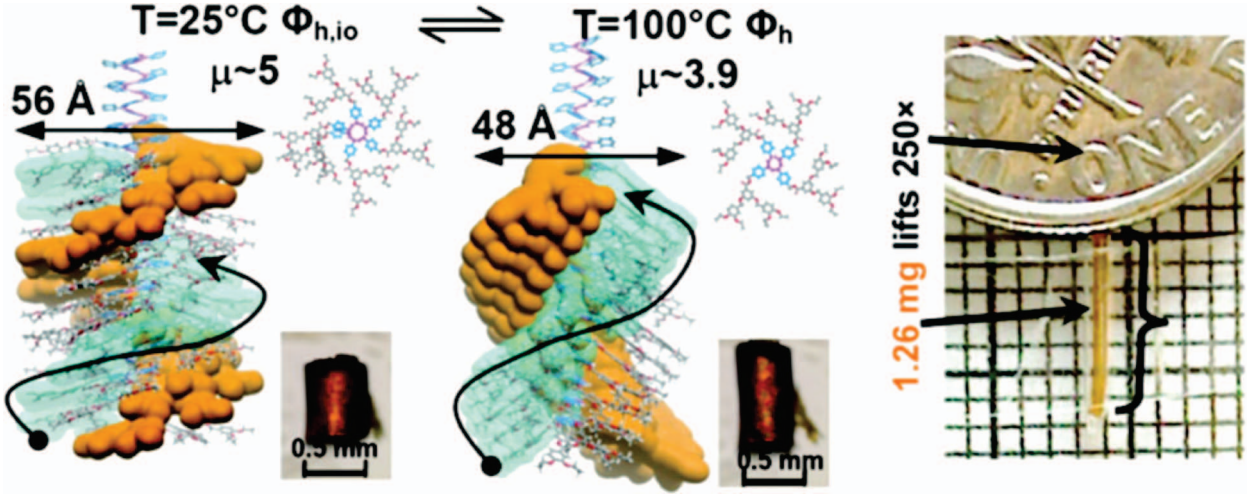

Figure 146. Nanomechanical function of poly[(3,4-3,5)16G2−4EBn]. Reprinted with permission from ref 576. Copyright 2008 American Chemical Society.

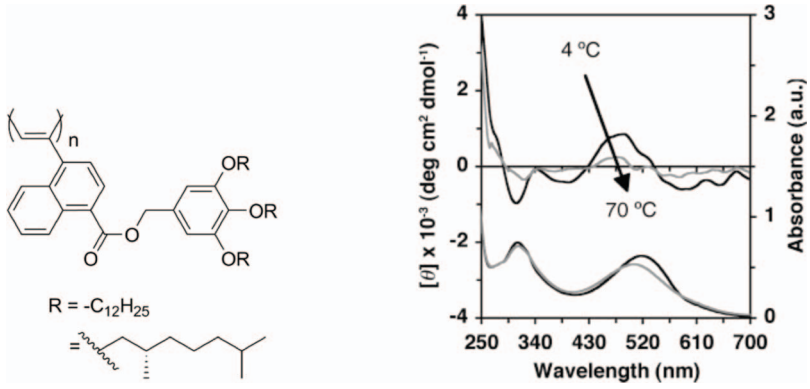

Figure 147. Structure of dendronized poly(1-naphthylacetylene)s (left) and CD/UV−vis of poly(1-naphthylacetylene) jacketed with (3,4,5)d*m*8G1 (right) in methylcyclohexane. Reprinted with permission from ref 579. Copyright 2007 John Wiley & Sons, Inc.

Meijer described another set of dendronized *cis*-PPAs. Here the macromonomer was a Percec-type (3,4,5)*n*G1 minidendron with achiral and branched chiral aliphatic side chains and a polymerizable acetylenic unit at the apex (Figure 143).[572] Stereoselective polymerization to form dendronized *cis*-PPA was achieved using $[Rh(nbd)Cl]_2$ as the catalyst. DSC/TOPM revealed that both chiral and achiral polymers exhibited a LC mesophase with identical textures. XRD suggested a bilayer architecture in the achiral polymer. Additionally, the film CD of the chiral polymer revealed exciton coupling. Thus, the chiral side chain induces a specific helical sense in the main chain.

Percec previously examined the polymers of Meijer and later reported more detailed studies in context of the Φ_h^{io} to Φ_h transition.[573,574] XRD showed that poly[(3,4,5)12G1−A] and poly[(3,4,5)d*m*8G1−A] assume a *cis*-cisoidal conformation at lower-temperature packing into a $\Phi_{r\text{-}c,\ k}$ lattice and that, at elevated temperature, a similar transition to a *cis*-transoidal conformation and a Φ_h lattice is observed. This is in contrast to a lamellar-type architecture reported by Meijer for poly[(3,4,5)12G1−A] at 50 °C.[572] CD/UV−vis spectroscopy suggested that the helical sense selection evident in poly[(3,4,5)d*m*812G1−A] is greater than in poly[(3,4-3,4)d*m*8−4EBn] and is persistent at much higher temperature. Further, poly[(3,4,5)d*m*8G1−A] has a 10% larger column stratum thickness than achiral poly[(3,4,5)12G1−A]. Such a difference was not observed for poly[(3,4-3,5)d*m*8G2−4EBn] and poly[(3,4-3,5)12G2−4EBn]. Thus, it seems that chiral communication in dendronized *cis*-PPA requires a critical level of stereocenter crowding in order to induce a structural distortion that selects the helical sense. This critical crowding occurs most efficiently when the stereocenter is in the polymer−dendron linkage or when the distance from the stereocenter to the main chain is short (i.e., a low generation number dendron side chain).

In addition to poly[(3,4-3,5)*n*G2−4EBn], it was also found that *cis*-PPA dendronized with a chiral phenylpropyl ether dendron poly[(4Pr-3,4,5Pr)12G1−4EO*−PA] also exhibits a Φ_h^{io} phase and the same thermoreversible $\Phi_h^{io}-\Phi_h$ transition (Figure 144).[575] As this was the first chiral dendronized *cis*-PPA to exhibit the $\Phi_h^{io}-\Phi_h$ transition, CD/UV−vis spectroscopy was able for the first time to characterize the helicity and assign it via negative exciton coupling to a right-handed helical sense (Figure 144).[575] Temperature-dependent CD/UV−vis experiments (Figure 145) demonstrate a limited hysteresis, only a small drop in magnitude from the first heating in later cycles, indicating that dendronization prevents decomposition of the polymer via 6π-electrocyclization even at elevated temperature and that the $\Phi_h^{io}-\Phi_h$ transition is completely reversible. It is worth noting that, even at very high temperature, helicity persists.

The unprecedented thermoreversible *cis*-cisoidal to *cis*-transoidal transition observed in poly[(3,4-3,5)*n*G2−4EBn] and poly[(4Pr-3,4,5Pr)12G1−EO*−PA] can be harnessed for complex nanomechanical function.[80,576−578] The elongation of the helix associated with the transition provides force directly along the helical axis. An oriented fiber of

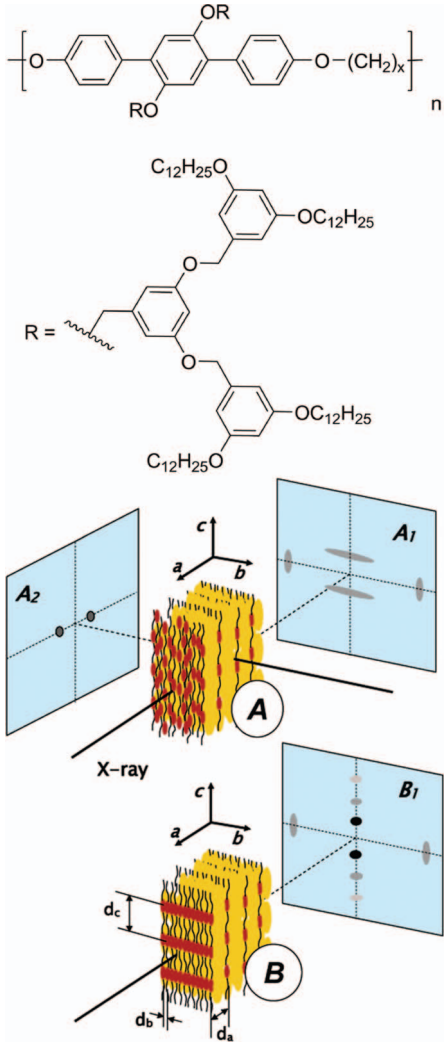

Figure 148. Structure and self-assembly of covalently dendronized polyterphenyl ethers. Reprinted with permission from ref 586. Copyright 2004 American Chemical Society.

1.26 mg of poly[(3,4-3,5)16G2−4EBn] is capable of lifting an object 250× its weight via the unraveling of its helical order triggered by temperature (Figure 146). Recooling below the $\Phi_h-\Phi_h^{io}$ transition temperature results in contraction of the fiber, providing a reversible extension−contraction process.

Chiral (poly[(3,4,5)dm8G1−1EN]) and achiral (poly[(3,4,5)-12G1−1EN]) dendronized poly(1-naphthylacetylene)s with very high *cis*-content were prepared using $[Rh(nbd)Cl]_2$ as a catalyst (Figure 147).[579] Both chiral and achiral polymers organize into columnar center-rectangular lattices ($\Phi_{r\text{-}c}$.) The dendronized poly(1-naphthylacetylenes) seem to exhibit greater stacking correlation, which can enhance chiral communication or allosteric regulation in bulk. Further, the pseudo-*ortho*-effect of the naphthalene side group prevents decomposition at high temperature due to 6π electrocyclization (Figure 139).[79,553,555,557,580,581]

Helical screw-sense induction has also been demonstrated via noncovalent interactions. Kato has reported that the helical sense of PPA bearing phosphonate side groups can be biased via the noncovalent interaction with chiral poly(L- or D-glutamic acid) dendrons.[582]

3.2.7. Main-Chain Polyethers and Polyesters

In 2002, using a phase-transfer catalyzed polyesterification technique pioneered by Percec[416] for the synthesis of main-chain liquid crystalline polyethers, Kallitsis reported the copolyetherification of $Br(CH_2)_xBr$ where $x = 8-12$ with 2′,5′-dendrido-*p*-terphenyl-4,4″-diol, where the dendron side chains were G1 and G2 Fréchet dendrons.[583−585] While some self-organization was evident via XRD, the structure of the polymer was not fully elaborated. To fully exploit the self-organization potential of the dendritic jacket, a further synthetic study was completed where the Fréchet dendrons were replaced with (3,5)12G1 and $(3,5)^2$12G2 Percec-type dendrons (Figure 148).[586] Here aliphatic−aromatic segregation induced a greater-degree of order as evidenced by DSC, Small-Angle Light Scattering (SALS), TOPM, and XRD.[587] Oriented fiber XRD exhibited 2D layering of dendron-jacketed terphenyl units and supported a N structure (Figure 148a) that is converted to an S phase (Figure 148b) upon annealing.

Lee reported the synthesis of *m*-linked rigid dendronized polymers via the polycondensation of bifunctional dendronized pentaphenylene with 4,4′-bis(bromomethyl)biphenyl (Scheme 42). The transition of *m*-linked rigid polymers from

Scheme 42. Synthesis of *m*-Linked Rigid Polymers (Reprinted with Permission from Ref 588; Copyright 2005 American Chemical Society)

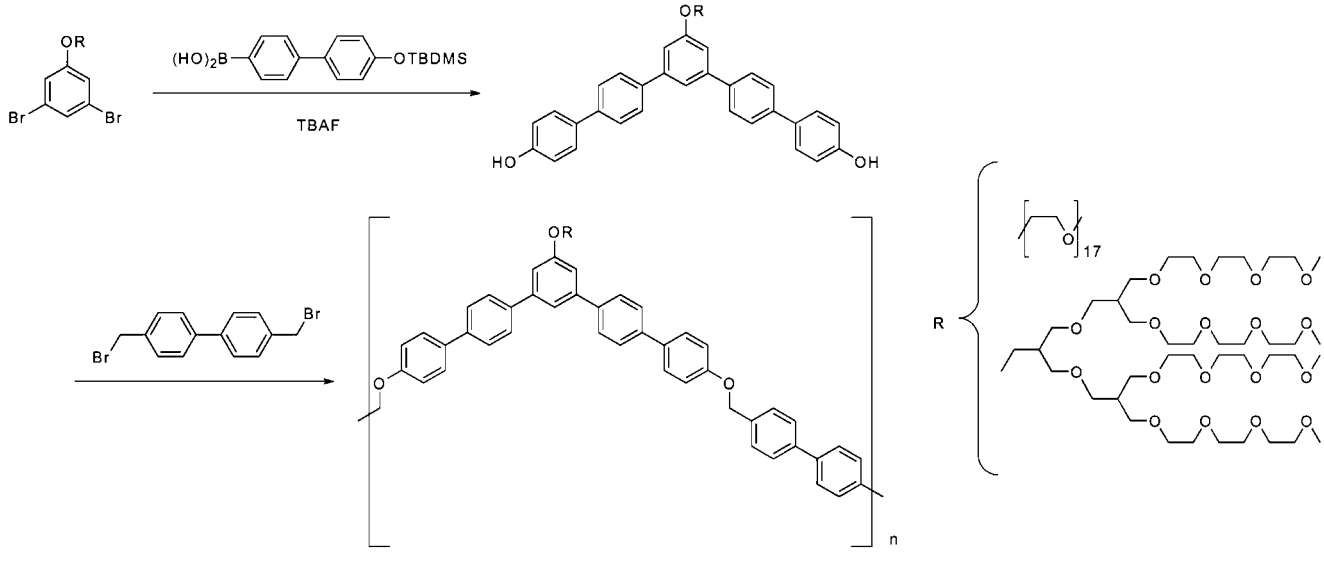

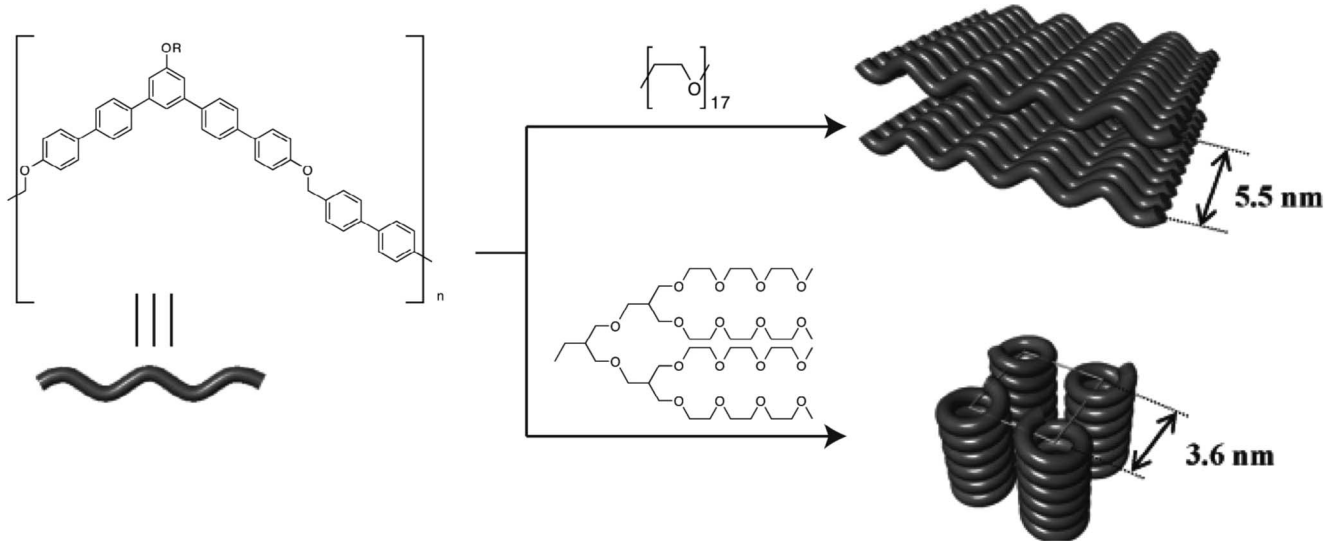

Figure 149. Structure and self-assembly of *m*-linked rigid dendronized polymers. Reprinted with permission from ref 588. Copyright 2005 American Chemical Society.

a lamellar architecture to a tetragonal columnar structure (*P*4*mm*) was mediated by the interchange of linear PEG side chain with a dendritic ethylene oxide side chain (Figure 149).[588]

Polyesters jacketed with hydroxy decorated bis(MPA)-dendrons have been prepared through a grafting-onto approach.[589] These poly(ε-caprolactone) based polymers are biocompatible and biodegradable and of interest for drug delivery. Various polyurethanes jacketed with G2−G4 Fréchet-type dendrons were prepared (Figure 150).[590] DSC revealed a T_g but no other thermal transitions indicating a lack of LC behavior. In spite of this, ordering was suggested by XRD and the structure formed was consistent with a BCC lattice. Addtionally, photoswitchable PAMAM-dendronized polyesters containing main-chain isomerizable azobenzene groups have been reported.[591]

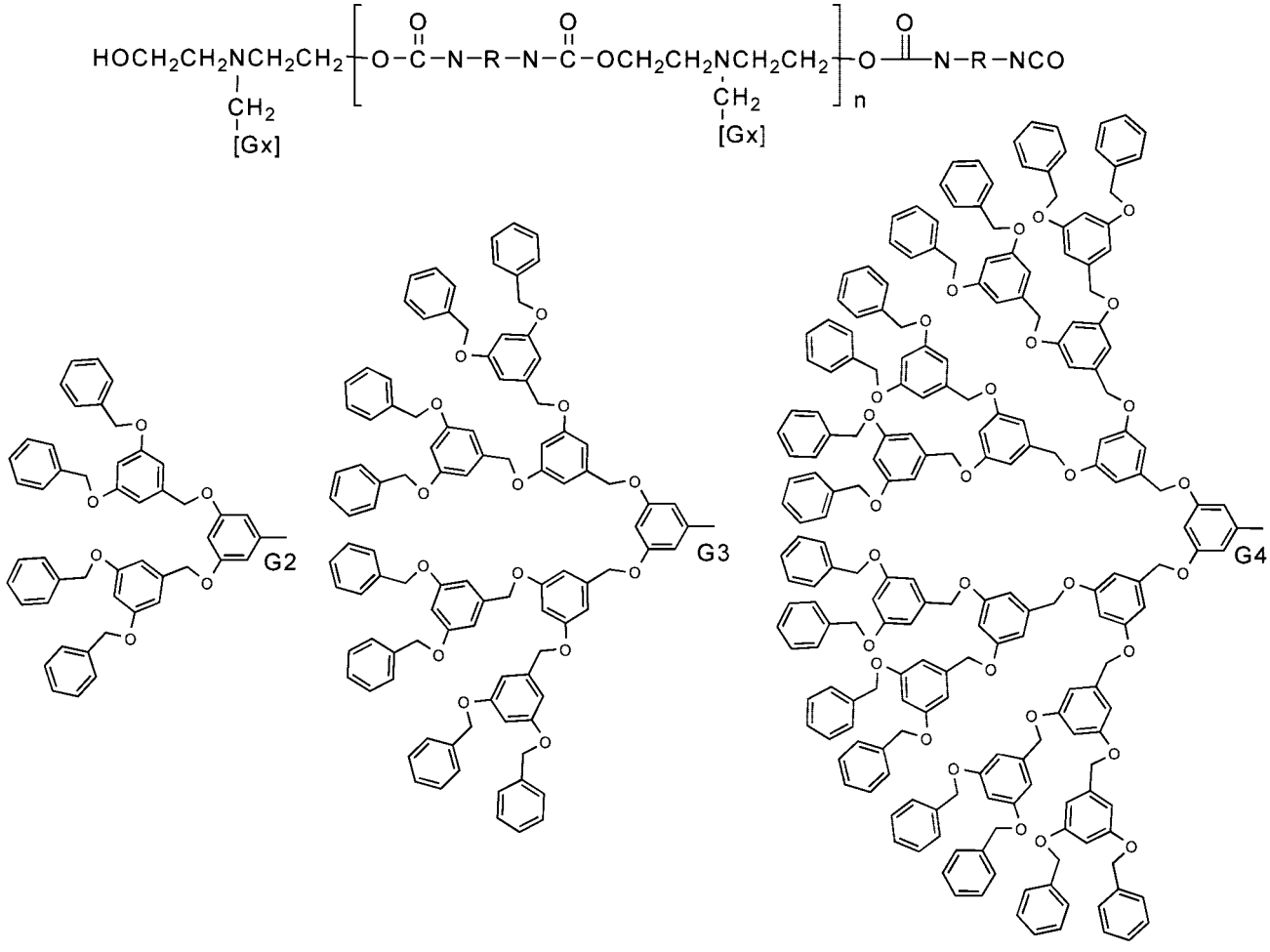

Figure 150. Dendronized polyurethanes.[590]

Scheme 43. Synthesis of Poly(phenylene) Jacketed with Fréchet Dendrons[592−594]

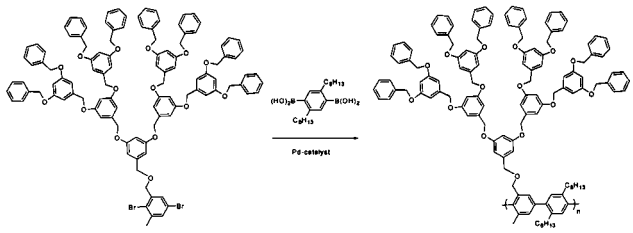

3.2.8. Rigid Conjugated Polymers

Schlüter has prepared poly(*p*-phenylene) jacketed with G1−G3 Fréchet dendrons via Suzuki polycondensation of a dendritic macromonomer (Scheme 43)[592−594] or through a grafting-onto approach.[592,595,596] The differently sized dendritics mediate varying degrees of disassembly and site-isolate of the poly(*p*-phenylene) core. In the case of G3 dendritic jacket, self-organization into arrays of nanorods was demonstrated through visualization by SFM.[592] Monte Carlo simulations on a similar system have suggested that, above generation three, the dendron begins to hinder the backbone conformation and provide for rigid-rod structures.[597] Schlüter was also able to show that asymmetrically dendronized amphiphilic poly(*p*-phenylene) forms LB monolayers at the air/water interface.[598,599]

Optically active *m*-linked dendronized poly(phenylene)s have also been prepared via Suzuki polycondensation of dendritic macromonomers and soluble spacer groups (Scheme 44).[600] The optical activity of the polymer is the result of (1*R*,2*S*)-ephedrine periphery units. The optical rotation of the polymer can be tuned by the number of spacer phenyl groups in the soluble linker. These polymers exhibit enhanced enantioselective catalysis of diethyl zinc additions.

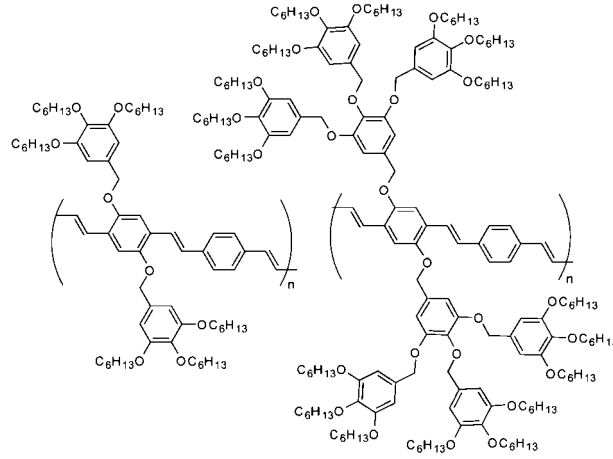

Figure 151. Dendronized poly(phenylene vinylene).[601]

Bao reported the Heck condensation of 2,5-bis(dendronized) 1,4-diiodobenzene with 1,4-divinyl benzene to form poly(phenylene vinylene) (PPV) decorated with Percec-type dendrons (Figure 151).[601] TOPM revealed N LC texture and XRD exhibited *d*-spacings consistent with varying

Scheme 44. Synthesis of *m*-Linked Poly(Phenylene) Jacketed with a Chiral Dendron[600]

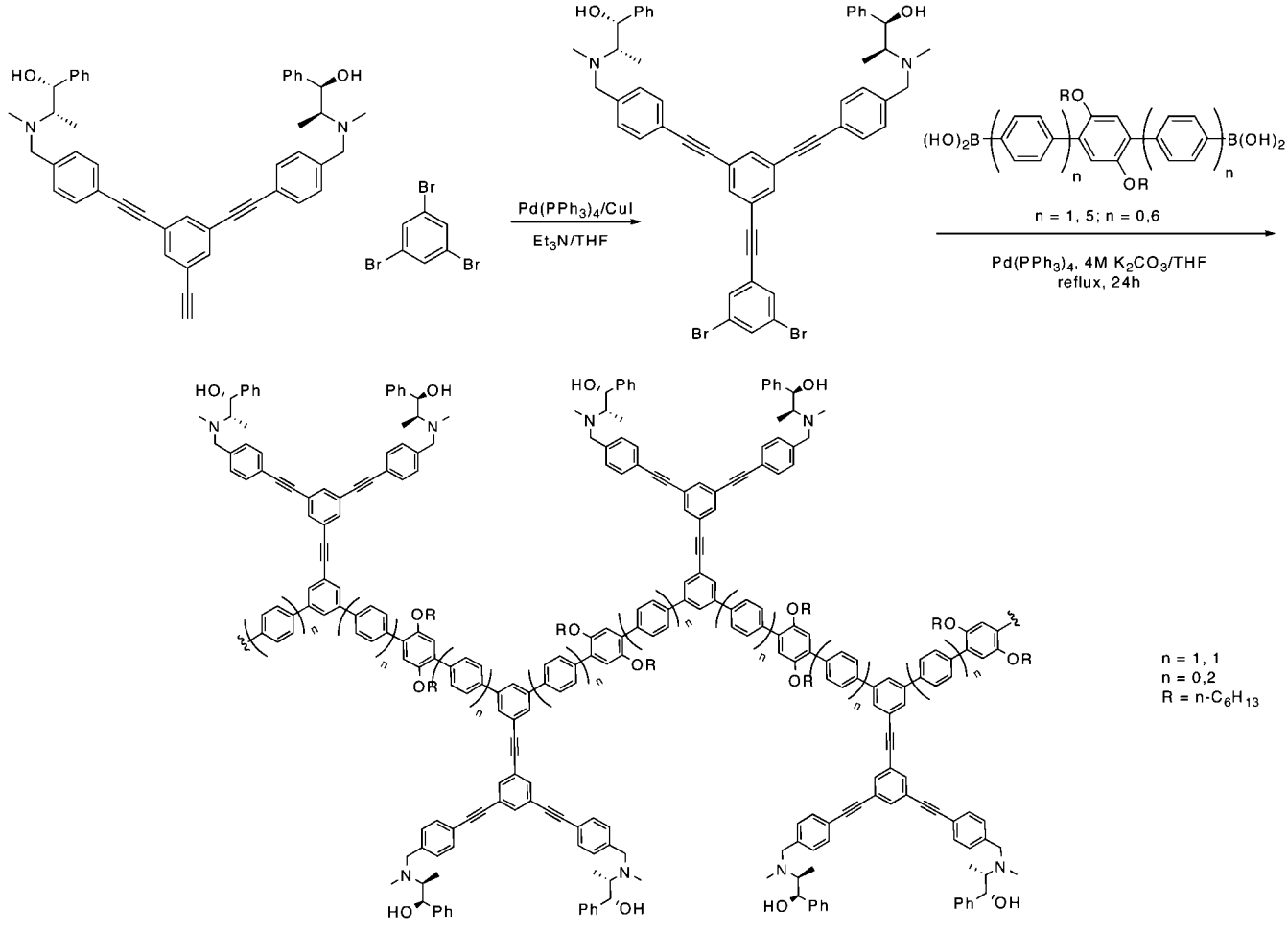

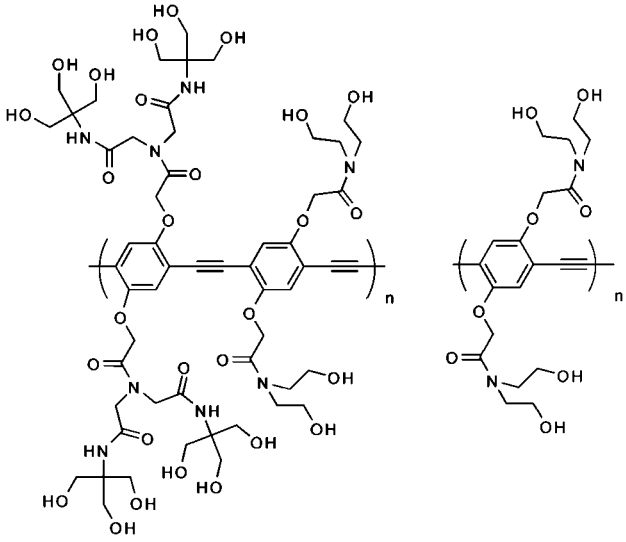

Figure 152. Dendronized poly(phenylene ethynylene)s.[608]

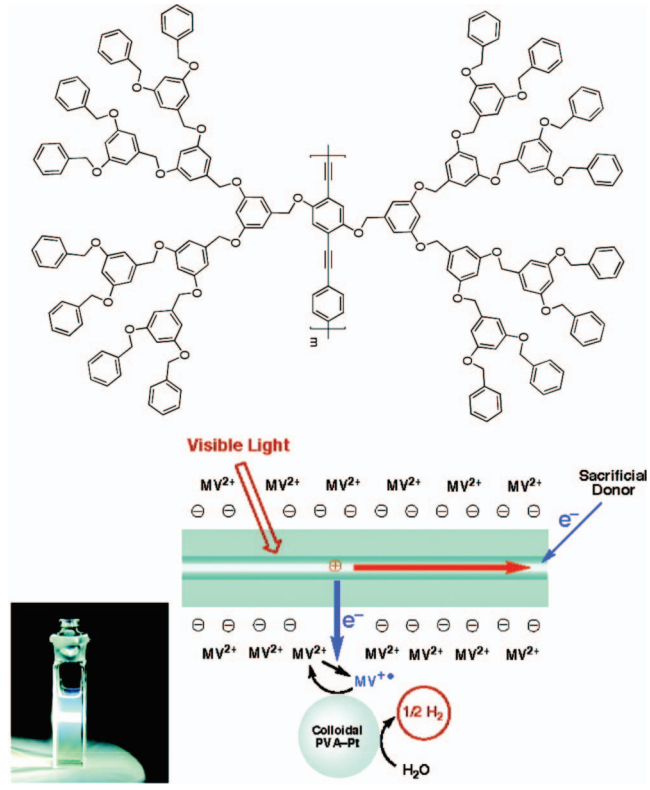

Figure 153. Photosplitting of water by dendronized poly(phenylene ethynylene)s in the presence of methyl viologen. Reprinted with permission from ref 612. Copyright 2004 American Chemical Society.

degrees of aliphatic interdigitation. Preliminary results showed limited change in UV−vis spectra in solution and film, suggesting limited chain-to-chain interaction through dendron-mediated disassembly. Later studies by Bao and Rothberg confirmed that the separation of the PPV chains via the bulky dendritic coating allowed for almost completely nonemissive interchain excitation and greatly enhanced bulk photoluminescence (PL).[602] Despite the steric bulk of dendritic side group, some degree of aggregation is still present and affects the PL.[603] Regardless, the presence of the N organization provided easy alignment of the dendronized PPV and fabrication into polymer light-emitting diodes (PLED)s.[604,605] Other examples of PPV jacketed with Fréchet-type[606] or phenylazomethine[607] dendrons have been reported.

Swager reported the synthesis of poly(phenylene ethynylene)s jacketed with Newkome hydrophilic dendrons via a dendritic macromonomer approach (Figure 152).[608,609] The polar dendritic side chains provide access to water-soluble conducting polymers. Aida reported the synthesis of poly(phenylene ethynylene) jacketed with Fréchet dendrons functionalized with neutral, cationic, and anionic surface groups for light-harvesting applications.[610−614] Poly(phenylene ethynylene)s with anionic surface groups in the presence of methyl viologen form a complex system that can be used in the light-driven reductive splitting of H_2O. This process is dependent on the 3-D order of the polymeric backbone into segregated planar arrays maximizing conjugation and suppressing quenching of the photoexcited state (Figure 153).[612]

Dendronized poly(enediyne)s were prepared via Glaser coupling approach using a macromonomer bearing two (3,4,5)12G1 side chains (Figure 154A).[615] XRD and TOPM results suggested N chain-segregated architectures via dendron-mediated disassembly of the rigid core. Other poly(enediyne)s and poly(enetetrayne)s jacketed with G1−G3 Fréchet dendrons (Figure 154B and C)[616,617] or G2 carbosilane[617] dendrons were prepared by Diederich. The dendritic side groups provide stability and dendron-mediated disassembly of the acetylenic backbone, but no self-organization was reported.

Fréchet was the first to report solution processable conducting polythiophene[127] with only dendron side chains as solubilizers.[618] Pentathiophene macromonomers with G2 or G3 benzyl-capped alkyl ether dendrons were prepared and polymerized via Stille coupling (Figure 155). Kumar reported an alternative approach to more densely dendronized polythiophene.[619] In this approach, a dendritic macromonomer was prepared from hydroxymethyl 3,4-ethylenedioxythiophene (EDOT). The dendritic EDOT monomer was electropolymerized to produce polythiophene with a G1 dendron attached to each monomer repeat unit (Figure 155).

Koeckelbergh recently prepared poly(dithienopyrrole)s with pendant Percec-type dendrons with chiral and achiral tails (Figure 156).[620] UV−vis spectroscopy was used to probe the helical folding of these polymers in solution. The highly oblique angle of the polymer chain suggests a large number of monomers per stratum layer resulting in a solenoid type structure. Donor−acceptor alternating copolymers of dendronized dithienopyrrole and nondendronized benzobisthiadiazole were also reported (Figure 157).[621]

Carter prepared the first fluorene homopolymers and alternating copolymers bis-jacketed with G1−G3 Fréchet dendrons via a Suzuki polycondensation *macromonomer* approach (Figure 158).[622] Fujiki reported the synthesis of the first fluorene homopolymers wherein the macromonomer was monoasymmetrically functionalized with a dendron, in this case a G2 Fréchet dendron, and a nondendritic side chain.[623] For polyfluorene, optimal PL quantum efficiency was achieved with G2 dendritic side groups, which hindered the formation of aggregate morphologies and provided site isolation. Shu also reported that the poly(fluorene)s jacketed G3 Fréchet dendrons may in fact have superior performance through improved suppression of aggregate and excimer formation via dendron-mediated disassembly.[624] Incorpora-

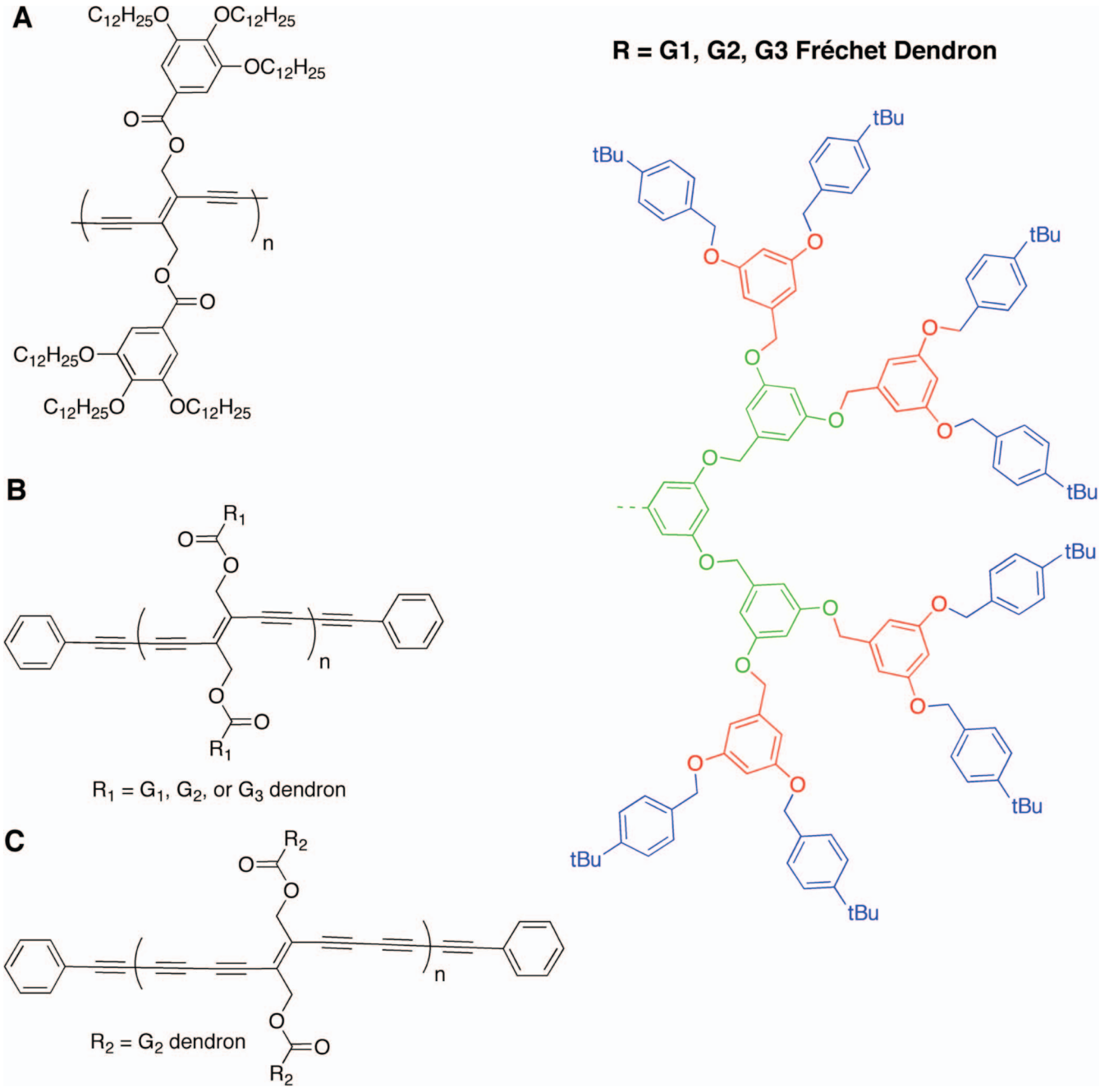

Figure 154. Dendronized poly(enediyne)s and poly(enetetrayne)s.[615−617]

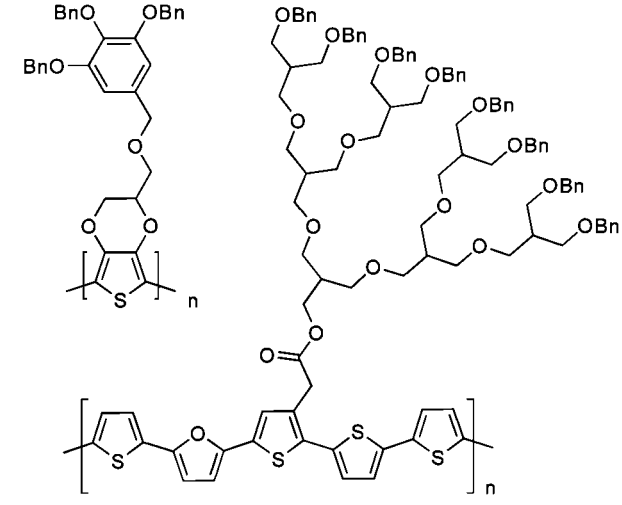

Figure 155. Structures of dendronized polythiophene.[618,619]

Figure 156. Structure and proposed solenoidal organization of Percec-dendronized poly(dithienopyrrole)s. Reprinted with permission from ref 620. Copyright 2008 American Chemical Society.

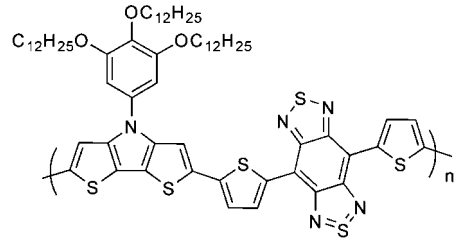

Figure 157. Dendronized poly(dithienopyrrole-*co*-benzobisthiadiazole)s.[621]

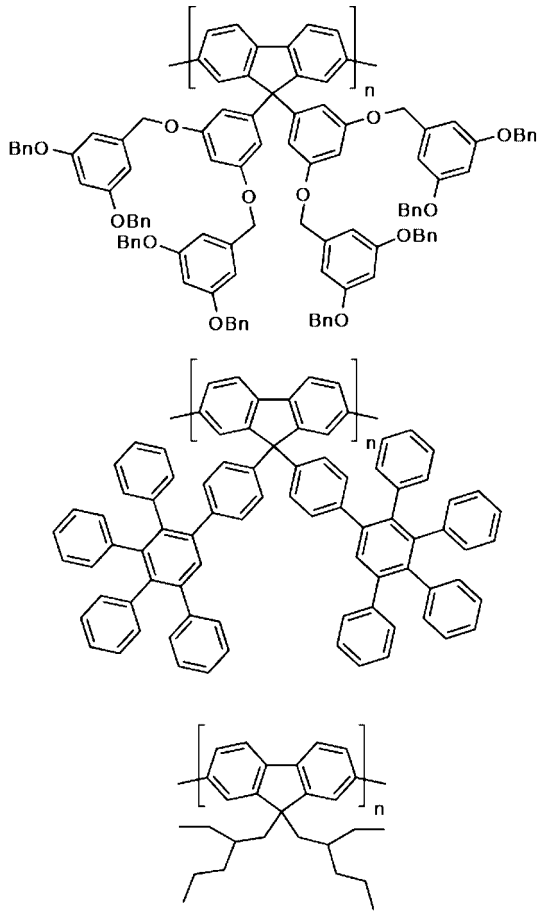

Figure 158. 9,9-Didendronized poly(fluorene)s.[622,626,627]

tion of branching sites in poly(fluorene)s jacketed with Fréchet dendrons leads to improved annealing stability and performance.[625] Müllen investigated the effect of dendronization in poly(fluorene)s on the spectral emission (Figure 158).[626−631] Contrary to previous assumptions, it was found that the structural disorder induced by these lower-generation but bulky dendrons resulted in line-broadening of the emission. Further, it was found that, in this case, dendronization enhanced interchain coupling via interaction at structural defects.

Alternating copolymers were prepared via Suzuki polycondensation of 2,7-bis(4,4,5,5-tetramethyl-1,3,2,-dioxaborolan-2-yl)-9,9-dihexylfluorene and 2,7-dibromo-9,9-bis(dendronized)fluorene, where the dendron is G1−G2 Fréchet dendron with oxadiazole peripheral functional groups (Figure 159).[632] G1 and G2 dendrons suppress the aggregation of the polyfluorene chains, and excitation of the periphery groups provides significant energy transfer to the backbone. Likewise, poly(fluorene-co-phenylene)s jacketed with Fréchet dendrons with cationic peripheries[633] or benzamide dendrons[634] inhibit $\pi-\pi$ interactions in aqueous media, allowing for extremely high fluorescence quantum yields (Figure 159).

Pu reported the synthesis of an early example of optically active dendronized polymers, (poly[(*R*)-1,1′-binaphthyl] bearing G1−G2 Fréchet-type dendrons, via dendritic macronomer that employed Ni-catalyzed coupling (Figure 160).[635] Lin also reported the synthesis of oligomers of (*R*)-1,1′-binaphthyl bearing G1−G3 Fréchet-type dendrons via a grafting-onto strategy (Figure 160).[636] CD/UV−vis measurements suggested an increase in the dihedral angle of the binaphthyl due to steric effects of the dendritic jacket.

Poly(isocyanide)s bearing a $(3,4,5)^2$12G2 or (4-3,4,5)12G1 Percec-type dendrons have been prepared through a dendritic macromonomer approach using a bimetallic Pd−Pt catalyst (Scheme 45).[637] While the $(3,4,5)^2$12G2 dendron exhibits spherical architecture, its attachment to the rigid poly(isocyanide) backbone mediates self-assembly into Φ_h phase as determined via XRD and TEM visualization. An exact assignment of the LC phase formed by poly(isocyanide) jacketed with (4-3,4,5)12G1 was not made.

A similar series of poly(isocyanide)s decorated with chiral (3,4)*n*G1 and (3,4,5)*n*G1 dendrons was prepared (Figure 161).[638] Polymers decorated with the (3,4,5)*n*G1 exhibited an LC phase as indicated by TOPM and XRD. CD/UV−vis spectroscopy suggests a helical model for the backbone. However, structure features and lattice packing were not fully determined.

Percec-type dendron $(3,4,5)^2$12G2 was attached to a terphenyldiamine via an aromatic spacer (Figure 162). Subsequent condensation polymerization with aromatic bisanhydride resulted in a dendronized polyimide. Alternatively, (3,4,5)12G1 was grafted-onto polyamides obtained from 4,4-hexafluoroisopropylidenedi(phthalic anhydride) and 4,4′-diamino-3,3′-dihydroxybiphenyl using a DCC mediated approach. Self-organization of this material was exploited for the preparation of N-aligned liquid crystal displays.[639,640]

3.2.9. Metallo-Linked Polymers

Self-organization has also been observed with dendronized coordination polymers. Lee reported the synthesis of *meta*-linked bispyridine ligand with dendritic oligo(ethylene oxide) side chains (Figure 163).[641] Formation of coordination polymers with $PdCl_2$ results in a zigzag lamellar architecture. On the other hand, coordination polymers formed with $CuCl_2$ result in oblique columnar assemblies. The columnar assembly results from a double-stranded helical conformation that may be stabilized by the formation of weak binuclear bridged Cu_2Cl_2 complexes.

Manners and Winnik have synthesized a library of dendronized poly(ferrocenylsilanes) prepared via the grafting-onto attachment of a diversity of (3,4,5)12G1 Percec-type dendrons to poly(chloromethylferrocenylsilanes) (PFS-Cl) (Figure 164).[642] While the Percec-type dendrons utilized often mediated self-organization in other cases, only glass transitions were observed in the polymers. However, the dendronized PFS does serve to isolate the iron-rich backbone and create novel metal−dendron rodlike architectures.

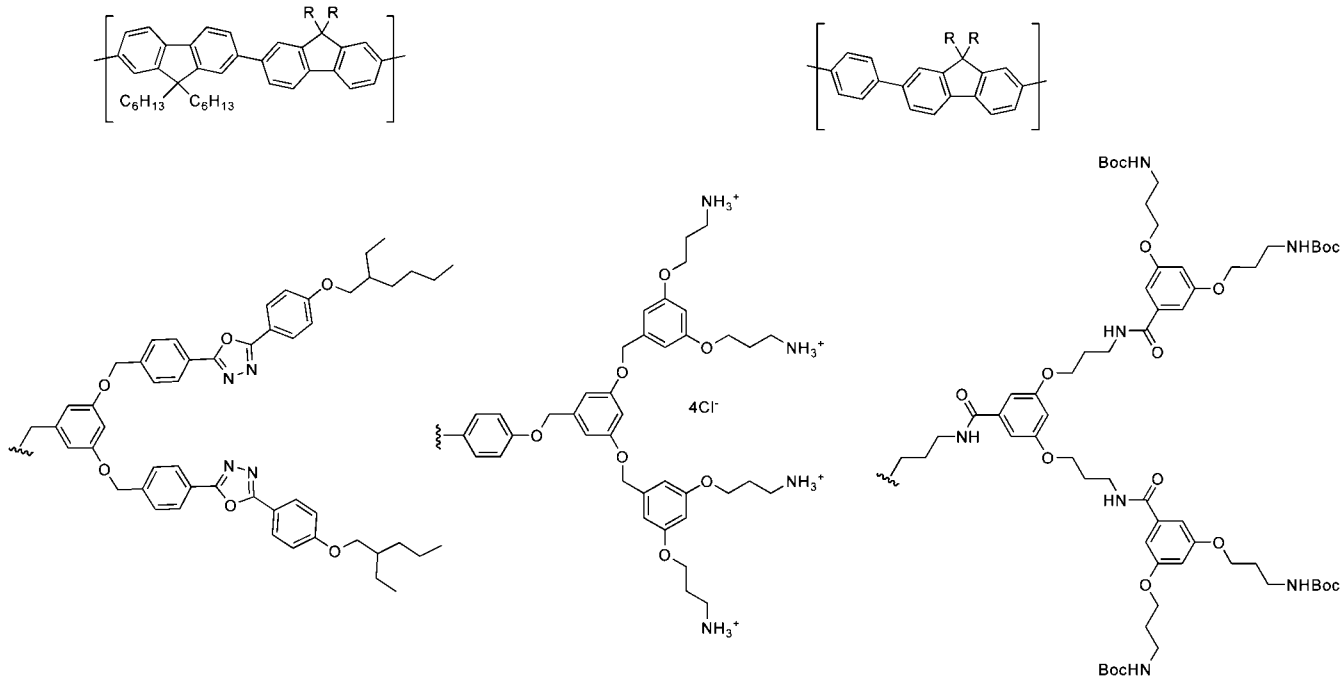

Figure 159. Dendronized polyfluorene bearing oxadiazole functionalized Fréchet dendron pendants (left) and poly(fluorene-co-phenylene) jacketed with Fréchet dendrons with cationic periphery or benzamide dendrons (right).[632−634]

Scheme 45. Synthesis of Poly(isocyanides) Jacketed with G2 Percec Dendrons[637]

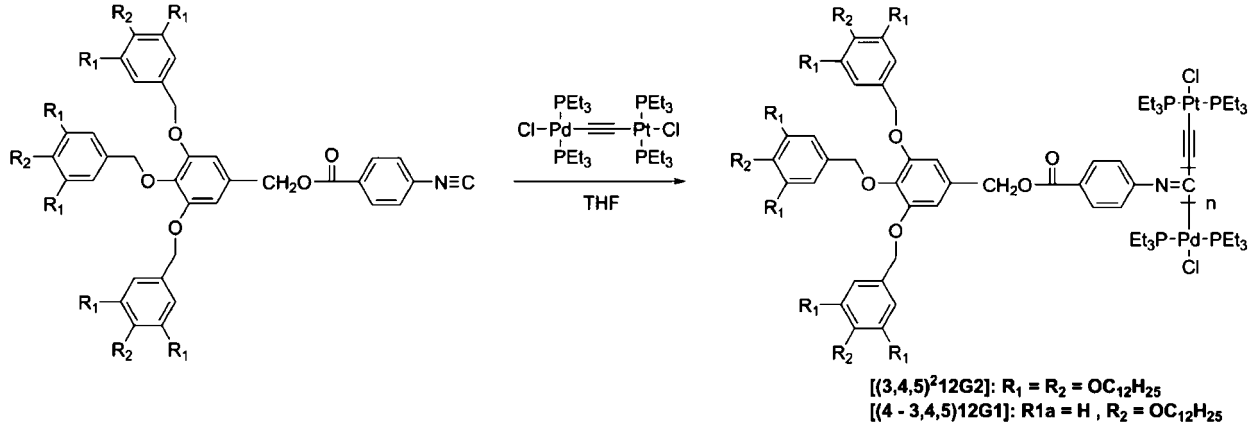

3.2.10. Biopolymers

Koltover has attached Fréchet-type dendrons with a diazo apex-functionality to the carboxylic acid residues of monodisperse poly(L-glutamic acid) (Figure 165).[643] Here dendronization of the poly-(L-glutamic acid) core stabilizes the α-helical conformation of the dendronized polymer. The dendron coat, as well the monodispersity of the backbone, mediates organization of the dendronized polymer into a Φ_h lattice.

Fréchet prepared a library of poly(L-lysine) dendronized with G1−G4 hydroxy-terminated bis(MPA)-dendrons prepared via a grafting-from approach by iterative treatment with the anhydride of isopropylidene-2,2-bis(oxymethyl)propionic acid (Figure 166).[644] Poly(L-lysine) on its own adopts a random-coil conformation; however, decoration of poly(L-lysine) with G1 or G2 dendrons results in an α-helical organization according to CD/UV−vis. The steric bulk of G3 and G4 dendrons prevents close helical back-folding and returns the polymer to its native coil state. An inverted strategy, wherein L-lysine dendronized polystyrene was prepared via a dendritic macromonomer approach, produced structures that could be visualized as nanorods.[645]

Schlüter and Rabe prepared complexes of DNA with a cationic dendronized polymer (Figure 167).[646] AFM imaging suggests a model of helical wrapping of the DNA around the more densely charged dendronized polymer. Increased salt concentration appears to decrease the pitch separation of the helical coil.[647]

Newkome has reported cellulose functionalized with branched aliphatic conifer Newkome dendrons[648] through reaction of the hydroxy groups with a dendron focally substituted with an isocyanate group (Figure 168),[649,650] which were utilized to fabricate CdS quantum dot assemblies.[651] Additionally, Heinze prepared cellulose with poly(aryl ester) dendrons and poly(aryl ester)/triazole dendrons via CDI coupling of the dendritic acid with hydroxyl group at the 2 and 6 position (Figure 168).[652] Heinze also reported cellulose that was click-functionalized with PAM-

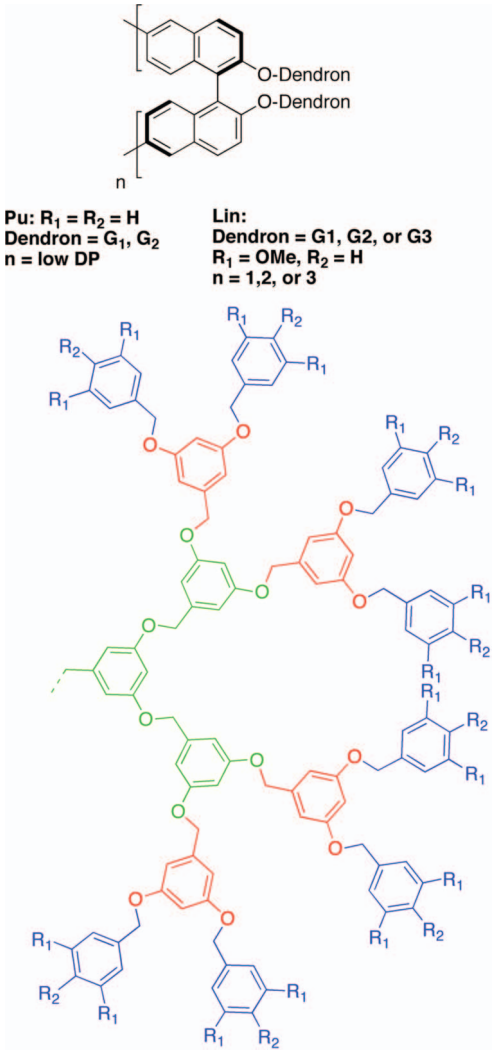

Figure 160. Dendronized poly[(*R*)-1,1′-binaphthyl].[635,636]

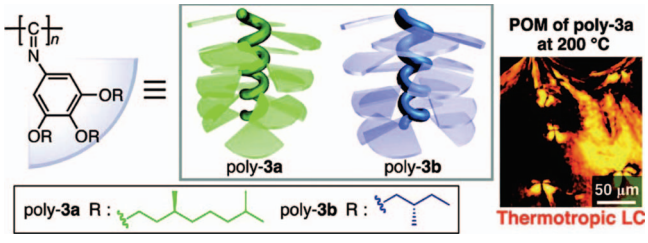

Figure 161. Poly(isocyanide)s jacketed with chiral Percec dendrons. Reprinted with permission from ref 638. Copyright 2008 American Chemical Society.

AM dendrons (Figure 168),[653] allowing for protein immobilization on the surface.[654] In addition, hydroxypropyl cellulose has been decorated with bis-(MPA) dendrons via grafting-from hydroxypropyl groups (Figure 168).[655,656] Carboxymethyl cellulose has been decorated with a trifunctional aminoamide dendron via grafting-onto carboxymethyl groups (Figure 168).[657] PAMAM/PPI dendrons have also been grafted-onto cyanoethyl cellulose (Figure 168).[658] Chitosan has been partially jacketed via a grafting-onto strategy with PAMAM[659,660] and aryl ether type dendrons[661] functionalized at the periphery with sialic acid (Figure 168).[662] No self-organization of dendronized cellulose or derivates was noted.

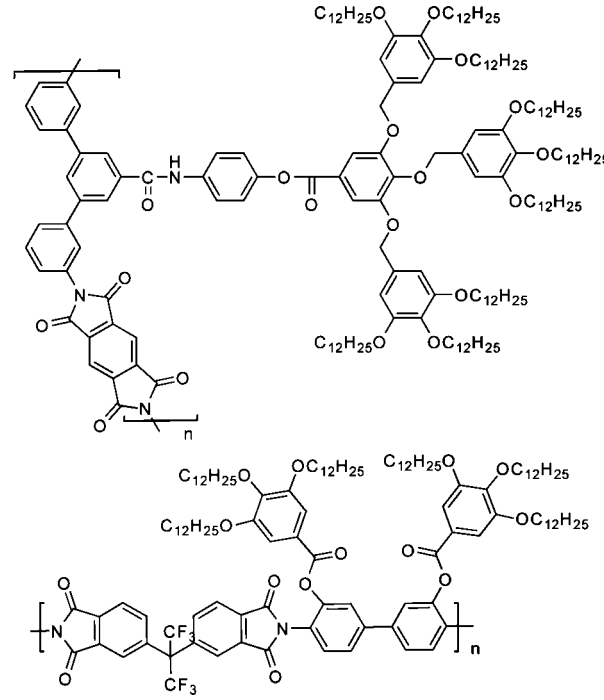

Figure 162. Poly(terphenylimide) jacketed with G2 Percec-type dendron (top)[639] and poly(imide) bisdendronized with G1 Percec-type dendron (bottom).[640]

3.2.11. Dendrons Attached to Polymers via Noncovalent Interactions

In some cases, it is more convenient to dendronize polymers in a noncovalent manner (Figure 1, second row middle). This process often provides synthetic simplicity and allows for structural manipulation through reversible environmental changes that effect molecular recognition.[663] Poly(4-vinylpyridine) (P4 VP) is often used as the polymeric main chain due to its readily accessible complexation with acidic functionalities. Noncovalent modification of P4 VP via Fréchet dendrons bearing a carboxylic acid apex mediates the formation of vesicular structure with lamellar walls (Figure 169).[664] The microsphere is believed to be the result of microphase segregation of the dendritic side chains into lamellae. Noncovalent modification of P4 VP occurs with (3,4,5)*n*G1. Additionally, PS_{192}-*b*-P4 VP_{181} was noncovalently modified with (3,4,5-4)8G1−COOH Percec-type hybrid dendron (referred to as TOB).[665] By increasing the ratio of (3,4,5-4)8G1−COOH relative to the number of pyridine binding sites, *x*, on the P4 VP block, a structural change from a coil−"jacketed" diblock-copolymer to a coil−column diblock-copolymer is observed, resulting in a diverse array of *structures-within-structures* (Figure 170). The neat diblock-copolymer without (3,4,5-4)8G1−COOH forms a S phase. Both the PS and P4 VP blocks have the same layer thickness, 43 nm. SAXS and WAXS reveal Φ_h-*within-lamallae* self-organization upon increasing the (3,4,5-4)8G1−COOH content to $x = 0.2$. In this case, the PS block is hexagonally packed, while the dendronized P4 VP block forms a local S arrangement. At $x = 0.5$, a face-centered cubic lattice with $Fm\bar{3}m$ symmetry is observed with the PS block forming the spheres, while the dendronized P4 VP block adopts a disordered Φ_h structure within the surround space. At $x = 0.7$, XRD indicates a tetragonally perforated lamellar-*within-columnar* structure composed of a body-centered tetragonal lattice ($I4/mmm$ symmetry) of ABAB layers (Figure 170 bottom).

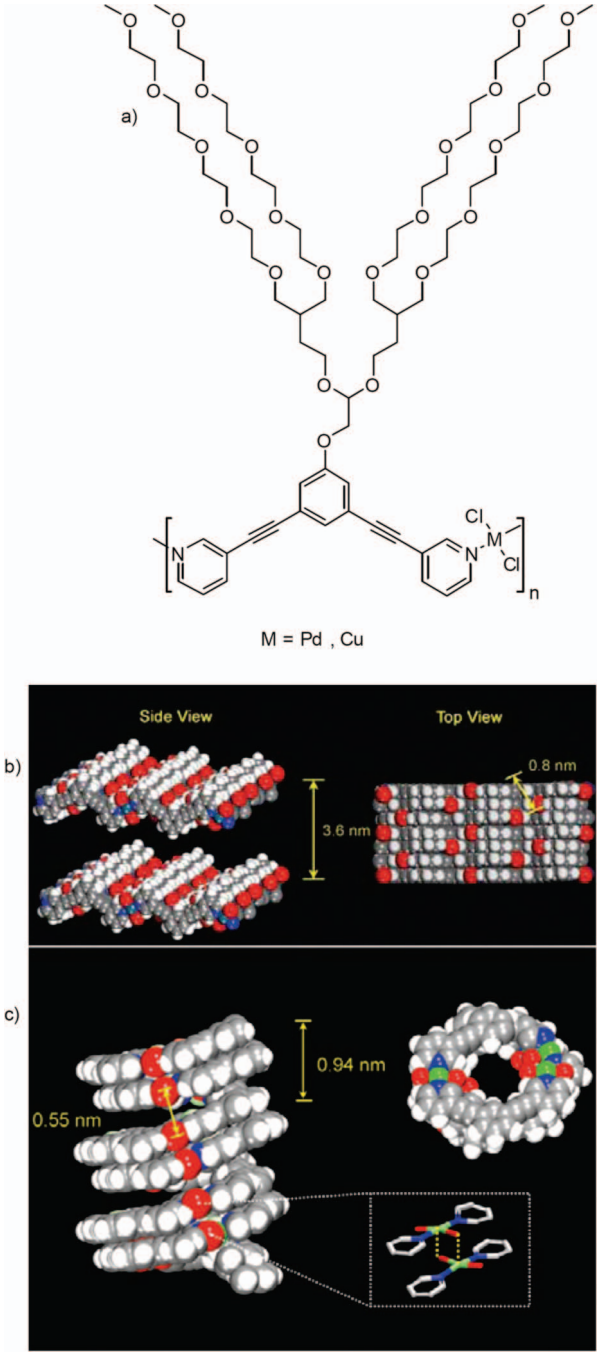

Figure 163. (a) Structure and self-assembly of (b) Pd and (c) Cu metallo-linked bispyridine dendrons. Reprinted with permission from ref 641. Copyright 2008 Wiley-VCH Verlag GmbH & Co. KGaA.

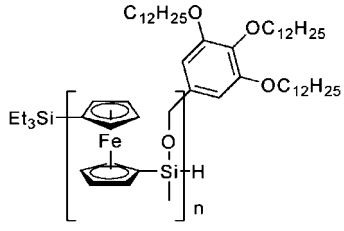

Figure 164. Dendronized poly(ferrocenylsilane).[642]

Percec-type dendrons with a diazo-linked sulfonic acid moiety also result in architectural modification (Figure 171).[666] At low degrees-of-neutralization (DN) of the pyridine side groups by the dendritic sulfonic acid, lamellar structures are detected by XRD. However, at higher loading levels (DN > 0.8), Φ_h organization emerges. Visualization of P4 VP noncovalently modified with dendritic sulfonic acids was achieved via AFM on an HOPG substrate.[667] Organization of the noncovalently dendronized P4 VP followed the 6-fold symmetry of HOPG surface (Figure 171).

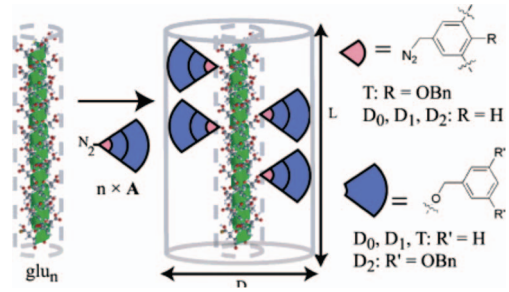

Figure 165. Fréchet-type dendrons grafted-onto monodisperse poly(L-glutamic acid). Reprinted with permission from ref 643. Copyright 2004 American Chemical Society.

Other nitrogen-bearing polymers have been utilized in the preparation of noncovalently dendronized polymers. Gin reported the synthesis of dendritic phosphonic acid (3,4,5)12G1−$CH_2P(O)(OH)_2$ via treatment of (3,4,5)12G1−CH_2Br with trimethylphosphite, followed by conversion of the resulting dimethylphosphonate to the phosphonic acid using trimethylsilane and triethylamine, followed by acidic workup.[668] Treatment of polyanaline with (3,4,5)12G1−$CH_2P(O)(OH)_2$ results in lyotropic S LC phases in DMF, water, and 1 M aqueous HCl (Figure 172). It was not determined whether interdigitated or tilted S phases phases were formed. Bulk conductivities were only in the semiconductor range due to what was suggested to be unfavorable conformations of the dry polyaniline backbone. Additionally, it was shown that (3,4,5)12G1−$CH_2P(O)(OH_2)$ forms lyotropic S phases when treated with aqueous NaOH.

Complexation of poly(ethylene imine) (PEI) and poly(allylamine hydrochloride) (PAH) with the carboxylic acid and potassium carboxylates of Percec-type (3,4,5)*n*G1 and (4-3,4,5)12G1 dendrons, respectively, mediated backbone organization (Figure 173).[669] Increasing the alkyl tail from 8 to 10 to 12 enlarged the size of self-assembled architecture as does switching from the (3,4,5) branching pattern to (4-3,4,5). However, the most dramatic change of architecture is mediated by the polymer backbone selection. PEI self-organizes exclusively into a lamellar architecture, while PAH self-organizes into a Φ_h lattice. Complexation of (3,4,5)*n*G1COOH to poly(ferrocenylsilane) with pendant trimethylammonium-bearing side chains (Figure 174) resulted in similar lamellar architectures.[670] Increased tail length from $n = 12$ to $n = 16$ improved stacking order.

Lin reported the synthesis of H-bond acceptor polymers and copolymers noncovalently jacketed with hydrogen-bond donor dendrons (Figure 175).[671] An alternating copolymer of hydrogen-bond accepting and light-emitting monomer, 1-{[4-(10-methacryloyloxydecyloxy)phenyl]ethynyl}-2,5-dimethoxy-4-[2-(4-pyridyl)ethynyl]benzene (PBB), and hole-transporting carbazole-containing monomer was prepared via free radical polymerization. Light emission can be tuned from blue to green via complexation with various generations of 1,3,4-oxadiazole containing dendrons.

In addition to acid−base complexes, other approaches to noncovalently dendron-jacketed polymers were explored. Stoddart reported acid−base switchable supramolecular dendronized polyacetylene and PS (see Figure 176).[672]

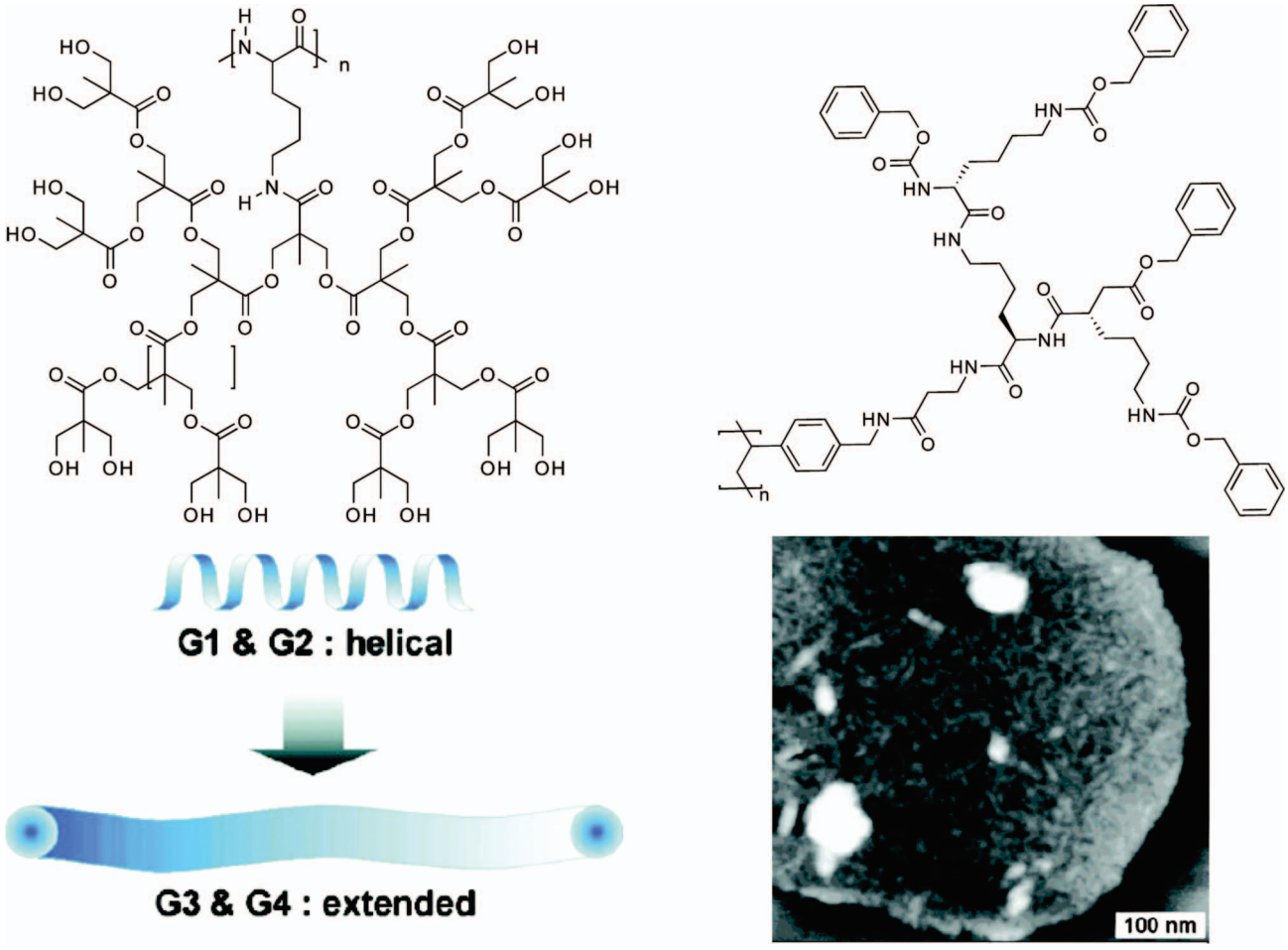

Figure 166. Poly(L-lysine) jacketed with bis(MPA)-aliphatic polyester dendrons (top) and PS jacketed with L-lysine dendrons (bottom). Reprinted with permission from refs 644 and 645. Copyright 2005 and 2006 American Chemical Society.

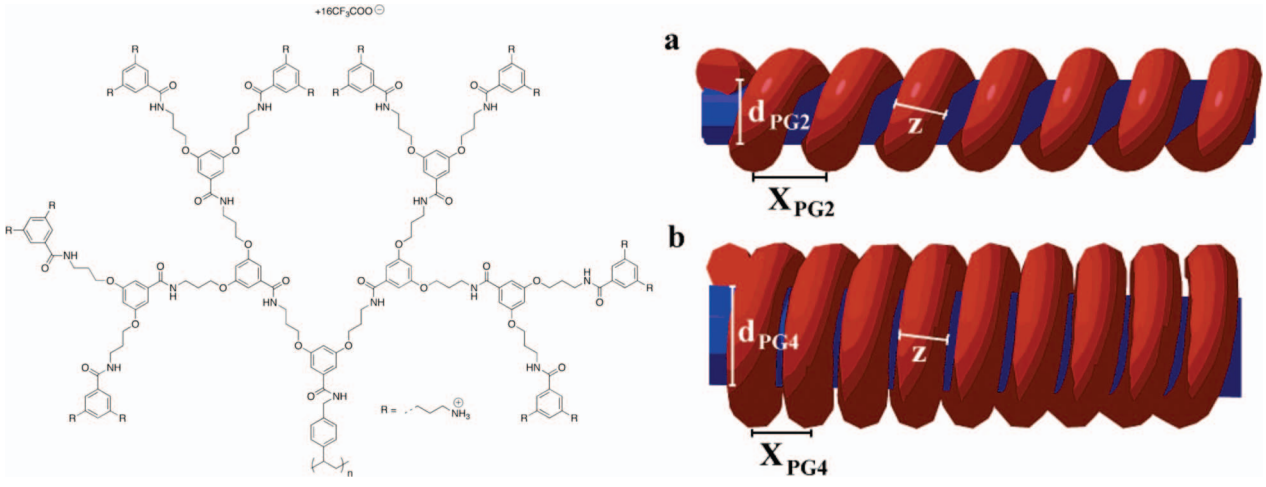

Figure 167. Coiling of DNA around cationic dendronized polystyrene. X is the helical pitch separation. Reprinted with permission from ref 646. Copyright 2002 American Chemical Society.

Polyacetylene and PS bearing dibenzo[24]crown-8 "eyes" were prepared via macromonomer and grafting-onto strategies, respectively. Treatment of these polymers bearing dibenzo[24]crown-8 "eyes" with Fréchet dendrons bearing dialkylammonium "hooks" induces a transition from a semiflexible "off" state to a rigid rodlike "on" state. The transition from the "off" to the "on" state and vice versa via modulation of the pH can be monitored via ^{1}H NMR, UV−vis spectroscopy, and light-scattering.

Additionally, Kallitsis developed an "attachment through coordination" approach to dendronized main-chain terphenyl polyethers (Figure 177).[673] Here, (3,5)12G1 and (3,5)^{2}12G2 Percec dendrons bearing a terpyridine (tpy) group at the apex were grafted-onto a polymer terphenyl ether polymer func-

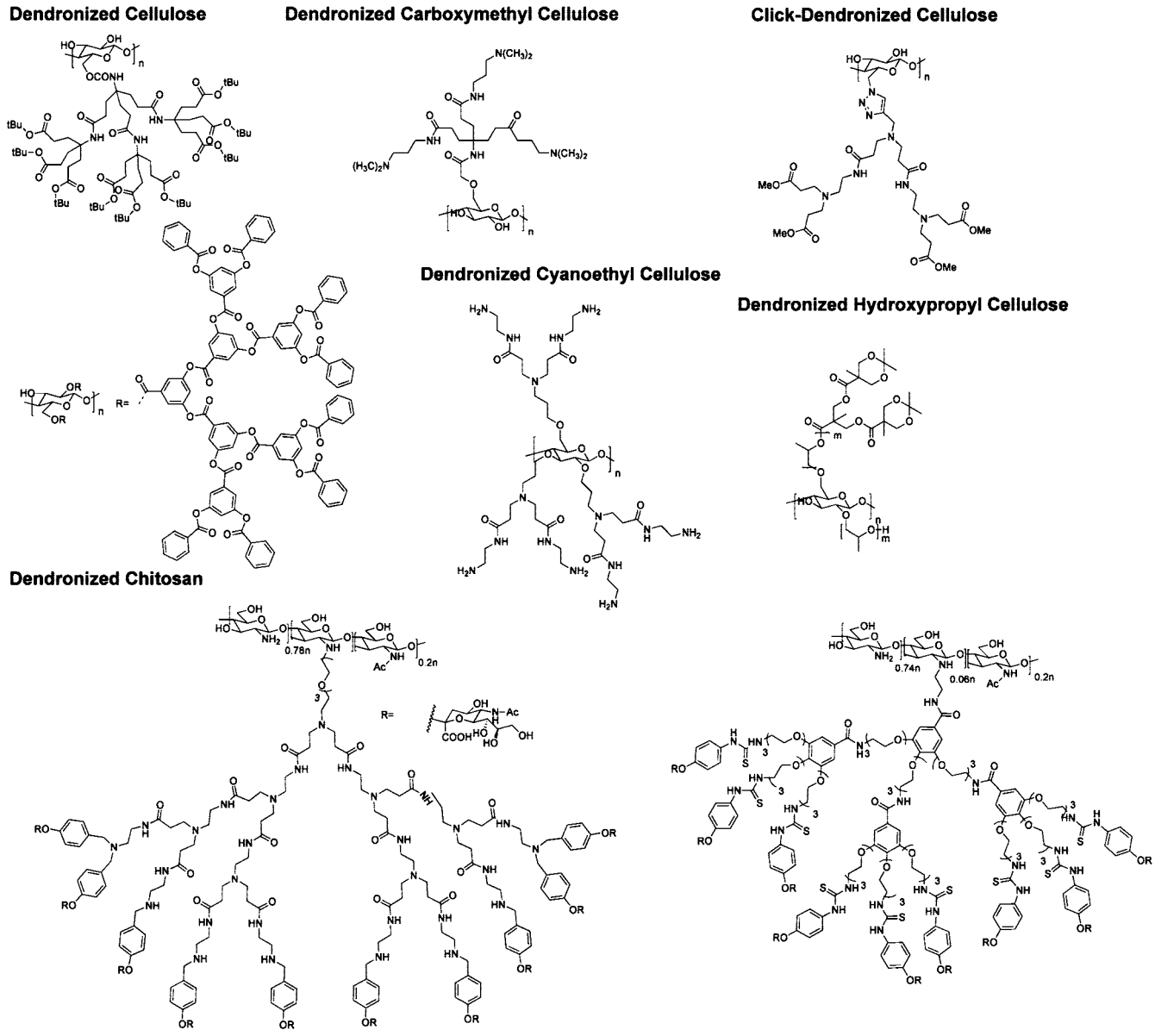

Figure 168. Structures of cellulose jacketed with conifer type Newkome dendrons,[649,650] cellulose jacketed with poly(aryl ether) dendrons,[652] dendron-jacketed carboxymethyl cellulose,[657] dendron-jacketed hydroxypropyl cellulose,[655,656] PAMAM-jacketed cyanoethyl cellulose,[658] click-dendronized cellulose,[653,654] and chitosan jacketed with sialic acid functionalized dendrons.[659−662]

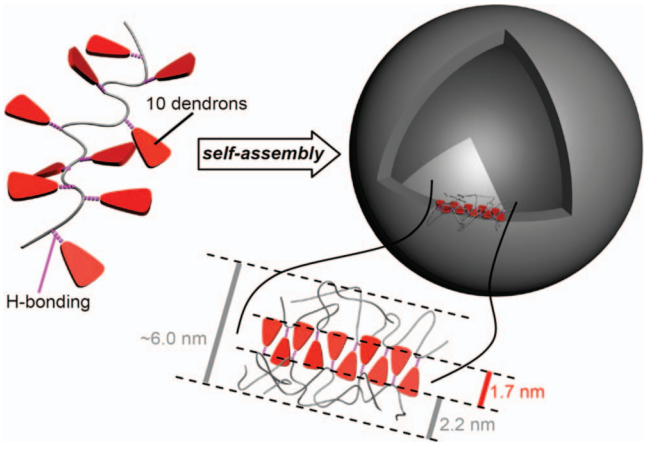

Figure 169. Noncovalent modification of P4 VP with Fréchet dendrons. Adapated from ref 664.

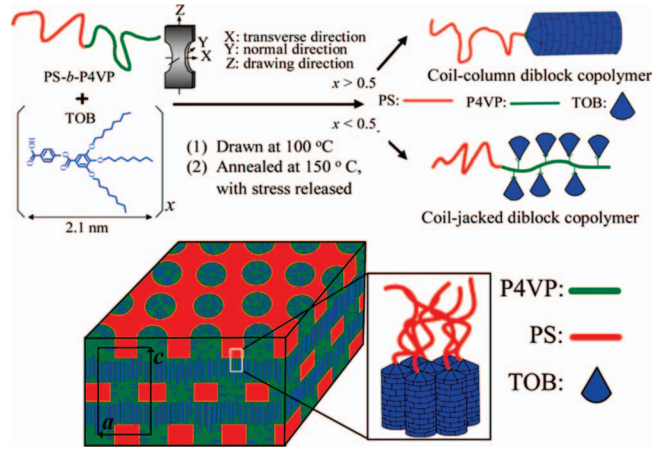

Figure 170. PS-*b*-P4 VP noncovalently functionalized with (3,4,5-4)8G1COOH (top) and schematic of the tetragonally perforated layer structure formed at $x = 0.7$. Reprinted with permission from ref 665. Copyright 2009 American Chemical Society.

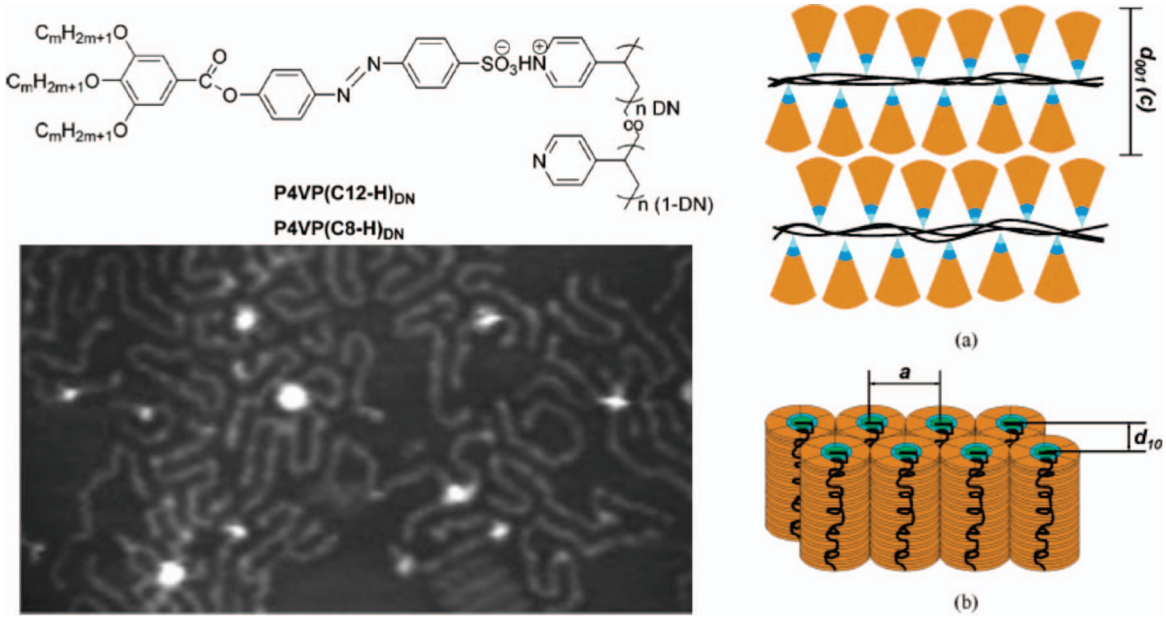

Figure 171. Structure, self-assembly, and visualization of P4 VP noncovalently modified by (3,4,5)*n*G1 Percec-type dendrons bearing sulfonic acid residues. Reprinted with permission from ref 666. Copyright 2006 American Chemical Society.

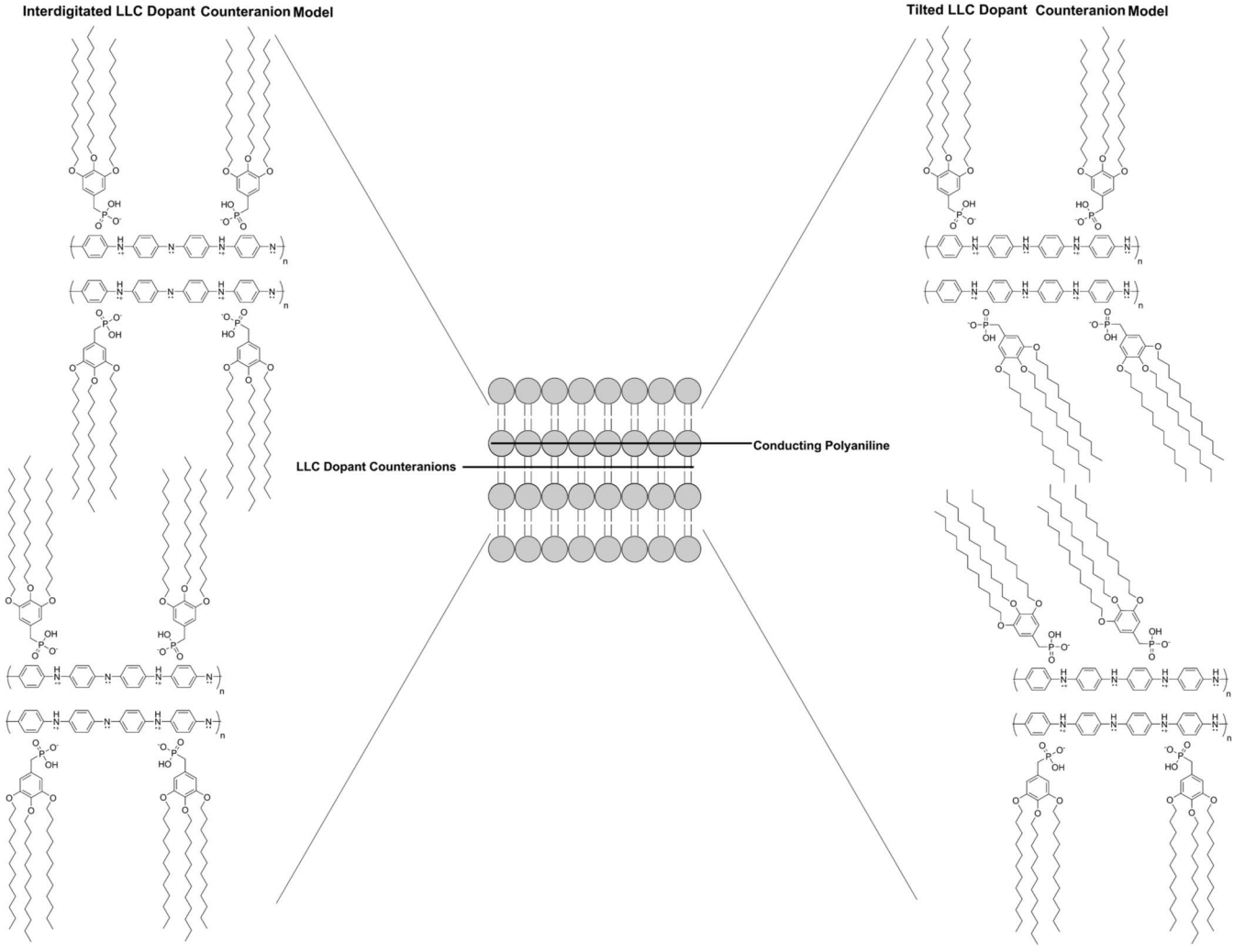

Figure 172. Possible models of lyotropic S phases formed from the complexation of (3,4,5)12G1−$CH_2P(O)(OH)_2$ with polyanaline. Adapted from ref 668.

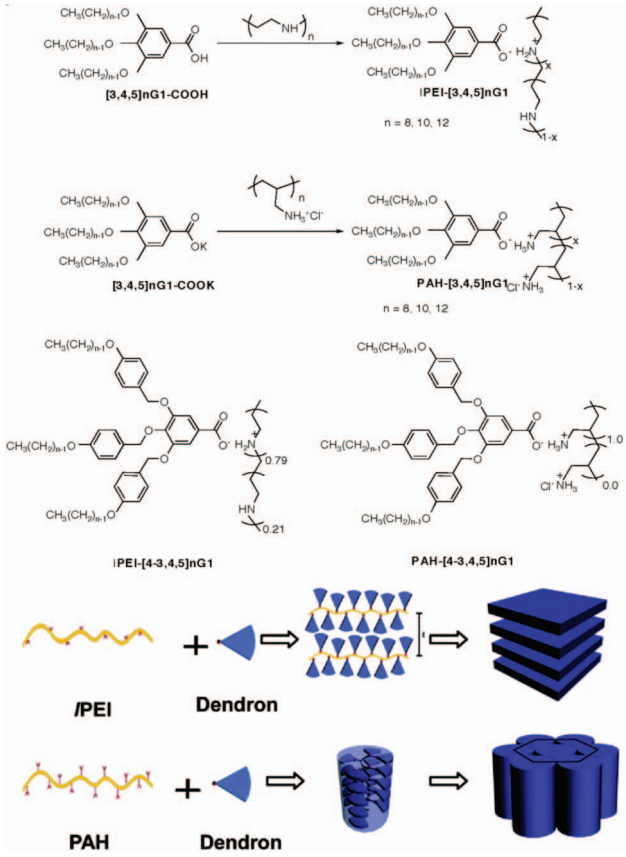

Figure 173. Structure and self-assembly of PEI and PAH noncovalently modified with Percec-type dendron. Reprinted with permission from ref 669. Copyright 2008 American Chemical Society.

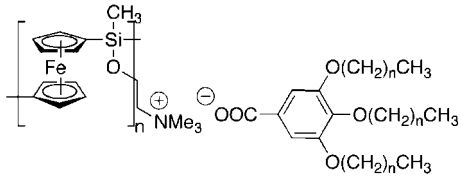

Figure 174. Noncovalently dendronized poly(ferrocenylsilane).[670]

tionalized with two tpy groups per terphenyl via a mutual coordination with Ru^{2+}. Alternatively, the same polymers can be prepared through the dendritic macromonomer approach where the dendron was precoordinated to the tpy-bearing terphenyl ether. The use of the metal-coordination induces the self-organized polymer with optical properties of tpy−Ru^{II}−tpy complex.

3.3. Linear Polymers Jacketed with Dendrons, Twin-Dendrons, and Janus-Dendrimers Attached via Their Periphery

For most dendron-jacketed polymers, the dendron is attached to the polymer at the dendron-apex (Figure 1, first row left and middle and second row left and Figure 178a). This is the most intuitive approach as the tapered dendron often forms a cylindrical coat around the polymer core. If the dendritic monomer self-assembles into supramolecular columns that self-organize, for example into a Φ_h lattice (Figure 178b), attachment of the dendron via the periphery (Figure 1, second row right and third row left, middle) to a polymer can result in similar self-organization. Here the polymer backbone occupies the interstitial space of the dendrons' lattice rather than being the center of the lattice elements. This approach creates network structures with the potential for enhanced mechanical properties.

Möller and Percec reported the first polymers prepared via the polymerization of dendrons at their periphery[674,675] (Figure 179) and their use as ion-selective membranes (Figure 180).[676−680] The membranes were prepared by fixing columns self-assembled from dendronized crown-ethers possessing one or more polymerizable moiety on the periphery in a methacrylate resin.[675] This process was termed "gel fixed supramolecular pores" (GFSP) (Figure 180) formation and is carried out in three distinct steps. First the pore-forming agent is dissolved in a mixture of mono- and bifunctional methacrylates. Controlled cooling causes the solute to organize into long cylindrical aggregates containing the self-assembled crown-ether units, resulting in gelation of the sample. In the final step, the solvent is polymerized in such a manner as to prevent destruction of the aggregates.[681] The resulted gel-fixed channels are capable of transporting alkali metal salts such as LiOTf.

Analogues of (4-3,4,5)12G1 branched aryl and aryl/naphthyl ether dendrons with oligo(ethylene oxide) apex groups were prepared with a methacrylate group at various positions in the aliphatic periphery (Figure 181a).[682] As discussed in section 2, dendrons of this topology have the propensity to self-assemble into Φ_h lattices. Free-radical polymerization of these macromonomers produced a networked Φ_h lattice, where the PMMA occupies the interstitial aliphatic domains of the lattice. As determined by XRD, the columnar diameter increases with increasing length of the oligo(ethylene oxide) apex unit. Addition of LiOTf forms a complex with the oligo(ethylene oxide apex), thereby stabilizing the column and thus providing for a durable ion-active membrane. Similarly, PMA jacketed with (3,4,5)12F8G1 dendrons bearing semifluorinated peripheries and ethylene oxide (EO) and benzo-15-crown-5 apex groups self-assembles into semifluorinated networks of Φ_h structures (Figure 181b).[683] Kim has also used this approach to generate nanoscale channels through the use of 3:1 complexes of G1 Percec-type dendrons with a benzotri(imidazole) core.[684] The 3:1 complex of dendron and benzotri(imidazole) self-organizes into a Φ_h lattice. Photopolymerization of the acrylates groups on the periphery of the dendrons fixes the columnar structures, and sonication allows for removal of the benzotri(imadazole), thereby generating a nanoporous structure.

On the basis of the technique developed in the Percec and Möller laboratories[674−683] and the precedent established for ion-conducting materials using dendronized crown-ether salt complexes,[210] Kato prepared 1-D ion-conductive polymer films via the periphery photopolymerization of Percec-type dendrons with ionic imadazolium apex moieties (Figure 182).[685] Self-assembly of dendritic macromonomer on NH_2 modified indium titanium oxide (ITO) or glass surfaces provided Φ_h structures homeotropically aligned on the surface, while self-assembly on unmodified ITO or glass surfaces under shear stress provided planar alignment of the Φ_h phase on the surface. Photopolymerization of the periphery acrylyl groups, using 2,2-dimethoxy-2-phenylacetophenone as the sensitizer, fixes the columnar assemblies

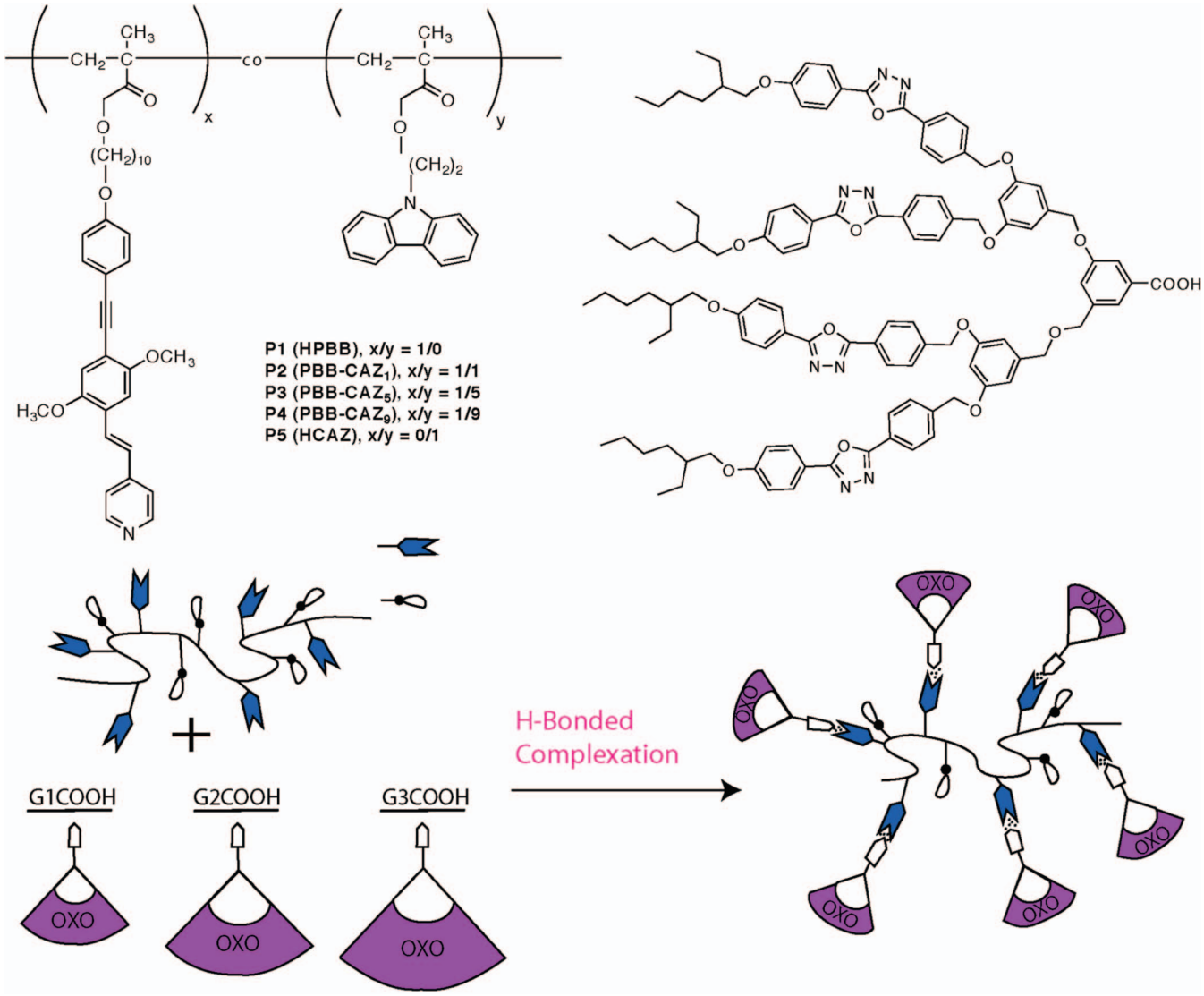

Figure 175. Noncovalent dendronization of light-emitting polymers hydrogen-bond acceptor polymers with hydrogen-bond donor 1,3,4-oxadiazole-containing dendrons. Adapted with permission from ref 671. Copyright 2008 American Chemical Society.

and provides 1-D ion-conductive materials with perpendicular or parallel alignment of the column on the surface (Figure 182). Anisotropic conductivity measurements were performed, and conductivities of 1.6×10^{-3} and 1.4×10^{-5} S cm^{-1} for conductivities parallel and perpendicular to the column axis, respectively, were obtained.[685] Retention of columnar ordering within the polymerized films was confirmed by XRD.

The helical columnar architecture is one of the most general in nature. However, more complex architectures often arise via helical bundling. Columnar bundles can be achieved via dendronized polymers through the incorporation of a covalent link between columns. Twin-dendritic benzamides composed of (3,4,5)12G1 dendrons [(3,4,5)12G1−BA] were shown to self-assemble in Φ_h lattices with Bragg reflections of about 23 Å.[297] Self-organization occurs via a mechanism of alternating stacking of twin-dendritic benzamides rotated 90° from one another along the columnar backbone. *N*-methylation of the amide results in the elimination of the Φ_h structure, suggesting that the self-assembly is mediated by an H-bonding along the long axis of the column. Free radical polymerization of a periphery methacrylate group produced PMA jacketed by (3,4,5)12G1−BA. As (3,4,5)12G1−BA is in fact a dendronized dendron, this dendronized polymer represents a distinct topology (Figure 1, row 3 middle) from those mentioned previously in this section. TOPM of this dendron-jacketed polymer exhibited a N texture, and XRD supported this assertion. It was hypothesized that the PMA jacketed with (3,4,5)12G1−BA forms three-cylinder bundles, with three columns stacked from twin-dendrons emanating from the central polymer chain (Figure 183). Architecturally similar both in shape and scale to natural proteins 3 and 4-α-helix bundles, columnar bundles prepared through periphery polymerization of twin-dendritic benzamides differ in that there is no inherent intracolumnar long-range helicity and that the polymer main chain does not run through the columnar axis.[686] With the main chain running through the intercolumnar space, which is often occupied by metallo-cofactor used in enzymatic activity, these synthetic columnar bundles are expected to serve only as structural analogues of α-helical bundles unable to mimic their catalytic function.

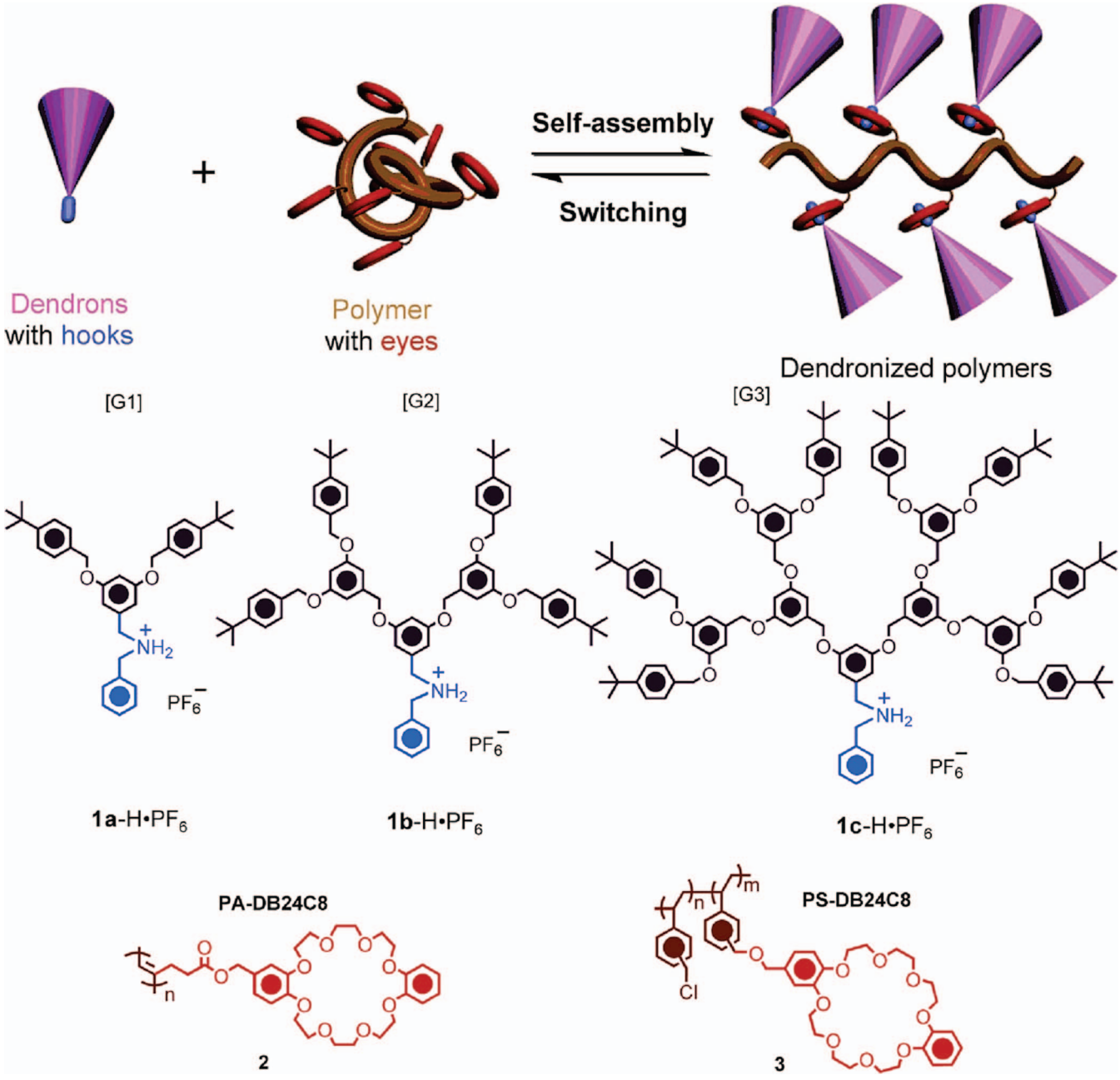

Figure 176. Acid−base switchable dendronized polymers composed of polyacetylene or PS backbones bearing dibenzo[24]crown-8 "eyes" and Fréchet dendrons bearing dialkylammonium "hooks". Reprinted with permission from ref 672. Copyright 2006 American Chemical Society.

Lack of Φ_h organization is attributed to the destabilizing vacancies in the superlattice. In forming a Φ_h lattice, the three helix-bundles would leave one-fourth of the lattice sites vacant (Figure 184).

Mixing of the polymer jacketed with three-column bundles with 20−60 mol % of (3,4,5)12G1−BA allows for filling of the lattice and intracolumnar gaps, thereby producing a Φ_h superlattice with Bragg reflections of ~45 Å, approximately twice the lattice spacing of the dendrons (Figure 185).

Self-assembly into columnar bundles is not restricted to (3,4,5)12G1−BA. (4-3,4,5)12G1−BA self-organizes into a Φ_h lattice via the same mechanism as (3,4,5)12G1−BA with a columnar diameter of 28.2 Å.[687] Free-radical polymerization of a methacrylate on the periphery of the twin-dendron produces a dendron-jacketed polymer that self-assembles into imperfect four-column bundles that exhibit a novel vesicular N_c phase with short-range Φ_h order. Here, one or more polymer chains form the center of macrofibrils composed of four-column bundles (Figure 186).

Addition of 20−30 mol % (4-3,4,5)12G1−BA to the dendronized polymer fills the intracolumnar gaps in the superstructure, providing for a Φ_h superlattice with 70−72 Å Bragg spacings (Figure 187).

Chow has reported a novel variant of the macromonomer strategy using diametrically bis(ethynyl) periphery-functionalized dendrimers.[688] The bis(ethynyl) groups readily polymerize with *trans*[$(Et_3P)_2PtCl_2$] to form linear dendritic

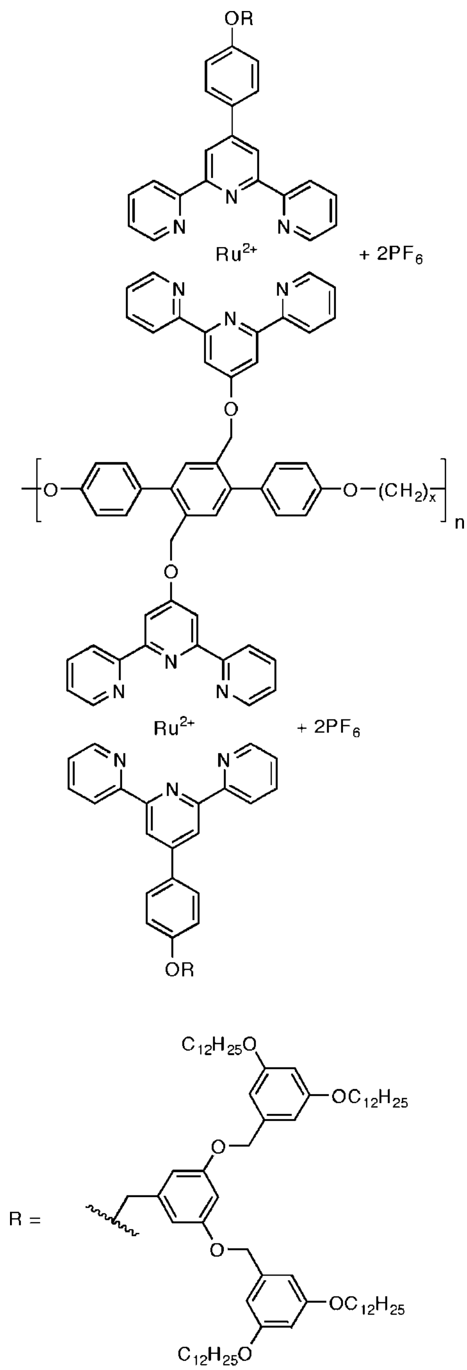

Figure 177. Dendronized main-chain terphenyl polyethers prepared via “attachment by coordination”.[673]

necklaces via an “outer sphere−outer sphere” connection (Figure 188). G1−G3 dendritic monomers were employed, achieving high molecular weight polymers with a DP that decreased with increasing generation number from 880 for G1 to 30 for G3. Alternatively, the use of tris(ethynyl) periphery-functionalized dendrons or copolymerization with a cross-linker results in dendritic network polymers.[689] This approach provides a unique structure wherein the organoplatinum main chain runs through the diameter of a discotic dendron. Self-organization should be evident in related systems constructed to match Percec-type or other self-assembling aryl ether dendrons. The effect of structural rigidity and dendron size on the synthesis of dendritic structures, dendronized polymers, and dendritic necklaces connected via $(Et_3P)_2PtCl_2$ was also investigated. Enhanced structural rigid and compact dendrimers tend to enforce linear polymerization, while bulkier and less rigid dendrons resulted in a greater degree of cylic oligomers.[690]

3.4. Dendron-Jacketed Block Copolymers

More recently, attention to dendron-jacketed block-copolymers (Figure 1, first row right) has been growing. Dendron-jacked block-copolymers exploit both dendron-mediated self-assembly and self-organization as well as the phase-segregation characteristics of the block-copolymer. Hammond reported the synthesis of PEO-*b*-PEI via the cationic polymerization of 2-ethyl-2-oxazoline initiated with PEO-Ts followed by hydrolysis.[692] PEI provided a regular grafting-from site for the divergent synthesis of PAMAM side chains (Scheme 46).

Xi reported the synthesis of rod−coil PEO-*b*-PDMA (PDMA = dendritic polymethylacrylate).[693] A PEO macroinitiator was extended with a G2 Fréchet dendritic methacrylate macromonomer via ATRP (Scheme 47).[694]

In solution, the block-copolymers were shown to produce a variety of spherical, rodlike, and spindly aggregates. The rod−coil architecture of PEO-*b*-PDMA could be converted to a rod−rod architecture through the formation of a pseudorotaxane inclusion complex with α-cylodextrin.[695] Poly(acrylic acid-*b*-DPS) (DPS = dendritic polystyrene) was also synthesized (Figure 189).[696]

The generation number of the Fréchet dendron of the PAA-*b*-DPS affected the gross morphology of the aggregates formed in DMF/water. PEO-*b*-PDMA jacketed with G2 Fréchet dendrons (Scheme 47)[697] or with Percec-type (4-3,4,5)12G1 dendrons (Scheme 48)[698] can be cast into films with honeycomb architecture, though no LC mesophase was observed. Other large scale morphologies were available in LB films cast of PEO-*b*-PDMA with Percec dendron side chains.[699]

PDMA-*b*-PEO-*b*-PDMA ABA triblock copolymers with Percec-type dendron side chains were also prepared (Figure 190).[700] Despite the Φ_h structure in the PDMA homopolymers, no LC phase was detected. However, in solution, aggregation into superhelical ribbons was noted.

AB block copolymers of poly(methoxy diethylene glycol methacrylate) or poly(*N*-isopropylacrylate) with poly(methacrylate) jacketed with G1 and G2 benzamide dendrons with anionic lipids coordinated to their surface NH_3 were prepared (Figure 191).[701] These block copolymers self-organize into hierarchical nanostructures, wherein there is lamellar segregation of the linear block from dendronized block. Within the dendronized block, suborganization into rectangular-within-lamellar, tetragonal-within-lamellar, hexagonal-within-lamellar, and lamellar-within-lamellar architectures (Figure 192).

Dendronized amphiphilic block copolymer poly[poly(ethylene oxide) methyl ether methacrylate]-*b*-(4-3,4,5)12G1−PS (P(PEOMA)-*b*-DPS) was prepared via ATRP of Percec-type dendritic macromonomer initiated with P(PEOMA) macroinitiator (Scheme 49).[702] The DPS homopolymer, P(PEOMA)-*b*-DPS, has varying block DP ratios as well as various PEOMA side-chain lengths all self-organized into Φ_h lattices. In solution, a variety of wormlike and vesicular structures were formed. In the case

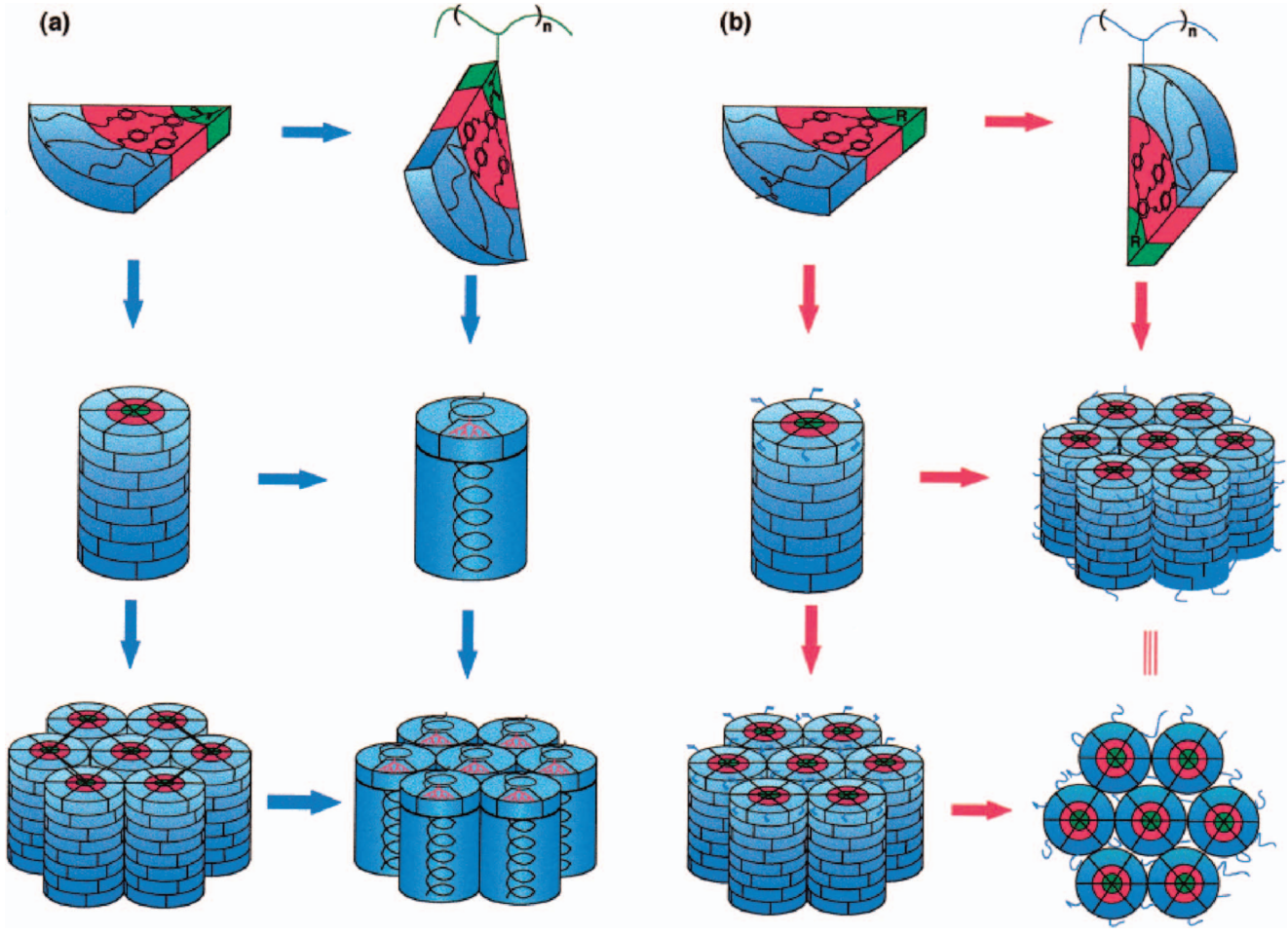

Figure 178. Dendrons attached to polymers via their apex and via their periphery. R-groups are defined in the following figures. Reprinted with permission from ref 683. Copyright 2002 Elsevier.

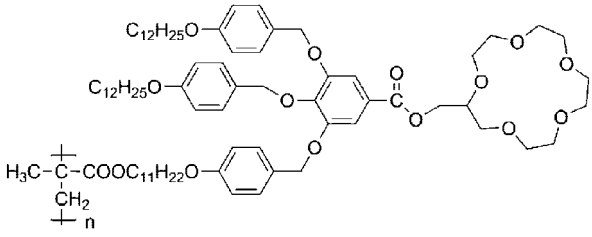

Figure 179. 15-Crown-5 functionalized Percec-type dendron attached to polymethacrylate via its periphery.[676,678,679]

of vesicular structures, a lamellar bilayer wall was proposed (Figure 193).

The architecture of PS can be modulated through noncovalent modification of a receptor modified block.[703] PS-*b*-PS/DAP was prepared where DAP (2,5-diamidopyridine) serves as binding receptor (Figure 194). PS-*b*-PS/DAP on its own assumes lamellar architecture. However, when treated with a Fréchet-type dendron bearing a complementary Thymine receptor at its apex, the lamellar architecture can be converted to cylindrical architectures. When G3 dendrons are utilized, spherical architectures can be obtained.

AB block copolymers of differentially dendronized diblock copolymers were reported (Figure 195).[704] While no evidence of self-organization was presented, this is an interesting example of a doubly dendritic rod−rod diblock architecture.

Block copolymers of dendronized and nondendronized poly(norbornene)s have been prepared via a dendritic macromonomer approach through ROMP using Ru(=CSPh)$Cl_2(P(Cy)_3)_2$ as catalyst.[705] Each dendritic side chain contains three ammonium groups that complex DNA and self-assemble into spherical complexes (Figure 196).

Block copolymers were also prepared via Suzuki condensation of 1,4-phenyl-diboronic acid and (*S*)-6,6′-dibromo-2,2′-didendron-substituted 1,1′-dinaphthyl (BINOL) (Figure 197).[706] The dinaphthyl in this case was decorated with either G1 or G2 Fréchet-type dendrons. The dendritic periphery isolated the conjugated backbone, allowing for high quantum efficiency. CD/UV−vis demonstrated multiple Cotton effects. Thus, it is possible that chirality is induced in both the backbone and dendritic portions. Random copolymers of the Fréchet dendronized dinaphthyl and 9,9-dihexylfluorene were prepared by another group.[707] CD/UV−vis spectroscopy indicated transfer of chirality from BINOL to fluorine regions.

4. Polymers and Oligomers Dendronized at Their Chain Ends

4.1. Synthetic Polymers and Oligomers Dendronized at Their Chain Ends

Attachment of dendrons to the chain ends of linear polymers or oligomers gives rise to a second topological class of dendronized polymers (Figure 1, third row right, fourth row, and fifth row left). This class has its own specific

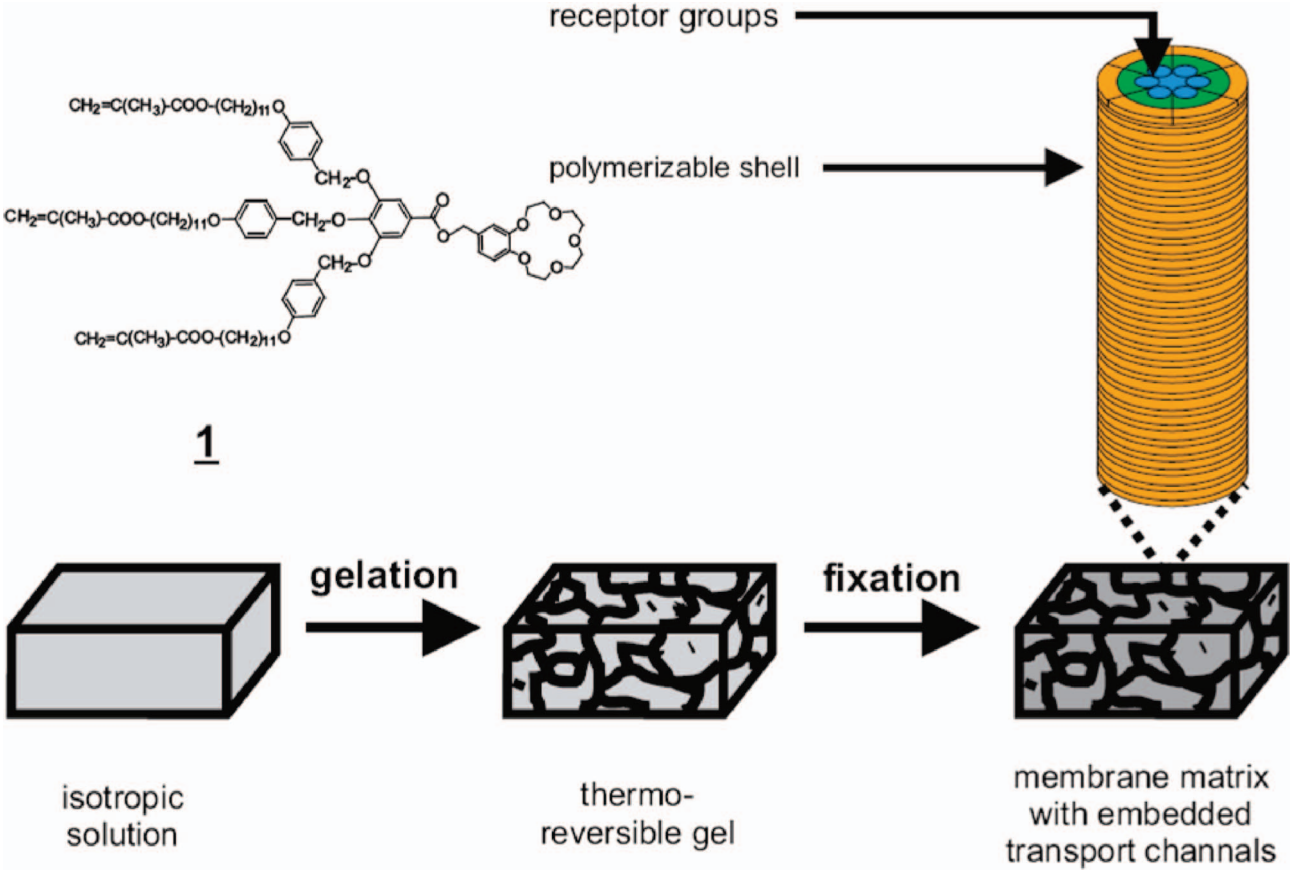

Figure 180. Ion channel formation by matrix copolymerization of trismethacroylyl functionalized dendron. Reprinted with permission from ref 680. Copyright 2000 Wiley-VCH Verlag GmbH & Co. KGaA.

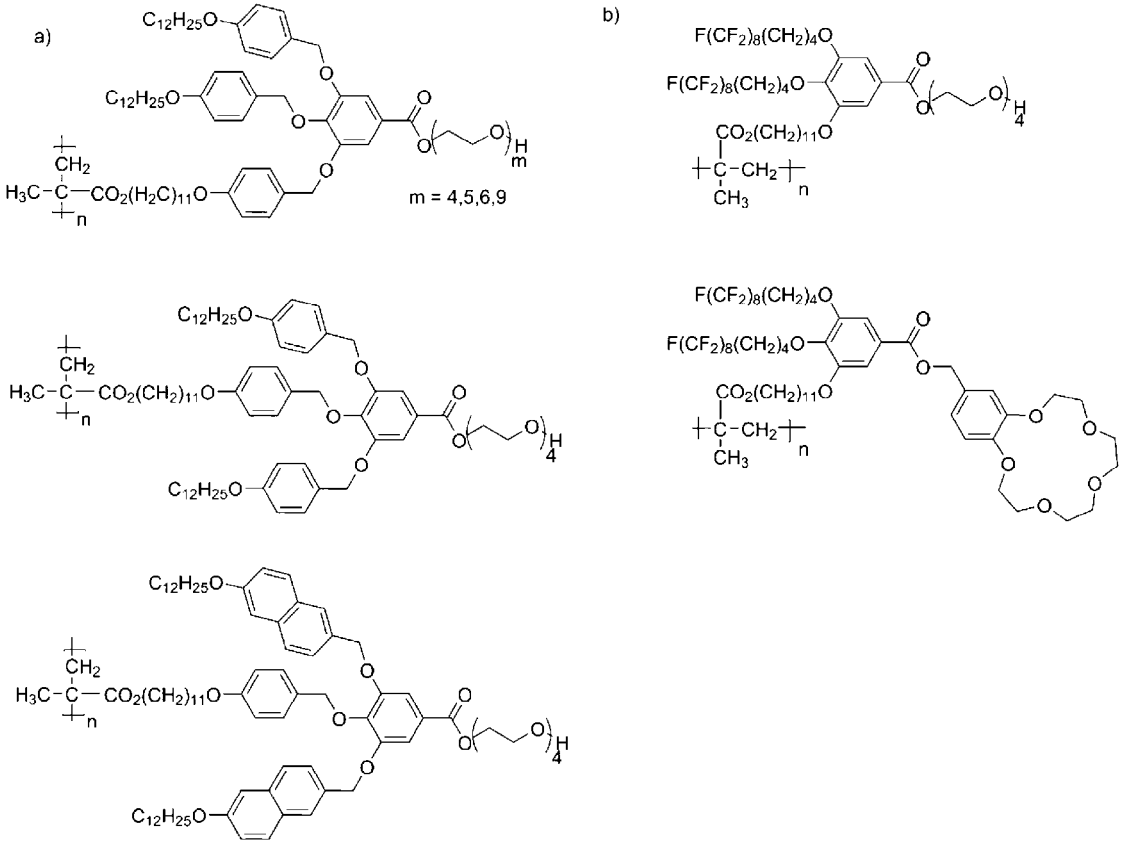

Figure 181. Structures of dendrons attached to polymers via their periphery.[297,682,683]

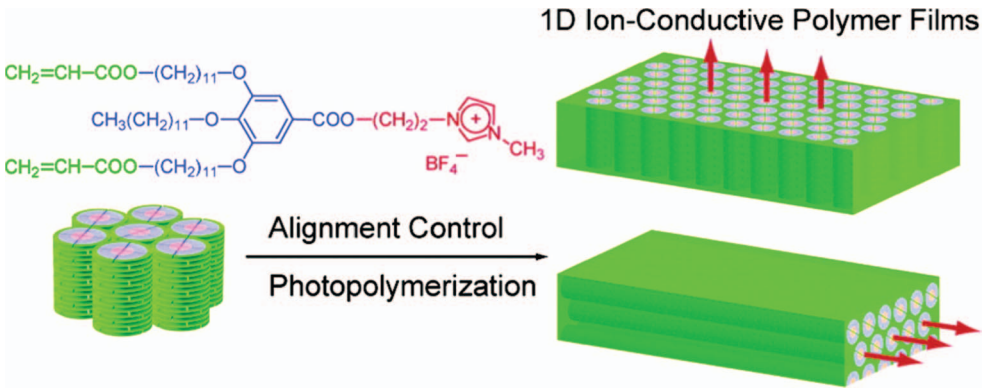

Figure 182. Photopolymerization of Percec-type dendrons with ionic apex groups photopolymerized at the periphery, producing 1-D ion-conductive films arranged parallel (bottom) and perpendicular (top) to the surface. Reprinted with permission from ref 685. Copyright 2006 American Chemical Society.

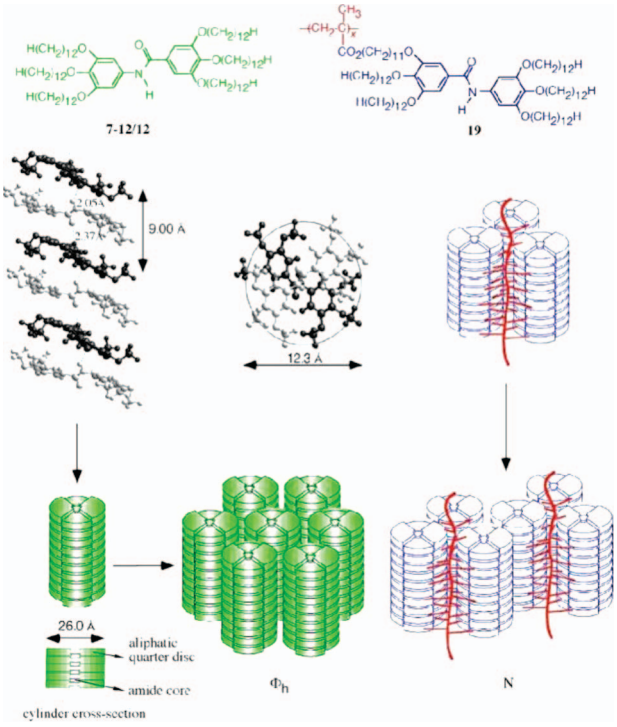

Figure 183. Self-assembly of twin-tapered dendrons and dendronized polymers into columns and three-column bundles. Reprinted with permission from ref 297. Copyright 1999 Wiley-VCH Verlag GmbH & Co. KGaA.

nomenclature, e.g., dendron-linear hybrids, dumbbells, bow-ties, barbells, Janus dendrons, and twin dendrons to name a few, which can be simplified according to the type of polymer or copolymer and the number of chain ends to which the dendron(s) are attached (Figure 198). In addressing the self-assembly and self-organization of polymers dendronized at their chain ends, the most broad distinction can be made between polymers dendronized at one chain end and polymers symmetrically or asymmetrically dendronized at both chain ends. Further subclassification of the main chain into flexible polymers, rigid polymers, and rigid-flexible block-copolymers is helpful in differentiating topology, architecture, and mechanisms of self-assembly and self-organization.

Both grafting-onto and grafting-from approaches were employed in the synthesis of linear polymers and oligomers dendronized at their chain ends as described in section

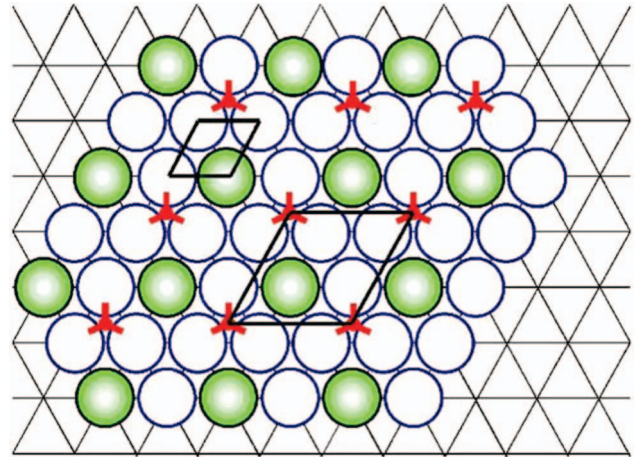

Figure 184. Lattice vacancies in hexagonal lattices produced via three-column bundles. Reprinted with permission from ref 297. Copyright 1999 Wiley-VCH Verlag GmbH & Co. KGaA.

3.1.1.[77] In the grafting-onto approach, dendrons prepared through a convergent strategy are attached to the chains ends of the linear polymer. In the grafting-from approach, G1 dendrons are attached to the chain ends of the linear polymer and subsequently elaborated to higher generation via a divergent growth strategy. Alternatively, a dendritic macroinitiator strategy can be employed, wherein a dendron prepared through a convergent strategy is functionalized at its apex with an initiator moiety. Polymerization of the dendritic macroinitiator under suitable conditions results in a linear polymer dendronized at one chain end. This process represents a strategy of linear polymers grafted-from the dendron.

Historically, the grafting-onto strategy was the first method to be used in the synthesis of linear polymers dendronized at their chain ends.[82] The synthesis of PS through living-anionic polymerization via potassium naphthylide, followed by modification of the living chain ends with 1,1-diphenylethylene, and quenching of the living α,ω-di(anionic) chain ends by Fréchet dendrons containing a benzyl bromide apex-functionality was reported in 1991 (Scheme 50, top).[708,709] Fréchet also reported the postpolymerization modification of PEO with Fréchet dendrons via Williamson etherification (Scheme 50, middle).[389,710−712] Additionally, Percec reported (4-3,4,5)12G1COOH grafted-onto in situ prepared oligo(ethylene oxide) monotosylate (Scheme 50 bottom).[208]

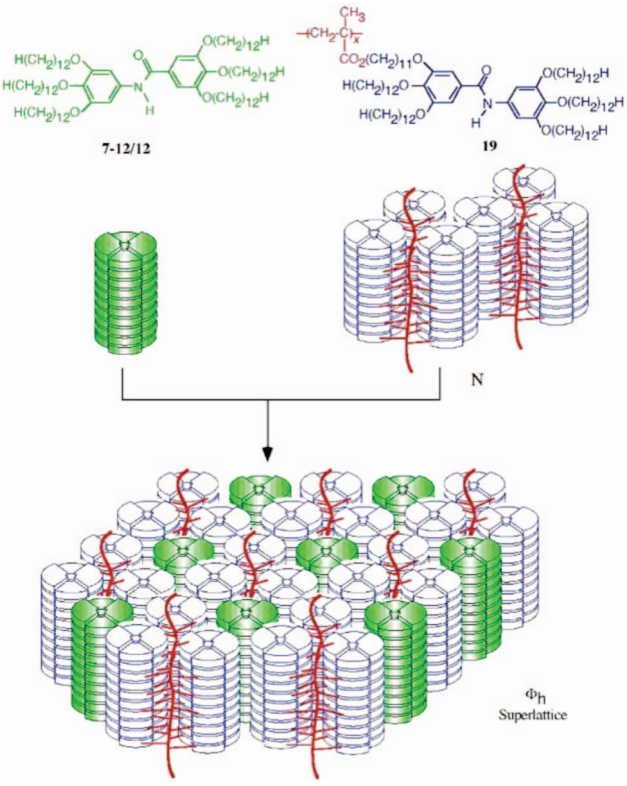

Figure 185. Superlattice of twin benzamide (BA), (3,4,5)12G1−BA, and its dendronized polymer containing a backbone jacketed with a bundle of three columns. Reprinted with permission from ref 297. Copyright 1999 Wiley-VCH Verlag GmbH & Co. KGaA.

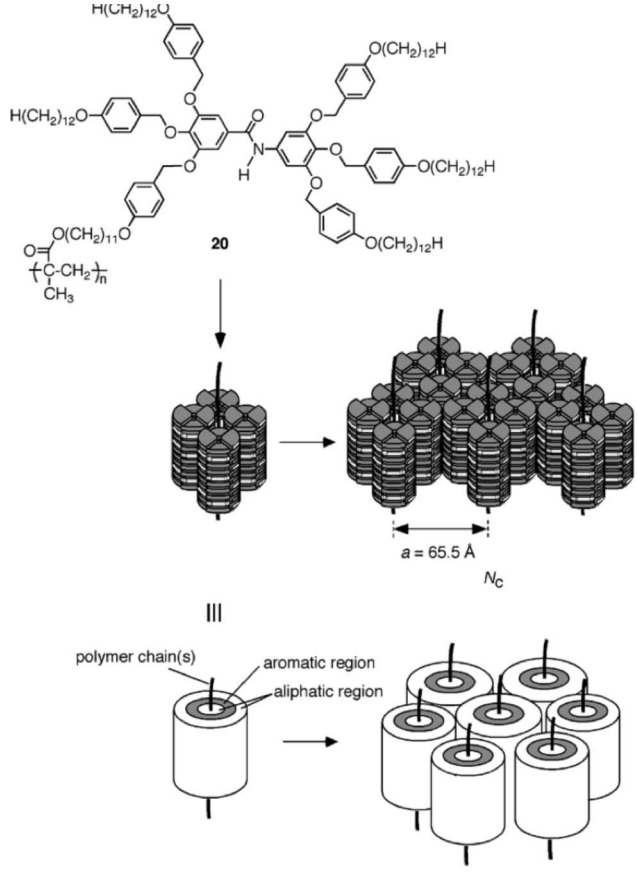

Figure 186. Vesicular N_c phase formed from four-column bundles. Reprinted with permission from ref 687. Copyright 2003 Wiley-VCH Verlag GmbH & Co. KGaA.

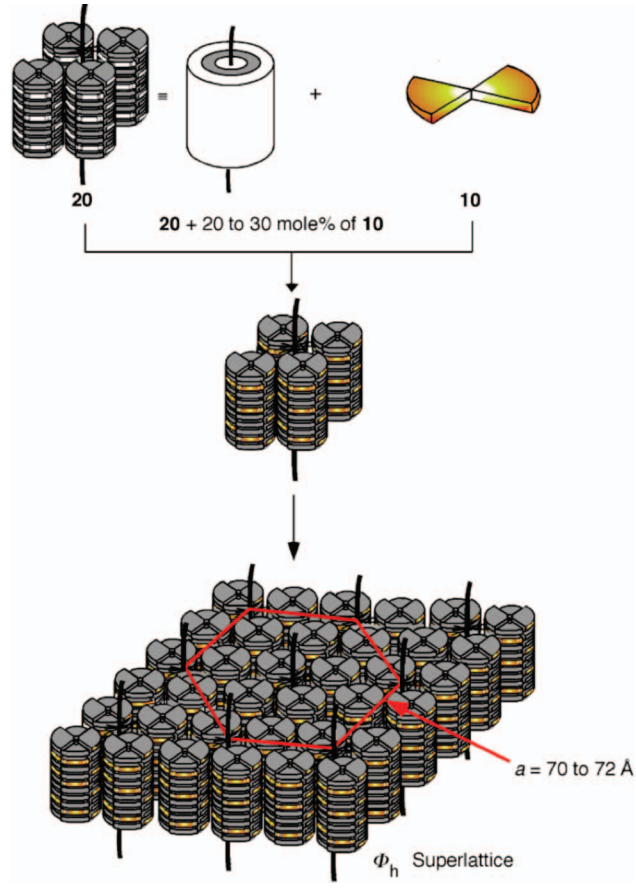

Figure 187. Superlattice formed from (4−3,4,5)12G1−BA and its dendronized polymer. Reprinted with permission from ref 687. Copyright 2003 Wiley-VCH Verlag GmbH & Co. KGaA.

Chapman was the first to adapt the grafting-from strategy for the synthesis of polymers dendronized at their chain ends in 1994. Poly(L-lysine) (PLL) dendrons were grown from a monofunctional PEO via sequential protection/deprotection (Scheme 51).[713] Later, Hammond used a similar synthetic strategy for the synthesis of PEO dendronized with PAMAM at one chain end (Scheme 52).[714−716]

Fréchet first reported the dendritic macroinitiator approach to the synthesis of chain-end dendronized linear polymers in 1994.[717,718] In the first example, a G4 Fréchet dendron functionalized at the apex with a potassium alkoxide was used as an initiator for the anionic ROP of ε-caprolactone (Scheme 53).[717] In a second example, a G4 Fréchet dendron was modified at its apex with a TEMPO-containing moiety or benzyl chloride and used as a dendritic macroinitiator for the NMP or ATRP of styrene, respectively (Scheme 54).

4.1.1. Flexible Polymers Dendronized at One Chain End. Dendron−Coil (DC)

Flexible polymers dendronized at one chain end (Figure 1, row 3 right, Figure 198, row 1 second from left) have drawn significant attention as they merge the interfacial properties of dendritic molecules with the processability of linear polymers.[712−714,718−731] Specifically, the use of a flexible polymer backbone increases entanglements and facilitates self-assembly into well-organized films.[714] Flexible PAMAM,[714,724] PPI,[719,726] PEG,[728,730,732−737] PLL,[713] and poly(carbosilane)[731] dendrons and stiffer Fréchet-type,[717,723,725,727,729] Percec-type carbazole functionalized benzyl ether[738] or poly(phenyl

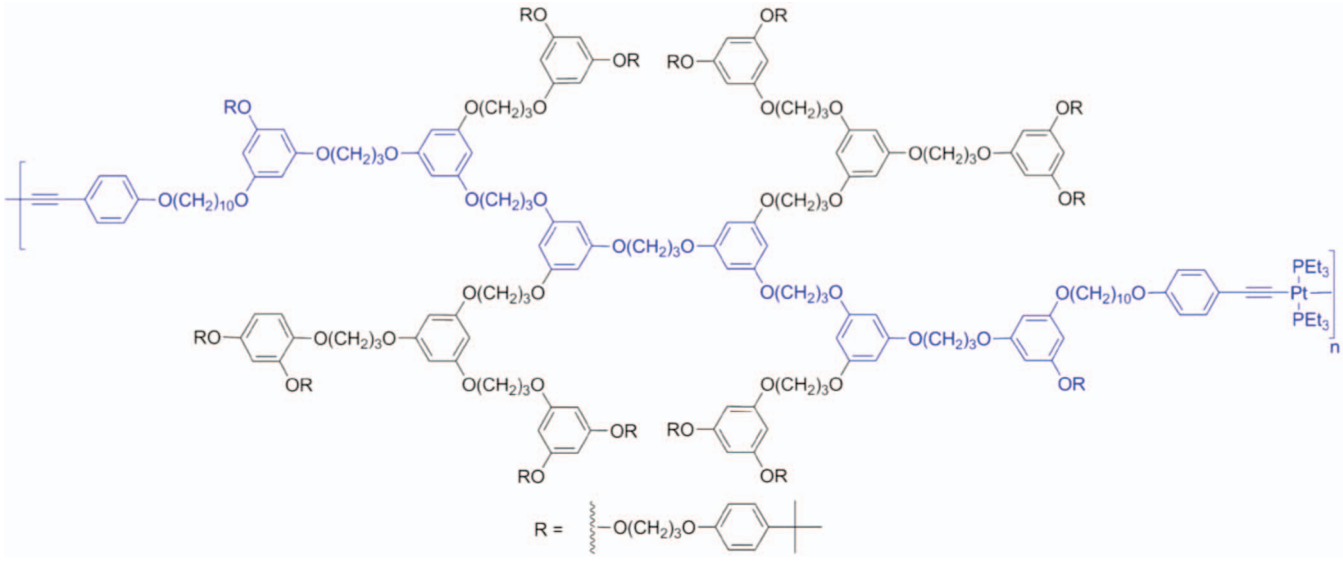

Figure 188. Example of a dendritic necklace.[691]

Scheme 46. Synthesis of PEO-*b*-PEI, with a Dendronized PEI Block[692]

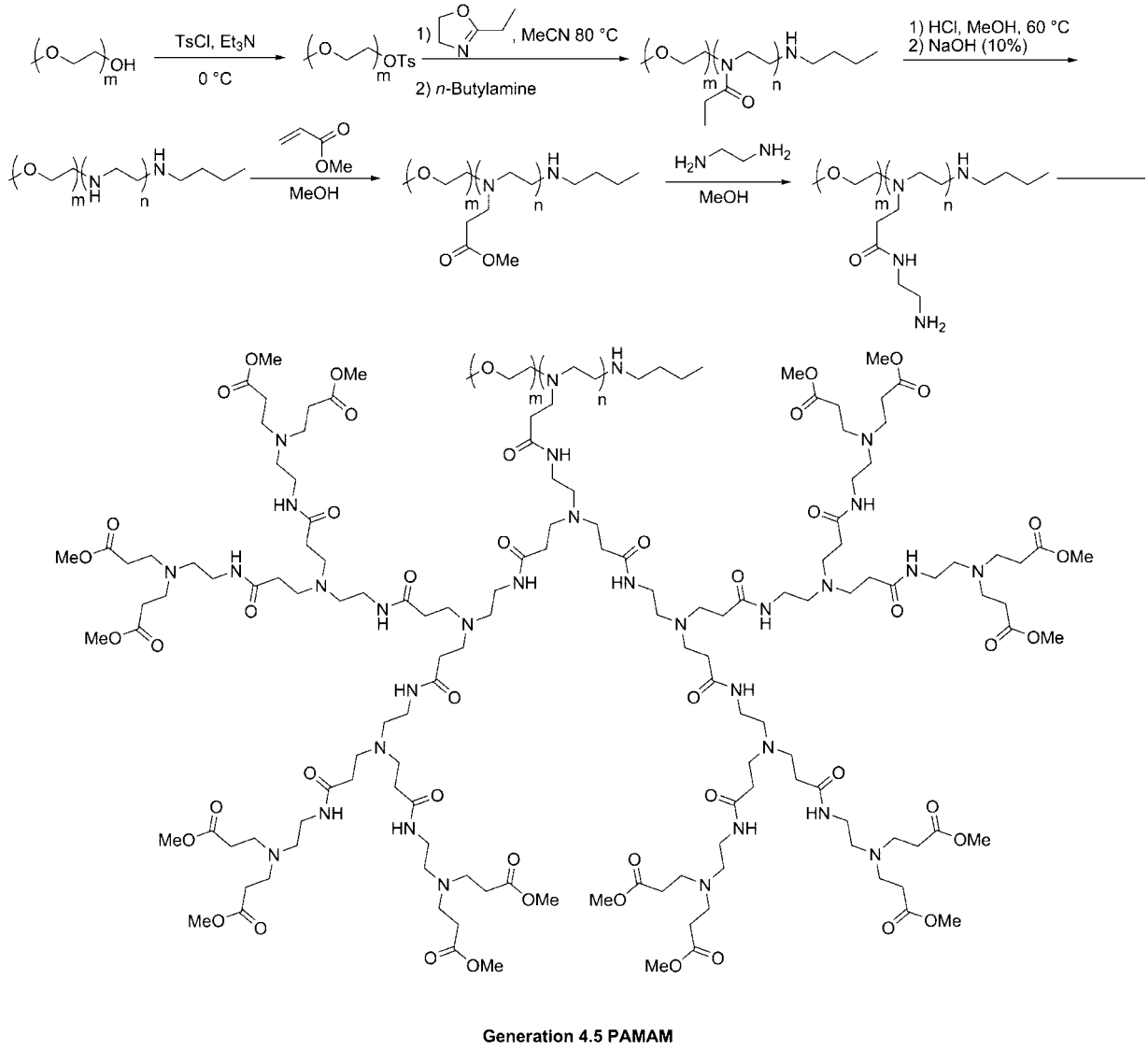

azomethine)[739] dendrons have been employed. The flexible linear polymer is most often PEO,[714,731−737] PS,[717,719,723,725,726] poly(methyl oxazoline),[724] poly(γ-*n*-dodecyl glutamate),[728] or poly(tetrafluoroethylene) (PTFE).[727] If the dendron com-

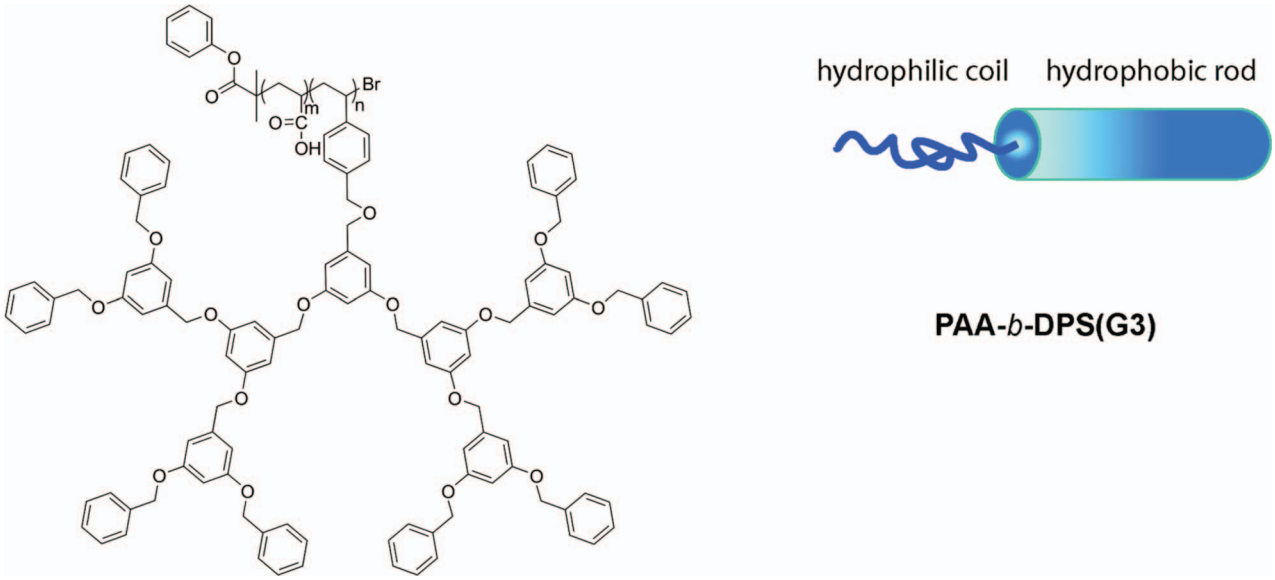

Figure 189. PAA-*b*-DPS dendronized with G3 Fréchet dendrons.[696]

Scheme 47. Synthesis of PEO-*b*-PDMA Dendronized with G2 Fréchet Dendrons; Adapted from Ref 693

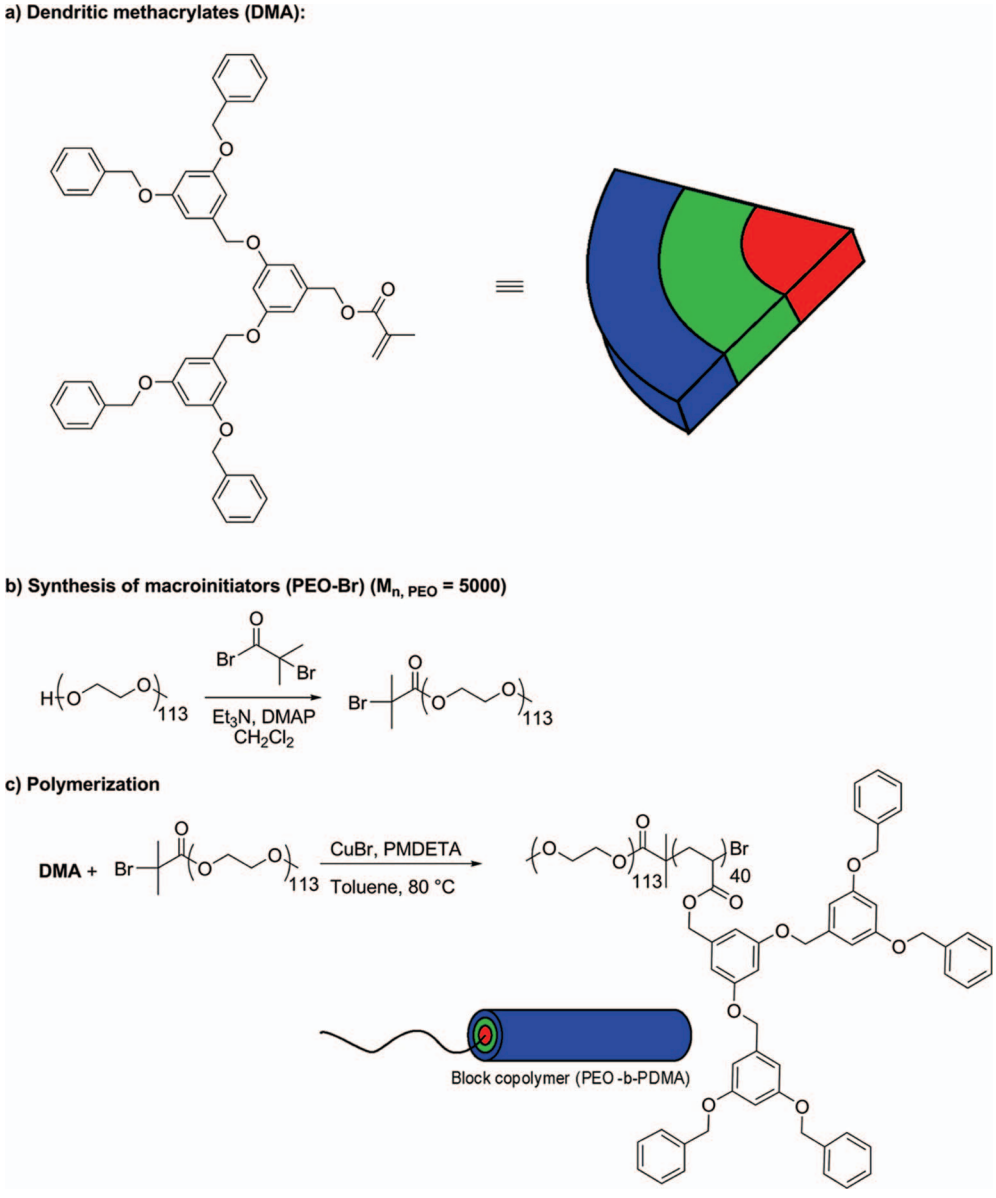

Scheme 48. Synthesis of PEO-*b*-PDMA Dendronized with (4-3,4,5)12G1; Adapted from Ref 698

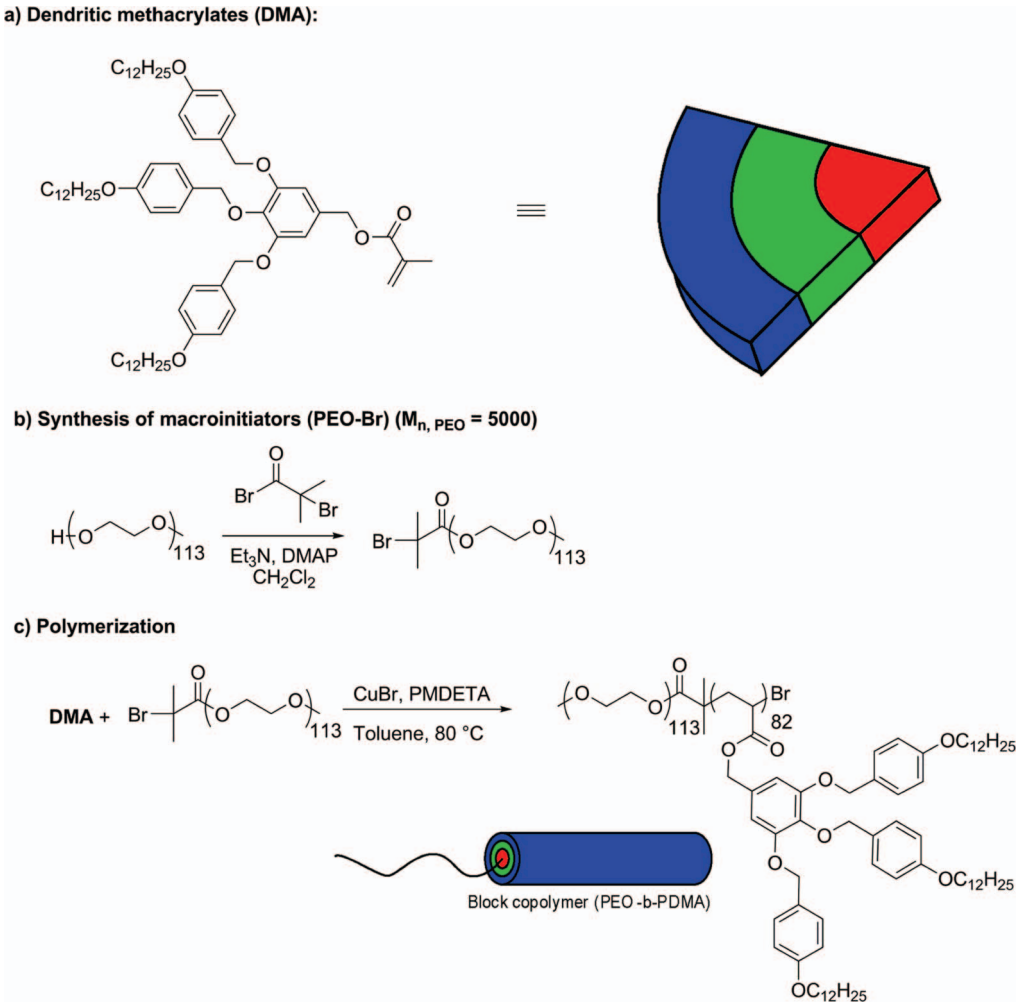

ponent is hydrophilic while the flexible chain is relatively hydrophobic (or vice versa), the chain-end dendronized polymer will act as a macromolecular amphiphile. The behavior of these chain-end dendronized polymeric amphiphiles has been studied experimentally and via computational modeling,[740] particularly for their use as polymeric surfactants[713,714,724] and other specific applications that rely on their self-assembly and self-organization in solution and bulk.[727,738,741−743]

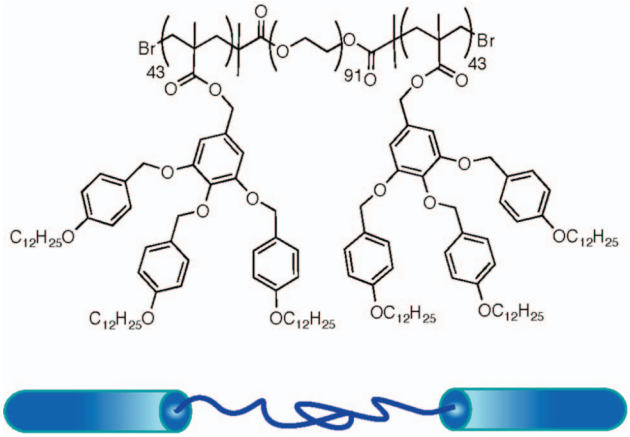

Figure 190. PDMA-*b*-PEO-*b*-PDMA dendronized with (4-3,4,5)12G1. Reprinted with permission from ref 700. Copyright 2005 American Chemical Society.

Percec prepared (4-3,4,5)12G1 grafted onto oligo(ethylene oxides) (Scheme 50, bottom).[208] Dendronized EO with free-hydroxyl chain ends self-assemble into supramolecular columns that self-organize into Φ_h^{io} and, at higher temperature, into Φ_h lattices. Dendronized EO with methyl-capped chain ends do not self-assemble or self-organize in Φ_h lattices, but only in Φ_h^{io} phases. This experiment demonstrates that a single H-bond can mediate the self-assembly process at higher temperatures. Moreover, experiments with LiOTf salts demonstrate the effect of ionic interaction in mediating the formation of a supramolecular backbone (Figure 199). (4-3,4,5)12G1−4EO has a T_m of 56 °C and a $T_{\Phi h\text{-}I}$ of 63 °C. (4-3,4,5)12G1−4EOMe has only a T_m of 46 °C. Poly[(4-3,4,5)12G14EO−MA] has a T_m of 48 °C and a $T_{\Phi h\text{-}I}$ of 113 °C. Addition of LiOTf to (4-3,4,5)12G1−4EOMe mediates the formation of Φ_h phase and increases the $T_{\Phi h\text{-}I}$ of all systems. It was found that, after the addition of ∼0.85 equiv of LiOTf, (4-3,4,5)12G1−4EOMe had the same $T_{\Phi h\text{-}I}$ as (4-3,4,5)12G1−4EO. Thus, 0.85 equiv of LiOTf is equivalent in effect to one H-bonding interaction. Further, it was shown that, after the addition of ∼0.65 equiv of LiOTf, (4-3,4,5)12G1−4EO had the same $T_{\Phi h\text{-}I}$ as poly[(4-3,4,5)12G1−4EO−MA]. Thus, the stabilizing effect of the covalent polymer backbone is equivalent to the stabilizing effect of the supramolecular backbone mediated by one H-bond plus 0.65 equiv of LiOTf.

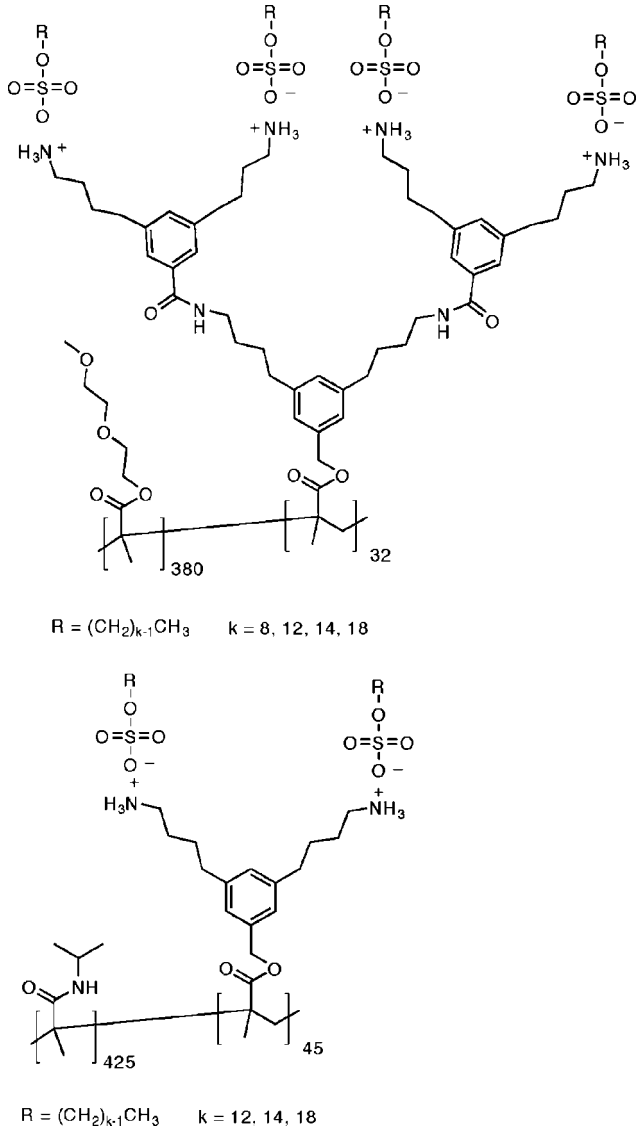

Figure 191. Structure of poly(methoxy diethyleneglycol methacrylate)-*b*-PDMA (top) and PNIPAM-*b*-PDMA (botto,). Reprinted with permission from ref 701. Copyright 2008 American Chemical Society.

The self-assembly of (4-3,4,5)12G1−2EO into tetramers on HOPG surfaces was studied via STM (Figure 200).[744] Chiral analogues, (*R*)-(4-3,4,5)12G1−2EO* and (*S*)-(4-3,4,5)12G1−2EO*, were prepared and their chiral self-assembly on surfaces was examined by STM (Figure 201).[745,746] When a racemic mixture was deposited on the surface of HOPG, segregation into enantiomeric domains was observed.

Amphiphilic chain-end dendronized polymers composed of a hydrophobic main chain and hydrophilic dendron exhibit complex morphology dependent on the type and generation of the hydrophilic dendron as well as the type and DP of the linear polymer. Meijer reported amphiphiles derived from PS chain end dendronized with acid-functionalized PPI.[721,747] Acid-functionalized PS was reduced to the corresponding alcohol and cyanoethylated. Reduction of the cyano group to the free amine provided a site for the divergent grafting-from synthesis of the PPI dendron headgroup via iterative cyanoethylation and reduction. The final PPI dendron was hydrolyzed under acidic conditions to furnish the carboxylic acid-functionalized PS−PPI molecules. This molecule and those like it strongly resemble the shape and structure of traditional molecular surfactants but with the size range of block-copolymers and, thus, can be categorized as types of macromolecular amphiphiles or surfactants (Scheme 55).

Meijer also reported PS chain end dendronized with standard G3−G5 PPI (Figure 202).[722] Lower generation PPI dendrons mediated the formation of inverse-micellar structures with the dendritic headgroup buried in the interior. Increasing generation induced a change from inverse micelles to micellar rods at G4 and standard micelles at G5.[719] Additionally, Gitsov reported pseudosemi-interpenetrating networks prepared from PS functionalized at one chain end with a G3 Fréchet-type dendron with ethyl−ester periphery groups.[748] The formation of the networked structure was achieved via transesterification of the peripheral ethyl−esters with PEG of various DP.

Several groups reported the self-organization of dendron−coil molecules in bulk via manipulation of the DP of the linear polymer segment[732−735] or generation number of the dendritic headgroup.[736] Hawker observed the lamellar and Φ_h self-organization of PS capped at one chain end with a G6 Fréchet dendron prepared through the dendritic macroinitiator route.[729] TEM suggested microphase segregation of the dendritic and linear segments (Figure 203). Self-organization of these molecules is particularly intriguing as the aryl ether dendron segment and the PS main chain have similar solvation properties and should be miscible.

Liu has reported the synthesis of poly(*N*-isopropylacrylamide) (PNIPAM) and PNIPAM−Py (Py = pyrene-functionalized butylacrylate) via RAFT using a G4 Fréchet dendron as a macroinitiator (Scheme 56).[749] These dendron−coils form micelles in aqueous environment with the dendrons buried in the interior. The thermoresponsive collapse of the micelle was detected through changes in the absorption and emission of the pyrene end groups.

Wiesner investigated a doubly hydrophilic PEO functionalized at one chain end with dendritic PEG and its complexes with LiOTf (Figure 204).[84,734−736] Systematic variation of the DP of the main PEO chain revealed a strong effect on self-organization. At DP = 31, crystalline and micellar *Cub* lattice were observed with and without LiOTf. At DP = 96, the polymer alone exhibited thermotropic Φ_h, Cub_{bi}, and lamellar architectures. Addition of LiOTf appears to destabilize and disassemble the lamellar phase. The thermoreversibility of the LiOTf doped structures allowed for facile study of ion transport in 1-D, 2-D, and 3-D network structures.[734] Earlier, ion-transport of LiOTf-doped dendronized crown-ethers was reported by Percec (see section 6.1).[674−676,678−681]

PEO dendronized at one chain end with hydrophobic PAMAM dendrons self-organizes in the aqueous phase into rodlike and spherical micellar structures.[750] PEO has also been dendronized at one or both chain ends with poly(γ-benzyl-L-glutamate) functionalized PAMAM via a grafting-onto click-chemistry route (Scheme 57, left).[751] PEO dendronized at one chain end with poly(γ-benzyl-L-glutamate)-functionalized PAMAM self-assembles in aqueous media to form nanoparticles (Scheme 57, right). A similar approach combining sequential ROP of ε-caprolactone, click attachment of a PAMAM dendron, and ROP of γ-benzyl-L-glutamate *N*-carboxyanhydride provided dendron-like polypeptide/poly(ε-caprolactone) block-copolymers.[752] Gitsov reported that PEO dendronized at one chain end with a G3 Fréchet-

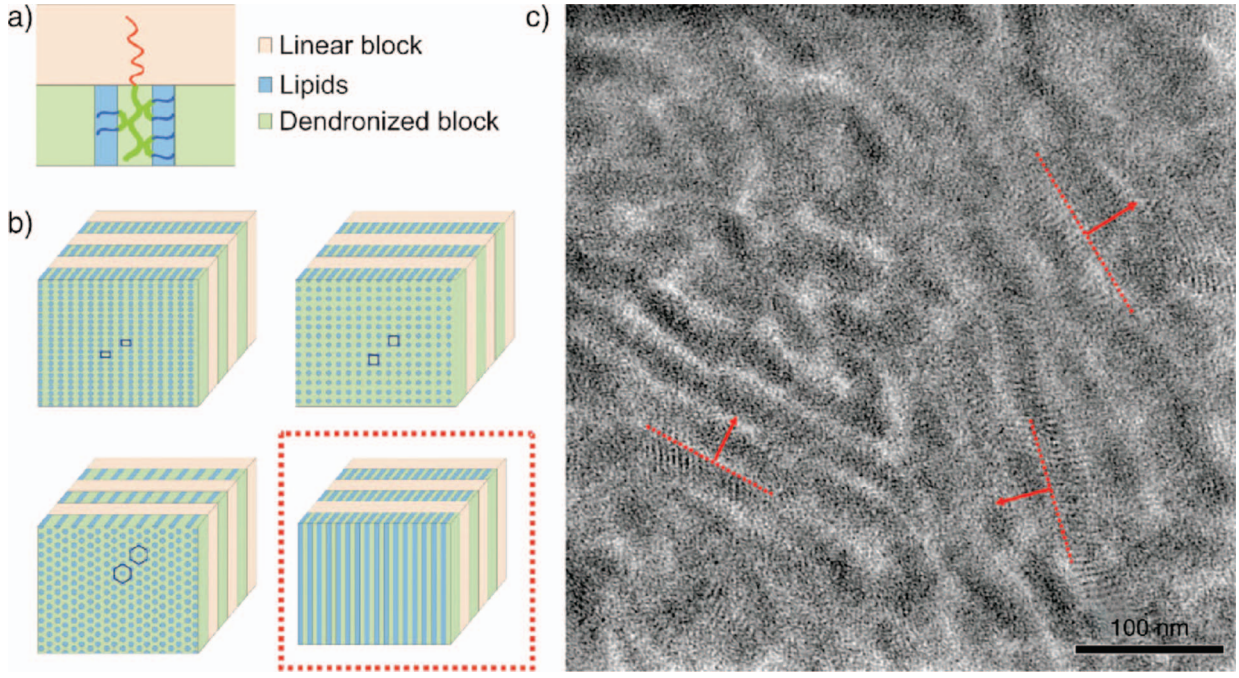

Figure 192. Multiscale self-organization of dendronized block copolymers. Reprinted with permission from ref 701. Copyright 2008 American Chemical Society.

Scheme 49. Synthesis of P(PEOMA)-*b*-DPS (Adapted with Permission from Ref 702; Copyright 2008 John Wiley & Sons, Inc.)

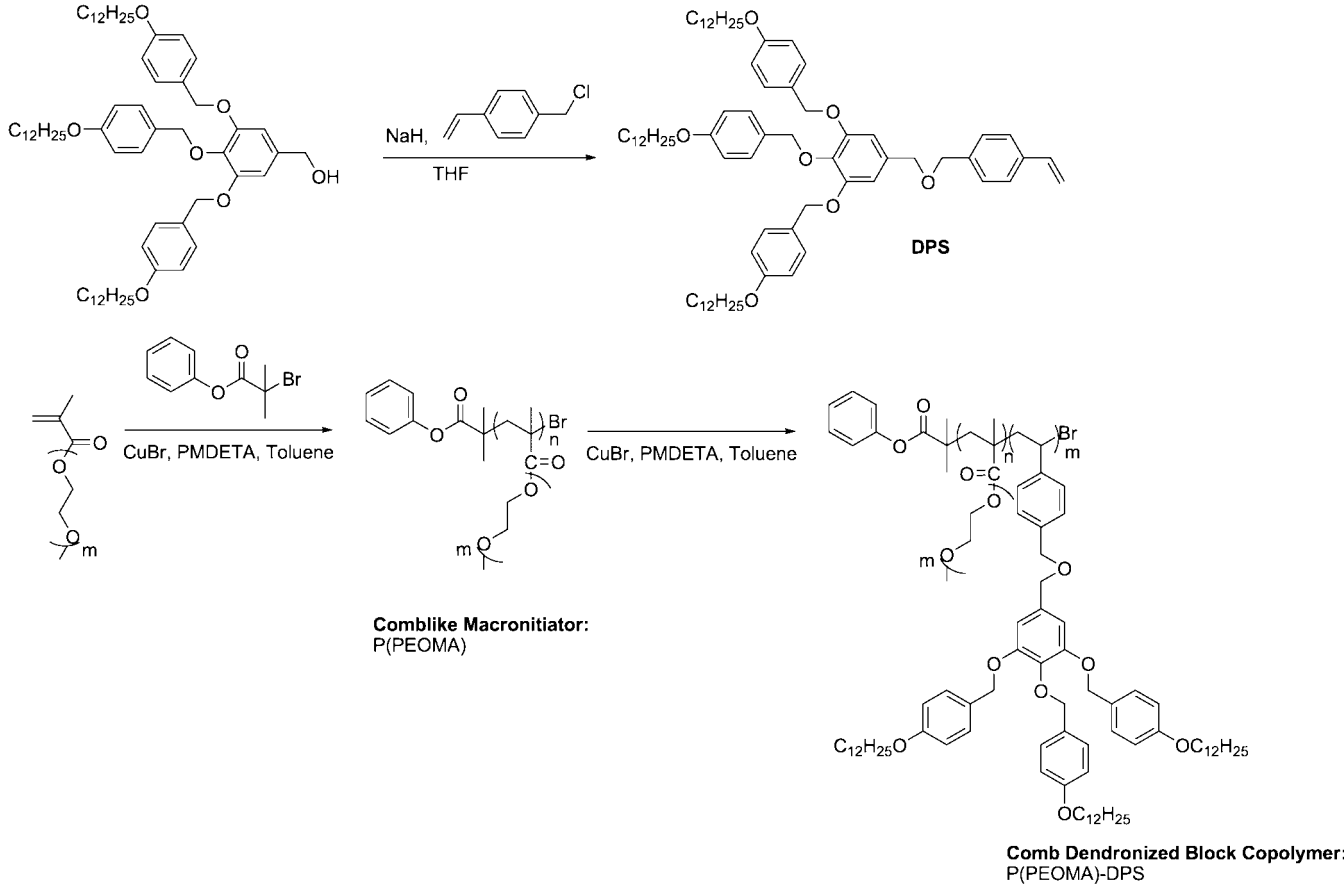

type dendron forms a micellar nanoreactor in water, capable of catalyzing the Diels−Alder reaction of anthracene and C_{60}.[753] Gitsov also demonstrated the ability of PEO dendronized at one or both chain ends with G3 Fréchet-type dendrons to bind and improve the catalytic activity to the oxidative enzyme laccase in aqueous solution.[754,755] The PEO dendronized at one chain end exhibited the best catalytic activity, rationalized as a combination of transport of reactive molecules to the catalytic site and isolation of each enzyme as a single catalytic species.

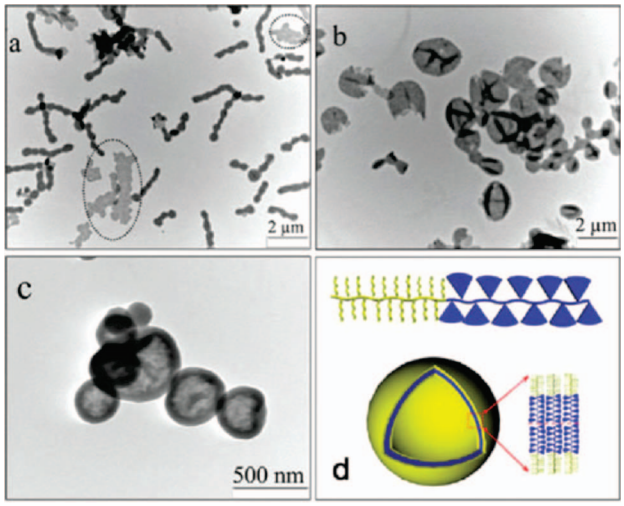

Figure 193. Solution aggregates of P(PEOMA)-DPS. Reprinted with permission from ref 702. Copyright 2008 John Wiley & Sons, Inc.

Gillies reported the formation of vesicles from poly(butadiene)-*b*-poly(ethylene oxide) (PBD-*b*-PEO) bearing surface-functional azides groups.[756] G3 aliphatic ester dendrons with surface-dye groups and apex alkyne functionality were grafted-onto the vesicle via click chemistry (Figure 205). The resulting dendronized PBD-*b*-PEO was visualizable via confocal laser scanning microscopy.

4.1.2. Rigid Polymers and Oligomers Dendronized at One Chain End. Dendron−Rod (DR)

Dendronization of a single chain end of rigid polymers (Figure 1, third row second from right, and Figure 198, first row left) such as oligo(*p*-phenylenes),[757−759] oligo(benzamides),[760] poly(phenylene ethynylene),[613] or poly(biphenyl esters)[761] also leads to a diverse array of self-organized architectures. Because of their rigid oblate shapes, the linear

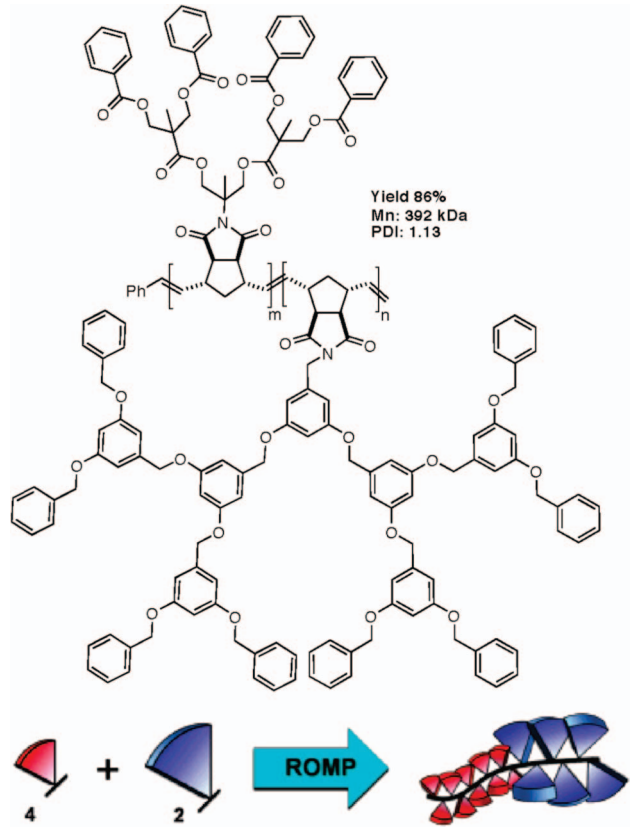

Figure 195. Structure and self-assembly of differentially dendronized AB block copolymers. Reprinted with permission from ref 704. Copyright 2007 American Chemical Society.

segments alone often exhibit N and S phases.[762,763] While higher DP rigid polymers exhibit poor solubility, even minimal chain-end dendronization of these rigid polymers can lead to significant improvements.

Investigation of rigid biphenyl-containing oligomers functionalized at one chain end with Percec-type dendrons (Figure

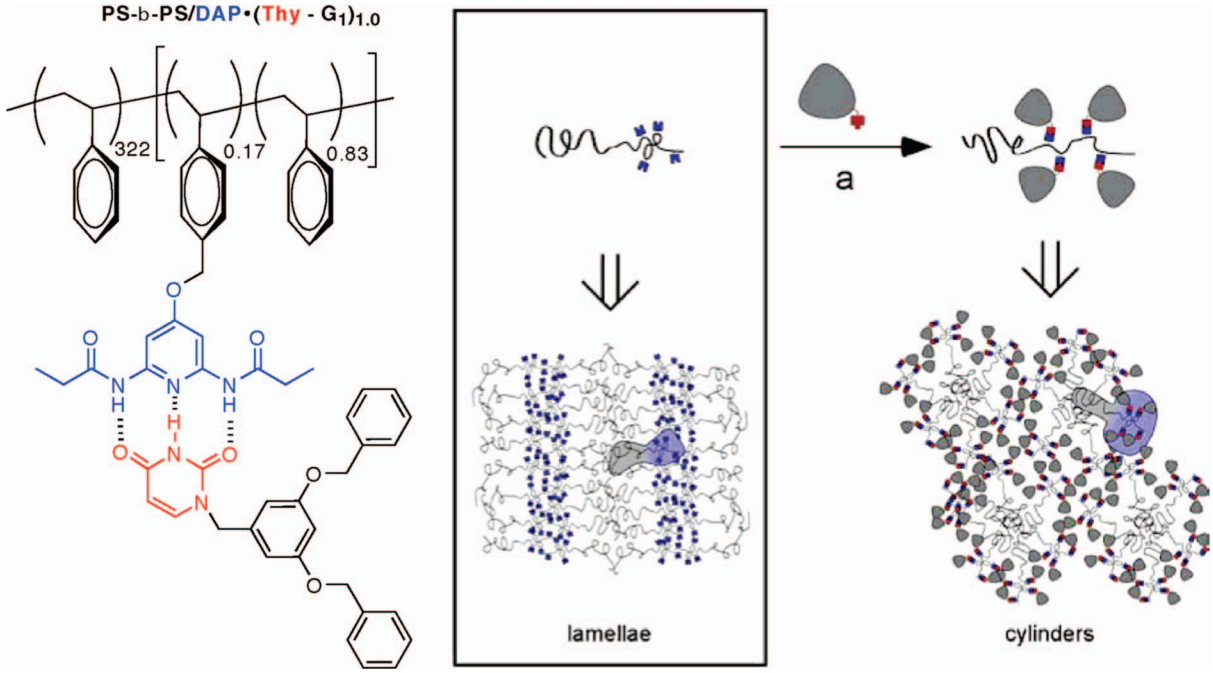

Figure 194. Self-organization of PS-*b*-PS/DAP noncovalently jacketed with Thy functionalized Fréchet dendrons. Reprinted with permission from ref 703. Copyright 2005 American Chemical Society.

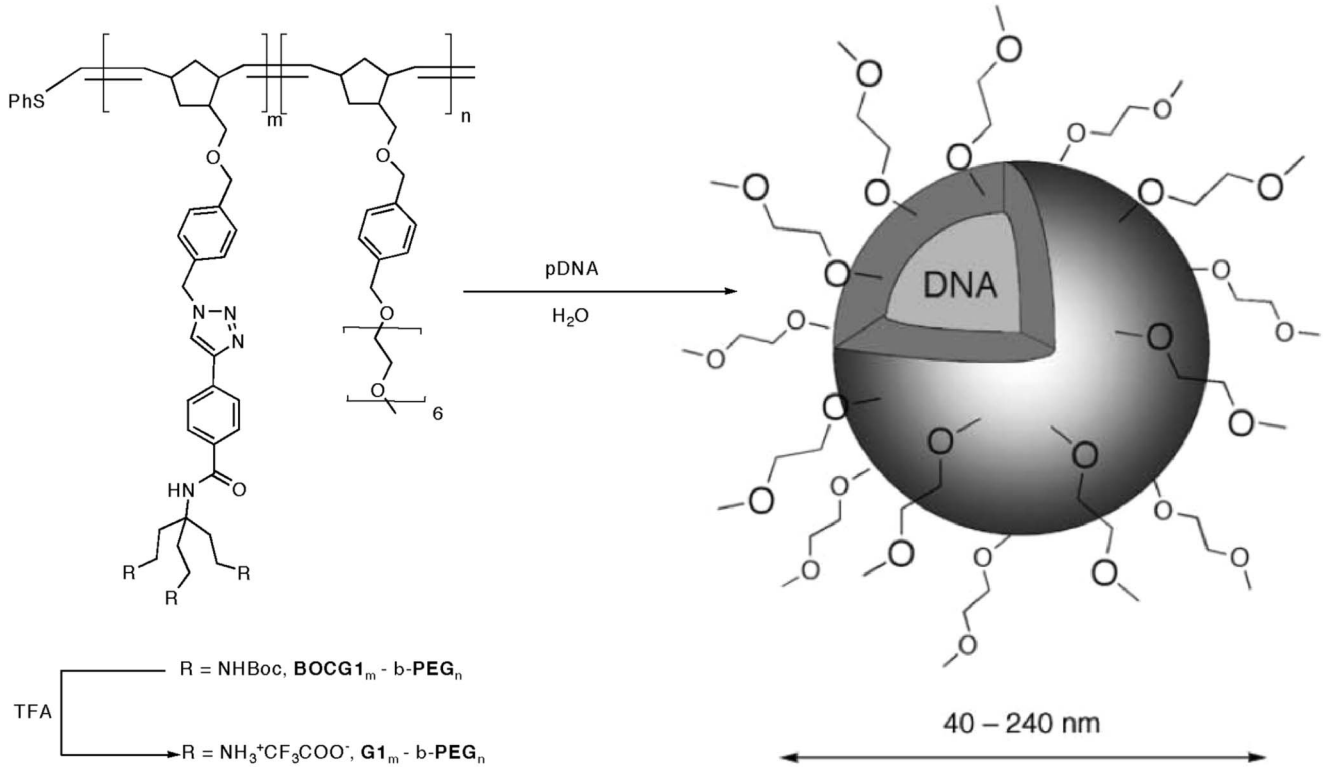

Figure 196. Complexes of poly(norbornene) block copolymers jacketed with cationic dendrons and DNA. Reprinted with permission from ref 705. Copyright 2008 Royal Society of Chemistry.

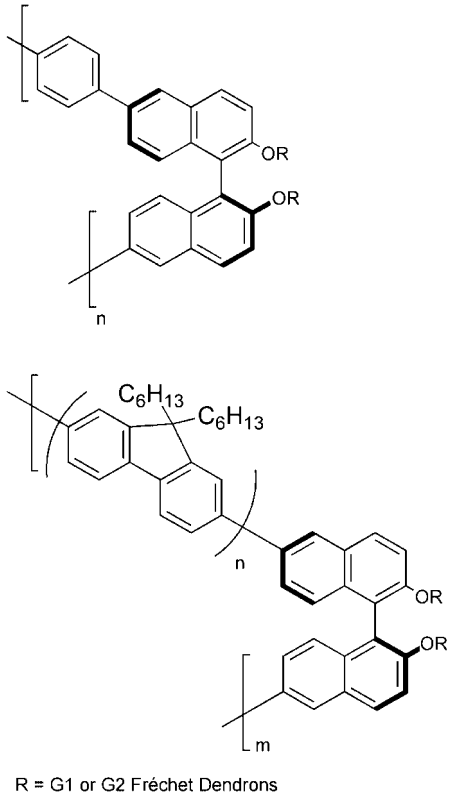

Figure 197. Dendronized poly(phenylene-*co*-bisnaphthol) and poly(fluorene-*co*-bisnaphthol).[706,707]

206) demonstrated that self-organization is mediated by a competition between lamellar assembly through $\pi-\pi$ stacking interactions of the rodlike segments and spherical assembly mediated by the dendron curvature (Figure 207).[761] As such, regardless of dendron structure or chain length, XRD suggested a bicontinuous *Cub* phase constituted of cylindrical arrays of stacked biphenyl units.

Lee investigated the aqueous-phase self-assembly of rigid oligomers dendronized at one chain end through DLS, static light scattering (SLS), TEM, and field-emission electron microscopy (FE-SEM).[757,758] In this study, hexa-*p*-phenylene was trisdendronized at one-chain end with dendritic PEG via a grafting-onto approach. Amphiphilic hexa-*p*-phenylenes bearing G2 PEG dendrons (DR5, Scheme 58) self-organized in bulk into a fully interdigitated bilayer S phase. Increasing the size of the head-groups by attachment of extra periphery EO groups (DR6, Scheme 58) results in increased steric interactions, thereby causing the lamellar architecture to break up into discrete heptameric bundles that self-organize into a 3-D primitive orthorhombic superlattice (Figure 208, left). In aqueous solution, DR6 self-assembles into the typical micellar structure expected for macromolecular amphiphiles (Figure 208, right). Subsequently, a study of the behavior of LB films of DR6 molecule on a solid substrate was performed.[757] Compression forces at the surface disrupted micelle formation and resulted in ribbonlike monolayers that were shown to collapse into unprecedented planar circular surface structures.

Dendronization of smaller rod subunits was also investigated. Phenylazo, naphthylimide azo, and phthalimide azo compounds was functionalized with PAMAM dendrons.[764] Azobenzene derivatives dendronized with poly(Gly-Asp) (Figure 209, top left) form photoreversible gels. CD/UV−vis experiments suggest chirality transfer indicative of supramolecular organization.[765] PAMAM dendronized carbazole (Figure 209, bottom), self-assembles into tubular and vesicular structures (Figure 209, right) (also see section 7.6).[766] XRD of the tubular structures suggested lamellar organization.

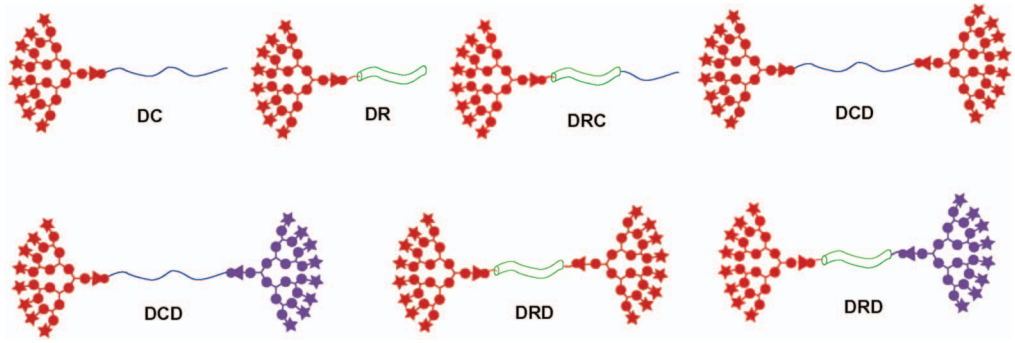

Figure 198. Topologies generated by polymers dendronized at their chain ends: dendron−rod (DR), dendron−coil (DC), dendron−rod−coil (DRC), symmetric or Janus dendron−coil−dendron (DCD), and symmetric or Janus dendron−rod−dendron (DRD).

Scheme 50. Synthesis of Linear Polymers Dendronized at Both Chains Ends Through Grafting-onto Strategies Involving Quenching of Living Chain Ends (Top)[708,709] or Post-Polymerization Modification (Bottom)[710−712]

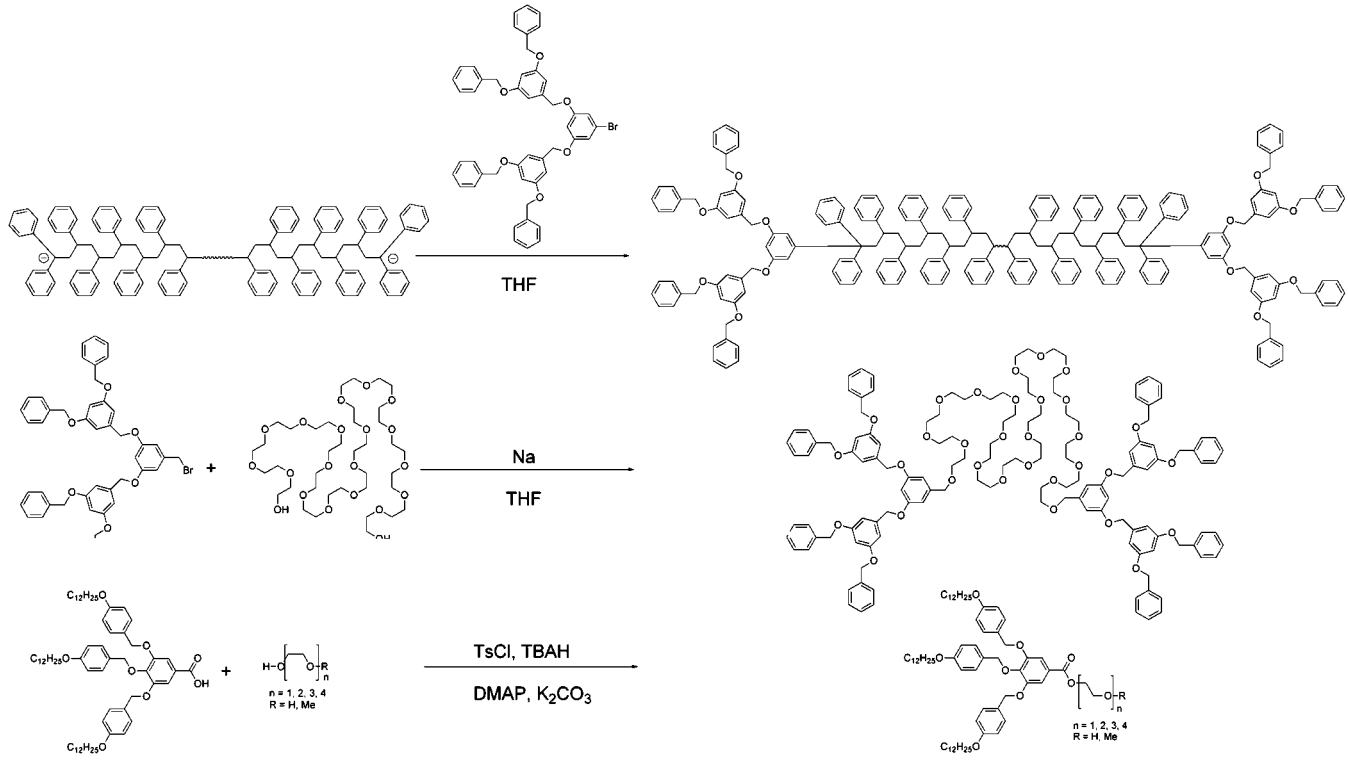

Kim reported another dendronized azobenzene that self-assembles into vesicular structures that can be photochemically triggered for release of guests (Figure 210).[767] Through self-assembly, these DRs can encapsulate calcein in the interior of the vesicle or Nile Red in the vesicular bilayer. Photocleavage of the azobenzene releases the guest from the interior or the bilayer. As will be discussed in a later chapter (section 11.3), Möller examined DRs containing sulfonate salt end groups on the azobenzene rod section.[768]

Recently, Yagai reported a DR composed of (3,4,5)12G1 dendron attached to an oligo(phenylene vinylene) (OPV) rod containing a barbituric acid H-bonding head-group (Figure 211).[769] Upon drop-casting or spin-coating from methylcyclohexane, a variety of morphologies was observed including closed nanorings, columnar nanocoils, and open-ended fibers. Upon heating the DR to 250 °C, a Φ_{r-c} phase was observed, which suggests a hexameric discotic assembly via H-bonding of the barbituric acid head-groups. It is proposed that, in solution, the hexameric species are dominant and behave as stacked nanorods. At low concentrations, the nanorods are short, leading to end-to-end interactions and thereby forming

Scheme 51. Divergent Strategies for the Synthesis of Linear Polymers Dendronized at One Chain End with L-Lysine Dendrons[713] (Left) and PAMAM Dendrons (Right)

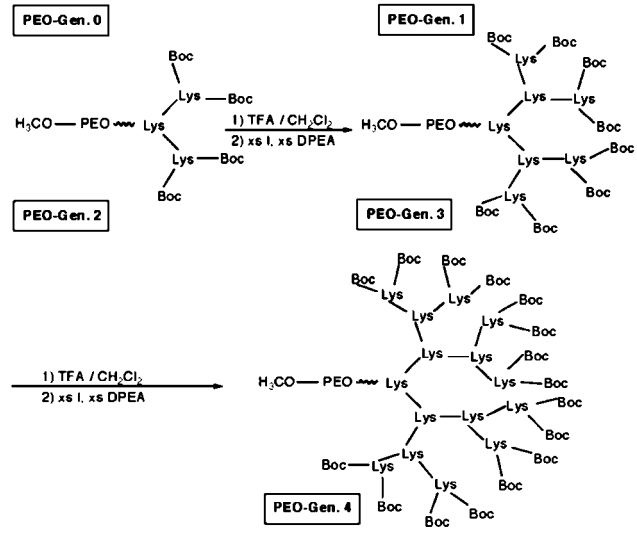

Scheme 52. Divergent Synthesis of PAMAM Dendrons from PEO[714−716]

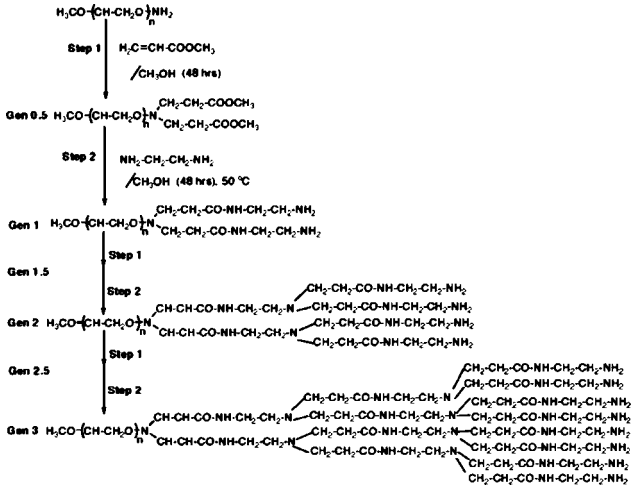

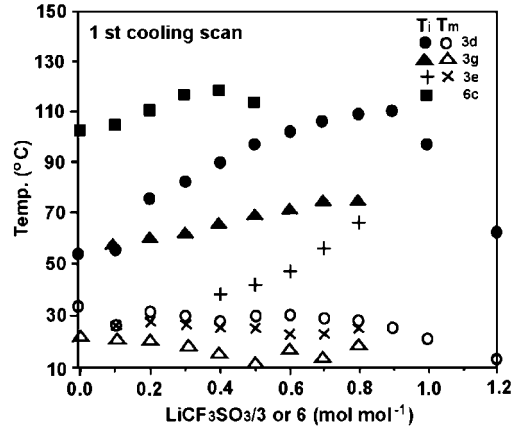

Figure 199. Effect of increasing LiOTf on the $T_{\Phi h\text{-}I}$ and T_m of (4-3,4,5)12G1−4EO (3d), (4-3,4,5)12G1−4EO−Me (3e), and poly[(4-3,4,5)12G1−4EO−MA]. Reprinted with permission from ref 208. Copyright 1993 Royal Society of Chemistry.

Scheme 53. ROP Polymerization of ε-Caprolactone Initiated with G4 Fréchet Dendron

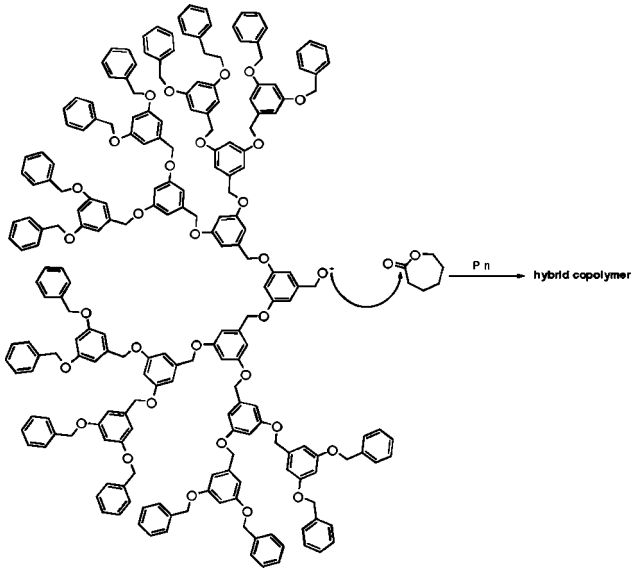

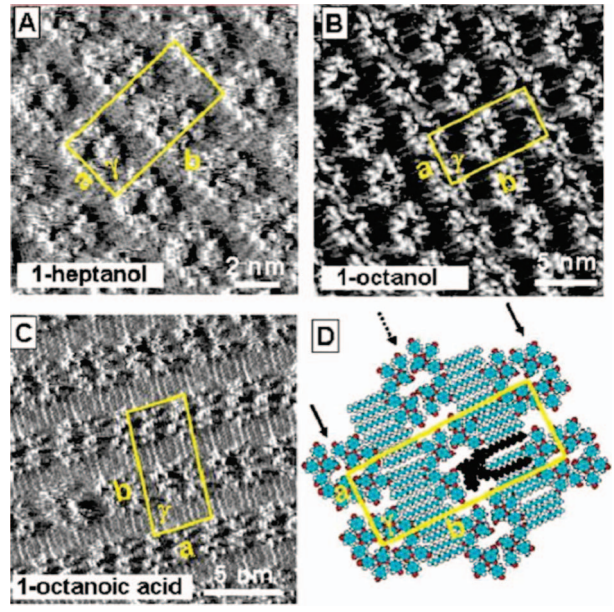

Figure 200. Solvent-dependent surface deposition of (4-3,4,5)12G1−2EO. Reprinted with permission from ref 744. Copyright 2006 American Chemical Society.

Scheme 54. Dendritic Macroinitiator Approach to PS Dendronized at One Chain End[718]

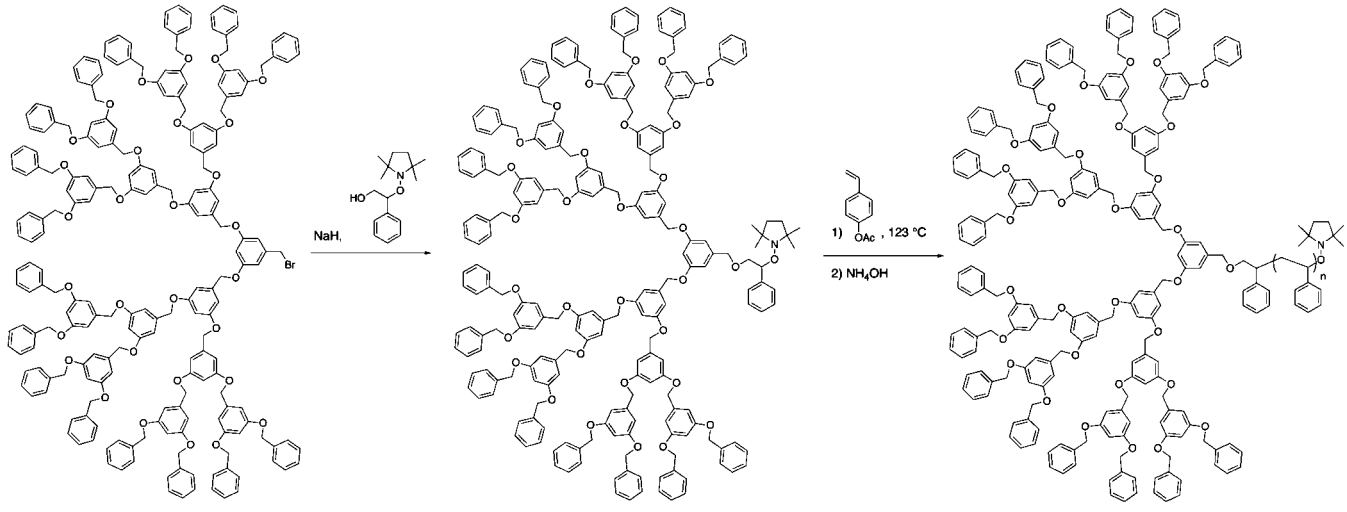

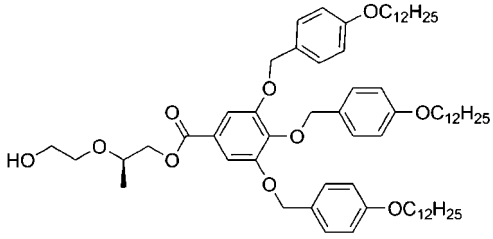

(R)-(4-3,4,5)12G$_1$-DEG*

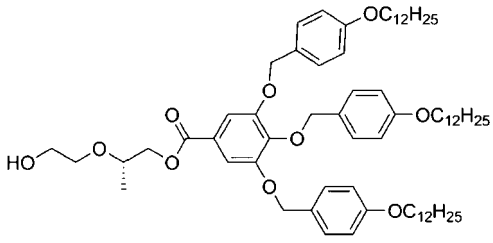

(S)-(4-3,4,5)12G$_1$-DEG*

Figure 201. Structures of chiral (4-3,4,5)12G1−2EO* used in surface studies.

closed nanorings. These rings can deform into coils or elongated fibers composed of DR dimers or tetramers.

Comb-polymers are often far less flexible than their linear backbones alone, resulting in rodlike behavior. Hammond reported a comblike poly(γ-*n*-dodecyl glutamate) modified at one chain end with dendritic PEG (Figure 212).[728] This macromolecular amphiphile was found to self-assemble into spherical micelles with the hydrophobic linear comb-polymer in the inner core and the dendritic PEG at the periphery. An unusually low CMC, even for polymeric amphiphiles, of 10^{-8} M and a 30.4 ± 1.2% (w/w% drug/polymer) loading capacity was observed.[728] Reduction of the size of the dendritic headgroup via removal of the PEO chains resulted in self-assembly into bilayer vesicular architecture (Figure 213).[770] Hammond also reported a biocompatible double-hydrophilic chain-end dendronized linear polymer composed of a linear poly(2-(2′-methoxyethoxy)ethyl methacrylate) (PEO2MA) main chain and a bis(MPA)-dendritic headgroup (Scheme 59).[737] Because of the oligo(ethylene oxide) side groups on the main chain, the chain-end dendronized polymer exhibited thermoresponsive properties, self-assembling into micelles only upon heating above the 50 °C LCST. The micelles were found to disrupt on cooling and regenerate on heating, making them suitable for active targeting in biological applications.

4.1.3. Block-Copolymers Containing Rigid and Flexible Segments Dendronized at One Chain End. Dendron−Rod−Coil (DRC) and Wedge−Coil

Copolymers composed of a rigid and a flexible block often self-organize due to their asymmetry. Introduction of a dendron at one chain end can further desymmetrize the structure and provide unique architectural morphology. The rigid segment can also spatially isolate the dendritic structure from the flexible segment, preventing its penetration into high-generation dendrons.[771] The flexible segment is essential for increasing the solubility of the chain-end dendronized block-copolymers as well as for facilitating mixing with linear polymer matrices.

Scheme 55. PS Dendronized at One Chain End with PPI and Its Self-Assembly in Aqueous Media into Wormlike Aggregates (Reprinted with Permission from Ref 721; Copyright 1995 American Chemical Society)

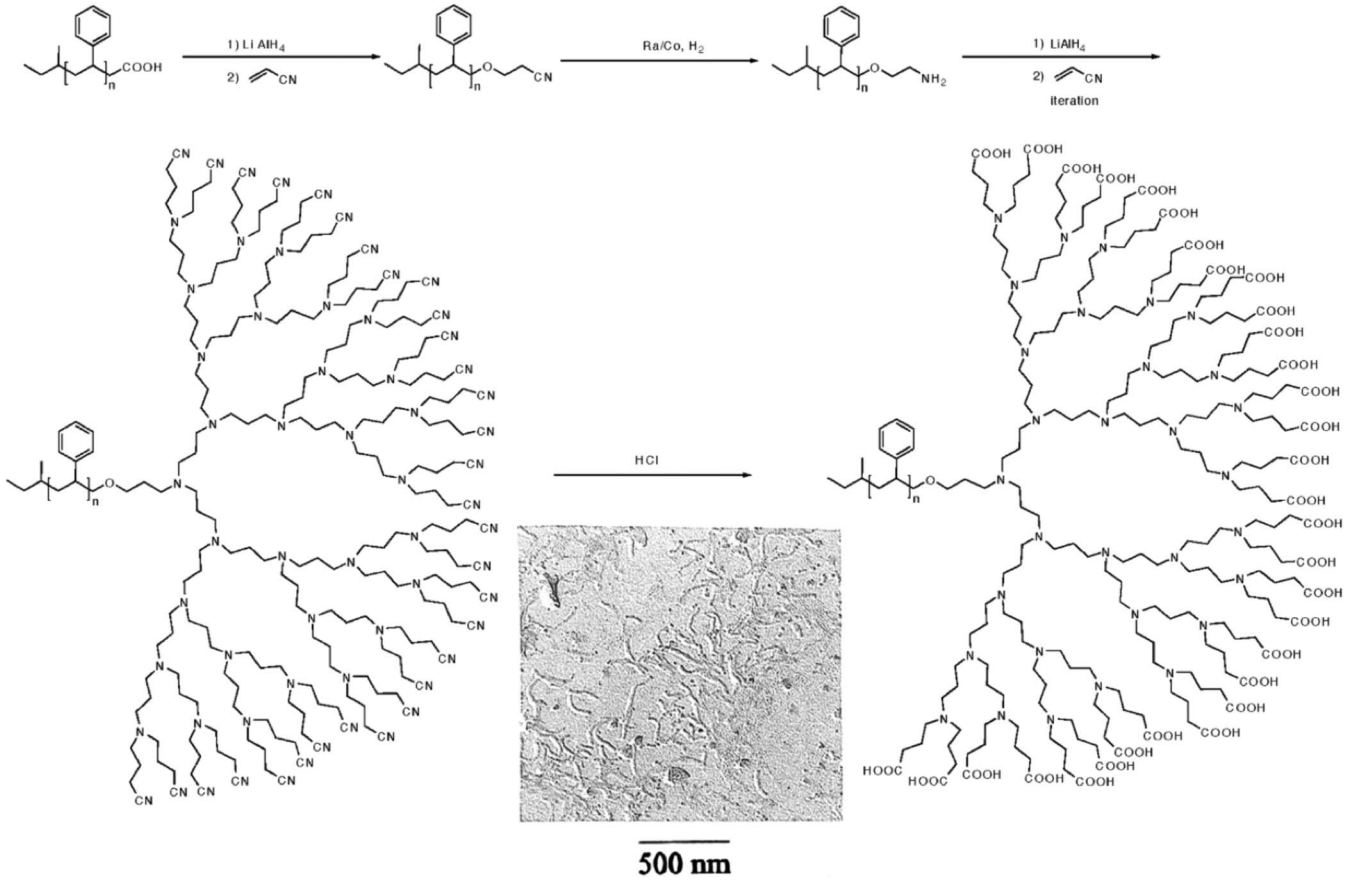

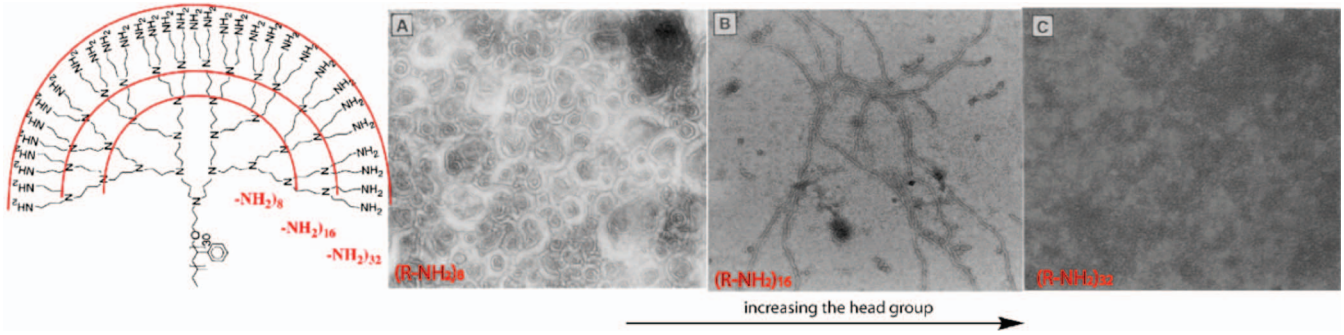

Figure 202. Structure and TEM images of the aggregates formed by PPI chain-end dendronized PS in water. Reprinted with permission from ref 722. Copyright 1995 American Association for the Advancement of Science.

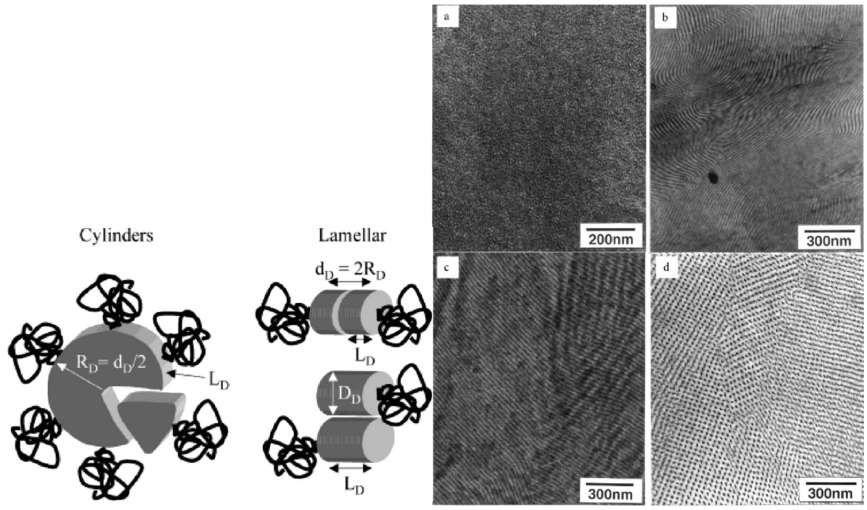

Figure 203. Model (left) and TEM (right) demonstrating the lamellar (b) and Φ_h (c and d) organization of PS dendronized at one end with G6-Fréchet-type dendron. Reprinted with permission from ref 725. Copyright 2002 American Chemical Society.

The first dendron−rod−coil (Figure 1, fourth row left, Figure 198, first row second from right), though not named as such, was reported by Malthête in 1986 (Figure 214).[194] This prototype DRC, a (4-3,4,5)12G1 dendron, was connected to a rodlike biphenyl unit, which in turn was connected to an aliphatic tail, and self-organizes into an N phase. Beyond breaking ground in dendron-linear hybrid structures, the existence of an enantiotropic biaxial N phase, N_b, was first advanced.

As discussed previously (section 2.2.1), inspired by the molecules of Malthête, Percec reported the synthesis and structural analysis of similar polymerizable dendrons (Figure 215).[195] Despite the structure similarities to Malthête's molecules, the polymerizable DRCs with a biphenyl rod-unit self-assemble into columnar architectures that self-organize into lamello-columnar Φ_{ob} lattices, while the naphthyl-containing DRC does not exhibit a LC phase. Additional related molecules are summarized in Figure 8.

Zeng reported the synthesis of a similar DRC to those of Malthête and Percec.[772] This DRC, composed of a (3,5)12G1 dendron attached to aryl ester/imine rod, terminated in a single alkyl tail, self-organizes into the first triply bicontinuous cubic lattice with $Ia\bar{3}m$ symmetry (Figure 216).

In 2001, Stupp reported chain-end dendronized rigid/flexible block copolymers and named them dendron rod−coils (DRCs).[773] The first DRCs prepared contained an oligo(isoprene) segment connected to an oligo(biphenyl) ester segment, which was capped with a variety of aryl-ester dendrons (Figure 217). Some DRC molecules where at least one −OH group was present on the benzyl ester formed gels in CH_2Cl_2 solution. TEM and AFM of gels, for example, those formed by DRC1 (Figure 217), indicated the formation of well-defined 1-D supramolecular objects with ribbonlike morphology (~10 nm wide, 1.5 nm thick, and several μm long). XRD with a synchrotron source showed no diffraction peaks, indicating limited aggregation or structural coherence. A model structure was synthesized containing the same dendritic unit as DRC1 but attached to only one biphenyl unit and no flexible isoprene unit (Figure 218). The crystal structure of the model molecule (Figure 218, bottom right) revealed nanoribbons containing tetrameric cycles stitched together along the axis of the ribbon by 8 hydrogen bonds. This hydrogen-bonded model was also suggested for the self-organization of DRC1 and related structures in CH_2Cl_2 solution (Figure 218, bottom).

DLS and SLS were used to analyze the self-assembly process of DRC1 in various solvents.[774] In 2-propanol, aggregation into rodlike structures occurred on a time scale of several minutes, while in ethyl acetate, aggregation proceeds more slowly. DRC1 is an effective organogelator mediating the formation of thermally irreversible gels in 15 other nonpolar solvents (CH_2Cl_2, CH_2Br_2, CH_2I_2, chloroform, bromoform, benzene, chlorobenzene, 1,3-dichlorobenzene, methanol, toluene, styrene, α-methylstyrene, ethyl meth-

Scheme 56. Synthesis of Dendronized PNIPAM-*b*-Py by RAFT[749]

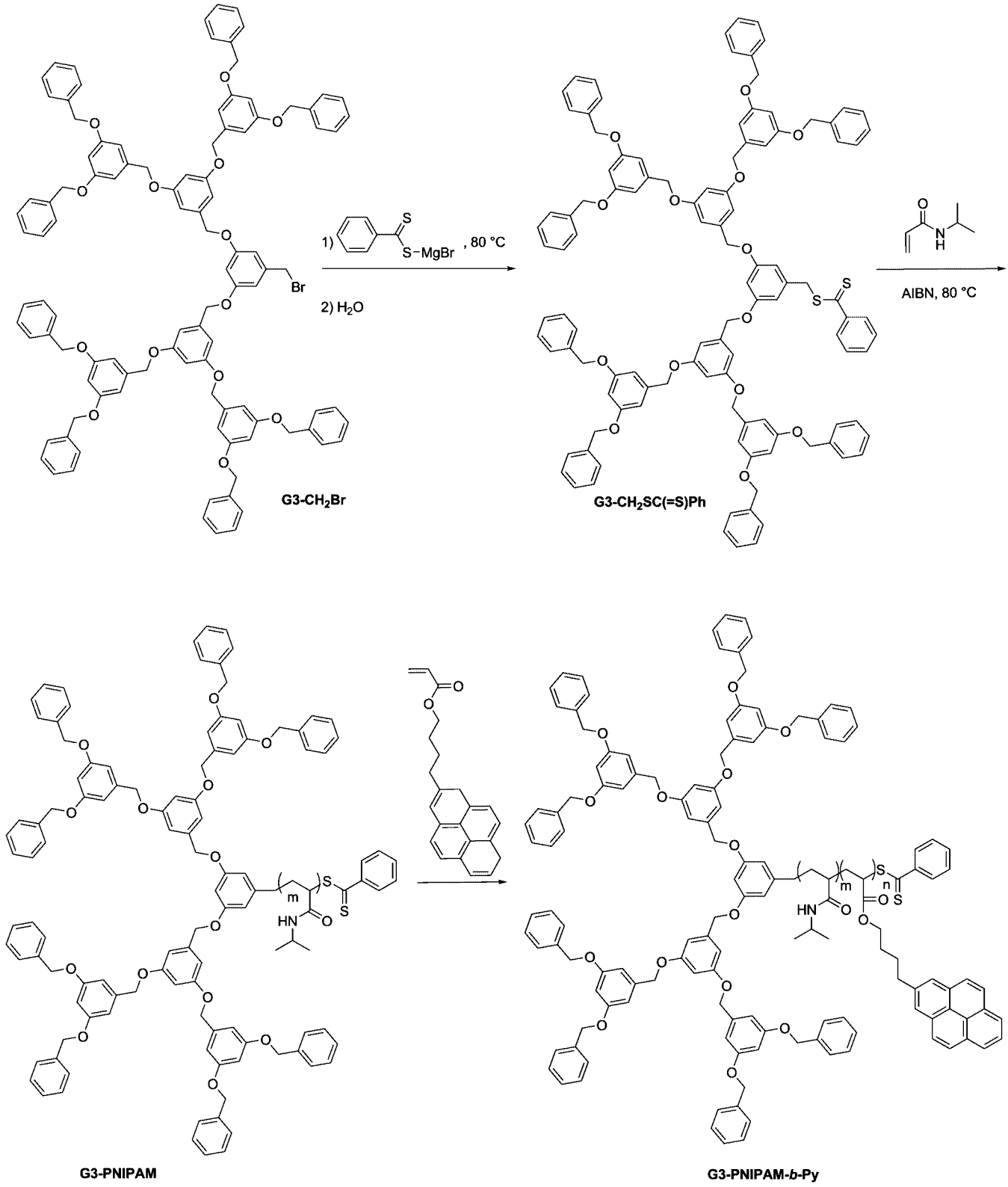

acrylate, 2-ethylhexyl methacrylate, hexyl methacrylate) at as little as 0.2% loading (w/w% DRC1/solvent).[775] Gelation is mediated by the formation of fibrous structures typically resembling flat nanoribbons, though in ethyl methacrylate (EMA) and 2-ethylhexyl methacrylate (EHMA) a helical-twist in the nanoribbons was observed. NMR experiments showed that both the solvent type as well as the structure of the DRC molecule affects nanoribbon formation and gelation. Strong interactions between dendritic and rodlike components result in their aggregation, while the flexible domain remains solvated after gelation.[775] Cooperative H-bonding and $\pi-\pi$ interactions as well as microphase segregation of the amphiphile are expected to strengthen the formation of the self-assembled structure in solution. Systematic modification of

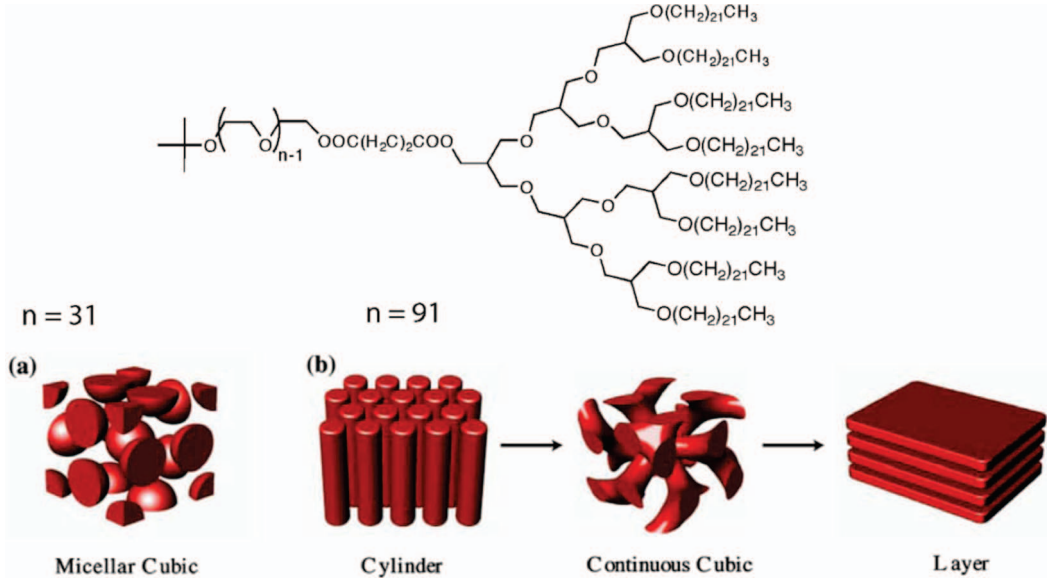

Figure 204. Self-assembly PEO with a single dendritic PEG chain end in bulk state. Reprinted with permission from ref 734. Copyright 2004 American Association for the Advancement of Science.

Scheme 57. Synthesis (Left) and Aqueous-Phase Self-Assembly (Right) of PEO Dendronized at Its Chain End via Click Chemistry (Reprinted with Permission from Ref 751; Copyright 2009 American Chemical Society)

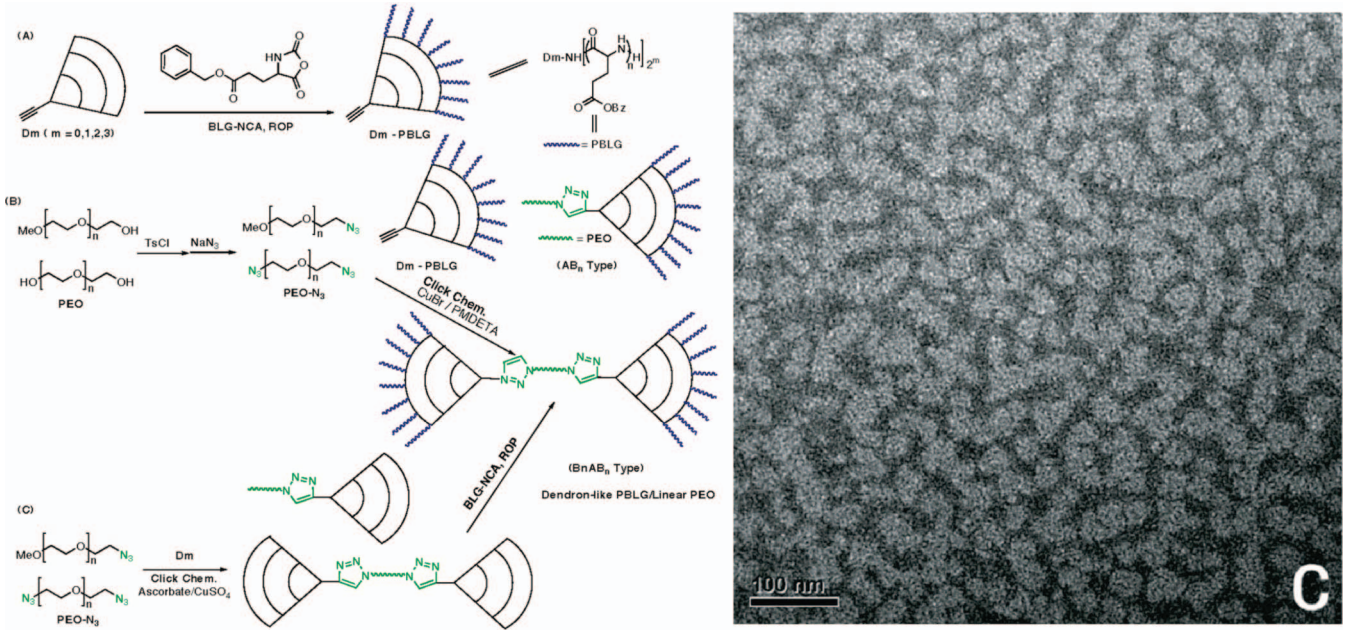

each segment of the DRC1 structure such as the number of HO− groups in the dendron, the number of biphenyl units in the rod unit, and different coil segments (variation of DP and degree of branching) revealed important structural requirements for the formation of the nanoribbons. As demonstrated previously,[773] at least 4 HO− groups per dendron were required for the formation of the H-bonded network. DRCs with no HO− groups gave isotropic solutions, while those with 2 HO− groups precipitated. XRD demonstrated the importance of the HO− groups in generating crystalline order inside the ribbon; a higher number of HO− groups induced more H-bond interactions in model compounds. The generation number of the dendron also influences the geometry of the DRC assemblies. Bulky higher-generation dendrons sterically inhibit self-assembly. TEM analysis of higher-generation dendrons (G2−G4) revealed only isolated aggregates.[83] The rodlike oligo(biphenyl ester) segment is essential as it stabilizes the assemblies via $\pi-\pi$ interactions. At least two biphenyl esters in the rodlike segment are needed to produce a weak gel. Further extension of rodlike segment to include 3−4 biphenyls induced self-assembly into purple birefringent self-supporting gels.

Stupp has also studied the ability of DRCs to template the self-assembly of other structures even when used in very small quantities.[776−779] Small amounts of DRC1 can induce the formation of gels in certain monomers such as styrene via the formation of nanoribbon architectures.[776] Polymerization of the soft-styrene gel produced a hard-ordered material with birefringent texture. The templating effect was

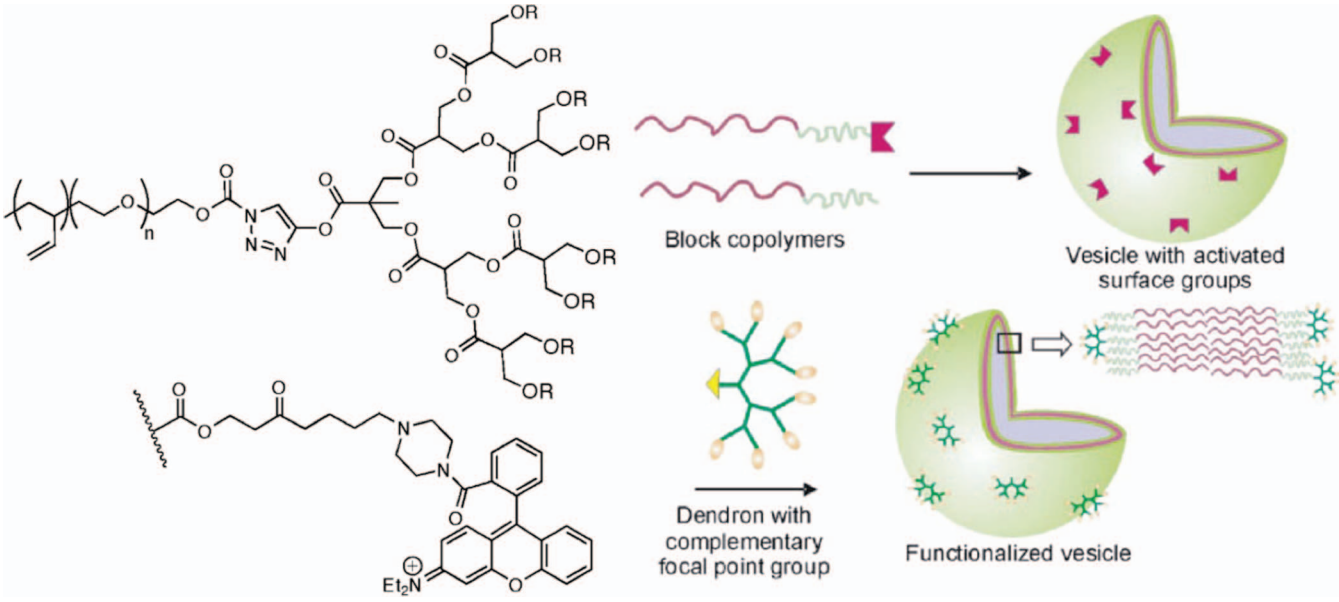

Figure 205. PBD-*b*-PEO dendronized with dye-bearing dendrons. Reprinted with permission from ref 756. Copyright 2007 Royal Society of Chemistry.

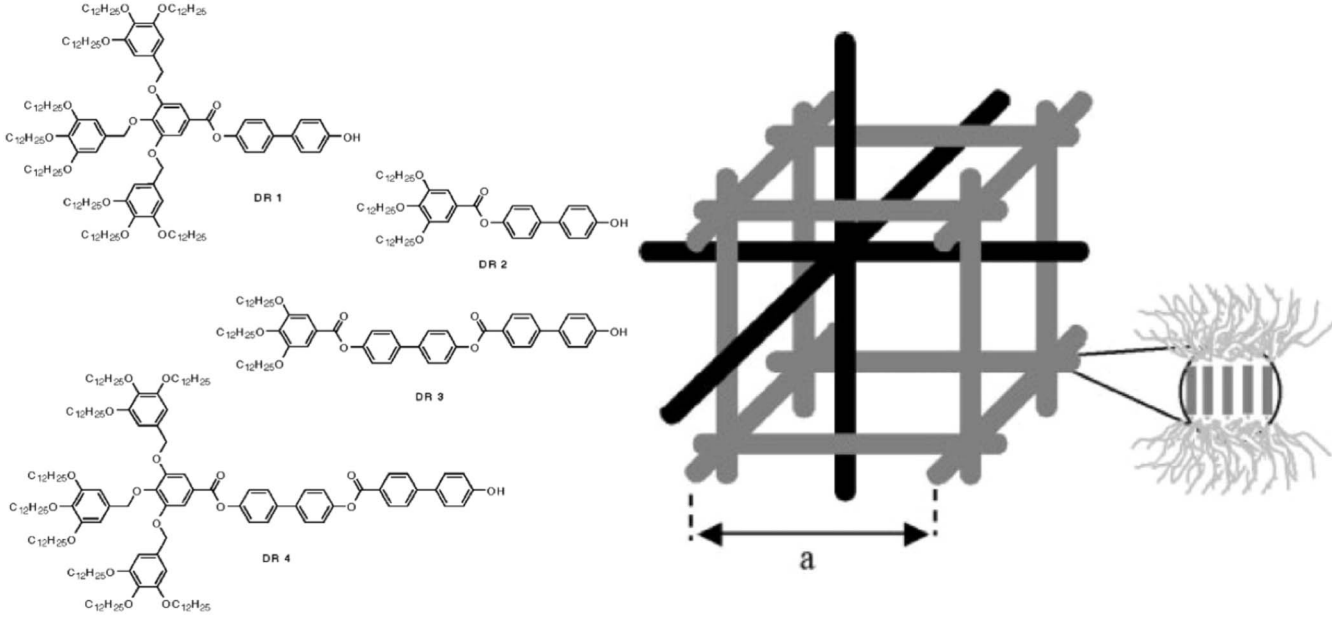

Figure 206. Structure of biphenyl-containing oligomers functionalized at one chain end with Percec-type dendrons and their self-organization into a bicontinuous cubic phase. Reprinted with permission from ref 761. Copyright 2003 John Wiley & Sons, Inc.

extended to the nanoscale morphological control of inorganic materials.[777,778] Free HO− groups in the DRC1 nanoribbon likely bind inorganic nanocrystalites such as CdS, ZnO, or TiO_2.[777] The twisted helical ribbons formed by DRC1 act as directing mediators for the formation of either a single helix, if the nucleation and growth is on one face, or a double-stranded coiled helix, if it is on both faces (Figure 219).[779] It was hypothesized that the formation of single versus double helical architectures is determined by the perfection of the twisted ribbons, which is further dependent on aging and conditions of gel formation. In a perfect twisted structure, both faces of the ribbon should be equivalent and, as a consequence, nucleation and growth occur on both sides, producing a double-helical architecture. Slightly coiled ribbons provide an increased exposure to the solvent on one face as compared to the other, creating the conditions for one-helix formation.

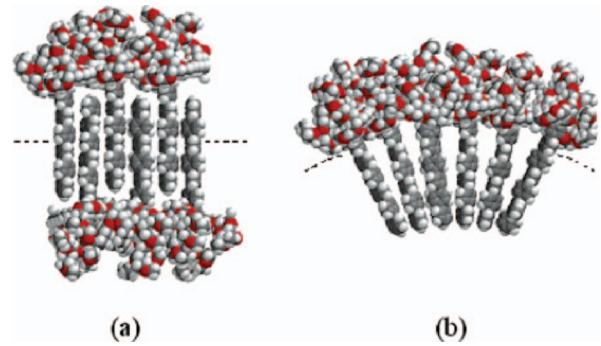

Figure 207. Competition between lamellar stacking (a) and spherical assembly (b) induced by dendron curvature. Reprinted with permission from ref 757. Copyright 2004 American Chemical Society.

Scheme 58. Dendron−Rod Structure Containing Amphiphilic Poly(ethylene oxide) Dendrons Attached to an Oligophenylene Rod[757]

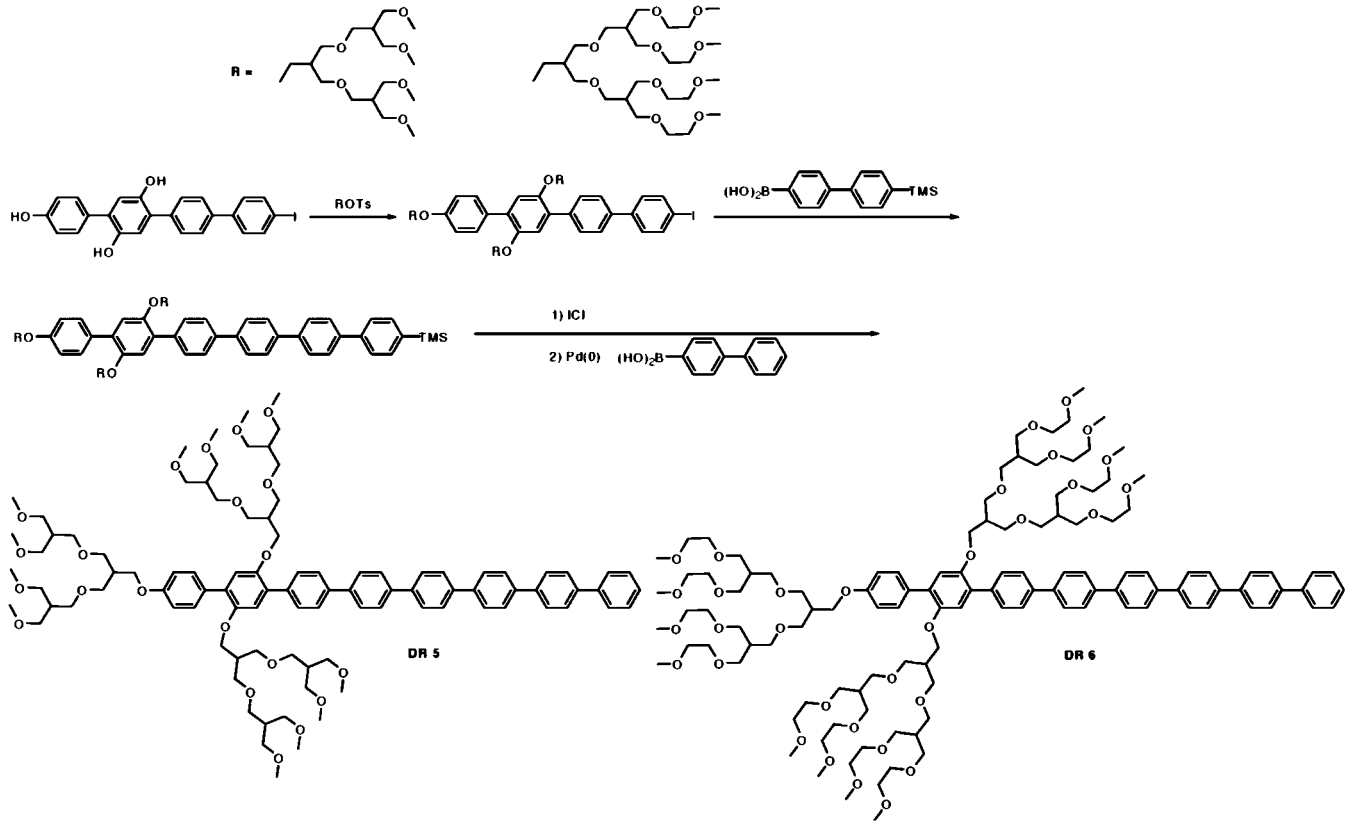

Replacement of the achiral oligo(isoprene) segment with a shorter chiral d*m*8 subunit resulted in the formation of helical nanoribbons. Helicity was confirmed by TEM and CD/UV−vis studies (Figure 220).[780] CD spectra of self-assembled *R*- and *S*-DRC showed mirror-image Cotton effects in the region of absorbance of biphenyl units as a result of the exciton coupling of the chromophore. The self-assembly process was found to be solvent-dependent, with helical ribbons being formed in acetonitrile while gelation did not occur in THF. The steric constraints imposed by chiral centers in the coil segment were believed to be responsible for the helical supramolecular assembly. Interestingly, similar helical nanoribbons could be derived from chiral branched peptide-containing structures (Figure 221).[781−783]

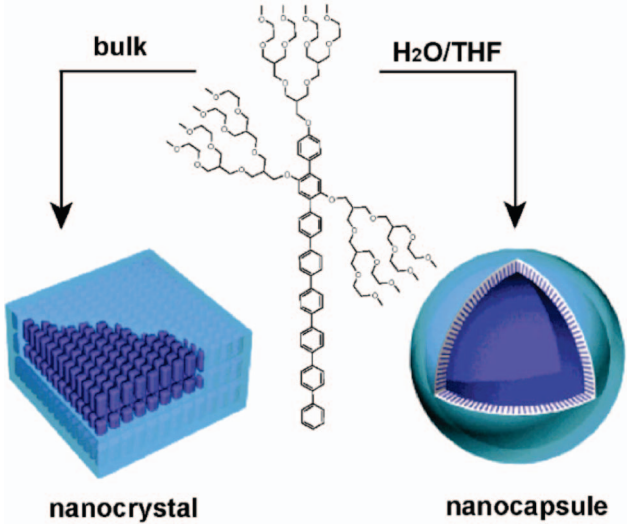

Figure 208. Self-assembled structures of DR6 molecules in bulk (left) and aqueous solution (right). Reprinted with permission from ref 757. Copyright 2004 American Chemical Society.

In addition to oligo(biphenyl esters), Stupp has investigated other rigid polymers in the rodlike segment including oligo(phenylene vinylene),[784] oligo(*p*-phenylene),[784,785] and oligo(thiophene) (Figure 222).[784] While oligo(biphenyl ester) has an interrupted electronic structure, oligo(phenylene vinylene) and oligo(thiophene) are fully conjugated structures and can be incorporated into a DRC molecule without disrupting their one-dimensional self-assembly into nanoribbons. These conjugated DRCs form conductive nanoribbons in solution. DRCs with an oligo(thiophene) rodlike segment (4T-DRC, Figure 222) exhibit a 3-order-of-magnitude increase in conductivity in the nanoribbon state (7.9×10^{-5} S/cm) as compared to the unassembled structure (8×10^{-8} S/cm). These conducting supramolecular polymers can be oriented macroscopically in external fields, providing uniaxially aligned films for electronic devices.[784]

Bardeen and Thayumanavan have designed dendrimers, rod−coils, DRs, and DRCs composed of (diarylamino)pyrene functionalized with Fréchet dendrons, benzthiadiazole rods, and polymethacrylate coils with naphthalene bisimide side chains for electron transfer (ET) applications (Figure 223, left).[786] In the absence of the coil, benzothiadiazole rods act as electron acceptors for photoinduced ET from the (diarylamino)pyrene periphery. In the full DRC molecule, the benzothiadazole rod acts as a sensitizer, transferring charge to the naphthalene bisimide side chains of the coil. The excited state is quenched via ET from the (diarylamino)py-

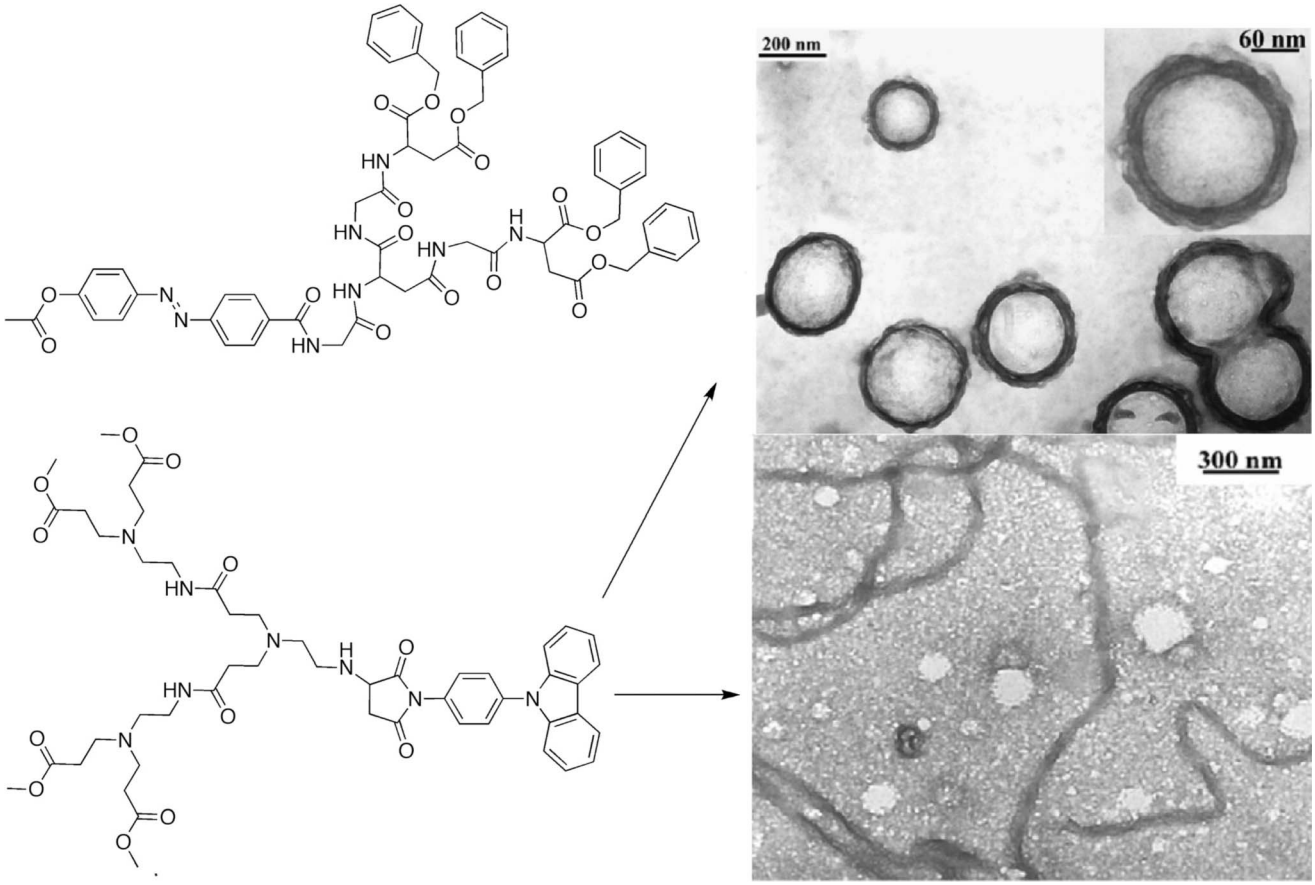

Figure 209. Dendronized azobenzene and carbazole. Reprinted with permission from ref 766. Copyright 2007 Elsevier.

rene periphery. The DRC exhibits greater charge-transfer efficiency than the truncated structures (Figure 223, right). It is not clear whether self-assembly or self-organization of the DRC contributes to its enhanced ET properties. Further, the comblike nature of the polymethacrylate imparts some rigidity, and thus, the self-assembly and self-organization, if occurring, may follow a mechanism more similar to DRs than DRCs.

As discussed in the previous chapter, perylene bisimides (PBI)s dendronized at one end and functionalized with a polymerizable aliphatic group at the other end have been prepared (section 3.2.2).[482] Here, self-assembly of the DRC-like dendritic macromonomer forms a micellar architecture, while coassembly of the DRC with bisdendronized PBIs results in much larger vesicular structures. Other water-soluble DRC and DRD dendronized PBIs were used to solubilize single-wall carbon nanotubes (SWCNT).[787] Recently, Guldi was able to characterize the metastable radical ion-pair states induced by the complexation of similar DRD dendronized PBIs to single-wall carbon nanotubes.[788]

Lee and co-workers investigated another set of DRC molecules that incorporates a rigid wedge and a flexible coil and named them wedge−coil molecules.[789] The wedge segment contains both Percec-type dendrons and a short oligo(*p*-phenylene) rigid-rod attached to a flexible (PEO) segment (Figure 224). TOPM, DSC, and XRD identified various LC phases dependent on the DP of PEO and the resulting modulation of microphase segregation and molecular shape. BCC lattices were observed at DP = 12, while *Cub* lattices were observed at DP =17. Further increases of the PEO length resulted in Φ_h symmetry at DP = 21, a perforated lamellar hexagonal at DP = 34, and S_A lamellar architecture at DP = 45 (Figure 224).[789]

Wedge−coil molecules form cylindrical nanofibers in both water and *n*-hexane. Moving from aqueous to *n*-hexanes solutions results in a conformational change from highly flexible coil-like character to stiff rodlike character.[785,790,791] In water, the core of the hexagonal micelles was occupied by the hydrophobic dendritic wedge. Steric effects frustrate the crystallization process and prevent dense packing inside the micelle, providing flexible cylindrical nanofibers. In *n*-hexanes, the PEO occupies the center of the micelle, thereby reducing steric frustration to crystallization providing rigid morphology. Wide-angle XRD showed sharp reflections indicating chain crystallization in nanofibers formed in *n*-hexanes. Increasing the chain length of the hydrophilic PEO causes a transition from long fibers to short fibers and ultimately to spherical micelles. Addition of an aromatic guest, Nile Red, to the cylindrical nanofibers induces a structural change to a flat ribbon architecture.[791] Nile Red serves as "molecular glue", intercalating between the aromatic wedges (Figure 225).

Replacement of the (3,4,5)14G1 Percec dendrons with dendritic PEG with oligo(ethylene oxide) (Scheme 60)[792] or glycosylated[793] tails groups and substitution of the PEO coil with a paraffin tail provided wedge−coil structures with inverted amphiphilic properties.

The glycosylated wedge−coil structure without an alkyl tail was found to self-organize in bulk into a Φ_h phase, but when a $-C_{22}H_{45}$ tail was attached, an S phase was ob-

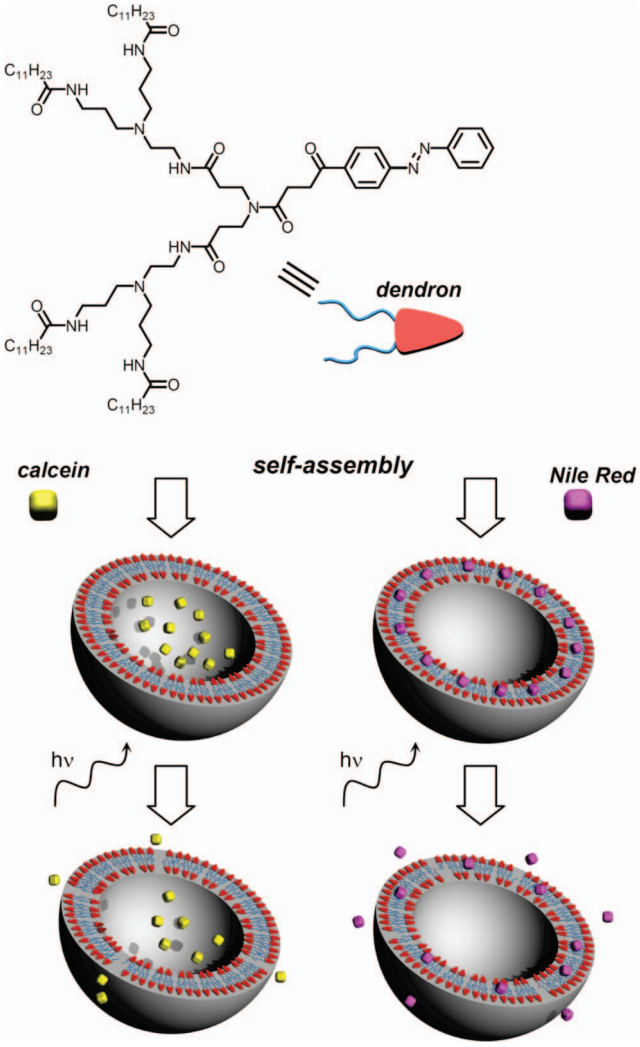

Figure 210. Structure of PAMAM-dendronized azobenzene (left), self-assembly, and photocontrolled encapsulation of guests molecules (right). Adapted from ref 767.

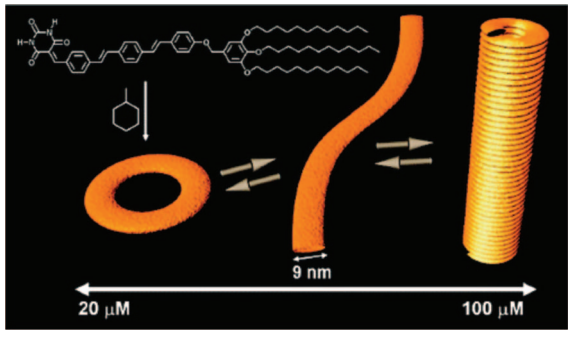

Figure 211. DR composed of (3,4,5)12G1 dendron, OPV rod, and barbituric acid head-group and its self-assembly into nanorings, nanofibers, and nanocoils. Reprinted with permission from ref 769. Copyright 2009 American Chemical Society.

served.[793] In aqueous solution, the glycosylated wedge−coil molecule self-assembled into well-defined nanofibers with a uniform diameter that could be reversibly transformed into spherical micelles upon addition of Nile Red "molecular glue". These stimuli-responsive nanofibers have potential biomedical applications.[793] The wedge−coil structure containing oligo(ethylene oxide) periphery groups was found to encapsulate hydrophobic guest molecules ($CHCl_3$ or Nile red) in aqueous media.[792] Increasing $CHCl_3$ content resulted in an increase of the nanocapsule diameter. It was suggested that strong interactions between the guest molecule and the flexible hydrophobic segment of the wedge−coil molecule and the otherwise poor solubility of the guest molecule in water facilitate the entrapment of the guest molecules inside the micelle. In bulk, self-assembled Φ_h architectures were observed for wedge−coils with small dendritic segments (rodlike molecules) and *Cub* phases for wedge−coils with larger dendritic segments (conelike molecules) (Figure 226).[792]

Grafting cholesterol chloroformate onto the surface of dendritic PEO produced a molecule similar structurally to DRCs, wherein the rod is composed of the fused 6,6,6,5-ABCD ring system and the coil is the aliphatic tail (Scheme 61).[794] Dendronized cholesterol self-assembles into micelles capable of solubilizing hydrophobic drugs such as paclitaxel.

4.1.4. Flexible Polymers Dendronized at Both Chain Ends. Dendron−Coil−Dendron (DCD)

The effect of dendronization of flexible polymers at both chain ends (Figure 1, fourth row second and third from left, Figure 198, first row right and second row left) has also been investigated. Flexible polymers bis(dendronized) with Fréchet,[708−710,795,796] PAMAM,[751,797] PLL,[798] citric acid,[799] or triazine[800] dendrons have been explored (Figure 227). In most cases, only the synthesis of the bisdendronized polymers were reported with little information provided about their self-assembly in either bulk or solution.[82,708−710] To the best of our knowledge, no studies relating to the self-assembly or self-organization of asymmetrically substituted DCDs have been reported (Figure 1, fourth row third from left, and Figure 198, second row left).

In 1993, Percec reported the synthesis of tetraethyleneglycol bisdendronized with (4-3,4,5)12G1COOH (Figure 228a).[208] The Percec-type DCD self-assembles into supramolecular columns that self-organize into Φ_h lattices. While this was the first example of a self-organizable DCD, the synthesis of [9]-*n*-[9] arborols, *n*-alkanes bisdendronized at their chain ends with G2 Newkome dendrons, and their reversible gel formation was reported by Newkome in 1986.[801] Later, ethylene glycol and ethylene diamine were bisdendronized with (3,4,5)12G1 and (3,4,5)*n*G1, respectively (Figure 228b).[309] Dendronized bisimides with longer chain alkyl tails were shown to self-organize into Φ_h phases, and a packing model was proposed wherein two bisimides form a single layer that is 90° from the neighboring stratum (Figure 228c).

Later, Kim reported the synthesis of twin alkyl functionalized dendrons connected via a short oligo(amide) linkage similar to PAMAM dendrons (Figure 229, left).[256] Like their monodendron counterparts, these DCDs self-assembled into gels composed of tubular aggregates in aqueous media. XRD suggests lamellar organization within the gel formed by the DCD composed of G1 dendrons (Figure 229D1) and Φ_h organization in the DCD composed of G2 dendrons (Figure 229D2). Later, a DCD with G3 dendron end-groups was prepared and shown to form lamellar vesicles in the gel state but columnar architecture upon cooling from the melt.[802] A model for self-organization into lamellar and columnar phases was proposed (Figure 229, right).

Wiesner reported the synthesis of PEO dendronized at both chain ends with dendritic PEG capped with aliphatic tails

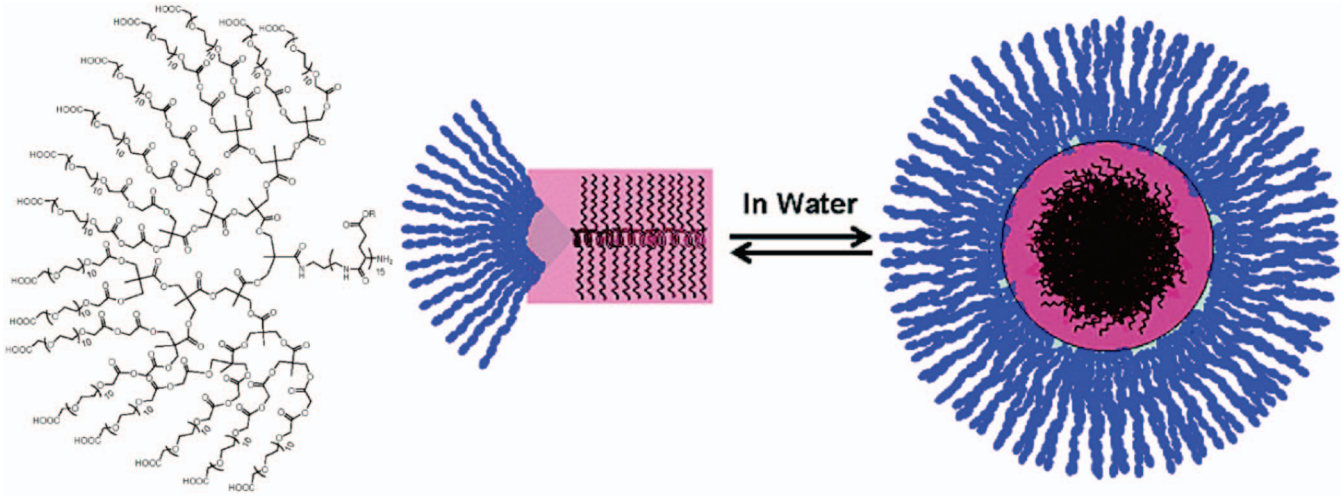

Figure 212. Structure (R = $-C_{12}H_{25}$) and self-assembly in solution of comb-polymer dendronized at one chain end. Reprinted with permission from ref 728. Copyright 2006 American Chemical Society.

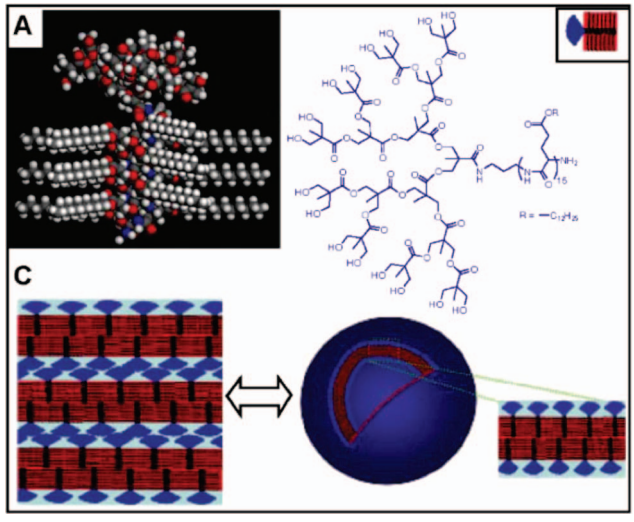

Figure 213. Bilayered vesicle formation by reducing the size of the dendritic headgroup. Reprinted with permission from ref 770. Copyright 2006 Royal Society of Chemistry.

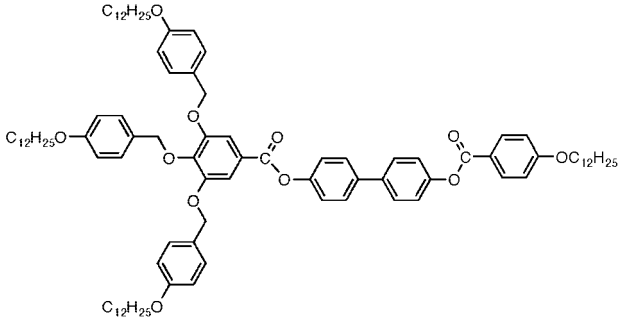

Figure 214. First DRC reported by Malthête.[194]

Scheme 59. Synthetic Route toward the Thermoresponsive Double Hydrophilic Chain-End Dendronized Polymers (a); Schematic Representation of Reversible Formation and Disruption of Micelles (b) (Reprinted with Permission from Ref 737; Copyright 2008 Royal Society of Chemistry)

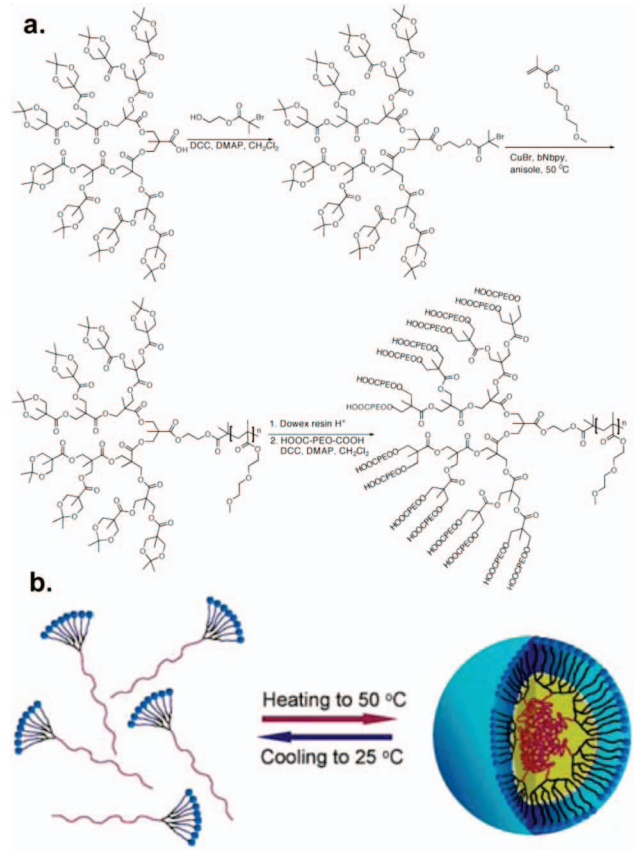

(Scheme 62, Figure 230).[732] PEO with DP = 49 capped at both ends with G2 hydrophobic dendrons resulted in self-assembly into columns that self-organize into Φ_h lattice. Maintaining the hydrophobic-to-hydrophilic ratio *f*, PEO with DP = 98 and capped at both ends with a G3 hydrophobic dendron was prepared. The larger dendronized polymer self-assembles into spheres that self-organize into a *Cub* lattice. It is clear that the volume fraction *f* alone does not dictate self-organized architecture and that the shape of the dendron is perhaps most significant. Similar DCDs where the hydrophobic dendrons were linked to the PEG core via succinic anhydride were reported. Self-organization into 2-D oblique lattices was observed.[803]

4.1.5. Rigid Polymers Symmetrically Dendronized at Both Chain Ends. Dendron−Rod−Dendron (DRD), Dumbbells

Often referred to as molecular dumbbells, rigid polymers (such as polyynes,[805] polythiophenes,[806−809] polyphenylenes,[810−813]

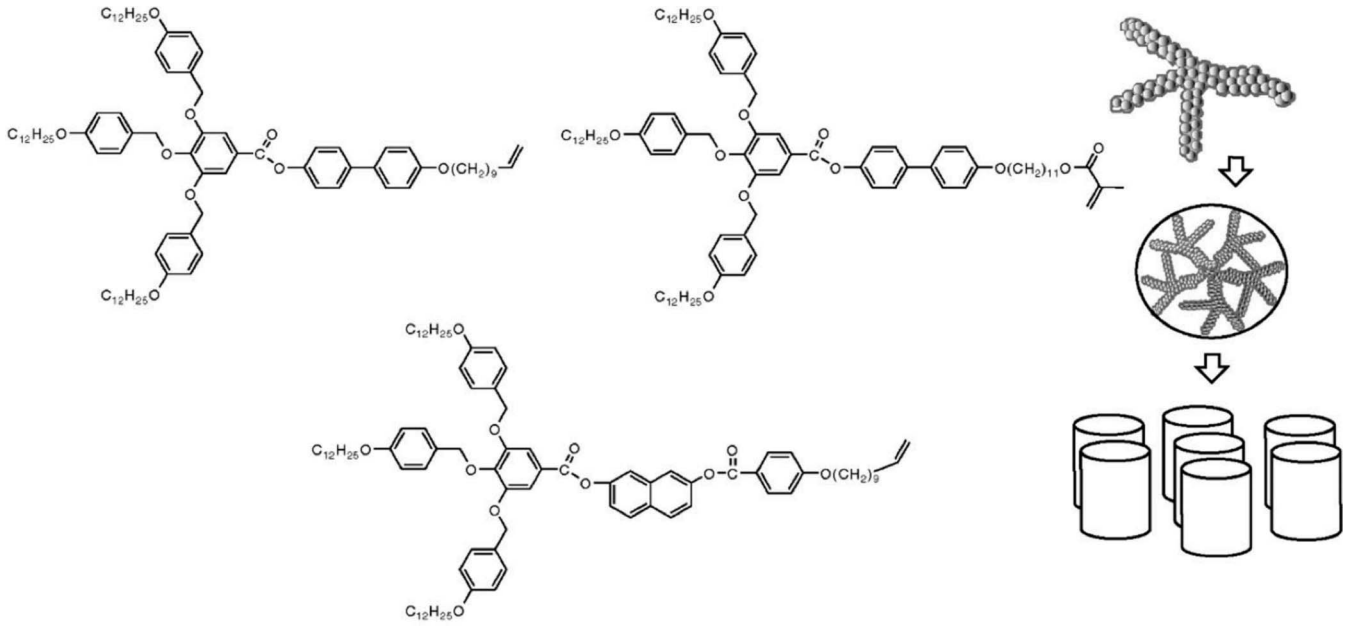

Figure 215. Polymerizable DRCs reported by Percec and their self-assembly in columnar structures. Adapted with permission from ref 205. Copyright 1992 Royal Society of Chemistry.

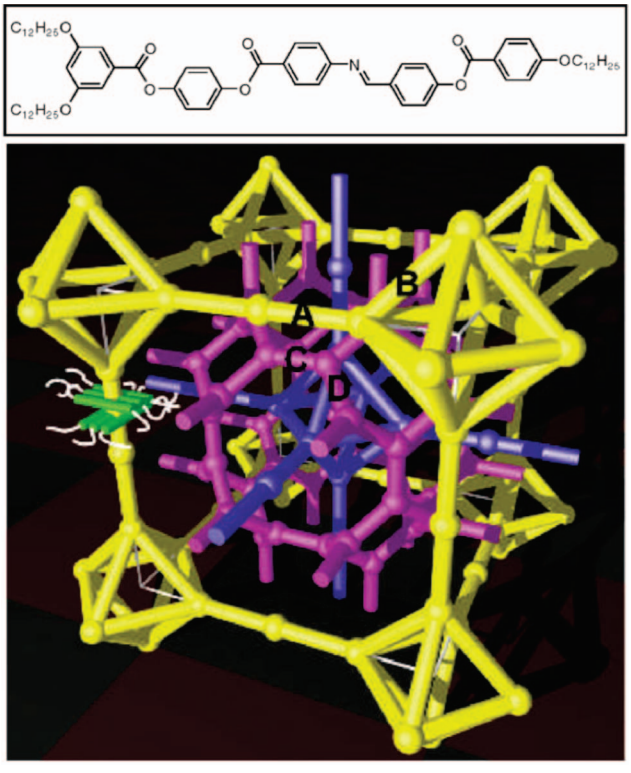

Figure 216. DRC (top) forming a triply continuous $Ia\bar{3}m$ network structure (bottom). Reprinted with permission from ref 772. Copyright 2005 Macmillan Publishers Ltd. (Nature).

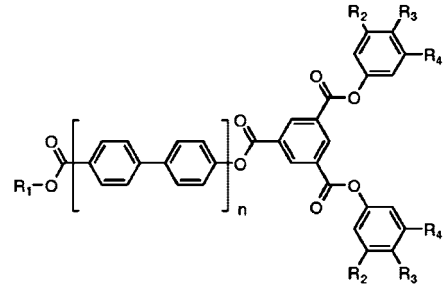

molecules	R_1	n	R_2	R_3	R_4	behavior in CH_2Cl_2
1	PI_9-$(CH_2)_2$-OCO	3	OH	H	OH	gel
2	PI_9-$(CH_2)_2$-OCO	3	H	H	OH	solution
3	PI_9-$(CH_2)_2$-OCO	3	H	H	OH	insoluble material
4	PI_9-$(CH_2)_2$-OCO	3	OH	OH	OH	gel
5	PI_9-$(CH_2)_2$-OCO	1	OH	H	OH	solution
6	PI_9-$(CH_2)_2$-OCO	2	OH	H	OH	weak gel
7	PI_9-$(CH_2)_2$-OCO	4	OH	H	OH	gel
8	PS_9-PB_9-$(CH_2)_2$-OCO	3	OH	H	OH	gel
9	PS_9-PB_9-$(CH_2)_2$-OCO	3	OH	H	OH	solution
10	PS_9-PB_9-$(CH_2)_2$-OCO	3	OH	H	OH	solution
11	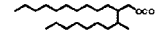	3	OH	H	OH	gel
12	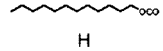	3	OH	H	OH	insoluble material
13	H	3	OH	H	OH	insoluble material
14	H	1	OH	H	OH	solution

Figure 217. Library of DRCs synthesized and their solution self-assembly. Adapted with permission from ref 773. Copyright 2001 American Chemical Society.

poly(phenylsulfones),[814] polymers with mixed polyaromatic segments[815−822] or rigid oligomers connected via donor−acceptor or H-bond interactions)[823] dendronized at both chains ends (Figure 1, fourth row right, fifth row left, and Figure 198, second row middle and right) have well-documented self-assembly and self-organization properties (Figure 231).

Self-organization in both bulk and solution of DRDs is influenced by steric interactions at the interface of the dendritic and rigid-rod segments, which can disrupt the strong $\pi-\pi$ interactions responsible for the self-assembly of the rigid block.[829] The first DRDs were reported by Malthête, wherein (4-3,4,5)12G1 and (3,4,5)12G1 dendrons were attached to oligo(benzylideneaniline) or biphenyl rod-units, respectively (Figure 232).[831,832] The DRD with (3,4,5)12G1 dendritic groups (Figure 232, top) self-organizes into a Φ_{ob} phase below 81.5 °C and Φ_h architecture above 81.5 °C. The DRD with (4-3,4,5)12G1 dendritic groups (Figure 232, bottom) self-organizes exclusively into a Φ_h lattice.

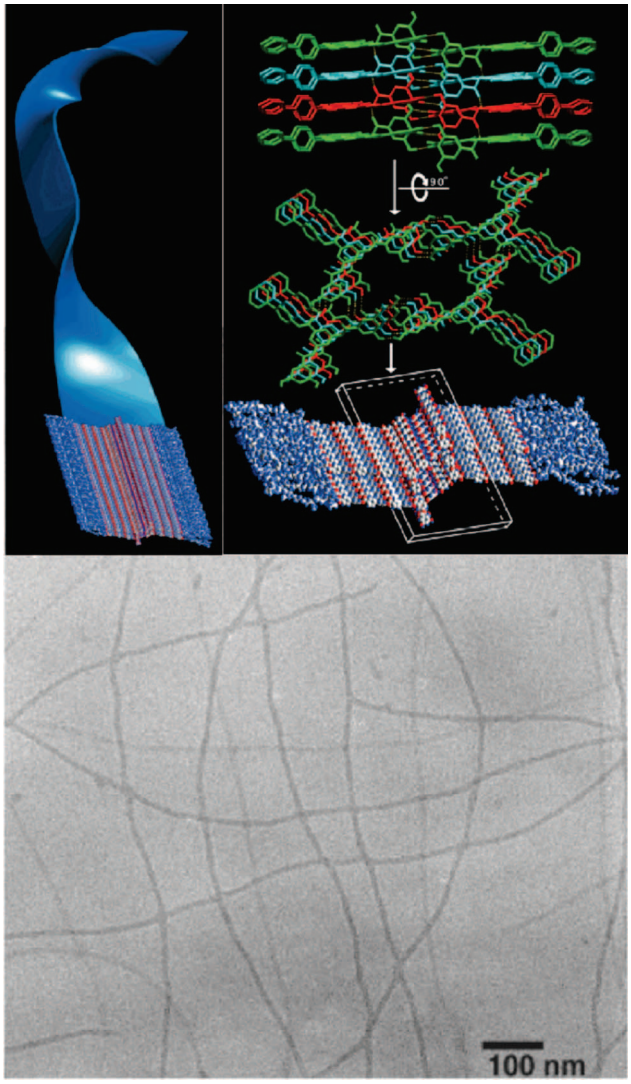

Figure 218. TEM of DRC nanoribbons (bottom), and the model of nanoribbon self-assembly in CH_2Cl_2 (top). Reprinted with permission from ref 773. Copyright 2001 American Chemical Society.

Malthête later reported another class of DRDs, termed diabolo-like molecules due to their resemblance to the children's toy (Figure 233).[833] For both $n = 1$ and $n = 2$, complex columnar mesophases were suggested by TOPM and XRD.

Fréchet reported the synthesis of polythiophene capped at both ends with Fréchet dendrons and its self-assembly in CH_2Cl_2. TEM and UV/vis studies indicated temperature-dependent self-assembly into nanorods with 20 nm diameter. Self-assembly was expected to follow a mechanism of chain planarization followed by $\pi-\pi$ stacking. The limited length of aggregates was thought to be due to steric effects of the dendrons (Figure 234).[806−809]

Lee investigated the self-assembly of several dumbbell structures containing dendritic PEO attached to both chain ends of an oligo(*p*-phenylene) rigid rod. These structures were found to self-assemble into helical nanofibers (Figure 235). Helix formation was attributed to the rotation of the rigid rods in the same direction in order to minimize the steric effects induced by the bulky dendritic segments.[810−813] Similar structures synthesized by the same group were

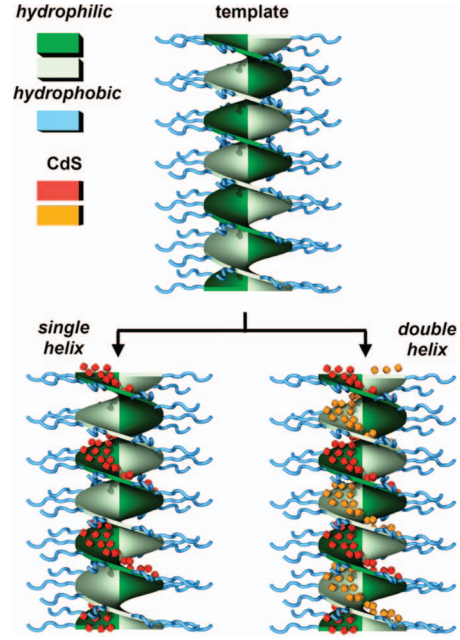

Figure 219. Template effect of the DRC1 twisted nanoribbon. Nucleation and growth on one face (top) or both faces (bottom) of the twisted ribbon result in the formation of single- or double-helical inorganic suprastructures. Adapted from ref 779.

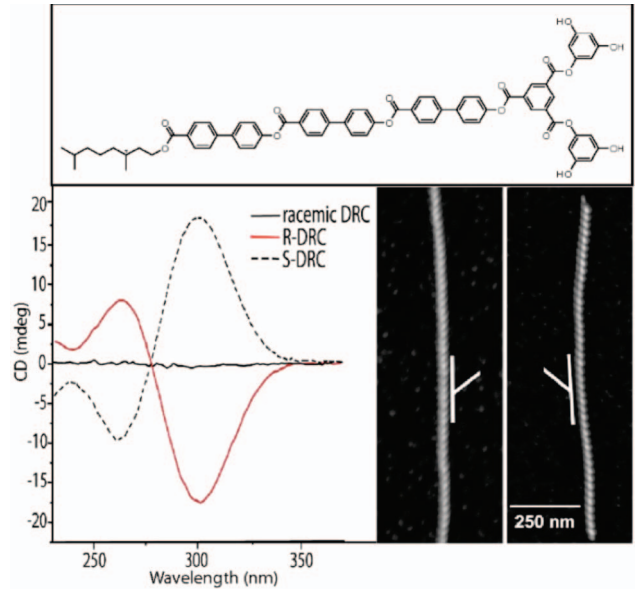

Figure 220. Self-assembling of (*R*)- and (*S*)-DRC3 in helical ribbons. CD spectra (left) and TEM (right) of the helical ribbons formed in acetonitrile reported. Reprinted with permission from ref 780. Copyright 2005 American Chemical Society.

found to spontaneously and reversibly transform from helical fibers into hollow nanocapsules after the addition of aromatic guest molecule, 4-bromonitrobenzene.[811] The guest molecule was presumed to selectively intercalate between the rod segments, increasing the distance between the vicinal rods and thus releasing the steric hindrance of the dendrons (Figure 236).[811]

Kato reported a similar class of oligo(*p*-phenylenes) trisdendronized at each chain end with (3,4,5)12G1 Percec dendrons (Figure 237).[834] With a single phenyl spacer, self-organization into a columnar phase was suggested by TOPM. With biphenyl, bipyridyl, or terphenyl spacers, no LC texture was observed, indicative of a *Cub* mesophase.

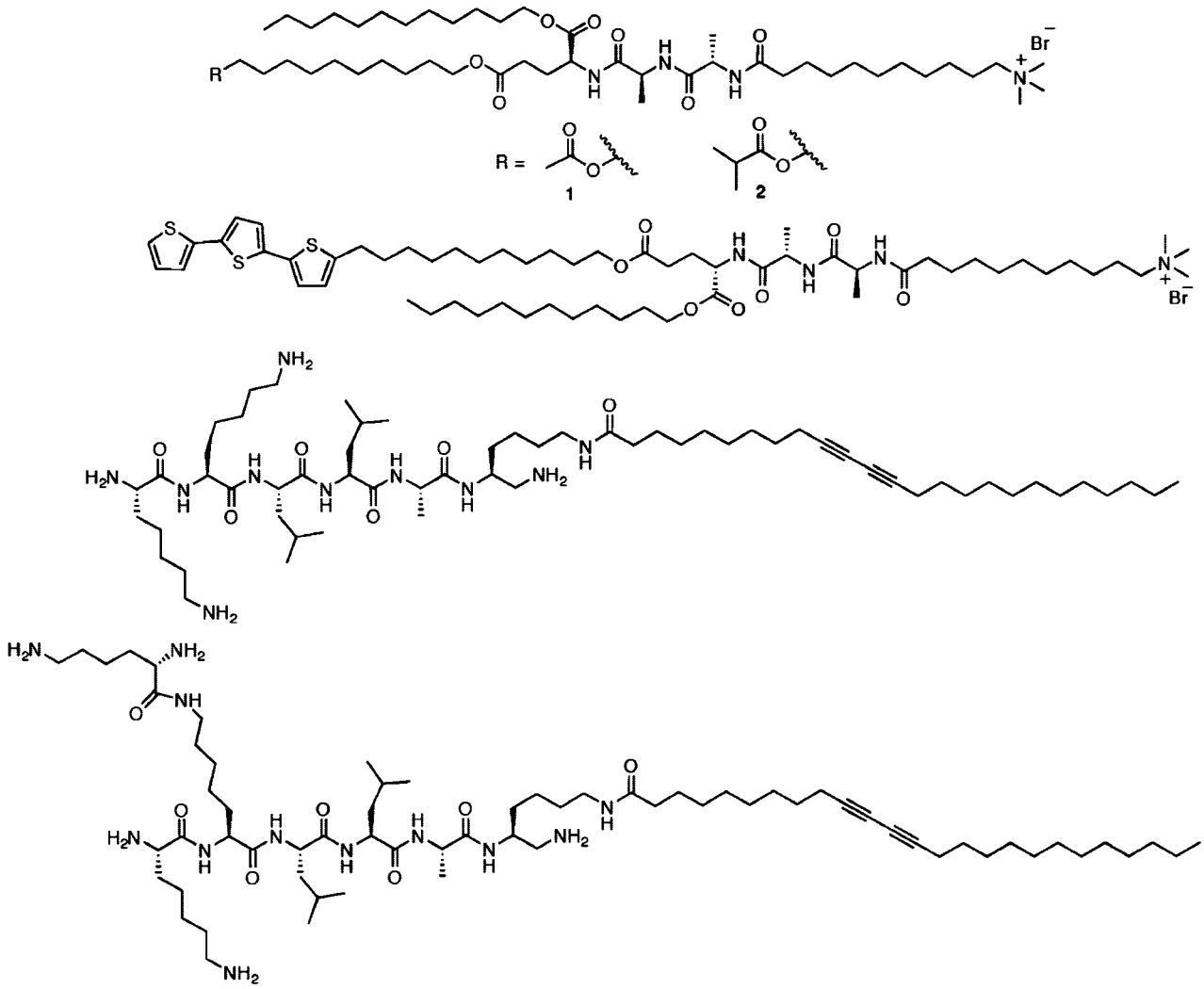

Figure 221. Branched peptides containing structures that form helical nanoribbons.[781−783]

As described in section 7.2, Kato also reported the 1,6-bis(phenylethynyl)pyrene dendronized with Percec-type (4-3,4,5-3,5)12G2 dendrons[835] The DRD self-assembles into columnar micellar assemblies that self-organize into a *Cub* lattice. Shearing of the sample results in a transformation to a columnar lattice with different π-stacked internal structure. This shear-mediated structural change induces a change in the luminescent properties of the LC.

Meijer and Schenning prepared chiral oligo(phenylene vinylene) (OPV) dumbbells constructed from DRs held together by hydrogen-bonding interactions.[826,836] (3,4,5)12G1 Percec-type dendrons were grafted-onto OPV capped with a 1-(4-amino-1,3,5-triazin-2-yl)-3-butylurea hydrogen-bonding donor/acceptor (Figure 238). The hydrogen-bonding donor−acceptor group mediates dimerization of the DR. The supramolecular dumbbell self-assembles in solution to form twisted columnar stacks. In mixed columns, energy is transferred efficiently from oligo(phenylene vinylene)s with shorter conjugation length to more highly conjugated equivalents.[837−845] Chemical cross-linking of the dendronized OPVs frustrates column formation and diminishes the efficiency of electron transfer (Figure 239).[846] The morphologies of films prepared from these chiral dendronized OPVs were also investigated.[847]

Other groups have investigated the self-organization in bulk of dumbbell amphiphiles through a combination of TOPM, DSC, and XRD.[810−816,823−827] Dumbbell structures containing oligo(diphenylene vinylene) capped at both chain ends with dendritic PEO dendritic units were found to self-assemble into a variety of phases depending on the dendron structure (Figure 240).

Dumbbells containing dibranched dendrons were found to self-assemble into primitive monoclinic-crystalline, BCC, and tetragonal lattices, while molecules containing tetra- and hexa-branched dendrons self-assembled only into BCC and tetragonal phases.[815]

Perylene bisimides and anthroquinones dendronized at both ends are also examples of the DRD topology. Since their rigid-rod segment is composed of a polyfused ring aromatic, they will be discussed in sections 7.3 and 7.6, respectively. As will be discussed in section 11.3, Kato prepared redox-active viologens dendronized with (3,4,5)*n*G1 (where n = 8, 12, 16) Percec-type dendrons, which also can be classified according to the DRD topology.[848]

4.1.6. Rigid Polymers Asymmetrically Dendronized at Both Chain Ends. Dendron−Rod−Dendron (DRD), Janus-Dumbbells

When a rodlike segment was asymmetrically capped with both hydrophilic and hydrophobic dendrons (Figure 1, fifth row left, and Figure 198, second row right), amphiphilic

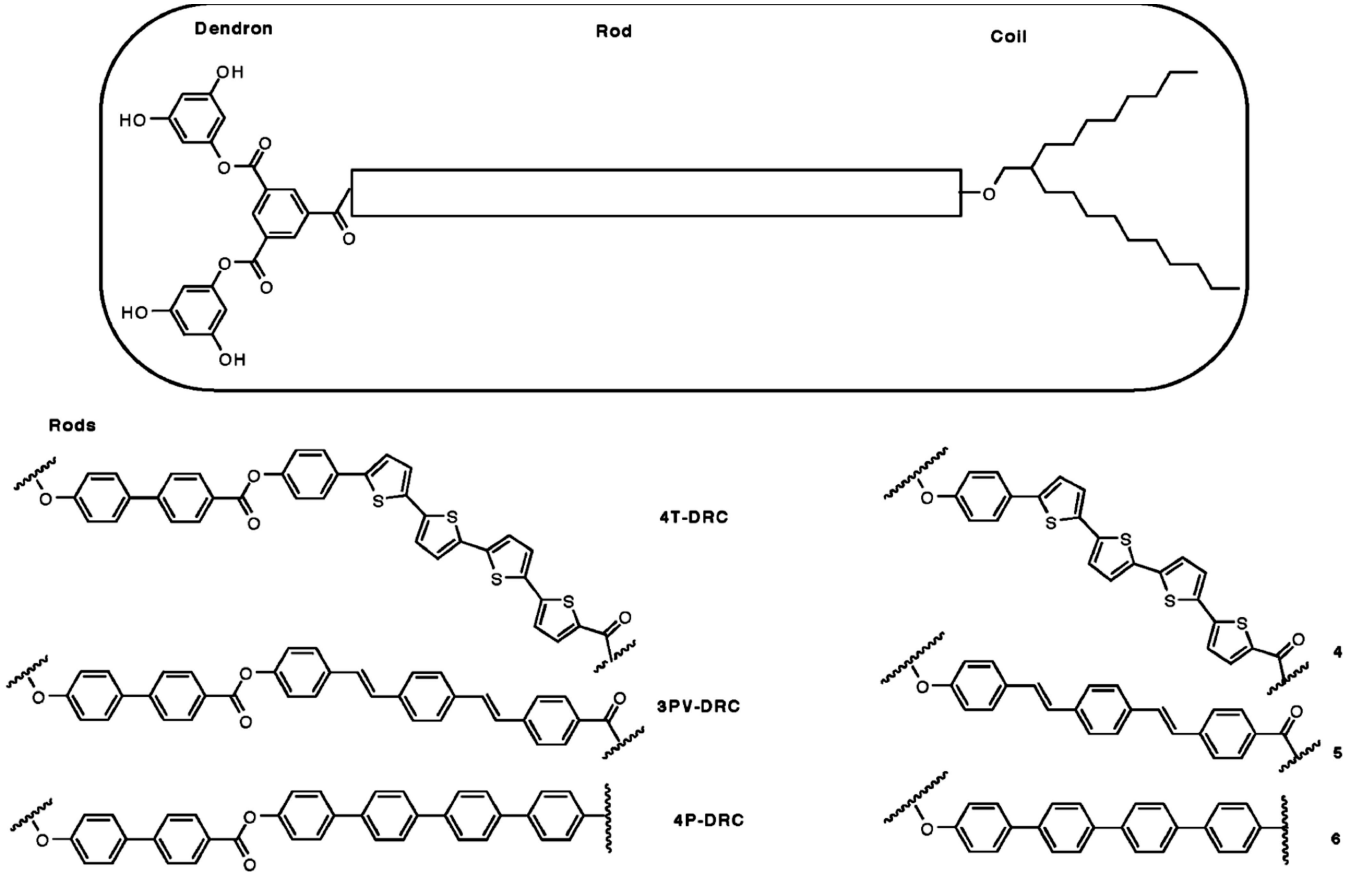

Figure 222. Structures of oligo(thiophene), oligo(phenylene vinylene), and oligo (*p*-phenylene) based DRCs. Adapted with permission from ref 784. Copyright 2004 American Chemical Society.

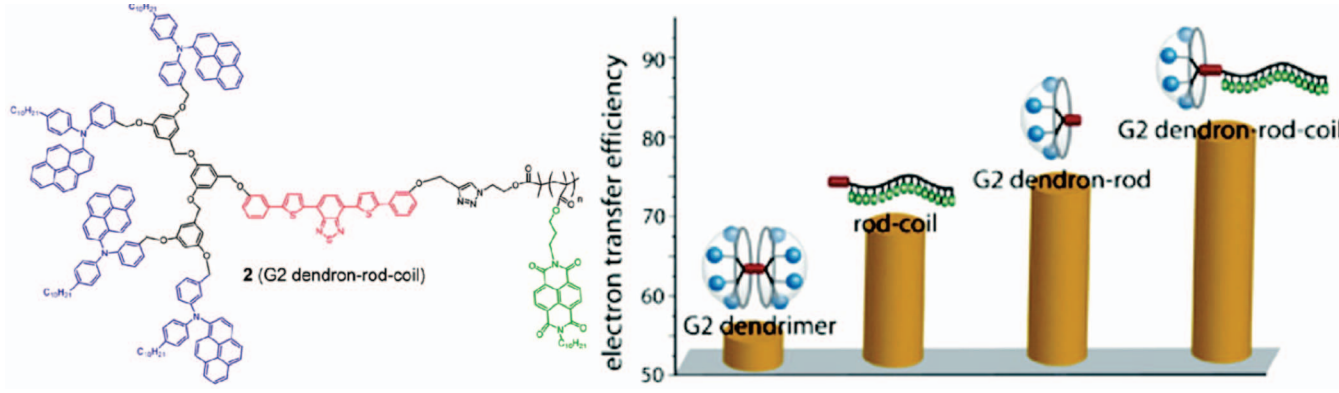

Figure 223. DRCs designed for ET (left) and their ET efficiency relative to similar structures (right). Reprinted with permission from ref 786. Copyright 2009 American Chemical Society.

structures were obtained. Lee investigated the self-assembly of these Janus-like dumbbell amphiphiles (Figure 241) in solution and observed a rich tapestry of morphologies dependent on the length of the aliphatic chains (microphase segregation) attached to the dendrons and the design of the rigid rod ($\pi-\pi$ interactions).[817−820]

Increasing the alkyl chain lengths resulted in a transition of the self-assembled architecture from closed spheres, to toroids, and finally to vesicles (Figure 242). Toroidal structures could be converted to 2D planar nets above their LCST. The delicate balance between the repulsive interactions of the amphiphiles and attractive $\pi-\pi$ interactions of the rods was considered to be responsible for the final structure observed.[815,816]

Lee also reported dumbbell-shaped dendron−rod−dendron amphiphiles (DRD 5−DRD 7, Figure 241) that self-assembled into a capsule structure with gated nanopores in the shell.[820] The nanopores were discovered also to undergo a thermoreversible transition from an open state to a closed state (Figure 243).

Toroidal structures were also observed in the LB films of amphiphilic DRDs composed of a dendritic PEO hydrophilic side and a (3,4,5)*n*G1 hydrophobic side (Figure 244).[849] Only with sufficiently large $C_{14}H_{29}$ tails are the unique 2D toroidal

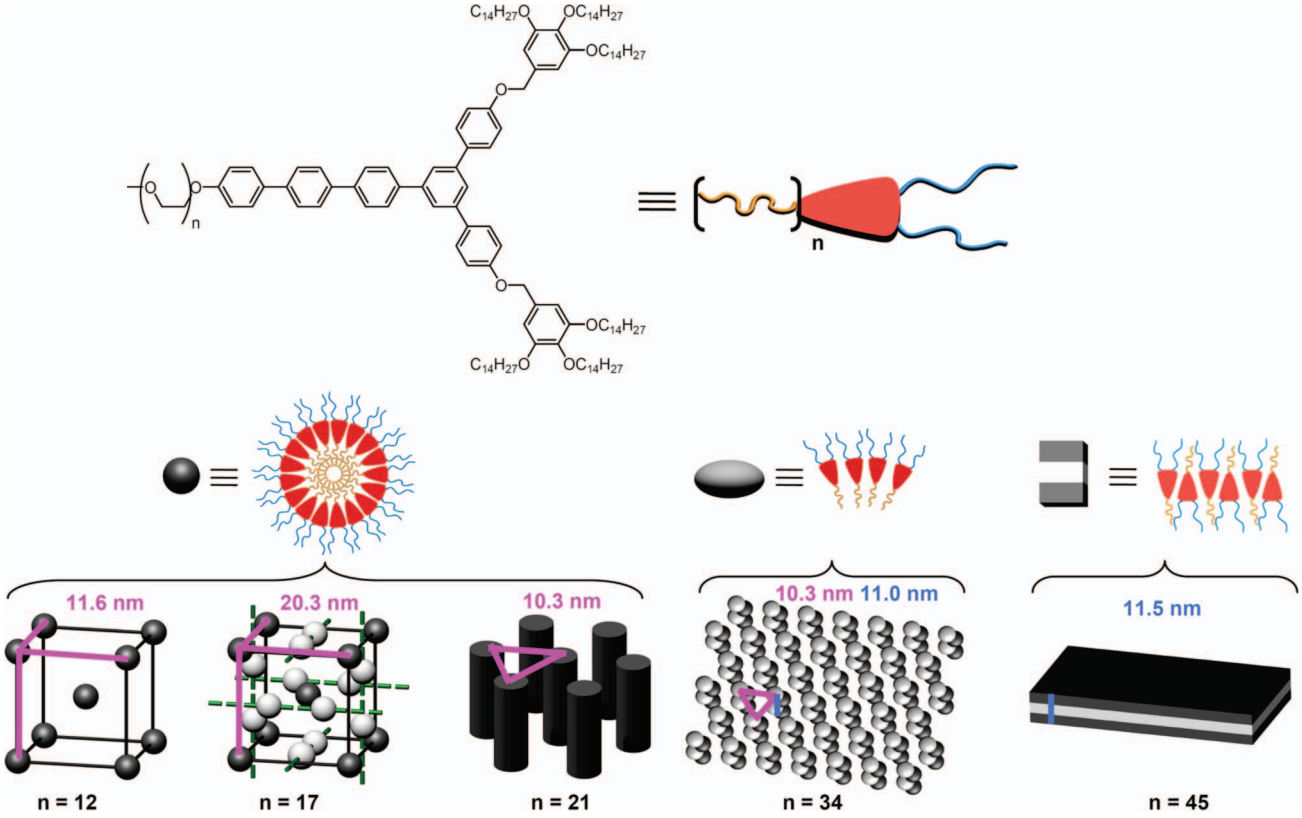

Figure 224. DP-dependent self-organization of wedge−coil molecules (top). Optical microscopy of Φ_h phase (left bottom) and Φ_h perforated lamellar phase (right bottom). Adapted from ref 789.

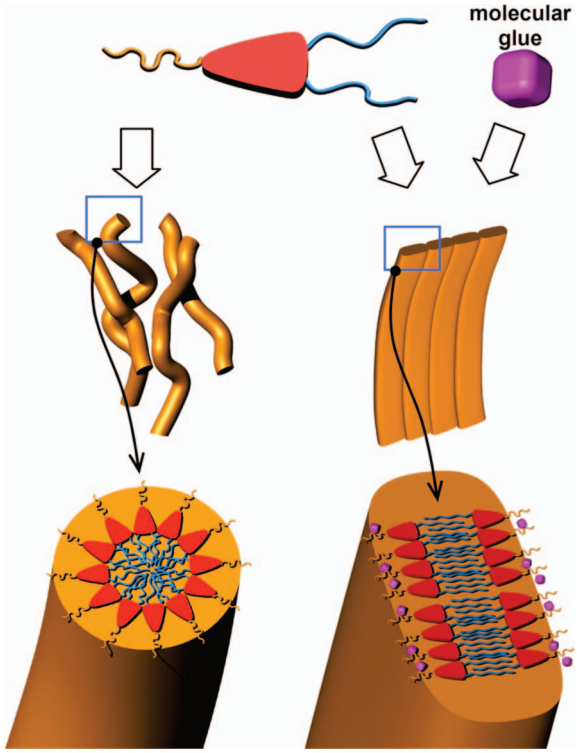

Figure 225. Nile Red as molecular glue for wedge−coil structures. Adapted from ref 791.

structures observed, indicating that, as in solution, the balance between hydrophobic and hydrophilic segments is a critical determinant of the self-assembled structure.

Diedrich reported amphiphilic/Janus-like dumbbells obtained by asymmetric attachment of both lipophilic and cationic Newkome-type dendrons to rigid phenylene−ethynylene units (Figure 245).[140,850−852] The structural design of these molecules was directed toward their use as synthetic vectors for gene transfection. Studies focused on the influence of the length of the alkyl chains and rigid rod or the size of the polar head-group on transfection efficiency of green fluorescent protein (GFP)-expressing plasmids into human cervical carcinoma (HeLa) cells.[140,850] Transfection efficiency depends heavily on the binding efficiency. Limited binding will result in poor surface protection of the plasmids and low transfection efficiency, while extremely high binding efficiency will prevent decomplexation after delivery. The number and type of alkyl chains in the lipophilic dendron was found to influence the binding affinity and transfection efficiency much more than changes to charged hydrophilic segment. Of the lipophilic dendrons investigated, those bearing three C_{12} chains had the highest activity. In addition to binding efficiency, in vitro and in vivo toxicity is also a major concern. Structural changes were also shown to have a large impact on cell viability. Compound **6** (Figure 245) with a longer rigid core exhibited a dramatic increase in toxicity as compared with compound **5** (Figure 245), while cholesteryl derivative does not damage cells even at high concentrations. Generally, higher-generation dendrons showed increased toxicity. However, compound **14** (Figure 245) had much lower toxicity, which was associated with low transfection activity.

It was determined that changes to the lipophilic dendron that resulted in lower activity were linked to a disruption of the self-assembly process and that the self-assembled morphology was inherently linked to gene transfection. Analysis of the self-assembly of amphiphilic DRDs in solution showed the formation of micelles and vesicles depending on the molecular curvature and shape. Molecules with large cur-

Scheme 60. Synthesis of Wedge−Coil Structures with EO-Hydrophilic Tails (Reprinted with Permission from Ref 792; Copyright 2004 American Chemical Society)

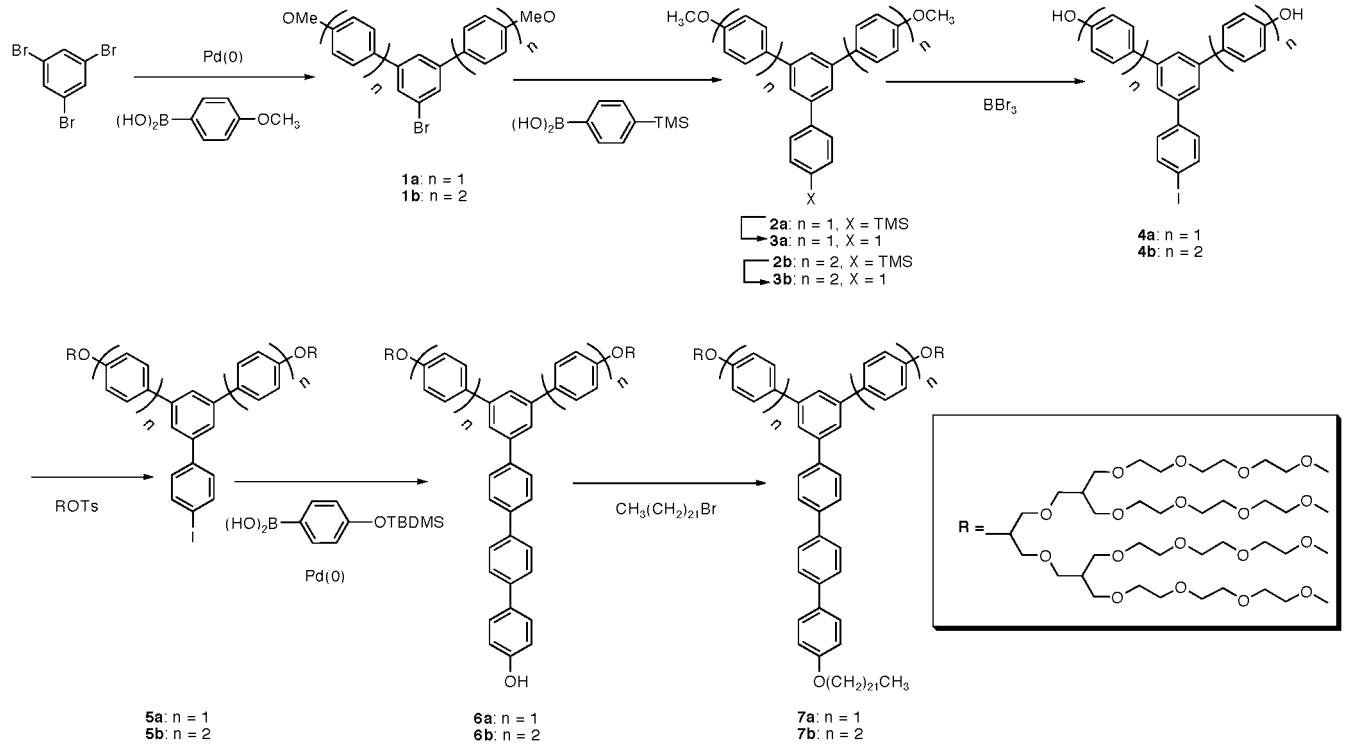

vature and conical shape, with larger cationic dendrons compared to the hydrophobic dendrons, self-assembled into relatively monodisperse spherical micelles, while structures with medium curvature and cylindrical shape self-assemble into unilamellar vesicles with broad size distribution. Differences in morphology were observed for self-assembly in pure water versus trisEDTA buffer. As a result of an environmentally dependent molecular shape, compound **10** (Figure 245) exhibited two morphologies, micelles in water and vesicles in aqueous buffer. In pure water with low ionic strength, cationic PAMAM-dendronized Janus-dumbbells adopt a conical shape, mediating self-assembly into micelles.

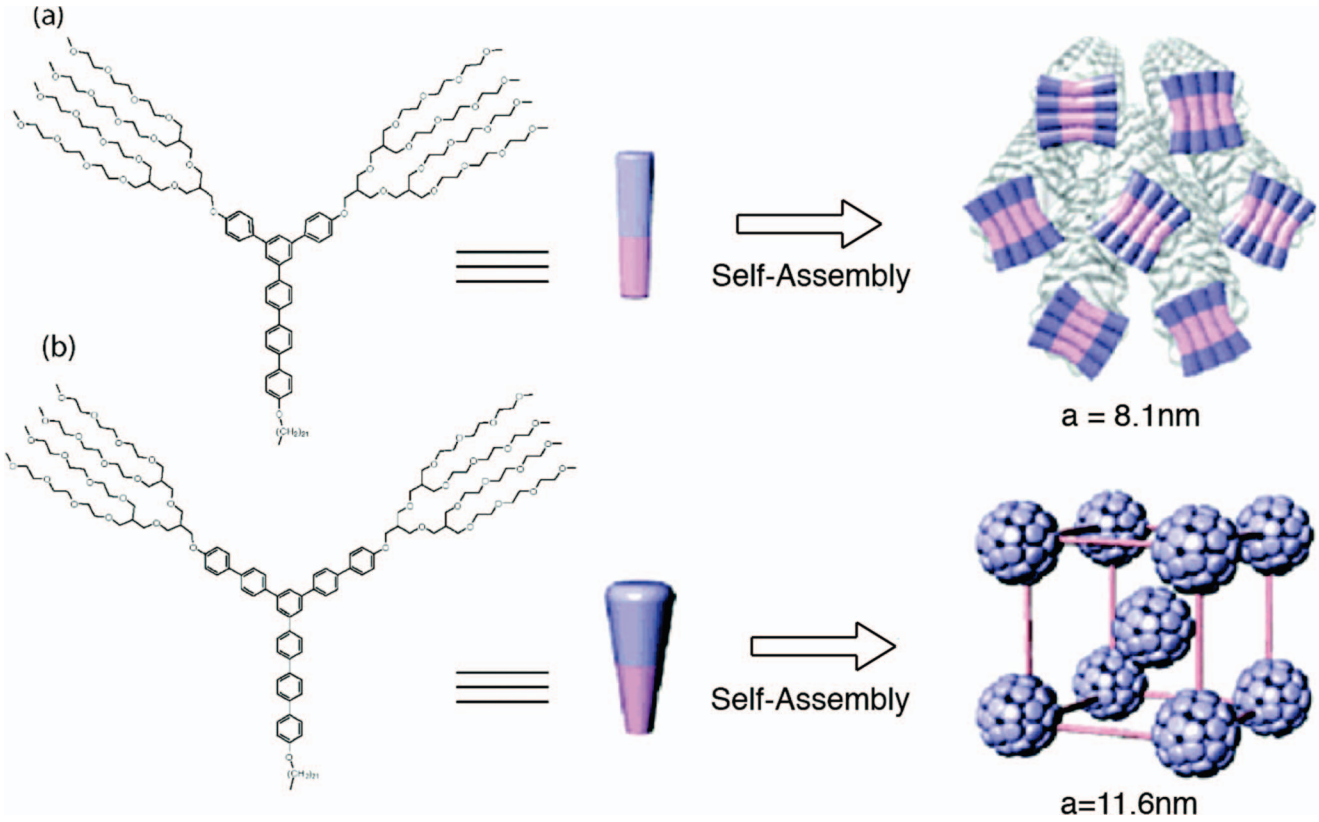

Figure 226. Effect of structure of dendritic structure on the self-assembly of wedge−coil molecules. Reprinted with permission from ref 792. Copyright 2004 American Chemical Society.

Scheme 61. Synthesis of Dendronized Cholesterol[794]

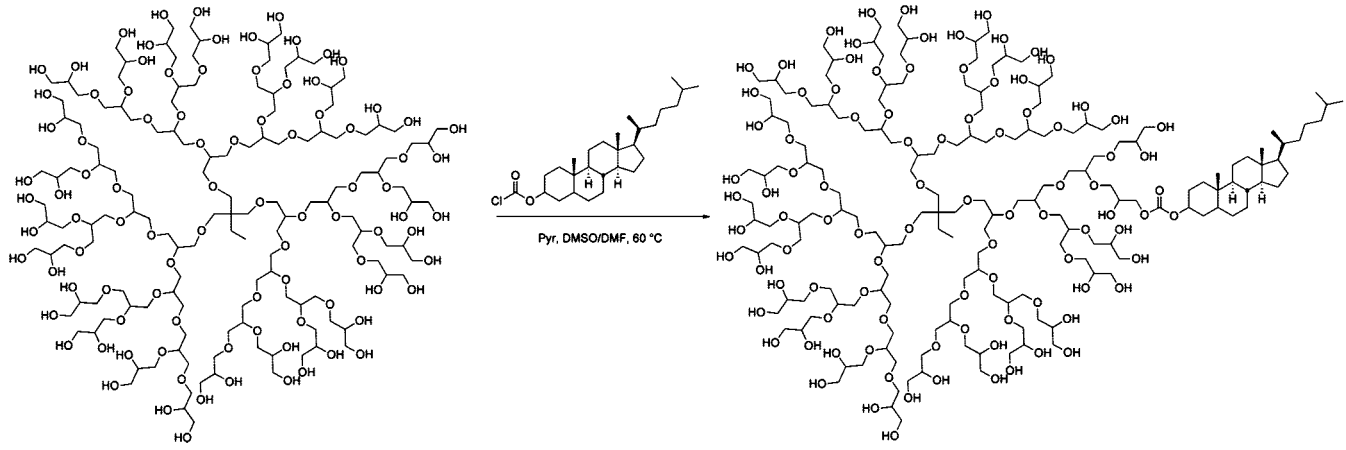

In trisEDTA buffer, the high ionic strength causes charge repulsion of the head-groups and a change in the molecular shape to that of a cylinder, resulting in vesicular self-assembled morphology. Addition of DNA induced the formation of multilamellar vesicles. The morphological change was dependent on the concentration of added DNA. Absorbed on the surface of the vesicles, the presence of DNA resulted in vesicle adhesion or branched vesicles (Figure 246).[852]

4.2. Biological Polymers and Oligomers Dendronized at Their Chain Ends

Biomacromolecules such as peptides, nucleotides, and carbohydrates provide useful building blocks for the design of supramolecular architectures. Topologically, biological polymers and oligomers functionalized at their chain ends follow the same classifications of their synthetic analogues as depicted in Figures 1 and 198. Driven by specific

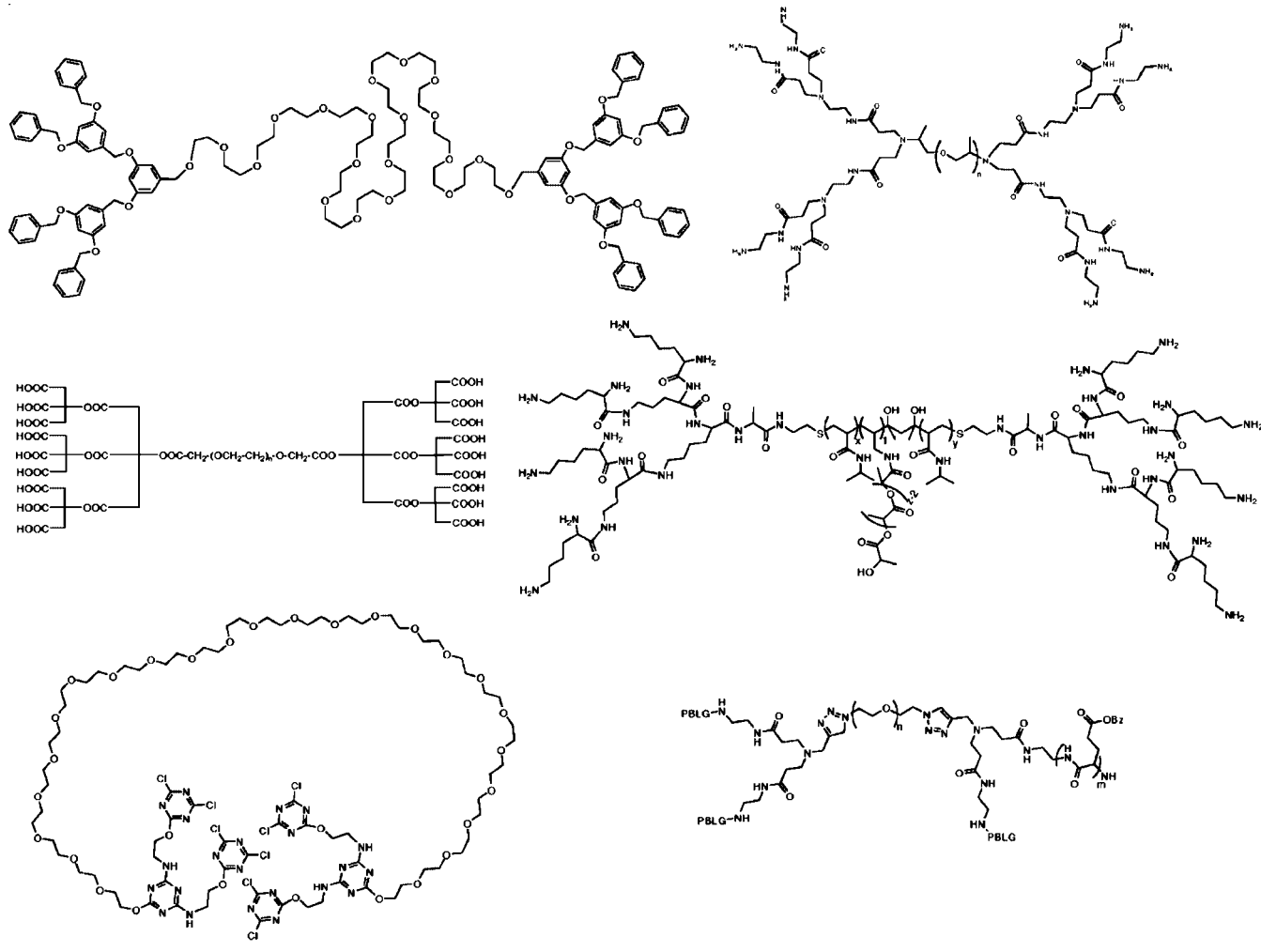

Figure 227. Representative structures of DCDs.[708−710,795−800]

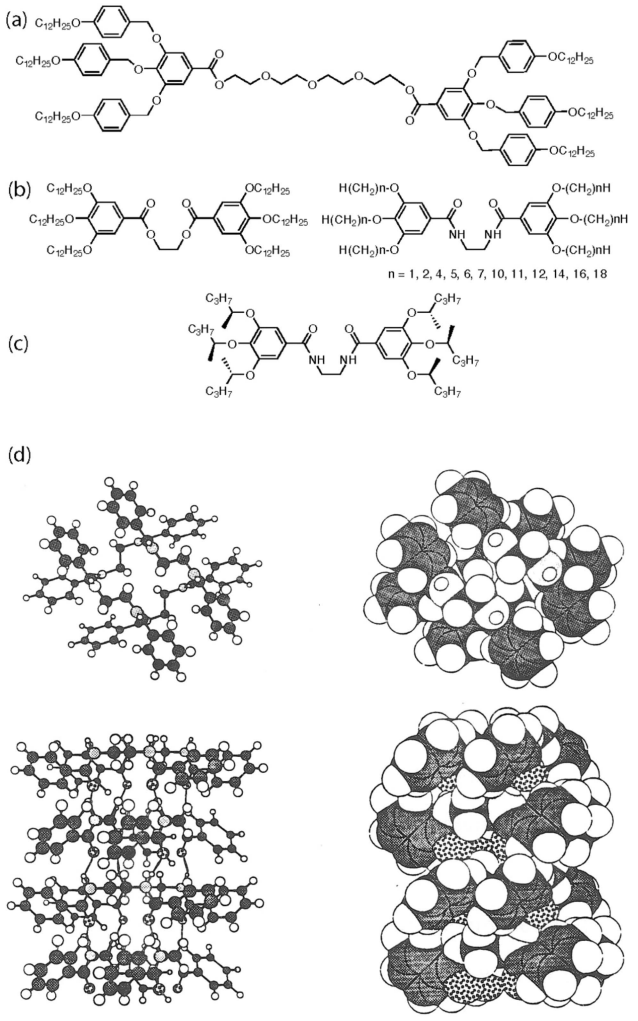

Figure 228. Percec-type dendron−coil−dendrons (a, b) and their model of self-assembly (c). Adapted with permission from the Ph.D. Thesis of James Arthur Heck, Case Western Reserve University, Cleveland, OH, 1995.

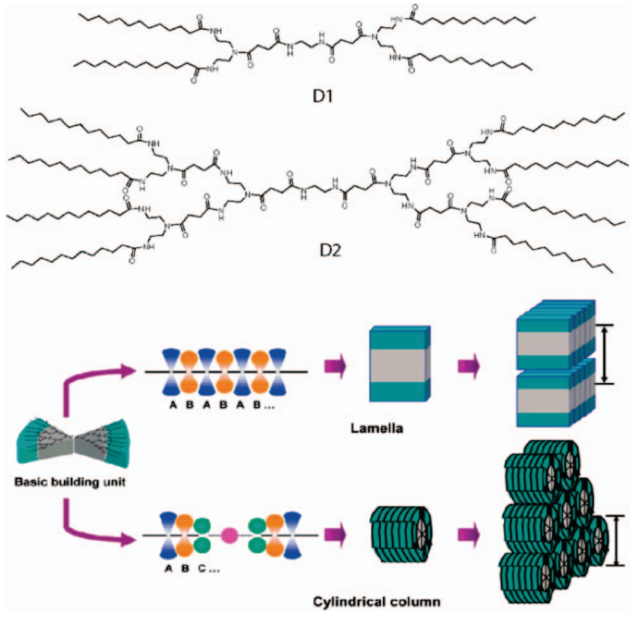

Figure 229. Hydrophobic DCDs (left) and their self-assembly into lamellar and columnar architectures. Reprinted with permission from ref 802. Copyright 2007 American Chemical Society.

Scheme 62. Synthesis of PEO Dendronized at Both Chain Ends with G2−G3 Hydrophobic Dendrons[733,804]

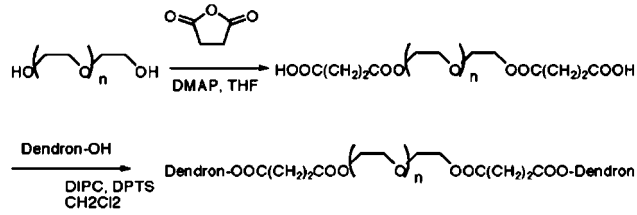

noncovalent interactions, which in isolation are weak but when combined are powerful, these simple molecules are capable of self-organizing into well-defined architectures with precise functionality. Progress in the design and understanding of the self-organization at both the molecular and supramolecular level has inspired the creation of new nanostructured materials. Toward this end, dendron−biomacromolecule conjugates based on peptides, nucleic acids, and carbohydrates have been of specific interest for their applications in the fields of tissue

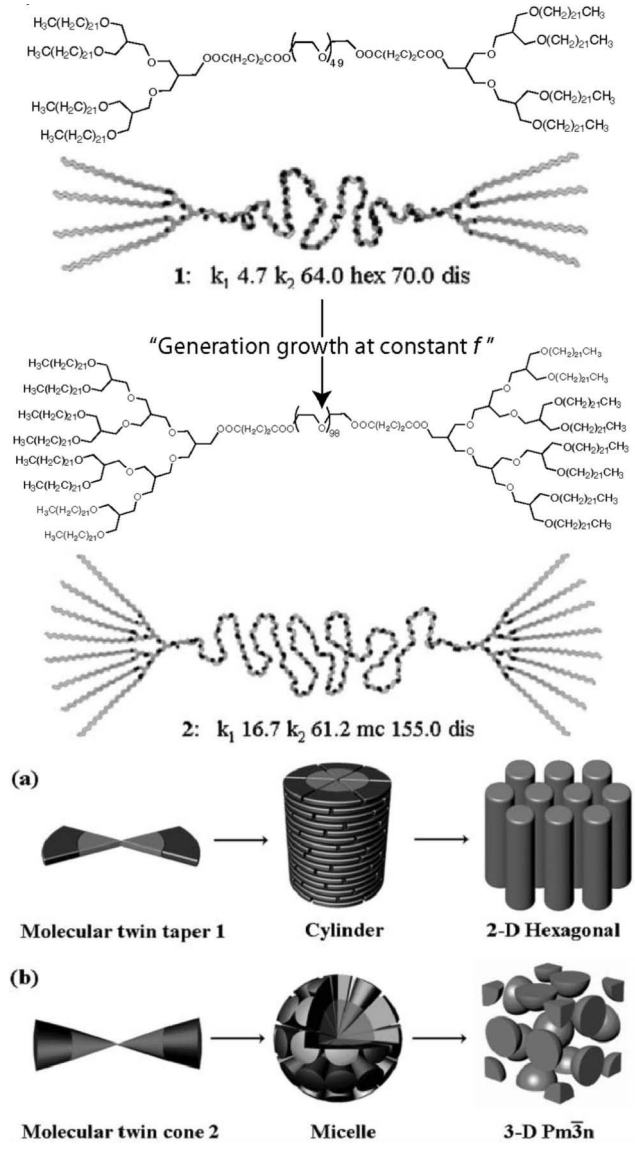

Figure 230. Structure and self-assembly of PEO dendronized at both chain ends with dendritic PEG capped with aliphatic tails. Reprinted with permission from ref 733. Copyright 2005 Royal Society of Chemistry.

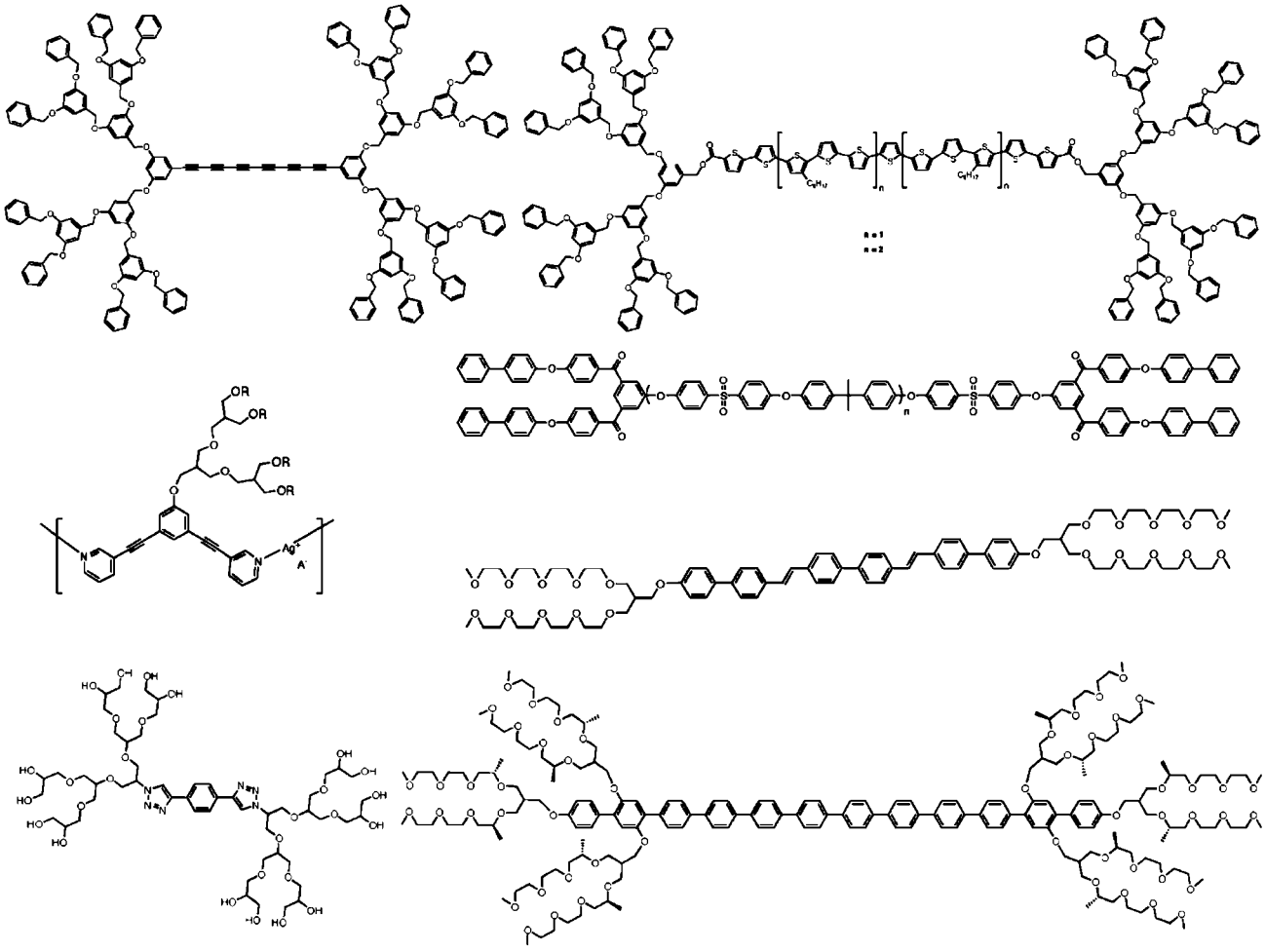

Figure 231. Dendron−rod−dendrons (DRD)s, Dumbbells.[805,809,810,814,815,823]

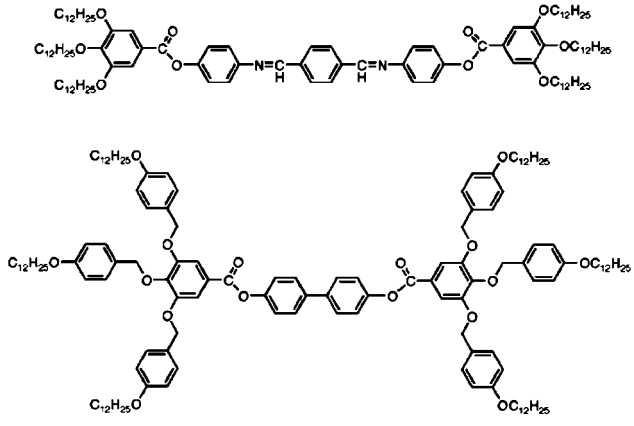

Figure 232. First DRDs reported by Malthête.[831,832]

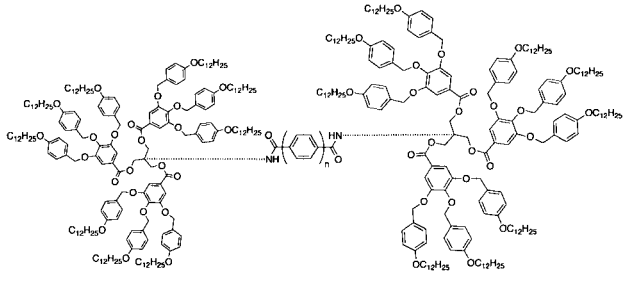

Figure 233. Malthête diabolo molecules.[833]

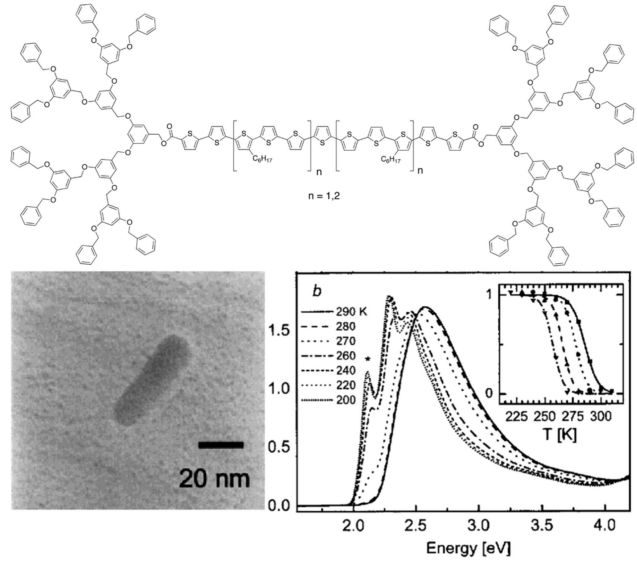

Figure 234. Polythiophene capped at both chain ends with Fréchet dendrons and their self-assembly into nanorods in CH_2Cl_2 as detected by TEM and UV/vis spectroscopy. Adapted with permission from ref 809. Copyright 2001 American Chemical Society.

engineering,[853] biomineralization, and regenerative medicine, as biosensors such as DNA microarrays and microchips, or as drug- and gene-delivery systems.

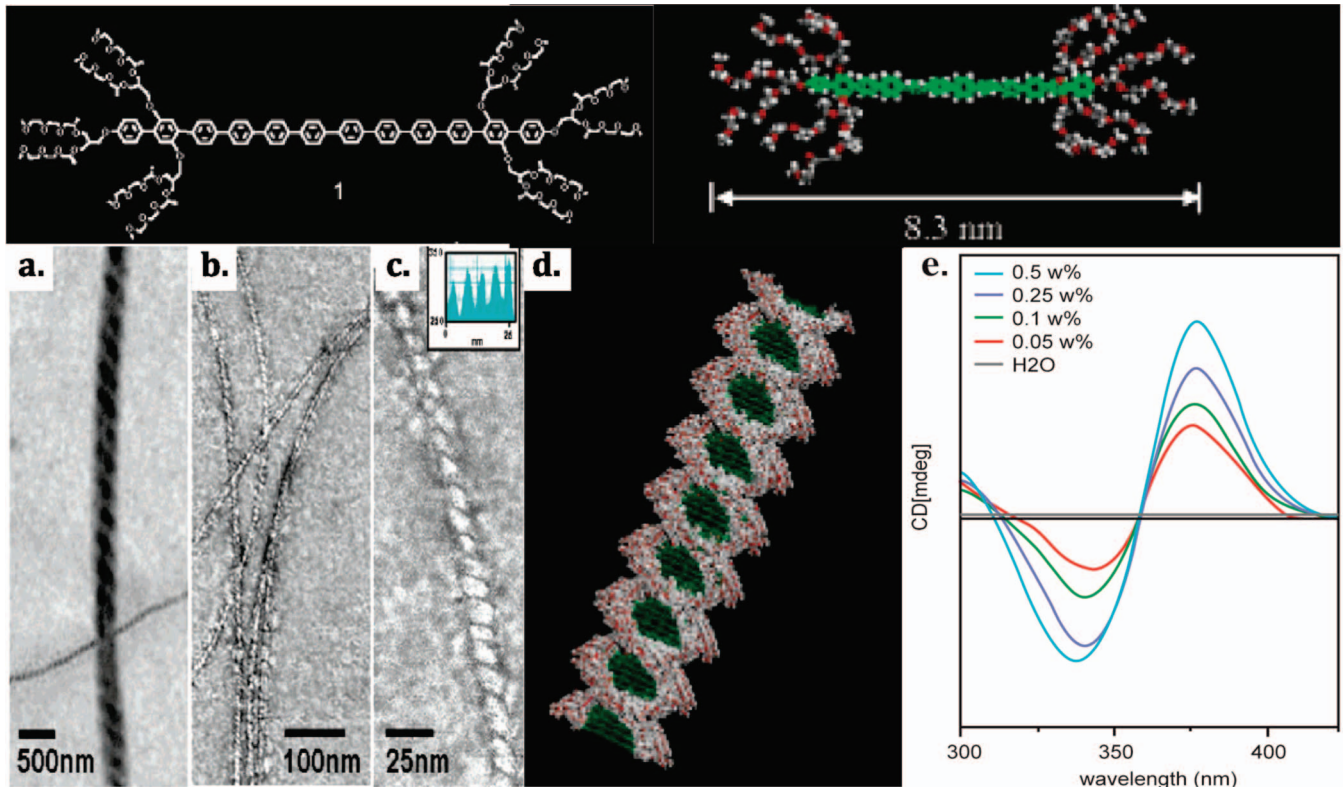

Figure 235. Self-assembly of poly(*p*-phenylene) capped at both chain ends with dendritic PEO into helical fibers as demonstrated by TEM (a−c) and circular dichroism at 25 °C (e). Schematic representation of the helical fiber (d). Adapted with permission from ref 810. Copyright 2005 American Chemical Society.

4.2.1. Poly(peptides) and Oligo(peptides) Dendronized at their Chain Ends. Dendron−Peptide Conjugates

Peptides dendronized at their chain ends are molecular structures containing well-defined constituents able to hierarchically self-organize into 3-D architectures. The two most important secondary structures derived from the self-assembly of peptides are α-helices and β-sheets. Both secondary structures are stabilized by periodic H-bonds of peptide backbone. In the α-helix, the peptide bond planes are parallel to the axis of the helix and each peptide forms two intramolecular hydrogen bonds. In β-sheets, a polypeptide chain is hydrogen bonded to another polypeptide chain aligned in a parallel or antiparallel direction.[854] In addition to the ability to program the internal architecture of the backbone, chain-end dendronized peptides also have the advantage that their amino acid constituents are biocompatible and their sequence space is vast.[121]

Stupp investigated the self-assembly of several chain-end dendronized peptides for potential applications as bioactive scaffolds for cell growth and tissue engineering. The dendron−peptide conjugates contained either dendritic PLL of different generations[855] and cholesteryl (L-lactic acid) as the rod segment or a hydrophobic alkyl tail covalently coupled at one chain end to a charged peptide sequence containing a β-sheet forming sequence and a bioactive segment at the other chain end. The latter group of molecules was classified as a peptide amphiphile.[856−859]

Peptide amphiphiles were found to self-assemble in water into micellar nanofibers (Figure 247).[856,860] Cross-linkage of the cysteine residues resulted in chemically robust fibers reversible only by reduction of the disulfide bonds back to free thiol groups.[856] This highly dynamic system was modified with different amino acids for various applications such as bladder tissue engineering[859] and mineralization.[856]

Meijer reported the synthesis and self-assembly of a peptide amphiphile based on oligo(phenylene vinylene) and glycinyl-alanyl-glycinyl-alanyl-glycine (GAGAG) or glycinyl-alanyl-asparagyl-prolyl-asparagyl-alanyl-alanyl-glycine (GANPNAAG) β-sheet oligopeptide sequences.[861] These systems were expected to generate 2-D and 3-D spatial orientation and packing due to the presence of the $\pi-\pi$ interactions from the oligo(phenylene vinylene) and hydrogen-bonding interactions from the peptide. The π-conjugated segment was used as an optical probe to study the self-assembly mechanism of peptides. A combination of scanning tunneling microscopy (STM), cryo-TEM, AFM, and optical studies were used for the investigation of the 2-D self-assembly at the liquid−solid interface and the self-assembly in solution. STM analysis of the 2D-self-assembly demonstrated the formation of the antiparallel β-sheet conformation (Figure 248) and showed that the peptide segment dictates the packing of the dendronized oligo(phenylene vinylene) units. Cryo-TEM and AFM confirmed the formation of the nanofibers in water.

Lee reported another class of dendron−peptide conjugates consisting of a functional peptide connected to a hydrophobic lipid dendrimer through a flexible ε-aminohexanoic acid linker (Figure 249).[862,863]

The functional peptide is a Tat cell-penetrating peptide (Tat CPP or Trojan horse peptide) consisting of highly charged lysine and arginine residues capable of translocation across the cell membrane with high efficiency. Tat CPP is a well-known protein derived from human immunodeficiency virus type-1 (HIV-1). The characteristics of the Tat peptide

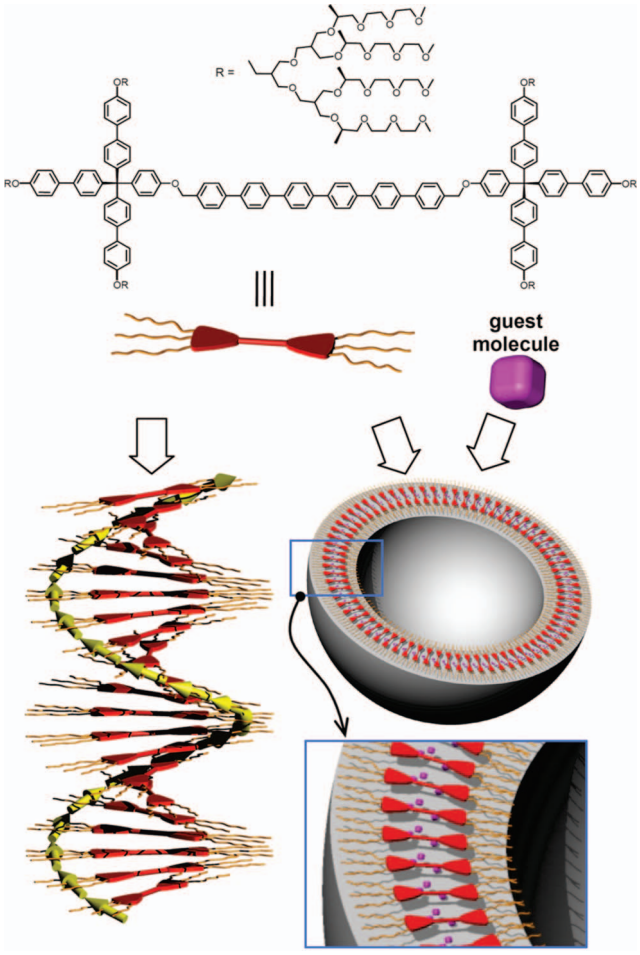

Figure 236. Representation of the reversible transformation of helical fibers into hollow spherical capsules. Adapted from ref 811.

could be exploited for delivery of bioactive molecules. For these purposes, the authors reported several dendron−peptide conjugates containing different generation dendritic lipids attached to the N-terminus of Tat CPP. The dendron−peptide conjugates were found to self-assemble in aqueous solution into different supramolecular structures from spherical micelles at low dendron generation number to short- and long-length cylindrical micelles at higher dendron generation number (Figure 250).

Parquette demonstrated that α-helical content could be observed in β-sheet forming oligopeptides through the replacement of two Ala residues with dendronized Ala.[864] When the two dendritic Ala residues are properly spaced in the oligopeptide, self-assembly into amyloid-like fibrillar structures that are capable of encapsulating Nile Red dye is observed. Only in this twisted β-sheet structure is chirality transferred from the peptide backbone to the dendron (Figure 251). Change in the pH, which effects both the peptidic and dendritic portions, results in disassembly of the fibrillar structure and formation of nanotubes and concomitant release of Nile Red.[865]

In contrast with the results of Meijer for dendronized oligo(phenylene vinylene)−peptide conjugates where peptides formed β-sheet self-assembled structures,[861] CD/UV−vis experiments for these molecules revealed only a random-coil conformation of the peptides inside the supramolecular nanostructures. Consequently, it was concluded

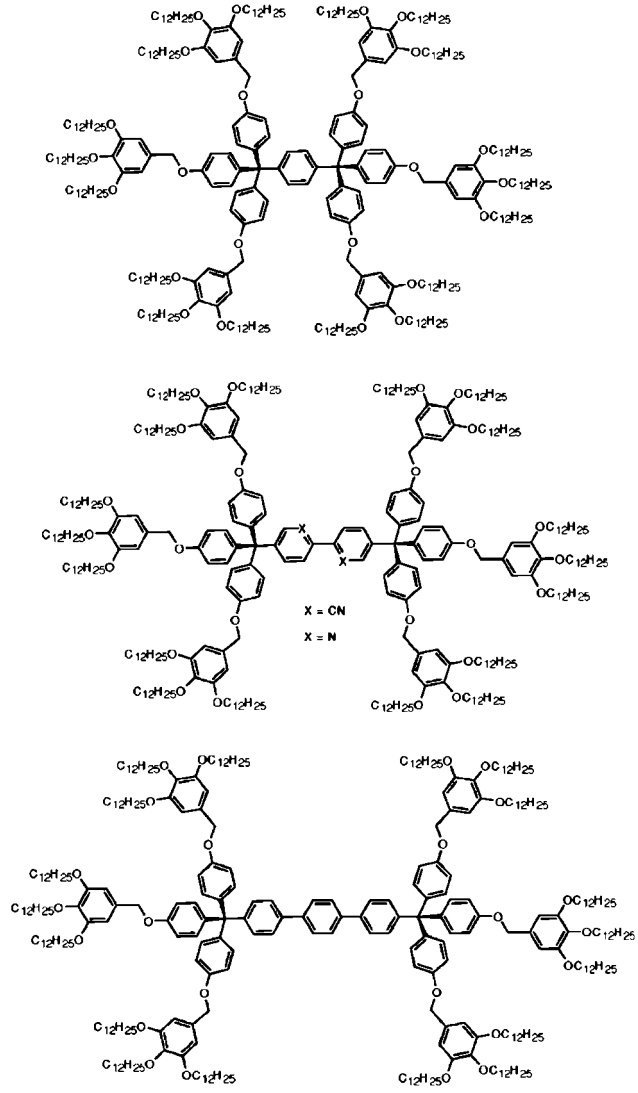

Figure 237. Oligo(*p*-phenylenes) trisdendronized at both chain ends with Percec-type dendrons.[834]

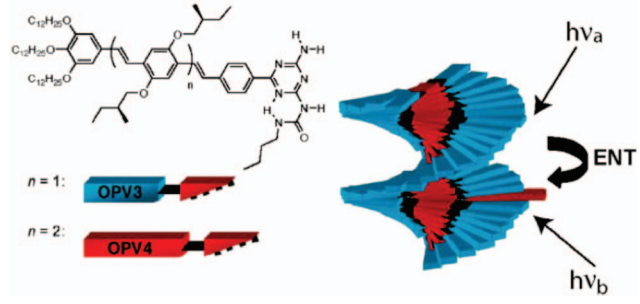

Figure 238. Supramolecular dumbbells based on oligo(phenylene vinylene) (left) and their self-assembly into twisted columnar stacks that mediate efficient energy transfer. Reprinted with permission from ref 840. Copyright 2003American Chemical Society.

that hydrophobic interactions are the only forces responsible for the self-assembly of the dendron−Tat CPP conjugates and that Tat CPP peptide retains its biological activity by not participating in the self-assembly process.

Manners reported the synthesis and self-assembly in solution of dendron−helical polypeptide conjugates (DHPs) consisting of either (4-3,4,5)12G1 or (3,4,5)^{2}12G2 Percec-type dendrons coupled to the polypeptide segment through

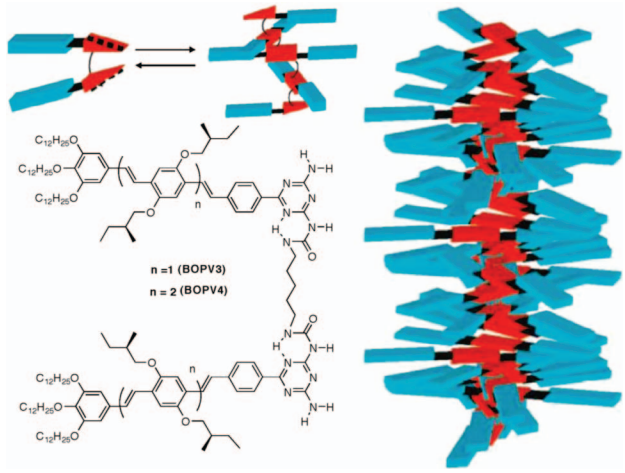

Figure 239. Cross-linked dendronized OPVs and frustrated columnar self-assembly. Reprinted with permission from ref 846. Copyright 2008 American Chemical Society.

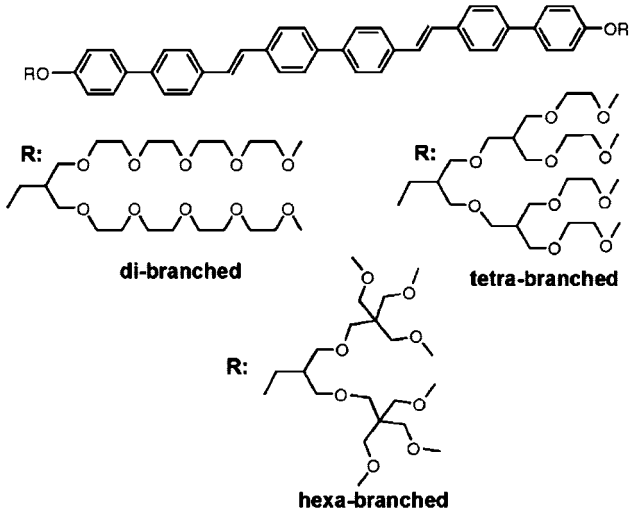

Figure 240. Dumbbell structures containing di-, tetra-, and hexa-branched dendrons.[815]

an oligo(ethylene oxide) chain.[866] The DHP molecules were synthesized using ring-opening polymerization (ROP) of γ-benzyl-L-glutamate *N*-carboxylanhydride (γ-Bn-Glu α-NCA) with the dendron serving as a macroinitiator (Scheme 63).

The DHPs exhibited solvent-dependent self-assembly. In toluene, thermoreversible gels composed of nanoribbons were observed, while in THF, lyotropic layered liquid crystals were found (Figure 252).

Since the gels retained their integrity and thermoreversibility in the presence of methanol, the authors concluded that hydrogen bonding was not important in the gelation process and the formation of nanoribbons, but rather the $\pi-\pi$ interactions between the benzyl side groups of the helices were found to be most critical. It was suggested that the block-copolymers stack in an antiparallel fashion so as to minimize the steric repulsion between the bulky dendrons. The same group reported a dif-917ferent design of the dendron−helical polypeptide conjugate by using flexible PLL dendrons of different generation numbers and similar helical peptide rod.[867] The resulting DHPs formed micelles in water and the morphology of the micelles was dependent on the size of the dendron. As the curvature increases from G1−G3 of the PLL dendron, the DHPs were found to form large helical aggregates with G1 PLL and vesicles and spherical micelles for G2 and G3 PLL.

Because of their biodegradability, several dendron−polypeptide conjugates were designed for use as organogelators[868,869] and dendritic macromonomers for in situ polymerization to secure cataract incisions.[870,871] These materials are able to spontaneously afford a hydrogel within a few minutes at room temperature and at neutral pH. This work, as well the use of these materials for ophthalmic and orthopedic applications, has been reviewed recently and will not be covered here.[138]

Self-assembled structures with vesicular morphologies received significant attention for their potential application in drug delivery and gene-transfer therapy.[872−874] The dendron−peptide conjugates used for these purposes were composed of PAMAM[872,873] or dendritic PLL[874,875] attached to a polypeptide chain (Figure 253). The dendritic PLL was further functionalized at the periphery with α-amino tetradecanoic acid. The alkyl amino groups were unmasked, giving a cationic nature to the dendron.

The lipid-modified cationic dendron was found to self-assemble in water into vesicular structures with Z-average diameter of ~300 nm. The cationic vesicles formed from highly lipidated PLL dendrons were named dendrisomes,[874] by analogy with polymersomes.[876] Investigation of the dendrisomes by TEM showed the wall thickness ranging from 6 to 10 nm, which, combined with molecular modeling, suggested a bilayer structure (Figure 254). The wall thickness and the high polydispersity of dendrisomes reported were found to be in the same range with polymersomes.[874,876]

4.2.2. DNA and Other Oligonucleotides Dendronized at Their Chain Ends. Dendron−Oligonucleotide Conjugates

Dendron−oligonucleotide conjugates and in particular DNA dendronized at its chain ends are two structures that are gaining significance especially for the fabrication of biosensors such as DNA microarrays and microchips,[124] in molecular medicine for gene expression studies, detection of nucleotide mutations, or genotyping of individuals in forensic applications, as well in gene therapy as part of gene-delivery vectors.[877]

DNA is an attractive framework for constructing self-assembling supramolecular architectures, due to its easily programmable self-recognition. DNA is a monodisperse polymer with an alternating phosphate-sugar backbone. Because of the ionic phosphate backbone, DNA has an overall negative charge that allows for ionic interactions with positively charged molecules. To each sugar unit is linked one of the four nucleobases, cytosine (C), guanine (G), adenine (A), or thymine (T), in a specific sequence. Hybridization of a single-stranded DNA (ssDNA or sense DNA) and its antiparallel complementary strand (antisense DNA) produces double-stranded DNA (dsDNA) that exhibit double-helix secondary structure. Hybridization is mediated through hydrogen-bonding recognition of Watson−Crick pairs (A−T and C−G). The fabrication of DNA microarrays takes advantage of the hybridization process (Figure 255).[125] A nucleic acid probe is typically immobilized at discrete positions on surface-activated slides. The microarray is treated with a target sample containing fluorescently labeled nucleic acids. The two components hybridize, forming dsDNA, and the degree of hybridization is quantified by fluorescence using a high-resolution scanning laser (Figure 255). Constant improvements to the design of DNA mi-

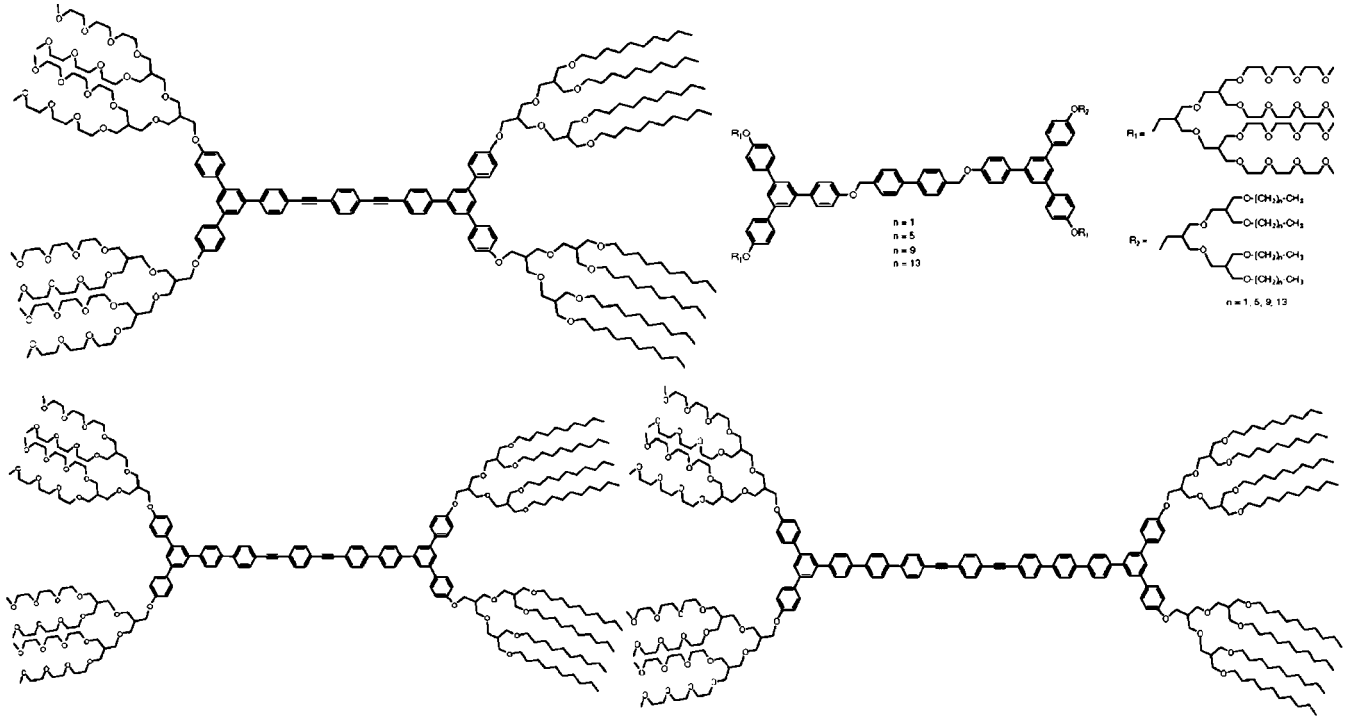

Figure 241. Dumbbell amphiphiles.[815−817]

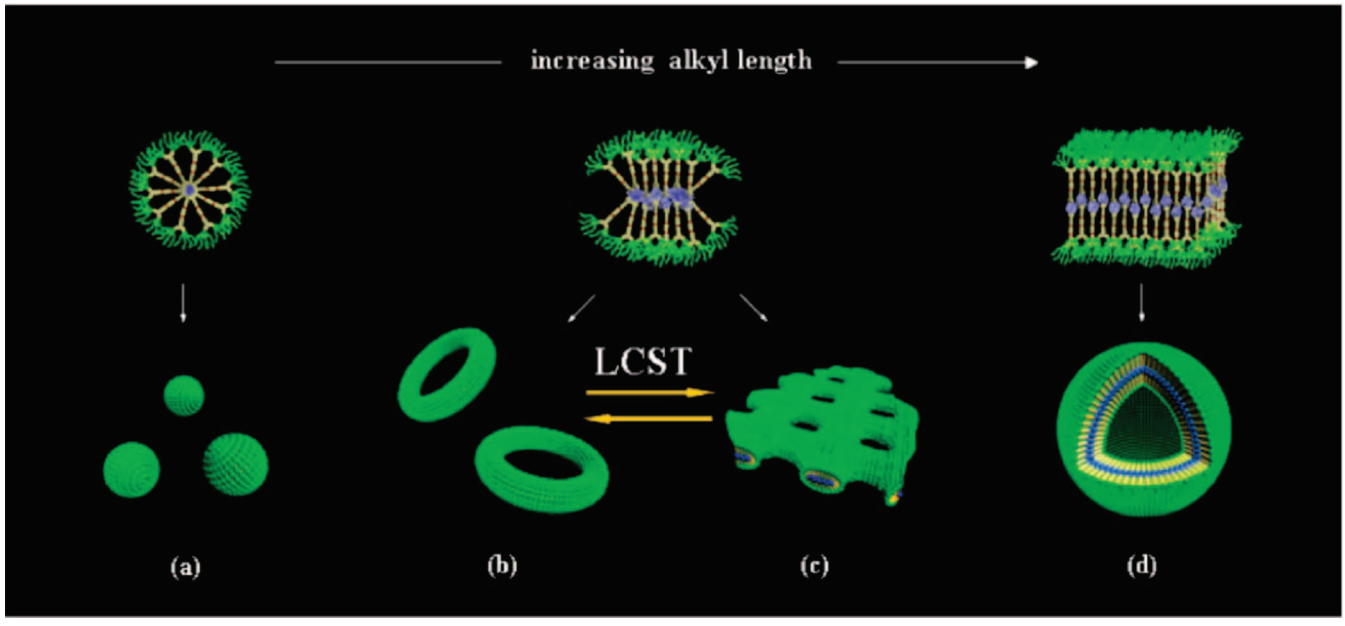

Figure 242. Effect of alkyl tail length on the supramolecular morphologies observed in dendron−rod−dendron amphiphiles: (a) closed spheres; (b) toroids; (c) 2-D planar nets; (d) vesicles with increasing the chain of the alkyl chain. Reprinted with permission from ref 818. Copyright 2007 American Chemical Society.

croarrays resulted in sophisticated devices with increased sensitivity. A first step in increasing the sensitivity involved the modification of the probe to increase DNA surface coverage. Although glass and silica provided good chemical resistance and low intrinsic fluorescence, they did not ensure a high surface coverage. Dendrimers and dendrons were considered the best candidates due to their numerous peripheral functionalities. Several reviews focused on the use of dendrimers and dendrons for the preparation of DNA microarrays, and this topic will not be covered here.[124,125]

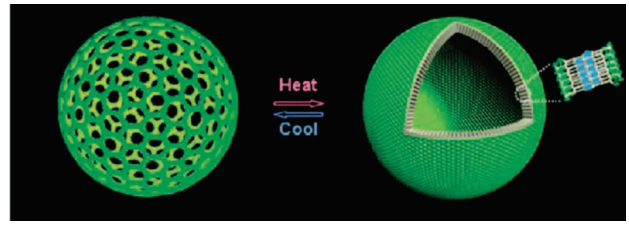

Figure 243. Illustration of the reversible open/closed gating motion in the lateral nanopores of the capsule. Reprinted with permission from ref 820. Copyright 2008 Wiley-VCH Verlag GmbH & Co. KGaA.

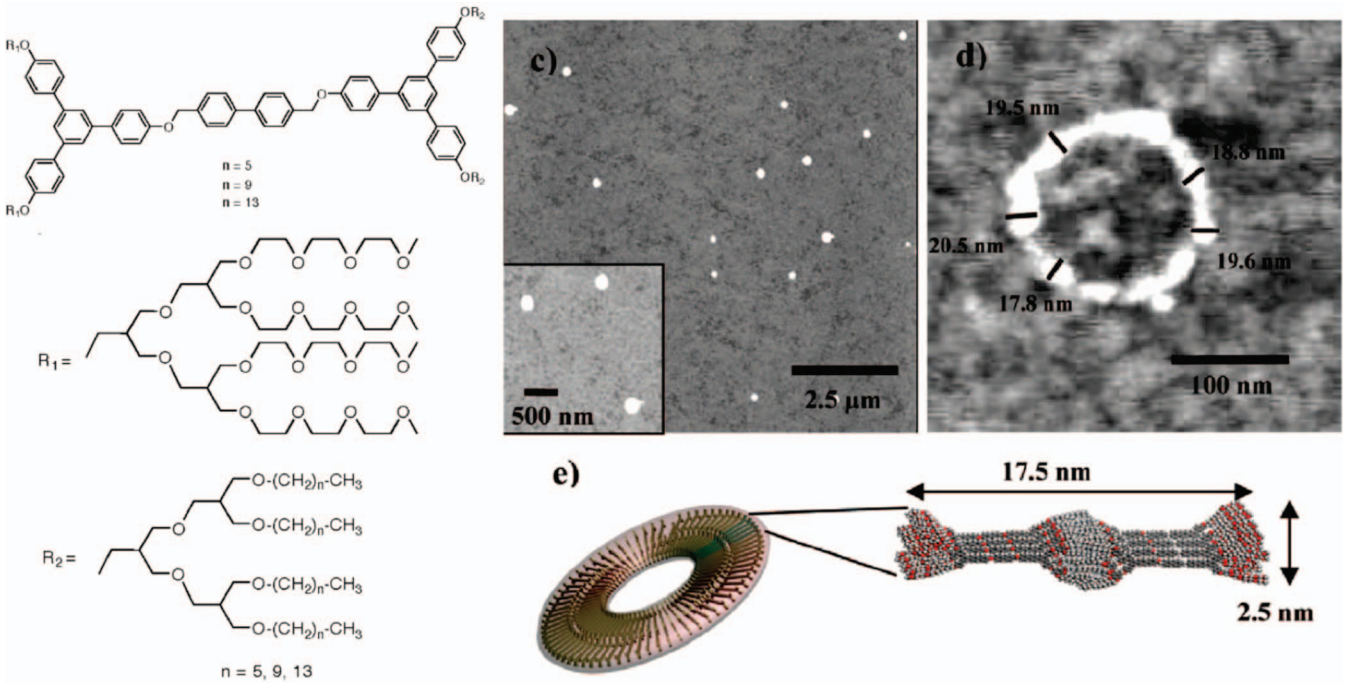

Figure 244. Structure (left) of DRDs forming toroids in LB films (right). Reprinted with permission from ref 849. Copyright 2008 American Chemical Society.

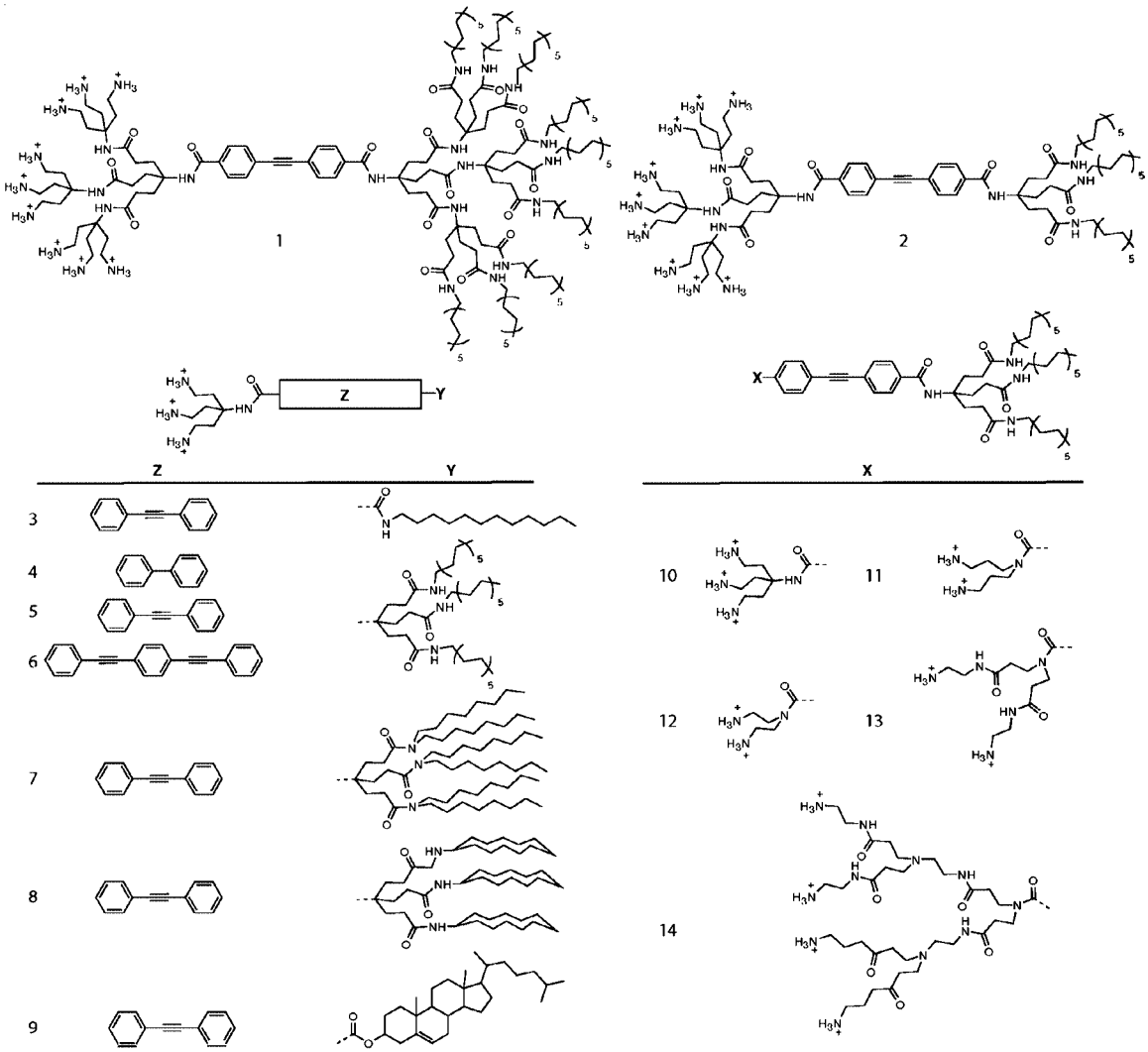

Figure 245. Janus-like DRD amphiphiles reported by Diederich.[140,850−852]

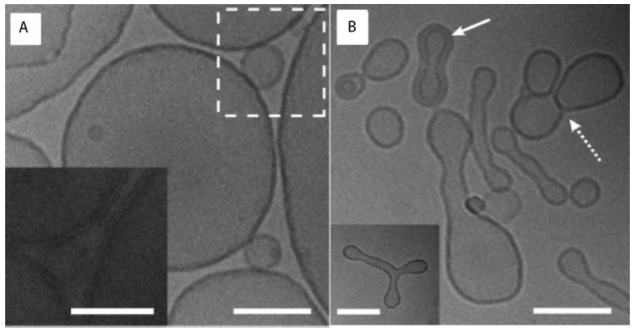

Figure 246. Cryo-TEM images of compound 10 in (a) trisEDTA buffer solution and (b) after the addition of DNA with the appearance of multilamellar vesicles (arrow) and the corresponding vesicle adhesion due to charged DNA (arrow with broken line) or branched vesicles (inset). Reprinted with permission from ref 852. Copyright 2007 American Chemical Society.

Dendron−DNA conjugates were synthesized either by covalent connection of the dendritic structure to the oligonucleotide chain or by noncovalent interactions such as hydrogen bonding (hybridization) or ionic interactions (complexation). Negatively charged DNA binds to polycationic structures based on either PAMAM,[135,878−881] PEI,[882−885] PPI,[886] or PLL[887−891] dendrons. Other dendritic structures reported for DNA complexation contained either polycationic phosphorus dendrimers,[892] triply branched spermine dendrimers,[893,894] or modified amphiphilic triply branched Newkome dendrons.[705,850,892] Complexes of DNA and dendritic structures, named dendriplexes,[895] like analogous DNA/liposome, lipoplexes,[896−898] and DNA/polymer complexes, polyplexes,[134,139,146,877] are important tools for gene delivery. Release of the DNA from the complex can be difficult when strong interactions between the DNA and the dendron are

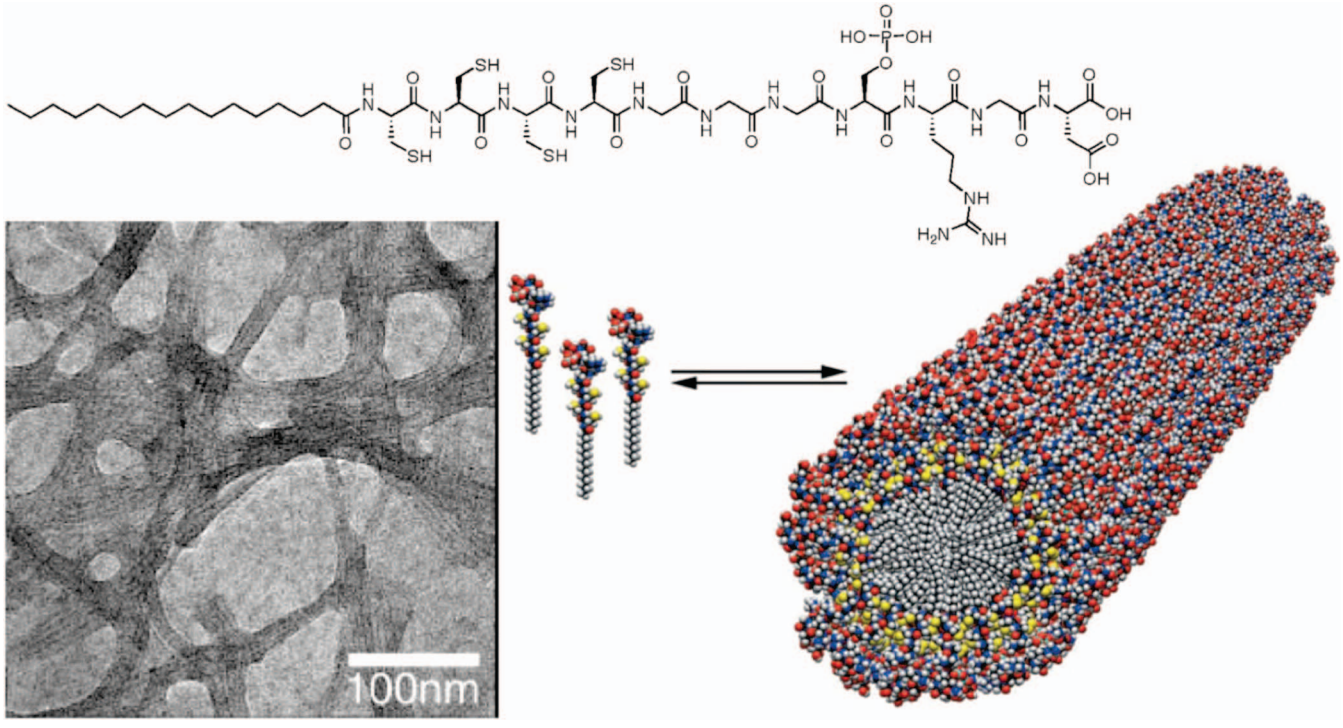

Figure 247. Chemical structure, TEM, and schematic representation of the self-assembly of peptide-amphiphile molecules. Reprinted with permission from ref 858. Copyright 2004 American Association for the Advancement of Science.

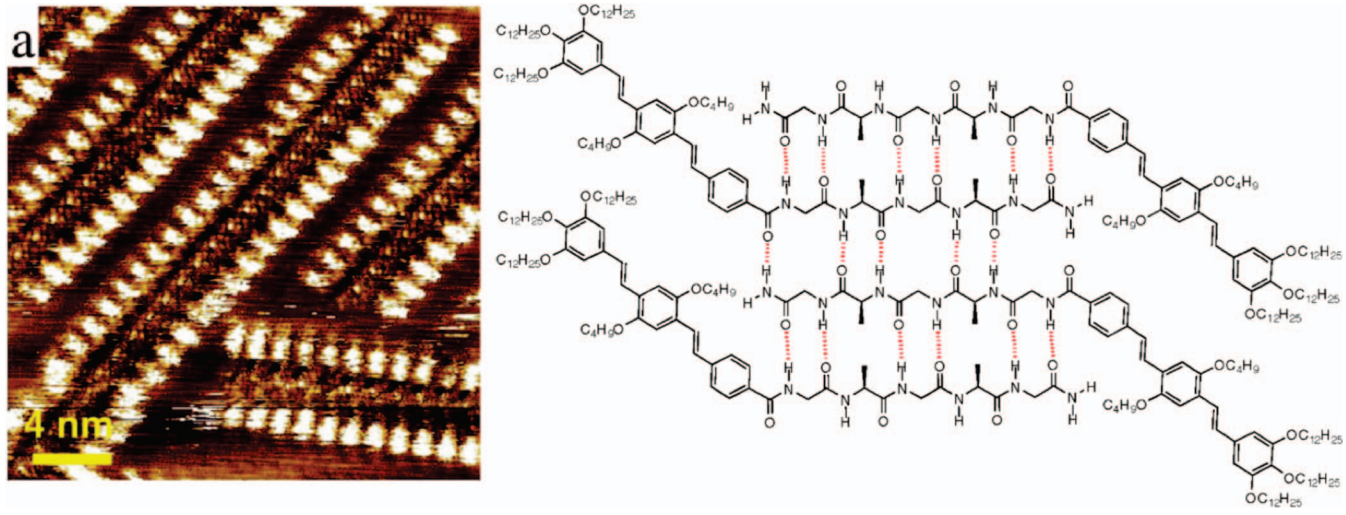

Figure 248. STM image of a dendronized peptide amphiphile at the liquid−solid interface of 1-octanoic acid and highly oriented pyrolytic graphite (HOPV) and the β-sheet formation by H-bonding between the peptide segments. Reprinted with permission from ref 861. Copyright 2008 American Chemical Society.

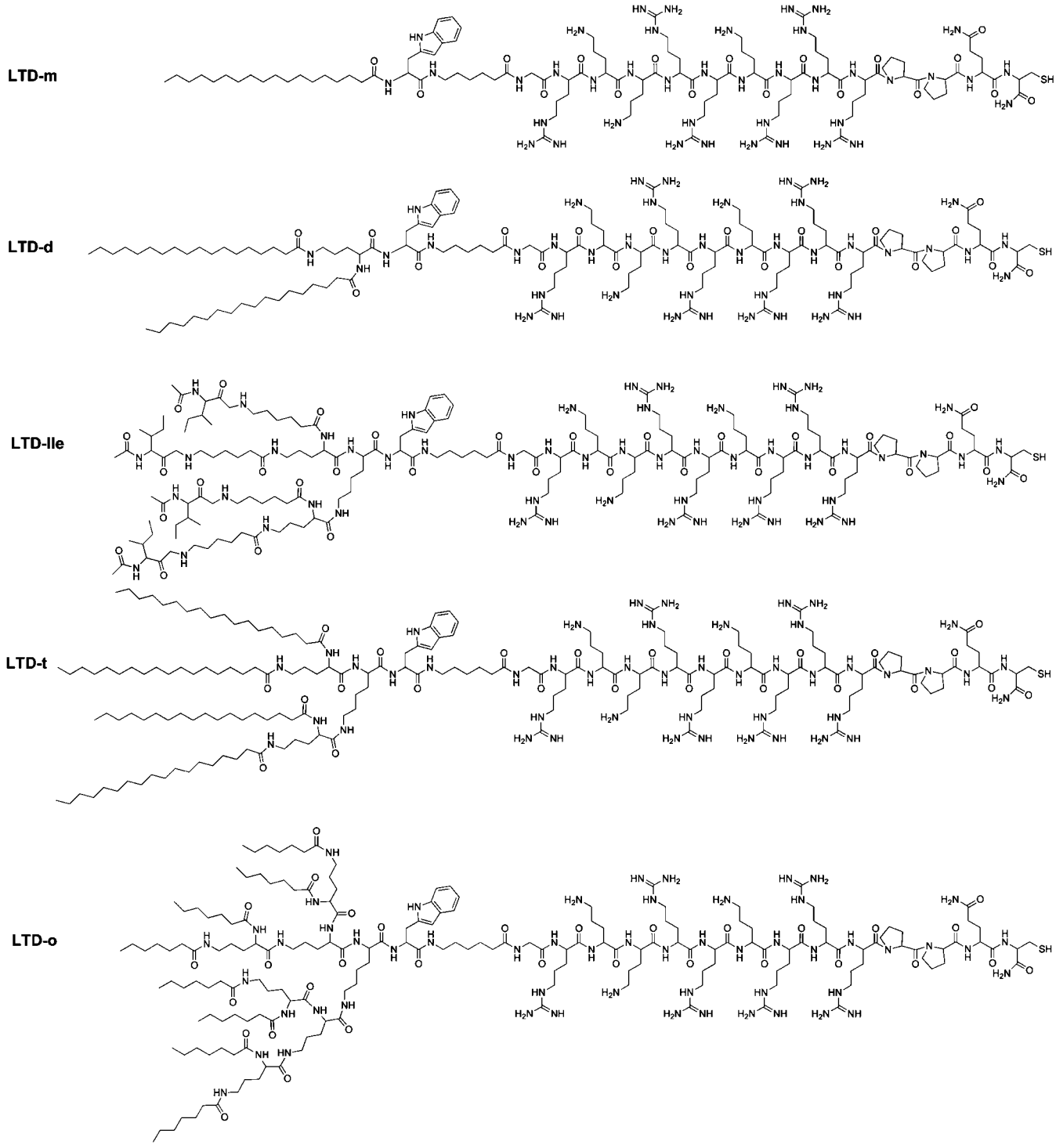

Figure 249. Dendron−peptide conjugates reported by Lee.[862]

present, resulting in low DNA transfer into the cell (low transfection efficiency).[899,900]

To overcome this problem, Konstiainen and Smith reported a series of photocleavable dendrons based on spermine chains connected to the dendritic structure through *o*-nitrobenzyl units (Figure 256a).[899] Degradation of the ester linkage to the *o*-nitrobenzyl unit under UV irradiation resulted in a controlled release of the DNA through the removal of the DNA-binding spermine groups from the surface of the dendron (Figure 256b,c). Generation 1 and 2 dendrons were found to bind DNA efficiently by electrostatic interactions and rapidly release the target under long-wavelength UV irradiation (λ = 350 nm).[899] Later, Kostiainen reported reduction-triggered release of PLL dendrons from DNA. Here, the oligo(spermine) units were attached to the periphery of PLL through a disulfide linkage.[901]

Several topologies may result from covalent interactions between dendrons and DNA (Figure 257, structures 2 and 5), as well from the hybridization process between dendritic structures containing sense and antisense DNA sequences (Figure 257, structures 3, 4, 6, and 7).

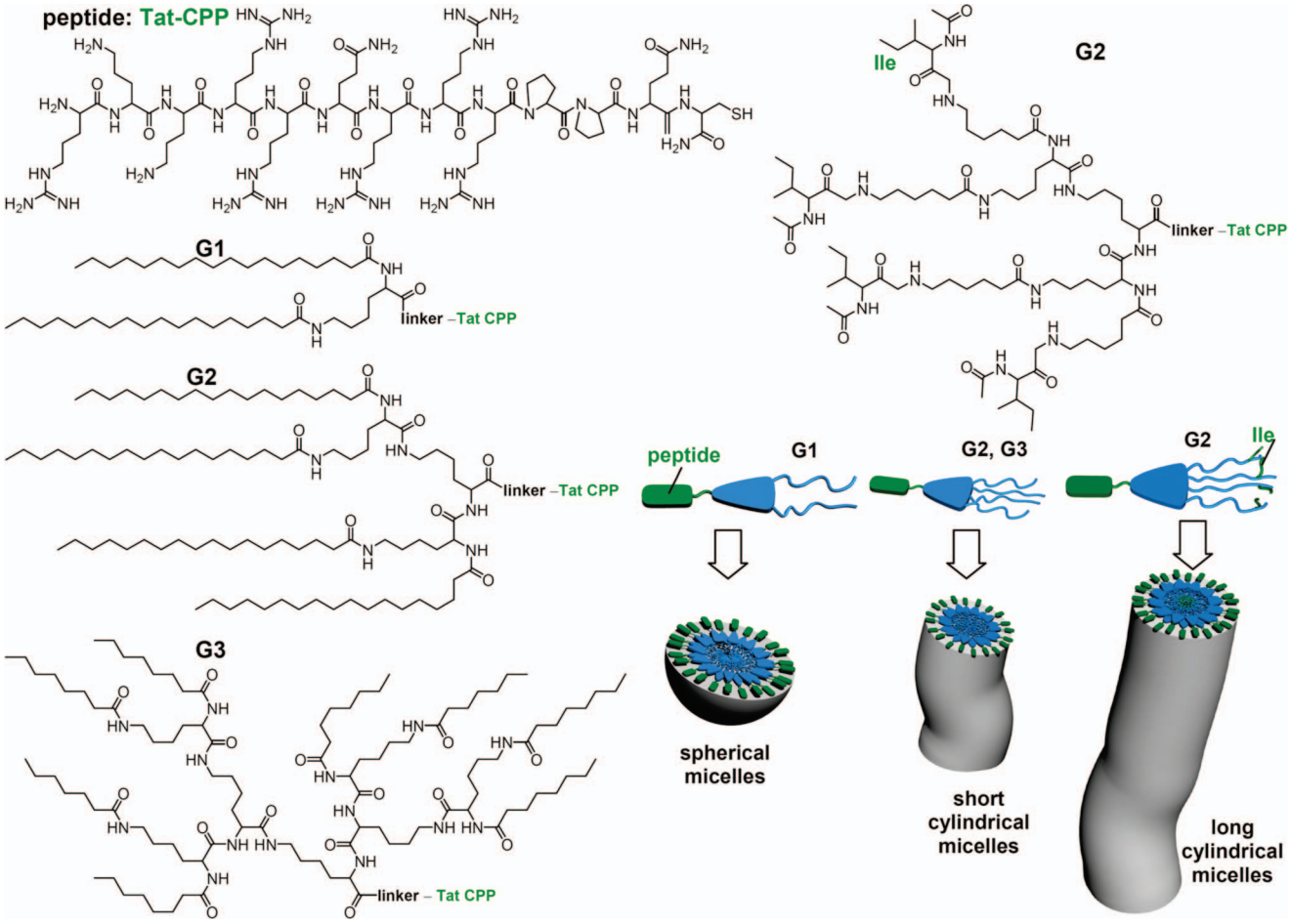

Figure 250. Self-assembly of chain-end dendronized Tat CPP. Adapted from ref 862.

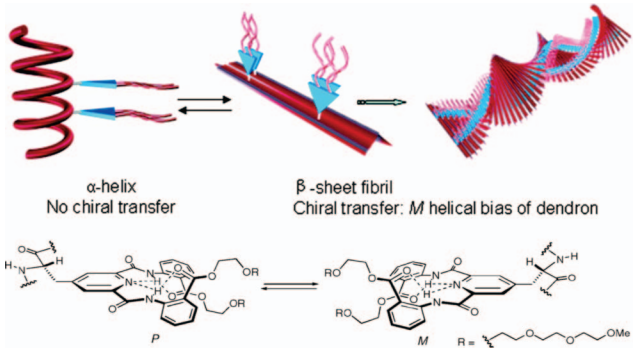

Figure 251. α-Helix and *β*-sheet fibril structures produced from doubly dendronized *β*-sheet forming peptides (top). *P* and *M* conformations of the pendent dendrons (bottom). Reprinted with permission from ref 864. Copyright 2007 American Chemical Society.

Damha reported in 1993 the first nucleic acid dendrimer (Figure 257, structure 1) by using a three-step convergent-growth procedure (Figure 258).[902] The first step involved the automatic solid-phase synthesis of single-stranded oligonucleotides on the surface of controlled-pore glass (CPG) with an automatic DNA synthesizer. In the second step, two adjacent oligonucleotide chains were coupled together to form a branching point using tetrazole-activated adenosine 2′,3′-bis(phosphoramidite). Finally, G1−G3 dendritic oligonucleotides were obtained by repetitive chain elongation and branching followed by cleavage of the dendrimer from the support.

Scheme 63. Synthesis of Dendron Helical Polypeptides[866]

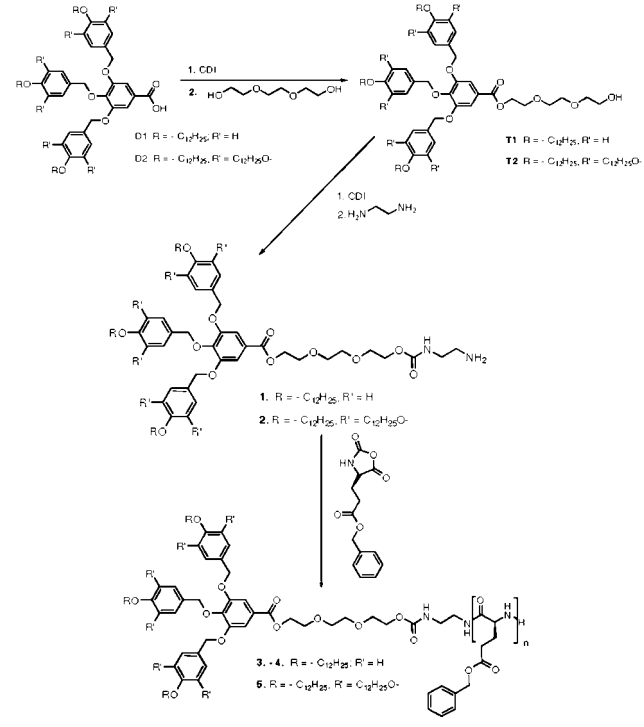

Damha also reported a divergent approach to the synthesis of nucleic acid dendrimers. Yields were expected to be higher

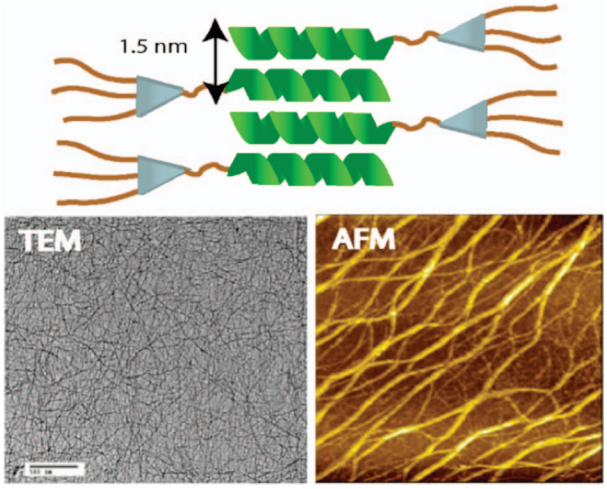

Figure 252. TEM and AFM images of nanoribbons formed and their schematic representation reported. Reprinted with permission from ref 866. Copyright 2006 Royal Society of Chemistry.

by removing the steric constraints present in the convergent approach.[903] Self-assembly of these structures was not reported.

Several groups reported the synthesis of dendron−oligonucleotide conjugates and their use as antisense oligonucleotide carriers, though their self-assembly was not thoroughly investigated.[259,904−908] In all cases, the solid support strategy was used for the growth of the oligonucleotide chain, either from a branching point, when the oligonucleotide was part of the dendritic structure (Figure 259),[904,905,907] or from a linear chain that was further attached to the dendron.[906,908]

Fréchet and Tomalia reported the synthesis and self-assembly of dendron−DNA conjugates based on polyester[259] and PAMAM dendrons, respectively.[906] The dendritic structures were connected to appropriate cDNA sequences (sDNA) that can further self-assemble through hybridization into well-defined double-helical supramolecular structures (Figure 260). The hybridized products were identified by polyacrylamide gel electrophoresis (PAGE), MALDI-TOF, and melting experiments. Dendrimer−DNA conjugates were reviewed recently[125] and will not be discussed in great detail.

4.2.3. Poly(saccharide)s and Oligo(saccharide)s Dendronized at Their Chain Ends. Dendron−Oligosaccharide Conjugates

Carbohydrates are one of the most abundant of the four classes of biomolecules, nucleic acids, proteins, lipids, and carbohydrates, and have the highest capacity to store information due to their high-density coding system.[115,117−119] Carbohydrates transfer information through molecular recognition by proteins called lectins or by other oligosaccharide molecules, enzymes, or antibodies. However, investigations have shown that such ligands and receptors exhibit weak binding affinities in cell-recognition processes.[909] The binding capacity is substantially enhanced through polyvalent interactions. Carbohydrates play an important role in bacterial and viral infections. They constitute the first contact for adhesion and tissue colonization by several pathogens expressing lectins.[910] Pathogens often bypass the recognition of the immune system by using self-carbohydrate structures to mask important receptors or antigenic determinants. For example, binding of the hyperbranched high mannose oligosaccharide ($Man_9GlcNAc_2$) present on HIV gp120 by

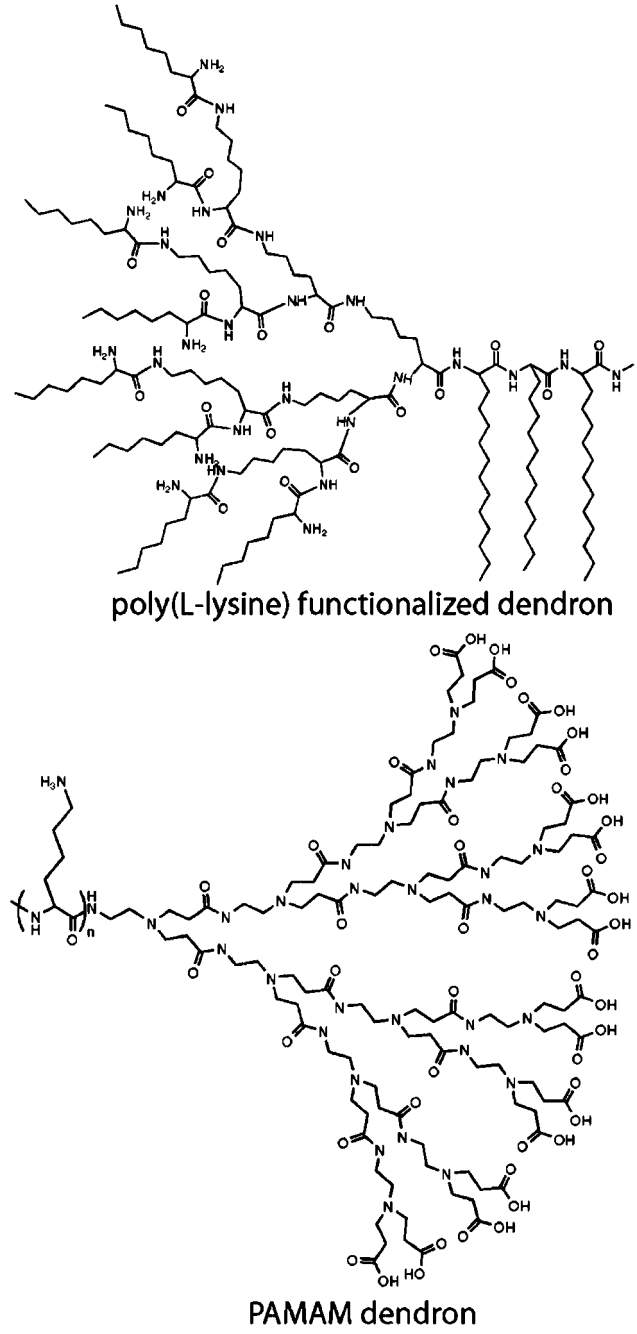

Figure 253. Amphiphilic dendron−peptide conjugates for vesicle formation.

dendritic cells allows for transport of the hidden HIV virus to the lymph nodes (Figure 261).[116,910]

The higher affinity of multisite carbohydrates to receptors as compared to simple monosaccharides indicates that the design of specific geometric arrangements of multiple sugar residues can provide access to materials with enhanced molecular recognition. Dendrimers and dendrons can be designed to incorporate multiple periphery sites for functionalization with carbohydrate units. Therefore, dendrimers and dendrons are ideal scaffolds for the synthesis of complex multicarbohydrate-containing architectures (sugar balls[911] or glycodendrimers[31,114,120,910,912−923]), dendrons (glycodendrons)[924−929] and their conjugates with peptides (glycopeptides)[930−937] which can potentially be used as antimicrobials and anti-inflammatory agents,[938−944] potential

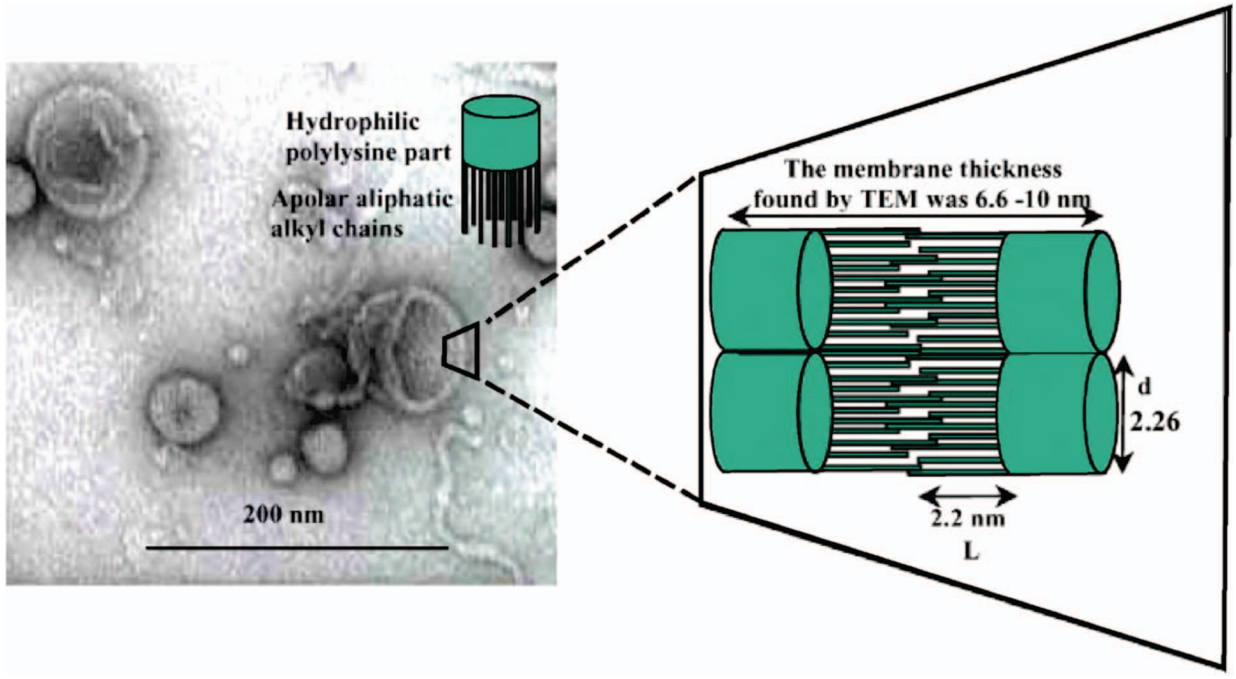

Figure 254. TEM of dendrisomes prepared by reverse-phase evaporation technique (left) and representation of the bilayer structure determined from molecular modeling. Reprinted with permission from ref 874. Copyright 2003 Elsevier.

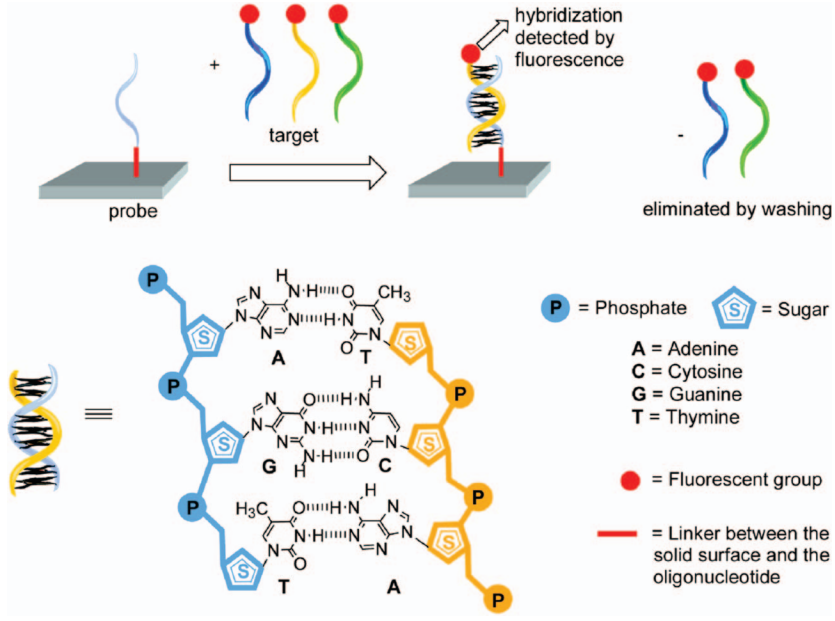

Figure 255. Principle of DNA chip or DNA array. Reprinted with permission from ref 124. Copyright 2007 MDPI.

vaccines,[928,945−949] glycomimetics[115,950] or as fluorescent probes in imaging.[926,951]

Roy reported the synthesis of homo- and heterobifunctional dendron−carbohydrate conjugates functionalized with up to 16 fucoside and/or galactoside residues (Scheme 64).[952] G1−G3 dendrons are prepared via a convergent approach. The periphery unit was synthesized via saponification of methyl 3,5-bis(2-azidoethoxy)benzoate. Higher-generation dendrons were generated by first reducing the periphery azide of methyl 3,5-bis(2-azidoethoxy)benzoate followed by coupling of the free amine termini with the periphery 3,5-bis(2-azidoethoxy)benzoic acid in the presence of benzotriazol-1-yloxy-tris(dimetylamino)phosphonium hexafluorophosphate (BOP). This process was repeated to achieve higher-generation dendrons. G1−G3 acid-apex dendrons were *endo*-functionalized at their periphery via amidation with $BocHN(CH_2)_3NH_2$ or converted to a twin dendrimer via bis(amidation) of 1,3-propyldiamine. Functionalization of the dendritic core with pro-2-ynyl α-L-(+)-fucose by CuAAC "click" approach provided fucoside-coated G1−G3 dendron−coil−dendron (Scheme 64). A similar approach was used to prepare D-galactose functionalized dendrimer.

The fucoside- and galactoside-functionalized dendrons were designed to specifically bind lectins found in *Pseudomonas aeruginosa*, a bacteria that afflicts immunocompromised and cystic fibrosis patients, and inactivate its cellular adhesion and prevent bacterial colonization. The two lectins localized

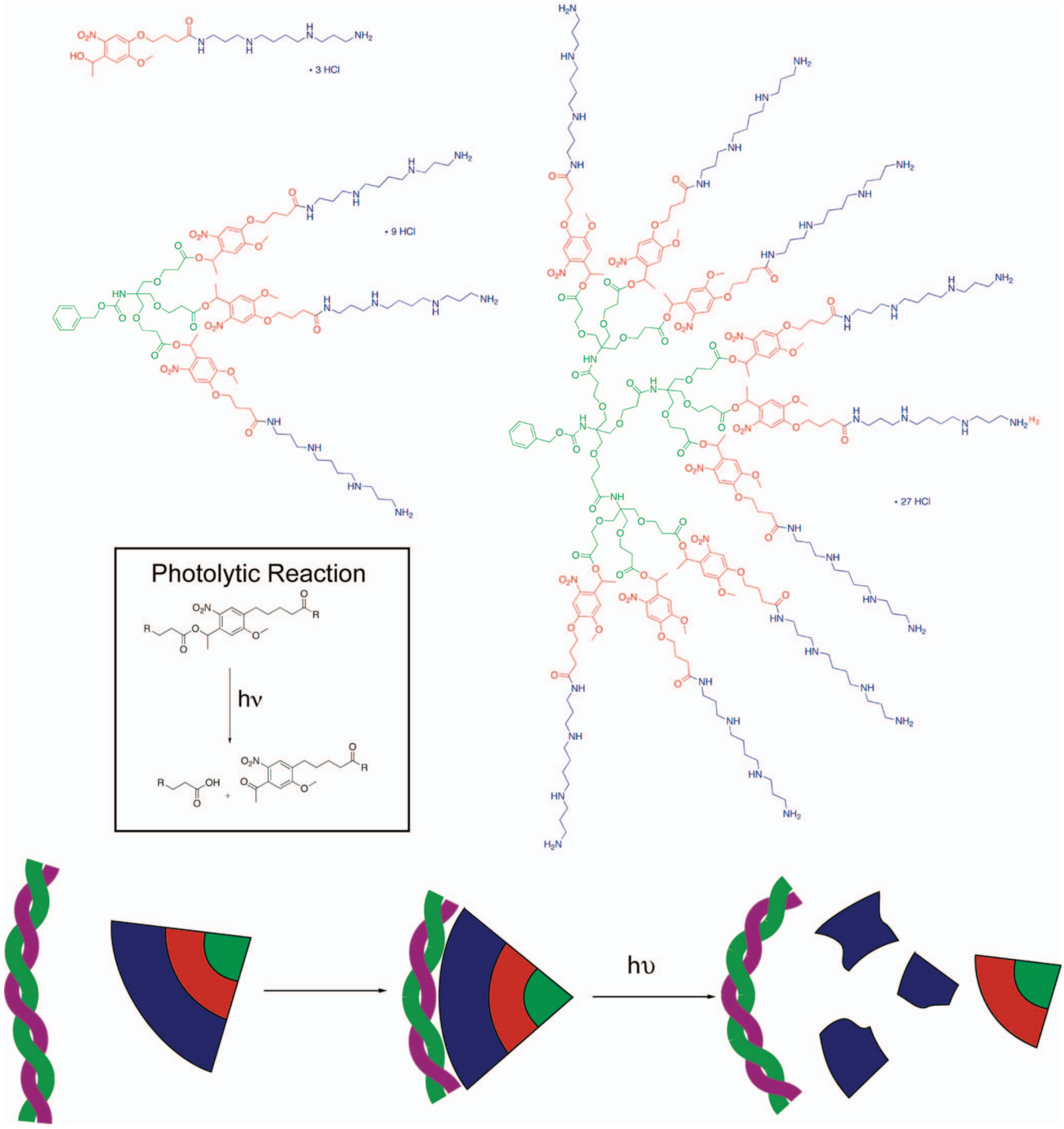

Figure 256. Photocleavable dendrons reported by Kostiainen and the products that resulted under photolysis (top). Representation of the release of DNA after decomplexation under UV irradiation (bottom). Adapted from ref 899.

on the outer membrane of the bacteria are specific for D-galactose and L-fucose. These synthetic glycoconjugates can block the cell adhesion by interacting with the lectins found in *Pseudomonas aeruginosa* bacteria. The relative binding and cross-linking abilities were determined by turbidimetric analysis. The densely glycosylated dendritic structures were found to rapidly bind the lectins conferring strong antiadhesion properties.

Lee and co-workers investigated triblock dendritic block molecules consisting of carbohydrates grafted-onto wedge-shaped aromatic units (Scheme 65).[793] The carbohydrate periphery enhanced water solubility and provided selectivity for bacterial cells. Glycosylated oligo-ether dendrons were prepared through the monoglycosylation of ethyleneglycol with commercially available peracetylated bromo-D-mannose, exchange of the acetyl protecting groups for a base-stable benzyl groups, and divergent etherification onto an oligo-ether dendron. The rigid aromatic segment was synthesized by successive Suzuki cross-coupling, onto which was grafted the dendritic glycoconjugate.

Investigation of the self-assembly behavior in bulk by TOPM, DSC, and XRD analysis demonstrated alkyl-tail length self-organization into Φ_h and S phases. The dendritic glycoconjugate containing an apex methoxy group self-

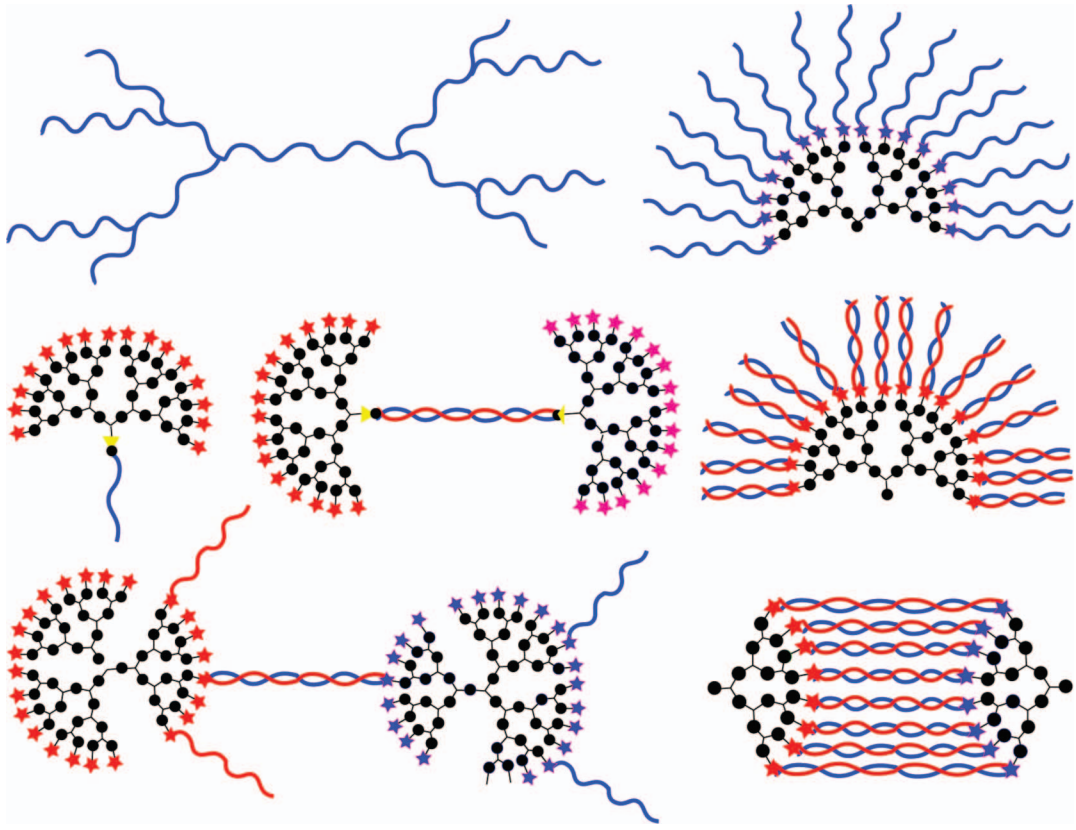

Figure 257. Topologies observed in dendritic−oligonucleotide conjugates. Adapted from ref 125.

assembles into carbohydrate-coated cylinders that self-organize into a Φ_h lattice (Figure 262). The dendritic glycodendron with long alkyl chain apex groups self-assembles into sheets that self-organize into an S phase. Comparison of extended molecular lengths versus layer lengths derived via XRD demonstrated interdigitation (Figure 262).

Investigation of the dendron−carbohydrate conjugates in aqueous solution by DLS, TEM, and fluorescence microscopy showed the self-assembly of both short- and long-chain terminated dendritic glycoconjugates in cylindrical micelles with uniform diameter of about 8−9 nm and length of several hundred nm. Addition of hydrophobic Nile red guest molecules to the wormlike micelles changed the cylindrical aggregates into spherical micelles (Figure 263). This effect was reversible, as removal of the guest molecules by extraction induced the change from spherical to cylindrical micelles. The entrapment of the guest molecule inside the micelle was mediated by strong hydrophobic interactions/low solubility of the guest in water and $\pi-\pi$ stacking between the guest and the amphiphilic molecule (Figure 264).[793]

Further investigation of the interaction of dendron−carbohydrate conjugates with bacterial cells such as *E. coli* showed the ability of both mannose-coated self-assembled structures to behave as multivalent ligands capable of binding to specific receptors on the cell surface. The size and the shape of the supramolecular architecture had a significant effect on the biological activity, resulting in different binding capacity to the *E. coli* cell. The spherical micelles were too short to cross-link to the pili of *E. coli*, only providing a limited effect on cell motility. However, the large cylindrical nanostructures exhibited a stronger binding and greater effect on cell motility.

Lee reported the synthesis and self-assembly behavior of carbohydrate-based dendrons attached to a β-sheet peptide block (Figure 265).[953,954] The conjugation of the polyvalent glycodendrons with β-sheet forming peptide blocks allowed the study of bacterial cell interaction on the self-assembly of β-sheet peptide conjugates into nanostructures.

A combination of CD/UV−vis, IR, DLS, TEM, and AFM revealed self-assembly into 1D-ribbonlike nanostructures. The size of the nanostructures was also dependent on the size of the dendritic structures. Bulky dendron attached to the peptide block (GP2) formed short nanostructures due to the steric crowding, while smaller linear coil−block molecules (GP1) self-assembled into long nanostructures (Figure 265). The inner core of the nanoribbons contained bilayered β-sheet peptide domains, while the outer edges comprised the mannose and triethylene glycol segments. The peptide segments were found to stack perpendicular to the ribbon axis with an antiparallel β-sheet arrangement. *E. coli* cells showed an increase in agglutination and cell motility with size of the interacting self-assembled structure. Quantitative measurement of degree of agglutination showed that GP2 had significantly lower agglutination compared with GP1. This result suggested that the length of the nanoribbons is important in the formation of bacterial clusters. The bacterial clusters were found to be stable over several days of incubation. No agglutination was observed during this time. The process was also demonstrated to be reversible through the addition of specific competitors such α-methyl-D-mannopyranoside. Complete predisposal of the bacterial cells into their mobile state was observed at the addition of high

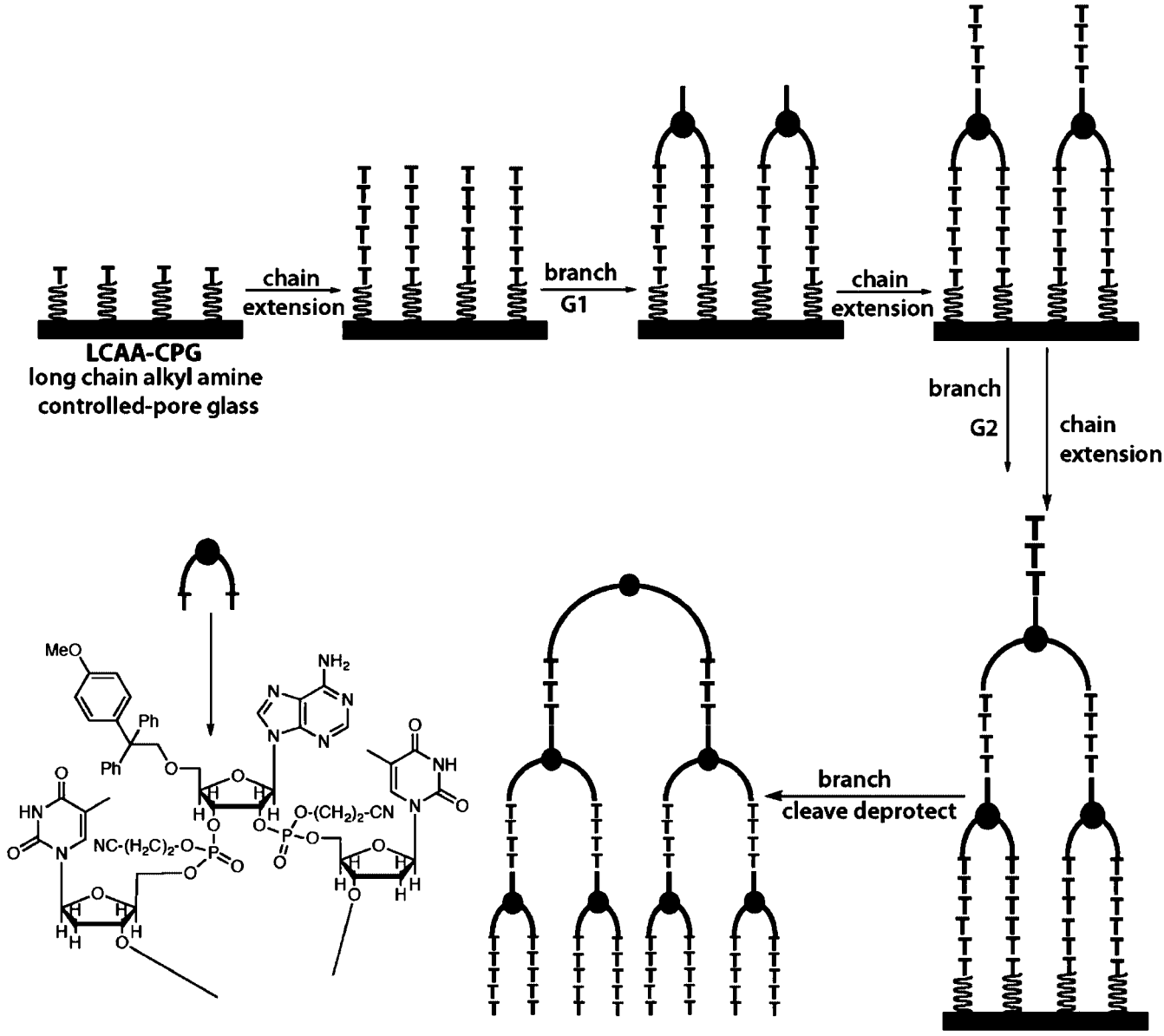

Figure 258. Schematic representation of the synthesis of nucleic acid dendrimer. Reprinted with permission from ref 902. Copyright 2003 American Chemical Society.

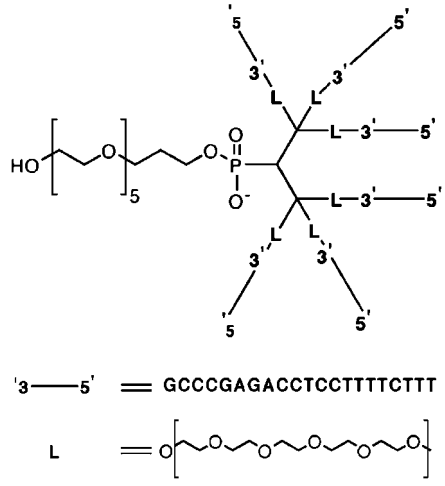

Figure 259. Dendron−DNA conjugate reported by Hussain.

concentrations of competitor over the agglutinated solution. Specificity of this binding process was demonstrated by the addition of a nonspecific competitor. In the presence of this competitor, no agglutination was detected. A mutant E.coli strain with knocked-out mannose-binding ability demonstrated the selectivity of the synthesized structures in the binding ability, as no agglutination or loss of motility was observed in this case with the knocked-out strain.

4.2.4. Solution-Phase Synthesis of Biopolymers Using Dendrons As a Chain-End Protecting Group and Solubilizer

While natural organisms can provide a variety of useful biopolymers, it is often essential to produce tailored oligonucleotide and oligopeptide sequences for biochemical studies or pharmaceutical applications. The laboratory synthesis of biopolymers with a specified sequence is a challenging process. As many useful biopolymers have high sequence lengths, nearly quantitative iterative procedures are required. Even a 99% yield per repeat unit would result in a 82% overall yield for a meager polymer of DP = 20, while a 90% yield per repeat unit would result in 12% overall yield. Additionally, the fidelity of the biopolymer sequence is

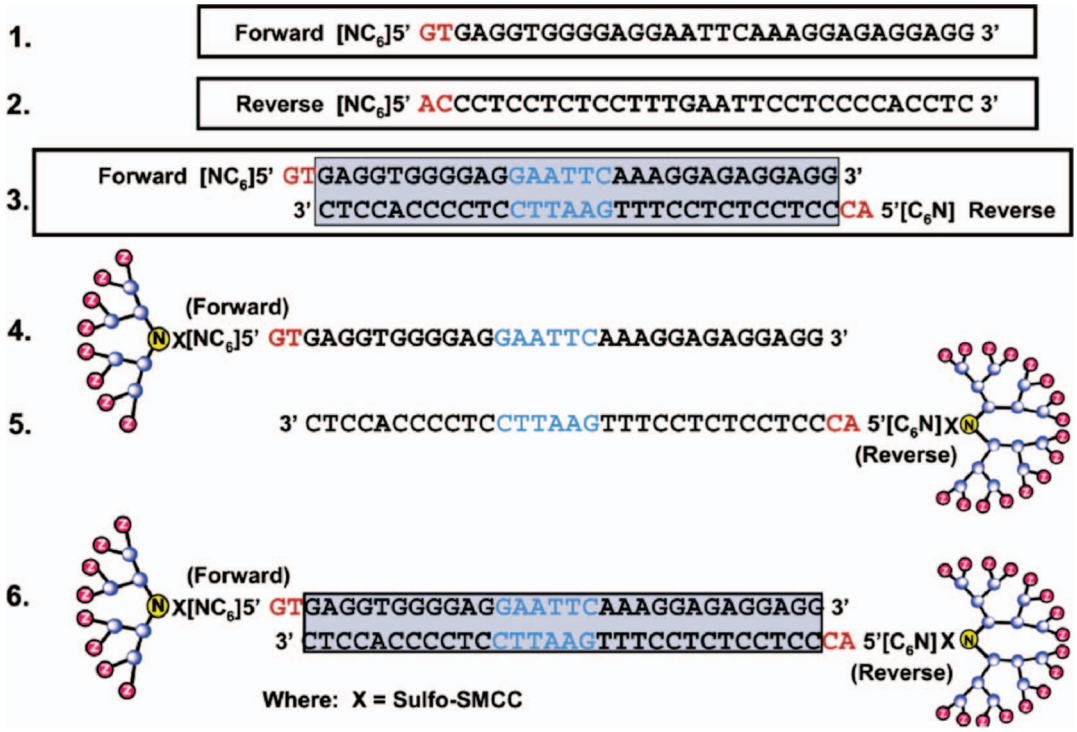

Figure 260. Schematic representation of dendron−DNA hybridization. Reprinted with permission from ref 906. Copyright 2004 American Chemical Society.

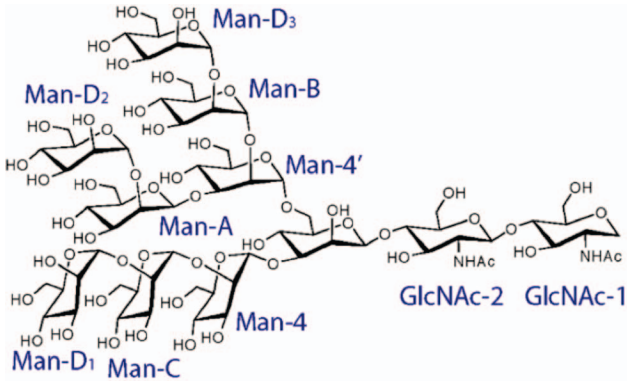

Figure 261. Hyperbranched high mannose oligosaccharide present on HIV gp 120.[910]

critical. Small changes in the sequence would result in drastically different molecular recognition and biological function. Thus, traditional solution-phase synthesis, where unreacted starting material must be removed via crude chromatographic techniques, is insufficient. As such, modern approaches to tailored biopolymer synthesis relies on either solid-phase synthesis (SPS) or solution-phase synthesis on fluorous or thermoresponsive support. In solid-phase synthesis, the growing chain is tethered to a macroscopic surface through a linker and subjected to iterative chain-expansion conditions.[955] As the growing chain can be easily removed from the reaction mixture, excess of highly reactive coupling reagents can be used. However, SPS suffers from difficulties at large scale and for reaction monitoring. In supported solution-phase synthesis, the temperature-dependent solubility of a support is used to facilitate simple isolation of the product, in this case, growing a polymer chain. Polymer support such as PEG or PNIPAM exhibit LCST behavior in water and some organic solvents, allowing for separation of the product as a solid.[956] Fluorous supports also allow for liquid−liquid extraction of the product via the fluorous phase.[290,957]

In 1963, Merrifield pioneered solid-phase peptide synthesis (SPPS) growing tetrameric peptide chains on a polymeric resin.[958] *t*-Boc protected amino acids were sequentially ligated using CDI as a coupling reagent. With only minor variation, this method is employed today for automated oligopeptide synthesis. In spite of the success of SPPS, there is still a need for effective solution-phase synthesis of oligopeptides. While many groups have focused on self-assembled structures obtained from dendron−peptide conjugates produced by conventional liquid- and solid-phase peptide synthesis, a few laboratories used dendrons to develop new synthetic methodologies.[959−962] Such methods included the synthesis of dendron−peptide conjugates through the combination of conventional ring-opening polymerization with click chemistry[960,961] as well as new techniques for peptide synthesis.[962] Tamiaki reported a new solution-phase concept for peptide synthesis. They simultaneously used G1−G2 Percec-type dendrons as C-terminus protecting groups and solubilizers in a new liquid-phase peptide synthesis (Scheme 66). (3,4,5)18G1−OH and $(3,4,5)^2$18G2−OH were prepared according to methods described by Percec.[314] The G1 dendritic alcohol was coupled to Fmoc-Ala−OH in 63% using 1-(3-dimethylaminopropyl)-3-ethylcarbodiimide (EDC) as a coupling reagent and 1-hydroxybenzotriazole (HOBt) as an additive. Efficient cleavage (92%) of the Fmoc group was achieved with piperidine. Use of Fmoc instead of *t*-Boc protecting groups allows for mild deprotection of the N-terminus without dendron cleavage. The process was repeated with Fmoc-Phe−OH and Fmoc-Leu−OH to achieve a tripeptide (Scheme 66). After each step, the oligopeptide attached to its dendron support could be isolated via size-exclusion chromotagrapy (SEC). After oligopeptide synthesis, the dendron must be removed. Three approaches to this cleavage were investigated: acidic conditions (HBr/AcOH or HCl/AcOEt) or H_2/Pd−C. Acidic

Scheme 64. Convergent Synthesis of Dendritic Core by "Click" Chemistry; Reagents: (i) LiOH, THF−H_2O; (ii) $BocHN(CH_2)_3NH_2$, BOP, DIPEA, DMF; (iii) Pd/C 10% H_2, MeOH; (iv) 4, BOP, DIPEA, DMF, $H_2N(CH_2)_3NH_2$; (v) BOP, DIPEA, DMF; (vi) $CuSO_4$, Sodium Ascorbate, THF, H_2O[952]

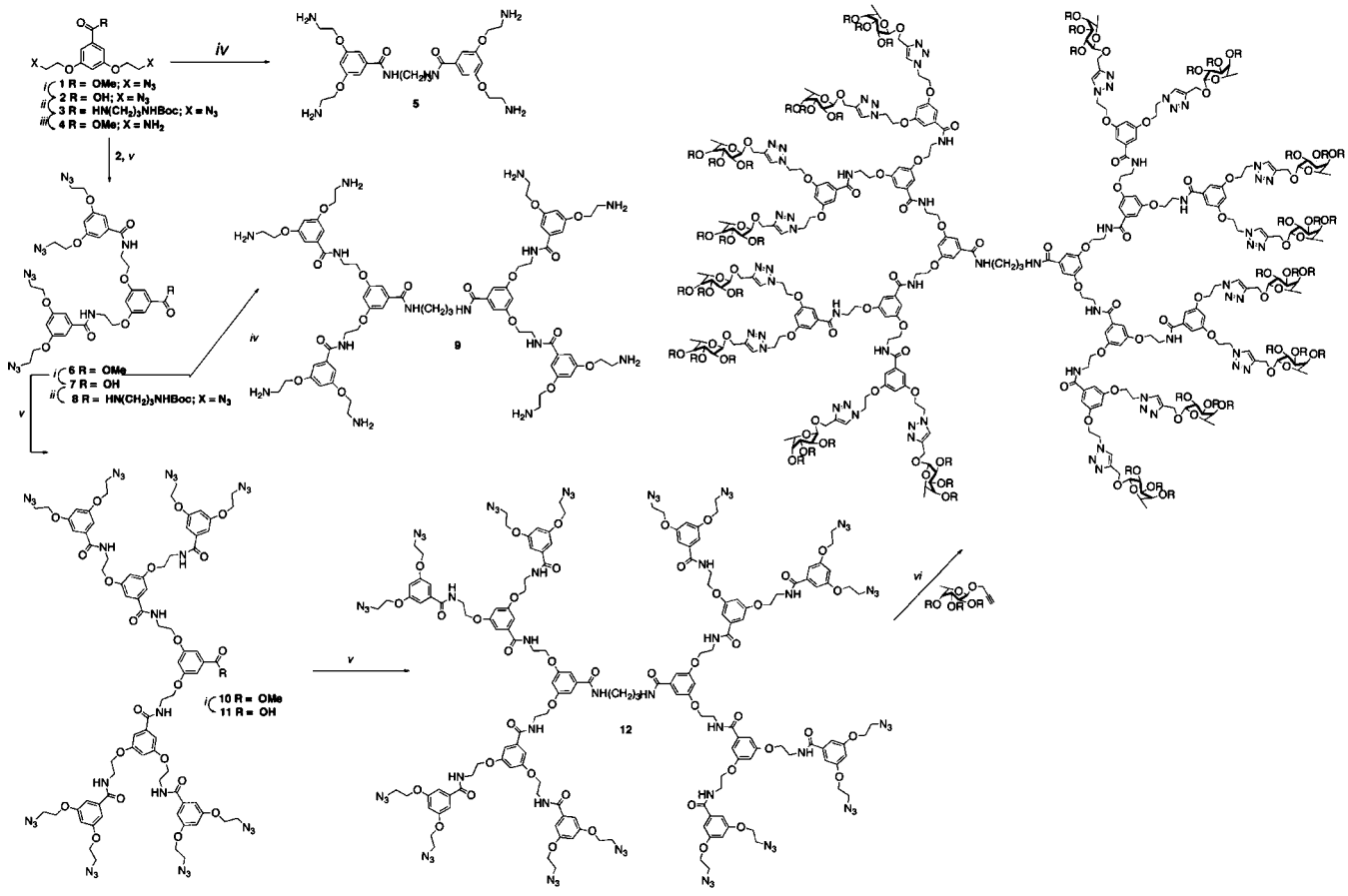

Scheme 65. Synthesis of Dendron−Carbohydrate Conjugate Reported by Lee[793]

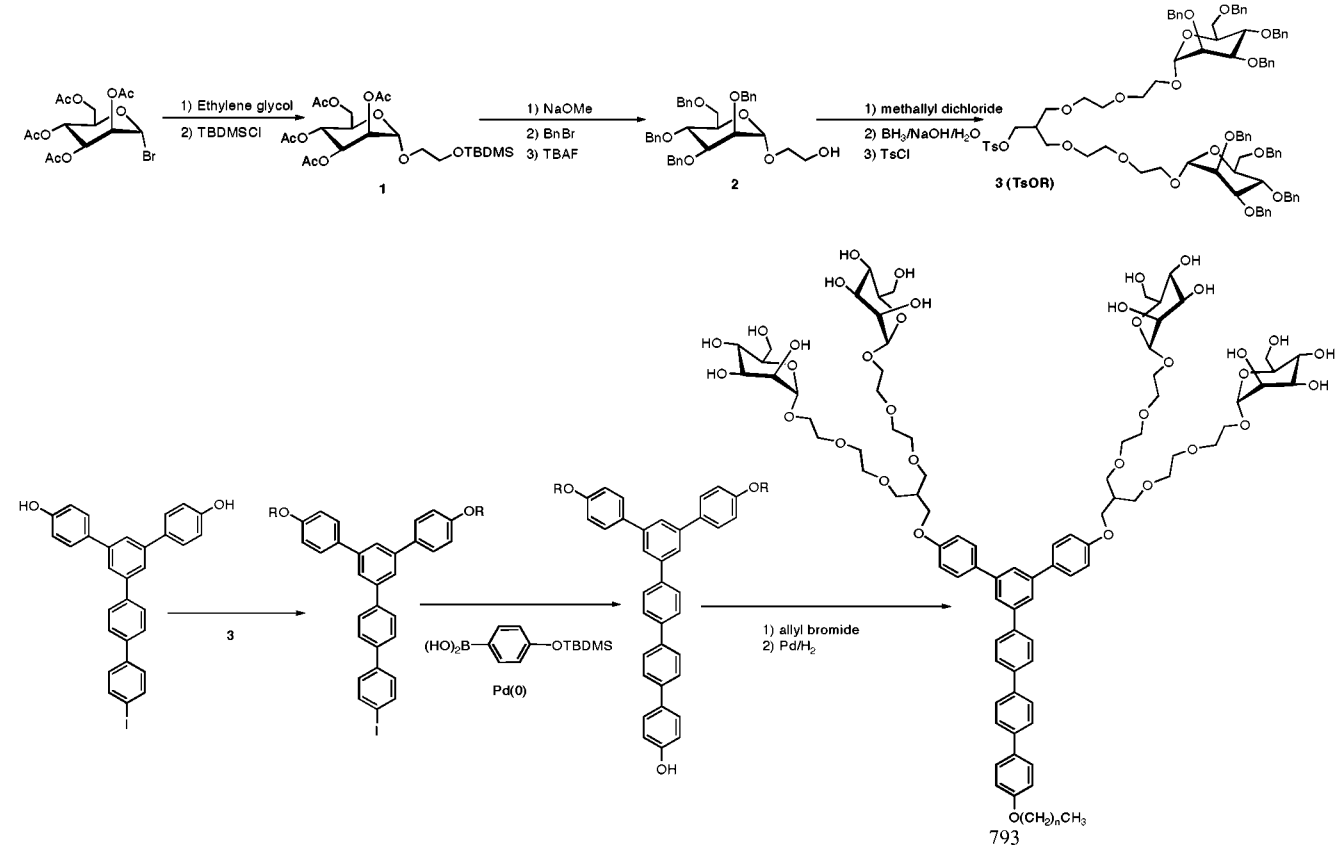

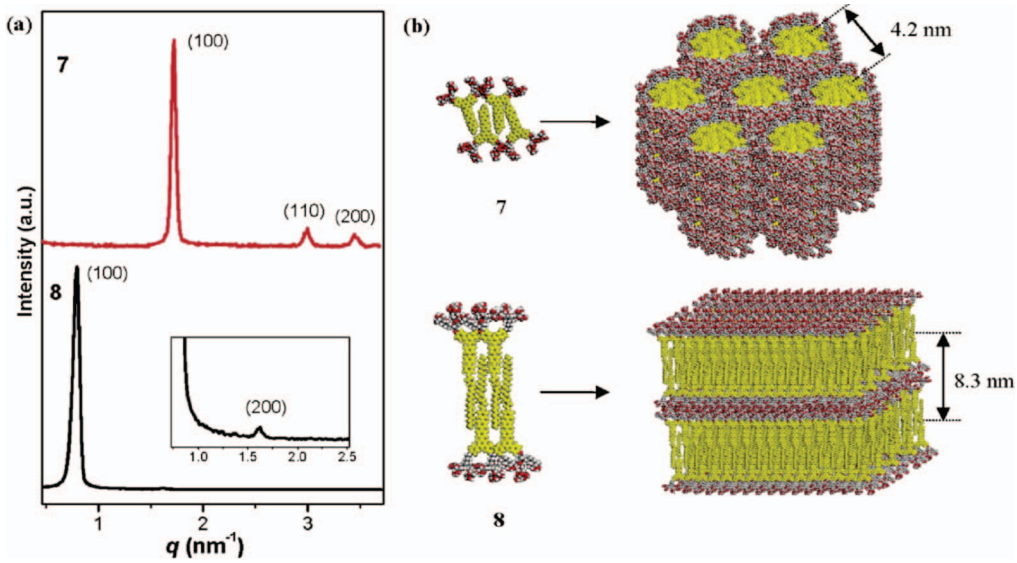

Figure 262. X-ray diffraction patterns (a) and representation of the self-assembly and self-organization of dendron−carbohydrate conjugates into Φ_h and S phases (b) reported by Lee. Reprinted with permission from ref 793. Copyright 2007 American Chemical Society.

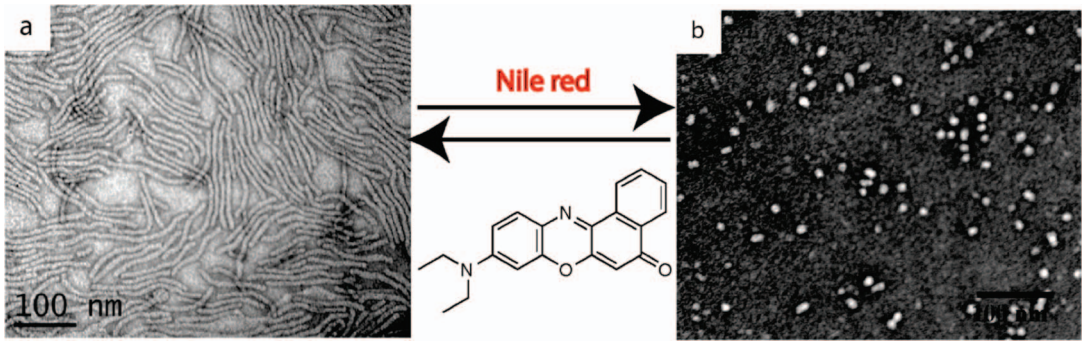

Figure 263. TEM images showing the transformation compound 8 (Scheme 65) from cylindrical to spherical micelles upon addition of Nile red. Reprinted with permission from ref 793. Copyright 2007 American Chemical Society.

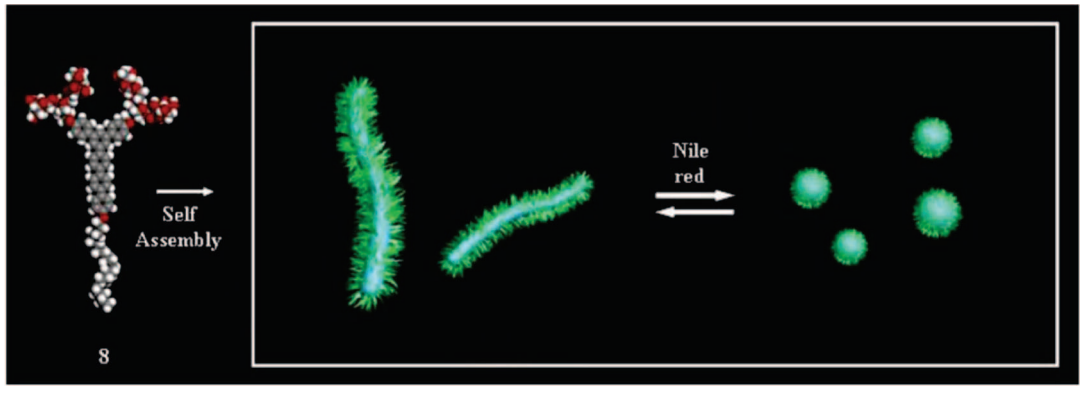

Figure 264. Schematic representation of the reversible transformation of cylindrical micelles into spherical micelles. Reprinted with permission from ref 793. Copyright 2007 American Chemical Society.

conditions quantitatively produced Fmoc-protected oligopeptide and regenerated (3,4,5)18G1−OH for further synthesis. Hydrogenation over Pd−C simultaneously removed the Fmoc group and the dendron. However, the hydrogenative cleavage of the dendron resulted in (3,4,5)18G1−H, which could not be used for further synthesis. No racemization of the peptide was observed during any of the deprotection. Additionally, higher-generation $(3,4,5)^2$18G2−OH was used as a solution-phase support, though with lower initial attachment yields (30%). While only dipeptides and tripeptides were reported and at relatively low yields, this approach demonstrates potential for dendrons as solution-phase supports for the synthesis of biopolymers and for other chemical transformations.

Typically, oligonucletoides are prepared through phosphoramidite chemistry.[963] In most modern and automated protocols, tritylated oligonucleotides are bound to PS beads, the 5′-hydroxyl group is detritylated and reacted with nucleoside phosporamidite. The resulting phosphorite triester is oxidized to the natural phosphate state. As with all solid-supported approaches, the phosphoramidite approach suffers from limited scale as well as difficulty in monitoring of

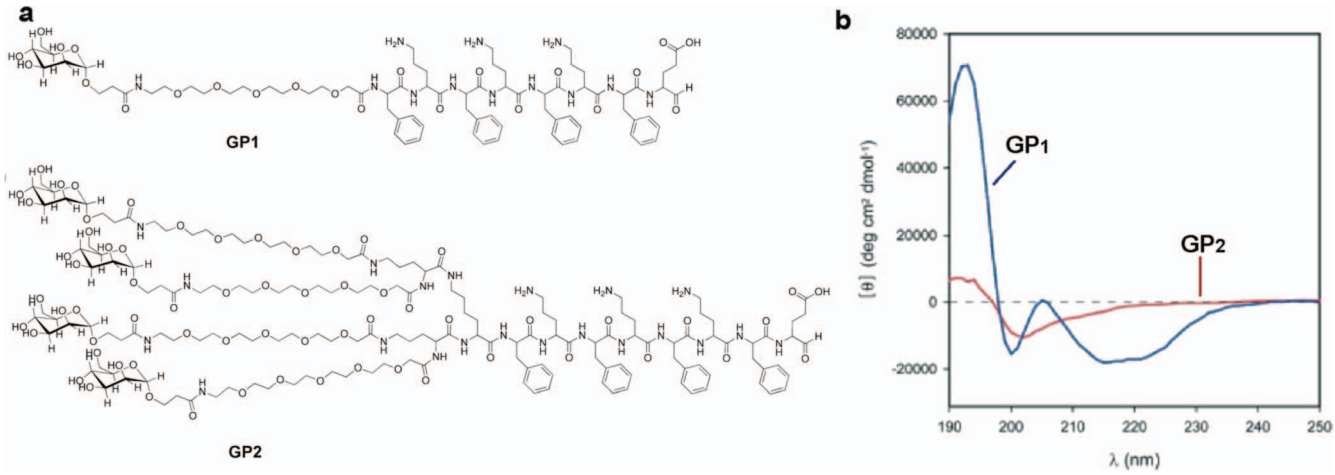

Figure 265. Structure and circular dichroism of glycoconjugates in water. Reprinted with permission from ref 953. Copyright 2007 American Chemical Society.

Scheme 66. Use of (3,4,5)^{2}18G2 Percec-Type Dendron As a Support for the Solution-Phase Synthesis of Polypeptides[962]

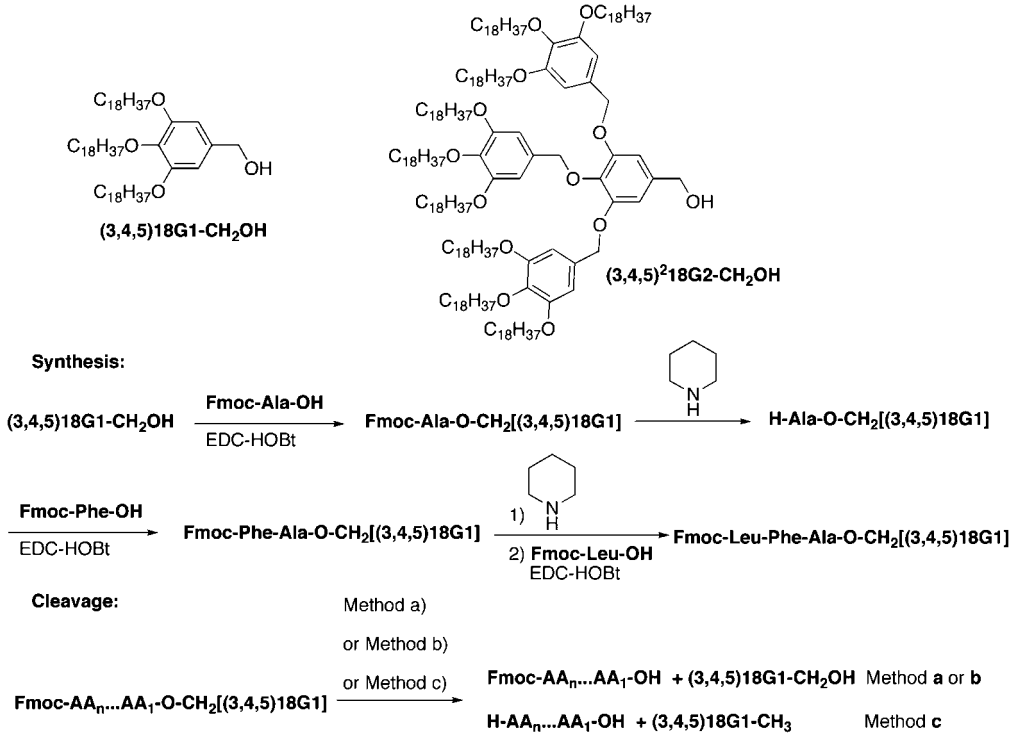

reaction progress. Wada has reported a new approach to nucleotide derivitives and oligonucleotides using fluorous dendrons as a solution-phase support and protecting group.[964−966] In the first example, Percec-type semifluorinated dendrons[367] were attached to Fmoc-Gly−OH using 2,4,6-collidine in a mixture of organic and fluorous solvents DMF/HFE-7100 in the presence of *o*-benzotriazole-*N*,*N*,*N*′,*N*′-tetramethyluroniumhexafluorophosphate (HBTU) or *N*-methyl-2-thiopyrrolidine (NMTP) as coupling agents (Scheme 67). The dendronized amino acid was purified by simple extraction with fluorous solvent perfluorohexane (FC-72), washing the fluorous layer with chloroform, and evaporation of FC-72. Removal of the Fmoc protecting group was achieved using 2% DBU in DMF. Coupling of the dendronized amino acid to thymidine nucleoside was achieved using similar 2,4,6-collidine, HBTU conditions in THF. This experiment demonstrated that Percec-type semifluorinated dendrons can be used as an alternative to solid-phase peptide synthesis (SPPS) protocol, especially for large-scale production and to monitor the reaction without terminating the synthesis. Additionally, it was determined that further chemistry of the oligonucleotide derivative was more effective when a linker was present between the bulky fluorous dendron support and the nucleotide derivative.

In a later patent application,[966] solution-phase synthesis of oligodeoxyribonucleotides was achieved using (3,4,5)11F8G1 and (3,4,5)^{2}11F8G2 supports (Scheme 68). In this iterative procedure, the fluorous support dendron is attached to the 3′-terminus of dimethoxy- or methoxytritylated nucleotide. The trityl group is removed using trifluoroacetic acid in perfluorhexane and another tritylated nucleotide is attached using 2-(benzotriazol-1-yloxy)-1,1-dimethyl-2-pyrrolidin-1-yl-1,3,2-diazaphospholidinium hexafluorophosphate (BOMP), bis(2-oxo-3-oxazolidinyl)phosphinic chloride (BOPCl), or 3-nitro-1,2,4-triazol-1-yl-tris(pyrrolidin-1-yl)phosphonium hexafluorophosphate (PyNTP) as a coupling reagent. At each step, the product is purified by fluorous phase separation.

Scheme 67. Synthesis of Fluorinated Dendron−Oligonucleotide Conjugate[964]

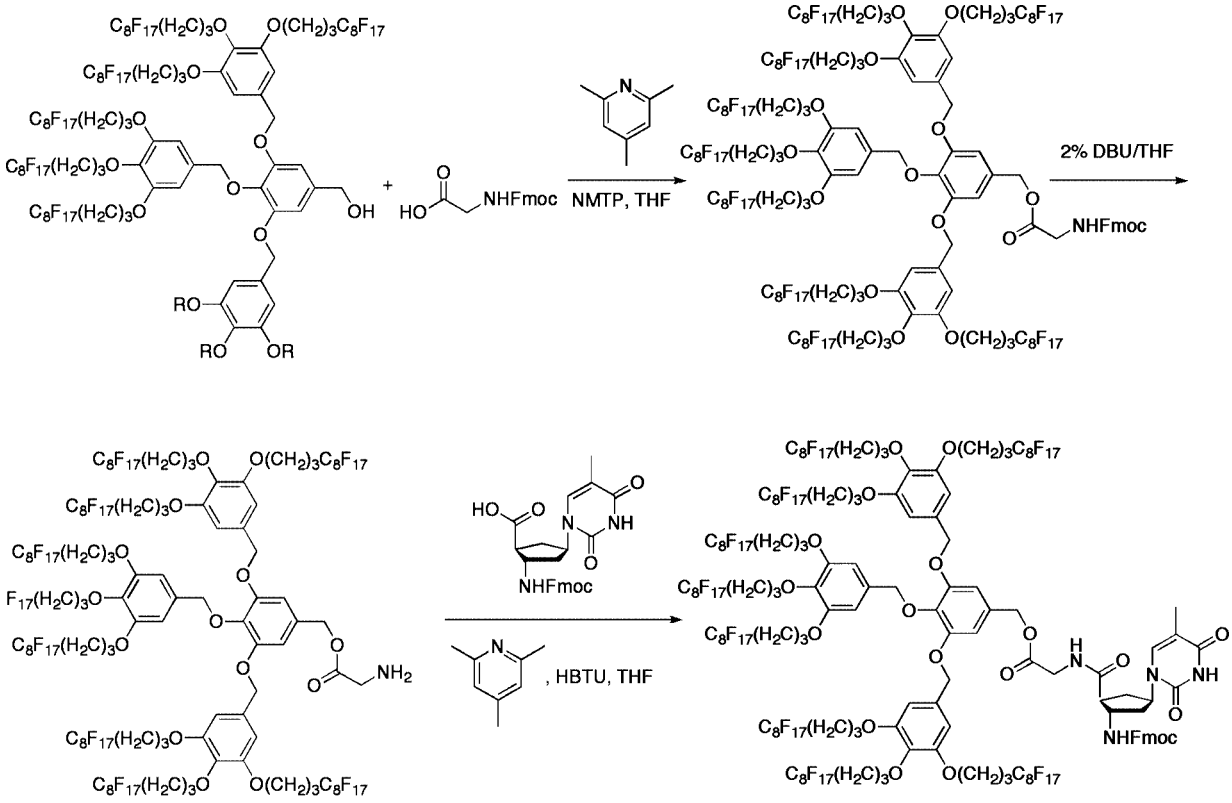

5. Dendronized Star Polymers

Dendronized star polymers (Figure 1, fifth row second from right) are a class of dendritic structures in which the dendrons are attached to a rigid or flexible core through three or more arms containing at least two monomer repeat units. Only star oligomers and polymers will be discussed. Some reference to representative star structures, which do not contain monomer repeat units between the focal point of the star and the dendron, will be made. Such structures can also be topologically classified as dendrimers, but their self-assembly mechanism is related to those of dendronized

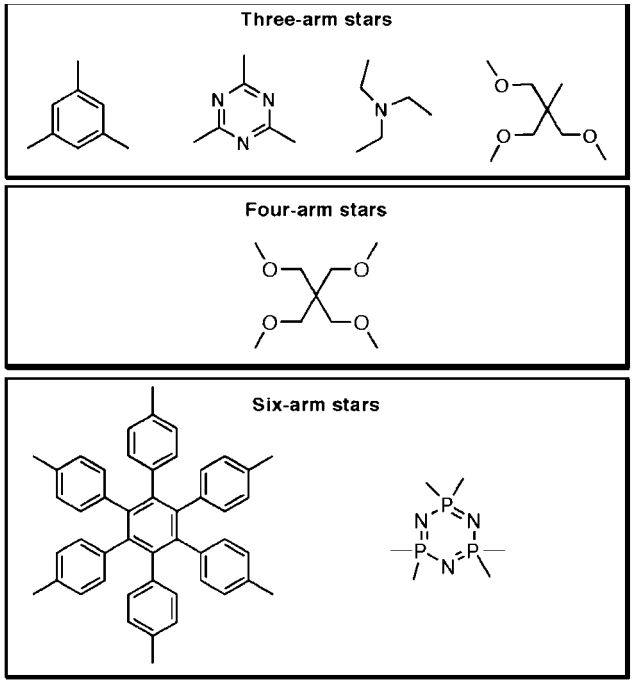

Figure 266. Different star topologies generated by the focal point of the star.

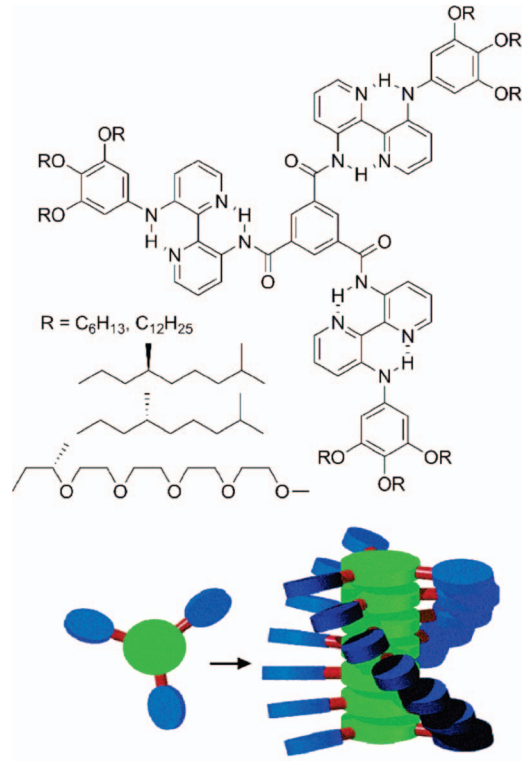

Figure 267. C_3 symmetric 3,3′-diacylamino-2,2′-dipyridine based dendrimer reported by Meijer. Reprinted with permission from ref 974. Copyright 2005 American Chemical Society.

Scheme 68. Fluorous Dendrons As Supports for Solution-Phase Synthesis of Oligopeptides[966]

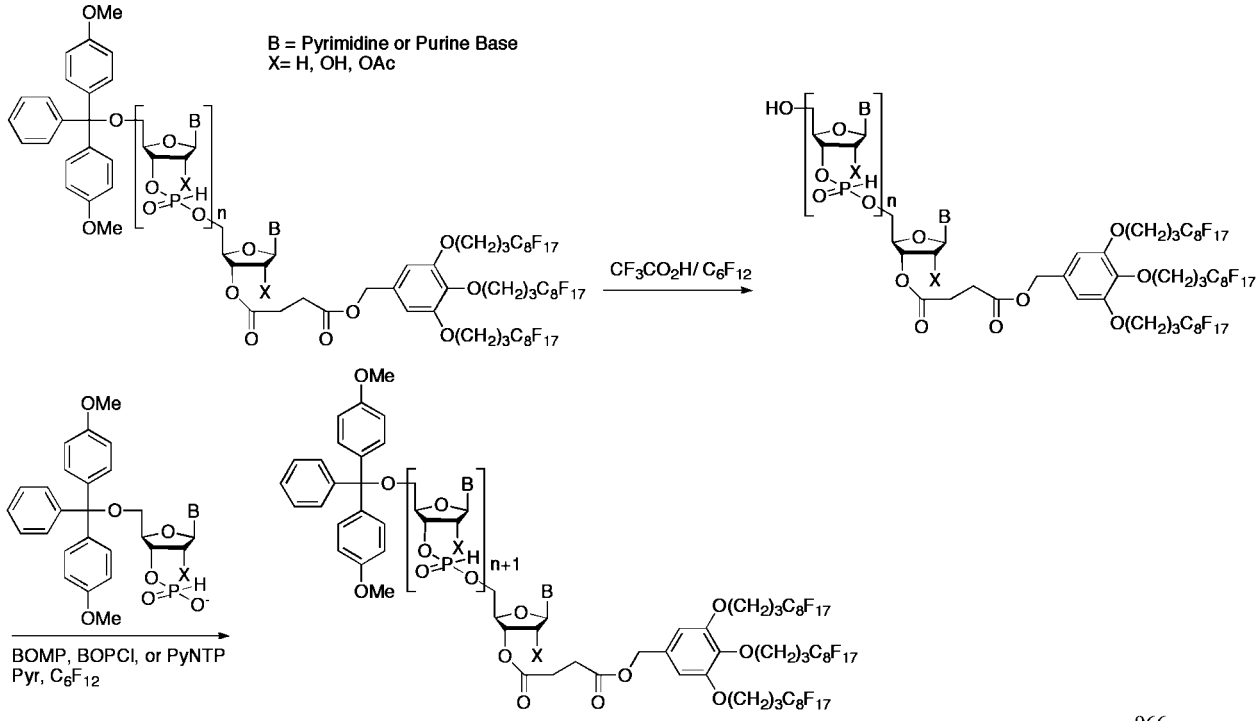

star polymers. Some of the earliest dendronized star polymers, benzyl ether dendrons attached to benzene hexanemethanol via a cyclotrimerization reaction, were reported by Fréchet.[967] Though no self-organization was observed in this example, often these molecules are constructed from conjugated cores or arms, which induce strong $\pi-\pi$ interactions. These interactions are often coupled with a symmetrical shape and a highly flexible geometry. The chemical nature of the core, the size of the structure, and its flexibility are important factors that dictate the self-assembly and self-organization of these molecules in different supramolecular architectures. Depending on the focal point of the star, self-assembly into three-, four-, or six-armed star polymers were reported (Figure 266). In many cases, the mechanism of self-assembly of dendronized star polymers can be viewed as a simplification of the self-assembly process of dendrons, in that the columnar strata are preformed via a covalent linkage at the core.

5.1. Dendronized Three-Armed Star Polymers

In 1993, Meijer reported the synthesis of chiral C_3 symmetric dendrimers[968,969] constructed from a 1,3,5-trisubstituted benzene core, a (3,4,5)*n*G1 periphery, and a 3,3′-di(acylamino)-2,2′-bipyridine linker (Figure 267).[970] These molecules exhibit a lyotropic N_c phase in dodecane solution[971] and Φ_h organization in bulk.[972] In the proposed model of self-assembly, the C_3 aromatic core forms a flat π-stacked column around which the dipyridine groups and pendent dendritic periphery groups form a titlted superhelix (Figure 267). Additionally, this C_3 dendrimer, as well as a library of related discotic molecules, forms organogels under certain conditions. Efficient transfer of chirality from the periphery of these molecules, mediated by intramolecular and intermolecular H-bonding and $\pi-\pi$ interactions, has been observed. Solution CD/UV−vis measurements have demonstrated that both "sergeant and soldiers"[973] and "majority rule"[974] apply.

Lehmann reported dendronized star polymers based on a phloroglucinol core and oligobenzoate arms with up to 4 monomer repeat units between the focal point of the star and the dendron (Scheme 69).[975−980]

The ester connectivity in these molecules provides structural flexibility. The unoccupied volume between the arms in the fully extended star-shape geometry coupled with the free rotation of the dendritic units around the C−O bond allow for the generation of different self-organized architectures (Figure 268).

TOPM, DSC, XRD, dilatometry, and solid-state NMR techniques were used to investigate the self-assembled structure in the bulk state. The symmetry of the dendronized star polymers and strong $\pi-\pi$ interactions between the aromatic units induced self-assembly into supramolecular columns that self-organize into Φ_h phases. However, the column diameter was considerably smaller than the diameter of the fully extended star-shape conformation (Figure 269). Several conformers were proposed for this molecule (Figure 269). An E-shaped conformation in the Φ_h was proposed as it minimizes empty space in the column. This conformation was confirmed by XRD of the helical crystal phase formed from the monotropic Φ_h phase after annealing at room temperature.[977,978]

Symmetrical dendronized star-shaped polymers self-organize at low temperatures in orthorhombic and body-centered phases, while at high temperatures, Φ_h phases are formed.[979] An increase of the length of the oligobenzoate arms resulted in an increase in the empty space for the planar star conformation and a decrease in the solid angle occupied by the E-shaped conformation. Lehmann also reported several structural variations of the dendronized star polymers by connecting different units to the phloroglucinol core and

Scheme 69. Synthesis of Symmetric (Left) and Asymmetric (Right) Dendronized Three-Armed Star Polymers[975,979,981]

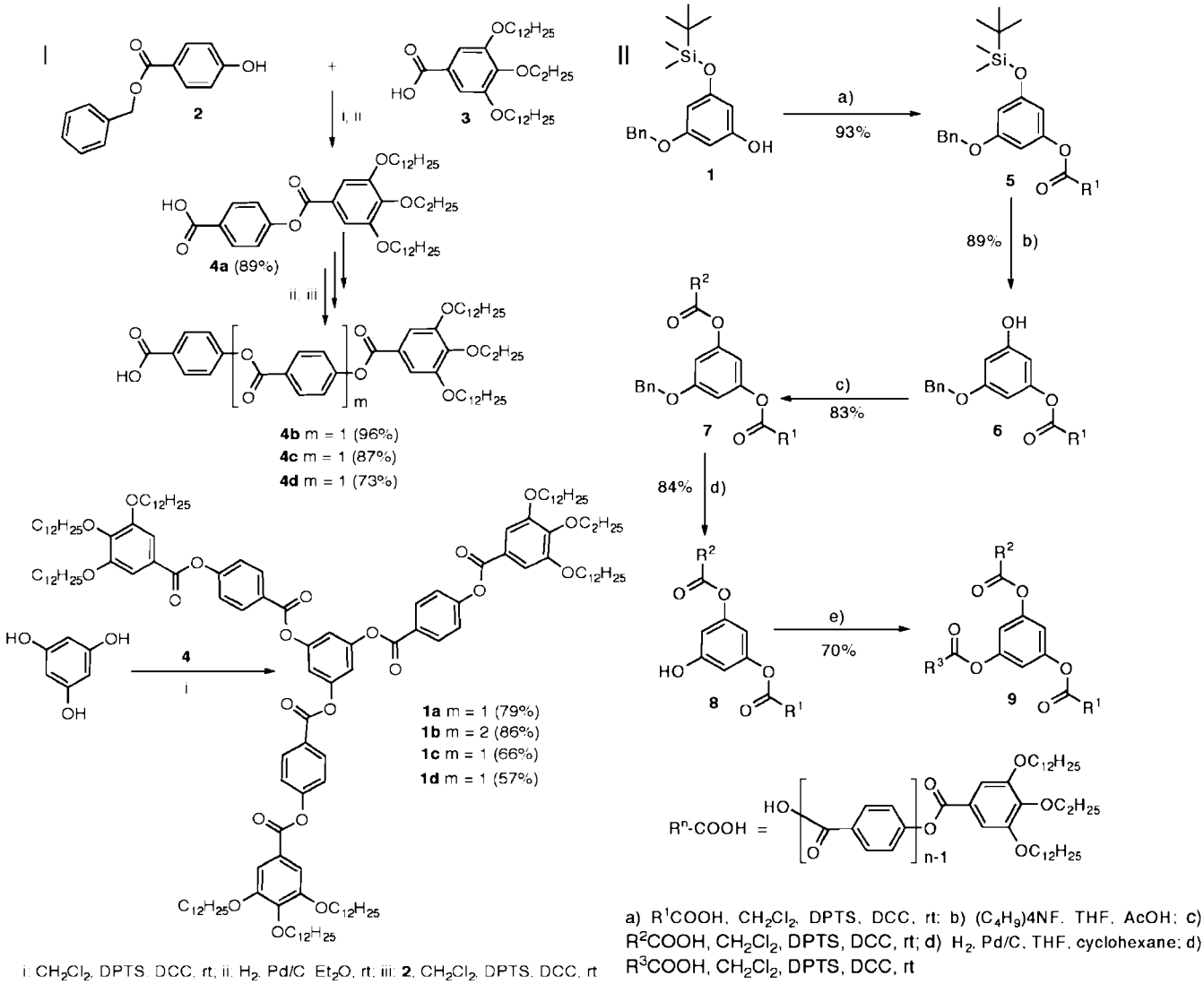

thus creating nonsymmetrical dendronized star-shaped polymers.[981−984] Self-organization of these molecules into *Cub* and BCC phases was demonstrated for molecules with large dissimilarity in the number of monomer repeat units (Scheme 69, right). The self-organization in *Cub* phases was attributed to the folding of oligobenzoate scaffold from a planar conformation into a conelike conformation (Figure 270). The structurally programmed adoption of wedgelike or conical conformations and subsequent arrangement into columnar and spherical structures, respectively, mimics the mechanism of self-assembly observed earlier in Percec-type dendrons.

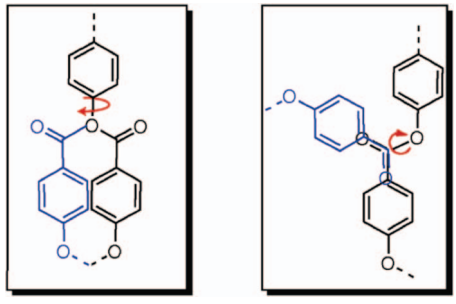

Figure 268. Rotation of the dendritic segment around the C−O bond. Adapted from ref 979.

Ivanov performed extensive XRD analysis of an example of star-shaped polymer of Lehmann (Figure 271).[985] Upon cooling from the isotropic phase, a metastable monotropic Φ_h was formed, which upon annealing at room temperature forms a stable rectangular crystal. XRD (Figure 271) clearly indicates a three-dimensional alignment, and the series of strong meridional reflections are indicative of helicity. The authors have suggested a hexameric cluster model for the columnar structures based off the E-shaped conformational model of the dendronized star (Figure 269). Spin-coated films of the dendronized star on Si wafers in the crystalline columnar state exhibited planar alignment, and some of the columnar features could be visualized by AFM. Films prepared on PTFE on the contrary exhibited hometropic alignment, and the effect of the annealing process on alignment was investigated through XRD, TOPM, and AFM.

Introduction of a naphthalene chromophore into a nonsymmetrical star-shaped mesogen generated a rich polymor-

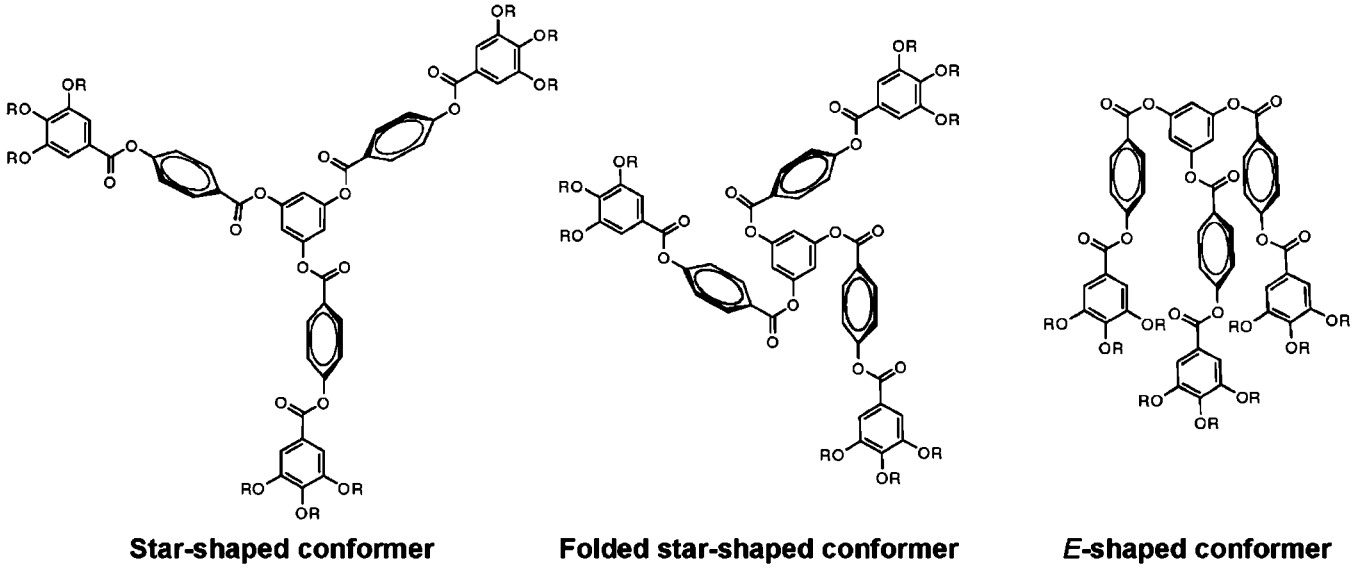

Figure 269. Possible conformers of dendronized star polymers.[979]

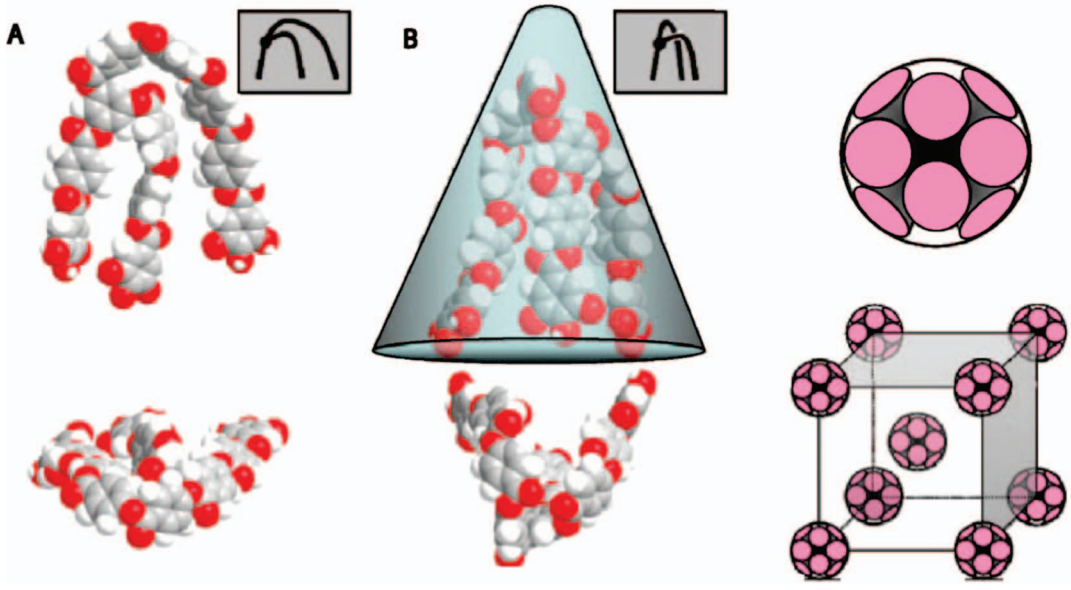

Figure 270. Molecular models without the aliphatic chains of the *E*-shaped conformer forming columnar phases (A), and the cone-shaped conformer that self-assembles into the *Cub* and BCC phases (B). Reprinted with permission from ref 982. Copyright 2008 American Chemical Society.

phism from Φ_h, Φ_r, lamellar, to *Cub* phases (Figure 272).[983] As in previous structures, the formation of the *Cub* phase was only observed in strongly nonsymmetric molecules with one arm considerably longer than the other three (Figure 272, 1d). Although naphthalene chromophores coupled with a semifluorinated dendron (Figure 272, 1b) were expected to mediate the segregation of the chromophores and provide access to electronic materials, the E-shaped conformation and the large intracolumnar separation due to the semifluorinated chains prevented the formation of ground-state aggregates as indicated by UV−vis.[983,984]

Meijer reported another class of dendronized three-armed star polymers based on 1,3,5-benzenetricarboxamide central core functionalized with chiral oligo(*p*-phenylene vinylene)s (OPVs) (Figure 273).[986] These structures were found to self-assemble in bulk and in solution. Self-assembly was dependent on a combination of $\pi-\pi$ and H-bonding interactions. Results obtained from IR, CD/UV−vis, and fluorescence studies suggested the presence of helical aggregates. The topology of the amide core strongly affects the stability and helicity of the fibers in solution, as well as the length of the fibrils at the surface of cast films. When bipyridine units were introduced into the core of star-shaped polymers, only limited chiral ordering was observed, though the aggregates remained stable over a large temperature range. The importance of molecular design in the amplification of chirality in star monomers has been recently reviewed.[100]

Goodman reported another star-shaped scaffold that was shown to assemble into collagen mimics.[987,988] Collagen, the most abundant protein in mammals, is composed of a Gly-Xaa-Yaa trimer (where Xaa is often proline or Yaa is often hydroxyproline). In collagen, three polypeptide strands each form left-handed helices that self-organize into a right-handed triple helix.[988] The star polymer reported by Goodman

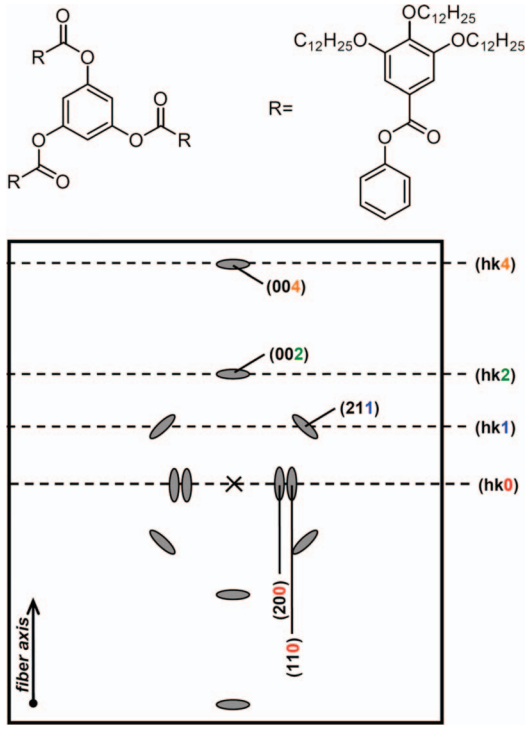

Figure 271. Dendronized 3-armed star and synchrotron XRD pattern by Ivanov. Adapted from ref 985.

incorporates three dendrons with (Gly-Pro-Nleu) tail groups, each of which serve as a mimic of the collagen triple helix, bound to a central trimesic acid (TMA) core (Figure 274). As hoped, the TMA[tris[(Gly-Pro-Nleu)$_6$-OMe]$_3$]$_3$ structure was found to self-assemble into a triple helical architecture similar to that of collagen. Helicity was confirmed by Optical Rotatory Dispersion (ORD) and CD/UV−vis measurements in water and helicity-enhancing ethylene glycol/water (2:1).[987] Cooperative thermal denaturation of the triple helix structure was monitored by CD/UV−vis spectroscopy and suggested that triple-helix formation is stabilized by intramolecular rather than intermolecular clustering (Figure 275).

Dendronized star-shaped structures containing triazine as a central core and **(3,4,5)G1** Percec-type dendrons without a monomer between them were reported (Figure 276).[989−992] These structures were found to self-assemble into supramolecular columns that self-organize into $\Phi_{r\text{-}c}$ and Φ_h lattices. The use of chiral tails in the dendron induced helical columnar structures.[990] Ishi-i reported the self-assembly of dendronized star-shaped triazines into columnar helical aggregates due to the cooperative effect of $\pi-\pi$ interactions between the triazine cores, hydrogen bonding between the amide connectors, and weak van der Waals interactions between the alkyl groups in nonpolar solvents. Additionally, a small amount of chiral stars was found to select the supramolecular helical sense of achiral stars through a sergeant-and-soldiers mechanism (Figure 276).[991] The helicity of the self-assembled structure was preserved after RCM mediated via Grubbs catalyst.

5.2. Dendronized Four-Arms Star Polymers

Malthête reported the first example of dendronized four-armed stars without monomeric repeat units based on a Pentaerythritol central core (Figure 278).[833,993] In spite of the tetrahedral geometry generated by the Pentaerythritol, these molecules self-assembled into supramolecular columns that

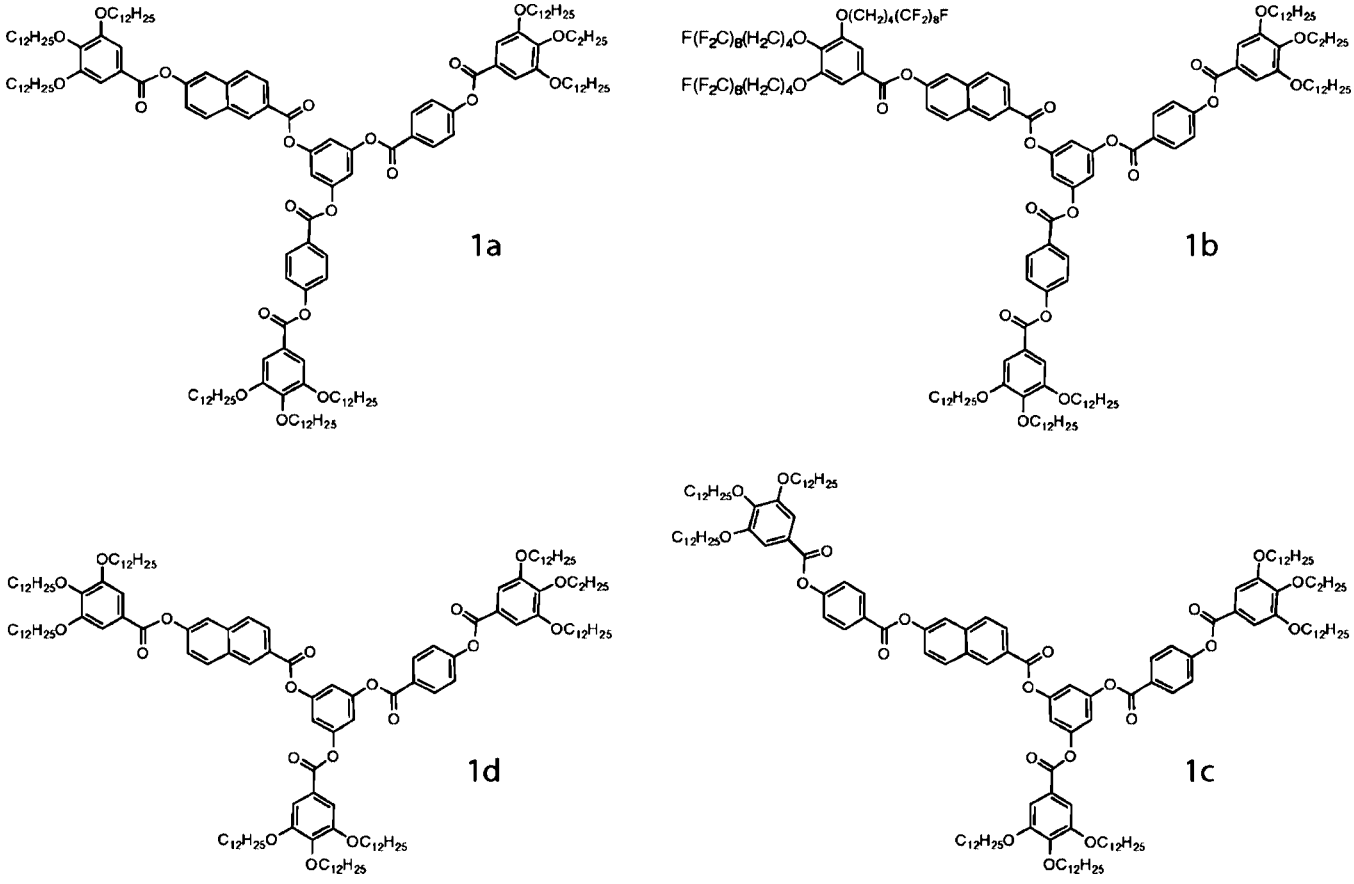

Figure 272. Asymmetric dendronized star polymers containing naphthalene groups.[983]

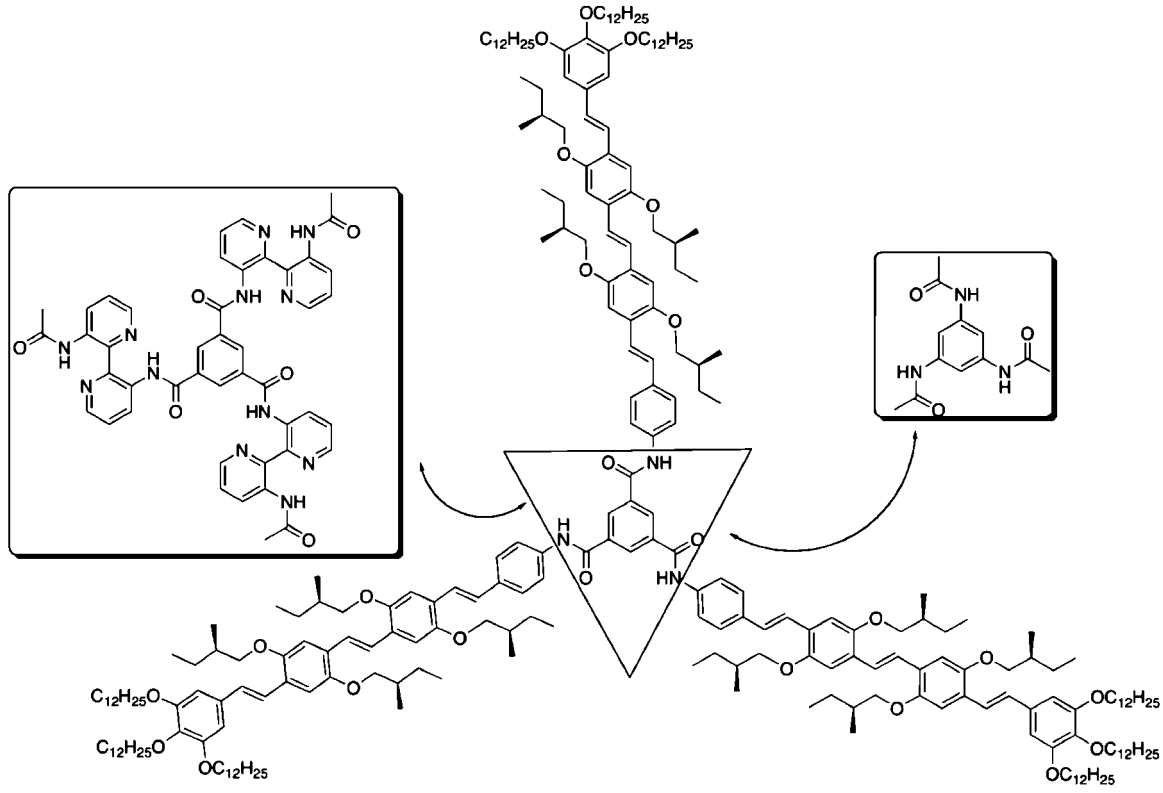

Figure 273. Dendronized star-shaped polymer based on oligo(*p*-phenylene vinylene)s reported by Meijer.[986]

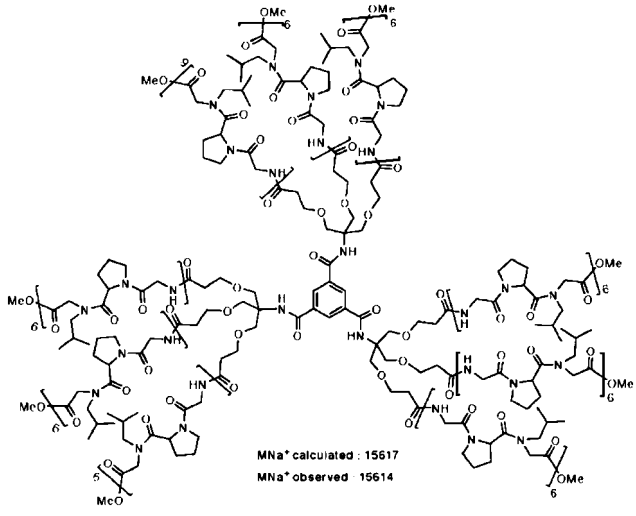

Figure 274. Collagen mimetic star-shaped polymer TMA[TRIS-[(Gly-Pro-Nleu)$_6$-OMe]$_3$]$_3$. Reprinted with permission from ref 987. Copyright 2002 American Chemical Society.

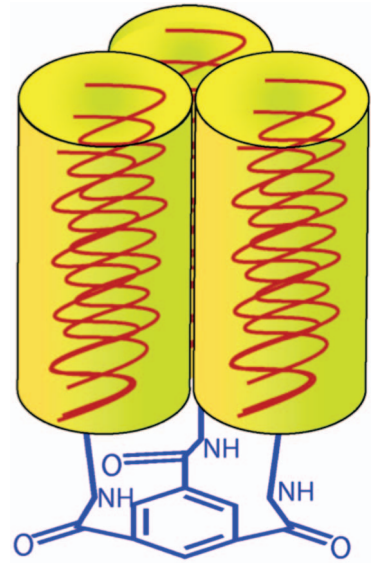

Figure 275. Schematic representation of the clustering of triple helices around the trimesic acid core. Reprinted with permission from ref 987. Copyright 2002 American Chemical Society.

self-organized in Φ_h phases. The $\pi-\pi$ interactions between the dendritic segments mediate the self-assembly process. Likewise, Fréchet reported four-armed star polymers with a Pentaerythritol core, G2-Fréchet dendron capped PEO arms.[994] The dendronized star polymers formed unimolecular micelles with solvent-dependent core−shell structures (Figure 277).

Tschierske reported similar structures to those of Malthête based on (3,4)*n*G1 nonfluorinated or semifluorinated dendrons connected to the four-armed cores by either polar ester and amide groups or by less polar ether units (Figure 278).[995,996]

Investigation of the self-assembly by TOPM, DSC, and XRD revealed organization of the semifluorinated phenylbenzoate units into enlarged polar regions. These regions exhibit enhanced self-interactions and assemble into supramolecular columns forming into Φ_h LC phases (Figure 279).[996] Two conformations of the central core are accessible in the dendronized Pentaerythritol derivatives: one with a tetrahedral arrangement of the dendrons and a conformer with a flat disklike arrangement of the dendritic structures. The flat conformation of the dendritic structures is reinforced by dipolar interaction of the polar linking groups and $\pi-\pi$ interactions of benzoate groups, as well as amphiphilic or fluorophobic effects mediated by the tail groups.

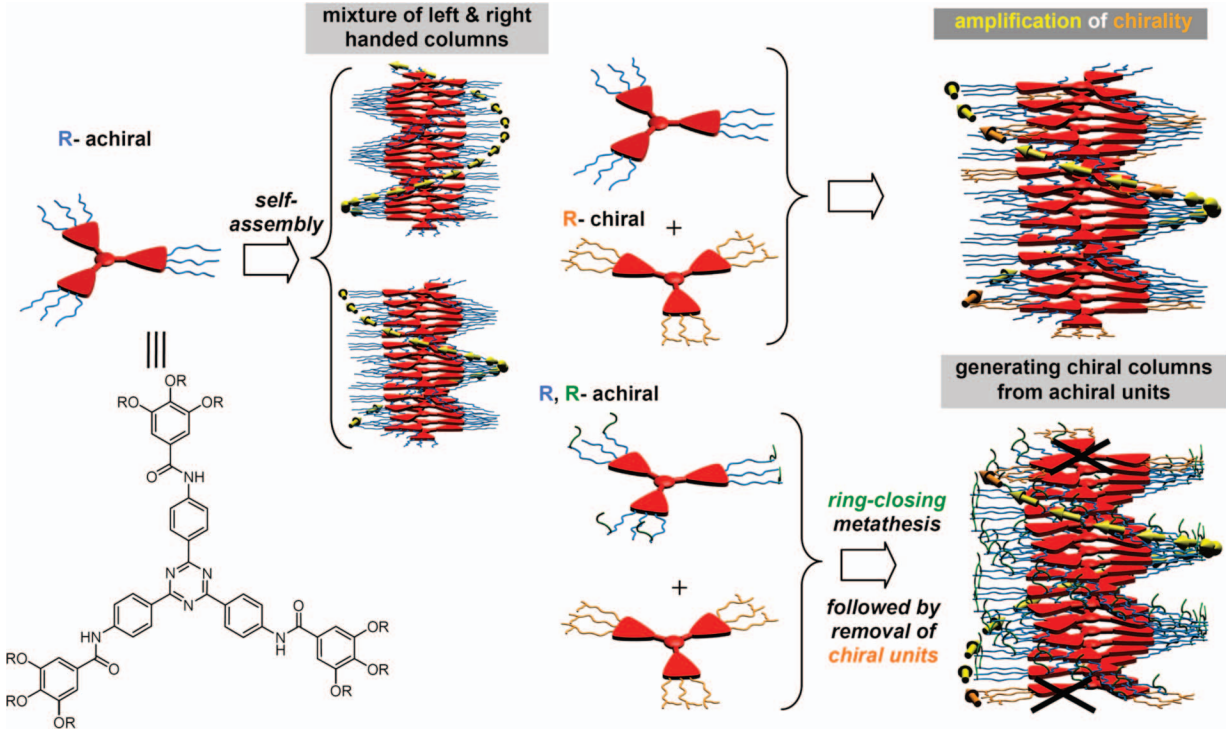

Figure 276. Structure of dendronized triazine stars and schematic representation of the sergeant-and-soldiers mechanism for chiral amplification in achiral aggregates. Adapted from ref 991. Copyright 2006 Wiley-VCH Verlag GmbH & Co. KGaA.

5.3. Dendronized Six-Armed Star Polymers

Meijer's laboratory reported the synthesis and self-assembly of dendronized six-armed star polymers based on OPV units attached to a hexa-arylbenzene central core (Scheme 70).[997]

XRD and TOPM suggested self-organization at room temperature in a highly ordered Φ_h superstructure as demonstrated by the large number of high-order reflections observed in the 2-D-WAXS pattern. CD/UV−vis was used to probe self-assembly in chloroform, heptane, and methylcyclohexane solutions. A bisignated Cotton effect with a positive sign at long wavelengths and negative sign at short wavelengths was observed in heptane, indicating that the chiral *S*-2-methylbutoxy side chains induce the organization of the OPV segments into right-handed helical aggregates (Figure 280). In each column, stars stack on top of each other to form right-handed helices (Figure 281). Each OPV arm is rotated out of the molecular plane by 3.3° as indicated by XRD. Temperature-dependent CD/UV−vis measurements in heptane showed no transitions even at 90 °C, indicating remarkably stable helical aggregates. However, in methylcyclohexane, a transition from the self-assembled state to the molecularly dissolved species was observed upon heating.[997] The heptane solution of the dendronized six-armed star molecule at concentrations above the threshold for solution self-assembly was deposited on both a silicon wafer and HOPG substrate. Surface analysis by SFM showed the presence of fibrils a few micrometers in length on silicon wafer and even shorter fibrils on the HOPG substrate. Supercoiled chiral nanoribbons with right-handed helical orientation were observed for regions with densely packed fibrils. The dendronized six-armed star polymer was also analyzed at the liquid−solid interface via STM. Organized monolayers with Φ_h packing and 2-D chirality were observed. They support the supramolecular model (Figure 281).

Dendronized six-armed stars were also obtained by functionalization of a cyclotriphosphazene core with (3,4,5)*n*G1 Percec-type dendrons through ester or amide connecting groups or through hydrogen bonding (Figure 282).[998−1000]

The design of cyclotriphosphazene central core allows for free rotation of the dendritic arms around the P−O−Ar bond. As a result, two conformations, rodlike and disklike, are accessible. Self-organization into Φ_r and Φ_h phases was observed over a wide temperature range. The incorporation of amide groups in the functional connectivity between dendron and core was expected to enhance intermolecular interaction through hydrogen bonding.[999] In molecules with amide linkages, solution FTIR demonstrated the presence of intramolecular hydrogen-bonding interactions between the arms of the same cyclophosphazene via a single sharp amide peak at 1645 cm^{-1}. A corresponding band in the neat state is indicative of intermolecular hydrogen-bonding, explaining the stabilization of the disklike conformer and of the supramolecular columns. XRD of the Φ_h mesophase showed a helical organization of the cyclotriphosphazenes inside the supramolecular columns.

Xu reported dendronized six-armed supramolecular stars through H-bond interactions (Figure 282, bottom). TOPM, DSC and XRD suggested a rodlike conformation for these molecules since only S and N phases were detected (Figure 283).

6. Dendronized Macrocycles

Macrocycles[1001−1007] pioneered the field of molecular recognition and supramolecular chemistry, exhibit biologically important functions, and give direct access to molecular building blocks predisposed to the formation of supramolecular architectures. Highly conjugated macrocycles possess photophysical and electronic properties, which when combined with self-organization results in functional materials

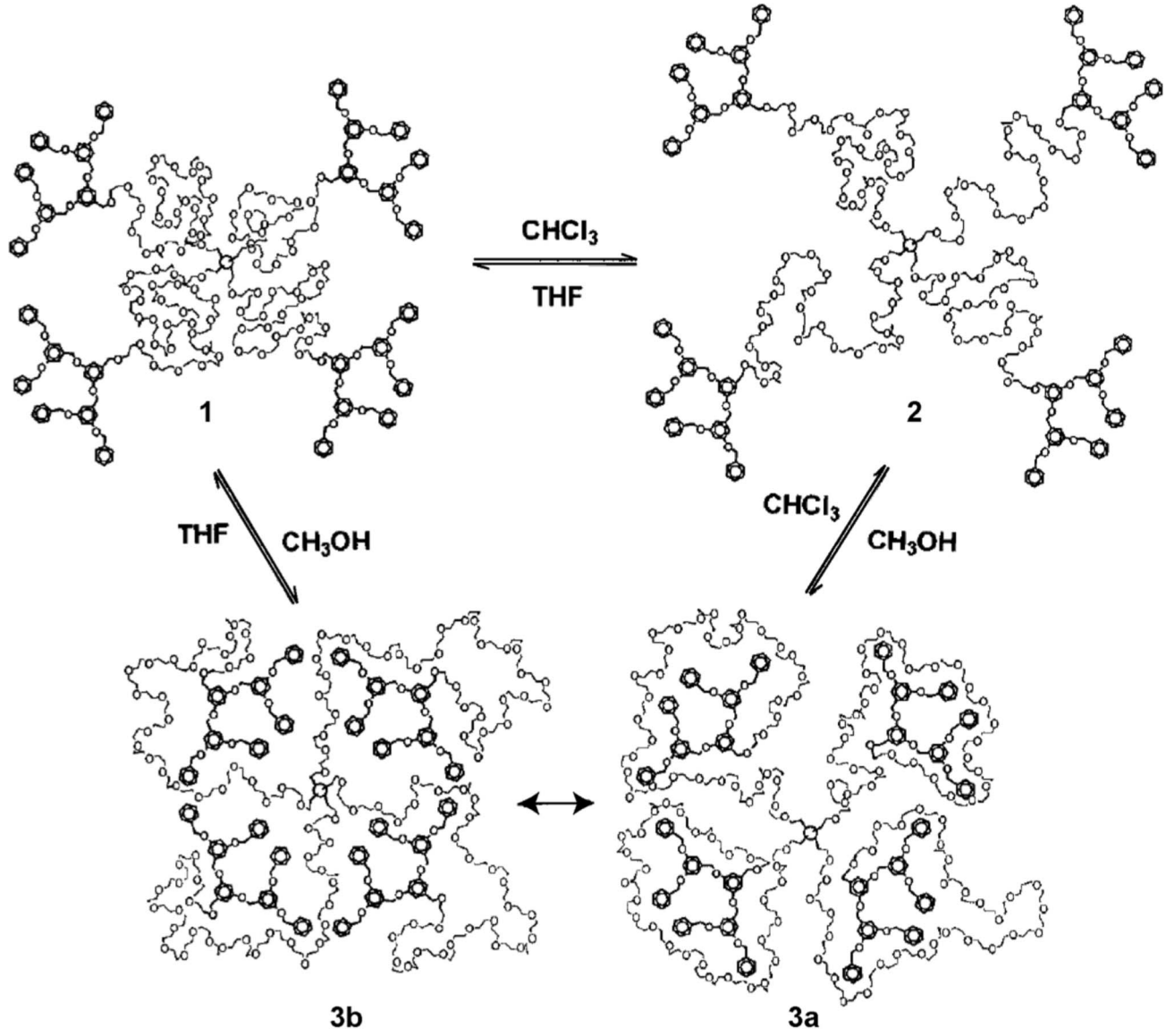

Figure 277. Solvent-dependent core−shell structures of dendronized 4-armed star polymers with Pentaerythritol core and dendronized PEO arms. Reprinted with permission from ref 994. Copyright 1996 American Chemical Society.

for use in optoelectronics and semiconductors. Macrocycles with heteroatoms in their structure have the ability to complex metal salts into their cavity. When decorated with self-assembling dendrons, macrocycles containing a transition metal may function as highly efficient catalysts. The ability of macrocycles to carry out photochemical and metal-catalyzed reactions is seen extensively in nature, for example, in photosynthesis and in metabolic enzymes such as photosystem II and cytochrome P450.[1008−1010] Macrocycles are also used medicinally for treatment of various diseases including HIV and cancer.[1011−1013] Self-assembly and self-organization of dendronized macrocycles has been studied extensively in both solution and bulk. Comprehensive reviews are available on macrocycle derivatives that self-organize into LC phases.[106,130,1014−1018] These subjects will not be covered here with the exception of limited illustrative examples. A more general review of discotic liquid crystals was reported by Laschat and Giesselmann.[107] This subsection will focus on the self-assembly and self-organization of dendronized macrocycles (Figure 1, fifth row middle to right). A large diversity of macrocycles were reported to self-organize in bulk when functionalized with dendrons (Figure 284).

6.1. Dendronized Crown-Ethers and Related Macrocycles

The first report of self-assembly and self-organization of dendronized crown-ethers was by Lehn, who used them to assemble synthetic mimics of transmembrane channels such as gramicidin A. A channel and bundle ("Chundle") model with rodlike topology was proposed (Figure 285).[1019]

Percec provided the first examples of self-assembly of dendrons functionalized with crown-ethers at their apex. Both benzo-15-crown-5 and 15-crown-5 were dendronized with Percec-type (3,4,5)12G1 and (4-3,4,5)12G1 dendrons, and their self-assembly was investigated by TOPM, DSC, and XRD (Figure 286).[210,212]

The crown-ether provided a functional *endo*-receptor capable of binding guests in their molecular cavities. The dendronized crown-ethers reported by Percec exhibited only crystalline

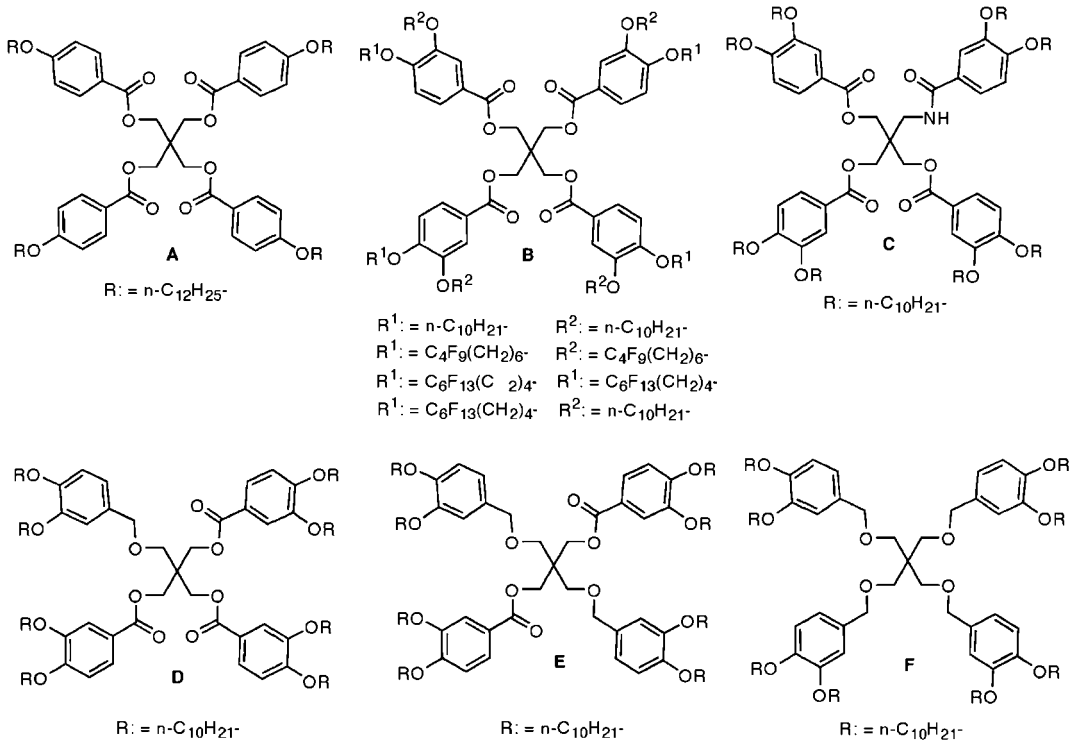

Figure 278. Dendronized four-armed stars reported by Malthête (A) and Tschierske (B−F).

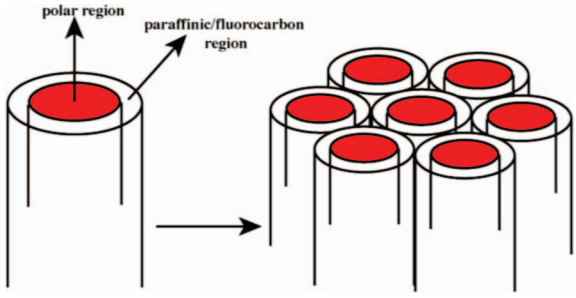

Figure 279. Core−shell model of the Φ_h self-organization. Adapted from ref 996.

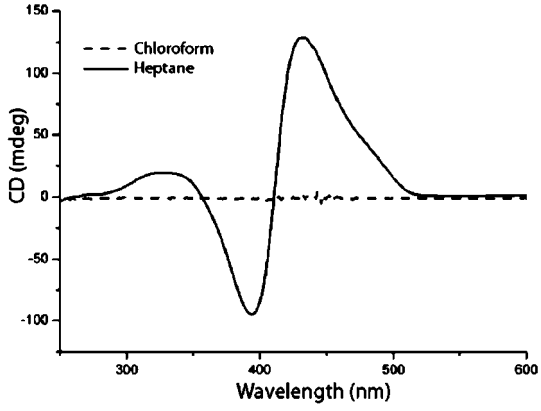

Figure 280. CD spectra of dendronized six-armed star polymer from Scheme 70. Reprinted with permission from ref 997. Copyright 2007 American Chemical Society.

Scheme 70. Dendronized Six-Armed Star OPV (Reprinted with Permission from Ref 997; Copyright 2007 American Chemical Society)

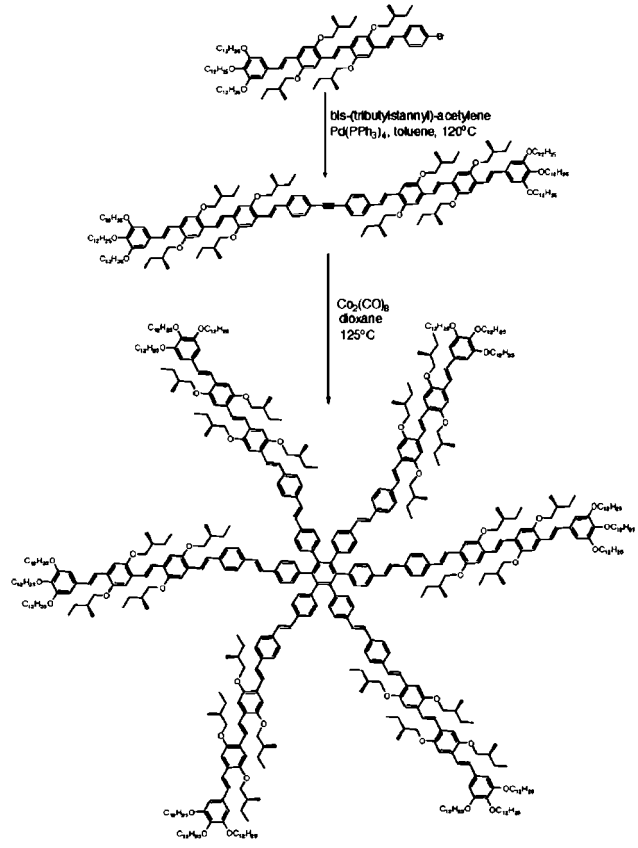

phases; however, complexation with sodium or potassium triflate destabilized the crystal phase, inducing self-assembly into a supramolecular column that self-organizes into a Φ_h phase. The self-assembly mechanism was proposed to be analogous to that of TMV (Figure 15),[229] and a detailed analogy of this molecular recognition directed self-assembly process has been presented.[227,228] TMV consists of a single strand of viral RNA and a single protein; its self-assembly is driven via molecular recognition at the surface of the protein (*exo*-recognition) and its subsequent self-organization is initiated by either a conformational change at a low pH or by interaction with the viral RNA.

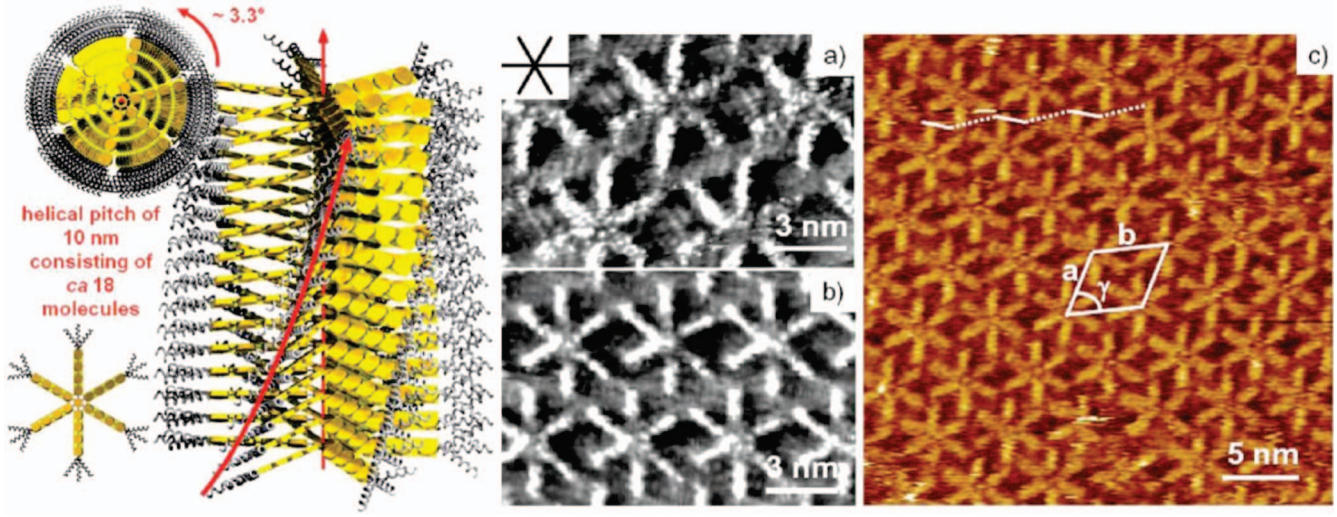

Figure 281. Supramolecular organization of the six-armed dendronized star into a helical column (left). Small-scale (a,b) and large-scale STM images (c) at the 1-phenyloctane−HOPG interface with the indication of the unit cell of chiral *p*6 *mm* symmetry. Reprinted with permission from ref 997. Copyright 2007 American Chemical Society.

XRD in tandem with molecular modeling was used to propose models for the intracolumnar packing of the 1:0.6 complex of (4-3,4,5)12G1−15C5 with $NaSO_2CF_3$. Three possible packing models were as follows: (a) crown-ether cavities aligned on the central column axis, forming a straight axial channel; (b) four macrocycles placed side-by-side within the column core; (c) five macrocycles placed side-by-side, inducing out-of-plane rotation of the crown-ether about the CH-Ph-crown-ether bond (Figure 287).

The molecular packing models for each column stratum were constructed, and their dimensions and theoretical densities were compared to the experimental values obtained from XRD and with experimental densities. The experimentally determined average distance from the center of the column cavity to the edge of the tails was 30.7 Å. This value is only slightly smaller than the calculated distance from the center to the edge of the column (33.8 Å). Placing all crown-ether apex-groups at the center of the column (Figure 287a) would result in a structure with lower than observed columnar diameter. Such a structure would exhibit only a 21% alkyl tail conformational shrinkage. Previous work demonstrated alkyl tail shrinkages of as much as 55% for similar compounds.[205,206] Packing four dendrons with the crown-ethers side-by-side would increase the columnar radius by 7.1 Å and would result in a more realistic alkyl tail shrinkage of 50% (Figure 287b). In the final model (Figure 287c), the packing of five dendrons per stratum resulted in a more efficient filling of space and gave an alkyl tail conformational shrinkage of around 52%, in good agreement with previous experimental data.[205,206] The three potential molecular models indicated theoretical densities of 0.19 g/cm^{-3} for the single crown-stacked column (Figure 287a), 0.75 g/cm^{-3} for the four-crown per stratum model (Figure 287b), and 0.94 g/cm^{-3} for the five-crown per stratum model. Comparison of these density values with measurements taken from a gradient density column along with theoretical density values for a hexagonal unit prism indicated a value of 5.8 molecules per strata, thereby eliminated the single crown-stacked and four-crown per stratum column models.[1020] As molecular models suggest only 5 molecules per stratum, a slightly higher stratum height than that reported in literature is likely.

From this model, it was suggested that the center of the column comprised either parallel channels or a multistranded helix. DC conductivity values in the range of 10^{-6}−10^{-5} S cm^{-1} were obtained, in line with ionic conductors.[442] Interestingly, there was little change in conductivity between the Φ_h phase and the isotropic liquid. The authors proposed that the similarity in conductivity arose from the retention of supramolecular column in the isotropic melt. Fast cooling to prevent crystallization of the Φ_h phase showed a significant drop in conductivity to the range of insulators below T_g. On the basis of XRD and conductivity measurements, a model of five parallel channels running through the center of the column was proposed with conductivity arising from ion migration within the channels. A change in the complexation ratio to 1:1.6 (4-3,4,5)12G1−15C5 to NaOTf resulted in columns with six macrocycles per stratum (Figure 288).

Following the discovery of ion transport within the supramolecular columns self-assembled from dendronized crown-ethers,[210] Möller and Percec used dendronized crown-ethers peripherally functionalized with dendrimers containing methacrylic groups on the periphery in order to construct alkali metal selective membranes (see section 3.3).[674−676,678−681]

Percec reported that the tendency to self-assemble into supramolecular architectures is much stronger for semifluorinated dendrons than for fully hydrogenated ones. This is due to the enhanced rigidity and lower solubility of highly fluorinated compounds in both polar and nonpolar solvents as well as its reduced miscibility with the aromatic part of the dendron (the fluorophobic or fluorous phase effect).[359] Dendronized crown-ethers peripherally functionalized with semifluorinated chains (Figure 289) exhibited enantiotropic thermotropic Φ_h and *Cub* mesophases with a high degree of thermodynamic control indicated by the small degree of supercooling (<0.4 °C) and excellent agreement between the enthalpy associated with the transition temperature on heating and cooling (~1 kcal mol^{-1}).

Hudson and Percec reported the direct visualization of the Φ_h structure of semifluorinated dendronized crown-ethers both in the homeotropic and planar arrangement by transmission electron microscopy (TEM), confirming the location of

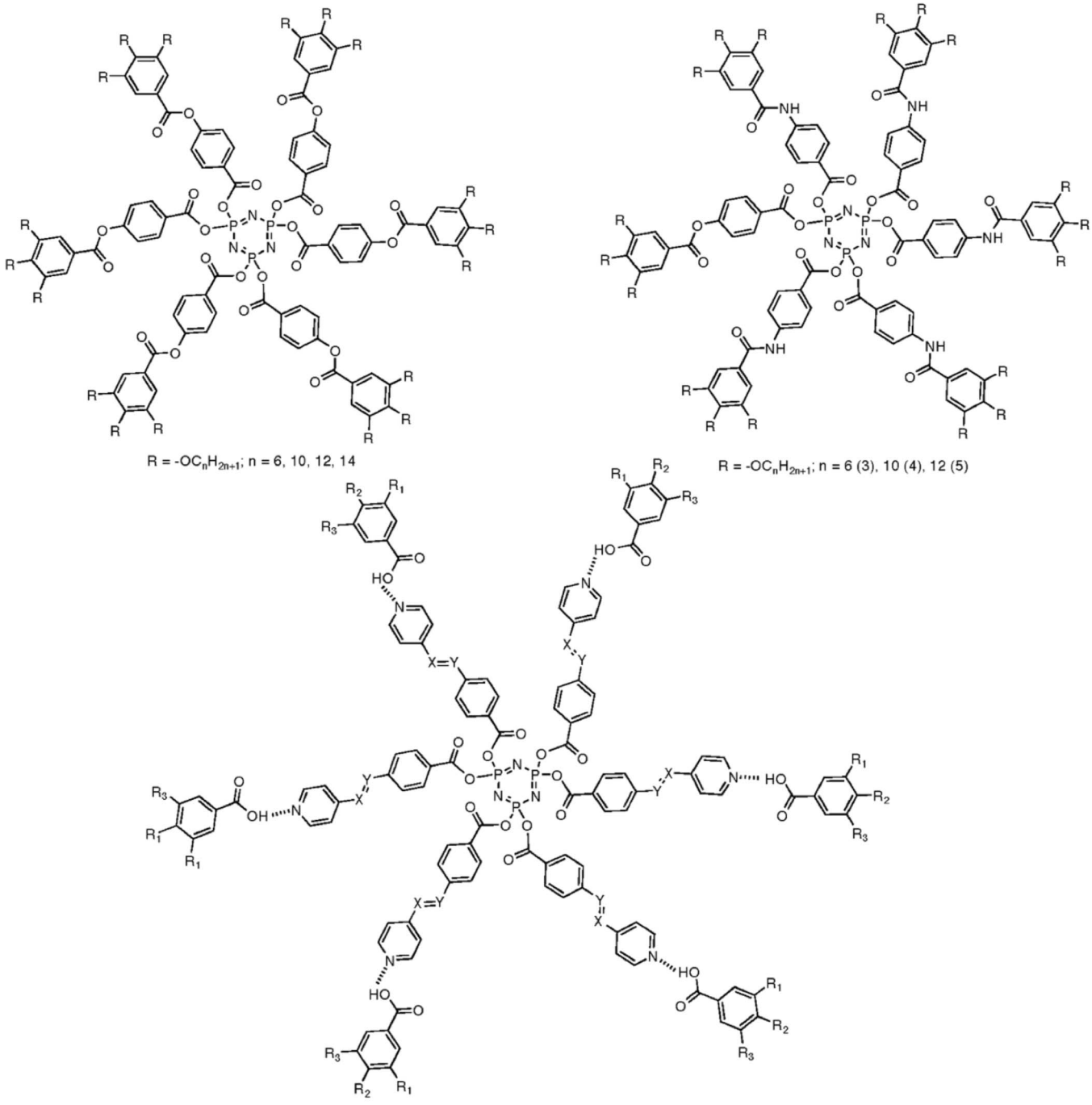

Figure 282. Dendronized six-armed star with cyclotriphosphazene cores.[998−1000]

the *endo*-receptor at the column center (Figure 17a,b). The analysis of the homeotropically arranged columns by electron-diffraction and TEM is in agreement with the electron-density map calculated from XRD (Figure 290a). This confirms the model of self-assembly and facilitated a molecular model to be advanced (Figure 290b,c). The quantitative "stiffness" of the supramolecular columns self-assembled from the two semifluorinated crown-ethers was also examined. The supramolecular columns generated from semifluorinated dendrons (3,4,5)12F8G1−B15C5 and (4-3,4,5)12F8G1−15C5 demonstrated a large increase in stiffness versus those generated from their perhydrogenated analogues.[306,1021] Additionally, the surface ordering of benzocrown-ethers functionalized with Percec-type dendrons in LB films were characterized by X-ray reflectivity experiments.[1022]

Following the discovery of the self-assembly of dendronized crown-ethers into supramolecular columns and their self-organization in a Φ_h phase, Percec synthesized libraries of benzo[15]crown-5 ethers dendronized with self-assembling dendrons. SAXS and WAXS in combination with molecular modeling were used to construct models of their self-organized structures (Figure 291).[443]

The effect of the *endo*-receptor on the self-assembly mechanism was demonstrated through the comparison of the structures formed from Percec-type dendrons *endo*-functionalized with benzocrown-ethers and compared with those of

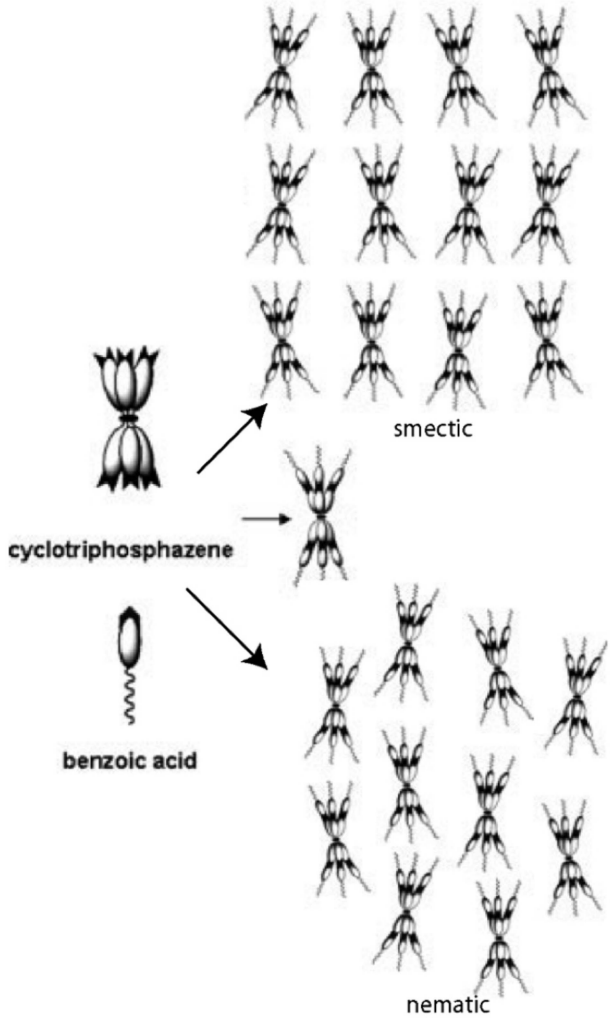

Figure 283. Self-assembly of dendronized six-armed supramolecular stars. Reprinted with permission from ref 1000. Copyright 2008 John Wiley and Sons, Inc.

identical monodendrons *endo*-functionalized with methyl esters and carboxylic acids. Dendrons functionalized with a benzocrown-ether at the focal point more frequently assume a disk shape, similar to those functionalized with methyl esters, rather than the conical shape often assumed by dendrons with H-bonding carboxylic acids apex moieties. One exception was in the case of (4-3,4)12G1−B15C5 where the bulkier B15C5 group results in a more symmetric dendron, and thus, it adopts a parallel-piped conformation for which an S_A phase was obtained.

Experiments were performed where the structures formed before and after addition of NaOTf were compared, providing insight into the role of complexation in the self-assembly process. Percec previously demonstrated that the solid angle of a monodendron is determined by both the volume of the apex and the aromatic branching architecture.[334,335] Dendrons with a large projection of solid angle α' maintained a tapered structure where a somewhat smaller projection of solid angle was observed. Tapered dendrons with a small projection of solid angle α' change into a parallel-piped. Conic dendrons with small values of α' change their shape into tapered dendrons, while conic dendrons with large values of α' remain conic. It was concluded that complexation (a) stabilizes the $Pm\bar{3}n$ cubic phase self-organized from spherical supramolecular dendrimers, which are self-assembled from conic dendrons; (b) stabilizes the S_A phase generated from parallel-piped dendrons; (c) has no effect on the stability of S_B phase of parallel-piped dendrons; (d) stabilizes the Φ_h self-organization from cylindrical supramolecular molecular dendrimers self-assembled from tapered dendrons; and (e) destabilizes the Φ_h self-organized from cylindrical supramolecular dendrimers self-assembled from half-disk dendrons.

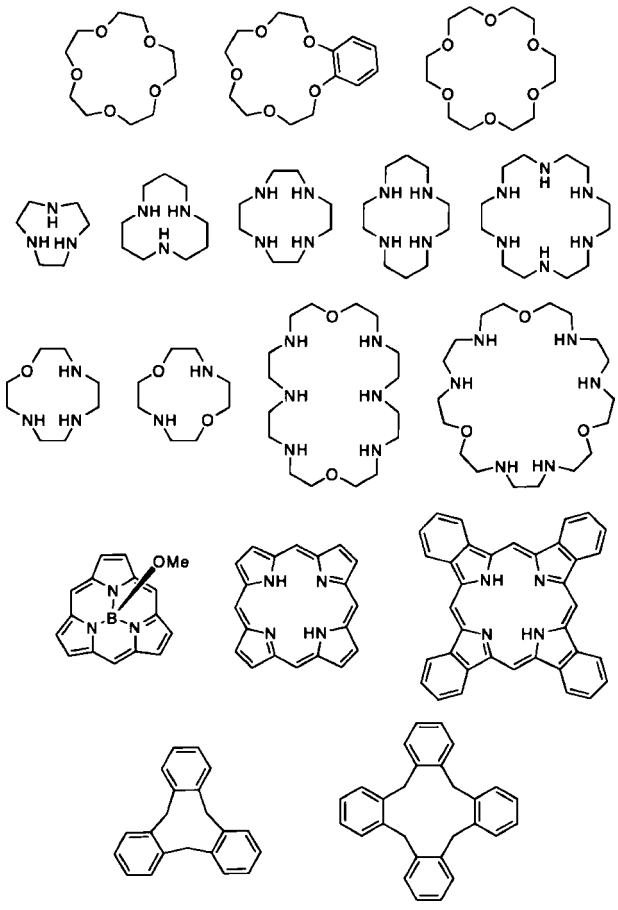

Figure 284. Macrocycles reported to self-assemble when functionalized with dendrons.

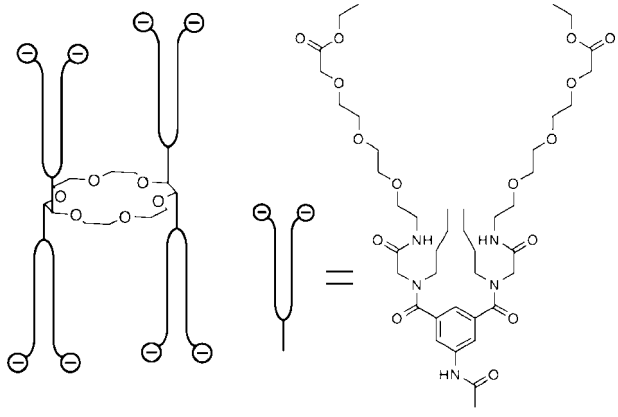

Figure 285. "Chundle" model of dendronized 18-crown-6 reported by Lehn.[1019]

Attempts were also made to correlate single crystal structures of dendronized crown-ethers to the self-organized state. Laschat synthesized a series of benzocrown-ethers substituted with two dendrons.[1023] Self-organization into Φ_h lattices was obtained, although only limited correlations could be drawn in between the single crystal structure and the self-organization in Φ_h phases.[1023,1024]

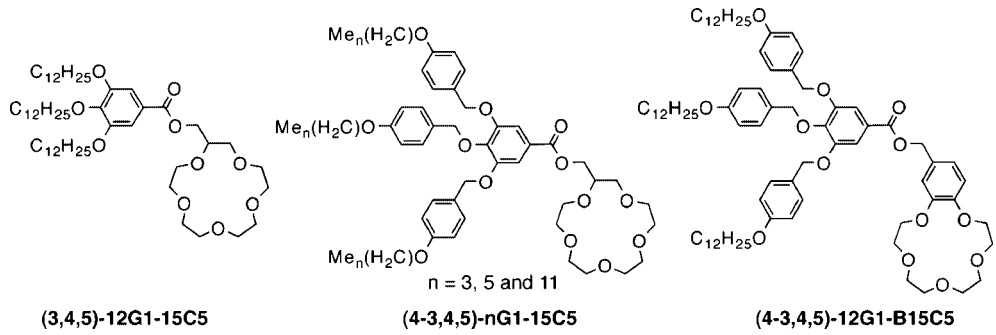

Figure 286. Dendronized 15-crown-5 and benzo-15-crown-5 reported by Percec.[210,212]

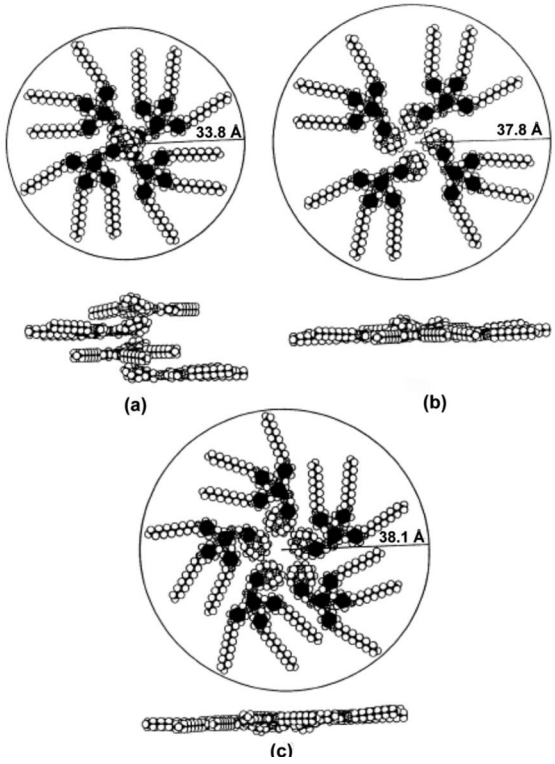

Figure 287. Columnar packing models with (a) one crown-ether per stratum, (b) four crown-ethers per stratum, (c) five crown-ethers per stratum. Reprinted with permission from ref 210. Copyright 1993 Royal Society of Chemistry.

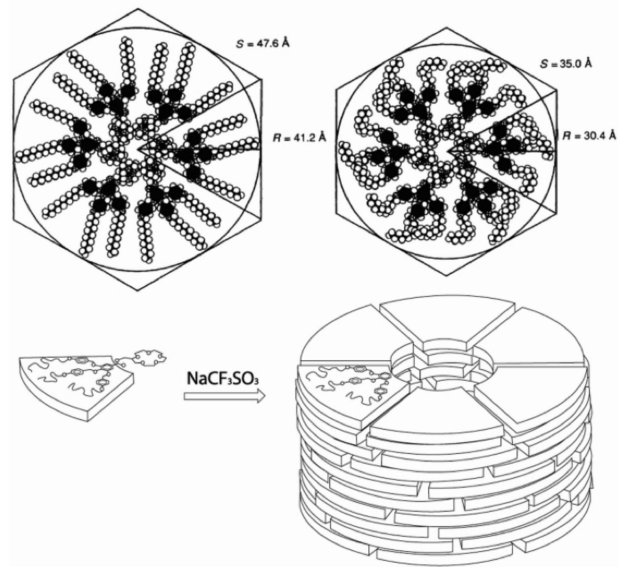

Figure 288. Model of self-assembly of the first dendronized crown-ethers with six macrocycles per stratum. Reprinted with permission from ref 212. Copyright 1994 Royal Society of Chemistry.

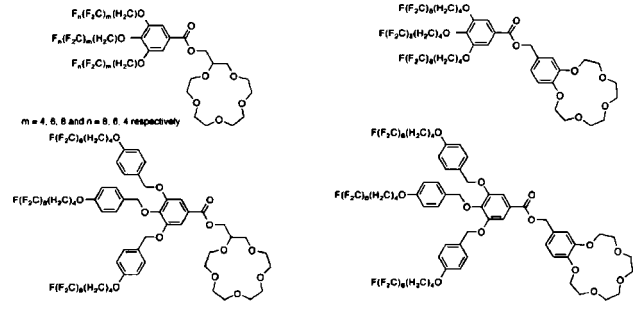

Figure 289. Dendronized crown-ethers with peripheral semifluorinated chains.[359]

Gitsov carried out an extensive study on the synthesis and functionalization of various crown-ethers with Fréchet-type dendrons. It was still possible to functionalize up to a G4 benzyl bromide dendron with a crown-ether bearing a single primary alcohol (Figure 292).[1025]

Structurally similar paracyclophanes were dendronized via a palladocyle linkage. Linear substitution (i.e., no branching point) resulted in lamellar phases, whereas 3,4-bis branched systems exhibited no self-assembly. Attachment of (3,4,5)10G1 dendrons via coordination to palladocyle-containing cyclophanes resulted in the self-organization into a Φ_h architecture (Figure 293).[1026] Dendronized cyclophanes (Figure 294) termed dendrophanes by Diederich were extensively studied as enzyme mimics for host−guest chemistry.[1027−1030] Additionally, the functionalization of cyclophanes with hydrophilic dendrons (Figure 294) imparts water solubility, allowing for aqueous-phase extraction of hydrophobic molecules such as anthracene.[1031]

In addition to self-organization in bulk, dendronized crown-ethers self-organize in gels and onto solid surfaces. Reversible assemblies of dendronized 18-crown-6 were reported by Smith through the binding of ammonium cations to the crown-ether apex. Using bisammonium cations, these dendronized crown-ethers were assembled into supramolecular dendritic gels (Scheme 71).[1032,1033] Tsukruk reported functionalization of crown-ethers with low-generation photochromic dendrons and their self-assembly on solid surfaces.[1034]

6.2. Dendronized Azacrown Macrocycles

Lehn reported the synthesis of the first dendronized macrocycles based on azacrown molecules and demon-

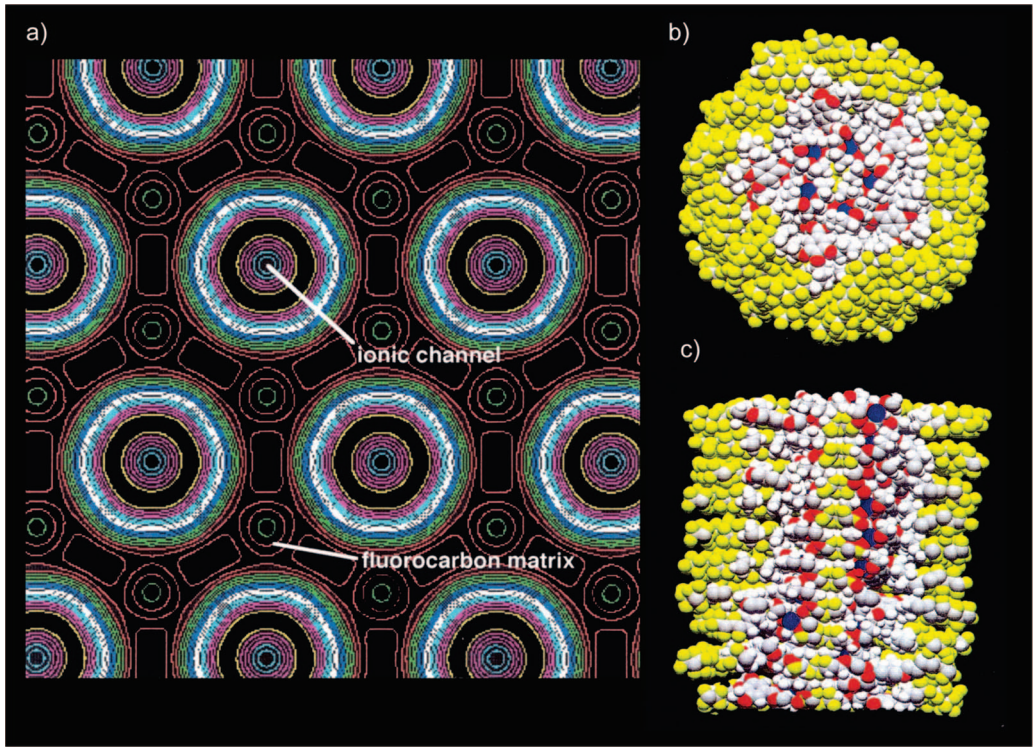

Figure 290. Electron-density map (a) of the self-organized lattice derived from (4-3,4,5)12F8G1−15C5 and the top (b) as well as side (c) views of the columnar model. Reprinted with permission from ref 306. Copyright 1996 American Chemical Society.

stratated that they generate a "tubular" mesophase self-organized into a Φ_h lattice (Figure 295).[1035−1037] The stability of the "tubular" mesophases was investigated by Ford, who found that crystallization could be obtained by pressing the sample between two glass surfaces at elevated temperatures for a period of one day.[1038,1039]

Dendronized azacrown structures (Figure 296) were less thoroughly investigated than their crown-ether counterparts. Lattermann investigated tri- and tetra-azacrown macrocycles. In most cases, Φ_h self-organized structures were obtained as evidenced by TOPM and XRD.[1040−1045] Ringsdorf investigated a series of cyclams and hexacyclens dendronized with G1 dendrons. In all cases, Φ_h phases were observed.[1046]

The formation of Φ_h phases from dendronized azacrowns has been a matter of some debate. Smith suggested that an equally feasible S ordering was possible based on the absence of higher-order reflections in the XRD in a series of hexacyclens.[1047,1048] Ringsdorf later demonstrated Φ_h phases based on XRD of the more conformationally restricted cyclen and its linear analogues.[1049] Later, self-assembly of azacrowns was harnessed by Aida to form nonheme metalloprotein mimics of monooxygenase and ribonucleotide reductase. Additionally, the dendronization of 1,4,7-triazacyclononane (TACN) with methoxy-functionalized Percec dendrons lead to a clear dendrimer effect on the stability of the bis(μ-oxo)dicopper toward oxidative self-decomposition (Figure 297).[1050]

Independent of their self-assembly, tetraazamacrocycles are of particular importance to radiology and diagnostic medicine. Gd^{III} complexes with tetraazamacrocycles or related noncyclic chelators are used intensively as MRI contrast agents.[1051−1053] While to date only low MW Gd^{III} complexes such as Gd^{III}DOTA and Gd^{III}DTPA (DOTA = 1,4,7,10-tetrazacyclododecane-14,6,10-tetraacetic acid and DTPA = diethylenetriaminepepntaaeyeic acid) have been approved for human use, dendrimer−Gd^{III} complexes are being developed into more effective MRI contrast agents and the field has been intensively reviewed.[25,134,1054−1056] Low molar mass Gd(III) contrast agents suffer from three major deficiencies. They lack site specificity, have low contrast efficiency, and are rapidly excreted by the renal system. Hydrophilic PAMAM and PLL dendimers are ideal candidates to improve on the performance of low MW Gd^{III} complexes, as they allow for incorporation of multiple tetrazamacrocycle or related Gd(III) binding sites at periphery as well as for parallel incorporation of cell-type specific targeting sites around the dendrimer periphery (Figure 298). Additionally dendrimers are less readily eliminated through the renal system than small molecules or even linear polymer. While not yet FDA approved, Schering has commercialized PLL−Gd^{III} complexes under the trade name Gadomer. In addition to Gd^{III} complexes for medical applications, Balzani, Maestri, and Vögtle reported the complexes of Cyclam dendronized with G1 and G2 Fréchet-type dendrons bearing peripheral naphthyl groups and lanthanide ions (Nd^{3+}, Eu^{3+}, Gd^{3+}, Tb^{3+}, and Dy^{3+}).[1057] In the uncomplex state, fluorescence of the naphthyl group is quenched by exciplex formation with cylam, while in the complexed state, the lanthanides suppress exciplex formation.

6.3. Dendronized Porphyrins and Phthalocyanines

Dendronized porphyrins and metalloporphyrins have been widely investigated due to their biocompatibility and have been reviewed by Aida.[130] Much work has been reported on the dynamic self-assembly of supramolecular porphyrin systems. This work was reviewed by Kobuke.[1058] The most recent and pertinent work involves the dendronization of triply fused metalloporphyrin dimers with **(3,4,5)G1** Percec

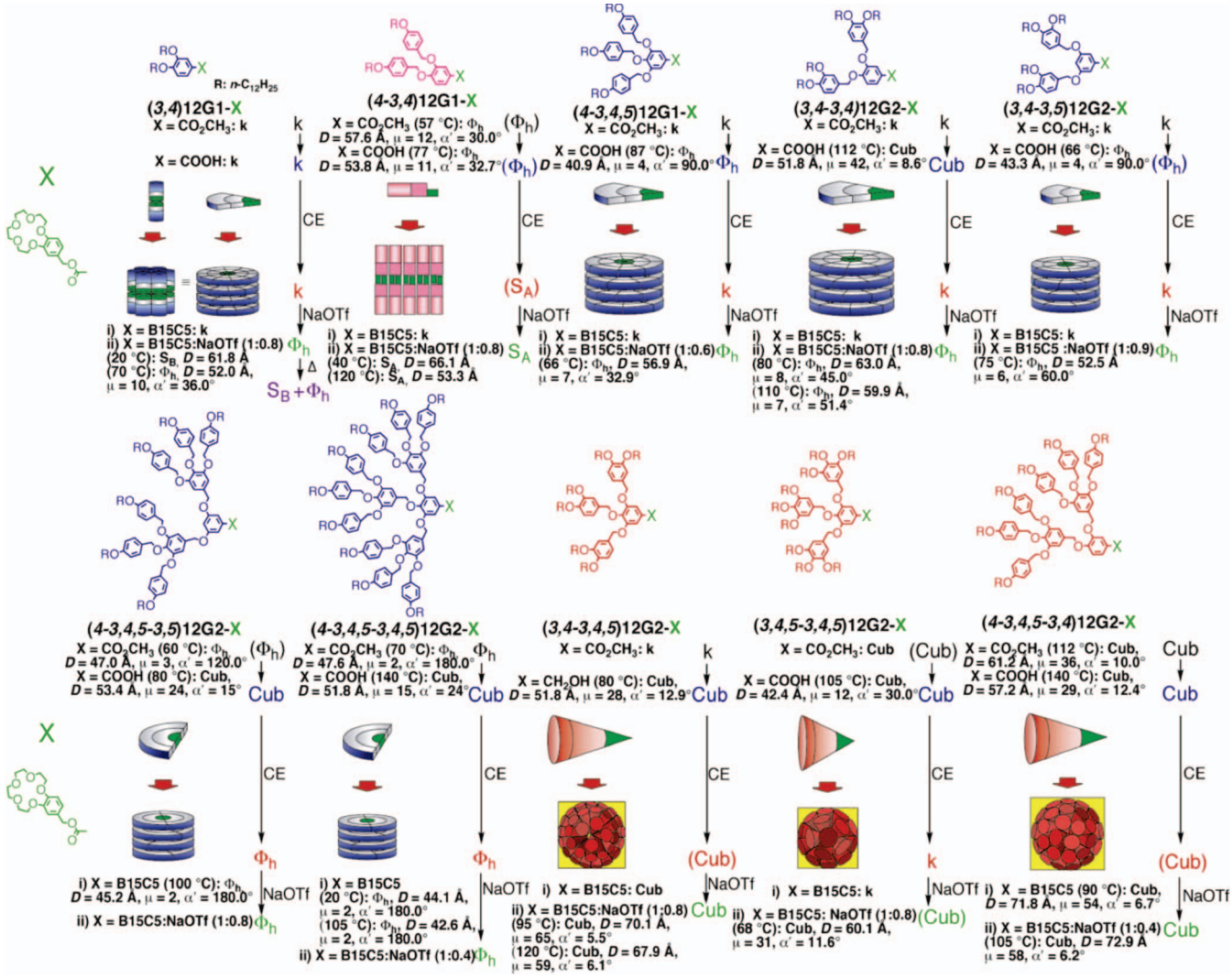

Figure 291. Structural and retrostructural analysis of a library of dendronized crown-ethers. Reprinted with permission from ref 443. Copyright 2002 Wiley-VCH Verlag GmbH & Co. KGaA.

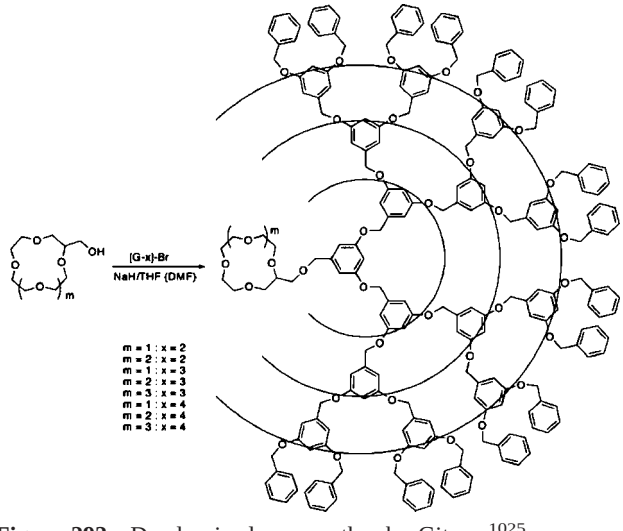

Figure 292. Dendronized crown-ether by Gitsov.[1025]

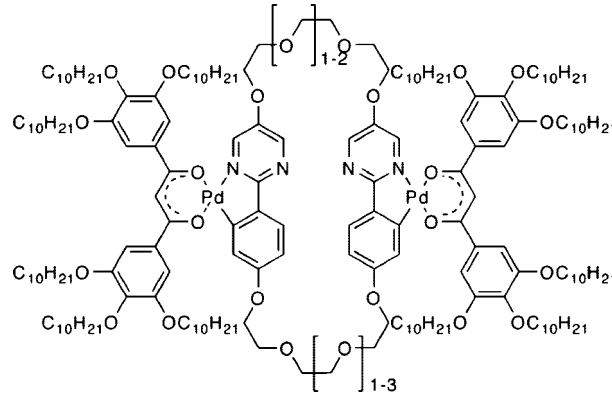

Figure 293. Dendronized paracyclophanes.[1026]

dendrons with aliphatic or EO tails by Aida (Figure 299).[1059] Aida also demonstrated chiral memory effects in the CD spectra of spin-coated films. J-aggregates formed by H-bonding of dendronized Zn-porphyrins retain the enantiomeric form dictated by the rotational direction of the spin-coating process (Figure 300). In solution, the formation of chiral aggregates formed from achiral dendronized porphyrins can be induced by torsional flows via clockwise or counterclockwise stirring.[1060] The reported compounds did not display optical activity in solution and represented the first examples of transformation of macroscopic spinning chirality into stable supramolecular chirality in the solid state (Figure 301).[1061] Zn-porphyrins tetra-functionalized with triazole-containing dendrons have also been reported.[1062]

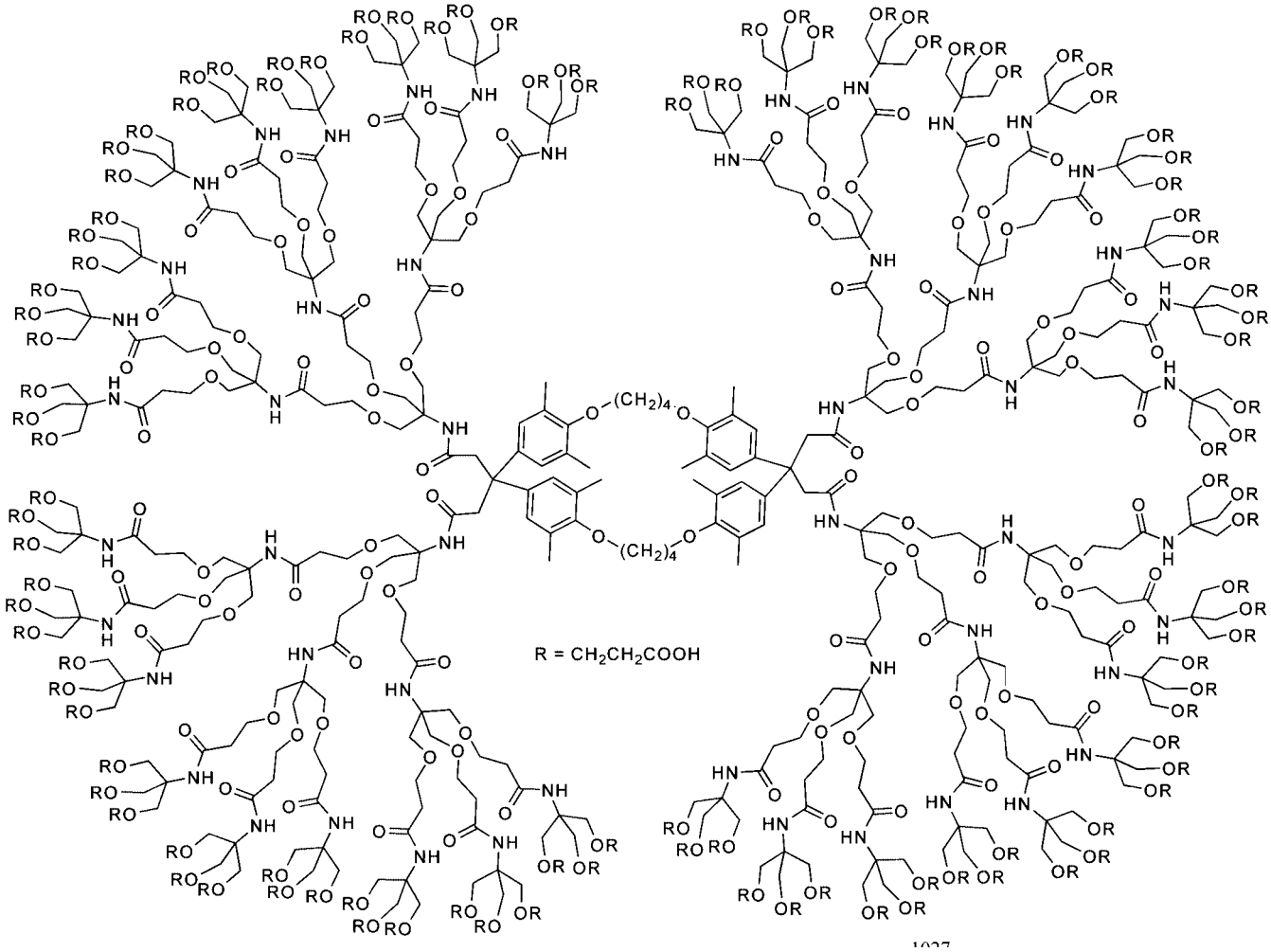

Figure 294. Cyclophane functionalized with G3 Newkome-type dendrons.[1027]

Scheme 71. Synthesis of Dendritic Crowns[1032]

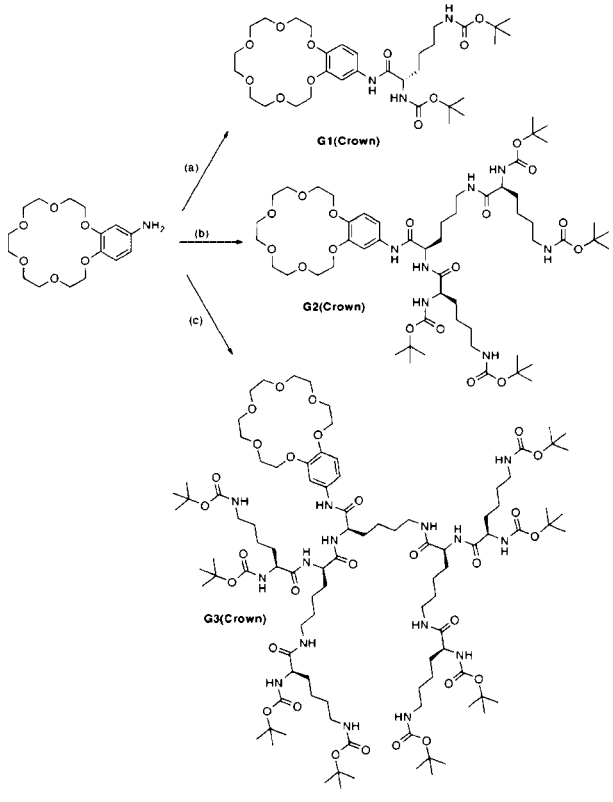

Sessler reported Zn-porphyrin and Zn-porphycene tetradendronized with (3,4)10G1 (Figure 302).[1063] While identical compounds tetrafunctionalized with decyloxybenzene formed only crystalline phases, lamello-columnar and $\Phi_{r\text{-}c}$ LC organization was noted for dendronized Zn-porphycene and Zn-porphyrin, respectively. Complexation of the dendronized Zn−porphycene with tetracyanoquinodimethane transformed the self-organized architecture from lamello-columnar to Φ_h.

To probe the natural rodlike self-assembly of bacteriochlorophyls, Würthner reported the synthesis of dendronized Zn 3^1-hydroxymethyl chlorins and Zn 3^1-hydroxyethyl chlorins (Figure 303).[1064] Self-assembly of natural bacteriochlorophylls into a tubular structure is believed to be mediated by $\pi-\pi$ interactions between the terpyrole rings, coordination of Zn center by the 3^1-hydroxyl group, and hydrogen bonding between the 3^1 hydroxy group and the 13^1 keto group. When the chlorin analogues were functionalized with dodecyloxyphenyl units, self-aggregation was not controlled. Dendronization with hydrophobic (3,5)12G1 or (3,4,5)12G1 resulted in self-assembly in nonpolar solvents into tubular aggregates as observed by AFM. Dendronization with (3,5)4EOMeG1 or (3,4,5)4EOMeG1 resulted in self-assembly in aqueous media. 3′-Methyl substitution hinders self-assembly into larger aggregates, and only small closed dimers or oligomers are observed. SFM studies of (3,5)12G1 dendronized 3^1-hydroxymethyl chlorin revealed the formation of two types of well-ordered π-stacked structures on HOPG

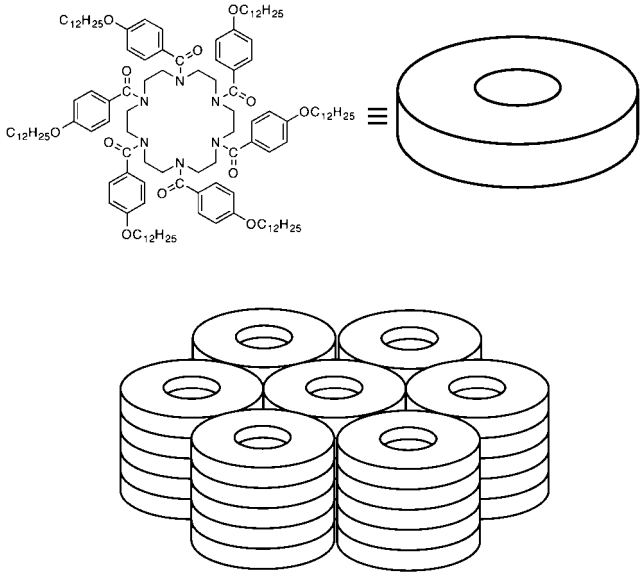

Figure 295. Schematic of the tubular mesophase reported by Lehn. Adapted with permission from ref 1035. Copyright 1985 Royal Society of Chemistry.

substrate, including an unprecedented side-by-side arrangement (Figure 304).[1065] In both phases, the aromatic cores are tilted relative to the surface.

Suslick substituted porphyrin macrocycles with 3,5-dicarboxybenzenes peripherally functionalized with hydrocarbon chains of different lengths (Figure 305).[1066] With the exception of the octyloxy-substituted compound, all compounds exhibited mesomorphic behavior. The orthogonal conformation of the phenyl rings in respect to the plane of the macrocycle creates a "pocket" on either side. The pocket permits axial ligation to species such as oxovanadium.

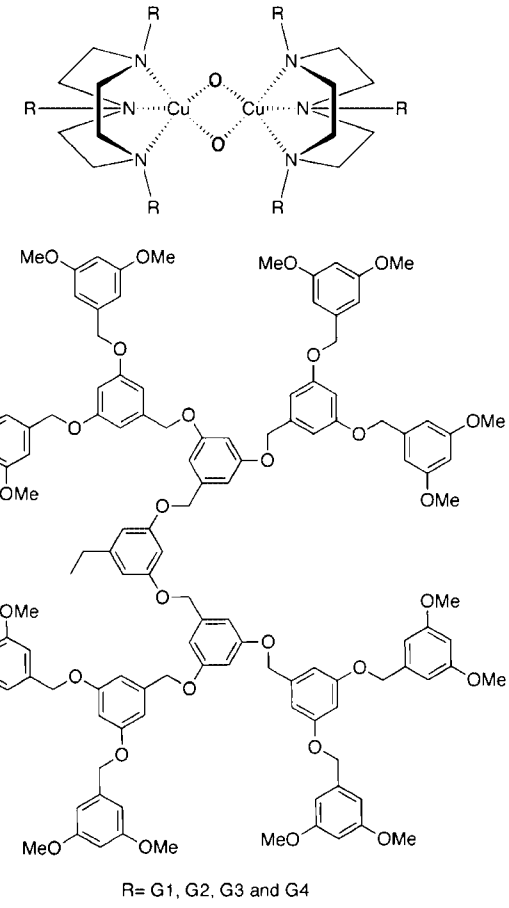

Figure 297. Dendronized 1,4,7-triazacyclononane.[1050]

Vanadyl derivatives show further destabilization of the crystal phase and exhibited a Φ_h phase over a 246 °C temperature range.[1066]

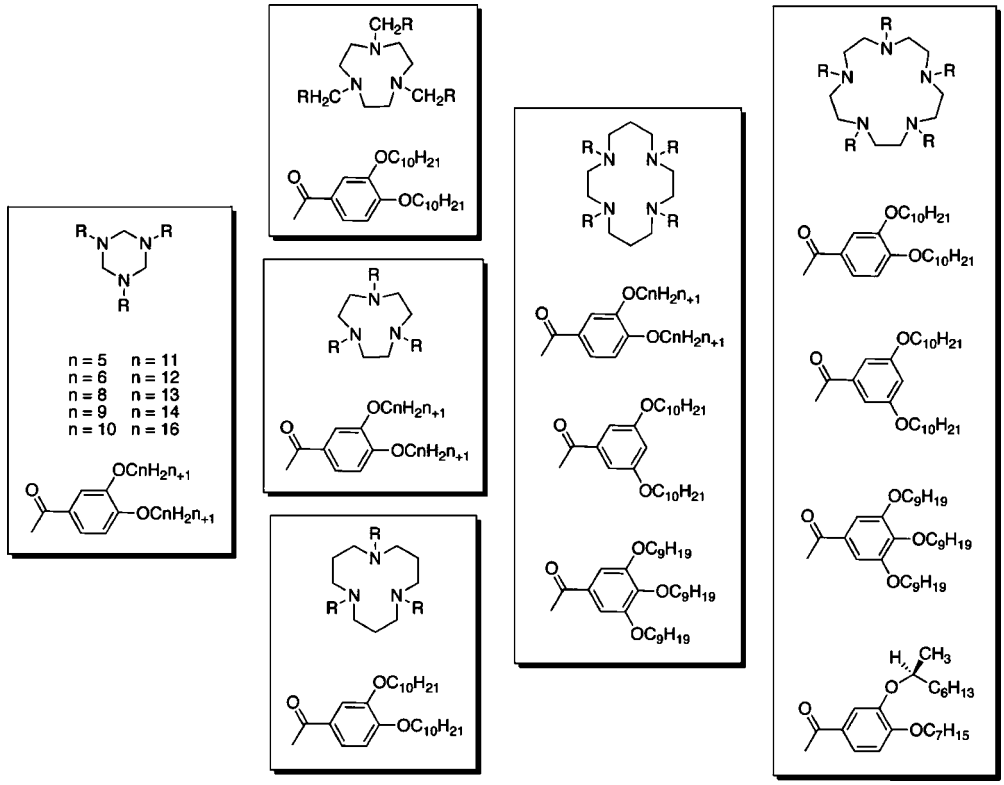

Figure 296. Classes of dendronized azacrown macrocycles.[1040−1049]

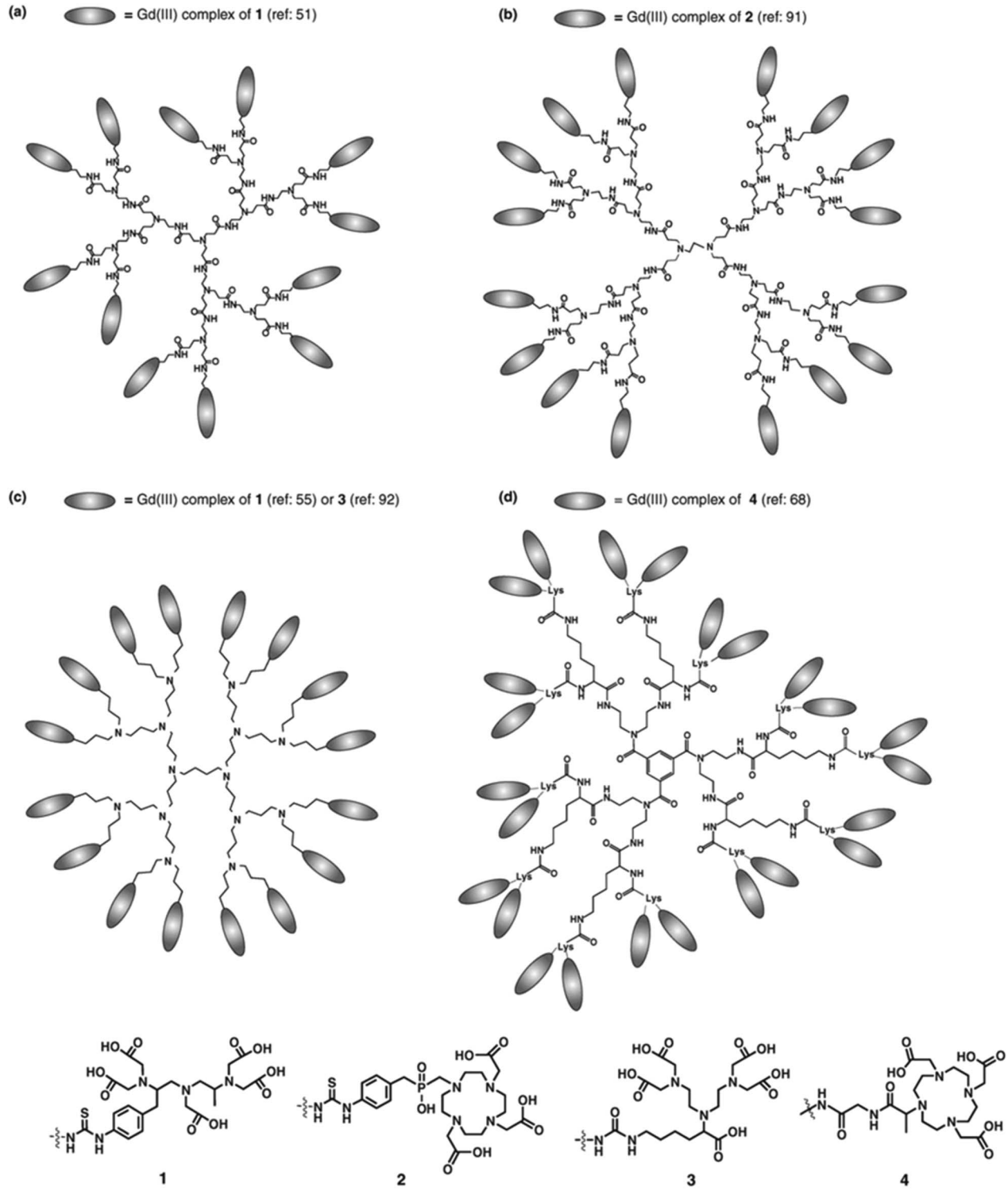

Figure 298. Dendritic MRI contrast agents incorporating multiple Gd^{III} binding sites. Reprinted with permission from ref 1056. Copyright 2007 Royal Society of Chemistry for the CNRS and RSC.

Porphyrins were dendronized with phenylene-based dendrons functionalized at the periphery with hydrocarbon chains (Figure 306).[1067] TOPM and XRD indicated the formation of Φ_r structures. Complexation with C_{60} resulted in 1:1 complex. Increased melting and isotropization temperatures were observed along with an unidentified LC phase. Φ_r phases were also reported in a series of porphyrins functionalized with Fréchet-type dendrons.[1068,1069]

Tsukube reported bis-pocketed porphyrins in the design of receptors for bimolecular guest accommodation.[1070] Dendronized thymine and pyridine guests were bound to a trisdendronized Zn metalloporphyrin bearing a diaminopyridine attached at the 5 position of the porphyrin macrocycle (Figure 307). Tsukube demonstrated that 90% of the receptor was bound to pyridine and 57% was bound to thymine, thus demonstrating proof of bimolecular guest accommodation. Diederich utilized the pocket obtained by 3,5- and 2,6-positions of the mesophenyls of 5,10,15,20-tetrakis(phenyl)porphyrin and 5,15-di(phenyl)porphyrin in the search for systems that will serve as models for hemoglobin.[1071]

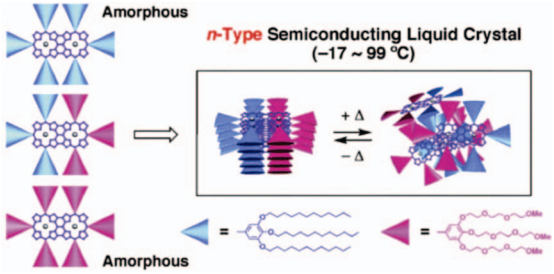

Figure 299. Dendronized porphyrin dimers. Reprinted with permission from ref 1059. Copyright 2008 American Chemical Society.

Hemin is one of the most readily accessible of all porphyrins, as it is isolated from blood. The first examples of dendronized hemin were reported by Velasco.[1072] Demetalation of hemin and functionalization of the macrocycle yielded the tetra acid. Esterification of the tetra acid with dendrons yielded the tetradendronized porphyrin bearing two flexible propionate linkers and two conformationally fixed α,β-unsaturated propionate linking groups (Figure 308).[1072]

At high temperature, a Φ_h phase was identified that, upon cooling, transformed into a second 2-D Φ_h lattice. Both phases were assigned by TOPM and XRD.[1072] Corresponding Zn metalloporphyrins were investigated. It was proposed that the second lower-temperature Φ_h phase was due to a change in the conformation of the phenyl propionate chains. In this phase, the $\pi-\pi$ interactions are partially broken and a less ordered phase was observed. Molecular models showed that the most stable conformation for the two phenyl propionate chains is an out-of-plane configuration rather than the planar conformation proposed for the high-temperature phase. This conformational change is not observed in the metalated compounds, where the loss of stronger $\pi-\pi$ interactions is not compensated by the more stable conformation of the two propyl chains. DSC experiments showed that the transformation from $\Phi_{h,1}$ to $\Phi_{h,2}$ was only complete after annealing at 25° over several hours.[1073,1074]

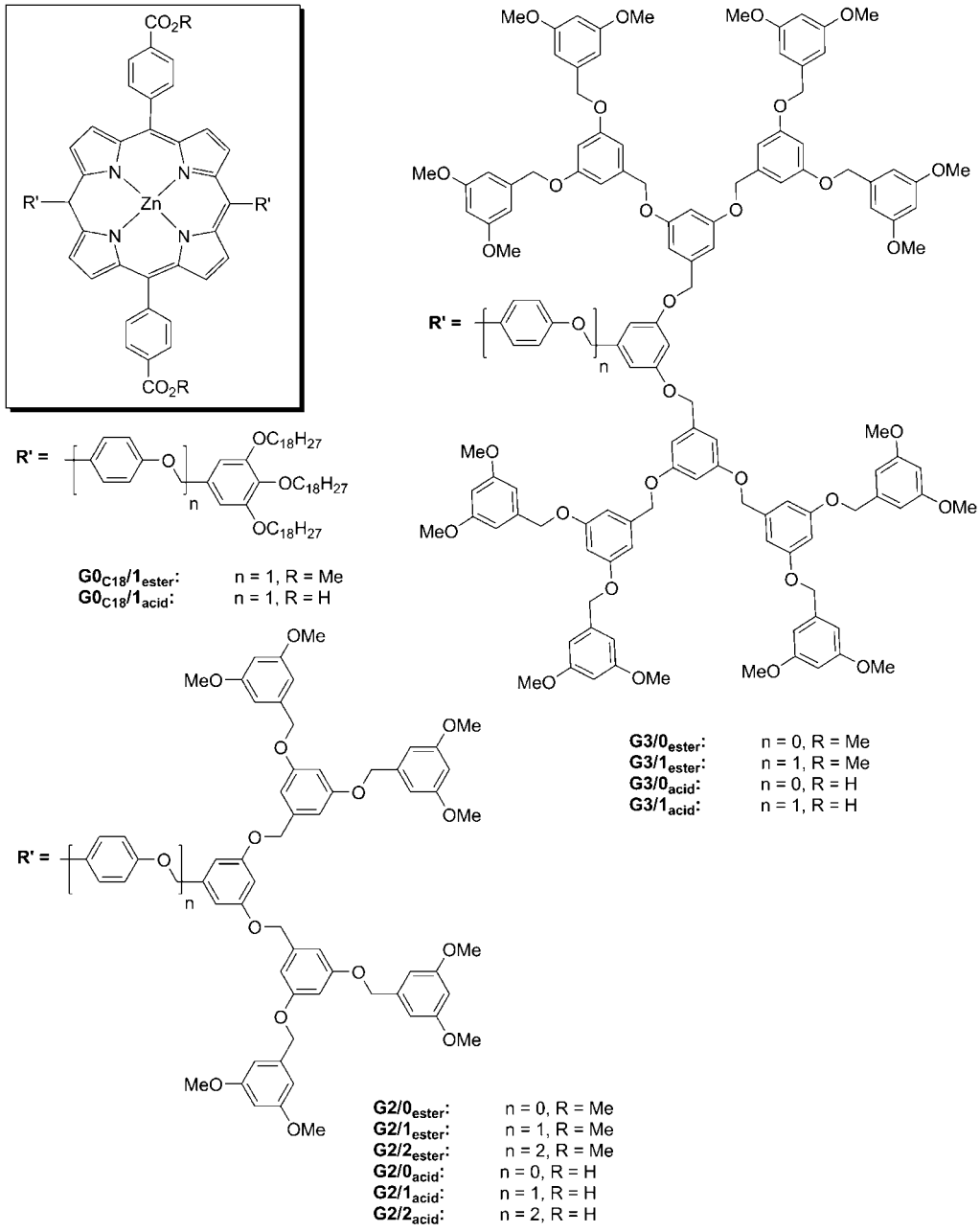

Figure 300. Structure of H-bonding dendronized Zn-porphyrins. Adapted from ref 1061.

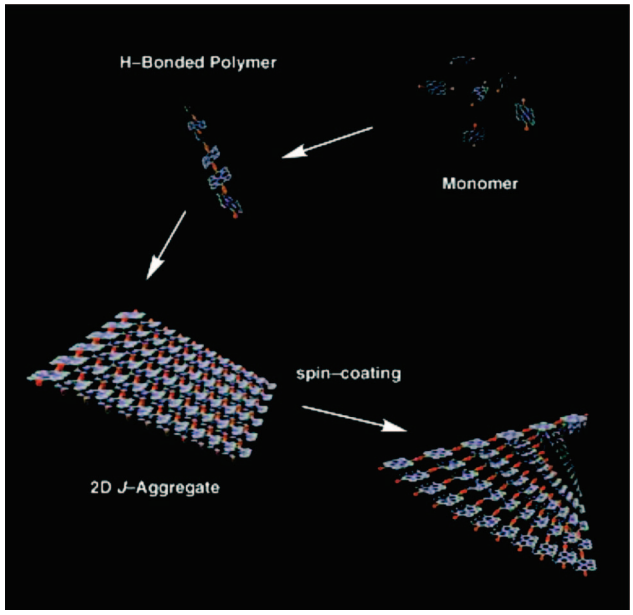

Figure 301. Proposed mechanism of self-assembly of porphyrin J-aggregates. Reprinted with permission from ref 1061. Copyright 2004 Wiley-VCH Verlag GmbH & Co. KGaA.

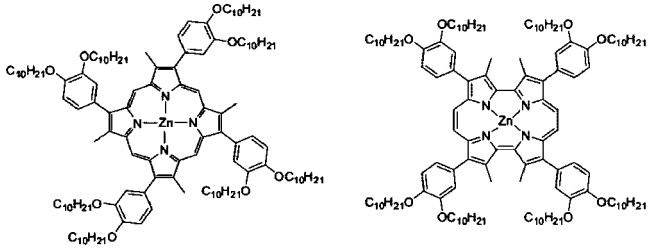

Figure 302. Dendronized Zn-porphyrins and porphycenes reported by Sessler.[1063]

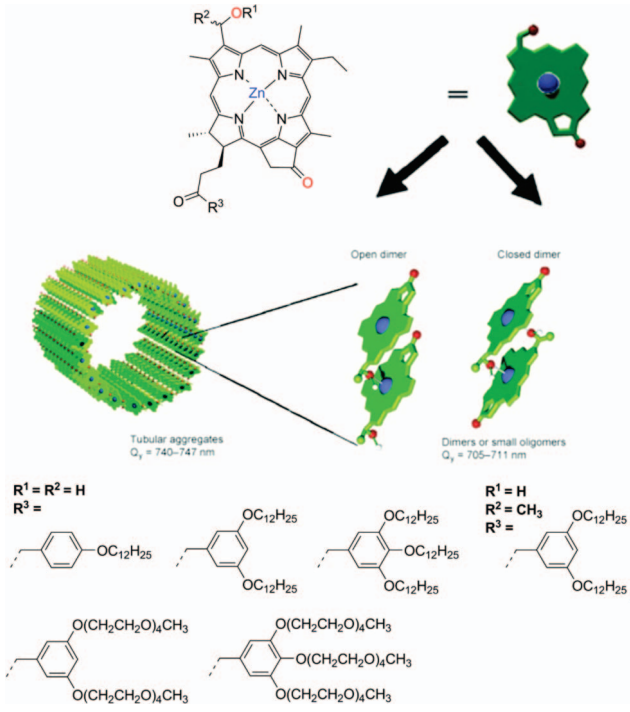

Figure 303. Structure and self-assembly of Zn 3[1]-hydroxymethyl chlorins and Zn 3[1]-hydroxyethyl chlorins. Adapted with permission from ref 1064. Copyright 2008 Wiley-VCH Verlag GmbH & Co. KGaA.

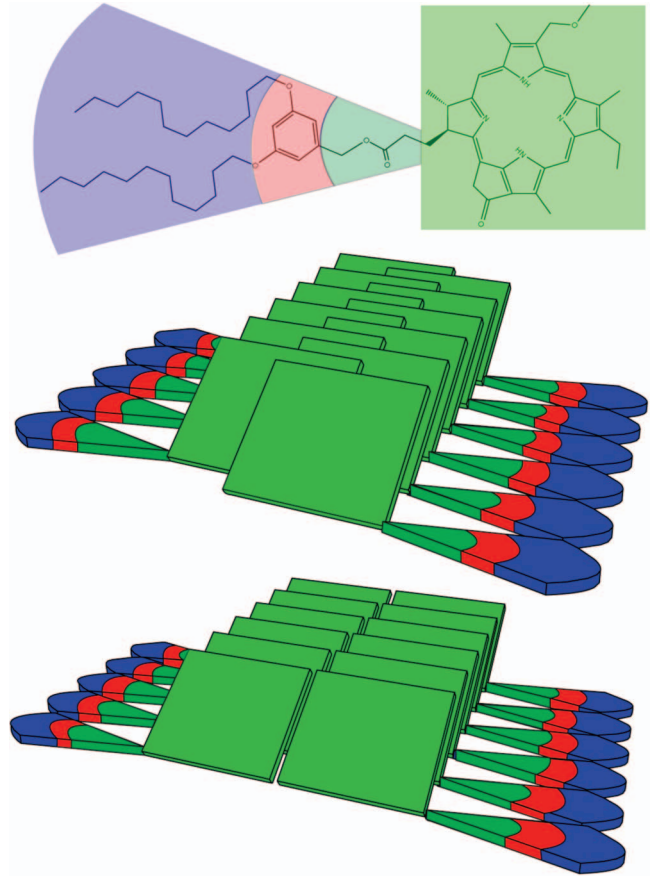

Figure 304. Self-assembly of dendronized chlorins on HOPG surfaces. Adapted from ref 1065.

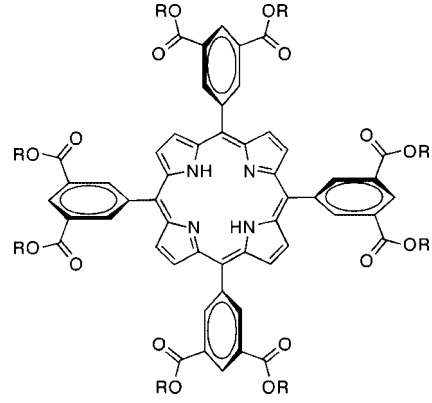

Figure 305. Porphyrins functionalized with 3,5-dicarboxy benzenes with different alkyl chain lengths.[1066]

The model was later refined by both solid-state XRD and solution-phase UV−vis and ^{1}H NMR experiments to propose a schematic model of the two Φ_h mesophases (Figure 309).[1075] The high-temperature phase is a classic representation of the Φ_h phase and is driven by the cofacial $\pi-\pi$ interactions of stacked macrocycles, with each macrocycle offset in both the H10−20 and H5−15 axis of the macrocycle. This model was first proposed by Sanders[1076] and demonstrated in a nondendronized β-substituted porphyrin by Costa and Dalcanale.[1077] The lower-temperature less-ordered phase arises from trimeric aggregates of macrocycles stabilized not only by cofacial $\pi-\pi$ interactions but also by CH$-\pi$ interactions arising from conformational changes in the phenyl propionic chain. At temperatures below 60 °C,

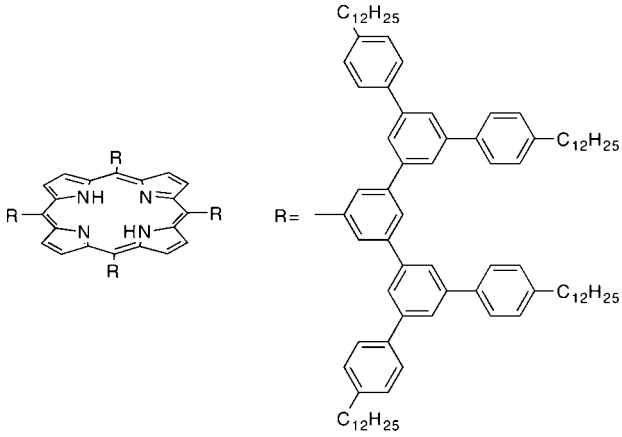

Figure 306. Porphyrins dendronized with phenylene dendrons. Reprinted with permission from ref 1067. Copyright 2002 American Chemical Society.

the $\pi-\pi$ stacking is not strong enough to offset the cost of the planar structure.[1075]

Vinogradov developed poly(L-glutamate) dendronized porphyrins and Newkome dendronized tetrabenzoporphyrin that can be utilized as pH nanosensors (Figure 310).[1078] These dendronized porphyrins and tetrabenzoporphyrins are membrane-impermeable and have nonoverlapping emission that is modulated by pH titration of porphyrin cores. Encapsulating the dendronized porphyrin, while keeping the dendronized tetrabenzoporphyrin, provides a spectroscopic method to measure proton transport across channeled membranes.[171,350]

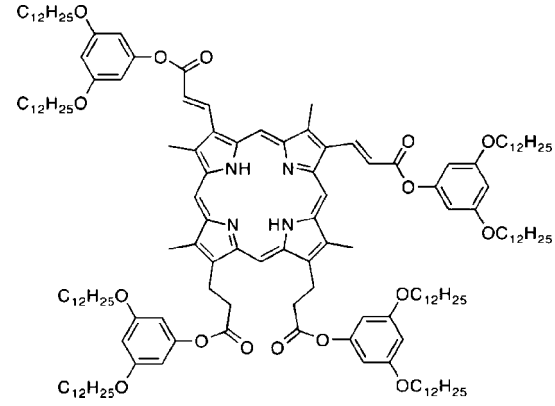

Figure 308. Dendronized Hemin.[1072]

Zimmerman developed a strategy for the functionalization of porphyrin with high-generation Haag−PEO dendrons via click chemistry (Figure 311).[1079] G4 PEO dendrons with azide apex functionality were attached-to porphyrins with G1 acetylene-functionalized benzyl ether dendrons via 1,3-Huisgen cyclization to form G5 hybrid dendrons. The surface cross-linking of the periphery via RCM has been reported.[1080]

In addition to porphyrins, recent attention has been focused on a relatively new class of subporphyrins.[1081] First synthesized by Osuka, subporphyrins consist of a bowl-shaped 14π aromatic cycle.[1082] The first dendronized subporphyrins were reported by Lu.[1083] Subporphyrins were dendronized with carbazole dendrons, and their photophysical properties were investigated (Figure 312). Although reasonable energy transfer efficiencies from dendron to subporphyrin were obtained, fluorescence quantum yields were only in the range

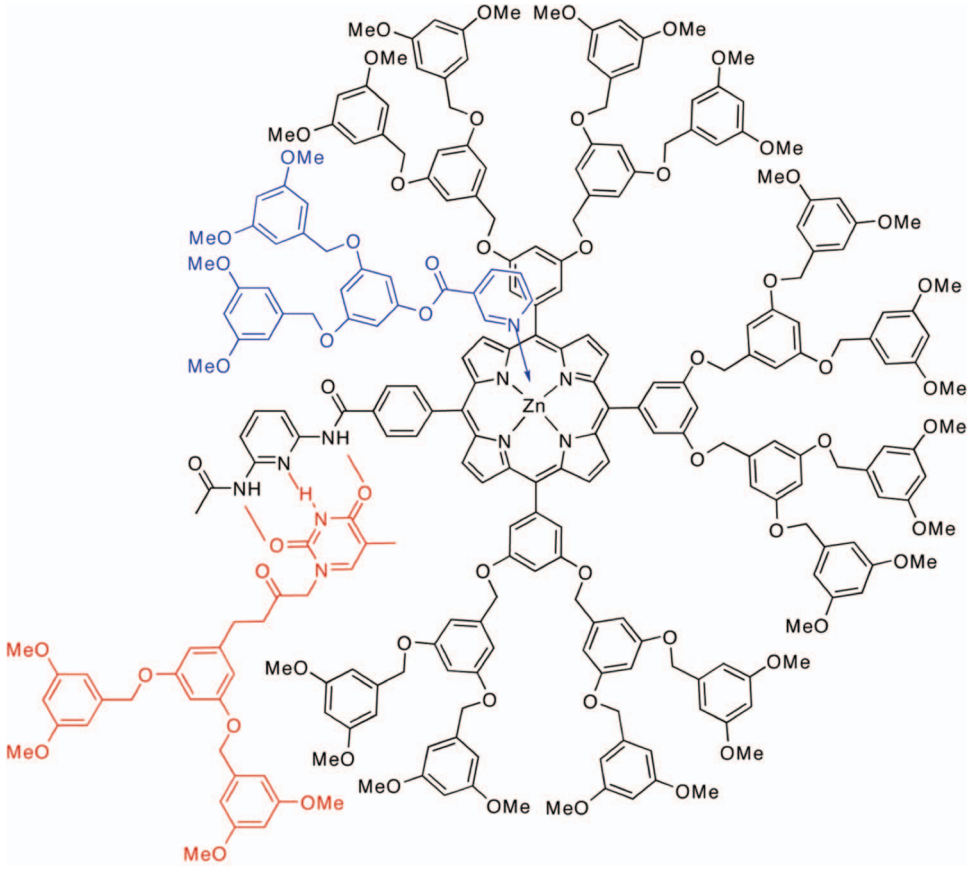

Figure 307. Bimolecular receptor dendronized porphyrin.[1070]

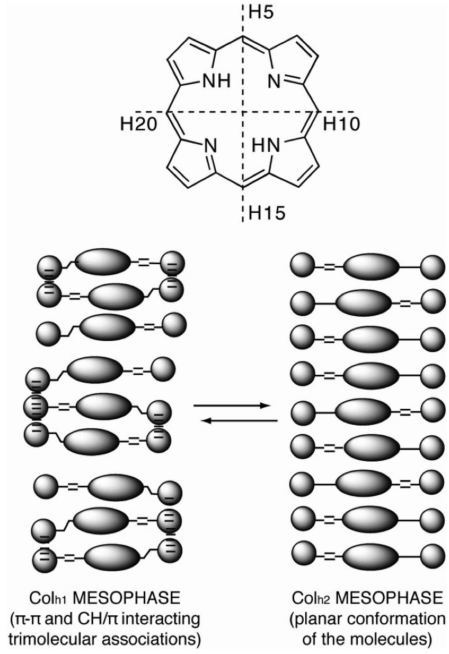

Figure 309. Schematic packing model of dendronized porphyrins at low temperature (left) and at high temperature (right). Reprinted with permission from ref 1075. Copyright 2008 American Chemical Society.

of 11−15%. A trend of decreasing efficiency with increased generation number was observed. In contrast to subporphyrins, Sessler reported dendronized cyclo[8]pyrroles that form Φ_h LC phases when combined with electron-deficient acceptors such as trinitrofluorenone, trinitrophenol, trinitrobenzene and trinitrotoluene (Figures 313 and 314).[1084]

In addition to porphyrins, subporphyrins, and cyclo[8]pyrroles, the self-assembly and self-organization of related phthalocyanines have also been investigated. Phthalocyanines structurally resemble benzoporphyrins but contain imine linkages. McKewon synthesized a series of phthalocyanines with varied substitution patterns and investigated the effect on self-organization with the aim of producing isotropic solid solutions in which the phthalocyanine cores are isolated from each other (Figure 315). Phthalocyanines peripherally substituted with Fréchet-type dendrons have been reported to display Φ_h phases over a wide range of temperatures, even in the absence of a hydrocarbon periphery, and were shown to resist crystallization over extended periods of time.[1085] Phthalocyanines asymmetrically substituted with Fréchet-type dendrons and EO have been synthesized, and all examples exhibited Φ_h phases that could be supercooled into a glassy state. Attachment of Fréchet-type dendrons to the axial positions of silicon phthalocyanine resulted in isotropic "solid solutions" with high T_g (Figure 315).[1086,1087] Kobayashi reported an asymmetric dendronized silicon phthalocyanine similar to those of McKewon that self-assembled into spherical micelles as observed by cryo-TEM (Figure 316).[1088] Ito also reported similar bis(dendronized) silicon−phthalocyanines with fullerodendrons.[1089]

Ivanov has also reported phthalocyanines functionalized with branched 12-pentacosane (Figure 317).[985] At low temperature, this dendronized phthalocyanine exhibits a Φ_r phase wherein the macrocycles are tilted 18° relative to the columnar axis. Upon heating, a reversible transition to Φ_h lattice is observed, wherein the title feature has disappeared.

6.4. Dendronized Cyclotriveratrylene and Cyclotetraveratrylene

The first examples of self-organizing cyclotriveratrylene (CTV) were reported independently in the same year by

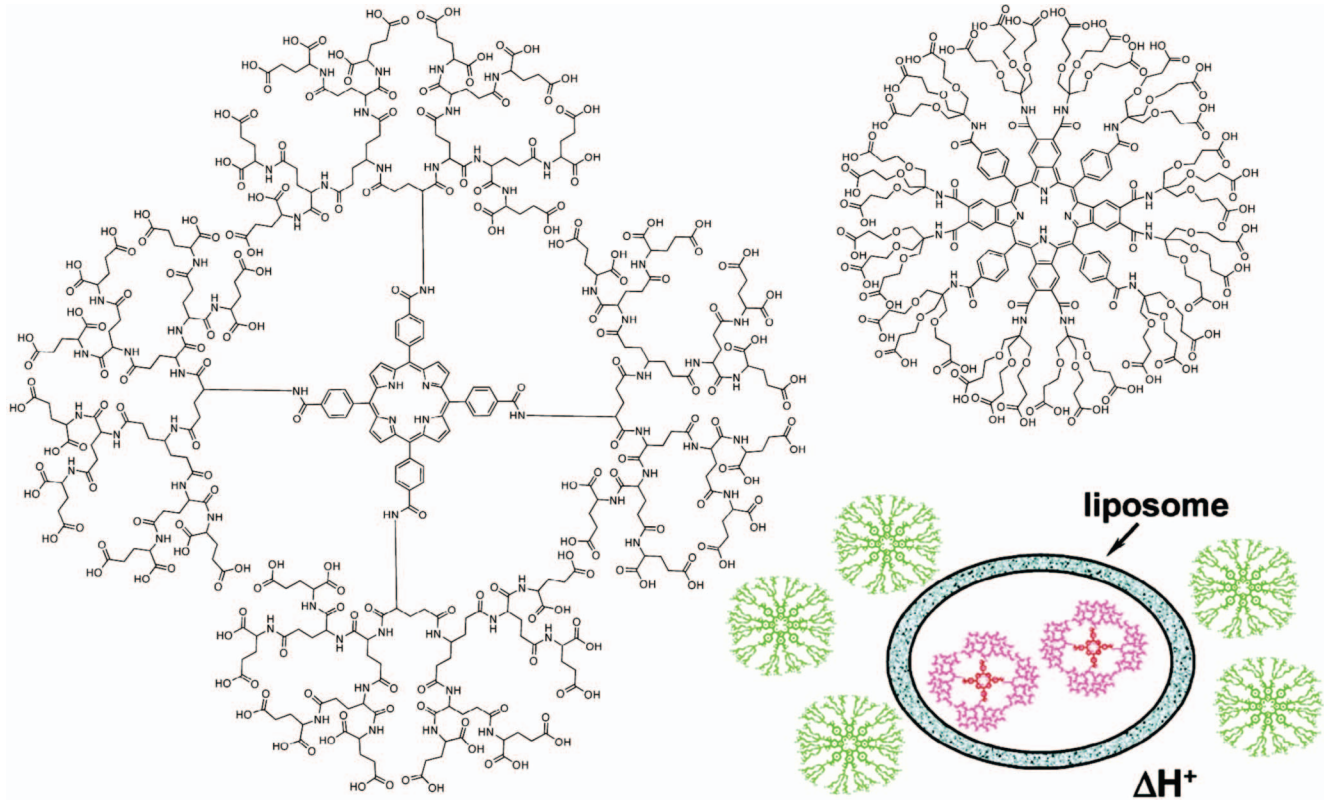

Figure 310. Structures of dendronized porphyrins and tetrabenzoporphyrins (top) and their use as colorimetric pH-responsive nanosensors in channeled membranes. Reprinted with permission from ref 1078. Copyright 2003 American Chemical Society.

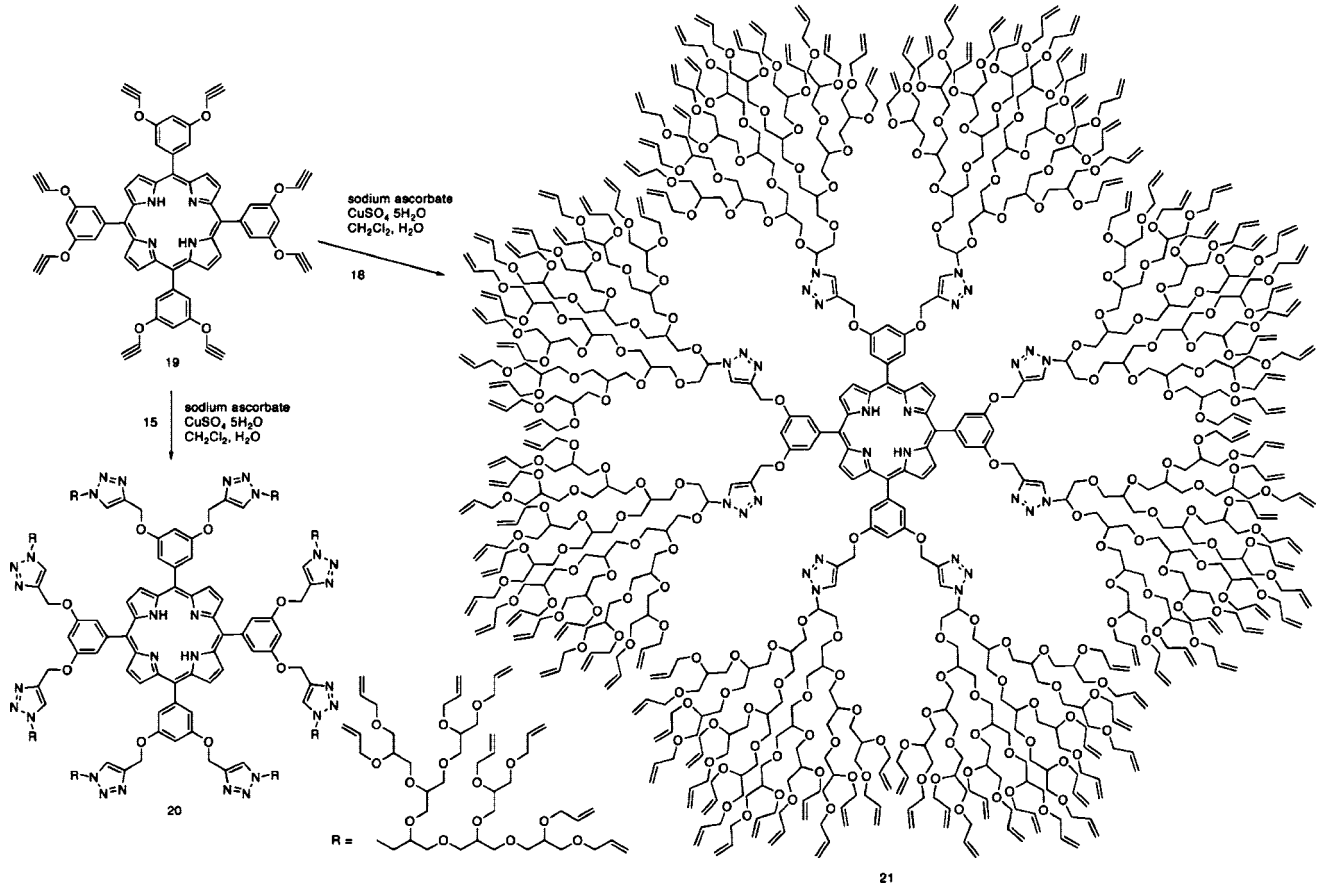

Figure 311. Synthesis of high-generation dendronized porphyrins via click chemistry.[1079]

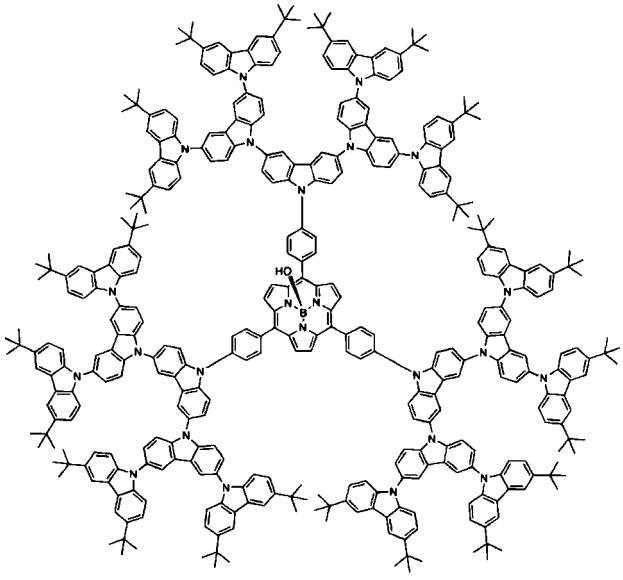

Figure 312. Subporphyrins dendronized with carbazole dendrons.[1083]

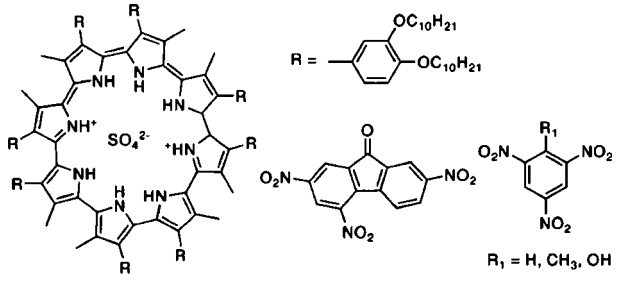

Figure 313. Cyclo[8]pyrroles and electron-deficient acceptors.[1084]

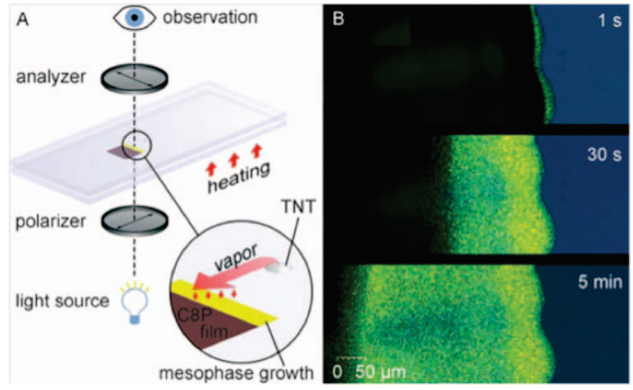

Figure 314. Mesophase formation on the complexation of dendronized cyclo[8]pyrroles with electron-deficient acceptors by Sessler. Reprinted with permission from ref 1084. Copyright 2007 Wiley-VCH Verlag GmbH & Co. KGaA.

Zimmermann and Malthête.[1090−1092] CTV with long alkyl tails was shown to self-assemble into structures that resemble the arrangement exhibited by crystalline CTV in its crystal state, and therefore, the phase was named pyramidal (Figure 318).[1090−1093]

Dendronization of CTV was investigated as a simple and direct route to producing ferroelectric materials.[1098] Dendronized, optically active CTV was synthesized, and its racemization in the LC state was investigated (Figure 319).[1098] In solution, the energy barrier to inversion of the CTV ring is about 27 kcal/mol (half-life, $\tau_{1/2}$, ~1 month at 20 °C).[1094] In dioxane at 100 °C, the first-order rate constant of inversion was determined to be 1.3×10^{-3} s^{-1} and an inversion barrier of 26.9 kcal/mol was determined, in line

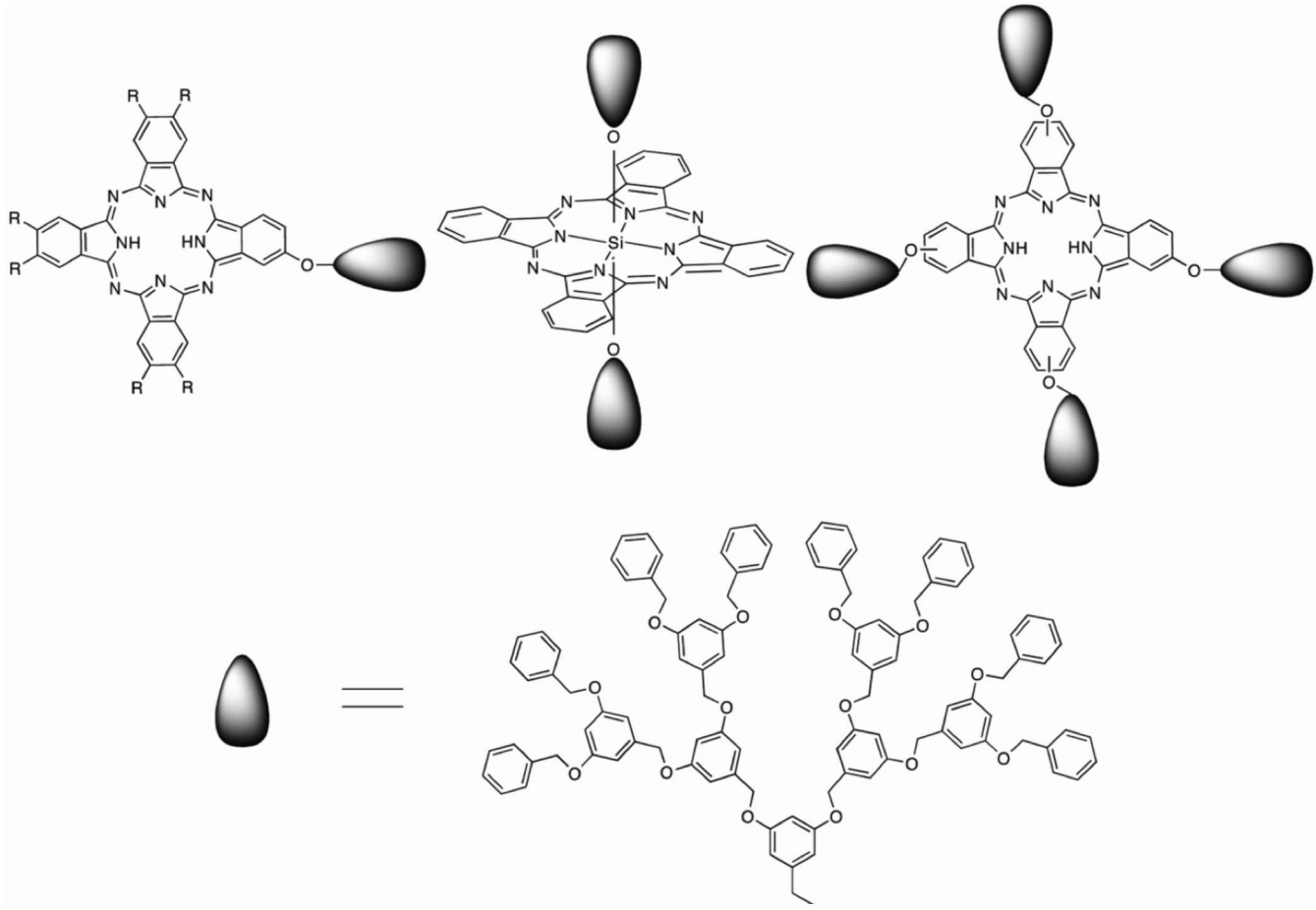

Figure 315. Classes of dendronized phthalocyanines.[1086,1087]

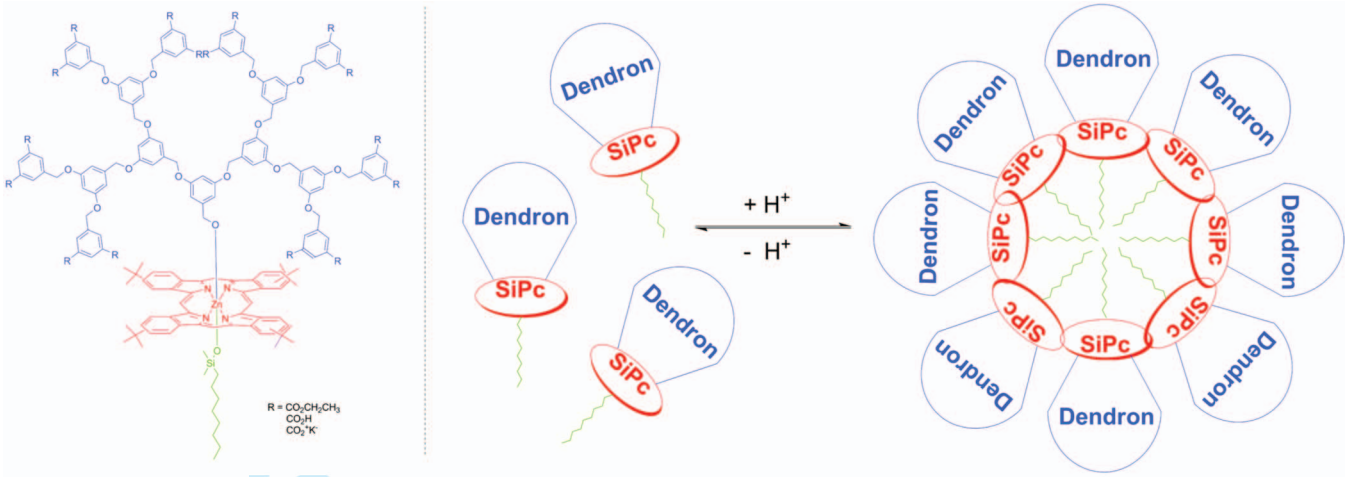

Figure 316. Micelle-forming dendronized phthalocyanines.[1088]

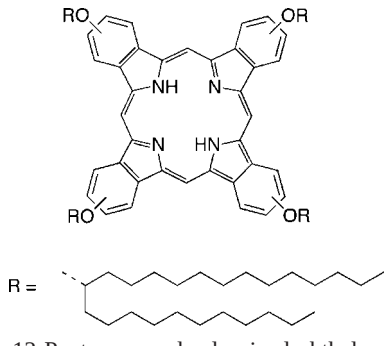

Figure 317. 12-Pentacosane dendronized phthalocyanine.[985]

with previous data obtained for CTV in solution. In the lower-temperature mesophases at 100 °C, the rate constant of inversion was found to be 2 orders of magnitude slower, 1.3×10^{-5} s^{-1}, with an inversion barrier of 30.3 kcal/mol. The racemization was found to be much faster at 130 °C with a rate constant of $\sim 3 \times 10^{-4}$ s^{-1}. The interlocking of the cones in the LC phases was shown to increase the inversion barrier by 3.4 kcal/mol over the solution phase. From this data, it was estimated that, at three degrees below T_I (149 °C), the estimated $\tau_{1/2}$ of a cone was 4 min. This temperature inversion was fast enough to allow for orientation in an electric field. Since the Φ_h pyramidal LC phase is

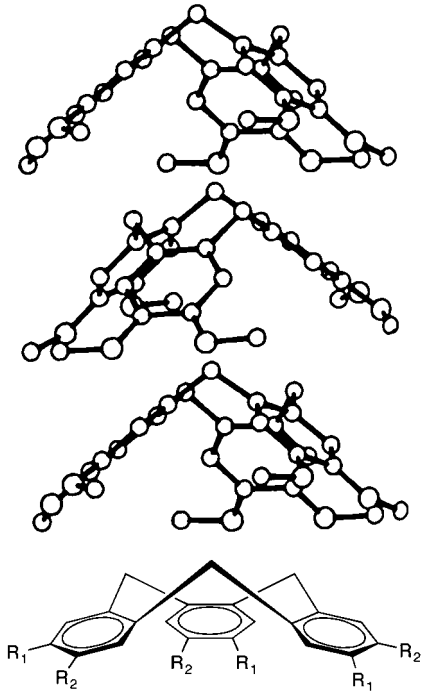

Figure 318. Crystal structure of crystalline CTV.[1093]

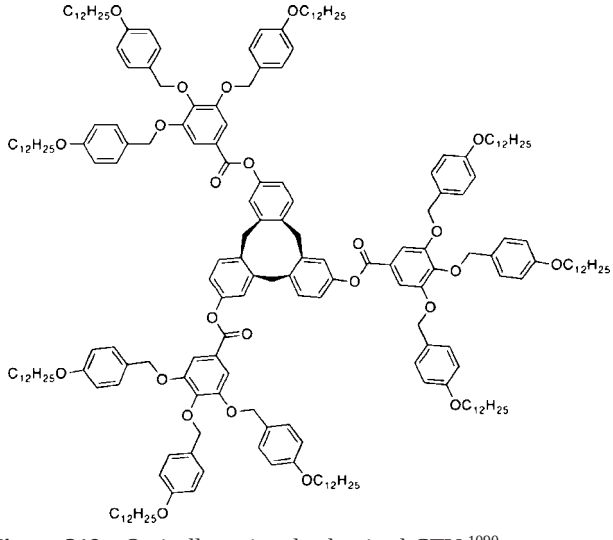

Figure 319. Optically active dendronized CTV.[1090]

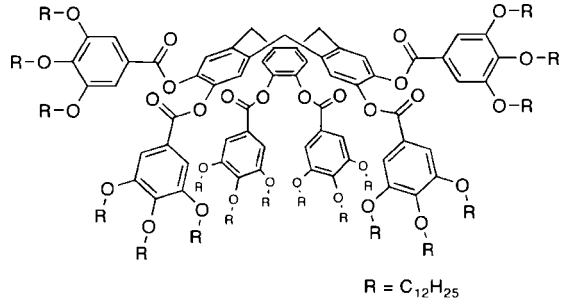

Figure 320. Dendronized CTV reported by Nierengarten.[1105]

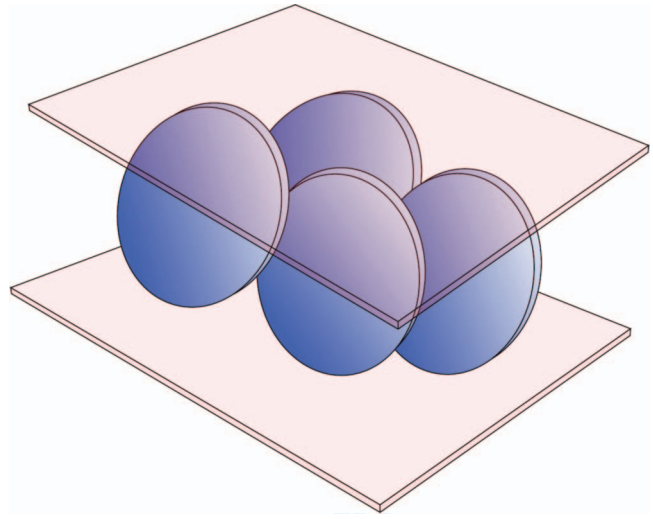

Figure 321. Proposed model for cybotactic ordering in the N phase of dendronized CTV from Figure 320. Adapted from ref 1105.

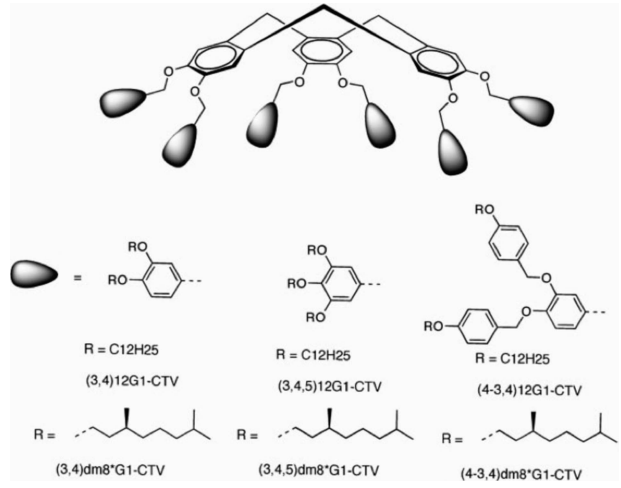

Figure 322. Dendronized CTV with both chiral and achiral tails. Reprinted with permission from ref 330. Copyright 2008 American Chemical Society.

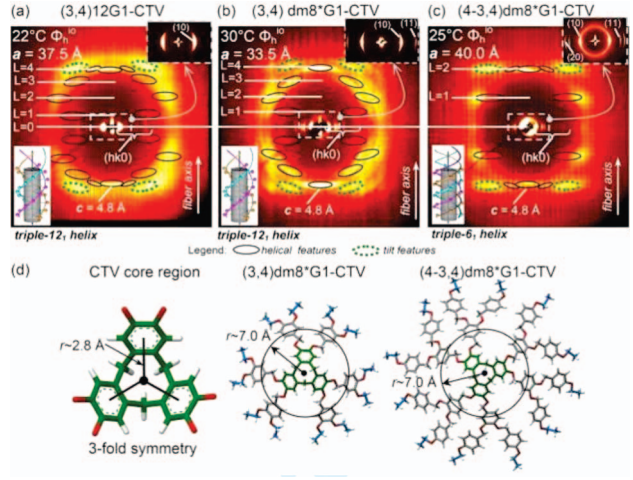

Figure 323. Experimental XRD and models of dendronized CTV. Reprinted with permission from ref 330. Copyright 2008 American Chemical Society.

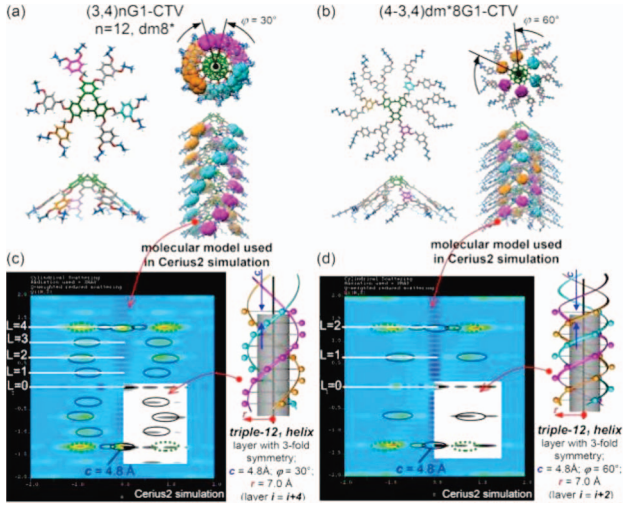

Figure 324. (a) Self-assembly of (3,4)*n*G1−CTV into a triple-12_1 helix, and (c) Cerius2 simulation of its diffractogram from the molecular model. (b) Self-assembly of (4-3,4)d*m**8G1−CTV into a triple 12_1 helix, and (d) Cerius2 simulation of its diffractogram from the molecular model. Reprinted with permission from ref 330. Copyright 2008 American Chemical Society.

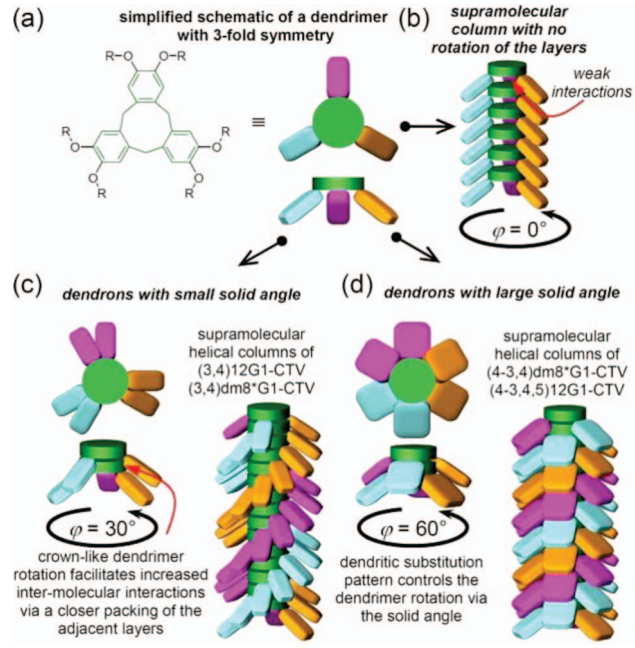

Figure 325. Schematic representation of the effect of solid angle on helical parameters of self-assembled dendronized CTV. Reprinted with permission from ref 330. Copyright 2008 American Chemical Society.

almost crystalline at room temperature (20 °C), it was proposed that, by quenching the Φ_h phase, orientation could be retained for many decades.[1090] Zimmermann investigated in detail the mechanism of inversion of nondendronized CTV macrocycles in both the mesomorphic and isotropic states. The inversion process in the plane perpendicular to the C_3 axis varied from a planar diffusion to discrete jumps dependent on peripheral substitution at the CTV core.[1095,1096]

Since the discovery of self-assembling dendronized CTV, LC CTV has been extensively investigated by a number of groups, most notably Nierengarten,[91,1097] Zimmermann,[1098−1100] Percec,[1101−1103] and Tschierske.[1104] However, the field of dendronized self-organizing CTV and cyclotetraveratrylene (CTTV) has been relatively untouched until recently. Nierengarten reported a dendronized CTV exhibiting an N-like phase (Figure 320).[1105] Diffuse reflection was suggested to be indicative of cybotactic behavior, a noted phenomenon in N liquid crystals[1106] where localized S ordering is observed over a small number of molecules. A model where dendronized CTV displayed short-range lamello-columnar order, i.e., S layers with the existence of columns oriented parallel to the S planes, was proposed (Figure 321). Nierengarten also reported the inclusion of C_{60} in a 2:1 host−guest complex. XRD of the mesophases formed by these compounds showed diffraction patterns indicative of a *Cub* phase. The lattice was deduced to be BCC as no extinction rule could be found to explain the number of missing low-angle reflections for either face-centered or simple *Cub* lattices. The absence of the [200] reflection and the presence of the [222] reflection suggested $I4_132$ symmetry.[1105] Nierengarten also reported the complexation of Fréchet dendronized CTV with C_{60},[1107,1108] but these CTV derivatives do not self-assemble. Similar dendronized resorcinarene complexes with C_{60} were also reported.[1109]

Percec reported libraries of CTV dendronized with self-assembling dendrons (Figure 322). Because of their rigid crown-conformation, the dendritic crowns generated from dendronized CTV were used as models for conformationally flexible dendritic crowns. An expanded version of Cochran, Crick, and Vand (CCV) helical diffraction theory[329] was applied to both flexible and rigid crowns, allowing for the determination of their atomic helical structure and demonstrating their self-assembly into helical pyramidal columns and self-organization into Φ_h and Φ_h^{io} lattices (Figure 323) and chiral supramolecular spheres.[330,1110] In addition, simulation of their fiber XRD by Cerius2 provided their molecular mechanisms of self-assembly. The CTV dendritic crown models facilitated the analysis of a library of dendronized polymers, dendrimers, and dendrons by the same combination of methods.[330]

Steric crowding at the periphery of the macrocycle was increased in a series of three Percec-type dendrons peripherally functionalized with dodecyl and (*S*)-d*m*8 tails [(3,4)*n*G1−CTV, (4-3,4)d*m*8G1−CTV, and (4-3,4,5)12G1−CTV]. Through the use of both chiral and achiral tails, the effect of the chirality on self-assembly and self-organization was examined. It was found that the introduction of a chiral tail to the periphery of the dendron resulted in selection of the handedness of the column but had little effect on other self-assembly parameters. In the case of (3,4)*n*G1CTV and (4-3,4)d*m*8G1−CTV, XRD studies showed the presence of a triple 12_1 helix (Figure 324), whereas the more sterically hindered (4-3,4,5)12G1−CTV exhibited a triple 6_1 helix (Figure 36).[330]

The difference in helix formation was explained by comparison of the dendron solid angles. Dendrons with a sharper projection of solid angle α' induced a smaller rotational angle φ, which in cooperation with the interlocking action of CTV controls the self-assembly of the helical column (Figure 325).[330]

Percec also reported a similar series of CTV dendronized with self-assembling dendrons bearing both chiral and achiral tails (Figure 326).[1110] Here chiral dendritic crowns were shown to self-assemble into chiral supramolecular spheres.

Compounds functionalized with (3,4)G1, (4-3,4)G1, and (4-3,4-3,5)G2 self-assembling dendrons (Figure 326) exhib-

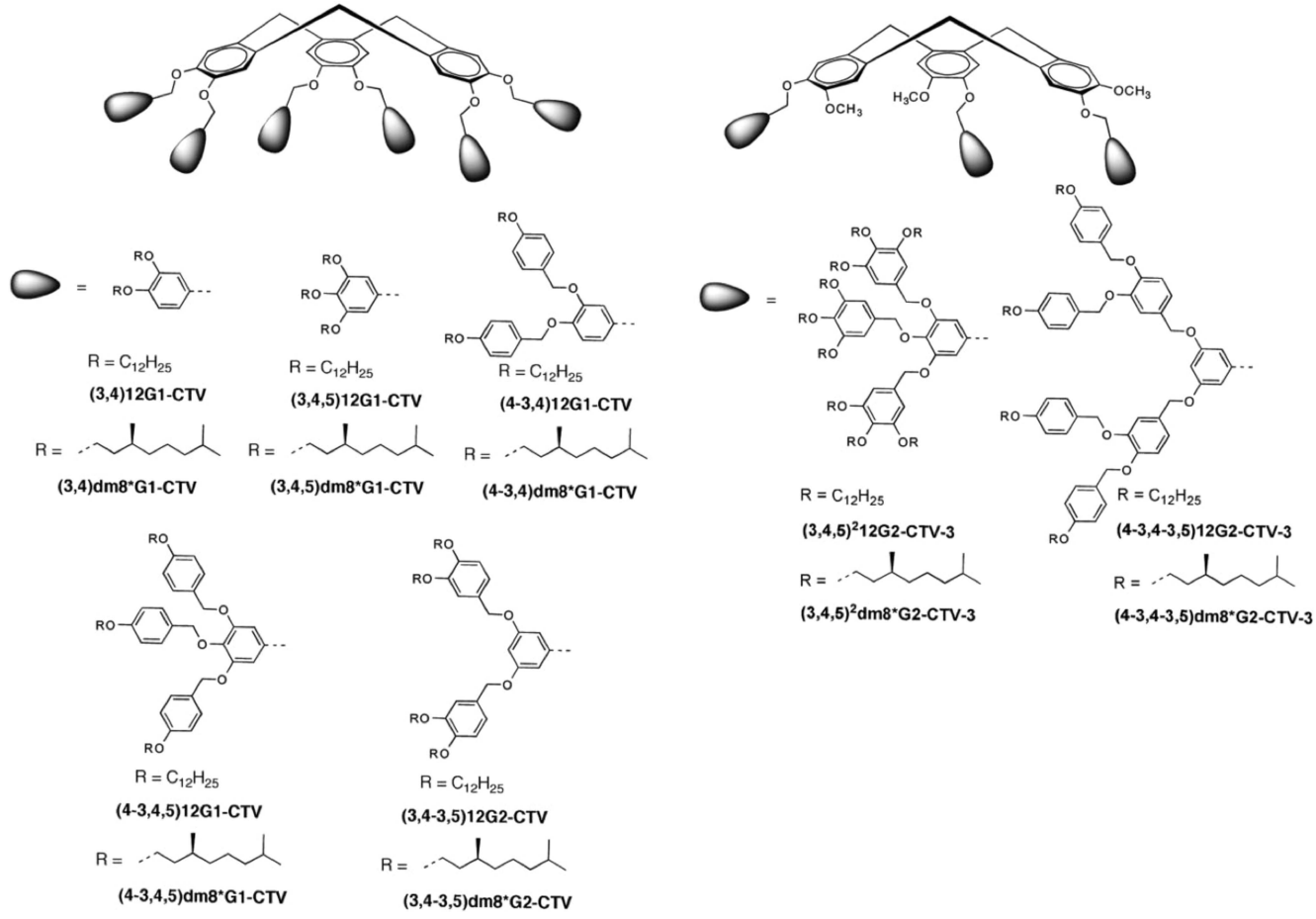

Figure 326. Dendronized CTV with both chiral and achiral tails. Reprinted with permission from ref 1110. Copyright 2008 American Chemical Society.

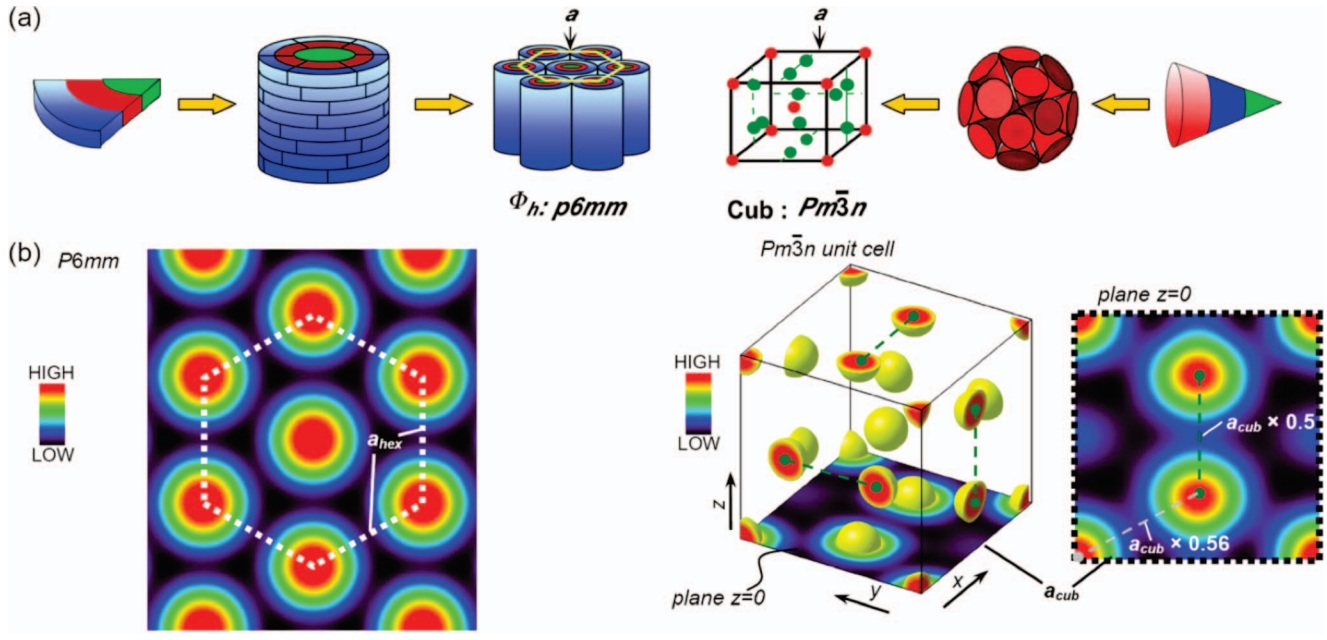

Figure 327. Reconstructed electron-density maps of hexagonal and cubic lattices exhibited by dendronized CTV. Reprinted with permission from ref 1110. Copyright 2008 American Chemical Society.

ited Φ_h lattices with and without intracolumnar helical order, Φ_h^{io}. Chiral and achiral compounds dendronized with (3,4,5)G1 dendrons (Figure 326) exhibited both Φ_h and *Cub* lattices. CTV functionalized with achiral (4-3,4,5)12G1 and (3,4-3,5)12G2 (Figure 326) dendrons exhibited both Φ_h and *Cub* lattices, whereas the chiral analogues displayed only *Cub* lattices. Finally, CTV decorated with $(3,4,5)^2$G2 dendrons (Figure 326) displayed only tetragonal lattices. In the

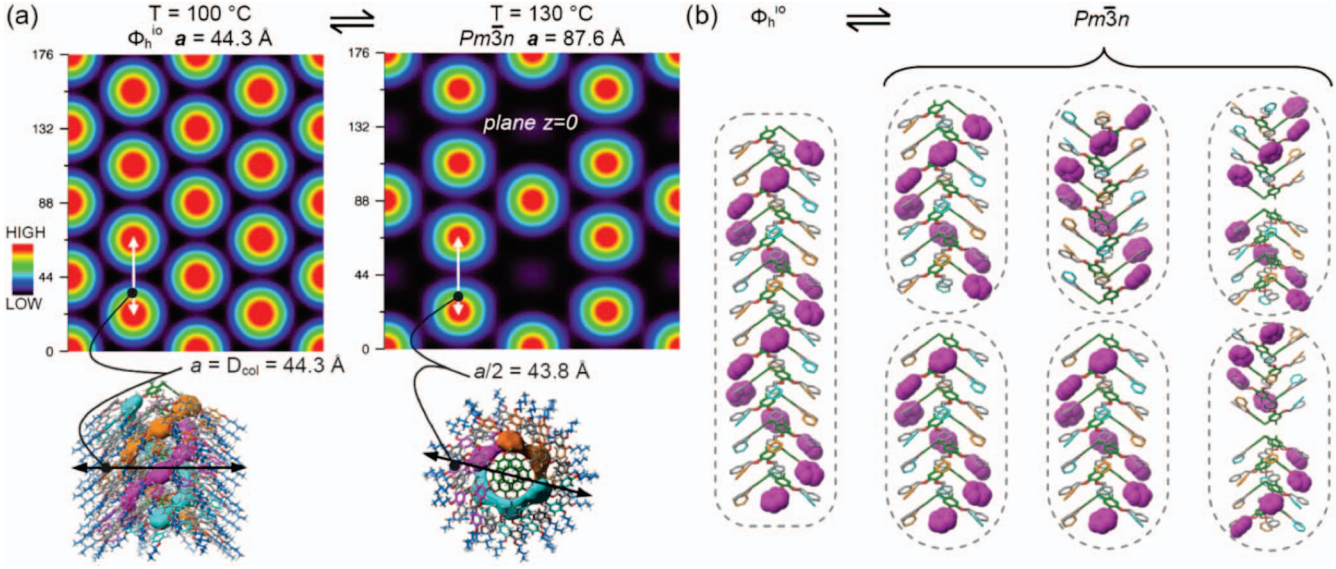

Figure 328. Proposed models for the formation of chiral spheres from helical columns. Reprinted with permission from ref 1110. Copyright 2008 American Chemical Society.

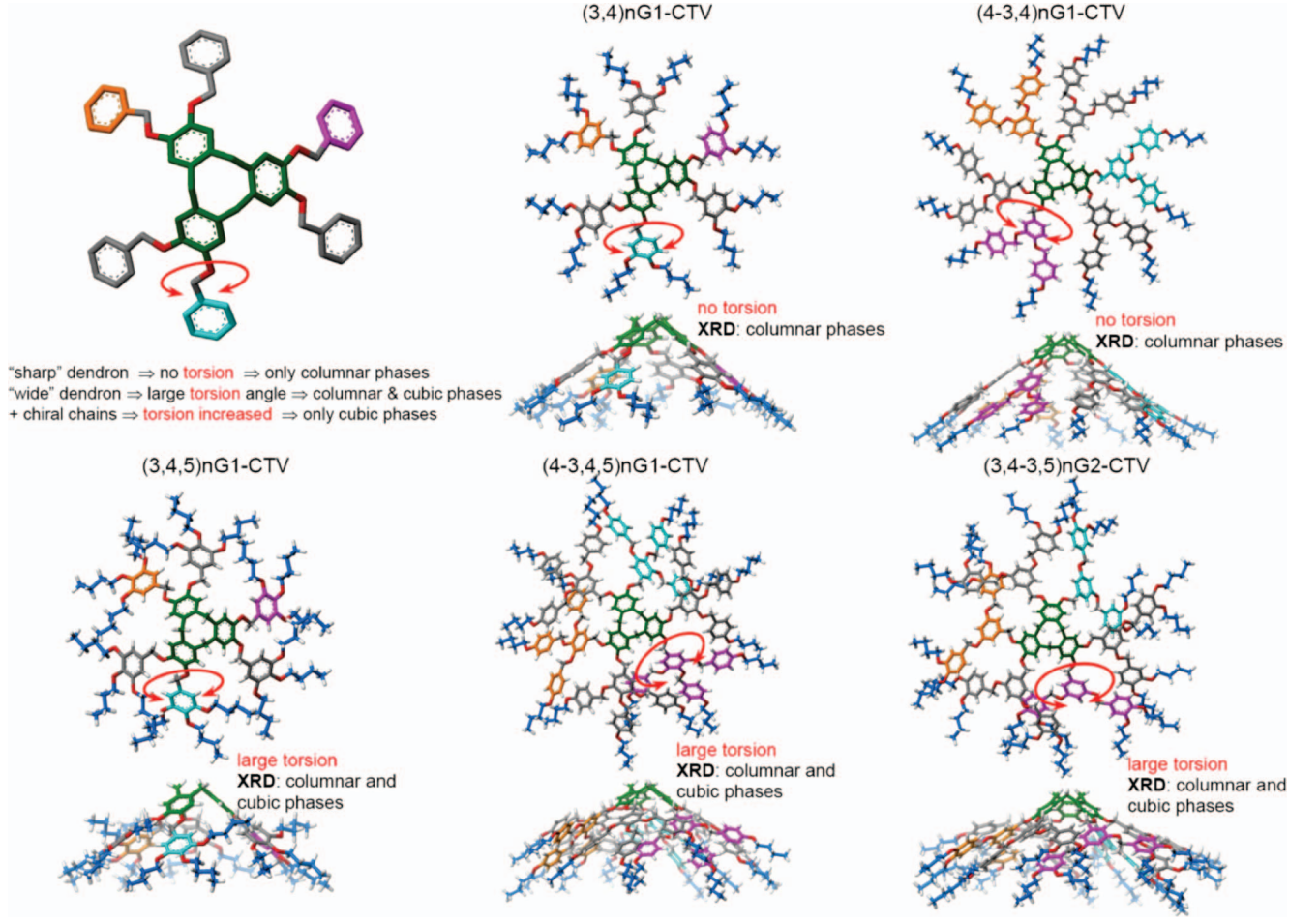

Figure 329. Relationship between solid angle and CTV dendron torsion angle in dendronized CTV. Reprinted with permission from ref 1110. Copyright 2008 American Chemical Society.

case of compounds displaying a transition from Φ_h to *Cub* lattices, the reconstructed electron-density maps showed a relationship between the lattice dimension of the Φ_h lattice and the *Cub* lattice of $a_{hex} \approx a_{cub}/2$ (Figure 327).[1110]

It was demonstrated that a crownlike conformation was adopted in the helical pyramidal columns and in supramolecular spheres. Three models of self-assembly were advanced.[1110] In each case, at one or more points along the helical pyramidal columns of dendritic crowns, the columns decouple and form shorter fragments (Figure 328).[1110]

Spherical objects arise from the transition from Φ_h to *Cub* phase. While the soft periphery of the self-assembled

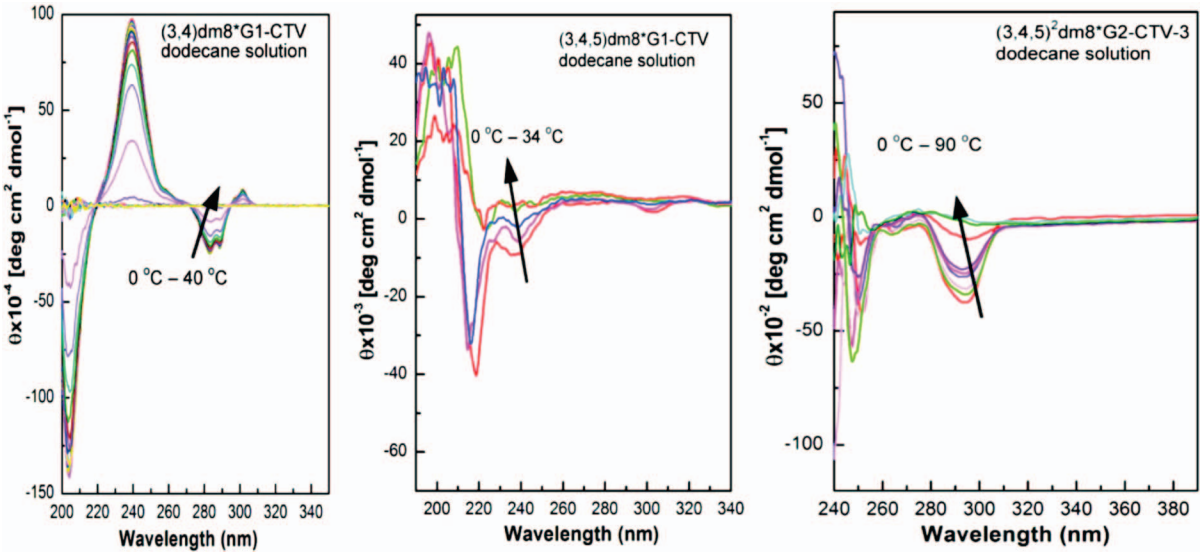

Figure 330. Solution CD spectra of chiral dendronized crowns that self-assemble into helical pyramidal columns (left) and chiral spheres (middle, right) that in the solid state pack into Φ_h^{io} (left), Cub_{Pm3n} (middle), and $P4_2/mnm$ lattices (right). The CD from the left figure is identical to the one in thin film. This indicates the persistence of the same structure in bulk and in solvophobic solvents and allows its structural analysis by XRD experiments. Reprinted with permission from ref 1110. Copyright 2008 American Chemical Society.

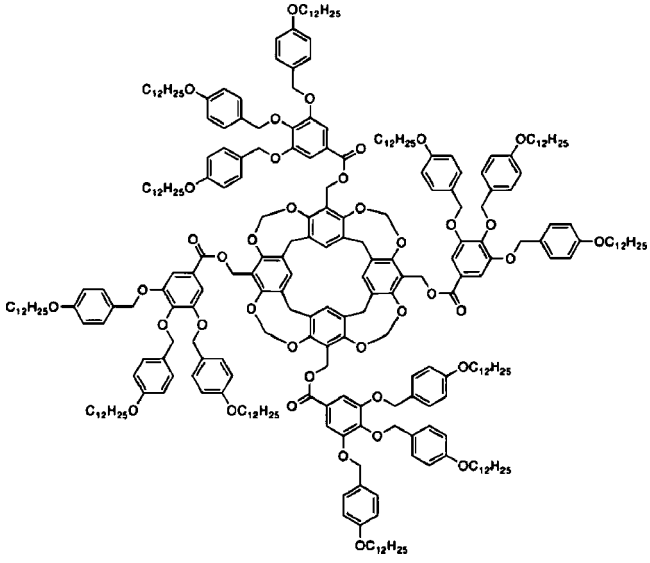

Figure 331. Cavitands dendronized with Percec-type self-assembling dendrons.[1111]

object is spherical arising from organization of the paraffin tails, the core retains a short helical pyramidal columnar structure. Therefore, the supramolecular sphere must retain to a certain extent the chirality of the parent helical pyramidal column. The decoupling may occur with a simultaneous inversion of the CTV macrocycle, although this was not necessarily the case in the simplest model. The loss of Φ_h self-organization along and the exclusive formation of the tetragonal lattices from the $(3,4,5)^2$G2 dendronized CTV was explained by the increased steric requirements of the dendrons. The increased steric bulk and, hence, a larger solid angle imposes a "minimum" torsion angle between dendron and CTV. The larger torsion angle predisposes the formation of supramolecular spheres over supramolecular columns (Figure 329).

Because of the isotropic nature of both the cubic and tetragonal lattices, it is not possible to demonstrate chirality in the structures by the XRD method using the

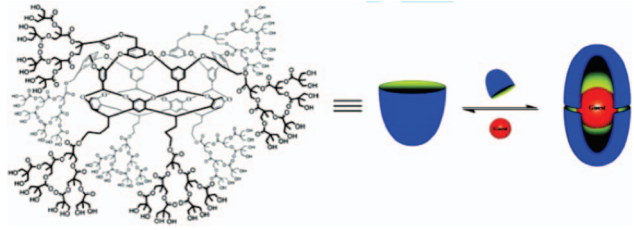

Figure 332. G3 bis(MPA)-dendronized cavitands. Reprinted with permission from ref 1112. Copyright 2008 American Chemical Society.

helical diffraction theory. However, CD spectra collected in both film and solution demonstrated amplified chirality in the self-assembled structures in both the cubic and tetragonal lattices, indicating a similar self-assembly mechanism to that seen in helical pyramidal columns (Figure 330). Mathematically a sphere cannot be chiral. However, the exterior or the interior of the supramolecular spheres[266,271,273−275,314,317,323,325,331,332,334−338,357] can be decorated with a chiral pathway such as an apple-peel, spherical helix, or loxodrome, and therefore, CD experiments in solution and solid state carried out on supramolecular spheres would display chirality. It was proposed that even supramolecular spherical dendrimers generated from achiral structures may self-assemble into chiral structures. However, they are racemic, and therefore, the detection of chirality is not accessible by CD experiments.[1110]

6.5. Other Dendronized Macrocycles

Other classes of macrocycles have been less intensively investigated. Nevertheless, they represent an important contribution to the understanding of self-assembly and self-organization of dendronized macrocycles.

6.5.1. Dendronized Cavitands

Cavitands displaying Φ_h phases were reported by Pirondini, based on resorcinarenes modified on their periphery with self-assembling Percec-type dendrons (Figure 331).[1111] Gray-

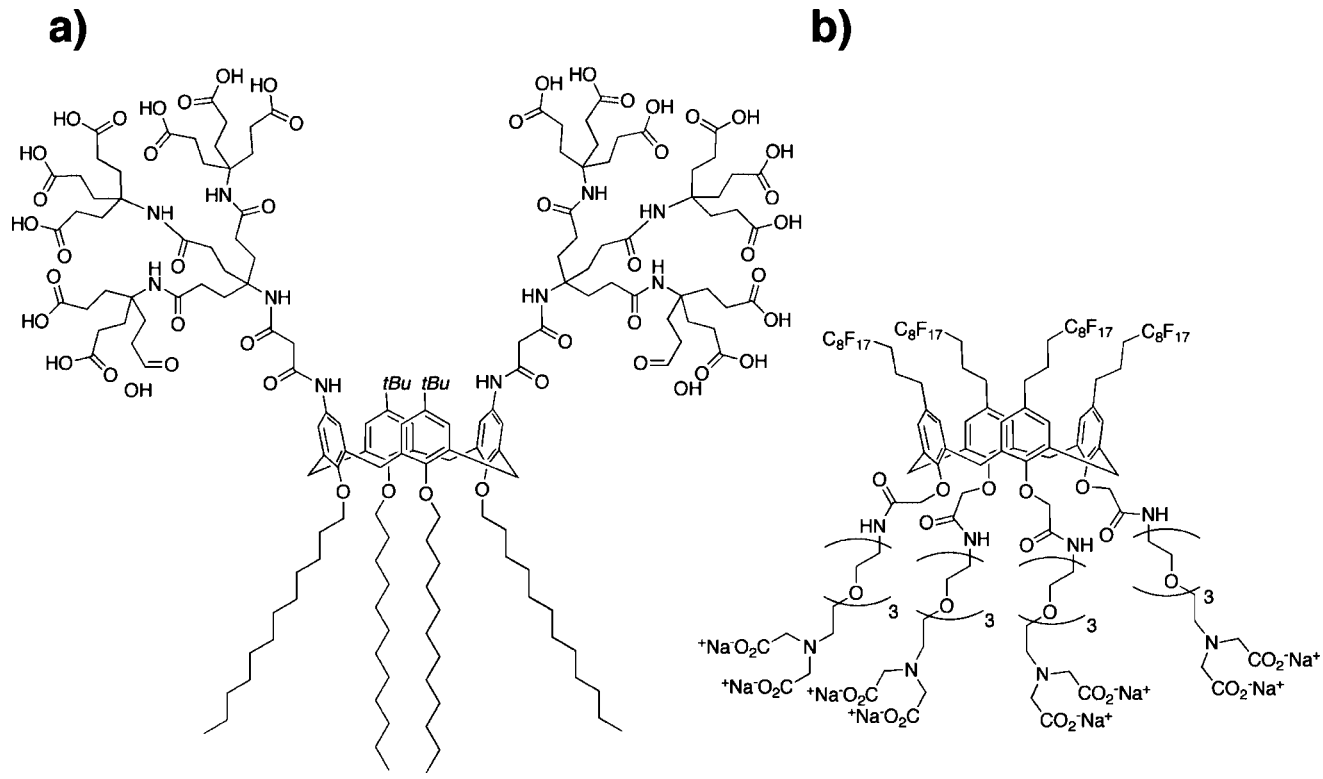

Figure 333. Synthesis of dendronized calix[4]arenes reported by Mecozzi.[1113,1114]

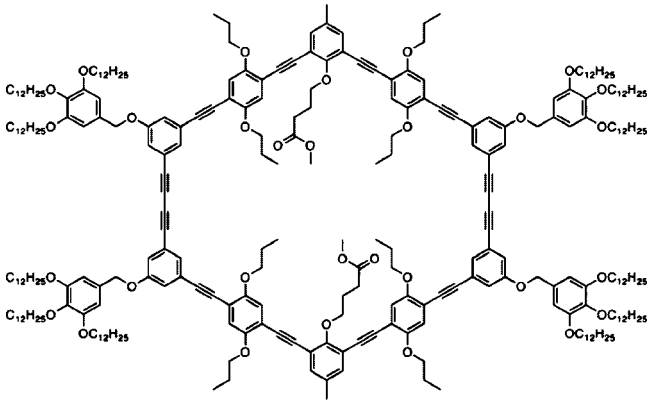

Figure 334. Dendronized phenylene acetylene macrocyclics.[1115]

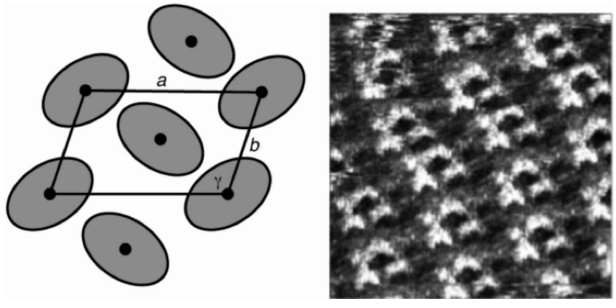

Figure 335. Proposed lattice for dendronized phenylene acetylenes along with STM image of self-assembled monolayer reported by Höger. Reprinted with permission from ref 1115. Copyright 2004 American Chemical Society.

son reported the synthesis of another cavitand dendronized with 8 G3 bis(MPA)-dendrons (Figure 332).[1112] In solution, two of these dendronized cavitands self-assemble around a lipophilic guest to form a capsule.

6.5.2. Dendronized Calixarenes

Calix[4]arenes are similar in structure to CTV. However, examples of self-assembling dendronized calix[4]arenes are much less common. Böttcher and Hirsch reported amphiphilic bis-dendronized calix[4]arenes, composed of two hydrophilic carboxylic acid terminated G2 Newkome-type dendrons on one face and four dodecyloxy tails on the other (Figure 333a).[1113] Self-assembly of these dendronized amphiphilic calix[4]arenes into persistent micelles was demonstrated via pulse gradient spin-echo NMR and cryo-TEM studies. Mecozzi also reported the synthesis and pH-dependent self-assembly of semifluorinated calix[4]arenes (Figure 333b).[1114] The formation of spherical micelles was demonstrated along with pH-dependent size control that was correlated to the change in the charged state of the molecule. While the branching in this molecule does not necessarily qualify it as dendronized calixarene, its self-assembly follows a similar mechanism to that of amphiphilic dendronized calix[4]arenes.

6.5.3. Dendronized Macrocyclic Oligo(phenylene)s and Oligo(phenylene acetylene)s

Höger reported the first example of self-assembling dendronized phenylene acetylene macrocyclics (Figure 334).[1115] Self-assembly of dendronized phenylacetylenes was investigated in both bulk state and in thin film on graphite by STM. XRD and electron diffraction investigations in the bulk and thin film indicated a monoclinic phase (Figure 335).[1116]

Lee reported tubular assemblies of rigid macrocyles functionalized with dendritic PEO dendrons (Figure 336).[1116] Structural investigation was carried out both in bulk and in aqueous solution by SAXS and TEM. Φ_r oblique phases were self-organized in bulk, whereas solution studies showed the formation of tubular structures (Figure 336). These molecules

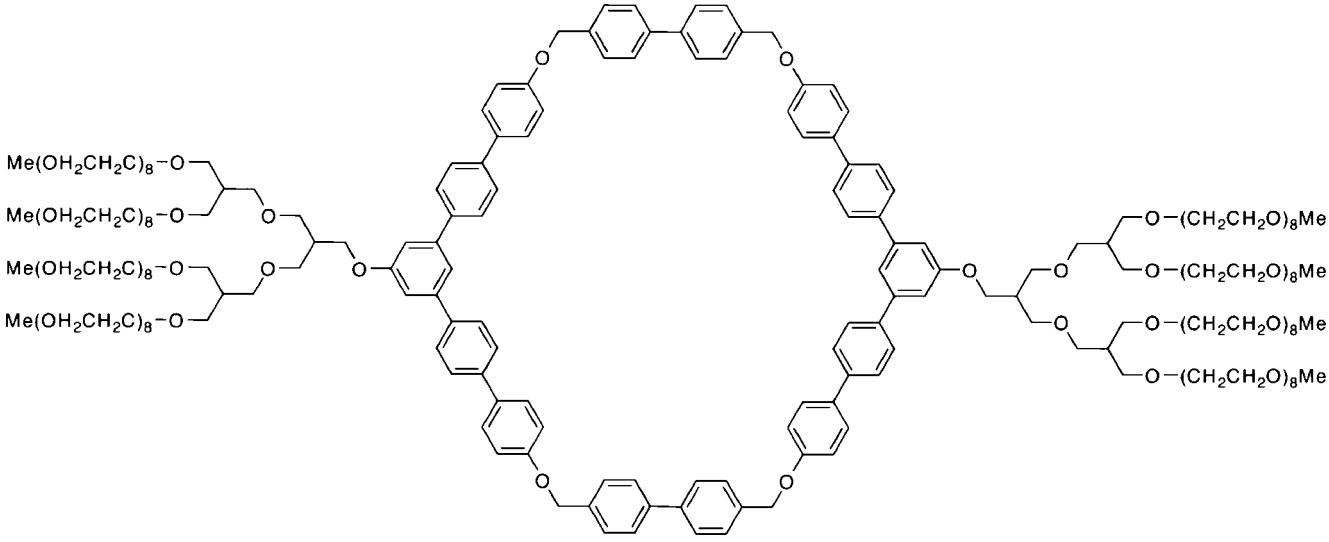

Figure 336. Structure of ethylene oxide dendronized macrocycles.[1116]

Scheme 72. Synthesis of Dendronized Donors Reported by Stang et al.[1117]

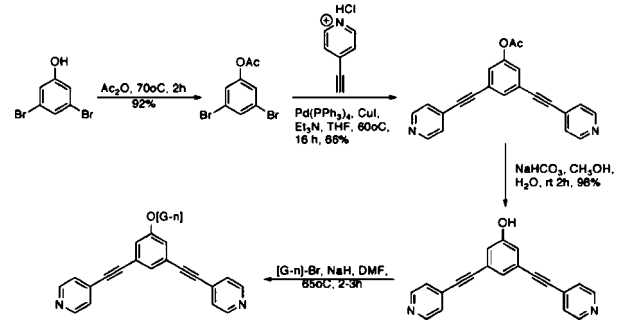

were able to solubilize single-walled nanotubes (SWCNT) in aqueous media via $\pi-\pi$ interactions.

6.5.4. Dendronized Supramolecular Macrocycles

Dendronized metallocycles of similar structure to phenylene acetylenes were reported by Stang.[1117] 3,5-Dibromophenol was coupled with 4-ethynylpyridine hydrochloride to yield the 3,5-bispyridylethynylphenyl ester. Subsequent

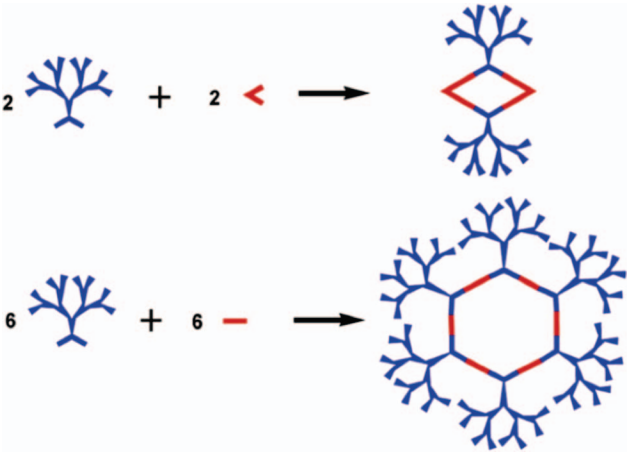

Figure 337. Schematic structure of metallocycles formed from bispyridyl donor subunits dendronized with Fréchet dendrons. Reprinted with permission from ref 1117. Copyright 2007 American Chemical Society.

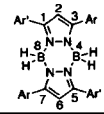

Compound	Number of peripheral chains	Chain length n	Substitution on phenyl rings	Ar	Ar'
4C10	4	10	4 and 4'	$H_{2n+1}C_nO$	$H_{2n+1}C_nO$
8C6-3,4	8	6	3,4 and 3',4'	$H_{2n+1}C_nO$ $H_{2n+1}C_nO$	$H_{2n+1}C_nO$ $H_{2n+1}C_nO$
8C10-3,4	8	10			
8C14-3,4	8	14			
8C10-3,5	8	10	3,5 and 3',5'	$H_{2n+1}C_nO$ $H_{2n+1}C_nO$	$H_{2n+1}C_nO$ $H_{2n+1}C_nO$
10C6	10	6	3,4 and 3',4',5'	$H_{2n+1}C_nO$ $H_{2n+1}C_nO$	$H_{2n+1}C_nO$ $H_{2n+1}C_nO$ $H_{2n+1}C_nO$
10C10	10	10			
10C14	10	14			
12C10unsym	12	10	2,3,4 and 3',4',5'	$H_{2n+1}C_nO$ $H_{2n+1}C_nO$ OC_nH_{2n+1}	$H_{2n+1}C_nO$ $H_{2n+1}C_nO$ $H_{2n+1}C_nO$
12C10sym	12	10	3,4,5 and 3',4',5'	$H_{2n+1}C_nO$ $H_{2n+1}C_nO$ $H_{2n+1}C_nO$	$H_{2n+1}C_nO$ $H_{2n+1}C_nO$ $H_{2n+1}C_nO$

Figure 338. Dendronized pyrazaboles. Reprinted with permission from ref 1118. Copyright 2000 American Chemical Society.

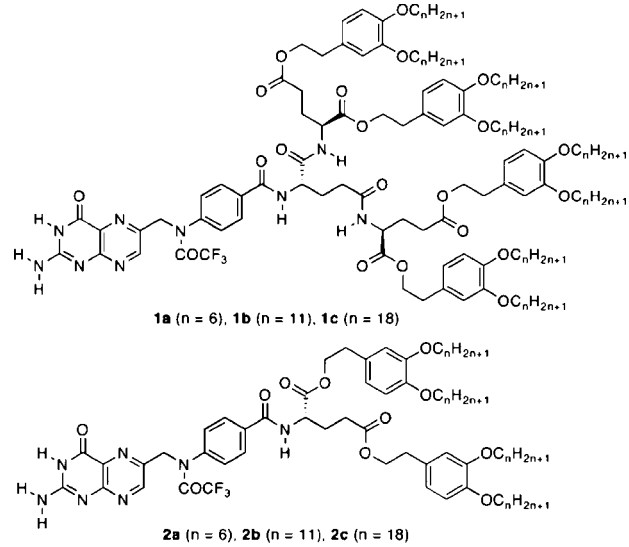

Figure 339. Structure of dendronized folic acid derivatives.[1124]

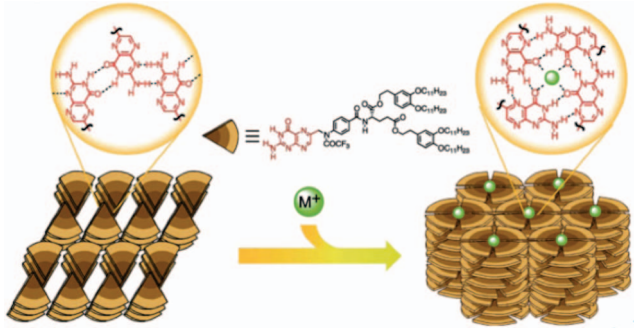

Figure 340. Transition of dendronized folates from S architectures to supramolecular macrocycles that self-organize into discotic Φ_h lattices via the addition of alkali metal salts. Reprinted with permission from ref 1121. Copyright 2002 American Association for the Advancement of Science.

saponification of the ester and functionalization with Fréchet dendrons yielded the dendritic donor subunits (Scheme 72).[1117]

Complexation of the dendronized bispyridiyls with 2,9-(trans-Pt(Pet$_3$)$_2$NO$_3$)$_2$-phenathrene resulted in the assembly of rhombohedral metallocycles with 60° and 120° angles (Figure 337, top). Expanded hexagonal metallocycles were obtained by combining the 120° donor with linear bis-acceptor 1,4-bis((PMe$_3$)$_2$-Pt(OTf))$_2$-benzene (Figure 337, bottom).[1117]

Serrano reported self-assembling pyrazaboles synthesized via the reaction of 3,5-dendronized pyrazaboles and borane (Figure 338).[1118] In most cases, self-organization in crystalline structures was observed, but in a few cases (8C$_{10}$-3,4, 10C$_{10}$, 12C$_{10unsym}$), distorted self-organization in Φ_h phases was observed.

Kato reported the synthesis of folic acid functionalized with hybrid dendrons composed of a G1 or G2 chiral L-glutamate periphery functionalized with Percec-type

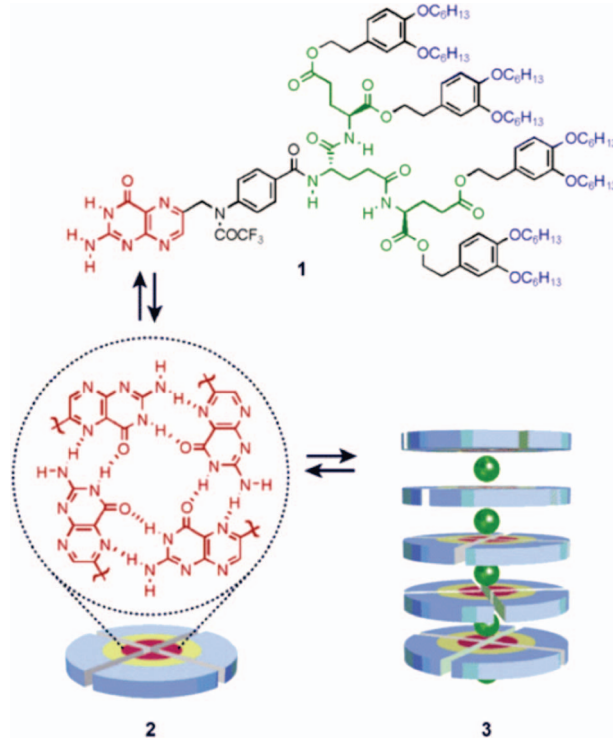

Figure 342. Dendronized supramolecular rosettes self-organized into columnar ion channels by Matile. Reprinted with permission from ref 1127. Copyright 2006 American Chemical Society.

(3,4)*n*G1 dendrons (Figure 339).[1119−1122] Self-assembly and self-organization of dendronized folic acid into lamellar and discotic columnar mesophases was observed. Self-assembly into discotic columnar phases proceeds through the formation of rosettes or "tetrameric supramolecular macrocycles" via H-bonding of the ring system. Transition from the S to Φ_h phase can be mediated by the addition of alkali metals

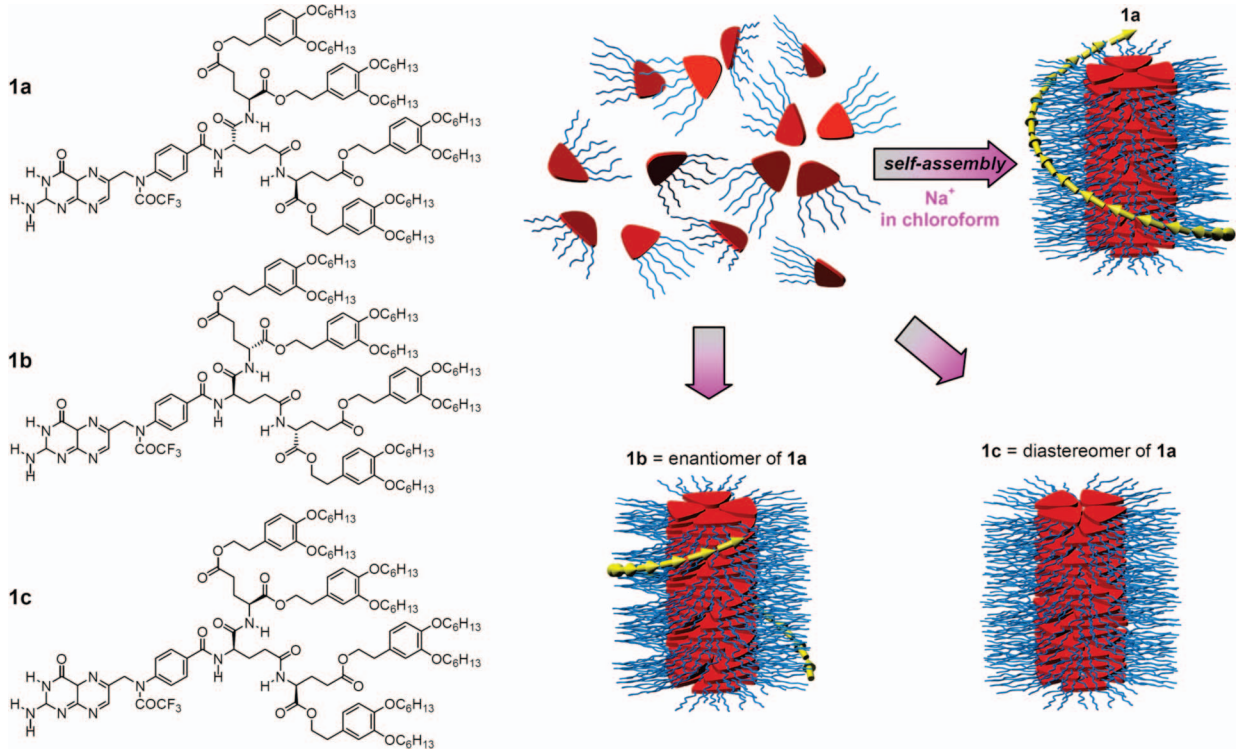

Figure 341. Structures of dendronized folate enantiomers and diastereomers (top) and their self-assembly into helical discotic columns (bottom). Adapted from ref 1125.

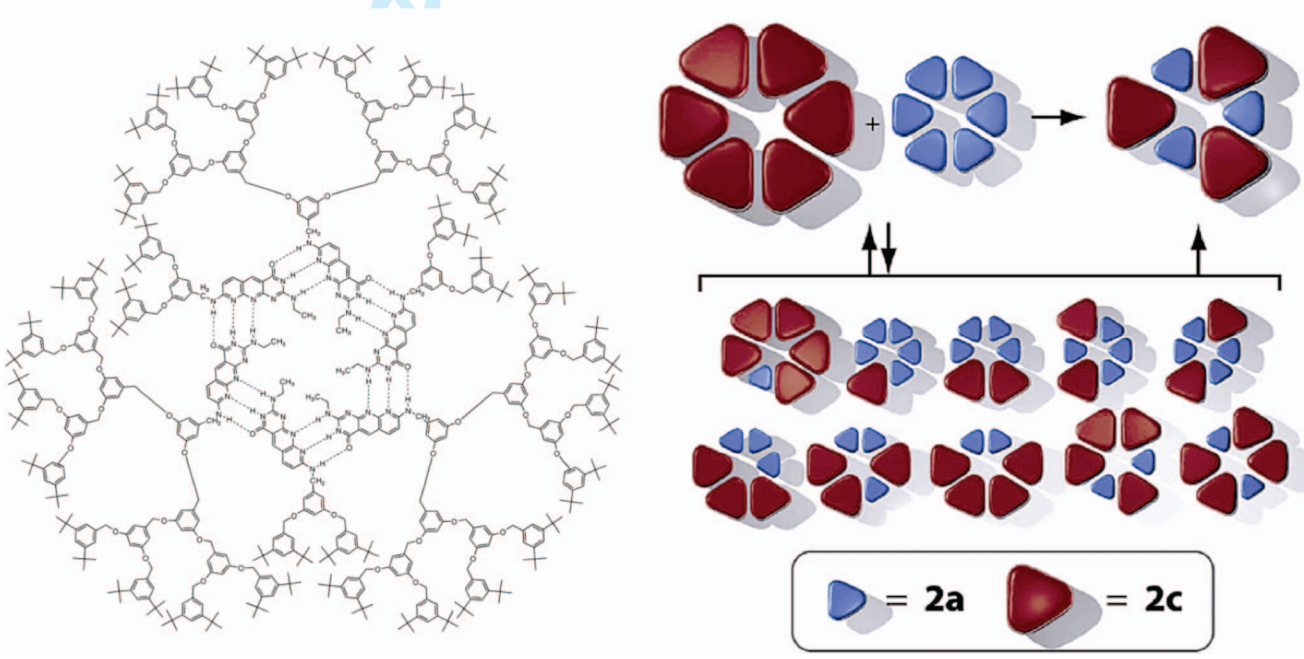

Figure 343. Dendronized DDA/AAD molecule and its self-assembly into mixed hexameric supramolecular macrocycles. Reprinted with permission from ref 1130. Copyright 2002 American Chemical Society.

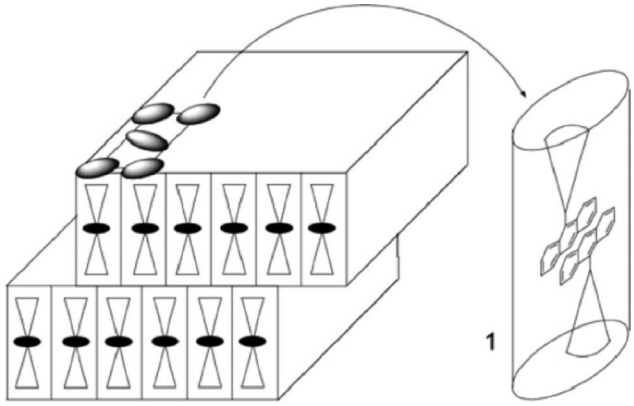

Figure 344. Schematic packing model of S_E phase of dendronized anthracene. Reprinted with permission from ref 1135. Copyright 2003 American Chemical Society.

Scheme 73. Photodimerization of Dendronized Anthracene (Reprinted with Permission from Ref 1135; Copyright 2003 American Chemical Society)

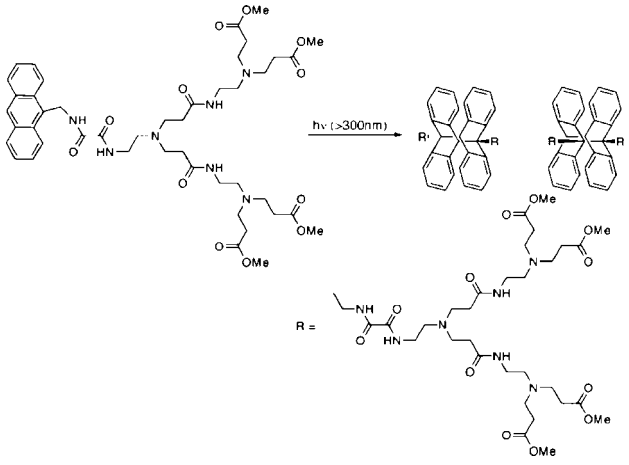

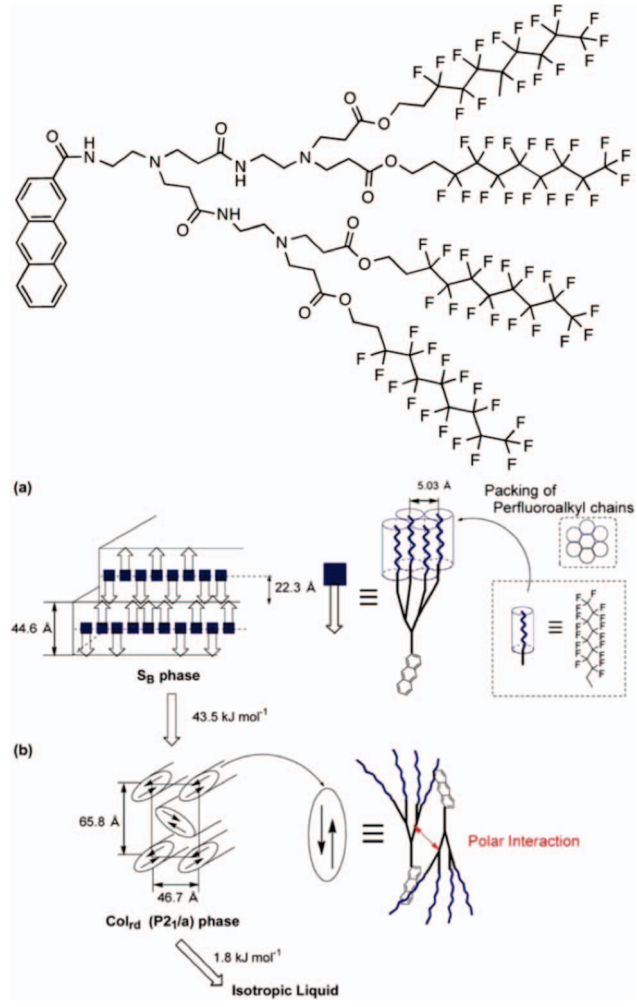

Figure 345. Dendronized anthracene (left) and packing models of the S_B (a) and $\Phi_{r\text{-}d}$ (b) phases. Reprinted with permission from ref 1136. Copyright 2006 Elsevier.

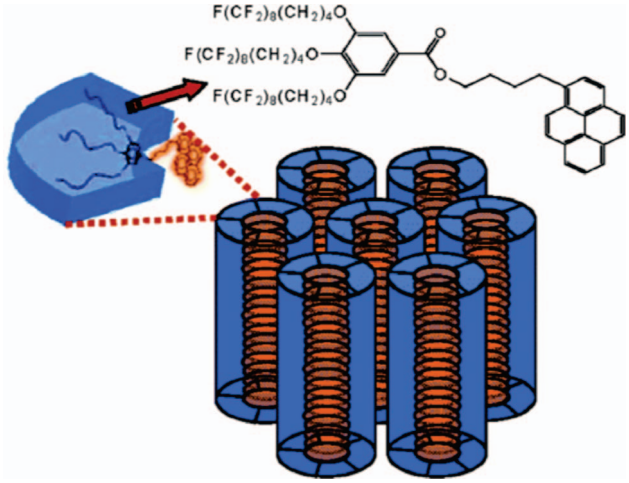

Figure 346. Schematic of self-assembly of dendronized pyrene into a Φ_h lattice. Reprinted with permission from ref 1138. Copyright 2006 American Chemical Society.

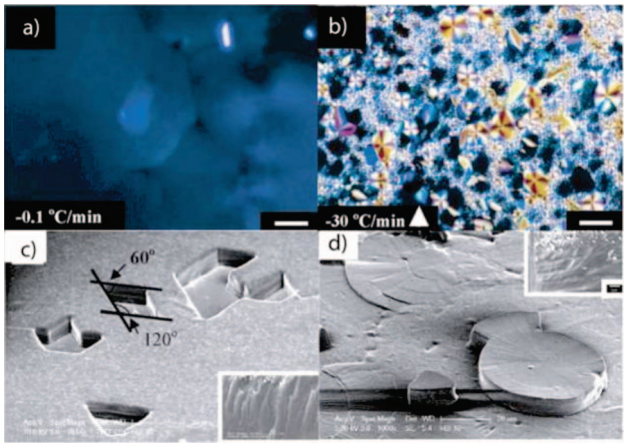

Figure 347. TOPM of dendronized pyrene films cooled at 0.1 and 30 °C min^{-1} (a) and (b), respectively. SEM images of dendronized pyrene films cooled at 0.1 and 30 °C min^{-1} (c) and (d). AFM indicating planar alignment of the Φ_h phase on Teflon-AF upon cooling at 0.1 °C min^{-1}. Reprinted with permission from ref 1138. Copyright 2006 American Chemical Society.

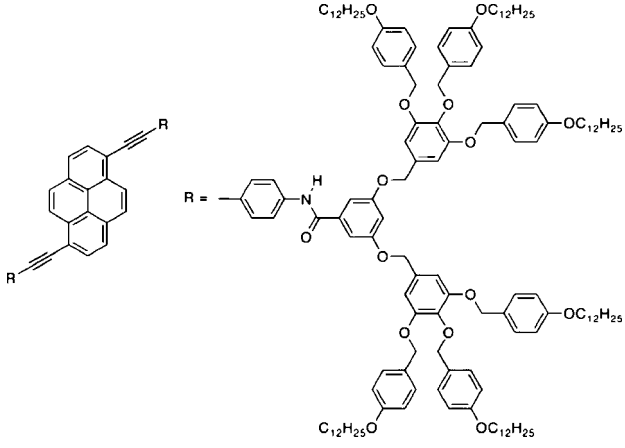

Figure 348. Dendronized pyrene acetylene.[835]

(Figure 340).[1123] Increasing the length of the alkyl tail results in thermotropic Φ_h and *Cub* phases.[1124] The *Cub* phase consists of spherical structures containing internal segmented columns that retain their structure and chirality. In polar

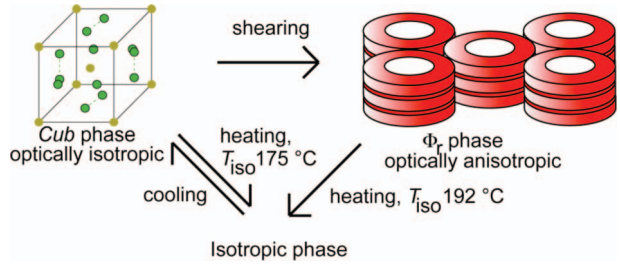

Figure 349. Schematic diagram showing shear-induced phase sequence by Kato. Adapted from ref 835.

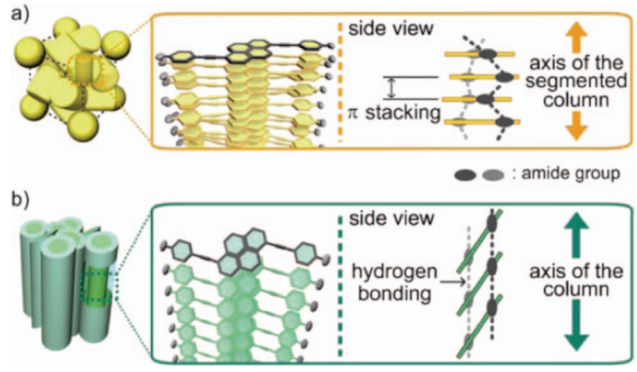

Figure 350. Schematic of pyrene packing within the metastable cubic phase and columnar phase by Kato et al. Reprinted with permission from ref 835. Copyright 2008 Wiley-VCH Verlag GmbH & Co. KGaA.

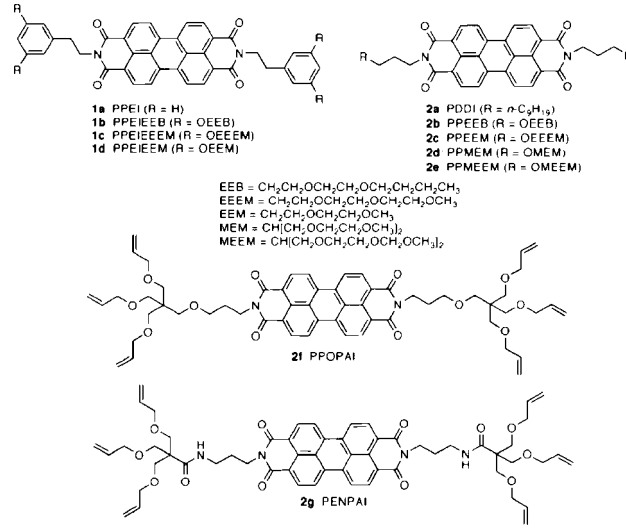

Figure 351. Dendronized PBI reported by Gregg.[1140]

solvents, supramolecular chirality is only observed in the presence of alkali salts (Figure 341), whereas in case of nonpolar solvents, lipophilic interactions are expected to mediate microphase segregation and allow for the expression of supramolecular chirality without alkali metal salt addition.[1125] Enantiomeric dendronized folates exhibit mirror image supramolecular chirality arising from opposite helical rotations of the tetrameric discs, while the diastereomers resulting from mismatched chiral glutamates do not express supramolecular chirality (Figure 342). De Mendoza and Nierengarten reported fullerodendrons with similar H-bonding apex groups.[1126] Only dimerization but no self-organization was observed.

Scheme 74. Dendronized PBI Reported by Würthner[1141]

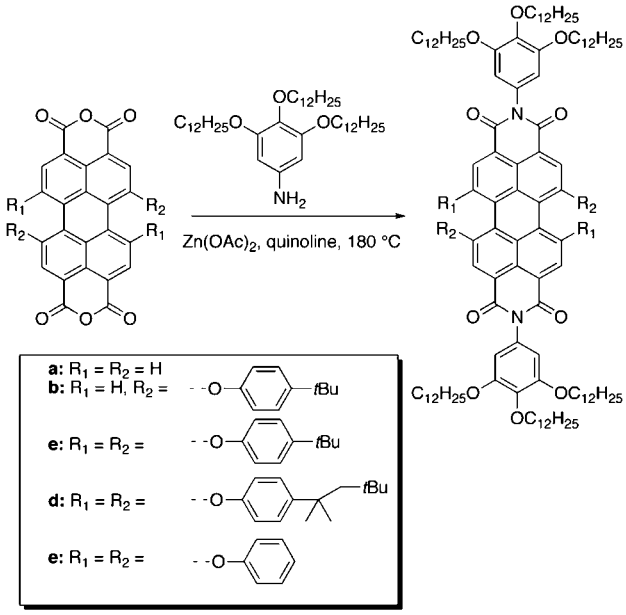

Self-assembled H-bonded rosettes were reported by Kato and Matile (Figure 342). Folate rosettes self-assemble into discs that stack into synthetic potassium channels.[1127]

Similarly, Lehn and Zimmerman reported the synthesis of dendronized phthalhydrazide lactams that self-assemble into discotic trimers and self-organize into columnar lattices.[1128] Later, Zimmerman reported the synthesis of hexameric dendronized supramolecular macrocycles.[1129−1131] Fused rings with H-bond donor/donor/acceptor (DDA) and acceptor/acceptor/donor (AAD) patterns (mimics of guanine/cytosine hydrogen-bonding patterns) fixed at 60 °C mediate self-assembly into hexameric rosettes. Dendronization of these DDA/AAD molecules provides a method for programmed self-assembly of dendronized supramolecular macrocycles (Figure 343). The stability of the hexamer decreases with increasing dendron size, due to steric interactions. Equal mixing of DDA/AAD molecules with low- and high-generation dendrons results in a single alternating hexameric supramolecular macrocycle that minimizes steric interactions

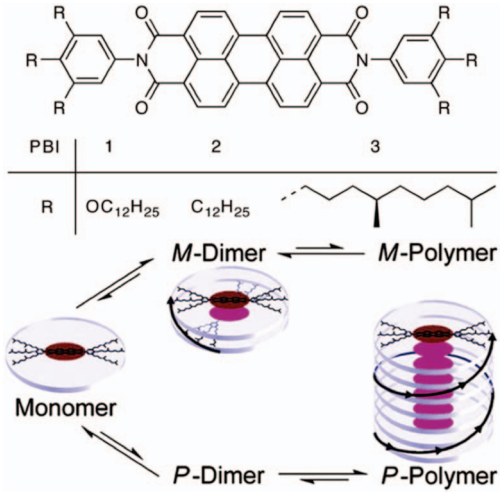

Figure 352. Structure of chiral PBI J-aggregates (left, 3) and self-assembly into M-dimers followed by P-polymers (right). Reprinted with permission from ref 1144. Copyright 2007 American Chemical Society.

(Figure 343). These supramolecular macrocyclics, however, do not self-organize.

7. Dendronized Polycycles

Polycycles contain multiple fused conjugated rings, instead of a single macrocyclic ring with a central cavity. Their aromatic nature has garnered intense interest.[1132] Polycyclic conjugated hydrocarbons are powerful molecular scaffolds for the design of self-assembling materials because of their rigid structure and often beneficial electronic and photophysical properties.[1133,1134] Many reviews have been dedicated to discotic LCs.[105,106,108] This chapter will cover only dendronized polycycles that self-assemble in bulk or solution. Topologically, dendronized polycycles (Figure 2, first row, left to second from right) share some of the symmetries of dendronized star polymers and dendronized macrocycles, but $\pi-\pi$ interactions are a more significant factor in self-assembly.

7.1. Dendronized Anthracene

The rigid three-ring structure of anthracene allows for the engineering of materials with both rodlike and disklike topologies. Takaguchi reported the synthesis and photodimerization of G2 PAMAM dendrons functionalized at the apex with anthracene (Scheme 73).[1135] Photodimerization in solution lead to a mixture of *syn*- and *anti*-isomers in a 3:7 ratio. Interestingly, photodimerization in the LC bulk state resulted in the *anti*-isomer exclusively. Analysis of the LC phase by XRD indicated S_E self-organization. XRD in conjunction with the LC phase photodimerization results suggested a model of self-organization with antiparallel packing within lamellae (Figure 344).[1135]

Takaguchi also reported anthracene dendronized with G2 PAMAM terminally functionalized with perfluoroalkyl tails and subsequent solution- and LC-phase photodimerization (Figure 345, left).[1136] The dendronized anthracene exhibited a S_B phase at room temperature (Figure 345a) and Φ_r phase with $P2_1/a$ symmetry at 60 °C composed of head-to-tail dimers (Figure 345b). In viscous media or the LC state, the singlet lifetime of the anthracene is not sufficient for the molecules to reorient themselves and so the ratio of head-to-head and head-to-tail photodimerization isomers reflects the ground-state distribution of parallel and antiparallel dimers.[1137] Photodimerization in the S_B phase resulted in a 65:35 mixture of head-to-head and head-to-tail regioisomers. The lack of specificity in the S_B phase was attributed to a degree of interdigitation of the anthracene groups within the bilayer. Photodimerization in fluorinated solvent resulted in exclusively head-to-head isomers with a 50:50 *syn*-to-*anti* ratio and was attributed to the formation of micellar aggregates in solution that exhibit parallel orientation.

7.2. Dendronized Pyrene

Jung reported the dendronization of pyrene with perfluorinated (3,4,5)12F8G1 Percec-type dendrons (Figure 346).[1138] A Φ_h phase was observed by TOPM and confirmed by XRD using synchrotron radiation. The effect of cooling on the formation of homeotropic alignment and the subsequent influence on photoluminescencent properties was investigated.[1138] The quality of alignment was confirmed by TOPM and SEM; cooling at a rate of 0.1 °C min^{-1} resulted in a highly uniform film with fragments exhibiting specific

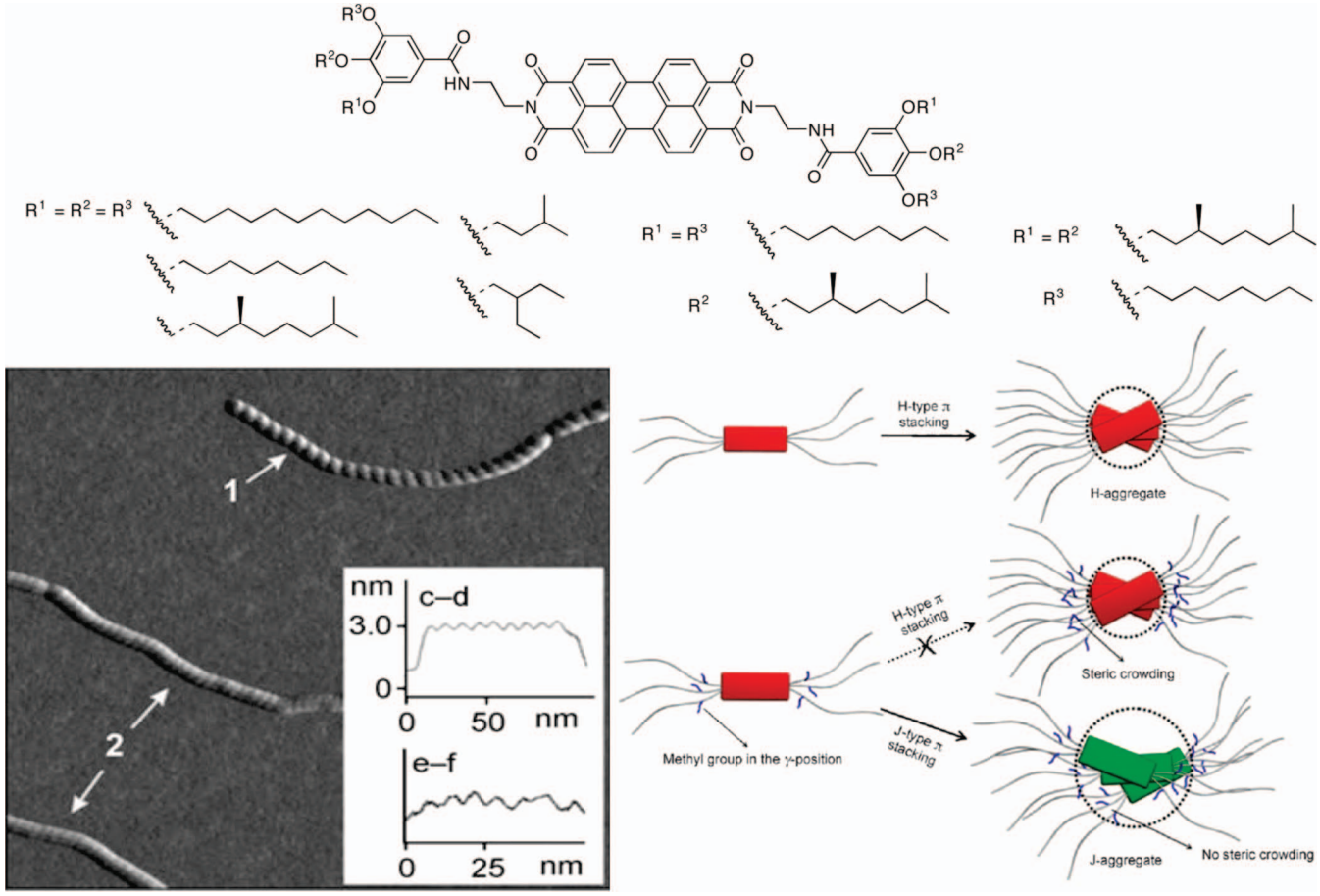

Figure 353. Dendronized PBI (top), their self-assembly in solution into twisted columnar fibers (bottom left), and a model for the self-assembly into H and J-aggregates (bottom right). Reprinted with permission from ref 1145. Copyright 2008 Wiley-VCH Verlag GmbH & Co. KGaA.

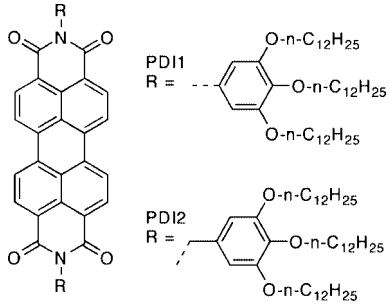

Figure 354. Dendronized PBIs analyzed by Marder.[1146]

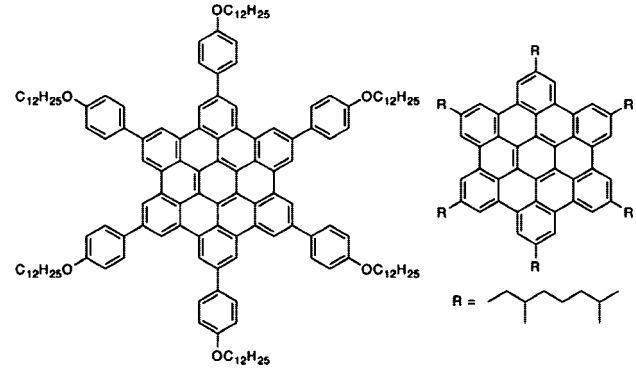

Figure 356. Hexabenzocoronenes that were mixed with dendronized PBIs.[1147]

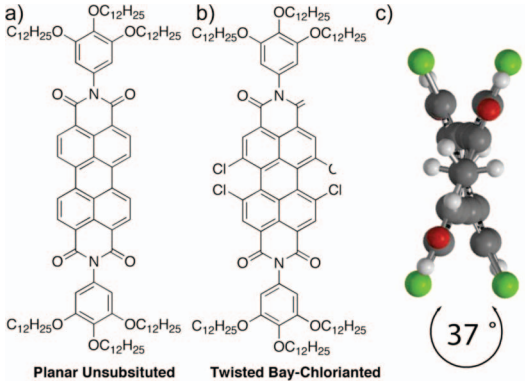

Figure 355. Planar dendronized PBI (a), compared with twisted bay-chlorinated dendronized PBI (b and c) by Würthner.[1147,1148]

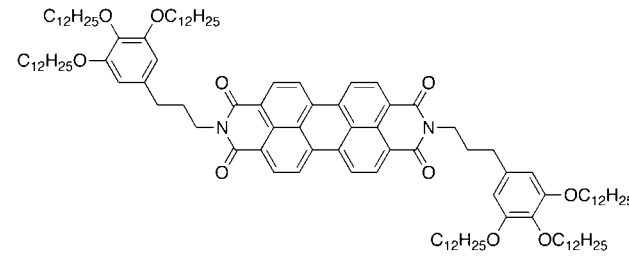

Figure 357. Dendronized PBI investigated by Singer and Percec.[1150]

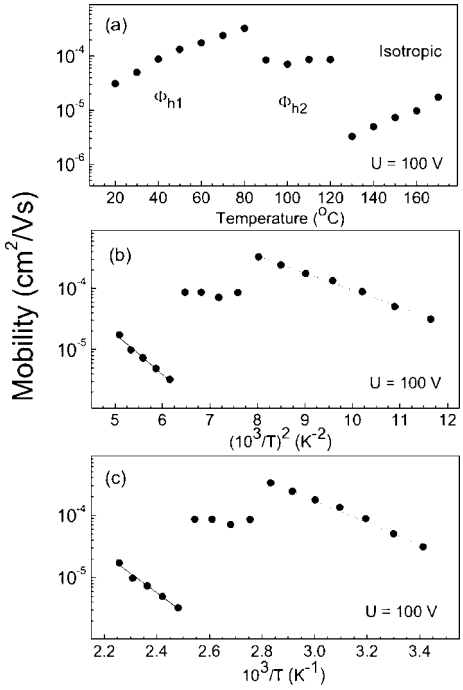

Figure 358. Temperature dependence of electron mobility in dendronized PBI along with the fits of models to the experimental data. Reprinted with permission from ref 1150. Copyright 2008 American Institute of Physics.

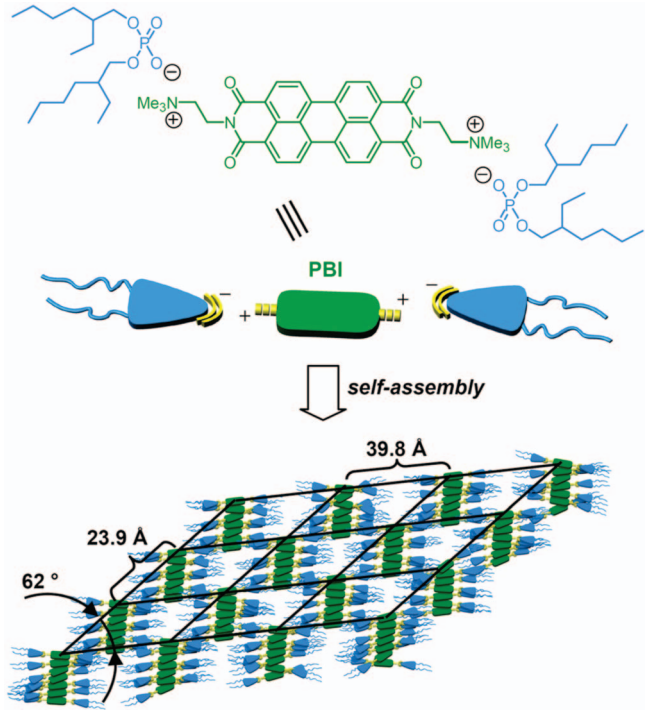

Figure 359. Structure (top) and self-organization of noncovalently dendronized PBIs. Adapted from ref 1151.

angles of 60° and 120°, indicative of hexagonal packing of the cylinders (Figure 347a and c). Cooling at a rate of 30 °C min^{-1} resulted in a less uniform film exhibiting spherulitic-like growth (Figure 347b and d). Samples exhibiting both homeotropic and planar alignment on fluorine-treated glass (Teflon-AF) were visualized by AFM. It was found that the perfection of structural conjugation arising from the quality of the aligned films was of much greater influence on photoluminescent properties than was the orientation of alignment relative to the substrate.[1138]

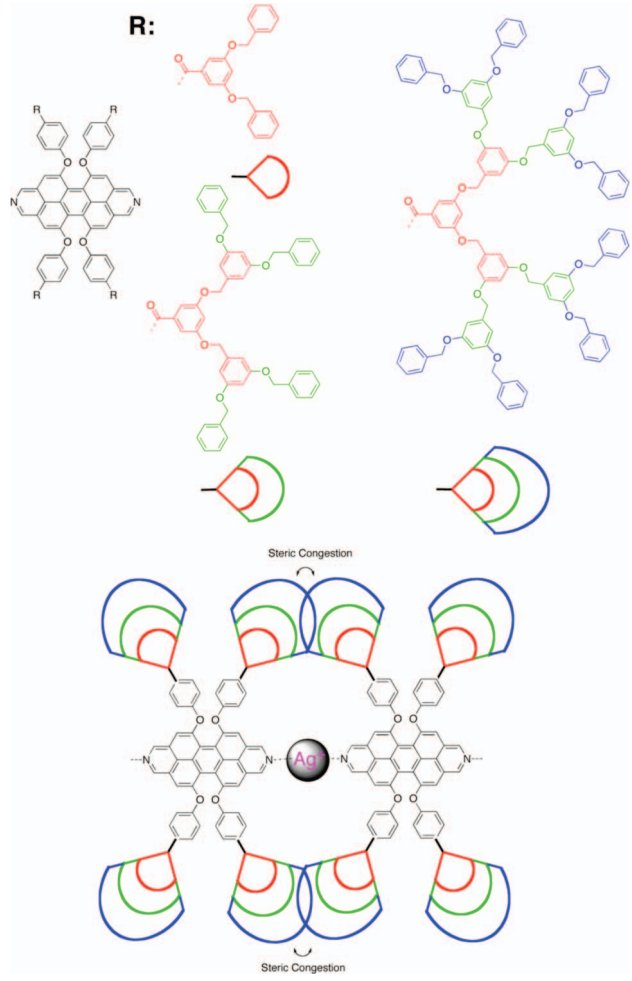

Figure 360. Dendronized 4-armed star with a diazadibenzoperylene core and their self-assembly into supramolecular polymers. Reprinted with permission from ref 1152. Copyright 2006 Wiley-VCH Verlag GmbH & Co. KGaA.

Kato reported dendronized 1,6-bis(phenylethynyl)pyrene functionalized with (4-3,4,5)12G1 Percec-type dendrons (Figure 348) exhibiting a shear-induced transition from *Cub* to a Φ_r phase with *P*2/*a* symmetry (Figure 349).[835] The metastable shear-induced Φ_r phase did not retransform to *Cub* on heating and exhibited a higher isotropization point than that of the thermotropic *Cub* phase (Figure 349). Photophysical properties of these two phases were investigated. A color change from yellow to blue−green was observed on shearing coupled with a decrease in emission lifetime. Thus, excimers present in the *Cub* phase were likely diminished in the Φ_r phase induced by shear. This was rationalized by diminished $\pi-\pi$ interactions in the molecular model of the Φ_r phase (Figure 350).

As discussed in section 3, Percec has reported the self-assembly and coassembly of pyrene and other fused aromatics dendronized with (3,4,5)12F8G1 with donor and acceptor polymers, thereby producing self-repairing complex electronic materials.[358] The self-organization of libraries of dendronized polycyclic acceptors[363] and donors[364] has also been investigated.

7.3. Dendronized Perylene Bisimides

LC perylene bisimides PBIs are an important class of dyes and organic semiconductor.[1139] Gregg reported the first dendronized LC PBIs.[1140] PBI was dendronized with both

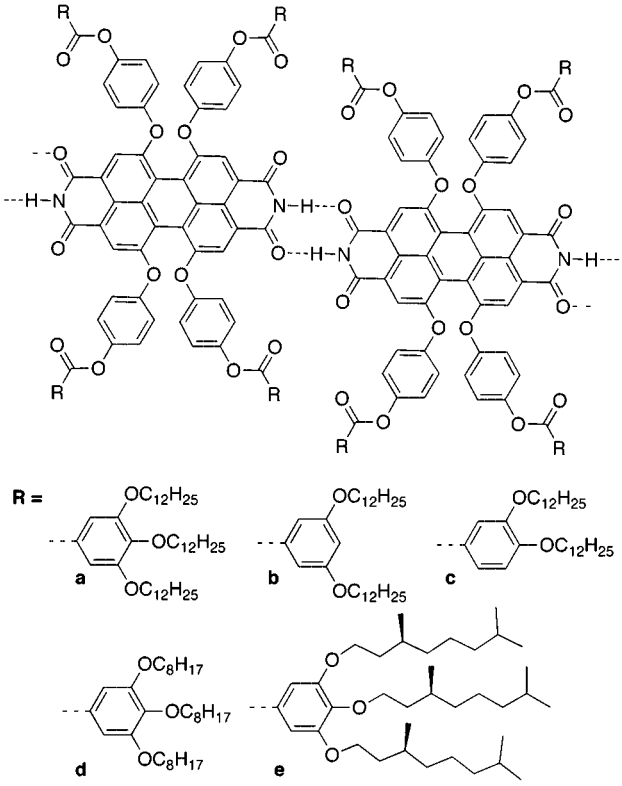

Figure 361. Four-armed star dendronized PBI that forms fluorescent J-aggegrates.[1153]

ethylene oxide dendrons and triallyl Pentaerythritol dendrons (Figure 351). While DSC thermograms provided evidence of probable ordered phases, their supramolecular structures were not investigated.

Würthner reported the synthesis of a series of PBIs dendronized with (3,4,5)12G1 (Scheme 74).[1141] J-type aggregates forming Φ_h thermotropic LC phases were observed over a broad temperature range as determined by XRD and TOPM analysis. Following the analysis of solvent-assisted nucleation in the self-assembly of oligophenylene vinylenes (OPVs),[1142,1143] Würthner investigated the self-assembly mechanism in solution of chiral dendronized PBI J-type aggregates into single helical columns.[1144] It was found that self-assembly proceeds via two different types of chiral aggregates (Figure 352). Stacked M-dimers favored left-handed assembly, while growth into P-polymers favored right-handed helicity. It was also observed that the use of chiral tails, as opposed to achiral tails, increased intracolumnar order, thereby enhancing charge transport in the bulk Φ_h phase.

Würthner also prepared perylene bisimides (PBI)s bis-dendronized with chiral and achiral (3,4,5)12G1 dendrons (Figure 353, left) connected via ethylene diamine.[1145] Self-assembly via π-stacking produces gels consisting of twisted columnar architectures (Figure 353, middle). For dendrons with nonbranched alkyl tails, π-stacking into H-aggregates was observed, while for dendrons with branched alkyl tails, π-stacking into J-aggregates was observed due to steric repulsion of the bulky branches (Figure 353, right). Mixtures of dendronized PBIs with branched and unbranched alkyl tails revealed only H-type stacks at low concentrations of dendronized PBIs with branched alkyl tails, but above a critical concentration J-aggregates predominated.

Marder[1146] reported on the charge mobility of the materials reported by Würthner (Figure 354). Charge mobilities were

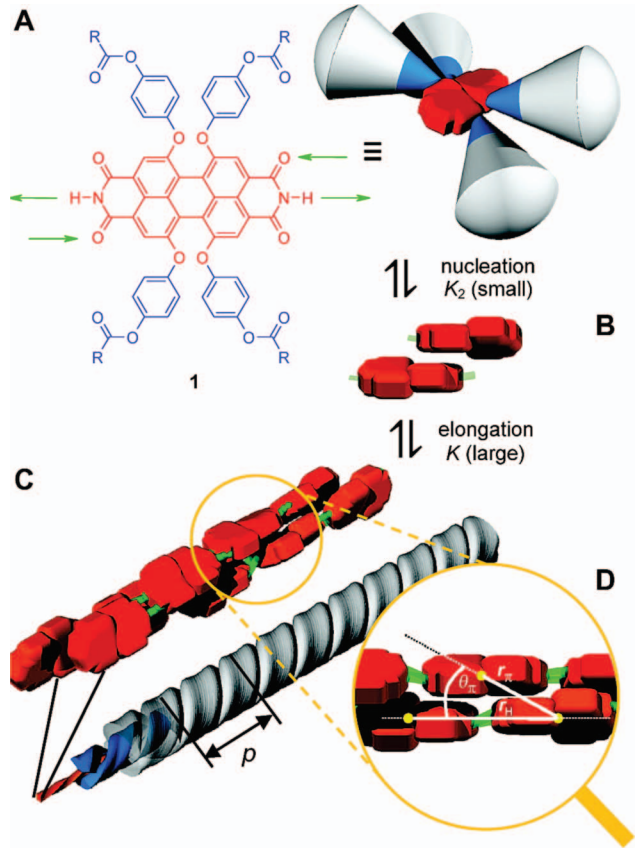

Figure 362. (a) Schematic for self-assembly of 4-armed-star dendronized PBI; (b) self-assembly mechanism depicting nucleation and elongation regimes; (c) model depicting stacked helical ribbons; and (d) depiction of the orientation of the J-aggregate. P is the helical pitch (~14 nm) of the fiber, and θ_π is the translational offset angle describing the orientation of the π-stacked dyes/fiber from the orientation of the aggregate. Reprinted with permission from ref 1153. Copyright 2009 American Chemical Society.

variable from device to device depending on domain size as observed by TOPM. In certain cases, mobilities greater than amorphous silicon were observed.[1146] Würthner also investigated the charge transport properties of dendronized PBIs, with particular attention to the effect of bay substitution (Figure 355a versus Figure 355b).[1147] XRD of dendronized PBI with chlorine bay-substitution could not be completely assigned; six out of eight peaks could be indexed as a Φ_r phase with lattice parameters $a = 24.5$ Å and $b = 18.0$ Å; however, two small additional peaks could not be assigned. TOPM experiments showed a texture indicative of an ordered columnar arrangement.[1147] Although the chlorinated derivatives displayed very similar charge transport properties to the nonhalogenated derivatives (2.0×10^{-2} cm^2 V^{-1} s^{-1}) charge carrier life times were increased by several orders of magnitude.[1147] Increased life times of charge carriers were attributed to two factors. First, cyclic voltammetry has shown that substitution at the bay positions with electron withdrawing groups increases electron affinity resulting in stabilized radical anions.[1148] Second the torsion angle from single crystal diffration[1148] of the chlorinated PBI is around 37° (Figure 355c). This twist was presumed to "lock" the $\pi-\pi$ stacks in a more ordered arrangement within the column. PBIs fuctionalized in their bay positions with thiophene dendrons were also synthesized and studied for p-type conductivity applications.[1149] Dendronized PBIs were mixed with substituted hexabenzocoronenes and the resulting

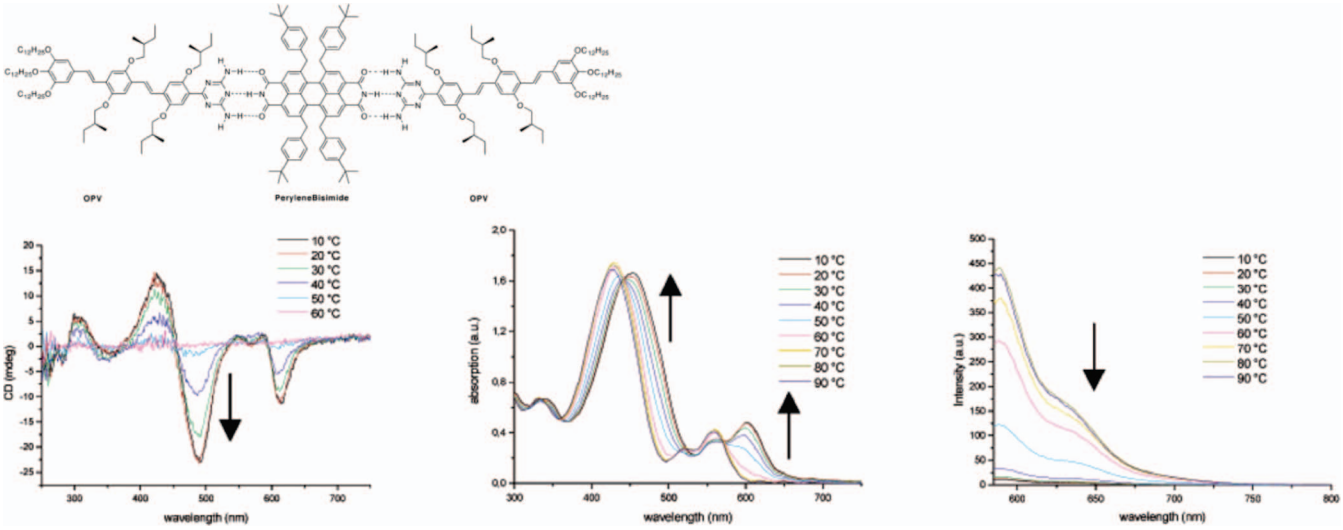

Figure 363. H-bonded self-assembly of PBI with dendronized OPV (top). Temperature-dependent CD, UV−vis, and fluorescence spectra, respectively. Reprinted with permission from ref 825. Copyright 2002 American Chemical Society.

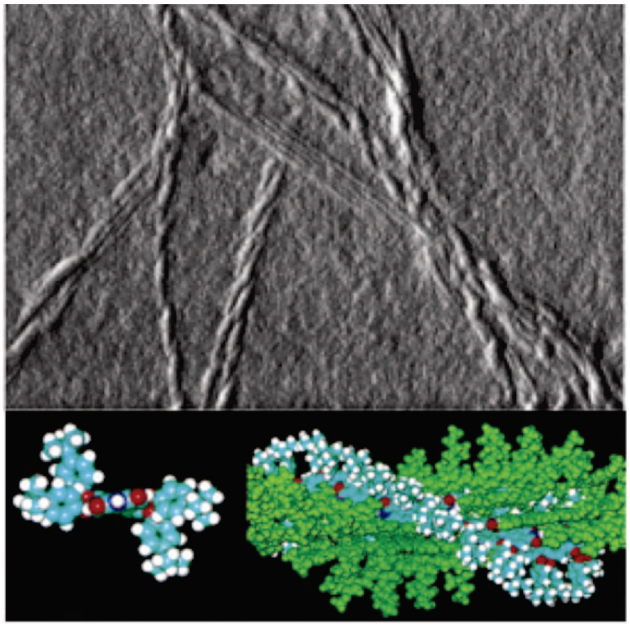

Figure 364. AFM of a spin-coated film of self-organized H-bonded PBI and dendronized OPV (top) and molecular model of self-assembly (bottom). Reprinted with permission from ref 825. Copyright 2002 American Chemical Society.

Scheme 75. Synthesis of Dendronized OPV: (a) Diisopropylethylamine, Dioxane, 100 °C, 120 h (15%); PBI Is Used for Coassembly by H-Bonding and $\pi-\pi$ Stacking[824]

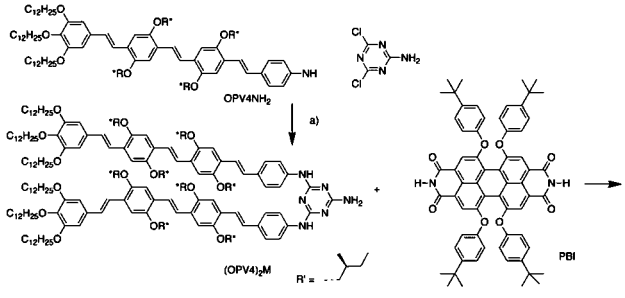

mixtures were investigated as potential photoconductors (Figure 356). It was concluded that mixing with hexabenzocoronenes increased charge carrier lifetime, thereby resulting in greater migration distances of photogenerated charges

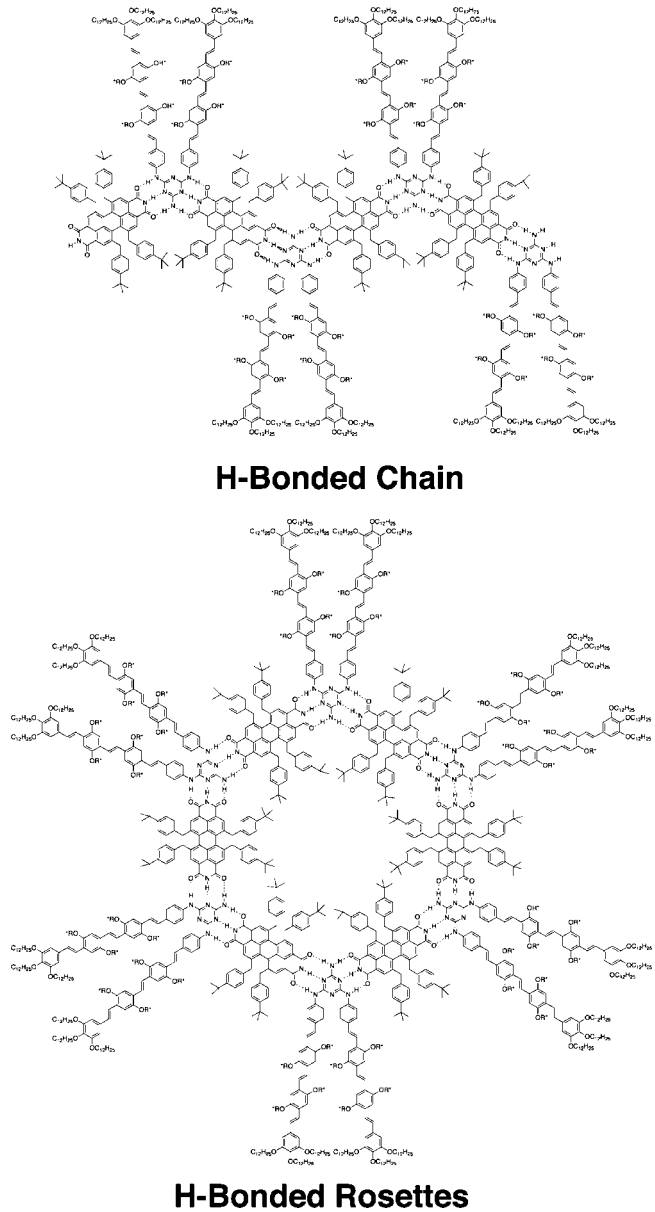

Figure 365. Self-assembled H-bonded chain (left) and rosette (right) of dendronized OPV and PBI.[824]

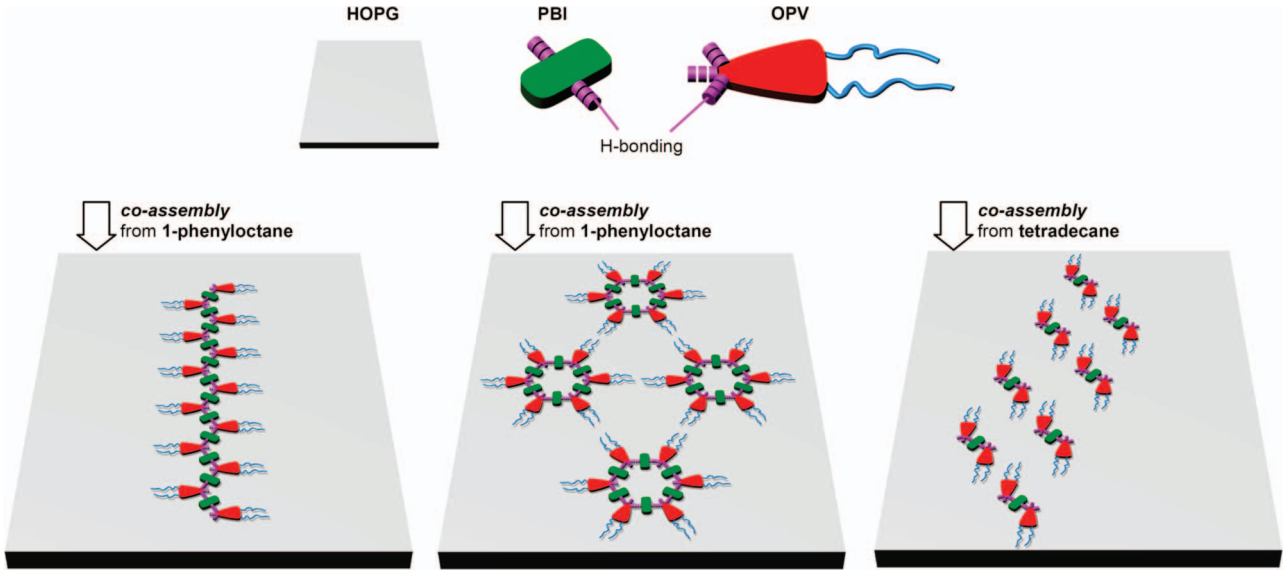

Figure 366. STM (top) of topologies of self-assembled structures formed from dendronized OPV H-bonded to PBIs and their corresponding molecular models of self-assembly into ribbons (bottom left) and rosettes (bottom center and right). Adapted from ref 824.

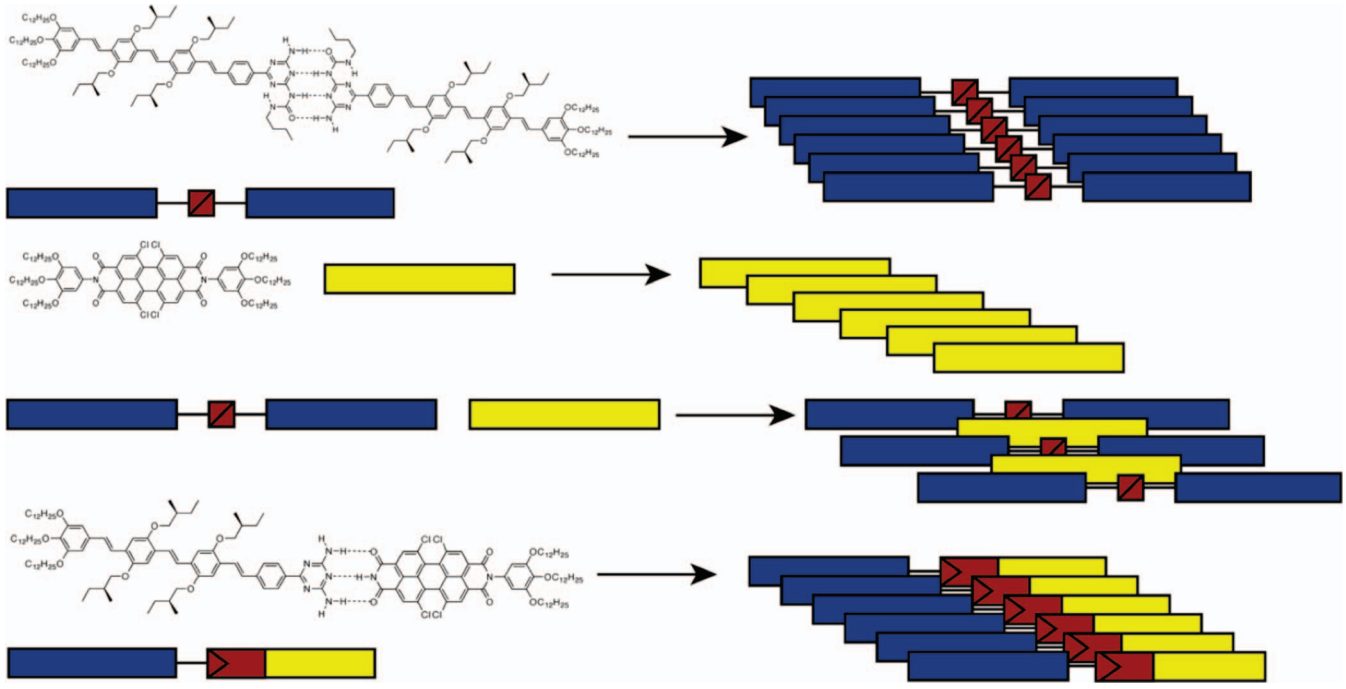

Figure 367. Dendronized OPV dimers, covalently and supramolecular dendronized PBIs, and mixtures thereof. Reprinted with permission from ref 1159. Copyright 2006 American Chemical Society.

and an increased number of charges reaching the collection electrode.[1147]

Singer and Percec also investigated long-range electron transport in (3,4,5)12G1 dendronized PBIs forming Φ_h lattices (Figure 357).[1150] Electron transport was investigated using time-of-flight (TOF) techniques. Increased order within the Φ_h phases resulted in orders of magnitude increases (Figure 358). The temperature and electric field dependence of charge transport was investigated using models of both free charge carrier hopping from sites with Gaussian distribution and energy and uncorrelated hopping of small polarons. It was concluded that static energetic and positional disorder was the greatest contributing factor to charge transport in both the I and Φ_h phases and that the model uncorrelated hopping of small polarons is at most a minor contributing phenomenon. It is notable that the authors were able to demonstrate reproducible and stable operation in air over several months.

Faul and Ikkala reported the self-organization of PBIs dendronized via noncovalent interactions (Figure 359).[1151] *N*,*N*′′-ethylenetrimethylammonium functionalized PBIs form ionic complexes with bis(2-ethylhexel)phosphate. In bulk, XRD suggested the formation of 2D oblique columnar architectures. When blended with PS, similar internal columnar order was observed, providing a strategy for architectural control of composite materials.

Würthner reported the synthesis of dendronized 4-armed stars with a diazadibenzoperylene core functionalized with G1−3 benzoic acid dendrons (Figure 360).[1152] The sp^2 nitrogen allows for the formation of supramolecular polymers via complexation with Ag^+ for G1 and G2 dendronized stars. The G3 benzoic acid dendron sterically inhibits supramo-

Scheme 76. Organogel-Forming Dendronized PBI Reported by Würthner[1160]

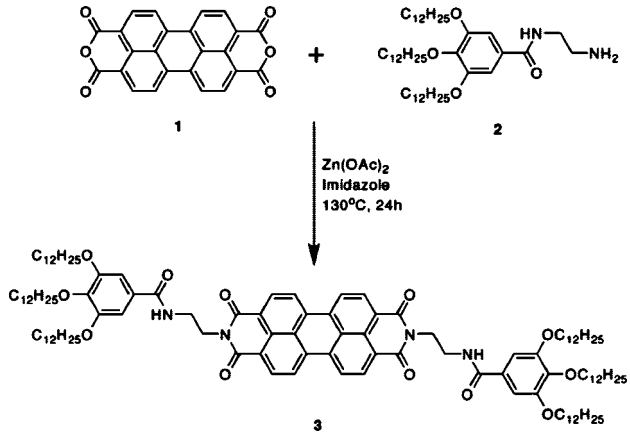

lecular polymerization. Supramolecular polymer formation could be directly visualized via AFM. During polymerization, spheres corresponding to individual stars were converted to rodlike entities. Recently, Würthner reported a series of dendronized 4-armed stars with PBI cores (Figure 361), and their self-assembly into twisted "double-cable" fibrous J-aggregates was confirmed via AFM and STM (Figure 362a,b).[1153,1154] The mechanism of self-assembly was carefully probed via a combination of UV−vis and CD spectroscopy, demonstrating that, contrary to all other PBI assemblies wherein "equal K" aggregation models[1155] were presumed, these J-aggregates appeared to follow a nucleation-elongation mechanism (Figure 362c). The nucleation process exhibits a significantly lower equilibrium constant for "dimerization" than the subsequent equilibrium constant for elongation. CD studies using a mixture of chiral and achiral dendronized PBIs also demonstrated chiral amplification through a sergeant-and-soldiers mechanism. Linear dichroism (LD) suggested an orientation of the PBI cores at an angle of less than 54.7° to the aggregate axis (Figure 362d).

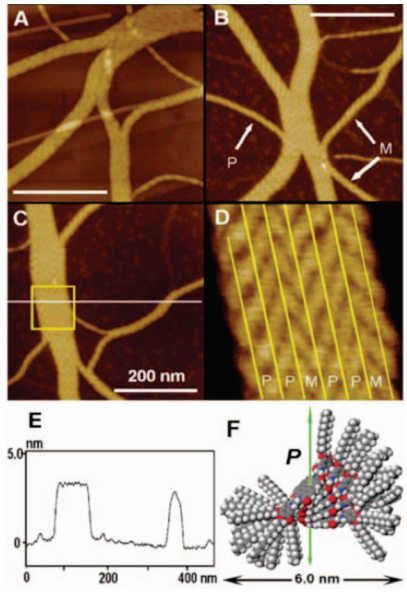

Figure 368. AFM images of self-organized dendronized perylene organogel spin coated onto HOPG (A) and mica (B). Left handed, M, and right-handed, P, configuration are shown (B). Zooming (D) in on the larger aggregates from (C) exhibits multiple configurations. (E) shows cross-sectional analysis of the white line in (D). (F) shows the model of the configuration of the P-aggreagate. Reprinted with permission from ref 1160. Copyright 2006 Royal Society of Chemistry.

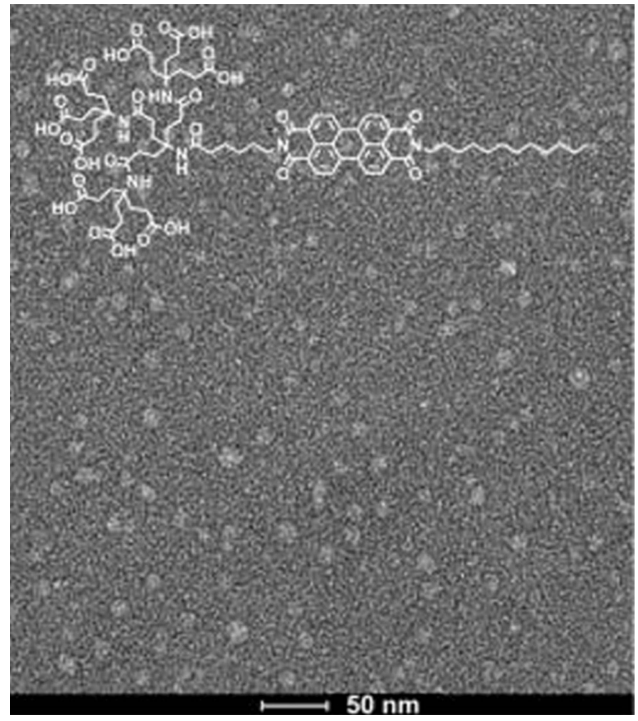

Figure 369. TEM of micellar structures formed from dendronized PBI amphiphile by Hirsch. Reprinted with permission from ref 1161. Copyright 2007 American Chemical Society.

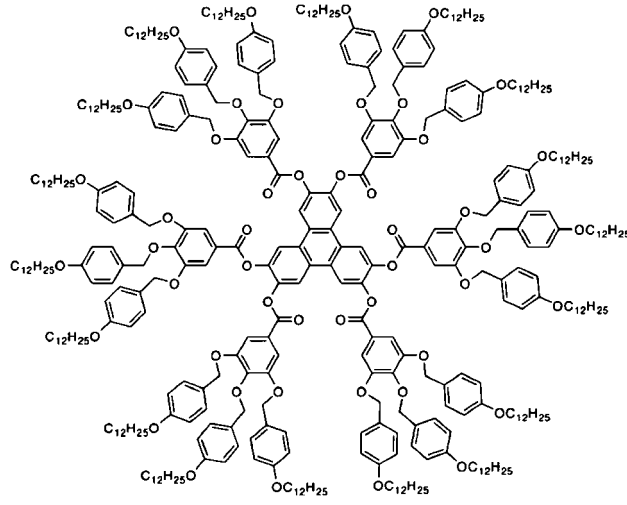

Figure 370. Dendronized triphenylene reported by Harris and Cheng.[1162]

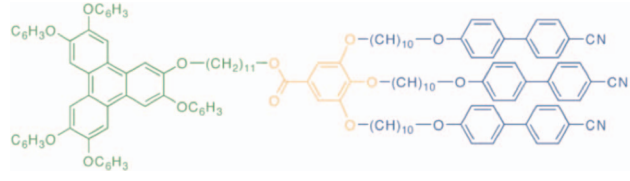

Figure 371. Dendronized triphenylene by Mehl. Reprinted with permission from ref 1163. Copyright 2004 Royal Society of Chemistry.

In addition to self-assembly in bulk or supramolecular homopolymerization in solution, dendronized PBIs have been shown to self-assemble with H-bonding to dendronized OPVs forming both supramolecular rosettes and supramolecular polymers. Würthner and Meijer reported the H-bonded self-assembly of PBIs and dendronized OPVs, which self-assemble in solution at temperatures below 50 °C as observed

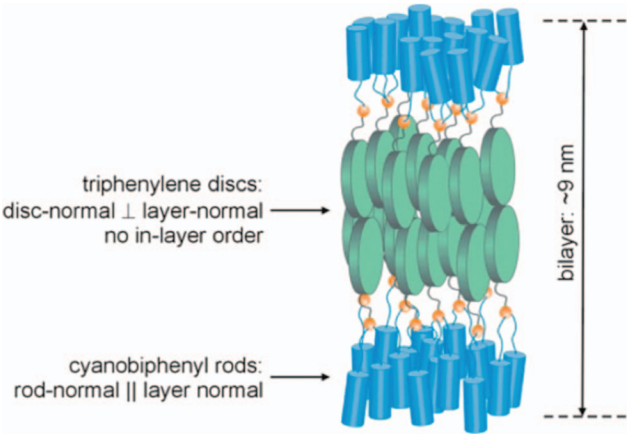

Figure 372. Schematic packing of dendronized triphenylene in the S phase by Mehl. Reprinted with permission from ref 1163. Copyright 2004 Royal Society of Chemistry.

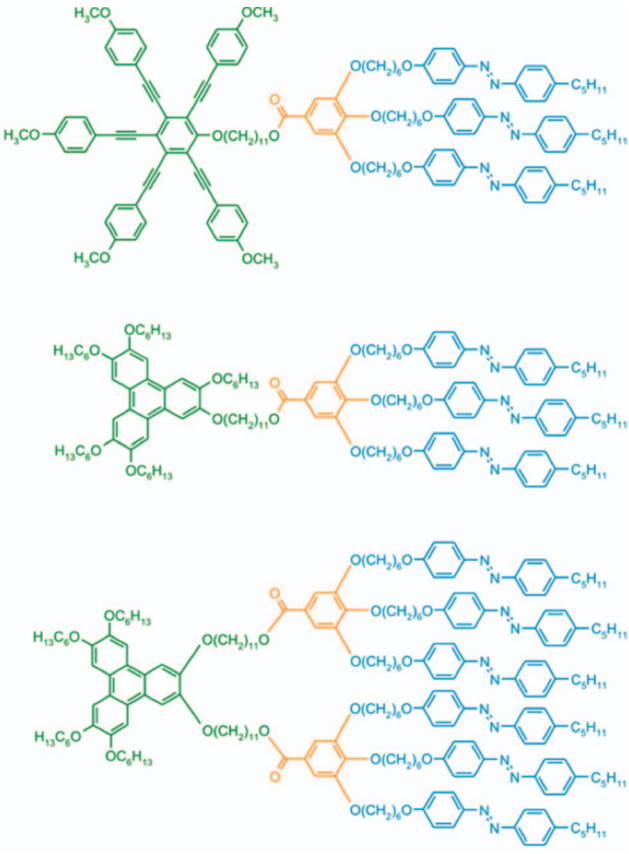

Figure 373. Dendronized discotic shape-amphiphiles. Reprinted with permission from ref 308. Copyright 2009 Royal Society of Chemistry.

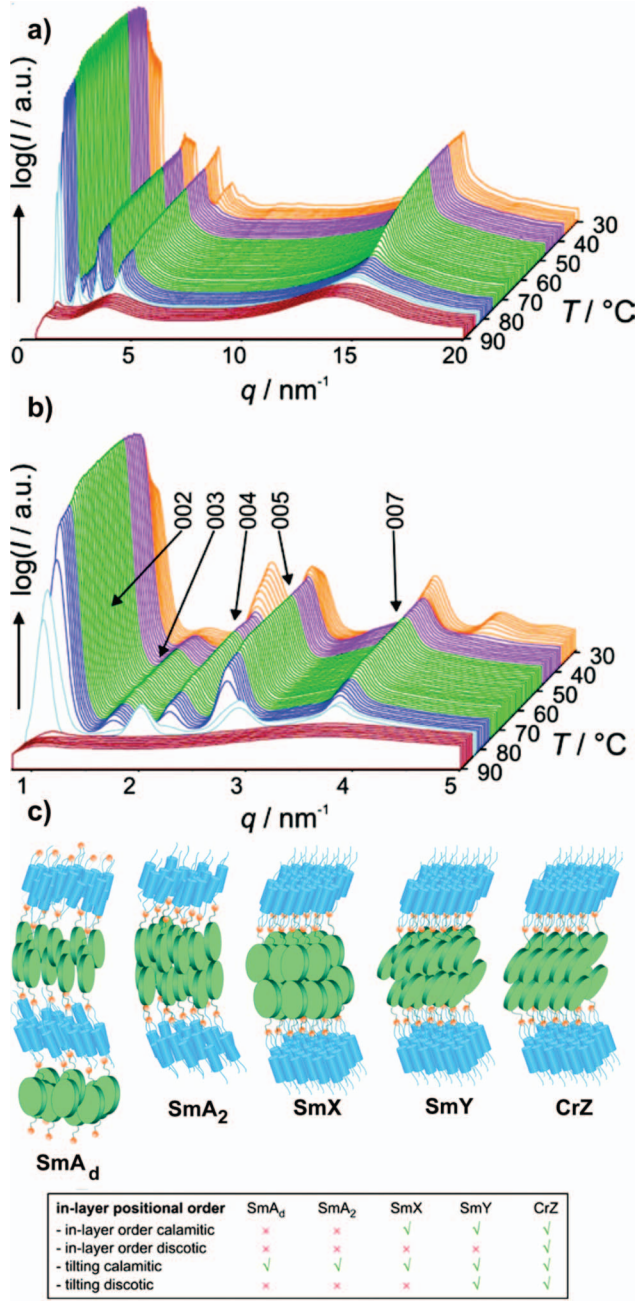

Figure 374. Full (a) experimental XRD-diffractogram and blow-up (b) of the small-angle region of compound 2 from Figure 373 and the corresponding models (c) of the S and crystalline phases: Sm_{Ad} (fully interdigitated bilayer), SmA_2 (bilayer without interdigitation), SmX phase, SmY phase, and crystal phase. Reprinted with permission from ref 308. Copyright 2009 Royal Society of Chemistry.

by temperature-dependent CD/UV−vis and fluorescence spectroscopy (Figure 363).[825] Visualization by AFM demonstrated self-assembly into helical fibers having a width of roughly 7 nm (Figure 364). Subsequently, Meijer and Würthner investigated these materials and their covalently linked analogues as possible supramolecular p−n heterojunctions with applications as photoconductors and as molecular diodes.[1156,1157]

By varying the structure of the dendronized OPV (Scheme 75), Würthner produced various self-assembled structures ranging from tapes to rosette fragments to full rosettes (Figure 365).[824] The self-assembled structures were visualized by STM (Figure 366), and their self-assembly was characterized by temperature-dependent CD/UV−vis spectroscopy. Würthner also reported similar systems where the PBI was replaced with naphthalene bisimide.[1158]

Würthner and Meijer investigated the self-assembly and ambipolar charge transport in a series of nonsymmetrical dendronized PBIs containing both H-bonded and covalently bonded dendrons, as well as symmetric dendronized OPV H-bonded dimers and the mixtures thereof (Figure 367).[1159] H-bonded dendronized OPV PBI complexes, H-bonded OPV dimers, and covalently dendronized PBIs were shown to act as field effect transistors (FET), while mixtures of H-bonded OPV dimers and covalently dendronized PBIs did not.

Table 6. Diffraction Data from the Diffractograms Presented in Figure 374 (Reprinted with Permission from Ref 308; Copyright 2009 Royal Society of Chemistry)

T/°C	phase	reflection	peak shape	q/nm^{-1}	d/Å
81	interdigitated SmA_d	001	s	0.95	66.1
		002	s	1.87	33.6
		003	s	2.79	22.5
		004	s	3.71	16.9
		B	d	3.89	16.2
		C	d	14.5	4.3
79	bilayer SmA_2	002	s	1.08	58.4
		003	s	1.58	39.8
		004	s	2.12	29.7
		005	s	2.65	23.8
		B	d	3.66	17.1
		007	s	3.71	17.0
		C	d	14.5	4.3
51	SmX	002	s	1.08	58.2
		003	s	1.58	39.8
		004	s	2.14	29.4
		005	s	2.64	23.8
		B	d	3.62	17.4
		007	s	3.72	16.9
		C_d	d	14.4	4.4
		C_s	s	14.7	4.27
40	SmY	002	s	1.09	57.7
		003	s	1.58	39.7
		004	s	2.14	29.3
		005	s	2.65	23.7
		B	d	3.63	17.3
		007	s	3.72	16.9
		C_d	d	14.5	4.3
		C_s	s	14.7	4.27

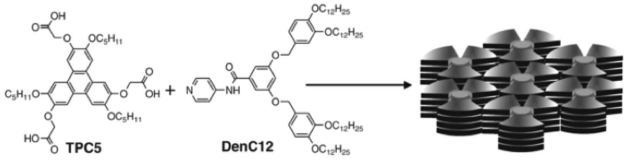

Figure 375. Dendronized triphenylene and H-bond mediated self-organization. Reprinted with permission from ref 1164. Copyright 2007 Japanese Chemical Society.

Scheme 77. Dendronized Triphenylene by Wang and Zhao (Reprinted with Permission from Ref 1165; Copyright 2007 Royal Society of Chemistry)

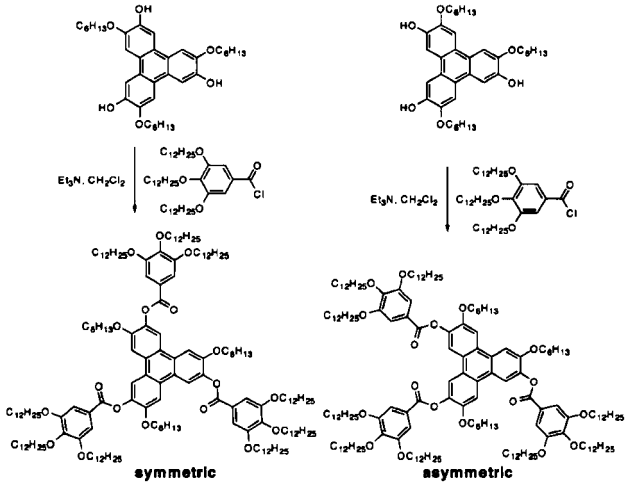

PBIs have been shown to form larger structures in solution such as networks, micelles, and vesicles. Würthner reported dendronized PBIs (Scheme 76) that self-assemble into interpenetrating networks of P and M type ribbons in a wide variety of solvents, forming organogels (Figure 368).[1160] Hirsch reported water-soluble PBIs functionalized with G2 Newkome-type dendrons (Figure 369).[1161] TEM experiments revealed micellar structures with a mean diameter of 16 nm in pH 7.2 phosphate-buffered water (Figure 369).

Würthner also reported dendronized amphiphilic PBIs and the control of their supramolecular structures generated by coself-assembly of both wedge- and dumbbell-shaped dendronized PBIs in THF−water mixtures (Figure 112) (see section 3.2.2).[482]

7.4. Dendronized Triphenylene

Harris and Cheng synthesized the first dendronized triphenylene functionalized with (4-3,4,5)12G1 Percec-type dendrons (Figure 370).[1162] While only DSC thermograms were reported, these dendronized triphenylenes were also characterized by XRD and TOPM. Three columnar phases were identified by WAXS, and the lowest temperature phase was assigned as Φ_h.

Mehl reported triphenylene monodendronized with cyanobiphenyl-functionalized AB_3 dendrons exhibiting thermodynamically stable S phases (Figure 371).[1163] The dendron and triphenylene precursors exhibit N and columnar phases, respectively. WAXS and SAXS suggested a bilayer packing model (Figure 372).

Mehl also reported other examples of dendronized polyaromatic diphenyldiazene containing "shape-amphiphiles" that self-organizes into both the N and S phases (Figure 373).[308] Of note, they reported the fine-tuning of order within sublayers by changing the aromatic and dendritic composition or through temperature variation (Figure 374 and Table 6).[308]

Takeoka reported triphenylene triacids mixed in 1:3 ratio with dendronized amino pyridine that self-assemble via H-bonding into supramolecular discs and self-organize into Φ_h lattices as demonstrated via FTIR and XRD analysis (Figure 375).[1164]

Wang and Zhao synthesized symmetrically and nonsymmetrically dendronized triphenylene and investigated the effect of substitution on self-assembly in bulk and on HOPG (Scheme 77).[1165] Symmetric isomers with C_3 symmetry self-assembled on HOPG surfaces and resulted in two distinct domain types. The first type of packing observed on HOPG was described as a classical honeycomb structure displaying a molecule at each of the six apexes. The second type of domain exhibited a close-packed structure forming a distorted hexagon with an additional molecule in the center of the hexagon. The nonsymmetric isomer exhibited only a single type of packing described as rectangular stripe packing.

In bulk, DSC indicated two-phase transitions for both isomers, which were assigned via XRD as k → Φ_h and Φ_h → I. The symmetrically substituted triphenylene displayed melting and clearing points that were both lower than those for the nonsymmetrically substituted isomer. The nonsymmetrically substituted isomer exhibited an enthalpy of 768 kJ mol^{-1} for the k → Φ_h compared to 39 kJ mol^{-1} for the symmetric isomer, whereas both enthalpies of isotropization were within 8 kJ mol^{-1}. The differences in enthalpy on melting correlate to the packing observed on HOPG wherein a more uniform single-domain structure was observed for the nonsymmetric isomer.

Percec recently reported the self-assembly of hexadendronized triphenylenes (Figure 376) into helical pyramidal columns and spheres (Figures 377 and 378) as described for CTV dendronized with Percec-type dendrons (see section 6.4).[324] (3,4-3,5)12G1−Tp and (4-3,4-3,5)12G1−Tp provided the first examples of self-assembled spheres with helical

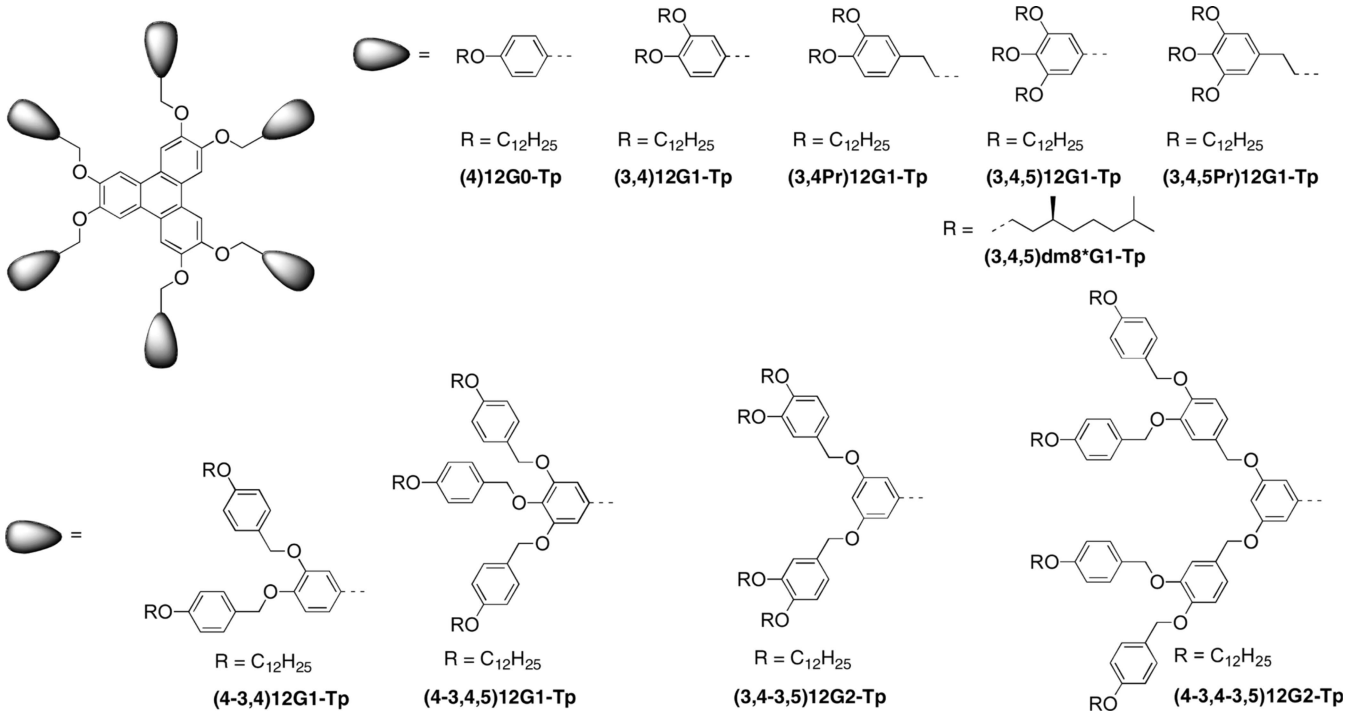

Figure 376. Triphenylenes hexafunctionalized with Percec-type dendrons. Reprinted with permission from ref 324. Copyright 2009 American Chemical Society.

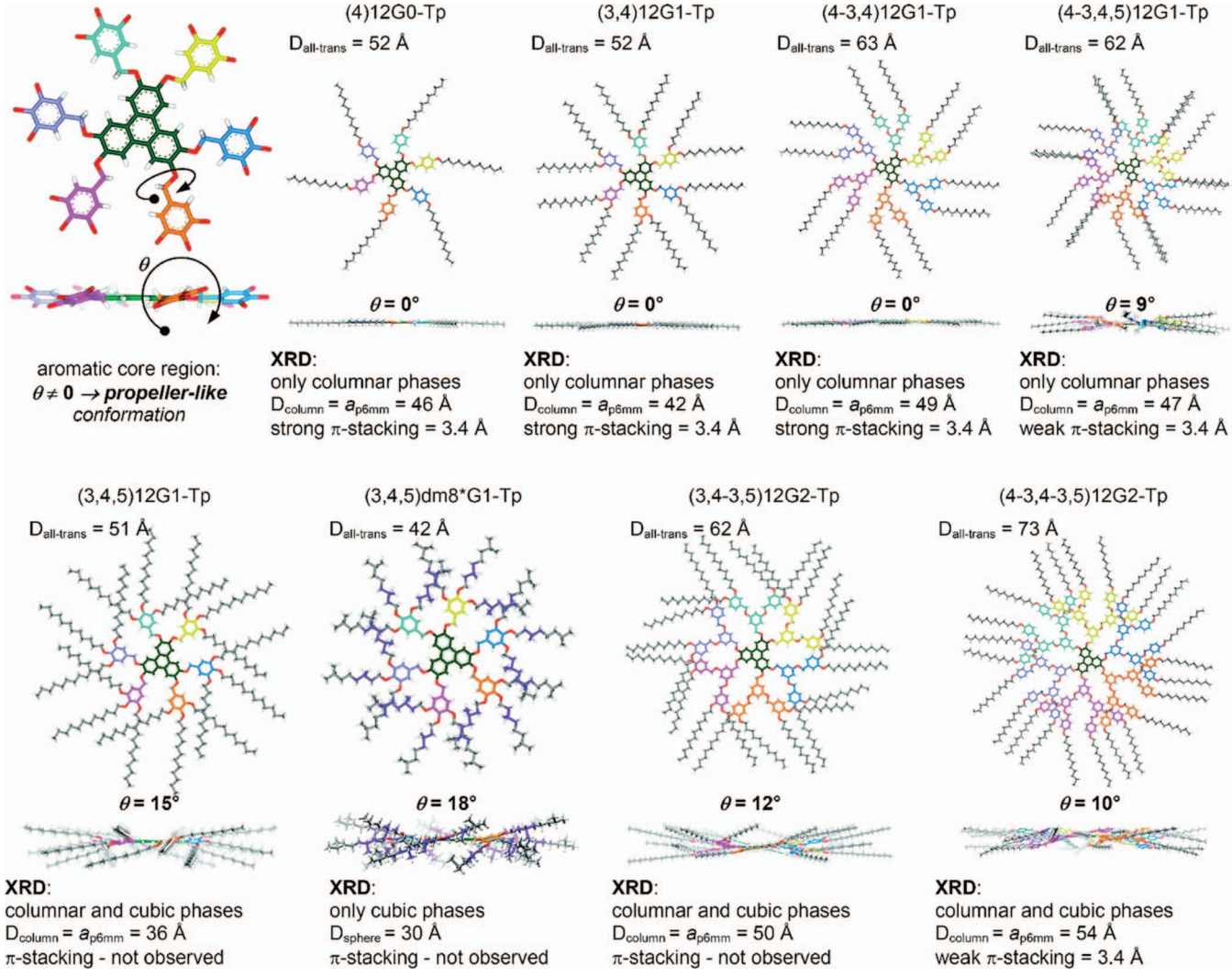

Figure 377. Self-assembly overview for dendronized triphenylenes. Reprinted with permission from ref 324. Copyright 2009 American Chemical Society.

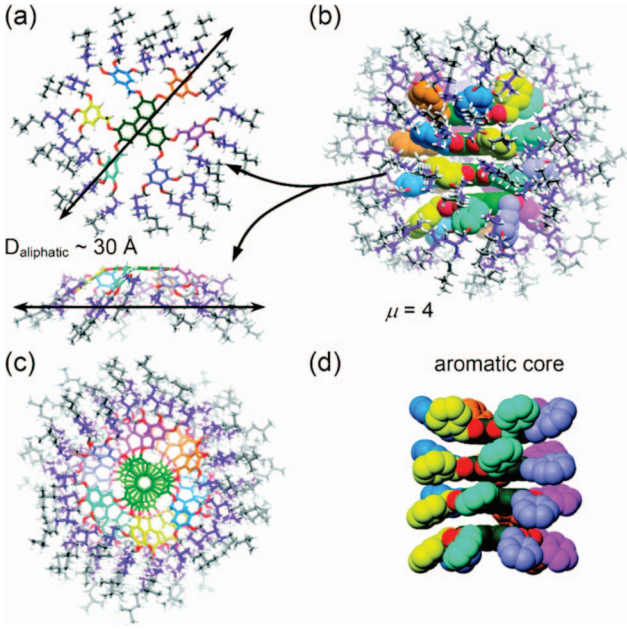

Figure 378. Self-assembly of dendronized triphenylenes into chiral spheres. (a) Top view of a singly crown-dendrimer. (b) Side-view of self-assembled sphere. (c) Top view of self-assembled sphere. (d) Side-view of self-assembled sphere only showing the helical aromatic cores. Reprinted with permission from ref 324. Copyright 2009 American Chemical Society.

Scheme 78. Synthesis of Dendronized tris[*N*-(3,4,5-Trimethoxyphenyl)]-1,4,5,8,9,12-hexaazatriphenylene-2,3,6,7,10,11-hexacarboxy Triimide[1166]

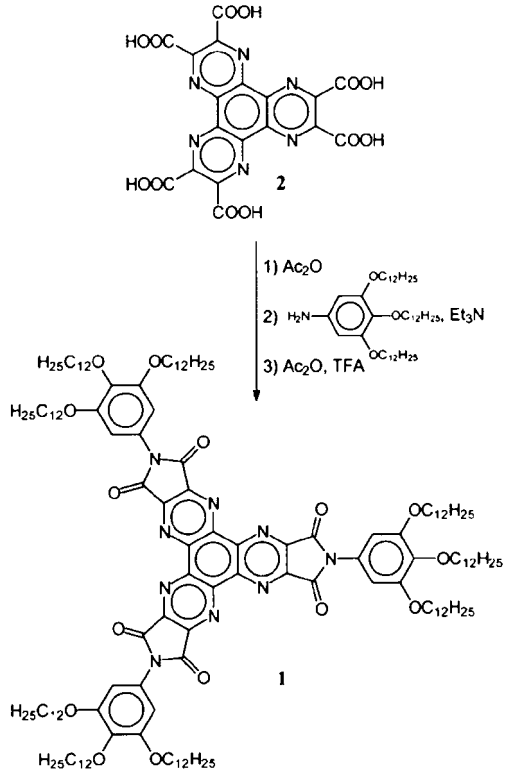

pyramidal internal structure that self-assemble into 12-fold QLC lattices. Furthermore, (3,4,5)12G1−Tp and (3,4,5)d*m*8*G1−Tp were shown to exhibit thermoreversible conversion upon heating from *Tet* to *Cub* lattices. In all previous examples of Percec-type dendrons or dendronized CTV, the phase order was *Cub* → *Tet*. (3,4,5)12G1−Tp also

Scheme 79. Dendronized Hexabenzocoronenes Reported by Müllen[1179]

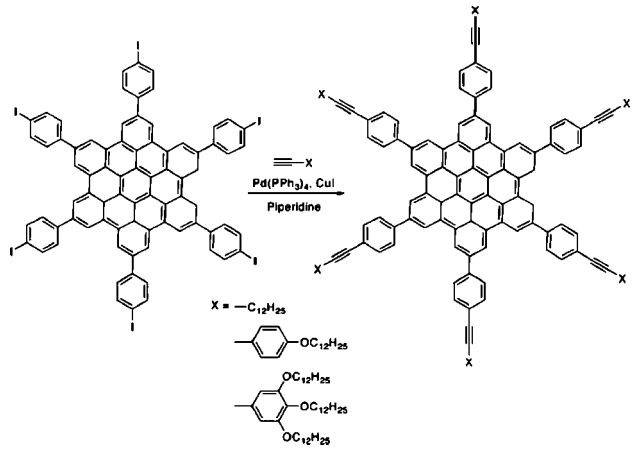

exhibited a low-temperature Φ_h phase. The incorporation of the branched chiral d*m*8* tail eliminated the Φ_h phase but provided amplification of chirality in the spherical phase as indicated by CD/UV−vis studies. Mixing of (3,4,5)12G1−Tp in 1:1 ratio with 2,4,7-trinitrofluorenone results in an EDA complex that self-assembles exclusively into a Φ_h lattice. The chirality of the self-assembled Electron Donor-Acceptor (EDA) complexes can be programmed through the use of L- or D-menthol-functionalized 2,4,7-trinitrofluorenone (TNF).

Additionally, Meijer reported a dendronized electron-deficient analogue of triphenylene and its photoinduced charge transport as an electron-acceptor material for photovoltaic devices (Scheme 78).[1166] DSC thermograms of this hexaazotriphenylene indicated a LC phase over a range of −24 to 269 °C, which was assigned by XRD as Φ_h. 50% w/w mixtures of this dendronized discotic acceptor with poly(3-hexylthiophene) were shown to exhibit photoinduced electron transfer by photoinduced absorption (PIA) and fluorescence spectroscopy.

7.5. Dendronized Hexabenzocoronene

The first synthesis of hexabenzocoronene was reported in 1958, and its crystal structure was reported in 1960.[1167,1168] Self-assembly and self-organization of hexabenzocoronenes has been investigated by Aida[1169−1173] and Müllen.[1174−1178] The first dendronized hexabenzocoronenes were reported by Müllen (Scheme 79).[1179] He developed a hexa(4-iodophenyl)-*peri*-hexabenzocoronene building block that could be elaborated to functional materials through Sonogashira cross-coupling with functional alkynes. In one example, the hexabenzocoronene core was dendronized via acetylene functionalized with (3,4,5)12G1.[1179]

Self-assembly in bulk was investigated by DSC, TOPM, and WAXS, though none of the samples displayed isotro-

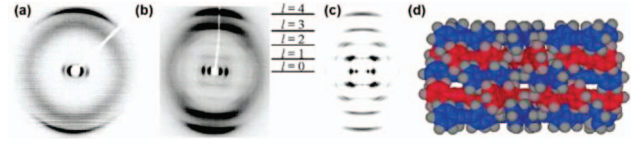

Figure 379. Experimental XRD diffraction patterns of 4-dodecyloxyphenyl substituted hexabenzocoronene (a) and (3,4,5)12G1 dendronized hexabenzocoronene (b) simulated 2D diffraction pattern of dendronized hexabenzocoronene (c); based on the model (d), each disk is rotated about the column axis successively by 15°. Reprinted with permission from ref 1179. Copyright 2004 American Chemical Society.

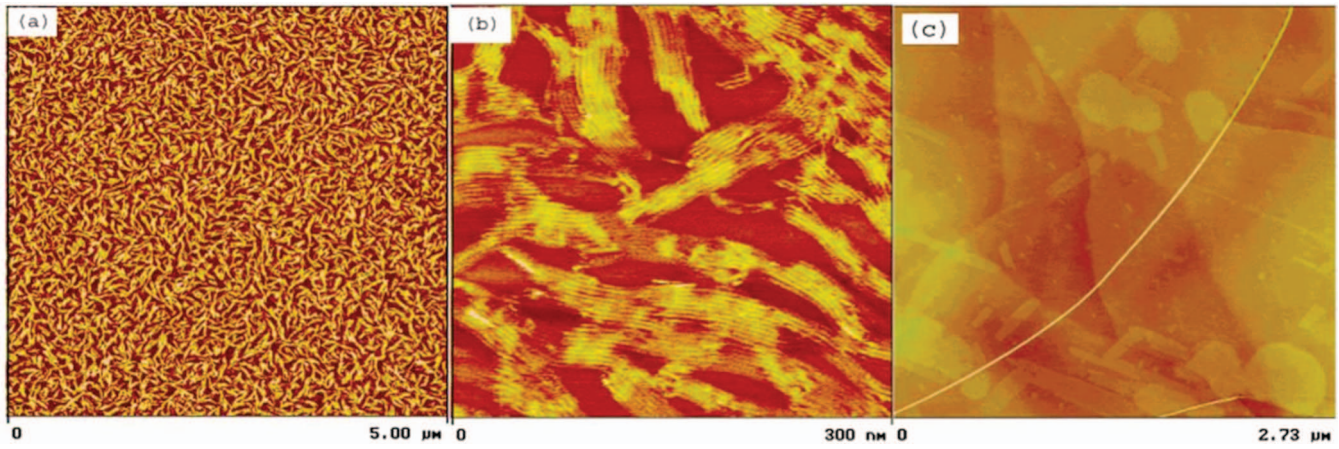

Figure 380. AFM images in tapping mode of dendronized hexabenzocoronene on HOPG surfaces: (a) spin-coated film 5 μm scan size; (b) spin-coated film 300 nm scan size; and (c) drop-cast film. Reprinted with permission from ref 1179. Copyright 2004 American Chemical Society.

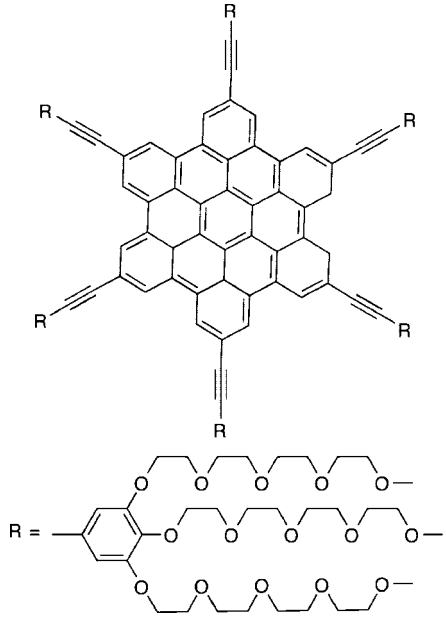

Figure 381. Water-soluble dendronized hexabenzocoronene reported by Müllen. Reprinted with permission from ref 1180. Copyright 2006 Royal Society of Chemistry.

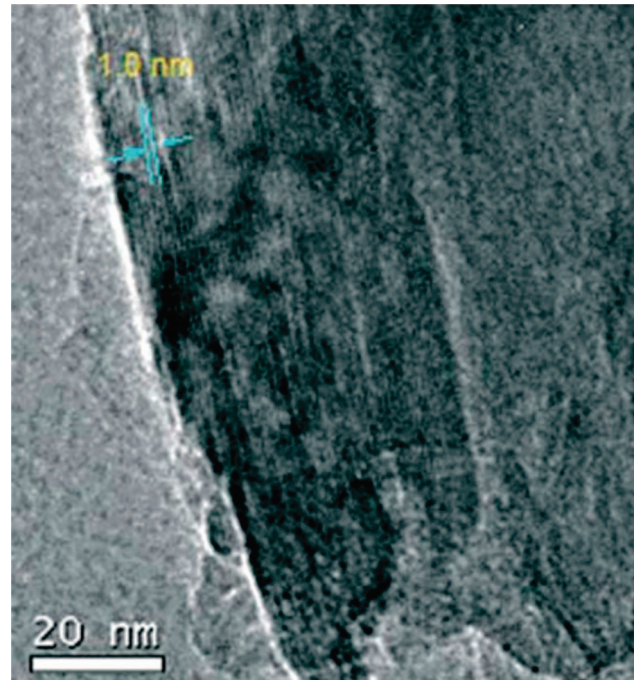

Figure 382. TEM of nanoporous silica templated by dendronized hexabenzocoronene. Reprinted with permission from ref 1180. Copyright 2006 Royal Society of Chemistry.

pization temperatures below 400 °C. Both helical and nonhelical Φ_h phases were identified along with a number of other unidentified columnar phases. XRD data was simulated for helical packing with discs rotated successively by 15° and was found to be in good agreement with experimental data (Figure 379).[1179]

Surface self-assembly was investigated by spin-coating absorption onto HOPG followed by AFM visualization. A variety of structures were observed including nanorods and nanoribbons. High magnification of the structures revealed stripelike domains consisting of single columns oriented parallel to the surface (Figure 380).[1179]

Recently, Müllen reported the synthesis of water-soluble hexabenzocoronene derivatives bearing oligo(ethylene oxide) functionalized dendrons (Figure 381).[1180] The DSC, TOPM, and XRD indicated columnar self-organization. Self-assembly in solution was confirmed by fluorescence spectroscopy. Fluorescence measurements in 1,1,2,2-tetrachloroethane showed well-resolved spectra of nonaggregated molecules. However, in polar protic solvents, only a single broad emission was observed, characteristic of aggregates formed by π-stacking. Sol−gel polymerization was carried out with tetraethoxysilane in HCl. XRD prior to calcination confirmed the maintenance of columns within the sol−gel. Following calcination, TEM analysis showed nanoporous silica containing 1D aligned channels (Figure 382).[1180]

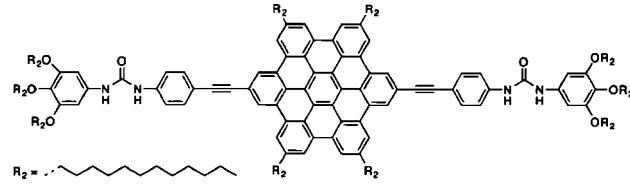

Figure 383. Dendronized ureido hexabenzocoronenes by Müllen.[1181]

Scheme 80. Hexabenzocoronene Nanotubes Dendronized with Fréchet-type Dendrons Reported by Aida (Reprinted with Permission from Ref 1182; Copyright 2008 American Chemical Society)

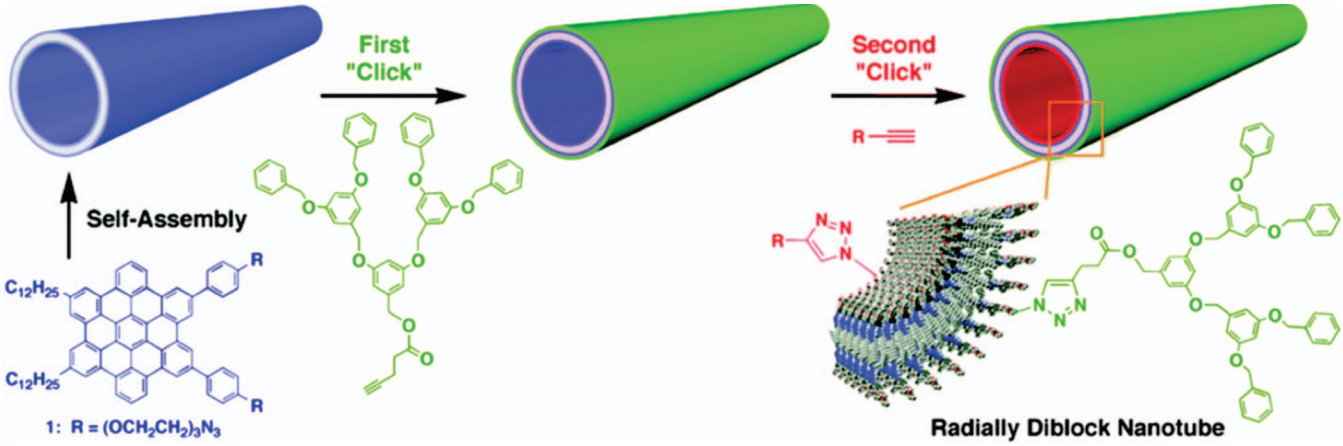

Müllen also reported the self-assembly of dendronized hexabenzocoronenes reinforced via H-bonding of ureido groups (Figure 383).[1181] Self-assembly in bulk was investigated by DSC and XRD. Organized phases were obtained. However, a unit cell for the supramolecular structure was not determined. Self-assembly in solution into fluorescent organogels was observed. Fluorescence was confirmed to arise from fibrillar structures within the organogel by laser scanning confocal microscopy.

Aida reported examples of self-assembling amphiphilic hexabenzocoronenes into graphitic nanotubular assemblies.[1169,1170,1172,1173] In a recent report, this method was extrapolated to produce dendronized hexabenzocoronenes via CuAAC click chemistry, forming radially diblock nanotubes (Scheme 80).[1182] Self-assembled amphiphilic hexabenzocoronenes with a 5-hexanitrile face were dendronized with G2 Fréchet with apical alkyne functionality via click chemistry. The aliphatic interior surface was treated with 5-hexyl-1-ol and subjected to a second click reaction to achieve radially diblock nanotubes. Through this technique, a soluble nanotube with densely tailored interior functionality was prepared.

Recently, Aida reported the self-assembly of corannulene, a π conjugated analogue of coronene, functionalized with (3,4,5)12G1 Percec-type dendrons (Figure 384).[1183] Corannulene is a bowl-shaped polycyclic that, unlike its coronene relative, possesses inversion flexibility at a rate of 2×10^5 s^{-1} and a net dipole of 2.5*D* that arises from nonequivalent electron density on the opposite faces of the polycycle. Aida demonstrated self-organization into a Φ_h phase behavior by

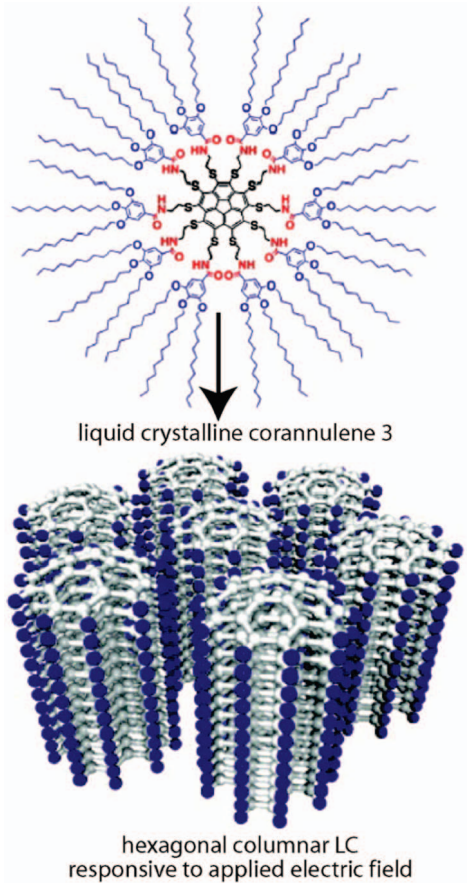

Figure 384. Self-assembly of dendronized corranulene and its homeotropic alignment under electric field. Reprinted with permission from ref 1183. Copyright 2009 American Chemical Society.

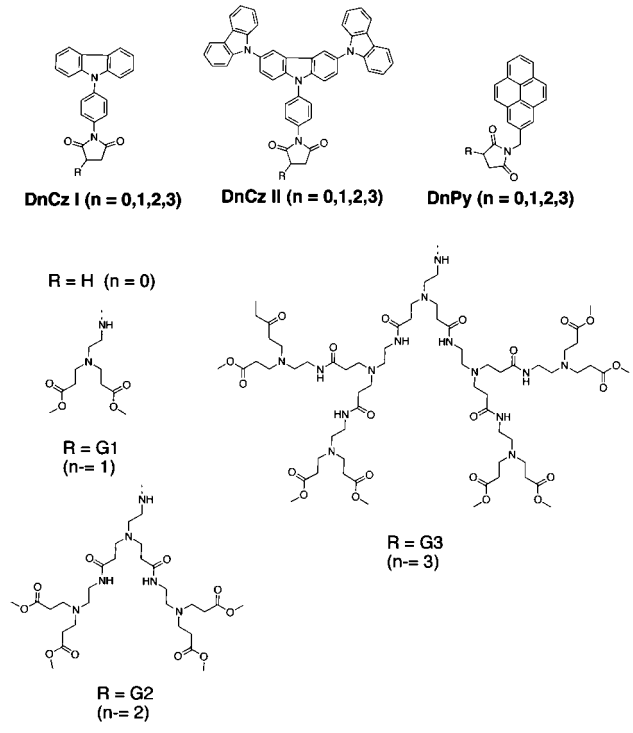

Figure 385. Dendronized chromophores reported by Wei.[766]

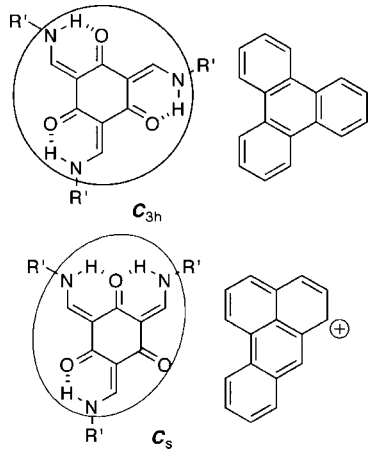

Figure 386. Tautomeric forms of TSANs C_{3h} symmetry analogous to triphenylene and C_s symmetry analogous to 6H-benz[de]anthracen-6-ylium. Reprinted with permission from ref 1184. Copyright 2007 American Chemical Society.

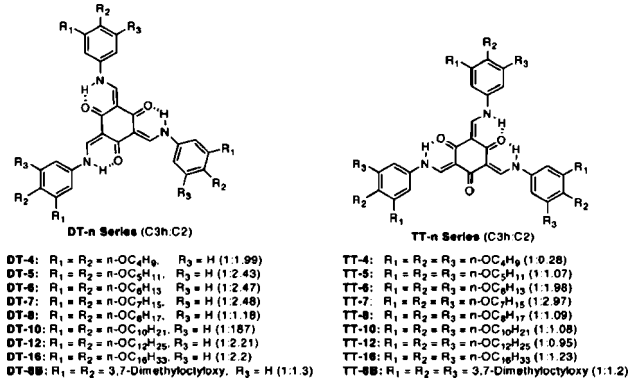

Figure 387. Dendronized TSANs reported by Yelamaggad. Reprinted with permission from ref 1184. Copyright 2007 American Chemical Society.

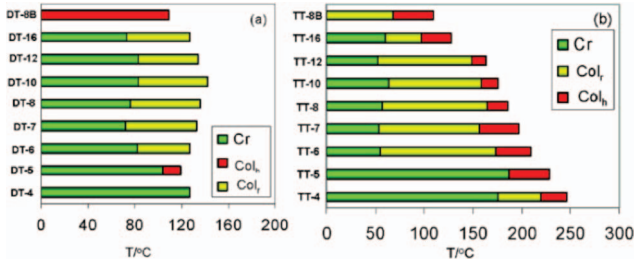

Figure 388. Effect of tail length on phase transitions reported by Yelamaggad. Reprinted with permission from ref 1184. Copyright 2007 American Chemical Society.

DSC, TOPM, and XRD and alignment in electric field to produce homeotropically aligned films on ITO surfaces.

7.6. Other Dendronized Polyaromatics

In addition to the major classes of dendronized polycycles described above, a number of other important examples of self-assembling and self-organizing dendronized polycycles have been prepared. Wei reported carbazoles and pyrenes chromophores functionalized with G1−G3 Newkome type dendrons (Figure 385), which self-assembled in aqueous solution into vesicular structures that transformed over a period of 7 days to form tubular aggregates (Figure 209).[766]

Yelamaggad reported dendronized tris(*N*-salideneaniline)s (TSANs).[1184] TSANs exist in two inseparable keto-enamine tautomers, one with C_{3h} rotational symmetry and one with

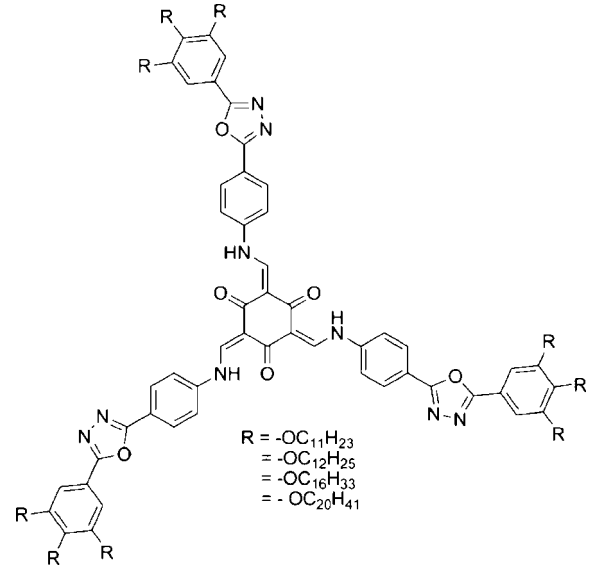

Figure 389. Oxadiazole-based TSANs.[1185]

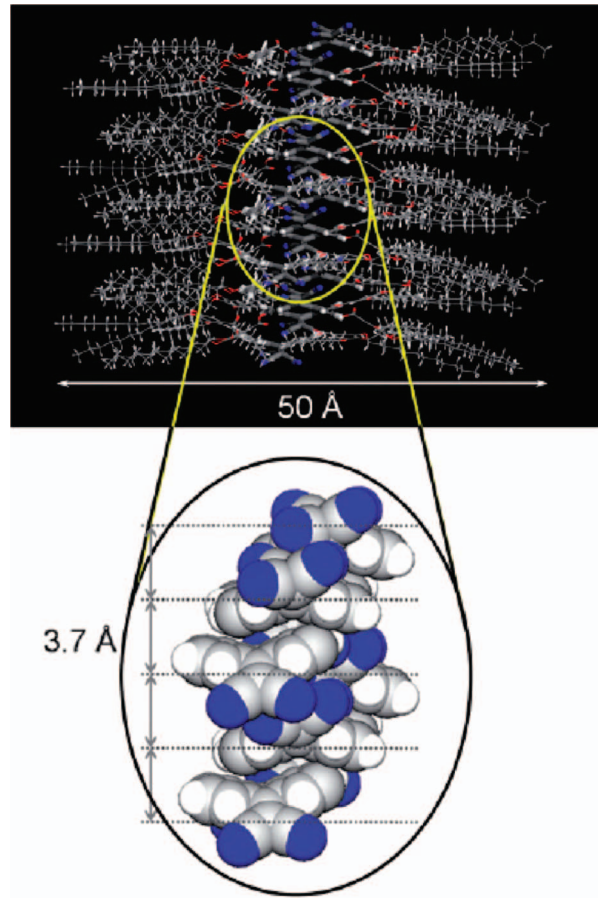

Figure 390. Self-assembly of (3,4,5)12G1 dendronized TCAQ. Reprinted with permission from ref 1187. Copyright 2008 Royal Society of Chemistry.

C_s symmetry. The C_{3h} tautomer is analogous to triphenylene whereas the C_s tautomer is analogous to 6H-benz[de]anthracen-6-ylium (Figure 386).[1184] TSANs were dendronized with (3,4)*n*G1 and (3,4,5)*n*G1 Percec-type dendrons (Figure 387). Self-assembly and self-organization were investigated by XRD, DSC, and TOPM. Increasing the length of alkyl tails tended to stabilize the Φ_r phase in the (3,4)*n*G1 dendronized TSANs and both the Φ_h and Φ_r phase in (3,4,5)*n*G1 dendronized TSANs (Figure 388). Branched alkyl tails

Scheme 81. Dendronized Anthraquinodimethane Reported by Kato[1187]

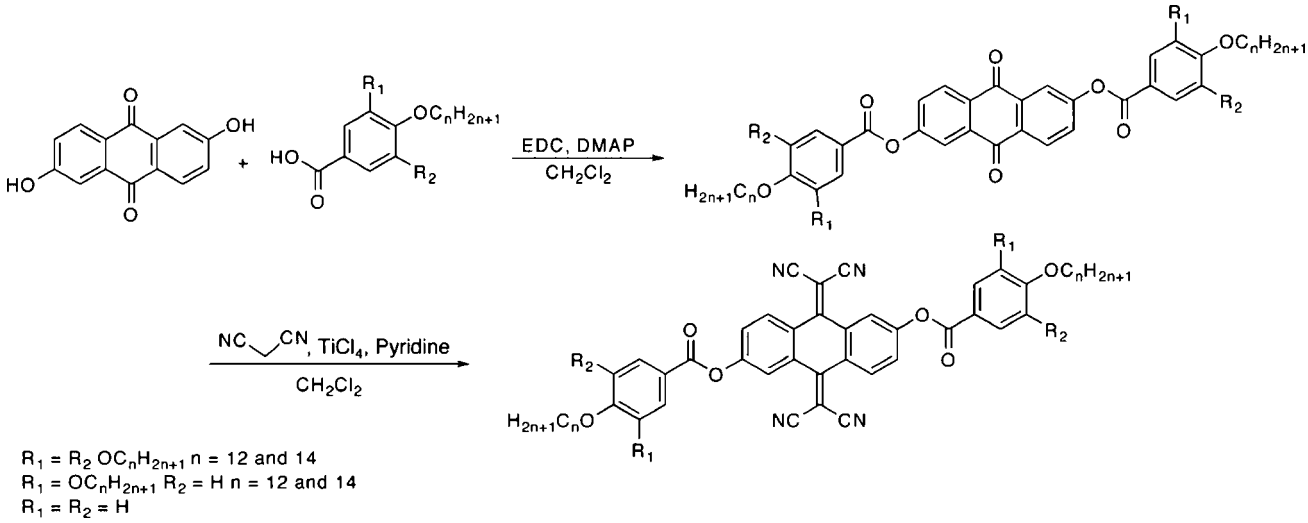

completely suppress the *k* phase and stabilize the Φ_h in (3,4)12G1 dendronized TSANs and the Φ_h and Φ_r phases in (3,4,5)12G1 dendronized TSANs. Subsequently, TSANs functionalized with oxadiazole containing dendrons have been prepared that also display self-organization into Φ_h phases (Figure 389).[1185] Through modification of the dendritic branch, the luminescence properties can be altered, while still maintaining similar 2-D organization.

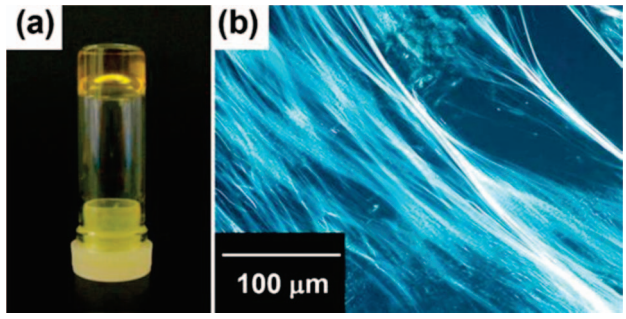

Figure 391. Organogel formed from dendronized tetracyanoanthraquinodimethane (a) and TOPM image of organogel fibrils (b). Reprinted with permission from ref 1187. Copyright 2007 Royal Society of Chemistry.

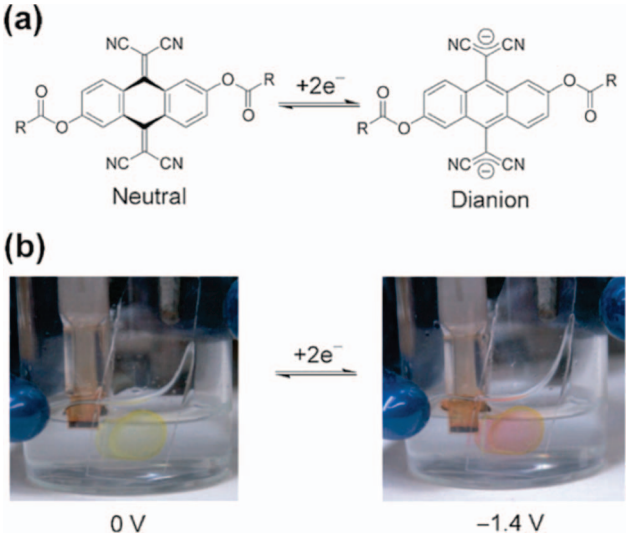

Figure 392. Redox reaction of dendronized tetracyanoanthraquinodimethane (a) and color change observed with change in redox state (b). Reprinted with permission from ref 1187. Copyright 2007 Royal Society of Chemistry.

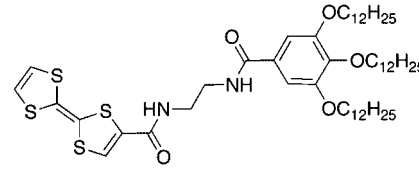

Figure 393. Dendronized TTF.[1188]

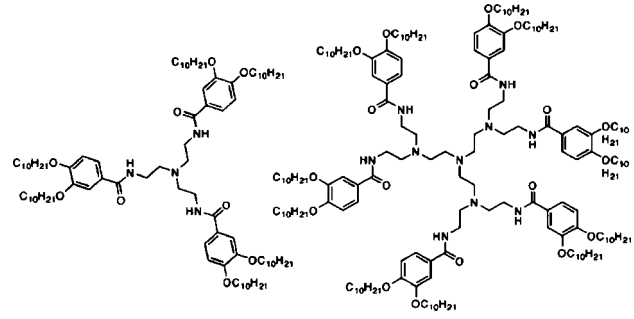

Figure 394. Dendronized PEI dendrimers functionalized at their periphery with (3,4)10G1.[1207]

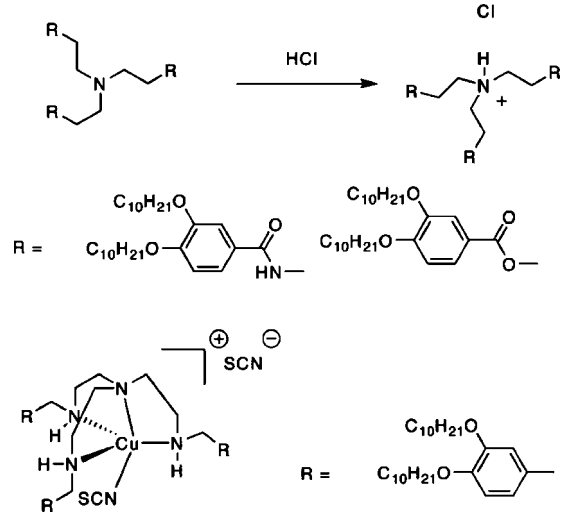

Figure 395. Protonation and metal complexation mediates self-organization in dendronized PEI dendrimers.[1207,1208]

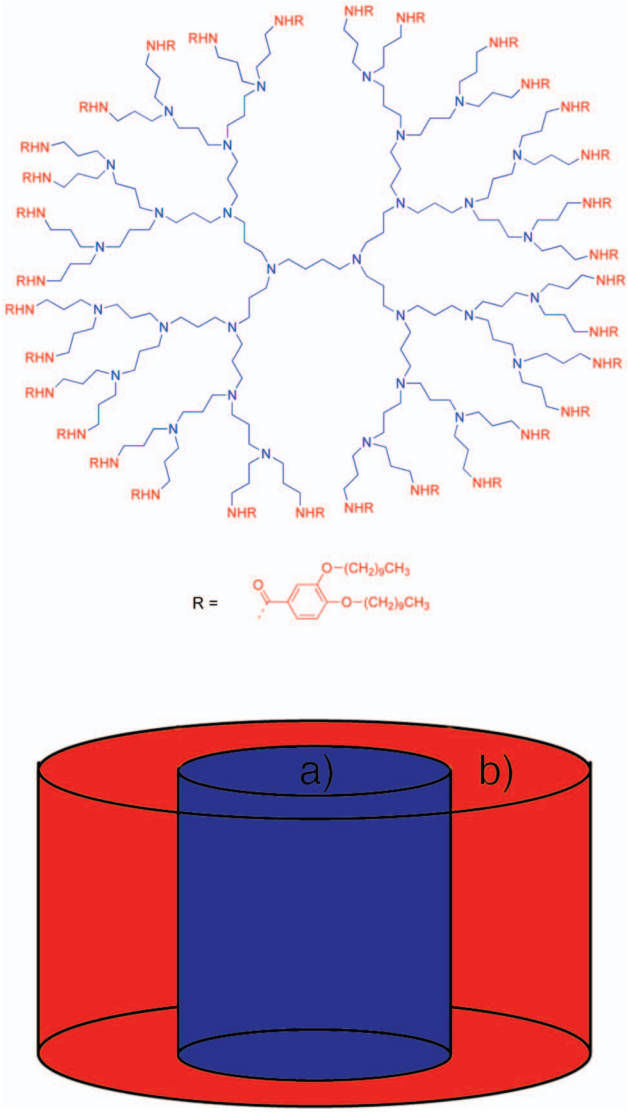

Figure 396. Dendronized PPL dendrimers and their self-assembly into core−shell supramolecular columns. Adapted from ref 1209 .

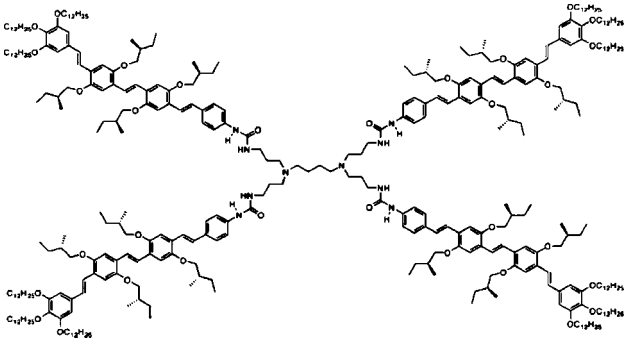

Figure 397. G1 PPI dendrimer functionalized with chiral (3,4,5)12G1 dendronized OPV.[1210]

Similar to previously reported structures,[1186] Kato reported the synthesis of tetracyanoanthraquinodimethane (TCAQ) and anthroquinone (AQ) bisdendronized with (3,4)12G1, (3,4)14G1, (3,4,5)12G1, and (3,4,5)14G1 Percec-type dendrons (Scheme 81).[1187] The effect of the polar cyano substituents on self-organization was pronounced. The relatively nonpolar dendronized AQs exhibit only crystalline, N, and S phases. While most of the bisdendronized TCAQs also form crystalline phases, TCAQ functionalized

Scheme 82. Synthesis of Octopus Dendronized Dendrons[1212,1213]

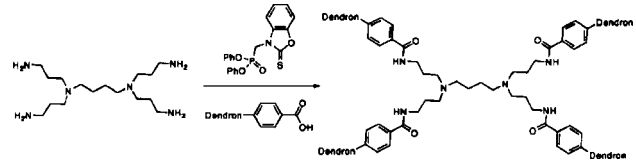

(3,4,5)*n*G1, where $n = 12$ or 14, self-organizes into Φ_h architectures exhibiting antiparallel orientation of roof-shaped TCAQ cores (Figure 390). Self-assembly in organic solvents was investigated. Only Φ_h forming dendronized tetracyanoanthraquinodimethanes exhibited gelation abilities (Figure 391a). In these cases, DSC showed a single reversible sol−gel transition. TOPM experiments revealed strongly birefringent fibrous aggregates (Figure 391b), and XRD showed a diffraction peak at 39.6 Å corresponding to the intercolumnar distance obtained from bulk samples. The evidence obtained indicated a retention of columnar structure within the organogel.The TCAQ cores are redox-active, and dendronized TCAQ exhibits electrochromic response in the reductive potential region. Redox experiments on thin films in the Φ_h phase exhibited reversible transition from the neutral species to the dianion with associated color change from yellow to red (Figure 392). Tetrathiafulvalene (TTF) dendronized with (3,4,5)12G1 (Figure 393) was also demonstrated to self-assemble into one-dimensional columns that mediate the formation of a fibrous gel in hexanes, which might serve as a conducting nanowire framework.[1188]

8. Dendronized Dendrimers and Dendrons

Most dendritic topologies consist of the attachment of a dendron to a linear or branched small molecule, oligomer, or polymer (Figures 1 and 2). Alternatively, dendronization of dendrimers and dendrons (Figure 2, row 1 right and row 2), specifically with dendrons that have intrinsic self-assembly capabilities, is a powerful strategy for the manipulation of molecular architectures and for the induction of self-assembly features in a nonself-assembling dendrimer or dendron. This strategy relies on the distortion of the original conformation of the dendron or dendrimer in a similar way as in the case of flexible backbones of side-chain LC S polymers.[1189−1206]

8.1. Dendrimers Dendronized on Their Periphery

Attachment of self-organizing dendrons to the periphery of amorphous or self-assembling dendrimers (Figure 2, row 2 left and second from left) often results in a dendronized dendrimer (aka hybrid dendrimers) with new self-assembly and self-organization capabilities.

8.1.1. Flexible Dendrimers Dendronized on Their Periphery

The synthesis of the first self-assembling dendronized dendrimers was demonstrated by Lattermann, wherein flexible and liquid PEI dendrimers were functionalized at their periphery with (3,4)10G1 Percec-type dendrons (Figure 394).[1207] LC phases were self-organized from dendronized G1 PEI dendrimer and other branched amines by reducing the flexibility of the compound via protonation of tertiary amines (Figure 395). The dendronized G2 PEI dendrimer exhibits a monotropic Φ_h phase, while the N-protonated

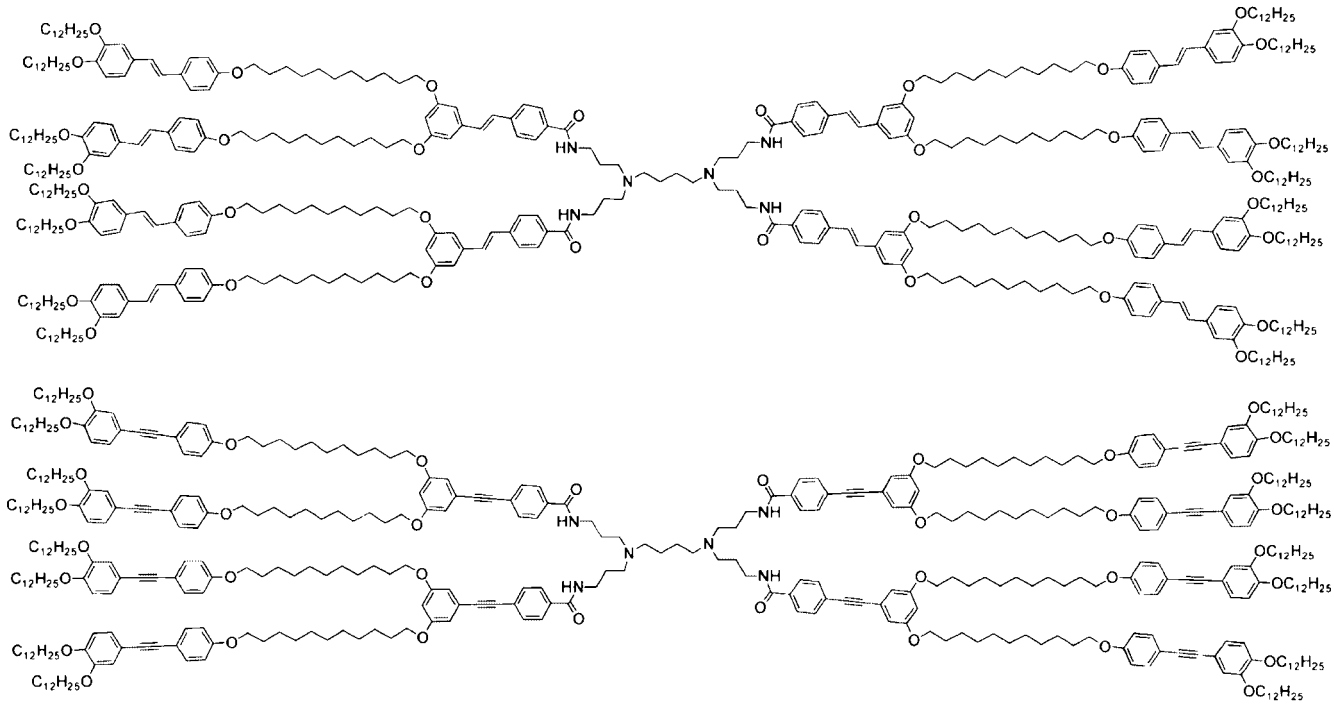

Figure 398. Octopus dendronized dendrimers with alkoxystilbenoid or alkoxytolanoid peripheries.[1212,1213]

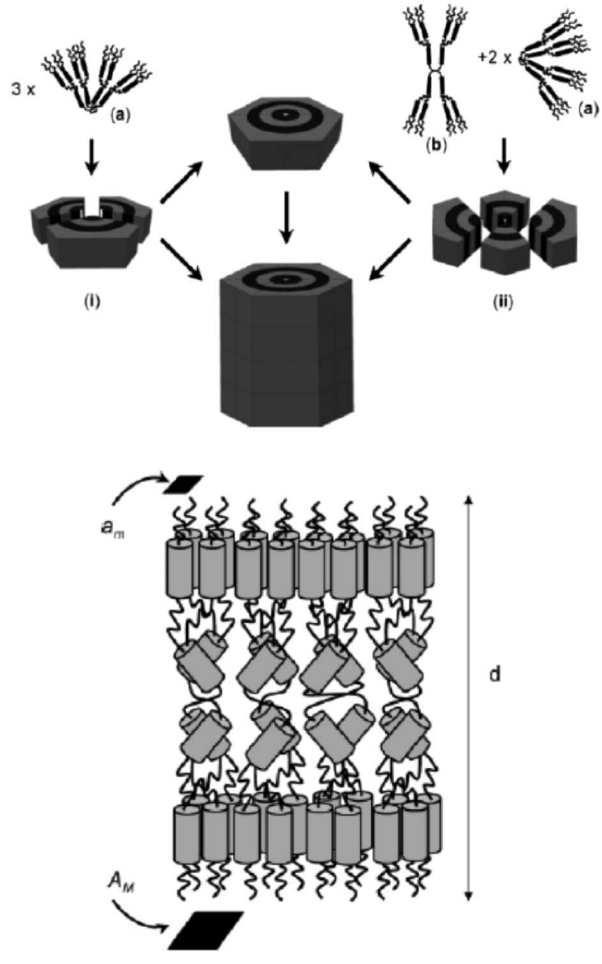

Figure 399. Two possible conformations of the (3,4-3,4) octopus dendronized dendrimers (a) and (b), and their self-assembly and self-organization into supramolecular columns and Φ_h phases (i) and (ii) (left) and self-organization of the (4-3,4) octopus dendronized dendrimers into S phases. Reprinted with permission from ref 1213. Copyright 2004 American Chemical Society.

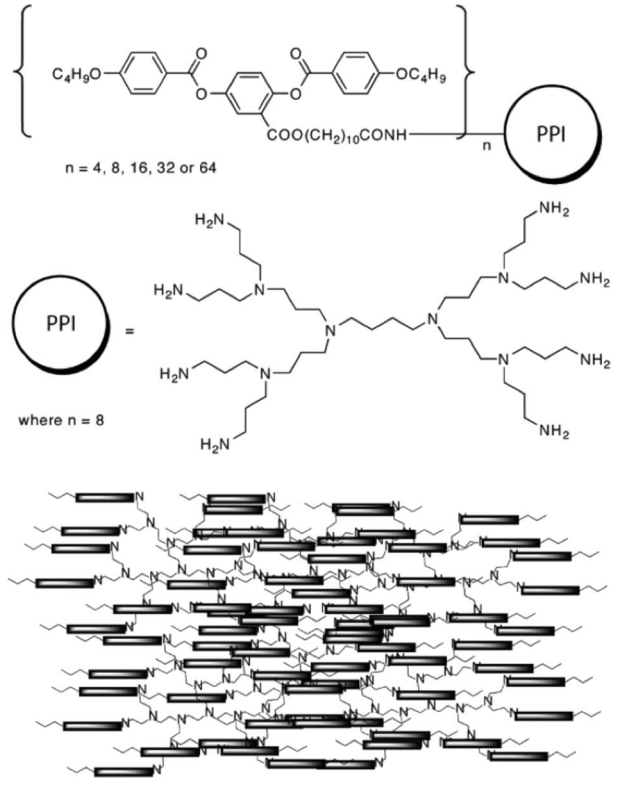

Figure 400. PPI LC dendrimers functionalized with dendrons generated from rodlike mesogenic repeat units (top) and their self-organization into N phases mediated by the rodlike mesogenic dendron units. Reprinted with permission from ref 1214. Copyright 2004 American Chemical Society.

derivative exhibits an enantiotropic S phase. Latterman also reported the formation of octahedral and trigonal bipyramidal complexes of the dendronized PEI dendrimers with Co, Ni, Cu, and Zn salts (Figure 395).[1208] XRD suggested Φ_h organization for most complexes, and thus these complexes were the first metallo-mesogenic dendronized dendrimers.

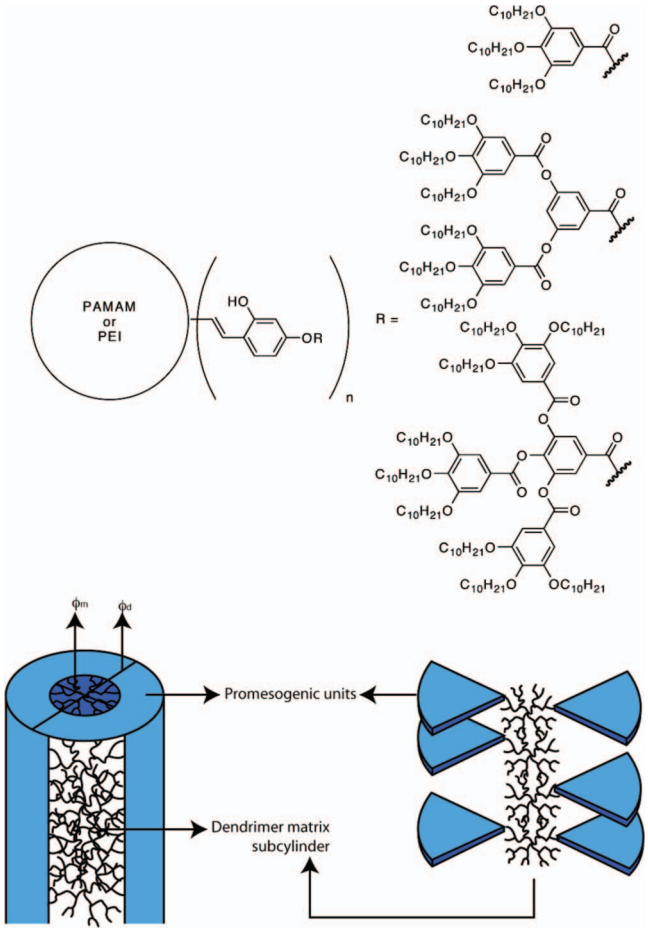

Figure 401. PAMAM and PEI dendronized with G1 and G2 Percec-type dendrons (left) and their self-organization into core−shell columns. Adapted with permission from ref 1219. Copyright 2005 American Chemical Society.

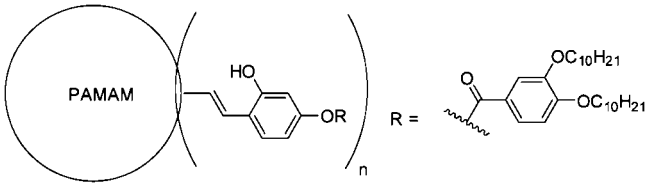

Figure 402. Partial dendronization of PAMAM with (3,4)10G1.[1220,1222]

Lattermann also reported dendronized G1−G5 PPI dendrimers substituted with (3,4)10G1 Percec-type dendrons at their periphery (Figure 396).[1209] Self-organization into a Φ_h phase was observed through the G4 PPI core. Core−shell columnar organization was achieved by stacking of disklike segments consisting of a polar core and a nonpolar shell. In the case of the G5 PPL core, no LC phase was observed. Most likely, a steric dense-packing limit was achieved for the discotic conformation, and thus, the typical PPI spheroid structure dominates.

Meijer modified G1, G3, and G5 PPI dendrimers at their periphery with (3,4,5)12G1 dendronized chiral OPV (Figure 397).[1210] Strong H-bonding but limited $\pi-\pi$ interactions were observed. In a previous report, Meijer proposed that dendrimers functionalized on their periphery with rodlike mesogens self-organize into lamellar structures where the rodlike portions and the dendrimeric core occupy different layers.[1211] XRD analysis of the Percec dendronized chiral OPV dendrimers and comparison to molecular models

Scheme 83. Selective Bifunctionalization of PPI Dendrons with Sulfonyl Halides and Fréchet Dendrons[1223]

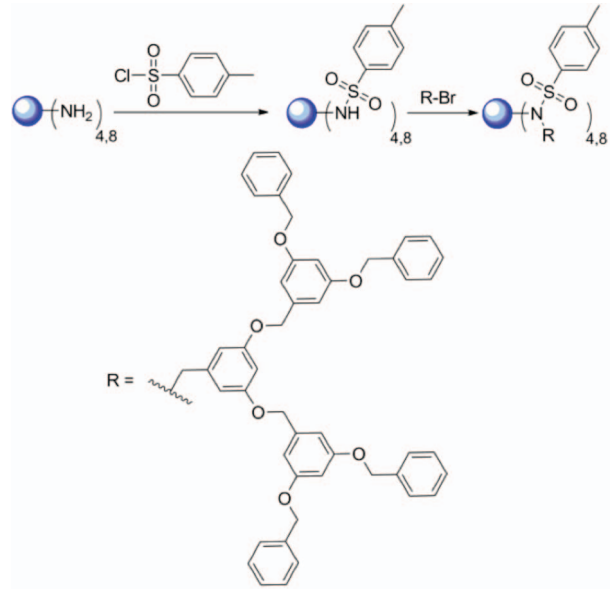

Scheme 84. Synthesis of POPAM Dendronized at the Periphery with PAMAM (Adapted with Permission from Ref 1224; Copyright 2008 American Chemical Society)

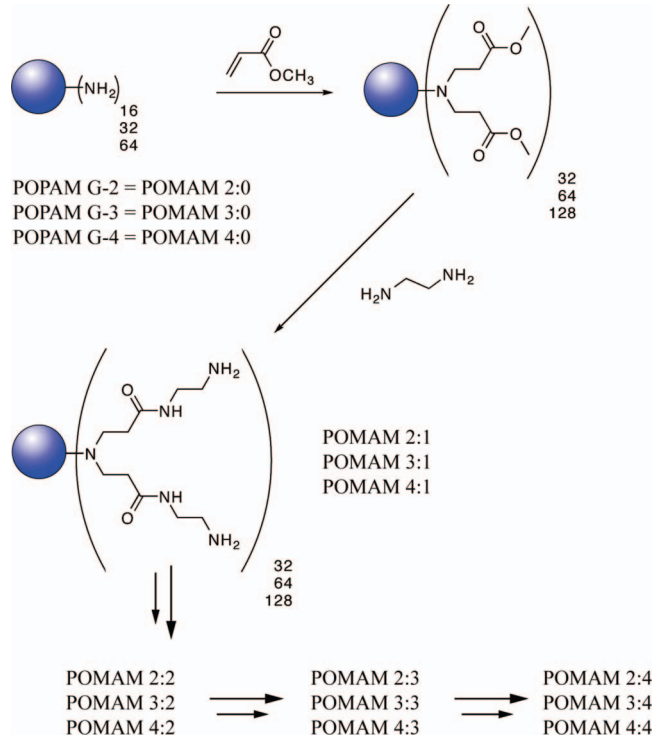

suggested the formation of interdigitated bilayer lamellar structures wherein flexible and conjugated segments were likewise separated.

Guillon reported the attachment of alkoxystilbenoid[1212] and alkoxytolanoid[1213] dendrons to first-generation PPI dendrimers via amidation of the dendritic acids with diphenyl(2,3-dihydro-2-thioxo-3-benzoxazolyl)phosphonate (Scheme 82 and Figure 398). These eight-armed "octopus" dendrimers exhibit either S_A, S_B, or Φ_h phases. In the Φ_h phase, the molecules adopt wedgelike or twinlike conformations (Figure 399) that self-assemble into supramolecular columns with an onionlike architecture due to the alternating aliphatic and aromatic domains. Dendrimers functionalized with stilbenoid

Scheme 85. Synthesis of Bis- and Trisdendronized TREN; Reagents and Conditions (i) THF.[1225]

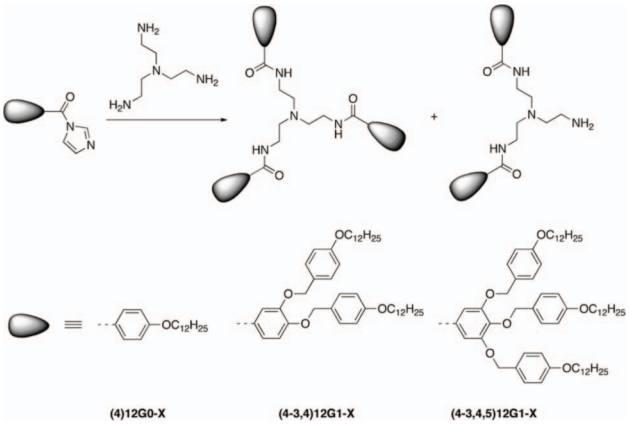

dendrons exclusively form a Φ_h phase. Dendrimers jacketed with tolanoid dendrons, with (3,4-3,4) architecture, also self-organize into onionlike Φ_h phases, while the use of tolanoid dendrons (4-3,4) architecture self-organizes into S_A or S_B phases (Figure 399).

Dendrons generated from rodlike mesogenic groups were attached to the surface of the amine groups of PPI dendrimers via the activation of their carboxylic groups as pentafluorophenyl carboxylates (Figure 400).[1214,1215] Because of the rodlike conformation of the peripheral dendritic units, only an N phase was observed. The synthesis of PPI dendrimers functionalized with a mixture of dendritic and nondendritic rods resulted in thermoreversible conversion between S and N phases.[1216] As will be described in section 11.2, Serrano also reported the noncovalent modification of PPI dendrimers via hydrogen bonding with (3,4)10G1COOH and (3,4,5)10G1COOH.[1217]

Covalent functionalization of the amine groups of PEI and PAMAM dendrimers with (3,4,5)10G1, (3,4,5-3,5)10G2, and $(3,4,5)^2$10G2 Percec-types dendrons was also accomplished via imine formation (Figure 401).[1218,1219] In all cases, even with G5 dendrimer cores, Φ_h self-organization was enforced by a shell of Percec-type dendrons that distort the conformation of the flexible dendrimer into a supramolecular cylinder.

(3,4)10G1 were attached to G1−G5 PAMAM dendrons (Figure 402).[1220,1221] In contrast to PAMAM peripherally functionalized with rodlike mesogens, PAMAM dendronized with even (3,4)10G1 dendrons, self-organizes into Φ_h rather than S phases. Increased branching induces a steric restriction on self-organization into S phases. Serrano also reported G4 PAMAM with 32 surface amine groups with varying degrees of dendronization with (3,4)10G1 (Figure 402) by grafting (3,4)12G1 in various proportions onto a G3 PAMAM dendrimer.[1222] At low surface coverage with 2−12 Percec-type dendrons, S_A and S_C phases were exclusively observed. With intermediate coverage, a mixture of S_A and Φ_r phases are observed. With high coverage, 28−32 Percec-type dendrons, Φ_r and Φ_h organization are found.

Selective bifunctionalization of terminal amine groups of PPI dendrimers with various sulfonyl chlorides and Fréchet dendritic bromides was reported by Vögtle, although self-organization was not reported (Scheme 83).[1223]

Likewise, Majoros reported a series of PPI dendrimers with a diaminobutane (DAB) core (POPAM) dendronized at the periphery with a PAMAM shell (Scheme 84) to form a hybrid POPAM−PAMAM dendron termed POMAM.[1224] As both PPI and PAMAM dendrimers are amorphous, no self-organization was expected or reported.

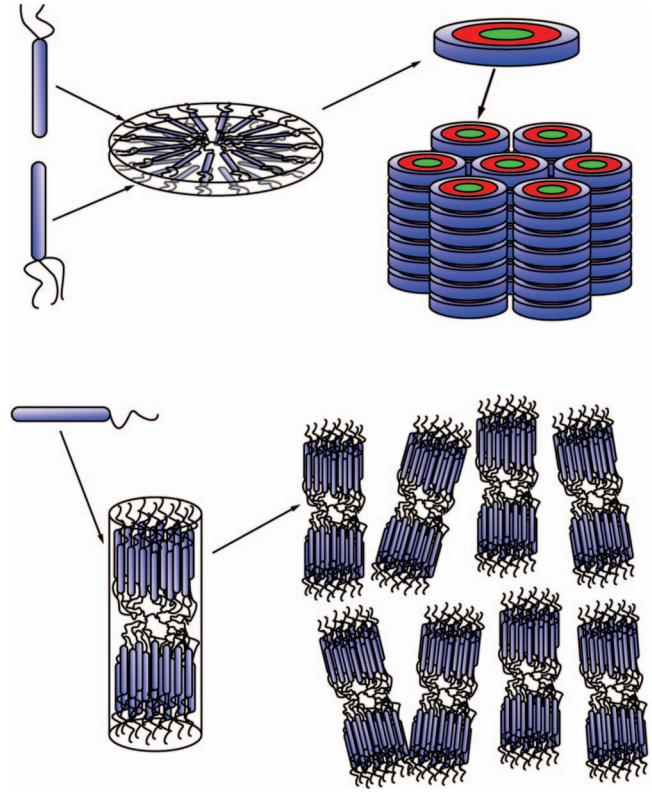

Figure 403. Minimal peripheral branching with promesogenic end-groups (3,4)10G1 and (3,4,5)12G1 induces Φ_h organization (top). Nonbranched end-groups result in S assemblies (bottom). Adapted with permission from ref 1221. Copyright 2001 Royal Society of Chemistry.

Percec reported the bis- and trisfunctionalization of TREN with a library of self-assembling dendrons (Scheme 85). The resulting compounds self-organize into Φ_h, $\Phi_{r\text{-}c}$, and *Cub* lattice. Thermoreversible Φ_h to *Cub* transitions exhibit an epitaxial relationship between the two phases (Figure 404).[1225]

Recently, Percec reported a library of dendronized dendrimers where the amine groups from the periphery of PPI {[DAB-$(NH_2)_n$] (n = 4 and 8)} were covalently functionalized with five different G1 and G2 AB_2 and AB_3 type self-assembling dendritic acids (Figure 405).[1226] Amidative functionalization was mediated by the peptide coupling agent 2-chloro-4,6-dimethoxy-1,3,5-triazine (CDMT)/*N*-methylmorpholine (NMM).

XRD analysis demonstrated that these dendronized dendrimers adopt a crownlike conformation that self-assembles into helical pyramidal supramolecular columns that self-organize into Φ_h and Φ_r 2-D lattices. In most cases, the number of supramolecular dendrimers per cylindrical column stratum was one (μ = 1). Only (4-3,4)12G_1−DAB−$(NHCO)_4$ requires 2 dendronized dendrimers (μ = 2) per column cross section. Both side-by-side and twinlike models for the packing (μ = 2) were proposed (Figure 406).

In this model, two tilted half-disklike dendronized dendrimers form a supramolecular crown. Each layer of the supramolecular crown is rotated 90° to generate a helical pyramidal column (Figure 406a, b, c). Alternatively, the

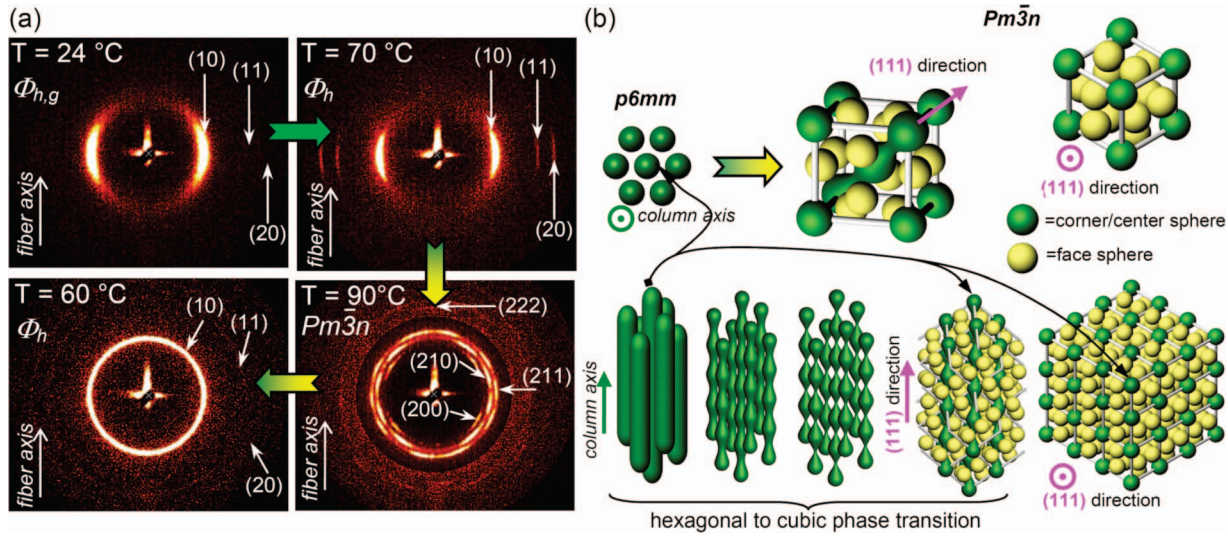

Figure 404. (a) Aligned fiber XRD and (b) models depicting the epitaxial relationship between the Φ_h and *Cub* phase. Reprinted with permission from ref 1225. Copyright 2008 Wiley-VCH Verlag GmbH & Co. KGaA.

dendrimers could adopt a twinlike conformation (Figure 406d). A supramolecular crown is generated by the orthogonal arrangement of a pair of twinlike dendronized dendrimers. The arrangement of the supramolecular crowns in twinlike conformations produces helical pyramidal columns (Figure 406e, f). XRD analysis has not been able to discriminate between these two models. However, comparison of molecular models with XRD have definitively confirmed that a full planar conformation and self-assembly into flat columns is not possible for $\mu = 1$, as well as that crownlike conformations that self-assemble into pyramidal columns with reduced diameter are most reasonable (Figure 407).

In all cases except (4-3,4)12G$_1$−DAB−(NHCO)$_4$, self-organized pyramidal columns underwent a transition to supramolecular spheres that self-organize into *Cub* lattices with *Pm*$\bar{3}$*n* and *P*4$_2$/*mnm* tetragonal symmetry. In the spherical self-assembly of dendronized DAB/PEI, the DAB/PEI dendrimer occupies the apex of sphere fragment such as a cone, a quarter, or one-half of a sphere and the outer shell is occupied by the Percec-type dendrons (Figure 407).

8.1.2. Rigid Dendrimers Dendronized on Their Periphery

Rigid dendritic macromolecules consisting of phenylacetylene repeat units were prepared by Moore.[1227,1228] Moore also reported the dendronization of phenylacetylene dendrimers with 3,5-phenyl carboxylates containing EO tails groups (Figure 408).[1229] These dendronized phenylacetylene dendrimers self-assembled into supramolecular columns that self-organize in a Φ_h lattice.

The synthesis of rigid stilbenoid dendrimers was simultaneously reported from two different laboratories.[1230,1231] Lehmann attached (3,4,5)12G1 Percec-type dendrons to the periphery of various generations of stilbenoid dendrimers (Scheme 86).[1231−1233] These dendronized dendrimers were synthesized by convergent synthesis, wherein *trans*-stilbene linkage of building blocks was achieved through Wittig−Horner reaction in conjunction with protection/deprotection of apex aldehydes. In solution, the stilbenoid dendrimers show a strong tendency to aggregate, which increases with generation number. In bulk state, mostly Φ_h and Φ_{ob} mesophases are formed for G1 and G2 dendrimers. At larger generations, intramolecular steric hindrance does not permit self-assembly into columns and only glasses or oils were found.

Recently, rigid core dendrimers based piperazine and triazine units[1234] were functionalized at their periphery with triazine dendrons bearing aliphatic tails. At G4, these dendronized dendrimers self-organize into Φ_h lattices (Figure 409).[1235]

8.2. Dendrons Dendronized at Their Apex

8.2.1. Dendrons Dendronized at Their Apex with Identical Dendrons: Twin Dendrons

The synthetic capabilities of self-assembling dendrons for the construction of complex supramolecular architectures and their self-organization into diverse lattices were demonstrated by hierarchical self-assembly and coassembly of twin-dendritic benzamides and by their corresponding polymers (see section 2) containing twin-dendritic benzamides as side groups (Figure 410a, b).[297,687] These twin-dendritic benzamides consist of two identical AB$_3$ Percec-type dendrons, (3,4,5)12G1 and (4-3,4,5)12G1, attached by an amide linkage (i.e., one dendron, dendronized at the apex) (Figure 2, row 2 middle) and self-assemble into cylindrical columns. The supramolecular columns are generated by an orthogonal H-bonded stack of dendritic units that self-organize into a Φ_h phase. The same twin-dendritic molecules attached to the polymethacrylate backbones (Figure 410c, d) self-assemble in a three- or four-cylinder bundle supramolecular dendrimer, which self-organizes in a N_c phase (see section 2).

The self-assembly of twin-dendritic benzamides depends on the ability of two successive molecules rotated by 90° to form a disklike shape and on the intermolecular hydrogen bonding between building blocks along the long axis of the supramolecular cylinder (Figure 411).[214]

Percec also reported the synthesis of semifluorinated twin benzamides (Figure 412).[1236] While the perhydrogenated analogues (Figure 411) exhibited a monotropic $\Phi_h \rightarrow \Phi_{r\text{-}c}$ transition that is observed only on cooling, the semifluorinated twin benzamide exhibits exclusively enantiotropic Φ_h organization (Figure 411). Furthermore, the rigidity of the semifluorinated alkyl tails mediates self-assembly into su-

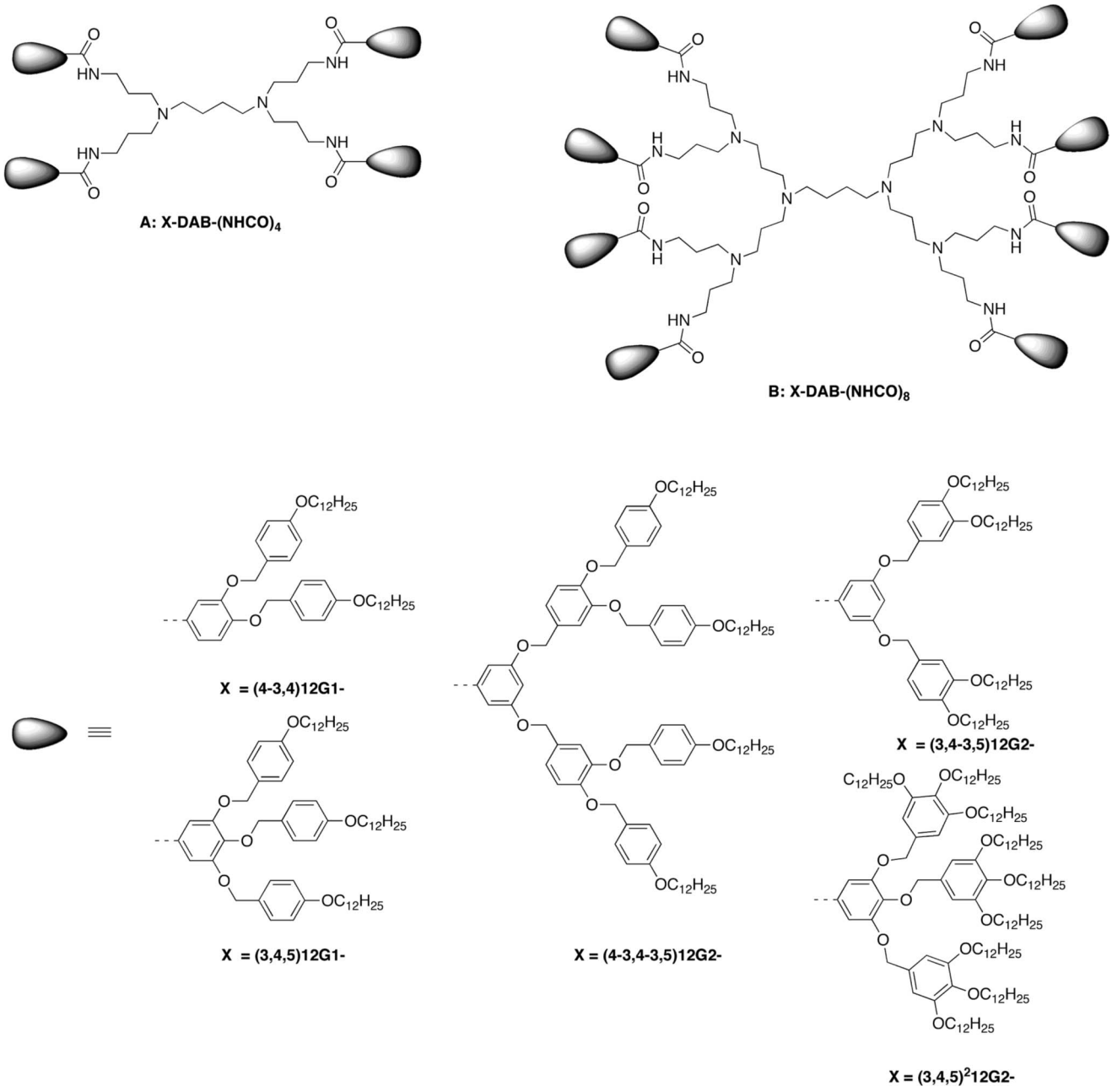

Figure 405. G1 and G2 PPI functionalized with a library of Percec-type dendrons.[1226]

pramolecular columns with $d = 33.5$ Å. These columns are 31% larger than their perhydrogenated analogues.

Recently, the twin-dendritic concept was employed to develop strategies for the design of more complex supramolecular assemblies[51,1225] and self-organizable thixotropic organogelators (Figure 413),[1237] The twin-dendron derived from tris(2-aminoethyl)amine (TREN), on which only two peripheral amines were selectively acylated with (4-3,4,5)12G1, exhibit $\Phi_{r\text{-}c}$, Φ_h, and *Cub* lattices. Close packing at the core of the twin-dendritic supramolecular columns facilitated H-bonds along the length of the column. A network of possible intra- and intermolecular hydrogen bonds were identified at the core of the resulting supramolecular column composed of the first-generation twin dendron (Figure 413).

A library of twin-dendritic organogelators was prepared through selective functionalization of primary amines of *N*-(3-aminopropyl)-1,3-propanediamine (APPDA) with various self-assembling tapered dendritic acids by using 1,1′-carbonyldiimidazole (CDI) as a coupling agent (Scheme 87).[1237] Subsequent modification of the APPDA linker provided an additional degree of structural diversity by which to tailor the self-assembly of the gelator.

These twin dendrons are able to gel various organic solvents. These gels are thixotropic; thus, shear force decreases the viscosity of the material, but upon cessation, the original gel structure returns. While elongated fibrillar supramolecular structures were implicated in gel formation, gels were obtained from compounds that self-assemble into lamellar, columnar, and spherical objects. The twin-dendritic gelators containing (4-3,4)12G1-dendritic units self-organize into a Φ_h lattice with internal order (Figure 414). The internal order is likely due to facile H-bonding, which creates a seam within the columnar structure. Dendrons with 3,4-disubsti-

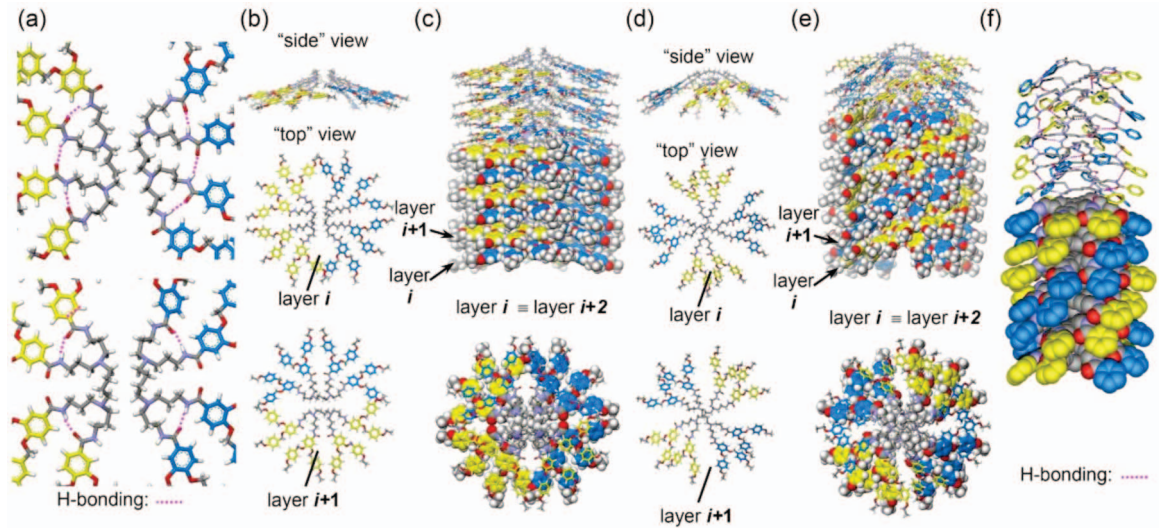

Figure 406. Two possible layer packing models based on the XRD data for the (4−3,4)12G_1-DAB-$(NHCO)_4$ dendrimer. Two dendronized dendrimers per layer in noncrossed configuration (a, b, c) and in crossed configuration (d, e, f). In (a, f) possible intra- or intermolecular H-bonding networks; (b, d) layer packing; (c, e) self-assembled supramolecular columns are shown. Reprinted with permission from ref 1226. Copyright 2009 L. P. P., Ltd.

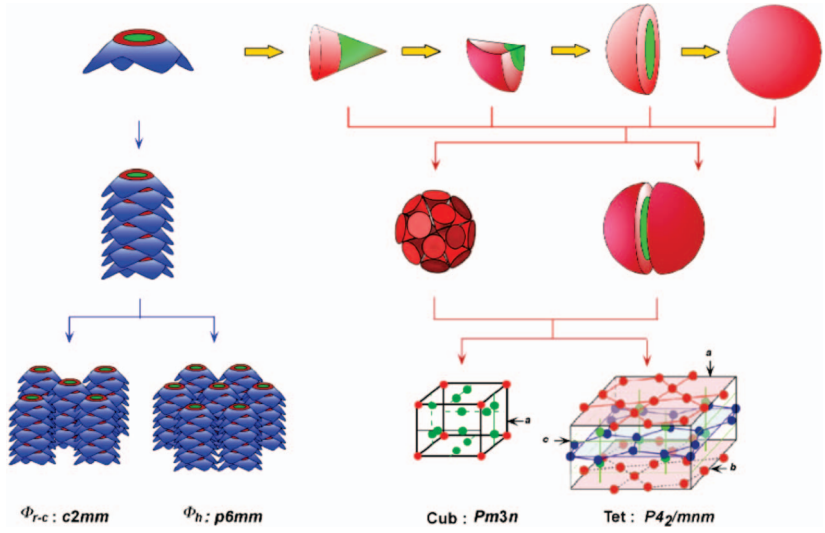

Figure 407. Self-assembly mechanism of dendronized PPI into pyramidal columns and spheres and their self-organization into period 2-D and 3-D lattices. Reprinted with permission from ref 1226. Copyright 2009 L. P. P., Ltd.

tuted branching units at the apex exhibit the greatest propensity to form gels and to impart thixotropic behavior, where the gel recovers its elasticity after being subjected to shear.

8.2.2. Dendrons Dendronized at Their Apex with Dissimilar Dendrons: Janus-Dendrimers

The overall organization of the supramolecular assemblies can be manipulated by the selective attachment at the apex of two totally different functionalities in one dendritic molecule ("Janus" dendrimer) (Figure 2, second row second from right). While the first Janus dendrimers were reported by Hawker and Fréchet[1238] during the synthesis of layered or segmented block codendrimers based on polyester and polyether dendritic fragments, the term Janus dendrimer was coined by Goodby.[65] Later, Fréchet reported the design strategy and synthesis of functional "bow-tie"-shaped hybrid dendrimers (Figure 415).[1239] These Janus-type dendrimers consist of two covalently attached and orthogonally protected polyester dendrons synthesized by a combination of convergent and divergent approaches.

Scheme 86. Synthesis of Stilbenoid Dendrimers[1231−1233]

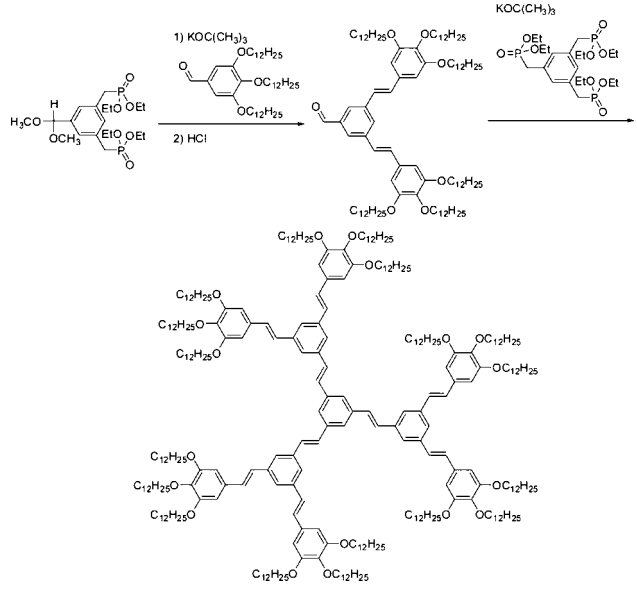

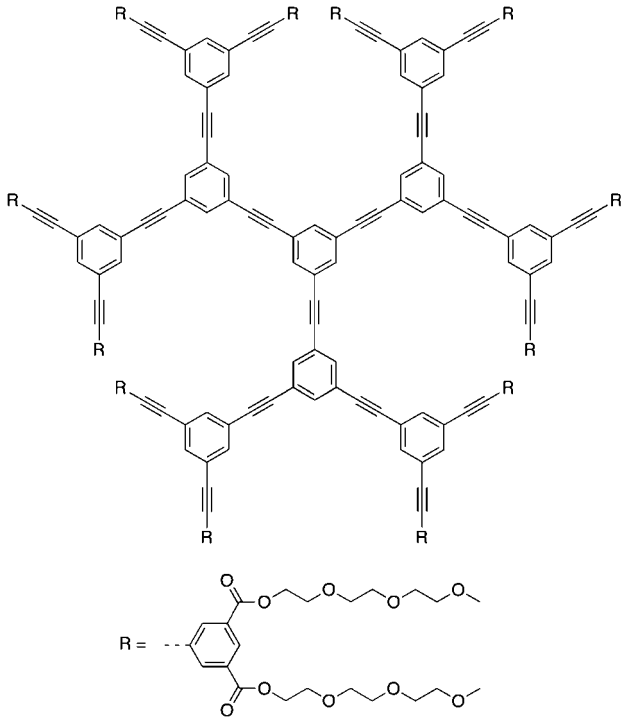

Figure 408. Phenylacetylene dendrimers dendronized with isophthalic acid bis-(2-[2-(2-methoxy−ethoxy)ethoxy]ethyl) esters on periphery.[1229]

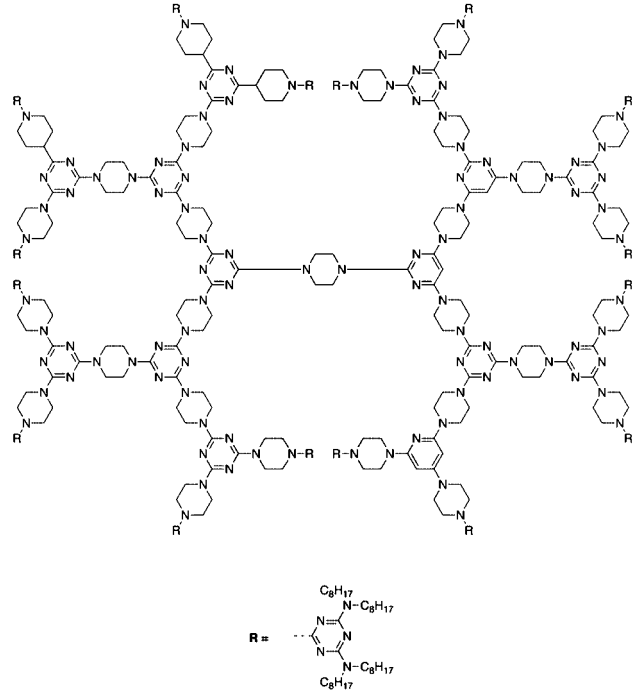

Figure 409. Dendronized piperazine/triazine dendrimers.[1235]

The first supramolecular self-organization behavior of Janus dendrons was demonstrated by Goodby.[1240,1241] Star-shaped hexamers, based on Pentaerythritol or tris(hydroxymethyl)aminomethane central scaffold were grafted with two different subunits to create Janus supramolecules containing two different hemispheres. One of the hemispheres contained three cyanobiphenyl (CB) end-groups, whereas the other lobe contained three chiral phenyl benzoate mesogenic moieties (Figure 416). The geometry of the attachment of the mesogens to the central scaffold and the nature of the connecting groups were explored as tools to create supramolecular systems with different hemispheres. End-on attached mesogens preferred the formation of S phases, whereas side-on appended mesogens favored N phases.

Amphiphilic Janus-dendritic molecules containing nonpolar alkoxy gallate ether and polar aliphatic arborol hemispheres (Figure 417a) were synthesized by a combination of protection−deprotection and divergent−convergent−divergent sequences.[1242] A liquid-phase approach to functionalized Janus dendrimers was also reported.[1243] These amphiphilic Janus dendrimers combine two functionally different surfaces, a nonpolar Fréchet-type dendron and a polar alcohol functionalized Fréchet-type dendron (Figure 417b). The potential application of these Janus dendrimers as a well-defined soluble support for liquid-phase organic synthesis was demonstrated in Pd-catalyzed Suzuki coupling reactions. Amorphous Janus dendrimers consisting of aliphatic polyester wedges with peripheral hydroxyl groups and chiral donor−acceptor azobenzene conjugates attached to Pentaerythritol core were also reported.[1244]

Majoral reported water-soluble fluorescent Janus dendrimers synthesized from hexafunctional cyclotriphosphazene dendrimers functionalized with ammonium groups on one side and dansyl derivatives on the other side (Figure 418).[1245] These dendrimers displayed bright fluorescence with emission maxima wavelength at around 495 nm, which is separated from the absorption area (∼345 nm).

A library of Janus-type amphiphilic dendrimers consisting of hydroxyl-containing poly(methallyl dichloride) (PMDC) and long alkyl-containing poly(urethane amide) (PUA) units were synthesized by Wegner (Figure 419).[1246] These Janus dendrimers were able to self-assemble into ribbonlike aggregates in toluene and produced three-dimensional networks behaving macroscopically as gels. The H-bonds between the hydroxyl groups on the periphery of the PMDC hemisphere generate an interdigitated layer structure. The hydrogen bonds of the PUA hemispheres bring the dimers together to form supramolecules with a ribbon-like structure. Hydrogen bonds in the *trans*-amide and urethane groups mediate a face-to-face arrangement between adjacent fan-shaped PUA blocks and growth of the ribbons along the direction perpendicular to the PUA face (Figure 419).

Guillon reported the synthesis and self-assembly of a library of Janus-type amphiphilic dendrimers derived from two differently functionalized dendrons.[1247,1248] One segment of the dendrimer was based on a hydrophobic (4-3,5)G1, or (3,4,5-3,5)12G2 dendron, and the other side was a hydrophilic benzamide dendron with polyhydroxyl-containing surface moieties (Figure 420). The generation of both dendritic fragments and the number of peripheral chains were modified independently, and their self-organization was examined. Φ_h lattices and *Cub* and BCC lattices were observed. Increasing the generation number of the hydrophobic segment and/or the number of peripheral aliphatic chains leads to an increase of the dendritic−aliphatic interface and selects for *Cub* and BCC over Φ_h phases.

Janus dendrimers were also exploited by Percec to generate more complex supramolecular structures (Figure 411).[1236] Semifluorination of one of the two dendrons of twin-dendritic benzamides (Figure 421) generates Janus dendrimers that change the mode of self-assembly from a single-layer supramolecular column to unprecedented bilayered pyramidal

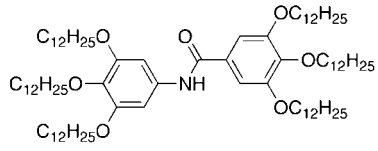

A: (3,4,5)12G1-(3,4,5)12G1-BzA

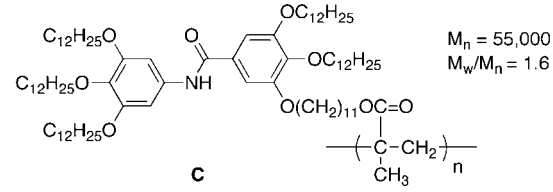

C

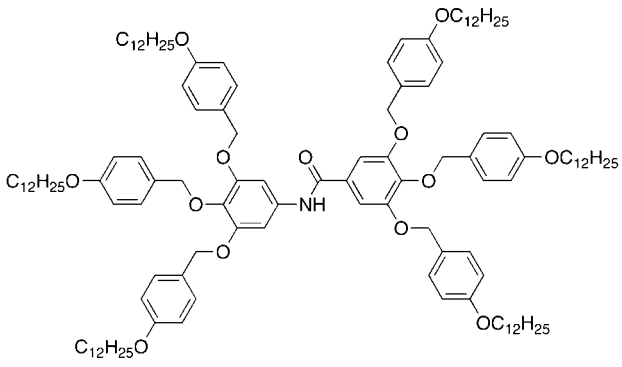

B: (4-3,4,5)12G1-(4-3,4,5)12G1-BzA

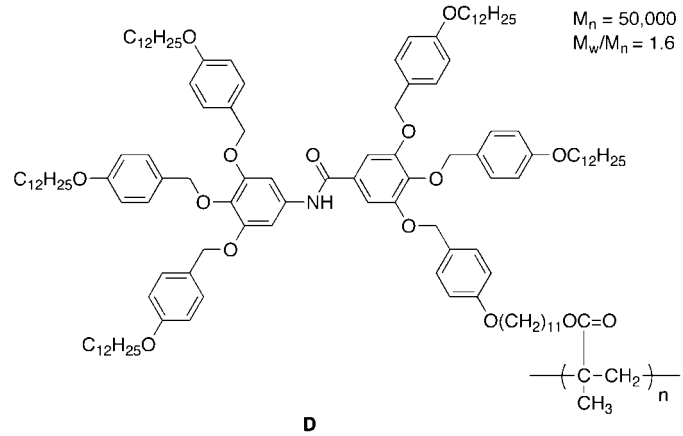

D

Figure 410. Examples of twin-dendritic benzamides and the corresponding dendronized polymers.[297,687]

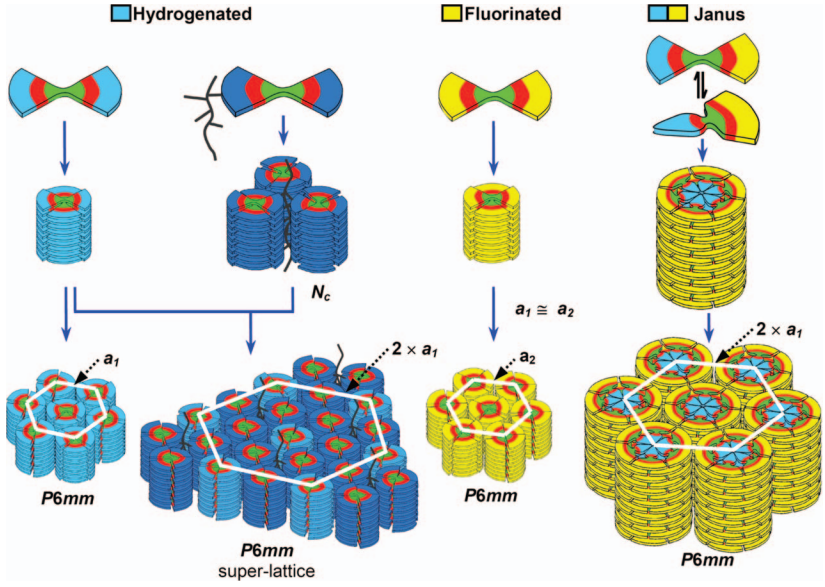

Figure 411. Self-assembly mechanism of twin-dendritic benzamides and Janus-benzamides. Reprinted with permission from ref 214. Copyright 2006 Royal Society.

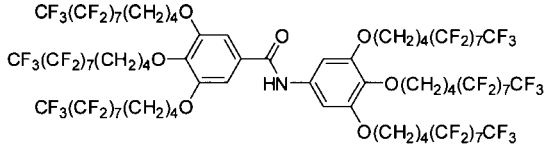

Figure 412. Semifluorinated twin-dendritic benzamide.[1236]

columns (Figure 422). The semifluorinated Janus-dendritic benzamides were synthesized by selectively replacing the aliphatic chains from the periphery of one of the two (3,4,5)12G1 or (4-3,4,5)12G1 dendrons of a twin-dendritic benzamide with semifluorinated chains (Figure 421). These Janus-dendritic benzamides self-assemble into supramolecular columns that self-organize into Φ_h lattices. The columns that are formed have twice the diameter of those of either hydrogenated or semifluorinated twin-dendritic benzamides.

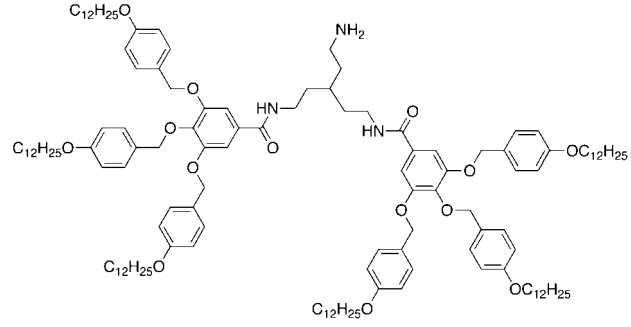

Figure 413. Example of twin dendrons based on self-assembling tapered dendrons.[1237]

The semifluorinated Janus-dendritic benzamides self-assemble into a bilayered disk or crown in which the semifluorinated regions are segregated from the hydrogenated

Scheme 87. Synthesis of Twin-Dendritic Organogelators: (i) 1,1-Carbodiimidazole (CDI), CH_2Cl_2; (ii) *N*-(3-Aminopropyl)-1,3-propanediamine (APPDA), THF; (iii) Succinic Anhydride, NEt_3, THF, 60 °C[1237]

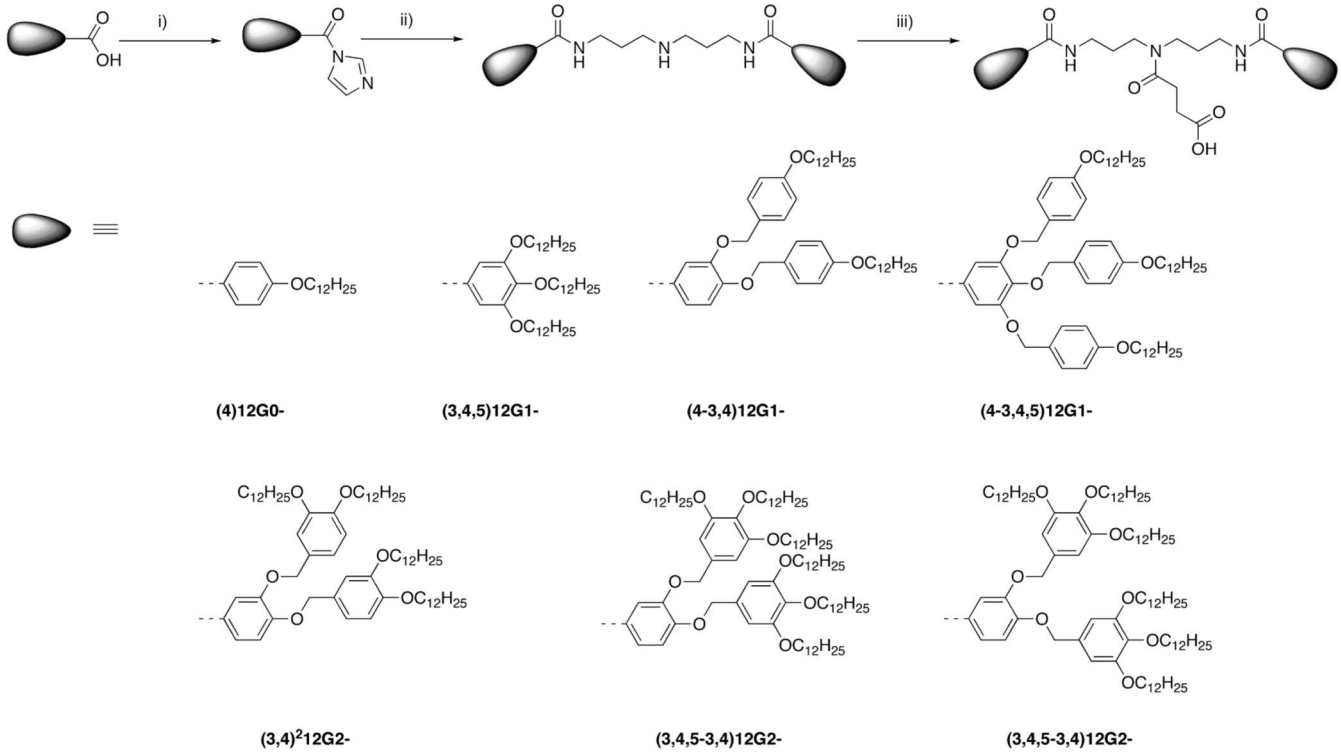

aliphatic regions. The bilayered disks and crowns contain the hydrogenated aliphatic chains in the core and the semifluorinated chains on the periphery, with the aromatic part of the molecules occupying the intermediate region. The disk- or crownlike aggregates generate a nonorthogonal stack of supramolecular helical pyramidal columns with amplified intermolecular hydrogen bonding (Figure 422).

As will be described in a subsequent subsection, Janus-type dendrons, dendrimers, and fullerodendrimers were also reported by Guillion (Figure 448).[1249,1250] These Janus-type fullerodendrons were composed of either (4-3,4,5-3,5)12G2 or (4-3,4,5-$(3,5)^2$)12G3 Percec-type dendrons linked to a poly(aryl ester) dendron functionalized with cyanobiphenyl groups.

9. Dendronized Rotaxanes and Catenanes

Dendronized rotaxanes, pseudorotaxanes, and catenanes (Figure 2, third row, left to middle) are intrinsically connected

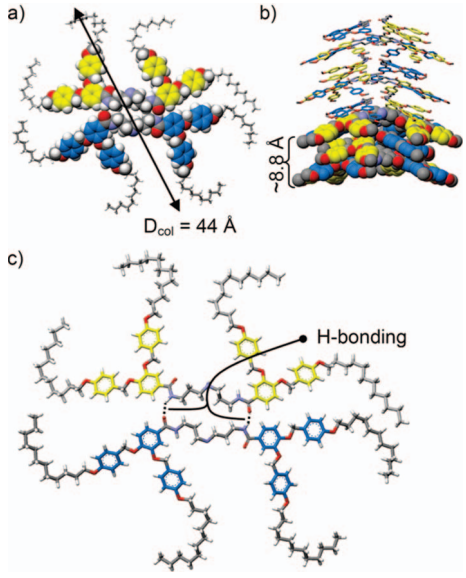

Figure 414. Top (a, b) and side (c) views of the molecular model constructed for twin-dendritic gelators self-assembled from (4-3,4)12G1-dendron. Reprinted with permission from ref 1237. Copyright 2008 Wiley-VCH Verlag GmbH & Co. KGaA.

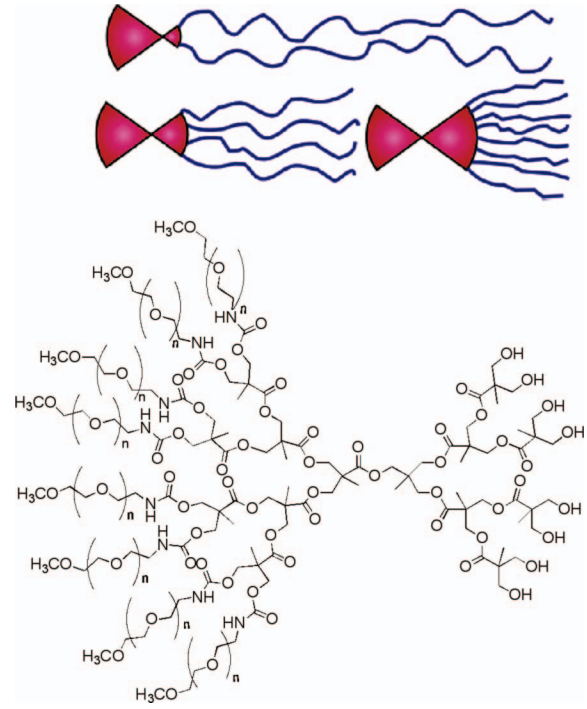

Figure 415. Schematic representation of different possible Janus-like bow-tie architecture (top) and example of Janus-type polyester−poly(ethylene oxide) bow-tie dendrimer. Reprinted with permission from ref 1239. Copyright 2002 American Chemical Society.

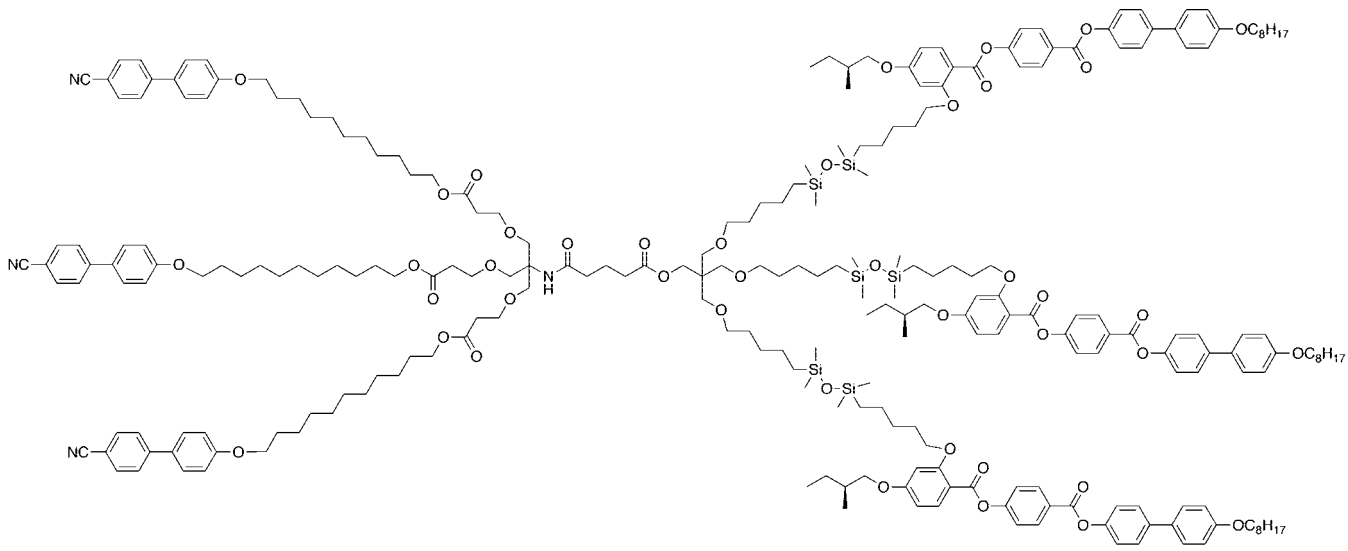

Figure 416. First LC Janus dendrimer.[1240]

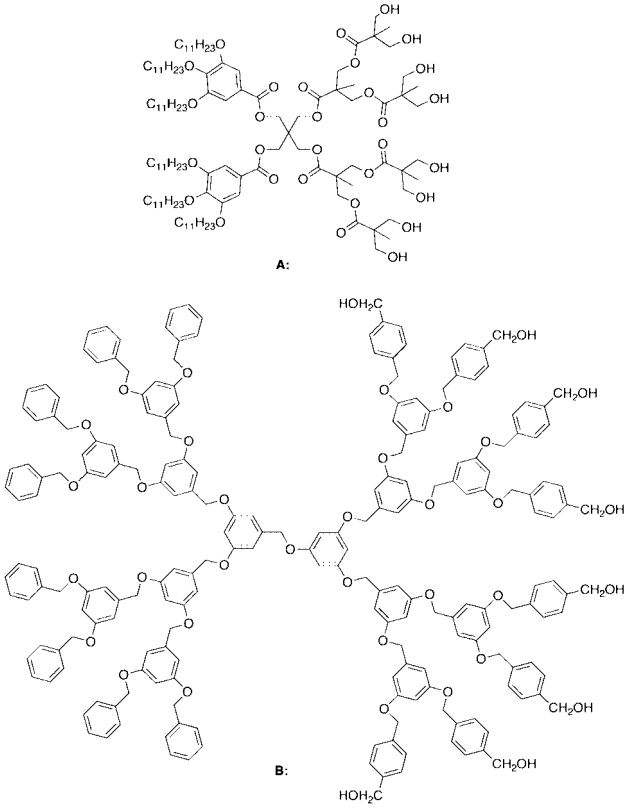

Figure 417. Amphiphilic Janus dendrimers.[1242]

to the previous topological classes. Dendronized catenanes are constructed of linked dendronized macrocycles, while dendronized rotaxanes and pseudorotaxanes are the supramolecular fusion of dendronized macrocycles and dendronized rods (DR)s. Most studies of dendronized rotaxanes, pseudorotaxanes, and catenanes focus on solution-phase self-assembly rather than bulk self-organization. The dynamic motion of these self-assembled systems make them promising targets for the construction of molecular machines.

9.1. Synthesis of Dendronized Rotaxanes

Numerous reports and extensive reviews[111,112] are available on the synthesis and self-assembly of rotaxanes and catenanes. In some studies, dendrons have been attached to either the wheel or axle of rotaxanes. The synthesis of dendronized rotaxanes may be divided into five methodologies: (i) threading and stoppering, (ii) stopper exchange, (iii) template-directed synthesis, (iv) dynamic-template-directed synthesis, and (v) slippage (Figure 423).

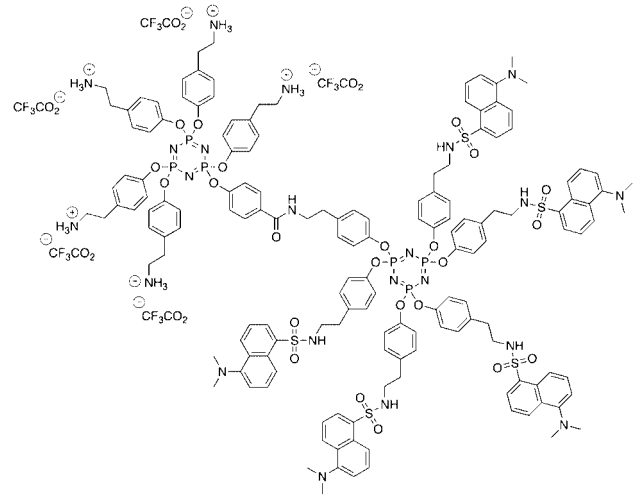

Figure 418. Water-soluble fluorescent Janus dendrimers.[1245]

9.1.1. Threading and Stoppering Approach

Stoddart reported the first dendronized rotaxanes synthesized via a threading and stoppering approach. By combining an aryl corand wheel and viologen axle, a pseudorotaxane was formed. Subsequent addition of dendritic stoppers resulted in a dumbbell-stoppered [2]rotaxane (Figure 424).[1251]

Stoddart also prepared a series of dendron-stoppered [2]rotaxanes, [3]rotaxanes, and [4]rotaxanes containing 1, 2, and 3 viologen units in the axle (Figure 425).

Dendronization has a pronounced effect on the properties of rotaxanes. Stoddart reported enhanced solubility of charged rotaxanes in organic solvents despite the hard nature of the bromide counterion. Enhanced solubility enabled the first study of solvent dependence on the shuttling of the macrocycle along the axle, demonstrating increased shuttling rate with increasing solvent polarity. Molecular dynamics experiments indicated that conformational changes induced by increased solvent polarity were responsible for the change in shuttling rate.[1251]

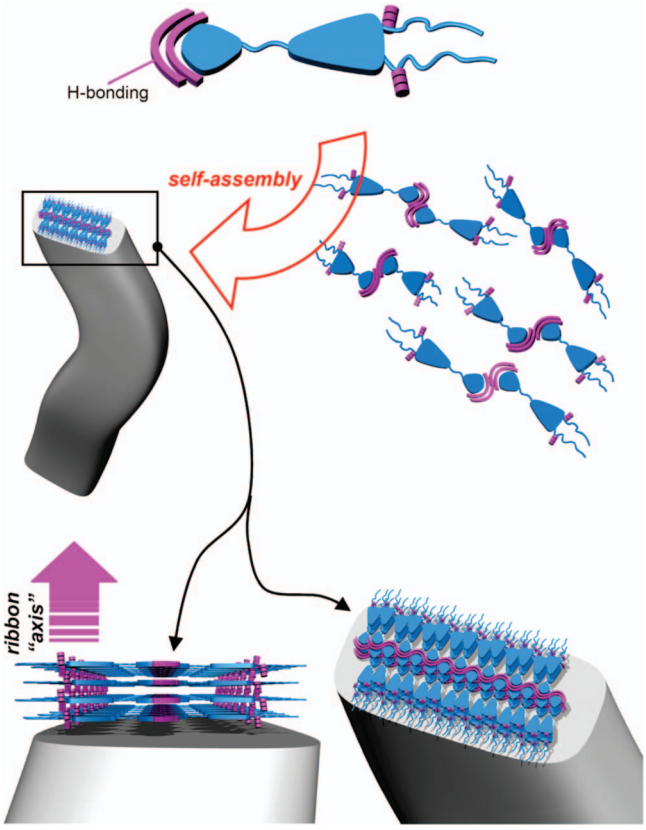

Figure 419. Structures (top) and proposed model (bottom) for ribbon formation of the Janus-type amphiphilic dendrimers.[1246]

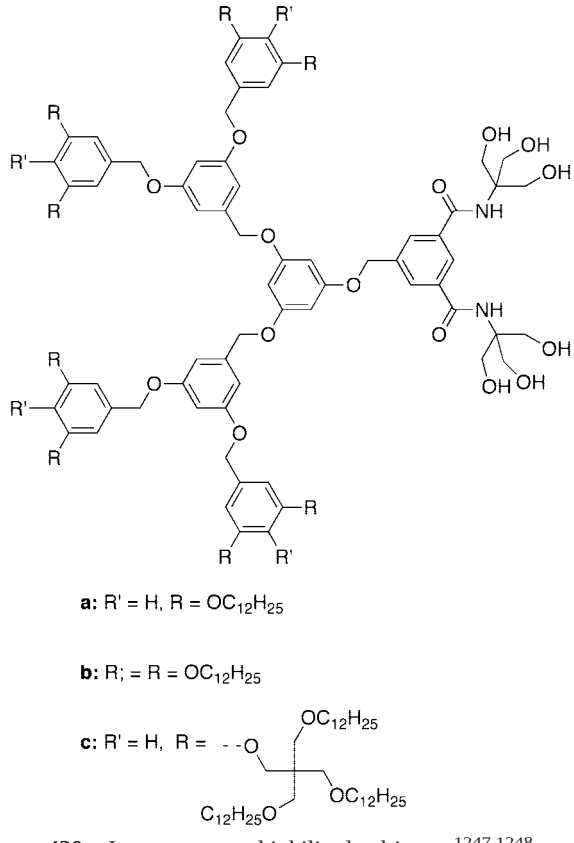

Figure 420. Janus-type amphiphilic dendrimers.[1247,1248]

9.1.2. Template-Directed Synthesis

Stoddart further expanded the concept of dendron-stoppered rotaxanes by the synthesis of an amphiphilic bistable

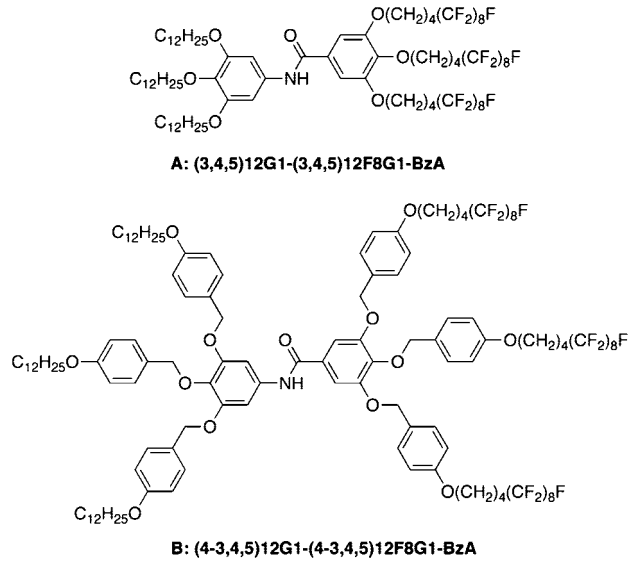

Figure 421. Examples of semifluorinated Janus-dendritic benzamides.[1236]

[2]rotaxane via template-directed synthesis. Here, the Fréchet-type dendron stoppers were replaced with an ethylene oxide-functionalized Percec-type dendron as the hydrophilic terminus and a triarylmethane as the hydrophobic terminus (Scheme 88).[1252] This structural modification coupled with the incorporation of both tetrathiafulvene (TTF) and 1,5-dioxynaphthalene (DNP) provides two binding sites for the cyclobis(paraquat-*p*-phenylene) wheel. The [2]rotaxanes were synthesized by first stoppering of the axle and second complexation of the open wheel to the TTF on the axle template. Template-directed covalent closure of the wheel with α,α′-dibromoxylene provided the intact [2]rotaxane. Cyclobis(paraquat-*p*-phenylene) complexation to TTF forms a green-colored complex, while the complex with DNP is red (Scheme 88).[1252]

The two isomers exist in a 1:1 equilibrium, giving a brown-colored material. The red complex was isolated by preparative thin-layer chromatography (TLC), and its isomerization to the equilibrium state was investigated by NMR. First-order kinetics were applied, and a rate constant of 2×10^{-5} s^{-1} for the isomerization was determined. Heating a 1:1 mixture to 425 K in d_6-dimethyl sulfoxide (d_6-DMSO) resulted in a shift in equilibrium in favor of the green complex in 1:9 ratio. The solution was quenched to 275 K, and the isomerization from green to red was investigated at 300 K. A first-order rate constant of 3×10^{-4} s^{-1} ($\Delta G^{\ddagger} \approx$ 22 kcal mol^{-1}) was determined for the slippage over the −SMe group of TTF.[1252] The electrochemical properties of dendron-capped [2]pseudorotaxanes with the same viologen-containing wheel were also investigated.[1253] Reversible switching of the system from the green- to the red-isomer could be achieved via oxidation of the TTF group to TTF^{+} or TTF^{2+}, thereby electrostatically destabilizing its interaction with the cationic viologen. This electrochemical switching of dendronized [2]rotaxanes has been exploited as a molecular electronics component of dynamic random access memory (DRAM).[1254] In this complex electrononic system, the hydrophilic Percec-type dendritic end-cap is used to electrochemically anchor the electrochemically switchable [2]rotaxane to the bottom Si nanowires of a nanowire-crossbar memory circuit. 0 or 1 bits (i.e., green or red) could be encoded and read using SEM.

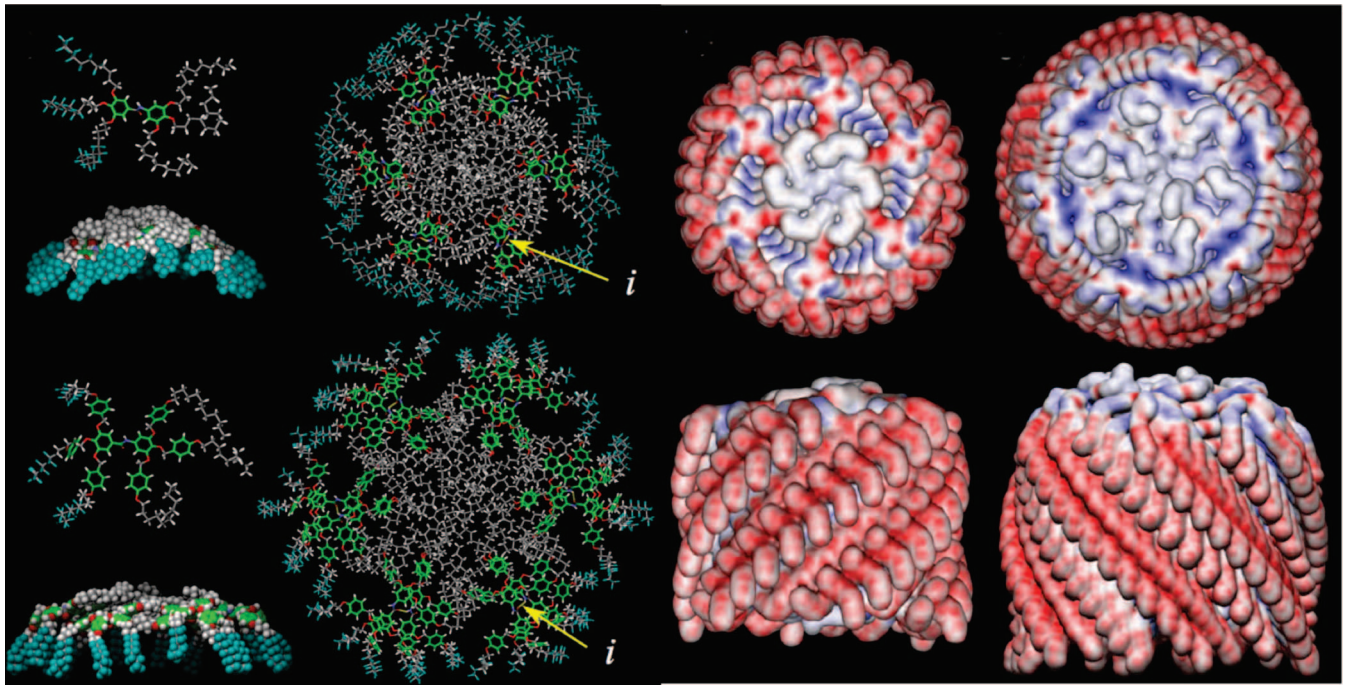

Figure 422. Molecular models of the bilayered supramolecular assembly of semifluorinated Janus-dendritic benzamide crowns. Reprinted with permission from ref 1236. Copyright 2005 Wiley-VCH Verlag GmbH & Co. KGaA.

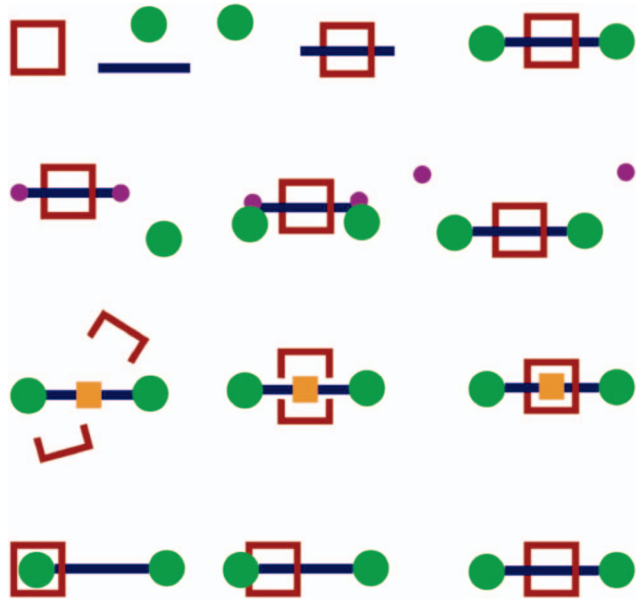

Figure 423. Schematic of rotaxane synthesis methodologies: (a) threading and stoppering, (b) stopper exchange, (c) template-/dynamic-template-directed synthesis, and (d) slippage.

A more comprehensive study of bistable amphiphilic [2]rotaxanes was also reported by Stoddart along with their [2]pseudorotaxane analogues.[1255] LC bistable [2]rotaxanes were synthesized by Stoddart and Kato via a thread-and-stopper approach using AB_3 dendron-containing mesogenic groups. This dendron was attached to the axle via click chemistry (Scheme 89).[1256]

Self-assembly of the LC dendronized [2]rotaxane was investigated by TOPM, DSC, and XRD. The [2]rotaxane self-organizes into an S_A phase as shown by XRD (Figure 426). Stoddart demonstrated the electrochemical switching of the wheel position between the TTF and naphthyl binding sites on the axle via reversible oxidation of TTF to its dication.[1256]

9.1.3. Dynamic-Template-Directed Synthesis

Stoddart reported a template-directed dynamic synthesis of mechanically interlocked dendrimers. Similar to the template-directed synthesis, the open wheel is templated to the preformed stoppered axle, but in this case, the closed wheel exists in a dynamic equilibrium with the open wheel. Once the equilibrium is achieved, the stopper may be chemically fixed. Stoddart mixed dendritic dialdehydes with 3 mol equiv of diamine and 1 mol equiv of dibenzylammonium salt in CD_3CN or CD_3NO_2 at room temperature (Scheme 90). Once equilibrium was reached, the kinetically labile dendrimers were fixed in place via reduction (Figure 427). This method afforded mechanically linked dendronized [2]rotaxane in excellent yield (90%).[1257] This methodology was later employed by Stoddart in the synthesis of combinatorial libraries of G0−G3 Fréchet-type dendrons.[1258]

9.1.4. Stopper-Exchange Synthesis

Stoddart prepared dendrimers with rotaxane-like mechanical branching via a stopper-exchange methodology (Scheme 91). Branched dibenzylammonium ions were threaded through cross-linked dibenzo[24]crown-8 and stoppered by conversion to bulky benzylic phosphonium ions. The benzylic phosphonium ions were later exchanged to Fréchet-type dendrons via Wittig olefination and subsequent hydrogenation.[1252] This methodology allowed the cross-linked [2]rotaxanes to be easily functionalized, without the formation of unthreaded products.[1259] Stoddart used the threading of dibenzylammonium ions through dibenzo[24]crown-8 to design the self-assembly of dendronized polymers with reversible control of the polymer architecture (see section 3.2.11).[672]

9.1.5. Slippage Synthesis

Slippage exploits the kinetic stability of the rotaxane complex. At high temperatures, the wheel can slip over an

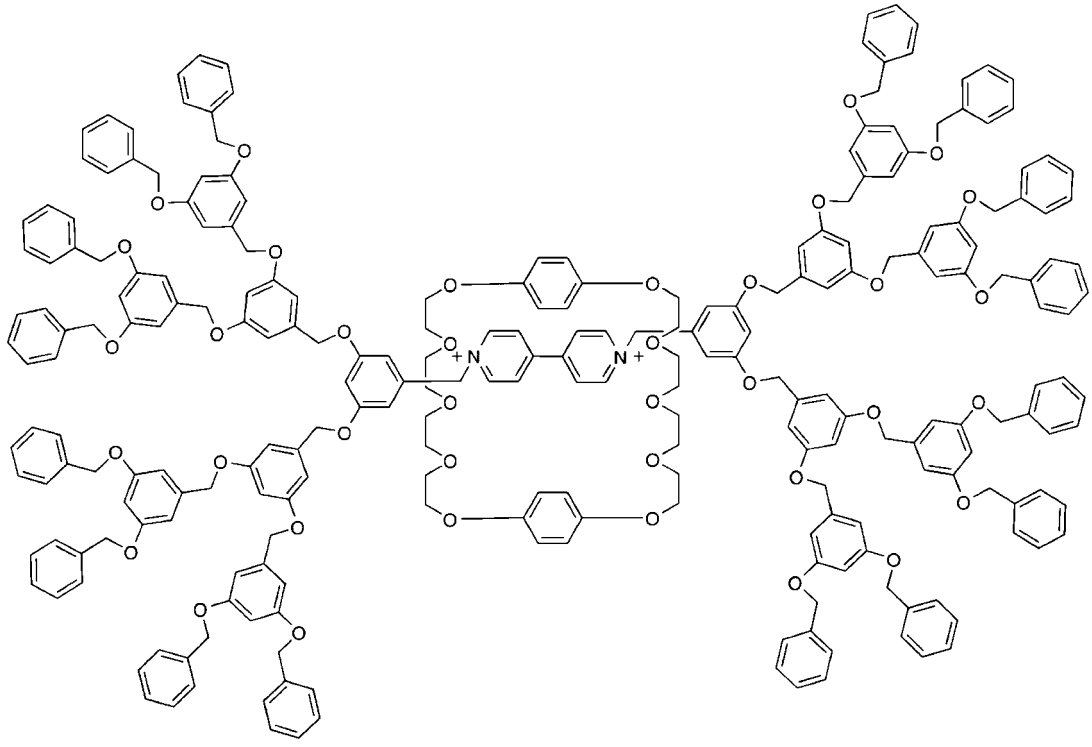

Figure 424. Dumbbell-stoppered rotaxane synthesized by Stoddart.[1251]

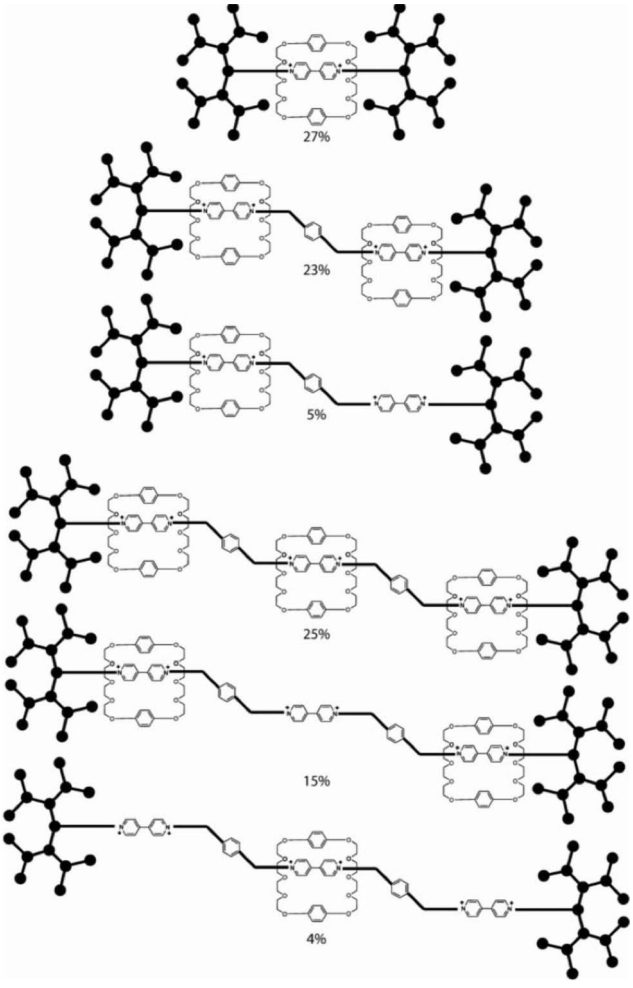

Figure 425. Dendronized rotaxanes. Reprinted with permission from ref 1251. Copyright 1996 American Chemical Society.

appropriately sized stopper on the axle terminus, and on cooling, it may become kinetically trapped as a rotaxane (Scheme 92). Stoddart used the slippage methodology to prepare triply branched dendronized [2]rotaxanes.[1260] A rod possessing a dialkylammonium ion of the form $RCH_2NH_2CH_2R'^+$ (where R = cyclohexane and R′ is a G2 Fréchet dendron) with a PF_6 counterion is locked inside the dendronized dibenzo[24]-crown-8 via cooling a warm solution in CH_2Cl_2. This process may be reversed by dissolving in CD_3SOCD_3 for 18 h.

9.1.6. Efficient Single-Pot Synthesis of Dendronized Rotaxanes

Cyclobis(paraquat-*p*-phenylene) ($CBPQT^{4+}$) is sensitive to most bases, nucleophiles, and reducing agents, and therefore, in order to design efficient high-yield routes to complex rotaxane materials containing this unit, a facile and mild methodology was required. Stoddart developed a stepwise protection−deprotection methodology to synthesize asymmetrical rotaxanes via a sequential Cu^I-catalyzed azide−alkyne cycloaddition (CuAAC) in a single-pot multistage reaction.[1261] He demonstrated excellent chemoselectivity between 3-trimethylsilyl-2-propynol and 1-octyne when treated with $CuSO_4$/ascorbic acid in the presence of 1-azidohexane (Scheme 93).[1261]

Stoddart also demonstrated the mild and quantitative deprotection of trimethylsilyl (TMS)-protected alkynes with 10 mol % aqueous $AgPF_6$ in 18 h at 40 °C. In the presence of $CBPQT^{4+}$, desilylation was slower; however, no decomposition of $CBPQT^{4+}$ was detected. Combination of the $CuSO_4$/ascorbic acid with $CBPQT^{4+}$ and $AgPF_6$ resulted in the reduction of $AgPF_6$ by Cu(I) (observed as a silver mirror) in conjunction with a reduction of $CBPQT^{4+}$ by ascorbic acid. This was circumvented by substitution of the Cu(I) catalytic system with Cu(0) nanopowder and $AgPF_6$ with

Scheme 88. Template-Directed Synthesis of Dendronized [2]Rotaxanes and the Structure of Red and Green Conformational Isomers[1252]

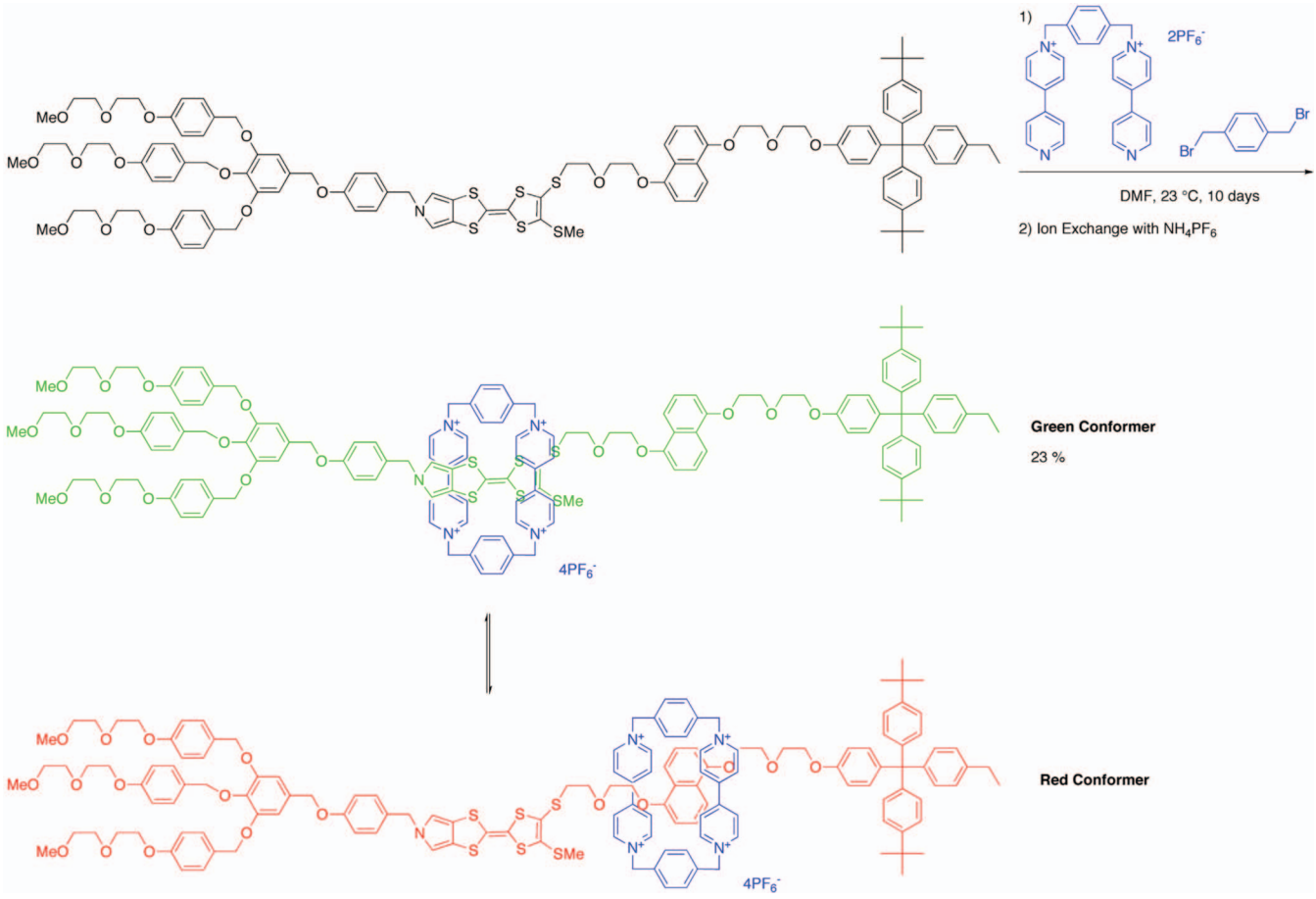

Scheme 89. LC Bistable Rotaxanes Synthesized by Stoddart[1256]

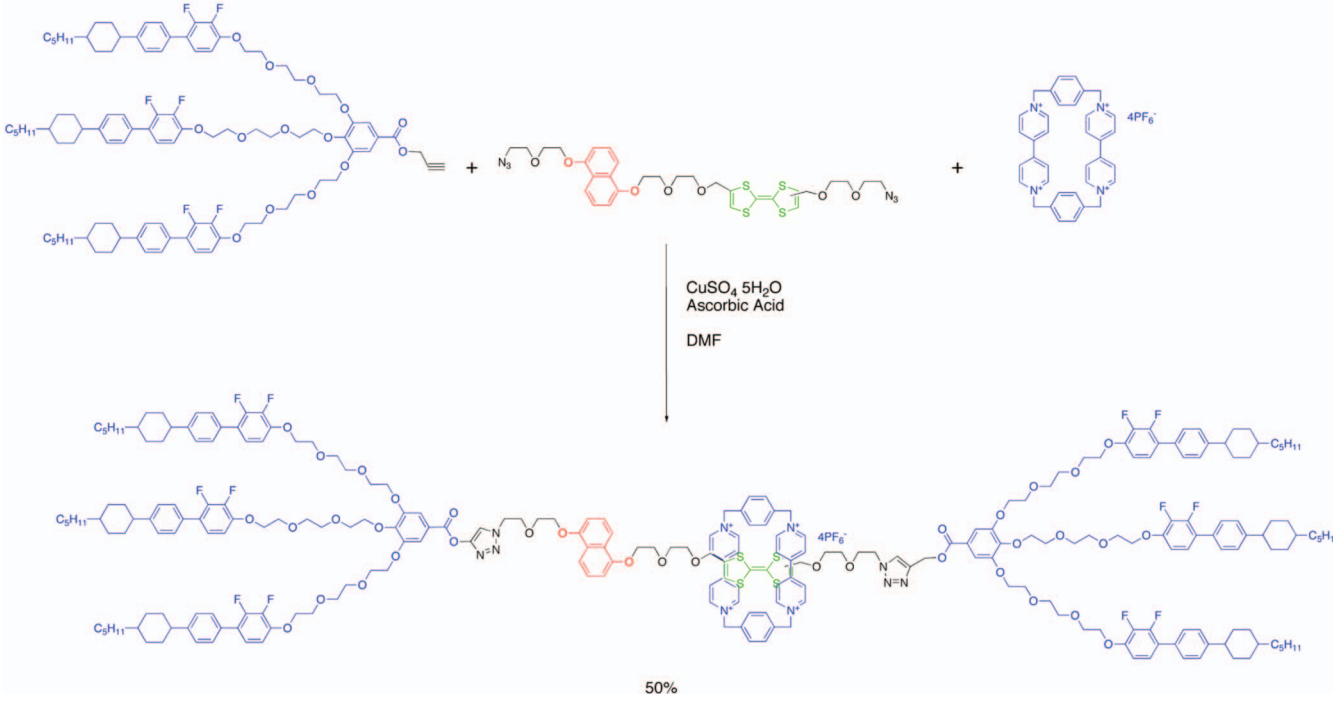

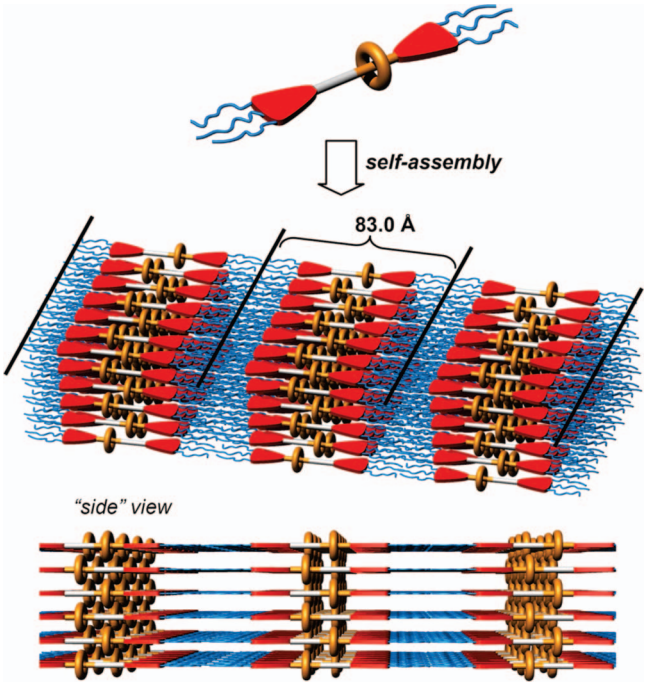

Figure 426. S_A phase for LC dendronized [2]rotaxanes from Scheme 89. Adapted from ref 1256.

$[Cu(MeCN)_4]PF_6$. Stoddart also demonstrated the use of this methodology to synthesize the three-armed dendronized [2]rotaxanes (Scheme 94).[1261]

9.2. Effect of Dendronization on the Self-Assembly of Rotaxanes

Dendronization has a profound effect on the self-assembly of rotaxane-based materials, as well as on the threading and dethreading mechanisms of rotaxanes and pseudorotaxanes. Gibson reported spontaneous self-assembly of triply branched [2]pseudorotaxanes in which dibenzo[24]crown-8 was dendronized with Fréchet-type dendrons.[1262] Self-assembly was driven by the molecular recognition of a three-armed star-shaped core containing dibenzylammonium salts with dibenzo[24]-crown-8 (Figures 428 and 429).

Evidence for the formation of a 1:3 complex was provided by ^1H NMR spectrometry.[1262] The rate of formation of the [2]pseudorotaxane was in the order of hours. When equilibrium conditions were achieved, the integration of the appropriate signals indicated a 1:3 complex (Figure 430).[1262]

MALDI-TOF experiments show mass peaks corresponding to the 1:1, 1:2, and 1:3 complexes. In each case, the PF_6 counterion was lost and additional peaks representing loss of benzyl groups from the periphery were observed.[1262] Later, Gibson et al. presented the synthesis of similar pseudorotaxanes for the formation of noncovalent polymers and poly(pseudorotaxane)s. The self-assembly was based on the same principle of the recognition of secondary dibenzylammonium cations by dibenzo[24]-crown-8.[1263]

Similar systems with wheels functionalized with Percec-type dendrons self-assemble to form 1:1, 1:2, and 1:3 pseudorotaxane complexes with a homotritopic axle (Figure 431).[1264] Association constants were measured for each stoichiometry and with dendrons of different generation number. It was found that the three ammonium sites act independently and that the association constant increases with

Scheme 90. Dynamic Templating of Mechanically Interlocked Dendrimers (Reprinted with Permission from Ref 1257; Copyright 2005 American Chemical Society)

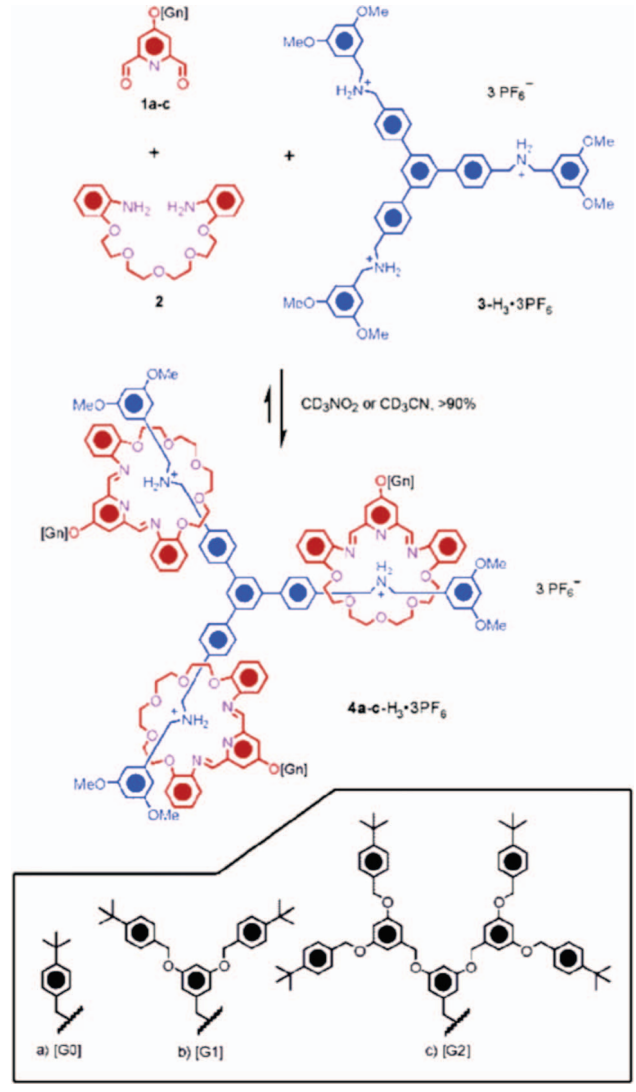

generation number. The increase in association constant was attributed to the increased encapsulation of the ionic core, screening the charges from the nonpolar bulk solvent.[1264]

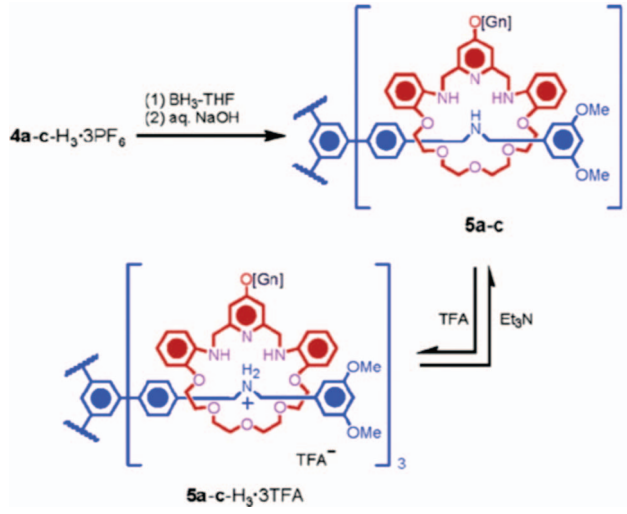

Figure 427. Fixing of mechanically linked dendrimers by reduction and protonation. Reprinted with permission from ref 1257. Copyright 2005 American Chemical Society.

Scheme 91. Synthesis of Dendrimers with Rotaxane-Like Mechanical Branching (Reprinted with Permission from Ref 1259; Copyright 2002 American Chemical Society)

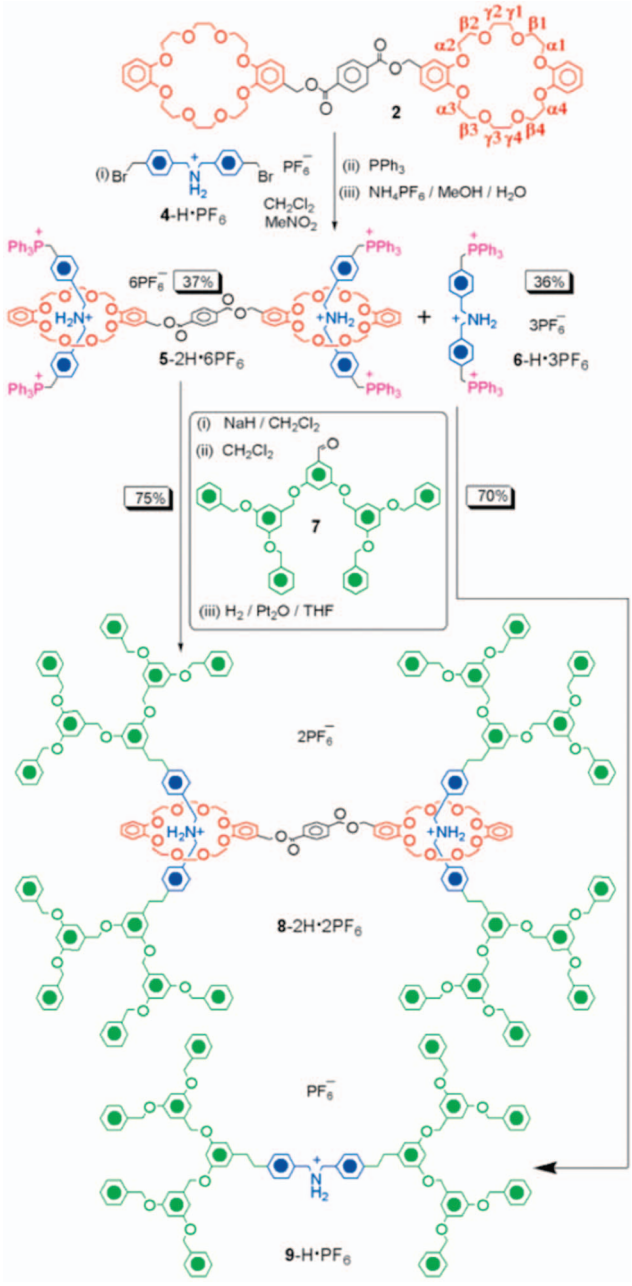

Mechanically linked fullerodendronized [2]pseudorotaxanes were also reported by Nierengarten.[1265]

Vögtle investigated the relationship between the spatial demand of Fréchet-type dendrons and deslipping in dendronized [2]rotaxanes. Generation two and three dendrons (Figure 432) were compared with two trityl stoppers, and their deslipping was monitored by NMR (Figure 433).[1266] All [2]rotaxanes were stable indefinitely at room temperature. However, from 80 to 150 °C, deslipping was observed. Though G2 Fréchet dendrons may appear to be more bulky than the trityl stoppers at elevated temperatures, the tri(*t*-butylphenyl)methyl stopper rethreads less readily than the G2 Fréchet-type stopper. The following empirical ranking was established G1 < D*t*BP < T1 < G2 < T2 < G3 (from Figure 433).[1266]

Scheme 92. Slippage-Based Synthesis of Dendronized [2]Rotaxane (Reprinted with Permission from Ref 1260; Copyright 2002 American Chemical Society)

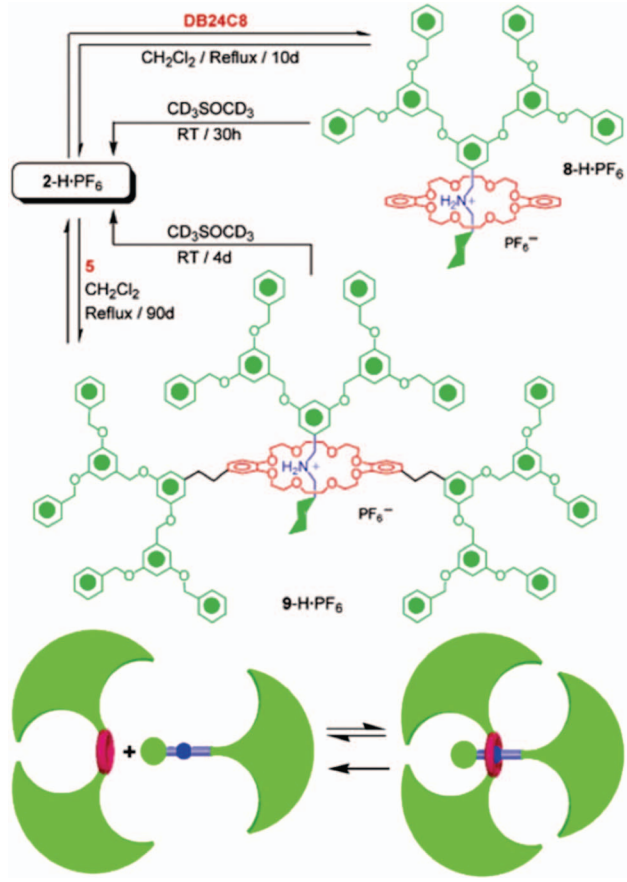

Scheme 93. Equimolar Amounts of 1, 2, and 3 Reacted for 16 h, Producing 1:99 Ratio of 4:5 with 96% Conversion[1261]

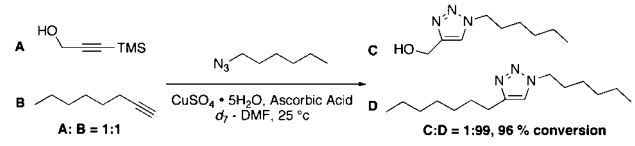

The strength of binding in dendronized [2]pseudorotaxanes was investigated by Kaifer.[1267] [2]Pseudorotaxanes dendronized with both Fréchet- and Newkome-type dendrons containing a single viologen unit bound to dibenzo[34]crown-10 were investigated (Figure 434). The interaction between dibenzo[34]-crown-10 and methyl viologen is well-known. Strong binding is mediated by electrostatic interaction of the crown-oxygens with the two positively charged nitrogens on viologen in conjunction with π donor−acceptor charge transfer complexes between the hydroquinol units and the bipyridinium.

The complex formed between viologen and dibenzo[34]crown-10 is only of modest stability and, therefore, is susceptible to interference from sterically demanding substituents. Fréchet-type dendrons did not affect complex stability, whereas a destabilizing effect was clear with Newkome-type dendrons. The rigidity of the Fréchet-type dendrons results in a more wedgelike conformation, whereas the flexibility of the Newkome-type dendrons allows them to encapsulate the viologen. Kaifer replaced the dibenzo[34]crown-10 with cucurbit[8]uril (CB8) and demonstrated redox-controlled self-

Scheme 94. One-Pot Three-Armed Rotaxane Synthesis[1261]

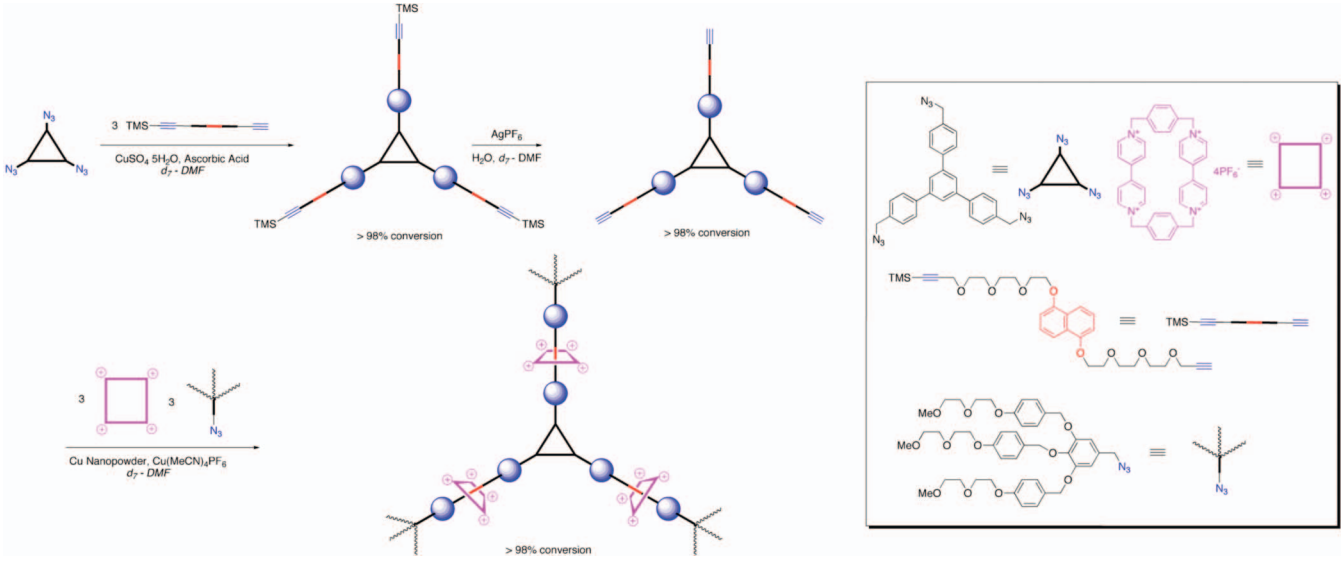

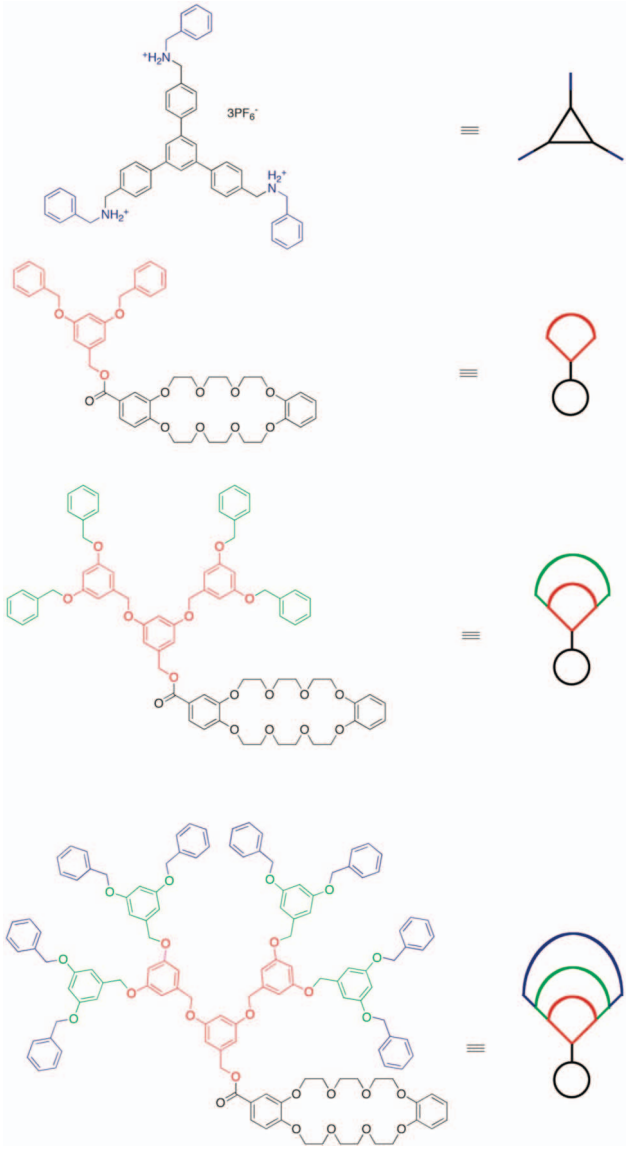

Figure 428. Components for the synthesis of dendronized pseudorotaxanes elaborated by Gibson.[1262]

assembly of dendronized dimeric [2]pseudorotaxanes (Figure 435).[1268] Here, one-electron reduction destabilizes the CB8 viologen donor/acceptor complex and allows for dimerization of the viologen radical cations within the CB8 scaffold. Oxidation releases one Newkome dendronized viologen from the wheel. Heterodimeric [2]pseudorotaxanes containing a

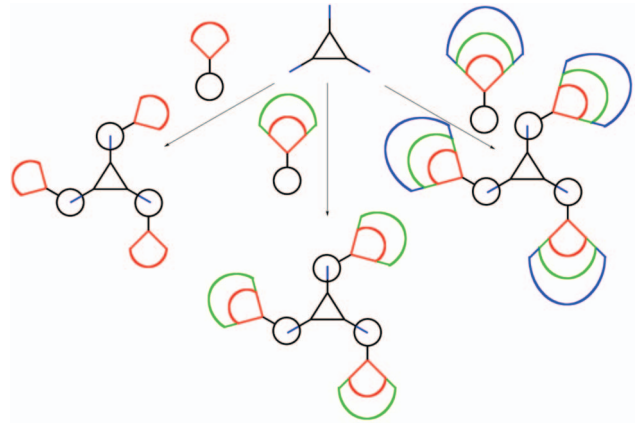

Figure 429. Self-assembly of pseudorotaxanes elaborated by Gibson.[1262]

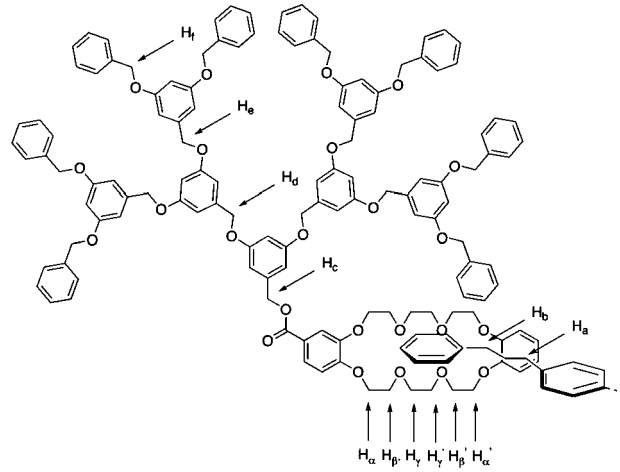

Figure 430. Designation of protons used for NMR assignment of pseudorotaxane.[1262]

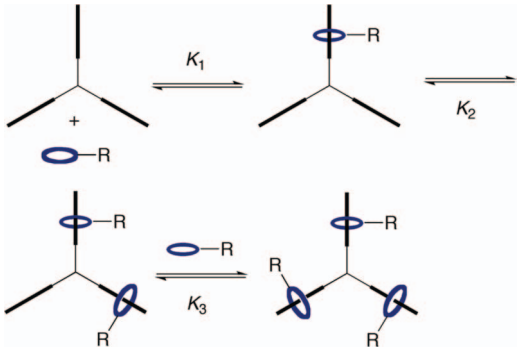

Figure 431. Self-assembly of pseudorotaxanes elaborated by Gibson. Reprinted with permission from ref 1264. Copyright 2002 American Chemical Society.

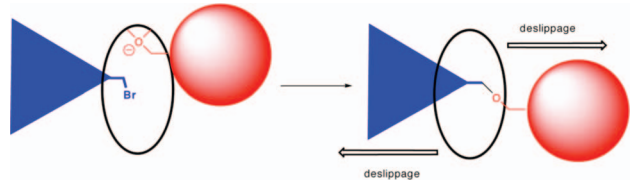

Figure 433. Deslipping of rotaxanes.[1266]

low-generation and high-generation dendronized viologen can be converted to the homodimeric low-generation dendronized [2]pseudorotaxanes via electrochemically induced exchange (Figure 436).[1269]

Using a similar methodology to Kaifer,[1268] Kim reported the use of click chemistry as a route to rotaxane dendrimers. G1−3 PAMAM were ligated to azide-functionalized methyl viologen and 2,5-dihydroxynaphthalene via CuAAC. A ternary charge-transfer complex was formed between the

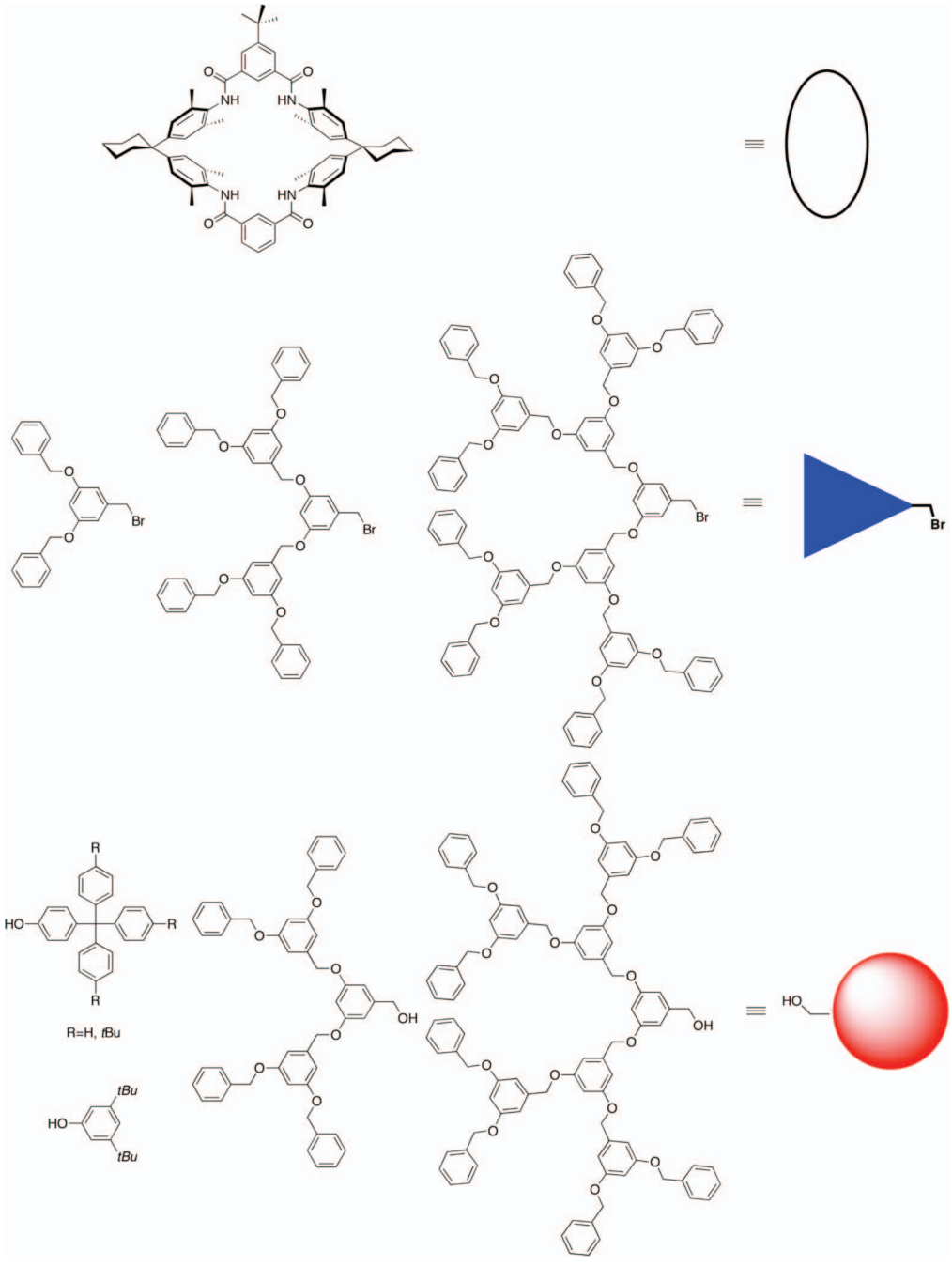

Figure 432. Dendritic bromides, wheel, and model axles used in deslippage studies.[1266]

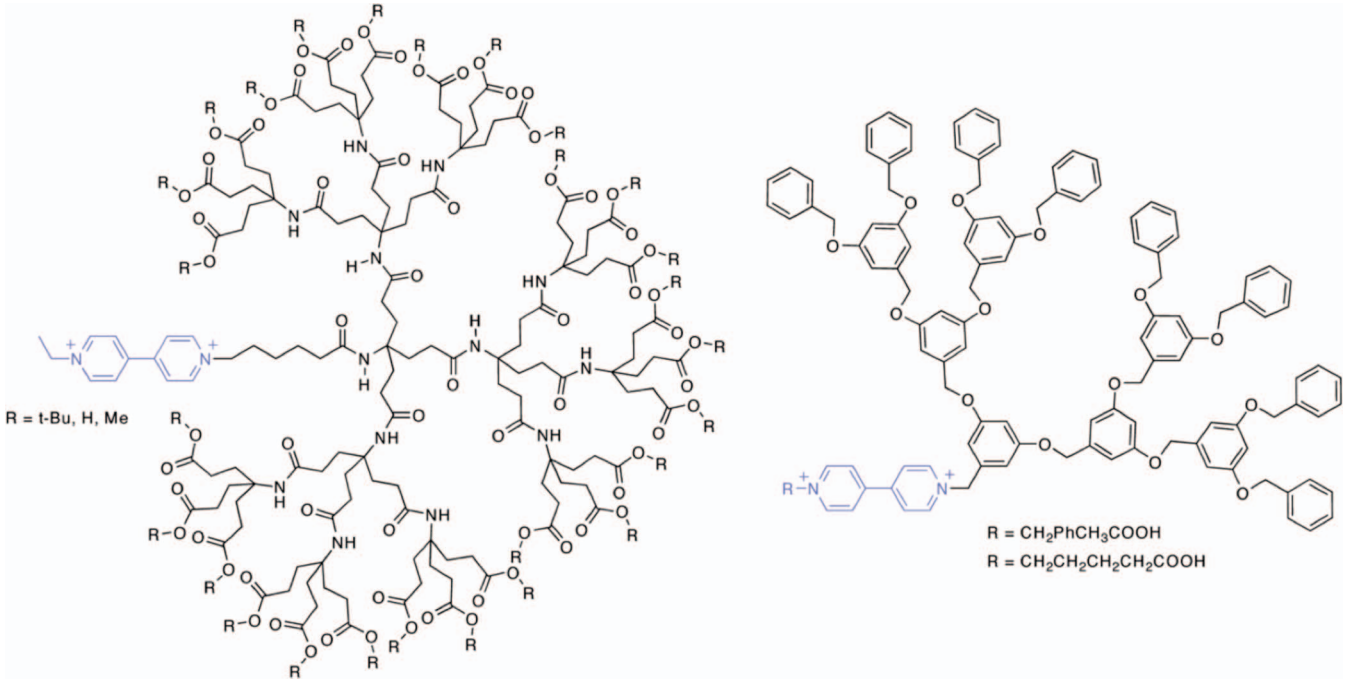

Figure 434. Fréchet and Newkome dendrons used in viologen binding studied by Kaifer. Reprinted with permission from ref 1267. Copyright 2005 American Chemical Society.

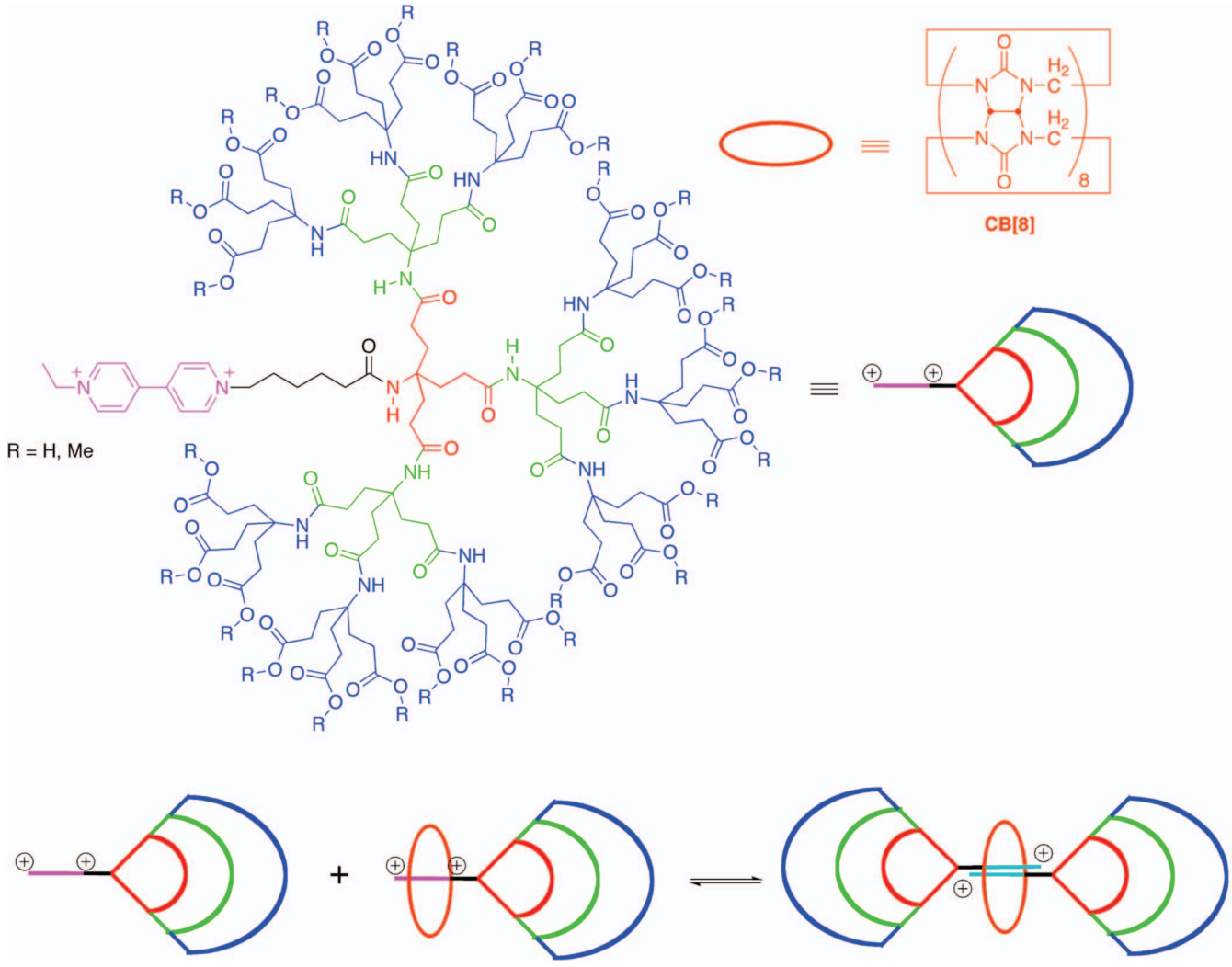

Figure 435. Cucurbit[8]uril-based dimeric [2]pseudorotaxanes and redox-controlled self-assembly. Reprinted with permission from ref 1268. Copyright 2004 Wiley-VCH Verlag GmbH & Co. KGaA.

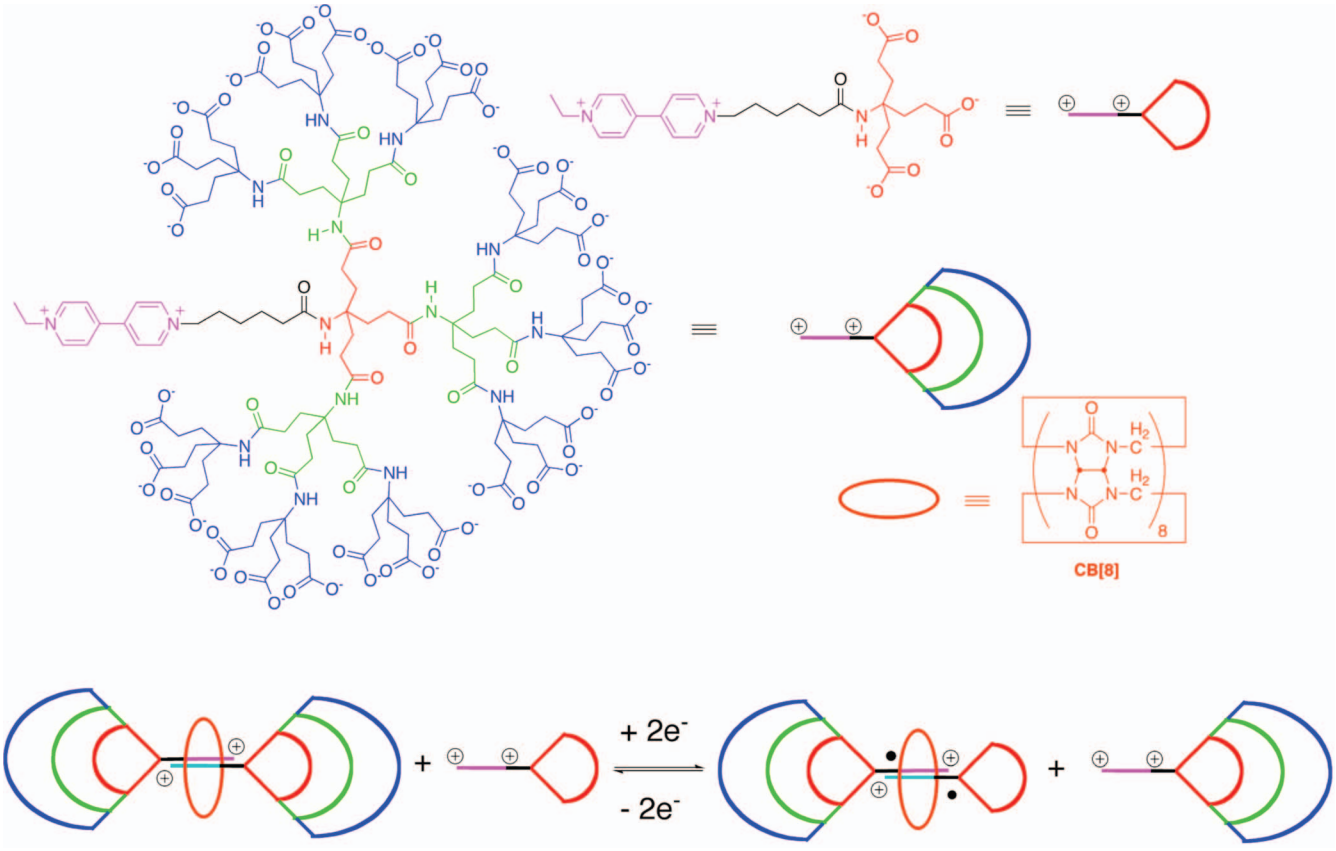

Figure 436. Electrochemical switching-based size selection by Kaifer.[1269]

Scheme 95. Supramolecular Click Chemistry Involved in the Synthesis of Rotaxane Dendrimers by Kim[1270]

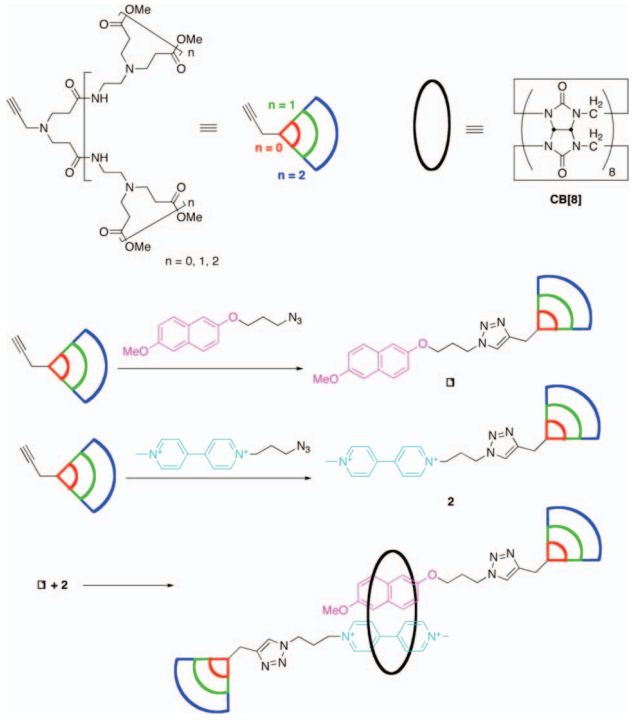

PAMAM dendronized methyl viologen and 2,6-dihydroxynaphthalene and CB8 (Scheme 95).[1270]

In a similar motif, Kim reported dendritic [2]pseudorotaxanes incorporating ring components in every branch.[1271] A homotritopic core extended viologen termini, and three dendrons bearing [2]pseudorotaxane peripheries and a 2,6-dihydroxynaphthalene apex form ternary charge-transfer complexes with CB8 (Figures 437 and 438).

Cyclodextrin has been used extensively as the macrocyclic host in rotaxane chemistry, though to a lesser extent for dendronized rotaxanes. Kim reported self-assembly of amide dendrons, which undergo a reversible transition from vesicles to nanotubes via addition or removal of cyclodextrin (Figure 439).[1272] Addition of cyclodextrin to amide dendrons *endo*-functionalized with pyrene results in the formation of [2]pseudorotaxane cyclodextrin-pyrene inclusion complex and induced a spontaneous transition from vesicular to nanotubular structure. Addition of poly(propylene glycol) to the cyclodextrin complex removed the cyclodextrin from the nanotube, and the reverse transformation of nanotubes to vesicles was observed (Figure 440).[1272] Cyclodextrins have also been used in the formation of pseudorotaxane dendronized polymers as discussed previously (see section 2).[695,1273]

9.3. Dendronized Catenanes and Molecular Knots

Vögtle reported molecular knots dendronized with Fréchet-type dendrons, termed dendroknots. Knots were prepared via supramolecular templating followed by amidative ring-closure with 4-hydroxy, benzyloxy, or dendronized 2,6-dicarbonyl chloride pyridine (Figure 441).[1274] Attempts to further dendronize the isophthalate unit (R′, Figure 441) resulted in low yields of knots and instead produced predominantly macrocycles and catenanes. XRD indicated the isophthalate units were buried inside the knot and, therefore, were intolerant to functionalization with bulky dendrons.[1275] Instead the pyridine units residing on the

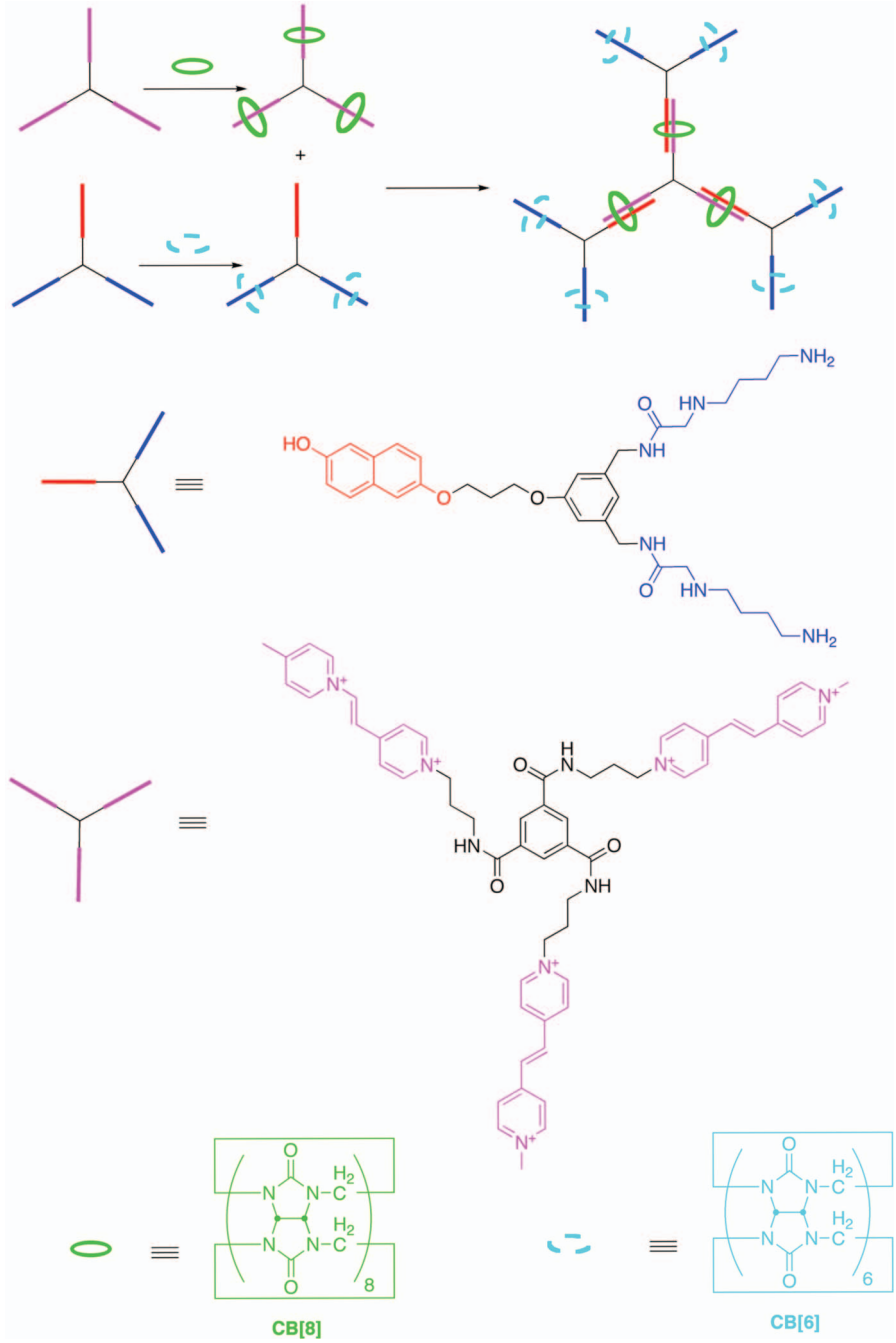

Figure 437. Components of dendritic pseudorotaxane elaborated by Kim.[1271]

periphery of the knot were functionalized yielding the molecular knots illustrated in Figure 28.[1274] Chiral separation of the first-generation dendronized knot was achieved using Chiralpak AD. CD/UV−vis was used to assess the supramolecular chirality of knots mono-, di-, and trisubstituted with first-generation dendrons.[1274] Vögtle also reported the synthesis of dendritic molecular knots via the cross-linking of trimeric knots (Scheme 96).[1276]

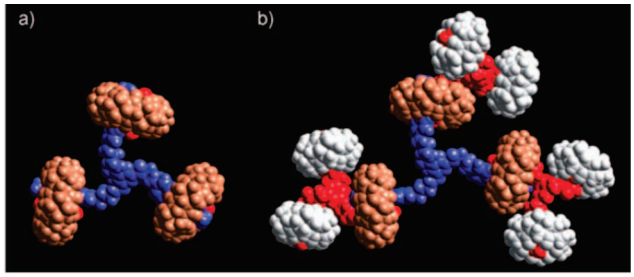

Figure 438. Energy-minimized molecular models of G1 (a) and G2 (b) dendritic pseudorotaxanes. Reprinted with permission from ref 1271. Copyright 2007 Wiley-VCH Verlag GmbH & Co. KGaA.

Vögtle also reported the synthesis and chiral resolution of dendron[2]phanes, dendro[2]rotaxanes, and dendro[2]catenanes by a similar methodology to that outlined above.[1277] LC catenanes using identical mesogens to those reported by Kato and Stoddart[1256] (Scheme 89) were also reported by Sauvage and Kato.[1278] The [2]catenanes incorporated a phenanthroline metal binding site in the central cavity, allowing for complexation with Cu (Figure 442). Both metal free and Cu-complexed compounds exhibited an S phase according to TOPM, DSC, and XRD (Figure 443).

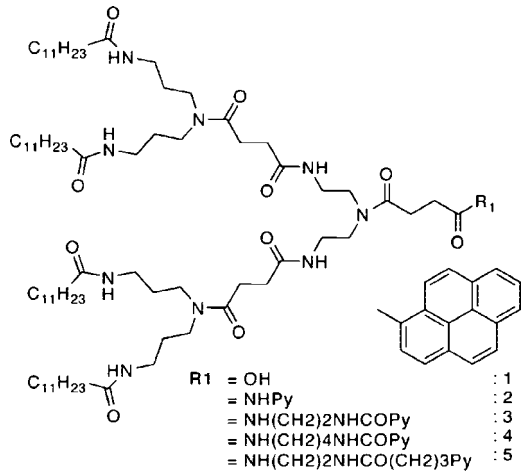

Figure 439. Vesicle-forming amide dendrons elaborated by Kim.[1272]

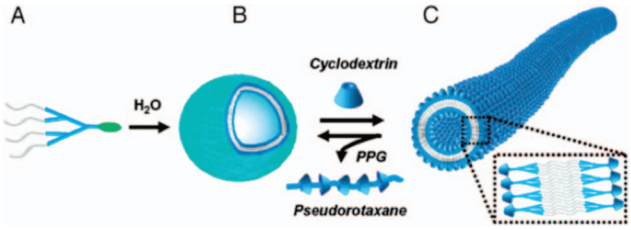

Figure 440. Reversible formation of vesicle and nanotubes. Reprinted with permission from ref 1272. Copyright 2006 PNAS.

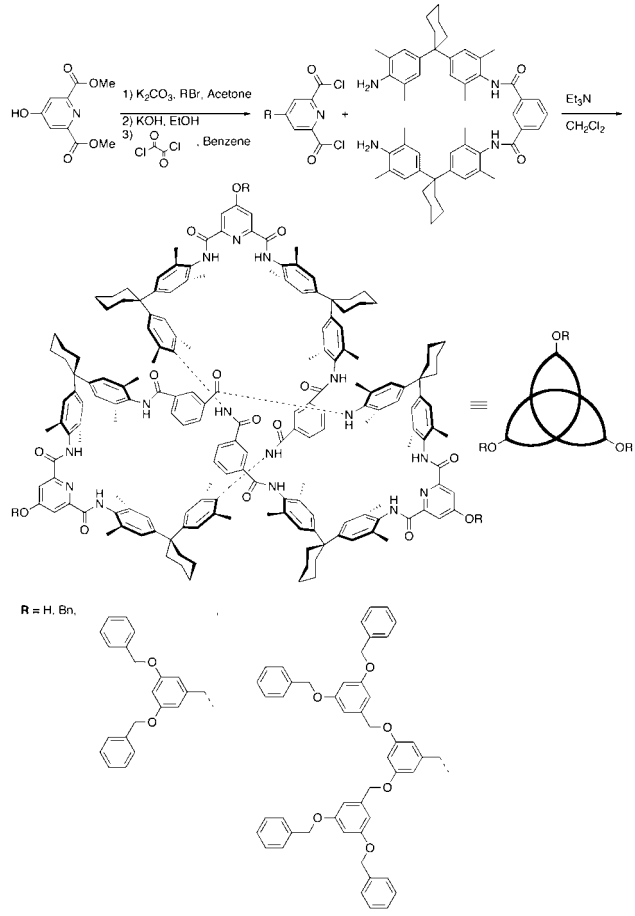

Figure 441. Dendronized knots synthesized by Vögtle.[1274]

10. Dendronized Fullerenes

C_{60}, the archetype of the fullerene family, is an intriguing target for molecular design on account of its highly symmetric truncated icosahedron/soccer-ball shape and its electronic properties. Dendronized fullerenes (Figure 2, third row second from right), first reported by Fréchet,[1279] have been the subject of many recent investigations. Self-assembling and self-organizing fullerenes were comprehensively reviewed by both Deschenaux and Nierengarten.[68,92,93] This section will serve to outline the important milestones in this field and bring the most recent advances up to date.

10.1. Covalently Dendronized Fullerenes

10.1.1. Synthesis of Dendronized Fullerenes

Despite the large number of C_{60} resonance structures, ab initio calculations and structural data demonstrate alternating bond character. Longer bonds are observed at the junctions between five- and six-member rings (5−6 junction), 1.46 Å, whereas shorter bonds are observed at the junction between two six-membered rings (6−6 junction), 1.40 Å. Effective bond alternation causes C_{60} to behave chemically like an electron-poor poly(alkene) rather than a "super-aromatic" system.[1280] Bond alternation can be exploited for the preparation of dendronized fullerenes via nucleophilic addition and cycloaddition.[86,1281] The Bingel reaction,[1282] a fullerene cyclopropanation, is one of the most versatile methodologies for the functionalization/dendronization of fullerenes.[87] In the Bingel reaction, α-haloketone or malonate are deprotonated to the enolate. The enolate

Scheme 96. Synthesis of Dendritic Knots[1276]

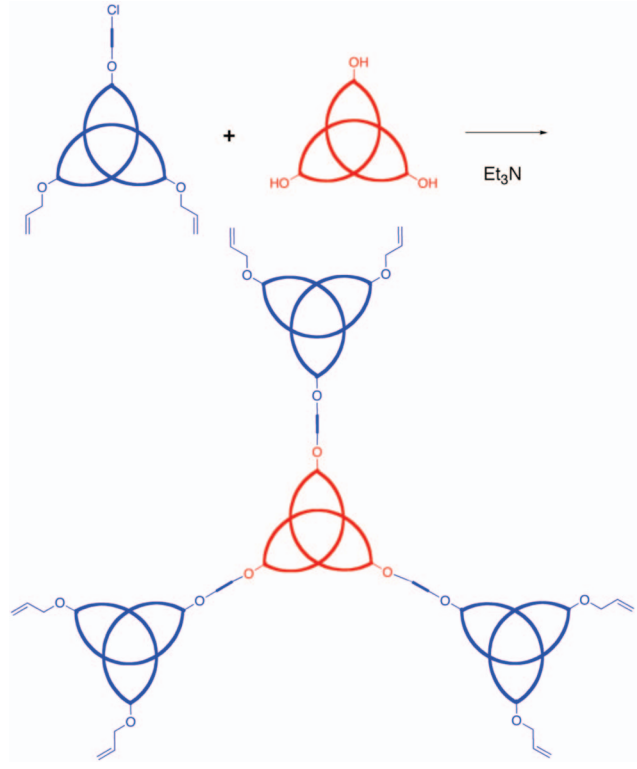

attacks the shorter, electrophilic C−C bond of a 6−6 junction of C_{60} to form a fullerene carbanion, which subsequently displaces the α-halide to form a methanofullerene. A

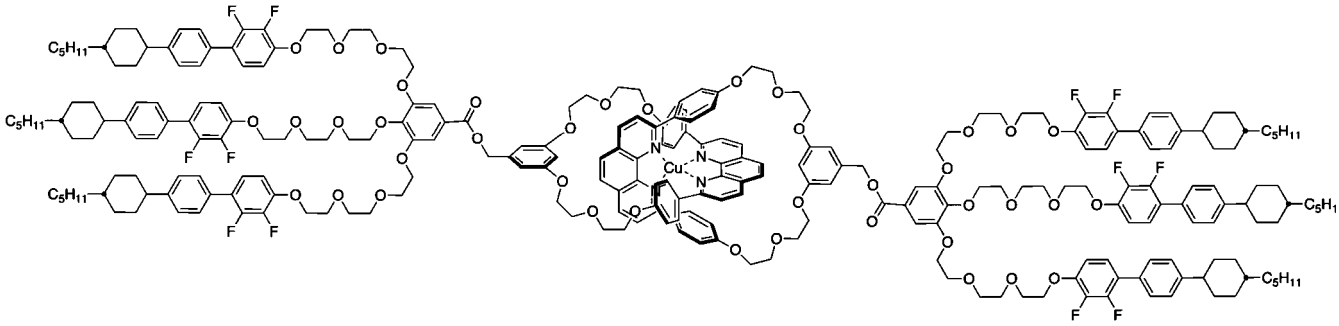

Figure 442. LC catenane of Sauvage and Kato.[1278]

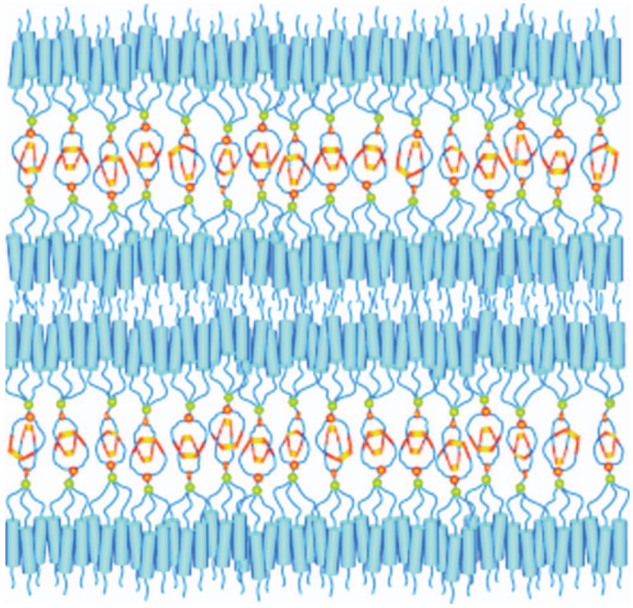

Figure 443. Schematic packing model for the S_A phase of liquid crystal catenanes. Reprinted with permission from ref 1278. Copyright 2007 Wiley-VCH Verlag GmbH & Co. KGaA.

Scheme 97. Mechanism of the Bingel Reaction[1282,87]

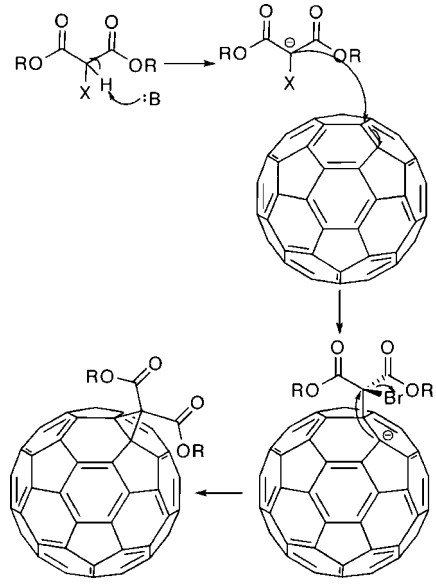

modified procedure utilizes an α-haloketone or malonate generated in situ from esters and ketones with either I_2 or CBr_4 and a base such as diaza(1,3)bicyclo[5.4.0]undecane (DBU) (Scheme 97).[1283−1286]

10.1.2. Self-Assembly and Self-Organization of Dendronized Fullerenes

Self-organizing dendronized fullerenes were prepared by the groups of Deschenaux and Guillon.[1287] A wide variety of compounds have been synthesized. Many of these self-organize in N, S, and columnar LC phases (Figures 444, 445, and 447).[1288−1290] Fullerodendrons bearing achiral rodlike mesogens on their periphery self-organize into S phases via interdigitation of rods. Side-on attachment of chiral-rodlike mesogens induces self-assembly into cholesteric phases. Attachment of (4-3,4,5-3,5)12G2, a dendron that self-assembles into supramolecular columns that self-organize into Φ_h phases, induces the organization of dendronized C_{60} into supramolecular columns. Attachment of (3,4,5)20G1 to C_{60} has been shown to mediate self-assembly into globular nanoflaked particles, which in conjunction with various thiols can be used to form superhydrophobic or superhydrophilic surfaces on Au (Figure 446).[1291] Likewise, attachment of a similar diacetylene-containing dendron results in lamellar structures that can be cross-linked to form water-repellant materials (Figure 446).[1292]

Guillon reported a series of Janus-type dendrimers functionalized with S-phase inducing poly(aryl ester) dendron bearing rodlike cyanobiphenyl mesogens on their periphery and one Φ_h inducing (4-3,4,5-(3,5)^n)12Gn+1 Percec-type dendron (Figure 448).[1249,1250] The Percec-type dendrons and the cyanobiphenyl-functionalized dendrons were attached to C_{60} via a 1,3-dipolar cycloaddition. When the size of Percec-type and cyanobiphenyl-terminated dendrons was balanced, Janus dendrimers and Janus fullerodendrimers exhibited S organization. When the Percec-type dendron was larger, $\Phi_{r\text{-}c}$ organization was observed (Figure 449).

Deschenaux utilized Janus-type dendronized fullerenes as acid-sensitive fluorescent probes. The Percec-type dendron was replaced with a phenylene vinylene dendron with dibutyl aniline periphery groups (Scheme 98). All compounds self-organized into S phases with a reversible acid-triggered switching in fluorescence emission from 498 to 710 nm.[1293] S_B phases were also reported by Ohta in a series of fullerodendrons periphery functionalized with cyanobiphenyl mesogens (Scheme 99).[1294]

In order to investigate the effect of fullerene on columnar lattice formation, a series of mono, twin, and Janus fullerodendrimers substituted with Percec-type dendrons that exhibit Φ_h and Φ_r self-organization were prepared through the Bingel reaction (Figure 450).[1295] The self-organized architecture of the fullerodendrons was dictated by the self-assembly of supramolecular discs derived from the parent dendritic malonate with little influence from the fullerene on phase structure (Figure 451).[1295] In most cases, Φ_h self-organization was observed. However, in the

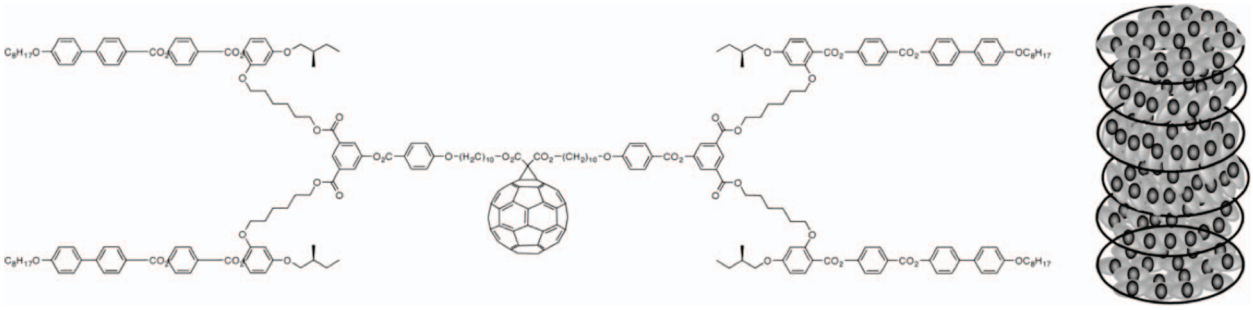

Figure 444. Schematic of chiral N phase self-organized from dendronized fullerene. Reprinted with permission from ref 1288. Copyright 2003 Royal Society of Chemistry.

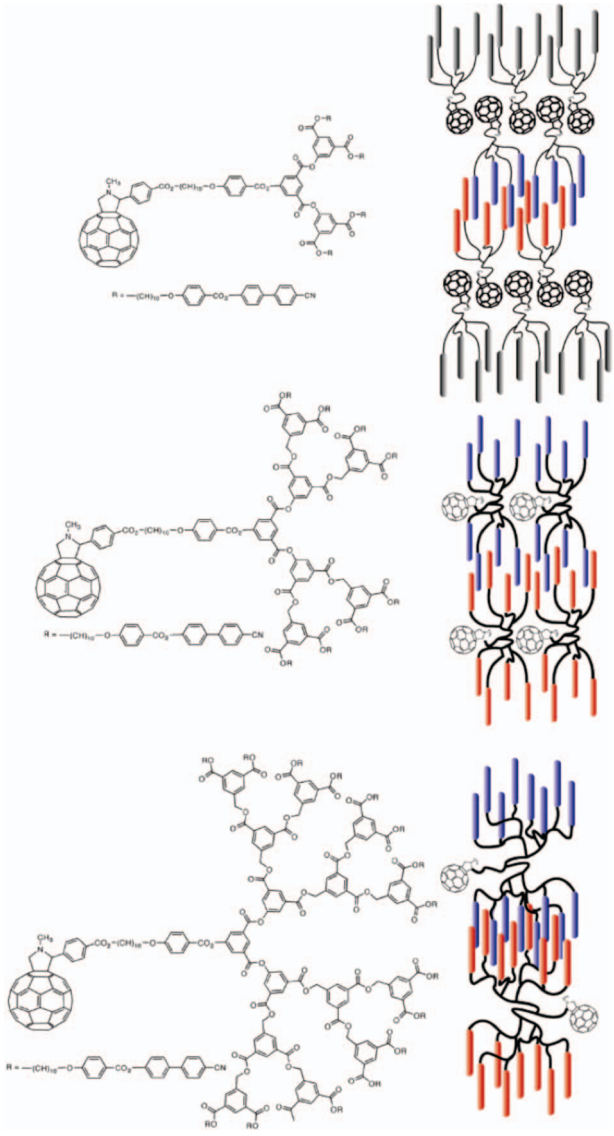

Figure 445. Schematic of S phases self-organized from dendronized fullerene. Reprinted with permission from ref 1289. Copyright 2005 American Chemical Society.

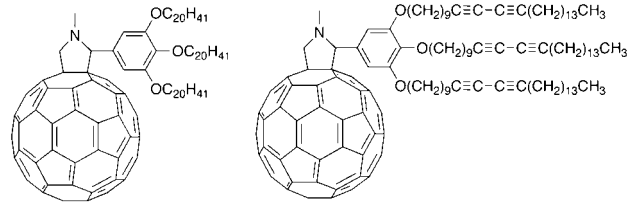

Figure 446. C_{60} dendronized with (3,4,5)20G1 and an analogous diacetylene-containing dendron.[1291,1292]

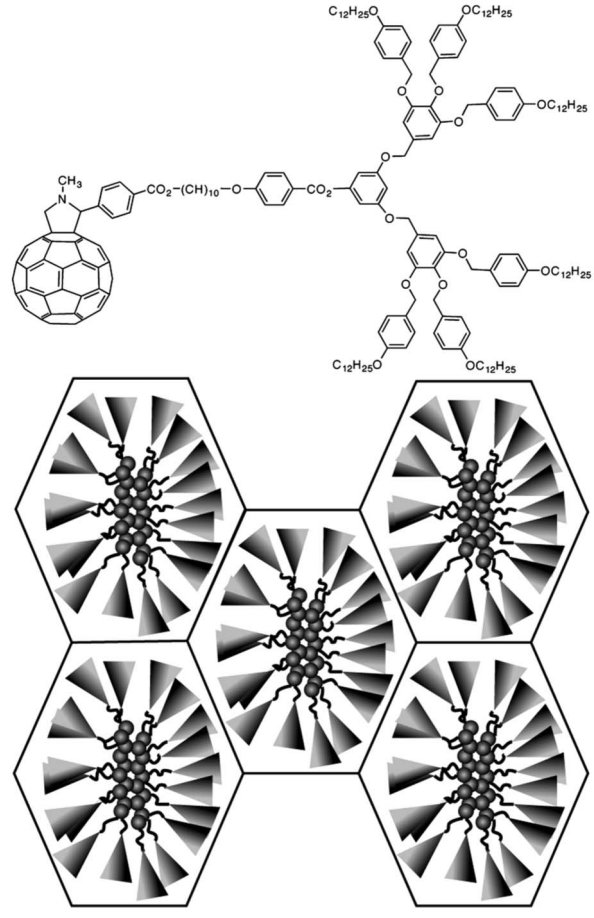

Figure 447. Schematic of columnar phase self-organized from dendronized fullerene. Reprinted with permission from ref 1290. Copyright 2006 American Chemical Society.

case of C_{60} dendronized with (4-3,4,5-3,5)12G2, Φ_r organization was observed, while that bisdendronized with (4-3,4,5-3,5)12G2 exhibited no mesomorphism.

Diederich also showed that the symmetry and size of C_{60} do not enhance the stability of the LC phase of self-assembling dendrons but diminish it (compound 2, Figure 452). Dense functionalization of the fullerene appears essential for LC phase formation (compounds 3 and 4, Figure 452).[1296] Photinos investigated the fullerodendrimers of Deschenaux through a simple cubic block model (Figure 453).[1295,1297] While crude, these models were in good agreement with experimentally obtained data for columnar packing of fullerodendrimers and correctly predicted the transition from Φ_h to S phases in the Janus systems

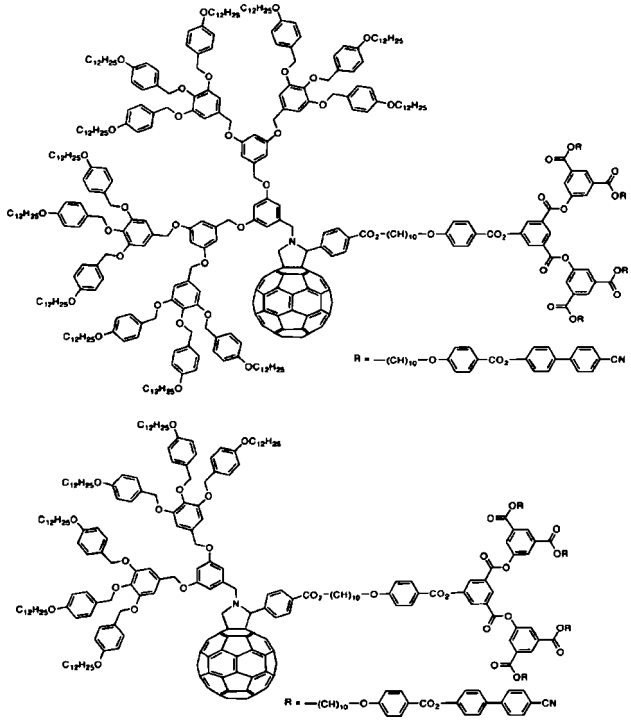

Figure 448. Janus-dendronized fullerene exhibiting $\Phi_{r\text{-}c}$ (top) and S self-organization (bottom).[1250]

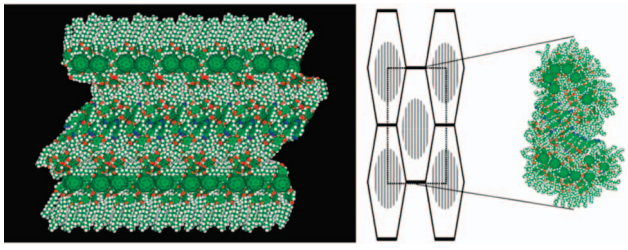

Figure 449. Models of S and $\Phi_{r\text{-}c}$ packing of Janus fulleroden-drimers. Reprinted with permission from ref 1249. Copyright 2007 American Chemical Society.

Scheme 98. Acid-Sensitive Fullerodendrons[1293]

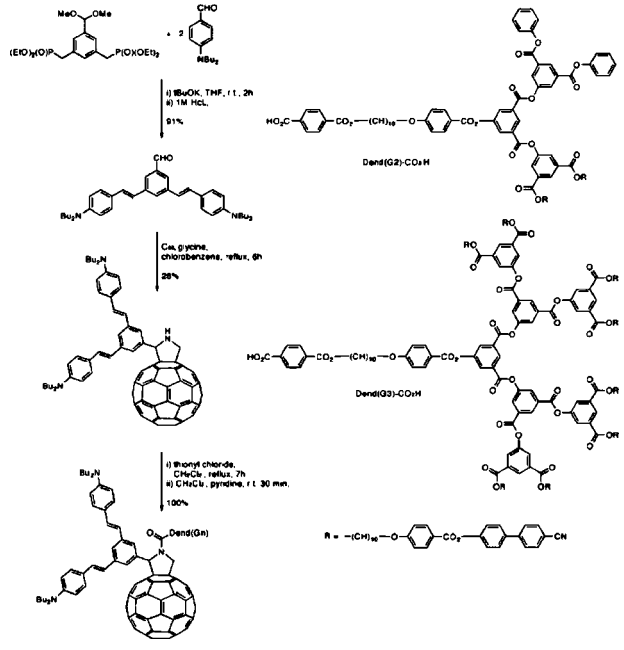

Scheme 99. Synthesis of Fullerodendrons Containing Cyanobiphenyl Groups Designed by Ohta[1294]

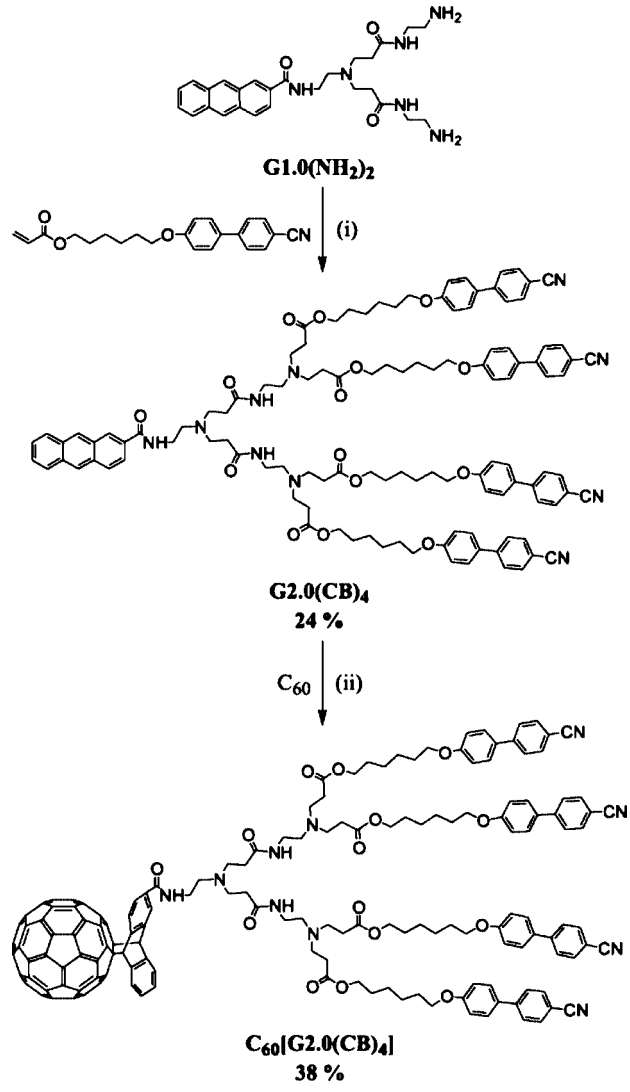

reported by Deschenaux, thereby demonstrating the strong connection between molecular shape and the self-assembled structure.

Kato reported the first dendritic fullerene derivatives that self-assemble and subsequently self-organize in various LC phases wherein organization was driven by $\pi-\pi$ interactions between the fullerene and adjacent aryl dendrons forming interlocked "shuttlecocks" (Figure 454).[1298,1299] Columnar orthorhombic crystals with P_{bca} space groups were obtained that, upon heating, could be transformed into thermotropic LCs with Φ_h organization. Contrary to most LC fullerodendrons, which only exhibit thermotropic mesophases, lyotropic phases of similar architecture were also observed (Figure 455).

The conductive properties of fullerenes have been investigated by Aida and Kato to synthesize photoconductive and electron-transport materials from dendronized fullerenes.[1300,1301] Aida reported amphiphilic dendronized fullerenes coupled to oligothiophene units that self-organize in a S_A phase (Figure 456).[1300] Kato reported electron transport and electrochemistry of dendronized fullerenes displaying long-range ordered layer structures (Figure 457).[1301] XRD suggested high-density packing of fullerenes within lamella. Electron mobility was $\sim 3 \times 10^{-3}$

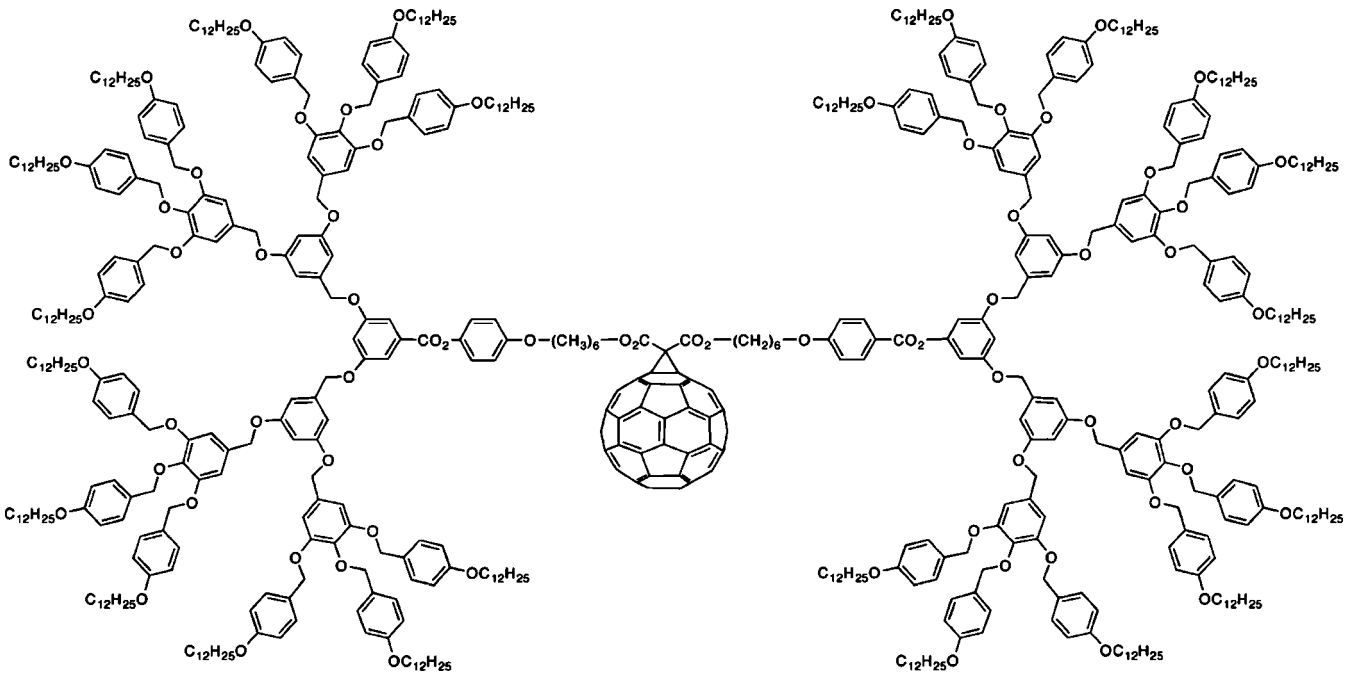

Figure 450. Twin-dendritic fullerene.[1295]

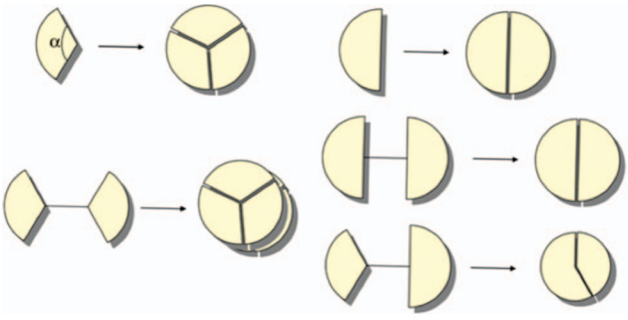

Figure 451. Janus fullerodendrons assume a discotic shape derived from their dendron structure that mediates self-assembly into columns. Reprinted with permission from ref 1295. Copyright 2008 Royal Society of Chemistry.

$cm^2\ V^{-1}$, at a field of 2×10^5 V cm^{-1}, in line with other S LC organic semiconductors.[1302,1303]

Zhao prepared fullerenes dendronized with Fréchet-type dendrons via click chemistry (Scheme 100).[1304] By varying the conditions under which the films were cast, the structure of the self-assembled structures could be controlled. Four distinct self-assembled objects were identified: multilayer cylinder, lamella, monolayer spherical micelles, and multilayer spherical micelles.

Formation of self-organized structures in aqueous solution derived from dendronized fullerenes is of great interest in nanobiotechnology as a model for the design of new therapeutic agents and drug delivery systems. Hirsch reported dendronized amphiphilic fullerenes that self-assemble into membranes and micelles and other structures.[1305−1309] These amphiphiles are composed of fullerenes bisfunctionalized with hydropillic G2-carboxylic terminated Newkome dendrons through a single malonate or malonamide linkage and ten alkyl tails via five malonate linkages (Figure 458). When the connection between the dendron and fullerene is through esters (Figure 458, X = O), a variety of structures can be formed.[1305−1308] However, when the connection is through a more rigid amide bond (Figure 458, X = NH), only micellar objects are observed.[1309] The micellar structures formed from these amphiphilic dendrons may be switched from rodlike to octomeric/globular micelles by increasing the pH (Figure 459). Hirsch also reported a hexakis-dendronized fullerene amphiphile (Figure 460).[1310] This amphiphile is composed of three hydrophilic G1-Newkome dendrons attached via three malonate linkages and a hydrophobic macrocycle. By restricting the size of the hydrophilic dendrons as well as decreasing the volume of the hydrophobic region by using cyclo-[3]-octylmalonate instead of straight-chain alkanes, extremely small persistent micelles were formed. Cryo-TEM and modeling studies suggest the formation of 5 nm hexameric micelles with D_3 symmetry (Figure 461). Hirsch also reported micellar self-assembled structures from diazabis[60]fullerene dendronized with mannpyranose-functionalized Newkome dendrons (Figure 462).[1311]

Conyers reported the first examples of unilamellar vesicles formed from dendronized fullerenes termed "buckysomes".[1312] A water-soluble dendronized fullerene previously reported by Hirsch (Figure 458) was used as a synthetic mimic for conventional phospholipids. Structures self-assembled in water were analyzed by both DLS and cryo-TEM (Figure 463). Little cytotoxicity was observed in kidney, liver, or macrophage cells as compared to phosphate-buffered saline standards.

10.2. Noncovalently Dendronized Fullerenes

Self-assembling noncovalently dendronized fullerenes have also been prepared via donor−acceptor interactions or other noncovalent interactions. As mentioned in section 6.4, Nierengarten reported 2:1 complexes of dendronized CTV and C_{60} that self-assemble into a cubic phase.[1107] Aida reported the construction of segregated arrays of donors and acceptors consisting of dendronized Zn-porphyrin acceptors and dendronized fullerene pyridine donors arranged around a petal-like core (Figure 464), which could be directly visualized by STM (Figure 465).[1313] The self-assembled wheel provided a charge-separation model similar to the

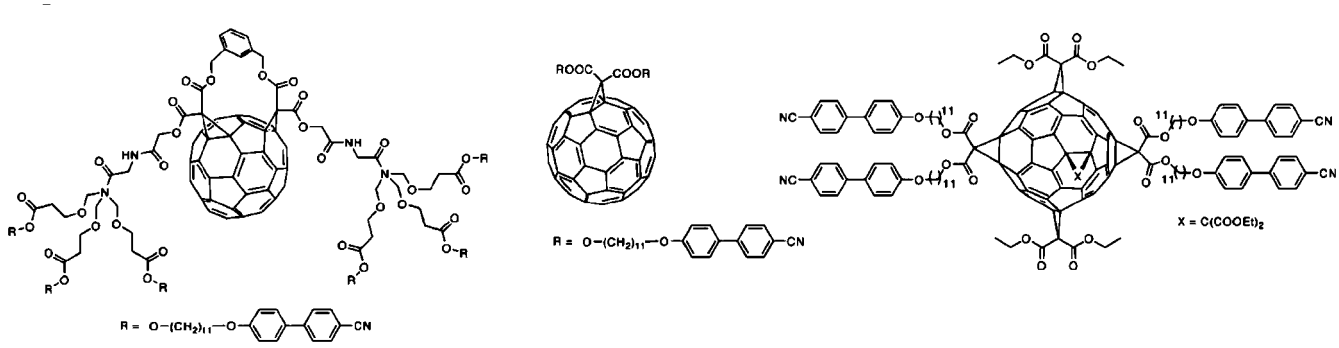

Figure 452. Dense functionalization of fullerodendrons is required for LC formation.[1296]

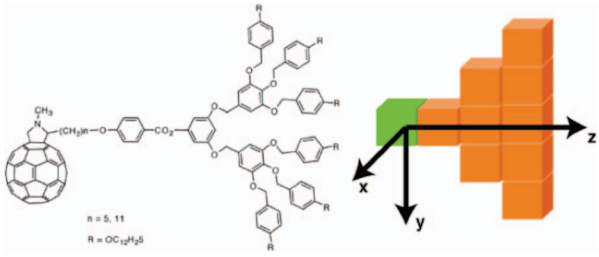

Figure 453. Dendronized fullerodendron (a) and the corresponding cubic block model (b). Reprinted with permission from ref 1297. Copyright 2008 American Chemical Society.

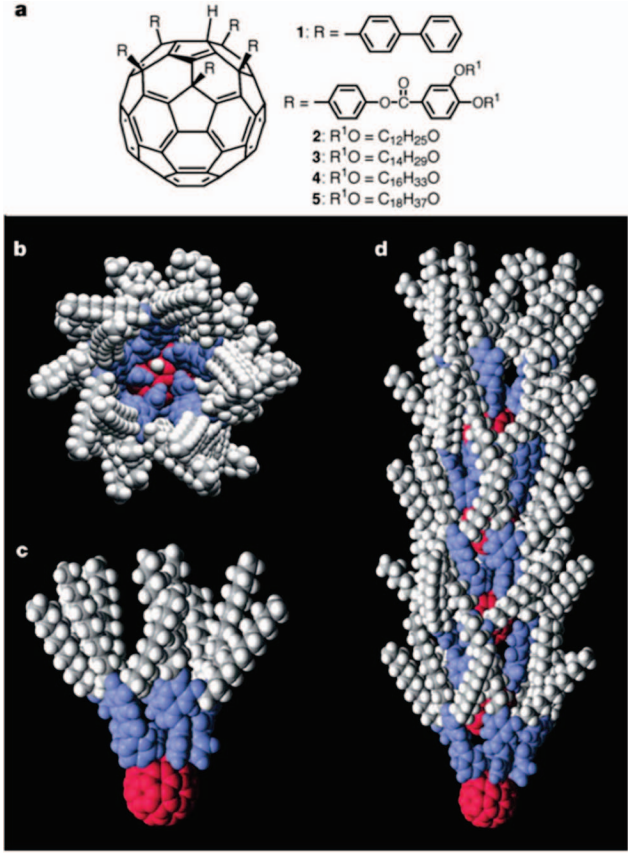

Figure 454. Structure of dendronized fullerenes (a). Molecular model of packing into shuttlecocks (b, c, d). Reprinted with permission from ref 1298. Copyright 2002 Macmillan Publishers Ltd. (Nature).

light-harvesting antenna LH1 and LH2 found in purple photosynthetic bacteria (Figure 466).[1314−1317]

Hirsch reported supramolecular dendrimers self-assembled from dendritic fullerene ligands and mediated by homotritopic Hamilton[1318] receptors (Figure 467).[1319] 2,6-Diaminopyridine containing Hamilton receptors are designed to bind substituted barbiturate molecules through multiple H-bonding sites. Here, the barbiturate was functionalized with a fullerene.

Dendronized fullerenes forming supramolecular dendrons have been reported by Matín.[1320] Periphery functionalization of the dendronized fullerene with TTF provides a concave receptor that is complementary to the fullerene

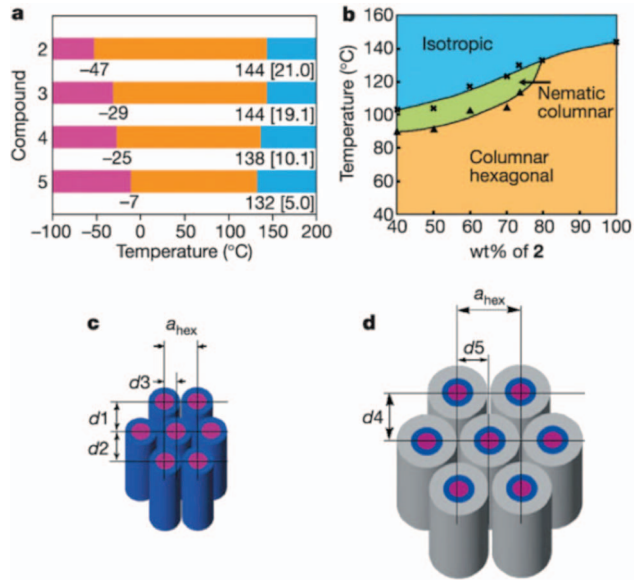

Figure 455. Thermotropic self-organization of dendronized fullerenes (a); pink = glassy, orange = Φ_h, blue = I. (b) Phase diagram for lyotropic self-organization of dendronized fullerenes. (c) Schematic packing in the crystalline phase of dendronized fullerene. (d) Schematic packing of the LC phase of dendronized fullerenes. Reprinted with permission from ref 1298. Copyright 2002 Nature Publishing Group.

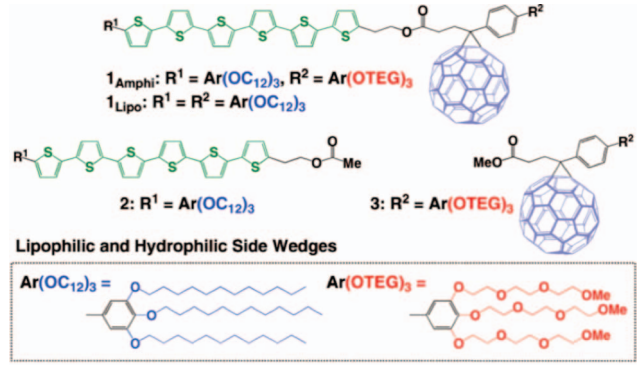

Figure 456. Amphiphilic fullerodendrons. Reprinted with permission from ref 1300. Copyright 2008 American Chemical Society.

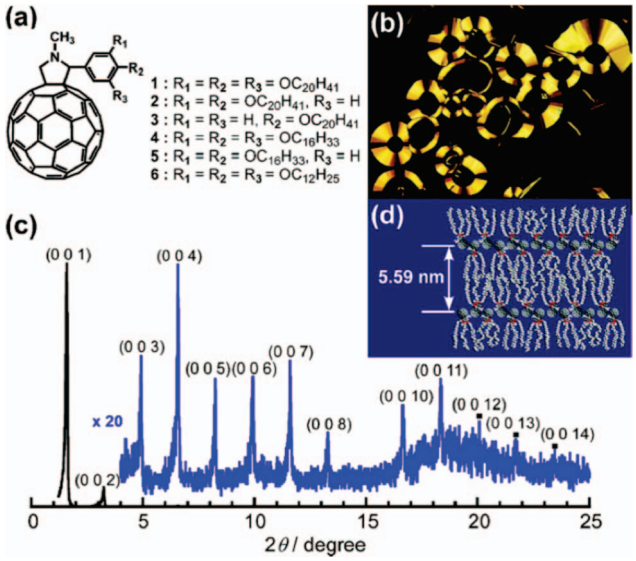

Figure 457. Fullerodendrons exhibiting highly ordered lamella. Reprinted with permission from ref 1301. Copyright 2008 American Chemical Society.

(Figure 468). MALDI-TOF showed formation of self-assembled oligomers in the gas phase up to hexamers (Figure 469).

Martin also demonstrated the disassembly of supramolecular dendrimers by titration with fullerene (Figure 470).[1321] Evidence for the formation of molecular aggregates of the dendrons of the self-assembled dendrimers in the absence of fullerene was presented by MALDI-TOF in the gas phase and NMR experiments in solution. Disassembly of supramolecular dendrimers was followed by UV−vis spectroscopy.

A number of other noteworthy examples of self-assembled fullerene dendron/dendrimer topologies have been reported in the literature. Hirsch reported the electrostatic assembly of fullerene−porphyrin conjugates as a step toward understanding the electron-transfer processes present in mitochondrial cytochrome c.[1322] Kono reported aqueous solubilization of fullerene via encapsulation at the periphery of dendrimers peripherally functionalized with cyclodextrin.[1323]

11. Dendronized Ionic Liquids

Ionic liquids (ILs) are fast gaining ground as "green" replacements for organic solvents in synthetic chemistry, because they have low volatility, are able to dissolve a wide range of organic and inorganic compounds, and are economical relative to organic solvents.[1324−1327] The field of ionic liquid crystals has been previously reviewed by Binnemans up to 2005. This section will serve to update the literature focusing only on dendronized ionic liquids (Figure 2, third row right).[1328] Dendron-mediated self-organization of ILs provides access to useful ion-conductive materials.

11.1. Imidazolium Salts

The most commonly studied dendronized ILs are the dendronized imidazolium salts of Kato.[1329,1330] The first report

Scheme 100. Synthesis of Dendronized Fullerenes via Click Chemistry[1304]

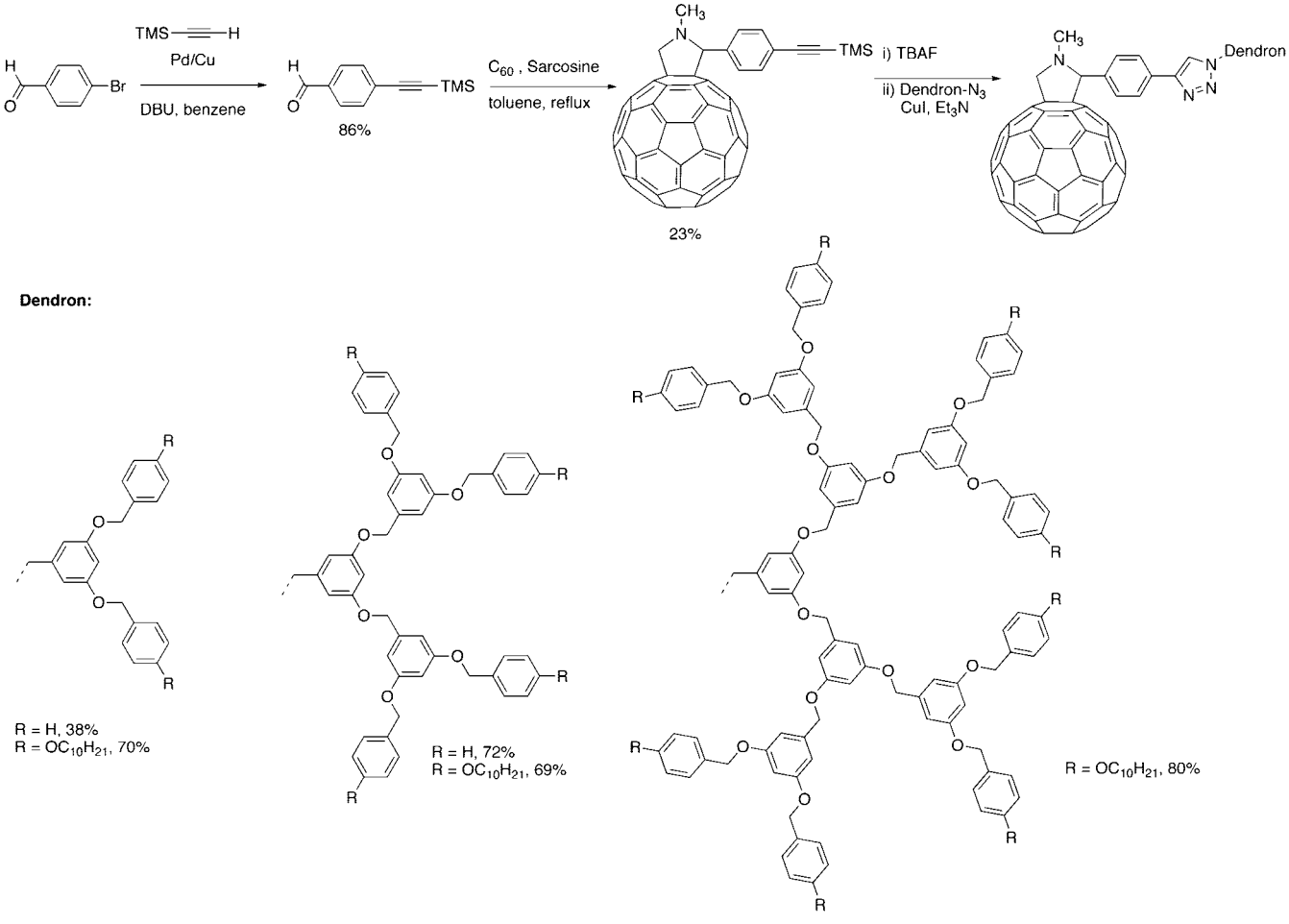

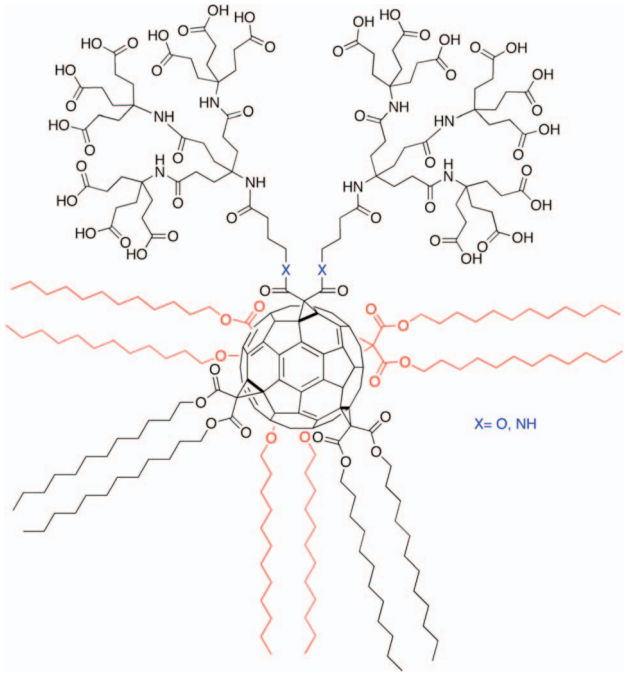

Figure 458. Structure of dendronized fullerene amphiphiles that form octameric/globular micelles.[1309]

of LC dendronized imidazolium salts by Kato investigated the relationship between both alkyl tail length and counterion on LC phase behavior (Figure 471 and Table 7). Melting

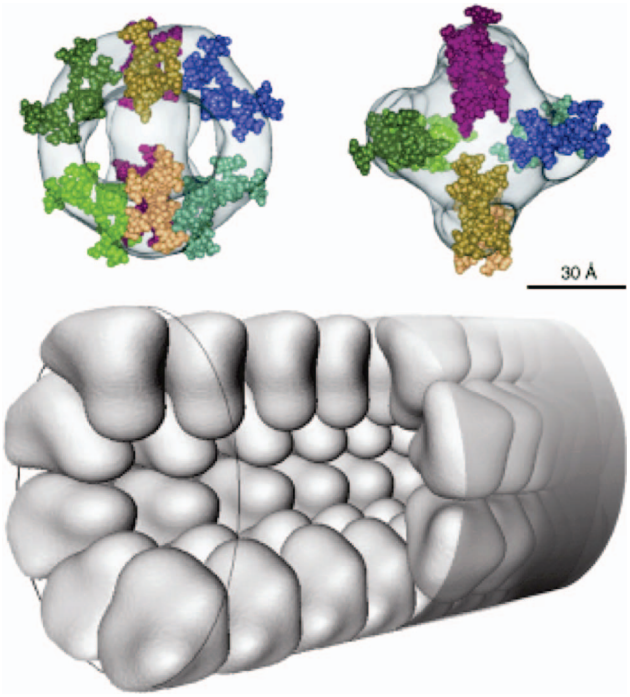

Figure 459. Schematic representations of globular and rodlike micelles formed by dendronized fullerenes. (top left) Eight head groups of the dendritic fullerene molecule in a C2-symmetrical mode. (top right) View tilted by 90° toward the front side. (bottom) Proposed model for the self-organization of dendronized fullerenes into micellar rods. Reprinted with permission from ref 1309. Copyright 2005 Wiley-VCH Verlag GmbH & Co. KGaA.

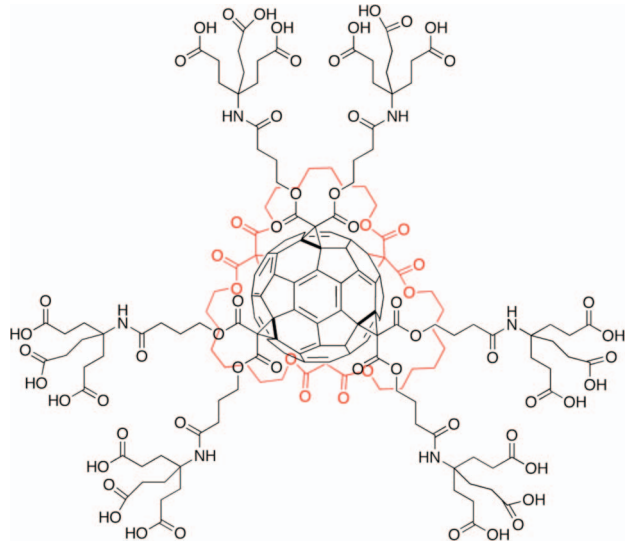

Figure 460. Hexadendronized fullerene amphiphile.[1310]

points and clearing points increase with alkyl tail length, while increasing size of the anion for octyl and dodecyl tails results in destabilization of mesophase formation. Ionic conductivity experiments were carried out on aligned samples, confirming anisotropic conductivities are higher parallel to the column axis than perpendicular.[1329]

As discussed in section 3.3, Kato later reported the preparation of 1D ion-conductive polymer films via dendronized ILs containing periphery polymerizable groups (Figure 182).[685] Kato also demonstrated enhanced anisotropic conductivities for noncovalently dendronized ILs (Figure 472).[1331] (3,4,5)12G1 and (3,4,5)8G1 Percec-type dendrons apex-functionalized with glycerol at the apex were mixed in various ratios with imidazolium salts. At low mole fraction

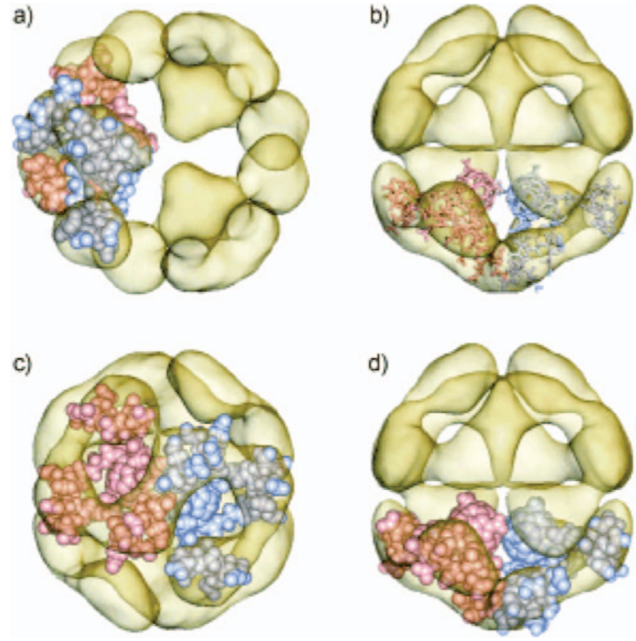

Figure 461. 3-D reconstructed spherical micelle and molecular fitting of hexakis dendronized fullerene amphiphiles. (a) CPK and (b) stick representations of two molecules viewed from the side (perpendicular to the C3 axis). (c) Same as in (b) but viewed along the C3 axis. (d) Same as in (b) but rotated by 90° about the C3 axis. Reprinted with permission from ref 1310. Copyright 2007 Wiley-VCH Verlag GmbH & Co. KGaA.

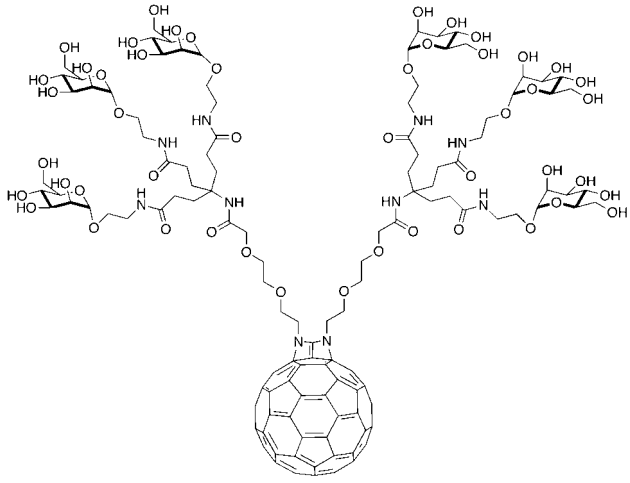

Figure 462. Dendronized fullerene peripherally functionalized with sugars.[1311]

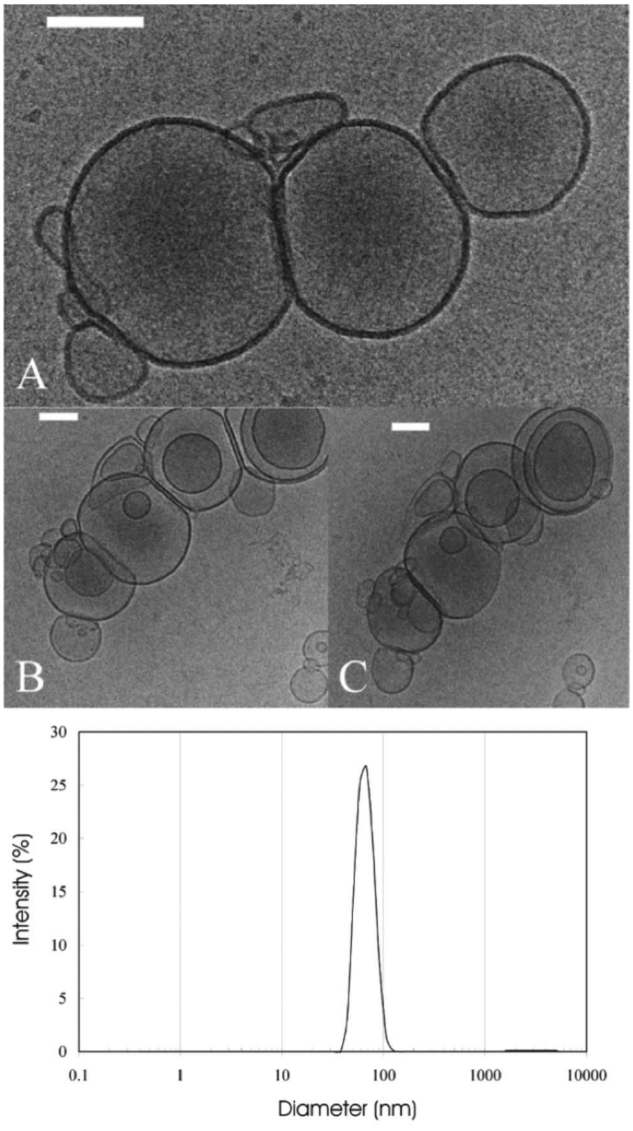

Figure 463. Cryo-TEM of buckysomes scale 100 nm. DLS of buckysomes in citrate buffer formed by hydration followed by extrusion. Reprinted with permission from ref 1312. Copyright 2007 Biomed.

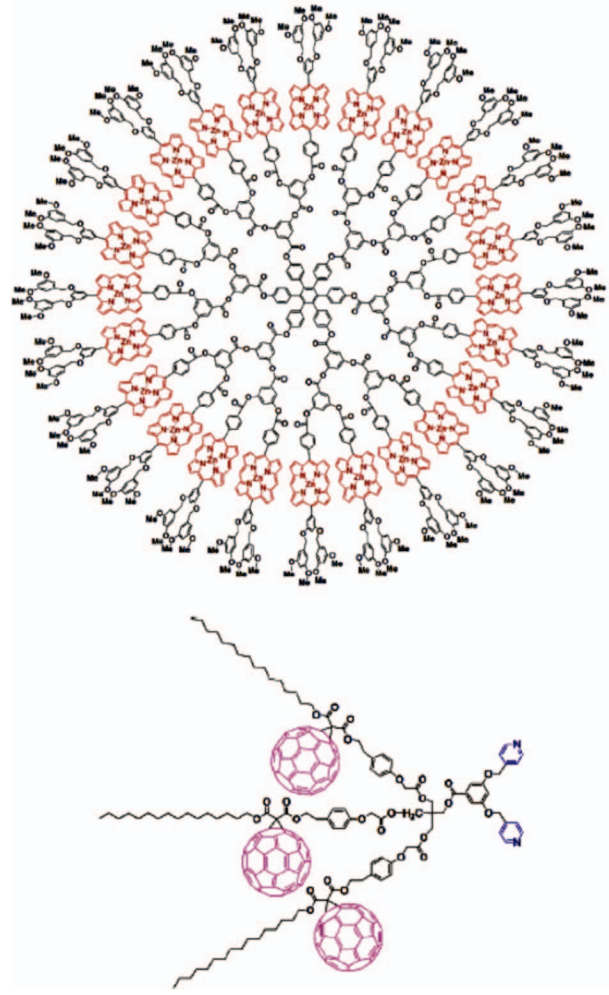

Figure 464. Donor−acceptor dendronized fullerene systems comprising Zn-porphyrin. Reprinted with permission from ref 1313. Copyright 2006 American Chemical Society.

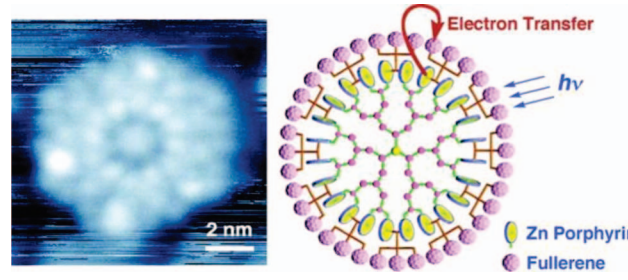

Figure 465. Ultrahigh vacuum (UHV)−STM image and schematic of petal-shaped porphyrin fullerene wheel. Reprinted with permission from ref 1313. Copyright 2006 American Chemical Society.

of imadazolium salts, micellar *Cub* phases were observed, while at higher loading levels, their self-assembly and self-organization into Φ_h was confirmed by XRD (Figure 472). In the Φ_h phase, anisotropic conductivity values were approximately 3.9×10^{-3} S cm^{-1}. This value is over 700 times higher than the conductivity of covalent analogues (5.3×10^{-6} S cm^{-1}) and was thought to be due to greater mobility of the ionic component in the noncovalent dendronized IL (Figure 472).[1331]

Kato also described the synthesis of ILs bearing L-glutamic acid dendrons that exhibit Φ_h phases at low temperature and a micellar *Cub* phase at high temperature (Figure 473).[1332] An order of magnitude increase in conductivity was observed

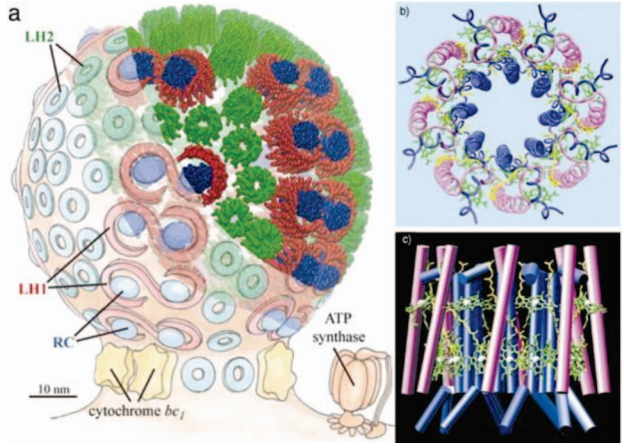

Figure 466. Spherical chromophore vesicle from R. spheroids constructed from AFM/LD data (a). Crystal structure of Light Harvesting Complex (LHC) 2 of *Rhodospirillum molishainum*. Reprinted with permission from ref 1316. Copyright 2007 PNAS.

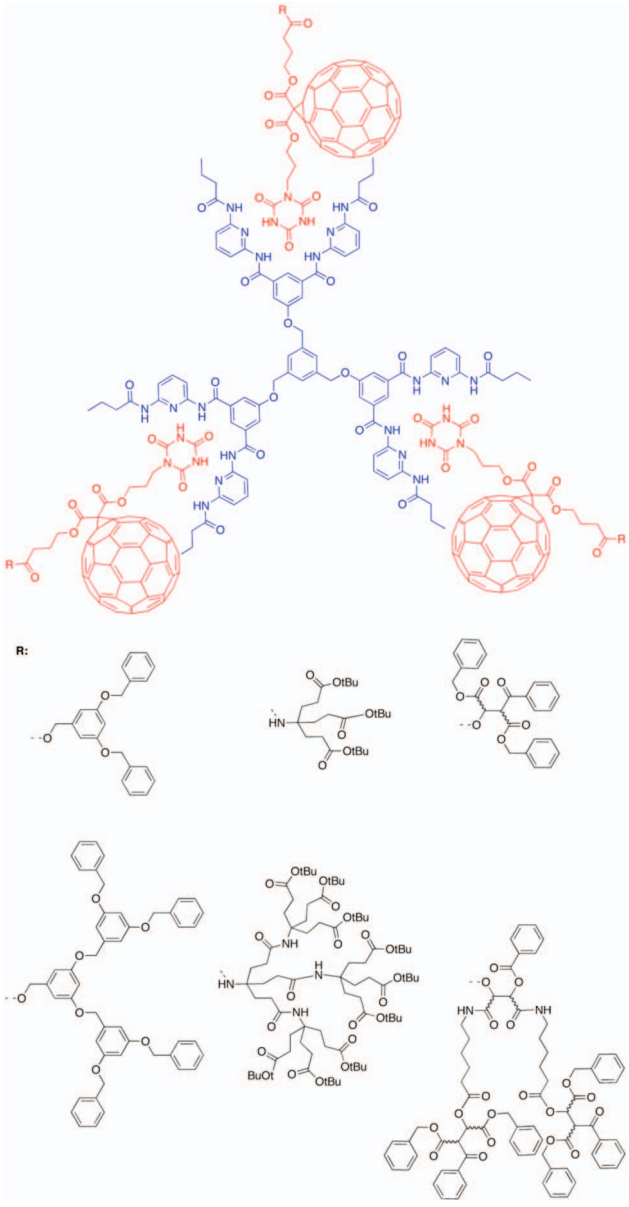

Figure 467. Dendronized fullerenes self-assembled via Hamilton receptors.[1319]

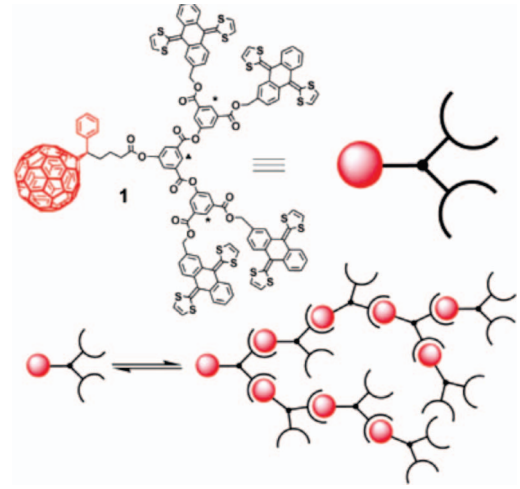

Figure 468. Self-assembled supramolecular dendron formed from dendronized fullerene. Reprinted with permission from ref 1320. Copyright 2008 American Chemical Society.

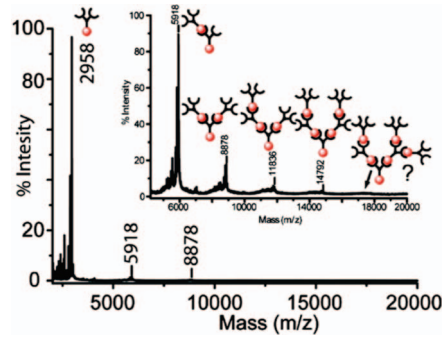

Figure 469. MALDI-TOF showing peaks for gas-phase oligomers of dendronized fullerene designed by Martin. Reprinted with permission from ref 1320. Copyright 2008 American Chemical Society.

in the Φ_h phase, allowing for temperature control switching of conduction from "on" to "off" (Figure 474).[1332]

Recently, Percec reported the synthesis and retrostructural analysis of a library of immidazolium, pyridinium, and onium salts functionalized with (3,4,5)12G1, (4-3,4,5)12G1, (3,4-3,5)12G2, (4-3,4-3,5)12G2, (4-3,4,5-3,5)12G2, and (3,4-$(3,5)^2$)12G3 dendrons (Figure 475).[1333] Through the application of the library approach to dendron construction, the principles of structural control for dendronized ILs was established. For the library of imidazolium salts, most structures, regardless of counteranion, self-assemble exclusively into supramolecular columns that self-organize into Φ_h lattices (Figure 476). However, (3,4-3,5)12G2$-CH_2Imz^+BF_4^-$,PF_6^- also exhibit $\Phi_{r\text{-}s}$ lattices, (3,4-3,5)12G2$-CH_2Imz^+Cl^-$ and (4-3,4,5-3,5)12G2$-CH_2Imz^+PF_6^-$ exhibit a thermoreversible *Cub* phase at higher temperature, and (3,4-$(3,5)^2$)12G3Imz^+Cl^- exhibits a thermoreversible *Tet* phase at elevated temperature. Interestingly, (3,4-$(3,5)^2$)12G3$Imz^+BF_4^-$,PF_6- self-assembles exclusively into spherical supramolecular dendrimers that self-organize into a *Tet* lattice. All onium salts functionalized with Percec-type dendrons self-organize into Φ_h lattices, except for (3,4,5)12G1$-CH_2Et_3N^+PF_6^-$, which self-organizes into a $\Phi_{r\text{-}s}$ lattice (Figure 477). Additionally, all pyridinium salts investigated self-organize into Φ_h lattices, though (3,4-3,5)12G2$CH_2Py^+Cl^-$ exhibits thermoreversible conversion

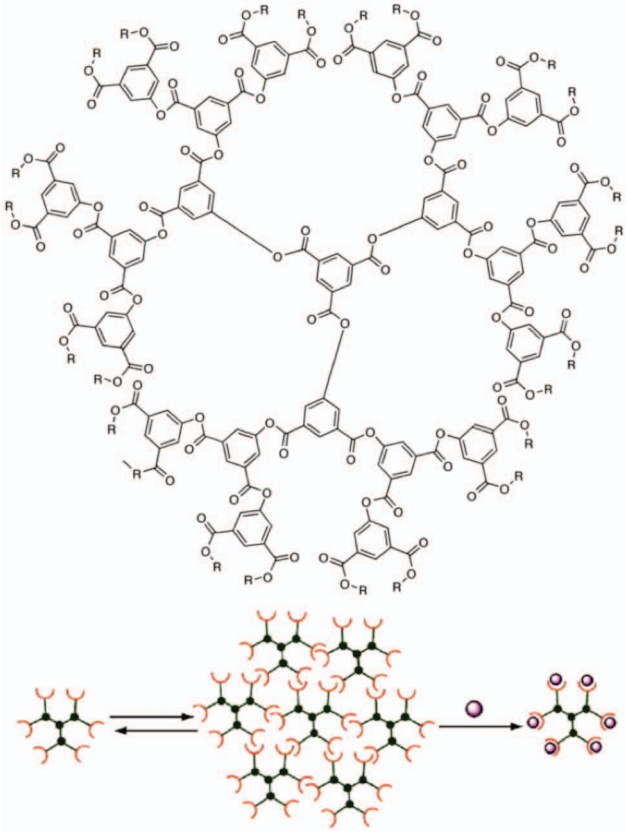

Figure 470. Self-assembly and disassembly of supramolecular dendrimers by Martin. Reprinted with permission from ref 1321. Copyright 2008 American Chemical Society.

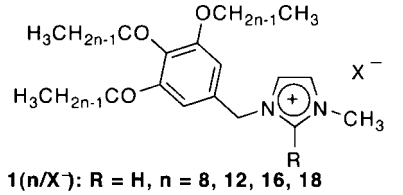

1(n/X⁻): R = H, n = 8, 12, 16, 18

1(12/X⁻): R = CH_3, n = 12

$X^- = BF_4^-, PF_6^-, CF_3SO_3^-, (CF_3SO_2)_2N^-$

Figure 471. Dendronized imidazolium salts.[1330]

to a *Cub* lattice (Figure 477). In general, it was observed that the T_{iso} decreases with the radius of the anion, though in the cases of the triethylammonium salts, the T_{iso} for Cl^- is lower than expected.

11.2. Onium Salts

Serrano reported ammonium salts of PPI dendrimers and (3,4,5)10G1COOH and (3,4)10G1COOH (Scheme 101).[1217] PPI dendrimers substituted with 4-decyloxybenzoic acid and (3,4)10G1COOH exhibited S_A phases, whereas salts with (3,4,5)10G1COOH exhibited Φ_r or Φ_h phases. This trend was observed regardless of the generation number of the parent PPI dendrimer. It was noted that the covalently bonded amide analogues prepared via the reaction of (3,4)12G1Cl and amino-terminated PPI dendrons exhibited columnar mesophases above 60 °C, whereas the ionic analogue displayed S_A phase at room temperature.

Table 7. Summary of Properties of Dendronized Ionic Liquids (Adapted with Permission from Ref 1330; Copyright 2007 Chemistry Society of Japan)

compound	first cooling[a]						second heating[a]			
1(8/BF_4^-)	I	130	Φ_h	−37	g	g	−29	Φ_h	133	I
1(12/BF_4^-)	I	182	Φ_h	8	k	k	17	Φ_h	83	I
1(16/BF_4^-)	I	175	Φ_h	33	k	k	74	Φ_h	177	I
1(18/BF_4^-)	I	145	Φ_h	60	k	k	88	Φ_h	148	I
1(8/PF_6^-)	I	73	Φ_h	−38	k	g	−33	Φ_h	78	I
1(12/PF_6^-)	I	147	Φ_h	5	k	k	12	Φ_h	151	I
1(16/PF_6^-)	I	167	Φ_h	48	k	k	55	Φ_h	167	I
1(18/PF_6^-)	I	162	Φ_h	60	k	k	68	Φ_h	161	I
1(8/$CF_3SO_3^-$)	I			−72	g	g	−56 I	−20	Cr 1	I
1(12/$CF_3SO_3^-$)	I	73	Φ_h	10	k	k	63			I
1(16/$CF_3SO_3^-$)	I	116	Φ_h	52	k	k	78	Φ_h	117	I
1(18/$CF_3SO_3^-$)	I	115	Φ_h	60	k	k	86	Φ_h	119	I
1(8/$(CF_3SO_3)_2N^-$)	I			−70	g	g	−58 I	−19	Cr 2	I
1(12/$(CF_3SO_3)_2N^-$)	I			13	k	k	37			I
1(16/$(CF_3SO_3)_2N^-$)	I	55	Φ_h	52	k	k	55	Φ_h	60	I
1(18/$(CF_3SO_3)_2N^-$)	I	76	Φ_h	63	k	k	66	Φ_h	77	I
2(12/BF_4^-)	I	177	Φ_h	10	k	k	19	Φ_h	174	I
2(12/PF_6^-)	I	157	Φ_h	5	k	k	58	Φ_h	155	I
2(12/$CF_3SO_3^-$)	I	83	Φ_h	13	k	k	66	Φ_h	85	I
2(18/$(CF_3SO_3)_2N^-$)	I			14	k	k	51			I

[a] Transition temperatures recorded at 10 °C/min.

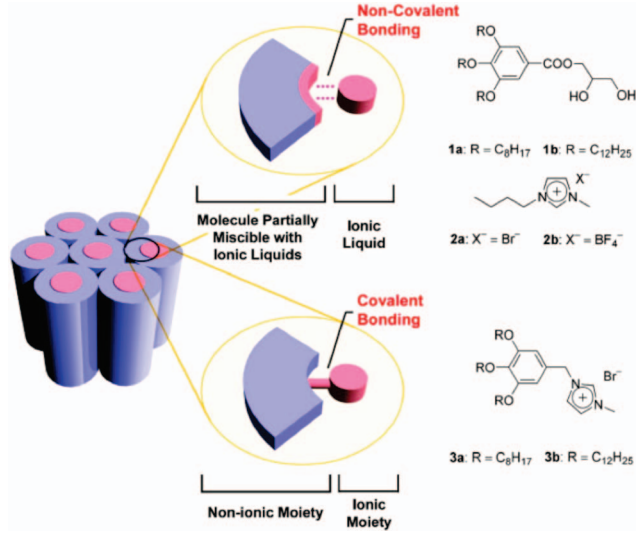

Figure 472. Self-assembly of noncovalently and covalently dendronized ILs. Reprinted with permission from ref 1331. Copyright 2008 American Chemical Society.

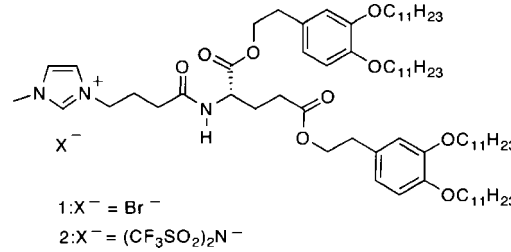

1:X^- = Br^-

2:X^- = $(CF_3SO_2)_2N^-$

Figure 473. Glutamic acid dendronized ionic liquids by Kato.[1332]

In addition to imidazolium salts, Kato described other dendronized ILs.[1334] The structurally simplest dendronized ILs were dendronized quaternary ammonium salts. The salts were shown to form LC *Cub* bicontinuous Cub_{bi} and Φ_h phases when dendronized with (3,4,5)*n*G1 Percec-type dendrons (Figure 478). Ionic conductivities of unaligned samples in the Cub_{bi} phase at room temperature exhibited higher

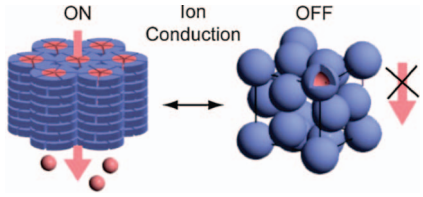

Figure 474. Self-organized switching in response to temperature from conducting to insulating of dendronized ionic liquids. Reprinted with permission from ref 1332. Copyright 2008 Japanese Society of Chemistry.

conductivities than analogues displaying Φ_h phases at room temperature (Figure 479).[1334] The structural and retrostructural analysis of supramolecular structures self-assembled from onium salts functionalized with Percec-type dendrons was described in section 11.1.

11.3. Pyridiniums and Viologens

Kato reported viologens bisdendronized with (3,4,5)*n*G1 Percec-type dendrons (Figure 480).[848] When the dendron contains octyl tails ($n = 8$), self-organization into Φ_h lattices is observed. Dodecyl ($n = 12$) and hexadecyl ($n = 16$) tails mediate self-organization into Φ_r phases. Other bisdendronized viologens have been reported, but self-organization was not noted.[1335] Stoddart and Venturi also reported polyviologen dendrimers that are capable of forming host−guest complexes with anionic dyes (Figure 481).[1336] Kato also reported dendronized tripodal pyridinium salts,[1337] which exhibited a Φ_r phase when the counterion is PF_6^-, a Φ_h phase when the counterion in BF_4^-, and the thermoreversible Φ_h and *Cub* phases when the counterion is Br^- (Figure 482). The structural and retrostructural analysis of

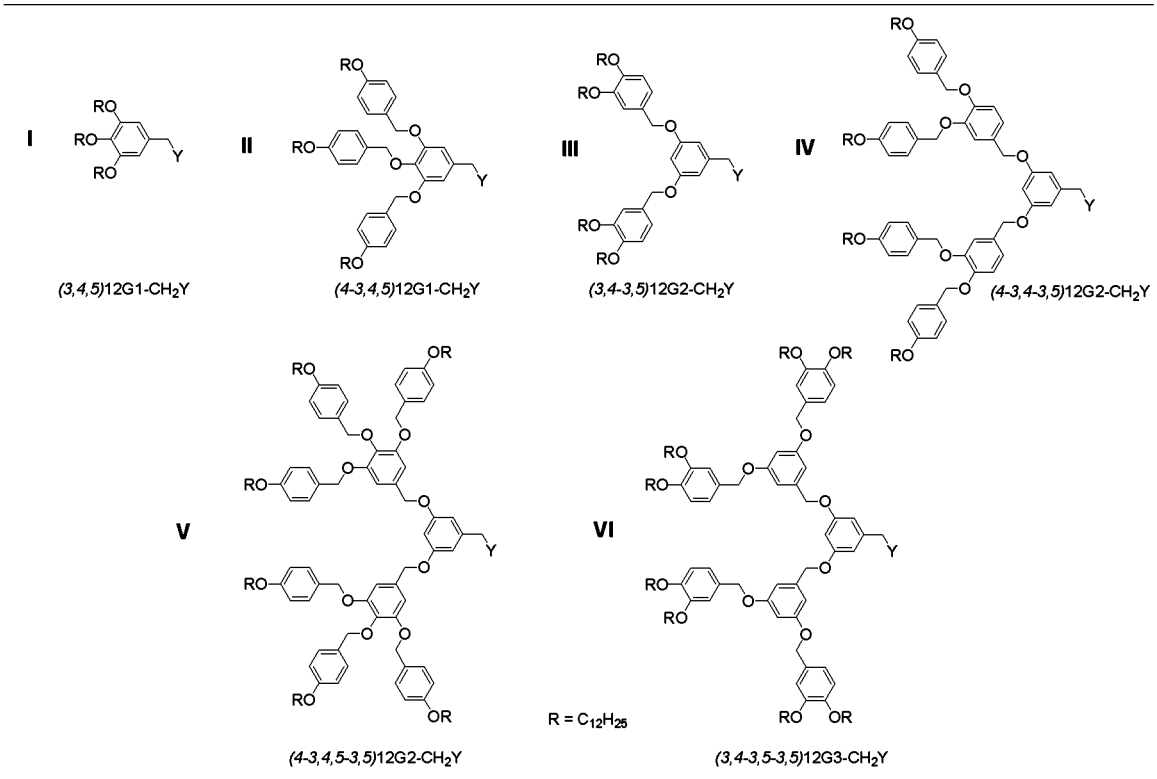

Y	I	II	III	IV	V	VI
	X⁻					
	**a** = Cl^- **b** = BF_4^- **c** = PF_6^-	**a** = Cl^- **b** = BF_4^- **c** = PF_6^-	**a** = Cl^- **b** = BF_4^- **c** = PF_6^-	**a** = Cl^- **b** = BF_4^- **c** = PF_6^-	**a** = Cl^- **b** = BF_4^- **c** = PF_6^-	**a** = Cl^- **b** = BF_4^- **c** = PF_6^-
$Et_3N^+X^-$	**d** = Cl^- **e** = BF_4^- **f** = PF_6^-	**d** = Cl^- **e** = BF_4^- **f** = PF_6^-	**d** = Cl^- **e** = BF_4^- **f** = PF_6^-			
$Pr_3N^+X^-$	**g** = Cl^-	**g** = Cl^-	**g** = Cl^-			
	**h** = Cl^-	**h** = Cl^-	**h** = Cl^-			

Figure 475. Library of imidazolium, pyridinium, and onium salts functionalized with Percec-type dendrons. Reprinted with permission from ref 1333. Copyright 2009 John Wiley & Sons, Inc.

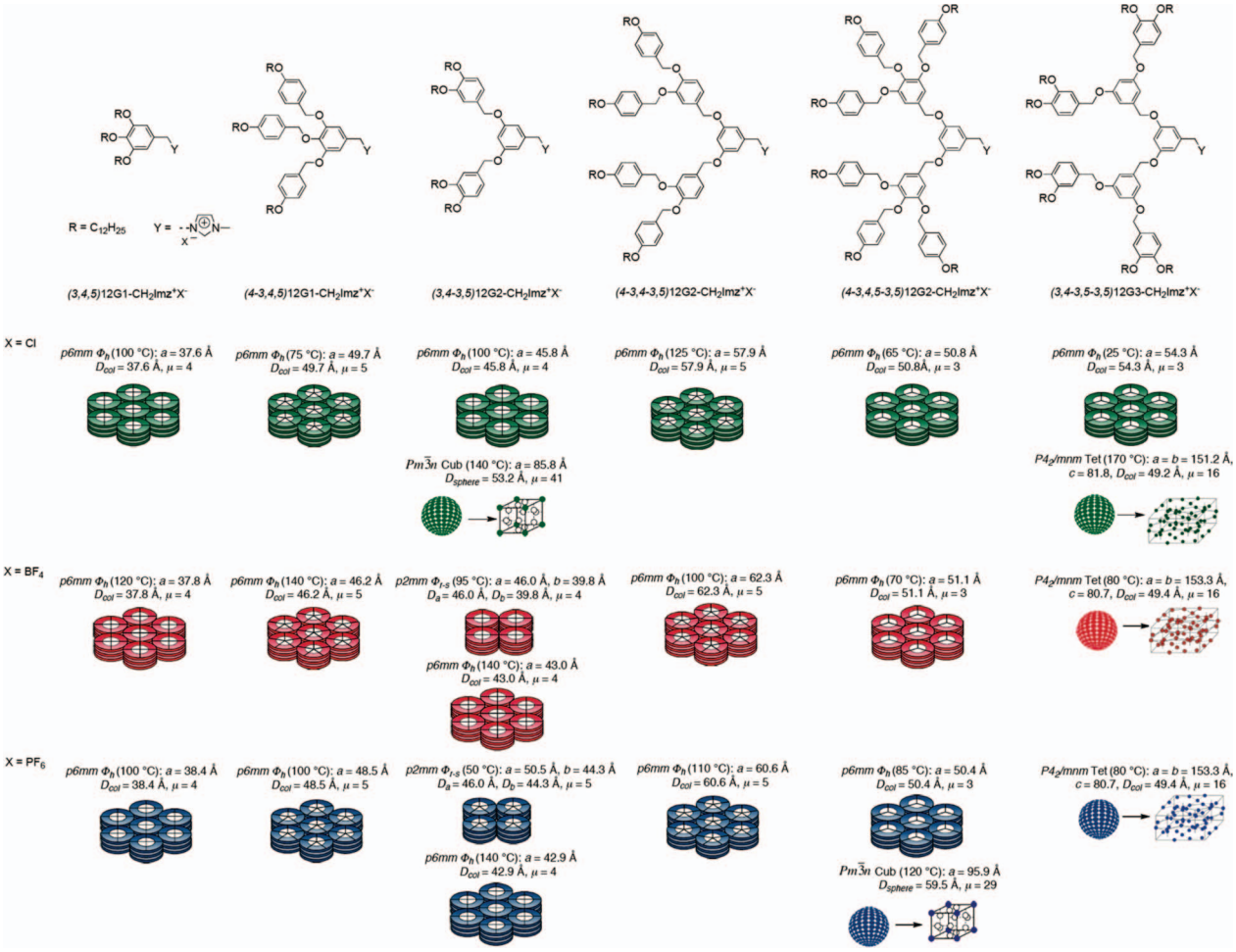

Figure 476. Retrostructural analysis of imidazolium salts functionalized with Percec-type dendrons. Reprinted with permission from ref 1333. Copyright 2009 John Wiley & Sons, Inc.

supramolecular structures self-assembled from pyridinium salts functionalized with Percec-type dendrons was described in section 11.1.

Möller investigated Percec-type dendron-rods containing sulfonate salt end-groups (Figure 483).[768] All structures exhibit LC phases by TOPM. Na salts exhibit phases with greater thermostability. SFM and gelation experiments indicated columnar superstructures.

11.4. Dendronized Metal Carboxylates

While no longer considered ILs because of their thermal instability and generally high melting points, self-assembling dendronized metal carboxylates are topologically related to modern ILs. As discussed previously (section 2.2.2), Percec reported that, while (3,4,5)*n*G1−COOH is a crystalline solid, (3,4,5)*n*G1COOX (X = Li, Na, K, Rb, and Cs) self-assembles into supramolecular spheres and columns that self-organize into BCC or *Cub* 3-D lattice and Φ_h or $\Phi_{r\text{-}c}$ 2-D lattices, respectively.[318] Unlike many other organic carboxylates, dendronized metal carboxylates as well as their predecessor dendronized crown-ethers/salt-complexes[210] (see section 6.1) are ionic liquids at room temperature.

Gin also reported the synthesis of (3,4,5)G1COOX (X = Na, Ni, Cd, Eu, Ce) Percec-type metal carboxylates with photopolymerizable acryloyl periphery groups.[1338−1343] Nanocomposites with PPV were obtained by preparing a mixture of 8:1:1 (3,4,5)G1COOX/PPV/2-hydroxy-2-methylpropiophenone (photoinitiator). The mixture was shown by XRD to exhibit inverse Φ_h self-organization, which was retained following photopolymerization (Scheme 102). This methodology was employed in the synthesis of Pd nanoparticles within the lyotropic LC polymer for use as a catalyst for the Heck reaction. Pd(0) nanoparticles were prepared via ion-exchange of Na^+ in the lyotrotpic LC polymer with $Pd^{II}Cl_2$(1,5-cyclooctadiene), followed by reduction with H_2 gas. Formation of the nanoparticles resulted in loss of order but provided good catalytic activity. 91−100% yield was achieved for the Heck coupling of activated aryl halides with styrene or butyl acrylate, though much lower conversion was observed for unactivated analogues.[1344]

Trivalent lanthanides (Ln)s have found extensive use in fiber-optics, most notably in Er-doped fiber amplifiers (EDFAs). Development of lanthanide-based molecular systems is often plagued by the inherent self-quenching effects of clustered lanthanides. Fréchet has reported site isolation of Ln^{3+} ions (Er^{3+}, Eu^{3+}, Tb^{3+}) in dendritic "molecular balls" exhibiting enhanced luminescence with increasing generation number in both bulk and solution (Figure 484).[1345,1346] This effect was attributed to an "antennae effect" involving ET from the dendritic ligands to the lanthanide core and a "shell effect" arising from the site isolation of Ln^{3+} provided by the dendron's coat. Similar systems were reported by Motoda

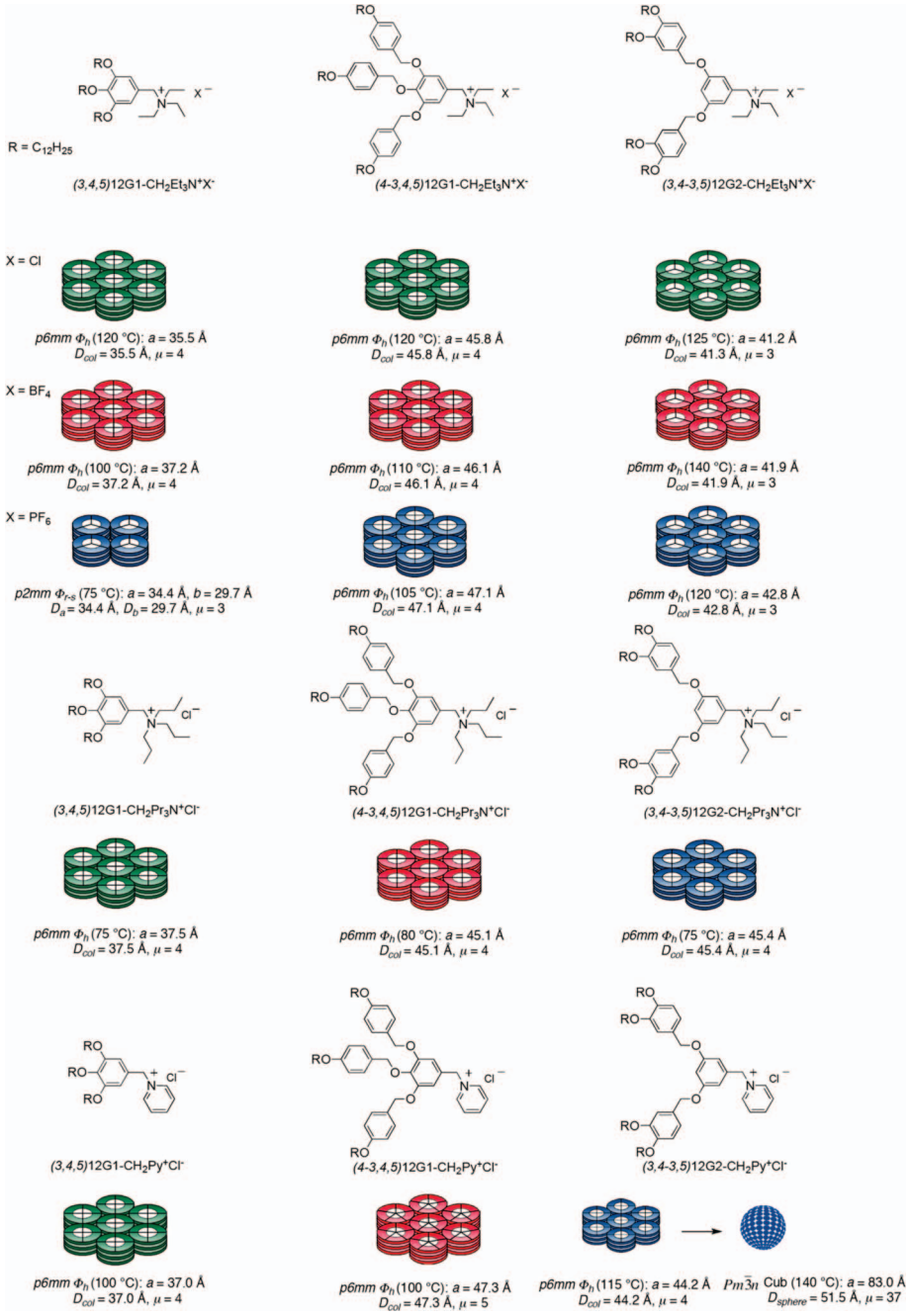

Figure 477. Retrostructural analysis of pyridinium and onium salts functionalized with Percec-type dendrons. Reprinted with permission from ref 1333. Copyright 2009 John Wiley & Sons, Inc.

Scheme 101. Dendronized PPI (Reprinted with Permission from Ref 1217; Copyright 2006 American Chemical Society)

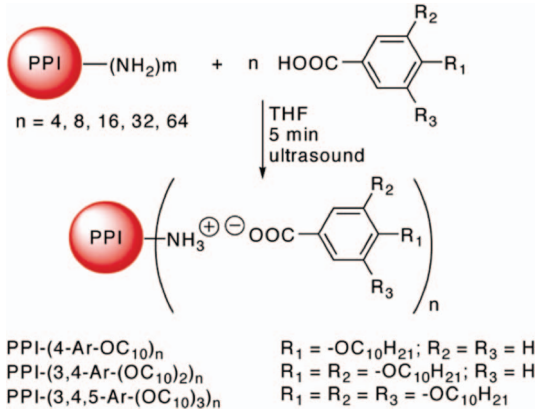

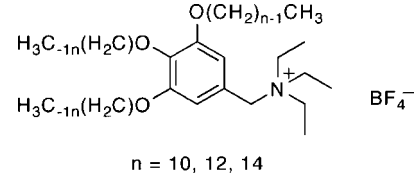

Figure 478. Dendronized quaternary ammonium salts. Reprinted with permission from ref 1334. Copyright 2007 American Chemical Society.

and Kawa for Fréchet-type dendrons with modified branching patterns[1347] and by Lindgren for bis(MPA) dendrons peripherally fuctionalized with pentafluorophenyl groups (Figure 485).[1348]

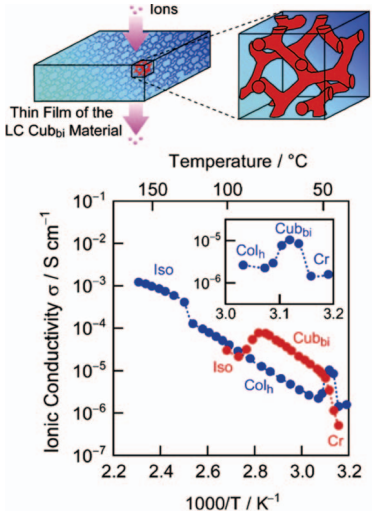

Figure 479. Ionic conductivity in self-organized dendronized ionic liquids by Kato et al. Reprinted with permission from ref 1334. Copyright 2007 American Chemical Society.

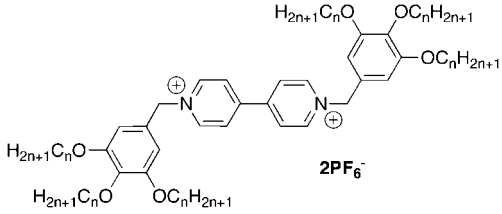

Figure 480. Bisdendronized viologen.[848]

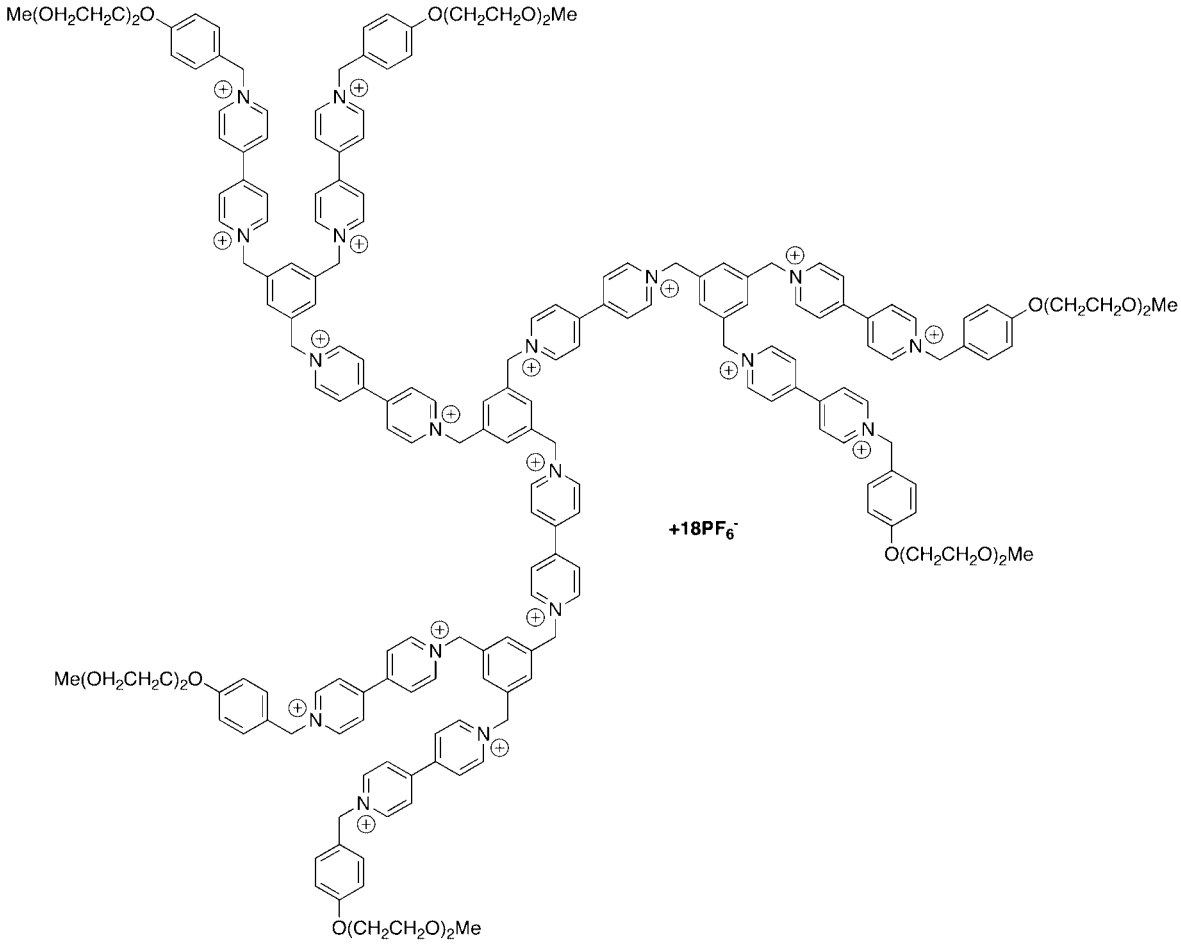

Figure 481. Dendritic polyviologen.[1336]

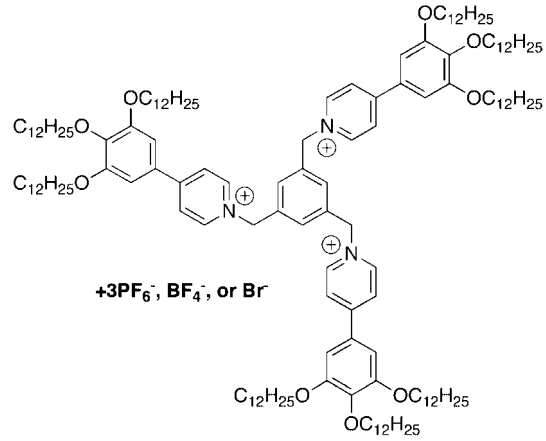

Figure 482. Dendronized tripodal pyridinium salts.[1337]

12. Applications

Self-organizable dendronized polymers, supramolecular polymers, and related topologies provide access to a large diversity of self-assembled and self-organized 3-D structures that have captivated the interest of many research groups. All such molecular assemblies provide insight into the molecular design strategies and principles of self-assembly and self-organization. In many cases, specific applications have been envisioned or even designed and demonstrated for these assemblies. Some of these applications have been reviewed previously.[39,43,95] In each dendronized topology section, notable applications were mentioned. As the unique functions provided through the nanoscale tailoring of struc-

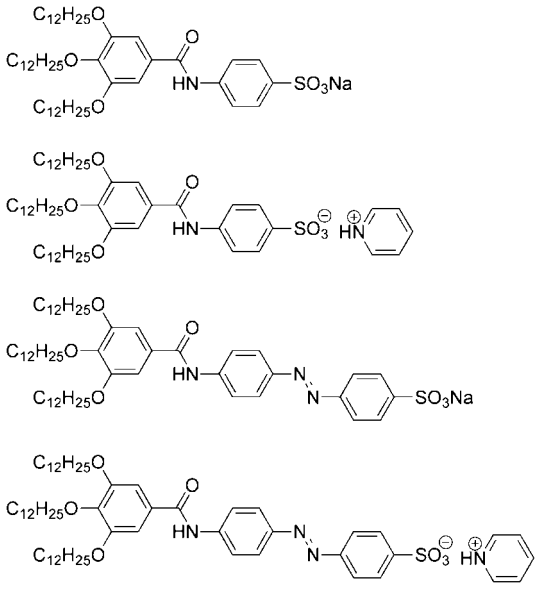

Figure 483. Sulfonate-capped DRs.[768]

ture through dendronization help to drive continued interest and development in this field, it is beneficial to organize the applications discussed above.[156,1349]

In 1959, Feynman suggested that "there is indeed plenty of room at the bottom"[1350] and heralded the age of nanotechnology. Feynman was convinced that the ultimate approach to nanoscale engineering would be through physical methods such as nanolithography and largely discounted the chemical approach to the problem. Feynman focused on the need for the development of tools to directly manipulate matter "atom-by-atom". However, nature has shown us how complex nanoscale function can be achieved through programmed self-assembly and self-organization.

12.1. Ionic, Electronic, Magnetic, and Electrooptical Applications

12.1.1. Ion-Conductive Materials

Percec-dendron jacketed methacrylates poly[(3,4,5)-12G1COO−*n*EO−MA] mixed with LiOTf demonstrate relatively high anisotropic ion conductivities along the axis of the Φ_h self-organized columns (Figure 93).[210,442] Crown-ethers and benzocrown-ethers dendronized with Percec-type dendrons were also found to exhibit high anisotropic ionic conductivities when treated with alkali salt (Figure 286),[210,212,442] which could be transformed into ion-selective membranes or organels via periphery polymerization (Figures 180 and 181).[297,680,682,683] Later, Kato replaced the ion-binding crown-ethers with imidazolium groups to create ion-conductive membranes that could be oriented parallel or perpendicular

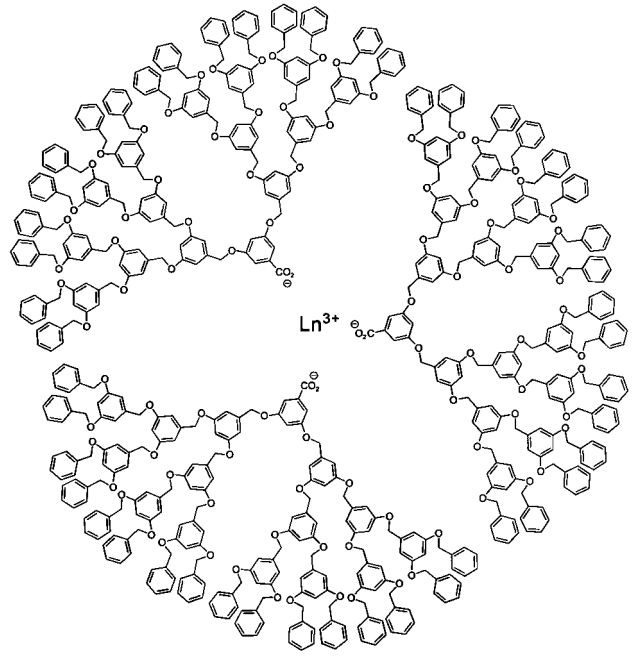

Figure 484. Fréchet-type dendritic lanthanide carboxylates.[1345,1346]

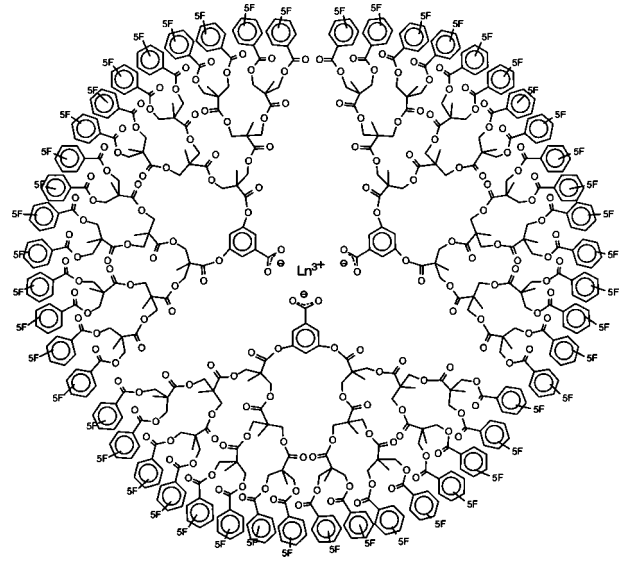

Figure 485. Lanthanide dendrons dendritic carboxylates reported by Lindgren.[1348]

Scheme 102. Polymerized Lyotropic LC Percec-type Metal Carboxylates; Adapted from Refs 1338−1343

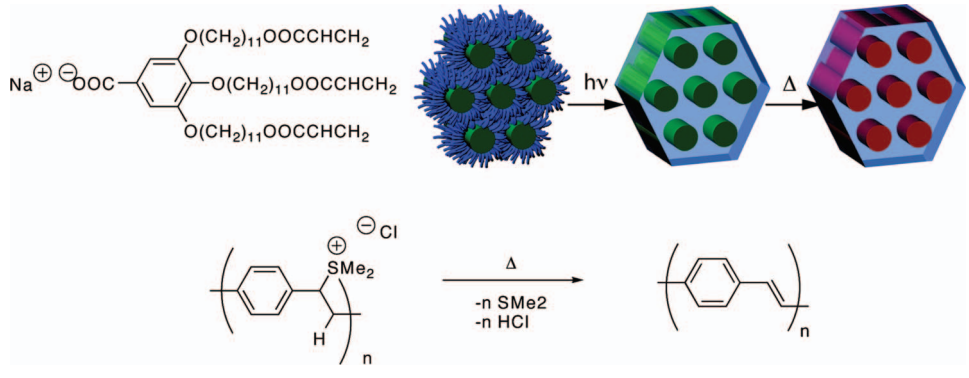

to ITO surfaces (Figure 182), much like Percec's earlier systems.[685] Dendronization of imidazolium with L-glutamic acid dendrons exhibit thermal switch between conductive Φ_h organization and nonconducting *Cub* organization (Figure 474).[1332] Conducting ILs composed of dendronized ammonium salts were also investigated by Kato (Figures 478 and 479).[1334] Wiesner has reported PEG dendron−coils[735,736] and dendron−coil−dendrons[734] that bind LiOTf to form 1-D, 2-D, and 3-D network ion-conducting materials (Figure 204).

12.1.2. Electron- or Hole-Conducting Materials

Self-assembly of electron-acceptor (Figure 82)[364] and electron-donor (Figure 80)[363] groups dendronized with semifluorinated Percec-type dendrons resulted in self-repairing (Figure 126) helical pyramidal columns. Mixtures of dendronized electron-acceptor and electron-donor with each other in a 1:1 ratio or with donor or acceptor polymers resulted in self-organized EDA columns capable of efficient electron and hole transport (for example, $\mu_{hole} = 2.3 \times 10^{-3}$ $cm^2\ V^{-1}\ s^{-1}$ and $\mu_{electron} = 7.5 \times 10^{-4}\ cm^2\ V^{-1}\ s^{-1}$) (Figure 125).[358] Similarly, dendronized TTF (Figure 393) has been shown to form fibrous gels with potential for electron-transport applications.[1188]

Using molecules originally designed by Würthner,[1141] dendronized PBI (Scheme 74) have been shown to self-organize into Φ_h lattices with electron mobility parallel to the columnar axis, which exceeds that of amorphous silicon.[1146] Charge carrier lifetimes were improved by bay-substitution, which improves intracolumnar ordering (Figure 355).[1147] Percec and Singer have also investigated electron mobility in other dendronized PBIs (Figure 357).[1150] Electron mobility was enhanced by orders of magnitude in the self-organized state (Figure 358). Würthner and Meijer have investigated PBIs functionalized with dendronized OPVs through H-bond as p-n heterojunctions for molecular diodes (Figure 363)[1156,1157] or as field-effect transistors (Figure 367).[1159] Stupp has investigated dendron−rod−coils containing a conjugated aromatic rod segment that self-assembles into nanoribbons (Figure 222).[784,785] When the rod-segment is an oligo(thiophene), a 3-order-of-magnitude increase in conductivity in the nanoribbon state was observed (7.9×10^{-5} S/cm), proving these materials are useful as aligned conducting materials. Kato showed relatively high electron mobilities for dendronized fullerenes with pendant oligothiophene groups (Figure 456).[1300−1303]

12.1.3. Light-Harvesting Materials

A variety of conjugated polymers including PPV[601−605] (Figure 151), poly(phenylene ethynylene)[608−612] (Figure 152), poly(enediynes) (Figure 154),[615−617] poly(thiophenes) (Figure 155),[618,619] poly(thienopyrolles) (Figures 156 and 157),[620,621] polyfluorenes (Figures 158 and 159),[622−634] polyisocyanides (Scheme 45 and Figure 161),[637,638] and conjugated aromatic polyimides[639,640] have been jacketed with dendrons, thereby mediating chain segregation and interruption of electronic coupling between chains, which results in quenching of the photoexcited state. By separating chains via dendron-mediated "disassembly", more effective candidates for PLED materials[126,128] can be prepared. Often the inherent LC N phase for the dendronized polymers allows for easy alignment of films to form LC display materials.[639,640] Schlüter showed that polymers dendronized with branched thiophenes retained the absorption and emission characteristics of the parent dendrons, demonstrating the ability to make processable electronic materials (Scheme 30).[480,481]

Bardeen and Thayumanavan have reported rod−coils, dendron−rods, and dendron−rod−coils composed of (diarylamino)pyrene functionalized Fréchet dendrons, benzothiadiazole rods, and polymethacrylate coils with naphthalene bisimide side chains for electron transfer (ET) or light-harvesting applications (Figure 223, left).[786] Optimal ET was achieved in the full dendron−coil structure. Dendronized fullerenes complexed to porphyrin containing dendrimers have been used as light-harvesting mimics of LH1 and LH2 (Figures 464 and 465).[1313]

Complexes of Fréchet-type and bis(MPA) carboxyates with lanthanides (Er^{3+}, Eu^{3+}, Tb^{3+}) have been investigated for fiber-optic applications (Figures 484 and 485).[1345−1348] An "antennae effect" wherein the dendritic ligand transfers energy efficiently to the metal core and a "shielding effect" that prevents aggregation of the lanthanide cations into clusters allow for improved performance. These systems are of particular interest for the design of signal amplifiers.

12.1.4. Nano-Patterned Materials for Information Storage

Semifluorinated Percec-type biphenyl methyl ether dendrons were shown to exhibit perpendicular alignment to magnetic fields (Figure 85).[368] Such systems have potential for magnetic data-storage devices.

Hawker reported the patterned photopolymerization of Fréchet dendritic macromonomers in a HMDI/PPT matrix.[484] The resulting material was a GRIN film useful for optical data storage (Figure 114). Similar patterning could be achieved via surface activation with AFM to produce anchoring sites for visualizable dendronized PS (Figure 118).[506] Other exotic dendronized polymers have been shown to exhibit NLO properties (Figure 122).[131,513−517,519]

Green and Choi[1254] demonstrated that on/off switchable dendronized [2]-rotaxanes prepared by Stoddart[1252] could be used as encodable memory units for DRAM. This approach allows for the construction of memory circuits over an order of magnitude smaller than existing lithographic methods.

12.2. Biomedical Applications

A number of dendronized systems self-assemble into micellar or vesicular topologies that have potential applications for medical imaging,[136] drug delivery,[133,134,136,1351,1352] and gene-transfer therapy.[137,380,482,664,702,737,756,761,766,770,792,793,811,815,816,850,872−875,1272,1273,1312,136] Additionally, self-immolative dendrons and dendrimers that do not self-assemble have been used for sensing applications wherein the signal is amplified via a dendritic chain reaction.[1353−1356]

12.2.1. Drug Delivery

AB_4 and AB_5 branched[275] Percec-type dendrons were shown to self-assemble into hollow spherical supramolecular dendrimers that can encapsulate guest molecules (Figure 64). Like the general class of micellar architectures, these structures have implication for drug delivery as well as for sensing applications. Phototriggered release of guests from within self-assembled micelles was achieved with dendronized azobenzene (Figure 210).[767] Unusually low CMCs and high drug loadings were demonstrated for micelles formed from poly(γ-*n*-dodecyl glutamate) modified at one

chain end with dendritic PEG (Figure 212).[728] Lee has reported micelles derived from dendron−rod−dendrons that undergo thermal conversion from a porous to a closed state (Figure 243).[820] Grayson has reported dendronized cavitands that can form dimerized capsules around a lipophilic guest molecule in solution (Figure 332).[1112] Lee has reported micelles and vesicles derived from dendronized Tat-CPP, a functional peptide that mediates translocation across membranes. Micelles and vesicles present Tat-CPP on the surface and are, therefore, of interest as drug-delivery vehicles (Figure 250).[862,863] Dendrisomes, DCs that form vesicular structures, have also been explored for drug-delivery applications (Figure 254).[874,875]

12.2.2. Gene-Transfer Therapy

Encapsulation or surface protection of DNA is useful for gene-transfer therapy. PAMAM dendrimers have been shown to bind DNA and enhance expression in mammalian cells.[906,1357−1362] Diedrich has reported effective gene-transfection of GFP in HeLa cells via self-assembling amphiphilic DRDs (Figure 245).[140,850−852] Self-assembly and gene transfection were shown to be related. Schlüter and Rabe have reported cationic dendronized PS, which forms a suprahelical structure around anionic DNA (Figure 167).[646,647] Block-copolymers of dendronized and nondendronized poly(norbornene) have also been shown to encapsulate DNA into spherical aggregates (Figure 196).[705] Molecules of similar structure to dendrisomes have also been utilized in DNA transfection experiments.[1363−1365]

12.2.3. Membrane Transport

Dendritic dipeptides have been shown to self-assembly in solution, bulk, and lipid bilayers into hollow channels (Figure 66).[171,312,350] These channels functionally mimic aquaporin, allowing for proton, water, and cation transport (Figure 67). Synthetic channels of this type have potential for sensing applications and as novel antibiotics. Vinogradov has used dendronized porphyrins and tetrabenzoporphyrins as membrane-impermeable pH sensors with no overlapping emission.[1078] Additionally, these systems have been used to detect proton transport across membranes (Figure 310).[171,312,350]

12.2.4. Cell-Structure Manipulation

Stupp has also reported the synthesis of dendronized bioconjugates that self-assemble into scaffolds for bladder tissue engineering and mineralization (Figure 247).[856−858]

Roy reported the synthesis of twin dendrons peripherally functionalized with fucoside and galactoside units. These systems were targeted to specifically bind lectins found in *Pseudomonas aeruginosa* and treat this bacterial infection in immuno-compromised and cystic fibrosis patients (Scheme 64).[952]

Lee reported dendron−wedges, functionalized at the periphery with mannose (Scheme 65).[793] Self-assembly into cylindrical and spherical micellar objects could be switched via the addition of Nile Red intercalating agent (Figure 264). The effect of micelle on *E. coli* cells was dependent on shape. Bacterial cell interaction was also observed for dendronized glycopeptides conjugates (Figure 265).[953,954]

12.3.5. Medical Imaging

Low MW Gd^{III} nondendronized complexes are already FDA approved as MRI contrasts agents.[134,1051−1053] PAMAM and PLL dendrimers peripherally functionalized with azamacrocycle or related Gd^{III} binding groups are currently being developed as next-generation contrast agents that take advantage of the inherent multivalency and low renal excretion rate.[25,1054−1056] Schering has commercialized PLL−Gd^{III} complexes (Gadomers).

12.3. Nanomechanical Applications

12.3.1. Control of Stiffness, Surface, and Solution Properties

The most primitive mechanical application is to alter the structural properties of a material. Dendron-jacketing of flexible polymers often results in a stiffening of the polymer backbone, providing the material with greater structural resilience.[445,1366] Hierarchical organization of these polymers into fibrils can result in improved properties (Figure 120).[510] Further, the dendronization of a polymer often mediates the formation of a persistent shape, be it a rigid-rod or a sphere (Figure 103). In some cases, dendronization provides for thermoresponsive or force-responsive shape change. Supramolecular polymers derived via the self-assembly and self-organization of Percec-type dendrons can be made more structurally rigid through semifluorination of the aliphatic tails (Figure 17).[306] The highly anisotropic viscoelastic properties[1367,1368] of willowlike dendrons were investigated.[1369] Additionally, Percec has reported twin-dendritic benzamides that self-organize in the gel state.[1237] These dendronized organogels display rare thixotropic behavior wherein the material reforms its self-organized structure after deformation by shear forces.

Kato reported 1,6-bis(phenylethynyl)pyrene bis-dendronized with Percec-type dendrons, which self-assemble into *Cub* lattices (Figure 349).[835] Shear induces the transformation of the lattice to a columnar phase with different optical absorption and emission. These shear-responsive materials can potentially be used as indicators of a mechanical deformation.

Self-assembly of dendronized polymers,[297,680,682,683] dendron−rods (Figures 483 and 252),[768,866,867] dendron−rod−coils (Figures 218 and 220),[773,780−783] and dendron−rod−dendrons (Scheme 76 and Figures 368 and 383)[1160,1181] into supramolecular fibers can allow for the synthesis of novel organic gels.[1370] In particular, the use of Stupp's dendron−rod−coils has allowed access to soft-organogels of styrene that could be converted to harder birefringent materials via subsequent polymerization.[776] Other hard materials could be formed via the binding of the helical ribbon dendron−rod−coil organogelators to inorganic nanocrystalites such as CdS, ZnO, or TiO_2 (Figure 219).[777−779]

Self-cleaning textiles have been prepared by grafting poly(glycidol methacrylate) from the surface of cellulose and *growing* G1−G2 perhydrogenated and perfluorinated dendrons *from* the ring-opened glycidol side chains (Scheme 35).[530] Perhydrogenated dendron side groups resulted in superhydrophobic materials, while perfluorinated dendron side groups were also oleophobic.

12.3.2. Nanomechanical Actuators

Nanomechanical actuators have been realized through the functionalization of *cis*-PPA with a variety of Percec-type dendrons (Figure 146).[576,577] Thermoreversible isomerization of a compressed *cis*-cisoidal helical dendronized PPA to higher-pitch *cis*-transoidal geometries, resulting in polymer expansion along the helical axis. This expansion can be harnessed as mechanical force, pushing objects 250× its own weight. Deuterated and periphery-modified poly[(3,4,5)12G1−4EO−MA] was suggested to exhibit cooperative rotation beneficial for molecular rotor applications (Figure 95).[434]

12.4. Chemical Synthesis

While not always relying on self-organization, dendronization of polymers and related topologies have been used to catalyze or control chemical reactions.[142,142] Dendronized topologies have been used as supports for single-site catalysis. Dendrimers offer many advantages over traditional polymer support catalysts such as enhanced solubility and precise size, allowing for physical separation and recycling. This has been examplifed by van Koten for the catalysis of the Kharasch reaction via silane dendrimers[1371] or Fréchet dendrons[1372] functionalized with arylnickel(II) complexes and by van Leeuwen for allylic alkylation using palladated carbosilane dendrimers.[1373] These dendron-supported catalysts can be effectively removed via nanofiltration techniques.[1374] Rodlike alternating copolymers of pyrrolidine jacketed with paraffin-capped bis(MPA)-dendrons and pyrrolidinopyridine were shown to catalyze the difficult esterification of tertiary alcohols with pivalic anhydride (Scheme 26).[457] Polystyrene jacketed with benzamide dendrons surface modified with Pt or Pd metallopincers formed nanorods suitable for the single-site catalysis of Aldol condensation reactions (Scheme 33).[496] Dendronized *m*-linked poly(phenylenes) peripherally functionalized with (1*R*, 2*S*)-ephedrine units (Scheme 44) have been shown to catalyze enantioselective diethyl zinc addition reactions.[600] Gin has reported the synthesis of Pd(0) nanoparticles inside a lyotropic LC matrix composed of photopolymerizable Percec-type metal carboxylates. This composite system was shown to efficiently catalyze the Heck coupling of activated aryl halides with styrene or butyl acrylate.[1344] Fujihara reported the synthesis of tri(4-hydroxy)phosphines functionalized with (3,4,5)12EOMe and (3,4,5-3,5)12EOMe, and their use as ligands for the Pd-catalyzed Suzuki cross-coupling of aryl chlorides and aryl boronic acids.[1375] Aida has also employed dendronized poly(phenylene ethynylene) surface functionalized with methyl viologen for the photosplitting of water in the presence of a colloidal Pt catalyst (Figure 153).[610,612] Gitsov has reported the acceleration of the Diels−Alder reaction of anthracene and C_{60} and the enzymatic oxidation of phenolic and polyaromatic compounds via the use of micellar-nanoreactors composed of PEG functionalized at one chain end with G3 Fréchet-type dendrons or their complexes with proteins, respectivaly.[753,754] Percec-type dendron, $(3,4,5)^2$18G2−OH, was used as a support for the solution-phase synthesis of polypeptides (Scheme 66).[962] Additionally, semifluorinated Percec-type dendron $(3,4,5)^2$12F8G2−OH was used as solubilizing chain ends in the fluorous-phase synthesis of oligonucleotides (Scheme 67).[964,964]

In some cases, dendron-mediated self-organization has been shown to affect reactivity. The self-assembly of Percec-type dendritic macromonomers into supramolecular aggregates or "nanoreactors" presenting an enhanced effective monomer concentration results in a 2−3-order-of-magnitude enhancement of the rate of polymerization (Figure 100).[390] In a similar vein, the dendritic macromonomer that self-assembles exclusively into spherical structures provides a method of unprecedented control in molecular distribution.[446] Once polymerization proceeds to a DP equal to the number of dendrons necessary to form a closed spherical structure, the rate of polymerization should slow considerably or even halt entirely, providing polydispersities very close to 1.0 (Figure 104). Dendronization of small molecules has also been shown to influence their reactivity. Dendronization of anthracene has been shown to control the stereochemistry of photodimerization reaction, in bulk and in solution (Scheme 73 and Figure 345).[1135−1137]

13. Conclusion and Outlook

This review covers all aspects related to dendron-mediated self-assembly, disassembly, and self-organization of complex systems, a field that emerged over a period of nearly 20 years. The evolution of this field was and will continue to be impacted by the development of simple and efficient methods and strategies for the design and synthesis of self-assembling dendrons and dendrimers with monodisperse and precise primary structure and of methods for the structural and retrostructural analysis of their supramolecular assemblies in bulk and in solution. These methods must ideally access in a rapid way libraries of self-assembling building blocks that ultimately are expected to predict the primary structure that will generate the 3-D supramolecular structure suitable to exhibit a particular function. Before molecular mechanisms for the transfer of structural information on all length scales will be elaborated, the use of libraries seems to be the only alternative avenue to this problem. The most ideal building blocks would need to display shape persistence in solution and in the solid state, since only this feature provides access to the use of complementary methods of structural analysis. Additionally, effective and robust methods for the attachment or incorporation of these self-assembling dendritic building blocks into all possible dendronized topologies are required (Figures 1 and 2).

In the early days of this field, it was believed that supramolecular structures generated from self-assembling dendrons, dendrimers, and other dendronized topologies are micellar. Recently, the transplant of methods for structural analysis from molecular biology to supramolecular chemistry demonstrated that this is not the case and that supramolecular dendrimers exhibit 3-D structures with the perfection and complexity resembling those of biological assemblies. While these discoveries are very enthusiastic, they also bring with them all the challenges associated with the structural analysis of giant synthetic supramolecular aggregates that resemble giant natural supramolecular complexes. Most supramolecular dendrimers are chiral even when they are constructed from nonchiral building blocks and are equipped with mechanisms that amplify chirality. This poses additional challenges associated with the understanding of the structural origin of chirality in different supramolecular structures via combinations of structurual analysis methods. This would be a simple problem if single crystals could be grown from giant supramolecular assemblies. However, just like in the case

of related biological assemblies, crystallographic experiments performed on simple crystal-like oriented fibers together with isomorphous labeling experiments are required to solve their structure.

While many supramolecular structures assembled from dendrimers and dendrons resemble some of the related morphologies generated from block-copolymers, they are much more complex and are not determined by the volume ratio between the dissimilar parts of the molcule. Therefore, theories must be developed to understand the principles of self-assembly of dendritic molecules. Unfortunately, research on this line is only in its early stages.[313,1376−1379]

Finally, one of the most neglected topics of this field concerns the mechanism of self-assembly. Fortunately, recent progress on this topic started to develop.[1142,1143,1380] Self-assembling dendrons and dendrimers are emerging into a powerful class of biologic mimics with numerous technological applications and, therefore, are associated with challenges emerging at the interface between organic and polymer chemistry, physics, molecular cell biology, structural biology, medicine, and nanoscience! Complete analysis of a new complex structure or system can take many years. This process sometimes can reduce the enthusiasm of the parallel synthetic efforts. However, without these tandem efforts, progress in this field will be only marginal. Very few properly analyzed complex structures and systems are available in the literature, and even a smaller fraction of synthetic supramolacular systems are analyzed according to current cababilities. Even so, they provided substantial advances in this field.

14. Glossary

α'	projection of solid angle
Φ_h	hexagonal columnar 2-D liquid crystalline phase with *p*6*mm* symmetry
Φ_h^{io}	hexagonal columnar 2-D with intracolumnar order
$\Phi_{h,k}$	hexagonal columnar crystalline phase
$\Phi_{r\text{-}c}$	rectangular-centered columnar 2-D liquid crystalline phase with *c*2*mm* symmetry
$\Phi_{r\text{-}c}^{k}$	rectangular columnar crystalline with *c*2*mm* symmetry
μ	number of tapered dendrons per supramolecular columnar stratum or number of conical dendrons per supramolecular spherical dendrimer
AFM	atomic force microscopy
AIBN	azobisisobutyronitrile
BCC	cubic BCC 3D lattice with $Im\bar{3}m$ symmetry
CDMT	2-chloro-4,6-dimethoxy-1,3,5-triazine
CD/UV−vis	circular dichroism/ultraviolet−visible spectroscopy
CMC	critical micelle concentration
Cub	cubic 3D lattice with $Pm\bar{3}n$ symmetry
Cub_{bi}	cubic gyroid bicontinuous phase with $Ia\bar{3}d$ symmetry
DAB	diaminobutane (same as PPI)
DOBOB	3,4,5-tris(*p*-dodecyloxybenzyloxy)benzoic acid
DCC	*N*,*N*′-dicyclohexylcarbodiimide
DLS	dynamic light scattering
dendritic purity	percentage of error-free dendrons
dm8	3,7-dimethyloctyl
DP	degree of polymerization
enantiotropic phase	thermodynamically stable LC phase with respect to the crystalline phase that is reversible upon both heating and cooling of the sample
EO	ethylene oxide
G*n*	generation *n*
H-bonding	hydrogen bonding
homeotropic alignment	alignment perpendicular to the surface
HOPG	highly ordered pyrolitic graphite
I	isotropic liquid
k	crystalline phase
LB	Langmuir−Blodgett film
LED	light-emitting diode
lyotropic liquid crystal	liquid crystals that form only upon the addition of solvent, and whose phase transitions are concentration-dependent
mesogenic group	rodlike group that mediates the formation of calamitic LC phases (N, S, etc.)
monotropic phase	thermodynamically metastable LC phase with respect to the crystalline phase that can be observed only upon cooling
M_n	number-average molecular weight
M_w	weight-average molecular weight
M_w/M_n	polydispersity index or molecular weight distribution
MPA	(methylol)propionic acid
N	nematic liquid crystalline phase
N_c	nematic columnar liquid crystalline phase
NMP	nitroxide-mediated polymerization
P4 VP	poly(4-vinylpyridine)
PAMAM	polyamidoamine dendrimer
PBI	perylene bisimide
PEI	poly(ethylene imine) dendrimer
PMA	in this case polymethacrylate, not poly(methyl acrylate), as is the usual meaning of the acronym
PPI	poly(propylene imine) dendrimer
PS	polystyrene
RCM	ring-closing metathesis
ROP	ring-opening polymerization
S	smectic liquid crystalline phase
SEM	scanning-electron microscopy
SLS	static-light scattering
TEM	transmission electron microscopy
TEMPO	2,2,6,6-tetramethylpiperidine-1-oxyl
thermotropic liquid crystal	bulk liquid crystal wherein phase transitions are temperature-dependent
TREN	tris(2-aminoethyl)amine
Tet	tetrahedral lattice with $P4_2/mnm$ symmetry
TMV	tobacco mosaic virus
TOPM	thermal optical polarized microscopy
tpy	terpyridine
XRD	X-ray diffraction

15. Acknowledgments

Financial support by the National Science Foundation (DMR-0548559 and DMR-0520020) and the P. Roy Vagelos Chair at Penn are gratefully acknowledged. BMR gratefully acknowledges funding from a NSF Graduate Research Fellowship and ACS Division of Organic Chemistry Graduate Fellowship (Roche). We also thank Dr. Juris Meija for the digital design of the composition Dendritic Dipeptide-Rose Window of the Chartres Cathedral incorporated in the Cover Art.

16. References

(1) Lehn, J.-M. *Proc. Natl. Acad. Sci. U.S.A.* **2002**, *99*, 4763.
(2) Lehn, J.-M. *Science* **2002**, *295*, 2400.
(3) Lehn, J.-M. *Rep. Prog. Phys.* **2004**, *67*, 249.
(4) Whitesides, G. M.; Grzybowski, B. A. *Science* **2002**, *295*, 2400.
(5) Whitesides, G. M; Ismagilov, R. F. *Science* **1999**, *264*, 89.
(6) Kauffman, S. A. *The Origins of Order. Self-Organization and Selection in Evolution*; Oxford University Press: Oxford, U.K., 1993.

(7) Kauffman, S. A. At Home in the Universe. In *The Search for Laws of Self-organization and Complexity*; Oxford University Press: Oxford, U.K., 1995.
(8) Coveney, P.; Highfield, R. Frontiers of Complexity. In *The Search for Order in a Chaotic World*; Fawcett Columbine: New York, 1995.
(9) Lewin, R. *Complexity—Life at the Edge of Chaos*; Collier Books: New York, 1992.
(10) Miller, A. D. *ChemBioChem* **2002**, *3*, 45.
(11) Ottino, J. M. *AIChE J.* **2003**, *49*, 292.
(12) Ottino, J. M. *Nature* **2004**, *427*, 399.
(13) Newkome, G. R.; Moorefield, C. N.; Vögtle, F. *Dendritic Molecules: Concepts Syntheses, and Applications*; Wiley-VCH: Weinheim, Germany, 1996.
(14) Newkome, G. R.; Moorefield, C. N.; Vögtle, F. *Dendrimers and Dendrons: Concepts Syntheses, and Perspectives*; Wiley-VCH: Weinheim, Germany, 2001.
(15) Fréchet, J. M. J.; Tomalia, D. A. *Dendrimers and Other Dendritic Polymers*; Wiley-VCH: Weinheim, Germany, 2001.
(16) Vögtle, F.; Richardt, G.; Werner, N. *Dendrimer Chemistry: Concepts, Synthesis, Properties, Applications*; Wiley-VCH: Weinheim, Germany, 2009.
(17) *Advances in Dendritic Molecules*, Vol. 1; Newkome, G. R., Ed.; JAI Press: Middlesex, England, 1994.
(18) *Advances in Dendritic Molecules*, Vol. 2; Newkome, G. R., Ed.; JAI Press: Middlesex, England, 1995.
(19) *Advances in Dendritic Molecules*, Vol. 3; Newkome, G. R., Ed.; JAI Press: Middlesex, England, 1996.
(20) *Advances in Dendritic Molecules*, Vol. 4; Newkome, G. R., Ed.; JAI Press: Middlesex, England, 1995.
(21) *Advances in Dendritic Molecules*, Vol. 5; Newkome, G. R., Ed.; JAI Press: Middlesex, England, 2002.
(22) *Dendrimers I*; Topics in Current Chemistry 197; Vögtle, F., Ed.; Springer-Verlag: New York, 1998.
(23) *Dendrimers II: Architecture, Nanostructure, and Supramoleculr Chemistry*; Topics in Current Chemistry 210; Vögtle, F., Ed.; Springer-Verlag: New York, 2000.
(24) *Dendrimers III: Design, Dimension, Function*; Topics in Current Chemistry 211; Vögtle, F., Ed.; Springer-Verlag: New York, 1998.
(25) *Dendrimers IV: Metal Coordination, Self Assembly, Catalysis*; Topics in Current Chemistry 217; Vögtle, F., Ed.; Springer-Verlag: New York, 2001.
(26) *Dendrimers V: Functional and Hyperbranched Building Blocks, Photophysical Properties, Applications in Materials and Life Sciences*; Topics in Current Chemistry 228; Vögtle, F., Ed.; Springer-Verlag: New York, 2003.
(27) Tomalia, D. A.; Durst, H. D. Genealogically Directed Synthesis: STARBURST/Cascade Dendrimers and Hyperbranched Structures. In *Supramolecular Chemistry I - Directed Synthesis and Molecular Recognition*; Topics in Current Chemistry 165; Weber, E., Ed.; Springer-Verlag: Berlin, 1993; pp 193−313.
(28) Mekelberger, H.-B.; Jaworek, W.; Vögtle, F. *Angew Chem., Int. Ed.* **1992**, *31*, 1571.
(29) Issberner, J.; Moors, R.; Vögtle, F. *Angew. Chem., Int. Ed. Engl.* **1994**, *33*, 2413.
(30) Fischer, M.; Vögtle, F. *Angew. Chem., Int. Ed.* **1999**, *38*, 885.
(31) Vögtle, F.; Gestermann, S.; Hesse, R.; Schwierz, H.; Windisch, B. *Prog. Polym. Sci.* **2000**, *25*, 987.
(32) Archut, A.; Vögtle, F. Dendritic Molecules—Historic Development and Future Applications. In *Handbook of Nanostructured Materials and Nanotechnology*; Nalwa, H. S., Ed.; Academic Press: New York, 2000; p 333.
(33) Ardoin, N.; Astruc, D. *Bull. Soc. Chim. France* **1995**, *132*, 875.
(34) Newkome, G. R.; Shreiner, C. D. *Polymer* **2008**, *49*, 1.
(35) Tomalia, D. A.; Naylor, A. M.; Goddard, W. A., III *Angew. Chem., Int. Ed. Engl.* **1990**, *29*, 138.
(36) Tomalia, D. A. *Adv. Mater.* **1994**, *6*, 529.
(37) Tomalia, D. A.; Majoros, I. *J. Macromol. Sci., Part C: Polym. Rev.* **2003**, *C43*, 411.
(38) Tomalia, D. A. *Sci. Am.* **1995**, *272*, 62.
(39) Balogh, L.; Tomalia, D. A.; Hagnauer, G. L. *Chem. Innov.* **2000**, 19.
(40) Grayson, S. M.; Fréchet, J. M. J. *Chem. Rev.* **2001**, *101*, 3819.
(41) Tomalia, D. A.; Fréchet, J. M. J. *J. Polym. Sci., Part A: Polym. Chem.* **2002**, *40*, 2719.
(42) Fréchet, J. M. J. *Proc. Natl. Acad. Sci. U.S.A.* **2002**, *99*, 4782.
(43) Fréchet, J. M. J. *J. Polym. Sci., Part A: Polym. Chem.* **2003**, *41*, 3713.
(44) Matthews, O. A.; Shipway, A. N.; Stoddard, J. F. *Prog. Polym. Sci.* **1998**, *23*, 1.
(45) Caminade, A.-M.; Laurent, R.; Majoral, J.-P. *Adv. Drug Deliv.* **2005**, *57*, 2130.
(46) Caminade, A.-M.; Turrin, C.-O.; Laurent, R.; Maraval, A.; Majoral, J.-P. *Curr. Org. Chem.* **2006**, *10*, 2333.
(47) Caminade, A.-M.; Turrin, C.-O.; Sutra, P.; Majoral, J.-P. *Curr. Opin. Colloid Interface Sci.* **2003**, *8*, 282.
(48) Majoral, J.-P.; Caminade, A. M. *Chem. Rev.* **1999**, *99*, 845.
(49) Zeng, F.; Zimmerman, S. C. *Chem. Rev.* **1997**, *97*, 1681.
(50) Smith, D. K.; Hirst, A. R.; Love, C. S.; Hardy, J. G.; Brignell, S. V.; Huang, B. *Prog. Polym. Sci.* **2005**, *30*, 220.
(51) Kim, Y.; Zimmerman, S. C. *Curr. Opin. Biol. Chem.* **1998**, *2*, 733.
(52) Emrick, T.; Fréchet, J. M. J. *Curr. Opin. Colloid Interface Sci.* **1999**, *4*, 15.
(53) Moore, J. S. *Curr. Opin. Colloid Interface Sci.* **1999**, *4*, 108.
(54) Elemans, J. A. A. W.; Rowan, A. E.; Nolte, R. J. M. *J. Mater. Chem.* **2003**, *13*, 2661.
(55) Al-Jamal, K. T.; Ramaswamy, C.; Florence, A. T. *Adv. Drug Delivery Rev.* **2005**, *57*, 2238.
(56) Hecht, S. *Mater. Today* **2005**, *8*, 48.
(57) Ponomarkenko, S. A.; Boiko, N. I.; Shibaev, V. P. *Polym. Sci., Ser. C.* **2001**, *43*, 1601.
(58) Donnio, B.; Guillon, D. *Adv. Polym. Sci.* **2006**, *201*, 45.
(59) Kim, Y. *Adv. Mater.* **1992**, *4*, 764.
(60) Neve, F. *Adv. Mater.* **1996**, *8*, 277.
(61) Lang, H.; Lühmann, B. *Adv. Mater.* **2001**, *13*, 1523.
(62) Guillon, D.; Deschenaux, R. *Curr. Opin. Solid State Mater. Sci.* **2002**, *6*, 515.
(63) Marcos, M.; Omenat, A.; Serrano, J. L. C. R. *Chimie* **2003**, *6*, 947.
(64) Barberá, J.; Donnio, B.; Gehringer, L.; Guillon, D.; Marcos, M.; Omenat, A.; Serrano, S. L. *J. Mater. Chem.* **2005**, *15*, 4093.
(65) Saez, I. M.; Goodby, J. W. *J. Mater. Chem.* **2005**, *15*, 26.
(66) Marcos, M.; Martín-Rapún, R.; Omenat, A.; Serrano, J. L. *Chem. Soc. Rev.* **2007**, *36*, 1889.
(67) Donnio, B.; Buathong, S.; Bury, I.; Guillon, D. *Chem. Soc. Rev.* **2007**, *36*, 1495.
(68) Deschenaux, R.; Donnio, B.; Guillon, D. *New J. Chem.* **2007**, *31*, 1064.
(69) Buathong, S.; Gehringer, L.; Donnio, B.; Guillon, D. C. R. *Chimie* **2009**, *12*, 138.
(70) Frey, H. *Angew. Chem., Int. Ed.* **1998**, *37*, 2193.
(71) Schlüter, A. D. *Top. Curr. Chem.* **1998**, *197*, 165.
(72) Schlüter, A. D.; Rabe, J. P. *Angew. Chem., Int. Ed.* **2000**, *39*, 864.
(73) Zhang, A.; Shu, L.; Bo, Z.; Schlüter, A. D. *Macromol. Chem. Phys.* **2003**, *204*, 328.
(74) Schlüter, A. D. C. R. *Chimie* **2003**, *6*, 843.
(75) Ishizu, K.; Tsubaki, K.; Mori, A.; Uchida, S. *Prog. Polym. Sci.* **2003**, *28*, 27.
(76) Schlüter, A. D. *Top. Curr. Chem.* **2005**, *245*, 151.
(77) Frauenrath, H. *Prog. Polym. Sci.* **2005**, *30*, 325.
(78) Zhang, A.; Sakamoto, J.; Schlüter, A. D. *Chimia* **2008**, *62*, 776.
(79) Rudick, J. G.; Percec, V. *New J. Chem.* **2007**, *13*, 1083.
(80) Rudick, J. G.; Percec, V. *Macromol. Chem. Phys.* **2008**, *209*, 1759.
(81) Rudick, J.G.; Percec, V. *Acc. Chem. Res.* **2008**, *41*, 1641.
(82) Gitsov, I. *J. Polym. Sci., Part A: Polym. Chem.* **2008**, *46*, 5295.
(83) Palmer, L. C.; Stupp, S. I. *Acc. Chem. Res.* **2008**, *41*, 1674.
(84) Cho, B. K.; Chung, Y. W.; Lee, B. I.; Han, K. H. *J. Inclusion Phenom. Macrocyclic Chem.* **2007**, *58*, 7.
(85) Lee, C. C.; Grenier, C.; Meijer, E. W.; Schenning, A. P. H. J. *Chem. Soc. Rev.* **2009**, *38*, 671.
(86) Prato, M.; Maggini, M. *Acc. Chem. Res.* **1998**, *31*, 519.
(87) Hirsch, A.; Vostrowsky, O. *Eur. J. Org. Chem.* **2001**, 829.
(88) Sanchez, L.; Martin, N.; Guldi, D. M. *Angew. Chem., Int. Ed.* **2005**, *44*, 5374.
(89) Guldi, D. M.; Zerbetto, F.; Georgakilas, V.; Prato, M. *Acc. Chem. Res.* **2005**, *38*, 38.
(90) Hahn, U.; Cardinali, F.; Nierengarten, J. F. *New J. Chem.* **2007**, *31*, 1128.
(91) Tashiro, K.; Aida, T. *Chem. Soc. Rev.* **2007**, *36*, 189.
(92) Nierengarten, J. F. *Fullerenes, Nanotubes, Carbon Nanostruct.* **2005**, *13*, 229.
(93) Perez, E. M.; Martin, N. *Chem. Soc. Rev.* **2008**, *37*, 1512.
(94) Seebach, D.; Rheiner, P. B.; Greiveldinger, G.; Butz, T.; Sellner, H. *Top. Curr. Chem.* **1998**, *197*, 125.
(95) Bosman, A. W.; Janssen, H. M.; Meijer, E. W. *Chem. Rev.* **1999**, *99*, 1665.
(96) Janssen, H. M.; Meijer, E. W. *Mater. Sci. Technol.* **1999**, *20*, 403.
(97) Green, M. M.; Park, J.-W.; Sato, T.; Teramoto, A.; Lifson, S.; Selinger, R. L. B.; Selinger, J. V. *Angew. Chem., Int. Ed.* **1999**, *38*, 3139.
(98) Hill, D. J.; Mio, M. J.; Prince, R. B.; Hughes, T. S.; Moore, J. S. *Chem. Rev.* **2001**, *101*, 3893.
(99) Green, M. M.; Cheon, K.-S.; Yang, S.-Y.; Park, J.-W.; Swansburg, S.; Liu, W. *Acc. Chem. Res.* **2001**, *34*, 672.
(100) Palmas, A. R. A.; Meijer, E. W. *Angew. Chem., Int. Ed.* **2007**, *46*, 8948.
(101) Ciferri, A. *Prog. Polym. Sci.* **1995**, *20*, 1081.
(102) Ciferri, A. *Trends Polym. Sci.* **1997**, *5*, 142.

(103) Cifferi, A. *Recent Res. Dev. Macromol.* **2002**, *6*, 129.
(104) Cifferi, A. *J. Macromol. Sci., Part C* **2003**, *C43*, 271.
(105) Bushby, R. J.; Lozman, O. R. *Curr. Opin. Colloid Interface Sci.* **2002**, *7*, 343.
(106) Kumar, S. *Chem. Soc. Rev.* **2006**, *35*, 83.
(107) Laschat, S.; Baro, A.; Steinke, N.; Giesselmann, F.; Hagele, C.; Scalia, G.; Judele, R.; Kapatsina, E.; Sauer, S.; Schreivogel, A.; Tosoni, M. *Angew. Chem., Int. Ed.* **2007**, *46*, 4832.
(108) Sergeyev, S.; Pisula, W.; Geerts, Y. H. *Chem. Soc. Rev.* **2007**, *36*, 1902.
(109) Eichhorn, H. *J. Porphyrins Phthalocyanines* **2000**, *4*, 88.
(110) Drain, C. M.; Varotto, A.; Radivojevic, I. *Chem. Rev.* **2009**, *109*, 1630.
(111) Stoddart, J. F.; Colquhoun, H. M. *Tetrahedron* **2008**, *64*, 8231.
(112) Balzani, V. *Pure Appl. Chem.* **2008**, *80*, 1631.
(113) *Catenanes, Rotaxanes, and Knots*; Sauvage, J. P., Dietrich-Buchecker, Eds.; Wiley-VCH: New York, 1999.
(114) Okada, M. *Prog. Polym. Sci.* **2001**, *26*, 67.
(115) Imberty, A.; Chambre, Y. M.; Roy, R. *Chem.—Eur. J.* **2008**, *14*, 7490.
(116) Chabre, Y. M.; Roy, R. *Curr. Top. Med. Chem.* **2008**, *8*, 1237.
(117) Niederhafner, P.; Sebestik, J.; Jezek, J. *J. Pept. Sci.* **2008**, *14*, 2.
(118) Niederhafner, P.; Sebestik, J.; Jezek, J. *J. Pept. Sci.* **2008**, *14*, 44.
(119) Niederhafner, P.; Sebestik, J.; Jezek, J. *J. Pept. Sci.* **2008**, *14*, 556.
(120) Cloninger, M. J. In *Molecular Recognition and Polymers: Control of Polymer Structure and Self-assembly*; Rotello, V. T. S., Ed.; John Wiley & Sons, Inc.: New York, 2008; Vol. 13, p 335.
(121) Niederhafner, P.; Sebestik, J.; Jezek, J. *J. Peptide Sci.* **2005**, *11*, 757.
(122) Higashi, N.; Koga, T. *Adv. Polym. Sci.* **2008**, *219*, 27.
(123) Lim, Y.-B; Lee, M. *J. Mater. Chem.* **2008**, *18*, 723.
(124) Caminade, A. M.; Padie, C.; Laurent, R.; Maraval, A.; Majoral, J. P. *Sensors* **2006**, *6*, 901.
(125) Caminade, A. M.; Turrin, C.-O.; Majoral, J. P. *Chem.—Eur. J.* **2008**, *14*, 7422.
(126) Grimsdale, A. C.; Chan, K. L.; Martin, R. E.; Jokisz, P. G.; Holmes, A. B. *Chem. Rev.* **2009**, *109*, 897.
(127) Mishra, A.; Ma, C.-Q.; Bäuerle, P. *Chem. Rev.* **2009**, *109*, 1141.
(128) Hwang, S.-H.; Moorfield, C. N.; Newkome, G. R. *Chem. Soc. Rev.* **2008**, *37*, 2543.
(129) Dykes, G. M. *J. Chem. Technol. Biotechnol.* **2001**, *76*, 903.
(130) Jiang, D. L.; Aida, T. *Prog. Polym. Sci.* **2005**, *30*, 403–422.
(131) Cho, M. J.; Choi, D. H.; Sullivan, P. A.; Akelaitis, A. J. P.; Dalton, L. R. *Prog. Polym. Sci.* **2008**, *33*, 1013.
(132) Bosman, A. W.; Jannsen, H. M.; Meijer, E. W. *Chem. Rev.* **1999**, *99*, 1665.
(133) Diederich, F.; Felber, B. *Proc. Natl. Acad. Sci. U.S.A.* **2002**, *99*, 4778.
(134) Stiriba, S. E.; Frey, H.; Haag, R. *Angew. Chem., Int. Ed.* **2002**, *41*, 1329.
(135) Dufes, C.; Uchegbu, I. F.; Schatzlein, A. G. *Adv. Drug Delivery Rev.* **2005**, *57*, 2177.
(136) Lee, C. C.; MacKay, J. A.; Fréchet, J. M. J. *Nat. Biotechnol.* **2005**, *23*, 1517.
(137) Parekh, H. S. *Curr. Pharm. Des.* **2007**, *13*, 2837.
(138) Grinstaff, M. W. *J. Polym. Sci., Part A: Polym. Chem.* **2008**, *46*, 383.
(139) Nguyen, D. N.; Green, J. J.; Chan, J. M.; Langer, R.; Anderson, D. G. *Adv. Mater.* **2008**, *20*, 1.
(140) Nieckowski, M. G.; Eisler, S.; Diederich, F. *New J. Chem.* **2007**, *31*, 1111.
(141) Shabat, D. *J. Polym. Sci., Part A: Polym. Chem.* **2006**, *44*, 1569.
(142) Albrecht, M.; van Koten, G. *Angew Chem., Int. Ed.* **2001**, *40*, 3750.
(143) Astruc, D.; Chardac, F. *Chem. Rev.* **2001**, *101*, 2991.
(144) Dahan, A.; Portnoy, M. *J. Polym. Sci., Part A: Polym. Chem.* **2005**, *43*, 235.
(145) Medina, S. H.; El-Sayed, M. E. H. *Chem. Rev.* **2009**, *109*, 3141.
(146) Tekade, R. K.; Kumar, P. V.; Jain, N. K. *Chem. Rev.* **2009**, *109*, 49.
(147) Balzani, V.; Campagna, S.; Denti, G.; Juris, A.; Serroni, S.; Venturi, M. *Acc. Chem. Res.* **1998**, *31*, 26.
(148) Newkome, G. R.; He, E.; Moorfield, C. N. *Chem. Rev.* **1999**, *99*, 1689.
(149) van Veggel, F. C. J. M.; Verboom, W.; Reinhoudt, D. N. *Chem. Rev.* **1994**, *94*, 279.
(150) Carothers, W. A. *Chem. Rev.* **1931**, *8*, 353.
(151) Percec, V.; Pugh, C. Oligomers. In *Encyclopedia of Polymer Science and Engineering*, 2nd ed.; Mark, H. F., Bikales, N., Overberger, C. G., Menges, G., Eds.; John Wiley & Sons: New York, 1987; Vol. 10, pp 430.
(152) Percec, V.; Pugh, C.; Nuyken, O.; Pask, S. D. Macromonomers, Oligomers, and Telechelics. In *Comprehensive Polymer Science*; Sir Allen, G., Bevington, J. C., Eds.; Pergamon: Oxford, U.K., 1989; Vol. 6, p 281.
(153) Percec, V.; Pugh, C. Oligomers. In *Encyclopedia of Polymer Science and Engineering*; Mark, H. F., Bikales, N., Overberger, C. G., Menges, G., Eds.; John Wiley & Sons: New York, 1990; p 432.
(154) Percec, V.; Tomazos, Molecular Engineering of Side Chain Liquid Crystalline Polymers. In *Contemporary Topics in Polymer Science*; Salamone, J. C., Riffle, J., Eds.; Plenum: New York, 1992; Vol. 7, p 247.
(155) Hikosaka, M.; Mabuchi, K.; Yonetake, K.; Masuko, T.; Ungar, G.; Percec, V. Liquid Crystallization Mechanism of Liquid Crystalline Polymers. In *Ordering in Macromolecular Systems*; Teramoto, A., Kosayahsi, M., Norisute, T., Eds.; Springer Verlag: New York, 1994; p 89.
(156) Klug, A. *Angew. Chem., Int. Ed. Engl.* **1983**, *22*, 565.
(157) Caspar, D. L. D.; Klug, A. *Cold Spring Harbor Symp. Quant. Biol.* **1962**, *27*, 1.
(158) Caspar, D. L. D. *Biophys. J.* **1980**, *32*, 103.
(159) Monod, J.; Changeux, J. P.; Jacob, F. *J. Mol. Biol.* **1963**, *6*, 306.
(160) Perutz, M. *Mechanisms of Cooperativity and Allosteric Regulation in Proteins*; Cambridge University Press: Cambridge, U.K., 1990.
(161) Evans, P. R. *Curr. Opin. Struct. Biol.* **1991**, *1*, 773.
(162) Steed, J. W.; Atwood, J. L. *Supramolecular Chemistry*; John Wiley & Sons: New York, 2000.
(163) Ma, J. C.; Dougherty, D. *Chem. Rev.* **1997**, *97*, 1303.
(164) Elmsley, J. *Chem. Soc. Rev.* **1980**, *9*, 91.
(165) Lehn, J.-M. *Angew. Chem., Int. Ed.* **1998**, *27*, 89.
(166) Hunter, C. A.; Sanders, J. K. M. *J. Am. Chem. Soc.* **1990**, *112*, 5525.
(167) Kim, E.; Paliwal, S.; Wilcox, C. S. *J. Am. Chem. Soc.* **1998**, *120*, 11192.
(168) Ulman, A. *Chem. Rev.* **1996**, *96*, 1533.
(169) Bates, F. S.; Fredrickson, G. H. *Phys. Today.* **1999**, 34.
(170) Percec, V.; Cho, W.-D. **2001**, unpublished results.
(171) Percec, V.; Dulcey, A. E.; Peterca, M.; Ilies, M.; Nummelin, S.; Sienkowska, M. J.; Heiney, P. A. *Proc. Nat. Acad. Sci. U.S.A.* **2006**, *103*, 2518.
(172) *Supramolecular Polymers*, 2nd ed.; Cifferi, A., Ed.; Taylor and Francis: New York, 2005.
(173) Ciferri, A. *J. Liq. Cryst.* **1999**, *26*, 489.
(174) Ciferri, A. *Macromol. Rapid Commun.* **2002**, *23*, 511.
(175) Ciferri, A. *Liq. Cryst.* **2004**, *31*, 1487.
(176) Tomalia, D. A. *J. Nanopart. Res.* **2009**, *11*, 1251.
(177) Flory, J. *J. Am. Chem. Soc.* **1941**, *63*, 3083.
(178) Flory, J. *J. Am. Chem. Soc.* **1941**, *63*, 3091.
(179) Flory, J. *J. Am. Chem. Soc.* **1941**, *63*, 3096.
(180) Flory, J. *J. Am. Chem. Soc.* **1952**, *74*, 2718.
(181) Rosen, B. M.; Wilson, D. A.; Wilson, C. J.; Peterca, M.; Won, B. C.; Huang, C.; Lipski, L. R.; Zeng, X.; Ungar, G.; Heiney, P. A.; Percec, V.; **2009**, submitted for publication.
(182) Buhleier, E.; Wehner, W.; Vögtle, F. *Synthesis* **1978**, 155.
(183) Denkewalter, R. G.; Kolc, J. F.; Lukasavage, W. J. U. S. Patent 4,360,646, 1979.
(184) Tomalia, D. A.; Dewald, J. R.; Hall, M. J.; Martin, S. J.; Smith, P. B. *Prepr. 1st SPSJ International Polymer Conference*, Kyoto, Japan, 1984; p *65*.
(185) Tomalia, D. A.; Baker, H.; Dewald, J.; Hall, M.; Kallos, S.; Martin, S.; Roeck, J.; Ryder, J.; Smith, P. *Polym J. (Tokyo)* **1985**, *17*, 117.
(186) Tomalia, D. A.; Dewald, J. R. U. S. Patent 4,507,466, 1985.
(187) Tomalia, D. A.; Dewald, J. R. U. S. Patent 4,558,120, 1985.
(188) Tomalia, D. A.; Dewald, J. R. U. S. Patent 4,568,737, 1986.
(189) Tomalia, D. A.; Baker, H.; Dewald, J.; Hall, M.; Kallos, G.; Martin, S.; Roeck, J.; Ryder, J.; Smith, P. *Macromolecules* **1986**, *19*, 2466.
(190) Newkome, G. R.; Yao, Z.; Baker, G. R.; Gupta, V. K. *J. Org. Chem.* **1985**, *50*, 2003.
(191) Fréchet, J. M. J.; Jiang, Y.; Hawker, C. J.; Philippides, A. E. *Proc. IUPAC Int. Symp., Macromol. (Seoul)* **1989**, 19.
(192) Hawker, C. J.; Fréchet, J. M. J. *J. Am. Chem. Soc.* **1990**, *112*, 7638.
(193) Miller, T. M.; Neenan, T. X. *Chem. Mater.* **1990**, *2*, 346.
(194) Malthête, J.; Leibert, L.; Levelut, A. M.; Galerne, Y. C. R. *Acad. Sci. Paris II* **1986**, *303*, 1073.
(195) Percec, V.; Heck, J. *Polym. Prepr. (Am. Chem. Soc., Div. Polym. Chem.)* **1989**, *30* (2), 450.
(196) Percec, V.; Heck, J. *J. Polym. Sci., Part A: Polym. Chem.* **1991**, *29*, 591.
(197) Percec, V.; Heck, J. *Polym. Bull.* **1990**, *24*, 255.
(198) Percec, V.; Heck, J. *Polym. Prepr. (Am. Chem. Soc., Div. Polym. Chem.)* **1991**, *32* (1), 263.
(199) Percec, V.; Heck, J. *Polym. Prepr. (Am. Chem. Soc., Div. Polym. Chem.)* **1991**, *32* (3), 698.
(200) Percec, V.; Heck, J. *Polym. Bull.* **1991**, *25*, 55.
(201) Percec, V.; Heck, J. *Polym. Bull.* **1991**, *25*, 431.
(202) Percec, V.; Heck, J.; Ungar, G. *Macromolecules* **1991**, *24*, 4957.

(203) Percec, V.; Heck, J.; Ungar, G. *Polym. Prepr. (Am. Chem. Soc., Div. Polym. Chem.)* **1992**, *33* (1), 152.
(204) Percec, V.; Heck, J. *Polym. Prepr. (Am. Chem. Soc., Div. Polym. Chem.)* **1992**, *33* (1), 217.
(205) Percec, V.; Lee, M.; Heck, J.; Blackwell, H. E.; Ungar, G.; Alvarez-Castillo, A. *J. Mater. Chem.* **1992**, *2*, 931.
(206) Percec, V.; Heck, J.; Lee, M.; Ungar, G.; Alvarez-Castillo, A. *J. Mater. Chem.* **1992**, *2*, 1033.
(207) Percec, V.; Heck, J.; Johannson, G. *Polym. Prepr. (Am. Chem. Soc., Div. Polym. Chem.)* **1993**, *34* (1), 116.
(208) Percec, V.; Heck, J.; Tomazos, D.; Falkenberg, F.; Blackwell, H.; Ungar, G. *J. Chem. Soc., Perkin Trans 1* **1993**, 2799.
(209) Percec, V.; Heck, J. A.; Tomazos, D.; Ungar, G. *J. Chem. Soc., Perkin Trans. 2* **1993**, 2381.
(210) Percec, V.; Johansson, G.; Heck, J.; Ungar, G.; Batty, S. V. *J. Chem. Soc., Perkin Trans. 1* **1993**, 1411.
(211) Kown, Y. K.; Chvalun, S.; Schneider, A.-I.; Blackwell, J.; Percec, V.; Heck, J. A. *Macromolecules* **1994**, *27*, 6129.
(212) Johansson, G.; Percec, V.; Ungar, G.; Abramic, D. *J. Chem. Soc., Perkin Trans. 1* **1994**, 447.
(213) Percec, V.; Tomazos, D.; Heck, J.; Blackwell, H.; Ungar, G. *J. Chem. Soc., Perkin Trans. 2* **1994**, 31.
(214) Percec, V. *Phil Trans. R. Soc. A.* **2006**, *364*, 2709.
(215) Percec, V.; Kawasumi, M. *Macromolecules* **1991**, *24*, 6318.
(216) Percec, V.; Kawasumi, M. *Polym. Prepr. (Am. Chem. Soc., Div. Polym. Chem.)* **1992**, *33* (1), 221.
(217) Percec, V.; Kawasumi, M. *Macromolecules* **1992**, *25*, 3843.
(218) Percec, V.; Kawasumi, M. *Polym. Prepr. (Am. Chem. Soc., Div. Polym. Chem.)* **1994**, *34* (1), 158.
(219) Percec, V.; Chu, P.; Kawasumi, M. *Macromolecules* **1994**, *27*, 4441.
(220) Percec, V.; Chu, P. *Polym. Prepr. (Am. Chem. Soc., Div. Polym. Chem.)* **1995**, *36* (1), 743.
(221) Percec, V.; Chu, P.; Ungar, G.; Zhou, J. *J. Am. Chem. Soc.* **1995**, *117*, 11441.
(222) Percec, V.; Chu, P.; Johansson, G.; Schlueter, D.; Ronda, J. C.; Ungar, G. *Polym. Prepr. (Am. Chem. Soc., Div. Polym. Chem.)* **1996**, *37* (1), 68.
(223) Bradley, D. *Science* **1995**, *270*, 1924.
(224) Percec, V.; Tomazos, D. Molecular Engineering of Liquid Crystalline Polymers. In *Comprehensive Polymer Science, First Supplement*; Allen, G., Ed.; Pergamon: Oxford, U.K., 1992; p 299.
(225) Percec, V.; Tomazos, D. *Indian. J. Technol.* **1993**, *31*, 339.
(226) Percec, V.; Heck, J.; Johansson, G.; Tomazos, D.; Ungar, G. *Macromol. Symp.* **1994**, *77*, 237.
(227) Percec, V.; Heck, J.; Johansson, G.; Tomazos, D.; Kawasumi, M.; Ungar, G. *J. Macromol. Sci. Pure Appl. Chem.* **1994**, *A31*, 1031.
(228) Percec, V.; Heck, J.; Johansson, G.; Tomazos, D.; Kawasumi, M.; Ungar, G. *J. Macromol. Sci. Pure Appl. Chem.* **1994**, *A31*, 1719.
(229) Percec, V.; Heck, J.; Johansson, G.; Tomazos, D.; Kawasumi, M.; Chu, P.; Ungar, G. *Mol. Cryst. Liq. Cryst.* **1994**, *254*, 137.
(230) Kwon, Y. K.; Danko, C.; Chvalun, S.; Blackwell, J.; Heck, J. A.; Percec, V. *Macromol. Symp.* **1994**, *87*, 103.
(231) Percec, V.; Johannson, G. *Macromol. Symp.* **1995**, *96*, 173.
(232) Percec, V. *Pure Appl. Chem.* **1995**, *67*, 2031.
(233) Percec, V. *J. Macromol. Sci. Pure Appl. Chem.* **1996**, *A33*, 1479.
(234) Percec, V.; Johansson, G.; Schleuter, D.; Ronda, J. C.; Ungar, G. *Macromol. Symp.* **1996**, *101*, 43.
(235) Percec, V. *Macromol. Symp.* **1997**, *117*, 267.
(236) Percec, V.; Ahn, C.-H.; Cho, W.-D.; Johansson, G.; Schlueter, D. *Macromol. Symp.* **1997**, *118*, 33.
(237) Percec, V. *Macromol. Symp.* **1997**, *118*, 663.
(238) Percec, V.; Johansson, G. In *Macromolecular Design of Polymeric Materials*; Hatada, K., Kitayama, T., Vogl, O., Eds.; Marcel Dekker, Inc.: New York, 1997; p 633.
(239) Percec, V. From Molecular to Macromolecular Liquid Crystals. In *Handbook of Liquid Crystal Research*; Collings, P. J., Patel, J. S., Eds.; Oxford University Press: Oxford, U.K., 1997; p 259.
(240) Lima-de-Faria, A. *Biosystems* **1997**, *43*, 115.
(241) Tomalia, D. A.; Dvornic, P. R. Dendritic Polymers, Divergent Synthesis (Starburst Polyamidoamine Dendrimers). In *Polymeric Materials Encycl.*; Salamone, J. C., Ed.; CRC Press: Boca Raton, FL, 1995; Vol. 3, D-E, pp 1814−1830.
(242) Tomalia, D. A.; Hall, M.; Hedstrand, D. M. *J. Am. Chem. Soc.* **1987**, *109*, 1601.
(243) de Gennes, P. G.; Hervet, H. *J. Phys., Lett.* **1983**, *44*, 351.
(244) Wörner, C.; Mülhaupt, R. *Angew. Chem., Int. Ed. Engl.* **1993**, *32*, 1306.
(245) de Brabander-van den Ber, E. M. M.; Meijer, E. W. *Angew. Chem., Int. Ed. Engl.* **1993**, *32*, 1308.
(246) Hummelen, J. C.; Van Dongen, J. L. J.; Meijer, E. W. *Chem.—Eur. J.* **1997**, *3*, 1489.
(247) Denkewalter, R. G.; Kolc, J.; Lukasavage, W. J. U. S. Patent 4,289,872, 1982.
(248) Denkewalter, R. G.; Kolc, J. F. Luksavage, W. J. U. S. Patent 4,410,688, 1983.
(249) Aharoni, S. M.; Crosby, C. R.; Walsh, E. K. *Macromolecules* **1982**, *15*, 1093.
(250) Tomalia D. A.; Dewald J. R. U.S. Patent 4,631,337, 1986.
(251) Friberg, S. E.; Podzimek, M.; Tomalia, D. A.; Hedstrand, D. M. *Mol. Cryst. Liq. Cryst.* **1988**, *164*, 157.
(252) Peterson, J.; Allikmaa, V.; Subbi, J.; Pehk, T.; Lopp, M. *Eur. Polym. J.* **2003**, *39*, 33.
(253) Pittelkow, M.; Christensen, J. B. *Org. Lett.* **2005**, *7*, 1295.
(254) Pittelkow, M.; Lewinsky, R.; Christensen, J. B. *Synthesis* **2002**, 2195.
(255) Pittelkow, M.; Lewinsky, R.; Christensen, J. B. *Org. Synth.* **2006**, *84*, 209.
(256) Kim, C.; Kim, K. T.; Chang, Y. *J. Am. Chem. Soc.* **2001**, *123*, 5586.
(257) Kim, C.; Lee, S. J.; Lee, I. H.; Kim, K. T.; Song, H. H.; Jeon, H.-J. *Chem. Mater.* **2003**, *15*, 3638.
(258) Ihre, H.; Hult, A.; Söderlind, E. *J. Am. Chem. Soc.* **1996**, *118*, 6388.
(259) Goh, S. L.; Francis, M. B.; Fréchet, J. M. J. *Chem. Commun.* **2002**, 2954.
(260) Newkome, G. R.; Lin, X. *Macromolecules* **1991**, *24*, 1443.
(261) Newkome, G. R.; Behera, R. K.; Moorefield, C. N.; Baker, G. R. *J. Org. Chem.* **1991**, *56*, 7162.
(262) Allcock, H. R.; Ravikiran, R.; O'Connor, S. J. M. *Macromolecules* **1997**, *30*, 3184.
(263) Haag, R.; Sunder, A.; Stumbé, J.-F. *J. Am. Chem. Soc.* **2000**, *122*.
(264) Jayaraman, M.; Fréchet, J. M. J. *J. Am. Chem. Soc.* **1998**, *120*, 12996.
(265) Balagurusamy, V. S. K.; Ungar, G.; Percec, V.; Johansson, G. *J. Am. Chem. Soc.* **1997**, *119*, 5783.
(266) Percec, V.; Cho, W.-D.; Ungar, G.; Yeardley, D. J. P. *J. Am. Chem. Soc.* **2001**, *123*, 1315.
(267) Yamakazi, N.; Washio, I.; Shibasaki, Y.; Ueda, M. *Org. Lett.* **2006**, *8*, 2321.
(268) Mulders, S. J. E.; Brouwer, A. J.; van der Meer, P. G. J.; Liskamp, R. M. J. *Tetrahedron Lett.* **1997**, *38*, 631.
(269) Klopsch, R.; Koch, S.; Schlüter, A. D. *Eur. J. Org. Chem.* **1998**, 1275.
(270) Neubert, I.; Schlüter, A. D. *Macromolecules* **1998**, *31*, 9372.
(271) Percec, V.; Cho, W.-D.; Möller, M.; Prokhorova, S. A.; Ungar, G.; Yeardley, D. J. P. *J. Am. Chem. Soc.* **2000**, *122*, 4249.
(272) Hersmis, M. C.; Spiering, A. J. H.; Waterval, R. J.; Meuldijk, J.; Vekeans, J. A. J. M.; Hulshof, l. A. *Org. Process Res. Dev.* **2001**, *5*, 54.
(273) Percec, V.; Peterca, M.; Sienkowska, M. J.; Ilies, M. A.; Aqad, E.; Smidrkal, J.; Heiney, P. A. *J. Am. Chem. Soc.* **2006**, *128*, 3324.
(274) Percec, V.; Holerca, M. N.; Nummellin, S.; Morrison, J. J.; Glodde, M.; Smidrkal, J.; Peterca, M.; Rosen, B. M.; Uchida, S.; Balagurusamy, V. S. K.; Sienkowska, M. J.; Heiney, P. A. *Chem.—Eur. J.* **2006**, *12*, 6216.
(275) Percec, V.; Won, B. C.; Peterca, M.; Heiney, P. A. *J. Am. Chem. Soc.* **2007**, *129*, 11265.
(276) Chandrasekhar, S. *Mol. Cryst. Liq. Cryst.* **1985**, *104*, 1.
(277) Yu, L. J.; Saupe, A. *Phys. Rev. Lett.* **1980**, *45*, 1000.
(278) Percec, V.; Keller, A. *Macromolecules* **1990**, *23*, 4347.
(279) Hughes, J. R.; Kothe, G.; Luckhurst, G. R. *J. Chem. Phys.* **1997**, *107*, 9252.
(280) Malthête, J.; Levulet, A. M.; Tinh, N. H. *J. Phys., Lett.* **1985**, *46*, L-875.
(281) Malthête, J.; Ting, N. H.; Levulet, A. M. *Chem. Soc., Chem. Commun.* **1986**, 1548.
(282) Levelut, A. M.; Malthête, J.; Destrade, C.; Tinh, N. H. *Liq. Cryst.* **1987**, *2*, 877.
(283) Guillon, D.; Skoulios, A.; Malthête, J. *Europhys. Lett.* **1987**, *3*, 67.
(284) Ribeiro, A. C.; Heinrich, B.; Cruz, C.; Nguyen, H. T.; Diele, S.; Schhroder, M. W.; Guillon, D. *Eur. Phys. J. E.* **2003**, *10*, 143.
(285) Guillon, D.; Donnio, B.; Bruce, D. W.; Cukiernik, F. D.; Rusjan, M. *Mol. Cryst. Liq. Cryst.* **2003**, *396*, 141.
(286) Donniom, B.; Heinrich, B.; Allouchi, H.; Kain, J.; Diele, S.; Guillon, D.; Bruce, D. W. *J. Am. Chem. Soc.* **2004**, *126*, 15258.
(287) Malthête, J.; Nguyen, H. T.; Destrade, C. *Liq. Cryst.* **1993**, *13*, 177.
(288) Nguyen, H. T.; Desstrade, C.; Malthête, J. *Adv. Mater.* **1997**, *9*, 5.
(289) Gharbia, M.; Garbia, A.; Nguyen, H. T.; Malthête, J. *Curr. Opin. Colloid Interface Sci.* **2002**, *7*, 312.
(290) Gladysz, J. A.; Curran, D. P. Horvath, I. T. *Handbook of Fluorous Chemistry*; Wiley-VCH: New York, 2004.
(291) Krafft, M. P. *J. Polym. Sci., Part A: Polym. Chem.* **2006**, *44*, 4251.
(292) Krafft, M. P.; Riess, J. G. *J. Polym. Sci., Part A: Polym. Chem.* **2007**, *45*, 1185.
(293) Percec, V.; Schlueter, D.; Kwon, Y. K.; Blackwell, J.; Möller, M.; Slangen, P. J. *Macromolecules* **1995**, *28*, 8807.
(294) Percec, V.; Schlueter, D.; Ungar, G. *Macromolecules* **1997**, *30*, 645.
(295) Johansson, G.; Percec, V.; Ungar, G.; Smith, K. *Chem. Mater.* **1997**, *9*, 164.

(296) Ungar, G.; Nobl, K. A.; Percec, V.; Johansson, G. *J. Mater. Sci.* **2000**, *35*, 5241.
(297) Percec, V.; Holerca, M. N.; Bera, T. K.; Ungar, G. *Polym. Mat. Sci. Eng.* **1998**, 234.
(298) Percec, V.; Ahn, C.-H.; Bera, T. K.; Ungar, G.; Yeardley, D. J. P. *Chem.—Eur. J.* **1999**, *5*, 1070.
(299) Robertson, D. E.; Farid, R. S.; Moser, C. C.; Urbauer, J. L.; Mulholland, S. E.; Pidikiti, R.; Lear, J. D.; Wand, A. J.; Degrado, W. F.; Dutton, P. L. *Nature* **1994**, *368*, 425.
(300) Heck, J. A. Supramolecular Polymers. M.S. Thesis, Case Western Reserve University, Cleveland, OH, 1993.
(301) Heck, J. A. Self-Assembly of Tubular Supramolecular Architectures via a Combination of Endo and Exo Recognition Process. Ph.D. Thesis, Case Western Reserve University, Cleveland, OH, 1995.
(302) Bawden, F. C.; Pirie, N. W.; Bernal, J. D.; Fankuchen, I. *Nature* **1937**, *138*, 1051.
(303) Klug, A. *Phil. Trans. R. Soc. B* **1999**, *354*, 531.
(304) Lindsey, J. S. *New. J. Chem.* **1991**, *15*, 153.
(305) Durham, A. C. H.; Finch, J. T.; Klug, A. *Nat. New. Biol.* **1971**, *229*, 37.
(306) Hudson, S. D.; Jung, H.-T.; Percec, V.; Cho, W.-D.; Johansson, G.; Ungar, G.; Balagurusamy, V. S. K. *Science* **1997**, *278*, 449.
(307) Sheiko, S. S.; Möller, M. *Chem. Rev.* **2001**, *101*, 4099.
(308) Kouwer, P. H. J.; Mehl, G. H. *J. Mater. Chem.* **2009**, *19*, 1564.
(309) Ungar, G.; Abramic, D.; Percec, V.; Heck, J. A. *Liq. Cryst.* **1996**, *21*, 73.
(310) Jung, H.-T.; Hudson, S. D.; Percec, V. *Mater. Res. Soc. Symp. Proc.* **1999**, *559*, 189.
(311) Jung, H.-T.; Kim, S. W.; Ko, Y. K.; Yoon, B. K.; Hudson, S. D.; Percec, V.; Holerca, M. N.; Cho, W.-D.; Mosier, P. E. *Macromolecules* **2002**, *35*, 3717.
(312) Percec, V.; Dulcey, A. E.; Balagurusamy, V. S. K.; Miura, Y.; Smidrkal, J.; Peterca, M.; Nummelin, S.; Edlund, U.; Hudson, S. D.; Heiney, P. A.; Duan, H.; Maganov, S. N.; Vinogradov, S. A. *Nature* **2004**, *430*, 764.
(313) Mezzenga, R.; Ruokolainen, J.; Canilho, N.; Kasëmi, E.; Schlüter, D. A.; Lee, W. B.; Fredrickson, G. H. *Soft Matter* **2009**, *5*, 92.
(314) Balagurusamy, V. S. K.; Ungar, G.; Percec, V.; Johansson, G. *J. Am. Chem. Soc.* **1997**, *119*, 1539.
(315) Diele, S. *Curr. Opin. Colloid Interface Sci.* **2002**, *7*, 333.
(316) Kutsumitzu, S. *Curr. Opin. Solid State Mater. Sci.* **2002**, *6*, 537.
(317) Percec, V.; Holerca, M. N.; Uchida, S.; Cho, W.-D.; Ungar, G.; Lee, Y.; Yeardley, D. J. P. *Chem.—Eur. J.* **2002**, *8*, 1106.
(318) Yeardley, D. J. P.; Ungar, G.; Percec, V.; Holerca, M. N.; Johansson, G. *J. Am. Chem. Soc.* **2000**, *122*, 1684.
(319) Duan, H.; Hudson, S. D.; Ungar, G.; Holerca, M. N.; Percec, V. *Chem.—Eur. J.* **2001**, *7*, 4134.
(320) Hudson, S. D.; Jung, H.-T.; Kewsuwan, P.; Percec, V.; Möller, M. *Liq. Cryst.* **1999**, *26*, 1493.
(321) Perutz, M. F.; Rossman, M. G.; Cullis, A. F.; Muirhead, H.; Will, G.; North, A. C. *Nature* **1960**, *185*, 416.
(322) Zeng, X.; Cseh, L.; Mehl, G. H.; Ungar, G. *J. Mater. Chem.* **2008**, *18*, 2953.
(323) Ungar, G.; Liu, Y.; Zeng, X.; Percec, V.; Cho, W.-D. *Science* **2003**, *299*, 1208.
(324) Percec, V.; Imam, M. R.; Peterca, M.; Wilson, D. A.; Graf, R.; Spiess, H.; Balagurusamy, V. S. K.; Heiney, P. A. *J. Am. Chem. Soc.* **2009**, *131*, 7682.
(325) Zeng, X.; Ungar, G.; Liu, Y.; Percec, V.; Dulcey, A. E.; Hobbs, J. K. *Nature* **2004**, *428*, 157.
(326) Mehl, G. H. *Angew. Chem., Int. Ed.* **2005**, *44*, 672.
(327) Ciao, M. *Nature* **2004**, *428*, 133.
(328) Zeng, X. *Curr. Opin. Colloid Interface Sci.* **2005**, *9*, 384.
(329) Cochran, W.; Crick, F. H. C.; Vand, V. *Acta Crystallogr.* **1952**, *5*, 581.
(330) Peterca, M.; Percec, V.; Imam, M. R.; Leonawat, P.; Morimitsu, K.; Heiney, P. A. *J. Am. Chem. Soc.* **2008**, *130*, 14840.
(331) Percec, V.; Cho, W.-D.; Mosier, P. E.; Ungar, G.; Yeardley, D. J. P. *J. Am. Chem. Soc.* **1998**, *120*, 11061.
(332) Percec, V.; Cho, W. D.; Ungar, G.; Yeardley, D. J. P. *Angew. Chem., Int. Ed.* **2000**, *39*, 1598.
(333) Naylor, A.; Goddard, W. A.; Kiefer, G. E.; Tomalia, D. A. *J. Am. Chem. Soc.* **1989**, *111*, 2339.
(334) Percec, V.; Cho, W.-D.; Ungar, G. *J. Am. Chem. Soc.* **2000**, *122*, 10273.
(335) Ungar, G.; Percec, V.; Holerca, M. N.; Johansson, G.; Heck, J. A. *Chem.—Eur. J.* **2000**, *6*, 1258.
(336) Creighton, T. E. *Proteins: Structures and Molecular Properties*, 2nd ed.; W. H. Freeman: New York, 1992.
(337) Whitford, D. *Proteins: Structure and Function*; John Wiley & Sons: New York, 2005.
(338) Percec, V.; Mitchell, C. M.; Cho, W.-D.; Uchida, S.; Glodde, M.; Ungar, G.; Zeng, X.; Liu, Y.; Balagursamy, V. S. K.; Heiney, P. A. *J. Am. Chem. Soc.* **2004**, *126*, 6078.
(339) Pao, W. J.; Zhang, F.; Heiney, P. A.; Mitchell, C.; Cho, W. D.; Percec, V. *Phys Rev. E* **2003**, *67*, 021601.
(340) Li, J.-F.; Crandall, K. A.; Chu, P.; Percec, V.; Petschek, R. G.; Rosenblatt, C. *Macromolecules* **1996**, *29*, 7813.
(341) Liu, Z.; Zhu, L.; Zhou, W.; Cheng, S. Z. D.; Percec, V.; Ungar, G. *Chem. Mater.* **2002**, *14*, 2384.
(342) Percec, V.; Chu, P.; Asandei, A. D. *Polym. Mater. Sci. Eng.* **1999**, *80*, 223.
(343) Percec, V.; Schlueter, D.; Ungar, G.; Cheng, S. Z. D.; Zhang, A. *Macromolecules* **1998**, *31*, 1745.
(344) Percec, V.; Golding, G. M.; Smidrkal, J.; Weichold, O. *J. Org. Chem.* **2004**, *69*, 3447.
(345) Percec, V.; Smidrkal, J.; Peterca, M.; Mitchell, C. M.; Nummellin, S.; Dulcey, A. E.; Sienkowska, M. J.; Heiney, P. A. *Chem.—Eur. J.* **2007**, *13*, 3989.
(346) Fox, J. M.; Huang, X.; Chieffi, A.; Buchwald, S. L. *J. Am. Chem. Soc.* **2000**, *122*, 1360.
(347) Elemans, J. A. A. W.; Boerakker, M. J.; Holder, S. J.; Rowan, A. E.; Cho, W. D.; Percec, V.; Nolter, R. J. M. *Proc. Natl. Acad. Sci. U.S.A.* **2002**, *99*, 5093.
(348) de Groot, B. L.; Grubmuller, H. *Science* **2001**, *294*, 2353.
(349) Dellago, C.; Naor, M. M.; Hummer, G. *Phys. Rev. Lett.* **2003**, *90*, 105902.
(350) Kaucher, M. S.; Peterca, M.; Dulcey, A. E.; Kim, A. J.; Vinogradov, S. A.; Hammer, D. A.; Heiney, P. A.; Percec, V. *J. Am. Chem. Soc.* **2007**, *129*, 11698.
(351) Kim, A. J.; Kaucher, M. S.; Davis, K. P.; Imam, M. R.; Christian, N. A.; Levine, D. A.; Peterca, M.; Bates, F. S.; Percec, V.; Hammer, D. A. Adv. Funct. Mater. 2009, in press.
(352) Percec, V.; Dulcey, A. E.; Peterca, M.; Ilies, M.; Sienkowska, M. J.; Heiney, P. A. *J. Am. Chem. Soc.* **2005**, *127*, 17902.
(353) Percec, V.; Dulcey, A. E.; Peterca, M.; Ilies, M.; Ladislaw, J.; Rosen, B. M.; Edlund, U.; Heiney, P. A. *Angew. Chem., Int. Ed.* **2005**, *44*, 6516.
(354) Percec, V.; Dulcey, A. E.; Peterca, M.; Adelman, P.; Samant, R.; Balagurusamy, V. S. K.; Heiney, P. A. *J. Am. Chem. Soc.* **2007**, *129*, 5992.
(355) Peterca, M.; Percec, V.; Dulcey, A. E.; Nummellin, S.; Korey, S.; Ilies, M.; Heiney, P. A. *J. Am. Chem. Soc.* **2006**, *128*, 6713.
(356) Percec, V.; Dulcey, A.; Peterca, M.; Ilies, M.; Miura, Y.; Edlund, U.; Heiney, P. A. *Aust. J. Chem.* **2005**, *58*, 472.
(357) Percec, V.; Peterca, M.; Dulcey, A. E.; Imam, M. R.; Hudson, S. D.; Nummelin, S.; Adelman, P.; Heiney, P. A. *J. Am. Chem. Soc.* **2008**, *130*, 13079.
(358) Percec, V.; Glodde, M.; Bera, T. K.; Miura, Y.; Shiyanovskaya, I.; Singer, K. D.; Balagurusamy, V. S. K.; Heiney, P. A.; Schnell, I.; Rapp, A.; Spiess, H.-W.; Hudson, S. D.; Duan, H. *Nature* **2002**, *419*, 384.
(359) Percec, V.; Johansson, G.; Ungar, G.; Zhou, J. *J. Am. Chem. Soc.* **1996**, *118*, 9855.
(360) Johansson, G.; Percec, V.; Ungar, G.; Zhou, J. P. *Macromolecules* **1996**, *29*, 646.
(361) Percec, V.; Glodde, M.; Johansson, G.; Balagurusamy, V. S. K.; Heiney, P. A. *Angew. Chem., Int. Ed.* **2003**, *42*, 4338.
(362) Tomalia, D. A. *Nat. Mater.* **2003**, *2*, 711.
(363) Percec, V.; Aqad, E.; Peterca, M.; Imam, M. R.; Glodde, M.; Bera, T. K.; Miura, Y.; Balagurusamy, V. S. K.; Ewbank, P. C.; Würthner, F.; Heiney, P. A. *Chem.—Eur. J.* **2007**, *13*, 3330.
(364) Percec, V.; Glodde, M.; Peterca, M.; Rapp, A.; Schnell, I.; Spiess, H. W.; Bera, T. K.; Miura, Y.; Balagurusamy, V. S. K.; Aqad, E.; Heiney, P. A. *Chem.—Eur. J.* **2006**, *12*, 6298.
(365) Shiyanovskaya, I.; Singer, K. D.; Percec, V.; Bera, T. K.; Miura, Y.; Glodde, M. *Phys. Rev. B* **2003**, *76*, 035204.
(366) Chvalun, S. N.; Shcherbina, M. A.; Yakunin, A. N.; Blackwell, J.; Percec, V. *Polym. Sci., Ser. A* **2007**, *49*, 158.
(367) Dukeson, D. R.; Ungar, G.; Balagurusamy, V. S. K.; Percec, V.; Johansson, G. A.; Glodde, M. *J. Am. Chem. Soc.* **2003**, *125*, 15974.
(368) Yoon, D. K.; Lee, S. R.; Kim, Y. H.; Choi, S.-M.; Jung, H.-T. *Adv. Mater.* **2006**, *18*, 509.
(369) Tomalia, D. A.; Kirchoff, P. M. U. S. Patent 4,694,064, 1987.
(370) Yin, R.; Zhu, Y.; Tomalia, D. A.; Ibuki, H. *J. Am. Chem. Soc.* **1998**, *120*, 2678.
(371) Hawker, C. J.; Fréchet, J. M. J. *Polymer* **1992**, *33*, 1507.
(372) Dramheim, G.; Ritter, H. *Macromol. Chem. Phys.* **1995**, *196*, 2211.
(373) Niggemann, M.; Ritter, H. *Acta Polym.* **1996**, *47*, 351.
(374) Neubert, I.; Amoulong-Kirstein, E.; Schlüter, A.-D.; Dautzengerg, H. *Macromol. Rapid Commun.* **1996**, *17*, 517.
(375) Neubert, I.; Klopsch, R.; Claussen, W.; Schlüter, A.-D. *Acta Polym.* **1996**, *47*, 455.

(376) Kim, H.-J.; Lim, Y.-B.; Lee, M. *J. Polym. Sci., Part A: Polym. Chem.* **2008**, *46*, 1925.
(377) Christopoulos, D. K.; Terzis, A. F.; Vanakaras, A. G.; Photinos, D. J. *J. Chem. Phys.* **2006**, *125*, 204907.
(378) Ding, Y.; Öttinger, H. C.; Schlüter, A. D.; Kröger, M. *J. Chem. Phys.* **2007**, *127*, 094904.
(379) Welch, P. M.; Welch, C. F. *Nano. Lett.* **2006**, *6*, 1922.
(380) Park, C.; Choi, K. S.; Song, Y.; Jeon, H.-J.; Song, H. H.; Chang, J. Y.; Kim, C. *Langmuir* **2006**, *22*, 3812.
(381) Makowski, L. *Biophys. J.* **1998**, *74*, 534.
(382) Chierotti, M. R.; Gobetto, R. *Chem. Commun.* **2008**, 1621.
(383) Pugh, C.; Percec, V. *Macromolecules* **1986**, *19*, 65.
(384) Rodriguez-Parada, J. M.; Percec, V. *Macromolecules* **1986**, *19*, 55.
(385) Percec, V.; Tomazos, D. *Adv. Mater.* **1992**, *4*, 548.
(386) Luo, J.; Liu, S.; Haller, M.; Liu, L.; Ma, H.; Jen, A. K. Y. *Adv. Mater.* **2002**, *14*, 1763.
(387) Chen, Y.-M.; Chen, C.-F.; Li, Y.-F.; Xi, F. *Macromol. Rapid Commun.* **1996**, *17*, 401.
(388) Neubert, I.; Klopsch, R.; Claussen, W.; Schlüter, A.-D. *Acta Polym.* **1996**, *47*, 455.
(389) Fréchet, J. M. J.; Gitsov, I. *Macromol. Symp.* **1995**, *98*, 441.
(390) Percec, V.; Ahn, C.-H.; Barboiu, B. *J. Am. Chem. Soc.* **1997**, *119*, 12978.
(391) Webster, O. W. *Science* **1991**, *251*, 887.
(392) Szwarc, M. *Nature* **1956**, *178*, 1168.
(393) Szwarc, M. *J. Polym. Sci., Part A: Polym. Chem.* **1998**, *56*, ix.
(394) Kennedy, J. P. *J. Polym. Sci., Part A: Polym. Chem.* **1999**, *37*, 2285.
(395) *Ring-Opening Polymerization: Mechanisms, Catalysis, Structure, Utility*; Brunelle, D. J., Ed.; Hanser Publishers: New York, 1993.
(396) Bielawski, C. W.; Grubbs, R. H. *Prog. Polym. Sci.* **2007**, *32*, 1.
(397) Webster, O. W.; Hertler, W. R.; Sogah, D. Y.; Farnham, W. B.; RajanBabu, T. V. *Polym. Prepr. (Am. Chem. Soc., Div. Polym. Chem.)* **1983**, *24*, 52.
(398) Hertler, W. R.; Sogah, D. Y.; Webster, O. W.; Trost, B. M. *Macromolecules* **1984**, *17*, 1415.
(399) Webster, O. W. *J. Polym. Sci., Part A: Polym. Chem.* **2000**, *38*, 2855.
(400) Solomon, D. H.; Rizzardo, E.; Cacioli, P. *Eur. Pat. Appl.* **1985**, *135280*.
(401) Hawker, C. J.; Bosman, A. W.; Harth, E. *Chem. Rev.* **2001**, *101*, 3661.
(402) Chiefari, J.; Chong, Y. K.; Ercole, F.; Krstina, J.; Jeffrey, J.; Le, T. P. T.; Mayadunne, R. T. A.; Meijs, G. F.; Moad, C. L.; Moad, G.; Rizzardo, E.; Thang, S. H. *Macromolecules* **1998**, *31*, 5559.
(403) Solomon, D. H. *J. Polym. Sci., Part A: Polym. Chem.* **2005**, *43*, 5748.
(404) Moad, G.; Rizzardo, E.; Thang, S. H. *Aust. J. Chem.* **2006**, *59*, 669.
(405) Zard, S. Z. *Angew. Chem., Int. Ed.* **1997**, *36*, 672.
(406) Perrier, S.; Takolpuckdee, P. *J. Polym. Sci., Part A: Polym. Chem.* **2005**, *43*, 5347.
(407) Wayland, B. B.; Poszmik, G.; Mukerjee, S. L.; Fryd, M. *J. Am. Chem. Soc.* **1994**, *116*, 7943.
(408) Wayland, B. B.; Basickes, L.; Mukerjee, S.; Wei, M.; Fryd, M. *Macromolecules* **1997**, *30*, 8109.
(409) Matyjaszewski, K.; Xia, J. *Chem. Rev.* **2001**, *101*, 2921.
(410) Percec, V.; Guliashvili, T.; Ladislaw, J. S.; Wistrand, A.; Stjerndahl, A.; Sienkowska, M. J.; Monteiro, M. J.; Sahoo, S. *J. Am. Chem. Soc.* **2006**, *128*, 14156.
(411) Rosen, B. M.; Percec, V. Chem. Rev. 2009, in press.
(412) Percec, V.; Popov, A. V.; Ramirez-Castillo, E.; Monteiro, M.; Barboiu, B.; Weichold, O.; Asandei, A. D.; Mitchell, C. M. *J. Am. Chem. Soc.* **2002**, *124*, 4940.
(413) Percec, V.; Popov, A. V.; Ramirez-Castillo, E.; Coelho, J. F. J.; Hinojosa-Falcon, L. A. *J. Polym. Sci., Part A: Polym. Chem.* **2004**, *42*, 6364.
(414) Yamago, S. *J. Polym. Sci., Part A: Polym. Chem.* **2006**, *44*, 1.
(415) Otsu, T. *J. Polym. Sci., Part A: Polym. Chem.* **2000**, *38*, 2121.
(416) Percec, V.; Shaffer, T. D.; Nava, H. *J. Polym. Sci.: Polym. Lett. Ed.* **1984**, *22*, 637.
(417) Schlüter, A. D. *J. Polym. Sci., Part A: Polym. Chem.* **2001**, *39*, 1533.
(418) Bunz, U. H. *Chem. Rev.* **2000**, *100*, 1605.
(419) Miyakoshi, R.; Yokoyama, A.; Yokozawa, T. *J. Polym. Sci., Part A: Polym. Chem.* **2008**, *46*, 753.
(420) Masuda, T.; Hasegawa, K. I.; Higashimura, T. *Macromolecules* **1974**, *7*, 728.
(421) Kishimoto, Y.; Eckerle, P.; Miyatake, T.; Ikariya, T.; Noyori, R. *J. Am. Chem. Soc.* **1994**, *116*, 12131.
(422) Liu, C.; Ringsdorf, H.; Ebert, M.; Kleppinger, R.; Wendorff, J. H. *Liq. Cryst.* **1989**, *5*, 1841.
(423) Malthêthe, J.; Tinh, N. H.; Levelut, A.-M. *J. Chem. Soc., Chem. Commun.* **1986**, 1548.
(424) Percec, V.; Heck, J. *Polym. Bull.* **1991**, *25*, 55.
(425) Ouall, N.; Méry, S.; Skoulios, A.; Noirez, L. *Macromolecules* **2000**, *33*, 6185.
(426) Kim, C.; Kang, S. *J. Polym Sci. Part A: Polym. Chem.* **2000**, *38*, 724.
(427) Kim, C.; Kwark, K. *J. Polym. Sci., Part A: Polym. Chem.* **2002**, *40*, 976.
(428) Lindsey, J. S. *New J. Chem.* **1991**, *15*, 153.
(429) Durham, A. C. H.; Finch, J. T.; Klug, A. *Nature New Biol.* **1971**, *229*, 37.
(430) Percec, V.; Heck, J.; Johansson, G.; Tomazos, G.; Kawasumi, K.; Chu, P.; Ungar, G. *Mol. Cryst. Liq. Cryst.* **1994**, *254*, 137.
(431) Shcherbina, M. A.; Chvalun, S. N.; Percec, V. *Polym. Sci., Ser. A* **2008**, *50*, 166.
(432) Li, J.-F.; Heck, J. A.; Percec, V.; Rosenblatt, C.; Collura, J. S.; Fisch, M. R. *J. Phys. II, France* **1994**, *4*, 1813.
(433) Tomazos, D.; Out, G.; Heck, J. A.; Johansson, G.; Percec, V.; Möller, M. *Liq. Cryst.* **1994**, *16*, 509.
(434) Zeng, E.; Jacob, K. I.; Polk, M. B. *Polymer* **2002**, *43*, 2169.
(435) Chvalun, S. N.; Kwon, Y. K.; Blackwell, J.; Percec, V. *Polym. Sci., Ser. A* **1996**, *38*, 1298.
(436) Chvalun, S. N.; Blackwell, J.; Cho, J. D.; Kwon, Y. K.; Percec, V.; Heck, J. A. *Polymer* **1998**, *39*, 4515.
(437) Kwon, Y. K.; Chvalun, S. N.; Blackwell, J.; Percec, V.; Heck, J. A. *Macromolecules* **1995**, *28*, 1552.
(438) Chvalun, S. N.; Shcherbina, M. A.; Bykova, I. V.; Blackwell, J.; Percec, V.; Kwon, Y. K.; Cho, J. D. *Polym. Sci., Ser. A* **2001**, *43*, 33.
(439) Chvalun, S. N.; Kwon, Y. K.; Blackwell, J.; Percec, V. *Polym. Sci., Ser. A* **1996**, *38*, 1298.
(440) Chvalun, S. N.; Blackwell, J.; Kwon, Y. K.; Percec, V. *Macromol. Symp.* **1997**, *118*, 663.
(441) Chvalun, S. N.; Blackwell, J.; Cho, J. D.; Bykova, I. V.; Percec, V. *Acta Polym.* **1999**, *50*, 51.
(442) Ungar, G.; Batty, S. V.; Percec, V.; Heck, J.; Johansson, G. *Adv. Mater. Opt. Electr.* **1994**, *4*, 303.
(443) Percec, V.; Cho, W.-D.; Ungar, G.; Yeardley, D. J. P. *Chem.—Eur. J.* **2002**, *8*, 2011.
(444) Percec, V.; Tomazos, D.; Heck, J.; Blackwell, H.; Ungar, G. *J. Chem. Soc., Perkin Trans. 2* **1994**, 31.
(445) Percec, V.; Ahn, C.-H.; Cho, W.-D.; Jamieson, A. M.; Kim, J.; Leman, T.; Scmidt, M.; Gerle, M.; Möller, M.; Prokhorova, S. A.; Sheiko, S. S.; Cheng, S. Z. D.; Zhang, A.; Ungar, G.; Yeardley, D. J. P. *J. Am. Chem. Soc.* **1998**, *120*, 8619.
(446) Percec, V.; Ahn, C. H.; Ungar, G.; Yeardley, D. J. P.; Möller, M.; Sheiko, S. S. *Nature* **1998**, *391*, 161.
(447) Frey, H. *Angew Chem., Int. Ed.* **1998**, *37*, 2193.
(448) Gu, D.; Jamieson, A. M.; Rosenblatt, C.; Tomazos, D.; Lee, M.; Percec, V. *Macromolecules* **1991**, *24*, 2385.
(449) Anderson, H. L. *Angew. Chem., Int. Ed.* **2000**, *39*, 2451.
(450) Prohorova, S. A.; Sheiko, S. S.; Möller, M.; Ahn, C.-H.; Percec, V. *Macromol. Rapid Commun.* **1998**, *19*, 359.
(451) Prokhorova, S. A.; Sheiko, S. S.; Mourran, A.; Azumi, R.; Beginn, U.; Zipp, G.; Ahn, C.-H.; Holerca, M. N.; Percec, V.; Möller, M. *Langmuir* **2000**, *16*, 6862.
(452) Wintermantel, M.; Gerle, M.; Fischer, K.; Schmidt, M.; Wataoka, I.; Urakawa, H.; Kajiwara, K.; Tsukahara, Y. *Macromolecules* **1996**, *29*, 978.
(453) Prokhorova, S. A.; Sheiko, S. S.; Ahn, C.-H.; Percec, V.; Möller, M. *Macromolecules* **1999**, *32*, 2653.
(454) Rapp, A.; Schnell, I.; Sebastiani, D.; Brown, S. P.; Percec, V.; Spiess, H. W. *J. Am. Chem. Soc.* **2003**, *125*, 13284.
(455) Spiess, H. W. *J. Polym. Sci., Part A: Polym. Chem.* **2004**, *42*, 5031.
(456) Percec, V.; Schlueter, D.; Ronda, J. C.; Johansson, G.; Ungar, G.; Zhou, J. P. *Macromolecules* **1996**, *29*, 1464.
(457) Liang, C. O.; Helms, B.; Hawker, C. J.; Fréchet, J. M. J. *Chem. Commun.* **2003**, 2524.
(458) Ronda, J. C.; Reina, J. A.; Cadiz, V.; Giamberini, N.; Nicolais, L. *J. Polym. Sci., Part A: Polym. Chem.* **2003**, *41*, 2918.
(459) Giamberini, M.; Ronda, J. C.; Reina, J. A. *J. Polym. Sci., Part A: Polym. Chem.* **2005**, *43*, 2099.
(460) Ronda, J. C.; Reina, J. A.; Giamberini, M. *J. Polym. Sci., Part A: Polym. Chem.* **2004**, *42*, 326.
(461) Giamberini, M.; Reina, J. A.; Ronda, J. C. *J. Polym. Sci., Part A: Polym. Chem.* **2006**, *44*, 1722.
(462) Bilibin, A.; Zorin, I.; Saratovsky, S.; Moukhina, I.; Egorova, G.; Girbasova, N. *Macromol. Symp.* **2003**, *199*, 197.
(463) Girbasova, N.; Aseyev, V.; Saratovsky, S.; Moukhina, I.; Tenhu, H.; Bilibin, A. *Macromol. Chem. Phys.* **2003**, *204*, 2258.
(464) Bushin, S. V.; Andreeva, L. N.; Girbasova, N. V.; Bezrukova, M. A.; Alyab'eva, V. P.; Tsvetkov, N. V.; Bilibin, A. Y. *Polym. Sci., Ser. A* **2007**, *49*, 843.
(465) Reemers, S.; Mela, P.; Mourran, A.; Magonov, S.; Keul, H.; Möller, M. *J. Polym. Sci., Part A: Polym. Chem.* **2007**, *45*, 614.

(466) Nyström, A. M.; Furó, I.; Malmström, E.; Hult, A. *J. Polym. Sci., Part A: Polym. Chem.* **2005**, *43*, 4496.
(467) Carlmark, A.; Malmström, E. E. *Macromolecules* **2004**, *37*, 7491.
(468) Malkoch, M.; Carlmark, A.; Woldegiorgis, A.; Hult, A.; Malmström, E. E. *Macromolecules* **2004**, *37*, 322.
(469) Benhabbour, S. R.; Parrott, M. C.; Gratton, S. E. A.; Adronov, A. *Macromolecules* **2007**, *40*, 5678.
(470) Jayaraman, A.; Ravindranath, R.; Subbiah, J.; Valiyaveettil, S. *Polym. Prepr. (Am. Chem. Soc., Div. Polym. Chem.)* **2005**, *46*, 490.
(471) Hietala, S.; Nyström, A.; Tenhu, H.; Hult, A. *J. Polym. Sci., Part A: Polym. Chem.* **2006**, *44*, 3674.
(472) Sindhu, S.; Jegadesan, S.; Parthiban, A.; Valiyaveettil, S. *J. Magn. Magn. Mat.* **2006**, *296*, 104.
(473) Nyström, A.; Hult, A. *J. Polym. Sci., Part A: Polym. Chem.* **2006**, *43*, 3852.
(474) Li, W.; Zhang, A.; Feldman, K.; Walde, P.; Schlüter, D. A. *Macromolecules* **2008**, *41*, 3659.
(475) Zhang, A.; Okrasa, L.; Pakula, T.; Schlüter, A. D. *J. Am. Chem. Soc.* **2004**, *126*, 6658.
(476) Canilho, N.; Kasëmi, E.; Mezzenga, R.; Schlüter, A. D. *J. Am. Chem. Soc.* **2006**, *128*, 13998.
(477) Canilho, N.; Kasëmi, E.; Schlüter, A. D.; Ruokolainen, J.; Mezzenga, R. *Macromol. Symp.* **2008**, *270*, 58.
(478) Canilho, N.; Kasëmi, E.; Schlüter, A. D.; Ruokolainen, J.; Mezzenga, R. *Macromolecules* **2007**, *40*, 7609.
(479) Zhaung, W.; Kasëmi, E.; Ding, Y.; Kröger, M.; Schlüter, A. D.; Rabe, J. P. *Adv. Mater.* **2008**, *20*, 3204.
(480) Sonar, P.; Benmansour, H.; Geiger, T.; Schlüter, A. D. *Polymer* **2007**, *48*, 4996.
(481) Xia, C.; Fan, X.; Locklin, J.; Advincula, R. C. *Org. Lett.* **2002**, *4*, 2067.
(482) Zhang, X.; Chen, Z.; Würthner, F. *J. Am. Chem. Soc.* **2007**, *129*, 4886.
(483) Zhang, A.; Rodríguez-Ropero, F.; Zanuy, D.; Alemán, C.; Meijer, E. W.; Schlüter, A. D. *Chem.—Eur. J.* **2008**, *14*, 6924.
(484) Khan, A.; Daugaard, A. E.; Bayles, A.; Koga, S.; Miki, Y.; Sato, K.; Enda, J.; Hvilsted, S.; Stucky, G. D.; Hawker, C. J. *Chem. Commun.* **2009**, 425.
(485) Grayson, S. M.; Fréchet, J. M. J. *Macromolecules* **2001**, *34*, 6542.
(486) Yoshida, M.; Fresco, Z. M.; Ohnishi; Fréchet, J. M. J. *Macromolecules* **2005**, *38*, 334.
(487) Das, J.; Yoshida, M.; Fresco, Z. M.; Choi, T.-L.; Fréchet, J. M. J.; Chakraborty, A. K. *J. Phys. Chem. B* **2005**, *109*, 6535.
(488) Helms, B.; Mynar, J. L.; Hawker, C. J.; Fréchet, J. M. J. *J. Am. Chem. Soc.* **2004**, *126*, 15020.
(489) Mynar, J. L.; Choi, T.-L.; Yoshida, M.; Kim, V.; Hawker, C. J.; Fréchet, J. M. J. *Chem. Commun.* **2005**, 5169.
(490) Wenzel, A.; Neubert; Schlüter, A. D. *Macromol. Chem. Phys.* **1998**, *199*, 745.
(491) Desai, A.; Atkinson, N.; Rivera, F.; Devonport, W.; Rees, I.; Branz, S. E.; Hawker, C. J. *J. Polym. Sci., Part A: Polym. Chem.* **2000**, *38*, 1033.
(492) Scrivanti, A.; Fasan, S.; Matteoli, U.; Seraglia, R.; Chessa, G. *Macromol. Chem. Phys.* **2000**, *201*, 326.
(493) Shu, L.; Gössl, I.; Rabe, J.; Schlüter, A. D. *Macromol. Chem. Phys.* **2002**, *203*, 2540.
(494) Kobshik, S.; Mikhailova, M.; Polushina, G.; Rjumtsev, E.; Kovshik, A.; Lezov, A. *J. Non-Cryst. Solids* **2005**, *351*, 2723.
(495) Bottcher, C.; Schade, B.; Ecker, C.; Rabe, J.; Shu, L.; Schlüter, A. D. *Chem.—Eur. J.* **2005**, *11*, 2923.
(496) Suijkerbuijk, B. M. J. M.; Shu, L.; Gebbink, R. J. M.; Schlüter, A. D.; van Koten, G. *Organometallics* **2003**, *22*, 4175.
(497) Zistler, A.; Koch, S.; Schlüter, A. D. *J. Chem. Soc., Perkins Trans. 1* **1999**, 501.
(498) Vetter, S.; Koch, S.; Schlüter, A. D. *J. Polym. Sci., Part A: Polym. Chem.* **2001**, *39*, 1940.
(499) Zhang, A. F.; Vetter, S.; Schlüter, A. D. *Macromol. Chem. Phys.* **2001**, *202*, 3301.
(500) Zhang, A. F.; Zhang, B.; Wachtersbach, E.; Schmidt, M.; Schlüter, A. D. *Chen.-Eur. J.* **2003**, *9*, 6083.
(501) Zhang, A.; Wei, L. H.; Schlüter, A. D. *Macromol. Rapid Commun.* **2004**, *25*, 799.
(502) Shu, L.; Schlüter, A. D. *Macromol. Chem. Phys.* **2000**, *201*, 239.
(503) Shu, L.; Schäfer, A.; Schlüter, A. D. *Macromolecules* **2000**, *33*, 4321.
(504) Shu, L.; Schlüter, A. D.; Ecker, C.; Severin, N.; Rabe, J. P. *Angew. Chem., Int. Ed.* **2001**, *40*, 4666.
(505) Ecker, C.; Severin, N.; Shu, L.; Schlüter, A. D.; Rabe, J. P. *Macromolecules* **2004**, *37*, 2484.
(506) Fresco, Z. M.; Suez, I.; Backer, S. A.; Fréchet, J. M. J. *J. Am. Chem. Soc.* **2004**, *126*, 8374.
(507) Moingeon, F.; Masson, P.; Méry, S. *Macromolecules* **2007**, *40*, 55.
(508) Moingeon, F.; Roeser, J.; Masson, P.; Arnaud, F.; Méry, S. *Chem. Commun.* **2008**, 1341.
(509) Zhang, Y.; Huang, J.; Chen, Y. *Macromolecules* **2005**, *38*, 5069.
(510) Feng, S.; Xiong, X.; Zhang, G.; Xia, N.; Chen, Y.; Wang, W. *Macromolecules* **2009**, *42*, 281.
(511) Boisselier, E.; Shun, A. C. K.; Ruiz, J.; Cloutet, E.; Belin, C.; Astruc, D. *New J. Chem.* **2009**, *33*, 246.
(512) Camponovo, J.; Ruiz, J.; Cloutet, E.; Astruc, D. *Chem.—Eur. J.* **2009**, *15*, 2990.
(513) Luo, J.; Liu, S.; Haller, M.; Li, H.; Kim, T.-D.; Kim, K.-S.; Tang, H.-Z.; Kang, S.-H.; Jang, S.-H.; Ma, H.; Dalton, L. R.; Jen, A. K.-Y. *Proc. SPIE* **2003**, *4991*, 520.
(514) Dalton, L. R. *J. Phys.: Condens. Matter* **2003**, *15*, R897.
(515) Luo, J.; Haller, M.; Li, H.; Tang, H.-Z.; Jen, A. K.-Y. *Macromolecules* **2004**, *37*, 248.
(516) Luo, J.; Ma, H.; Jen, A. K.-Y. *C. R. Chim.* **2003**, *6*, 895.
(517) Luo, J.; Haller, M.; Ma, H.; Liu, S.; Kim, T.-D.; Tian, Y.; Chen, B.; Jang, S.-H.; Dalton, L. R.; Jen, A. K.-Y. *J. Phys. Chem. B* **2004**, *108*, 8523.
(518) Franc, G.; Kakkar, A. K. *Chem.—Eur. J.* **2009**, *15*, 5630.
(519) Kim, T. D.; Luo, J.; Tian, Y.; Ka, J.-W.; Tucker, N. M.; Haller, M.; Kang, J.-W.; Jen, A. K.-Y. *Macromolecules* **2006**, *39*, 1676.
(520) Chvalun, S. N.; Scherbina, M. A.; Bykova, I. V.; Blackwell, J.; Percec, V. *Polym. Sci., Ser. A* **2002**, *44*, 2134.
(521) Chvalun, S. N.; Shcherbina, M. A.; Bykova, I. V.; Blackwell, J.; Percec, V. *Polym. Sci., Ser. A* **2002**, *44*, 1281.
(522) Meijer, E. W.; Schenning, A. P. H. J. *Nature* **2002**, *419*, 353.
(523) Wang, J.; Mao, G.; Ober, C. K.; Kramer, E. J. *Macromolecules* **1997**, *30*, 1906.
(524) Muthukumar, M.; Ober, C. K.; Thomas, E. L. *Science* **1997**, *277*, 1225.
(525) Xiang, M.; Yang, S.; Ober, C. K. *Polym. Prepr. (Am. Chem. Soc., Div. Polym. Chem.)* **1998**, *39* (2), 974.
(526) Ober, C. K.; Xiang, M.; Char, K.; Genzer, J.; Sivaniah, E.; Kramer, E. J.; Fisher, D. *Proc. Am. Chem Soc., Div. Polym. Mat. Sci. Eng.* **1999**, *80*, 100.
(527) Xiang, M.; Li, X.; Ober, C. K.; Char, K.; Genzer, J.; Sivaniah, E.; Kramer, E. J.; Fischer, D. A. *Macromolecules* **2000**, *33*, 6106.
(528) Genzer, J.; Sivaniah, E.; Kramer, E. J.; Wang, J.; Xiang, M.; Char, K.; Ober, C. K.; Bubeck, R. A.; Fischer, D. A.; Graupe, M.; Colorado, R.; Shmakova, O. E.; Lee, T. R. *Macromolecules* **2000**, *33*, 6068.
(529) Sivaniah, E.; Genzer, J.; Fredrickson, G. H.; Kramer, E. J.; Xiang, M.; Li, X.; Ober, C.; Magonov, S. *Langmuir* **2001**, *17*, 4342.
(530) Nyström, D.; Lindqvistt, J.; Östtmark, E.; Antoni, P.; Carlmark, A.; Hult, A.; Malmström, E. *ACS. Appl. Mater. Int.* **2009**, *1*, 816.
(531) Percec, V.; Holerca, M. N.; Möller, M.; Prokorova, S. *Polym. Prepr. (Am. Chem. Soc., Div. Polym. Chem.)* **1999**, *40* (1), 492.
(532) Stewart, G. M.; Fox, M. A. *Chem. Mater.* **1998**, *10*, 860.
(533) Percec, V.; Schlueter, D. *Macromolecules* **1997**, *30*, 5783.
(534) Buchowicz, W.; Holerca, M. N.; Percec, V. *Macromolecules* **2001**, *34*, 3842.
(535) Percec, V.; Holerca, M. N. *Biomacromolecules* **2000**, *1*, 6.
(536) Gu, A.; Jamieson, M.; Kawasumi, M.; Lee, M.; Percec, V. *Macromolecules* **1992**, *25*, 2151.
(537) Liu, Z.; Zhu, L.; Shen, Z.; Zhou, W.; Cheng, S. Z. D.; Percec, V.; Ungar, G. *Macromolecules* **2002**, *35*, 9426.
(538) Nyström, A.; Malkoch, M.; Furó, I.; Nyström, D.; Unal, K.; Antoni, P.; Vamvounis, G.; Hawker, C.; Wooley, K.; Malmstöm, E.; Hult, A. *Macromolecules* **2006**, *29*, 7241.
(539) Boydston, A. J.; Holcombe, T. W.; Unruh, D. A.; Fréchet, J. M. J.; Grubbs, R. H. *J. Am. Chem. Soc.* **2009**, *131*, 5388.
(540) Stebani, U.; Lattermann, G. *Macromol. Rep.* **1995**, *A32*, 385.
(541) Stebani, U.; Lattermann, G.; Festag, R.; Wittenberg, M.; Wendorff, J. H. *J. Mater. Chem.* **1995**, *5*, 2247.
(542) Fischer, H.; Ghosh, S. S.; Heiney, P. A.; Maliszewskyj, N. C.; Plesnivy, T.; Ringsdorf, H.; Seitz, M. *Angew. Chem., Int. Ed. Engl.* **1995**, *34*, 795.
(543) Seitz, M.; Plesnivy, T.; Schimossek, K.; Edelmann, M.; Ringsdorf, H.; Fischer, H.; Uyama, H.; Kobayashi, S. *Macromolecules* **1996**, *29*, 6560.
(544) Fischer, H.; Plesnivy, T.; Ringsdorf, H.; Seitz, M. *Chem. Commun.* **1995**, 1615.
(545) Percec, V.; Holerca, M. N.; Uchida, S.; Magonov, S. N.; Yeardley, D. J. P.; Ungar, G.; Duan, H.; Hudson, S. D. *Biomacromolecules* **2001**, 706.
(546) Percec, V.; Holerca, M. N.; Uchida, S.; Yeardley, D. J. P.; Ungar, G. *Biomacromolecules* **2001**, *2*, 729.
(547) Simionescu, C. I.; Percec, V.; Dumitrescu, S. *J. Polym. Sci.: Polym. Chem. Ed.* **1977**, *15*, 2497.
(548) Simionescu, C. I.; Dumitrescu, S.; Percec, V. *J. Polym. Sci.: Polym. Symp.* **1978**, *64*, 209–227.

(549) Simionescu, C. I.; Percec, V. *J. Polym. Sci.: Polym. Lett. Ed.* **1979**, *17*, 421.
(550) Simionescu, C. I.; Percec, V. *J. Polym. Sci.: Polym. Symp.* **1980**, *67*, 43.
(551) Simionescu, C. I.; Percec, V. *J. Polym. Sci.: Polym. Chem. Ed.* **1980**, *18*, 147.
(552) Simionescu, C. I.; Percec, V. *Prog. Polym. Sci.* **1982**, *8*, 133.
(553) Percec, V.; Rinaldi, P. *Polym. Bull.* **1983**, *9*, 548.
(554) Percec, V. *Polym. Bull.* **1983**, *10*, 1.
(555) Percec, V.; Rinaldi, P. L. *Polym. Bull.* **1983**, *9*, 582.
(556) Morino, K.; Maeda, K.; Okamoto, Y.; Yashima, E.; Sato, T. *Chem.—Eur. J.* **2002**, *8*, 5112.
(557) Percec, V.; Rudick, J. G.; Aqad, E. *Macromolecules* **2005**, *38*, 7205.
(558) Kaneko, T.; Horie, T.; Asano, M.; Aoki, T.; Oikawa, E. *Macromolecules* **1997**, *30*, 3118.
(559) Kaneko, T.; Asano, M.; Yamamoto, K.; Aoki, T. *Polym. J.* **2001**, *33*, 879.
(560) Aoki, T.; Kaneko, T. *Polym. J.* **2005**, *37*, 717.
(561) Wu, C.; Malinin, S. V.; Tretiak, S.; Chernyak, V. Y. *Nature Phys.* **2006**, *2*, 631.
(562) Percec, V.; Obata, M.; Rudick, J. G.; De, B. B.; Glodde, M.; Bera, T.; Magonov, S. N.; Balagurusamy, V. S. K.; Heiney, P. A. *J. Polym. Sci., Part A: Polym. Chem.* **2002**, *40*, 3509.
(563) Dumitrescu, S.; Percec, V.; Simionescu, C. I. *J. Polym. Sci.: Polym. Chem. Ed.* **1977**, *15*, 2893.
(564) Percec, V.; Rudick, J. G.; Peterca, M.; Wagner, M.; Obata, M.; Mitchell, C. M.; Cho, W.-D.; Balagurusamy, V. S. K.; Heiney, P. A. *J. Am. Chem. Soc.* **2005**, *127*, 15257.
(565) Bishop, L. M.; Barbarow, J. E.; Bergman, R. G.; Trauner, D. *Angew. Chem. Int. Ed.* **2008**, *47*, 8100.
(566) Percec, V.; Rudick, J. G.; Aqad, E. *Macromolecules* **2005**, *38*, 7205.
(567) Nakano, T.; Okamoto, Y. *Chem. Rev.* **2001**, *101*, 4013.
(568) Cornelissen, J. J. L.; Rowan, A. E.; Nolte, R. J. M.; Sommerdijk, N. A. J. M. *Chem. Rev.* **2001**, *101*, 4039.
(569) Yashima, E.; Maeda, K.; Nisimura, T. *Chem.—Eur. J.* **2004**, *10*, 42.
(570) Percec, V.; Rudick, J. G.; Wagner, M.; Obata, M.; Mitchell, C. M.; Cho, W.-D.; Magonov, S. N. *Macromolecules* **2006**, *39*, 7342.
(571) Percec, V.; Rudick, J. G.; Peterca, M.; Staley, S. R.; Wagner, M.; Obata, M.; Mitchell, C. M.; Cho, W.-D.; Balagurusamy, V. S. K.; Lowe, J. N.; Glodde, M.; Weichold, O.; Chung, K. J.; Ghionni, N.; Magonov, S. N.; Heiney, P. A. *Chem.—Eur. J.* **2006**, *12*, 5731.
(572) Schenning, A. P. H. J.; Fransen, M.; Meijer, E. W. *Macromol. Rapid Commun.* **2002**, *23*, 265.
(573) Lemon, L. Synthesis and polymerization of arylacetylene monomers. M.S. Thesis, Case Western Reserve University, Cleveland, OH, 1996.
(574) Percec, V.; Aqad, E.; Peterca, M.; Rudick, J. G.; Lemon, L.; Ronda, J. C.; De, B. B.; Heiney, P. A.; Meijer, E. W. *J. Am. Chem. Soc.* **2006**, *128*, 16365.
(575) Percec, V.; Peterca, M.; Rudick, J. G.; Aqad, E.; Imam, M. R.; Heiney, P. A. *Chem.—Eur. J.* **2007**, *13*, 9572.
(576) Percec, V.; Rudick, J. G.; Peterca, M.; Heiney, P. A. *J. Am. Chem. Soc.* **2008**, *130*, 7503.
(577) Feringa, B. L.; Browne, W. R. *Nat. Nanotechnol.* **2008**, *3*, 383.
(578) Rudick, J. G.; Percec, V. *Macromol. Chem. Phys.* **2008**, *209*, 1760.
(579) Percec, V.; Rudick, J. G.; Peterca, M.; Aqad, E.; Imam, M. R.; Heiney, P. A. *J. Polym. Sci., Part A: Polym. Chem.* **2007**, *45*, 4974.
(580) Percec, V.; Rudick, J. G.; Nombel, P.; Buchowiscz, W. *J. Polym. Sci., Part A: Polym. Chem.* **2002**, *40*, 3212.
(581) Percec, V.; Rudick, J. G. *Macromolecules* **2005**, *38*, 7241.
(582) Kamikawa, Y.; Kato, T.; Onouchi, H.; Kashiwagi, D.; Maeda, K.; Yashima, E. *J. Polym. Sci., Part A: Polym. Chem.* **2004**, *42*, 4580.
(583) Andreopoulou, A. K.; Kallitsis, J. K. *Macromolecules* **2002**, *35*, 5808.
(584) Kallitsis, J. K.; Andreopoulou, A. K. *J. Polym. Sci., Part B: Polym. Phys.* **2003**, *41*, 2485.
(585) Pistolis, G.; Andreopoulou, A. K.; Malliaris, A.; Kallitsis, J. K. *Macromolecules* **2004**, *37*, 1524.
(586) Andreopoulou, A. K.; Carbonnier, B.; Kallitsis, J. K.; Pakula, T. *Macromolecules* **2004**, *37*, 3576.
(587) Carbonnier, B.; Andreopoulou, A. K.; Pakula, T.; Kallitsis, J. *Macromol. Chem. Phys.* **2005**, *206*, 66.
(588) Ryu, J.-H.; Bae, J.; Lee, M. *Macromolecules* **2005**, *38*, 2050.
(589) Lee, C. C.; Grayson, S. M.; Fréchet, J. M. J. *J. Polym. Sci., Part A: Polym. Chem.* **2004**, *42*, 3563.
(590) Jahromi, S.; Coussens, B.; Meijerink, N.; Braam, A. W. M. *J. Am. Chem. Soc.* **1998**, *120*, 9753.
(591) Ghosh, S.; Banthia, A. *J. Polym Sci., Part A: Polym. Chem.* **2001**, *39*, 4182.
(592) Claussen, W.; Schulte, N.; Schlüter, A. D. *Macromol. Rapid Commun.* **1995**, *16*, 89.
(593) Karakaya, B.; Claussen, W.; Gessler, K.; Saenger, W.; Schlüter, A. D. *J. Am. Chem. Soc.* **1997**, *119*, 3296.
(594) Stocker, W.; Karakaya, B.; Scürman, B. L.; Rabe, J. P.; Schlüter, A. D. *J. Am. Chem. Soc.* **1998**, *120*, 7691.
(595) Schlüter, A. D. *Polym. Prepr. (Am. Chem. Soc., Div. Polym. Chem.)* **1995**, *36* (1), 745.
(596) Karakaya, B.; Claussen, W.; Schäfer, A.; Lehmann, A.; Schlüter, A. D. *Acta Polym.* **1996**, *47*, 79.
(597) Christopoulos, D. K.; Photinos, D. J.; Stimson, L. M.; Terzis, A. F.; Vanakaras, A. G. *J. Mater. Chem.* **2003**, *13*, 2756.
(598) Bo, Z.; Rabe, J. P.; Schlüter, A. D. *Angew. Chem., Int. Ed.* **1999**, *38*, 2370.
(599) Bo, Z.; Zhang, C.; Severin, N.; Rabe, J. P.; Schlüter, A. D. *Macromolecules* **2000**, *33*, 2688.
(600) Hu, Q.-S.; Sun, C.; Monaghan, C. E. *Tet. Lett.* **2002**, *43*, 927.
(601) Bao, Z.; Amundson, K. R.; Lovinger, A. J. *Macromolecules* **1998**, *31*, 8647.
(602) Jakubiak, R.; Bao, Z.; Rothberg, L. *Synth. Met.* **2000**, *114*, 61.
(603) Jakubiak, R.; Bao, Z.; Rothberg, L. J. *Synth. Met.* **2001**, *116*, 41.
(604) Bao, Z.; Chen, L.; Lovinger, A.; Sapjeta, J.; Jakubiak, R. *Rothberg Proc. Am. Chem Soc., Div. Polym. Mater. Sci. Eng.* **2000**, *83*, 288.
(605) Rothberg, L. J.; Bao, Z. *J. Phys.: Condens. Matter* **2002**, *14*, 12261.
(606) Jiang, J.; Liu, H.; Zhao, Y.; Chen, C.; Xi, F. *Synth. Met.* **2002**, *132*, 1.
(607) Kimoto, A.; Masachika, K.; Cho, J.-S.; Higuchi, M.; Yamamoto, K. *Org. Lett.* **2004**, *6*, 1179.
(608) Kuroda, K.; Swager, T. *Chem. Commun.* **2003**, 26.
(609) Kuroda, K.; Swager, T. *Macromolecules* **2004**, *37*, 716.
(610) Sato, T.; Jiang, D.-L.; Aida, T. *J. Am. Chem. Soc.* **1999**, *121*, 10658.
(611) Li, W.-S.; Jiang, D.-L.; Aida, T. *Angew. Chem., Int. Ed.* **2004**, *43*, 2943.
(612) Jiang, D.-L.; Choi, C.-K.; Honda, K.; Li, W.-S.; Yuzawa, T.; Aida, T. *J. Am. Chem. Soc.* **2004**, *126*, 12084.
(613) Masuo, S.; Yoshikawa, H.; Asahi, T.; Masuhara, H.; Sato, T.; Jiang, D.-L.; Aida, T. *J. Phys. Chem. B* **2001**, *105*, 2885.
(614) Masuo, S.; Yoshikawa, H.; Asahi, T.; Masuhara, H.; Sato, T.; Jiang, D.-L.; Aida, T. *J. Phys. Chem. B* **2002**, *106*, 905.
(615) Nierengarten, J.-F.; Guillon, D.; Heinrich, B.; Nicoud, J.-F. *Chem. Commun.* **1997**, 1233.
(616) Schenning, A. P. H. J.; Martin, R. E.; Ito, M.; Diederich, F.; Boudon, C.; Gisselbrecht, J.-P.; Gross, M. *Chem. Commun.* **1998**, 1013.
(617) Schenning, A. P. H. J.; Arndt, J.-D.; Ito, M.; Stoddart, A.; Schreiber, M.; Siemsen, P.; Martin, R. E.; Boudon, C.; Gisselbrecht, J.-P.; Gross, M.; Gramlich, V.; Diederich, F. *Helv. Chim. Acta* **2001**, *84*, 296.
(618) Malenfant, P. R. L.; Fréchet, J. M. J. *Macromolecules* **2000**, *33*, 3634.
(619) Krishnamoorthy, K.; Ambade, A. V.; Mishra, S. P.; Kanungo, M.; Contractor, A. Q.; Kumar, A. *Polymer* **2002**, *43*, 6465.
(620) Vanormelingen, W.; Van den Bergh, K.; Verbiest, T.; Koeckelberghs, G. *Macromolecules* **2008**, *41*, 5582.
(621) Steckler, T. T.; Zhang, X.; Hwang, J.; Honeyager, R.; Ohira, S.; Zhang, X.-H.; Grant, A.; Ellinger, S.; Odom, S. A.; Sweat, D.; Tanner, D. B.; Rinzler, A. G.; Barlow, S.; Brédas, J.-L.; Kippelen, B.; Marder, S. R.; Reynolds, J. R. *J. Am. Chem. Soc.* **2009**, *131*, 2824.
(622) Marsitzky, D.; Vestberg, R.; Blainey, P.; Tang, B. T.; Hawker, C. J.; Carter, K. R. *J. Am. Chem. Soc.* **2001**, *123*, 6965.
(623) Tang, H. Z; Fujiki, M.; Zhang, Z.-B.; Torimitsu, K.; Montonaga, M. *Chem. Commun.* **2001**, 2426.
(624) Chou, C.-H.; Shu, C.-F. *Macromolecules* **2002**, *35*, 9673.
(625) Tsai, L.-R.; Li, C.-W.; Chen, Y. *J. Polym. Sci., Part A: Polym. Chem.* **2008**, *46*, 5945.
(626) Setayesh, S.; Grimsdale, A. C.; Weil, T.; Enkelmann, V.; Müllen, K.; Meghdadi, F.; List, E. J. W.; Leising, G. *J. Am. Chem. Soc.* **2001**, *123*, 946.
(627) Becker, S.; Ego, C.; Grimsdale, A. C.; List, E. J. W.; Marsitzky, D.; Pogantsch, A.; Setayesh, S.; Leising, G.; Müllen, K. *Synth. Met.* **2002**, *125*, 73.
(628) Pogantsch, A.; Wenzl, F. P.; List, E. J. W.; Leising, G.; Grimsdale, A. C.; Müllen, K. *Adv. Mater.* **2002**, *14*, 1061.
(629) Lupton, J. M.; Schouwink, P.; Keivanidis, P. E.; Grimsdale, A. C.; Müllen, K. *Adv. Funct. Mater.* **2003**, *13*, 154.
(630) Pogantsch, A.; Gadermaier, C.; Cerullo, G.; Lanzani, G.; Scherf, U.; Grimsdale, A. C.; Müllen, K.; List, E. J. W. *Synth. Met.* **2003**, *139*, 847.
(631) Pogantsch, A.; Wenzl, F. P.; Scherf, U.; Grimsdale, A. C.; Müllen, K. *J. Chem. Phys.* **2003**, *119*, 6904.
(632) Wu, C.-W.; Tsai, C.-M.; Lin, H.-C. *Macromolecules* **2006**, *39*, 4298.
(633) Yu, M.; Liu, L.; Wang, S. *J. Polym. Sci., Part A: Polym. Chem.* **2008**, *46*, 7462.
(634) Zhu, B.; Han, Y.; Sun, M.; Bo, Z. *Macromolecules* **2007**, *40*, 4494.

(635) Wyatt, S. R.; Hu, Q.-S.; Yan, X.-L.; Bare, W. D.; Pu, L. *Macromolecules* **2001**, *34*, 7983.
(636) Ma, L.; Lee, S. J.; Lin, W. *Macromolecules* **2002**, *35*, 6178.
(637) Tian, Y.; Kamata, K.; Yoshida, H.; Iyoda, T. *Chem.—Eur. J.* **2006**, *12*, 584.
(638) Kajitani, T.; Lin, H.; Nagai, K.; Okoshi, K.; Onouchi, H.; Yashima, E. *Macromolecules* **2009**, *42*, 560.
(639) Tsuda, Y.; Kuwahara, R.; Lee, B. J.; Oh, J.-M. *Polym. Prep. (Am. Chem. Soc., Div. Polym. Chem.)* **1999**, *40*, 1215.
(640) Tsuda, Y.; Kuwahara, R.; Oh, J.-M. *Trans. Mater. Res. Soc. Jpn.* **2004**, *29*, 267.
(641) Kim, H.-J.; Lee, E.; Kim, M.; Kim, M.-C.; Lee, M.; Sim, E. *Chem.—Eur. J.* **2008**, *14*, 3883.
(642) Kim, K. T.; Han, J.; Ryu, C. Y.; Sun, F. C.; Sheiko, S. S.; Winnik, M. A.; Manners, I. *Macromolecules* **2006**, *39*, 7922.
(643) Zhuravel, M. A.; David, N. E.; Nguyen, S. T.; Koltover, I. *J. Am. Chem. Soc.* **2004**, *126*, 9882.
(644) Lee, C. C.; Fréchet, J. M. J. *Macromolecules* **2006**, *39*, 476.
(645) Lübbert, A.; Nguyen, T. Q.; Sun, F.; Sheiko, S. S.; Klok, H.-A. *Macromolecules* **2005**, *38*, 2064.
(646) Gössel, I.; Shu, L.; Schlüter, A. D.; Rabe, J. P. *J. Am. Chem. Soc.* **2002**, *124*, 6860.
(647) Gössel, I.; Shu, L.; Schlüter, A. D.; Rabe, J. P. *Single. Mol.* **2002**, *3*, 315.
(648) Newkome, G. R.; Kotta, K.; Moorefield, C. N. *Chem.—Eur. J.* **2006**, *12*, 3726.
(649) Hassan, M. L.; Moorefield, C. N.; Newkome, G. R. *Macromol. Rapid Commun.* **2004**, *25*, 1999.
(650) Hassan, M. L.; Moorefield, C. N.; Kotta, K.; Newkome, G. R. *Polymer* **2005**, 8947.
(651) Hwang, S. H.; Moorefield, C. N.; Wang, P.; Jeong, K.-U.; Cheng, S. Z. D.; Kotta, K. K.; Newkome, G. R. *Chem. Commun.* **2006**, 3495.
(652) Pohl, M.; Schaller, J.; Mesiter, F.; Heinze, T. *Macromol. Symp.* **2008**, *262*, 119.
(653) Heinze, T.; Schöbitz, M.; Pohl, M.; Meister, F. *J. Polym. Sci., Part A: Polym. Chem.* **2008**, *46*, 3853.
(654) Pohl, M.; Michaelis, N.; Meister, F.; Heinze, T. *Biomacromolecules* **2009**, *10*, 382.
(655) Östmark, E.; Lindqvist, J.; Nyström, D.; Maimstöm, E. *Biomacromolecules* **2007**, *8*, 3815.
(656) Östmark, E.; Harrison, S.; Wooley, K. L.; Malmström, E. E. *Biomacromolecules* **2007**, *8*, 1138.
(657) Zhang, C.; Price, L. M.; Daly, W. H. *Biomacromolecules* **2006**, *7*, 139.
(658) Hassan, M. L. *J. Appl. Polym. Sci.* **2006**, *101*, 2079.
(659) Sashiwa, H.; Shigemasa, Y.; Roy, R. *Macromolecules* **2000**, *33*, 6913.
(660) Sashiwa, H.; Shigemasa, Y.; Roy, R. *Carbohydr. Polym.* **2002**, *49*, 195.
(661) Sashiwa, H.; Shigemasa, Y.; Roy, R. *Macromolecules* **2001**, *34*, 3905.
(662) Niederhanfner, P.; Sebestik, J.; Jezek, J. *J. Pept. Sci.* **2008**, *14*, 44.
(663) Hammong, M. R.; Mezzenga, R. *Soft Matter* **2008**, *4*, 952.
(664) Xie, D.; Jiang, M.; Zhang, G.; Chen, D. *Chem.—Eur. J.* **2007**, *13*, 3346.
(665) Chuang, W.-T.; Sheu, H.-S.; Jeng, U. S.; Wu, H.-H.; Hong, P.-D.; Lee, J. J. *Chem. Mater.* **2009**, *21*, 975.
(666) Zhu, X.; Beginn, U.; Möller, M.; Gaerba, R. I.; Anokhin, D. V.; Ivanov, D. A. *J. Am. Chem. Soc.* **2006**, *128*, 16928.
(667) Albrecht, K.; Gallyamov, M.; Zhu, X.; Moeller, M. *Macromol. Chem. Phys.* **2007**, *208*, 1409.
(668) Hammond, S. R.; Zhou, W.-J.; Gin, D. L.; Avlyanov, J. K. *Liq. Cryst.* **2002**, *9*, 1151.
(669) Cheng, Z.; Ren, B.; Shan, H.; Liu, X.; Tong, Z. *Macromolecules* **2008**, *41*, 2656.
(670) Cheng, Z.; Ren, B.; Zhao, D.; Liu, X.; Tong, Z. *Macromolecules* **2009**, *42*, 2762.
(671) Yang, P.-J.; Wu, C.-W.; Sahu, D.; Lin, H.-C. *Macromolecules* **2008**, *41*, 9692.
(672) Leung, K. C.-F.; Mendes, P. M.; Magonov, S. N.; Northrop, B. H.; Kim, S.; Patel, K.; Flood, A. H.; Tseng, H.-R.; Stoddart, J. F. *J. Am. Chem. Soc.* **2006**, *128*, 10707.
(673) Andreopoulou, A. K.; Kallitsis, J. K. *Eur. J. Org. Chem.* **2005**, 4448.
(674) Percec, V.; Zipp, G.; Johansson, G.; Beginn, U.; Möller, M. *Macromol. Chem. Phys.* **1997**, *198*, 265.
(675) Beginn, U.; Zipp, G.; Möller, M.; Johansson, G.; Percec, V. *Macromol. Chem. Phys.* **1997**, *198*, 2839.
(676) Gankema, H.; Hempenius, M. A.; Möller, M.; Johansson, G.; Percec, V. *Macromol. Symp.* **1996**, *102*, 381.
(677) Beginn, U.; Zipp, G.; Möller, M. *J. Polym. Sci., Part A: Polym. Chem.* **1999**, *38*, 631.
(678) Beginn, U.; Zipp, G.; Möller, M. *Chem.—Eur. J.* **2000**, *6*, 2016.
(679) Beginn, U.; Zipp, G.; Mourran, A.; Walther, P.; Möller, M. *Adv. Mater.* **2000**, *12*, 513.
(680) Beginn, U.; Zipp, G.; Möller, M. *Adv. Mater.* **2000**, *12*, 510.
(681) Gankema, H.; Hempenius, M. A.; Möller, M. *Rec. Trac. Chim.* **1994**, *113*, 241.
(682) Percec, V.; Bera, T. K. *Biomacromolecules* **2002**, *3*, 167.
(683) Percec, V.; Bera, T. K. *Tetrahedron* **2002**, *58*, 4031.
(684) Lee, H.-Y.; Lee, H.; Ko, Y. H.; Chang, Y. J.; Oh, N.-K.; Zin, W.-C.; Kim, K. *Angew. Chem., Int. Ed.* **2001**, *40*, 2669.
(685) Yoshio, M.; Kagata, T.; Hoshino, K.; Mukai, T.; Ohno, H.; Kato, T. *J. Am. Chem. Soc.* **2006**, *128*, 5570.
(686) Weber, P. C.; Salemme, F. R. *Nature* **1980**, *287*, 82.
(687) Percec, V.; Bera, T. K.; Glodde, M.; Fu, Q.; Balagurusamy, V. S. K.; Heiney, P. A. *Chem.—Eur. J.* **2003**, *9*, 921.
(688) Chow, H.-K.; Leung, C.-F.; Li, W.; Wong, K.-W.; Xi, L. *Angew. Chem., Int. Ed.* **2003**, *42*, 4919.
(689) Chow, H.-K.; Leung, C.-F.; Xi, L.; Lau, L. W. M. *Macromolecules* **2004**, *37*, 3595.
(690) Cheung, S.-Y.; Chow, H.-K.; Ngai, T.; Wei, X. *Chem.—Eur. J.* **2009**, *15*, 2278.
(691) Chow, H.-K.; Leung, C.-F.; Li, W.; Wong, K.-W.; Xi, L. *Angew. Chem., Int. Ed.* **2003**, *42*, 4919.
(692) Santini, C. M. B.; Johnson, M. A.; Boedicker, J. Q.; Hatton, T. A.; Hammond, P. T. *J. Polym. Sci., Part A: Polym. Chem.* **2004**, *42*, 2784.
(693) Cheng, C.-X.; Tang, R. P.; Xi, F. *J. Polym. Sci., Part A: Polym. Chem.* **2005**, *43*, 2291.
(694) Chen, C. X.; Tang, R. P.; Zhao, Y. L.; Xi, F. *J. Appl. Polym. Sci.* **2004**, *91*, 2733.
(695) Cheng, C.; Tang, R.; Xi, F. *Macromol. Rapid Commun.* **2005**, *26*, 744.
(696) Yi, Z.; Zhang, Y.; Chen, Y.; Xi, F. *Macromol. Rapid Commun.* **2008**, *29*, 757.
(697) Cheng, C. X.; Tian, Y.; Shi, Y. Q.; Tang, R. P.; Xi, F. *Langmuir* **2005**, *21*, 6576.
(698) Cheng, C.; Tian, Y.; Shi, Y.; Tang, R.; Xi, F. *Macromol. Rapid Commun.* **2005**, *26*, 1266.
(699) Cheng, C.-X.; Jiao, T.-F.; Tang, R.-P.; Chen, E. Q.; Liu, M.-H.; Xi, F. *Macromolecules* **2006**, *39*, 6327.
(700) Cheng, C.-X.; Huang, Y.; Tang, R.-P.; Chen, E.-q.; Xi, F. *Macromolecules* **2005**, *38*, 3044.
(701) Li, C.; Schlüter, A. D.; Zhang, A.; Mezzenga, R. *Adv. Mater.* **2008**, *20*, 4530.
(702) Yi, Z.; Liu, X.; Jiao, Q.; Chen, E.; Chen, Y.; Xi, F. *J. Polym. Sci., Part A: Polym. Chem.* **2008**, *46*, 4205.
(703) Shenhar, R.; Xu, H.; Frankamp, B. L.; Goel, D.; Sanyal, A.; Rotello, V. M. *J. Am. Chem. Soc.* **2005**, *127*, 16318.
(704) Rajaram, S.; Choi, T.-L.; Rolandi, M.; Fréchet, J. M. J. *J. Am. Chem. Soc.* **2007**, *129*, 9619.
(705) Wigglesworth, T. J.; Teixeira, F.; Axthelm, F.; Eisler, S.; Csaba, N. S.; Merkle, H. P.; Meier, W.; Diederich, F. *Org. Biomol. Chem.* **2008**, *6*, 1905.
(706) Jiang, J.; Liu, H.-W.; Zhao, Y.-L.; Chen, C.-F.; Xi, F. *J. Polym. Sci., Part A: Polym. Chem.* **2002**, *40*, 1167.
(707) Liu, Z.-T.; He, Y.-M.; Wang, Z. J.; Feng, Y.; Fan, Q.-H. *J. Polym. Sci., Part A: Polym. Chem.* **2008**, *46*, 886.
(708) Gitsov, I.; Wooley, K. L.; Hawker, C. J.; Fréchet, J. M. J. *J. Polym. Prepr. (Am. Chem. Soc., Div. Polym. Chem.)* **1991**, *32*, 631.
(709) Gitsov, I.; Fréchet, J. M. J. *Macromolecules* **1994**, *27*, 7309.
(710) Gitsov, I.; Fréchet, J. M. J. *Macromolecules* **1993**, *26*, 6536.
(711) Gitsov, I.; Wooley, K. L.; Fréchet, J. M. J. *Angew. Chem., Int. Ed.* **1992**, *31*, 1200.
(712) Gitsov, I.; Wooley, K. L.; Hawker, C. J.; Ivanova, P. T.; Fréchet, J. M. J. *Macromolecules* **1993**, *26*, 5621.
(713) Chapman, T. M.; Hillyer, G. L.; Mahan, E. J.; Shaffer, K. A. *J. Am. Chem. Soc.* **1994**, *116*, 11195.
(714) Iyer, J.; Fleming, K.; Hammond, P. T. *Macromolecules* **1998**, *31*, 8757.
(715) Iyer, J.; Hammond, P. T. *Langmuir* **1999**, *15*, 1299.
(716) Johnson, M. A.; Iyer, J.; Hammond, P. T. *Macromolecules* **2004**, *37*, 2490.
(717) Gitsov, I.; Ivanova, P. T.; Fréchet, J. M. J. *Macromol. Rapid Commun.* **1994**, *15*, 387.
(718) Leduc, M. R.; Hawker, C. J.; Dao, J.; Fréchet, J. M. J. *J. Am. Chem. Soc.* **1996**, *118*, 11111.
(719) Fernandez-Megia, E.; Correa, J.; Riguera, R. *Biomacromolecules* **2006**, *7*, 3104.
(720) Namazi, H.; Adeli, M. *Polymer* **2005**, *46*, 10788.
(721) Vanhest, J. C. M.; Baars, M.; Elissenroman, C.; Vangenderen, M. H. P.; Meijer, E. W. *Macromolecules* **1995**, *28*, 6689.
(722) Vanhest, J. C. M.; Delnoye, D. A. P.; Baars, M.; Vangenderen, M. H. P.; Meijer, E. W. *Science* **1995**, *268*, 1592.

(723) Matyjaszewski, K.; Shigemoto, T.; Frechet, J. M. J.; Leduc, M. *Macromolecules* **1996**, *29*, 4167.
(724) Aoi, K.; Motoda, A.; Okada, M.; Imae, T. *Macromol. Rapid Commun.* **1997**, *18*, 945.
(725) Leduc, M. R.; Hayes, W.; Fréchet, J. M. J. *J. Polym. Sci., Part A: Polym. Chem.* **1998**, *36*, 1.
(726) Román, C.; Fischer, H. R.; Meijer, E. W. *Macromolecules* **1999**, *32*, 5525.
(727) Jang, S. S.; Lin, S. T.; Cagin, T.; Molinero, V.; Goddard, W. A. *J. Phys. Chem. B* **2005**, *109*, 10154.
(728) Tian, L.; Hammond, P. T. *Chem. Mater.* **2006**, *18*, 3976.
(729) Mackay, M. E.; Hong, Y.; Jeong, M.; Tande, B. M.; Wagner, N. J.; Hong, S.; Gido, S. P.; Vestberg, R.; Hawker, C. J. *Macromolecules* **2002**, *35*, 8391.
(730) Newkome, G. R.; Kotta, K. K.; Mishra, A.; Moorefield, C. N. *Macromolecules* **2004**, *37*, 8262.
(731) Chang, Y.; Kwon, Y. C.; Lee, S. C.; Kim, C. *Macromolecules* **2000**, *33*, 4496.
(732) Wang, L. L.; Meng, Z. L.; Yu, Y. L.; Meng, Q. W.; Chen, D. Z. *Polymer* **2008**, *49*, 1199.
(733) Cho, B. K.; Jain, A.; Gruner, S. M.; Wiesner, U. *Chem. Commun.* **2005**, 2143.
(734) Cho, B. K.; Jain, A.; Gruner, S. M.; Wiesner, U. *Science* **2004**, *305*, 1598.
(735) Cho, B. K.; Jain, A.; Gruner, S. M.; Wiesner, U. *Chem. Mater.* **2007**, *19*, 3611.
(736) Chung, Y. W.; Lee, J. K.; Zin, W. C.; Cho, B. K. *J. Am. Chem. Soc.* **2008**, *130*, 7139.
(737) Lee, H.-I.; Lee, J. A.; Poon, Z.; Hammond, P. T. *Chem. Commun.* **2008**, 3726.
(738) Patton, D. L.; Taranekar, P.; Fulghum, T.; Advincula, R. *Macromolecules* **2008**, *41*, 6703.
(739) Gao, Y.; Zhang, X. W.; Yang, M.; Zhang, X. J.; Wang, W.; Wegner, G.; Burger, C. *Macromolecules* **2007**, *40*, 2606.
(740) Lee, W. B.; Elliott, R.; Mezzanga, R.; Fredrickson, G. H. *Macromolecules* **2009**, *42*, 849.
(741) Meyers, S. R.; Juhn, F. S.; Griset, A. P.; Luman, N. R.; Grinstaff, M. W. *J. Am. Chem. Soc.* **2008**, *130*, 14444.
(742) Ling, F. H.; Lu, V.; Svec, F.; Fréchet, J. M. J. *J. Org. Chem.* **2002**, *67*, 1993.
(743) Vestberg, R.; Piekarski, A. M.; Pressly, E. D.; Berkel, K. Y. V.; Malcoch, M.; Gerbac, J.; Ueno, N.; Hawker, C. J. *J. Polym. Sci., Part A: Polym. Chem.* **2008**, *47*, 1237.
(744) Mamdouh, W.; Uji-i, H.; Ladislaw, J. S.; Dulcey, A. E.; Percec, V.; De Schryver, F. C.; De Feyter, S. *J. Am. Chem. Soc.* **2006**, *128*, 317.
(745) Mamdouh, W.; Uji-i, H.; Dulcey, A. E.; Percec, V.; De Feyter, S.; De Schryver, F. C. *Langmuir* **2004**, *20*, 7678.
(746) De Feyter, S.; Uji-I, H.; Mamdoih, W.; Miura, Y.; Zhang, J.; Jonkeijm, P.; Schenning, A. P. H. J.; Meijer, E. W.; Chen, Z.; Würthner, F.; Schuurmans, N.; van Esch, J.; Feringa, B.; Dulcey, A. E.; Percec, V.; De Schryver, F. C. *Int. J. Nanotech.* **2006**, *3*, 462.
(747) van Hest, J. C. M.; Delnoye, D. A. P.; Baars, M. W. P. L.; Elissen-Román, C.; van Genderen, M. H. P.; Meijer, E. W. *Chem.—Eur. J.* **1996**, *2*, 1616.
(748) Gitsov, I.; Zhu, C. *J. Am. Chem. Soc.* **2003**, *125*, 11228.
(749) Ge, Z.; Luo, S.; Liu, S. *J. Polym. Sci., Part A: Polym. Chem.* **2006**, *44*, 1357.
(750) Kim, K. T.; Lee, I. H.; Park, C.; Song, Y.; Kim, C. *Macromol. Res.* **2004**, *12*, 528.
(751) Peng, S.-M.; Chen, Y.; Hua, C.; Dong, C.-M. *Macromolecules* **2009**, *42*, 104.
(752) Hua, C.; Dong, C.-M.; Wei, Y. *Biomacromolecules* **2009**, *10*, 1140.
(753) Simonyan, A.; Gitsov, I. *Langmuir* **2008**, *24*, 11431.
(754) Gitsov, I.; Hamzik, J.; Ryan, J.; Simonyan, A.; Nakas, J. P.; Omori, S.; Krastanov, A.; Cohen, T.; Tanenbaum, S. W. *Biomacromolecules* **2008**, *9*, 804.
(755) Gitsov, I.; Simonyan, A.; Krastanov, A.; Tanenbaum, S. *Green Oxidation of Steroids in Nano-Reactors Assembled from Laccase and Linear-Dendritic Copolymers Polymer Biocatalysis and Biomaterials*; Cheng, H. N., Gross, R. A., Eds.;ACS Symposium Series Vol. *999*; American Chemical Society: Washington, DC, 2008; pp 110−128.
(756) Li, B.; Martin, A. L.; Gillies, E. R. *Chem. Commun.* **2007**, 5217.
(757) Yoo, Y.-S.; Choi, J.-H.; Song, J. H.; Oh, N.-K.; Zin, W.-C.; Park, S.; Chang, T.; Lee, M. *J. Am. Chem. Soc.* **2004**, *126*, 6294.
(758) Holzmueller, J.; Genson, K. L.; Park, Y.; Yoo, Y.-S.; Park, M.-H.; Lee, M.; Tsukruk, V. *Langmuir* **2005**, *21*, 6392.
(759) Ryu, J. H.; Hong, D. J.; Lee, M. *Chem. Commun.* **2008**, 1043.
(760) Ito, Y.; Washio, I.; Ueda, M. *Macromolecules* **2008**, *41*, 2778.
(761) Lecommandoux, S.; Klok, H. A.; Sayar, M.; Stupp, S. I. *J. Polym. Sci., Part A: Polym. Chem.* **2003**, *41*, 3501.
(762) Demus, D.; Richter, L. *Textures of Liquid Crystals*; Verlag Chemie: Weinheim, Germany, 1978.
(763) Gray, G. W.; Goodby, J. W. *Smectic Liquid Crystals: Textures and Structures*; Leonard Hill: Glasgow, Scotland, 1984.
(764) Cheon, K.-S.; Kazmaier, P. M.; Keum, S.-R.; Park, K.-T.; Buncel, E. *Can. J. Chem.* **2004**, *82*, 551.
(765) Ji, Y.; Kuang, G.-C.; Jia, X.-R.; Chen, E.-Q.; Wang, B.-B.; Li, W.-S.; Wei, Y.; Lei, J. *Chem. Commun.* **2007**, 4233.
(766) Wang, B.-B.; Li, W.-S.; Jia, X.-R.; Gao, M.; Ji, Y.; Zhang, X.; Li, Z.-C.; Jiang, L.; Wei, Y. *J. Colloid Interface Sci.* **2007**, *314*, 289.
(767) Park, C.; Lim, J.; Yun, M.; Kim, C. *Angew. Chem., Int. Ed.* **2008**, *47*, 2959.
(768) Zhu, X.; Tartsch, B.; Beginn, U.; Möller, M. *Chem.—Eur. J.* **2004**, *10*, 3871.
(769) Yagai, S.; Kubota, S.; Saito, H.; Unoike, K.; Karatsu, T.; Kitamura, A.; Ajayaghosh, A.; Kenesato, M.; Kikkawa, Y. *J. Am. Chem. Soc.* **2009**, *131*, 5408.
(770) Tian, L.; Nguyen, P.; Hammond, P. T. *Chem. Commun.* **2006**, 3489.
(771) Zubarev, E. R.; Stupp, S. I. *J. Am. Chem. Soc.* **2002**, *124*, 5762.
(772) Zeng, X.; Ungar, G.; Impéror-Clerc, M. *Nat. Mater.* **2005**, *4*, 562.
(773) Zubarev, E. R.; Pralle, M. U.; Sone, E. D.; Stupp, S. I. *J. Am. Chem. Soc.* **2001**, *123*, 4105.
(774) de Gans, B. J.; Wiegand, S.; Zubarev, E. R.; Stupp, S. I. *J. Phys. Chem. B* **2002**, *106*, 9730.
(775) Zubarev, E. R.; Sone, E. D.; Stupp, S. I. *Chem.—Eur. J.* **2006**, *12*, 7313.
(776) Zubarev, E. R.; Pralle, M. U.; Sone, E. D.; Stupp, S. I. *Adv. Mater.* **2002**, *14*, 198.
(777) Li, L. M.; Beniash, E.; Zubarev, E. R.; Xiang, W. H.; Rabatic, B. M.; Zhang, G. Z.; Stupp, S. I. *Nat. Mater.* **2003**, *2*, 689.
(778) Sone, E. D.; Zubarev, E. R.; Stupp, S. I. *Angew. Chem., Int. Ed.* **2002**, *41*, 1706.
(779) Sone, E. D.; Zubarev, E. R.; Stupp, S. I. *Small* **2005**, *1*, 694.
(780) Messmore, B. W.; Sukerkar, P. A.; Stupp, S. I. *J. Am. Chem. Soc.* **2005**, *127*, 7992.
(781) Li, L. S.; Jiang, H. Z.; Messmore, B. W.; Bull, S. R.; Stupp, S. I. *Angew. Chem., Int. Ed.* **2007**, *46*, 5873.
(782) Tsai, W. W.; Li, L. S.; Cui, H. G.; Jiang, H. Z.; Stupp, S. I. *Tetrahedron* **2008**, *64*, 8504.
(783) Hsu, L.; Cvetanovich, G. L.; Stupp, S. I. *J. Am. Chem. Soc.* **2008**, *130*, 3892.
(784) Messmore, B. W.; Hulvat, J. F.; Sone, E. D.; Stupp, S. I. *J. Am. Chem. Soc.* **2004**, *126*, 14452.
(785) Liu, L.; Kim, J. K.; Lee, M. *ChemPhysChem* **2008**, *9*, 1585.
(786) Nantalaksakul; Mueller, A.; Klaikherd, A.; Bardeen, C. J.; Thayumanavan, S. *J. Am. Chem. Soc.* **2009**, *131*, 2727.
(787) Backes, C.; Scmidt, C. D.; Hauke, F.; Böttcher, C.; Hirsch, A. *J. Am. Chem. Soc.* **2009**, *131*, 2172.
(788) Ehli, C.; Oelsner, C.; Guldi, D. M.; Mateo-Alonso, A.; Prato, M.; Schmidt, C.; Backes, C.; Hauke, F.; Hirsch, A. *Nat. Chem.* **2009**, *1*, 243.
(789) Kim, J. K.; Hong, M. K.; Ahn, J. H.; Lee, M. *Angew. Chem., Int. Ed.* **2005**, *44*, 328.
(790) Kim, J. K.; Lee, E.; Lee, M. *Angew. Chem., Int. Ed.* **2006**, *45*, 7353.
(791) Lee, E.; Kim, J. K.; Lee, M. *Angew. Chem., Int. Ed.* **2008**, *47*, 6375.
(792) Jang, C. J.; Ryu, J. H.; Lee, J. D.; Sohn, D.; Lee, M. *Chem. Mater.* **2004**, *16*, 4226.
(793) Ryu, J.-H.; Lee, E.; Lim, Y.-B; Lee, M. *J. Am. Chem. Soc.* **2007**, *129*, 4808.
(794) Ooya, T.; Huh, K. M.; Saitoh, M.; Tamiya, E.; Park, K. *Sci. Tech. Adv. Mater.* **2005**, *6*, 452.
(795) Emerick, T.; Hayes, W.; Frechet, J. M. J. *J. Polym. Sci., Part A: Polym. Chem.* **1999**, *37*, 3748.
(796) Duan, X.; Yuan, F.; Wen, X.; Yang, M.; He, B.; Wang, W. *Macromol. Chem. Phys.* **2004**, *205*, 1410.
(797) Nguyen, P. M.; Hammond, P. T. *Langmuir* **2006**, *22*, 7825.
(798) Kim, Y. S.; Gil, E. S.; Lowe, T. L. *Macromolecules* **2006**, *39*, 7805.
(799) Namazi, H.; Adeli, M. *Eur. Polym. J.* **2003**, *39*, 1491.
(800) Namazi, H.; Adeli, M. *J. Polym. Sci., Part A: Polym. Chem.* **2005**, *43*, 28.
(801) Newkome, G. R.; Baker, G. R.; Saunder, M. J.; Russo, P. S.; Gupta, V. K.; Yao, Z.-Q.; Miller, J. E.; Bouillion, K. *J. Chem. Soc., Chem. Commun.* **1986**, 752.
(802) Jeon, H.-J.; Kang, M. K.; Park, C.; Kim, K. T.; Chang, J. Y.; Kim, C.; Song, H. H. *Langmuir* **2007**, *23*, 13109.
(803) Lee, E.; Lee, B.-I.; Kim, S.-H.; Lee, J.-K.; Zin, W.-C.; Cho, B.-K. *Macromolecules* **2009**, *42*, 4134.
(804) Cho, B.-K.; Jain, A.; Mahajan, S.; Ow, H.; Gruner, S. M.; Wiesner, U. *J. Am. Chem. Soc.* **2004**, *126*, 4070.
(805) Gibtner, T.; Hampel, F.; Gisselbrecht, J.-P.; Hirsch, A. *Chem.—Eur. J.* **2002**, *8*, 408.
(806) Malenfant, P. R. L.; Groenendaal, L.; Fréchet, J. M. J. *J. Am. Chem. Soc.* **1998**, *120*, 10990.

(807) Apperloo, J. J.; Janssen, R. A. J.; Malenfant, P. R. L.; Fréchet, J. M. J. *Macromolecules* **2000**, *33*, 7038.
(808) Apperloo, J. J.; Malenfant, P. R. L.; Fréchet, J. M. J.; Janssen, R. A. J. *Synth. Met.* **2001**, 1259.
(809) Apperloo, J. J.; Janssen, R. A. J.; Malenfant, P. R. L.; Fréchet, J. M. J. *J. Am. Chem. Soc.* **2001**, *123*, 6916.
(810) Bae, J.; Choi, J.-H.; Oh, N.-K.; Kim, B.-S; Lee, M. *J. Am. Chem. Soc.* **2005**, *127*, 9668.
(811) Ryu, J. H.; Kim, H. J.; Huang, Z. G.; Lee, E.; Lee, M. *Angew. Chem., Int. Ed.* **2006**, *45*, 5304.
(812) Ryu, J. H.; Tang, L.; Lee, E.; Kim, H.-J.; Lee, M. *Chem.—Eur. J.* **2008**, *14*, 871.
(813) Huang, Z.; Liu, L.; Lee, E.; Lee, M. *Bull. Korean Chem. Soc.* **2008**, *29*, 1485.
(814) Osano, K.; Turner, R. S. *J. Polym. Sci., Part A: Polym. Chem.* **2008**, *46*, 958.
(815) Lee, M.; Jeong, Y. S.; Cho, B. K.; Oh, N. K.; Zin, W. C. *Chem.—Eur. J.* **2002**, *8*, 876.
(816) Jin, L. Y.; Bae, J.; Ryu, J.-H.; Lee, M. *Angew. Chem., Int. Ed.* **2006**, *45*, 650.
(817) Lee, E.; Jeong, Y.-H.; Kim, J.-K.; Lee, M. *Macromolecules* **2007**, *40*, 8355.
(818) Kim, J.-K.; Lee, E.; Jeong, Y.-H.; Lee, J.-K.; Zin, W.-C.; Lee, M. *J. Am. Chem. Soc.* **2007**, *129*, 6082.
(819) Kim, J.-K.; Lee, E.; Huang, Z.; Lee, M. *J. Am. Chem. Soc.* **2006**, *128*, 14022.
(820) Kim, J.-K.; Lee, E.; Lim, Y.-B.; Lee, M. *Angew. Chem., Int. Ed.* **2008**, *47*, 4662.
(821) Kim, H. J.; Jung, E. Y.; Jin, L. Y.; Lee, M. *Macromolecules* **2008**, *41*, 6066.
(822) Miller, S.; Schlechte, J. S. *Polym. Prepr. (Am. Chem. Soc., Div. Polym. Chem.)* **2000**, *41*, 323.
(823) Kim, H.-J.; Zin, W.-C.; Lee, M. *J. Am. Chem. Soc.* **2004**, *126*, 7009.
(824) Hoeben, F. J. M.; Zhang, J.; Lee, C. C.; Pouderoijen, M. J.; Wolffs, M.; Würthner, F.; Schenning, A.; Meijer, E. W.; De Feyter, S. *Chem.—Eur. J.* **2008**, *14*, 8579.
(825) Schenning, A.; von Herrikhuyzen, J.; Jonkheijm, P.; Chen, Z.; Würthner, F.; Meijer, E. W. *J. Am. Chem. Soc.* **2002**, *124*, 10252.
(826) Hoeben, F. J. M.; Herz, L. M.; Daniel, C.; Jonkheijm, P.; Schenning, A.; Silva, C.; Meskers, S. C. J.; Beljonne, D.; Phillips, R. T.; Friend, R. H.; Meijer, E. W. *Angew. Chem., Int. Ed.* **2004**, *43*, 1976.
(827) Jonkheijm, P.; Miura, A.; Zdanowska, M.; Hoeben, F. J. M.; De Feyter, S.; Schenning, A.; De Schryver, F. C.; Meijer, E. W. *Angew. Chem., Int. Ed.* **2004**, *43*, 74.
(828) Hoeben, F. J. M.; Jonkheijm, P.; Meijer, E. W.; Schenning, A. *Chem. Rev.* **2005**, *105*, 1491.
(829) Cho, B.-K.; Kim, H.-J.; Chung, Y.-W.; Lee, B.-I.; Lee, M. *Adv. Polym. Sci.* **2008**, *219*, 69.
(830) Wyszorgrodzka, M.; Haag, R. *Chem.—Eur. J.* **2008**, *14*, 9202.
(831) Malthête, J.; Levelut, A.-M.; Nguyen Huu, T. *J. Phys. Lett., Paris* **1985**, *46*, L875.
(832) Malthête, J.; Collet, A.; Levelut, A.-M. *Liq. Cryst.* **1989**, *5*, 123.
(833) Malthête, J.; Levelut, A.-M. *Adv. Mater.* **1991**, *3*, 94.
(834) Hatano, T.; Kato, T. *Tetrahedron* **2008**, *64*, 8368.
(835) Sagara, Y.; Kato, T. *Angew Chem., Int. Ed.* **2008**, *47*, 5175.
(836) Schenning, A. P. H. J.; Jonkheijm, P.; Peeters, E.; Meijer, E. W. *J. Am. Chem. Soc.* **2001**, *123*, 409.
(837) Hoeben, F. J. M.; Schenning, A. P. H. J.; Meijer, E. W. *ChemPhysChem* **2005**, *6*, 2337.
(838) Spano, F. C.; Meskers, S. C. J.; Hennebicq, E.; Beljonne, D. *J. Am. Chem. Soc.* **2007**, *129*, 7044.
(839) Herz, L. M.; Daniel, C.; Silva, C.; Hoeen, F. J. M.; Schenning, A. P. H. J.; Meijer, E. W.; Friend, R. H.; Phillips, R. T. *Phys. Rev. B* **2003**, *68*, 045203.
(840) Daniel, C.; Herz, L. M.; Silva, C.; Hoeben, F. J. M.; Schenning, A. P. H. J.; Meijer, E. W. Phys. Rev. B 2003, *235212*.
(841) Daniel, C.; Herz, L. M.; Silva, C.; Hoeben, F. J. M.; Schenning, A. P. H. J.; Meijer, E. W. *Synth. Met.* **2004**, *147*, 29.
(842) Daniel, C.; Makereel, F.; Herz, L. M.; Hoeben, F. J. M.; Jonkheijm, P.; Schenning, A. P. H. J.; Meijer, E. W.; Friend, R. H.; Silva, C. *J. Chem. Phys.* **2005**, *123*, 084902.
(843) Deljonne, D.; Hennebicq, E.; Daniel, C.; Herz, L. M.; Silva, C.; Scholes, G. D.; Hoeben, F. J. M.; Jonkheijkm, P.; Schenning, P. H. J.; Meskers, S. C. J.; Phillips, R. T.; Friend, R. H.; Meijer, E. W. *J. Phys. Chem. B* **2005**, *109*, 10594.
(844) Chang, M. H.; Hoeben, F. J. M.; Jonkheijm, P.; Schenning, A. P. H. J.; Meijer, E. W.; Silva, C.; Herz, L. M. *Chem. Phys. Lett.* **2006**, *418*, 196.
(845) Daniel, C.; Westenhoff, S.; Makereel, M.; Friend, R. H.; Beljonne, D.; Herz, L. M.; Silva, C. *J. Phys. Chem. C* **2007**, *111*, 19111.
(846) Daniel, C.; Makereel, F.; Herz, L. M.; Hoeben, F. J. M.; Jonkeijm, P.; Schenning, A. P. H. J.; Meijer, E. W.; Silva, C. *J. Chem. Phys.* **2008**, *129*, 104701.
(847) Jonkheijm, P.; van Duren, J. K. J.; Kemerink, M.; Janssen, R. A. J.; Schenning, A. P. H. J.; Meijer, E. E. *Macromolecules* **2006**, *39*, 784.
(848) Tanabe, K.; Yasuda, T.; Yoshio, M.; Kato, T. *Org. Lett.* **2007**, *9*, 4271.
(849) Liu, L.; Kim, J.-K.; Gunawidjaja, R.; Tsukruk, V. V.; Lee, M. *Langmuir* **2008**, *24*, 12340.
(850) Joester, D.; Losson, M.; Pugin, R.; Heinzelmann, H.; Walter, E.; Merkle, H. P.; Diederich, F. *Angew. Chem., Int. Ed.* **2003**, *42*, 1486.
(851) Guillot, M.; Eisler, S.; Weller, K.; Merkle, H. P.; Gallani, J.-L.; Diederich, F. *Org. Biomol. Chem.* **2006**, *4*, 766.
(852) Nieckowski, M. G.; Joester, D.; Stöhr, M.; Losson, M.; Adrian, M.; Wagner, B.; Kansy, M.; Heinzelmann, H.; Pugin, R.; Diederich, F.; Gallani, J.-L. *Langmuir* **2007**, *23*, 737.
(853) Zhang, L.; Webster, T. J. *Nano Today* **2009**, *4*, 66.
(854) Higashi, N.; Koga, T. *Adv. Polym. Sci.* **2008**, *219*, 28.
(855) Klok, H. A.; Hwang, J. J.; Hartgerink, J. D.; Stupp, S. I. *Macromolecules* **2002**, *35*, 6101.
(856) Hartgerink, J. D.; Beniash, E.; Stupp, S. I. *Science* **2001**, *294*, 1684.
(857) Hartgerink, J. D.; Beniash, E.; Stupp, S. I. *Proc. Natl. Acad. Sci. U.S.A.* **2002**, *99*, 5133.
(858) Silva, G. A.; Czeisler, C.; Niece, K. L.; Beniash, E.; Harrington, D. A.; Kessler, J. A.; Stupp, S. I. *Science* **2004**, *303*, 1352.
(859) Harrington, D. A.; Cheng, E. Y.; Guler, M. O.; Lee, L. E; Donovan, J. L.; Claussen, R. C.; Stupp, S. I. *J. Biomed. Mater. Res., Part A* **2006**, 157.
(860) Lim, Y.-B.; Moon, K.-S.; Lee, M. *Chem. Soc. Rev.* **2009**, *38*, 925.
(861) Matmour, R.; De Cat, I.; George, S. J.; Adriaens, W.; Leclere, P.; Bomans, P. H. H.; Sommerdijk, N.; Gielen, J. C.; Christianen, P. C. M.; Heldens, J. T.; van Hest, J. C. M.; Lowik, D.; De Feyter, S.; Meijer, E. W.; Schenning, A. *J. Am. Chem. Soc.* **2008**, *130*, 14576.
(862) Lim, Y.-B; Lee, E.; Lee, M. *Angew. Chem., Int. Ed.* **2007**, *46*, 9011.
(863) Moon, K.-S.; Lee, E.; Lim, Y.-b.; Lee, M. *Chem. Commun.* **2008**, 4001.
(864) Shao, H.; Lockman, J. W.; Parquette, J. R. *J. Am. Chem. Soc.* **2007**, *129*, 1884.
(865) Shao, H.; Parquette, J. R. *Angew. Chem., Int. Ed.* **2009**, *48*, 2525.
(866) Kim, K. T.; Park, C.; Kim, Ch.; Winnik, M. A.; Manners, I. *Chem. Commun.* **2006**, 1372.
(867) Kim, K. T.; Winnik, M. A.; Manners, I. *Soft Matter* **2006**, 957.
(868) Hirst, A. R.; Smith, D. K.; Harrington, J. P. *Chem.—Eur. J.* **2005**, *11*, 6552.
(869) Ji, Y.; Luo, Y.-F.; Jia, X.-R.; Chen, E.-Q.; Huang, Y.; Ye, C.; Wang, B.-B.; Zhou, Q.-F.; Wei, Y. *Angew. Chem., Int. Ed.* **2005**, *44*, 6025.
(870) Wathier, M.; Jung, P. J.; Carnahan, M. A.; Kim, T.; Grinstaff, M. W. *J. Am. Chem. Soc.* **2004**, *126*, 12744.
(871) Wathier, M.; Johnson, S.; Kim, T.; Grinstaff, M. W. *Bioconjugate Chem.* **2006**, *17*, 873.
(872) Harada, A.; Kawamura, M.; Matsuo, K.; Takahashi, T.; Kono, K. *Bioconjugate Chem.* **2006**, *17*, 3.
(873) Harada, A.; Nakanishi, K.; Ichimura, S.; Kojima, C.; Kono, K. *J. Polym. Sci., Part A: Polym. Chem.* **2009**, *47*, 1217.
(874) Jamal, K. T. A.; Sakthivel, T.; Florence, A. T. *Int. J. Pharm.* **2003**, *254*, 33.
(875) Jamal, K. T. A.; Sakthivel, T.; Florence, A. T. *J. Pharm. Sci.* **2005**, *94*, 102.
(876) Discher, B. M.; Won, Y.-Y.; Ege, D. S.; Lee, J. C.-M.; Bates, F. S.; Discher, D. E.; Hammer, D. A. *Science* **1999**, *284*, 1143.
(877) Ciftci, K.; Gupte, A. In *Pharmaceutical Biotechnology*, 2nd ed.; Crommelin, D. J. A., Sindelar, R. D., Ed.; Taylor & Francis Group, LLC: New York, 2006; Vol. 13, p 333.
(878) Haensler, J.; Szoka, F. C. *Bioconjugate Chem.* **1993**, *4*, 372.
(879) Plank, C.; Mechtler, K.; Szoka, F. C.; Wagner, E. *Hum. Gene Ther.* **1996**, *7*, 1437.
(880) Bielinska, A. U.; Chen, C. L.; Johnson, J.; Baker, J. R. *Bioconjugate Chem.* **1999**, *10*, 843.
(881) Luo, D.; Haverstick, K.; Belcheva, N.; Han, E.; Saltzman, W. *Macromolecules* **2002**, *35*, 3456.
(882) Godbey, W. T.; Wu, K. K.; Mikos, A. G. *J. Controlled Release* **1999**, *60*, 149.
(883) Lemkine, G. F.; Demeneix, B. A. *Curr. Opin. Mol. Ther.* **2001**, *3*, 178.
(884) Trubetskoy, V. S.; Wong, S. C; Subbotin, V.; Budker, V. G.; Loomis, A.; Hagstrom, J. E.; Wolff, J. A. *Gene Ther.* **2003**, *10*, 261.
(885) Kircheis, R.; Blessing, T.; Brunner, S.; Wightman, L.; Wagner, E. *J. Controlled Release* **2001**, *72*, 165.
(886) Zinselmeyer, B. H.; Mackay, S. P.; Schatzlein, A. G.; Uchegbu, I. F. *Pharm. Res.* **2002**, *19*, 960.
(887) Read, M. L.; Etrych, T.; Ulbrich, K.; Seymour, L. W. *FEBS Lett.* **1999**, *461*, 96.

(888) Ohsaki, M.; Okuda, T.; Wada, A.; Hirayama, T.; Niidome, T.; Aoyagi, H. *Bioconjugate Chem.* **2002**, *13*, 510.
(889) Aral, C.; Akbuga, J. *J. Pharm. Pharm. Sci.* **2003**, *6*, 321.
(890) Xiang, J. J.; Tang, J. Q.; Zhu, S. G.; Nie, X. M.; Lu, H. B.; Shen, S. R.; Li, X. L.; Tang, K.; Zhou, M.; Li, G. Y. *J. Gene Med.* **2003**, *5*, 803.
(891) Jeon, E.; Kim, H. D.; Kim, J. S. *J. Biomed. Mater. Res.* **2003**, *66*, 854.
(892) Padié, C.; Maszewska, M.; Majchrzak, K.; Nawrot, B.; Caminade, A.-M.; Majoral, J.-P. *New J. Chem.* **2009**, *33*, 318.
(893) Konstiainen, M. A.; Hardy, J. G.; Smith, D. K. *Angew. Chem., Int. Ed.* **2005**, *44*, 2556.
(894) Hardy, J. G.; Konstiainen, M. A.; Smith, D. K.; Gabrielson, N. P.; Pack, D. W. *Bioconjugate Chem.* **2006**, *17*, 172.
(895) Ramaswamy, C.; Sakthivel, T.; Wilderspin, A. F.; Florence, A. T. *Int. J. Pharm.* **2003**, *254*, 17.
(896) Behr, J.-P. *Tetrahedron Lett.* **1986**, *27*, 5861.
(897) Behr, J.-P. *Biconjugate Chem.* **1994**, *5*, 382.
(898) Felgner, P. L.; Gadek, T. R.; Holm, M.; Roman, R.; Chan, H. W.; Wenz, M.; Northrop, J. P.; Ringold, G. M.; Danielsen, M. *Proc. Natl. Acad. Sci. U.S.A.* **1987**, *84*, 7413.
(899) Konstiainen, M. A.; Smith, D. K.; Ikalla, O. *Angew. Chem., Int. Ed.* **2007**, *46*, 7600.
(900) Zelphati, O.; Scoka, F. C. *Proc. Natl. Acad. Sci. U.S.A.* **1996**, *93*, 11493.
(901) Kostiainen, M. A.; Rosilo, H. *Chem.—Eur. J.* **2009**, *15*, 5656.
(902) Hudson, R. H. E.; Damha, M. J. *J. Am. Chem. Soc.* **1993**, *115*, 2119.
(903) Hudson, R. H. E.; Robidoux, S.; Damha, M. J. *Tetrahedron Lett.* **1998**, *39*, 1299.
(904) Shchepinov, M. S.; Udalova, I. A.; Bridgman, A. J.; Southern, E. M. *Nucleic Acids Res.* **1997**, *25*, 4447.
(905) Shchepinov, M. S.; Mir, K. U.; Elder, J. K.; Frank-Kamenetskii, M. D.; Southern, E. M. *Nucleic Acids Res.* **1999**, *27*, 3035.
(906) DeMattei, C. R.; Huang, B.; Tomalia, D. A. *Nano Lett.* **2004**, *4*, 771.
(907) Hussain, M.; Shchepinov, M. S.; Sohail, M.; Benter, I. F.; Hollins, A. J.; Southern, E. M.; Akhtar, S. *J. Controlled Release* **2004**, *99*, 139.
(908) Bell, S. A.; McLean, M. E.; Oh, S. K.; Tichy, S. E.; Zhang, W.; Corn, R. M.; Crooks, R. M.; Simanek, E. E. *Bioconjugate Chem.* **2003**, *14*, 488.
(909) Varki, A. C., R.; Esko, J.; Freeze, H.; Hart, G.; Marth, J. *Essentials of Glycobiology*, 2nd ed.; Cold Spring Harbor Laboratory Press: New York, 1999.
(910) Roy, R. *Trends Glycosci. Glycotech.* **2003**, *15*, 291.
(911) Aoi, K.; Itoh, K.; Okada, M. *Macromolecules* **1995**, *28*, 5391.
(912) Ashton, P. R.; Boyd, S. E.; Brown, C. L.; Jayaraman, N.; Nepogodiev, S. A.; Stoddart, J. F. *Chem.—Eur. J.* **1996**, *2*, 1115.
(913) Ashton, P. R.; Boyd, S. E.; Brown, C. L.; Jayaraman, N.; Stoddart, J. F. *Angew. Chem., Int. Ed.* **1997**, *36*, 732.
(914) Ashton, P. R.; Boyd, S. E.; Brown, C. L.; Nepogodiev, S. A.; Meijer, E. W.; Peerlings, H. W. I.; Stoddart, J. F. *Chem.—Eur. J.* **1997**, *3*, 974.
(915) Jayaraman, N.; Nepogodiev, S. A.; Stoddart, J. F. *Chem.—Eur. J.* **1997**, *3*, 1193.
(916) Andre, S.; Ortega, P. J. C.; Perez, M. A.; Roy, R.; Gabius, H. J. *Glycobiology* **1999**, *9*, 1253.
(917) Turnbull, W. B.; Pease, A. R.; Stoddart, J. F. *ChemBioChem* **2000**, *1*, 70.
(918) Backinowsky, L. V.; Abronina, P. I.; Shashkov, A. S.; Grachev, A. A.; Kochetkov, N. K.; Nepogodiev, S. A.; Stoddart, J. F. *Chem.—Eur. J.* **2002**, *8*, 4412.
(919) Turnbull, W. B.; Kalovidouris, S. A.; Stoddart, J. F. *Chem.—Eur. J.* **2002**, *8*, 2988.
(920) Kalovidouris, S. A.; Turnbull, W. B.; Stoddart, J. F. *Can. J. Chem.* **2002**, *80*, 983.
(921) Thoma, G.; Katopodis, A. G.; Voelcker, N.; Duthaler, R. O.; Streiff, M. B. *Angew. Chem., Int. Ed.* **2002**, *41*, 3195.
(922) Rockendorf, N.; Lindhorst, T. K. *Top. Curr. Chem.* **2001**, *217*, 201.
(923) Ballardini, R.; Colonna, B.; Gandolfi, M. T.; Kalovidouris, S. A.; Orzel, L.; Raymo, F. M.; Stoddart, J. F. *Eur. J. Org. Chem.* **2003**, 288.
(924) Page, D.; Zanini, D.; Roy, R. *Bioorg. Med. Chem.* **1996**, *4*, 1949.
(925) Andre, S.; Pieters, R. J.; Vrasidas, I.; Kaltner, H.; Kuwabara, L.; Liu, F. T.; Liskamp, R. M. J.; Gabius, H. J. *ChemBioChem* **2001**, *2*, 822.
(926) Krist, P.; Vannucci, L.; Kuzma, M.; Man, P.; Sadalapure, K.; Patel, A.; Bezouska, K.; Pospisil, M.; Petrus, L.; Lindhorst, T. K.; Kren, V. *ChemBioChem* **2004**, *5*, 445.
(927) Nelson, A.; Stoddart, J. F. *Carbohydr. Res.* **2004**, *339*, 2069.
(928) Bewley, C. A.; Otero-Qintero, S. *J. Am. Chem. Soc.* **2001**, *123*, 3892.
(929) Hada, N.; Sato, K.; Jin, Y.; Takeda, T. *Chem. Pharm. Bull.* **2005**, *53*, 1131.
(930) Roberge, J. Y.; Beebe, X.; Danishefsky, S. J. *Science* **1995**, *269*, 202.
(931) Kuduk, S. D.; Schwarz, J. B.; Chen, X. T.; Glunz, P. W.; Sames, D.; Ragupathi, G.; Livingston, P. O.; Danishefsky, S. J. *J. Am. Chem. Soc.* **1998**, *120*, 12474.
(932) Dudkin, V. Y.; Miller, J. S.; Danishefsky, S. J. *J. Am. Chem. Soc.* **2004**, *126*, 736.
(933) Warren, J. D.; Miller, J. S.; Keding, S. J.; Danishefsky, S. J. *J. Am. Chem. Soc.* **2004**, *126*, 6576.
(934) Sato, K.; Hada, N.; Takeda, T. *Carbohydr. Res.* **2006**, *341*, 836.
(935) Kolomiets, E.; Johansson, E. M. V.; Renaudet, O.; Darbre, T.; Reymond, J. L. *Org. Lett.* **2007**, *9*, 1465.
(936) Dudkin, V. Y.; Miller, J. S.; Dudkina, A. S.; Antczak, C.; Scheinberg, D. A.; Danishefsky, S. J. *J. Am. Chem. Soc.* **2008**, *130*, 13598.
(937) Huang, W.; Li, C.; Li, B.; Umekawa, M.; Yamamoto, K.; Zhang, X.; Wang, L.-X. *J. Am. Chem. Soc.* **2009**, *131*, 2214.
(938) Arosio, D.; Vrasidas, I.; Valentini, P.; Liskamp, R. M.; Pieters, R. J.; Bernardi, A. *Org. Biomol. Chem.* **2004**, *2*, 2113.
(939) Pukin, A. V.; Branderhorst, H. M.; Sisu, C.; Weijers, C. A.; Gilbert, M.; Liskamp, R. M.; Visser, G. M.; Zuilof, H.; Pieters, R. J. *ChemBioChem.* **2007**, *77*, 7497.
(940) Kanda, V.; Kitov, P.; Bundle, D. R.; McDermott, M. T. *Anal. Chem.* **2005**, *77*, 7497.
(941) Nishikawa, K.; Matsuoka, K.; Kita, E.; Okabe, N.; Mizuguchi, M.; Hino, K.; Miyazawa, S.; Yamasaki, C.; Aoki, J.; Takashima, S.; Yamakawa, Y.; Nishijima, M.; Terunuma, D.; Kuzuhara, H.; Natori, Y. *Proc. Natl. Acad. Sci. U.S.A.* **2002**, *99*, 7669.
(942) Nishikawa, K.; Matsuoka, K.; Watanabe, M.; Igai, K.; Hino, K.; Hatano, K.; Yamada, A.; Abe, N.; Terunuma, D.; Kuzuhara, H.; Natori, Y. *J. Infect. Dis.* **2005**, *191*, 2097.
(943) Reuter, J. D.; Myc, A.; Hayes, M. M.; Gan, Z.; Roy, R.; Qin, D.; Yin, R.; Pihler, L. T.; Esfand, R.; Tomalia, D. A.; Baker, J. R. *Bioconjugate Chem.* **1999**, *10*, 271.
(944) Sun, X. L. *Curr. Med. Chem.* **2007**, *14*, 2304.
(945) Ragupathi, G.; Coltart, D. M.; Williams, L. J.; Koide, F.; Kagan, E.; Allen, J.; Harris, C.; Glunz, P. W.; Livingston, P. O.; Danishefsky, S. J. *Proc. Natl. Acad. Sci. U.S.A.* **2002**, *99*, 13699.
(946) Krauss, I. J.; Joyce, J. G.; Finnefrock, A. C.; Song, H. C.; Dudkin, V. Y.; Geng, X.; Warren, J. D.; Chastain, M.; Shiver, J. W.; Danishefsky, S. J. *J. Am. Chem. Soc.* **2007**, *129*, 11042.
(947) Joyce, J. G.; Krauss, I. J.; Song, H. C.; Opalka, D. W.; Grimm, K. M.; Nahas, D. D.; Esser, M. T.; Hrin, R.; Feng, M. Z.; Dudkin, V. Y.; Chastain, M.; Shiver, J. W.; Danishefsky, S. J. *Proc. Natl. Acad. Sci. U.S.A.* **2008**, *105*, 15684.
(948) Warren, J. D.; Geng, X. D.; Danishefsky, S. J. *Top. Curr. Chem.* **2007**, *267*, 109.
(949) Wang, S. K.; Liang, P. H.; Astronomo, R. D.; Hsu, T. L.; Hsieh, S. L.; Burton, D. R.; Wong, C. H. *Proc. Natl. Acad. Sci. U.S.A.* **2008**, *105*, 3690.
(950) Elsner, K.; Boysen, M. M. K.; Lindhorst, T. K. *Carbohydr. Res.* **2007**, *342*, 1715.
(951) Kantchev, E. A. B.; Chang, C. C.; Cheng, S. F.; Roche, A. C.; Chang, D. K. *Org. Biomol. Chem.* **2008**, *6*, 1377.
(952) Deguise, I.; Lagnoux, D.; Roy, R. *New J. Chem.* **2007**, *31*, 1321.
(953) Lim, Y.-B.; Park, S.; Lee, E.; Jeong, H.; Ryu, J.-H.; Lee, M. S.; Lee, M. *Biomacromolecules* **2007**, *8*, 1404.
(954) Lim, Y.-B.; Lee, E.; Yoon, Y.-R.; Lee, M. S.; Lee, M. *Angew. Chem., Int. Ed.* **2008**, *47*, 4525.
(955) Liu, J.; Toy, P. J. *Chem. Rev.* **2009**, *109*, 815.
(956) Bergbreiter, D. E.; Tian, J.; Hongfra, C. *Chem. Rev.* **2009**, *109*, 530.
(957) Zhang, W. *Chem. Rev.* **2009**, *109*, 749.
(958) Merrifield, R. B. *J. Am. Chem. Soc.* **1963**, *85*, 2149.
(959) Parrish, B.; Breitenkamp, R. B.; Emrick, T. *J. Am. Chem. Soc.* **2005**, *127*, 7404.
(960) Peng, S.-M.; Chen, Y.; Hua, C.; Dong, C.-M. *Macromolecules* **2009**, *42*, 104.
(961) Hua, C.; Peng, S.-M.; Dong, C.-M. *Macromolecules* **2008**, *41*, 6686.
(962) Tamiaki, H.; Obata, T.; Azefu, Y.; Toma, K. *Bull. Chem. Soc. Jpn.* **2001**, *74*, 733.
(963) Beaucage, S. L.; Iyer, R. P. *Tetrahedron* **1992**, *48*, 2223.
(964) Threlfall, R.; Cosstick, R.; Wada, T. *Nucleic Acids Symp. Ser.* **2008**, *52*, 337.
(965) Wada, T.; Narita, R.; Kato, Y.; Saigo, K. *International Symposium on Fluorous Technologies*, Bordeaux, France, 3−6 July 2005; p 22.
(966) Wada, T.; Ryouichi, N.; Yukiko, K.; Saigo, K. PCT patent application, WO2005070859, **2005**
(967) Hecht, S.; Fréchet, J. M. J. *J. Am. Chem. Soc.* **1999**, *121*, 4084.

(968) Huang, B.; Prantil, M. A.; Gustafson, T. L.; Parquette, J. R. *J. Am. Chem. Soc.* **2003**, *125*, 14518.
(969) Lockman, J. W.; Paul, N. M.; Parquette, J. R. *Prog. Polym. Sci.* **2005**, *30*, 423.
(970) Palmans, A. R. A.; Vekemans, J. A. J. M.; Fischer, H.; Hikmet, R. A. M.; Meijer, E. W. *Chem.—Eur. J.* **1997**, *3*, 300.
(971) Palmans, A. R. A.; Vekemans, J. A. J. M.; Hikamet, R. A.; Fischer, H.; Meijer, E. W. *Adv. Mater.* **1998**, *10*, 873.
(972) van Gorp, J. J.; Venkemans, J. A. J. M.; Meijer, E. W. *J. Am. Chem. Soc.* **2002**, *124*, 14759.
(973) Palmans, A. R. A.; Vekemans, J. A. J. M.; Havinga, E. E.; Meijer, E. W. *Angew. Chem., Int. Ed.* **1997**, *36*, 2648.
(974) van Gestel, J.; Palmans, A. R. A.; Titulaer, B.; Venkemans, J. A. J. M.; Meijer, E. W. *J. Am. Chem. Soc.* **2005**, *127*, 5490.
(975) Lehmann, M.; Gearba, R. I.; Koch, M. H. J.; Ivanov, D. A. *Chem. Mater.* **2004**, *16*, 374.
(976) Gemming, S.; Popov, I.; Lehmann, M. *Philos. Mag. Lett.* **2007**, *87*, 883.
(977) Gearba, R. I.; Bondar, A. I.; Lehmann, M.; Goderis, B.; Bras, W.; Koch, M. H. J.; Ivanov, D. A. *Adv. Mater.* **2005**, *17*, 671.
(978) Gearba, R. I.; Anokhin, D. V.; Bondar, A. I.; Bras, W.; Jahr, M.; Lehmann, M.; Ivanov, D. A. *Adv. Mater.* **2007**, *19*, 815.
(979) Lehmann, M.; Jahr, M.; Donnio, B.; Graf, R.; Gemming, S.; Popov, I. *Chem.—Eur. J.* **2008**, *14*, 3562.
(980) Lehmann, M. *Chem.—Eur. J.* **2009**, *15*, 3638.
(981) Lehmann, M.; Jahr, M. *Org. Lett.* **2006**, *8*, 721.
(982) Lehmann, M.; Jahr, M. *Chem. Mater.* **2008**, *20*, 5453.
(983) Lehmann, M.; Jahr, M.; Gutmann, J. *J. Mater. Chem.* **2008**, *18*, 2995.
(984) Lehmann, M.; Jahr, M.; Grozema, F. C.; Abellon, R. D.; Siebbeles, L. D. A.; Muller, M. *Adv. Mater.* **2008**, *20*, 4414.
(985) Gearba, R. I.; Anokhin, D. V.; Bondar, A. I.; Bras, W.; Jahr, M.; Lehmann, M.; Ivanov, D. A. *Adv. Mater.* **2007**, *19*, 815.
(986) Herrikhuyzen, J. H.; Jonkheijm, P.; Schenning, A. P. H. J.; Meijer, E. W. *Org. Biomol. Chem.* **2006**, *4*, 1539.
(987) Kinberger, G. A.; Cai, W.; Goodman, M. *J. Am. Chem. Soc.* **2002**, *124*, 15162.
(988) Cai, W.; Wong, D.; Kinberger, G. A.; Kwok, S. W.; Taulane, J. P.; Goodman, M. *Bioorg. Chem.* **2007**, *35*, 327.
(989) Pieterse, K.; Lauritsen, A.; Schenning, A. P. H. J.; Vekemans, J. A. J. M.; Meijer, E. W. *Chem.—Eur. J.* **2003**, *9*, 5597.
(990) Lee, H.; Kim, D.; Lee, H.-K.; Qiu, W.; Oh, N.-K.; Zin, W.-C.; Kim, K. *Tetrahedron Lett.* **2004**, *45*, 1019.
(991) Ishi-I, T.; Kuwahara, R.; Takata, A.; Jeong, Y.; Sakurai, K.; Mataka, S. *Chem.—Eur. J.* **2006**, *12*, 763.
(992) Lee, C.-H.; Yamamoto, T. *Tetrahedron Lett.* **2001**, *42*, 3993.
(993) Malthête, J. *New. J. Chem.* **1996**, *20*, 925.
(994) Gitsov, I.; Fréchet, J. M. J. *J. Am. Chem. Soc.* **1996**, *118*, 3785.
(995) Pegenau, A.; Cheng, X. H.; Tschierske, C.; Göring, P.; Diele, S. *New J. Chem.* **1999**, *23*, 465.
(996) Pegenau, A.; Hegmann, T.; Tschierske, C.; Diele, S. *Chem.—Eur. J.* **1999**, *5*, 1643.
(997) Tomovic, Z.; Van Dongen, J.; George, S. J.; Xu, H.; Pisula, W.; Leclere, P.; Smulders, M. M. J.; De Feyter, S.; Meijer, E. W.; Schenning, A. *J. Am. Chem. Soc.* **2007**, *129*, 16190.
(998) Barbera, J.; Bardaji, M.; Jimenez, J.; Laguna, A.; Martinez, M. P.; Oriol, L.; Serrano, J. L.; Zaragozano, I. *J. Am. Chem. Soc.* **2005**, *127*, 8994.
(999) Barbera, J.; Jimenez, J.; Laguna, A.; Oriol, L.; Perez, S.; Serrano, J. L. *Chem. Mater.* **2006**, *18*, 5437.
(1000) Xu, J.; Ling, T. C.; He, C. *J. Polym. Sci., Part A: Polym. Chem.* **2008**, *46*, 4691.
(1001) Pedersen, C. J. *J. Am. Chem. Soc.* **1967**, *89*, 2495.
(1002) Pedersen, C. J. *J. Am. Chem. Soc.* **1967**, *89*, 7017.
(1003) Dietrich, B.; Lehn, J. M.; Sauvage, J. P. *Tetrahedron Lett.* **1967**, 2885.
(1004) Dietrich, B.; Lehn, J. M.; Sauvage, J. P. *Tetrahedron Lett.* **1967**, 2889.
(1005) Lehn, J.-M. *Supramolecular Chemistry*; Wiley-VCH: New York, 1995.
(1006) Kyba, E. P.; Siegel, M. G.; Sousa, L. R.; Sogah, G. D. Y.; Cram, D. J. *J. Am. Chem. Soc.* **1973**, *95*, 2691.
(1007) Cram, D. J.; Cram, J. M. *Science* **1974**, *183*, 803.
(1008) Dandliker, P. J.; Diderich, F.; Zingg, A.; Gisselbrecht, J.-P.; Gross, M.; Louati, A.; Sanford, E. *Helv. Chim. Acta* **1997**, *80*, 1773.
(1009) Rowland, P.; Blaney, F. E.; Smyth, M. G.; Jones, J. J.; Leydon, V. R.; Oxbrow, A. K.; Lewis, C. J.; Tennant, M. G.; Modi, S.; Eggleston, D. S.; Chenery, R. J.; Bridges, A. M. *J. Biol. Chem.* **2006**, *281*, 7614.
(1010) Biesiadka, J.; Loll, B.; Kern, J.; Irrgang, K. D.; Zouni, A. *Phys. Chem. Chem. Phys.* **2004**, *6*, 4733.
(1011) Valks, G. C.; McRobbie, G.; Lewis, E. A.; Hubin, T. J.; Hunter, T. M.; Sadler, P. J.; Pannecouque, C.; De Clercq, E.; Archibald, S. J. *J. Med. Chem.* **2006**, *49*, 6162.
(1012) Khan, A.; Greenman, J.; Archibald, S. J. *Curr. Med. Chem.* **2007**, *14*, 2257.
(1013) Hudson, R.; Boyle, R. W. *J. Porphyrins Phthalocyanines* **2004**, *8*, 954.
(1014) Diederich, F. *Chimia* **2001**, *55*, 821.
(1015) Smith, D. K.; Diederich, F. *Chem.—Eur. J.* **1998**, *4*, 1353.
(1016) Smith, D. K.; Diederich, F. *Top. Curr. Chem.* **2000**, *210*, 183.
(1017) Caminade, A.-M.; Wei, Y.; Majoral, J.-P. C. R. *Chimie* **2009**, *12*, 105.
(1018) Blake, A. J.; Bruce, D. W.; Fallis, I. A.; Parsons, S.; Richtzenhain, H.; Ross, S. A.; Schroder, M. *Philos. Trans. R. Soc. London, Ser. A* **1996**, *354*, 395.
(1019) Jullien, L.; Lehn, J. M. *Tetrahedron Lett.* **1988**, *29*, 3803.
(1020) Safinya, C. R.; Liang, K. S.; Varady, W. A.; Clark, N. A.; Andersson, G. *Phys. Rev. Lett.* **1984**, *53*, 1172.
(1021) Jung, H. T.; Kim, S. O.; Hudson, S. D.; Percec, V. *Appl. Phys. Lett.* **2002**, *80*, 395.
(1022) Pao, W.-J.; Stetzer, M. R.; Heiney, P. A.; Cho, W.-D.; Percec, V. *J. Phys. Chem. B* **2001**, *105*, 2170.
(1023) Schultz, A.; Laschat, S.; Saipa, A.; Giesselmann, F.; Nimtz, M.; Schulte, J. L.; Baro, A.; Miehlich, B. *Adv. Funct. Mater.* **2004**, *14*, 163.
(1024) Steinke, N.; Frey, W.; Baro, A.; Laschat, S.; Drees, C.; Nimtz, M.; Hagele, C.; Giesselmann, F. *Chem.—Eur. J.* **2006**, *12*, 1026.
(1025) Gitsov, I.; Ivanova, P. T. *Chem. Commun.* **2000**, 269.
(1026) Hegmann, T.; Neumann, B.; Kain, J.; Diele, S.; Tschierske, C. *J. Mater. Chem.* **2000**, *10*, 2244.
(1027) Wallimann, P.; Seiler, P.; Diederich, F. *Helv. Chim. Acta* **1996**, *79*, 779.
(1028) Wallimann, P.; Mattei, S.; Selier, P.; Diederich, F. *Helv. Chim. Acta* **1997**, *80*, 2368.
(1029) Kenda, B.; Diederich, F. *Angew. Chem., Int. Ed.* **1998**, *37*, 3154.
(1030) Habicher, T.; Diederich, F.; Gramlich, V. *Helv. Chim. Acta* **1999**, *82*, 1066.
(1031) Diederich, F. *Angew. Chem., Int. Ed.* **1988**, *27*, 362.
(1032) Dykes, G. M.; Smith, D. K. *Tetrahedron* **2003**, *59*, 3999.
(1033) Brignell, S. V.; Smith, D. K. *New J. Chem.* **2007**, *31*, 1243.
(1034) Sidorenko, A.; Houphouet-Boigny, C.; Villavicencio, O.; McGrath, D. V.; Tsukruk, V. V. *Thin Solid Films* **2002**, *410*, 147.
(1035) Lehn, J. M.; Malthête, J.; Levelut, A. M. *J. Chem. Soc., Chem. Commun.* **1985**, 1794.
(1036) Malthête, J.; Levelut, A. M.; Lehn, J. M. *J. Chem. Soc., Chem. Commun.* **1992**, 1434.
(1037) Malthête, J.; Poupinet, D.; Vilanove, R.; Lehn, J. M. *J. Chem. Soc., Chem. Commun.* **1989**, 1016.
(1038) Tatarsky, D.; Banerjee, K.; Ford, W. T. *Chem. Mater.* **1990**, *2*, 138.
(1039) Zhao, M. Y.; Ford, W. T.; Idziak, S. H. J.; Maliszewskyj, N. C.; Heiney, P. A. *Liq. Cryst.* **1994**, *16*, 583.
(1040) Lattermann, G. *Liq. Cryst.* **1989**, *6*, 619.
(1041) Facher, A.; Stebani, U.; Lattermann, G.; Diele, S.; Neundorf, M. *Liq. Cryst.* **1998**, *25*, 441.
(1042) Lattermann, G.; Schmidt, S.; Kleppinger, R.; Wendorff, J. H. *Adv. Mater.* **1992**, *4*, 30.
(1043) Stebani, U.; Lattermann, G.; Wittenberg, M.; Festag, R.; Wendorff, J. H. *Adv. Mater.* **1994**, *6*, 572.
(1044) Lattermann, G.; Schmidt, S.; Gallot, B. *J. Chem. Soc., Chem. Commun.* **1992**, 1091.
(1045) Stebani, U.; Lattermann, G.; Wittenberg, M.; Wendorff, J. H. *J. Mater. Chem.* **1997**, *7*, 607.
(1046) Mertesdorf, C.; Ringsdorf, H. *Liq. Cryst.* **1989**, *5*, 1757.
(1047) Idziak, S. H. J.; Maliszewskyj, N. C.; Heiney, P. A.; McCauley, J. P.; Sprengeler, P. A.; Smith, A. B. *J. Am. Chem. Soc.* **1991**, *113*, 7666.
(1048) Idziak, S. H. J.; Maliszewskyj, N. C.; Vaughan, G. B. M.; Heiney, P. A.; Mertesdorf, C.; Ringsdorf, H.; McCauley, J. P.; Smith, A. B. *J. Chem. Soc., Chem. Commun.* **1992**, 98.
(1049) Seitz, M.; Plesnivy, T.; Schimossek, K.; Edelmann, M.; Ringsdorf, H.; Fischer, H.; Uyama, H.; Kobayashi, S. *Macromolecules* **1996**, *29*, 6560.
(1050) Enomoto, M.; Aida, T. *J. Am. Chem. Soc.* **1999**, *121*, 874.
(1051) Caravan, P.; Ellison, J. J.; McMurry, T. J.; Lauffer, R. B. *Chem. Rev.* **1999**, *99*, 2293.
(1052) Kim, J.-H.; Park, K.; Nam, H. Y.; Lee, S.; Kim, K.; Kwon, I. C. *Prog. Polym. Sci.* **2007**, *32*, 1031.
(1053) Que, E. L.; Domaille, D. W.; Chang, C. J. *Chem. Rev.* **2008**, *108*, 1517.
(1054) Vennditto, V. J.; Regino, C. A. S.; Brechbiel, M. W. *Mol. Pharm.* **2005**, *2*, 302.
(1055) Barret, T.; Kobayashi, H.; Brechbiel, M.; Choyke, P. L. *Eur. J. Rad.* **2006**, *60*, 353.

(1056) Langereis, S.; Dirksen, A.; Hackeng, T. M.; can Genderen, M. H. P.; Meijer, E. W. *New J. Chem.* **2007**, *31*, 1152.
(1057) Saudan, C.; Ceroni, P.; Bicinelli, V.; Maestri, M.; Balzani, V.; Gorka, M.; Lee, S.-K.; van Heyst, J.; Vögtle, F. *J. Chem. Soc., Dalton. Trans.* **2004**, 1597.
(1058) Satake, A.; Kobuke, Y. *Tetrahedron* **2005**, *61*, 13.
(1059) Sakurai, T.; Shi, K.; Sato, H.; Tashiro, K.; Osuka, A.; Saeki, A.; Seki, S.; Tagawa, S.; Sasaki, S.; Masunaga, H.; Osaka, K.; Takata, M.; Aida, T. *J. Am. Chem. Soc.* **2008**, *130*, 13812.
(1060) Tsuda, A.; Alam, Md. A.; Harada, T.; Yamaguchi, T.; Ishii, N.; Aida, T. *Angew. Chem., Int. Ed.* **2007**, *46*, 8198.
(1061) Yamaguchi, T.; Kimura, T.; Matsuda, H.; Aida, T. *Angew. Chem., Int. Ed.* **2004**, *43*, 6350.
(1062) Kimura, M.; Nakano, Y.; Adachi, N.; Tatewaki, Y.; Shirai, H.; Kobayashi, N. *Chem.—Eur. J.* **2009**, *15*, 2617.
(1063) Stêpiañ, M.; Donnio, B.; Sessler, J. L. *Chem.—Eur. J.* **2007**, *13*, 6853.
(1064) Huber, V.; Sengupta, S.; Würthner, F. *Chem.—Eur. J.* **2008**, *14*, 7791.
(1065) Huber, V.; Lysetka, M.; Würthner, F. *Small* **2007**, *3*, 1007.
(1066) Patel, B. R.; Suslick, K. S. *J. Am. Chem. Soc.* **1998**, *120*, 11802.
(1067) Kimura, M.; Saito, Y.; Ohta, K.; Hanabusa, K.; Shirai, H.; Kobayashi, N. *J. Am. Chem. Soc.* **2002**, *124*, 5274.
(1068) Li, J. Z.; Xin, H.; Li, M. *Liq. Cryst.* **2006**, *33*, 913.
(1069) Li, J. Z.; Tang, T.; Li, F.; Li, M. *Dyes Pigm.* **2008**, *77*, 395.
(1070) Shinoda, S.; Ohashi, M.; Tsukube, H. *Chem.—Eur. J.* **2007**, *13*, 81.
(1071) Felber, B.; Diederich, F. *Helv. Chim. Acta* **2005**, *88*, 120.
(1072) Castella, M.; Lopez-Calahorra, F.; Velasco, D.; Finkelmann, H. *Chem. Commun.* **2002**, 2348.
(1073) Segade, A.; Castella, M.; Lopez-Calahorra, F.; Velasco, D. *Chem. Mater.* **2005**, *17*, 5366.
(1074) Segade, A.; Lopez-Calahorra, F.; Velasco, D. *Mol. Cryst. Liq. Cryst.* **2005**, *439*, 2067.
(1075) Segade, A.; Lopez-Calahorra, F.; Velasco, D. *J. Phys. Chem. B* **2008**, *112*, 7395.
(1076) Hunter, C. A.; Sanders, J. K. M. *J. Am. Chem. Soc.* **1990**, *112*, 5525.
(1077) Paganuzzi, V.; Guatteri, P.; Riccardi, P.; Sacchelli, T.; Barbera, J.; Costa, M.; Dalcanale, E. *Eur. J. Org. Chem.* **1999**, 1527.
(1078) Finikova, O.; Galkin, A.; Rozhkov, V.; Cordero, M.; Hägerhäll, C.; Vinogradov, S. *J. Am. Chem. Soc.* **2003**, *125*, 4882.
(1079) Elmer, S. L.; Man, S.; Zimmerman, S. C. *Eur. J. Org. Chem.* **2008**, 3845.
(1080) Lemcoff, N. G.; Spurlin, T. A.; Gewirth, A. A.; Zimmeran, S. C.; Beil, J. B.; Elmer, S. L.; Vandeveer, H. G. *J. Am. Chem. Soc.* **2004**, *126*, 11420.
(1081) Inokuma, Y.; Osuka, A. *Dalton Trans.* **2008**, *]?>*, *]?>*, 2517.
(1082) Torres, T. *Angew. Chem., Int. Ed.* **2006**, *45*, 2834.
(1083) Xu, T. H.; Lu, R.; Liu, X. L.; Chen, P.; Qiu, X. P.; Zhao, Y. Y. *Eur. J. Org. Chem.* **2008**, 1065.
(1084) Stepien, M.; Donnio, B.; Sessler, J. L. *Angew. Chem., Int. Ed.* **2007**, *46*, 1431.
(1085) Brewis, M.; Clarkson, G. J.; Holder, A. M.; McKeown, N. B. *Chem. Commun.* **1998**, 969.
(1086) McKeown, N. B. *Adv. Mater.* **1999**, *11*, 67.
(1087) Brewis, M.; Clarkson, G. J.; Helliwell, M.; Holder, A. M.; McKeown, N. B. *Chem.—Eur. J.* **2000**, *6*, 4630.
(1088) Uchiyama, T.; Ishii, K.; Nonomura, T.; Kobayashi, N.; Isoda, S. *Chem.—Eur. J.* **2003**, *9*, 5757.
(1089) El-Khouly, M. E.; Kang, E. S.; Kay, K.-Y.; Choi, C. S.; Aaraki, Y.; Ito, O. *Chem.—Eur. J.* **2007**, *13*, 2854.
(1090) Zimmerman, H.; Poupko, R.; Luz, Z.; Billard, J. *Naturfortsch* **1985**, *40*, 149.
(1091) Levelut, A. M.; Malthête, J.; Collet, A. *J. Phys. (Paris)* **1986**, 351.
(1092) Malthête, J.; Collet, A. *J. Am. Chem. Soc.* **1987**, *109*, 7544.
(1093) Malthête, J.; Collet, A. *Nouv. J. Chim.* **1985**, *9*, 151.
(1094) Canceill, J.; Collet, A.; Gottarelli, G. *J. Am. Chem. Soc.* **1984**, *106*, 5997.
(1095) Zamir, S.; Luz, Z.; Poupko, R.; Alexander, S.; Zimmermann, H. *J. Chem. Phys.* **1991**, *94*, 5927.
(1096) Poupko, R.; Luz, Z.; Spielberg, N.; Zimmermann, H. *J. Am. Chem. Soc.* **1989**, *111*, 6094.
(1097) Eckert, J. F.; Byrne, D.; Nicoud, J. F.; Oswald, L.; Nierengarten, J. F.; Numata, M.; Ikeda, A.; Shinkai, S.; Armaroli, N. *New J. Chem.* **2000**, *24*, 749.
(1098) Zimmermann, H.; Poupko, R.; Luz, Z.; Billard, J. *Liq. Cryst.* **1988**, *3*, 759.
(1099) Kranig, W.; Spiess, H. W.; Zimmermann, H. *Liq. Cryst.* **1990**, *7*, 123.
(1100) Spielberg, N.; Sarkar, M.; Luz, Z.; Poupko, R.; Billard, J.; Zimmermann, H. *Liq. Cryst.* **1993**, *15*, 311.
(1101) Percec, V.; Cho, C. G.; Pugh, C. *Macromolecules* **1991**, *24*, 3227.
(1102) Percec, V.; Cho, C. G.; Pugh, C.; Tomazos, D. *Macromolecules* **1992**, *25*, 1164.
(1103) Percec, V.; Cho, C. G.; Pugh, C. *J. Mater. Chem.* **1991**, *1*, 217.
(1104) Budig, H.; Diele, S.; Goring, P.; Paschke, R.; Sauer, C.; Tschierske, C. *J. Chem. Soc., Chem. Commun.* **1994**, 2359.
(1105) Felder, D.; Heinrich, B.; Guillon, D.; Nicoud, J. F.; Nierengarten, J. F. *Chem.—Eur. J.* **2000**, *6*, 3501.
(1106) Karahaliou, P. K.; Kouwer, P. H. J.; Meyer, T.; Mehl, G. H.; Photinos, D. J. *J. Phys. Chem. B* **2008**, *112*, 6550.
(1107) Nierengarten, J.-F.; Oswald, L.; Eckert, J.-F.; Nicoud, J.-F.; Armaroli, N. *Tetraheron Lett.* **1999**, *40*, 5681.
(1108) Nirengarten, J.-F. *Fullerenes, Nanotubes, Carbon Nanostruct.* **2005**, *13*, 299.
(1109) Márquez, A. G.; Nava, M. G.; Chavez, J. G. D.; Klimova, E.; Klimova, T.; García, M. M. *Fullerenes, Nanotubes, Carbon Nanostruct.* **2006**, *14*, 357.
(1110) Percec, V.; Imam, M. R.; Peterca, M.; Wilson, D. A.; Heiney, P. A. *J. Am. Chem. Soc.* **2009**, *131*, 1294.
(1111) Pirondini, L.; Vecchi, G.; Negri, S.; Di Blasi, A.; Massera, C.; Dalcanale, E. *Collect. Czech. Chem. Commun.* **2004**, *69*, 1362.
(1112) Gilies, M. D.; Liu, S.; Emanuel, R. L.; Gibb, B. C.; Grayson, S. M. *J. Am. Chem. Soc.* **2008**, *130*, 14430.
(1113) Kellerman, M.; Bauer, W.; Hirsch, A.; Schade, B.; Ludwig, K.; Böttcher, C. *Angew. Chem., Int. Ed.* **2004**, *43*, 2959.
(1114) Martin, O.; Mecozzi, S. *Supramol. Chem.* **2005**, *17*, 9.
(1115) Fischer, M.; Lieser, G.; Rapp, A.; Schnell, I.; Mamdouh, W.; De Feyter, S.; De Schryver, F. C.; Hoger, S. *J. Am. Chem. Soc.* **2004**, *126*, 214.
(1116) Ryu, J. H.; Oh, N. K.; Lee, M. *Chem. Commun.* **2005**, 1770.
(1117) Yang, H.; Hawkridge, A. M.; Huang, A. D.; Das, N.; Bunge, S. D.; Muddiman, D. C.; Stang, P. J. *J. Am. Chem. Soc.* **2007**, *129*, 2120.
(1118) Barberá, J.; Giméz, R.; Serrano, J. L. *Chem. Mater.* **2000**, *12*, 481.
(1119) Kanie, K.; Yasuda, T.; Ujiie, S.; Kato, T. *Chem. Commun.* **2000**, 1899.
(1120) Kanie, K.; Yasuda, T.; Nishii, M.; Ujiie, S.; Kato, T. *Chem. Lett.* **2001**, 480.
(1121) Kato, T. *Science* **2002**, *295*, 2414.
(1122) Kato, T.; Fréchet, J. M. J. *Liq. Cryst.* **2006**, *33*, 1429.
(1123) Kanie, K.; Nishii, M.; Yasuda, T.; Taki, T.; Ujiie, S.; Kato, T. *J. Mater. Chem.* **2001**, *11*, 2875.
(1124) Kato, T.; Matsuoka, T.; Nishii, M.; Kamikawa, Y.; Kanie, K.; Nishimura, T.; Yashima, E.; Ujiie, S. *Angew Chem., Int. Ed.* **2004**, *43*, 1969.
(1125) Kamikawa, Y.; Nishii, M.; Kato, T. *Chem.—Eur. J.* **2004**, *10*, 5942.
(1126) Hahn, U.; González, J. J.; Huerta, E.; Segura, M.; Eckert, J.-F.; Cardinali, F.; de Mendoza, J.; Nierengarten, J.-F. *Chem.—Eur. J.* **2005**, *11*, 6666.
(1127) Sakai, N.; Kamikawa, Y.; Nishii, M.; Matsuoka, T.; Kato, T.; Matile, S. *J. Am. Chem. Soc.* **2006**, *128*, 2218.
(1128) Suárez, M.; Lehn, J.-M.; Zimmerman, S. C.; Skoulios, A.; Heinrich, B. *J. Am. Chem. Soc.* **1998**, *120*, 9526.
(1129) Kolotuchin, S. V.; Zimmerman, S. C. *J. Am. Chem. Soc.* **1998**, *120*, 9092.
(1130) Ma, Y.; Kolotuchin, S. V.; Zimmerman, S. C. *J. Am. Chem. Soc.* **2002**, *124*, 13757.
(1131) Jin, S.; Ma, Y.; Zimmerman, C. S.; Cheng, S. Z. D. *Chem. Mater.* **2004**, *16*, 2975.
(1132) Randic, M. *Chem. Rev.* **2003**, *103*, 3449.
(1133) Wu, J. S.; Pisula, W.; Müllen, K. *Chem. Rev.* **2007**, *107*, 718.
(1134) Hoeben, F. J. M.; Jonkheijm, P.; Meijer, E. W.; Schenning, A. *Chem. Rev.* **2005**, *105*, 1491.
(1135) Takaguchi, Y.; Tajima, T.; Yanagimoto, Y.; Tsuboi, S.; Ohta, K.; Motoyoshiya, J.; Aoyama, H. *Org. Lett.* **2003**, *5*, 1677.
(1136) Yanagimoto, Y.; Takaguchi, Y.; Sako, Y.; Tsuboi, S.; Ichihara, M.; Ohta, K. *Tetrahedron* **2006**, *62*, 8373.
(1137) Lin, Y. C.; Weiss, R. G. *Liq. Cryst.* **1989**, *4*, 367.
(1138) Kim, Y. H.; Yoon, D. K.; Lee, E. H.; Ko, Y. K.; Jung, H. T. *J. Phys. Chem. B* **2006**, *110*, 20836.
(1139) Schmidt-Mende, L.; Fechtenkotter, A.; Müllen, K.; Moons, E.; Friend, R. H.; MacKenzie, J. D. *Science* **2001**, *293*, 1119.
(1140) Cormier, R. A.; Gregg, B. A. *Chem. Mater.* **1998**, *10*, 1309.
(1141) Würthner, F.; Thalacker, C.; Diele, S.; Tschierske, C. *Chem.—Eur. J.* **2001**, *7*, 2245.
(1142) Jonkheijm, P.; van der Schoot, P.; Schenning, A.; Meijer, E. W. *Science* **2006**, *313*, 80.
(1143) Percec, V.; Ungar, G.; Peterca, M. *Science* **2006**, *313*, 55.
(1144) Dehm, V.; Chen, Z. J.; Baumeister, U.; Prins, P.; Siebbeles, L. D. A.; Würthner, F. *Org. Lett.* **2007**, *9*, 1085.
(1145) Ghosh, S.; Li, X.-Q.; Stepanenko, V.; Würthner, F. *Chem.—Eur. J.* **2008**, *14*, 11343.
(1146) An, Z. S.; Yu, J. S.; Jones, S. C.; Barlow, S.; Yoo, S.; Domercq, B.; Prins, P.; Siebbeles, L. D. A.; Kippelen, B.; Marder, S. R. *Adv. Mater.* **2005**, *17*, 2580.

(1147) Debije, M. G.; Chen, Z. J.; Piris, J.; Neder, R. B.; Watson, M. M.; Müllen, K.; Würthner, F. *J. Mater. Chem.* **2005**, *15*, 1270.
(1148) Chen, Z. J.; Debije, M. G.; Debaerdemaeker, T.; Osswald, P.; Würthner, F. *ChemPhysChem* **2004**, *5*, 137.
(1149) Fischer, M. K. R.; Kaiser, T. E.; Würthner, F.; Bäuerle, P. *J. Mater. Chem.* **2009**, *19*, 1129.
(1150) Duzhko, V.; Aqad, E.; Imam, M. R.; Peterca, M.; Percec, V.; Singer, K. D. *Appl. Phys. Lett.* **2008**, *92*, 113312.
(1151) Laiho, A.; Smarsly, B. M.; Faul, C. F. J.; Ikkala, O. *Adv. Funct. Mater.* **2008**, *18*, 1890.
(1152) Würthner, F.; Stepanenko, V.; Sautter, A. *Angew. Chem., Int. Ed.* **2006**, *45*, 1939.
(1153) Kaiser, T. E.; Wang, H.; Stepanenko, V.; Würthner, F. *Angew. Chem., Int. Ed.* **2007**, *46*, 5541.
(1154) Kaiser, T. E.; Stepanenko, V.; Würthner, F. *J. Am. Chem. Soc.* **2009**, *131*, 6719.
(1155) Martin, R. B. *Chem. Rev.* **1996**, *96*, 3043.
(1156) Würthner, F.; Chen, Z. J.; Hoeben, F. J. M.; Osswald, P.; You, C. C.; Jonkheijm, P.; von Herrikhuyzen, J.; Schenning, A.; van der Schoot, P.; Meijer, E. W.; Beckers, E. H. A.; Meskers, S. C. J.; Janssen, R. A. J. *J. Am. Chem. Soc.* **2004**, *126*, 10611.
(1157) Uji-i, H.; Miura, A.; Schenning, A.; Meijer, E. W.; Chen, Z. J.; Würthner, F.; De Schryver, F. C.; Van der Auweraer, M.; De Feyter, S. *ChemPhysChem* **2005**, *6*, 2389.
(1158) De Cat, I.; Roger, C.; Lee, C. C.; Hoeben, F. J. M.; Pouderoijen, M. J.; Schenning, A.; Würthner, F.; De Feyter, S. *Chem. Commun.* **2008**, 5496.
(1159) Jonkheijm, P.; Stutzmann, N.; Chen, Z. J.; de Leeuw, D. M.; Meijer, E. W.; Schenning, A.; Würthner, F. *J. Am. Chem. Soc.* **2006**, *128*, 9535.
(1160) Li, X. Q.; Stepanenko, V.; Chen, Z. J.; Prins, P.; Siebbeles, L. D. A.; Würthner, F. *Chem. Commun.* **2006**, 3871.
(1161) Schmidt, C. D.; Boettcher, C.; Hirsch, A. *Eur. J. Org. Chem.* **2007**, 5497.
(1162) Wang, H.; Shen, Z.; Ge, J. J.; Cheng, S. Z. D.; Harris, F. W. *Polym. Prepr. (Am. Chem. Soc., Div. Polym. Chem.)* **1999**, *40* (1), 486.
(1163) Kouwer, P. H. J.; Pourzand, J.; Mehl, G. H. *Chem. Commun.* **2004**, 66.
(1164) Ishihara, S.; Furuki, Y.; Takeoka, S. *Chem. Lett.* **2007**, *36*, 282.
(1165) Ma, X. J.; Yang, Y. L.; Deng, K.; Zeng, Q. D.; Wang, C.; Zhao, K. Q.; Hu, P.; Wang, B. Q. *ChemPhysChem* **2007**, *8*, 2615.
(1166) Pieterse, K.; van Hal, P. A.; Kleppinger, R.; Vekemans, J.; Janssen, R. A. J.; Meijer, E. W. *Chem. Mater.* **2001**, *13*, 2675.
(1167) Robertson, J.; Trotter, J. *J. Chem. Soc.* **1961**, 1280.
(1168) Robertson, J. M.; White, J. G. *J. Chem. Soc.* **1945**, 607.
(1169) Jin, W.; Fukushima, T.; Niki, M.; Kosaka, A.; Ishii, N.; Aida, T. *Proc. Natl. Acad. Sci. U.S.A.* **2005**, *102*, 10801.
(1170) Aida, T.; Fukushima, T. *Phil. Trans. R. Soc. London, Ser. A* **2007**, *365*, 1539.
(1171) Yamamoto, Y.; Fukushima, T.; Saeki, A.; Seki, S.; Tagawa, S.; Ishii, N.; Aida, T. *J. Am. Chem. Soc.* **2007**, *129*, 9276.
(1172) Hara, T.; Furukawa, K.; Nakamura, T.; Yamamoto, Y.; Kosaka, A.; Jin, W. S.; Fukushima, T.; Aida, T. *J. Phys. Soc. Jpn.* **2008**, 77.
(1173) Yamamoto, T.; Fukushima, T.; Kosaka, A.; Jin, W.; Yamamoto, Y.; Ishii, N.; Aida, T. *Angew. Chem., Int. Ed.* **2008**, *47*, 1672.
(1174) Biasutti, M. A.; Rommens, J.; Vaes, A.; De Feyter, S.; De Schryver, F. D.; Herwig, P.; Müllen, K. *Bull. Soc. Chim. Belg.* **1997**, *106*, 659.
(1175) Rohr, U.; Schlichting, P.; Bohm, A.; Gross, M.; Meerholz, K.; Brauchle, C.; Müllen, K. *Angew. Chem., Int. Ed.* **1998**, *37*, 1434.
(1176) Thunemann, A. F.; Ruppelt, D.; Burger, C.; Müllen, K. *J. Mater. Chem.* **2000**, *10*, 1325.
(1177) Rohr, U.; Kohl, C.; Müllen, K.; van de Craats, A.; Warman, J. *J. Mater. Chem.* **2001**, *11*, 1789.
(1178) Rieger, R.; Kastler, M.; Enkelmann, V.; Müllen, K. *Chem.—Eur. J.* **2008**, *14*, 6322.
(1179) Wu, J. S.; Watson, M. D.; Zhang, L.; Wang, Z. H.; Müllen, K. *J. Am. Chem. Soc.* **2004**, *126*, 177.
(1180) Wu, J. S.; Li, J. X.; Kolb, U.; Müllen, K. *Chem. Commun.* **2006**, 48.
(1181) Don, X.; Pisula, W.; Wu, J.; Bodwell, G. J.; Müllen, K. *Chem.—Eur. J.* **2008**, *14*, 240.
(1182) Mynar, J. L.; Yamamoto, T.; Kosaka, A.; Fukushima, T.; Ishii, N.; Aida, T. *J. Am. Chem. Soc.* **2008**, *130*, 1530.
(1183) Miyajima, D.; Tashuiro, K.; Araoka, F.; Takazoe, H.; Kim, J.; Kato, K.; Takata, M.; Aida, T. *J. Am. Chem. Soc.* **2009**, *131*, 44.
(1184) Yelamaggad, C. V.; Achalkumar, A. S.; Rao, D. S. S.; Prasad, S. K. *J. Org. Chem.* **2007**, *72*, 8308.
(1185) Yelamaggad, C. V.; Achalkumar, A. S.; Rao, D. S. S.; Prasad, S. K. *J. Org. Chem.* **2009**, *74*, 3168.
(1186) Metzger, R. M.; Wiser, D. C.; Laidlaw, R. K.; Takassi, M. A.; Mattern, D. L.; Panetta, C. A. *Langmuir* **1990**, *6*, 350.
(1187) Isoda, K.; Yasuda, T.; Kato, T. *J. Mater. Chem.* **2008**, *18*, 4522.
(1188) Kitahara, T.; Shirakawa, M.; Kawano, S.; Beginn, U.; Fujita, N.; Shinkai, S. *J. Am. Chem. Soc.* **2005**, *127*, 14980.
(1189) Rodriguez-Parada, J. M.; Percec, V. *J. Polym. Sci., Part A: Polym. Chem.* **1986**, *24*, 1363.
(1190) Pugh, C.; Percec, V. *Polym. Bull.* **1986**, *16*, 513.
(1191) Hsu, C. S.; Rodriguez-Parada, J. M.; Percec, V. *J. Polym. Sci., Part A: Polym. Chem.* **1987**, *25*, 2425.
(1192) Hsu, C. S.; Percec, V. *Polym. Bull.* **1987**, *17*, 49.
(1193) Hsu, C. S.; Percec, V. *Makromol. Chem. Rapid Commun.* **1987**, *8*, 331.
(1194) Percec, V.; Hahn, B. *J. Polym. Sci., Part A: Polym. Chem.* **1989**, *27*, 2367.
(1195) Percec, V.; Tomazos, D.; Pugh, C. *Macromolecules* **1989**, *22*, 3229.
(1196) Perry, B. C.; Hahn, B.; Percec, V.; Koenig, J. *Polymer* **1990**, *31*, 721.
(1197) Percec, V.; Tamazos, D. *Polymer* **1990**, *31*, 1658.
(1198) Percec, V.; Hahn, B.; Ebert, M.; Wendorff, J. H. *Macromolecules* **1990**, *23*, 2092.
(1199) Percec, V.; Keller, A. *Macromolecules* **1990**, *23*, 4347.
(1200) Gu, D.; Jamieson, A. M.; Rosenblatt, C.; Tomazos, D.; Lee, M.; Percec, V. *Macromolecules* **1991**, *24*, 2385.
(1201) Percec, V.; Lee, M. *Macromolecules* **1991**, *24*, 2780.
(1202) Gedde, U. W.; Jonsson, H.; Hult, A.; Percec, V. *Polymer* **1992**, *33*, 4352.
(1203) Percec, V.; Tomazos, D. *J. Mater. Chem.* **1993**, *3*, 633.
(1204) Percec, V.; Tomazos, D. *J. Mater. Chem.* **1993**, *3*, 643.
(1205) Gu, D.; Smith, S. R.; Jamieson, A. M.; Lee, M.; Percec, V. *J. Phys II (France)* **1993**, *3*, 937.
(1206) Zhong, Z. Z.; Gordon, W. L.; Schuele, D. E.; Akins, R. B.; Percec, V. *Mol. Cryst. Liq. Cryst.* **1994**, *238*, 129.
(1207) Stebani, U.; Lattermann, G. *Adv. Mater.* **1995**, *7*, 578.
(1208) Stebani, U.; Lattermann, G.; Wittenberg, M.; Wendorff, J. H. *Angew. Chem., Int. Ed.* **1996**, *35*, 1858.
(1209) Cameron, J. H.; Facher, A.; Lattermann, G.; Diele, S. *Adv. Mater.* **1997**, *9*, 398.
(1210) Precup-Blaga, F. S.; Schenning, A. P. H. J.; Meijer, E. W. *Macromolecules* **2003**, *36*, 565.
(1211) Baars, M. W. P. L.; van Boxtel, M. C. W.; Bastiaansen, C. W. M.; Broer, D. J.; Söntjens, S. H. M.; Meijer, E. W. *Adv. Mater.* **2000**, *12*, 715.
(1212) Gehringer, L.; Guillon, D.; Donnio, B. *Macromolecules* **2003**, *36*, 5593.
(1213) Gehringer, L.; Bourgogne, C.; Guillon, D.; Donnio, B. *J. Am. Chem. Soc.* **2004**, *126*, 3856.
(1214) Pastor, L.; Barberá, J.; McKenna, M.; Marcos, M.; Martín-Rapún, R.; Serrano, J.-L.; Luckhurst, G. R.; Mainal, A. *Macromolecules* **2004**, *37*, 9386.
(1215) Barberá, J.; Giménez, R.; Marcos, M.; Serrano, J. L. *Liq. Cryst.* **2002**, *29*, 309.
(1216) Martín-Rapún, R.; Marcos, M.; Omenat, A.; Serrano, J.-L.; Luckhurst, G. R.; Mainal, A. *Chem. Mater.* **2004**, *16*, 4969.
(1217) Marcos, M.; Martín-Rapún, R.; Omenat, A.; Barberá, J.; Serrano, J. L. *Chem. Mater.* **2006**, *18*, 1206.
(1218) Rueff, J.-M.; Barberá, J.; Marcos, M.; Omenat, A.; Martín-Rapún, R.; Donnio, B.; Guillon, D.; Serrano, J. L. *Chem. Mater.* **2006**, *18*, 249.
(1219) Donnio, B.; Barberá, J.; Giménez, R.; Guillon, D.; Marcos, M.; Serrano, J. L. *Macromolecules* **2002**, *35*, 370.
(1220) Marcos, M.; Giménez, R.; Serrano, J. L.; Donnio, B.; Heinrich, B.; Guillon, D. *Chem.—Eur. J.* **2001**, *7*, 1006.
(1221) Barberá, J.; Donnio, B.; Giménez, R.; Guillon, D.; Marcos, M.; Omenat, A.; Serrano, J. L. *J. Mater. Chem.* **2001**, *11*, 2808.
(1222) Rueff, J.-M.; Barberá, J.; Donnio, B.; Guillon, D.; Marcos, M.; Serrano, J. L. *Macromolecules* **2003**, *36*, 8368.
(1223) Archut, A.; Gestermann, S.; Hesse, R.; Kauffmann, C.; Vögtle, F. *Synlett* **1998**, 546.
(1224) Majoros, I. J.; Williams, C. R.; Tomalia, D. A.; Baker, J. R. *Macromolecules* **2008**, *41*, 8372.
(1225) Percec, V.; Rudick, J. G.; Peterca, M.; Yurchenko, M. E.; Smidrkal, J.; Heiney, P. A. *Chem.—Eur. J.* **2008**, *14*, 3355.
(1226) Percec, V.; Imam, M. R.; Peterca, M.; Cho, W.-D.; Heiney, P. A. *Isr. J. Chem.* **2008**, *49*, 55.
(1227) Moore, J. S.; Xu, Z. *Macromolecules* **1991**, *24*, 5893.
(1228) Xu, Z.; Kahr, M.; Walker, K. L.; Wilkins, C. L.; Moore, J. S. *J. Am. Chem. Soc.* **1994**, *116*, 4537.
(1229) Pesak, D. J.; Moore, J. S. *Angew. Chem., Int. Ed.* **1997**, *36*, 1636.
(1230) Deb, S. K.; Maddux, T. M.; Yu, L. *J. Am. Chem. Soc.* **1997**, *119*, 9079.
(1231) Meier, H.; Lehmann, M. *Angew. Chem., Int. Ed.* **1998**, *37*, 643.
(1232) Meier, H.; Lehmann, M.; Kolb, U. *Chem.—Eur. J.* **2000**, *6*, 2462.
(1233) Lehmann, M.; Schartel, B.; Hennecke, M.; Meier, H. *Tetrahedron* **1999**, *55*, 13377.

(1234) Steffensen, M. B.; Hollink, E.; Kuschel, F.; Bauer, M.; Simanek, E. E. *J. Polym. Sci., Part A: Polym. Chem.* **2006**, *44*, 3411.
(1235) Lai, L.-L; Lee, C.-H.; Wang, L.-Y.; Cheng, K.-L.; Hsu, H.-F. *J. Org. Chem.* **2008**, *73*, 485.
(1236) Percec, V.; Imam, M. R.; Bera, T. K.; Balagurusamy, V. S. K.; Peterca, M.; Heiney, P. A. *Angew. Chem., Int. Ed.* **2005**, *44*, 4739.
(1237) Percec, V.; Rudick, J. G.; Peterca, M.; Yurchenko, M. E.; Smidrkal, J.; Heiney, P. A. *Chem.—Eur. J.* **2008**, *14*, 909.
(1238) Hawker, C. J.; Fréchet, J. M. J. *J. Am. Chem. Soc.* **1992**, *114*, 8405.
(1239) Gillies, E. R.; Fréchet, J. M. J. *J. Am. Chem. Soc.* **2002**, *124*, 14137.
(1240) Saez, I. M.; Goodby, J. W. *Chem. Commun.* **2003**, 1726.
(1241) Saez, I. M.; Goodby, J. W. *Chem.—Eur. J.* **2003**, *9*, 4869.
(1242) Ropponen, J.; Nummelin, S.; Rissanen, K. *Org. Lett.* **2004**, *6*, 2495.
(1243) Feng, Y.; He, Y.-M.; Zhao, L.-W.; Huang, Y.-Y.; Fan, Q.-H. *Org. Lett.* **2007**, *9*, 2261.
(1244) Tuuttila, T.; Lipsonen, J.; Lahtinen, M.; Huuskonen, J.; Rissanen, K. *Tetrahedron* **2008**, *64*, 10590.
(1245) Fuchs, S.; Pla-Quintana, A.; Mazeres, S.; Caminade, A.-M.; Majoral, J.-P. *Org. Lett.* **2008**, *10*, 4751.
(1246) Yang, M.; Zhang, Z.; Yuan, F.; Wang, W.; Hess, S.; Lienkamp, K.; Lieberwirth, I.; Wegner, G. *Chem.—Eur. J.* **2008**, *14*, 3330.
(1247) Bury, I.; Heinrich, B.; Bourgogne, C.; Guillon, D.; Donnio, B. *Chem.—Eur. J.* **2006**, *12*, 8396.
(1248) Bury, I.; Donnio, B.; Gallani, J.-L.; Guillon, D. *Langmuir* **2007**, *23*, 619.
(1249) Scanu, D.; Yevlampieva, N. P.; Deschenaux, R. *Macromolecules* **2007**, *40*, 1133.
(1250) Lenoble, J.; Campidelli, S.; Maringa, N.; Donnio, B.; Guillon, D.; Yevlampieva, N.; Deschenaux, R. *J. Am. Chem. Soc.* **2007**, *129*, 9941.
(1251) Amabilino, D. B.; Ashton, P. R.; Balzani, V.; Brown, C. L.; Credi, A.; Frechet, J. M. J.; Leon, J. W.; Raymo, F. M.; Spencer, N.; Stoddart, J. F.; Venturi, M. *J. Am. Chem. Soc.* **1996**, *118*, 12012.
(1252) Jeppesen, J. O.; Perkins, J.; Becher, J.; Stoddart, J. F. *Angew. Chem., Int. Ed.* **2001**, *40*, 1216.
(1253) Srinivasan, K.; Rajakumar, P. *Synthesis* **2005**, *16*, 2772.
(1254) Green, J. E.; Choi, J. W.; Boukai, A.; Bunimovich, Y.; Johnston-Halperin, E.; Delonno, E.; Luo, Y.; Sheriff, B. A.; Xu, K.; Shin, Y. S.; Tseng, H.-R.; Stoddart, J. F.; Heath, J. R. *Nature* **2007**, *445*, 414.
(1255) Jeppesen, J. O.; Nielsen, K. A.; Perkins, J.; Vignon, S. A.; Di Fabio, A.; Ballardini, R.; Gandolfi, M. T.; Venturi, M.; Balzani, V.; Becher, J.; Stoddart, J. F. *Chem.—Eur. J.* **2003**, *9*, 2982.
(1256) Aprahamian, I.; Yasuda, T.; Ikeda, T.; Saha, S.; Dichtel, W. R.; Isoda, K.; Kato, T.; Stoddart, J. F. *Angew. Chem., Int. Ed.* **2007**, *46*, 4675.
(1257) Leung, K. C. F.; Arico, F.; Cantrill, S. J.; Stoddart, J. F. *J. Am. Chem. Soc.* **2005**, *127*, 5808.
(1258) Leung, K. C. F.; Arico, F.; Cantrill, S. J.; Stoddart, J. F. *Macromolecules* **2007**, *40*, 3951.
(1259) Elizarov, A. M.; Chiu, S.-H.; Glink, P. T.; Stoddart, F. J. *Org. Lett.* **2002**, 679.
(1260) Elizarov, A. M.; Chang, T.; Chiu, S. H.; Stoddart, J. F. *Org. Lett.* **2002**, *4*, 3565.
(1261) Spruell, J. M.; Dichtel, W. R.; Heath, J. R.; Stoddart, J. F. *Chem.—Eur. J.* **2008**, *14*, 4168.
(1262) Yamaguchi, N.; Hamilton, L. M.; Gibson, H. W. *Angew. Chem., Int. Ed.* **1998**, *37*, 3275.
(1263) Gibson, H. W.; Hamilton, L.; Yamaguchi, N. *Polym. Adv. Technol.* **2000**, *11*, 791.
(1264) Gibson, H. W.; Yamaguchi, N.; Hamilton, L.; Jones, J. W. *J. Am. Chem. Soc.* **2002**, *124*, 4653.
(1265) Nirengarten, J.-F.; Hahn, U.; Trabolsi, A.; Herschbach, H.; Cardinali, F.; Elhabiri, M.; Leize, E.; Dorssalaer, A. V.; Albrecht-Gary, A.-M. *Chem.—Eur. J.* **2006**, *12*, 3365.
(1266) Hubner, G. M.; Nachtsheim, G.; Li, Q. Y.; Seel, C.; Vögtle, F. *Angew. Chem., Int. Ed.* **2000**, *39*, 1269.
(1267) Ong, W.; Grindstaff, J.; Sobransingh, D.; Toba, R.; Quintela, J. M.; Peinador, C.; Kaifer, A. E. *J. Am. Chem. Soc.* **2005**, *127*, 3353.
(1268) Moon, K.; Grindstaff, J.; Sobransingh, D.; Kaifer, A. E. *Angew. Chem., Int. Ed.* **2004**, *43*, 5496.
(1269) Wang, W.; Kaifer, A. E. *Angew. Chem., Int. Ed.* **2006**, *45*, 7042.
(1270) Lee, J. W.; Han, S. C.; Kim, J. H.; Ko, Y. H.; Kim, K. *Bull. Korean Chem. Soc.* **2007**, *28*, 1837.
(1271) Kim, S. Y.; Ko, Y. H.; Lee, J. W.; Sakamoto, S.; Yamaguchi, K.; Kim, K. *Chem. Asian J.* **2007**, *2*, 747.
(1272) Park, C.; Lee, I. H.; Lee, S.; Song, Y.; Rhue, M.; Kim, C. *Proc. Natl. Acad. Sci. U.S.A.* **2006**, *103*, 1199.
(1273) Li, J.; Yang, C.; Li, H. Z.; Wang, X.; Goh, S. H.; Ding, J. L.; Wang, D. Y.; Leong, K. W. *Adv. Mater.* **2006**, *18*, 2969.
(1274) Recker, J.; Muller, W. M.; Muller, U.; Kubota, T.; Okamoto, Y.; Nieger, M.; Vögtle, F. *Chem.—Eur. J.* **2002**, *8*, 4434.
(1275) Safarowsky, O.; Nieger, M.; Frohlich, R.; Vogtle, F. *Angew. Chem., Int. Ed.* **2000**, *39*, 1616.
(1276) Lukin, O.; Kubota, T.; Okamoto, Y.; Kaufmann, A.; Vögtle, F. *Chem.—Eur. J.* **2004**, *10*, 2804.
(1277) Reuter, C.; Pawlitzki, G.; Worsdorfer, U.; Plevoets, M.; Mohry, A.; Kubota, T.; Okamoto, Y.; Vögtle, F. *Eur. J. Org. Chem.* **2000**, 3059.
(1278) Baranoff, E. D.; Voignier, J.; Yasuda, T.; Heitz, V.; Sauvage, J. P.; Kato, T. *Angew. Chem., Int. Ed.* **2007**, *46*, 4680.
(1279) Wooley, K. L.; Hawker, C. J.; Frechet, J. M. J.; Wudl, F.; Srdanov, G.; Shi, S.; Li, C.; Kao, M. *J. Am. Chem. Soc.* **1993**, *115*, 9836.
(1280) Birkett, P. R.; Hitchcock, P. B.; Kroto, H. W.; Taylor, R.; Walton, D. R. M. *Nature* **1991**, *357*, 479.
(1281) Bingel, C. *Chem. Ber.* **1993**, *126*, 1957.
(1282) Bingel, C. *Chem. Ber.* **1993**, *126*, 1957.
(1283) Hirsch, A.; Brettreich, M. *Fullerenes Chemistry and Reactions*; Wiley-VCH Verlag GmbH & Co: Weinheim, Germany, 2005.
(1284) Nierengarten, J. F.; Gramlich, V.; Cardullo, F.; Diederich, F. *Angew. Chem., Int. Ed. Engl.* **1996**, *35*, 2101.
(1285) Nierengarten, J. F.; Nicoud, J. F. *Tetrahedron Lett.* **1997**, *38*, 7737.
(1286) Camps, X.; Hirsch, A. *J. Chem. Soc., Perkin Trans. 1* **1997**, 1595.
(1287) Donnio, B.; Buathong, S.; Bury, I.; Guillon, D. *Chem. Soc. Rev.* **2007**, *36*, 1495.
(1288) Campidelli, S.; Eng, C.; Saez, I. M.; Goodby, J. W.; Deschenaux, R. *Chem. Commun.* **2003**, 1520.
(1289) Campidelli, S.; Lenoble, J.; Barbera, J.; Paolucci, F.; Marcaccio, M.; Paolucci, D.; Deschenaux, R. *Macromolecules* **2005**, *38*, 7915.
(1290) Lenoble, J.; Maringa, N.; Campidelli, S.; Donnio, B.; Guillon, D.; Deschenaux, R. *Org. Lett.* **2006**, *8*, 1851.
(1291) Shen, Y.; Wang, J.; Kuhlmann, U.; Hildebrandt, P.; Ariga, K.; Möhwald, H.; Kurth, D. G.; Nakanishi, T. *Chem.—Eur. J.* **2009**, *15*, 2763.
(1292) Wang, J.; Shen, Y.; Kessel, S.; Fernandes, P.; Yoshida, K.; Yigai, S.; Kurth, D. G.; Möhwald, H.; Nakanishi, T. *Angew. Chem., Int. Ed.* **2009**, *48*, 2166.
(1293) Perez, L.; Lenoble, J.; Barbera, J.; de la Cruz, P.; Deschenaux, R.; Langa, F. *Chem. Commun.* **2008**, 4590.
(1294) Sako, Y.; Takaguchi, Y.; Ichihara, M.; Ohta, K. *Sen-I Gakkaishi* **2008**, *64*, 324.
(1295) Maringa, N.; Lenoble, J.; Donnio, B.; Guillon, D.; Deschenaux, R. *J. Mater. Chem.* **2008**, *18*, 1524.
(1296) Tirelli, N.; Cardullo, F.; Habicher, T.; Suter, U. W.; Diederich, F. *J. Chem Soc., Perkin Trans. 2* **2000**, 193.
(1297) Peroukidis, S. D.; Vanakaras, A. G.; Photinos, D. J. *J. Phys. Chem. B* **2008**, *112*, 12761.
(1298) Sawamura, M.; Kawai, K.; Matsuo, Y.; Kanie, K.; Kato, T.; Nakamura, E. *Nature* **2002**, *419*, 702.
(1299) Matsuo, Y.; Muramatsu, A.; Kamikawa, Y.; Kato, T.; Nakamura, E. *J. Am. Chem. Soc.* **2006**, *128*, 9586.
(1300) Li, W. S.; Yamamoto, Y.; Fukushima, T.; Saeki, A.; Seki, S.; Tagawa, S.; Masunaga, H.; Sasaki, S.; Takata, M.; Aida, T. *J. Am. Chem. Soc.* **2008**, *130*, 8886.
(1301) Nakanishit, T.; Shen, Y.; Wang, J.; Yagai, S.; Funahashi, M.; Kato, T.; Fernandes, P.; Mohwald, H.; Kurth, D. G. *J. Am. Chem. Soc.* **2008**, *130*, 9236.
(1302) Tuladhar, S. M.; Poplavskyy, D.; Choulis, S. A.; Durrant, J. R.; Bradley, D. D. C.; Nelson, J. *Adv. Funct. Mater.* **2005**, *15*, 1171.
(1303) Yoshimoto, N.; Hanna, J. *J. Mater. Chem.* **2003**, *13*, 1004.
(1304) Mahmud, I. M.; Zhou, N. Z.; Wang, L.; Zhao, Y. M. *Tetrahedron* **2008**, *64*, 11420.
(1305) Brettreich, B.; Hirsch, A. *Tetrahedron Lett.* **1998**, *39*, 2731.
(1306) Brettreich, B.; Burghardt, S.; Böttcher, C.; Bayerl, T.; Bayerl, S.; Hirsch, A. *Angew. Chem., Int. Ed.* **2000**, *39*, 1845.
(1307) Maierhofer, A. P.; Brettreich, M.; Burghardt, S.; Vostrowsky, O.; Hirsch, A.; Langridge, S.; Bayerl, T. M. *Langmuir* **2000**, *16*, 8884.
(1308) Braun, M.; Atalick, S.; Guldi, D. S.; Lanig, H.; Brettreich, B.; Burghardt, S.; Hatzimarinaki, M.; Ravanelli, E.; Prato, M.; Van Eldik, R.; Hirsch, A. *Chem.—Eur. J.* **2003**, *9*, 3867.
(1309) Burghardt, S.; Hirsch, A.; Schade, B.; Ludwig, K.; Bottcher, C. *Angew. Chem., Int. Ed.* **2005**, *44*, 2976.
(1310) Schade, B.; Ludwig, K.; Bottcher, C.; Hartnagel, U.; Hirsch, A. *Angew. Chem., Int. Ed.* **2007**, *46*, 4393.
(1311) Kato, H.; Bottcher, C.; Hirsch, A. *Eur. J. Org. Chem.* **2007**, 2659.
(1312) Partha, R.; Lackey, M.; Hirsch, A.; Ward Casscells, S.; Conyers, J. L. J. Nanobiotechnol. 2007, *5*.
(1313) Li, W. S.; Kim, K. S.; Jiang, D. L.; Tanaka, H.; Kawai, T.; Kwon, J. H.; Kim, D.; Aida, T. *J. Am. Chem. Soc.* **2006**, *128*, 10527.
(1314) Bahatyrova, S.; Frese, R. N.; Siebert, C. A.; Olsen, J. D.; van der Werf, K. O.; van Grondelle, R.; Niederman, R. A.; Bullough, P. A.; Otto, C.; Hunter, C. N. *Nature* **2004**, *430*, 1058.
(1315) Frese, R. N.; Siebert, C. A.; Niederman, R. A.; Hunter, C. N.; Otto, C.; van Grondelle, R. *Proc. Natl. Acad. Sci. U.S.A.* **2004**, *101*, 17994.

(1316) Sener, M. K.; Olsen, J. D.; Hunter, C. N.; Schulten, K. *Proc. Natl. Acad. Sci. U.S.A.* **2007**, *104*, 15723.
(1317) Koepke, J.; Hu, X. C.; Muenke, C.; Schulten, K.; Michel, H. *Structure* **1996**, *4*, 581.
(1318) Chang, S. K.; Hamilton, A. D. *J. Am. Chem. Soc.* **1988**, *110*, 1318.
(1319) Hager, K.; Hartnagel, U.; Hirsch, A. *Eur. J. Org. Chem.* **2007**, 1942.
(1320) Fernandez, G.; Perez, E. M.; Sanchez, L.; Martin, N. *J. Am. Chem. Soc.* **2008**, *130*, 2410.
(1321) Fernandez, G.; Sanchez, L.; Perez, E. M.; Martin, N. *J. Am. Chem. Soc.* **2008**, *130*, 10674.
(1322) Hartnagel, U.; Balbinot, D.; Jux, N.; Hirsch, A. *Org. Biomol. Chem.* **2006**, *4*, 1785.
(1323) Kojima, C.; Toi, Y.; Harada, A.; Kono, K. *Bioconjugate Chem.* **2008**, *19*, 2280.
(1324) Seddon, K. R. *J. Chem. Technol. Biotechnol.* **1997**, *68*, 351.
(1325) Welton, T. *Chem. Rev.* **1999**, *99*, 2071.
(1326) Sheldon, R. *Chem. Commun.* **2001**, 2399.
(1327) Plechkova, N. V.; Seddon, K. R. *Chem. Soc. Rev.* **2008**, *37*, 123.
(1328) Binnemans, K. *Chem. Rev.* **2005**, *105*, 4148.
(1329) Yoshio, M.; Mukai, T.; Ohno, H.; Kato, T. *J. Am. Chem. Soc.* **2004**, *126*, 994.
(1330) Yoshio, M.; Ichikawa, T.; Shimura, H.; Kagata, T.; Hamasaki, A.; Mukai, T.; Ohno, H.; Kato, T. *Bull. Chem. Soc. Jpn.* **2007**, *80*, 1836.
(1331) Shimura, H.; Yoshio, M.; Hoshino, K.; Mukai, T.; Ohno, H.; Kato, T. *J. Am. Chem. Soc.* **2008**, *130*, 1759.
(1332) Yazaki, S.; Kamikawa, Y.; Yoshio, M.; Hamasaki, A.; Mukai, T.; Ohno, H.; Kato, T. *Chem. Lett.* **2008**, *37*, 538.
(1333) Imam, M. R.; Peterca, M.; Edlund, U.; Balagursamy, V. S. K.; Percec, V. *J. Polym. Sci., Part A: Polym. Chem.* **2009**, *47*, 4165.
(1334) Ichikawa, T.; Yoshio, M.; Hamasaki, A.; Mukai, T.; Ohno, H.; Kato, T. *J. Am. Chem. Soc.* **2007**, *129*, 10662.
(1335) Bhattacharya, P.; Kaifer, A. E. *J. Org. Chem.* **2008**, *73*, 5693.
(1336) Ronconi, C. M.; Stoddart, J. F.; Balzani, V.; Baroncini, M.; Ceroni, P.; Giansante, C.; Venturi, M. *Chem.—Eur. J.* **2008**, *14*, 8365.
(1337) Tanabe, K.; Yasuda, T.; Kato, T. *Chem. Lett.* **2008**, *37*, 1208.
(1338) Smith, R. C.; Fischer, W. M.; Gin, D. L. *J. Am. Chem. Soc.* **1997**, *119*, 4092.
(1339) Deng, H.; Gin, D. L.; Smith, R. C. *J. Am. Chem. Soc.* **1998**, *120*, 3522.
(1340) Gin, D. L.; Grey, D. H.; Smith, R. C.; Deng, H.; Kim, E.; Juang, E.; Baxter, B. C. *Polym. Mater. Sci. Eng.* **1999**, *80*, 5.
(1341) Juang, E.; Schwartz, K. B.; Deng, H.; Reimer, J. A.; Gin, D. L. *Polym. Mater. Sci. Eng.* **1999**, 384.
(1342) Gin, D. L.; Gray, D. H.; Smith, R. C. *Synlett* **1999**, 1509.
(1343) Resel, R.; Leising, G; Markart, P.; Kriechbaum, M.; Smith, R.; Gin, D. *Macromol. Chem. Phys.* **2000**, *201*, 1128.
(1344) Ding, J. H.; Gin, D. L. *Chem. Mater.* **2000**, *12*, 22.
(1345) Kawa, M.; Fréchet, J. M. J. *Thin Solid Films* **1998**, *331*, 259.
(1346) Kawa, M.; Fréchet, J. M. J. *Chem. Mater.* **1998**, *10*, 286.
(1347) Kawa, K.; Motoda, M. *Kobunshi Ronbunshu* **2000**, *12*, 855.
(1348) Pitois, C.; Hult, A.; Lindgren, M. *J. Lumin.* **2005**, *111*, 265.
(1349) Lehn, J.-M. *Angew. Chem., Int. Ed.* **1988**, *27*, 89.
(1350) Feynman, R. *J. Microelectromech. Sys.* **1992**, *1*, 60.
(1351) Tekade, R. K.; Kumar, P. V.; Jain, N. K. *Chem. Rev.* **2009**, *109*, 49.
(1352) Duncan, R.; Izzo, L. *Adv. Drug Delivery Rev.* **2005**, *57*, 2215.
(1353) Amir, R. J.; Pessah, N.; Shamis, M.; Shabat, D. *Angew. Chem., Int. Ed.* **2003**, *42*, 4494.
(1354) Haba, K.; Popkov, M.; Shamis, M.; Lerner, R. A.; Barbas, C. F., III; Shabat, D. *Angew. Chem., Int. Ed.* **2005**, *44*, 716.
(1355) Sagi, A.; Segal, E.; Satchi-Fainaro, R.; Shabat, D. *Bioorg. Med. Chem.* **2007**, *15*, 3720.
(1356) Sella, E.; Shabat, D. *J. Am. Chem. Soc.* **2009**, *131*, 9934.
(1357) Kukowska-Latallo, J. F.; Bielinksa, A. U.; Johnson, J.; Spindler, R.; Tomalia, D. A.; Baker, J. R. *Proc. Acad. Nat. Sci. U.S.A.* **1996**, *93*, 4897.
(1358) Bielinska, A. U.; Kukowska-Latallo, J. F.; Johnson, J.; Tomalia, D. A.; Baker, J. R. *Nucl. Acid Res.* **1996**, *24*, 2176.
(1359) Chen, W.; Turro, N. J.; Tomalia, D. A. *Langmuir* **2000**, *16*, 15.
(1360) Ottiavani, M. F.; Furini, F.; Casani, A.; Turro, N. J.; Jockusch, S.; Tomalia, D. A.; Messori, L. *Macromolecules* **2000**, *33*, 7842.
(1361) Braun, C. S.; Vetro, J. A.; Tomalia, D. A.; Koe, G. S.; Koe, J. G.; Middaugh, C. R. *J. Pharm. Sci.* **2005**, *94*, 423.
(1362) Braun, C. S.; Fisher, M. T.; Tomalia, D. A.; Koe, G. S.; Koe, J. G.; Middaugh, C. R. *Biophys. J.* **2005**, *88*, 4146.
(1363) Shah, D. S.; Sakthivel, T.; Toth, I.; Florence, A. T.; Wilderspin, A. F. *Int. J. Pharm.* **2000**, *208*, 41.
(1364) Bayele, H. K.; Sakthivel, T.; O'Donell, M.; Pasi, K. J.; Wilderspin, A. F.; Lee, C. A.; Toth, I.; Florence, A. T. *J. Pharm. Sci.* **2005**, *94*, 446.
(1365) Toth, I.; Sakthivel, T.; Wilderspin, A. F.; Bayele, H.; O'Donnel, M.; Perry, D. J.; Pasi, K. J.; Lee, C. A.; Florence, A. T. S. I. P. *Pharm. Sci.* **1999**, *9*, 93.
(1366) Förster, S.; Neubert, I.; Schlüter, A. D.; Lindner, P. *Macromolecules* **1999**, *32*, 4043.
(1367) Chen, L.; Jamieson, A. M.; Kawasumi, M.; Percec, V. *J. Polym. Sci., Part B: Polm. Phys.* **1995**, *33*, 1213.
(1368) Chiang, Y.-C.; Jamieson, A. M.; Kawasumi, M.; Percec, V. *Macromolecles* **1997**, *30*, 1992.
(1369) Jin, J.; Fisch, M. R.; Mahajan, M. P.; Crandall, K. A.; Chu, P.; Huang, C.-Y.; Percec, V.; Petschek, R. G.; Rosenblatt, C. *Eur. Phys. J. B* **1998**, *5*, 251.
(1370) Hirst, A. R.; Escuder, B.; Miravet, J. F.; Smith, D. K. *Angew. Chem., Int. Ed.* **2008**, *47*, 8002.
(1371) Knapen, J. W. J.; van der Made, A. W.; de Wilde, J. C.; van Leeuwen, P. W. N. M.; Wijkens, P.; Grove, D. M.; van Koten, G. *Nature* **1994**, *372*, 659.
(1372) Albrecht, M.; Hovestad, N. J.; Boersma, J.; van Koten, G. *Chem.—Eur. J.* **2001**, *7*, 1289.
(1373) De Groot, D.; Eggeling, E. B.; de Wilde, J. C.; Koojiman, H.; van Haaren, R. J.; van der Made, A. W.; Spek, A. L.; Vogt, D.; Reek, J. N. H.; Kamer, P. C. J.; van Leeuwen, P. W. N. M. *Chem. Commun.* **1999**, 1623.
(1374) Dijkstra, H. P.; van Klink, G. P. M.; van Koten, G. *Acc. Chem. Res.* **2002**, *35*, 798.
(1375) Fujihara, T.; Yoshida, S.; Terao, J.; Tsuji, Y. *Org. Lett.* **2009**, *11*, 2121.
(1376) Snir, Y.; Kamien, R. D. *Science* **2005**, *307*, 1067.
(1377) Ziherl, P.; Kamien, R. D. *J. Phys. Chem. B* **2001**, *105*, 10147.
(1378) Cagin, T.; Wang, G.; Martin, R.; Zamanakos, G.; Vaidehi, N.; Mainz, D. T.; Goddard, W. A. *Comp. Theor. Polym. Sci.* **2001**, *11*, 345.
(1379) Li, Y.; Lin, S.-T.; Goddard, W. A. *J. Am. Chem. Soc.* **2004**, *126*, 1872.
(1380) de Greef, T. F. A.; Smulders, M. M. J.; Wolffs, M.; Schenning, A. P. H. J.; Sijbesma, R. P.; Meijer, E. J. Chem. Rev. 2009, *131*, in press.

CR900157Q